Paul A. Tipler
Ralph A. Llewellyn

MODERN PHYSICS

Fifth Edition

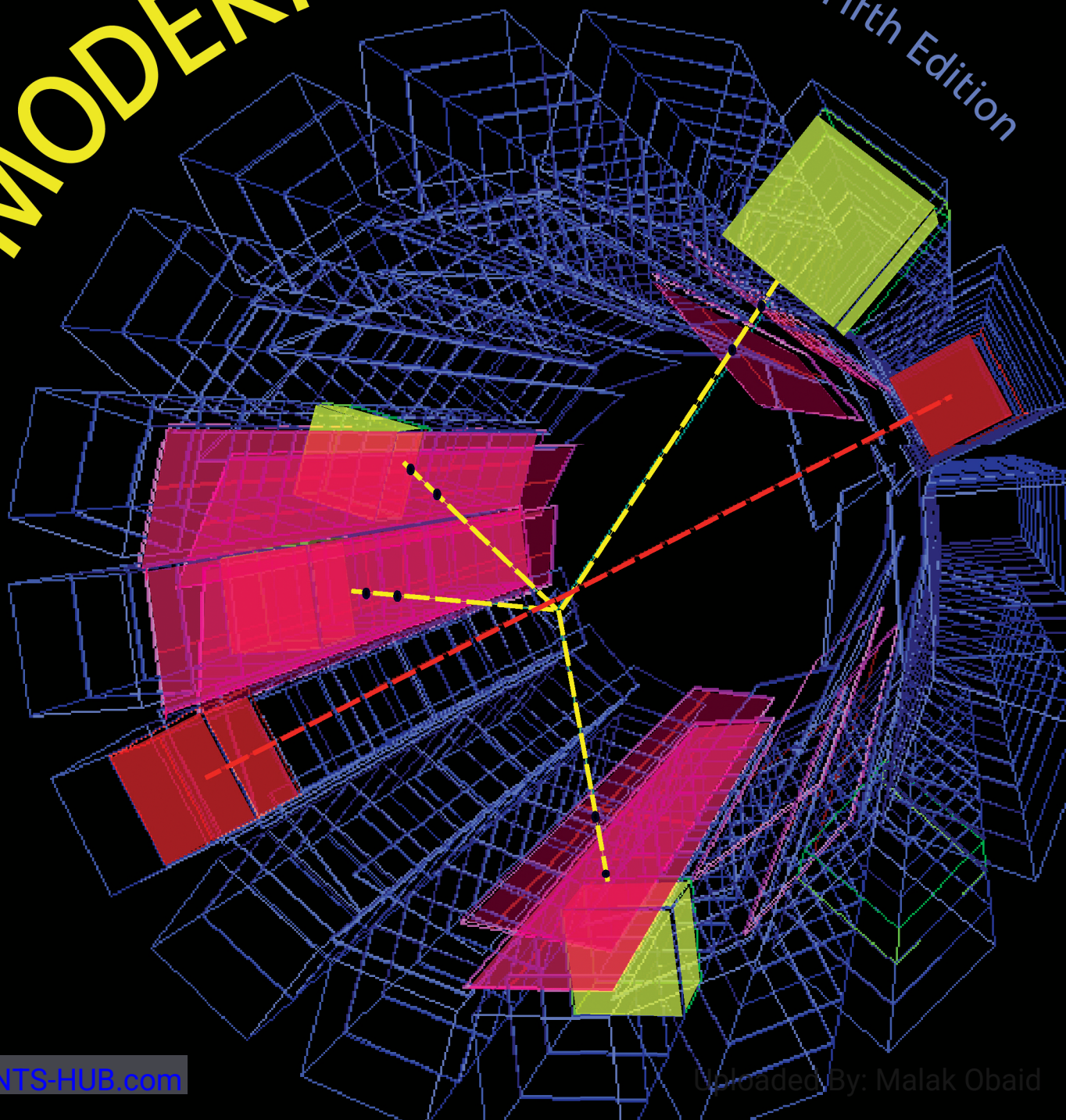

STUDENTS-HUB.com
Uploaded By: Malak Obaid

Publisher: Clancy Marshall
Senior Acquisitions Editor: Jessica Fiorillo
Marketing Manager: Anthony Palmiotto
Media Editors: Jeanette Picerno and Samantha Calamari
Supplements Editor and Editorial Assistant: Janie Chan
Senior Project Editor: Mary Louise Byrd
Cover and Text Designer: Diana Blume
Photo Editor: Ted Szczepanski
Photo Researcher: Rae Grant
Senior Illustration Coordinator: Bill Page
Production Coordinator: Paul W. Rohloff
Illustrations and Composition: Preparé
Printing and Binding: Quebecor Printing

Library of Congress Control Number: 2007931523

ISBN-13: 978-0-7167-7550-8
ISBN-10: 0-7167-7550-6

© 2008 by Paul A. Tipler and Ralph A. Llewellyn
All rights reserved.

Printed in the United States of America

First printing

W. H. Freeman and Company
41 Madison Avenue
New York, NY 10010
Houndmills, Basingstoke RG21 6XS, England
www.whfreeman.com

STUDENTS-HUB.com Uploaded By: Malak Obaid

MODERN PHYSICS

Fifth Edition

Paul A. Tipler
Formerly of Oakland University

Ralph A. Llewellyn
University of Central Florida

W. H. Freeman and Company • New York

STUDENTS-HUB.com

Uploaded By: Malak Obaid

This page intentionally left blank

STUDENTS-HUB.com Uploaded By: Malak Obaid

Contents

PART 1 Relativity and Quantum Mechanics: The Foundations of Modern Physics 1

CHAPTER 1 Relativity I 3

1-1 The Experimental Basis of Relativity 4
Michelson-Morley Experiment 11
1-2 Einstein's Postulates 11
1-3 The Lorentz Transformation 17
Calibrating the Spacetime Axes 28
1-4 Time Dilation and Length Contraction 29
1-5 The Doppler Effect 41
Transverse Doppler Effect 44
1-6 The Twin Paradox and Other Surprises 45
The Case of the Identically Accelerated Twins 48
Superluminal Speeds 52

CHAPTER 2 Relativity II 65

2-1 Relativistic Momentum 66
2-2 Relativistic Energy 70
From Mechanics, Another Surprise 80
2-3 Mass/Energy Conversion and Binding Energy 81
2-4 Invariant Mass 84

The indicates material that appears only on the Web site: www.whfreeman.com/tiplermodernphysics5e.

The indicates material of high interest to students.

STUDENTS-HUB.com Uploaded By: Malak Obaid

2-5 General Relativity 97
Deflection of Light in a Gravitational Field 100
Gravitational Redshift 103
Perihelion of Mercury's Orbit 105
Delay of Light in a Gravitational Field 105

CHAPTER 3 Quantization of Charge, Light, and Energy 115

3-1 Quantization of Electric Charge 115
3-2 Blackbody Radiation 119
3-3 The Photoelectric Effect 127
3-4 X Rays and the Compton Effect 133
Derivation of Compton's Equation 138

CHAPTER 4 The Nuclear Atom 147

4-1 Atomic Spectra 148
4-2 Rutherford's Nuclear Model 150
Rutherford's Prediction and Geiger and Marsden's Results 156
4-3 The Bohr Model of the Hydrogen Atom 159
Giant Atoms 168
4-4 X-Ray Spectra 169
4-5 The Franck-Hertz Experiment 174
A Critique of Bohr Theory and the "Old Quantum Mechanics" 176

CHAPTER 5 The Wavelike Properties of Particles 185

5-1 The de Broglie Hypothesis 185
5-2 Measurements of Particle Wavelengths 187
5-3 Wave Packets 196
5-4 The Probabilistic Interpretation of the Wave Function 202
5-5 The Uncertainty Principle 205
The Gamma-Ray Microscope 206
5-6 Some Consequences of the Uncertainty Principle 208

STUDENTS-HUB.com Uploaded By: Malak Obaid

5-7 Wave-Particle Duality 212
Two-Slit Interference Pattern 213

CHAPTER 6 The Schrödinger Equation 221

6-1 The Schrödinger Equation in One Dimension 222
6-2 The Infinite Square Well 229
6-3 The Finite Square Well 238
Graphical Solution of the Finite Square Well 241
6-4 Expectation Values and Operators 242
Transitions Between Energy States 246
6-5 The Simple Harmonic Oscillator 246
Schrödinger's Trick 249
Parity 250
6-6 Reflection and Transmission of Waves 250
Alpha Decay 258
NH_3 Atomic Clock 260
Tunnel Diode 260

CHAPTER 7 Atomic Physics 269

7-1 The Schrödinger Equation in Three Dimensions 269
7-2 Quantization of Angular Momentum and Energy in the Hydrogen Atom 272
7-3 The Hydrogen Atom Wave Functions 281
7-4 Electron Spin 285
Stern-Gerlach Experiment 288
7-5 Total Angular Momentum and the Spin-Orbit Effect 291
7-6 The Schrödinger Equation for Two (or More) Particles 295
7-7 Ground States of Atoms: The Periodic Table 297
7-8 Excited States and Spectra of Atoms 301
Multielectron Atoms 303
The Zeeman Effect 303
Frozen Light 304

STUDENTS-HUB.com Uploaded By: Malak Obaid

CHAPTER 8 Statistical Physics 315

8-1 Classical Statistics: A Review 316
Temperature and Entropy 319
A Derivation of the Equipartition Theorem 324
8-2 Quantum Statistics 328
8-3 The Bose-Einstein Condensation 335
Liquid Helium 336
8-4 The Photon Gas: An Application of Bose-Einstein Statistics 344
8-5 Properties of a Fermion Gas 351

PART 2 Applications of Quantum Mechanics and Relativity 361

CHAPTER 9 Molecular Structure and Spectra 363

9-1 The Ionic Bond 364
9-2 The Covalent Bond 369
Other Covalent Bonds 375
9-3 Other Bonding Mechanisms 375
9-4 Energy Levels and Spectra of Diatomic Molecules 379
9-5 Scattering, Absorption, and Stimulated Emission 390
9-6 Lasers and Masers 396

CHAPTER 10 Solid State Physics 413

10-1 The Structure of Solids 413
10-2 Classical Theory of Conduction 422
10-3 Free-Electron Gas in Metals 426
10-4 Quantum Theory of Conduction 430
Thermal Conduction—The Quantum Model 434
10-5 Magnetism in Solids 434
Spintronics 437
10-6 Band Theory of Solids 438
Energy Bands in Solids—An Alternate Approach 445

STUDENTS-HUB.com Uploaded By: Malak Obaid

10-7 Impurity Semiconductors 445
Hall Effect 449
10-8 Semiconductor Junctions and Devices 452
How Transistors Work 457
10-9 Superconductivity 458
Flux Quantization 462
Josephson Junction 466

CHAPTER 11 Nuclear Physics 477

11-1 The Composition of the Nucleus 478
11-2 Ground-State Properties of Nuclei 480
Liquid-Drop Model and the Semiempirical Mass Formula 489
11-3 Radioactivity 492
Production and Sequential Decays 495
11-4 Alpha, Beta, and Gamma Decay 495
Energetics of Alpha Decay 498
The Mössbauer Effect 505
11-5 The Nuclear Force 506
Probability Density of the Exchange Mesons 512
11-6 The Shell Model 513
Finding the "Correct" Shell Model 516
11-7 Nuclear Reactions 516
11-8 Fission and Fusion 526
Nuclear Power 530
Interaction of Particles and Matter 536
11-9 Applications 537
Radiation Dosage 549

CHAPTER 12 Particle Physics 561

12-1 Basic Concepts 562
12-2 Fundamental Interactions and the Force Carriers 570
A Further Comment About Interaction Strengths 577

STUDENTS-HUB.com Uploaded By: Malak Obaid

12-3 Conservation Laws and Symmetries 580
When Is a Physical Quantity Conserved? 583
Resonances and Excited States 591
12-4 The Standard Model 591
Where Does the Proton Get Its Spin? 595
12-5 Beyond the Standard Model 605
Neutrino Oscillations and Mass 609
Theories of Everything 610

CHAPTER 13 Astrophysics and Cosmology 619

13-1 The Sun 619
Is There Life Elsewhere? 630
13-2 The Stars 630
The Celestial Sphere 636
13-3 The Evolution of Stars 639
13-4 Cataclysmic Events 644
13-5 Final States of Stars 647
13-6 Galaxies 653
13-7 Cosmology and Gravitation 662
13-8 Cosmology and the Evolution of the Universe 664
"Natural" Planck Units 673

Appendix A Table of Atomic Masses AP-1
Appendix B Mathematical Aids AP-16
B1 Probability Integrals AP-16
B2 Binomial and Exponential Series AP-18
B3 Diagrams of Crystal Unit Cells AP-19
Appendix C Electron Configurations AP-20
Appendix D Fundamental Physical Constants AP-26
Appendix E Conversion Factors AP-30
Appendix F Nobel Laureates in Physics AP-31

Answers AN-1
Index I-1

STUDENTS-HUB.com Uploaded By: Malak Obaid

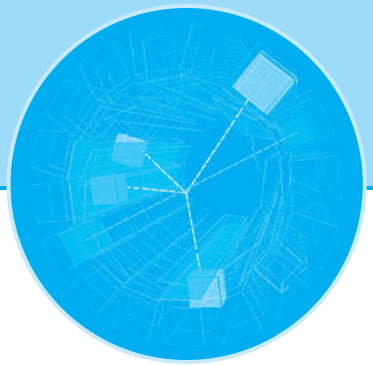

Preface

In preparing this new edition of *Modern Physics,* we have again relied heavily on the many helpful suggestions from a large team of reviewers and from a host of instructor and student users of the earlier editions. Their advice reflected the discoveries that have further enlarged modern physics in the early years of this new century and took note of the evolution that is occurring in the teaching of physics in colleges and universities. As the term *modern physics* has come to mean the physics of the modern era—relativity and quantum theory—we have heeded the advice of many users and reviewers and preserved the historical and cultural flavor of the book while being careful to maintain the mathematical level of the fourth edition. We continue to provide the flexibility for instructors to match the book and its supporting ancillaries to a wide variety of teaching modes, including both one- and two-semester courses and media-enhanced courses.

Features

The successful features of the fourth edition have been retained, including the following:

- The logical structure—beginning with an introduction to relativity and quantization and following with applications—has been continued. Opening the book with relativity has been endorsed by many reviewers and instructors.
- As in the earlier editions, the end-of-chapter problems are separated into three sets based on difficulty, with the least difficult also grouped by chapter section. More than 10 percent of the problems in the fifth edition are new. The first edition's *Instructor's Solutions Manual* (*ISM*) with solutions, not just answers, to all end-of-chapter problems was the first such aid to accompany a physics (and not just a modern physics) textbook, and that leadership has been continued in this edition. The ISM is available in print or on CD for those adopting *Modern Physics,* fifth edition, for their classes. As with the previous edition, a paperback *Student's Solution Manual* containing one-quarter of the solutions in the ISM is also available.
- We have continued to include many examples in every chapter, a feature singled out by many instructors as a strength of the book. As before, we frequently use combined quantities such as hc, $\hbar c$, and ke^2 in eV · nm to simplify many numerical calculations.
- The summaries and reference lists at the end of every chapter have, of course, been retained and augmented, including the two-column format of the summaries, which improves their clarity.

STUDENTS-HUB.com
Uploaded By: Malak Obaid

- We have continued the use of real data in figures, photos of real people and apparatus, and short quotations from many scientists who were key participants in the development of modern physics. These features, along with the Notes at the end of each chapter, bring to life many events in the history of science and help counter the too-prevalent view among students that physics is a dull, impersonal collection of facts and formulas.
- More than two dozen Exploring sections, identified by an atom icon and dealing with text-related topics that captivate student interest such as superluminal speed and giant atoms, are distributed throughout the text.
- The book's Web site includes 30 MORE sections, which expand in depth on many text-related topics. These have been enthusiastically endorsed by both students and instructors and often serve as springboards for projects and alternate credit assignments. Identified by a laptop icon , each is introduced with a brief text box.
- More than 125 questions intended to foster discussion and review of concepts are distributed throughout the book. These have received numerous positive comments from many instructors over the years, often citing how the questions encourage deeper thought about the topic.
- Continued in the new edition are the Application Notes. These brief notes in the margins of many pages point to a few of the many benefits to society that have been made possible by a discovery or development in modern physics.

New Features

A number of new features are introduced in the fifth edition:

- The "Astrophysics and Cosmology" chapter that was on the fourth edition's Web site has been extensively rewritten and moved into the book as a new Chapter 13. Emphasis has been placed on presenting scientists' current understanding of the evolution of the cosmos based on the research in this dynamic field.
- The "Particle Physics" chapter has been substantially reorganized and rewritten focused on the remarkably successful Standard Model. As the new Chapter 12, it immediately precedes the new "Astrophysics and Cosmology" chapter to recognize the growing links between these active areas of current physics research.
- The two chapters concerned with the theory and applications of nuclear physics have been integrated into a new Chapter 11, "Nuclear Physics." Because of the renewed interest in nuclear power, that material in the fourth edition has been augmented and moved to a MORE section of the Web.
- Recognizing the need for students on occasion to be able to quickly review key concepts from classical physics that relate to topics developed in modern physics, we have added a new Classical Concept Review (CCR) to the book's Web site. Identified by a laptop icon in the margin near the pertinent modern physics topic of discussion, the CCR can be printed out to provide a convenient study support booklet.
- The *Instructor's Resource* CD for the fifth edition contains all the illustrations from the book in both PowerPoint and JPEG format. Also included is a gallery of the astronomical images from Chapter 13 in the original image colors.
- Several new MORE sections have been added to the book's Web site, and a few for which interest has waned have been removed.

STUDENTS-HUB.com Uploaded By: Malak Obaid

Organization and Coverage

This edition, like the earlier ones, is divided into two parts: Part 1, "Relativity and Quantum Mechanics: The Foundation of Modern Physics," and Part 2, "Applications." We continue to open Part 1 with the two relativity chapters. This location for relativity is firmly endorsed by users and reviewers. The rationale is that this arrangement avoids separation of the foundations of quantum mechanics in Chapters 3 through 8 from its applications in Chapters 9 through 12. The two-chapter format for relativity provides instructors with the flexibility to cover only the basic concepts or to go deeper into the subject. Chapter 1 covers the essentials of special relativity and includes discussions of several paradoxes, such as the twin paradox and the pole-in-the-barn paradox, that never fail to excite student interest. Relativistic energy and momentum are covered in Chapter 2, which concludes with a mostly qualitative section on general relativity that emphasizes experimental tests. Because the relation $E^2 = p^2c^2 + (mc^2)^2$ is the result most needed for the later applications chapters, it is possible to omit Chapter 2 without disturbing continuity. Chapters 1 through 8 have been updated with a number of improved explanations and new diagrams. Several classical foundation topics in those chapters have been moved to the Classical Concept Review or recast as MORE sections. Many quantitative topics are included as MORE sections on the Web site. Examples of these are the derivation of Compton's equation (Chapter 3), the details of Rutherford's alpha-scattering theory (Chapter 4), the graphical solution of the finite square well (Chapter 6), and the excited states and spectra of two-electron atoms (Chapter 7). The comparisons of classical and quantum statistics are illustrated with several examples in Chapter 8, and unlike the other chapters in Part 1, Chapter 8 is arranged to be covered briefly and qualitatively if desired. This chapter, like Chapter 2, is not essential to the understanding of the applications chapters of Part 2 and may be used as an applications chapter or omitted without loss of continuity.

Preserving the approach used in the previous edition, in Part 2 the ideas and methods discussed in Part 1 are applied to the study of molecules, solids, nuclei, particles, and the cosmos. Chapter 9 ("Molecular Structure and Spectra") is a broad, detailed discussion of molecular bonding and the basic types of lasers. Chapter 10 ("Solid-State Physics") includes sections on bonding in metals, magnetism, and superconductivity. Chapter 11 ("Nuclear Physics") is an integration of the nuclear theory and applications that formed two chapters in the fourth edition. It focuses on nuclear structure and properties, radioactivity, and the applications of nuclear reactions. Included in the last topic are fission, fusion, and several techniques of age dating and elemental analysis. The material on nuclear power has been moved to a MORE section, and the discussion of radiation dosage continues as a MORE section. As mentioned above, Chapter 12 ("Particle Physics") has been substantially reorganized and rewritten with a focus on the Standard Model and revised to reflect the advances in that field since the earlier editions. The emphasis is on the fundamental interactions of the quarks, leptons, and force carriers and includes discussions of the conservation laws, neutrino oscillations, and supersymmetry. Finally, the thoroughly revised Chapter 13 ("Astrophysics and Cosmology") examines the current observations of stars and galaxies and qualitatively integrates our discussions of quantum mechanics, atoms, nuclei, particles, and relativity to explain our present understanding of the origin and evolution of the universe from the Big Bang to dark energy.

STUDENTS-HUB.com Uploaded By: Malak Obaid

The Research Frontier

Research over the past century has added abundantly to our understanding of our world, forged strong links from physics to virtually every other discipline, and measurably improved the tools and devices that enrich life. As was the case at the beginning of the last century, it is hard for us to foresee in the early years of this century how scientific research will deepen our understanding of the physical universe and enhance the quality of life. Here are just a few of the current subjects of frontier research included in *Modern Physics,* fifth edition, that you will hear more of in the years just ahead. Beyond these years there will be many other discoveries that no one has yet dreamed of.

- **The Higgs boson**, the harbinger of mass, may now be within our reach at Brookhaven's Relativistic Heavy Ion Collider and at CERN with completion of the Large Hadron Collider. (Chapter 12)
- **The neutrino mass question** has been solved by the discovery of neutrino oscillations at the Super-Kamiokande and SNO neutrino observatories (Chapters 2, 11, and 12), but the magnitudes of the masses and whether the neutrino is a Majorana particle remain unanswered.
- **The origin of the proton's spin**, which may include contributions from virtual strange quarks, still remains uncertain. (Chapter 11)
- **The Bose-Einstein condensates**, which suggest atomic lasers and super–atomic clocks are in our future, were joined in 2003 by **Fermi-Dirac condensates,** wherein pairs of fermions act like bosons at very low temperatures. (Chapter 8)
- **It is now clear that dark energy** accounts for 74 percent of the mass/energy of the universe. Only 4 percent is baryonic (visible) matter. The remaining 22 percent consists of as yet unidentified **dark matter** particles. (Chapter 13)
- **The predicted fundamental particles of supersymmetry (SUSY)**, an integral part of grand unification theories, will be a priority search at the Large Hadron Collider. (Chapters 12 and 13)
- **High-temperature superconductors reached critical temperatures greater than 130 K a few years ago and doped fullerenes compete with cuprates for high-T_c records,** but a theoretical explanation of the phenomenon is not yet in hand. (Chapter 10)
- **Gravity waves from space** may soon be detected by the upgraded Laser Interferometric Gravitational Observatory (LIGO) and several similar laboratories around the world. (Chapter 2)
- **Adaptive-optics telescopes, large baseline arrays, and the Hubble telescope** are providing new views deeper into space of the very young universe, revealing that the expansion is speeding up, a discovery supported by results from the Sloan Digital Sky Survey and the Wilkinson Microwave Anisotropy Project. (Chapter 13)
- **Giant Rydberg atoms**, made accessible by research on tunable dye lasers, are now of high interest and may provide the first direct test of the correspondence principle. (Chapter 4)
- **The search for new elements has reached $Z = 118$,** tantalizingly near the edge of the "island of stability." (Chapter 11)

Many more discoveries and developments just as exciting as these are to be found throughout *Modern Physics,* fifth edition.

STUDENTS-HUB.com Uploaded By: Malak Obaid

Some Teaching Suggestions

This book is designed to serve well in either one- or two-semester courses. The chapters in Part 2 are independent of one another and can be covered in any order. Some possible one-semester courses might consist of

- Part 1, Chapters 1, 3, 4, 5, 6, 7; and Part 2, Chapters 11, 12
- Part 1, Chapters 3, 4, 5, 6, 7, 8; and Part 2, Chapters 9, 10
- Part 1, Chapters 1, 2, 3, 4, 5, 6, 7; and Part 2, Chapter 9
- Part 1, Chapters 1, 3, 4, 5, 6, 7; and Part 2, Chapters 11, 12, 13

Possible two-semester courses might consist of

- Part 1, Chapters 1, 3, 4, 5, 6, 7; and Part 2, Chapters 9, 10, 11, 12, 13
- Part 1, Chapters 1, 2, 3, 4, 5, 6, 7, 8; and Part 2, Chapters 9, 10, 11, 12, 13

There is tremendous potential for individual student projects and alternate credit assignments based on the Exploring and, in particular, the MORE sections. The latter will encourage students to search for related sources on the Web.

Acknowledgments

Many people contributed to the success of the earlier editions of this book, and many more have helped with the development of the fifth edition. We owe our thanks to them all. Those who reviewed all or parts of this book, offering suggestions for the fifth edition, include

Marco Battaglia
University of California–Berkeley

Mario Belloni
Davidson College

Eric D. Carlson
Wake Forest University

David Cinabro
Wayne State University

Carlo Dallapiccola
University of Massachusetts–Amherst

Anthony D. Dinsmore
University of Massachusetts–Amherst

Ian T. Durham
Saint Anselm College

Jason J. Engbrecht
St. Olaf College

Brian Fick
Michigan Technological University

Massimiliano Galeazzi
University of Miami

Hugh Gallagher
Tufts University

Richard Gelderman
Western Kentucky University

Tim Gfroerer
Davidson College

Torgny Gustafsson
Rutgers University

Scott Heinekamp
Wells College

Adrian Hightower
Occidental College

Mark Hollabaugh
Normandale Community College

Richard D. Holland II
Southern Illinois University at Carbondale

Bei-Lok Hu
University of Maryland–College Park

Dave Kieda
University of Utah

Steve Kraemer
Catholic University of America

Wolfgang Lorenzon
University of Michigan

STUDENTS-HUB.com Uploaded By: Malak Obaid

Bryan A. Luther
Concordia College at Moorhead
Catherine Mader
Hope College
Kingshuk Majumdar
Berea College
Peter Moeck
Portland State University
Robert M. Morse
University of Wisconsin–Madison
Igor Ostrovskii
University of Mississippi at Oxford
Anne Reilly
College of William and Mary
David Reitze
University of Florida
Mark Riley
Florida State University
Nitin Samarth
Pennsylvania State University
Kate Scholberg
Duke University
Ben E. K. Sugerman
Goucher College
Rein Uritam
Physics Department
Boston College
Ken Voss
University of Miami
Thad Walker
University of Wisconsin–Madison
Barry C. Walker
University of Delaware
Eric Wells
Augustana College
William R. Wharton
Wheaton College
Weldon J. Wilson
University of Central Oklahoma
R. W. M. Woodside
University College of Fraser Valley

We also thank the reviewers of the fourth and third editions. Their comments significantly influenced and shaped the fifth edition as well. For the fourth edition they were Darin Acosta, University of Florida; Jeeva Anandan, University of South Carolina; Gordon Aubrecht, Ohio State University; David A. Bahr, Bemidji State University; Patricia C. Boeshaar, Drew University; David P. Carico, California Polytechnic State University at San Luis Obispo; David Church, University of Washington; Wei Cui, Purdue University; Snezana Dalafave, College of New Jersey; Richard Gass, University of Cincinnati; David Gerdes, University of Michigan; Mark Hollabaugh, Normandale Community College; John L. Hubisz, North Carolina State University; Ronald E. Jodoin, Rochester Institute of Technology; Edward R. Kinney, University of Colorado at Boulder; Paul D. Lane, University of St. Thomas; Fernando J. Lopez-Lopez, Southwestern College; Dan MacIsaac, Northern Arizona University; Robert Pompi, SUNY at Binghamton; Warren Rogers, Westmont College; George Rutherford, Illinois State University; Nitin Samarth, Pennsylvania State University; Martin A. Sanzari, Fordham University; Earl E. Scime, West Virginia University; Gil Shapiro, University of California at Berkeley; Larry Solanch, Georgia College & State University; Francis M. Tam, Frostburg State University; Paul Tipton, University of Rochester; K. Thad Walker, University of Wisconsin at Madison; Edward A. Whittaker, Stevens Institute of Technology; Stephen Yerian, Xavier University; and Dean Zollman, Kansas State University.

For the third edition, reviewers were Bill Bassichis, Texas A&M University; Brent Benson, Lehigh University; H. J. Biritz, Georgia Institute of Technology; Patrick Briggs, The Citadel; David A. Briodo, Boston College; Tony Buffa, California Polytechnic State University at San Luis Obispo; Duane Carmony, Purdue University; Ataur R. Chowdhury, University of Alaska at Fairbanks; Bill Fadner, University of Northern Colorado; Ron Gautreau, New Jersey Institute of Technology; Charles Glashauser,

STUDENTS-HUB.com Uploaded By: Malak Obaid

Rutgers–The State University of New Jersey; Roger Hanson, University of Northern Iowa; Gary G. Ihas, University of Florida; Yuichi Kubota, University of Minnesota; David Lamp, Texas Tech University; Philip Lippel, University of Texas at Arlington; A. E. Livingston, University of Notre Dame; Steve Meloma, Gustavus Adolphus College; Benedict Y. Oh, Pennsylvania State University; Paul Sokol, Pennsylvania State University; Thor F. Stromberg, New Mexico State University; Maurice Webb, University of Wisconsin at Madison; and Jesse Weil, University of Kentucky.

All offered valuable suggestions for improvements, and we appreciate their help.

In addition, we give a special thanks to all the physicists and students from around the world who took time to send us kind words about the third and fourth editions and offered suggestions for improvements.

Finally, though certainly not least, we are grateful for the support, encouragement, and patience of our families throughout the project. We especially want to thank Mark Llewellyn for his preparation of the *Instructor's Solutions Manual* and the *Student's Solutions Manual* and for his numerous helpful suggestions from the very beginning of the project, Eric Llewellyn for his photographic and computer-generated images, David Jonsson at Uppsala University for his critical reading of every chapter of the fourth edition, and Jeanette Picerno for her imaginative work on the Web site. Finally, to the entire *Modern Physics* team at W. H. Freeman and Company goes our sincerest appreciation for their skill, hard work, understanding about deadlines, and support in bringing it all together.

Paul A. Tipler,
Berkeley, California

Ralph A. Llewellyn,
Oviedo, Florida

STUDENTS-HUB.com Uploaded By: Malak Obaid

This page intentionally left blank

STUDENTS-HUB.com Uploaded By: Malak Obaid

PART 1

Relativity and Quantum Mechanics: The Foundations of Modern Physics

The earliest recorded systematic efforts to assemble knowledge about motion as a key to understanding natural phenomena were those of the ancient Greeks. Set forth in sophisticated form by Aristotle, theirs was a natural philosophy (i.e., physics) of explanations deduced from assumptions rather than experimentation. For example, it was a fundamental assumption that every substance had a "natural place" in the universe. Motion then resulted when a substance was trying to reach its natural place. Time was given a similar absolute meaning, as moving from some instant in the past (the creation of the universe) toward some end goal in the future, its natural place. The remarkable agreement between the deductions of Aristotelian physics and motions observed throughout the physical universe, together with a nearly total absence of accurate instruments to make contradictory measurements, led to acceptance of the Greek view for nearly 2000 years. Toward the end of that time a few scholars had begun to deliberately test some of the predictions of theory, but it was Italian scientist Galileo Galilei who, with his brilliant experiments on motion, established for all time the absolute necessity of experimentation in physics and, coincidentally, initiated the disintegration of Aristotelian physics. Within 100 years Isaac Newton had generalized the results of Galileo's experiments into his three spectacularly successful laws of motion, and the natural philosophy of Aristotle was gone.

With the burgeoning of experimentation, the following 200 years saw a multitude of major discoveries and a concomitant development of physical theories to explain them. Most of the latter, then as now, failed to survive increasingly sophisticated experimental tests, but by the dawn of the twentieth century Newton's theoretical explanation of the motion of mechanical systems had been joined by equally impressive laws of electromagnetism and thermodynamics as expressed by Maxwell, Carnot, and others. The remarkable success of these laws led many scientists to believe that description of the physical universe was complete. Indeed, A. A. Michelson, speaking to scientists near the end of the nineteenth century, said, "The grand underlying principles have been firmly established . . . the future truths of physics are to be looked for in the sixth place of decimals."

STUDENTS-HUB.com

Uploaded By: Malak Obaid

Such optimism (or pessimism, depending on your point of view) turned out to be premature, as there were already vexing cracks in the foundation of what we now refer to as classical physics. Two of these were described by Lord Kelvin, in his famous Baltimore Lectures in 1900, as the "two clouds" on the horizon of twentieth-century physics: the failure of theory to account for the radiation spectrum emitted by a blackbody and the inexplicable results of the Michelson-Morley experiment. Indeed, the breakdown of classical physics occurred in many different areas: the Michelson-Morley null result contradicted Newtonian relativity, the blackbody radiation spectrum contradicted predictions of thermodynamics, the photoelectric effect and the spectra of atoms could not be explained by electromagnetic theory, and the exciting discoveries of x rays and radioactivity seemed to be outside the framework of classical physics entirely. The development of the theories of quantum mechanics and relativity in the early twentieth century not only dispelled Kelvin's "dark clouds," they provided answers to all of the puzzles listed here and many more. The applications of these theories to such microscopic systems as atoms, molecules, nuclei, and fundamental particles and to macroscopic systems of solids, liquids, gases, and plasmas have given us a deep understanding of the intricate workings of nature and have revolutionized our way of life.

In Part 1 we discuss the foundations of the physics of the modern era, relativity theory, and quantum mechanics. Chapter 1 examines the apparent conflict between Einstein's principle of relativity and the observed constancy of the speed of light and shows how accepting the validity of both ideas led to the special theory of relativity. Chapter 2 discusses the relations connecting mass, energy, and momentum in special relativity and concludes with a brief discussion of general relativity and some experimental tests of its predictions. In Chapters 3, 4, and 5 the development of quantum theory is traced from the earliest evidences of quantization to de Broglie's hypothesis of electron waves. An elementary discussion of the Schrödinger equation is provided in Chapter 6, illustrated with applications to one-dimensional systems. Chapter 7 extends the application of quantum mechanics to many-particle systems and introduces the important new concepts of electron spin and the exclusion principle. Concluding the development, Chapter 8 discusses the wave mechanics of systems of large numbers of identical particles, underscoring the importance of the symmetry of wave functions. Beginning with Chapter 3, the chapters in Part 1 should be studied in sequence because each of Chapters 4 through 8 depends on the discussions, developments, and examples of the previous chapters.

STUDENTS-HUB.com Uploaded By: Malak Obaid

CHAPTER 1

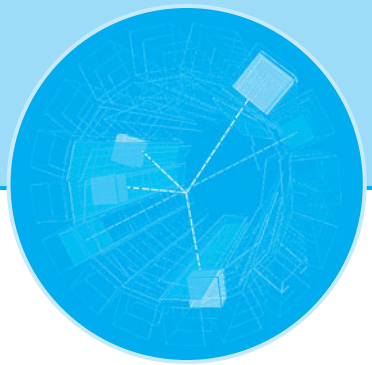

Relativity I

1-1 The Experimental Basis of Relativity 4
1-2 Einstein's Postulates 11
1-3 The Lorenz Transformation 17
1-4 Time Dilation and Length Contraction 29
1-5 The Doppler Effect 41
1-6 The Twin Paradox and Other Surprises 45

The relativistic character of the laws of physics began to be apparent very early in the evolution of classical physics. Even before the time of Galileo and Newton, Nicolaus Copernicus[1] had shown that the complicated and imprecise Aristotelian method of computing the motions of the planets, based on the assumption that Earth was located at the center of the universe, could be made much simpler, though no more accurate, if it were assumed that the planets move about the Sun instead of Earth. Although Copernicus did not publish his work until very late in life, it became widely known through correspondence with his contemporaries and helped pave the way for acceptance a century later of the heliocentric theory of planetary motion. While the Copernican theory led to a dramatic revolution in human thought, the aspect that concerns us here is that it did not consider the location of Earth to be special or favored in any way. Thus, the laws of physics discovered on Earth could apply equally well with any point taken as the center—i.e., the same equations would be obtained regardless of the origin of coordinates. This invariance of the equations that express the laws of physics is what we mean by the term *relativity*.

We will begin this chapter by investigating briefly the relativity of Newton's laws and then concentrate on the theory of relativity as developed by Albert Einstein (1879–1955). The theory of relativity consists of two rather different theories, the special theory and the general theory. The special theory, developed by Einstein and others in 1905, concerns the comparison of measurements made in different frames of reference moving with constant velocity relative to each other. Contrary to popular opinion, the special theory is not difficult to understand. Its consequences, which can be derived with a minimum of mathematics, are applicable in a wide variety of situations in physics and engineering. On the other hand, the general theory, also developed by Einstein (around 1916), is concerned with accelerated reference frames and gravity. Although a thorough understanding of the general theory requires more sophisticated mathematics (e.g., tensor analysis), a number of its basic ideas and important predictions can be discussed at the level of this book. The general theory is of great importance in cosmology and in understanding events that occur in the

STUDENTS-HUB.com Uploaded By: Malak Obaid

vicinity of very large masses (e.g., stars) but is rarely encountered in other areas of physics and engineering. We will devote this chapter entirely to the special theory (often referred to as *special relativity*) and discuss the general theory in the final section of Chapter 2, following the sections concerned with special relativistic mechanics.

1-1 The Experimental Basis of Relativity

Classical Relativity

In 1687, with the publication of the *Philosophiae Naturalis Principia Mathematica,* Newton became the first person to generalize the observations of Galileo and others into the laws of motion that occupied much of your attention in introductory physics. The second of Newton's three laws is

$$\mathbf{F} = m\frac{d\mathbf{v}}{dt} = m\mathbf{a} \qquad \textbf{1-1}$$

where $d\mathbf{v}/dt = \mathbf{a}$ is the acceleration of the mass m when acted upon by a net force $\mathbf{F}$. Equation 1-1 also includes the first law, the *law of inertia*, by implication: if $\mathbf{F} = 0$, then $d\mathbf{v}/dt = 0$ also, i.e., $\mathbf{a} = 0$. (Recall that letters and symbols in boldface type are vectors.)

As it turns out, Newton's laws of motion only work correctly in *inertial reference frames*, that is, reference frames in which the law of inertia holds.[2] They also have the remarkable property that they are *invariant*, or unchanged, in any reference frame that moves with constant velocity relative to an inertial frame. Thus, all inertial frames are equivalent—there is no special or favored inertial frame relative to which absolute measurements of space and time could be made. Two such inertial frames are illustrated in Figure 1-1, arranged so that corresponding axes in S and S' are parallel and S' moves in the $+x$ direction at velocity $\mathbf{v}$ for an observer in S (or S moves in the $-x'$

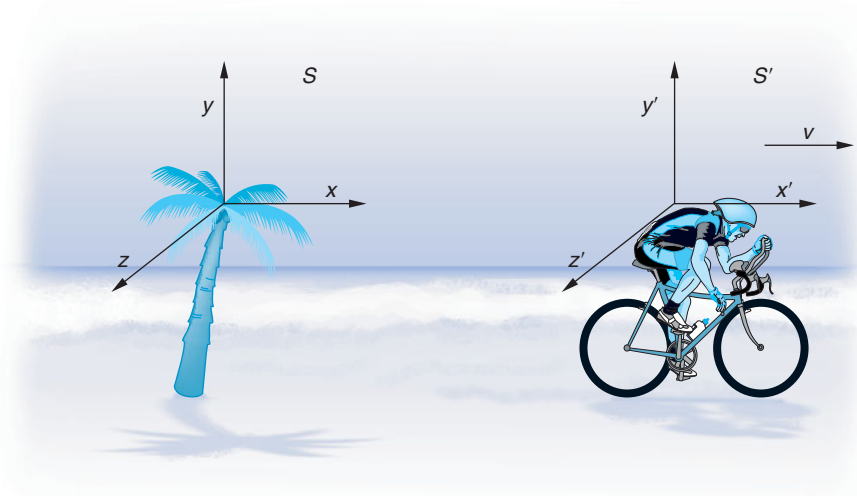

Figure 1-1 Inertial reference frame S is attached to Earth (the palm tree) and S' to the cyclist. The corresponding axes of the frames are parallel, and S' moves at speed v in the $+x$ direction of S.

STUDENTS-HUB.com Uploaded By: Malak Obaid

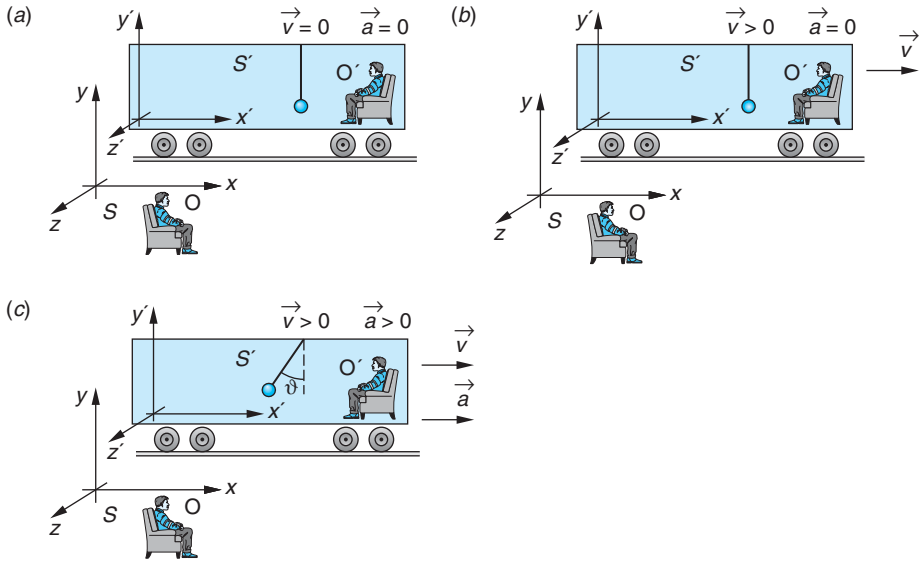

Figure 1-2 A mass suspended by a cord from the roof of a railroad boxcar illustrates the relativity of Newton's second law, $\mathbf{F} = m\mathbf{a}$. The only forces acting on the mass are its weight $m\mathbf{g}$ and the tension $\mathbf{T}$ in the cord. (*a*) The boxcar sits at rest in *S*. Since the velocity $\mathbf{v}$ and the acceleration $\mathbf{a}$ of the boxcar (i.e., the system S') are both zero, both observers see the mass hanging vertically at rest with $\mathbf{F} = \mathbf{F}' = 0$. (*b*) As S' moves in the $+x$ direction with $\mathbf{v}$ constant, both observers see the mass hanging vertically but moving at $\mathbf{v}$ with respect to O in *S* and at rest with respect to the S' observer. Thus, $\mathbf{F} = \mathbf{F}' = 0$. (*c*) As S' moves in the $+x$ direction with $\mathbf{a} > 0$ with respect to *S*, the mass hangs at an angle $\vartheta > 0$ with respect to the vertical. However, it is still at rest (i.e., in equilibrium) with respect to the observer in S', who now "explains" the angle ϑ by adding a pseudoforce $\mathbf{F}_p$ in the $-x'$ direction to Newton's second law.

direction at velocity $-\mathbf{v}$ for an observer in S'). Figures 1-2 and 1-3 illustrate the conceptual differences between inertial and noninertial reference frames. Transformation of the position coordinates and the velocity components of *S* into those of S' is the *Galilean transformation*, Equations 1-2 and 1-3, respectively.

$$x' = x - vt \qquad y' = y \qquad z' = z \qquad t' = t \tag{1-2}$$

$$u'_x = u_x - v \qquad u'_y = u_y \qquad u'_z = u_z \tag{1-3}$$

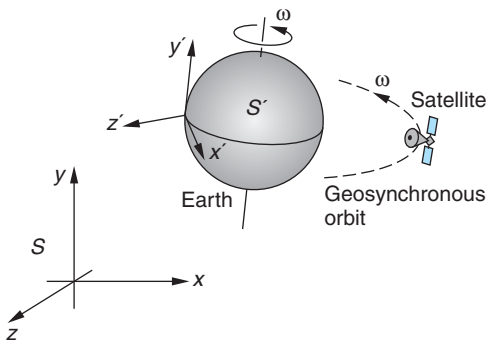

Figure 1-3 A geosynchronous satellite has an orbital angular velocity equal to that of Earth and, therefore, is always located above a particular point on Earth; i.e., it is at rest with respect to the surface of Earth. An observer in *S* accounts for the radial, or centripetal, acceleration $\mathbf{a}$ of the satellite as the result of the net force $\mathbf{F}_G$. For an observer O′ at rest on Earth (in S'), however, $\mathbf{a}' = 0$ and $\mathbf{F}'_G \neq m\mathbf{a}'$. To explain the acceleration being zero, observer O′ must add a pseudoforce $\mathbf{F}_p = -\mathbf{F}_G$.

STUDENTS-HUB.com Uploaded By: Malak Obaid

Notice that differentiating Equation 1-3 yields the result $a' = a$ since $dv/dt = 0$ for constant v. Thus, $\mathbf{F} = m\mathbf{a} = \mathbf{F}'$. This is the invariance referred to above. Generalizing this result:

> Any reference frame that moves at constant velocity with respect to an inertial frame is also an inertial frame. Newton's laws of mechanics are invariant in all reference systems connected by a Galilean transformation.

Speed of Light

In about 1860 James Clerk Maxwell summarized the experimental observations of electricity and magnetism in a consistent set of four concise equations. Unlike Newton's laws of motion, Maxwell's equations are not invariant under a Galilean transformation between inertial reference frames (Figure 1-4). Since the Maxwell equations predict the existence of electromagnetic waves whose speed would be a particular value, $c = 1/\sqrt{\mu_0 \epsilon_0} = 3.00 \times 10^8$ m/s, the excellent agreement between this number and the measured value of the speed of light[3] and between the predicted polarization properties of electromagnetic waves and those observed for light provided strong confirmation of the assumption that light was an electromagnetic wave and, therefore, traveled at speed c.[4]

That being the case, it was postulated in the nineteenth century that electromagnetic waves, like all other waves, propagated in a suitable material medium. The implication of this postulate was that the medium, called the *ether*, filled the entire universe, including the interior of matter. (The Greek philosopher Aristotle had first suggested that the universe was permeated with "ether" 2000 years earlier.) In this way the remarkable opportunity arose to establish experimentally the existence of the all-pervasive ether by measuring the speed of light c' relative to Earth as Earth moved relative to the ether at speed v, as would be predicted by Equation 1-3. The value of c was given by the Maxwell equations, and the speed of Earth relative to the ether, while not known, was assumed to be at least equal to its orbital speed around the Sun, about 30 km/s. Since the maximum observable effect is of the order v^2/c^2 and given this assumption $v^2/c^2 \approx 10^{-8}$, an experimental accuracy of about 1 part in 10^8 is necessary in order to detect Earth's motion relative to the ether. With a single exception, equipment and

Classical Concept Review

The concepts of classical relativity, frames of reference, and coordinate transformations—all important background to our discussions of special relativity—may not have been emphasized in many introductory courses. As an aid to a better understanding of the concepts of modern physics, we have included the *Classical Concept Review* on the book's Web site. As you proceed through *Modern Physics*, the icon in the margin will alert you to potentially helpful classical background pertinent to the adjacent topics.

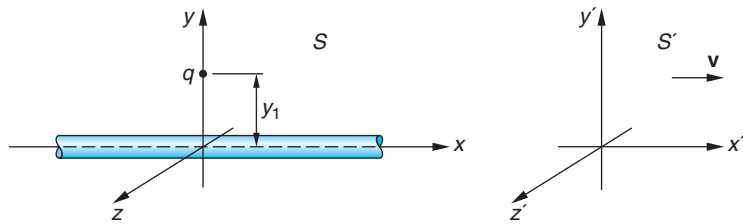

Figure 1-4 The observers in S and S' see identical electric fields $2k\lambda/y_1$ at a distance $y_1 = y_1'$ from an infinitely long wire carrying uniform charge λ per unit length. Observers in both S and S' measure a force $2kq\lambda/y_1$ on q due to the line of charge; however, the S' observer measures an additional force $-\mu_0\lambda v^2 q/(2\pi y_1)$ due to the magnetic field at y_1' arising from the motion of the wire in the $-x'$ direction. Thus, the electromagnetic force does not have the same form in different inertial systems, implying that Maxwell's equations are *not* invariant under a Galilean transformation.

STUDENTS-HUB.com Uploaded By: Malak Obaid

techniques available at the time had an experimental accuracy of only about 1 part in 10^4, woefully insufficient to detect the predicted small effect. That single exception was the experiment of Michelson and Morley.[5]

Questions

1. What would the relative velocity of the inertial systems in Figure 1-4 need to be in order for the S' observer to measure no net electromagnetic force on the charge q?
2. Discuss why the very large value for the speed of the electromagnetic waves would imply that the ether be rigid, i.e., have a large bulk modulus.

The Michelson-Morley Experiment

All waves that were known to nineteenth-century scientists required a medium in order to propagate. Surface waves moving across the ocean obviously require the water. Similarly, waves move along a plucked guitar string, across the surface of a struck drumhead, through Earth after an earthquake, and, indeed, in all materials acted upon by suitable forces. The speed of the waves depends on the properties of the medium and is derived *relative to the medium*. For example, the speed of sound waves in air, i.e., their absolute motion relative to still air, can be measured. The Doppler effect for sound in air depends not only on the relative motion of the source and listener, but also on the motion of each relative to still air. Thus, it was natural for scientists of that time to expect the existence of some material like the ether to support the propagation of light and other electromagnetic waves *and* to expect that the absolute motion of Earth through the ether should be detectable, despite the fact that the ether had not been observed previously.

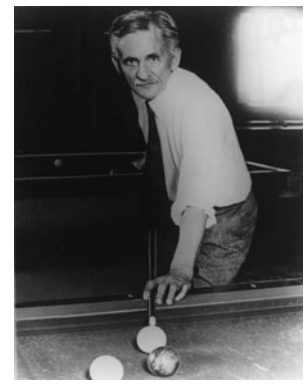

Albert A. Michelson, here playing pool in his later years, made the first accurate measurement of the speed of light while an instructor at the U.S. Naval Academy, where he had earlier been a cadet. [*AIP Emilio Segrè Visual Archives.*]

Michelson realized that although the effect of Earth's motion on the results of any "out-and–back" speed of light measurement, such as shown generically in Figure 1-5, would be too small to measure directly, it should be possible to measure v^2/c^2 by a difference measurement, using the interference property of the light waves as a sensitive "clock." The apparatus that he designed to make the measurement is called the *Michelson interferometer*. The purpose of the Michelson-Morley experiment was to measure the speed of light relative to the interferometer (i.e., relative to Earth), thereby detecting Earth's motion through the ether and thus verifying the latter's existence. To illustrate how the interferometer works and the reasoning behind the experiment, let us first describe an analogous situation set in more familiar surroundings.

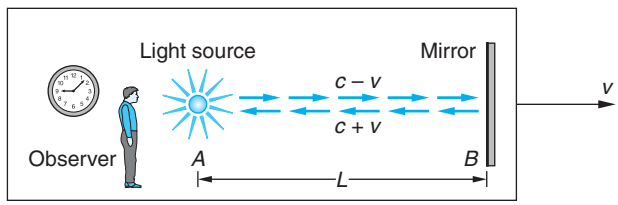

Figure 1-5 Light source, mirror, and observer are moving with speed v relative to the ether. According to classical theory, the speed of light c, relative to the ether, would be $c - v$ relative to the observer for light moving from the source toward the mirror and $c + v$ for light reflecting from the mirror back toward the source.

STUDENTS-HUB.com Uploaded By: Malak Obaid

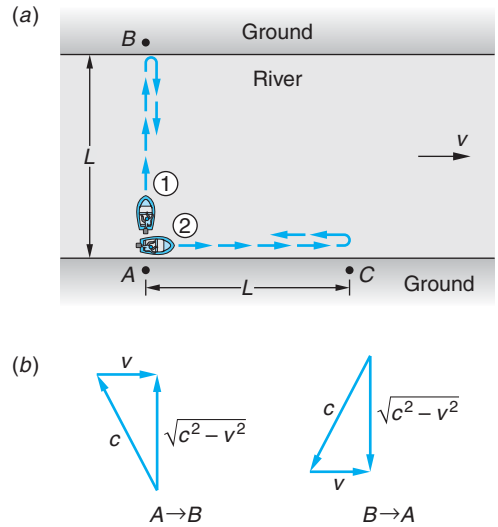

Figure 1-6 (*a*) The rowers both row at speed c in still water. (See Example 1-1.) The current in the river moves at speed v. Rower 1 goes from A to B and back to A, while rower 2 goes from A to C and back to A. (*b*) Rower 1 must point the bow upstream so that the sum of the velocity vectors $\mathbf{c} + \mathbf{v}$ results in the boat moving from A directly to B. His speed relative to the banks (i.e., points A and B) is then $(c^2 - v^2)^{1/2}$. The same is true on the return trip.

EXAMPLE 1-1 A Boat Race Two equally matched rowers race each other over courses as shown in Figure 1-6*a*. Each oarsman rows at speed c in still water; the current in the river moves at speed v. Boat 1 goes from A to B, a distance L, and back. Boat 2 goes from A to C, also a distance L, and back. A, B, and C are marks on the riverbank. Which boat wins the race, or is it a tie? (Assume $c > v$.)

SOLUTION

The winner is, of course, the boat that makes the round trip in the shortest time, so to discover which boat wins, we compute the time for each. Using the classical velocity transformation (Equations 1-3), the speed of 1 relative to the ground is $(c^2 - v^2)^{1/2}$, as shown in Figure 1-6*b*; thus the round-trip time t_1 for boat 1 is

$$t_1 = t_{A\to B} + t_{B\to A} = \frac{L}{\sqrt{c^2 - v^2}} + \frac{L}{\sqrt{c^2 - v^2}} = \frac{2L}{\sqrt{c^2 - v^2}}$$
$$= \frac{2L}{c\sqrt{1 - \dfrac{v^2}{c^2}}} = \frac{2L}{c}\left(1 - \frac{v^2}{c^2}\right)^{-1/2} \approx \frac{2L}{c}\left(1 + \frac{1}{2}\frac{v^2}{c^2} + \cdots\right) \qquad \textbf{1-4}$$

where we have used the binomial expansion. Boat 2 moves downstream at speed $c + v$ relative to the ground and returns at $c - v$, also relative to the ground. The round-trip time t_2 is thus

$$t_2 = \frac{L}{c + v} + \frac{L}{c - v} = \frac{2Lc}{c^2 - v^2}$$
$$= \frac{2L}{c}\frac{1}{1 - \dfrac{v^2}{c^2}} \approx \frac{2L}{c}\left(1 + \frac{v^2}{c^2} + \cdots\right) \qquad \textbf{1-5}$$

STUDENTS-HUB.com Uploaded By: Malak Obaid

which, you may note, is the same result obtained in our discussion of the speed of light experiment in the Classical Concept Review.

The difference Δt between the round-trip times of the boats is then

$$\Delta t = t_2 - t_1 \approx \frac{2L}{c}\left(1 + \frac{v^2}{c^2}\right) - \frac{2L}{c}\left(1 + \frac{1}{2}\frac{v^2}{c^2}\right) \approx \frac{Lv^2}{c^3} \qquad \textbf{1-6}$$

The quantity Lv^2/c^3 is always positive; therefore, $t_2 > t_1$ and rower 1 has the faster average speed and wins the race.

The Results Michelson and Morley carried out the experiment in 1887, repeating with a much-improved interferometer an inconclusive experiment that Michelson alone had performed in 1881 in Potsdam. The path length L on the new interferometer (Figure 1-7) was about 11 meters, obtained by a series of multiple reflections. Michelson's interferometer is shown schematically in Figure 1-8*a*. The field of view seen by the observer consists of parallel alternately bright and dark interference bands, called *fringes*, as illustrated in Figure 1-8*b*. The two light beams in the interferometer are exactly analogous to the two boats in Example 1-1, and Earth's motion through the ether was expected to introduce a time (phase) difference as given by

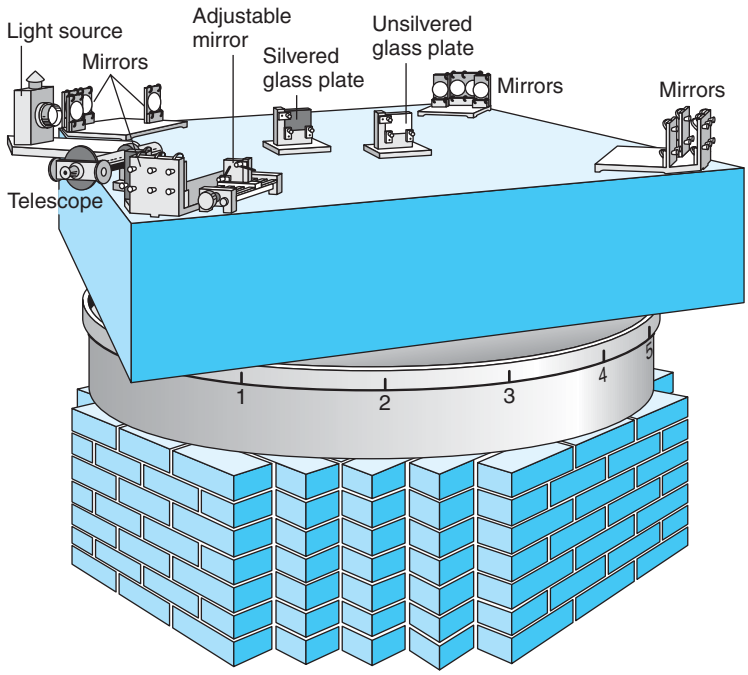

Figure 1-7 Drawing of Michelson-Morley apparatus used in their 1887 experiment. The optical parts were mounted on a 5 ft square sandstone slab, which was floated in mercury, thereby reducing the strains and vibrations during rotation that had affected the earlier experiments. Observations could be made in all directions by rotating the apparatus in the horizontal plane. [*From R. S. Shankland, "The Michelson-Morley Experiment," Copyright © November 1964 by Scientific American, Inc. All rights reserved.*]

STUDENTS-HUB.com Uploaded By: Malak Obaid

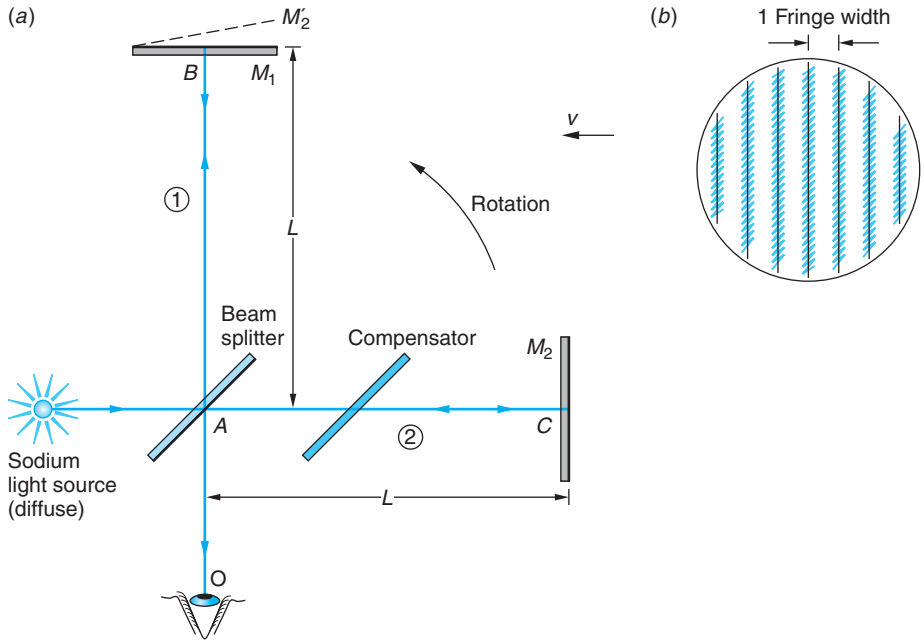

Figure 1-8 Michelson interferometer. (*a*) Yellow light from the sodium source is divided into two beams by the second surface of the partially reflective beam splitter at *A*, at which point the two beams are exactly in phase. The beams travel along the mutually perpendicular paths 1 and 2, reflect from mirrors M_1 and M_2, and return to *A*, where they recombine and are viewed by the observer. The compensator's purpose is to make the two paths of equal optical length, so that the lengths *L* contain the same number of light waves, by making both beams pass through two thicknesses of glass before recombining. M_2 is then tilted slightly so that it is not quite perpendicular to M_1. Thus, the observer O sees M_1 and M_2', the image of M_2 formed by the partially reflecting second surface of the beam splitter, forming a thin wedge-shaped film of air between them. The interference of the two recombining beams depends on the number of waves in each path, which in turn depends on (1) the length of each path and (2) the speed of light (relative to the instrument) in each path. Regardless of the value of that speed, the wedge-shaped air film between M_1 and M_2' results in an increasing path length for beam 2 relative to beam 1, looking from left to right across the observer's field of view; hence, the observer sees a series of parallel interference fringes as in (*b*), alternately yellow and black from constructive and destructive interference, respectively.

Equation 1-6. Rotating the interferometer through 90° doubles the time difference and changes the phase, causing the fringe pattern to shift by an amount ΔN. An improved system for rotating the apparatus was used in which the massive stone slab on which the interferometer was mounted floated on a pool of mercury. This dampened vibrations and enabled the experimenters to rotate the interferometer without introducing mechanical strains, both of which would cause changes in *L* and hence a shift in the fringes. Using a sodium light source with $\lambda = 590$ nm and assuming $v = 30$ km/s (i.e., Earth's orbital speed), ΔN was expected to be about 0.4 of the width of a fringe, about 40 times the minimum shift (0.01 fringe) that the interferometer was capable of detecting.

STUDENTS-HUB.com Uploaded By: Malak Obaid

To Michelson's immense disappointment and that of most scientists of the time, the expected shift in the fringes did not occur. Instead, the shift observed was only about 0.01 fringe, i.e., approximately the experimental uncertainty of the apparatus. With characteristic reserve, Michelson described the results thus:[6]

> The actual displacement [of the fringes] was certainly less than the twentieth part [of 0.4 fringe], and probably less than the fortieth part. But since the displacement is proportional to the square of the velocity, the relative velocity of the earth and the ether is probably less than one-sixth the earth's orbital velocity and certainly less than one-fourth.

Michelson and Morley had placed an upper limit on Earth's motion relative to the ether of about 5 km/s. From this distance in time it is difficult for us to appreciate the devastating impact of this result. The then-accepted theory of light propagation could not be correct, and the ether as a favored frame of reference for Maxwell's equations was not tenable. The experiment was repeated by a number of people more than a dozen times under various conditions and with improved precision, and no shift has ever been found. In the most precise attempt, the upper limit on the relative velocity was lowered to 1.5 km/s by Georg Joos in 1930 using an interferometer with light paths much longer than Michelson's. Recent, high-precision variations of the experiment using laser beams have lowered the upper limit to 15 m/s.

Michelson interferometers with arms as long as 4 km are currently being used in the search for gravity waves. See Section 2-5.

More generally, on the basis of this and other experiments, we must conclude that Maxwell's equations are correct and that the speed of electromagnetic radiation is the same in all inertial reference systems independent of the motion of the source relative to the observer. This invariance of the speed of light between inertial reference frames means that there must be some relativity principle that applies to electromagnetism as well as to mechanics. That principle cannot be Newtonian relativity, which implies the dependence of the speed of light on the relative motion of the source and observer. It follows that the Galilean transformation of coordinates between inertial frames cannot be correct but must be replaced with a new coordinate transformation whose application preserves the invariance of the laws of electromagnetism. We then expect that the fundamental laws of mechanics, which were consistent with the old Galilean transformation, will require modification in order to be invariant under the new transformation. The theoretical derivation of that new transformation was a cornerstone of Einstein's development of special relativity.

More

A more complete description of the *Michelson-Morley experiment*, its interpretation, and the results of very recent versions can be found on the home page: www.whfreeman.com/tiplermodernphysics5e. See also Figures 1-9 through 1-11 here, as well as Equations 1-7 through 1-10.

1-2 Einstein's Postulates

In 1905, at the age of 26, Albert Einstein published several papers, among which was one on the electrodynamics of moving bodies.[11] In this paper, he postulated a more general principle of relativity that applied to the laws of both electrodynamics and mechanics. A consequence of this postulate is that absolute motion cannot be detected

STUDENTS-HUB.com Uploaded By: Malak Obaid

by any experiment. We can then consider the Michelson apparatus and Earth to be at rest. No fringe shift is expected when the interferometer is rotated 90°, since all directions are equivalent. The null result of the Michelson-Morley experiment is therefore to be expected. It should be pointed out that Einstein did not set out to explain the Michelson-Morley experiment. His theory arose from his considerations of the theory of electricity and magnetism and the unusual property of electromagnetic waves that they propagate in a vacuum. In his first paper, which contains the complete theory of special relativity, he made only a passing reference to the experimental attempts to detect Earth's motion through the ether, and in later years he could not recall whether he was aware of the details of the Michelson-Morley experiment before he published his theory.

The theory of special relativity was derived from two postulates proposed by Einstein in his 1905 paper:

Postulate 1. The laws of physics are the same in all inertial reference frames.

Postulate 2. The speed of light in a vacuum is equal to the value c, independent of the motion of the source.

Postulate 1 is an extension of the Newtonian principle of relativity to include all types of physical measurements (not just measurements in mechanics). It implies that no inertial system is preferred over any other; hence, absolute motion cannot be detected. Postulate 2 describes a common property of all waves. For example, the speed of sound waves does not depend on the motion of the sound source. When an approaching car sounds its horn, the frequency heard increases according to the Doppler effect, but the speed of the waves traveling through the air does not depend on the speed of the car. The speed of the waves depends only on the properties of the air, such as its temperature. The force of this postulate was to include light waves, for which experiments had found no propagation medium, together with all other waves, whose speed *was* known to be independent of the speed of the source. Recent analysis of the light curves of gamma-ray bursts that occur near the edge of the observable universe have shown the speed of light to be independent of the speed of the source to a precision of one part in 10^{20}.

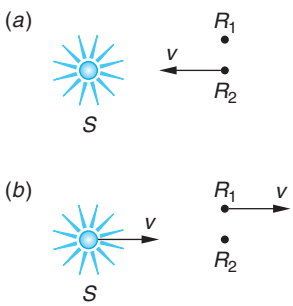

Figure 1-12 (*a*) Stationary light source S and a stationary observer R_1, with a second observer R_2 moving toward the source with speed v. (*b*) In the reference frame in which the observer R_2 is at rest, the light source S and observer R_1 move to the right with speed v. If absolute motion cannot be detected, the two views are equivalent. Since the speed of light does not depend on the motion of the source, observer R_2 measures the same value for that speed as observer R_1.

Although each postulate seems quite reasonable, many of the implications of the two together are surprising and seem to contradict common sense. One important implication of these postulates is that every observer measures the same value for the speed of light independent of the relative motion of the source and observer. Consider a light source S and two observers R_1, at rest relative to S, and R_2, moving toward S with speed v, as shown in Figure 1-12*a*. The speed of light measured by R_1 is $c = 3 \times 10^8$ m/s. What is the speed measured by R_2? The answer is *not* $c + v$, as one would expect based on Newtonian relativity. By postulate 1, Figure 1-12*a* is equivalent to Figure 1-12*b*, in which R_2 is at rest and the source S and R_1 are moving with speed v. That is, since absolute motion cannot be detected, it is not possible to say which is really moving and which is at rest. By postulate 2, the speed of light from a moving source is independent of the motion of the source. Thus, looking at Figure 1-12*b*, we see that R_2 measures the speed of light to be c, just as R_1 does. This result, that all observers measure the same value c for the speed of light, is often considered an alternative to Einstein's second postulate.

This result contradicts our intuition. Our intuitive ideas about relative velocities are approximations that hold only when the speeds are very small compared with the speed of light. Even in an airplane moving at the speed of sound, it is not possible to measure the speed of light accurately enough to distinguish the difference between the results c and $c + v$, where v is the speed of the plane. In order to make such a

STUDENTS-HUB.com Uploaded By: Malak Obaid

distinction, we must either move with a very great velocity (much greater than that of sound) or make extremely accurate measurements, as in the Michelson-Morley experiment, and when we do, we will find, as Einstein pointed out in his original relativity paper, that the contradictions are "only apparently irreconcilable."

Events and Observers

In considering the consequences of Einstein's postulates in greater depth, i.e., in developing the theory of special relativity, we need to be certain that meanings of some important terms are crystal clear. First, there is the concept of an *event*. A physical event is something that happens, like the closing of a door, a lightning strike, the collision of two particles, your birth, or the explosion of a star. Every event occurs at some point in space and at some instant in time, but it is very important to recognize that events are independent of the particular inertial reference frame that we might use to describe them. Events do not "belong" to any reference frame.

Events are described by *observers* who do belong to particular inertial frames of reference. Observers could be people (as in Section 1-1), electronic instruments, or other suitable recorders, but for our discussions in special relativity we are going to be very specific. Strictly speaking, the observer will be an array of recording clocks located throughout the inertial reference system. It may be helpful for you to think of the observer as a person who goes around reading out the memories of the recording clocks or receives records that have been transmitted from distant clocks, but always keep in mind that in reporting events, such a person is strictly limited to summarizing the data collected from the clock memories. The travel time of light precludes him from including in his report distant events that he may have seen by eye! It is in this sense that we will be using the word *observer* in our discussions.

Each inertial reference frame may be thought of as being formed by a cubic three-dimensional lattice made of identical measuring rods (e.g., meter sticks) with a recording clock at each intersection as illustrated in Figure 1-13. The clocks are all identical, and we, of course, want them all to read the "same time" as one another at any instant; i.e., they must be *synchronized*. There are many ways to accomplish synchronization of the clocks, but a very straightforward way, made possible by the second postulate, is to use one of the clocks in the lattice as a standard, or *reference clock*. For convenience we will also use the location of the reference clock in the lattice as the coordinate origin for the reference frame. The reference clock is started with its indicator (hands, pointer, digital display) set at zero. At the instant it starts, it also sends out a flash of light that spreads out as a spherical wave in all directions. When the flash from the reference clock reaches the lattice clocks 1 meter away (notice that in Figure 1-13 there are six of them, two of which are off the edges of the figure), we want their indicators to read the time required for light to travel 1 m (= 1/299,792,458 s). This can be done simply by having an observer at each clock set that time on the indicator and then having the flash from the reference clock start them as it passes. The clocks 1 m from the origin now display the same time as the reference clock; i.e., they are all synchronized. In a similar fashion, all of the clocks throughout the inertial frame can be synchronized since the distance of any clock from the reference clock can be calculated from the space coordinates of its position in the lattice and the initial setting of its indicator will be the corresponding travel time for the reference light flash. This procedure can be used to synchronize the clocks in any inertial frame, *but* it does not synchronize the clocks in reference frames that move with respect to one another. Indeed, as we shall see shortly, clocks in relatively moving frames cannot in general be synchronized with one another.

(*Top*) Albert Einstein in 1905 at the Bern, Switzerland, patent office. [*Hebrew University of Jerusalem Albert Einstein Archives, courtesy AIP Emilio Segrè Visual Archives.*] (*Bottom*) Clock tower and electric trolley in Bern on Kramstrasse, the street on which Einstein lived. If you are on the trolley moving away from the clock and look back at it, the light you see must catch up with you. If you move at nearly the speed of light, the clock you see will be slow. In this, Einstein saw a clue to the variability of time itself. [*Underwood & Underwood/CORBIS.*]

STUDENTS-HUB.com Uploaded By: Malak Obaid

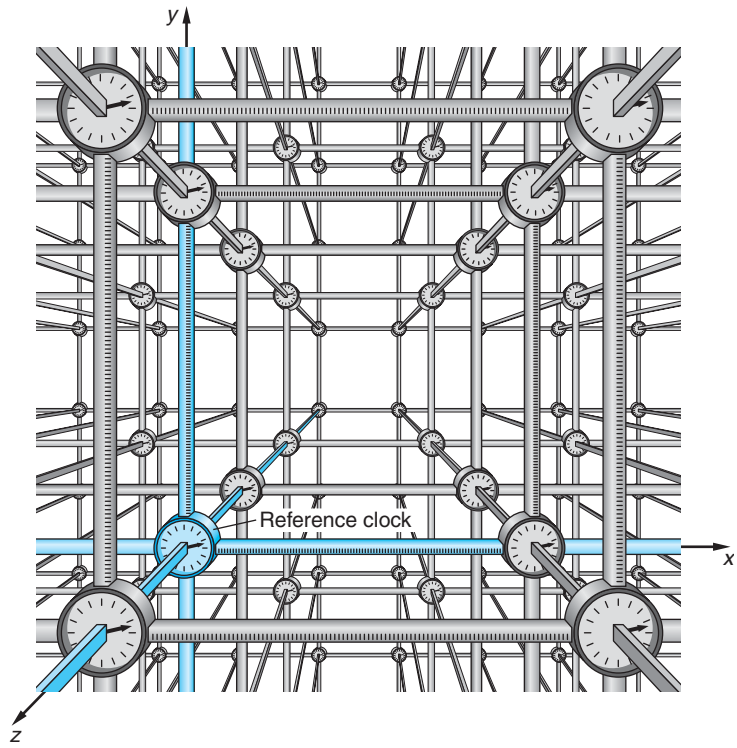

Figure 1-13 Inertial reference frame formed from a lattice of measuring rods with a clock at each intersection. The clocks are all synchronized using a reference clock. In this diagram the measuring rods are shown to be 1 m long, but they could all be 1 cm, 1 μm, or 1 km as required by the scale and precision of the measurements being considered. The three space dimensions are the clock positions. The fourth spacetime dimension, time, is shown by indicator readings on the clocks.

When an event occurs, its location and time are recorded instantly by the nearest clock. Suppose that an atom located at $x = 2$ m, $y = 3$ m, $z = 4$ m in Figure 1-13 emits a tiny flash of light at $t = 21$ s on the clock at that location. That event is recorded in space and in time or, as we will henceforth refer to it, in the *spacetime* coordinate system with the numbers (2,3,4,21). The observer may read out and analyze these data at his leisure, within the limits set by the information transmission time (i.e., the light travel time) from distant clocks. For example, the path of a particle moving through the lattice is revealed by analysis of the records showing the particle's time of passage at each clock's location. Distances between successive locations and the corresponding time differences make possible the determination of the particle's velocity. Similar records of the spacetime coordinates of the particle's path can, of course, also be made in any inertial frame moving relative to ours, but to compare the distances and time intervals measured in the two frames requires that we consider carefully the relativity of simultaneity.

Relativity of Simultaneity

Einstein's postulates lead to a number of predictions about measurements made by observers in inertial frames moving relative to one another that initially seem very strange, including some that appear paradoxical. Even so, these predictions have been experimentally verified; and nearly without exception, every paradox is resolved by an understanding of the *relativity of simultaneity*, which states that

> Two spatially separated events simultaneous in one reference frame are not, in general, simultaneous in another inertial frame moving relative to the first.

STUDENTS-HUB.com Uploaded By: Malak Obaid

A corollary to this is that

> Clocks synchronized in one reference frame are not, in general, synchronized in another inertial frame moving relative to the first.

What do we mean by simultaneous events? Suppose two observers, both in the inertial frame S at different locations A and B, agree to explode bombs at time t_o (remember, we have synchronized all of the clocks in S). The clock at C, equidistant from A and B, will record the arrival of light from the explosions at the same instant, i.e., simultaneously. Other clocks in S will record the arrival of light from A or B first, depending on their locations, but after correcting for the time the light takes to reach each clock, the data recorded by each would lead an observer to conclude that the explosions were simultaneous. *We will thus define two events to be simultaneous in an inertial reference frame if the light signals from the events reach an observer halfway between them at the same time as recorded by a clock at that location*, called a local clock.

Einstein's Example To show that two events that are simultaneous in frame S are not simultaneous in another frame S' moving relative to S, we use an example introduced by Einstein. A train is moving with speed v past a station platform. We have observers located at A', B', and C' at the front, back, and middle of the train. (We consider the train to be at rest in S' and the platform in S.) We now suppose that the train and platform are struck by lightning at the front and back of the train and that the lightning bolts are simultaneous in the frame of the platform (S; Figure 1-14*a*). That is, an observer located at C halfway between positions A and B, where lightning strikes, observes the two flashes at the same time. It is convenient to suppose that the

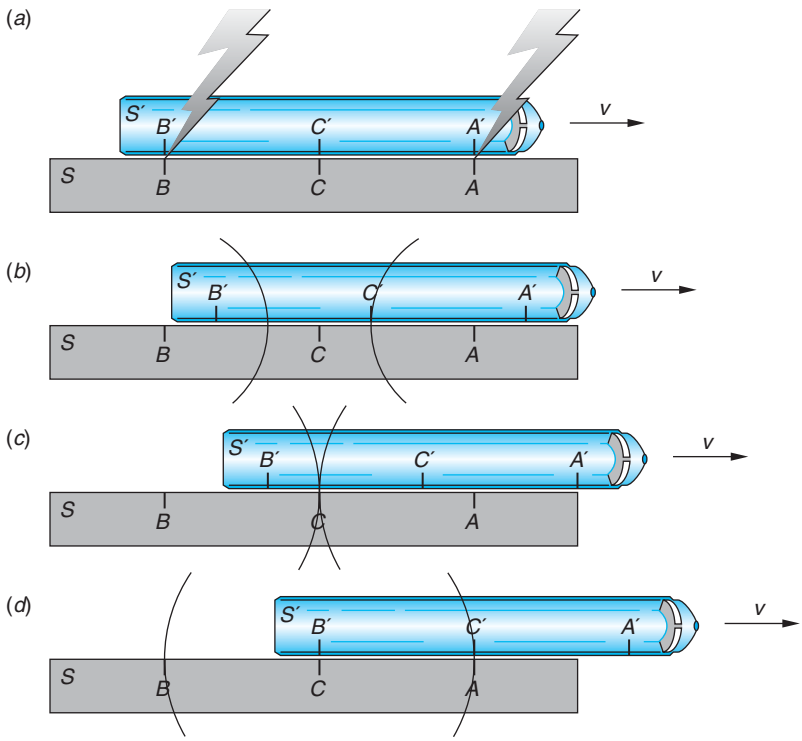

Figure 1-14 Lightning bolts strike the front and rear of the train, scorching both the train and the platform, as the train (frame S') moves past the platform (system S) at speed v. (*a*) The strikes are simultaneous in S, reaching the C observer located midway between the events at the same instant as recorded by the clock at C as shown in (*c*). In S' the flash from the front of the train is recorded by the C' clock, located midway between the scorch marks on the train, before that from the rear of the train (*b* and *d*, respectively). Thus, the C' observer concludes that the strikes were not simultaneous.

STUDENTS-HUB.com Uploaded By: Malak Obaid

lightning scorches both the train and the platform so that the events can be easily located in each reference frame. Since C' is in the middle of the train, halfway between the places on the train that are scorched, the events are simultaneous in S' only if the clock at C' records the flashes at the same time. However, the clock at C' records the flash from the front of the train before the flash from the back. In frame S, when the light from the front flash reaches the observer at C', the train has moved some distance toward A, so that the flash from the back has not yet reached C', as indicated in Figure 1-14*b*. The observer at C' must therefore conclude that the events are not simultaneous, but that the front of the train was struck before the back. Figures 1-14*c* and 1-14*d* illustrate, respectively, the subsequent simultaneous arrival of the flashes at C and the still-later arrival of the flash from the rear of the train at C'. As we have discussed, all observers in S' on the train will agree with the observer C' when they have corrected for the time it takes light to reach them.

The corollary can also be demonstrated with a similar example. Again consider the train to be at rest in S' that moves past the platform, at rest in S, with speed v. Figure 1-15 shows three of the clocks in the S lattice and three of those in the S' lattice. The clocks in each system's lattice have been synchronized in the manner that was described earlier, but those in S are not synchronized with those in S'. The observer at C midway between A and B on the platform announces that light sources at A and B will flash when the clocks at those locations read t_o (Figure 1-15*a*). The observer at C', positioned midway between A' and B', notes the arrival of the light flash from the front of the train (Figure 1-15*b*) *before* the arrival of the one from the rear (Figure 1-15*d*). Observer C' thus concludes that if the flashes were each emitted at t_o on the local clocks, as announced, then the clocks at A and B are not synchronized. All observers in S' would agree with that conclusion after correcting for the time of light travel. The clock located at C records the arrival of the two flashes simultaneously, of course, since the clocks in S are synchronized (Figure 1-15*c*).

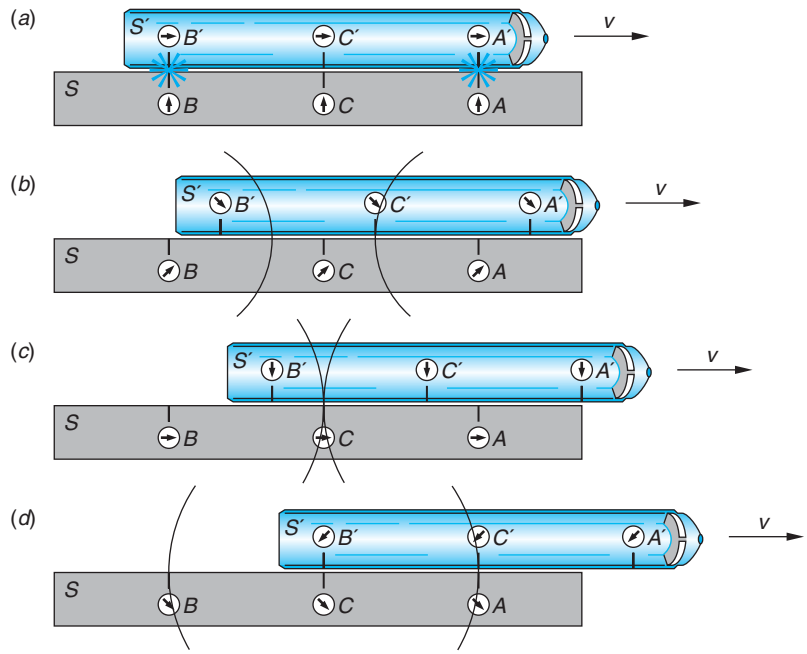

Figure 1-15 (*a*) Light flashes originate simultaneously at clocks A and B, synchronized in S. (*b*) The clock at C', midway between A' and B' on the moving train, records the arrival of the flash from A before the flash from B shown in (*d*). Since the observer in S announced that the flashes were triggered at t_o on the local clocks, the observer at C' concludes that the local clocks at A and B did not read t_o simultaneously; i.e., they were not synchronized. The simultaneous arrival of the flashes at C is shown in (*c*).

STUDENTS-HUB.com Uploaded By: Malak Obaid

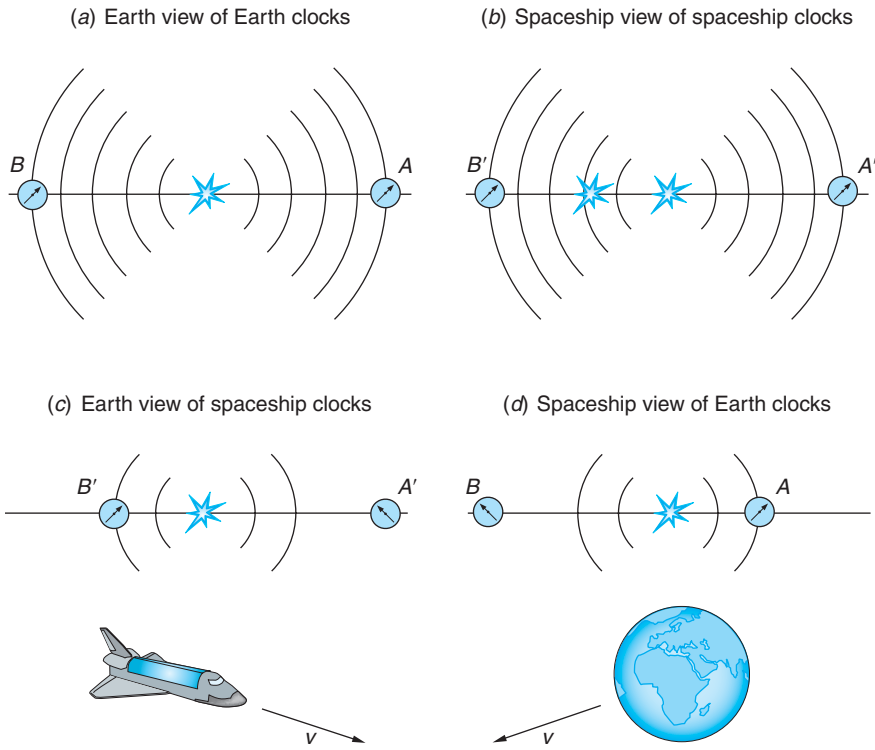

Figure 1-16 A light flash occurs on Earth midway between two Earth clocks. At the instant of the flash the midpoint of a passing spaceship coincides with the light source. (*a*) The Earth clocks record the lights' arrival simultaneously and are thus synchronized. (*b*) Clocks at both ends of the spaceship also record the lights' arrival simultaneously (Einstein's second postulate) and they, too, are synchronized. (*c*) However, the Earth observer sees the light reach the clock at B' *before* the light reaches the clock at A'. Since the spaceship clocks read the same time when the light arrives, the Earth observer concludes that the clocks at A' and B' are not synchronized. (*d*) The spaceship observer similarly concludes that the Earth clocks are not synchronized.

Notice, too, in Figure 1-15 that C' also concludes that the clock at A is ahead of the clock at B. This is important, and we will return to it in more detail in the next section. Figure 1-16 illustrates the relativity of simultaneity from a different perspective.

Questions

3. In addition to that described above, what would be another possible method of synchronizing all of the clocks in an inertial reference system?
4. Using Figure 1-16*d*, explain how the spaceship observer concludes that Earth clocks are not synchronized.

1-3 The Lorentz Transformation

We now consider a very important consequence of Einstein's postulates, the general relation between the spacetime coordinates x, y, z, and t of an event as seen in reference frame S and the coordinates x', y', z', and t' of the same event as seen in reference frame S', which is moving with uniform velocity relative to S. For simplicity we will

STUDENTS-HUB.com Uploaded By: Malak Obaid

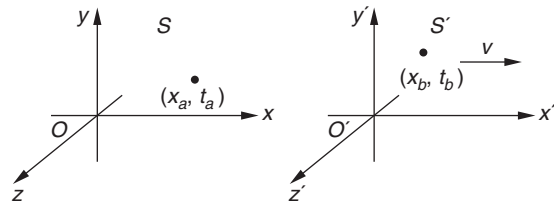

Figure 1-17 Two inertial frames S and S' with the latter moving at speed v in $+x$ direction of system S. Each set of axes shown is simply the coordinate axes of a lattice like that in Figure 1-13. Remember, there is a clock at each intersection. A short time before, the times represented by this diagram O and O' were coincident and the lattices of S and S' were intermeshed.

consider only the special case in which the origins of the two coordinate systems are coincident at time $t = t' = 0$ and S' is moving, relative to S, with speed v along the x (or x') axis and with the y' and z' axes parallel, respectively, to the y and z axes, as shown in Figure 1-17. As we discussed earlier (Equation 1-2), the classical Galilean coordinate transformation is

$$x' = x - vt \qquad y' = y \qquad z' = z \qquad t' = t \tag{1-2}$$

which expresses coordinate measurements made by an observer in S' in terms of those measured by an observer in S. The inverse transformation is

$$x = x' + vt' \qquad y = y' \qquad z = z' \qquad t = t'$$

and simply reflects the fact that the sign of the relative velocity of the reference frames is different for the two observers. The corresponding classical velocity transformation was given in Equation 1-3 and the acceleration, as we saw earlier, is invariant under a Galilean transformation. (For the rest of the discussion we will ignore the equations for y and z, which do not change in this special case of motion along the x and x' axes.) These equations are consistent with experiment as long as v is much less than c.

It should be clear that the classical velocity transformation is not consistent with the Einstein postulates of special relativity. If light moves along the x axis with speed c in S, Equation 1-3 implies that the speed in S' is $u'_x = c - v$ rather than $u'_x = c$. The Galilean transformation equations must therefore be modified to be consistent with Einstein's postulates, but the result must reduce to the classical equations when v is much less than c. We will give a brief outline of one method of obtaining the relativistic transformation that is called the *Lorentz transformation*, so named because of its original discovery by H. A. Lorentz.[12] We assume the equation for x' to be of the form

$$x' = \gamma(x - vt) \tag{1-11}$$

where γ is a constant that can depend upon v and c but not on the coordinates. If this equation is to reduce to the classical one, γ must approach 1 as v/c approaches 0. The inverse transformation must look the same except for the sign of the velocity:

$$x = \gamma(x' + vt') \tag{1-12}$$

With the arrangement of the axes in Figure 1-17, there is no relative motion of the frames in the y and z directions; hence $y' = y$ and $z' = z$. However, insertion of the as yet unknown multiplier γ modifies the classical transformation of time, $t' = t$. To see

STUDENTS-HUB.com Uploaded By: Malak Obaid

this, we substitute x' from Equation 1-11 into Equation 1-12 and solve for t'. The result is

$$t' = \gamma\left[t + \frac{(1 - \gamma^2)}{\gamma^2}\frac{x}{v}\right] \qquad \textbf{1-13}$$

Now let a flash of light start from the origin of S at $t = 0$. Since we have assumed that the origins coincide at $t = t' = 0$, the flash also starts at the origin of S' at $t' = 0$. The flash expands from *both* origins as a spherical wave. The equation for the wave front according to an observer in S is

$$x^2 + y^2 + z^2 = c^2t^2 \qquad \textbf{1-14}$$

and according to an observer in S', it is

$$x'^2 + y'^2 + z'^2 = c^2t'^2 \qquad \textbf{1-15}$$

where both equations are consistent with the second postulate. Consistency with the first postulate means that the relativistic transformation that we seek must transform Equation 1-14 into Equation 1-15 and vice versa. For example, substituting Equations 1-11 and 1-13 into 1-15 results in Equation 1-14 *if*

$$\gamma = \frac{1}{\sqrt{1 - \dfrac{v^2}{c^2}}} = \frac{1}{\sqrt{1 - \beta^2}} \qquad \textbf{1-16}$$

where $\beta = v/c$. Notice that $\gamma = 1$ for $v = 0$ and $\gamma \longrightarrow \infty$ for $v = c$. How this is done is illustrated in Example 1-2 below.

EXAMPLE 1-2 **Relativistic Transformation Multiplier γ** Show that γ must be given by Equation 1-16 if Equation 1-15 is to be transformed into Equation 1-14 consistent with Einstein's first postulate.

SOLUTION

Substituting Equations 1-11 and 1-13 into Equation 1-15 and noting that $y' = y$ and $z' = z$ in this case yields

$$\gamma^2(x - vt)^2 + y^2 + z^2 = c^2\gamma^2\left[t + \frac{1 - \gamma^2}{\gamma^2}\frac{x}{v}\right]^2 \qquad \textbf{1-17}$$

To be consistent with the first postulate, Equation 1-15 must be identical to 1-12. This requires that the coefficient of the x^2 term in Equation 1-17 be equal to 1, that of the t^2 term be equal to c^2, and that of the xt term be equal to 0. Any of those conditions can be used to determine γ, and all yield the same result. Using, for example, the coefficient of x^2, we have from Equation 1-17 that

$$\gamma^2 - c^2\gamma^2\frac{(1 - \gamma^2)^2}{\gamma^4v^2} = 1$$

STUDENTS-HUB.com Uploaded By: Malak Obaid

which can be rearranged to

$$-c^2\frac{(1-\gamma^2)^2}{\gamma^2 v^2} = (1-\gamma^2)$$

Canceling $1-\gamma^2$ on both sides and solving for γ yields

$$\gamma = \frac{1}{\sqrt{1-\dfrac{v^2}{c^2}}}$$

With the value for γ found in Example 1-2, Equation 1-13 can be written in a somewhat simpler form, and with it the complete Lorentz transformation becomes

$$\begin{aligned} x' &= \gamma(x-vt) & y' &= y \\ t' &= \gamma\left(t-\frac{vx}{c^2}\right) & z' &= z \end{aligned} \qquad \textbf{1-18}$$

and the inverse

$$\begin{aligned} x &= \gamma(x'+vt') & y &= y' \\ t &= \gamma\left(t'+\frac{vx'}{c^2}\right) & z &= z' \end{aligned} \qquad \textbf{1-19}$$

with

$$\gamma = \frac{1}{\sqrt{1-\beta^2}}$$

EXAMPLE 1-3 **Transformation of Time Intervals** The arrivals of two cosmic-ray μ leptons (muons) are recorded by detectors in the laboratory, one at time t_a at location x_a and the second at time t_b at location x_b in the laboratory reference frame, S in Figure 1-17. What is the time interval between those two events in system S', which moves relative to S at speed v?

SOLUTION

Applying the time coordinate transformation from Equation 1-18,

$$\begin{aligned} t'_b - t'_a &= \gamma\left(t_b-\frac{vx_b}{c^2}\right) - \gamma\left(t_a-\frac{vx_a}{c^2}\right) \\ t'_b - t'_a &= \gamma(t_b-t_a) - \frac{\gamma v}{c^2}(x_b-x_a) \end{aligned} \qquad \textbf{1-20}$$

We see that the time interval measured in S' depends not just on the corresponding time interval in S, but also on the spatial separation of the clocks in S that measured the interval. This result should not come as a total surprise, since we have

STUDENTS-HUB.com Uploaded By: Malak Obaid

already discovered that although the clocks in S are synchronized with each other, they are not, in general, synchronized for observers in other inertial frames.

Special Case 1

If the two events happen to occur at the same location in S, i.e., $x_a = x_b$, then $(t_b - t_a)$, the time interval measured on a clock located at the events, is called the *proper time interval*. Notice that since $\gamma > 1$ for all frames moving relative to S, the proper time interval is the *minimum* time interval that can be measured between those events.

Special Case 2

Does an inertial frame exist for which the events described above would be measured as being simultaneous? Since the question has been asked, you probably suspect that the answer is yes, and you are right. The two events will be simultaneous in a system S'' for which $t''_b - t''_a = 0$, i.e., when

$$\gamma(t_b - t_a) = \frac{\gamma v}{c^2}(x_b - x_a)$$

or when

$$\beta = \frac{v}{c} = \left(\frac{t_b - t_a}{x_b - x_a}\right)c \qquad \textbf{1-21}$$

Notice that $(x_b - x_a)/c$ = time for a light beam to travel from x_a to x_b; thus we can characterize S'' as being that system whose speed relative to S is that fraction of c given by the time interval between the events divided by the travel time of light between them. (Note, too, that $c(t_b - t_a) > (x_b - x_a)$ implies that $\beta > 1$, a nonphysical situation that we will discuss in Section 1-4.)

While it is possible for us to get along in special relativity without the Lorentz transformation, it has an application that is quite valuable: it enables the spacetime coordinates of events measured by the measuring rods and clocks in the reference frame of one observer to be translated into the corresponding coordinates determined by the measuring rods and clocks of an observer in another inertial frame. As we will see in Section 1-4, such transformations lead to some startling results.

Relativistic Velocity Transformations

The transformation for velocities in special relativity can be obtained by differentiation of the Lorentz transformation, keeping in mind the definition of the velocity. Suppose a particle moves in S with velocity $\mathbf{u}$ whose components are $u_x = dx/dt$, $u_y = dy/dt$, and $u_z = dz/dt$. An observer in S' would measure the components $u'_x = dx'/dt'$, $u'_y = dy'/dt'$, and $u'_z = dz'/dt'$. Using the transformation equations, we obtain

$$dx' = \gamma(dx - v\,dt) \qquad dy' = dy$$

$$dt' = \gamma\left(dt - \frac{v\,dx}{c^2}\right) \qquad dz' = dz$$

STUDENTS-HUB.com Uploaded By: Malak Obaid

from which we see that u'_x is given by

$$u'_x = \frac{dx'}{dt'} = \frac{\gamma(dx - v\,dt)}{\gamma\left(dt - \dfrac{v\,dx}{c^2}\right)} = \frac{(dx/dt - v)}{1 - \dfrac{v}{c^2}\dfrac{dx}{dt}}$$

or

$$u'_x = \frac{u_x - v}{1 - \dfrac{v u_x}{c^2}} \qquad \textbf{1-22}$$

and, if a particle has velocity components in the y and z directions, it is not difficult to find the components in S' in a similar manner.

$$u'_y = \frac{u_y}{\gamma\left(1 - \dfrac{v u_x}{c^2}\right)} \qquad u'_z = \frac{u_z}{\gamma\left(1 - \dfrac{v u_z}{c^2}\right)}$$

Remember that this form of the velocity transformation is specific to the arrangement of the coordinate axes in Figure 1-17. Note, too, that when $v \ll c$, i.e., when $\beta = v/c \approx 0$, the relativistic velocity transforms reduce to the classical velocity addition of Equation 1-3. Likewise, the inverse velocity transformation is

$$u_x = \frac{u'_x + v}{\left(1 + \dfrac{v u'_x}{c^2}\right)} \qquad u_y = \frac{u'_y}{\gamma\left(1 + \dfrac{v u'_x}{c^2}\right)} \qquad u_z = \frac{u'_z}{\gamma\left(1 + \dfrac{v u'_x}{c^2}\right)} \qquad \textbf{1-23}$$

EXAMPLE 1-4 **Relative Speeds of Cosmic Rays** Suppose that two cosmic ray protons approach Earth from opposite directions, as shown in Figure 1-18*a*. The speeds relative to Earth are measured to be $v_1 = 0.6c$ and $v_2 = -0.8c$. What is Earth's velocity relative to each proton, and what is the velocity of each proton relative to the other?

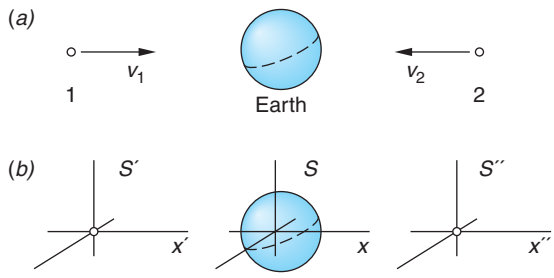

Figure 1-18 (*a*) Two cosmic ray protons approach Earth from opposite directions at speeds v_1 and v_2 with respect to Earth. (*b*) Attaching an inertial frame to each particle and Earth enables one to visualize the several relative speeds involved and apply the velocity transformation correctly.

SOLUTION

Consider each particle and Earth to be inertial reference frames S', S'', and S with their respective x axes parallel as in Figure 1-18*b*. With this arrangement $v_1 = u_{1x} = 0.6c$ and $v_2 = u_{2x} = -0.8c$. Thus, the speed of Earth measured in S' is $v'_{Ex} = -0.6c$ and the speed of Earth measured in S'' is $v''_{Ex} = 0.8c$.

STUDENTS-HUB.com Uploaded By: Malak Obaid

To find the speed of proton 2 with respect to proton 1, we apply Equation 1-22 to compute u'_{2x}, i.e., the speed of particle 2 in S'. Its speed in S has been measured to be $u_{2x} = -0.8c$, where the S' system has relative speed $v_1 = 0.6c$ with respect to S. Thus, substituting into Equation 1-22, we obtain

$$u'_{2x} = \frac{-0.8c - (0.6c)}{1 - (0.6c)(-0.8c)/c^2} = \frac{-1.4c}{1.48} = -0.95c$$

and the first proton measures the second to be approaching (moving in the $-x'$ direction) at $0.95c$.

The observer in S'' must of course make a consistent measurement, i.e., find the speed of proton 1 to be $0.95c$ in the $+x''$ direction. This can be readily shown by a second application of Equation 1-22 to compute u''_{1x}:

$$u''_{1x} = \frac{0.6c - (-0.8c)}{1 - (0.6c)(-0.8c)/c^2} = \frac{1.4c}{1.48} = 0.95c$$

Questions

5. The Lorentz transformation for y and z is the same as the classical result: $y = y'$ and $z = z'$. Yet the relativistic velocity transformation does not give the classical result $u_y = u'_y$ and $u_z = u'_z$. Explain.
6. Since the velocity components of a moving particle are different in relatively moving frames, the *directions* of the velocity vectors are also different in general. Explain why the fact that observers in S and S' measure different directions for a particle's motion is not an inconsistency in their observations.

Spacetime Diagrams

The relativistic discovery that time intervals between events are not the same for all observers in different inertial reference frames underscores the four-dimensional character of spacetime. With the diagrams that we have used thus far, it is difficult to depict and visualize on the two-dimensional page events that occur at different times, since each diagram is equivalent to a snapshot of spacetime at a particular instant. Showing events as a function of time typically requires a series of diagrams, such as Figures 1-14, 1-15, and 1-16, but even then our attention tends to be drawn to the space coordinate systems rather than the events, whereas it is the *events* that are fundamental. This difficulty is removed in special relativity with a simple yet powerful graphing method called the *spacetime diagram*. (This is just a new name given to the t vs. x graphs that you first began to use when you discussed motion in introductory physics.) On the spacetime diagram we can graph both the space and time coordinates of many events in one or more inertial frames, albeit with one limitation. Since the page offers only two dimensions for graphing, we suppress, or ignore for now, two of the space dimensions, in particular y and z. With our choice of the relative motion of inertial frames along the x axis, $y' = y$ and $z' = z$ anyhow. (This is one of the reasons we made that convenient choice a few pages back, the other reason being mathematical simplicity.) This means that for the time being, we are limiting our attention to one space dimension and to time, i.e., to events that occur, regardless of

STUDENTS-HUB.com Uploaded By: Malak Obaid

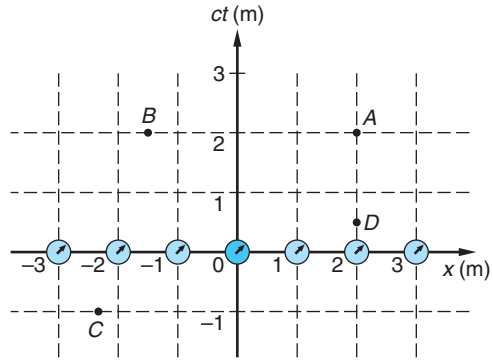

Figure 1-19 Spacetime diagram for an inertial reference frame S. Two of the space dimensions (y and z) are suppressed. The units on both the space and time axes are the same, meters. A meter of time means the time required for light to travel one meter, i.e., 3.3×10^{-9} s.

when, along one line in space. Should we need the other two dimensions, e.g., in a consideration of velocity vector transformations, we can always use the Lorentz transformation equations.

In a spacetime diagram the space location of each event is plotted along the x axis horizontally and the time is plotted vertically. From the three-dimensional array of measuring rods and clocks in Figure 1-13, we will use only those located on the x axis, as in Figure 1-19. (See, things are simpler already!) Since events that exhibit relativistic effects generally occur at high speeds, it will be convenient to multiply the time scale by the speed of light (a constant), which enables us to use the same units and scale on both the space and time axes, e.g., meters of distance and meters of light travel time.[13] The time axis is, therefore, c times the time t in seconds, i.e., ct. As we will see shortly, this choice prevents events from clustering about the axes and makes possible the straightforward addition of other inertial frames into the diagram.

As time advances, notice that in Figure 1-19 each clock in the array moves vertically upward along the dotted lines. Thus, as events A, B, C, and D occur in spacetime, one of the clocks of the array is at (or very near) each event when it happens. Remember that the clocks in the reference frame are synchronized, and so the difference in the readings of clocks located at each event records the *proper time interval* between the events. (See Example 1-3.) In the figure, events A and D occur at the same place ($x = 2$ m) but at different times. The time interval between them measured on clock 2 is the proper time interval since clock 2 is located at *both* events. Events A and B occur at different locations but at the same time (i.e., simultaneously in this frame). Event C occurred before the present since $ct = -1$ m. For this discussion we will consider the time that the coordinate origins coincide, $ct = ct' = 0$, to be the present.

Worldlines in Spacetime Particles moving in space trace out a line in the spacetime diagram called the *worldline* of the particle. The worldline is the "trajectory" of the particle on a ct versus x graph. To illustrate, consider four particles moving in space (not spacetime) as shown in Figure 1-20*a*, which shows the array of synchronized clocks on the x axis and the space trajectories of four particles, each starting at $x = 0$ and moving at some constant speed during 3 m of time. Figure 1-20*b* shows the worldline for each of the particles in spacetime. Notice that constant speed means that the worldline has constant slope; i.e., it is a straight line (slope $= \Delta t/\Delta x = 1/(\Delta x/\Delta t) = 1/\text{speed}$).

STUDENTS-HUB.com Uploaded By: Malak Obaid

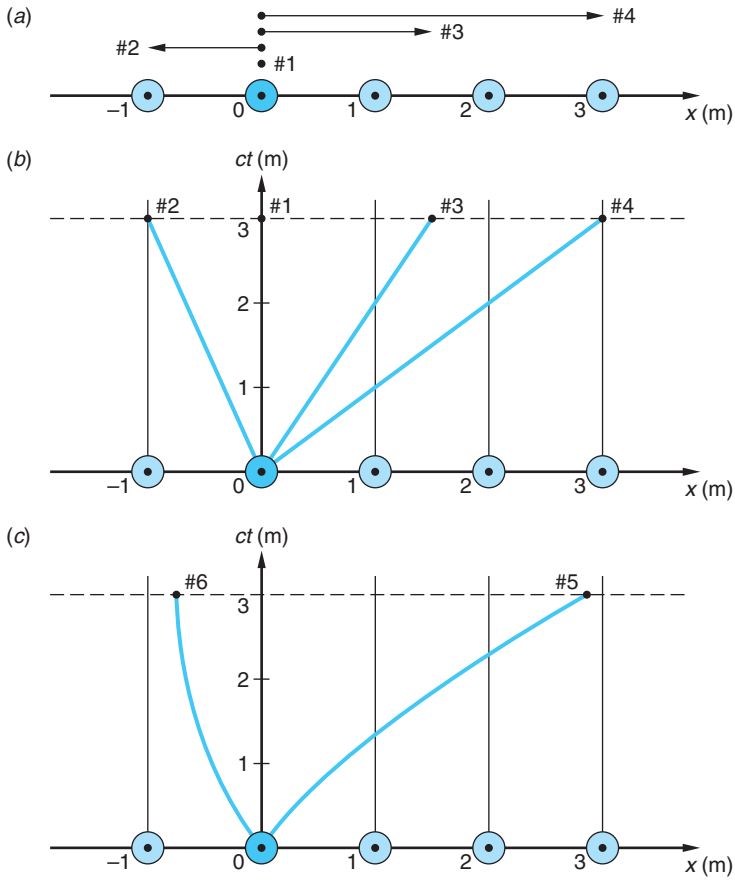

Figure 1-20 (*a*) The space trajectories of four particles with various constant speeds. Note that particle 1 has a speed of zero and particle 2 moves in the $-x$ direction. The worldlines of the particles are straight lines. (*b*) The worldline of particle 1 is also the ct axis since that particle remains at $x = 0$. The constant slopes are a consequence of the constant speeds. (*c*) For accelerating particles 5 and 6 [not shown in (*a*)], the worldlines are curved, the slope at any point yielding the instantaneous speed.

That was also the case when you first encountered elapsed time versus displacement graphs in introductory physics. Even then, you were plotting spacetime graphs and drawing worldlines! If the particle is accelerating—either speeding up like particle 5 in Figure 1-20*c* or slowing down like particle 6—the worldlines are curved. Thus, the worldline is the record of the particle's travel through spacetime, giving its speed (= 1/slope) and acceleration (= 1/rate at which the slope changes) at every instant.

EXAMPLE 1-5 Computing Speeds in Spacetime Find the speed u of particle 3 in Figure 1-20.

SOLUTION

The speed $u = \Delta x/\Delta t = 1/\text{slope}$, where we have $\Delta x = 1.5 - 0 = 1.5$ m and $\Delta ct = c \cdot \Delta t = 3.0 - 0 = 3.0$ m (from Figure 1-20). Thus, $\Delta t = (3.0/c) = (3.0/3.0 \times 10^8) = 10^{-8}$ s and $u = 1.5\text{ m}/10^{-8}\text{ s} = 0.5c$.

The speed of particle 4, computed as shown in Example 1-5, turns out to be c, the speed of light. (Particle 4 is a light pulse.) The slope of its worldline $\Delta(ct)/\Delta x = 3\text{ m}/3\text{ m} = 1$. Similarly, the slope of the worldline of a light pulse moving in the $-x$ direction is -1. Since relativity limits the speed of particles with mass to less than c,

STUDENTS-HUB.com Uploaded By: Malak Obaid

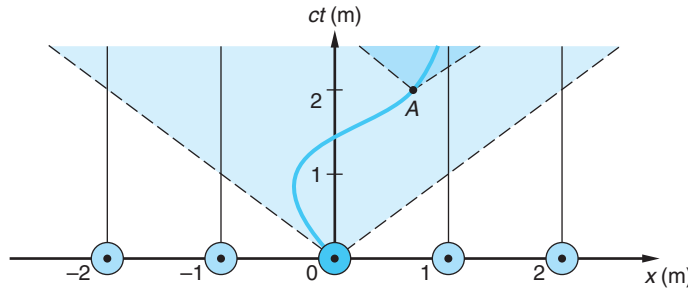

Figure 1-21 The speed-of-light limit to the speeds of particles limits the slopes of worldlines for particles that move through $x = 0$ at $ct = 0$ to the shaded area of spacetime, i.e., to slopes < -1 and $> +1$. The dashed lines are worldlines of light flashes moving in the $-x$ and $+x$ directions. The curved worldline of the particle shown has the same limits at every instant. Notice that the particle's speed = 1/slope.

as we will see in Chapter 2, the slopes of worldlines for particles that move through $x = 0$ at $ct = 0$ are limited to the larger shaded triangle in Figure 1-21. The same limits to the slope apply at every point along a particle's worldline, such as point A on the curved spacetime trajectory in Figure 1-21. This means that the particle's possible worldlines for times greater than $ct = 2$ m must lie within the heavily shaded triangle.

Analyzing events and motion in inertial systems that are in relative motion can now be accomplished more easily than with diagrams such as Figures 1-14 through 1-18. Suppose we have two inertial frames S and S' with S' moving in the $+x$ direction of S at speed v as in those figures. The clocks in both systems are started at $t = t' = 0$ (the present) as the two origins $x = 0$ and $x' = 0$ coincide, and, as before, observers in each system have synchronized the clocks in their respective systems. The spacetime diagram for S is, of course, like that in Figure 1-19, but how does S' appear in that diagram, i.e., with respect to an observer in S? Consider that as the origin of S' (i.e., the point where $x' = 0$) moves in S, its worldline is the ct' axis since the ct' axis is the locus of all points with $x' = 0$ (just as the ct axis is the locus of points with $x = 0$.) Thus, the slope of the ct' axis as seen by an observer in S can be found from Equation 1-18, the Lorentz transformation, as follows:

$$x' = \gamma(x - vt) = 0 \qquad \text{for} \qquad x' = 0$$

or

$$x = vt = (v/c)(ct) = \beta ct$$

and

$$ct = (1/\beta)x$$

which says that the slope (in S) of the worldline of the point $x' = 0$, the ct' axis, is $1/\beta$. (See Figure 1-22*a*.)

In the same manner, the x' axis can be located using the fact that it is the locus of points for which $ct' = 0$. The Lorentz transformation once again provides the slope:

$$t' = \gamma\left(t - \frac{vx}{c^2}\right) = 0$$

$$\text{or} \qquad t = \frac{vx}{c^2} \qquad \text{and} \qquad ct = \frac{v}{c}x = \beta x$$

Thus, the slope of the x' axis as measured by an observer in S is β, as shown in Figure 1-22*a*. Don't be confused by the fact that the x axes don't look parallel anymore. They are still parallel in *space*, but this is a *spacetime* diagram. It shows motion in both

STUDENTS-HUB.com Uploaded By: Malak Obaid

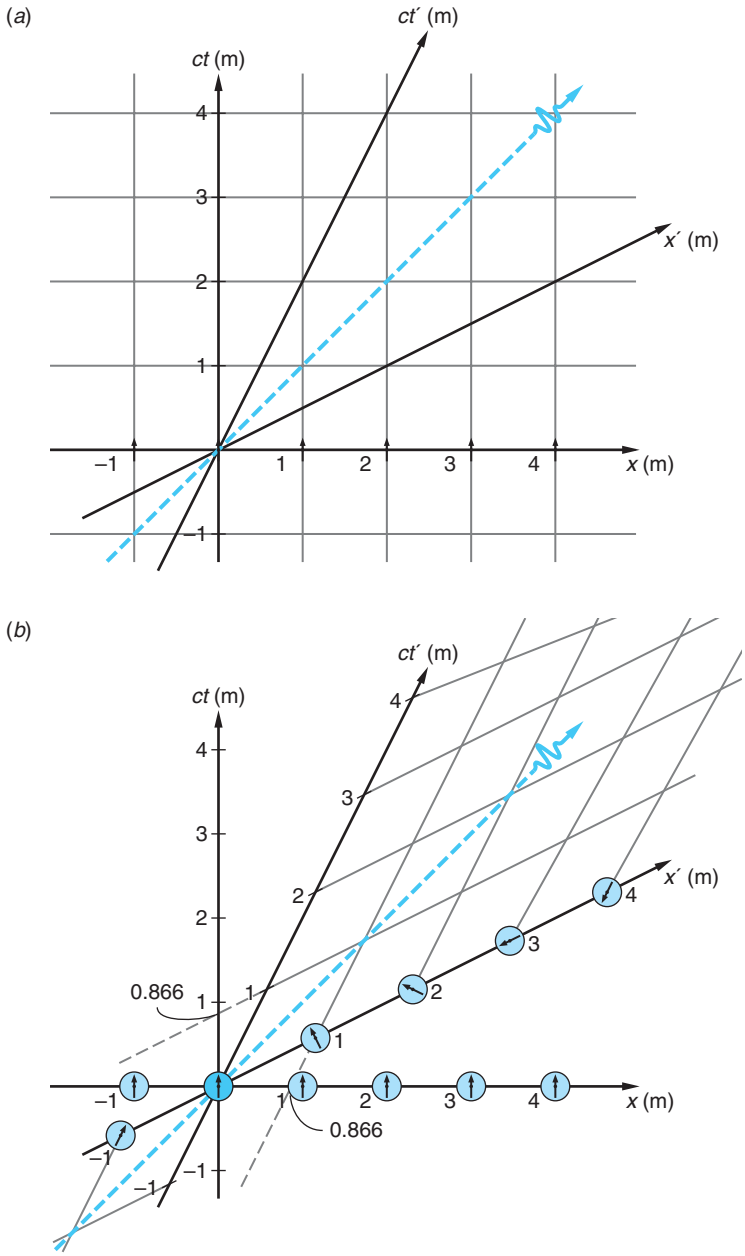

Figure 1-22 Spacetime diagram of S showing S' moving at speed $v = 0.5c$ in the $+x$ direction. The diagram is drawn with $t = t' = 0$ when the origins of S and S' coincided. The dashed line shows the worldline of a light flash that passed through the point $x = 0$ at $t = 0$ heading in the $+x$ direction. Its slope equals 1 in both S and S'. The ct' and x' axes of S' have slopes of $1/\beta = 2$ and $\beta = 0.5$, respectively. (*a*) Calibrating the axes of S' as described in the text allows the grid of coordinates to be drawn on S'. Interpretation is facilitated by remembering that (*b*) shows the system S' as it is observed in the spacetime diagram of S.

space and time. For example, the clock at $x' = 1$ m in Figure 1-22*b* passed the point $x = 0$ at about $ct = -1.5$ m as the x' axis of S' moved both upward and to the right in S. Remember, as time advances, the array of synchronized clocks and measuring rods that are the x axis also move upward, so that, for example, when $ct = 1$, the origin of S' ($x' = 0$, $ct' = 0$) has moved $vt = (v/c)ct = \beta ct$ to the right along the x axis.

Question

7. Explain how the spacetime diagram in Figure 1-22*b* would appear drawn by an observer in S'.

STUDENTS-HUB.com Uploaded By: Malak Obaid

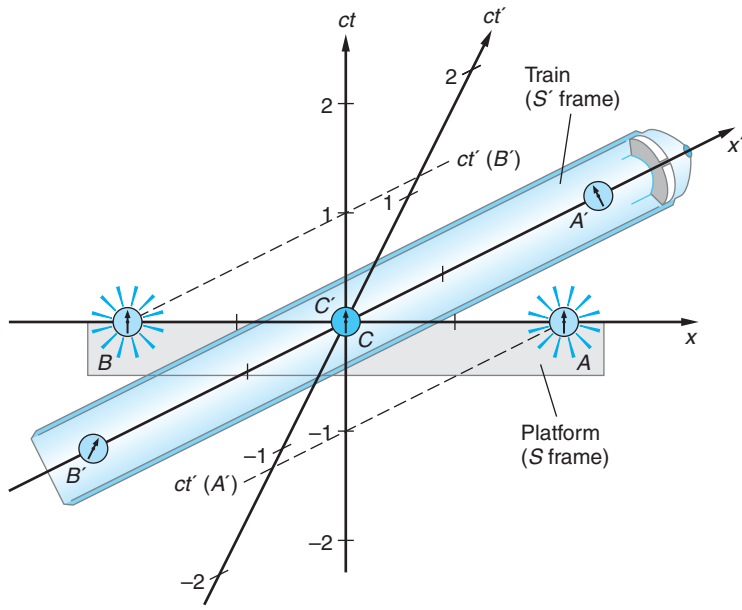

Figure 1-23 Spacetime equivalent of Figure 1-15, showing the spacetime diagram for the system S in which the platform is at rest. Measurements made by observers in S' are read from the primed axes.

EXAMPLE 1-6 Simultaneity in Spacetime Use the train-platform example of Figure 1-15 and a suitable spacetime diagram to show that events simultaneous in one frame are not simultaneous in a frame moving relative to the first. (This is the corollary to the relativity of simultaneity that we first demonstrated in the previous section using Figure 1-15.)

SOLUTION

Suppose a train is passing a station platform at speed v and an observer C at the midpoint of the platform, system S, announces that light flashes will be emitted at clocks A and B located at opposite ends of the platform at $t = 0$. Let the train, system S', be a rocket train with $v = 0.5c$. As in the earlier discussion, clocks at C and C' both read 0 as C' passes C. Figure 1-23 shows this situation. It is the spacetime equivalent of Figure 1-15.

Two events occur, the light flashes. The flashes are simultaneous in S since both occur at $ct = 0$. In S', however, the event at A occurred at $ct'(A')$ (see Figure 1-23), about 1.2 ct' units *before* $ct' = 0$, and the event at B occurred at $ct'(B')$, about 1.2 ct' units *after* $ct' = 0$. Thus, the flashes are not simultaneous in S' and A occurs before B, as we also saw in Figure 1-15.

EXPLORING
Calibrating the Spacetime Axes

By calibrating the coordinate axes of S' consistent with the Lorentz transformation, we will be able to read the coordinates of events and calculate space and time intervals between events as measured in both S and S' directly from the diagram, in addition to calculating them from Equations 1-18 and 1-19. The calibration of the S' axes is

STUDENTS-HUB.com Uploaded By: Malak Obaid

straightforward and is accomplished as follows. The locus of points, e.g., with $x' = 1$ m, is a line parallel to the ct' axis through the point $x' = 1$ m, $ct' = 0$, just as we saw earlier that the ct' axis was the locus of those points with $x' = 0$ through the point $x' = 0$, $ct' = 0$. Substituting these values into the Lorentz transformation for x', we see that the line through $x' = 1$ m intercepts the x axis, i.e., the line where $ct = 0$ at

$$\begin{aligned} x' &= \gamma(x - vt) = \gamma(x - \beta ct) \\ 1 &= \gamma x \qquad \text{or} \qquad x = 1/\gamma = \sqrt{1 - \beta^2} \end{aligned} \tag{1-24}$$

or, in general,

$$x = x'\sqrt{1 - \beta^2}$$

In Figure 1-22*b*, where $\beta = 0.5$, the line $x' = 1$ m intercepts the x axis at $x = 0.866$ m. Similarly, if $x' = 2$ m, $x = 1.73$ m; if $x' = 3$ m, $x = 2.60$ m; and so on.

The ct' axis is calibrated in a precisely equivalent manner. The locus of points with $ct' = 1$ m is a line parallel to the x' axis through the point $ct' = 1$ m, $x' = 0$. Using the Lorentz transformation, the intercept of that line with the ct axis (where $x = 0$) is found as follows:

$$t' = \gamma(t - vx/c^2)$$

which can also be written as

$$ct' = \gamma(ct - \beta x) \tag{1-25}$$

or $ct' = \gamma ct$ for $x = 0$. Thus, for $ct' = 1$ m, we have $1 = \gamma ct$ or $ct = (1 - \beta^2)^{1/2}$ and, again in general, $ct = ct'(1 - \beta^2)^{1/2}$. The $x' \cdot ct'$ coordinate grid is shown in Figure 1-22*b*.

Notice in Figure 1-22*b* that the clocks located in S' are *not* found to be synchronized by observers in S, even though they are synchronized in S'. This is exactly the conclusion that we arrived at in the discussion of the lightning striking the train and platform. In addition, those with positive x' coordinates are behind the S' reference clock and those with negative x' coordinates are ahead, the differences being greatest for those clocks farthest away. This is a direct consequence of the Lorentz transformation of the time coordinate—i.e., when $ct = 0$ in Equation 1-25, $ct' = -\gamma\beta x$. Note, too, that the slope of the worldline of the light beam equals 1 in S' as well as in S, as required by the second postulate.

1-4 Time Dilation and Length Contraction

The results of correct measurements of the time and space intervals between events do not depend upon the kind of apparatus used for the measurements or on the events themselves. We are free therefore to choose any events and measuring apparatus that will help us understand the application of the Einstein postulates to the results of measurements. As you have already seen from previous examples, convenient events in relativity are those that produce light flashes. A convenient, simple such clock is a *light clock*, pictured schematically in Figure 1-24. A photocell detects the light pulse and sends a voltage pulse to an oscilloscope, which produces a vertical deflection of the oscilloscope's trace. The phosphorescent material on the face of the oscilloscope tube gives a persistent light that can be observed visually, photographed, or recorded electronically. The time between two light flashes is determined by measuring the

STUDENTS-HUB.com Uploaded By: Malak Obaid

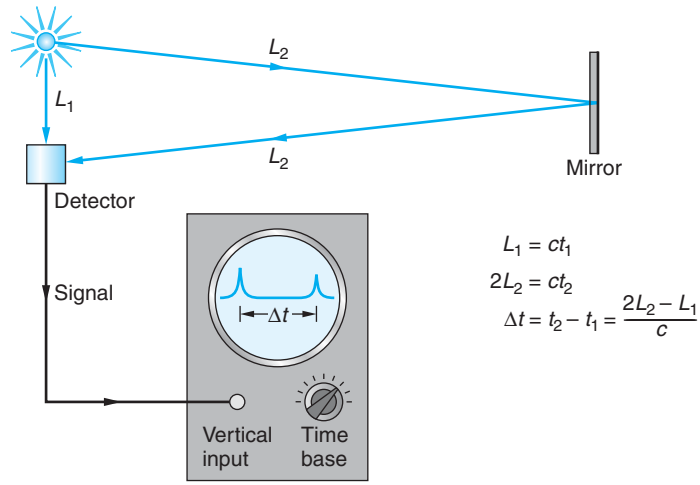

Figure 1-24 Light clock for measuring time intervals. The time is measured by reading the distance between pulses on the oscilloscope after calibrating the sweep speed.

distance between pulses on the scope and knowing the sweep speed. Such clocks can easily be calibrated and compared with other types of clocks. Although not drawn as in Figure 1-24, the clocks used in explanations in this section may be thought of as light clocks.

Time Dilation (or Time Stretching)

We first consider an observer A' at rest in frame S' a distance D from a mirror, also in S', as shown in Figure 1-25*a*. She triggers a flash gun and measures the time interval $\Delta t'$ between the original flash and the return flash from the mirror. Since light travels with speed c, this time is $\Delta t' = (2D)/c$.

Now consider these same two events, the original flash of light and the returning flash, as observed in reference frame S, with respect to which S' is moving to the right with speed v. The events happen at two different places, x_1 and x_2, in frame S because between the original flash and the return flash observer A' has moved a horizontal distance $v\Delta t$, where Δt is the time interval between the events measured in S.

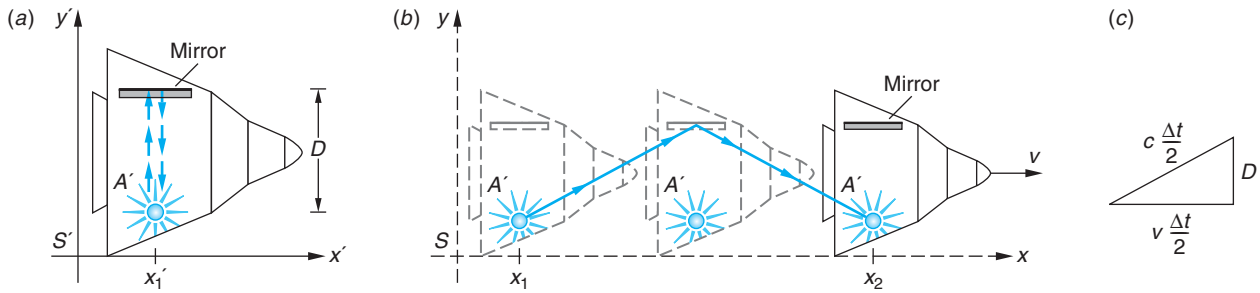

Figure 1-25 (*a*) Observer A' and the mirror are in a spaceship at rest in frame S'. The time it takes for the light pulse to reach the mirror and return is measured by A' to be $2D/c$. (*b*) In frame S, the spaceship is moving to the right with speed v. If the speed of light is the same in both frames, the time it takes for the light to reach the mirror and return is longer than $2D/c$ in S because the distance traveled is greater than $2D$. (*c*) A right triangle for computing the time Δt in frame S.

STUDENTS-HUB.com Uploaded By: Malak Obaid

In Figure 1-25*b*, a space diagram, we see that the path traveled by the light is longer in S than in S'. However, by Einstein's postulates, light travels with the same speed c in frame S as it does in frame S'. Since it travels farther in S at the same speed, it takes longer in S to reach the mirror and return. The time interval between flashes in S is thus longer than it is in S'. We can easily calculate Δt in terms of $\Delta t'$. From the triangle in Figure 1-25*c*, we see that

$$\left(\frac{c\Delta t}{2}\right)^2 = D^2 + \left(\frac{v\Delta t}{2}\right)^2$$

or

$$\Delta t = \frac{2D}{\sqrt{c^2 - v^2}} = \frac{2D}{c}\frac{1}{\sqrt{1 - v^2/c^2}}$$

Using $\Delta t' = 2D/c$, we have

$$\Delta t = \frac{\Delta t'}{\sqrt{1 - v^2/c^2}} = \gamma \Delta t' = \gamma\tau \qquad \textbf{1-26}$$

where $\tau = \Delta t'$ is the *proper time interval* that we first encountered in Example 1-3. Equation 1-26 describes *time dilation*; i.e., it tells us that the observer in frame S always measures the time interval between two events to be longer (since $\gamma > 1$) than the corresponding interval measured on the clock located at both events in the frame where they occur at the same location. Thus, observers in S conclude that the clock at A' in S' runs slow since that clock measures a smaller time interval between the two events. Notice that the faster S' moves with respect to S, the larger is γ, and the slower the S' clocks will tick. It appears to the S observer that time is being stretched out in S′.

Be careful! The *same* clock must be located at each event for $\Delta t'$ to be the proper time interval τ. We can see why this is true by noting that Equation 1-26 can be obtained directly from the inverse Lorentz transformation for t. Referring again to Figure 1-25 and calling the emission of the flash event 1 and its return event 2, we have that

$$\Delta t = t_2 - t_1 = \gamma\left(t'_2 + \frac{vx'_2}{c^2}\right) - \gamma\left(t'_1 + \frac{vx'_1}{c^2}\right)$$

$$\Delta t = \gamma(t'_2 - t'_1) + \frac{\gamma v}{c^2}(x'_2 - x'_1)$$

or

$$\Delta t = \gamma \Delta t' + \frac{\gamma v}{c^2}\Delta x' \qquad \textbf{1-27}$$

If the clock that records t'_2 and t'_1 is located at the events, then $\Delta x' = 0$. If that is not the case, however, $\Delta x' \neq 0$ and $\Delta t'$, though certainly a valid measurement, is not a proper time interval. Only a clock located *at* an event *when* it occurs can record a proper time interval.

STUDENTS-HUB.com Uploaded By: Malak Obaid

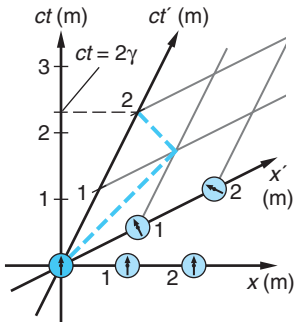

Figure 1-26 Spacetime diagram illustrating time dilation. The dashed line is the worldline of a light flash emitted at $x' = 0$ and reflected back to that point by a mirror at $x' = 1$ m. $\beta = 0.5$.

EXAMPLE 1-7 Spatial Separation of Events Two events occur at the same point x'_0 at times t'_1 and t'_2 in S', which moves with speed v relative to S. What is the spatial separation of these events measured in S?

SOLUTION

1. The location of the events in S is given by the Lorentz inverse transformation Equation 1-19:
$$x = \gamma(x' + vt')$$

2. The spatial separation of the two events $\Delta x = x_2 - x_1$ is then
$$\Delta x = \gamma(x'_0 + vt'_2) - \gamma(x'_0 + vt'_1)$$

3. The $\gamma x'_0$ terms cancel:
$$\Delta x = \gamma v(t'_2 - t'_1) = \gamma v \Delta t'$$

4. Since $\Delta t'$ is the proper time interval τ, Equation 1-26 yields
$$\Delta x = v\gamma\tau = v\Delta t$$

5. Using the situation in Figure 1-26 as a numerical example, where $\beta = 0.5$ and $\gamma = 1.15$, we have
$$\Delta x = \gamma\frac{v}{c}\Delta(ct') = (1.15)(0.5)(2) = 1.15 \text{ m}$$

EXAMPLE 1-8 The Pregnant Elephant[14] Elephants have a gestation period of 21 months. Suppose that a freshly impregnated elephant is placed on a spaceship and sent toward a distant space jungle at $v = 0.75c$. If we monitor radio transmissions from the spaceship, how long after launch might we expect to hear the first squealing trumpet from the newborn calf?

SOLUTION

1. In S', the rest frame of the elephant, the time interval from launch to birth, is $\tau = 21$ months. In the Earth frame S the time interval is Δt_1, given by Equation 1-26:
$$\Delta t_1 = \gamma\tau = \frac{1}{\sqrt{1 - \beta^2}}\tau = \frac{1}{\sqrt{1 - (0.75)^2}}(21 \text{ months}) = 31.7 \text{ months}$$

2. At that time the radio signal announcing the happy event starts toward Earth at speed c, but from where? Using the result of Example 1-7, since launch the spaceship has moved Δx in S, given by
$$\Delta x = \gamma vt = \gamma\beta ct = (1.51)(0.75)(21\ c \cdot \text{months}) = 23.8\ c \cdot \text{months}$$
where $c \cdot$ month is the distance light travels in one month.

3. Notice that there is no need to convert Δx into meters since our interest is in how long it will take the radio signal to travel this distance in S. That time is Δt_2, given by
$$\Delta t_2 = \Delta x/c = 23.8\ c \cdot \text{months}/c = 23.8 \text{ months}$$

4. Thus, the good news will arrive at Earth at time Δt after launch where
$$\Delta t = \Delta t_1 + \Delta t_2 = 31.7 + 23.8 = 55.5 \text{ months}$$

STUDENTS-HUB.com Uploaded By: Malak Obaid

Remarks: *This result, too, is readily obtained from a spacetime diagram. Figure 1-27 illustrates the general appearance of the spacetime diagram for this example, showing the elephant's worldline and the worldline of the radio signal.*

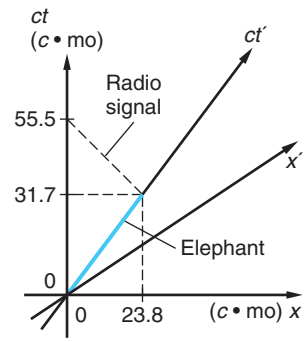

Figure 1-27 Sketch of the spacetime diagram for Example 1-8. β = 0.75. The colored line is the worldline of the pregnant elephant. The worldline of the radio signal is the dashed line at 45° toward the upper left.

Question

8. You are standing on a corner and a friend is driving past in an automobile. Both of you note the times when the car passes two different intersections and determine from your watch readings the time that elapses between the two events. Which of you has determined the proper time interval?

The time dilation of Equation 1-26 is easy to see in a spacetime diagram such as Figure 1-26, using the same round trip for a light pulse used above. Let the light flash leave $x' = 0$ at $ct' = 0$ when the S and S' origins coincided. The flash travels to $x' = 1$ m, reflects from a mirror located there, and returns to $x' = 0$. Let $\beta = 0.5$. The dotted line shows the worldline of the light beam, reflecting at ($x' = 1$, $ct' = 1$) and returning to $x' = 0$ at $ct' = 2$ m. Note that the S observer records the latter event at $ct > 2$ m; i.e., the observer in S sees the S' clock running slow.

Experimental tests of the time dilation prediction have been performed using macroscopic clocks, in particular, accurate atomic clocks. In 1975, C. O. Alley conducted a test of both general and special relativity in which a set of atomic clocks were carried by a U.S. Navy antisubmarine patrol aircraft while it flew back and forth over the same path for 15 hours at altitudes between 8000 m and 10,000 m over Chesapeake Bay. The clocks in the plane were compared by laser pulses with an identical group of clocks on the ground. (See Figure 1-13 for one way such a comparison might be done.) Since the experiment was primarily intended to test the gravitational effect on clocks predicted by general relativity (see Section 2-5), the aircraft was deliberately flown at the rather sedate average speed of 270 knots (140 m/s) = $4.7 \times 10^{-7}c$ to minimize the time dilation due to the relative speeds of the clocks. Even so, after Alley deducted the effect of gravitation as predicted by general relativity, the airborne clocks lost an average of 5.6×10^{-9} s due to the relative speed during the 15-hour flight. This result agrees with the prediction of special relativity, 5.7×10^{-9} s, to within 2 percent, even at this low relative speed. The experimental results leave little basis for further debate as to whether traveling clocks of all kinds lose time on a round trip. They do.

Length Contraction

A phenomenon closely related to time dilation is *length contraction*. The length of an object measured in the reference frame in which the object is at rest is called its *proper length* L_p. In a reference frame in which the object is moving, the measured length parallel to the direction of motion is shorter than its proper length. Consider a rod at rest in the frame S' with one end at x'_2 and the other end at x'_1, as illustrated in Figure 1-28. The length of the rod in this frame is its proper length $L_p = x'_2 - x'_1$. Some care must

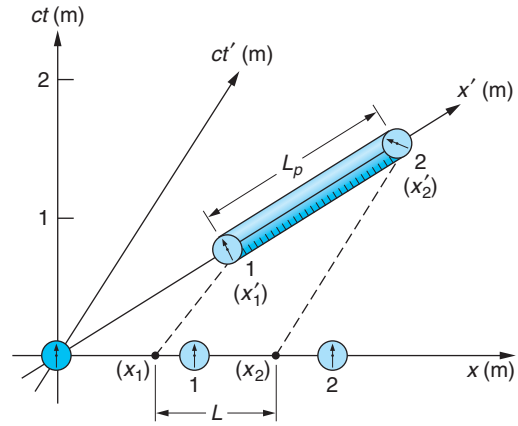

Figure 1-28 A measuring rod, a meter stick in this case, lies at rest in S' between $x'_2 = 2$ m and $x'_1 = 1$ m. System S' moves with $\beta = 0.79$ relative to S. Since the rod is in motion, S must measure the locations of the ends of the rod x_2 and x_1 simultaneously in order to have made a valid length measurement. L is obviously shorter than L_p. By direct measurement from the diagram (use a millimeter scale) $L/L_p = 0.61 = 1/\gamma$.

STUDENTS-HUB.com Uploaded By: Malak Obaid

be taken to find the length of the rod in frame S. In this frame, the rod is moving to the right with speed v, the speed of frame S'. The length of the rod in frame S is *defined* as $L = x_2 - x_1$, where x_2 is the position of one end at some time t_2 and x_1 is the position of the other end *at the same time* $t_1 = t_2$ as measured in frame S. Since the rod is at rest in S', t'_2 need not equal t'_1. Equation 1-18 is convenient to use to calculate $x_2 - x_1$ at some time t because it relates x, x', and t, whereas Equation 1-19 is not convenient because it relates x, x', and t':

$$x'_2 = \gamma(x_2 - vt_2) \qquad \text{and} \qquad x'_1 = \gamma(x_1 - vt_1)$$

Since $t_2 = t_1$, we obtain

$$x'_2 - x'_1 = \gamma(x_2 - x_1)$$

$$x_2 - x_1 = \frac{1}{\gamma}(x'_2 - x'_1) = \sqrt{1 - \frac{v^2}{c^2}}(x'_2 - x'_1)$$

or

$$L = \frac{1}{\gamma}L_p = \sqrt{1 - \frac{v^2}{c^2}}L_p \qquad \textbf{1-28}$$

Thus, the length of a rod is smaller when it is measured in a frame with respect to which it is moving. Before Einstein's paper was published, Lorentz and G. FitzGerald had independently shown that the null result of the Michelson-Morley experiment could be explained by assuming that the lengths in the direction of the interferometer's motion contracted by the amount given in Equation 1-28. For that reason, the length contraction is often called the *Lorentz-FitzGerald contraction*.

EXAMPLE 1-9 Speed of S' A stick that has a proper length of 1 m moves in a direction parallel to its length with speed v relative to you. The length of the stick as measured by you is 0.914 m. What is the speed v?

SOLUTION

1. The length of the stick measured in a frame relative to which it is moving with speed v is related to its proper length by Equation 1-28: $L = \dfrac{L_p}{\gamma}$

2. Rearranging to solve for γ: $\gamma = \dfrac{L_p}{L}$

3. Substituting the values of L_p and L: $\gamma = \dfrac{1\text{ m}}{0.914\text{ m}} = \dfrac{1}{\sqrt{1 - v^2/c^2}}$

4. Solving for v:

$$\sqrt{1 - v^2/c^2} = 0.914$$

$$1 - v^2/c^2 = (0.914)^2 = 0.835$$

$$v^2/c^2 = 1 - 0.835 = 0.165$$

$$v^2 = 0.165c^2$$

$$v = 0.406c$$

STUDENTS-HUB.com Uploaded By: Malak Obaid

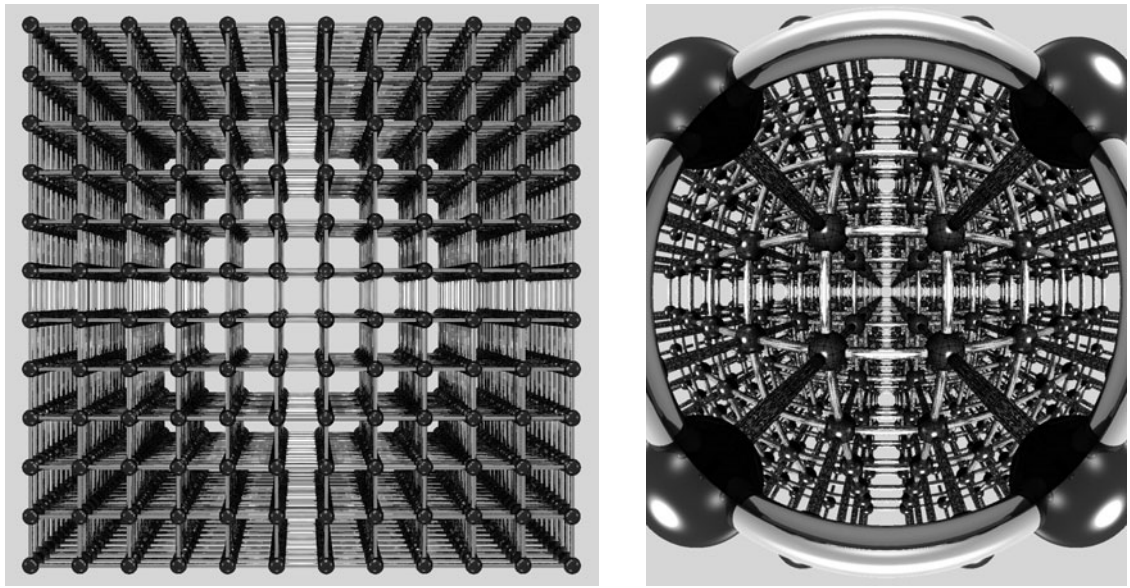

Figure 1-29 The appearance of rapidly moving objects depends on both length contraction in the direction of motion and the time when the observed light left the object. (*a*) The array of clocks and measuring rods that represents S' as viewed by an observer in S with $\beta = 0$. (*b*) When S' approaches the S observer with $\beta = 0.9$, the distortion of the lattice becomes apparent. This is what an observer on a cosmic-ray proton might see as it passes into the lattice of a face-centered-cubic crystal such as NaCl. [*P.-K. Hsiung, R. Dunn, and C. Cox. Courtesy of C. Cox, Adobe Systems, Inc., San Jose, CA.*]

It is important to remember that the relativistic contraction of moving lengths occurs only parallel to the relative motion of the reference frames. In particular, observers in relatively moving systems measure the same values for lengths in the y and y' and in the z and z' directions perpendicular to their relative motion. The result is that observers measure different shapes and angles for two- and three-dimensional objects. (See Example 1-10 and Figures 1-29 and 1-30.)

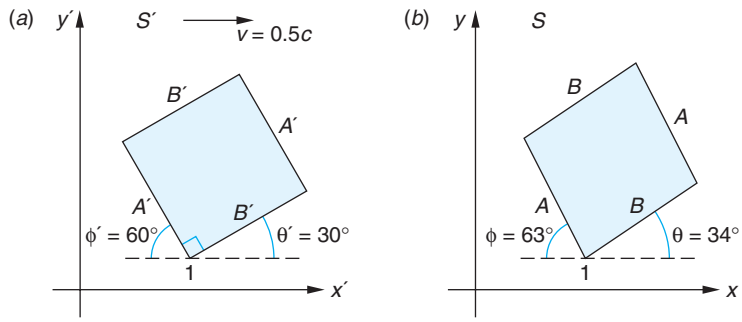

Figure 1-30 Length contraction distorts the shape and orientation of two- and three-dimensional objects. The observer in S measures the square shown in S' as a rotated parallelogram.

STUDENTS-HUB.com Uploaded By: Malak Obaid

EXAMPLE 1-10 The Shape of a Moving Square Consider the square in the $x'y'$ plane of S' with one side making a 30° angle with the x' axis, as in Figure 1-30*a*. If S' moves with $\beta = 0.5$ relative to S, what is the shape and orientation of the figure in S?

SOLUTION

The S observer measures the x components of each side to be shorter by a factor $1/\gamma$ than those measured in S'. Thus, S measures

$$A = [\cos^2 30 + \sin^2 30/\gamma^2]^{1/2} A' = 0.968A'$$
$$B = [\sin^2 30 + \cos^2 30/\gamma^2]^{1/2} B' = 0.901B'$$

Since the figure is a square in S', $A' = B'$. In addition, the angles between B and the x axis and between A and the x axis are given by, respectively,

$$\theta = \tan^{-1}\left[\frac{B' \sin 30}{B' \cos 30/\gamma}\right] = \tan^{-1}\left[\gamma \frac{\sin 30}{\cos 30}\right] = 33.7°$$

$$\phi = \tan^{-1}\left[\frac{A' \cos 30}{A' \sin 30/\gamma}\right] = \tan^{-1}\left[\gamma \frac{\cos 30}{\sin 30}\right] = 63.4°$$

Thus, S concludes from geometry that the interior angle at vertex 1 is not 90°, but $180° - (63.4° + 33.7°) = 82.9°$—i.e., the figure is not a square, but a parallelogram whose shorter sides make 33.7° angles with the x axis! Its shape and orientation in S are shown in Figure 1-30*b*.

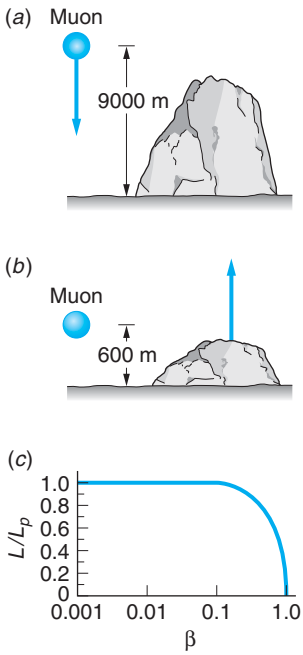

Figure 1-31 Although muons are created high above Earth and their mean lifetime is only about 2 μs when at rest, many appear at Earth's surface. (*a*) In Earth's reference frame, a typical muon moving at $0.998c$ has a mean lifetime of 30 μs and travels 9000 m in this time. (*b*) In the reference frame of the muon, the distance traveled by Earth is only 600 m in the muon's lifetime of 2 μs. (*c*) L varies only slightly from L_p until v is of the order of $0.1c$. $L \to 0$ as $v \to c$.

Muon Decay

An interesting example of both time dilation and length contraction is afforded by the appearance of muons as secondary radiation from cosmic rays. Muons decay according to the statistical law of radioactivity:

$$N(t) = N_0 e^{(-t/\tau)} \qquad \textbf{1-29}$$

where N_0 is the original number of muons at time $t = 0$, $N(t)$ is the number remaining at time t, and τ is the mean lifetime (a proper time interval), which is about 2 μs for muons. Since muons are created (from the decay of pions) high in the atmosphere, usually several thousand meters above sea level, few muons should reach sea level. A typical muon moving with speed $0.998c$ would travel only about 600 m in 2 μs. However, the lifetime of the muon measured in Earth's reference frame is increased according to time dilation (Equation 1-26) by the factor $1/(1 - v^2/c^2)^{1/2}$, which is 15 for this particular speed. The mean lifetime measured in Earth's reference frame is therefore 30 μs, and a muon with speed $0.998c$ travels about 9000 m in this time. From the muon's point of view, it lives only 2 μs, but the atmosphere is rushing past it with a speed of $0.998c$. The distance of 9000 m in Earth's frame is thus contracted to only 600 m in the muon's frame, as indicated in Figure 1-31.

It is easy to distinguish experimentally between the classical and relativistic predictions of the observations of muons at sea level. Suppose that we observe 10^8 muons at an altitude of 9000 m in some time interval with a muon detector. How many would

STUDENTS-HUB.com Uploaded By: Malak Obaid

we expect to observe at sea level in the same time interval? According to the nonrelativistic prediction, the time it takes for these muons to travel 9000 m is (9000 m)/$0.998c \approx 30$ μs, which is 15 lifetimes. Substituting $N_0 = 10^8$ and $t = 15\tau$ into Equation 1-29, we obtain

$$N = 10^8 e^{-15} = 30.6$$

We would thus expect all but about 31 of the original 100 million muons to decay before reaching sea level.

According to the relativistic prediction, Earth must travel only the contracted distance of 600 m in the rest frame of the muon. This takes only 2 μs = 1τ. Therefore, the number of muons expected at sea level is

$$N = 10^8 e^{-1} = 3.68 \times 10^7$$

Thus relativity predicts that we would observe 36.8 million muons in the same time interval. Experiments of this type have confirmed the relativistic predictions.

The Spacetime Interval

Experiments with muons moving near the speed of light are performed at many accelerator laboratories throughout the world despite their short mean life. Time dilation results in much longer mean lives relative to the laboratory, providing plenty of time to do experiments.

We have seen earlier in this section that time intervals and lengths (= space intervals), quantities that were absolutes, or invariants, for relatively moving observers using the classical Galilean coordinate transformation, are not invariants in special relativity. The Lorentz transformation and the relativity of simultaneity lead observers in inertial frames to conclude that lengths moving relative to them are contracted and time intervals are stretched, both by the factor γ. The question naturally arises: Is there *any* quantity involving the space and time coordinates that is invariant under a Lorentz transformation? The answer to that question is yes, and as it happens, we have already dealt with a special case of that invariant quantity when we first obtained the correct form of the Lorentz transformation. It is called the *spacetime interval*, or usually just the *interval*, Δs, and is given by

$$(\Delta s)^2 = (c\Delta t)^2 - [\Delta x^2 + \Delta y^2 + \Delta z^2] \qquad \textbf{1-30}$$

or, specializing it to the one-space-dimensional systems that we have been discussing,

$$(\Delta s)^2 = (c\Delta t)^2 - (\Delta x)^2 \qquad \textbf{1-31}$$

It may help to think of Equations 1-30 and 1-31 like this:

$$[\text{interval}]^2 = [\text{separation in time}]^2 - [\text{separation in space}]^2$$

The interval Δs is the only measurable quantity describing pairs of events in spacetime for which observers in all inertial frames will obtain the same numerical value. The negative sign in Equations 1-30 and 1-31 implies that $(\Delta s)^2$ may be positive, negative, or zero depending on the relative sizes of the time and space separations. With the sign of $(\Delta s)^2$, nature is telling us about the causal relation between the two events. Notice that whichever of the three possibilities characterizes a pair for one observer, it does so for all observers since Δs is invariant. The interval is called *timelike* if the time separation is the larger and *spacelike* if the space separation predominates. If the two terms are equal, so that $\Delta s = 0$, then it is called *lightlike*.

STUDENTS-HUB.com Uploaded By: Malak Obaid

Timelike Interval Consider a material particle[15] or object, e.g., the elephant in Figure 1-27, that moves relative to S. Since no material particle has ever been measured traveling faster than light, particles always travel less than 1 m of distance in 1 m of light travel time. We saw that to be the case in Example 1-8, where the time interval between launch and birth of the baby was 31.7 months on the S clock, during which time the elephant had moved a distance of $23.8c \cdot$ months. Equation 1-31 then yields $(c\Delta t)^2 - (\Delta x)^2 = (31.7c)^2 - (23.8c)^2 = (21.0c)^2 = (\Delta s)^2$, and the interval in S is $\Delta s = 21.0\ c \cdot$ months. The time interval term being the larger, Δs is a timelike interval and we say that material particles have *timelike worldlines*. Such worldlines lie within the shaded area of the spacetime diagram in Figure 1-21. Note that in the elephant's frame S' the separation in space between the launch and birth is zero and Δt is 21.0 months. Thus $\Delta s = 21.0\ c \cdot$ months in S', too. That is what we mean by the interval being invariant: observers in both S and S' measure the same number for the separation of the two events in spacetime.

The proper time interval τ between two events can be determined from Equations 1-31 using space and time measurements made in *any* inertial frame since we can write that equation as

$$\frac{\Delta s}{c} = \sqrt{(\Delta t)^2 - (\Delta x/c)^2}$$

Since $\Delta t = \tau$ when $\Delta x = 0$—i.e., for the time interval recorded on a clock in a system moving such that the clock is located at each event as it occurs—in that case

$$\sqrt{(\Delta t)^2 - (\Delta x/c)^2} = \sqrt{\tau^2 - 0} = \tau = \frac{\Delta s}{c} \qquad \textbf{1-32}$$

Notice that this yields the correct proper time $\tau = 21.0$ months in the elephant example.

Spacelike Interval When two events are separated in space by an interval whose square is greater than the value of $(c\Delta t)^2$, then Δs is called *spacelike*. In that case it is convenient for us to write Equation 1-31 in the form

$$(\Delta s)^2 = (\Delta x)^2 - (c\Delta t)^2 \qquad \textbf{1-33}$$

so that, as with timelike intervals, $(\Delta s)^2$ is not negative.[16] Events that are spacelike occur sufficiently far apart in space and close together in time that no inertial frame could move fast enough to carry a clock from one event to the other. For example, suppose two observers in Earth frame S, one in San Francisco and one in London, agree to each generate a light flash at the same instant, so that $c\Delta t = 0$ m in S and $\Delta x = 1.08 \times 10^7$ m. For *any* other inertial frame $(c\Delta t)^2 > 0$, and we see from Equation 1-33 that $(\Delta x)^2$ must be greater than $(1.08 \times 10^7)^2$ in order that Δs be invariant. In other words, 1.08×10^7 m is as close in space as the two events can be in any system; consequently, it will not be possible to find a system moving fast enough to move a clock from one event to the other. A speed greater than c, in this case infinitely greater, would be needed. Notice that the value of $\Delta s = L_p$, the proper length. Just as with the proper time interval τ, measurements of space and time intervals in any inertial system can be used to determine L_p.

STUDENTS-HUB.com Uploaded By: Malak Obaid

Lightlike (or Null) Interval The relation between two events is *lightlike* if Δs in Equation 1-31 equals zero. In that case

$$c\Delta t = \Delta x \qquad \textbf{1-34}$$

and a light pulse that leaves the first event as it occurs will just reach the second as it occurs.

The existence of the lightlike interval in relativity has no counterpart in the world of our everyday experience, where the geometry of space is Euclidean. In order for the distance between two points in space to be zero, the separation of the points in each of the three space dimensions must be zero. However, in spacetime the interval between two events may be zero, even though the intervals in space and time may individually be quite large. Notice, too, that pairs of events separated by lightlike intervals have both the proper time interval and proper length equal to zero since $\Delta s = 0$.

Things that move at the speed of light[17] have lightlike worldlines. As we saw earlier (see Figure 1-22), the worldline of light bisects the angles between the ct and x axes in a spacetime diagram. Timelike intervals lie in the shaded areas of Figure 1-32 and share the common characteristic that their relative order in time is the same for observers in all inertial systems. Events A and B in Figure 1-32 are such a pair. Observers in both S and S' agree that A occurs *before* B, although they of course measure different values for the space and time separations. Causal events, i.e., events that depend upon or affect one another in some fashion, such as your birth and that of your mother, have timelike intervals. On the other hand, the temporal order of events with spacelike intervals, such as A and C in Figure 1-32, depends upon the relative motion of the systems. As you can see in the diagram, A occurs before C in S, but C occurs first in S'. Thus, the relative order of pairs of events is absolute in the shaded areas but elsewhere may be in either order.

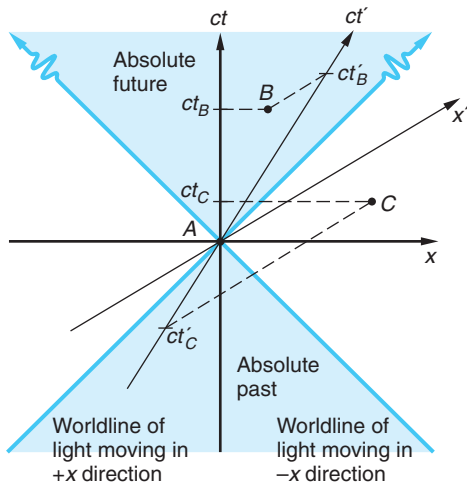

Figure 1-32 The relative temporal order of events for pairs characterized by timelike intervals, such as A and B, is the same for all inertial observers. Events in the upper shaded area will all occur in the future of A; those in the lower shaded area occurred in A's past. Events whose intervals are spacelike, such as A and C, can be measured as occurring in either order, depending on the relative motion of the frames. Thus, C occurs after A in S but before A in S'.

STUDENTS-HUB.com Uploaded By: Malak Obaid

Question

9. In 1987 light arrived at Earth from the explosion of a star (a supernova) in the Large Magellanic Cloud, a small companion galaxy to the Milky Way, located about 170,000 $c \cdot$ y away. Describe events that together with the explosion of the star would be separated from it by (a) a spacelike interval, (b) a lightlike interval, and (c) a timelike interval.

EXAMPLE 1-11 Characterizing Spacetime Intervals Figure 1-33 is the spacetime diagram of a laboratory showing three events, the emission of light from an atom in each of three samples.

1. Determine whether the interval between each of the three possible pairs of events is timelike, spacelike, or lightlike.
2. Would it have been possible in any of the pairs for one of the events to have been caused by the other? If so, which?

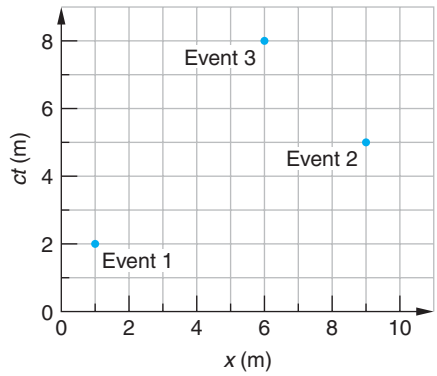

Figure 1-33 A spacetime diagram of three events whose intervals Δs are found in Example 1-11.

SOLUTION

1. The spacetime coordinates of the events are

event	ct	x
1	2	1
2	5	9
3	8	6

and for the three possible pairs 1 and 2, 2 and 3, and 1 and 3 we have

pair	$c\Delta t$	Δx	$(c\Delta t)^2$	$(\Delta x)^2$	
1 & 2	5–2	9–1	9	64	spacelike
2 & 3	8–5	6–9	9	9	lightlike
1 & 3	8–2	6–1	36	25	timelike

2. Yes, event 3 may possibly have been caused by either event 1 since 3 is in the absolute future of 1, or event 2, since 2 and 3 can just be connected by a flash of light.

STUDENTS-HUB.com Uploaded By: Malak Obaid

1-5 The Doppler Effect

In the Doppler effect for sound the change in frequency for a given velocity v depends on whether it is the source or receiver that is moving with that speed. Such a distinction is possible for sound because there is a medium (the air) relative to which the motion takes place, and so it is not surprising that the motion of the source or the receiver relative to the still air can be distinguished. Such a distinction between motion of the source or receiver cannot be made for light or other electromagnetic waves in a vacuum as a consequence of Einstein's second postulate; therefore, the classical expressions for the Doppler effect cannot be correct for light. We will now derive the relativistic Doppler effect equations that are correct for light.

Consider a light source moving toward an observer or receiver at A in Figure 1-34a at velocity v. The source is emitting a train of light waves toward receivers A and B while approaching A and receding from B. Figure 1-34b shows the spacetime

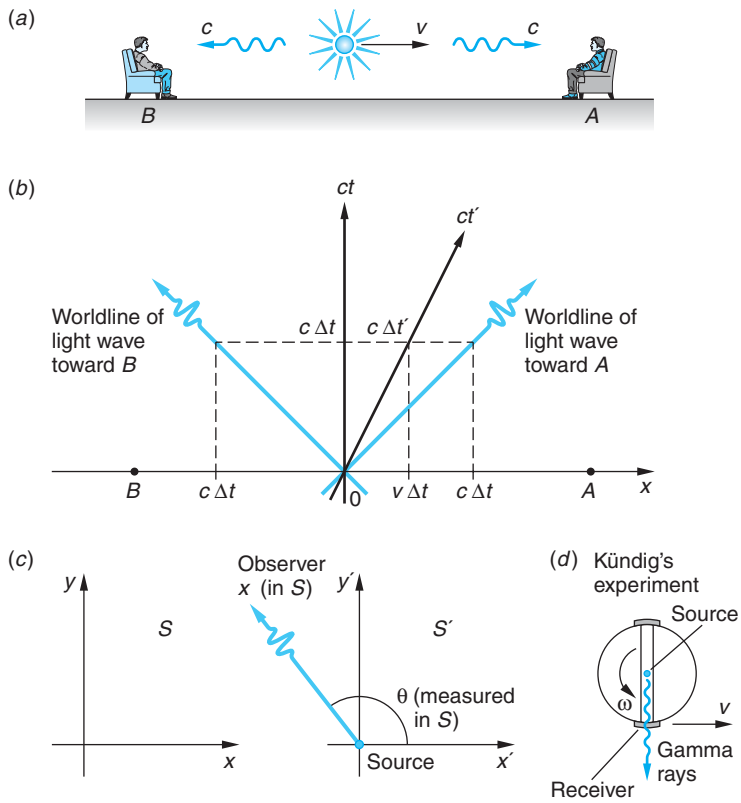

Figure 1-34 The Doppler effect in light, as in sound, arises from the relative motion of the source and receiver; however, the independence of the speed of light on that motion leads to different expressions for the frequency shift. (a) A source approaches observer A and recedes from observer B. The spacetime diagram of the system S in which A and B are at rest and the source moves at velocity $\mathbf{v}$ illustrates the two situations. (b) The source located at $x' = 0$ (the x' axis is omitted) moves along its worldline, the ct' axis. The N waves emitted toward A in time Δt occupy space $\Delta x = c\Delta t - v\Delta t$, whereas those headed for B occupy $\Delta x = c\Delta t + v\Delta t$. In three dimensions the observer in S may see light emitted at some angle θ with respect to the x axis as in (c). In that case a transverse Doppler effect occurs. (d) Kündig's apparatus for measuring the transverse Doppler effect.

STUDENTS-HUB.com Uploaded By: Malak Obaid

diagram of S, the system in which A and B are at rest. The source is located at $x' = 0$ (x' axis is not shown), and, of course, its worldline is the ct' axis. Let the source emit a train of N electromagnetic waves in each direction beginning when the S and S' origins were coincident. First, let's consider the train of waves headed toward A. During the time Δt over which the source emits the N waves, the first wave emitted will have traveled a distance $c\Delta t$ and the source itself a distance $v\Delta t$ in S. Thus, the N waves are seen by the observer at A to occupy a distance $c\Delta t - v\Delta t$ and, correspondingly, their wavelength λ is given by

$$\lambda = \frac{c\Delta t - v\Delta t}{N}$$

and the frequency $f = c/\lambda$ is

$$f = \frac{c}{\lambda} = \frac{cN}{(c - v)\Delta t} = \frac{1}{1 - \beta}\frac{N}{\Delta t}$$

The frequency of the source in S', called the *proper frequency*, is given by $f_0 = c/\lambda' = N/\Delta t'$, where $\Delta t'$ is measured in S', the rest system of the source. The time interval $\Delta t' = \tau$ is the proper time interval since the light waves, in particular the first and the Nth, are all emitted at $x' = 0$; hence $\Delta x' = 0$ between the first and the Nth in S'. Thus, Δt and $\Delta t'$ are related by Equation 1-26 for time dilation, so $\Delta t = \gamma\Delta t'$, and when the source and receiver are moving toward each other, the observer A in S measures the frequency

$$f = \frac{1}{1 - \beta}\frac{f_0\Delta t'}{\Delta t} = \frac{f_0}{1 - \beta}\frac{1}{\gamma} \qquad \textbf{1-35}$$

or

$$f = \frac{\sqrt{1 - \beta^2}}{1 - \beta}f_0 = \sqrt{\frac{1 + \beta}{1 - \beta}}f_0 \qquad \text{(approaching)} \qquad \textbf{1-36}$$

This differs from the classical equation only in the addition of the time dilation factor. Note that $f > f_0$ for the source and observer approaching each other. Since for visible light this corresponds to a shift toward the blue part of the spectrum, it is called a *blueshift*.

Suppose the source and receiver are moving away from each other, as for observer B in Figure 1-34*b*. Observer B, in S, sees the N waves occupying a distance $c\Delta t + v\Delta t$, and the same analysis shows that observer B in S measures the frequency

$$f = \frac{\sqrt{1 - \beta^2}}{1 + \beta}f_0 = \sqrt{\frac{1 - \beta}{1 + \beta}}f_0 \qquad \text{(receding)} \qquad \textbf{1-37}$$

The use of Doppler radar to track weather systems is a direct application of special relativity.

Notice that $f < f_0$ for the observer and source receding from each other. Since for visible light this corresponds to a shift toward the red part of the spectrum, it is called a *redshift*. It is left as a problem for you to show that the same results are obtained when the analysis is done in the frame in which the source is at rest.

In the event that $v \ll c$ (i.e., $\beta \ll 1$), as is often the case for light sources moving on Earth, useful (and easily remembered) approximations of Equations 1-36 and 1-37 can be obtained. Using Equation 1-36 as an example and rewriting it in the form

$$f = f_0(1 + \beta)^{1/2}(1 - \beta)^{-1/2}$$

STUDENTS-HUB.com Uploaded By: Malak Obaid

the two quantities in parentheses can be expanded by the binomial theorem to yield

$$f = f_0\left(1 + \frac{1}{2}\beta - \frac{1}{8}\beta^2 + \ldots\right)\left(1 + \frac{1}{2}\beta + \frac{3}{8}\beta^2 + \ldots\right)$$

Multiplying out and discarding terms of higher order than β yields

$$f/f_0 \approx 1 + \beta \qquad \text{(approaching)}$$

and, similarly,

$$f/f_0 \approx 1 - \beta \qquad \text{(receding)}$$

and $|\Delta f/f_0| \approx \beta$ in both situations, where $\Delta f = f_0 - f$.

EXAMPLE 1-12 **Rotation of the Sun** The Sun rotates at the equator once in about 25.4 days. The Sun's radius is 7.0×10^8 m. Compute the Doppler effect that you would expect to observe at the left and right limbs (edges) of the Sun near the equator for light of wavelength $\lambda = 550$ nm $= 550 \times 10^{-9}$ m (yellow light). Is this a redshift or a blueshift?

SOLUTION

The speed of limbs v = (circumference)/(time for one revolution) or

$$v = \frac{2\pi R}{T} = \frac{2\pi(7.0 \times 10^8)\text{ m}}{25.4\text{ d} \cdot 3600\text{ s/h} \cdot 24\text{ h/d}} = 2000\text{ m/s}$$

$v \ll c$, so we may use the approximation equations. Using $\Delta f/f_0 \approx \beta$, we have that $\Delta f \approx \beta f_o = \beta c/\lambda_o$, or $\Delta f \approx 2000/550 \times 10^{-9} = 3.64 \times 10^9$ Hz. Since $f_o = c/\lambda_o = (3 \times 10^8\text{ m/s})/(550 \times 10^{-9}) = 5.45 \times 10^{14}$ Hz, Δf represents a fractional change in frequency of β, or about one part in 10^5. It is a redshift for the receding limb, a blueshift for the approaching one.

Doppler Effect of Starlight

In 1929 E. P. Hubble became the first astronomer to suggest that the universe is expanding.[18] He made that suggestion and offered a simple equation to describe the expansion on the basis of measurements of the Doppler shift of the frequencies of light emitted toward us by distant galaxies. Light from distant galaxies is always shifted toward frequencies lower than those emitted by similar sources nearby. Since the general expression connecting the frequency f and wavelength λ of light is $c = f\lambda$, the shift corresponds to longer wavelengths. As noted above, the color red is on the longer-wavelength side of the visible spectrum (see Chapter 4), so the *redshift* is used to describe the Doppler effect for a receding source. Similarly, *blueshift* describes light emitted by stars, typically stars in our galaxy, that are approaching us.

Astronomers define the redshift of light from astronomical sources by the expression $z = (f_o - f)/f$, where f_o = frequency measured in the frame of the star or galaxy and f = frequency measured at the receiver on Earth. This allows us to write $\beta = v/c$ in terms of z as

$$\beta = \frac{(z+1)^2 - 1}{(z+1)^2 + 1} \qquad \textbf{1-38}$$

STUDENTS-HUB.com Uploaded By: Malak Obaid

Equation 1-37 is the appropriate one to use for such calculations, rather than the approximations, since galactic recession velocities can be quite large. For example, the quasar 2000-330 has a measured $z = 3.78$, which implies from Equation 1-38 that it is receding from Earth due to the expansion of space at $0.91c$. (See Chapter 13.)

EXAMPLE 1-13 Redshift of Starlight The longest wavelength of light emitted by hydrogen in the Balmer series (see Chapter 4) has a wavelength of $\lambda_o = 656$ nm. In light from a distant galaxy, this wavelength is measured as $\lambda = 1458$ nm. Find the speed at which the galaxy is receding from Earth.

SOLUTION

1. The recession speed is the v in $\beta = v/c$. Since $\lambda > \lambda_o$, this is a redshift and Equation 1-37 applies:
$$f = \sqrt{\frac{1-\beta}{1+\beta}} f_0$$

2. Rewriting Equation 1-37 in terms of the wavelengths:
$$f = \sqrt{\frac{1-\beta}{1+\beta}} = \frac{f}{f_0} = \frac{\lambda_o}{\lambda}$$

3. Squaring both sides and substituting values for λ_o and λ:
$$\frac{1-\beta}{1+\beta} = \left(\frac{\lambda_0}{\lambda}\right)^2 = \left(\frac{656 \text{ nm}}{1458 \text{ nm}}\right)^2 = 0.202$$

4. Solving for β:
$$1 - \beta = (0.202)(1 + \beta)$$
$$1.202\beta = 1 - 0.202 = 0.798$$
$$\beta = \frac{0.798}{1.202} = 0.664$$

5. The galaxy is thus receding at speed v, where
$$v = c\beta = 0.664c$$

EXPLORING
Transverse Doppler Effect

Our discussion of the Doppler effect in Section 1-5 involved only one space dimension, wherein the source, observer, and the direction of the relative motion all lie on the x axis. In three space dimensions, where they may not be colinear, a more complete analysis, though beyond the scope of our discussion, makes only a small change in Equation 1-35. If the source moves along the positive x axis but the observer views the light emitted at some angle θ with the x axis, as shown in Figure 1-34c, Equation 1-35 becomes

$$f = \frac{f_0}{\gamma} \frac{1}{1 - \beta \cos\theta} \qquad \textbf{1-35}a$$

When $\theta = 0$, this becomes the equation for the source and receiver approaching, and when $\theta = \pi$, the equation becomes that for the source and receiver receding. Equation 1-35a also makes the quite surprising prediction that even when viewed perpendicular

STUDENTS-HUB.com Uploaded By: Malak Obaid

to the direction of motion, where $\theta = \pi/2$, the observer will still see a frequency shift, the so-called *transverse Doppler effect*, $f = f_0/\gamma$. Note that $f < f_0$ since $\gamma > 1$. It is sometimes referred to as the second-order Doppler effect and is the result of time dilation of the moving source. [The general derivation of Equation 1-35*a* can be found in the French (1968), Resnick (1992), and Ohanian (2001) references at the end of the chapter.]

Following a suggestion first made by Einstein in 1907, Kündig in 1962 made an excellent quantitative verification of the transverse Doppler effect.[19] He used 14.4-keV gamma rays emitted by a particular isotope of Fe as the light source (see Chapter 11). The source was at rest in the laboratory, on the axis of an ultracentrifuge, and the receiver (an Fe absorber foil) was mounted on the ultracentrifuge rim, as shown in Figure 1-34*d*. Using the extremely sensitive frequency measuring technique called the Mössbauer effect (see Chapter 11), Kündig found a transverse Doppler effect in agreement with the relativistic prediction within ±1 percent over a range of relative speeds up to about 400 m/s.

1-6 The Twin Paradox and Other Surprises

The consequences of Einstein's postulates—the Lorentz transformation, relativistic velocity addition, time dilation, length contraction, and the relativity of simultaneity—lead to a large number of predictions that are unexpected and even startling when compared with our experiences in a macroscopic world where $\beta \approx 0$ and geometry obeys the Euclidean rules. Still other predictions seem downright paradoxical, with relatively moving observers obtaining equally valid but apparently totally inconsistent results. This chapter concludes with the discussion of a few such examples that will help you hone your understanding of special relativity.

Twin Paradox

Perhaps the most famous of the paradoxes in special relativity is that of the twins or, as it is sometimes called, the clock paradox. It arises out of time dilation (Equation 1-26) and goes like this. Homer and Ulysses are identical twins. Ulysses travels at a constant high speed to a star beyond our solar system and returns to Earth while his twin, Homer, remains at home. When the traveler Ulysses returns home, he finds his twin brother much aged compared to himself—in agreement, we will see, with the prediction of relativity. The paradox arises out of the contention that the motion is relative and either twin could regard the other as the traveler, in which case each twin should find the other to be younger than he and we have a logical contradiction—a paradox. Let's illustrate the paradox with a specific example. Let Earth and the destination star be in the same inertial frame S. Two other frames S' and S'' move relative to S at $v = +0.8c$ and $v = -0.8c$, respectively. Thus, $\gamma = 5/3$ in both cases. The spaceship carrying Ulysses accelerates quickly from S to S', then coasts with S' to the star, again accelerates quickly from S' to S'', coasts with S'' back to Earth, and brakes to a stop alongside Homer.

It is easy to analyze the problem from Homer's point of view on Earth. Suppose, according to Homer's clock, Ulysses coasts in S' for a time interval $\Delta t = 5$ y and in S'' for an equal time. Thus, Homer is 10 y older when Ulysses returns. The time interval in S' between the events of Ulysses' leaving Earth and arriving at the star is shorter because it is a proper time interval. The time it takes to reach the star by Ulysses' clock is

$$\Delta t' = \frac{\Delta t}{\gamma} = \frac{5 \text{ y}}{5/3} = 3 \text{ y}$$

STUDENTS-HUB.com Uploaded By: Malak Obaid

Since the same time is required for the return trip, Ulysses will have recorded 6 y for the round trip and will be 4 y younger than Homer upon his return.

The difficulty in this situation seems to be for Ulysses to understand why his twin aged 10 y during his absence. If we consider Ulysses as being at rest and Homer as moving away, Homer's clock should run slow and measure only $3/\gamma = 1.8$ y, and it appears that Ulysses should expect Homer to have aged only 3.6 years during the round trip. This is, of course, the paradox. Both predictions can't be right. However, this approach makes the incorrect assumption that the twins' situations are symmetrical and interchangeable. They are not. Homer remains in a single inertial frame, whereas Ulysses *changes* inertial frames, as illustrated in Figure 1-35*a*, the spacetime diagram for Ulysses' trip. While the turnaround may take only a minute fraction of the total time, it is absolutely essential if the twins clocks are to come together again so that we can compare their ages (readings).

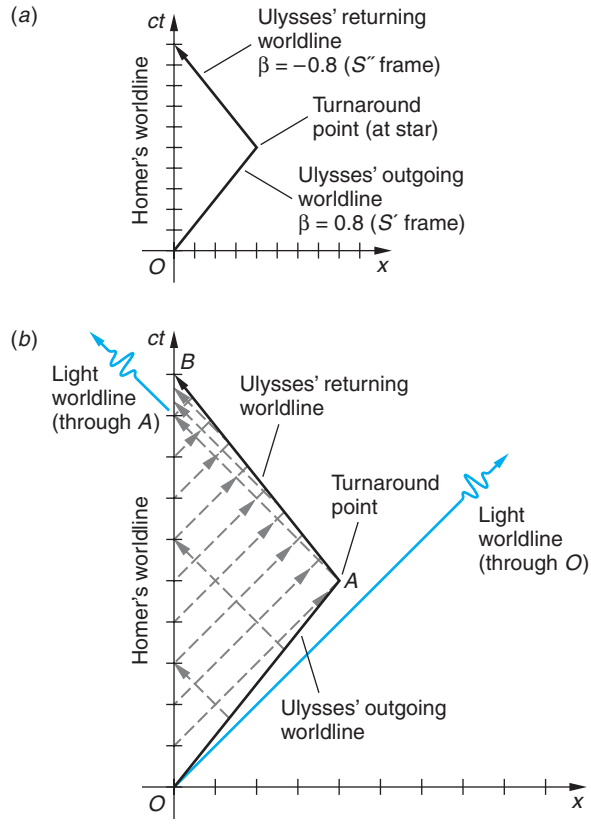

Figure 1-35 (*a*) The spacetime diagram of Ulysses' journey to a distant star in the inertial frame in which Homer and the star are at rest. (*b*) Divisions on the *ct* axis correspond to years on Homer's clock. The broken lines show the paths (worldlines) of light flashes transmitted by each twin with a frequency of 1/year on his clock. Note the markedly different frequencies at the receivers.

STUDENTS-HUB.com Uploaded By: Malak Obaid

A correct analysis can be made using the invariant interval Δs from Equation 1-31 rewritten as

$$\left(\frac{\Delta s}{c}\right)^2 = (\Delta t)^2 - \left(\frac{\Delta x}{c}\right)^2$$

where the left side is constant and equal to $(\tau)^2$, the proper time interval squared, and the right side refers to measurements made in any inertial frame. Thus, Ulysses along each of his worldlines in Figure 1-35*a* has $\Delta x = 0$ and, of course, measures $\Delta t = \tau = 3$ y, or 6 y for the round trip. Homer, on the other hand, measures

$$(\Delta t)^2 = (\tau)^2 + \left(\frac{\Delta x}{c}\right)^2$$

and since $(\Delta x/c)^2$ is always positive, he always measures $\Delta t > \tau$. In this situation $\Delta x = 0.8c\Delta t$, so

$$(\Delta t)^2 = (3\text{ y})^2 + (0.8c\Delta t/c)^2$$

or

$$(\Delta t)^2(0.36) = (3)^2$$

$$\Delta t = \frac{3}{0.6} = 5\text{ y}$$

or 10 y for the round trip, as we saw earlier. The reason that the twins' situations cannot be treated symmetrically is because the special theory of relativity can predict the behavior of accelerated systems, such as Ulysses at the turnaround, provided that in the formulation of the physical laws we take the view of an inertial, i.e., unaccelerated, observer such as Homer. That's what we have done. Thus, we cannot do the same analysis in the rest frame of Ulysses' spaceship because it does not remain in an inertial frame during the round trip; hence, it falls outside of the special theory, and no paradox arises. The laws of physics can be reformulated so as to be invariant for accelerated observers, which is the role of general relativity (see Chapter 2), but the result is the same: Ulysses returns younger than Homer by just the amount calculated above.

EXAMPLE 1-14 **Twin Paradox and the Doppler Effect** This example, first suggested by C. G. Darwin,[20] may help you understand what each twin sees during Ulysses' journey. Homer and Ulysses agree that once each year, on the anniversary of the launch date of Ulysses' spaceship (when their clocks were together), each twin will send a light signal to the other. Figure 1-35*b* shows the light signals each sends. Based on our discussion above, Homer sends 10 light flashes (the *ct* axis, Homer's worldline, is divided into 10 equal interval corresponding to the 10 years of the journey on Homer's clock) and Ulysses sends 6 light flashes (each of Ulysses' worldlines is divided into 3 equal intervals corresponding to 3 years on Ulysses' clock). Note that each transmits his final light flash as they are reunited at *B*. Although each transmits light signals with a frequency of 1 per year, they obviously do not receive them at that frequency. For example, Ulysses sees no signals from Homer during the first three years! How can we explain the observed frequencies?

STUDENTS-HUB.com Uploaded By: Malak Obaid

SOLUTION

The Doppler effect provides the explanation. As the twins (and clocks) recede from each other the frequency of their signals is reduced from the proper frequency f_0 according to Equation 1-37 and we have

$$\frac{f}{f_0} = \sqrt{\frac{1-\beta}{1+\beta}} = \sqrt{\frac{1-0.8}{1+0.8}} = \frac{1}{3}$$

which is exactly what both twins see (refer to Figure 1-35*b*): Homer receives 3 flashes in the first 9 years and Ulysses 1 flash in his first 3 years; i.e., $f = (1/3)f_0$ for both.

After the turnaround they are approaching each other and Equation 1-38 yields

$$\frac{f}{f_0} = \sqrt{\frac{1+\beta}{1-\beta}} = \sqrt{\frac{1+0.8}{1-0.8}} = 3$$

and again this agrees with what the twins see: Homer receives 3 flashes during the final (10th) year and Ulysses receives 9 flashes during his final 3 years; i.e., $f = 3f_0$ for both.

Question

10. The different ages of the twins upon being reunited are an example of the relativity of simultaneity that was discussed earlier. Explain how that accounts for the fact that their biological clocks are no longer synchronized.

More

It is the relativity of simultaneity, not their different accelerations, that is responsible for the age difference between the twins. This is readily illustrated in *The Case of the Identically Accelerated Twins*, which can be found on the home page: www.whfreeman.com/tiplermodernphysics5e. See also Figure 1-36 here.

The Pole and Barn Paradox

An interesting problem involving length contraction, reported initially by W. Rindler, involves putting a long pole into a short barn. One version, from E. F. Taylor and J. A. Wheeler,[22] goes as follows. A runner carries a pole 10 m long toward the open front door of a small barn 5 m long. A farmer stands near the barn so that he can see both the front and the back doors of the barn, the latter being a closed swinging door, as shown in Figure 1-37*a*. The runner carrying the pole at speed v enters the barn, and at some instant the farmer sees the pole completely contained in the barn and closes the

STUDENTS-HUB.com Uploaded By: Malak Obaid

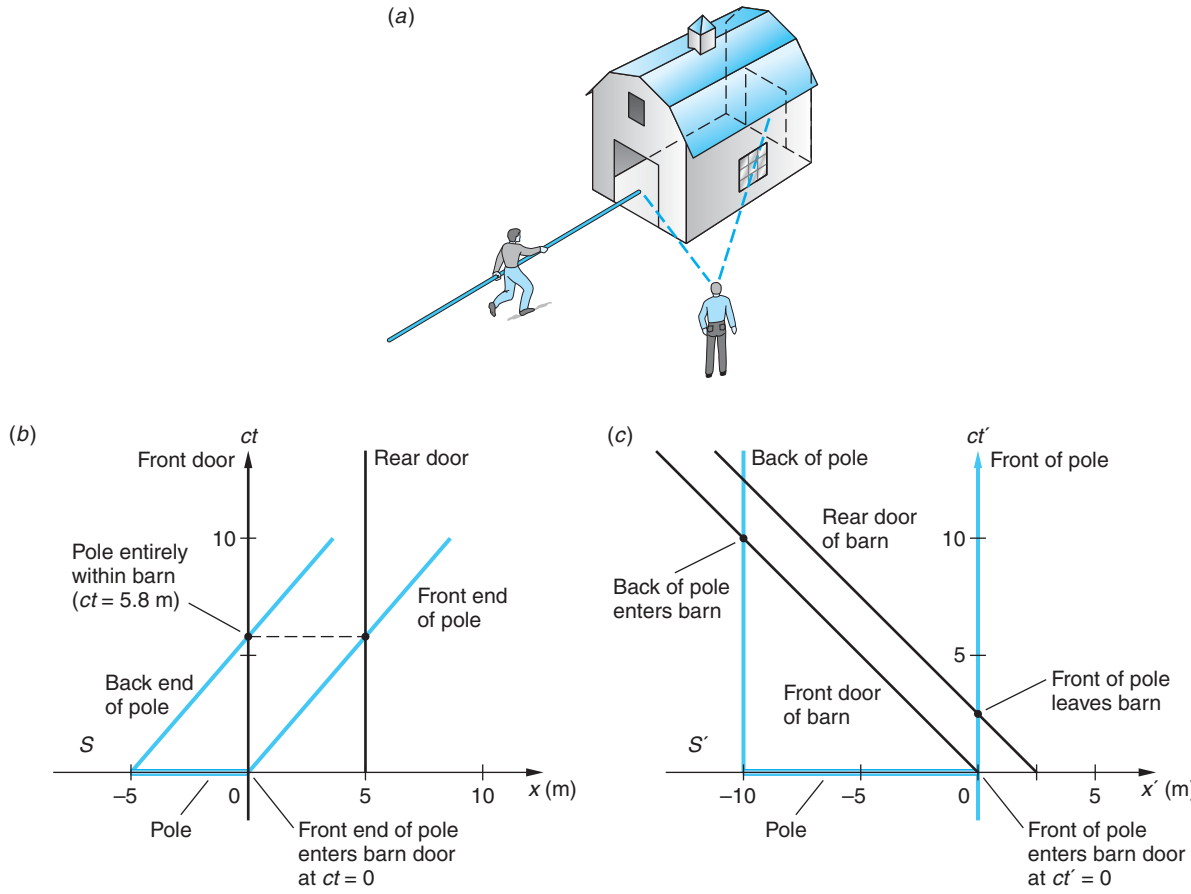

Figure 1-37 (*a*) A runner carrying a 10-m pole moves quickly enough so that the farmer will see the pole entirely contained in the barn. The spacetime diagrams from the point of view of the farmer's inertial frame (*b*) and that of the runner (*c*). The resolution of the paradox is in the fact that the events of interest, shown by the large dots in each diagram, are simultaneous in S but not in S'.

front door, thus putting a 10-m pole into a 5-m barn. The minimum speed of the runner v that is necessary for the farmer to accomplish this feat can be computed from Equation 1-28, giving the relativistic length contraction $L = L_p/\gamma$, where L_p = proper length of the pole (10 m) and L = length of the pole measured by the farmer, to be equal to the length of the barn (5 m). Therefore, we have

$$\gamma = \frac{1}{\sqrt{1 - v^2/c_2}} = \frac{L_p}{L} = \frac{10}{5}$$

$$1 - v^2/c^2 = (5/10)^2$$

$$v^2/c^2 = 1 - (5/10)^2 = 0.75$$

$$v = 0.866c \quad \text{or} \quad \beta = 0.866$$

STUDENTS-HUB.com Uploaded By: Malak Obaid

A paradox seems to arise when this situation is viewed in the rest system of the runner. For him the pole, being at rest in the same inertial system, has its proper length of 10 m. However, the runner measures the length of the barn to be

$$L = L_p/\gamma = 5\sqrt{1 - \beta^2}$$
$$L = 2.5 \text{ m}$$

How can he possibly fit the 10-m pole into the length-contracted 2.5-m barn? The answer is that he can't, and the paradox vanishes, but how can that be? To understand the answer, we need to examine two events—the coincidences of both the front and back ends of the pole, respectively, with the rear and front doors of the barn—in the inertial frame of the farmer and in that of the runner.

These are illustrated by the spacetime diagrams of the inertial frame S of the farmer and barn (Figure 1-37*b*) and that of the runner S' (Figure 1-37*c*). Both diagrams are drawn with the front end of the pole coinciding with the front door of the barn at the instant the clocks are started. In Figure 1-37*b* the worldlines of the barn doors are, of course, vertical, while those of the two ends of the pole make an angle $\theta = \tan^{-1}(1/\beta) = 49.1°$ with the x axis. Note that in S the front of the pole reaches the rear door of the barn at $ct = 5 \text{ m}/0.866 = 5.8 \text{ m}$ *simultaneous* with the arrival of the back end of the pole at the front door; i.e., at that instant in S the pole is entirely contained in the barn.

In the runner's rest system S' it is the worldlines of the ends of the pole that are vertical, while those of the front and rear doors of the barn make angles of 49.1° with the $-x'$ axis (since the barn moves in the $-x'$ direction at v). Now we see that the rear door passes the front of the pole at $ct' = 2.5 \text{ m}/0.866 = 2.9 \text{ m}$, but the front door of the barn doesn't reach the rear of the pole until $ct' = 10 \text{ m}/0.866 = 11.5 \text{ m}$. Thus, the first of those two events occurs *before* the second, and the runner never sees the pole entirely contained in the barn. Once again, the relativity of simultaneity is the key—events simultaneous in one inertial frame are not necessarily simultaneous when viewed from another inertial frame.

Now let's consider a different version of this paradox, the one initially due to W. Rindler. Suppose the barn's back wall were made of thick, armor-plate steel and had no door. What do the farmer and the runner see then? Once again, in the farmer's (and the barn's) rest frame, the instant the front of the pole reaches the armor plate, the farmer shuts the door and the 10-m pole is instantaneously contained in the 5-m barn. However, in the *next* instant (assuming that the pole doesn't break) it must either bend (i.e., rotate in spacetime) or break through the armor plate. Since this is relativity, the runner must come to the same conclusion in his rest frame as the 2.5-m barn races toward him at $\beta = 0.866$. But now when the armor plate back wall contacts the front of the pole, the barn continues to move at $\beta = 0.866$, taking the front of the pole with it and leaving at that instant 7.5 m of the pole still outside the barn. Yet like the farmer, the runner must also see the 10-m pole entirely contained within the 2.5-m barn. How can that be? Like this: the instant the tip of the pole hits the steel plate, that information (an elastic shock wave) begins to propagate down the pole. Even if the wave were to propagate at the speed of light c, it will take $10 \text{ m}/3.0 \times 10^8 \text{ m/s} = 3.33 \times 10^{-8} \text{ s}$ to reach the back of the pole. In the meantime, the barn door must move only 7.5 m to reach the back of the pole and does so in only $7.5 \text{ m}/(0.866 \times 3.0 \times 10^8 \text{ m/s}) = 2.89 \times 10^{-8} \text{ s}$. Thus, the runner, in agreement with the farmer, sees the 10-m pole entirely contained within the 2.5-m barn—at least briefly!

STUDENTS-HUB.com Uploaded By: Malak Obaid

Question

11. In the discussion where the barn's back wall was made from armor-plate steel and had no door, do the farmer and the runner both see the pole entirely contained in the barn, no matter what their relative speed is? Explain.

Headlight Effect

We have made frequent use of Einstein's second postulate asserting that the speed of light is independent of the source motion for all inertial observers; however, the same is not true for the *direction* of light. Consider a light source in S' that emits light uniformly in all directions. A beam of that light emitted at an angle θ' with respect to the x' axis is shown in Figure 1-38*a*. During a time $\Delta t'$ the x' displacement of the beam is $\Delta x'$, and these are related to θ' by

$$\frac{\Delta x'}{c\Delta t'} = \frac{\Delta x'}{\Delta(ct')} = \cos\theta' \qquad \textbf{1-39}$$

The direction of the beam relative to the x axis in S is similarly given by

$$\frac{\Delta x}{\Delta(ct)} = \cos\theta \qquad \textbf{1-40}$$

Applying the inverse Lorentz transformation to Equation 1-40 yields

$$\cos\theta = \frac{\Delta x}{c\Delta t} = \frac{\gamma(\Delta x' + v\Delta t')}{c\gamma(\Delta t' + v\Delta x'/c^2)}$$

Dividing the numerator and denominator by $\Delta t'$ and then by c, we obtain

$$\cos\theta = \frac{(\Delta x'/\Delta t' + v)}{c\left(1 + \frac{v}{c^2}\Delta x'/\Delta t'\right)} = \frac{\Delta x'/\Delta(ct') + v/c}{1 + \frac{v}{c}\cdot\frac{\Delta x'}{\Delta(ct')}}$$

and substituting from Equation 1-39 yields

$$\cos\theta = \frac{\cos\theta' + \beta}{1 + \beta\cos\theta'} \qquad \textbf{1-41}$$

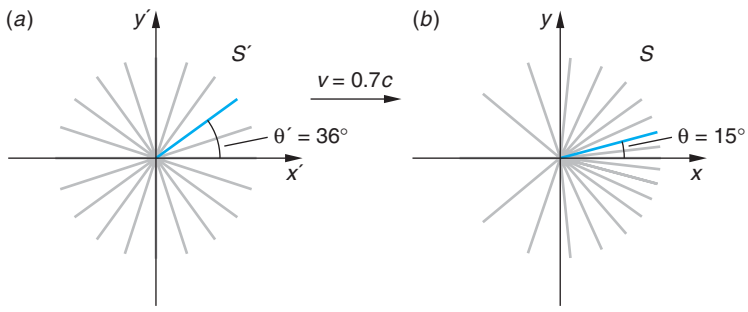

Figure 1-38 (*a*) The source at rest in S' moves with $\beta = 0.7$ with respect to S. (*b*) Light emitted uniformly in S' appears to S concentrated into a cone in the forward direction. Rays shown in (*a*) are 18° apart. Rays shown in (*b*) make angles calculated from Equation 1-41. The two colored rays shown are corresponding ones.

STUDENTS-HUB.com Uploaded By: Malak Obaid

Considering the half of the light emitted by the source in S' into the forward hemisphere, i.e., rays with θ' between $\pm\pi/2$, note that Equation 1-41 restricts the angles θ measured in S for those rays (50 percent of all the light) to lie between $\theta = \pm\cos^{-1}\beta$. For example, for $\beta = 0.5$, the observer in S would see half of the total light emitted by the source in S' to lie between $\theta = \pm 60°$, i.e., in a cone of half angle 60° whose axis is along the direction of the velocity of the source. For values of β near unity θ is very small, e.g., $\beta = .99$ yields $\theta = 8.1°$. This means that the observer in S sees half of all the light emitted by the source to be concentrated into a forward cone with that half angle. (See Figure 1-38*b*.) Note, too, that the remaining 50 percent of the emitted light is distributed throughout the remaining 344° of the two-dimensional diagram.[23] As a result of the headlight effect, light from a directly approaching source appears far more intense than that from the same source at rest. For the same reason, light from a directly receding source will appear much dimmer than that from the same source at rest. This result has substantial applications in experimental particle physics and astrophysics.

In determining the brightness of stars and galaxies, a critical parameter in understanding them, astronomers must correct for the headlight effect, particularly at high velocities relative to Earth.

Question

12. Notice from Equation 1-41 that some light emitted by the moving source into the rear hemisphere is seen by the observer in S as having been emitted into the forward hemisphere. Explain how that can be, using physical arguments.

EXPLORING
Superluminal Speeds

We conclude this chapter with a few comments about things that move faster than light. The Lorentz transformations (Equations 1-18 and 1-19) have no meaning in the event that the relative speeds of two inertial frames exceed the speed of light. This is generally taken to be a prohibition on the moving of mass, energy, and information faster than c. However, it is possible for certain processes to proceed at speeds greater than c and for the speeds of moving objects to appear to be greater than c without contradicting relativity theory. A common example of the first of these is the motion of the point where the blades of a giant pair of scissors intersect as the scissors are quickly closed, sometimes called the scissors paradox. Figure 1-39 shows the situation. A long straight rod (one blade) makes an angle θ with the x axis (the second blade) and moves in the $-y$ direction at constant speed $v_y = \Delta y/\Delta t$. During time Δt, the intersection of the blades, point P, moves to the right a distance Δx. Note from the figure that

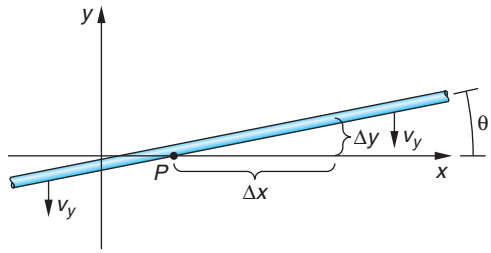

Figure 1-39 As the long straight rod moves vertically downward, the intersection of the "blades," point P, moves toward the right at speed $v_p = \Delta x/\Delta t$. In terms of v_y and θ, $v_p = v_y/\tan\theta$.

STUDENTS-HUB.com Uploaded By: Malak Obaid

$\Delta y/\Delta x = \tan\theta$. The speed with which P moves to the right is

$$v_p = \Delta x/\Delta t = \frac{\Delta x}{\Delta y/v_y} = \frac{v_y \Delta x}{\Delta x \tan\theta} \qquad \textbf{1-42}$$

or

$$v_p = \frac{v_y}{\tan\theta}$$

Since $\tan\theta \to 0$ as $\theta \to 0$, it will always be possible to find a value of θ close enough to zero so that $v_p > c$ for any (nonzero) value of v_y. As real scissors are closed, the angle gets progressively smaller, so in principle all that one needs for $v_p > c$ are long blades so that $\theta \to 0$.

Question

13. Use a diagram like Figure 1-32 to explain why the motion of point P cannot be used to convey information to observers along the blades.

The point P in the scissors paradox is, of course, a geometrical point, not a material object, so it is perhaps not surprising that it could appear to move at speeds greater than c. As an example of an object with mass appearing to do so, consider a tiny meteorite moving through space directly toward you at high speed v. As it enters Earth's atmosphere, about 9 km above the surface, frictional heating causes it to glow and the first light from the glow starts toward your eye. After some time Δt the frictional heating has evaporated all of the meteorite's matter, the glow is extinguished, and its final light starts toward your eye, as illustrated in Figure 1-40. During the time between the first and the final glow, the meteorite traveled a distance $v\Delta t$. During that same time interval light from the first glow has traveled toward your eye a distance $c\Delta t$. Thus, the space interval between the first and final glows is given by

$$\Delta y = c\Delta t - v\Delta t = \Delta t(c - v)$$

and the visual time interval at your eye Δt_{eye} between the arrival of the first and final light is

$$\Delta t_{\text{eye}} = \Delta y/c = \frac{\Delta t(c - v)}{c} = \Delta t(1 - \beta)$$

and, finally, the apparent visual speed v_a that you record is

$$v_a = \frac{v\Delta t}{\Delta t_{\text{eye}}} = \frac{v\Delta t}{\Delta t(1 - \beta)} = \frac{\beta c}{1 - \beta} \qquad \textbf{1-43}$$

Clearly, $\beta = 0.5$ yields $v_a = c$ and any larger β yields $v_a > c$. For example, a meteorite approaching you at $v = 0.8c$ is perceived to be moving at $v_a = 4c$. Certain galactic

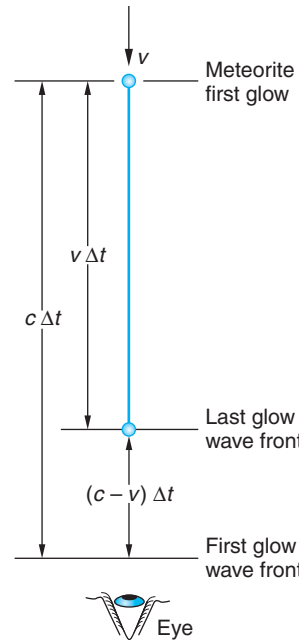

Figure 1-40 A meteorite moves directly toward the observer's eye at speed v. The spatial distance between the wave fronts is $(c - v)\Delta t$ as they move at c, so the time interval between their arrival at the observer is not Δt, but Δt_{eye}, which is $(c - v)\Delta t/c = (1 - \beta)\Delta t$, and the apparent speed of approach is $v_a = v\Delta t/\Delta t_{\text{eye}} = \beta c/(1 - \beta)$.

STUDENTS-HUB.com Uploaded By: Malak Obaid

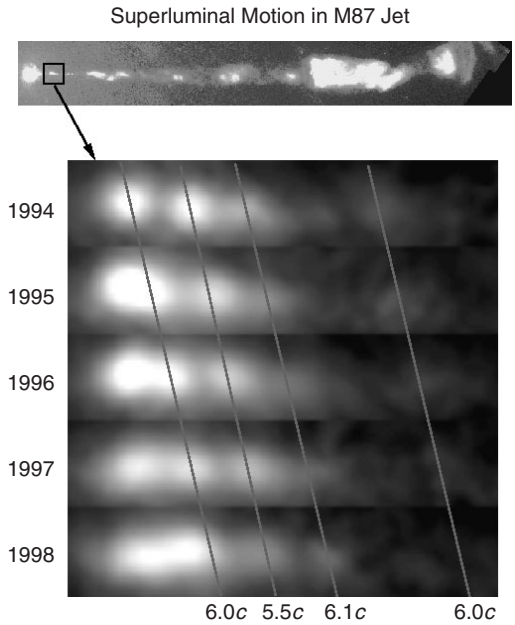

Figure 1-41 Superluminal motion has been detected in a number of cosmic objects. This sequence of images taken by the Hubble Space Telescope shows apparent motion at six times the speed of light in galaxy M87. The jet streaming from the galaxy's nucleus (the bright round region at the far left in the bar image at the top) is about 5000 $c \cdot$ y long. The boxed region is enlarged. The slanting lines track the moving features and indicate the apparent speeds in each region. [*John Biretta, Space Telescope Science Institute.*]

structures may also be observed to move at superluminal speeds, as the sequence of images of the jet from galaxy M87 in Figure 1-41 illustrates.

As a final example of things that move faster than c, it has been proposed that particles with mass might exist whose speeds would always be faster than light speed. One basis for this suggestion is an appealing symmetry: ordinary particles always have $v < c$, and photons and other massless particles have $v = c$, so the existence of particles with $v > c$ would give a sort of satisfying completeness to the classification of particles. Called *tachyons*, their existence would present relativity with serious but not necessarily insurmountable problems of infinite creation energies and causality paradoxes, e.g., alteration of history. (See the next example.) No compelling theoretical arguments preclude their existence and eventual discovery; however, to date, all experimental searches for tachyons[24] have failed to detect them, and the limits set by those experiments indicate that it is highly unlikely they exist.

EXAMPLE 1-15 **Tachyons and Reversing History** Use tachyons and an appropriate spacetime diagram to show how the existence of such particles might be used to change history and, hence, alter the future, leading to a paradox.

SOLUTION

In a spacetime diagram of the laboratory frame S the worldline of a particle with $v > c$ created at the origin traveling in the $+x$ direction makes an angle less than 45° with the x axis; i.e., it is below the light worldline, as shown in Figure 1-42. After some time the tachyon reaches a tachyon detector mounted on a spaceship moving rapidly away at $v < c$ in the $+x$ direction. The spaceship frame S' is shown in the figure at P. The detector immediately creates a new tachyon, sending it off in the $-x'$ direction and, of course, into the future of S', i.e., with $ct' > 0$. The second tachyon returns to the laboratory at $x = 0$ but at a time *ct before* the first tachyon was emitted, having traveled into the past of S to point M, where $ct < 0$. Having sent an object into our own past, we would then have the ability to alter events that occur after M and produce causal contradictions. For example, the laboratory tachyon detector could be coupled to equipment that created the first tachyon via a computer programmed to

STUDENTS-HUB.com Uploaded By: Malak Obaid

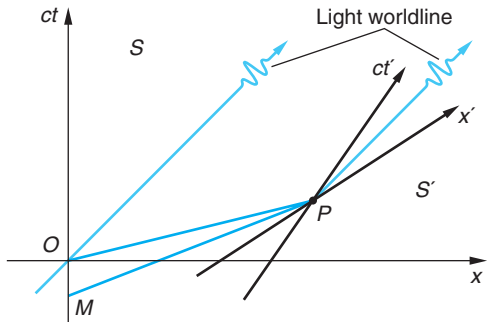

Figure 1-42 A tachyon emitted at O in S, the laboratory frame, catches up with a spaceship moving at high speed at P. Its detection triggers the emission of a second tachyon at P back toward the laboratory at $x = 0$. The second tachyon arrives at the laboratory at $ct < 0$, i.e., before the emission of the first tachyon.

cancel emission of the first tachyon if the second tachyon is detected. (Shades of *The Terminator*!) It is logical that contradictions such as this, together with the experimental results referred to above, lead to the conclusion that faster-than-light particles do not exist.

As mentioned above, one attraction (or specter) associated with objects moving faster than light is the prospect of altering history via time travel. We close this chapter on relativity by illustrating one such paradox in Figure 1-43.

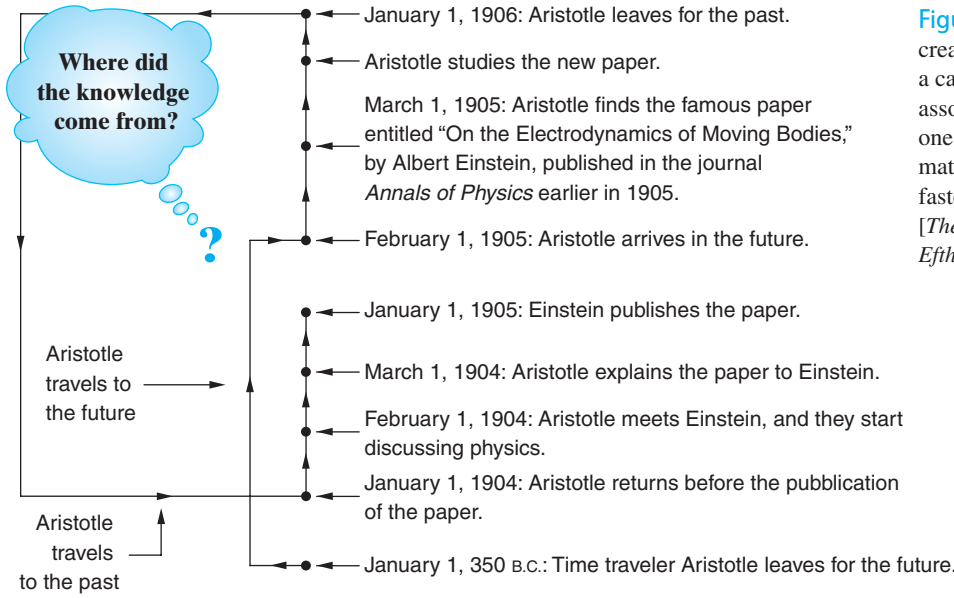

Figure 1-43 The knowledge creation paradox illustrates a causality problem associated with time travel, one possible consequence of material objects moving faster than light speed. [*The authors thank Costas Efthimiou for this example.*]

Summary

TOPIC	RELEVANT EQUATIONS AND REMARKS	
1. Classical relativity		
Galilean transformation	$x' = x - vt \quad y' = y \quad z' = z \quad t' = t$	**1-2**
Newtonian relativity	Newton's laws are invariant in all systems connected by a Galilean transformation.	

STUDENTS-HUB.com Uploaded By: Malak Obaid

TOPIC	RELEVANT EQUATIONS AND REMARKS
2. Einstein's postulates	The laws of physics are the same in all inertial reference frames. The speed of light is c, independent of the motion of the source.
3. Relativity of simultaneity	Events simultaneous in one reference frame are not in general simultaneous in any other inertial frame.
4. Lorentz transformation	$x' = \gamma(x - vt)y' = y\ z' = z$ **1-18** $t' = \gamma(t - vx/c^2)$ with $\gamma = (1 - v^2/c^2)^{-1/2}$
5. Time dilation	Proper time is the time interval τ between two events that occur at the same space point. If that interval is $\Delta t' = \tau$, then the time interval in S is $\Delta t = \gamma \Delta t' = \gamma\tau$ where $\gamma = (1 - v^2/c^2)^{-1/2}$ **1-26**
6. Length contraction	The proper length of a rod is the length L_p measured in the rest system of the rod. In S, moving at speed v with respect to the rod, the length measured is $L = L_p/\gamma$ **1-28**
7. Spacetime interval	All observers in inertial frames measure the same interval Δs between pairs of events in spacetime, where $(\Delta s)^2 = (c\Delta t)^2 - (\Delta x)^2$ **1-31**
8. Doppler effect	
Source/ observer approaching	$f = \sqrt{\dfrac{1 + \beta}{1 - \beta}}\, f_0$
Source/ observer receding	$f = \sqrt{\dfrac{1 - \beta}{1 + \beta}}\, f_0$

General References

The following general references are written at a level appropriate for readers of this book.

Bohm, D., *The Special Theory of Relativity*, W. A. Benjamin, New York, 1965.

French, A. P., *Special Relativity*, Norton, 1968. Includes an excellent discussion of the historical basis of relativity.

Gamow, G., *Mr. Tompkins in Paperback*, Cambridge University Press, Cambridge, 1965. Contains the delightful Mr. Tompkins stories. In one of these Mr. Tompkins visits a dream world where the speed of light is only about 10 mi/h and relativistic effects are quite noticeable.

Lorentz, H. A., A. Einstein, H. Minkowski, and W. Weyl, *The Principle of Relativity: A Collection of Original Memoirs on the Special and General Theory of Relativity* (trans. W. Perrett and J. B. Jeffery), Dover, New York, 1923. A delightful little book containing Einstein's original paper ["On the Electrodynamics of Moving Bodies," *Annalen der Physik*, **17** (1905)] and several other original papers on special relativity.

Ohanian, H. C., *Special Relativity: A Modern Introduction*, Physics Curriculum & Instruction, 2001.

Pais, A., *Subtle Is the Lord . . .* , Oxford University Press, Oxford, 1982.

Resnick, R., and D. Halliday, *Basic Concepts in Relativity and Early Quantum Theory,* 2d ed., Macmillan, 1992.

Rindler, W., *Essential Relativity*, Van Nostrand Reinhold, New York, 1969.

Taylor, E. F., and J. A. Wheeler, *Spacetime Physics,* 2d ed., W. H. Freeman and Co. 1992. This is a good book with many examples, problems, and diagrams.

STUDENTS-HUB.com Uploaded By: Malak Obaid

Notes

1. Polish astronomer, 1473–1543. His book describing heliocentric (i.e., Sun-centered) orbits for the planets was published only a few weeks before his death. He had hesitated to release it for many years, fearing that it might be considered heretical. It is not known whether or not he saw the published book.

2. Events are described by measurements made in a coordinate system that defines a frame of reference. The question was, Where is the reference frame in which the law of inertia is valid? Newton knew that no rotating system, e.g., Earth or the Sun, would work and suggested the distant "fixed stars" as the fundamental inertial reference frame.

3. The speed of light is exactly 299,792,458 m/s. The value is set by the definition of the standard meter as being the distance light travels in 1/299,792,458 s.

4. Over time, an entire continuous spectrum of electromagnetic waves has been discovered, ranging from extremely low-frequency (radio) waves to extremely high-frequency waves (gamma rays), all moving at speed c.

5. Albert A. Michelson (1852–1931), an American experimental physicist whose development of precision optical instruments and their use in precise measurements of the speed of light and the length of the standard meter earned him the Nobel Prize in 1907. Edward W. Morley (1838–1923), an American chemist and physicist and professor at Western Reserve College when Michelson was a professor at the nearby Case School of Applied Science.

6. Albert A. Michelson and Edward W. Morley, *The American Journal of Science*, **XXXIV**, no. 203, November 1887.

7. Note that the width depends on the small angle between M_2' and M_1. A very small angle results in relatively few wide fringes, a larger angle in many narrow fringes.

8. Since the source producing the waves, the sodium lamp, was at rest relative to the interferometer, the frequency would be constant.

9. T. S. Jaseja, A. Javan, J. Murray, and C. H. Townes, *Physical Review*, **133**, A1221 (1964).

10. A. Brillet and J. Hall, *Physical Review Letters*, **42**, 549 (1979).

11. *Annalen der Physik*, **17**, 841(1905). For a translation from the original German, see the collection of original papers by Lorentz, Einstein, Minkowski, and Weyl (Dover, New York, 1923).

12. Hendrik Antoon Lorentz (1853–1928), Dutch theoretical physicist, discovered the Lorentz transformation empirically while investigating the fact that Maxwell's equations are not invariant under a Galilean transformation, although he did not recognize its importance at the time. An expert on electromagnetic theory, he was one of the first to suggest that atoms of matter might consist of charged particles whose oscillations could account for the emission of light. Lorentz used this hypothesis to explain the splitting of spectral lines in a magnetic field discovered by his student Pieter Zeeman, with whom he shared the 1902 Nobel Prize.

13. One meter of light travel time is the *time* for light to travel 1 m, i.e., $ct = 1$ m, or $t = 1\text{ m}/3.00 \times 10^8\text{ m/s} = 3.3 \times 10^{-9}$ s. Similarly, 1 cm of light travel time is $ct = 1$ cm, or $t = 3.3 \times 10^{-11}$ s, and so on.

14. This example is adapted from a problem in H. Ohanian, *Modern Physics* (Englewood Cliffs, NJ: Prentice Hall, 1987).

15. Any particle that has mass.

16. Equation 1-31 would lead to imaginary values of Δs for spacelike intervals, an apparent problem. However, the geometry of spacetime is not Euclidean, but Lorentzian. While a consideration of Lorentz geometry is beyond the scope of this chapter, suffice it to say that it enables us to write $(\Delta s)^2$ for spacelike intervals as in Equation 1-33.

17. There are only two such things: photons (including those of visible light), which will be introduced in Chapter 3, and gravitons, which are the particles that transmit the gravitational force.

18. Edwin P. Hubble, *Proceedings of the National Academy of Sciences*, **15**, 168 (1929).

19. Walter Kündig, *Physical Review*, **129**, 2371 (1963).

20. C. G. Darwin, *Nature*, **180**, 976 (1957).

21. S. P. Boughn, *American Journal of Physics*, **57**, 791 (1989).

22. E. F. Taylor and J. A. Wheeler, *Spacetime Physics*, 2d ed. (New York: W. H. Freeman and Co., 1992).

23. Seen in three space dimensions by the observer in S, 50 percent of the light is concentrated in 0.06 steradian of 4π-steradian solid angle around the moving source.

24. T. Alväger and M. N. Kreisler, "Quest for Faster-Than-Light Particles," *Physical Review*, **171**, 1357 (1968).

25. Paul Ehrenfest (1880–1933), Austrian physicist and professor at the University of Leiden (the Netherlands), longtime friend and correspondent of Einstein, about whom, upon his death, Einstein wrote, "[He was] the best teacher in our profession I have ever known."

26. This experiment is described in J. C. Hafele and R. E. Keating, *Science*, **177**, 166 (1972). Although not as accurate as the experiment described in Section 1-4, its results supported the relativistic prediction.

27. R. Shaw, *American Journal of Physics*, **30**, 72 (1962).

STUDENTS-HUB.com Uploaded By: Malak Obaid

Problems

Level I

Section 1-1 The Experimental Basis of Relativity

1-1. In episode 5 of Star Wars, the Empire's spaceships launch probe droids throughout the galaxy to seek the base of the Rebel Alliance. Suppose a spaceship moving at 2.3×10^8 m/s toward Hoth (site of the rebel base) launches a probe droid toward Hoth at 2.1×10^8 m/s relative to the spaceship. According to Galilean relativity, (*a*) What is the speed of the droid relative to Hoth? (*b*) If rebel astronomers are watching the approaching spaceship through a telescope, will they see the probe before it lands on Hoth?

1-2. In one series of measurements of the speed of light, Michelson used a path length L of 27.4 km (17 mi). (*a*) What is the time needed for light to make the round trip of distance $2L$? (*b*) What is the classical correction term in seconds in Equation 1-5, assuming Earth's speed is $v = 10^{-4}c$? (*c*) From about 1600 measurements, Michelson arrived at a result for the speed of light of 299,796 $\pm$ 4 km/s. Is this experimental value accurate enough to be sensitive to the correction term in Equation 1-5?

1-3. A shift of one fringe in the Michelson-Morley experiment would result from a difference of one wavelength or a change of one period of vibration in the round-trip travel of the light when the interferometer is rotated by 90°. What speed would Michelson have computed for Earth's motion through the ether had the experiment seen a shift of one fringe?

1-4. In the "old days" (circa 1935) pilots used to race small, relatively high-powered airplanes around courses marked by a pylon on the ground at each end of the course. Suppose two such evenly matched racers fly at airspeeds of 130 mph. (Remember, this was a long time ago!) Each flies one complete round trip of 25 miles, *but* their courses are perpendicular to each other and there is a 20-mph wind blowing steadily parallel to one course. (*a*) Which pilot wins the race and by how much? (*b*) Relative to the axes of their respective courses, what headings must the two pilots use?

1-5. Paul Ehrenfest[25] suggested the following thought experiment to illustrate the dramatically different observations that might be expected, dependent on whether light moved relative to a stationary ether or according to Einstein's second postulate:

> Suppose that you are seated at the center of a huge dark sphere with a radius of 3×10^8 m and with its inner surface highly reflective. A source at the center emits a very brief flash of light that moves outward through the darkness with uniform intensity as an expanding spherical wave.

What would you see during the first 3 seconds after the emission of the flash if (*a*) the sphere moved through the ether at a constant 30 km/s and (*b*) if Einstein's second postulate is correct?

1-6. Einstein reported that as a boy he wondered about the following puzzle. If you hold a mirror at arm's length and look at your reflection, what will happen as you begin to run? In particular, suppose you run with speed $v = 0.99c$. Will you still be able to see yourself? If so, what would your image look like, and why?

1-7. Verify by calculation that the result of the Michelson-Morley experiment places an upper limit on Earth's speed relative to the ether of about 5 km/s.

1-8. Consider two inertial reference frames. When an observer in each frame measures the following quantities, which measurements made by the two observers *must* yield the same results? Explain your reason for each answer.

(*a*) The distance between two events
(*b*) The value of the mass of a proton
(*c*) The speed of light
(*d*) The time interval between two events
(*e*) Newton's first law
(*f*) The order of the elements in the periodic table
(*g*) The value of the electron charge

STUDENTS-HUB.com Uploaded By: Malak Obaid

Section 1-2 Einstein's Postulates

1-9. Assume that the train shown in Figure 1-14 is 1.0 km long as measured by the observer at C' and is moving at 150 km/h. What time interval between the arrival of the wave fronts at C' is measured by the observer at C in S?

1-10. Suppose that A', B', and C' are at rest in frame S', which moves with respect to S at speed v in the $+x$ direction. Let B' be located exactly midway between A' and C'. At $t' = 0$ a light flash occurs at B' and expands outward as a spherical wave. (*a*) According to an observer in S', do the wave fronts arrive at A' and C' simultaneously? (*b*) According to an observer in S, do the wave fronts arrive at A' and C' simultaneously? (*c*) If you answered no to either (*a*) or (*b*), what is the difference in their arrival times and at which point did the front arrive first?

Section 1-3 The Lorentz Transformation

1-11. Make a graph of the relativistic factor $\gamma = 1/(1 - v^2/c^2)^{1/2}$ as a function of $\beta = v/c$. Use at least 10 values of β ranging from 0 up to 0.995.

1-12. Two events happen at the same point x'_0 in frame S' at times t'_1 and t'_2. (*a*) Use Equation 1-19 to show that in frame S, the time interval between the events is greater than $t'_2 - t'_1$ by a factor γ. (*b*) Why is Equation 1-18 less convenient than Equation 1-19 for this problem?

1-13. Suppose that an event occurs in inertial frame S with coordinates $x = 75$ m, $y = 18$ m, $z = 4.0$ m at $t = 2.0 \times 10^{-5}$ s. The inertial frame S' moves in the $+x$ direction with $v = 0.85c$. The origins of S and S' coincided at $t = t' = 0$. (*a*) What are the coordinates of the event in S'? (*b*) Use the inverse transformation on the results of (*a*) to obtain the original coordinates.

1-14. Show that the null effect of the Michelson-Morley experiment can be accounted for if the interferometer arm parallel to the motion is shortened by a factor of $(1 - v^2/c^2)^{1/2}$.

1-15. Two spaceships are approaching each other. (*a*) If the speed of each is $0.9c$ relative to Earth, what is the speed of one relative to the other? (*b*) If the speed of each relative to Earth is 30,000 m/s (about 100 times the speed of sound), what is the speed of one relative to the other?

1-16. Starting with the Lorentz transformation for the components of the velocity (Equation 1-23), derive the transformation for the components of the acceleration.

1-17. Consider a clock at rest at the origin of the laboratory frame. (*a*) Draw a spacetime diagram that illustrates that this clock ticks slow when observed from the reference frame of a rocket moving with respect to the laboratory at $v = 0.8c$. (*b*) When 10 s have elapsed on the rocket clock, how many have ticked by on the lab clock?

1-18. A light beam moves along the y' axis with speed c in frame S', which is moving to the right with speed v relative to frame S. (*a*) Find u_x and u_y, the x and y components of the velocity of the light beam in frame S. (*b*) Show that the magnitude of the velocity of the light beam in S is c.

1-19. A particle moves with speed $0.9c$ along the x'' axis of frame S'', which moves with speed $0.9c$ in the positive x' direction relative to frame S'. Frame S' moves with speed $0.9c$ in the positive x direction relative to frame S. (*a*) Find the speed of the particle relative to frame S'. (*b*) Find the speed of the particle relative to frame S.

Section 1-4 Time Dilation and Length Contraction

1-20. Use the binomial expansion to derive the following results for values of $v \ll c$ and use when applicable in the problems that follow.

$$(a) \qquad \gamma \approx 1 + \frac{1}{2}\frac{v^2}{c^2}$$

$$(b) \qquad \frac{1}{\gamma} \approx 1 - \frac{1}{2}\frac{v^2}{c^2}$$

$$(c) \qquad \gamma - 1 \approx 1 - \frac{1}{\gamma} \approx \frac{1}{2}\frac{v^2}{c^2}$$

1-21. How great must the relative speed of two observers be for their time-interval measurements to differ by 1 percent (see Problem 1-20)?

STUDENTS-HUB.com Uploaded By: Malak Obaid

1-22. A *nova* is the sudden, brief brightening of a star (see Chapter 13). Suppose Earth astronomers see two novas occur simultaneously, one in the constellation Orion (the Hunter) and the other in the constellation Lyra (the Lyre). Both nova are the same distance from Earth, $2.5 \times 10^3\ c \cdot y$, and are in exactly opposite directions from Earth. Observers on board an aircraft flying at 1000 km/h on a line from Orion toward Lyra see the same novas, but note that they are not simultaneous. (*a*) For the observers on the aircraft, how much time separates the nova? (*b*) Which one occurs first? (Assume Earth is an inertial reference frame.)

1-23. A meter stick moves parallel to its length with speed $v = 0.6c$ relative to you. (*a*) Compute the length of the stick measured by you. (*b*) How long does it take for the stick to pass you? (*c*) Draw a spacetime diagram from the viewpoint of your frame with the front of the meter stick at $x = 0$ when $t = 0$. Show how the answers to (*a*) and (*b*) are obtained from the diagram.

1-24. The proper mean lifetime of π mesons (pions) is 2.6×10^{-8} s. If a beam of such particles has speed $0.9c$, (*a*) What would their mean life be as measured in the laboratory? (*b*) How far would they travel (on the average) before they decay? (*c*) What would your answer be to part (*b*) if you neglected time dilation? (*d*) What is the interval in spacetime between creation of a typical pion and its decay?

1-25. You have been posted to a remote region of space to monitor traffic. Near the end of a quiet shift, a spacecraft streaks past. Your laser-based measuring device reports the spacecraft's length to be 85 m. The identification transponder reports it to be the NCXXB-12, a cargo craft of proper length 100 m. In transmitting your report to headquarters, what speed should you give for this spacecraft?

1-26. The light clock in the spaceship in Figure 1-25 uses a light pulse moving up the *y*-axis to reflect back from a mirror as the ship moves along the *x*-axis. Suppose instead the light pulse moves along the x'-axis between $x' = 0$ and a mirror at $x' = L$. (*a*) What is the time required for the pulse to make a round trip in the rest system of the spaceship? (*b*) What is the round-trip time in the laboratory frame? (*c*) Does the result in (*b*) agree with that expected from time dilation? Justify your answer.

1-27. Two spaceships pass each other traveling in opposite directions. A passenger on ship *A*, which she knows to be 100 m long, notes that ship *B* is moving with a speed of $0.92c$ relative to *A* and that the length of *B* is 36 m. What are the lengths of the two spaceships measured by a passenger in *B*?

1-28. A meter stick at rest in S' is tilted at an angle of 30° to the x' axis. If S' moves at $\beta = 0.8$, how long is the meter stick as measured in *S* and what angle does it make with the *x* axis?

1-29. A rectangular box at rest in S' has sides $a' = 2$ m, $b' = 2$ m, and $c' = 4$ m and is oriented as shown in Figure 1-44. S' moves with $\beta = 0.65$ with respect to the laboratory frame *S*. (*a*) Compute the volume of the box in S' and in *S*. (*b*) Draw an accurate diagram of the box as seen by an observer in *S*.

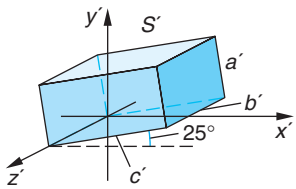

Figure 1-44

Section 1-5 The Doppler Effect

1-30. How fast must you be moving toward a red light ($\lambda = 650$ nm) for it to appear yellow ($\lambda = 590$ nm)? green ($\lambda = 525$ nm)? blue ($\lambda = 460$ nm)?

1-31. A distant galaxy is moving away from us at speed 1.85×10^7 m/s. Calculate the fractional red shift $(\lambda' - \lambda_0)/\lambda_0$ of the light from this galaxy.

1-32. The light from a nearby star is observed to be shifted toward the blue by 2 percent, i.e., $f_{obs} = 1.02 f_0$. Is the star approaching or receding from Earth? How fast is it moving? (Assume motion is directly toward or away from Earth to avoid superluminal speeds.)

1-33. Stars typically emit the red light of atomic hydrogen with wavelength 656.3 nm (called the H_α spectral line). Compute the wavelength of that light observed at Earth from stars receding directly from us with relative speed $v = 10^{-3}c$, $v = 10^{-2}c$, and $v = 10^{-1}c$.

Section 1-6 The Twin Paradox and Other Surprises

1-34. Heide boards a spaceship and travels away from Earth at a constant velocity $0.45c$ toward Betelgeuse (a red giant star in the constellation Orion). One year later on Earth clocks, Heide's twin, Hans, boards a second spaceship and follows her at a constant velocity of $0.95c$ in the

STUDENTS-HUB.com Uploaded By: Malak Obaid

same direction. (*a*) When Hans catches up to Heide, what will be the difference in their ages? (*b*) Which twin will be older?

1-35. You point a laser flashlight at the Moon, producing a spot of light on the Moon's surface. At what minimum angular speed must you sweep the laser beam in order for the light spot to streak across the Moon's surface with speed $v > c$? Why can't you transmit information between research bases on the Moon with the flying spot?

1-36. A clock is placed in a satellite that orbits Earth with a period of 108 min. (*a*) By what time interval will this clock differ from an identical clock on Earth after 1 y? (*b*) How much time will have passed on Earth when the two clocks differ by 1.0 s? (Assume special relativity applies and neglect general relativity.)

1-37. Einstein used trains for a number of relativity thought experiments since they were the fastest objects commonly recognized in those days. Let's consider a train moving at $0.65c$ along a straight track at night. Its headlight produces a beam with an angular spread of 60° according to the engineer. If you are standing alongside the track (rails are 1.5 m apart), how far from you is the train when you see its approaching headlight suddenly disappear?

Level II

1-38. In 1971 four portable atomic clocks were flown around the world in jet aircraft, two eastbound and two westbound, to test the time dilation predictions of relativity.[26] (*a*) If the westbound plane flew at an average speed of 1500 km/h relative to the surface, how long would it have had to fly for the clock on board to lose 1 second relative to the reference clock on the ground at the U.S. Naval Observatory? (*b*) In the actual experiment the planes circumflew Earth once and the observed discrepancy of the clocks was 273 ns. What was the average speed of each plane?

1-39. "Ether drag" was among the suggestions made to explain the null result of the Michelson-Morley experiment (see More section). The phenomenon of stellar aberration refutes this proposal. Suppose Earth moves relative to the ether at velocity $\boldsymbol{v}$ and a light beam (e.g., from a star) approaches Earth at an angle θ with respect to $\boldsymbol{v}$. (*a*) Show that the angle of approach in Earth's reference frame θ' is given by

$$\tan\theta' = \frac{\sin\theta}{\cos\theta + v/c}$$

(*b*) θ' is the stellar aberration angle. If $\theta = 90°$, by how much does θ' differ from 90°?

1-40. A friend of yours who is the same age as you travels to the star Alpha Centauri, which is 4 $c \cdot$ y away, and returns immediately. He claims that the entire trip took just 6 years. (*a*) How fast did he travel? (*b*) How old are you when he returns? (*c*) Draw a spacetime diagram that verifies your answers to (*a*) and (*b*).

1-41. A clock is placed in a satellite that orbits Earth with a period of 90 min. By what time interval will this clock differ from an identical clock on Earth after 1 year? (Assume that special relativity applies.)

1-42. In frame S, event B occurs 2 μs after event A and at $\Delta x = 1.5$ km from event A. (*a*) How fast must an observer be moving along the $+x$ axis so that events A and B occur simultaneously? (*b*) Is it possible for event B to precede event A for some observer? (*c*) Draw a spacetime diagram that illustrates your answers to (*a*) and (*b*). (*d*) Compute the spacetime interval and proper distance between the events.

1-43. A burst of π^+ mesons travels down an evacuated beam tube at Fermilab moving at $\beta = 0.92$ with respect to the laboratory. (*a*) Compute γ for this group of pions. (*b*) The proper mean lifetime of pions is 2.6×10^{-8} s. What mean lifetime is measured in the lab? (*c*) If the burst contained 50,000 pions, how many remain after the group has traveled 50 m down the beam tube? (*d*) What would be the answer to (*c*) ignoring time dilation?

1-44. H. A. Lorentz suggested 15 years before Einstein's 1905 paper that the null effect of the Michelson-Morley experiment could be accounted for by a contraction of that arm of the interferometer lying parallel to Earth's motion through the ether to a length $L = L_p(1 - v^2/c^2)^{-1/2}$. He thought of this, incorrectly, as an actual shrinking of matter. By about how many atomic diameters would the material in the parallel arm of the interferometer have had to shrink in order

STUDENTS-HUB.com Uploaded By: Malak Obaid

to account for the absence of the expected shift of 0.4 of a fringe width? (Assume the diameter of atoms to be about 10^{-10} m.)

1-45. Observers in reference frame S see an explosion located at $x_1 = 480$ m. A second explosion occurs 5 μs later at $x_2 = 1200$ m. In reference frame S', which is moving along the $+x$ axis at speed v, the explosions occur at the same point in space. (*a*) Draw a spacetime diagram describing this situation. (*b*) Determine v from the diagram. (*c*) Calibrate the ct' axis and determine the separation in time in μs between the two explosions as measured in S'. (*d*) Verify your results by calculation.

1-46. Two spaceships, each 100 m long when measured at rest, travel toward each other with speeds of $0.85c$ relative to Earth. (*a*) How long is each ship as measured by someone on Earth? (*b*) How fast is each ship traveling as measured by an observer on the other? (*c*) How long is one ship when measured by an observer on the other? (*d*) At time $t = 0$ on Earth, the fronts of the ships are together as they just begin to pass each other. At what time on Earth are their ends together? (*e*) Sketch accurately scaled diagrams in the frame of one of the ships showing the passing of the other ship.

1-47. If v is much less than c, the Doppler frequency shift is approximately given by $\Delta f/f_0 = \pm\beta$, both classically and relativistically. A radar transmitter-receiver bounces a signal off an aircraft and observes a fractional increase in the frequency of $\Delta f/f_0 = 8 \times 10^{-7}$. What is the speed of the aircraft? (Assume the aircraft to be moving directly toward the transmitter.)

1-48. The null result of the Michelson-Morley experiment could be explained if the speed of light depended on the motion of the source relative to the observer. Consider a binary eclipsing star system, that is, a pair of stars orbiting their common center of mass with Earth lying in the orbital plane of the system, as is very nearly the case for the binary system Algol (see More section about the Michelson-Morley experiment). Assume that the stars in the system have circular orbits with a period of 115 days and that one of the stars' orbital speed is 32 km/s (about the same as Earth's orbital speed around the Sun). If the suggestion above were true, astronomers would simultaneously see two images of the star in opposition, i.e., on opposite sides of its orbit. What is the minimum distance L from Earth to the binary for this phenomenon to occur?

1-49. Frames S and S' are moving relative to each other along the x and x' axes. They set their clocks to $t = t' = 0$ when their origins coincide. In frame S, event 1 occurs at $x_1 = 1\ c \cdot$y and $t_1 = 1$ y and event 2 occurs at $x_2 = 2.0\ c \cdot$y and $t_2 = 0.5$ y. These events occur simultaneously in frame S'. (*a*) Find the magnitude and direction of the velocity of S' relative to S. (*b*) At what time do both of these events occur as measured in S'? (*c*) Compute the spacetime interval Δs between the events. (*d*) Is the interval spacelike, timelike, or lightlike? (*e*) What is the proper distance L_p between the events?

1-50. Do Problem 1-49 parts (*a*) and (*b*) using a spacetime diagram.

1-51. An observer in frame S standing at the origin observes two flashes of colored light separated spatially by $\Delta x = 2400$ m. A blue flash occurs first, followed by a red flash 5 μs later. An observer in S' moving along the x axis at speed v relative to S also observes the flashes 5 μs apart and with a separation of 2400 m, but the red flash is observed first. Find the magnitude and direction of v.

1-52. A cosmic-ray proton streaks through the lab with velocity $0.85c$ at an angle of 50° with the $+x$ direction (in the xy plane of the lab). Compute the magnitude and direction of the proton's velocity when viewed from frame S' moving with $\beta = 0.72$.

Level III

1-53. A meter stick is parallel to the x axis in S and is moving in the $+y$ direction at constant speed v_y. From the viewpoint of S show that the meter stick will appear tilted at an angle θ' with respect to the x' axis of S' moving in the $+x$ direction at $\beta = 0.65$. Compute the angle θ' measured in S'.

1-54. The equation for the spherical wave front of a light pulse that begins at the origin at time $t = 0$ is $x^2 + y^2 + z^2 - (ct)^2 = 0$. Using the Lorentz transformation, show that such a light pulse also has a spherical wave front in S' by showing that $x'^2 + y'^2 + z'^2 - (ct')^2 = 0$ in S'.

1-55. An interesting paradox has been suggested by R. Shaw[27] that goes like this. A very thin steel plate with a circular hole 1 m in diameter centered on the y axis lies parallel to the xz plane

STUDENTS-HUB.com Uploaded By: Malak Obaid

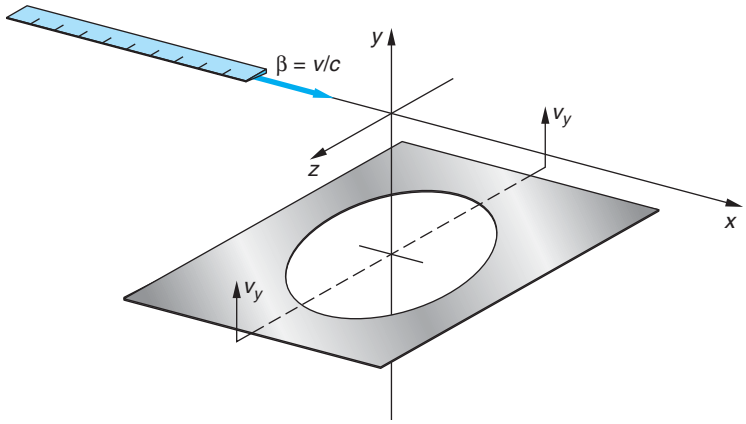

Figure 1-45

in frame S and moves in the $+y$ direction at constant speed v_y as illustrated in Figure 1-45. A meter stick lying on the x axis moves in the $+x$ direction with $\beta = v/c$. The steel plate arrives at the $y = 0$ plane at the same instant that the center of the meter stick reaches the origin of S. Since the meter stick is observed by observers in S to be contracted, it passes through the 1-m hole in the plate with no problem. A paradox appears to arise when one considers that an observer in S', the rest system of the meter stick, measures the diameter of the hole in the plate to be contracted in the x dimension and, hence, becomes too small to pass the meter stick, resulting in a collision. Resolve the paradox. Will there be a collision?

1-56. Two events in S are separated by a distance $D = x_2 - x_1$ and a time $T = t_2 - t_1$. (*a*) Use the Lorentz transformation to show that in frame S', which is moving with speed v relative to S, the time separation is $t_2 - t_1 = \gamma(T - vD/c^2)$. (*b*) Show that the events can be simultaneous in frame S' only if D is greater than cT. (*c*) If one of the events is the *cause* of the other, the separation D must be less than cT since D/c is the smallest time that a signal can take to travel from x_1 to x_2 in frame S. Show that if D is less than cT, t_2' is greater than t_1' in all reference frames. (*d*) Suppose that a signal could be sent with speed $c' > c$ so that in frame S the cause precedes the effect by the time $T = D/c'$. Show that there is then a reference frame moving with speed v less than c in which the effect precedes the cause.

1-57. Two observers agree to test time dilation. They use identical clocks and one observer in frame S' moves with speed $v = 0.6c$ relative to the other observer in frame S. When their origins coincide, they start their clocks. They agree to send a signal when their clocks read 60 min and to send a confirmation signal when each receives the other's signal. (*a*) When does the observer in S receive the first signal from the observer in S'. (*b*) When does he receive the confirmation signal? (*c*) Make a table showing the times in S when the observer sent the first signal, received the first signal, and received the confirmation signal. How does this table compare with one constructed by the observer in S'?

1-58. The compact disk in a CD-ROM drive rotates with angular speed ω. There is a clock at the center of the disk and one at a distance r from the center. In an inertial reference frame, the clock at distance r is moving with speed $u = r\omega$. Show that from time dilation in special relativity, time intervals Δt_o for the clock at rest and Δt_r for the moving clock are related by

$$\frac{\Delta t_r - \Delta t_o}{\Delta t_o} \approx \frac{r^2\omega^2}{2c^2} \qquad \text{if } r\omega \ll c$$

1-59. Two rockets, A and B, leave a space station with velocity vectors $\mathbf{v}_A$ and $\mathbf{v}_B$ relative to the station frame S, perpendicular to each other. (*a*) Determine the velocity of A relative to B, $\mathbf{v}_{BA}$. (*b*) Determine the velocity of B relative to A, $\mathbf{v}_{AB}$. (*c*) Explain why $\mathbf{v}_{AB}$ and $\mathbf{v}_{BA}$ do not point in opposite directions.

1-60. Suppose a system S consisting of a cubic lattice of meter sticks and synchronized clocks, e.g., the eight clocks closest to you in Figure 1-13, moves from left to right (the $+x$ direction) at high speed. The meter sticks parallel to the x direction are, of course, contracted and the cube

STUDENTS-HUB.com Uploaded By: Malak Obaid

would be *measured* by an observer in a system S' to be foreshortened in that direction. However, recalling that your eye constructs images from light waves that reach it simultaneously, not those leaving the source simultaneously, sketch what your eye would *see* in this case. Scale contractions and show any angles accurately. (Assume the moving cube to be farther than 10 m from your eye.)

1-61. Figure 1-11*b* (in the More section about the Michelson-Morley experiment) shows an eclipsing binary. Suppose the period of the motion is T and the binary is a distance L from Earth, where L is sufficiently large so that points A and B in Figure 1-11*b* are a half orbit apart. Consider the motion of one of the stars and (*a*) show that the star would appear to move from A to B in time $T/2 + 2Lv/(c^2 - v^2)$ and from B to A in time $T/2 - 2Lv/(c^2 - v^2)$, assuming classical velocity addition applies to light, i.e., that emission theories of light were correct. (*b*) What rotational period would cause the star to appear to be at both A and B simultaneously?

1-62. Show that if a particle moves at an angle θ with respect to the x axis with speed u in system S, it moves at an angle θ' with the x' axis in S' given by

$$\tan\theta' = \frac{\sin\theta}{\gamma(\cos\theta - v/u)}$$

1-63. Like jets emitted from some galaxies (see Figure 1-41), some distant astronomical objects can appear to travel at speeds greater than c across our line of sight. Suppose distant galaxy AB15 moving with velocity v at an angle θ with respect to the direction toward Earth emits two bright flashes of light separated by time Δt on the galaxy AB15 local clock. Show that (*a*) the time interval $\Delta t_{\text{Earth}} = \Delta t(1 - \beta\cos\theta)$ and (*b*) the apparent speed of AB15 measured by observers on Earth is $v_{\text{app}} = \dfrac{\Delta x_{\text{Earth}}}{\Delta t_{\text{Earth}}} = \dfrac{\beta\sin\theta}{1 - \beta\cos\theta}$. (*c*) For $\beta = 0.75$, compute the value of θ for which $v_{\text{app}} = c$.

STUDENTS-HUB.com Uploaded By: Malak Obaid

CHAPTER 2

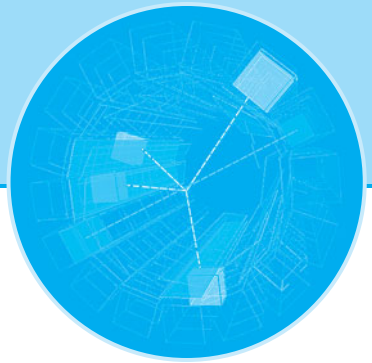

Relativity II

2-1 Relativistic Momentum 66
2-2 Relativistic Energy 70
2-3 Mass/Energy Conversion and Binding Energy 81
2-4 Invariant Mass 84
2-5 General Relativity 97

In the opening section of Chapter 1, we discussed the classical observation that, if Newton's second law, $\mathbf{F} = m\mathbf{a}$, holds in a particular reference frame, it also holds in any other reference frame that moves with constant velocity relative to it, i.e., in any inertial frame. As shown in Section 1-1, the Galilean transformation (Equation 1-2) leads to the same accelerations $a'_x = a_x$ in both frames, and forces such as those due to stretched springs are also the same in both frames. However, according to the Lorentz transformation, accelerations are not the same in two such reference frames. If a particle has acceleration a_x and velocity u_x in frame S, its acceleration in S', obtained by computing du'_x/dt' from Equation 1-22, is

$$a'_x = \frac{a_x}{\gamma^3(1 - vu_x/c^2)^3} \qquad \textbf{2-1}$$

Thus, F/m must transform in a similar way, or else Newton's second law, $\mathbf{F} = m\mathbf{a}$, does not hold.

It is reasonable to expect that $\mathbf{F} = m\mathbf{a}$ does *not* hold at high speeds, for this equation implies that a constant force will accelerate a particle to unlimited velocity if it acts for a long time. However, if a particle's velocity were greater than c in some reference frame S, we could not transform from S to the rest frame of the particle because γ becomes imaginary when $v > c$. We can show from the velocity transformation that, if a particle's velocity is less than c in some frame S, it is less than c in all frames moving relative to S with $v < c$. This result leads us to expect that particles never have speeds greater than c. Thus, we expect that Newton's second law $\mathbf{F} = m\mathbf{a}$ is not relativistically invariant. We will, therefore, need a new law of motion, but one that reduces to Newton's classical version when $\beta(=v/c) \rightarrow 0$, since $\mathbf{F} = m\mathbf{a}$ is consistent with experimental observations when $\beta \ll 1$.

In this chapter we will explore the changes in classical dynamics that are dictated by relativity theory, directing particular attention to the same concepts around which classical mechanics was developed, namely, mass, momentum, and energy. We will

STUDENTS-HUB.com
Uploaded By: Malak Obaid

find these changes to be every bit as dramatic as those we encountered in Chapter 1, including a Lorentz transformation for momentum and energy and a new invariant quantity to stand beside the invariant spacetime interval Δs. Then, in the latter part of the chapter, we will briefly turn our attention to noninertial, or accelerated, reference frames, the realm of the theory of general relativity.

2-1 Relativistic Momentum

Among the most powerful fundamental concepts that you have studied in physics until now are the ideas of conservation of momentum and conservation of total energy. As we will discuss a bit further in Chapter 12, each of these fundamental laws arises because of a particular symmetry that exists in the laws of physics. For example, the conservation of total energy in classical physics is a consequence of the symmetry, or invariance, of the laws of physics to translations in time. As a consequence, Newton's laws work exactly the same way today as they did when he first wrote them down. The conservation of momentum arises from the invariance of physical laws to translations in space. Indeed, Einstein's first postulate and the resulting Lorentz transformation (Equations 1-18 and 1-19) guarantee this latter invariance in all inertial frames.

The simplicity and universality of these conservation laws leads us to seek equations for relativistic mechanics, replacing Equation 1-1 and others, that are consistent with momentum and energy conservation and are also invariant under a Lorentz transformation. However, it is straightforward to show that the momentum, as formulated in classical mechanics, does not result in relativistic invariance of the law of conservation of momentum. To see that this is so, we will look at an isolated collision between two masses, where we avoid the question of how to transform forces because the net external force is zero. In classical mechanics, the total momentum $\mathbf{p} = \Sigma m_i \mathbf{u}_i$ is conserved. We will see that relativistically, conservation of the quantity $\Sigma m_i \mathbf{u}_i$ is an approximation that holds only at low speeds.

Consider one observer in frame S with a ball A and another in S' with ball B. The balls each have mass m and are identical when measured at rest. Each observer throws his ball along his y axis with speed u_0 (measured in his own frame) so that the balls collide.[1] Assuming the balls to be perfectly elastic, each observer will see his ball rebound with its original speed u_0. If the total momentum is to be conserved, the y component must be zero because the momentum of each ball is merely reversed by the collision. However, if we consider the relativistic velocity transformation, we can see that the quantity mu_y does not have the same magnitude for each ball as seen by either observer.

Let us consider the collision as seen in frame S (Figure 2-1*a*). In this frame ball A moves along the y axis with velocity $u_{yA} = u_0$. Ball B has x component of velocity $u_{xB} = v$ and y component

$$u_{yB} = u'_{yB}/\gamma = -u_0\sqrt{1 - v^2/c^2} \qquad \textbf{2-2}$$

Here we have used the velocity transformation (Equation 1-22) and the facts that u'_{yB} is just $-u_0$ and $u'_{xB} = 0$. We see that the y component of the velocity of ball B is smaller in magnitude than that of ball A. The quantity $(1 - v^2/c^2)^{1/2}$ comes from the time dilation factor. The time taken for ball B to travel a given distance along the y axis in S is greater than the time measured in S' for the ball to travel this same distance.

STUDENTS-HUB.com Uploaded By: Malak Obaid

Thus, in S the total y component of classical momentum is not zero. Since the y components of the velocities are reversed in an elastic collision, momentum as defined by $\mathbf{p} = \Sigma m\mathbf{u}$ is not conserved in S. Analysis of this problem in S' leads to the same conclusion (Figure 2-1*b*), since the roles of A and B are simply interchanged.[2] In the classical limit $v \ll c$, momentum is conserved, of course, because in that limit $\gamma \approx 1$ and $u_{yB} \approx u_0$.

The reason for defining momentum as $\Sigma m\mathbf{u}$ in classical mechanics is that this quantity is conserved when there is no external force, as in our collision example. We now see that this quantity is conserved only in the approximation $v \ll c$. We will define the *relativistic momentum* $\mathbf{p}$ of a particle to have the following properties:

1. $\mathbf{p}$ is conserved in collisions.
2. $\mathbf{p}$ approaches $m\mathbf{u}$ as u/c approaches zero.

Let's apply the first of these conditions to the collision of the two balls that we just discussed, noting two important points. First, for each observer in Figure 2-1, the speed of each ball is unchanged by the elastic collision. It is either u_0 (for the observer's own ball) or $(u_y^2 + v^2)^{1/2} = u$ (for the other ball). Second, the failure of the conservation of momentum in the collision we described can't be due to the velocities because we used the Lorentz transformation to find the y components. It must have something to do with the mass! Let us write down the conservation of the y component of the momentum *as observed in S*, keeping the masses of the two balls straight by writing $m(u_0)$ for the S observer's own ball and $m(u)$ for the S' observer's ball.

$$\underset{\text{(before collision)}}{m(u_0)u_0 - m(u)u_{yB}} = \underset{\text{(after collision)}}{-m(u_0)u_0 + m(u)u_{yB}} \qquad \textbf{2-3}$$

Equation 2-3 can be readily rewritten as

$$\frac{m(u)}{m(u_0)} = \frac{u_0}{u_{yB}} \qquad \textbf{2-4}$$

If u_0 is small compared to the relative speed v of the reference frames, then it follows from Equation 2-2 that $u_{yB} \ll v$ and, therefore, $u \approx v$.

If we can now imagine the limiting case where $u_0 \to 0$, i.e., where each ball is at rest in its "home" frame so that the collision becomes a "grazing" one as B moves past A at speed $v = u$, then we conclude from Equations 2-2 and 2-4 that in order for Equation 2-3 to hold, i.e., for the momentum to be conserved,

$$\frac{m(u = v)}{m(u_0 = 0)} = \frac{u_0}{u_0\sqrt{1 - v^2/c^2}}$$

or

$$m(u) = \frac{m}{\sqrt{1 - v^2/c^2}} \qquad \textbf{2-5}$$

Equation 2-5 says that the observer in S *measures* the mass of ball B, moving relative to him at speed u, as equal to $1/(1 - v^2/c^2)^{1/2}$ times the rest mass of the ball, or its mass measured in the frame in which it is at rest. Notice that observers always measure the mass of an object that is in motion with respect to them to be larger than the value measured when the object is at rest.

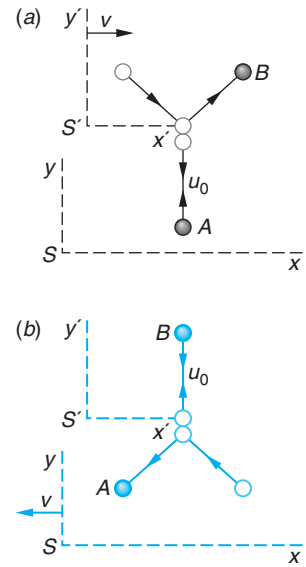

Figure 2-1 (*a*) Elastic collision of two identical balls as seen in frame S. The vertical component of the velocity of ball B is u_0/γ in S if it is u_0 in S'. (*b*) The same collision as seen in S'. In this frame, ball A has vertical component of velocity u_0/γ.

The design and construction of large particle accelerators throughout the world, such as CERN's LHC, are based directly on the relativistic expressions for momentum and energy.

STUDENTS-HUB.com Uploaded By: Malak Obaid

Thus, we see that the law of conservation of momentum will be valid in relativity, provided that we write the momentum **p** of an object with rest mass m moving with velocity **u** relative to an inertial system S to be

$$\mathbf{p} = \frac{m\mathbf{u}}{\sqrt{1 - u^2/c^2}} \qquad \textbf{2-6}$$

where u is the speed of the particle. We therefore take this equation as the definition of relativistic momentum. It is clear that this definition meets our second criterion because the denominator approaches 1 when u is much less than c. From this definition, the momenta of the two balls A and B in Figure 2-1 as seen in S are

$$p_{yA} = \frac{mu_0}{\sqrt{1 - u_0^2/c^2}} \qquad p_{yB} = \frac{mu_{yB}}{\sqrt{1 - (u_{xB}^2 + u_{yB}^2)/c^2}}$$

where $u_{yB} = u_0(1 - v^2/c^2)^{1/2}$ and $u_{xB} = v$. It is similarly straightforward to show that $p_{yB} = -p_{yA}$. Because of the similarity of the factor $1/\sqrt{1 - u^2/c^2}$ and γ in the Lorentz transformation, Equation 2-6 is often written

$$\mathbf{p} = \gamma m\mathbf{u} \quad \text{with} \quad \gamma = \frac{1}{\sqrt{1 - u^2/c^2}} \qquad \textbf{2-7}$$

This use of the symbol γ for two different quantities causes some confusion; the notation is standard, however, and simplifies many of the equations. We will use this notation except when we are also considering transformations between reference frames. Then, to avoid confusion, we will write out the factor $1/(1 - u^2/c^2)^{1/2}$ and reserve γ for $1/(1 - v^2/c^2)^{1/2}$, where v is the relative speed of the frames. Figure 2-2 shows a graph of the magnitude of **p** as a function of u/c. The quantity $m(u)$ in Equation 2-5 is sometimes called the *relativistic mass*; however, we will avoid using the term or a symbol for relativistic mass: in this book *m always* refers to the mass

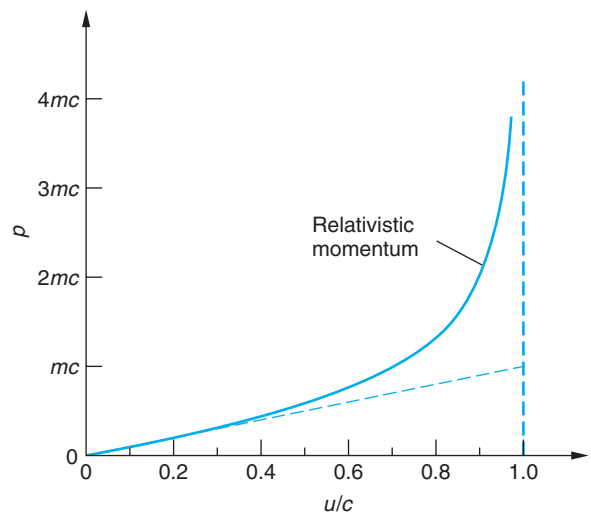

Figure 2-2 Relativistic momentum as given by Equation 2-6 versus u/c, where u = speed of the object relative to an observer. The magnitude of the momentum p is plotted in units of mc. The fainter dashed line shows the classical momentum mu for comparison.

STUDENTS-HUB.com Uploaded By: Malak Obaid

measured in the rest frame. In this we are following Einstein's view. In a letter to a colleague in 1948 he wrote:[3]

> It is not good to introduce the concept of mass $M = m/(1 - v^2/c^2)^{1/2}$ of a body for which no clear definition can be given. It is better to introduce no other mass than "the rest mass" m. Instead of introducing M, it is better to mention the expression for the momentum and energy of a body in motion.

EXAMPLE 2-1 Measured Values of Moving Mass For what value of u/c will the measured mass of an object γm exceed the rest mass by a given fraction f?

SOLUTION

From Equation 2-5 we see that

$$f = \frac{\gamma m - m}{m} = \gamma - 1 = \frac{1}{\sqrt{1 - u^2/c^2}} - 1$$

Solving for u/c,

$$1 - u^2/c^2 = \frac{1}{(f + 1)^2} \longrightarrow u^2/c^2 = 1 - \frac{1}{(f + 1)^2}$$

or

$$u/c = \frac{\sqrt{f(f + 2)}}{f + 1}$$

from which we can compute the table of values below or the value of u/c for any other f. Note that the value of u/c that results in a given fractional increase f in the measured value of the mass is independent of m. A diesel locomotive moving at a particular u/c will be observed to have the same f as a proton moving with that u/c.

f	u/c	Example
10^{-12}	1.4×10^{-6}	jet fighter aircraft
5×10^{-9}	0.0001	Earth's orbital speed
0.0001	0.014	50-eV electron
0.01 (1%)	0.14	quasar 3C273
1.0 (100%)	0.87	quasar 0Q172
10	0.996	muons from cosmic rays
100	0.99995	some cosmic ray protons

EXAMPLE 2-2 Momentum of a Rocket A high-speed interplanetary probe with a mass $m = 50{,}000$ kg has been sent toward Pluto at a speed $u = 0.8c$. What is its momentum as measured by Mission Control on Earth? If, preparatory to landing on Pluto, the probe's speed is reduced to $0.4c$, by how much does its momentum change?

STUDENTS-HUB.com Uploaded By: Malak Obaid

SOLUTION

1. Assuming that the probe travels in a straight line toward Pluto, its momentum along that direction is given by Equation 2-6:

$$p = \frac{mu}{\sqrt{1 - u^2/c^2}} = \frac{(50{,}000\ \text{kg})(0.8c)}{\sqrt{1 - (0.8c)^2/c^2}}$$
$$= 6.7 \times 10^4\, c \cdot \text{kg} = 2.0 \times 10^{13}\ \text{kg} \cdot \text{m/s}$$

2. When the probe's speed is reduced, the momentum declines along the relativistic momentum curve in Figure 2-2. The new value is computed from the ratio:

$$\frac{p_{0.4c}}{p_{0.8c}} = \frac{m(0.4c)/\sqrt{1 - (0.4)^2}}{m(0.8c)/\sqrt{1 - (0.8)^2}}$$
$$= \frac{1}{2}\frac{\sqrt{1 - (0.8)^2}}{\sqrt{1 - (0.4)^2}}$$
$$= 0.33$$

3. The reduced momentum $p_{0.4c}$ is then given by

$$p_{0.4c} = 0.33 p_{0.8c}$$
$$= (0.33)(6.7 \times 10^4\, c \cdot \text{kg})$$
$$= 2.2 \times 10^4\, c \cdot \text{kg}$$
$$= 6.6 \times 10^{12}\ \text{kg} \cdot \text{m/s}$$

Remarks: Notice from Figure 2-2 that the incorrect classical value of $p_{0.8c}$ would have been $4.0 \times 10^4\ c \cdot \text{kg}$. Also, while the probe's speed was decreased to 1/2 its initial value, the momentum was decreased to 1/3 of the initial value.

Question

1. In our discussion of the inelastic collision of balls A and B, the collision was a "grazing" one in the limiting case. Suppose instead that the collision is a "head-on" one along the x axis. If the speed of S' (i.e., ball B) is low, say, $v = 0.1c$, what would a spacetime diagram of the collision look like?

2-2 Relativistic Energy

As noted in the preceding section, the fundamental character of the principle of conservation of total energy leads us to seek a definition of total energy in relativity that preserves the invariance of that conservation law in transformations between inertial systems. As with the definition of the relativistic momentum, Equation 2-6, we will require that the *relativistic total energy* E satisfy two conditions:

1. The total energy E of any isolated system is conserved.
2. E will approach the classical value when u/c approaches zero.

Let us first find a form for E that satisfies the second condition and then see if it also satisfies the first. We have seen that the quantity $m\mathbf{u}$ is not conserved in collisions but that $\gamma m\mathbf{u}$ is, with $\gamma = 1/(1 - u^2/c^2)^{1/2}$. We have also noted that Newton's second

STUDENTS-HUB.com Uploaded By: Malak Obaid

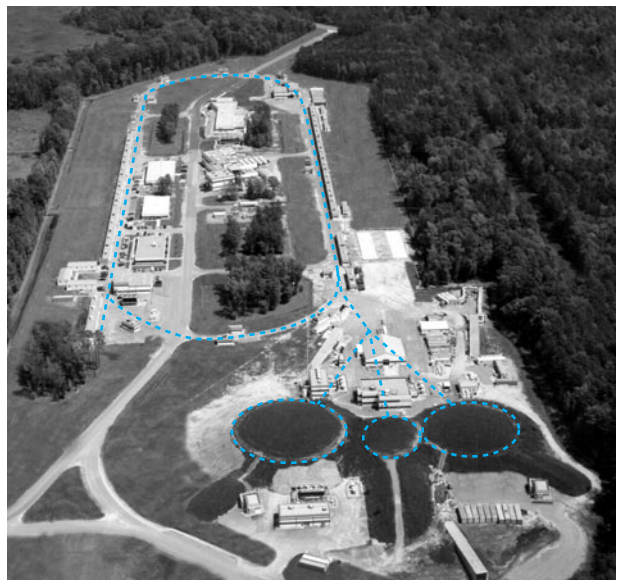

Aerial view of the Jefferson Laboratory's Continuous Electron Beam Accelerator Facility (CEBAF) in Virginia. The dashed line indicates the location of the underground accelerator, where electrons are accelerated to 6 GeV and reach speeds of more than 99.99 percent of the speed of light. The circles outline the experiment halls, also underground. [*Thomas Jefferson National Accelerator Facility/U.S. Department of Energy.*]

law in the form $\mathbf{F} = m\mathbf{a}$ cannot be correct relativistically, one reason being that it leads to the conservation of $m\mathbf{u}$. We can get a hint of the relativistically correct form of the second law by writing it $\mathbf{F} = d\mathbf{p}/dt$. This equation is relativistically correct *if* the relativistic momentum $\mathbf{p}$ is used. We thus define the force in relativity to be

$$\mathbf{F} = \frac{d\mathbf{p}}{dt} = \frac{d(\gamma m\mathbf{u})}{dt} \qquad \textbf{2-8}$$

Now, as in classical mechanics, we will define kinetic energy E_k as the work done by a net force in accelerating a particle from rest to some velocity u. Considering motion in one dimension only, we have

$$E_k = \int_{u=0}^{u} F\,dx = \int_0^u \frac{d(\gamma mu)}{dt}dx = \int_0^u u\,d(\gamma mu)$$

using $u = dx/dt$. The computation of the integral in this equation is not difficult but requires a bit of algebra. It is left as an exercise (Problem 2-2) to show that

$$d(\gamma mu) = m\left(1 - \frac{u^2}{c^2}\right)^{-3/2} du$$

Substituting this into the integrand of the equation for E_k above, we obtain

$$E_k = \int_0^u u\,d(\gamma mu) = \int_0^u m\left(1 - \frac{u^2}{c^2}\right)^{-3/2} u\,du$$

$$= mc^2\left(\frac{1}{\sqrt{1 - u^2/c^2}} - 1\right)$$

or

$$E_k = \gamma mc^2 - mc^2 \qquad \textbf{2-9}$$

STUDENTS-HUB.com Uploaded By: Malak Obaid

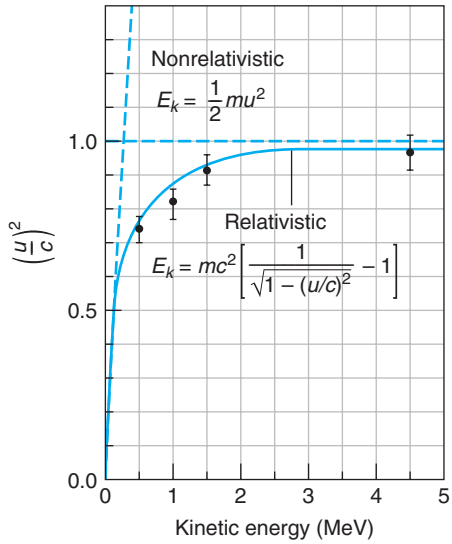

Figure 2-3 Experimental confirmation of the relativistic relation for kinetic energy. Electrons were accelerated to energies up to several MeV in large electric fields, and their velocities were determined by measuring their time of flight over 8.4 m. Note that when the velocity $u \ll c$, the relativistic and nonrelativistic (i.e., classical) relations are indistinguishable. [*W. Bertozzi, American Journal of Physics,* ***32****, 551 (1964).*]

Equation 2-9 defines the *relativistic kinetic energy*. Notice that, as we warned earlier, E_k is *not* $mu^2/2$ or even $\gamma mu^2/2$. This is strikingly evident in Figure 2-3. However, consistent with our second condition on the relativistic total energy E, Equation 2-9 does approach $mu^2/2$ when $u \ll c$. We can check this assertion by noting that for $u/c \ll 1$, expanding γ by the binomial theorem yields

$$\gamma = \left(1 - \frac{u^2}{c^2}\right)^{-1/2} = 1 + \frac{1}{2}\frac{u^2}{c^2} + \cdots$$

and thus

$$E_k = mc^2\left(1 + \frac{1}{2}\frac{u^2}{c^2} + \cdots - 1\right) \approx \frac{1}{2}mu^2$$

The expression for kinetic energy in Equation 2-9 consists of two terms. One term, γmc^2, depends on the speed of the particle (through the factor γ), and the other term, mc^2, is independent of the speed. The quantity mc^2 is called the *rest energy* of the particle, i.e., the energy associated with the rest mass m. The relativistic total energy E is then defined as the sum of the kinetic energy and the rest energy.

$$E = E_k + mc^2 = \gamma mc^2 = \frac{mc^2}{\sqrt{1 - u^2/c^2}} \qquad \textbf{2-10}$$

Thus, the work done by a net force increases the energy of the system from the rest energy mc^2 to γmc^2 (or increases the measured mass from m to γm).

For a particle at rest relative to an observer, $E_k = 0$, and Equation 2-10 becomes perhaps the most widely recognized equation in all of physics, Einstein's famous $E = mc^2$. When $u \ll c$, Equation 2-10 can be written as

$$E = \frac{1}{2}mu^2 + mc^2$$

STUDENTS-HUB.com Uploaded By: Malak Obaid

Before the development of relativity theory, it was thought that mass was a conserved quantity;[4] consequently, m would always be the same before and after an interaction or event and mc^2 would therefore be constant. Since the zero of energy is arbitrary, we are always free to include an additive constant; therefore, our definition of the relativistic total energy reduces to the classical kinetic energy for $u \ll c$ and our second condition on E is satisfied.[5]

Be very careful to understand Equation 2-10 correctly. It defines the total energy E, and E is what we are seeking to conserve for isolated systems in all inertial frames, *not* E_k and *not* mc^2. Remember, too, the distinction between *conserved* quantities and *invariant* quantities. The former have the same value before and after an interaction in a particular reference frame. The latter have the same value when measured by observers in different reference frames. Thus, we are not requiring observers in relatively moving inertial frames to measure the same values for E, but rather that E be unchanged in interactions as measured in each frame. To assist us in showing that E as defined by Equation 2-10 is conserved in relativity, we will first see how E and $\mathbf{p}$ transform between inertial reference frames.

Lorentz Transformation of E and $\mathbf{p}$

Consider a particle of rest mass m that has an arbitrary velocity $\mathbf{u}$ with respect to frame S, as shown in Figure 2-4. System S' is a second inertial frame moving in the $+x$ direction. The particle's momentum and energy are given in the S and S' systems, respectively, by,

In S:

$$\begin{aligned} E &= \gamma mc^2 \\ p_x &= \gamma m u_x \\ p_y &= \gamma m u_y \\ p_z &= \gamma m u_z \end{aligned} \qquad \textbf{2-11}$$

where

$$\gamma = 1/\sqrt{1 - u^2/c^2}$$

In S':

$$\begin{aligned} E' &= \gamma' mc^2 \\ p'_x &= \gamma' m u'_x \\ p'_y &= \gamma' m u'_y \\ p'_z &= \gamma' m u'_z \end{aligned} \qquad \textbf{2-12}$$

where

$$\gamma' = 1/\sqrt{1 - u'^2/c^2}$$

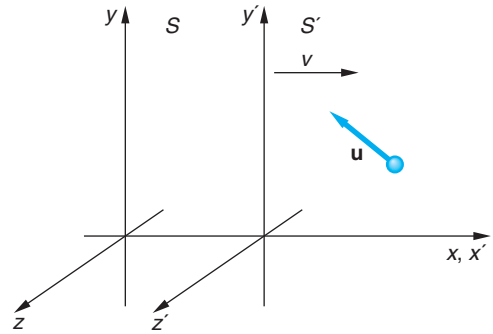

Figure 2-4 Particle of mass m moves with velocity $\mathbf{u}$ measured in S. System S' moves in the $+x$ direction at speed v. The Lorentz velocity transformation makes possible determination of the relations connecting measurements of the total energy and the components of the momentum in the two frames of reference.

Developing the Lorentz transformation for E and $\mathbf{p}$ requires that we first express γ' in terms of quantities measured in S. (We could just as well express γ in terms of primed quantities. Since this is relativity, it makes no difference which we choose.) The result is

$$\frac{1}{\sqrt{1 - u'^2/c^2}} = \gamma \frac{(1 - vu_x/c^2)}{\sqrt{1 - u^2/c^2}} \quad \text{where now} \quad \gamma = \frac{1}{\sqrt{1 - v^2/c^2}} \qquad \textbf{2-13}$$

STUDENTS-HUB.com Uploaded By: Malak Obaid

Substituting Equation 2-13 into the expression for E' in Equation 2-12 yields

$$E' = \frac{mc^2}{\sqrt{1 - u'^2/c^2}} = \gamma\left[\frac{mc^2}{\sqrt{1 - u^2/c^2}} - \frac{mc^2 v u_x/c^2}{\sqrt{1 - u^2/c^2}}\right]$$

The first term in the brackets you will recognize as E, and the second term, canceling the c^2 factors, as vp_x from Equation 2-11. Thus, we have

$$E' = \gamma(E - vp_x) \qquad \textbf{2-14}$$

Similarly, substituting Equation 2-13 and the velocity transformation for u'_x into the expression for p'_x in Equations 2-12 yields

$$p'_x = \frac{mu'_x}{\sqrt{1 - u'^2/c^2}} = \gamma\left[\frac{mu_x}{\sqrt{1 - u^2/c^2}} - \frac{mv}{\sqrt{1 - u^2/c^2}}\right]$$

The first term in the brackets is p_x from Equation 2-11, and, because $m(1 - u^2/c^2)^{-1/2} = E/c^2$, the second term is vE/c^2. Thus, we have

$$p'_x = \gamma(p_x - vE/c^2) \qquad \textbf{2-15}$$

Using the same approach, we can show (Problem 2-46) that

$$p'_y = p_y \quad \text{and} \quad p'_z = p_z$$

Together these relations are the *Lorentz transformation for momentum and energy*:

$$\begin{aligned} p'_x &= \gamma(p_x - vE/c^2) & p'_y &= p_y \\ E' &= \gamma(E - vp_x) & p'_z &= p_z \end{aligned} \qquad \textbf{2-16}$$

The inverse transformation is

$$\begin{aligned} p_x &= \gamma(p'_x + vE'/c^2) & p_y &= p'_y \\ E &= \gamma(E' + vp'_x) & p_z &= p'_z \end{aligned} \qquad \textbf{2-17}$$

with

$$\gamma = \frac{1}{\sqrt{1 - v^2/c^2}} = \frac{1}{\sqrt{1 - \beta^2}}$$

Note the striking similarity between Equations 2-16 and 2-17 and the Lorentz transformation of the space and time coordinates, Equations 1-18 and 1-19. The momentum $\mathbf{p}(p_x, p_y, p_z)$ transforms in relativity exactly like $\mathbf{r}(x, y, z)$, and the total energy E transforms like the time t. We will return to this remarkable result and related matters shortly, but first let's do some examples and then, as promised, show that the energy as defined by Equation 2-10 is conserved in relativity.

EXAMPLE 2-3 **Transforming Energy and Momentum** Suppose a micrometeorite of mass 10^{-9} kg moves past Earth at a speed of $0.01c$. What values will be measured for the energy and momentum of the particle by an observer in a system S' moving relative to Earth at $0.5c$ in the same direction as the micrometeorite?

STUDENTS-HUB.com Uploaded By: Malak Obaid

SOLUTION

Taking the direction of the micrometeorite's travel to be the x axis, the energy and momentum as measured by the Earth observer are, using the $u \ll c$ approximation of Equation 2-10:

$$E \approx \frac{1}{2}mu^2 + mc^2 = 10^{-9}\,\text{kg}[(0.01c)^2/2 + c^2]$$

$$E \approx 1.00005 \times 10^{-9}c^2\,\text{J}$$

and

$$p_x = mu_x = (10^{-9}\,\text{kg})(0.01c) = 10^{-11}c\,\text{kg}\cdot\text{m/s}$$

For this situation $\gamma = 1.1547$, so in S' the measured values of the energy and momentum will be

$$E' = \gamma(E - vp_x) = (1.1547)[1.00005 \times 10^{-9}c^2 - (0.5c)(10^{-11}c)]$$

$$E' = (1.1547)(1.00005 \times 10^{-9} - 0.5 \times 10^{-11})c^2$$

$$E' = 1.14898 \times 10^{-9}c^2\,\text{J}$$

and

$$p'_x = \gamma(p_x - vE/c^2) = (1.1547)[10^{-11}c - (0.5c)(1.00005 \times 10^{-9}c^2)/c^2]$$

$$p'_x = (1.1547)(10^{-11} - 5.00025 \times 10^{-10})c$$

$$p'_x = -5.66 \times 10^{-10}\,c\,\text{kg}\cdot\text{m/s} = -56.6 \times 10^{-11}\,c\,\text{kg}\cdot\text{m/s}$$

Thus, the observer in S' measures a total energy nearly 15 percent larger and a momentum more than 50 times greater and in the $-x$ direction.

EXAMPLE 2-4 A More Difficult Lorentz Transformation of Energy Suppose that a particle with mass m and energy E is moving toward the origin of a system S such that its velocity $\mathbf{u}$ makes an angle α with the y axis, as shown in Figure 2-5. Using the Lorentz transformation for energy and momentum, determine the energy E' of the particle measured by an observer in S', which moves relative to S so that the particle moves along the y' axis.

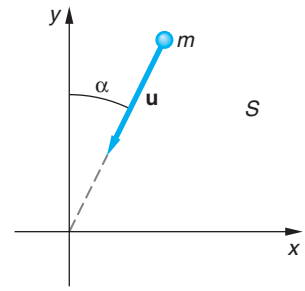

Figure 2-5 The system discussed in Example 2-4.

SOLUTION

System S' moves in the $-x$ direction at speed $u\sin\alpha$, as determined from the Lorentz velocity transformation for $u'_x = 0$. Thus, $v = -u\sin\alpha$. Also,

$$E = mc^2/\sqrt{1 - u^2/c^2} \qquad p = mu/\sqrt{1 - u^2/c^2}$$

and from the latter,

$$p = -\left(mu/\sqrt{1 - u^2/c^2}\right)\sin\alpha$$

In S' the energy will be

$$E' = \gamma(E - vp_x)$$

$$= \frac{1}{\sqrt{1 - v^2/c^2}}[E - (u\sin\alpha)\left(m - \mu/\sqrt{1 - v^2/c^2}\right)\sin\alpha]$$

$$= \frac{1}{\sqrt{1 - u^2\sin^2\alpha/c^2}}[E - \left(m/\sqrt{1 - u^2/c^2}\right)u^2\sin^2\alpha]$$

STUDENTS-HUB.com Uploaded By: Malak Obaid

Multiplying the second term in the brackets by c^2/c^2 and factoring an E from both terms yield

$$E' = E\sqrt{1 - (u^2/c^2)\sin\alpha}$$

Since $u < c$ and $\sin^2\alpha \leq 1$, we see that $E' < E$, except for $\alpha = 0$ when $E' = E$, in which case S and S' are the same system. Note, too, that for $\alpha > 0$, if $u \to c$, $E' \to E\cos\alpha$. As we will see later, this is the case for light.

Question

2. Recalling the results of the measurements of time and space intervals by observers in motion relative to clocks and measuring rods, discuss the results of corresponding measurements of energy and momentum changes.

Conservation of Energy

As with our discussion of momentum conservation in relativity, let us consider a collision of two identical particles, each with rest mass m. This time, for a little variety, we will let the collision be completely inelastic—i.e., when the particles collide, they stick together. In the system S', called the *zero momentum frame*, the particles approach each other along the x' axis with equal speeds u—hence equal and opposite momenta—as illustrated in Figure 2-6*a*. In this frame the collision results in the formation of a composite particle of mass M at rest in S'. If S' moves with respect to a second frame S at speed $v = u$ in the x direction, then the particle on the right before the collision will be at rest in S and the composite particle will move to the right at speed u in that frame. This situation is illustrated in Figure 2-6*b*.

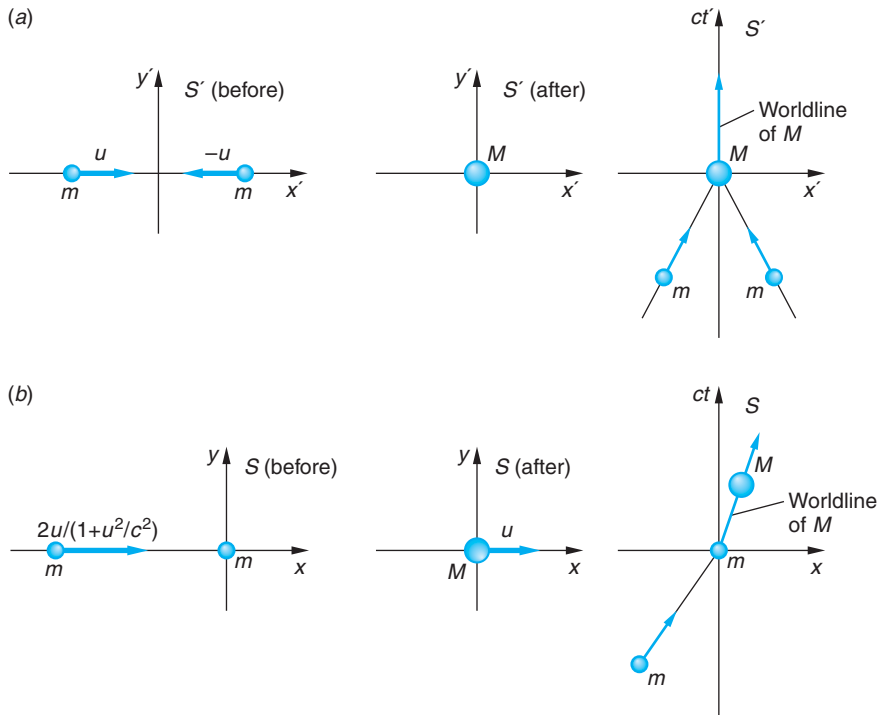

Figure 2-6 Inelastic collision of two particles of equal rest mass m. (*a*) In the zero momentum frame S' the particles have equal and opposite velocities and hence momenta. After the collision, the composite particle of mass M is at rest in S'. The diagram on the far right is the spacetime diagram of the collision from the viewpoint of S'. (*b*) In system S the frame S' is moving to the right at speed u so that the particle on the right is at rest in S, while the left one moves at $2u/(1 + u^2/c^2)$. After collision, the composite particle moves to the right at speed u. Again, the spacetime diagram of the interaction is shown on the far right. All diagrams are drawn with the collision occurring at the origin.

STUDENTS-HUB.com Uploaded By: Malak Obaid

Using the total energy as defined by Equation 2-10, we have in S':

Before collision:

$$E'_{\text{before}} = \frac{mc^2}{\sqrt{1 - u^2/c^2}} + \frac{mc^2}{\sqrt{1 - u^2/c^2}} = \frac{2mc^2}{\sqrt{1 - u^2/c^2}} \qquad \textbf{2-18}$$

After collision:

$$E'_{\text{after}} = Mc^2 \qquad \textbf{2-19}$$

Energy will be conserved in S' if $E'_{\text{before}} = E'_{\text{after}}$, i.e., if

$$\frac{2mc^2}{\sqrt{1 - u^2/c^2}} = Mc^2 \qquad \textbf{2-20}$$

This is ensured by the validity of conservation of momentum, in particular by Equation 2-5, and so energy is conserved in S'. (The validity of Equation 2-20 is important and not trivial. We will consider it in more detail in Example 2-7.) To see if energy as we have defined it is also conserved in S, we transform to S using the inverse transform, Equation 2-17. We then have in S:

Before collision:

$$E_{\text{before}} = \gamma(E'_{\text{before}} + vp'_x)$$

$$E_{\text{before}} = \gamma\left(\frac{2mc^2}{\sqrt{1 - u^2/c^2}} + up'_x\right)$$

$$E_{\text{before}} = \left(\frac{2mc^2}{\sqrt{1 - u^2/c^2}}\right) \quad \text{since} \quad p'_x = 0 \qquad \textbf{2-21}$$

After collision:

$$E_{\text{after}} = \gamma(Mc^2 + up'_x) = \gamma Mc^2 \quad \text{since again} \quad p'_x = 0 \qquad \textbf{2-22}$$

The energy will be conserved in S and, therefore, the law of conservation of energy will hold in all inertial frames if $E_{\text{before}} = E_{\text{after}}$, i.e., if

$$\gamma\left(\frac{2mc^2}{\sqrt{1 - u^2/c^2}}\right) = \gamma Mc^2 \qquad \textbf{2-23}$$

which, like Equation 2-20, is ensured by Equation 2-5. Thus, we conclude that the energy as defined by Equation 2-10 is consistent with a relativistically invariant law of conservation of energy, satisfying the first of the conditions set forth at the beginning of this section. While this demonstration was not a general one, since that is beyond the scope of our discussions, you may be assured that our conclusion is quite generally valid.

Question

3. Explain why the result of Example 2-4 does not mean that energy conservation is violated.

STUDENTS-HUB.com Uploaded By: Malak Obaid

EXAMPLE 2-5 **Mass of Cosmic Ray Muons** In Chapter 1, muons produced as secondary particles by cosmic rays were used to illustrate both the relativistic length contraction and time dilation resulting from their high speed relative to observers on Earth. That speed is about $0.998c$. If the rest energy of a muon is 105.7 MeV, what will observers on Earth measure for the total energy of a cosmic ray–produced muon? What will they measure for its mass?

SOLUTION

The electron volt (eV), the amount of energy acquired by a particle with electric charge equal in magnitude to that on an electron (e) accelerated through a potential difference of 1 volt, is a convenient unit in physics, as you may have learned. It is defined as

$$1.0\text{ eV} = 1.602 \times 10^{-19}\text{ C} \times 1.0\text{ V} = 1.602 \times 10^{-19}\text{ J} \qquad \textbf{2-24}$$

Commonly used multiples of the eV are the keV (10^3 eV), the MeV (10^6 eV), the GeV (10^9 eV), and the TeV (10^{12} eV). Many experiments in physics involve the measurement and analysis of the energy and/or momentum of particles and systems of particles, and Equation 2-10 allows us to express the masses of particles in energy units rather than the SI unit of mass, the kilogram. That and the convenient size of the eV facilitate[6] numerous calculations. For example, the mass of an electron is 9.11×10^{-31} kg. Its rest energy is given by

$$E = mc^2 = 9.11 \times 10^{-31}\text{ kg} \cdot c^2 = 8.19 \times 10^{-14}\text{ J}$$

or

$$E = 8.19 \times 10^{-14}\text{ J} \times \frac{1}{1.602 \times 10^{-19}\text{ J/eV}} = 5.11 \times 10^5\text{ eV}$$

or

$$E = 0.511\text{ MeV} \quad \textbf{rest energy} \text{ of the electron}$$

The mass of the particle is often expressed with the same number thus:

$$m = \frac{E}{c^2} = 0.511\text{ MeV}/c^2 \quad \textbf{mass} \text{ of the electron}$$

Now, applying the above to the muons produced by cosmic rays, each has a total energy E given by

$$E = \gamma mc^2 = \frac{1}{\sqrt{1 - (0.998c)^2/c^2}} \times 105.7\,\frac{\text{MeV}}{c^2} \times c^2$$

$$E = 1670\text{ MeV}$$

and a measured mass (see Equation 2-5) of

$$\gamma m = E/c^2 = 1670\text{ MeV}/c^2$$

The dependence of the measured mass on the speed of the particle has been verified by numerous experiments. Figure 2-7 illustrates a few of those results.

STUDENTS-HUB.com Uploaded By: Malak Obaid

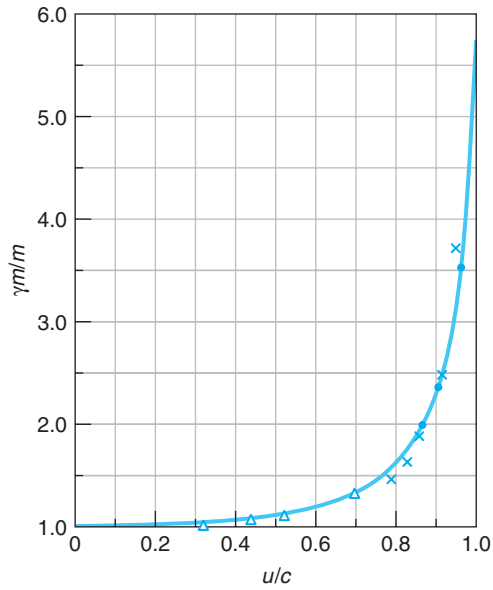

Figure 2-7 A few of the many experimental measurements of the mass of electrons as a function of their speed u/c. The data points are plotted onto Equation 2-5, the solid line. The data points represent the work of W. Kaufmann (×, 1901), A. H. Bucherer (Δ, 1908), and W. Bertozzi (●, 1964). Note that Kaufmann's work preceded the appearance of Einstein's 1905 paper on special relativity. Kaufmann used an incorrect mass for the electron and interpreted his results as support for classical theory. [*Adapted from Figure 3-4 in R. Resnick and D. Halliday, Basic Concepts in Relativity and Early Quantum Theory, 2d ed. (New York: Macmillan, 1992).*]

EXAMPLE 2-6 Change in the Solar Mass Compute the rate at which the Sun is losing mass, given that the mean radius R of Earth's orbit is 1.50×10^8 km and the intensity of solar radiation at Earth (called the solar constant) is 1.36×10^3 W/m^2.

SOLUTION

1. The conversion of mass into energy, a consequence of conservation of energy in relativity, is implied by Equation 2-10. With $u = 0$ that equation becomes

$$E = mc^2$$

2. Assuming that the Sun radiates uniformly over a sphere of radius R, the total power radiated by the Sun is given by

$$\begin{aligned} P &= (\text{area of the sphere})(\text{solar constant}) \\ &= (4\pi R^2)(1.36 \times 10^3 \text{ W/m}^2) \\ &= 4\pi(1.50 \times 10^{11} \text{ m})^2(1.36 \times 10^3 \text{ W/m}^2) \\ &= 3.85 \times 10^{26} \text{ J/s} \end{aligned}$$

3. Thus, every second the Sun emits 3.85×10^{26} J, which, from Equation 2-10, is the result of converting an amount of mass given by

$$\begin{aligned} m &= E/c^2 \\ &= \frac{3.85 \times 10^{26} \text{ J}}{(3.00 \times 10^8 \text{ m/s})^2} \\ &= 4.3 \times 10^9 \text{ kg} \end{aligned}$$

Remarks: *Thus, the Sun is losing 4.3×10^9 kg of mass (about 4 million metric tons) every second! If this rate of mass loss remains constant (which it will for the next few billion years) and with a fusion mass-to-energy conversion efficiency of about 1 percent, the Sun's present mass of about 2.0×10^{30} kg will "only" last for about 10^{11} more years!*

STUDENTS-HUB.com Uploaded By: Malak Obaid

EXPLORING
From Mechanics, Another Surprise

One consequence of the fact that Newton's second law, $\mathbf{F} = m\mathbf{a}$, is not relativistically invariant is yet another surprise—the lever paradox. Consider a lever of mass m at rest in S (Figure 2-8). Since the lever is at rest, the net torque τ_{net} due to the forces $\mathbf{F}_x$ and $\mathbf{F}_y$ is zero, i.e. (using magnitudes):

$$\tau_{net} = \tau_x + \tau_y = -F_x b + F_y a = 0$$

and therefore

$$F_x b = F_y a$$

An observer in system S' moving with $\beta = 0.866$ ($\gamma = 2$) with respect to S sees the lever moving in the $-x'$ direction and measures the torque to be

$$\begin{aligned}\tau'_{net} &= \tau'_x + \tau'_y = -F'_x b' + F'_y a' = -F_x b + (F_y/2)(a/2) \\ &= -F_x b + F_x b/4 = -(3/4)F_x b \neq 0\end{aligned}$$

where $F'_x = F_x$ and $F'_y = F_y/2$ (see Problem 2-53) and the lever is rotating!

The resolution of the paradox was first given by the German physicist Max von Laue (1879–1960). Recall that the net torque is the rate of change of the angular momentum $\mathbf{L}$. The S' observer measures the work done per unit time by the two forces as

For F'_x: $$-F'_x v = -F_x v$$

For F'_y: zero, since F'_y is perpendicular to the motion

and the change in mass Δm per unit time of the moving lever is

$$\frac{\Delta m}{\Delta t'} = \frac{\Delta E/c^2}{\Delta t'} = \frac{1}{c^2}\frac{\Delta E}{\Delta t'} = -\frac{1}{c^2}F_x v$$

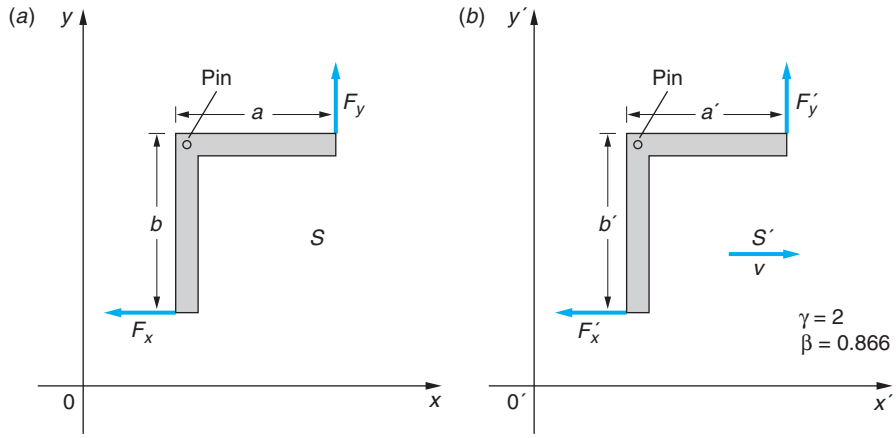

Figure 2-8 (*a*) A lever in the *xy* plane of system S is free to rotate about the pin P but is held at rest by the two forces F_x and F_y. (*b*) The same lever as seen by an observer in S' that is moving with instantaneous speed v in the $+x$ direction. For the S' observer the lever is moving in the $-x'$ direction.

STUDENTS-HUB.com Uploaded By: Malak Obaid

The S' observer measures a change in the magnitude of angular momentum per unit time given by

$$\tau_{net} = \frac{\Delta L'}{\Delta t'} = \frac{b\Delta p'}{\Delta t'} = \frac{bv\Delta m}{\Delta t'}$$

Substituting for $\Delta m/\Delta t'$ from above yields

$$\tau'_{net} = \frac{\Delta L'}{\Delta t'} = bv\frac{-F_x v}{c^2} = -bF_x\frac{v^2}{c^2} = -bF_x\beta^2 = -\frac{3}{4}F_x b$$

As a result of the motion of the lever relative to S', an observer in that system sees the force F'_x doing net work on the lever, thus changing the angular momentum over time, and the paradox vanishes. (The authors thank Costas Efthimiou for bringing this paradox to our attention.)

2-3 Mass/Energy Conversion and Binding Energy

The identification of the term mc^2 as rest energy is not merely a convenience. Whenever additional energy ΔE in any form is stored in an object, the mass of the object is increased by $\Delta E/c^2$. This is of particular importance whenever we want to compare the mass of an object that can be broken into constituent parts with the mass of the parts (for example, an atom containing a nucleus and electrons, or a nucleus containing protons and neutrons). In the case of the atom, the mass changes are usually negligibly small (see Example 2-8). However, the difference between the mass of a *nucleus* and that of its constituent parts (protons and neutrons) is often of great importance.

As an example, consider Figure 2-9*a* in which two particles, each with mass m, are moving toward each other with speeds u. They collide with a spring that compresses and locks shut. (The spring is merely a device for visualizing energy storage.) In the Newtonian mechanics description, the original kinetic energy $E_k = 2\left(\frac{1}{2}mu^2\right)$ is converted into potential energy of the spring U. When the spring is unlocked, the potential energy reappears as kinetic energy of the particles. In relativity theory, the internal energy of the system, $E_k = U$, appears as an increase in the rest mass of the system. That is, the mass of the system M is now greater than $2m$ by E_k/c^2. (We will derive this result in the next example.) This change in mass is too small to be observed for ordinary-size masses and springs, but it is easily observed in transformations that involve nuclei. For example, in the fission of a ^{235}U nucleus, the energy released as kinetic energy of the fission fragments is an appreciable fraction of the rest energy of the original nucleus. (See Example 11-19.) This energy can be calculated by measuring the difference between the mass of the original system and the total mass of the fragments. Einstein was the first to point out this possibility in 1905, even before the discovery of the atomic nucleus, at the end of a very short paper that followed his famous article on relativity.[7] After deriving the theoretical equivalence of energy and mass, he wrote:

> It is not impossible that with bodies whose energy content is variable to a high degree (e.g., with radium salts) the theory may be successfully put to the test.

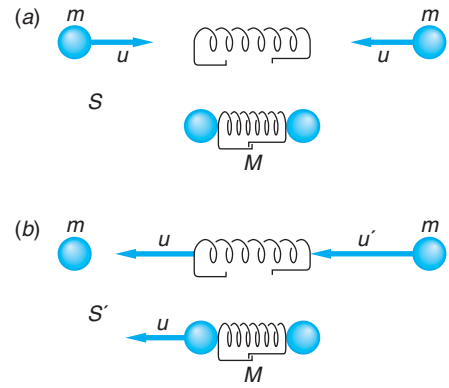

Figure 2-9 Two objects colliding with a massless spring that locks shut. The total rest mass of the system M is greater than that of the parts $2m$ by the amount E_k/c^2, where E_k is the internal energy, which in this case is the original kinetic energy. (*a*) The event as seen in a reference frame S in which the final mass M is at rest. (*b*) The same event as seen in a frame S' moving to the right at speed u relative to S, so that one of the initial masses is at rest.

The relativistic conversion of mass into energy is the fundamental energy source in the nuclear reactor–based systems that produce electricity in 30 nations and in large naval vessels and nuclear submarines.

STUDENTS-HUB.com Uploaded By: Malak Obaid

EXAMPLE 2-7 **Change in the Rest Mass of the Two-Particle and Spring System of Figure 2-9** Derive the increase in the rest mass of a system of two particles in a totally inelastic collision. Let m be the mass of each particle so that the total mass of the system is $2m$ when the particles are at rest and far apart, and let M be the rest mass of the system when it has internal energy E_k. The original kinetic energy in the reference frame S (Figure 2-9*a*) is

$$E_k = 2mc^2(\gamma - 1) \qquad \textbf{2-25}$$

SOLUTION

In a perfectly inelastic collision, momentum conservation implies that both particles are at rest after collision in this frame, which is the center-of-mass frame. The total kinetic energy is therefore lost. We wish to show that if momentum is to be conserved in any reference frame moving with a constant velocity relative to S, the total mass of the system must increase by Δm, given by

$$\Delta m = \frac{E_k}{c^2} = 2m(\gamma - 1) \qquad \textbf{2-26}$$

We therefore wish to show that the total mass of the system with internal energy is M, given by

$$M = 2m + \Delta m = 2\gamma m \qquad \textbf{2-27}$$

To simplify the mathematics, we chose a second reference frame S' moving to the right with speed $v = u$ relative to frame S so that one of the particles is initially at rest, as shown in Figure 2-9*b*. The initial speed of the other particle in this frame is

$$u' = \frac{u - v}{1 - uv/c^2} = \frac{-2u}{1 + u^2/c^2} \qquad \textbf{2-28}$$

After collision, the particles move together with speed u toward the left (since they are at rest in S). The initial momentum in S' is

$$p'_i = \frac{mu'}{\sqrt{1 - u'^2/c^2}} \quad \text{to the left}$$

The final momentum is

$$p'_f = \frac{Mu}{\sqrt{1 - u^2/c^2}} \quad \text{to the left}$$

Using Equation 2-28 for u', squaring, dividing by c^2, and adding -1 to both sides gives

$$1 - \frac{u'^2}{c^2} = 1 - \frac{4u^2/c^2}{(1 + u^2/c^2)^2} = \frac{(1 - u^2/c^2)^2}{(1 + u^2/c^2)^2}$$

Then

$$p'_i = \frac{m[2u/(1 + u^2/c^2)]}{(1 - u^2/c^2)/(1 + u^2/c^2)} = \frac{2mu}{(1 - u^2/c^2)}$$

STUDENTS-HUB.com Uploaded By: Malak Obaid

Conservation of momentum in frame S' requires that $p'_f = p'_i$, or

$$\frac{Mu}{\sqrt{1 - u^2/c^2}} = \frac{2mu}{1 - u^2/c^2}$$

Solving for M, we obtain

$$M = \frac{2m}{\sqrt{1 - u^2/c^2}} = 2\gamma m$$

which is Equation 2-27. Thus, the measured value of M would be $2\gamma m$.

If the latch in Figure 2-9*b* were to suddenly come unhooked, the two particles would fly apart with equal momenta, converting the rest mass Δm back into kinetic energy. The derivation is similar to that in Example 2-7.

Mass and Binding Energy

When a system of particles is held together by attractive forces, energy is required to break up the system and separate the particles. The magnitude of this energy E_b is called the *binding energy* of the system. An important result of the special theory of relativity that we will illustrate by example in this section is

> The mass of a bound system is less than that of the separated particles by E_b/c^2, where E_b is the binding energy.

In atomic and nuclear physics, masses and energies are typically given in atomic mass units (u) and electron volts (eV) rather than in standard SI units of kilograms and joules. The u is related to the corresponding SI units by

$$1 \text{ u} = 1.66054 \times 10^{-27} \text{ kg} = 931.494 \text{ MeV}/c^2 \qquad \textbf{2-29}$$

(The eV was defined in terms of the joule in Equation 2-24.) The rest energies of some elementary particles and a few light nuclei are given in Table 2-1, from which you can see by comparing the sums of the masses of the constituent particles with the nuclei listed that the mass of a nucleus is not the same as the sum of the masses of its parts.

The simplest example of nuclear binding energy is that of the deuteron, ^{2}H, which consists of a neutron and a proton bound together. Its rest energy is 1875.613 MeV. The sum of the rest energies of the proton and neutron is 938.272 + 939.565 = 1877.837 MeV. Since this is greater than the rest energy of the deuteron, the deuteron cannot *spontaneously* break up into a neutron and a proton without violating conservation of energy. The binding energy of the deuteron is 1877.837 − 1875.613 = 2.224 MeV. In order to break up a deuteron into a proton and a neutron, at least 2.224 MeV must be added. This can be done by bombarding deuterons with energetic particles or electromagnetic radiation. If a deuteron is formed by combination of a neutron and a proton (fusion; see Chapter 11), the same amount of energy is released.

STUDENTS-HUB.com Uploaded By: Malak Obaid

Table 2-1 Rest energies of some elementary particles and light nuclei

Particle	Symbol	Rest energy (MeV)
Photon	γ	0
Neutrino (antineutrino)	ν ($\overline{\nu}$)	$<2.8 \times 10^{-6}$
Electron (positron)	e or e^- (e^+)	0.5110
Muon	μ^- μ^+	105.7
Pi mesons (pions)	π^- (π^0) π^+	139.6 (135) 139.6
Proton	p	938.272
Neutron	n	939.565
Deuteron	^{2}H or d	1875.613
Helion	^{3}He or h	2808.391
Alpha	^{4}He or α	3727.379

EXAMPLE 2-8 **Binding Energy of the Hydrogen Atom** The binding energies of atomic electrons to the nuclei of atoms are typically of the order of 10^{-6} times those characteristic of particles in the nuclei; consequently, the mass differences are correspondingly smaller. The binding energy of the hydrogen atom (the energy needed to remove the electron from the atom) is 13.6 eV. How much mass is lost when an electron and a proton form a hydrogen atom?

SOLUTION

The mass of the proton plus that of the electron must be greater than that of the hydrogen atom by

$$\frac{13.6 \text{ eV}}{931.5 \text{ MeV/u}} = 1.46 \times 10^{-8} \text{ u}$$

This mass difference is so small that it is usually neglected.

2-4 Invariant Mass

In Chapter 1 we discovered that as a consequence of Einstein's relativity postulates, the coordinates for space and time are linearly dependent on one another in the Lorentz transformation that connects measurements made in different inertial reference frames. Thus, the time t became a coordinate, in addition to the space coordinates x, y, and z, in the four-dimensional relativistic "world" that we call spacetime. We note in passing that the geometry of spacetime was not the familiar Euclidean geometry of our three-dimensional world, but the four-dimensional Lorentz geometry. The difference became apparent when one compared the computation of the distance r between two points in space with that of the interval between two events in spacetime. The former is, of course, the vector $\mathbf{r}$, whose magnitude is given by $r^2 = x^2 + y^2 + z^2$. The vector $\mathbf{r}$ is unchanged (invariant) under a Galilean transformation in space, and quantities that transform like $\mathbf{r}$ are also vectors. The latter we called the spacetime interval Δs, and its magnitude, as we have seen, is given by

$$(\Delta s)^2 = (c\Delta t)^2 - [(\Delta x)^2 + (\Delta y)^2 + (\Delta z)^2] \qquad \textbf{2-30}$$

STUDENTS-HUB.com Uploaded By: Malak Obaid

The interval Δs is the four-dimensional analog of $\mathbf{r}$ and therefore is called a *four-vector*. Just as x, y, and z are the components of the three-vector $\mathbf{r}$, the components of the four-vector Δs are Δx, Δy, Δz, and $c\Delta t$. We have seen that Δs is also invariant under a Lorentz transformation in spacetime. Correspondingly, any quantity that transforms like Δs—i.e., is invariant under a Lorentz transformation—will also be a four-vector. The physical significance of the invariant interval Δs is quite profound: for timelike intervals $\Delta s/c = \tau$ (the proper time interval), for spacelike intervals $\Delta s = L_p$ (the proper length), and the proper intervals can be found from measurements made in *any* inertial frame.[8]

In the relativistic energy and momentum we have components of another four-vector. In the preceding sections we saw that the momentum and energy, defined by Equations 2-6 and 2-10, respectively, were not only both conserved in relativity, but also together satisfied the Lorentz transformation, Equations 2-16 and 2-17, with the components of the momentum $\mathbf{p}(p_x, p_y, p_z)$ transforming like the space components of $\mathbf{r}(x, y, z)$ and the energy transforming like the time t. The questions then are, What invariant four-vectors are they components of? and, What is its physical significance? The answers to both turn out to be easy to find and yield for us yet another relativistic surprise. By squaring Equations 2-6 and 2-10, you can readily verify that

$$E^2 = (pc)^2 + (mc^2)^2 \qquad \textbf{2-31}$$

This very useful relation we will rearrange slightly to

$$(mc^2)^2 = E^2 - (pc)^2 \qquad \textbf{2-32}$$

Comparing the form of Equation 2-32 with that of Equation 2-30 and knowing that E and $\mathbf{p}$ transform according to the Lorentz transformation, we see that *the magnitude of the invariant energy/momentum four-vector is the rest energy of the mass m*! Thus, observers in all inertial frames will measure the same value for the rest energy of isolated systems and, since c is constant, the same value for the mass. Note that only in the rest frame of the mass m, i.e., the frame where $\mathbf{p} = 0$, are the rest energy and the total energy equal. Even though we have written Equation 2-31 for a single particle, we could as well have written the equations for momentum and energy in terms of the total momentum and total energy of an entire ensemble of noninteracting particles with arbitrary velocities. We would only need to write down Equations 2-6 and 2-10 for each particle and add them together. Thus, the Lorentz transformation for momentum and energy, Equations 2-16 and 2-17, holds for any system of particles and so therefore does the invariance of the rest energy expressed by Equation 2-32.

We may state all of this more formally by saying that the *kinematic* state of the system is described by the four-vector Δs where

$$(\Delta s)^2 = (c\Delta t)^2 - [(\Delta x)^2 + (\Delta y)^2 + (\Delta z)^2]$$

and its *dynamic* state is described by the energy/momentum four-vector mc^2, given by

$$(mc^2)^2 = E^2 - (pc)^2$$

The next example illustrates how this works.

STUDENTS-HUB.com Uploaded By: Malak Obaid

EXAMPLE 2-9 Rest Mass of Moving Object A particular object is observed to move through the laboratory at high speed. Its total energy and the components of its momentum are measured by lab workers to be (in SI units) $E = 4.5 \times 10^{17}$ J, $p_x = 3.8 \times 10^8$ kg · m/s, $p_y = 3.0 \times 10^8$ kg · m/s, and $p_z = 3.0 \times 10^8$ kg · m/s. What is the object's rest mass?

SOLUTION A

From Equation 2-32 we can write

$$\begin{aligned}(mc^2)^2 &= (4.5 \times 10^{17})^2 - [(3.8 \times 10^8 c)^2 + (3.0 \times 10^8 c)^2 + (3.0 \times 10^8 c)^2] \\ &= (4.5 \times 10^{17})^2 - [1.4 \times 10^{17} + 9.0 \times 10^{16} + 9.0 \times 10^{16}]c^2 \\ &= 2.0 \times 10^{35} - 2.9 \times 10^{34} \\ &= 1.74 \times 10^{35}\ \text{J}^2 \\ m &= (1.74 \times 10^{35}\ \text{J}^2)^{1/2}/c^2 = 4.6\ \text{kg}\end{aligned}$$

SOLUTION B

A slightly different but sometimes more convenient calculation that doesn't involve carrying along large exponentials makes use of Equation 2-32 divided by c^4:

$$m^2 = \left(\frac{E}{c^2}\right)^2 - \left(\frac{p}{c}\right)^2 \qquad \textbf{2-33}$$

Notice that this is simply a unit conversion, expressing each term in (mass)^2 units—e.g., kg^2 when E and p are in SI units:

$$\begin{aligned}m^2 &= \left(\frac{4.5 \times 10^{17}}{c^2}\right)^2 - \left[\left(\frac{3.8 \times 10^8}{c}\right)^2 + \left(\frac{3.0 \times 10^8}{c}\right)^2 + \left(\frac{3.0 \times 10^8}{c}\right)^2\right] \\ &= (5.0)^2 - [(1.25)^2 + (1.0)^2 + (1.0)^2] \\ &= 25 - 3.56 \\ m &= (21.4)^{1/2} = 4.6\ \text{kg}\end{aligned}$$

In the example, we determined the rest energy and mass of a rapidly moving object using measurements made in the laboratory without the need to be in the system in which the object was at rest. This ability is of enormous benefit to nuclear, particle, and astrophysicists, whose work regularly involves particles moving at speeds close to that of light. For particles or objects whose rest mass is known, we can use the invariant magnitude of the energy/momentum four-vector to determine the values of other dynamic variables, as illustrated in the next example.

EXAMPLE 2-10 Speed of a Fast Electron The total energy of an electron produced in a particular nuclear reaction is measured to be 2.40 MeV. Find the electron's momentum and speed in the laboratory frame. (The rest mass of an electron is 9.11×10^{-31} kg and its rest energy is 0.511 MeV.)

SOLUTION

The magnitude of the momentum follows immediately from Equation 2-31:

$$\begin{aligned}pc &= \sqrt{E^2 - (mc^2)^2} = \sqrt{(2.40\ \text{MeV})^2 - (0.511\ \text{MeV})^2} \\ &= 2.34\ \text{MeV} \\ p &= 2.34\ \text{MeV}/c\end{aligned}$$

STUDENTS-HUB.com Uploaded By: Malak Obaid

where we have again made use of the convenience of the eV as an energy unit. The resulting momentum unit MeV/c can be readily converted to SI units by converting the MeV to joules and dividing by c, i.e.,

$$1 \text{ MeV}/c = \frac{1.602 \times 10^{-13} \text{ J}}{2.998 \times 10^{8} \text{ m/s}} = 5.34 \times 10^{-22} \text{ kg} \cdot \text{m/s}$$

Therefore, the conversion to SI units is easily done, if desired, and yields

$$p = 2.34 \text{ MeV}/c \times \frac{5.34 \times 10^{-22} \text{ kg} \cdot \text{m/s}}{1 \text{ MeV}/c}$$

$$p = 1.25 \times 10^{-21} \text{ kg} \cdot \text{m/s}$$

The speed of the particle is obtained by noting from Equation 2-32 or from Equations 2-6 and 2-10 that

$$\frac{u}{c} = \frac{pc}{E} = \frac{2.34 \text{ MeV}}{2.40 \text{ MeV}} = 0.975 \qquad \textbf{2-34}$$

or

$$u = 0.975c$$

It is extremely important to recognize that the invariant rest energy in Equation 2-32 is that of the *system* and that its value is *not* the sum of the rest energies of the particles of which the system is formed, if the particles move relative to one another. Earlier we used numerical examples of the binding energy of atoms and nuclei that illustrated this fact by showing that the masses of the atoms and nuclei were less than the sum of the masses of their constituents by an amount Δmc^2 that equaled the observed binding energy, but those were systems of interacting particles—i.e., there were forces acting between the constituents. A difference exists, even when the particles do not interact. To see this, let us focus our attention on specifically *what* mass is invariant.

Consider two identical noninteracting particles, each of rest mass $m = 4$ kg moving toward each other along the x axis of S with momentum $p_x = 3c \cdot \text{kg}$, as illustrated in Figure 2-10*a*. The energy of each particle, using Equation 2-33, is

$$E/c^2 = \sqrt{m^2 + (p/c)^2} = \sqrt{(4)^2 + (3)^2} = 5 \text{ kg}$$

Thus, the total energy of the system is $5c^2 + 5c^2 = 10c^2$ kg, since the energy is a scalar. Similarly, the total momentum of the system is $3c \cdot \text{kg} - 3c \cdot \text{kg} = 0$, since the momentum is a vector and the momenta are equal and opposite. The rest mass of the system is then

$$m = \sqrt{(E/c^2)^2 - (p/c)^2} = \sqrt{(10)^2 - 0^2} = 10 \text{ kg}$$

Hence, the system mass of 10 kg is *greater* than the sum of the masses of the two particles, 8 kg. (This is in contrast to bound systems, such as atoms, where the system mass is *smaller* than the total of the constituents.) This difference is not binding energy, since the particles are noninteracting. Neither does the 2 kg "mass difference" reside equally with the two particles. In fact, it doesn't reside in any particular place but is a property of the entire system. The correct interpretation is that the mass *of the system* is 10 kg.

Although the invariance of the energy/momentum four-vector guarantees that observers in other inertial frames will also measure 10 kg as the mass of the system, let us allow for a skeptic or two and transform to another system S', e.g., the one shown in Figure 2-10*c*, just to be sure.

STUDENTS-HUB.com Uploaded By: Malak Obaid

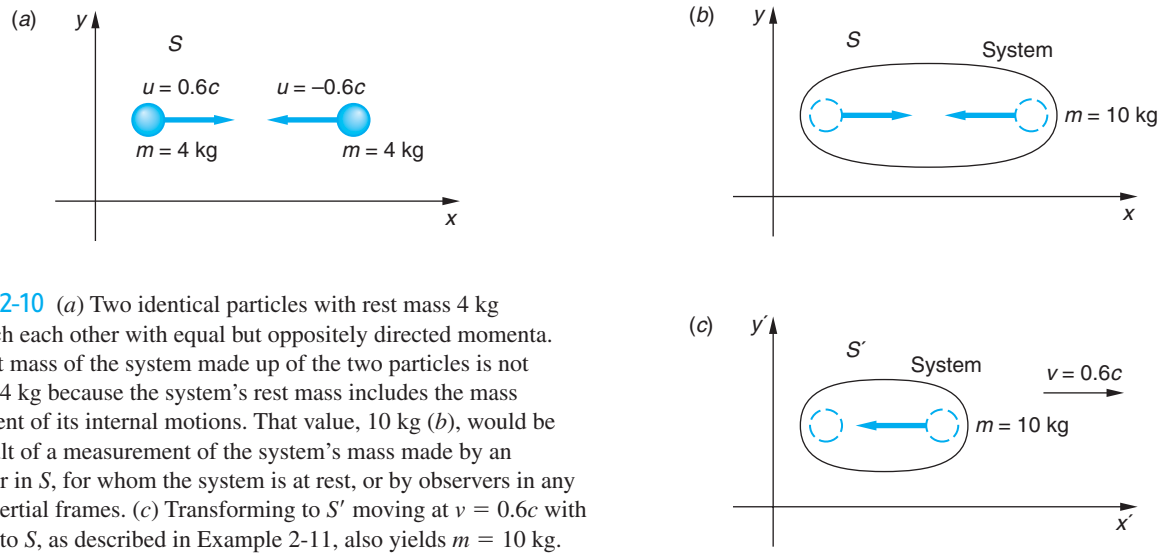

Figure 2-10 (*a*) Two identical particles with rest mass 4 kg approach each other with equal but oppositely directed momenta. The rest mass of the system made up of the two particles is not 4 kg + 4 kg because the system's rest mass includes the mass equivalent of its internal motions. That value, 10 kg (*b*), would be the result of a measurement of the system's mass made by an observer in *S*, for whom the system is at rest, or by observers in any other inertial frames. (*c*) Transforming to S' moving at $v = 0.6c$ with respect to *S*, as described in Example 2-11, also yields $m = 10$ kg.

EXAMPLE 2-11 Lorentz Transformation of System Mass For the system illustrated in Figure 2-10, show that an observer in S', which moves relative to *S* at $\beta = 0.6$, also measures the mass of the system to be 10 kg.

SOLUTION

1. The mass m measured in S' is given by Equation 2-33, which in this case is

$$m = [(E'/c^2)^2 - (p'_x/c)^2]^{1/2}$$

2. E' is given by Equation 2-16:

$$\begin{aligned} E' &= \gamma(E - vp_x) \\ &= \frac{1}{\sqrt{1 - (0.6)^2}}(10c^2 - 0.6c \times 0) \\ &= (1.25)(10c^2) \\ &= 12.5\ c^2 \cdot \text{kg} \end{aligned}$$

3. p'_x is also given by Equation 2-16:

$$\begin{aligned} p'_x &= \gamma(p_x - vE/c^2) \\ &= (1.25)[0 - (0.6c)(10c^2)/c^2] \\ &= -7.5\ c \cdot \text{kg} \end{aligned}$$

4. Substituting E' and p'_x into Equation 2-33 yields

$$\begin{aligned} m &= [(12.5c^2/c^2)^2 - (-7.5c/c)^2]^{1/2} \\ &= [(12.5)^2 - (-7.5)^2]^{1/2} \\ &= 10 \text{ kg} \end{aligned}$$

Remarks: *This result agrees with the value measured in S. The speed of S' chosen for this calculation, $v = 0.6c$, is convenient in that one of the particles constituting the system is at rest in S'; however, that has no effect on the generality of the solution.*

STUDENTS-HUB.com Uploaded By: Malak Obaid

Thus, we see that it is the rest energy of any isolated system that is invariant, whether that system is a single atom or the entire universe. And based on our discussions so far, we note that the system's rest energy may be greater than, equal to, or less than the sum of the rest energies of the constituents depending on their relative velocities and the detailed character of any interactions between them.

Questions

4. Suppose two loaded boxcars, each of mass $m = 50$ metric tons, roll toward each other on level track at identical speeds u, collide, and couple together. Discuss the mass of this system before and after the collision. What is the effect of the magnitude of u on your discussion?
5. In 1787 Count Rumford (1753–1814) tried unsuccessfully to measure an increase in the weight of a barrel of water when he increased its temperature from 29°F to 61°F. Explain why, relativistically, you would expect such an increase to occur, and outline an experiment that might, in principle, detect the change. Since Count Rumford preceded Einstein by about 100 years, why might he have been led to such a measurement?

Massless Particles

Equation 2-32 formally allows positive, negative, and zero values for $(mc^2)^2$, just as was the case for the spacetime interval $(\Delta s)^2$. We have been tacitly discussing positive cases so far in this section; a discussion of possible negative cases we will defer until Chapter 12. Here we need to say something about the $mc^2 = 0$ possibility. Note first of all that the idea of zero rest mass has no analog in classical physics since classically $E_k = mu^2/2$ and $\mathbf{p} = m\mathbf{u}$. If $m = 0$, then the momentum and kinetic energy are always zero too, and the "particle" seems to be nothing at all, experiencing no second-law forces, doing no work, and so forth. However, for $mc^2 = 0$, Equation 2-32 states that in relativity

$$E = pc \quad (\text{for } m = 0) \qquad \textbf{2-35}$$

and, together with Equation 2-34, that $u = c$, i.e., *a particle whose mass is zero moves at the speed of light*. Similarly, a particle whose speed is measured to be c will have $m = 0$ and satisfy $E = pc$.

We must be careful, however, because Equation 2-32 was obtained from the relativistic definitions of E and $\mathbf{p}$:

$$E = \gamma mc^2 = \frac{mc^2}{\sqrt{1 - u^2/c^2}} \qquad \mathbf{p} = \gamma m\mathbf{u} = \frac{m\mathbf{u}}{\sqrt{1 - u^2/c^2}}$$

As $u \to c$, $1/\sqrt{1 - u^2/c^2} \to \infty$; however, since m is also approaching zero, the quantity γm, which is tending toward $0/0$, can (and does) remain defined. Indeed, there is ample experimental evidence for the existence of particles with $mc^2 = 0$.

Current theories suggest the existence of three such particles. Perhaps the most important of these and the one thoroughly verified by experiment is the *photon*, a particle of electromagnetic radiation (i.e., light). Classically, electromagnetic radiation was interpreted via Maxwell's equations as a wave phenomenon, its energy and momentum being distributed continuously throughout the space occupied by the wave.

STUDENTS-HUB.com Uploaded By: Malak Obaid

It was discovered around 1900 that the classical view of light required modification in certain situations, the change being a confinement of the energy and momentum of the radiation into many tiny packets or bundles, which were referred to as photons. Photons move at light speed, of course, and, as we have noted, are required by relativity to have $mc^2 = 0$. Recall that the spacetime interval Δs for light is also zero. Strictly speaking, of course, the second of Einstein's relativity postulates prevents a Lorentz transformation to the rest system of light since light moves at c relative to all inertial frames. Consequently, the term *rest mass* has no operational meaning for light.

EXAMPLE 2-12 Rest Energy of a System of Photons Remember that the rest energy of a system of particles is not the sum of the rest energies of the individual particles if they move relative to one another. This applies to photons too! Suppose two photons, one with energy 5 MeV and the second with energy 2 MeV, approach each other along the x axis. What is the rest energy of this system?

SOLUTION

The momentum of the 5-MeV photon is (from Equation 2-35) $p_x = 5\ \text{MeV}/c$ and that of the 2-MeV photon is $p_x = -2\ \text{MeV}/c$. Thus, the energy of the system is $E = 5\ \text{MeV} + 2\ \text{MeV} = 7\ \text{MeV}$ and its momentum is $p = 5\ \text{MeV}/c - 2\ \text{MeV}/c = 3\ \text{MeV}/c$. From Equation 2-32 the system's rest energy is

$$mc^2 = \sqrt{(7\ \text{MeV})^2 - (3\ \text{MeV})^2} = 6.3\ \text{MeV}\ !!$$

A second particle whose rest energy is zero is the *gluon*. This massless particle transmits or carries the strong interaction between *quarks*, which are the "building blocks" of all fundamental particles, including protons and neutrons. The existence of gluons is well established experimentally. We will discuss quarks and gluons further in Chapter 12. Finally, there are strong theoretical reasons to expect that gravity is transmitted by a massless particle called the *graviton*, which is related to gravity in much the same way that the photon is related to the electromagnetic field. Gravitons, too, move at speed c. While direct detection of the graviton is beyond our current and foreseeable experimental capabilities, major international cooperative experiments are currently under way to detect gravity waves. (See Section 2-5.)

Until about the beginning of this century a fourth particle, the *neutrino*, was also thought to have zero rest mass. However, substantial experimental evidence collected by the Super-Kamiokande (Japan) and SNO (Canada) imaging neutrino detectors, among others, made it clear that neutrinos are not massless. We discuss neutrino mass and its implications further in Chapters 11 and 12.

Creation and Annihilation of Particles

The relativistic equivalence of mass and energy implies still another remarkable prediction that has no classical counterpart. As long as momentum and energy are conserved in the process,[9] elementary particles with mass can combine with their *antiparticles*, the masses of both being completely converted to energy in a process called *annihilation*. An example is that of an ordinary electron. An electron can orbit briefly with its antiparticle, called a *positron*,[10] but then the two unite, mutually annihilating and producing two or three photons. The two-photon version of this process is shown schematically in Figure 2-11. Positrons are produced naturally by cosmic rays in the upper atmosphere and as the result of the decay of certain radioactive nuclei. P. A. M. Dirac predicted their existence in 1928 while investigating the invariance of the energy/momentum four-vector.

STUDENTS-HUB.com Uploaded By: Malak Obaid

Figure 2-11 (*a*) A positron orbits with an electron about their common center of mass, shown by the dot between them. (*b*) After a short time, typically of the order of 10^{-10} s for the case shown here, the two annihilate, producing two photons. The orbiting electron-positron pair, suggestive of a miniature hydrogen atom, is called *positronium*.

If the speeds of both the electron and the positron $u \ll c$ (not a requirement for the process, but it makes the following calculation clearer), then the total energy of each particle is $E = mc^2 = 0.511$ MeV. Therefore, the total energy of the system in Figure 2-11*a* before annihilation is $2mc^2 = 1.022$ MeV. Also from the diagram, the momenta of the particles are always opposite and equal, and so the total momentum of the system is zero. Conservation of momentum then requires that the total momentum of the two photons produced also be zero, i.e., that they move in opposite directions relative to the original center of mass and have equal momenta. Since $E = pc$ for photons, then they must also have equal energy. Conservation of energy then requires that the energy of each photon be 0.511 MeV. (Photons are usually called *gamma rays* when their energies are a few hundred keV or higher.) Notice from Example 2-12 that the magnitude of the energy/momentum four-vector (the rest energy) is not zero, even though both of the final particles are photons. In this case it equals the rest energy of the initial system. Analysis of the three-photon annihilation, although the calculation is a bit more involved, is similar.

By now you will not be surprised to learn that the reverse process, the creation of mass from energy, can also occur under the proper circumstances. The conversion of mass and energy works both ways. The energy needed to create the new mass can be provided by the kinetic energy of another massive particle or by the "pure" energy of a photon. In either case, in determining what particles might be produced with a given amount of energy, it is important to be sure, as was the case with annihilation, that the appropriate conservation laws are satisfied. As we will discuss in detail in Chapter 12, this restricts the creation process for certain kinds of particles (including electrons, protons, and neutrons) to producing only particle-antiparticle pairs. This means, for example, that the energy in a photon cannot be used to create a single electron but must produce an electron-positron pair.

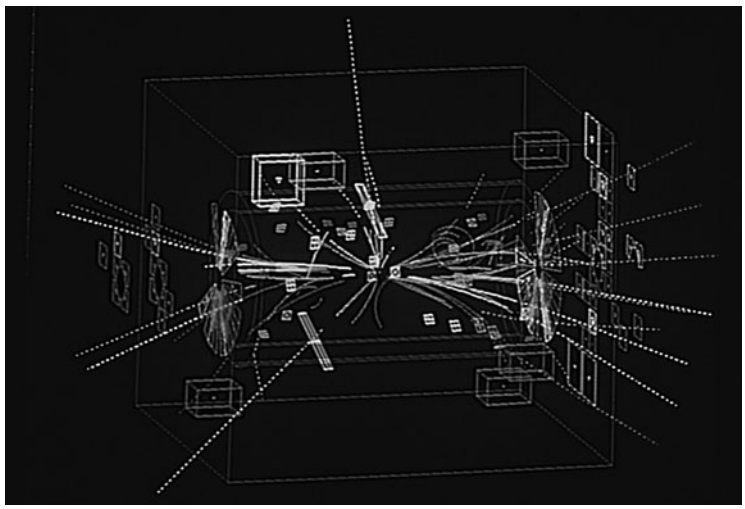

Decay of a Z into an electron-positron pair in the UA1 detectors at CERN. This is the computer image of the first Z event recorded (30 April 1983). The newly created pair leave the central detector in opposite directions at nearly the speed of light. [*CERN.*]

STUDENTS-HUB.com Uploaded By: Malak Obaid

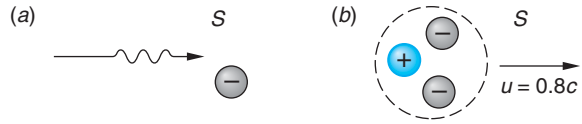

Figure 2-12 (*a*) A photon of energy E and momentum $p = E/c$ encounters an electron at rest. The photon produces an electron-positron pair (*b*), and the group move off together at speed $u = 0.8c$.

To see how relativistic creation of mass goes, let us consider a particular situation, the creation of an electron-positron pair from the energy of a photon. The photon moving through space encounters, or "hits," an electron at rest in frame S, as illustrated in Figure 2-12*a*.[11] Usually the photon simply scatters, but occasionally a pair is created. Encountering the existing electron is important since it is not possible for the photon to produce spontaneously the two rest masses of the pair and also conserve momentum. (See Problem 2-45.) Some other particle must be nearby, not to provide energy to the creation process, but to acquire some of the photon's initial momentum. In this case we have selected an electron for this purpose because it provides a neat example, but almost any particle would do. (See Example 2-13.)

While near the electron, the photon suddenly disappears, and an electron-positron pair appears. The process must occur very fast since the photon, moving at speed c, will travel across a region as large as an atom in about 10^{-19} s. Let's suppose that the details of the interaction that produced the pair are such that the three particles all move off together toward the right in Figure 2-12*b* with the same speed u—i.e., they are all at rest in S', which moves to the right with speed u relative to S.[12] What must the energy E_γ of the photon be for this particular electron-positron pair to be created? To answer this question, we first write the conservation of energy and momentum:

Before pair creation	**After pair creation**
$E_i = E_\gamma + mc^2$	$E_f = E_i = E_\gamma + mc^2$
$p_i = \dfrac{E_\gamma}{c}$	$p_f = p_i = \dfrac{E_\gamma}{c}$

where mc^2 = rest energy of an electron. In the final system after pair creation the total rest energy is $3mc^2$ in this case. We know this because the invariant rest energy equals the sum of the rest energies of the *constituent* particles (the original electron and the pair) in the system where they do not move relative to one another, i.e., in S'. So in S' we have for the system after pair creation

$$(3mc^2)^2 = E^2 - (pc)^2$$

$$9(mc^2)^2 = (E_\gamma + mc^2)^2 - \left(\frac{E_\gamma c}{c}\right)^2$$

$$9(mc^2)^2 = E_\gamma^2 + 2E_\gamma mc^2 + (mc^2)^2 - E_\gamma^2$$

Noting that the E_γ^2 terms cancel and dividing the remaining terms by mc^2, we see that

$$E_\gamma = 4mc^2$$

STUDENTS-HUB.com Uploaded By: Malak Obaid

Thus, the initial photon needs energy equal to 4 electron rest energies in order to create 2 new electron rest masses in this case. Why is the "extra" energy needed? Because the three electrons in the final system share momentum E_γ/c, they must *also* have kinetic energy E_k given by

$$E_k = E - 3mc^2 = (E_\gamma + mc^2) - 3mc^2$$
$$= 4mc^2 + mc^2 - 3mc^2 = 2mc^2$$

or the initial photon must provide the $2mc^2$ necessary to create the electron and positron masses and the additional $2mc^2$ of kinetic energy that they and the existing electron share as a result of momentum conservation. The speed u at which the group of particles moves in S can be found from $u/c = pc/E$ (Equation 2-34):

$$u/c = \frac{\left(\frac{E_\gamma}{c} \times c\right)}{(E_\gamma + mc^2)} = \frac{4mc^2}{5mc^2} = 0.8$$

The portion of the incident photon's energy that is needed to provide kinetic energy in the final system is reduced if the mass of the existing particle is larger than that of an electron and, indeed, can be made negligibly small, as illustrated in the following example.

EXAMPLE 2-13 Threshold for Pair Production What is the minimum or threshold energy that a photon must have in order to produce an electron-positron pair?

SOLUTION

The energy E_γ of the initial photon must be

$$E_\gamma = mc^2 + E_{k-} + mc^2 + E_{k+} + E_{kM}$$

where mc^2 = electron rest energy, E_{k-} and E_{k+} are the kinetic energies of the electron and positron, respectively, and E_{kM} = kinetic energy of the existing particle of mass M. Since we are looking for the threshold energy, consider the limiting case where the pair is created at rest in S, i.e., $E_{k-} = E_{k+} = 0$ and correspondingly $p_- = p_+ = 0$. Therefore, momentum conservation requires that

$$p_{\text{initial}} = E_\gamma/c = p_{\text{final}} = \frac{Mu}{\sqrt{1 - u^2/c^2}}$$

where u = speed of recoil of the mass M. Since the masses of single atoms are in the range of 10^3 to 10^5 MeV/c^2 and the value of E_γ at the threshold is clearly less than 2 MeV (i.e., it must be less than the value $E_\gamma = 4mc^2 = 2.044$ MeV, the speed with which M recoils from the creation event is quite small compared with c, even for the smallest M available, a single proton! (See Table 2-1.) Thus, the kinetic energy $E_{kM} \approx \frac{1}{2}mu^2$ becomes negligible, and we conclude that the minimum energy E_γ of the initial photon that can produce an electron-positron pair is $2mc^2$, i.e., that needed just to create the two rest masses.

STUDENTS-HUB.com Uploaded By: Malak Obaid

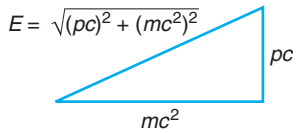

Figure 2-13 Triangle showing the relation between energy, momentum, and rest mass in special relativity. *Caution:* Remember that E and pc are not relativistically invariant. The invariant is mc^2.

Some Useful Equations and Approximations

$$E^2 = (pc)^2 + (mc^2)^2 \qquad \textbf{2-31}$$

Extremely Relativistic Case The triangle shown in Figure 2-13 is sometimes useful in remembering this result. If the energy of a particle is much greater than its rest energy mc^2, the second term on the right of Equation 2-31 can be neglected, giving the useful approximation

$$E \approx pc \qquad \text{for} \qquad E \gg mc^2 \qquad \textbf{2-36}$$

This approximation is accurate to about 1 percent or better if E is greater than about $8mc^2$. Equation 2-36 is the exact relation between energy and momentum for particles with zero rest mass.

From Equation 2-36 we see that the momentum of a high-energy particle is simply its total energy divided by c. A convenient unit of momentum is MeV/c. The momentum of a charged particle is usually determined by measuring the radius of curvature of the path of the particle moving in a magnetic field. If the particle has charge q and a velocity $\mathbf{u}$, it experiences a force in a magnetic field $\mathbf{B}$ given by

$$\mathbf{F} = q\mathbf{u} \times \mathbf{B}$$

where $\mathbf{F}$ is perpendicular to the plane formed by $\mathbf{u}$ and $\mathbf{B}$ and hence is always perpendicular to $\mathbf{u}$. Since the magnetic force is always perpendicular to the velocity, it does no work on the particle (the work-energy theorem also holds in relativity), so the energy of the particle is constant. From Equation 2-10 we see that if the energy is constant, γ must be a constant, and therefore the speed u is also constant. So

$$\mathbf{F} = q\mathbf{u} \times \mathbf{B} = \frac{d\mathbf{p}}{dt} = \frac{d(\gamma m\mathbf{u})}{dt} = \gamma m\frac{d\mathbf{u}}{dt}$$

For the case $\mathbf{u} \perp \mathbf{B}$, the particle moves in a circle with centripetal acceleration u^2/R. (If $\mathbf{u}$ is not perpendicular to $\mathbf{B}$, the path is a helix. Since the component of $\mathbf{u}$ parallel to $\mathbf{B}$ is unaffected, we will only consider motion in a plane.) We then have

$$quB = m\gamma\left|\frac{du}{dt}\right| = m\gamma\left(\frac{u^2}{R}\right)$$

or

$$BqR = m\gamma u = p \qquad \textbf{2-37}$$

This is the same as the nonrelativistic expression except for the factor of γ. Figure 2-14 shows a plot of BqR/mu versus u/c. It is useful to rewrite Equation 2-37 in terms of practical but mixed units; the result is

$$p = 300\,BR\left(\frac{q}{e}\right) \qquad \textbf{2-38}$$

where p is in MeV/c, B is in tesla, and R is in meters.

STUDENTS-HUB.com Uploaded By: Malak Obaid

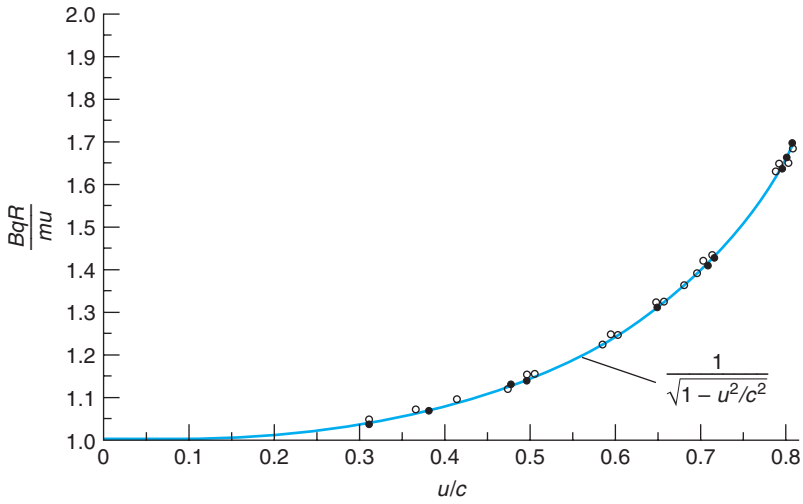

Figure 2-14 BqR/mu versus u/c for particle of charge q and mass m moving in a circular orbit of radius R in a magnetic field B. The agreement of the data with the curve predicted by relativity theory supports the assumption that the force equals the time rate of change of relativistic momentum. [*Adapted from I. Kaplan, Nuclear Physics, 2d ed., Reading, MA: Addison-Wesley Publishing Company, Inc., 1962; by permission.*]

EXAMPLE 2-14 **Electron in a Magnetic Field** What is the approximate radius of the path of a 30-MeV electron moving in a magnetic field of 0.05 tesla (= 500 gauss)?

SOLUTION

1. The radius of the path is given by rearranging Equation 2-38 and substituting $q = e$:

$$R = \frac{p}{300\,B}$$

2. In this situation the total energy E is much greater than the rest energy mc^2:

$$E = 30 \text{ MeV} \gg mc^2 = 0.511 \text{ MeV}$$

3. Equation 2-36 may then be used to determine p:

$$p \approx E/c = 30 \text{ MeV}/c$$

4. Substituting this approximation for p into Equation 2-38 yields

$$R = \frac{30 \text{ MeV}/c}{(300)(0.05)} = 2 \text{ m}$$

Remarks: *In this case the error made by using the approximation, Equation 2-36, rather than the exact solution, Equation 2-31, is only about 0.01 percent.*

Nonrelativistic Case Nonrelativistic expressions for energy, momentum, and other quantities are often easier to use than the relativistic ones, so it is important to know when these expressions are accurate enough. As $\gamma \to 1$, all the relativistic expressions approach the classical ones. In most situations, the kinetic energy or the total energy is given, so that the most convenient expression for calculating γ is, from Equation 2-10,

$$\gamma = \frac{E}{mc^2} = 1 + \frac{E_k}{mc^2} \qquad \textbf{2-39}$$

STUDENTS-HUB.com Uploaded By: Malak Obaid

When the kinetic energy is much less than the rest energy, γ is approximately 1 and nonrelativistic equations can be used. For example, the classical approximation $E_k \approx (1/2)mu^2 = p^2/2m$ can be used instead of the relativistic $E_k = (\gamma - 1)mc^2$ if E_k is much less than mc^2. We can get an idea of the accuracy of these expressions by expanding γ, using the binomial expansion as was done in Section 2-2, and examining the first term that is *neglected* in the classical approximation. We have

$$\gamma = \left(1 - \frac{u^2}{c^2}\right)^{1/2} \approx 1 + \frac{1}{2}\frac{u^2}{c^2} + \frac{3}{8}\frac{u^4}{c^4} + \cdots$$

and

$$E_k = (\gamma - 1)mc^2 \approx \frac{1}{2}mu^2 + \frac{3}{2}\frac{\left(\frac{1}{2}mu^2\right)^2}{mc^2} + \cdots$$

Then

$$\frac{E_k - \frac{1}{2}mu^2}{E_k} \approx \frac{3}{2}\frac{E_k}{mc^2}$$

For example, if $E_k/mc^2 \approx 1$ percent, the error in using the approximation $E_k \approx (1/2)mu^2$ is about 1.5 percent.

At very low energies, the velocity of a particle can be obtained from its kinetic energy $E_k \approx (1/2)mu^2$ just as in classical mechanics. At very high energies, the velocity of a particle is very near c and the following approximation is sometimes useful (see Problem 2-28):

$$\frac{u}{c} \approx 1 - \frac{1}{2\gamma^2} \qquad \text{for} \quad \gamma \gg 1 \tag{2-40}$$

An exact expression for the velocity of a particle in terms of its energy and momentum was obtained in Example 2-10.

$$\frac{u}{c} = \frac{pc}{E} \tag{2-41}$$

This expression, of course, is not useful if the approximation $E \approx pc$ has already been made.

EXAMPLE 2-15 **Different Particles, Same Energy** An electron and a proton are each accelerated through 10×10^6 V. Find γ, the momentum, and the speed for each.

SOLUTION

Since each particle has a charge of e, each acquires a kinetic energy of 10 MeV. This is much greater than the 0.511 MeV rest energy of the electron and much less than the 938.3 MeV rest energy of the proton. We will calculate the momentum and speed of each particle exactly and then by means of the nonrelativistic (proton) or the extreme relativistic (electron) approximations.

1. We first consider the electron. From Equation 2-39 we have

$$\gamma = 1 + \frac{E_k}{mc^2} = 1 + \frac{10 \text{ MeV}}{0.511 \text{ MeV}} = 20.57$$

STUDENTS-HUB.com Uploaded By: Malak Obaid

Since the total energy is $E_k + mc^2 = 10.511$ MeV, we have, from the magnitude of the energy/momentum four-vector (Equation 2-31),

$$pc = \sqrt{E^2 - (mc^2)^2} = \sqrt{(10.511)^2 - (0.511)^2}$$
$$= 10.50 \text{ MeV}$$

The exact calculation then gives $p = 10.50$ MeV$/c$. The high-energy or extreme relativistic approximation $p \approx E/c = 10.50$ MeV is in good agreement with the exact result. If we use Equation 2-34, we obtain for the speed $u/c = pc/E = 10.50$ MeV$/10.51$ MeV $= 0.999$. On the other hand, the approximation of Equation 2-40 gives

$$\frac{u}{c} \approx 1 - \frac{1}{2}\left(\frac{1}{\gamma}\right)^2 = 1 - \frac{1}{2}\left(\frac{1}{20.57}\right)^2 = 0.999$$

2. For the proton, the total energy is $E_k + mc^2 = 10$ MeV $+ 938.3$ MeV $= 948.3$ MeV. From Equation 2-39 we obtain $\gamma = 1 + E_k/mc^2 = 1 + 10/938.3 = 1.01$. Equation 2-31 gives for the momentum

$$pc = \sqrt{E^2 - (mc^2)^2} = \sqrt{(948.3)^2 - (938.3)^2}$$
$$p = 137.4 \text{ MeV}/c$$

The nonrelativistic approximation gives

$$E_k \approx \frac{1}{2}mu^2 = \frac{(mu)^2}{2m} \approx \frac{p^2}{2m} = \frac{p^2c^2}{2mc^2}$$

or

$$pc \approx \sqrt{2mc^2E_k} = \sqrt{(2)(938.3)(10)}$$
$$p = 137.0 \text{ MeV}/c$$

The speed can be determined from Equation 2-34 exactly or from $p = mu$ approximately. From Equation 2-34 we obtain

$$\frac{u}{c} = \frac{pc}{E} = \frac{137.4}{948.3} = 0.1449$$

From $p \approx mu$, the nonrelativistic expression for p, we obtain

$$\frac{u}{c} \approx \frac{pc}{mc^2} = \frac{137.0}{938.3} = 0.1460$$

2-5 General Relativity

The generalization of relativity to noninertial reference frames by Einstein in 1916 is known as the *general theory of relativity*. This theory is much more difficult mathematically than the special theory of relativity, and there are fewer situations in which it can be tested. Nevertheless, its importance in the areas of astrophysics and cosmology and the need to take account of its predictions in the design of such things as global navigation systems[13] calls for its inclusion here. A full description of the general theory uses tensor analysis at a quite sophisticated level, well beyond the scope of this book,

STUDENTS-HUB.com Uploaded By: Malak Obaid

so we will be limited to qualitative or, in some instances, semiquantitative discussions. An additional purpose to the discussion that follows is to give you something that few people will ever have, namely, an acquaintance with one of the most remarkable of all scientific accomplishments and a bit of a feel for the man who did it.

The sensitivity of modern electronic devices is so exceptional that general relativistic effects are included in the design of such systems as the Global Positioning System.

Einstein's development of the general theory of relativity was not motivated by any experimental enigma. Instead, it grew out of his desire to include the descriptions of *all* natural phenomena within the framework of the special theory. By 1907 he realized that he could accomplish that goal with the single exception of the law of gravitation. About that exception he said,[14]

> I felt a deep desire to understand the reason behind this [exception].

The "reason" came to him, as he said later, while he was sitting in a chair in the patent office in Bern. He described it like this:[15]

> Then there occurred to me the happiest thought of my life, in the following form. The gravitational field has only a relative existence in a way similar to the electric field generated by electromagnetic induction. *Because for an observer falling freely from the roof of a house there exists*—at least in his immediate surroundings—*no gravitational field* [Einstein's italics]. . . . The observer then has the right to interpret his state as "at rest."

Out of this "happy thought" grew the *principle of equivalence* that became Einstein's fundamental postulate for general relativity.

Principle of Equivalence

The basis of the general theory of relativity is what we may call Einstein's third postulate, the principle of equivalence, which states:

> A homogeneous gravitational field is completely equivalent to a uniformly accelerated reference frame.

This principle arises in a somewhat different form in Newtonian mechanics because of the apparent identity of gravitational and inertial mass. In a uniform gravitational field, all objects fall with the same acceleration g independent of their mass because the gravitational force is proportional to the (gravitational) mass while the acceleration varies inversely with the (inertial) mass. That is, the mass m in

$$\mathbf{F} = m\mathbf{a} \quad \text{(inertial } m\text{)}$$

and that in

$$\mathbf{F} = \frac{GMm}{r^2}\hat{\mathbf{r}} \quad \text{(gravitational } m\text{)}$$

appear to be identical in classical mechanics, although classical theory provides no explanation for this equality. For example, near Earth's surface, $F_G = GMm/r^2 = m_{\text{grav}}g = m_{\text{inertial}}a = F$. Recent experiments have shown that $m_{\text{inertial}} = m_{\text{grav}}$ to better than one part in 10^{12}.

To understand what the equivalence principle means, consider a compartment in space far away from any matter and undergoing uniform acceleration $\mathbf{a}$ as shown in Figure 2-15*a*. If people in the compartment drop objects, they fall to the "floor" with acceleration $\mathbf{g} = -\mathbf{a}$. If they stand on a spring scale, it will read their "weight" of magnitude ma. No mechanics experiment can be performed *within* the compartment

STUDENTS-HUB.com Uploaded By: Malak Obaid

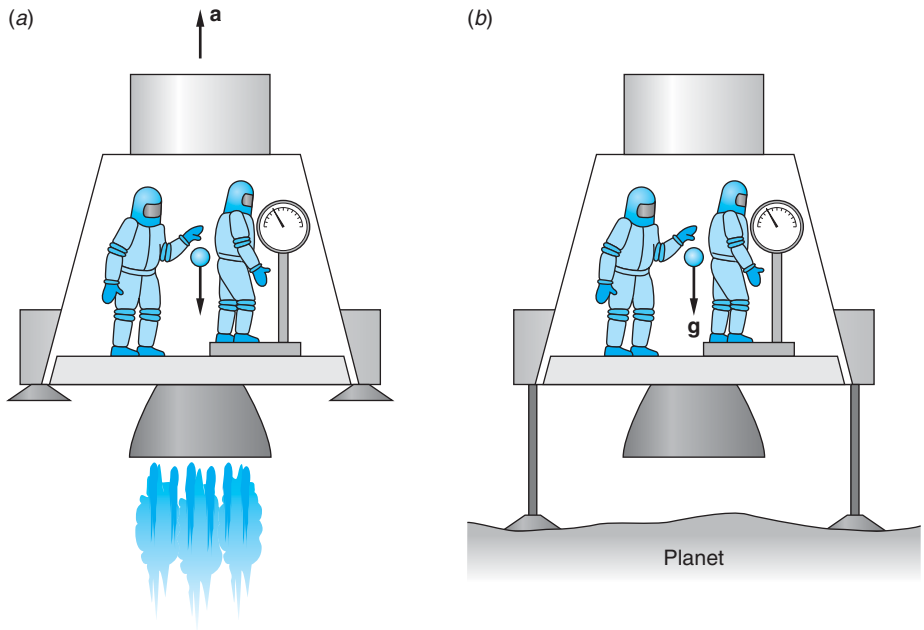

Figure 2-15 Results from experiments in a uniformly accelerated reference frame (*a*) cannot be distinguished from those in a uniform gravitational field (*b*) if the acceleration **a** and gravitational field **g** have the same magnitude.

that will distinguish whether the compartment is actually accelerating in space or is at rest (or moving with uniform velocity) in the presence of a uniform gravitational field $\mathbf{g} = -\mathbf{a}$.

Einstein broadened the principle of equivalence to apply to *all* physical experiments, not just to mechanics. In effect, he assumed that there is no experiment of any kind that can distinguish uniformly accelerated motion from the presence of a gravitational field. A direct consequence of the principle is that $m_{\text{inertial}} = m_{\text{grav}}$ is a requirement, not a coincidence. The principle of equivalence extends Einstein's first postulate, the principle of relativity, to *all* reference frames, noninertial (i.e., accelerated) as well as inertial. It follows that there is no absolute acceleration of a reference frame. Acceleration, like velocity, is only relative.

Question

6. For his 76th (and last) birthday Einstein received a present designed to demonstrate the principle of equivalence. It is shown in Figure 2-16. The object is, starting with the ball hanging down as shown to put the ball into the cup with a method that works every time (as opposed to random shaking). How would you do it? (*Note:* When it was given to Einstein, he was delighted and did the experiment correctly immediately.)

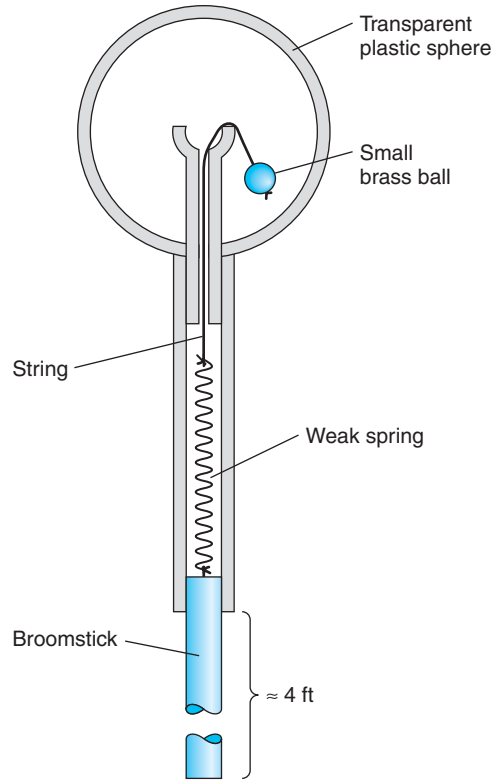

Figure 2-16 Principle of equivalence demonstrator given to Einstein by E. M. Rogers. The object is to put the hanging brass ball into the cup by a technique that always works. The spring is weak, too weak to pull the ball in as it stands, and is stretched even when the ball is in the cup. The transparent sphere, about 10 cm in diameter, does not open. [*From A. P. French, Albert Einstein: A Centenary Volume, Harvard University Press, Cambridge, Mass. (1979).*]

STUDENTS-HUB.com Uploaded By: Malak Obaid

Some Predictions of General Relativity

In his first paper on general relativity, in 1916, Einstein was able to explain quantitatively a discrepancy of long standing between the measured and (classically) computed values of the advance of the perihelion of Mercury's orbit, about 43 arc seconds/century. It was the first success of the new theory. A second prediction, the bending of light in a gravitational field, would seem to be more difficult to measure owing to the very small effect. However, it was accurately confirmed less than five years later when Arthur Eddington measured the deflection of starlight passing near the limb of the Sun during a total solar eclipse. The theory also predicts the slowing of light itself and the slowing of clocks—i.e., frequencies—in gravitational fields, both effects of considerable importance to the determination of astronomical distances and stellar recession rates. The predicted slowing of clocks, called gravitational redshift, was demonstrated by Pound and co-workers in 1960 in Earth's gravitational field using the ultrasensitive frequency measuring technique of the Mössbauer effect (see Chapter 11). The slowing of light was conclusively measured in 1971 by Shapiro and co-workers using radar signals reflected from several planets. Two of these experimental tests of relativity's predictions, bending of light and gravitational redshift, are discussed in the Exploring sections that follow. The perihelion of Mercury's orbit and the delay of light are discussed in More sections on the book's Web page. Many other predictions of general relativity are subjects of active current research. Two of these, black holes and gravity waves, are discussed briefly in the concluding paragraphs of this chapter.

EXPLORING
Deflection of Light in a Gravitational Field

This relativistic effect results in gravitational lenses in the cosmos that focus light from extremely distant galaxies, greatly improving their visibility in telescopes, both on Earth and in orbit.

With the advent of special relativity, several features of the Newtonian law of gravitation $F_G = GMm/r^2$ became conceptually troublesome. One of these was the implication from the relativistic concept of mass-energy equivalence that even particles with zero rest mass should exhibit properties such as weight and inertia, thought of classically as masslike; classical theory does not include such particles. According to the equivalence principle, however, light, too, would experience the gravitational force. Indeed, the deflection of a light beam passing through the gravitational field near a large mass was one of the first consequences of the equivalence principle to be tested experimentally.

To see why a deflection of light would be expected, consider Figure 2-17, which shows a beam of light entering an accelerating compartment. Successive positions of the compartment are shown at equal time intervals. Because the compartment is accelerating, the distance it moves in each time interval increases with time. The path of the beam of light, as observed from inside the compartment, is therefore a parabola. But according to the equivalence principle, there is no way to distinguish between an accelerating compartment and one with uniform velocity in a uniform gravitational field. We conclude, therefore, that a beam of light will accelerate in a gravitational field as do objects with rest mass. For example, near the surface of Earth light will fall with acceleration 9.8 m/s^2. This is difficult to observe because of the enormous speed of light. For example, in a distance of 3000 km, which takes about 0.01 second to cover, a beam of light should fall about 0.5 mm. Einstein pointed out that the deflection of a light beam in a gravitational field might be observed when light from a distant star passes close to the Sun.[16] The deflection, or bending, is computed as follows.

STUDENTS-HUB.com Uploaded By: Malak Obaid

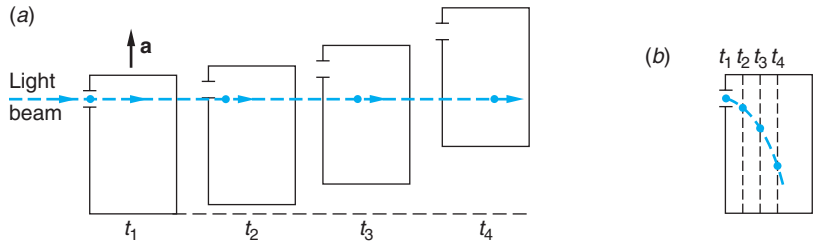

Figure 2-17 (*a*) Light beam moving in a straight line through a compartment that is undergoing uniform acceleration. The position of the light beam is shown at equally spaced times t_1, t_2, t_3, t_4. (*b*) In the reference frame of the compartment, the light travels in a parabolic path, as would a ball were it projected horizontally. Note that in both (*a*) and (*b*) the vertical displacements are greatly exaggerated for emphasis.

Rewriting the spacetime interval Δs (Equation 2-32) in differential form and converting the space Cartesian coordinates to polar coordinates (in two dimensions, since the deflection occurs in a plane) yields

$$ds^2 = c^2\,dt^2 - (dr^2 + r^2\,d\theta^2) \qquad \textbf{2-42}$$

Einstein showed that this expression is slightly modified in the presence of a (spherical, nonrotating) mass M to become

$$ds^2 = \gamma(r)^2 c^2\,dt^2 - dr^2/\gamma(r)^2 - r^2\,d\theta^2 \qquad \textbf{2-43}$$

where $\gamma(r) = (1 - 2GM/c^2 r)^{1/2}$, with G = universal gravitational constant and r = distance from the mass M. The factor $\gamma(r)$ is roughly analogous to the γ of special relativity. In the following Exploring section on gravitational redshift, we will describe how $\gamma(r)$ arises. For now, $\gamma(r)$ can be thought of as correcting for *gravitational time dilation* (the first term on the right of Equation 2-43) and *gravitational length contraction* (the second term).

This situation is illustrated in Figure 2-18, which shows the light from a distant star just grazing the edge of the Sun. The gravitational deflection of light (with mass $\gamma m = E/c^2$) can be treated as a refraction of the light. The speed of light is reduced to $\gamma(r)c$ in the vicinity of the mass M since $\gamma(r) < 1$ (see Equation 2-43), thus bending the wave fronts, and hence the beam, toward M. This is analogous to the deflection of starlight toward Earth's surface as a result of the changing density—hence index of refraction—of the atmosphere. By integrating Equation 2-43 over the entire trajectory of the light beam (recall that $ds = 0$ for light) as it passes by M, the total deflection α is found to be[17]

$$\alpha = 4GM/c^2R \qquad \textbf{2-44}$$

where R = distance of closest approach of the beam to the center of M. For a beam just grazing the Sun, $R = R_\odot$ = solar radius = 6.96×10^8 m. Substituting the values for G and the solar mass ($M = 1.99 \times 10^{30}$ kg) yields $\alpha = 1.75$ arc second.[18]

Ordinarily, of course, the brightness of the Sun prevents astronomers (or anyone else) from seeing stars close to the limbs (edges) of the Sun, except during a total eclipse. Einstein completed the calculation of α in 1915, and in 1919 expeditions were organized by Eddington[19] at two points along the line of totality of a solar eclipse, both of which were successful in making measurements of α for several stars and testing the predicted $1/R_\odot$ dependence of α. The measured values of α for grazing beams at the two sites were:

At Sobral (South America): $\alpha = 1.98 \pm 0.12$ arc seconds
At Principe Island (Africa): $\alpha = 1.61 \pm 0.30$ arc seconds

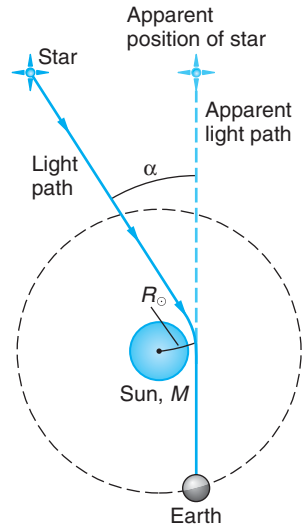

Figure 2-18 Deflection (greatly exaggerated) of a beam of starlight due to the gravitational attraction of the Sun.

STUDENTS-HUB.com Uploaded By: Malak Obaid

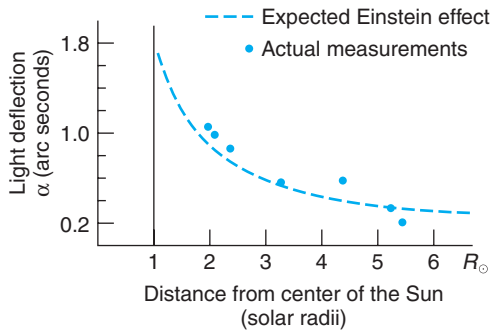

Figure 2-19 The deflection angle α depends on the distance of closest approach $R_\odot$ according to Equation 2-44. Shown here is a sample of the data for 7 of the 13 stars measured by the Eddington expeditions. The agreement with the relativistic prediction is apparent.

their average agreeing with the general relativistic prediction to within about 2 percent. Figure 2-19 illustrates the agreement of the $1/R_\odot$ dependence with Equation 2-44. (Einstein learned of the successful measurements via a telegram from H. A. Lorentz.) Since 1919, many measurements of α have been made during eclipses. Since the development of radio telescopes, which are not blinded by sunlight and hence don't require a total eclipse, many more measurements have been made. The latest data agree with the deflection predicted by general relativity to within about 0.1 percent.

The gravitational deflection of light is being put to use by modern astronomers via the phenomenon of *gravitational lensing* to help in the study of galaxies and other large masses in space. Light from very distant galaxies passing near or through other galaxies or clusters of galaxies between the source and Earth can be bent so as to reach Earth in much the same way that light from an object on a bench in the laboratory can be refracted by a glass lens and thus reach the eye of an observer. An intervening galaxy or cluster of galaxies can thus produce images of the distant source, even ones magnified and distorted, just as the glass lens can. Figure 2-20*a* will serve as a reminder of a refracting lens in the laboratory, while Figure 2-20*b* illustrates the corresponding action

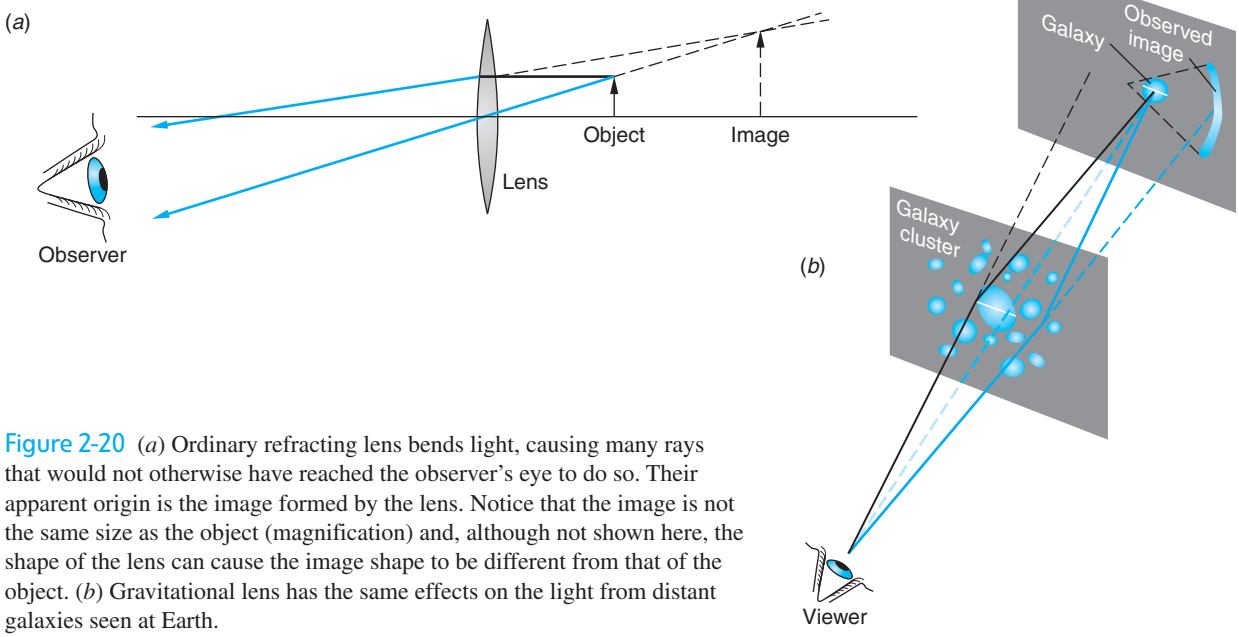

Figure 2-20 (*a*) Ordinary refracting lens bends light, causing many rays that would not otherwise have reached the observer's eye to do so. Their apparent origin is the image formed by the lens. Notice that the image is not the same size as the object (magnification) and, although not shown here, the shape of the lens can cause the image shape to be different from that of the object. (*b*) Gravitational lens has the same effects on the light from distant galaxies seen at Earth.

STUDENTS-HUB.com Uploaded By: Malak Obaid

of a gravitational lens. The accompanying photograph shows the images of several distant galaxies drawn out into arcs by the lens effect of the cluster of galaxies in the center. The first confirmed discovery of images formed by a gravitational lens, the double image of the quasar QSO 0957, was made in 1979 by D. Walsh and his co-workers. Since then, astronomers have found many such images. Their discovery and interpretation is currently an active area of research. Gravitational lensing was recently used to help image the first apparent findings of dark matter in this cosmos. (See Chapter 13.)

EXPLORING
Gravitational Redshift

A second prediction of general relativity concerns the rates of clocks and the frequencies of light in a gravitational field. As a specific case that illustrates the gravitational redshift as a direct consequence of the equivalence principle, suppose we consider two identical light sources (A and A') and detectors (B and B') located in identical spaceships (S and S') as illustrated in Figure 2-21. The spaceship S' in Figure 2-21*b* is located far from any mass. At time $t = 0$, S' begins to accelerate, and simultaneously an atom in the source A' emits a light pulse of its characteristic frequency f_0. During the time $t(= h/c)$ for the light to travel from A' to B', B' acquires a speed $v = at = gh/c$, and the detector B', receding from the original location of A', measures the frequency of the incoming light to be *f redshifted* by a fractional amount $(f_0 - f)/f_0 \approx \beta$ for $v \ll c$. (See Section 1-5.) Thus,

$$(f_0 - f)/f_0 = \Delta f/f \approx \beta = v/c = gh/c^2 \qquad \textbf{2-45}$$

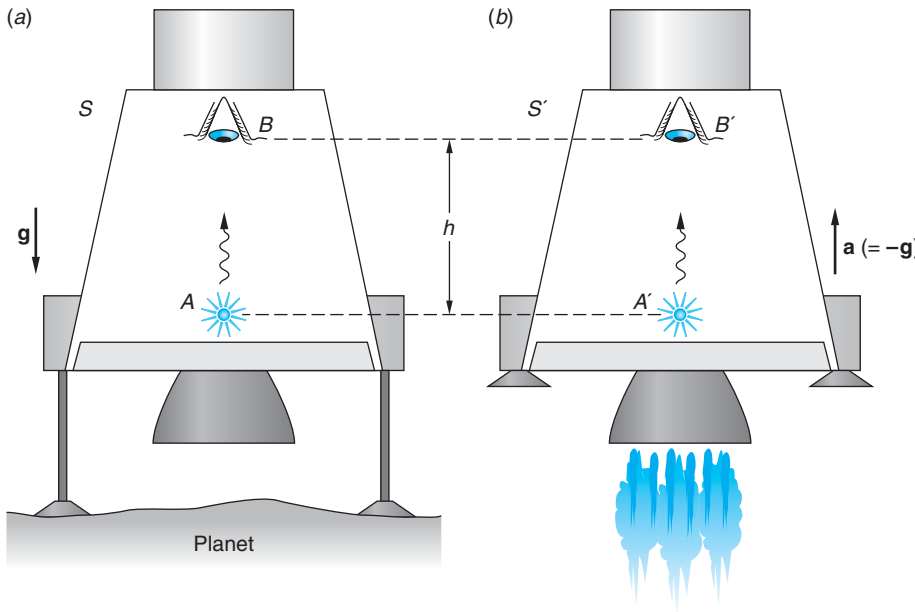

Figure 2-21 (*a*) System S is at rest in the gravitational field of the planet. (*b*) Spaceship S', far from any mass, accelerates with $\mathbf{a} = -\mathbf{g}$.

STUDENTS-HUB.com Uploaded By: Malak Obaid

Notice that the right side of Equation 2-45 is equal to the gravitational potential (i.e., the gravitational potential energy per unit mass) $\Delta\phi = gh$ between A and B, divided by c^2. According to the equivalence principle, the detector at B in S must also measure the frequency of the arriving light to be f, even though S is at rest on the planet and, therefore, the shift cannot be due to the Doppler effect! Since the vibrating atom that produced the light pulse at A can be considered to be a clock and since no "cycles" of the vibration are lost on the pulse's trip from A to B, the observer at B must conclude that the clock at A runs slow, compared with an identical clock (or an identical atom) located at B. Since A is at the lowest potential, the observer concludes that *clocks run more slowly the lower the gravitational potential*. This shift of clock rates to lower frequencies, hence longer wavelengths, in lower gravitational potentials is the *gravitational redshift*.

In the more general case of a spherical, nonrotating mass M, the change in gravitational potential between the surface at some distance R from the center and a point at infinity is given by

$$\Delta\phi = \int_R^\infty \frac{GM}{r^2}\,dr = GM(-1/r)\Big|_R^\infty = \frac{GM}{R} \qquad \textbf{2-46}$$

and the factor by which gravity shifts the light frequency is found from

$$\Delta f/f_0 = (f_0 - f)/f_0 = GM/c^2R$$

or

$$f/f_0 = 1 - GM/c^2R \quad \text{(gravitational redshift)} \qquad \textbf{2-47}$$

Notice that if the light is moving the other way, i.e., from high to low gravitational potential, the limits of integration in Equation 2-46 are reversed and Equation 2-47 becomes

$$f/f_0 = 1 + GM/c^2R \quad \text{(gravitational blueshift)} \qquad \textbf{2-48}$$

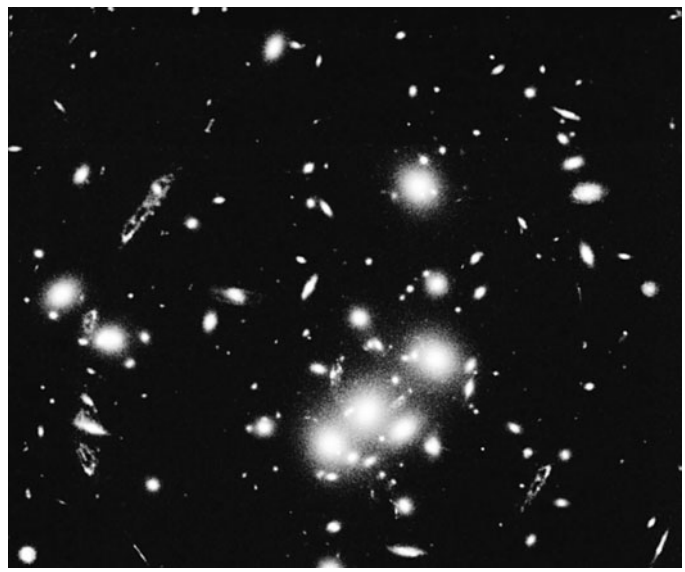

Images of distant galaxies are drawn out into arcs by the massive cluster of galaxies Abell 2218, whose enormous gravitational field acts as a lens to magnify, brighten, and distort the images. Abell 2218 is about 2 billion $c \cdot$ y from Earth. The arcs in this January 2000 Hubble Space Telescope photograph are images of galaxies 10 to 20 billion $c \cdot$ y away. [*NASA, A. Fruchter; ERO Team.*]

STUDENTS-HUB.com Uploaded By: Malak Obaid

Analyzing the frequency of starlight for gravitational effects is exceptionally difficult because several shifts are present. For example, the light is gravitationally redshifted as it leaves the star and blueshifted as it arrives at Earth. The blueshift near Earth is negligibly small with current measuring technology; however, the redshift due to the receding of nearby stars and distant galaxies from us as a part of the general expansion of the universe is typically much larger than gravitational effects and, together with thermal frequency broadening in the stellar atmospheres, results in large uncertainties in measurements. Thus, it is quite remarkable that the relativistic prediction of Equation 2-48 has been tested in the relatively small gravitational field of Earth. R. V. Pound and his co-workers,[20] first in 1960 and then again in 1964 with improved precision, measured the shift in the frequency of 14.4-keV gamma rays emitted by ^{57}Fe falling through a height h of only 22.5 m. Using the Mössbauer effect, an extremely sensitive frequency shift measuring technique developed in 1968, Pound's measurements agreed with the predicted fractional blueshift $gh/c^2 = 2.45 \times 10^{-15}$ to within 1 percent. Equations 2-47 and 2-48 have been tested a number of times since then—using atomic clocks carried on aircraft, as described in Section 1-4, and, in 1980, by R. F. C. Vessot and his co-workers using a precision microwave transmitter carried to 10,000 km from Earth by a space probe. The results of these tests, too, agree with the relativistically predicted frequency shift, the latter to 1 part in 14,000.

Question

7. The frequency f in Equation 2-47 can be shifted to zero by an appropriate value of M/R. What would be the corresponding value of R for a star with the mass of the Sun? Speculate on the significance of this result.

More

The inability of Newtonian gravitational theory to correctly account for the observed rate at which the major axis of Mercury's orbit precessed about the Sun was a troubling problem, pointing as it did to some subtle failure of the theory. Einstein's first paper on general relativity, the *Perihelion of Mercury's Orbit*, quantitatively explained the advance of Mercury's orbit, setting the stage for general relativity to supplant the old Newtonian theory. A clear description of the relativistic explanation is on the home page: www.whfreeman.com/tiplermodernphysics5e. See also Equations 2-49 through 2-51 here, as well as Figure 2-22 and Table 2-2.

More

General relativity includes a gravitational interaction for particles with zero rest mass, such as photons, which are excluded in Newtonian theory. One consequence is the prediction of a *Delay of Light in a Gravitational Field*. This phenomenon and its subsequent observation are described qualitatively on the home page: www.whfreeman.com/tiplermodernphysics5e. See also Equation 2-52 here, as well as Figures 2-23 and 2-24.

Black Holes Black holes were first predicted by J. R. Oppenheimer and H. Snyder in 1939. According to the general theory of relativity, if the density of an object such as a star is great enough, the gravitational attraction will be so large that nothing can escape

STUDENTS-HUB.com Uploaded By: Malak Obaid

from its surface, not even light or other electromagnetic radiation. It is as if space itself were being drawn inward faster than light could move outward through it. A remarkable property of such an object is that nothing that happens inside it can be communicated to the outside world. This occurs when the gravitational potential at the surface of the mass M becomes so large that the frequency of radiation emitted at the surface is redshifted to zero. From Equation 2-47 we see that the frequency will be zero when the radius of the mass has the critical value $R_G = GM/c^2$. This result is a consequence of the principle of equivalence, but Equation 2-47 is a $v \ll c$ approximation. A precise derivation of the critical value of the radius R_G, called the *Schwarzschild radius*, yields

$$R_G = \frac{2MG}{c^2} \qquad \textbf{2-53}$$

For an object with mass equal to that of our Sun to be a black hole, its radius would be about 3 km. A large number of black holes have been identified by astronomers in recent years, one of them in the center of the Milky Way. (See Chapter 13.)

An interesting historical note is that Equation 2-53 was first derived by nineteenth-century French physicist Pierre Laplace using Newtonian mechanics to compute the escape velocity v_e from a planet of mass M before anyone had ever heard of Einstein or black holes. The result, derived in first-year physics courses by setting the kinetic energy of the escaping object equal to the gravitational potential energy at the surface of the planet (or star), is

$$v_e = \sqrt{\frac{2GM}{r}}$$

Setting $v_e = c$ gives Equation 2-53. Laplace obtained the correct result by making two fundamental errors that just happened to cancel each other!

Gravitational Waves Einstein's formulation of general relativity in 1916 explicitly predicted the existence of gravitational radiation. He showed that, just as accelerated electric charges generate time-dependent electromagnetic fields in space—i.e., electromagnetic waves—accelerated masses would create time-dependent gravitational fields in space—i.e., *gravitational waves*—that propagate from their source at the speed of light. The gravitational waves are propagating ripples, or distortions of spacetime. Figure 2-25 illustrates gravitational radiation emitted by two merging black holes distorting the otherwise flat "fabric" of spacetime.

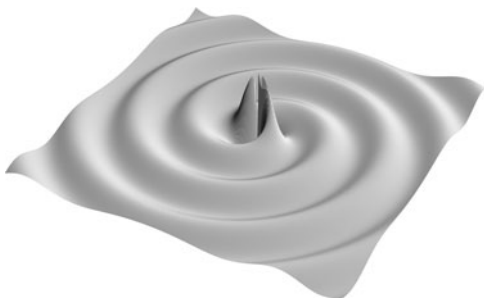

Figure 2-25 Gravitational waves, intense ripples in the fabric of spacetime, are expected to be generated by a merging binary system of neutron stars or black holes. The amplitude decreases with distance due to the $1/R$ falloff and because waves farther from the source were emitted at an earlier time, when the emission was weaker. [*Courtesy of Patrick Brady.*]

The best experimental evidence that exists so far in support of the gravitational wave prediction is indirect. In 1974 R. A. Hulse and J. H. Taylor[24] discovered the first binary pulsar, i.e., a pair of neutron stars orbiting each other, one of which was emitting periodic flashes of electromagnetic radiation (pulses). In an exquisitely precise experiment they showed that the gradual decrease in the orbital period of the pair was in good agreement with the general relativistic prediction for the rate of loss of gravitational energy via the emission of gravitational waves.

Experiments are currently under way in several countries to *directly* detect gravitational waves arriving at Earth. One of the most promising is LIGO (*L*aser *I*nterferometer *G*ravitational-Wave *O*bservatory), a pair of large Michelson interferometers with Fabry-Perot cavities at the Livingston Observatory in Louisiana and the

STUDENTS-HUB.com Uploaded By: Malak Obaid

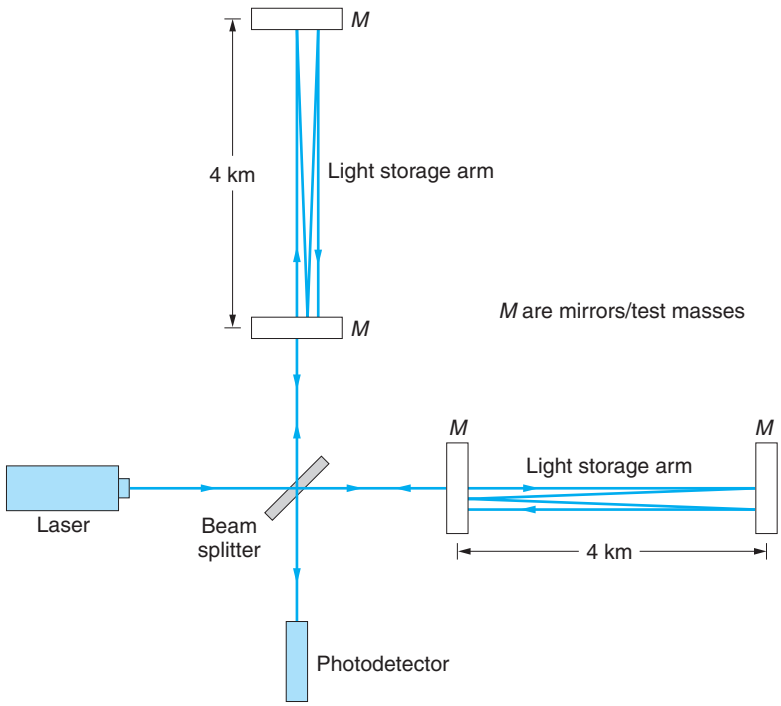

Figure 2-26 The LIGO detectors are equal-arm Michelson interferometers. The mirrors, each 25 cm in diameter by 10 cm thick and isolated from Earth's motions, are also the test masses of the gravitational wave detector. Arrival of a gravitational wave would change the length of each arm by about the diameter of an atomic nucleus and result in light signal at the photodetector.

Hanford Observatory 3002 km away in Washington, operating in coincidence. Figure 2-26 illustrates one of the LIGO interferometers. Each arm is 4 km long. The laser beams are reflected back and forth in the cavities, making about 75 round trips along each arm and recombining at the photodetector, making the effective lengths of the arms about 400 km. (A half-size but equally sensitive instrument using Fabry-Perot cavities is also housed at the Hanford Observatory.) The arrival of a gravitational wave would stretch one arm of the interferometer by about 1/1000 of the diameter of a proton and squeeze the other arm by the same minuscule amount! Nonetheless, that tiny change in the lengths is sufficient to change very slightly the relative phase of the recombining laser beams and produce a signal at the detector. The two LIGO interferometers must record the event within 10 ms of each other for the signal to be interpreted as a gravitational wave, that being the travel time between the two observatories for a gravitational wave moving at speed c. LIGO completed its two-year, low-sensitivity initial operational phase and went online in mid-2002. By 2005 LIGO had completed two science runs that included observations on 28 pulsars. (See Chapter 13.) At this writing a third science run with improved sensitivity is under way, operating jointly with GEO 600, a similar gravitational wave interferometer in Germany. A third gravitational wave observatory, Virgo, in Italy, is currently being commissioned and will soon join the search. These instruments are by far the most sensitive scientific instruments ever built. So far, none of the half-dozen or so experiments under way around the world has detected a gravitational wave.[25]

This application of Michelson's interferometer may well lead to the first direct detection of "ripples" or waves in spacetime.

An enormous amount remains to be learned about the predictions and implications of general relativity—not just about such things as black holes and gravity waves, but also, for example, about gravity and spacetime in the very early universe,

STUDENTS-HUB.com Uploaded By: Malak Obaid

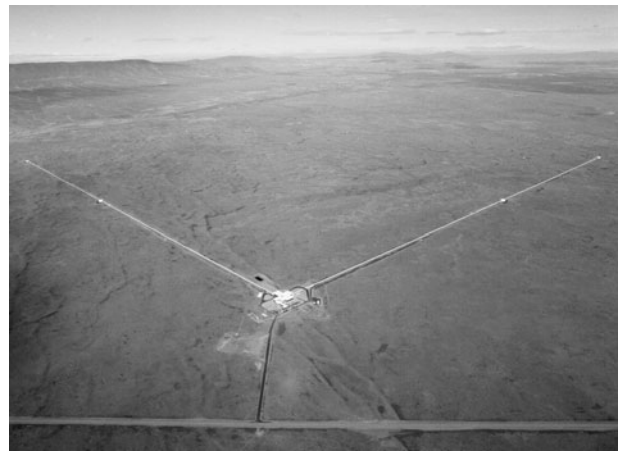

Aerial view of the LIGO gravitational wave interferometer near Hanford, Washington. Each of the two arms is 4 km long. [*CalTech/LIGO.*]

when forces were unified and the constituents were closely packed. These and other fascinating matters are investigated more specifically in the areas of astrophysics and cosmology (Chapter 13) and particle physics (Chapter 12), fields of research linked by general relativity, perhaps the grandest of Einstein's great scientific achievements.

Question

8. Speculate on what the two errors made by Laplace in deriving Equation 2-53 might have been.

Summary

TOPIC	RELEVANT EQUATIONS AND REMARKS	
1. Relativistic momentum	$\mathbf{p} = \gamma m\mathbf{u}$	**2-7**
	The relativistic momentum is conserved and approaches $m\mathbf{u}$ for $v \ll c$. $\gamma = (1 - u^2/c^2)^{-1/2}$ in Equation 2-7, where u = particle speed in S.	
2. Relativistic energy	$E = \gamma mc^2$	**2-10**
Total energy	The relativistic total energy is conserved.	
Kinetic energy	$E_k = \gamma mc^2 - mc^2$	**2-9**
	mc^2 is the rest energy. $\gamma = (1 - u^2/c^2)^{-1/2}$ in Equations 2-9 and 2-10.	
3. Lorentz transformation for E and $\mathbf{p}$.	$p'_x = \gamma(p_x - vE/c^2) \quad p'_y = p_y$ $E' = \gamma(E - vp_x) \quad p'_z = p_z$	**2-16**
	where v = relative speed of the systems and $\gamma = (1 - v^2/c^2)^{-1/2}$	
4. Mass/energy conversion	Whenever additional energy ΔE in any form is stored in an object, the rest mass of the object is increased by $\Delta m = \Delta E/c^2$.	
5. Invariant mass	$(mc^2) = E^2 - (pc)^2$	**2-32**
	The energy and momentum of any system combine to form an invariant four-vector whose magnitude is the rest energy of the ma˜ss m.	

STUDENTS-HUB.com Uploaded By: Malak Obaid

TOPIC	RELEVANT EQUATIONS AND REMARKS
6. Force in relativity	The force $\mathbf{F} = m\mathbf{a}$ is not invariant in relativity. Relativistic force is defined as $\mathbf{F} = \frac{d\mathbf{p}}{dt} = \frac{d(\gamma m\mathbf{u})}{dt}$ **2-8**
7. General relativity	
Principle of equivalence	A homogeneous gravitational field is completely equivalent to a uniformly accelerated reference frame.

General References

The following general references are written at a level appropriate for readers of this book.

Bohm, D., *The Special Theory of Relativity*, W. A. Benjamin, New York, 1965.

French, A. P., *Albert Einstein: A Centenary Volume*. Harvard University Press, Cambridge, Mass., 1979. An excellent collection of contributions from many people about Einstein's life and work.

Lorentz, H. A., A. Einstein, H. Minkowski, and W. Weyl, *The Principle of Relativity: A Collection of Original Memoirs on the Special and General Theory of Relativity* (trans. W. Perrett and J. B. Jeffery), Dover, New York, 1923. Two of Einstein's papers reprinted here are of interest in connection with this chapter: "On the Electrodynamics of Moving Bodies" [*Annalen der Physik*, **17** (1905)], and "Does the Inertia of a Body Depend upon Its Energy Content?" [*Annalen der Physik*, **17** (1905)].

Ohanian, H. C., *Special Relativity: A Modern Introduction,* Physics Curriculum & Instruction, 2001.

Pais, A., *Subtle Is the Lord . . .* , Oxford University Press, Oxford, 1982.

Resnick, R., *Introduction to Relativity*, Wiley, New York, 1968.

Resnick, R., and D. Halliday, *Basic Concepts in Relativity and Early Quantum Theory,* 2d ed., Macmillan, New York, 1992.

Rosser, W. G. V., *The Theory of Relativity*, Butterworth, London, 1964.

Taylor, E. F., and J. A. Wheeler, *Spacetime Physics,* 2d ed., W. H. Freeman and Co., 1992. A good book with many examples, problems, and diagrams.

Notes

1. This *Gedankenexperiment* (thought experiment) is based on one first suggested by G. N. Lewis and R. C. Tolman, *Philosophical Magazine*, **18**, 510, (1909).

2. You can see that this is so by rotating Figure 2-1*a* through 180° in its own plane; it then matches Figure 2-1*b* exactly.

3. C. G. Adler, *American Journal of Physics*, **55**, 739 (1987).

4. This idea grew out of the results of the measurements of masses in chemical reactions in the nineteenth century, which, within the limits of experimental uncertainties of the time, were always observed to conserve mass. The conservation of energy had a similar origin in the experiments of James Joule (1818–1889) as interpreted by Hermann von Helmholtz (1821–1894). This is not an unusual way for conservation laws to originate; they still do it this way.

5. The approximation of Equation 2-10 used in this discussion was, of course, not developed from Newton's equations. The rest energy mc^2 has no classical counterpart.

6. "Facilitates" means that we don't have to make frequent unit conversions or carry along large powers of 10 with nearly every factor in many calculations. However, a word of caution is in order. Always remember that the eV is *not* a basic SI unit. When making calculations whose results are to be in SI units, don't forget to convert the eV!

7. A. Einstein, *Annalen der Physik*, **17**, 1905.

8. Strictly speaking, the time component should be written $ic\Delta t$, where $i = (-1)^{1/2}$. The i is the origin of the minus sign in the spacetime interval, as well as in Equation 2-32 for the energy/momentum four-vector and other four-vectors in both special and general relativity. Its inclusion was a contribution of Hermann Minkowski (1864–1909), a Russian-German mathematician who developed the geometric interpretation of relativity and who was one of Einstein's professors at Zurich. Consideration of the four-dimensional geometry is beyond the scope of our discussions, so we will not be concerned with the i.

STUDENTS-HUB.com Uploaded By: Malak Obaid

9. Other conservation laws must also be satisfied, e.g., electric charge, angular momentum.
10. The positron is a particle with the same mass as an ordinary electron but with a positive electric charge of the same magnitude as that carried by the electron. It and other antiparticles will be discussed in Chapters 11 and 12.
11. Since electrons are thought to be point particles, i.e., they have no space dimensions, it isn't clear what it means to "hit" an electron. Think of it as the photon close to the electron's location, hence within its strong electric field.
12. Such a system is called a *polyelectron*. It is analogous to an ionized hydrogen molecule much as positronium is analogous to a hydrogen atom. (See Figure 2-12 caption.)
13. Satellite navigation systems, e.g., the Global Positioning System, are now so precise that the minute corrections arising primarily from the general relativistic time dilation must be taken into account by the system's programs.
14. From Einstein's lecture in Kyoto in late 1922. See A. Pais, *Subtle Is the Lord . . .* (Oxford: Oxford University Pres, 1982).
15. From an unpublished paper now in the collection of the Pierpont Morgan Library in New York. See Pais (1982).
16. Einstein inquired of the astronomer George Hale (after whom the 5-m telescope on Palomar Mountain is named) in 1913 whether such minute deflections could be measured near the Sun. The answer was no, but a corrected calculation two years later doubled the predicted deflection and brought detection to within the realm of possibility.
17. This is not a simple integration. See, e.g., Adler et al., *Introduction to General Relativity* (New York: McGraw-Hill, 1963).
18. Both Newtonian mechanics and special relativity predict half this value. The particle-scattering formula used in Chapter 4 to obtain Equation 4-3, applied to the gravitational deflection of a photon of mass $h\nu/c^2$ by the solar mass $M_\odot$ at impact parameter b equal to the solar radius $R_\odot$, shows how this value arises.
19. A copy of Einstein's work (he was then in Berlin) was smuggled out of Germany to Eddington in England so that he could plan the project. Germany and England were then at war. Arthur S. Eddington was at the time director of the prestigious Cambridge Observatory. British authorities approved the eclipse expeditions to avoid the embarrassment of putting such a distinguished scientist as Eddington, a conscientious objector, into a wartime internment camp.
20. See, e.g., R. V. Pound and G. A. Rebka, Jr., *Physical Review Letters*, **4**, 337 (1960).
21. These values are relative to the fixed stars.
22. A. Einstein, "The Foundation of the General Theory of Relativity," *Annalen der Physik*, **49**, 769 (1916).
23. I. I. Shapiro et al., *Physical Review Letters*, **26**, 1132 (1971).
24. R. A. Hulse and J. H. Taylor, *Astrophysical Journal*, **195**, L51 (1975).
25. Gravity wave detectors outside the U.S. are the TAMA 300 (Japan), GEO600 (Germany), and Virgo (Italy). NASA and the European Space Agency are designing a space-based gravity-wave detector, LISA, that will have arms 5 million kilometers long. The three satellites that LISA will comprise are scheduled for launch in 2011.

Problems

Level I

Section 2-1 Relativistic Momentum and Section 2-2 Relativistic Energy

2-1. Show that $p_{yA} = -p_{yB}$, where p_{yA} and p_{yB} are the relativistic momenta and speeds of the balls in Figure 2-1, given by

$$p_{yA} = \frac{mu_0}{\sqrt{1 - u_0^2/c^2}} \qquad p_{yB} = \frac{mu_{yB}}{\sqrt{1 - (u_{xB}^2 + u_{yB}^2)/c^2}}$$

$$u_{yB} = -u_0\sqrt{1 - v^2/c^2} \qquad u_{xB} = v$$

2-2. Show that $d(\gamma mu) = m(1 - u^2/c^2)^{-3/2}\, du$.
2-3. An electron of rest energy $mc^2 = 0.511$ MeV moves with respect to the laboratory at speed u = 0.6c. Find (*a*) γ, (*b*) p in units of MeV/c, (*c*) E, and (*d*) E_k.
2-4. How much energy would be required to accelerate a particle of mass m from rest to a speed of (*a*) 0.5 c, (*b*) 0.9 c, and (*c*) 0.99 c? Express your answers as multiples of the rest energy.
2-5. Two 1-kg masses are separated by a spring of negligible mass. They are pushed together, compressing the spring. If the work done in compressing the spring is 10 J, find the change in mass of the system in kilograms. Does the mass increase or decrease?

STUDENTS-HUB.com Uploaded By: Malak Obaid

2-6. At what value of u/c does the measured mass of a particle exceed its rest mass by (*a*) 10%, (*b*) a factor of 5, and (*c*) a factor of 20?

2-7. A cosmic ray proton is moving at such a speed that it can travel from the Moon to Earth in 1.5 s. (*a*) At what fraction of the speed of light is the proton moving? (*b*) What is its kinetic energy? (*c*) What value would be measured for its mass by an observer in Earth's reference frame? (*d*) What percent error is made in the kinetic energy by using the classical relation? (The Earth-Moon distance is 3.8×10^5 km. Ignore Earth's rotation.)

2-8. How much work must be done on a proton to increase its speed from (*a*) $0.15c$ to $0.16c$? (*b*) $0.85c$ to $0.86c$? (*c*) $0.95c$ to $0.96c$? Notice that the change in the speed is the same in each case.

2-9. The Relativistic Heavy Ion Collider (RHIC) at Brookhaven is colliding fully ionized gold (Au) nuclei accelerated to an energy of 200 GeV per nucleon. Each Au nucleus contains 197 nucleons. (*a*) What is the speed of each Au nucleus just before collision? (*b*) What is the momentum of each at that instant? (*c*) What energy and momentum would be measured for one of the Au nuclei by an observer in the rest system of the other Au nucleus?

2-10. (*a*) Compute the rest energy of 1 g of dirt. (*b*) If you could convert this energy entirely into electrical energy and sell it for 10 cents per kilowatt-hour, how much money would you get? (*c*) If you could power a 100-W lightbulb with the energy, for how long could you keep the bulb lit?

2-11. An electron with rest energy of 0.511 MeV moves with speed $u = 0.2c$. Find its total energy, kinetic energy, and momentum.

2-12. A proton with rest energy of 938 MeV has a total energy of 1400 MeV. (*a*) What is its speed? (*b*) What is its momentum?

2-13. The orbital speed of the Sun relative to the center of the Milky Way is about 250 km/s. By what fraction do the relativistic and Newtonian values differ for (*a*) the Sun's momentum and (*b*) the Sun's kinetic energy?

2-14. An electron in a hydrogen atom has a speed about the proton of 2.2×10^6 m/s. (*a*) By what percent do the relativistic and Newtonian values of E_k differ? (*b*) By what percent do the momentum values differ?

2-15. Suppose that you seal an ordinary 60-W lightbulb and a suitable battery inside a transparent enclosure and suspend the system from a very sensitive balance. (*a*) Compute the change in the mass of the system if the lamp is on continuously for one year at full power. (*b*) What difference, if any, would it make if the inner surface of the container were a perfect reflector?

Section 2-3 Mass/Energy Conversion and Binding Energy

2-16. Use Appendix A and Table 2-1 to find how much energy is needed to remove one proton from a ^{4}He atom, leaving a ^{3}H atom plus a proton and an electron.

2-17. Use Appendix A and Table 2-1 to find how much energy is required to remove one of the neutrons from a ^{3}H atom to yield a ^{2}H atom plus a neutron.

2-18. The energy released when sodium and chlorine combine to form NaCl is 4.2 eV. (*a*) What is the increase in mass (in unified mass units) when a molecule of NaCl is dissociated into an atom of Na and an atom of Cl? (*b*) What percentage of error is made in neglecting this mass difference? (The mass of Na is about 23 u and that of Cl is about 35.5 u.)

2-19. In a nuclear fusion reaction two ^{2}H atoms are combined to produce one ^{4}He. (*a*) Calculate the decrease in rest mass in unified mass units. (*b*) How much energy is released in this reaction? (*c*) How many such reactions must take place per second to produce 1 W of power?

2-20. An elementary particle of mass M completely absorbs a photon, after which its mass is $1.01M$. (*a*) What was the energy of the incoming photon? (*b*) Why is that energy greater than $0.01Mc^2$?

2-21. When a beam of high-energy protons collides with protons at rest in the laboratory (e.g., in a container of water or liquid hydrogen), neutral pions (π^0) are produced by the reaction $p + p \rightarrow p + p + \pi^0$. Compute the threshold energy of the protons in the beam for this reaction to occur. (See Table 2-1 and Example 2-11.)

STUDENTS-HUB.com Uploaded By: Malak Obaid

2-22. The energy released in the fission of a ^{235}U nucleus is about 200 MeV. How much rest mass (in kg) is converted to energy in this fission?
2-23. The temperature of the Sun's core is about 1.5×10^7 K. Assuming the core to consist of atomic hydrogen gas and recalling that temperature measures the average kinetic energy of the atoms, compute (*a*) the thermal energy of 1 kg of the gas and (*b*) the mass associated with this energy ($\overline{E}_k = 3kT/2$, where k is the Boltzmann constant; see Chapter 3).

Section 2-4 Invariant Mass

2-24. Compute the force exerted on the palm of your hand by the beam from a 1.0-W flashlight (*a*) if your hand absorbs the light, and (*b*) if the light reflects from your hand. What would be the mass of a particle that exerts that same force in each case if you hold it at Earth's surface?
2-25. An electron-positron pair combined as positronium is at rest in the laboratory. The pair annihilate, producing a pair of photons (gamma rays) moving in opposite directions in the lab. Show that the invariant rest energy of the gamma rays is equal to that of the electron pair.
2-26. Show that Equation 2-31 can be written $E = mc^2(1 + p^2/m^2c^2)^{1/2}$ and use the binomial expansion to show that, when pc is much less than mc^2, $E \approx mc^2 + p^2/2m$.
2-27. An electron of rest energy 0.511 MeV has a total energy of 5 MeV. (*a*) Find its momentum in units of MeV/c. (*b*) Find u/c.
2-28. Make a sketch of the total energy of an electron E as a function of its momentum p. (See Equations 2-36 and 2-39 for the behavior of E at large and small values of p.)
2-29. What is the speed of a particle that is observed to have momentum 500 MeV/c and energy 1746 MeV? What is the particle's mass (in MeV/c^2)?
2-30. An electron of total energy 4.0 MeV moves perpendicular to a uniform magnetic field along a circular path whose radius is 4.2 cm. (*a*) What is the strength of the magnetic field B? (*b*) By what factor does γm exceed m?
2-31. A proton is bent into a circular path of radius 2 m by a magnetic field of 0.5 T. (*a*) What is the momentum of the proton? (*b*) What is its kinetic energy?

Section 2-5 General Relativity

2-32. Compute the deflection angle α for light from a distant star that would, according to general relativity, be measured by an observer on the Moon as the light grazes the edge of Earth.
2-33. A set of twins work in the Sears Tower, a very tall office building in Chicago. One works on the top floor and the other works in the basement. Considering general relativity, which twin will age more slowly? (*a*) They will age at the same rate. (*b*) The twin who works on the top floor will age more slowly. (*c*) The twin who works in the basement will age more slowly. (*d*) It depends on the building's speed. (*e*) None of the previous choices is correct.
2-34. Jupiter makes 8.43 orbits/century and exhibits an orbital eccentricity $\epsilon = 0.048$. Jupiter is 5.2 AU from the Sun (see footnote for Table 2-2 in the More section) and has a mass 318 times the Earth's 5.98×10^{24} kg. What does general relativity predict for the rate of precession of Jupiter's perihelion? (It has not yet been measured.) (The astronomical unit AU = the mean Earth-Sun distance = 1.50×10^{11} m.)
2-35. A synchronous satellite "parked" in orbit over the equator is used to relay microwave transmissions between stations on the ground. To what frequency must the satellite's receiver be tuned if the frequency of the transmission from Earth is exactly 9.375 GHz? (Ignore all Doppler effects.)
2-36. A particular distant star is found to be 92 $c \cdot$ y from Earth. On a direct line between us and the star and 35 $c \cdot$ y from the distant star is a dense white dwarf star with a mass equal to 3 times the Sun's mass $M_\odot$ and a radius of 104 km. Deflection of the light beam from the distant star by the white dwarf causes us to see it as a pair of circular arcs like those shown in Figure 2-20(*b*). Find the angle 2α formed by the lines of sight to the two arcs.

Level II

2-37. A clock is placed on a satellite that orbits Earth with a period of 90 min at an altitude of 300 km. By what time interval will this clock differ from an identical clock on Earth after 1 year? (Include both special and general relativistic effects.)

STUDENTS-HUB.com Uploaded By: Malak Obaid

2-38. Referring to Example 2-11, find the total energy E' as measured in S' where $p' = 0$.

2-39. In the Stanford linear collider, small bundles of electrons and positrons are fired at each other. In the laboratory's frame of reference, each bundle is about 1 cm long and 10 μm in diameter. In the collision region, each particle has energy of 50 GeV, and the electrons and positrons are moving in opposite directions. (*a*) How long and how wide is each bundle in its own reference frame? (*b*) What must be the minimum proper length of the accelerator for a bundle to have both its ends simultaneously in the accelerator in its own reference frame? (The actual length of the accelerator is less than 1000 m.) (*c*) What is the length of a positron bundle in the reference frame of the electron bundle? (*d*) What are the momentum and energy of the electrons in the rest frame of the positrons?

2-40. The rest energy of a proton is about 938 MeV. If its kinetic energy is also 938 MeV, find (*a*) its momentum and (*b*) its speed.

2-41. A spaceship of mass 10^6 kg is coasting through space when suddenly it becomes necessary to accelerate. The ship ejects 10^3 kg of fuel in a very short time at a speed of $c/2$ relative to the ship. (*a*) Neglecting any change in the rest mass of the system, calculate the speed of the ship in the frame in which it was initially at rest. (*b*) Calculate the speed of the ship using classical Newtonian mechanics. (*c*) Use your results from (*a*) to estimate the change in the rest mass of the system.

2-42. A clock (or a light-emitting atom) located at Earth's equator moves at about 463 m/s relative to one located at the pole. The equator clock is also about 21 km farther from the center of Earth than the pole clock due to Earth's equatorial bulge. For an inertial reference frame centered on Earth, compute the time dilation effect for each clock as seen by an observer at the other clock. Show that the effects nearly cancel and that, as a result, the clocks read very close to the same time. (Assume that g is constant over the 21 km of the equatorial bulge.)

2-43. Professor Spenditt, oblivious to economics and politics, proposes the construction of a circular proton accelerator around Earth's circumference using bending magnets that provide a magnetic field of 1.5 T. (*a*) What would be the kinetic energy of protons orbiting in this field in a circle of radius R_E? (*b*) What would be the period of rotation of these protons?

2-44. In ancient Egypt the annual flood of the Nile was predicted by the rise of Sirius (the Dog Star). Sirius is one of a binary pair whose companion is a white dwarf. Orbital analysis of the pair indicates that the dwarf's mass is 2×10^{30} kg (i.e., about one solar mass). Comparison of spectral lines emitted by the white dwarf with those emitted by the same element on Earth shows a fractional frequency shift of 7×10^{-4}. Assuming this to be due to a gravitational redshift, compute the density of the white dwarf. (For comparison, the Sun's density is 1409 kg/m^3.)

2-45. Show that the creation of an electron-positron pair (or any particle-antiparticle pair, for that matter) by a single photon is not possible in isolation, i.e., that additional mass (or radiation) must be present. (*Hint:* Use the conservation laws.)

2-46. With inertial systems S and S' arranged with their corresponding axes parallel and S' moving in the $+x$ direction, it was apparent that the Lorentz transformation for y and z would be $y' = y$ and $z' = z$. The transformations for the y and z components of the momentum are not so apparent, however. Show that, as stated in Equations 2-16 and 2-17, $p'_y = p_y$ and $p'_z = p_z$.

Level III

2-47. Two identical particles of rest mass m are each moving toward the other with speed u in frame S. The particles collide inelastically with a spring that locks shut (see Figure 2-9) and come to rest in S, and their initial kinetic energy is transformed into potential energy. In this problem you are going to show that the conservation of momentum in reference frame S', in which one of the particles is initially at rest, requires that the total rest mass of the system after the collision be $2m/(1 - u^2/c^2)^{1/2}$. (*a*) Show that the speed of the particle not at rest in frame S' is

$$u' = \frac{2u}{1 + u^2/c^2}$$

and use this result to show that

$$\sqrt{1 - \frac{u'^2}{c^2}} = \frac{1 - u^2/c^2}{1 + u^2/c^2}$$

STUDENTS-HUB.com Uploaded By: Malak Obaid

(b) Show that the initial momentum in frame S' is $p' = 2mu/(1 - u^2/c^2)$. (c) After the collision, the composite particle moves with speed u in S' (since it is at rest in S). Write the total momentum after the collision in terms of the final rest mass M, and show that the conservation of momentum implies that $M = 2m/(1 - u^2/c^2)^{1/2}$. ($d$) Show that the total energy is conserved in each reference frame.

2-48. An antiproton $\bar{p}$ has the same rest energy as a proton. It is created in the reaction $p + p \rightarrow p + p + p + \bar{p}$. In an experiment, protons at rest in the laboratory are bombarded with protons of kinetic energy E_k, which must be great enough so that kinetic energy equal to $2mc^2$ can be converted into the rest energy of the two particles. In the frame of the laboratory, the total kinetic energy cannot be converted into rest energy because of conservation of momentum. However, in the zero-momentum reference frame in which the two initial protons are moving toward each other with equal speed u, the total kinetic energy can be converted into rest energy. (a) Find the speed of each proton u such that the total kinetic energy in the zero-momentum frame is $2mc^2$. (b) Transform to the laboratory's frame in which one proton is at rest, and find the speed u' of the other proton. (c) Show that the kinetic energy of the moving proton in the laboratory's frame is $E_k = 6mc^2$.

2-49. In a simple thought experiment, Einstein showed that there is mass associated with electromagnetic radiation. Consider a box of length L and mass M resting on a frictionless surface. At the left wall of the box is a light source that emits radiation of energy E, which is absorbed at the right wall of the box. According to classical electromagnetic theory, this radiation carries momentum of magnitude $p = E/c$. (a) Find the recoil velocity of the box such that momentum is conserved when the light is emitted. (Since p is small and M is large, you may use classical mechanics.) (b) When the light is absorbed at the right wall of the box, the box stops, so the total momentum remains zero. If we neglect the very small velocity of the box, the time it takes for the radiation to travel across the box is $\Delta t = L/c$. Find the distance moved by the box in this time. (c) Show that if the center of mass of the system is to remain at the same place, the radiation must carry mass $m = E/c^2$.

2-50. A pion spontaneously decays into a muon and a muon antineutrino according to (among other processes) $\pi^- \rightarrow \mu^- + \bar{\nu}_\mu$. Recent experimental evidence indicates that the mass m of the $\bar{\nu}_\mu$ is no larger than about 190 keV/c^2 and may be as small as zero. Assuming that the pion decays at rest in the laboratory, compute the energies and momenta of the muon and muon antineutrino (a) if the mass of the antineutrino were zero and (b) if its mass were 190 keV/c^2. The mass of the pion is 139.56755 MeV/c^2 and the mass of the muon is 105.65839 MeV/c^2. (See Chapters 11 and 12 for more on the neutrino mass.)

2-51. Use Equation 2-47 to obtain the gravitational redshift in terms of the wavelength λ. Use that result to determine the shift in wavelength of light emitted by a white dwarf star at 720.00 nm. Assume the white dwarf has the same mass as the Sun (1.99×10^{30} kg) but a radius equal to only 1 percent of the solar radius $R_\odot$ ($R_\odot = 6.96 \times 10^8$ m).

2-52. For a particle moving in the xy plane of S, show that the y' component of the acceleration is given by

$$a'_y = \frac{a_y}{\gamma^2(1 - u_x v/c^2)^2} + \frac{a_x u_y v/c^2}{\gamma^2(1 - u_x v/c^2)^3}$$

2-53. Consider an object of mass m at rest in S acted upon by a force F with components F_x and F_y. System S' moves with instantaneous velocity v in the $+x$ direction. Defining the force with Equation 2-8 and using the Lorentz velocity transformation, show that (a) $F'_x = F_x$ and (b) $F'_y = F_y/\gamma$. (*Hint:* See Problem 2-52.)

2-54. An unstable particle of mass M decays into two identical particles, each of mass m. Obtain an expression for the velocities of the two decay particles in the lab frame (a) if M is at rest in the lab and (b) if M has total energy $4mc^2$ when it decays and the decay particles move along the direction of M.

STUDENTS-HUB.com Uploaded By: Malak Obaid

CHAPTER 3

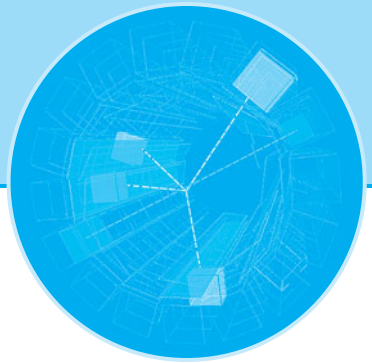

Quantization of Charge, Light, and Energy

3-1 Quantization of Electric Charge 115
3-2 Blackbody Radiation 119
3-3 The Photoelectric Effect 127
3-4 X Rays and the Compton Effect 133

The idea that all matter is composed of tiny particles, or atoms, dates to the speculations of the Greek philosopher Democritus[1] and his teacher Leucippus in about 450 B.C. However, little attempt was made to correlate such speculations with observations of the physical world until the seventeenth century. Pierre Gassendi, in the mid-seventeenth century, and Robert Hooke, somewhat later, attempted to explain states of matter and the transitions between them with a model of tiny, indestructible solid objects flying in all directions. But it was Avogadro's hypothesis, advanced in 1811, that all gases at a given temperature contain the same number of molecules per unit volume, that led to great success in the interpretation of chemical reactions and to development of kinetic theory in about 1900. Avogadro's hypothesis made possible quantitative understanding of many bulk properties of matter and led to general (though not unanimous) acceptance of the molecular theory of matter. Thus, matter is not continuous, as it appears, but is *quantized* (i.e., discrete) on the microscopic scale. Scientists of the day understood that the small size of the atom prevented the discreteness of matter from being readily observable.

In this chapter, we will study how three additional great quantization discoveries were made: (1) electric charge, (2) light energy, and (3) energy of oscillating mechanical systems. The quantization of electric charge was not particularly surprising to scientists in 1900; it was quite analogous to the quantization of mass. However, the quantization of light energy and mechanical energy, which are of central importance in modern physics, were revolutionary ideas.

3-1 Quantization of Electric Charge

Early Measurements of e and e/m

The first estimates of the order of magnitude of the electric charges found in atoms were obtained from Faraday's law. The work of Michael Faraday (1791–1867) in the early to mid-1800s stands out even today for its vision, experimental ingenuity, and thoroughness. The story of this self-educated blacksmith's son who rose from errand boy and

STUDENTS-HUB.com Uploaded By: Malak Obaid

bookbinder's apprentice to become the director of the distinguished Royal Institution of London and the foremost experimental investigator of his time is a fascinating one. One aspect of his work concerned the study of the conduction of electricity in weakly conducting solutions. His discovery that the same quantity of electricity, F, now called the *faraday* and equal to about 96,500 C, always decomposes one gram-ionic weight, that is, Avogadro's number N_A, of monovalent ions leads to the reasonable conclusion that each monovalent ion carries the same electric charge, e, and therefore

$$F = N_A e \qquad \textbf{3-1}$$

Equation 3-1 is called Faraday's law of electrolysis. While F was readily measurable, neither N_A nor e could be experimentally determined at the time. Faraday was aware of this but could not determine either quantity. Even so, it seemed logical to expect that electric charge, like matter, was not continuous, but consisted of particles of some discrete minimum charge. In 1874, G. J. Stoney[2] used an estimate of N_A from kinetic theory to compute the value of e from Equation 3-1 to be about 10^{-20} C; however, direct measurement of the value of e had to await an ingenious experiment conducted by R. A. Millikan a third of a century later.

Meanwhile, Pieter Zeeman, in 1896, obtained the first evidence for the existence of atomic particles with a specific charge-to-mass ratio by looking at the changes in the discrete *spectral lines* emitted by atoms when they were placed in a strong magnetic field. He discovered that the individual spectral lines split into three very closely spaced lines of slightly different frequencies when the atoms were placed in the magnetic field. (This phenomenon is called the *Zeeman effect* and will be discussed further in Chapter 7.) Classical electromagnetic theory relates the slight differences in the frequencies of adjacent lines to the charge-to-mass ratio of the oscillating charges producing the light.

From his measurements of the splitting, Zeeman calculated q/m to be about 1.6×10^{11} C/kg, which compares favorably with the presently accepted value, 1.759×10^{11} C/kg (see Appendix D). From the polarization of the spectral lines, Zeeman concluded that the oscillating particles were negatively charged.

Discovery of the Electron: J. J. Thomson's Experiment

The year following Zeeman's work, J. J. Thomson[3] measured the q/m value for the so-called cathode rays that were produced in electrical discharges in gases and pointed out that, if their charge was Faraday's charge e as determined by Stoney, then their mass was only a small fraction of the mass of a hydrogen atom. Two years earlier J. Perrin had collected cathode rays on an electrometer and found them to carry a negative electric charge.[4] Thus, with his measurement of q/m for the cathode rays, Thomson had, in fact, discovered the *electron.* That direct measurement of e/m of electrons by J. J. Thomson in 1897, a little over a century ago, can be justly considered to mark the beginning of our understanding of atomic structure.

Measurement of e/m When a uniform magnetic field of strength B is established perpendicular to the direction of motion of charged particles, the particles move in a circular path. The radius R of the path can be obtained from Newton's second law by setting the magnetic force quB equal to the mass m times the centripetal acceleration u^2/R, where u is the speed of the particles:

$$quB = \frac{mu^2}{R} \quad \text{or} \quad \mathrm{R} = \frac{\mathrm{mu}}{qB} \quad \text{and} \quad \frac{q}{m} = \frac{u}{RB} \qquad \textbf{3-2}$$

STUDENTS-HUB.com Uploaded By: Malak Obaid

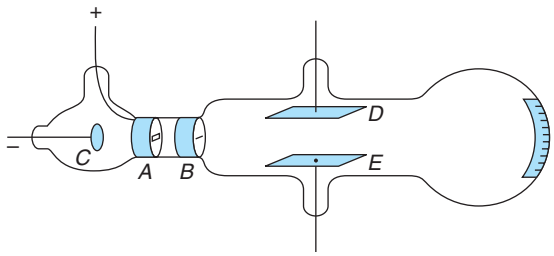

Figure 3-1 J. J. Thomson's tube for measuring e/m. Electrons from the cathode C pass through the slits at A and B and strike a phosphorescent screen. The beam can be deflected by an electric field between the plates D and E or by a magnetic field (not shown) whose direction is perpendicular to the electric field between D and E. From the deflections measured on a scale on the tube at the screen, e/m can be determined. [*From J. J. Thomson, "Cathode Rays," Philosophical Magazine (5),* ***44****, 293 (1897).*]

Thomson performed two e/m experiments of somewhat different designs. The second, more reproducible of the two has become known as the *J. J. Thomson experiment* (Figure 3-1). In this experiment he adjusted perpendicular B and $\mathscr{E}$ fields so that the particles were undeflected. This allowed him to determine the speed of the electrons by equating the magnitudes of the magnetic and electric forces and then to compute $e/m(\equiv q/m)$ from Equation 3-2:

$$quB = q\mathscr{E} \quad \text{or} \quad u = \frac{\mathscr{E}}{B} \qquad \textbf{3-3}$$

Thomson's technique for controlling the direction of the electron beam with "crossed" electric and magnetic fields was subsequently applied in the development of cathode ray tubes used in oscilloscopes and the picture tubes of television receivers.

Thomson's experiment was remarkable in that he measured e/m for a subatomic particle using only a voltmeter, an ammeter, and a measuring rod, obtaining the result 0.7×10^{11} C/kg. Present-day particle physicists routinely use the modern equivalent of Thomson's experiment to measure the momenta of elementary particles.

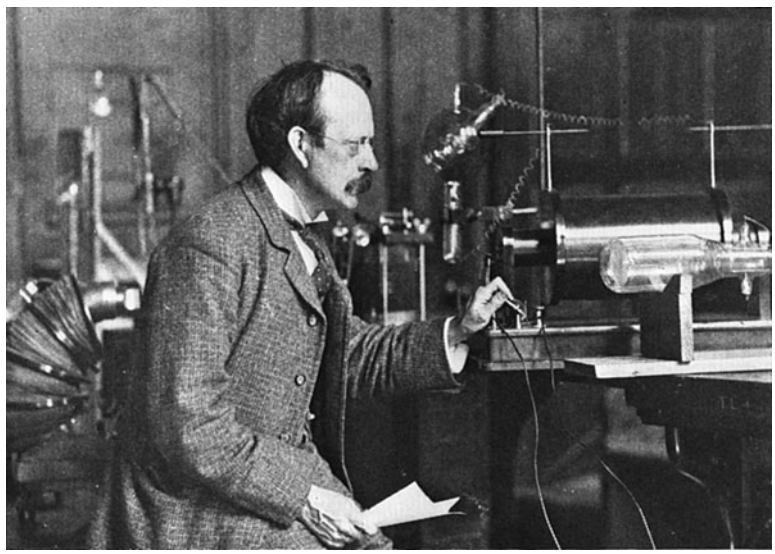

J. J. Thomson in his laboratory. He is facing the screen end of an e/m tube; an older cathode ray tube is visible in front of his left shoulder. [*Courtesy of Cavendish Laboratory.*]

STUDENTS-HUB.com Uploaded By: Malak Obaid

Thomson repeated the experiment with different gases in the tube and different metals for cathodes and always obtained the same value for e/m within his experimental uncertainty, thus showing that these particles are common to all metals. The agreement of these results with Zeeman's led to the unmistakable conclusion that these particles—called *corpuscles* by Thomson and later called *electrons* by Lorentz—which have one unit of negative charge e and a mass about 2000 times less than the mass of the lightest known atom were constituents of *all* atoms.

Questions

1. One advantage of Thomson's evidence over others' (such as Faraday's or Zeeman's) was its directness. Another was that it was not just a statistical inference. How does the Thomson experiment show that e/m is the same for a large number of the particles?
2. Thomson noted that his values for e/m were about 2000 times larger than those for the lightest known ion, that of hydrogen. Could he tell from his data whether this was the result of the electron having either a greater charge or a smaller mass than the hydrogen ion?

Measuring the Electric Charge: Millikan's Experiment

The fact that Thomson's e/m measurements always yielded the same results regardless of the materials used for the cathodes or the kind of gas in the tube was a persuasive argument that the electrons all carried one unit e of negative electric charge. Thomson initiated a series of experiments to determine the value of e. The first of these experiments, which turned out to be very difficult to do with high precision, was carried out by his student J. S. E. Townsend. The idea was simple: a small (but visible) cloud of identical water droplets, each carrying a single charge e, was observed to drift downward in response to the gravitational force. The total charge on the cloud $Q = Ne$ was measured, as were the mass of the cloud and the radius of a single drop. Finding the radius allowed calculation of N, the total number of drops in the cloud, and, hence, the value of e.

The accuracy of Thomson's method was limited by the uncertain rate of evaporation of the cloud. In addition, the assumption that each droplet contained a single charge could not be verified. R. A. Millikan tried to eliminate the evaporation problem by using a field strong enough to hold the top surface of the cloud stationary so that he could observe the rate of evaporation and correct for it. That, too, turned out to be very difficult, but then he made a discovery of enormous importance, one that allowed him to measure directly the charge of a single electron! Millikan described his discovery in the following words:

> It was not found possible to balance the cloud as had been originally planned, but it was found possible to do something much better: namely, to hold individual charged drops suspended by the field for periods varying from 30 to 60 seconds. I have never actually timed drops which lasted more than 45 seconds, although I have several times observed drops which in my judgment lasted considerably longer than this. The drops which it was found possible to balance by an electric field always carried multiple charges, and the difficulty experienced in balancing such drops was less than had been anticipated.[5]

STUDENTS-HUB.com Uploaded By: Malak Obaid

The discovery that he could see individual droplets and that droplets suspended in a vertical electric field sometimes suddenly moved upward or downward, evidently because they had picked up a positive or negative ion, led to the possibility of observing the charge of a single ion. In 1909, Millikan began a series of experiments that not only showed that charges occurred in integer multiples of an elementary unit e, but measured the value of e to about 1 part in 1000. To eliminate evaporation, he used oil drops sprayed into dry air between the plates of a capacitor (Figure 3-2). These drops were already charged by the spraying process, i.e., by friction in the spray nozzle, and during the course of the observation they picked up or lost additional charges. By switching the direction of the electric field between the plates, a drop could be moved up or down and observed for several hours. When the charge on a drop changed, the velocity of the drop with the field "on" changed also. Assuming only that the terminal velocity of the drop was proportional to the force acting on it (this assumption was carefully checked experimentally), Millikan's oil drop experiment[6] gave conclusive evidence that electric charges always occur in integer multiples of a fundamental unit e, whose value he determined to be 1.601×10^{-19} C. The currently accepted value[7] is $1.60217653 \times 10^{-19}$ C. An expanded discussion of Millikan's experiment is included in the Classical Concept Review.

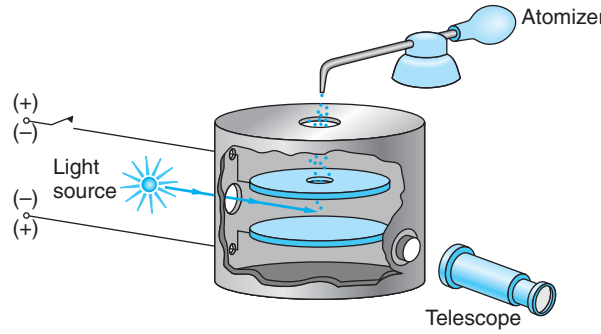

Figure 3-2 Schematic diagram of Millikan's oil drop experiment. The drops are sprayed from an atomizer and pick up a static charge, a few falling through the hole in the top plate. Their fall due to gravity and their rise due to the electric field between the capacitor plates can be observed with the telescope. From measurements of the rise and fall times, the electric charge on a drop can be calculated. The charge on a drop could be changed by exposure to x rays from a source (not shown) mounted opposite the light source.

3-2 Blackbody Radiation

The first clue to the quantum nature of radiation came from the study of thermal radiation emitted by opaque bodies. When radiation falls on a opaque body, part of it is reflected and the rest is absorbed. Light-colored bodies reflect most of the visible radiation incident on them, whereas dark bodies absorb most of it. The absorption part of the process can be described briefly as follows. The radiation absorbed by the body increases the kinetic energy of the constituent atoms, which oscillate about their equilibrium positions. Since the average translational kinetic energy of the atoms determines the temperature of the body, the absorbed energy causes the temperature to rise. However, the atoms contain charges (the electrons), and they are accelerated by the oscillations. Consequently, as required by electromagnetic theory, the atoms emit electromagnetic radiation, which reduces the kinetic energy of the oscillations and tends to reduce the temperature. When the rate of absorption equals the rate of emission, the temperature is constant, and we say that the body is in thermal equilibrium with its surroundings. A good absorber of radiation is therefore also a good emitter.

The electromagnetic radiation emitted under these circumstances is called *thermal radiation.* At ordinary temperatures (below about 600°C) the thermal radiation emitted by a body is not visible; most of the energy is concentrated in wavelengths much longer than those of visible light. As a body is heated, the quantity of thermal radiation emitted increases, and the energy radiated extends to shorter and shorter wavelengths. At about 600°–700°C there is enough energy in the visible spectrum so that the body glows and becomes a dull red, and at higher temperatures it becomes bright red or even "white hot."

STUDENTS-HUB.com Uploaded By: Malak Obaid

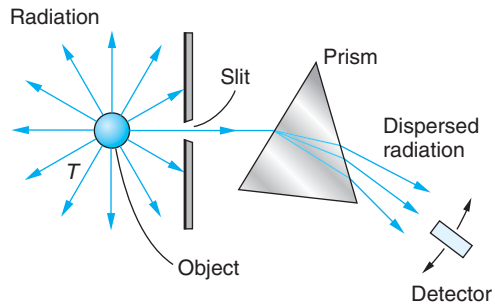

Figure 3-3 Radiation emitted by the object at temperature T that passes through the slit is dispersed according to its wavelengths. The prism shown would be an appropriate device for that part of the emitted radiation in the visible region. In other spectral regions other types of devices or wavelength-sensitive detectors would be used.

A body that absorbs *all* radiation incident on it is called an *ideal blackbody.* In 1879 Josef Stefan found an empirical relation between the power radiated by an ideal blackbody and the temperature:

$$R = \sigma T^4 \qquad \textbf{3-4}$$

where R is the power radiated per unit area, T is the absolute temperature, and $\sigma = 5.6703 \times 10^{-8}\ \mathrm{W/m^2K^4}$ is a constant called Stefan's constant. This result was also derived on the basis of classical thermodynamics by Ludwig Boltzmann about five years later, and Equation 3-4 is now called the Stefan-Boltzmann law. Note that the power per unit area radiated by a blackbody depends only on the temperature and not on any other characteristic of the object, such as its color or the material of which it is composed. Note, too, that R tells us the *rate* at which energy is emitted by the object. For example, doubling the absolute temperature of an object, e.g., a star, increases the energy flow out of the object by a factor of $2^4 = 16$. An object at room temperature (300°C) will double the rate at which it radiates energy as a result of a temperature increase of only 57°C. Thus, the Stefan-Boltzmann law has an enormous effect on the establishment of thermal equilibrium in physical systems.

Objects that are not ideal blackbodies radiate energy per unit area at a rate less than that of a blackbody at the same temperature. For those objects the rate does depend on properties in addition to the temperature, such as color and the composition of the surface. The effects of those dependencies are combined into a factor called the *emissivity* ϵ which multiplies the right side of Equation 3-4. The values of ϵ, which is itself temperature dependent, are always less than unity.

Like the total radiated power R, the *spectral distribution* of the radiation emitted by a blackbody is found empirically to depend *only* on the absolute temperature T. The spectral distribution is determined experimentally as illustrated schematically in Figure 3-3. With $R(\lambda)\,d\lambda$ the power emitted per unit area with wavelength between λ and $\lambda + d\lambda$, Figure 3-4 shows the measured spectral distribution function $R(\lambda)$ versus λ for several values of T ranging from 1000 K to 6000 K.

The $R(\lambda)$ curves in Figure 3-4 are quite remarkable in several respects. One is that the wavelength at which the distribution has its maximum value varies inversely with the temperature:

$$\lambda_m \propto \frac{1}{T}$$

or

$$\lambda_m T = \text{constant} = 2.898 \times 10^{-3}\ \mathrm{m \cdot K} \qquad \textbf{3-5}$$

STUDENTS-HUB.com Uploaded By: Malak Obaid

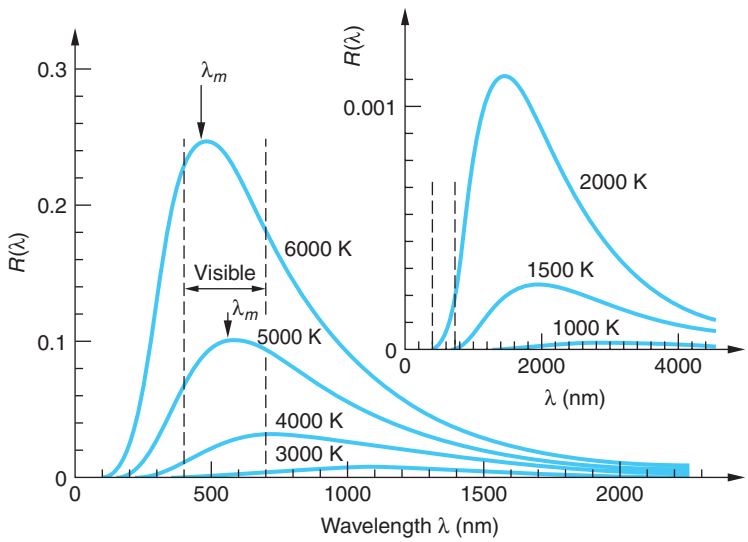

Figure 3-4 Spectral distribution function $R(\lambda)$ measured at different temperatures. The R (λ) axis is in arbitrary units for comparison only. Notice the range of λ in the visible spectrum. The Sun emits radiation very close to that of a blackbody at 5800 K. λ_m is indicated for the 5000-K and 6000-K curves.

This result is known as Wien's displacement law. It was obtained by Wien in 1893. Examples 3-1 and 3-2 illustrate its application.

EXAMPLE 3-1 How Big Is a Star? Measurement of the wavelength at which the spectral distribution $R(\lambda)$ from a certain star is maximum indicates that the star's surface temperature is 3000 K. If the star is also found to radiate 100 times the power $P_\odot$ radiated by the Sun, how big is the star? (The symbol $\odot$ = Sun.) The Sun's surface temperature is 5800 K.

SOLUTION

If the Sun and the star both radiate as blackbodies (astronomers nearly always make that assumption, based on, among other things, the fact that the solar spectrum is very nearly that of an ideal blackbody), their surface temperatures from Equation 3-5 are 5800 K and 3000 K, respectively. Measurement also indicates that $P_{\text{star}} = 100\,P_\odot$. Thus, from Equation 3-4 we have

$$R_{\text{star}} = \frac{P_{\text{star}}}{(\text{area})_{\text{star}}} = \frac{100\,P_\odot}{4\pi r_{\text{star}}^2} = \sigma T_{\text{star}}^4$$

and

$$R_\odot = \frac{P_\odot}{(\text{area})_\odot} = \frac{P_\odot}{4\pi r_\odot^2} = \sigma T_\odot^4$$

So we have

$$r_{\text{star}}^2 = 100\,r_\odot^2\left(\frac{T_\odot}{T_{\text{star}}}\right)^4$$

$$r_{\text{star}} = 10\,r_\odot\left(\frac{T_\odot}{T_{\text{star}}}\right)^2 = 10\left(\frac{5800}{3000}\right)^2 r_\odot$$

$$r_{\text{star}} = 37.4\,r_\odot$$

Since $r_\odot = 6.96 \times 10^8$ m, this star has a radius of about 2.6×10^{10} m, or about half the radius of the orbit of Mercury. This star is a red giant (see Chapter 13).

STUDENTS-HUB.com Uploaded By: Malak Obaid

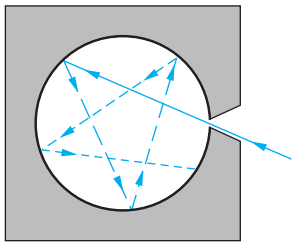

Figure 3-5 A small hole in the wall of a cavity approximating an ideal blackbody. Radiation entering the hole has little chance of leaving before it is completely absorbed within the cavity.

Rayleigh-Jeans Equation

The calculation of the distribution function $R(\lambda)$ involves the calculation of the energy density of electromagnetic waves in a cavity. Materials such as black velvet or lampblack come close to being ideal blackbodies, but the best practical realization of an ideal blackbody is a small hole leading into a cavity (such as a keyhole in a closet door; Figure 3-5). Radiation incident on the hole has little chance of being reflected back out of the hole before it is absorbed by the walls of the cavity. The power radiated *out* of the hole is proportional to the total energy density U (the energy per unit volume of the radiation in the cavity). The proportionality constant can be shown to be $c/4$, where c is the speed of light.[8]

$$R = \frac{1}{4}cU \qquad \textbf{3-6}$$

Similarly, the spectral distribution of the power emitted from the hole is proportional to the spectral distribution of the energy density in the cavity. If $u(\lambda)\,d\lambda$ is the fraction of the energy per unit volume in the cavity in the range $d\lambda$, then $u(\lambda)$ and $R(\lambda)$ are related by

$$R(\lambda) = \frac{1}{4}cu(\lambda) \qquad \textbf{3-7}$$

The energy density distribution function $u(\lambda)$ can be calculated from classical physics in a straightforward way. The method involves finding the number of modes of oscillation of the electromagnetic field in the cavity with wavelengths in the interval $d\lambda$ and multiplying by the average energy per mode. The result is that the number of modes of oscillation per unit volume, $n(\lambda)$, is independent of the shape of the cavity and is given by

$$n(\lambda) = 8\pi\lambda^{-4} \qquad \textbf{3-8}$$

According to classical kinetic theory, the average energy per mode of oscillation is kT, the same as for a one-dimensional harmonic oscillator, where k is the Boltzmann constant. Classical theory thus predicts for the energy density distribution function

$$u(\lambda) = kT\,n(\lambda) = 8\pi kT\lambda^{-4} \qquad \textbf{3-9}$$

This prediction, initially derived by Lord Rayleigh,[9] is called the *Rayleigh-Jeans equation.* It is illustrated in Figure 3-6.

At very long wavelengths the Rayleigh-Jeans equation agrees with the experimentally determined spectral distribution, but at short wavelengths this equation predicts that $u(\lambda)$ becomes large, approaching infinity as $\lambda \longrightarrow 0$, whereas experiment shows (see Figure 3-4) that the distribution actually approaches zero as $\lambda \longrightarrow 0$. This enormous disagreement between the experimental measurement of $u(\lambda)$ and the prediction of the fundamental laws of classical physics at short wavelengths was called the *ultraviolet catastrophe.* The word *catastrophe* was not used lightly; Equation 3-9 implies that

$$\int_0^\infty u(\lambda)\,d\lambda \longrightarrow \infty \qquad \textbf{3-10}$$

That is, every object would have an infinite energy density, which observation assures us is not true.

STUDENTS-HUB.com Uploaded By: Malak Obaid

Planck's Law

In 1900 the German physicist Max Planck[10] announced that by making somewhat strange assumptions, he could derive a function $u(\lambda)$ that agreed with the experimental data. He first found an empirical function that fit the data and then searched for a way to modify the usual calculation so as to predict his empirical formula. We can see the type of modification needed if we note that, for any cavity, the shorter the wavelength, the more standing waves (modes) will be possible. Therefore, as $\lambda \rightarrow 0$ the number of modes of oscillation approaches infinity, as evidenced in Equation 3-8. In order for the energy density distribution function $u(\lambda)$ to approach zero, we expect the average energy per mode to depend on the wavelength λ and approach zero as λ approaches zero, rather than be equal to the value kT predicted by classical theory.

Parenthetically, we should note that those working on the ultraviolet catastrophe at the time—and there were many besides Planck—had no a priori way of knowing whether the number of modes $n(\lambda)$ or the average energy per mode kT (or both) was the source of the problem. Both were correct classically. Many attempts were made to rederive each so as to solve the problem. As it turned out, it was the average energy per mode (that is, kinetic theory) that was at fault.

Classically, the electromagnetic waves in the cavity are produced by accelerated electric charges in the walls of the cavity vibrating as simple harmonic oscillators. Recall that the radiation emitted by such an oscillator has the same frequency as the oscillation itself. The average energy for a one-dimensional simple harmonic oscillator is calculated classically from the energy distribution function, which in turn is found from the Maxwell-Boltzmann distribution function. That energy distribution function has the form (see Chapter 8)

$$f(E) = Ae^{-E/kT} \tag{3-11}$$

where A is a constant and $f(E)$ is the fraction of the oscillators with energy equal to E. The average energy $\overline{E}$ is then found, as is any weighted average, from

$$\overline{E} = \int_0^\infty E f(E)\, dE = \int_0^\infty EAe^{-E/kT}\, dE \tag{3-12}$$

with the result $\overline{E} = kT$, as was used by Rayleigh and others.

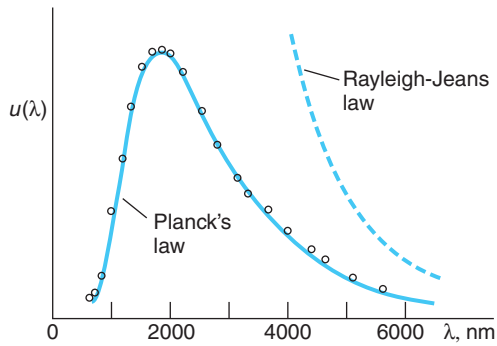

Figure 3-6 Comparison of Planck's law and the Rayleigh-Jeans equation with experimental data at $T = 1600$ K obtained by W. W. Coblenz in about 1915. The $u(\lambda)$ axis is linear. [*Adapted from F. K. Richmyer, E. H. Kennard, and J. N. Cooper, Introduction to Modern Physics, 6th ed., McGraw-Hill, New York (1969), by permission.*]

STUDENTS-HUB.com Uploaded By: Malak Obaid

Planck found that he could derive his empirical formula by calculating the average energy $\overline{E}$ assuming that the energy of the oscillating charges, and hence the radiation that they emitted, was a discrete variable; i.e., that it could take on only the values $0, \epsilon, 2\epsilon, \ldots, n\epsilon$ where n is an integer; and further, that E was proportional to the frequency of the oscillators and, hence, to that of the radiation. Planck therefore wrote the energy as

$$E_n = n\epsilon = nhf \quad n = 0, 1, 2, \ldots \tag{3-13}$$

where the proportionality constant h is now called *Planck's constant.* The Maxwell-Boltzmann distribution (Equation 3-11) then becomes

$$f_n = Ae^{-E_n/kT} = Ae^{-n\epsilon/kT} \tag{3-14}$$

where A is determined by the normalization condition that the sum of all fractions f_n must, of course, equal 1, i.e.,

$$\sum_{n=0}^{\infty} f_n = A\sum_{n=0}^{\infty} e^{-n\epsilon/kT} = 1 \tag{3-15}$$

The average energy of an oscillator is then given by the discrete-sum equivalent of Equation 3-12:

$$\overline{E} = \sum_{n=0}^{\infty} E_n f_n = \sum_{n=0}^{\infty} E_n A e^{-E_n/kT} \tag{3-16}$$

Calculating the sums in Equations 3-15 and 3-16 (see Problem 3-58) yields the result

$$\overline{E} = \frac{\epsilon}{e^{\epsilon/kT} - 1} = \frac{hf}{e^{hf/kT} - 1} = \frac{hc/\lambda}{e^{hc/lkT} - 1} \tag{3-17}$$

Multiplying this result by the number of oscillators per unit volume in the interval $d\lambda$ given by Equation 3-8, we obtain for the energy density distribution function of the radiation in the cavity

$$u(\lambda) = \frac{8\pi hc\lambda^{-5}}{\epsilon^{hc/\lambda kT} - 1} \tag{3-18}$$

This function, called *Planck's law,* is sketched in Figure 3-6. It is clear from the figure that the result fits the data quite well.

For very large λ, the exponential in Equation 3-18 can be expanded using $e^x \approx 1 + x + \ldots$ for $x \ll 1$, where $x = hc/\lambda kT$. Then

$$e^{hc/\lambda kT} - 1 \approx \frac{hc}{\lambda kT}$$

and

$$u(\lambda) \longrightarrow 8\pi\lambda^{-4}kT$$

STUDENTS-HUB.com Uploaded By: Malak Obaid

which is the Rayleigh-Jeans formula. For short wavelengths, we can neglect the 1 in the denominator of Equation 3-18, and we have

$$u(\lambda) \longrightarrow 8\pi hc\lambda^{-5}e^{-hc/\lambda kT} \longrightarrow 0$$

as $\lambda \longrightarrow 0$. The value of the constant in Wein's displacement law also follows from Planck's law, as you will show in Problem 3-23.

The value of Planck's constant, h, can be determined by fitting the function given by Equation 3-18 to the experimental data, although direct measurement (see Section 3-3) is better but more difficult. The presently accepted value is

$$h = 6.626 \times 10^{-34}\ \text{J}\cdot\text{s} = 4.136 \times 10^{-15}\ \text{eV}\cdot\text{s} \qquad \textbf{3-19}$$

Planck tried at length to reconcile his treatment with classical physics but was unable to do so. The fundamental importance of the quantization assumption implied by Equation 3-13 was suspected by Planck and others but was not generally appreciated until 1905. In that year Einstein applied the same ideas to explain the photoelectric effect and suggested that, rather than being merely a mysterious property of the oscillators in the cavity walls and blackbody radiation, quantization was a fundamental characteristic of light energy.

EXAMPLE 3-2 Peak of the Solar Spectrum The surface temperature of the Sun is about 5800 K, and measurements of the Sun's spectral distribution show that it radiates very nearly like a blackbody, deviating mainly at very short wavelengths. Assuming that the Sun radiates like an ideal blackbody, at what wavelength does the peak of the solar spectrum occur?

The electromagnetic spectrum emitted by incandescent bulbs is a common example of blackbody radiation, the amount of visible light being dependent on the temperature of the filament. Another application is the pyrometer, a device that measures the temperature of a glowing object, such as molten metal in a steel mill.

SOLUTION

1. The wavelength at the peak, or maximum intensity, of an ideal blackbody is given by Equation 3-5:

$$\lambda_m T = \text{constant} = 2.898 \times 10^{-3}\ \text{m}\cdot\text{K}$$

2. Rearranging and substituting the Sun's surface temperature yield

$$\lambda_m = (2.898 \times 10^{-3}\ \text{m}\cdot\text{K})/T = \frac{2.898 \times 10^{-3}\ \text{m}\cdot\text{K}}{5800\ \text{K}}$$

$$= \frac{2.898 \times 10^{6}\ \text{nm}\cdot\text{K}}{5800\ \text{K}} = 499.7\ \text{nm}$$

where $1\ \text{nm} = 10^{-9}\ \text{m}$.

Remarks: *This value is near the middle of the visible spectrum.*

EXAMPLE 3-3 Average Energy of an Oscillator What is the average energy $\overline{E}$ of an oscillator that has a frequency given by $hf = kT$ according to Planck's calculation?

SOLUTION

$$\overline{E} = \frac{\epsilon}{e^{\epsilon/kT} - 1} = \frac{kT}{e^{1} - 1} = 0.582\,kT$$

Remarks: *Recall that according to classical theory, $\overline{E} = kT$ regardless of the frequency.*

STUDENTS-HUB.com Uploaded By: Malak Obaid

EXAMPLE 3-4 **Stefan-Boltzmann from Planck** Show that the total energy density in a blackbody cavity is proportional to T^4 in accordance with the Stefan-Boltzmann law.

SOLUTION

The total energy density is obtained from the distribution function (Equation 3-18) by integrating over all wavelengths:

$$U = \int_0^\infty u(\lambda)\, d\lambda = \int_0^\infty \frac{8\pi hc\lambda^{-5}}{e^{hc/\lambda kT} - 1}\, d\lambda$$

Define the dimensionless variable $x = hc/\lambda kT$. Then $dx = -(hc/\lambda^2 kT)\, d\lambda$ or $d\lambda = -\lambda^2(kT/hc)\, dx$. Then

$$U = -\int_0^\infty \frac{8\pi hc\lambda^{-3}}{e^x - 1}\left(\frac{kT}{hc}\right) dx = 8\pi hc\left(\frac{kT}{hc}\right)^4 \int_0^\infty \frac{x^3}{e^x - 1}\, dx$$

Since the integral is now dimensionless, this shows that U is proportional to T^4. The value of the integral can be obtained from tables; it is $\pi^4/15$. Then $U = (8\pi^5 k^4/15h^3c^3)T^4$. This result can be combined with Equations 3-4 and 3-6 to express Stefan's constant in terms of π, k, h, and c (see Problem 3-13).

A dramatic example of an application of Planck's law on the current frontier of physics is in tests of the Big Bang theory of the formation and present expansion of the universe. Current cosmological theory holds that the universe originated in an extremely high-temperature explosion of space, one consequence of which was to fill the infant universe with radiation whose spectral distribution must surely have been that of an ideal blackbody. Since that time, the universe has expanded to its present size and cooled to its present temperature T_{now}. However, it should still be filled with radiation whose spectral distribution should be that characteristic of a blackbody at T_{now}.

In 1965, Arno Penzias and Robert Wilson discovered radiation of wavelength 7.35 cm reaching Earth with the same intensity from all directions in space. It was soon recognized that this radiation could be a remnant of the Big Bang fireball, and measurements were subsequently made at other wavelengths in order to construct an experimental energy density $u(\lambda)$ versus λ graph. The most recent data from the Cosmic Background Explorer (COBE) satellite, shown in Figure 3-7, and by the

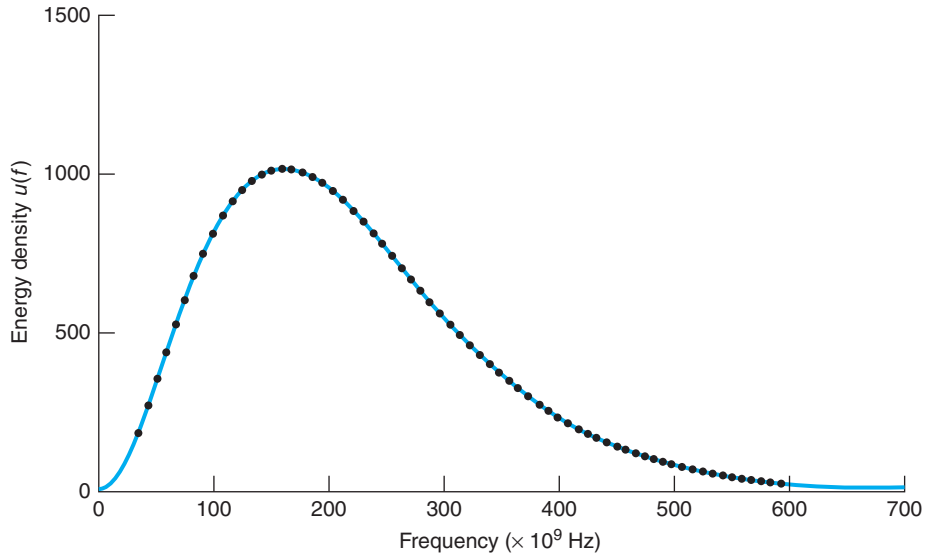

Figure 3-7 The energy density spectral distribution of the cosmic microwave background radiation. The solid line is Planck's law with $T = 2.725$ K. These measurements (the black dots) were made by the COBE satellite.

STUDENTS-HUB.com Uploaded By: Malak Obaid

Wilkinson Microwave Anisotropy Probe (WMAP) have established the temperature of the background radiation field at 2.725 ± 0.001 K. The excellent agreement of the data with Planck's equation, indeed, the best fit that has ever been measured, is considered to be very strong support for the Big Bang theory (see Chapter 13).

3-3 The Photoelectric Effect

It is one of the ironies in the history of science that in the famous experiment of Heinrich Hertz[11] in 1887, in which he produced and detected electromagnetic waves, thus confirming Maxwell's wave theory of light, he also discovered the photoelectric effect, which led directly to the particle description of light. Hertz was using a spark gap in a tuned circuit to generate the waves and another similar circuit to detect them. He noticed accidentally that when the light from the generating gap was shielded from the receiving gap, the receiving gap had to be made shorter in order for the spark to jump the gap. Light from any spark that fell on the terminals of the gap facilitated the passage of the sparks. He described the discovery with these words:

> In a series of experiments on the effects of resonance between very rapid electric oscillations that I had carried out and recently published, two electric sparks were produced by the same discharge of an induction coil, and therefore simultaneously. One of these sparks, spark *B*, was the discharge spark of the induction coil, and served to excite the primary oscillation. I occasionally enclosed spark *B* in a dark case so as to make observations more easily, and in so doing I observed that the maximum spark length became decidedly smaller inside the case than it was before.[12]

The unexpected discovery of the photoelectric effect annoyed Hertz because it interfered with his primary research, but he recognized its importance immediately and interrupted his other work for six months in order to study it in detail. His results, published later that year, were then extended by others. It was found that negative particles were emitted from a clean surface when exposed to light. P. Lenard in 1900 deflected them in a magnetic field and found that they had a charge-to-mass ratio of the same magnitude as that measured by Thomson for cathode rays: the particles being emitted were electrons.

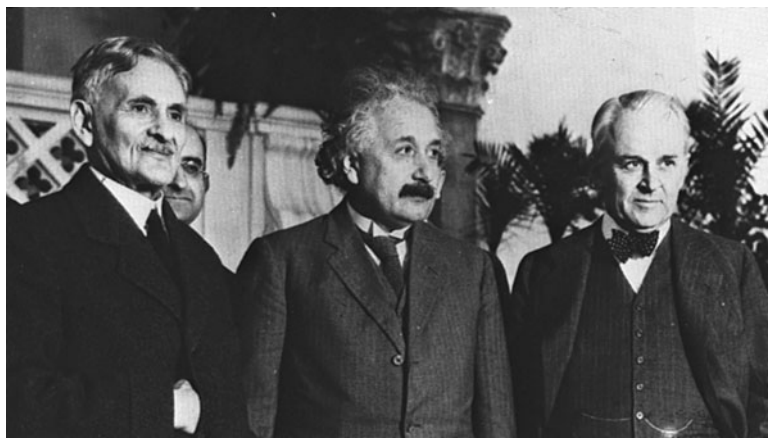

Albert A. Michelson, Albert Einstein, and Robert A. Millikan at a meeting in Pasadena, California, in 1931. [*AP/Wide World Photos.*]

STUDENTS-HUB.com Uploaded By: Malak Obaid

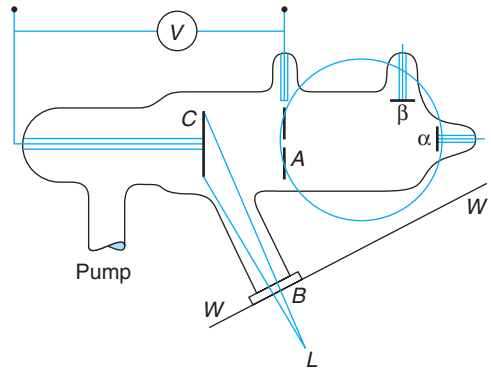

Figure 3-8 Schematic diagram of the apparatus used by P. Lenard to demonstrate the photoelectric effect and to show that the particles emitted in the process were electrons. Light from the source *L* strikes the cathode *C*. Photoelectrons going through the hole in anode *A* are recorded by the electrometer connected to α. A magnetic field, indicated by the circular pole piece, could deflect the particles to a second electrometer connected to β, making possible the establishment of the sign of the charges and their e/m ratio. [*P. Lenard, Annalen der Physik,* ***2****, 359 (1900).*]

Figure 3-8 shows a schematic diagram of the basic apparatus used by Lenard. When light *L* is incident on a clean metal surface (cathode *C*), electrons are emitted. If some of these electrons that reach the anode *A* pass through the small hole, a current results in the external electrometer circuit connected to α. The number of the emitted electrons reaching the anode can be increased or decreased by making the anode positive or negative with respect to the cathode. Letting *V* be the potential difference between the cathode and anode, Figure 3-9*a* shows the current versus *V* for two values of the intensity of light incident on the cathode. When *V* is positive, the electrons are attracted to the anode. At sufficiently large *V* all the emitted electrons reach the anode and the current reaches its maximum value. Lenard observed that the maximum current was proportional to the light intensity, an expected result since doubling the energy per unit time incident on the cathode should double the number of electrons emitted. Intensities too low to provide the electrons with the energy necessary to escape from the metal should result in no emission of electrons. However, in contrast with the classical expectation, there was no minimum intensity below which the current was absent. When *V* is negative, the electrons are repelled from the anode. Then only electrons with initial kinetic energy $mv^2/2$ greater than $e|V|$ can reach the anode. From Figure 3-9*a* we see that if *V* is less than $-V_0$, no electrons reach the anode. The potential V_0 is called the *stopping potential.* It is related to the maximum kinetic energy of the emitted electrons by

$$\left(\frac{1}{2}mv^2\right) = eV_0 \qquad \textbf{3-20}$$

The experimental result, illustrated by Figure 3-9*a,* that V_0 is independent of the incident light intensity was surprising. Apparently, increasing the rate of energy falling on the cathode does not increase the maximum kinetic energy of the emitted electrons, contrary to classical expectations. In 1905 Einstein offered an explanation of this result in a remarkable paper in the same volume of *Annalen der Physik* that contained his papers on special relativity and Brownian motion.

STUDENTS-HUB.com Uploaded By: Malak Obaid

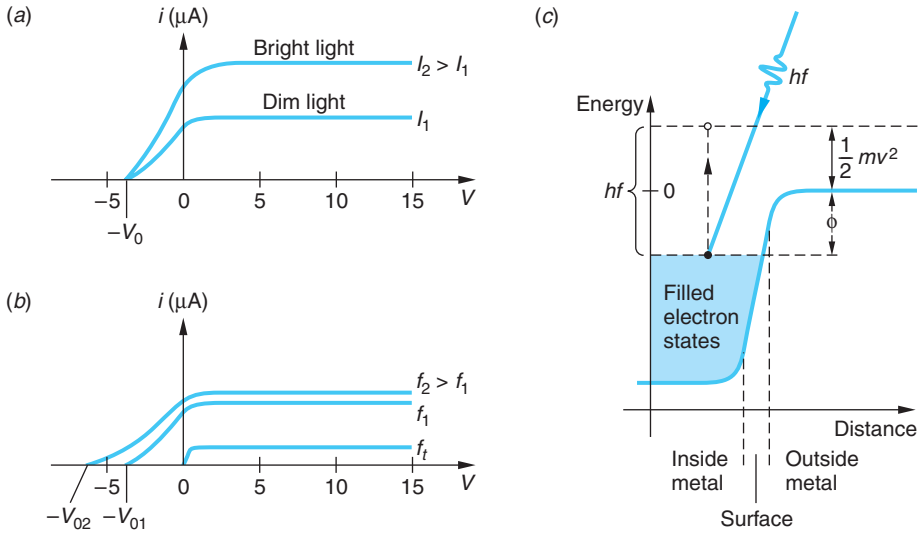

Figure 3-9 (*a*) Photocurrent i versus anode voltage V for light of frequency f with two intensities I_1 and I_2, where $I_2 > I_1$. The stopping voltage V_0 is the same for both. (*b*) For constant I, Einstein's explanation of the photoelectric effect indicates that the magnitude of the stopping voltage should be greater for f_2 than f_1, as observed, and that there should be a threshold frequency f_t below which no photoelectrons were seen, also in agreement with experiment. (*c*) Electron potential energy curve across the metal surface. An electron with the highest energy in the metal absorbs a photon of energy hf. Conservation of energy requires that its kinetic energy after leaving the surface be $hf - \phi$.

Einstein assumed that the *energy quantization used by Planck in solving the blackbody radiation problem was, in fact, a universal characteristic of light.* Rather than being distributed evenly in the space through which it propagated, light energy consisted of discrete quanta, each of energy hf. When one of these quanta, called a *photon,* penetrates the surface of the cathode, all of its energy may be absorbed completely by a single electron. If ϕ is the energy necessary to remove an electron from the surface (ϕ is called the *work function* and is a characteristic of the metal), the maximum kinetic energy of an electron leaving the surface will be $hf - \phi$ as a consequence of energy conservation; see Figure 3-9*c*. (Some electrons will have less than this amount because of energy lost in traversing the metal.) Thus, the stopping potential should be given by

$$eV_0 = \left(\frac{1}{2}mv^2\right)_{\max} = hf - \phi \qquad \textbf{3-21}$$

Equation 3-21 is referred to as the photoelectric effect equation. As Einstein noted,

> If the derived formula is correct, then V_0, when represented in Cartesian coordinates as a function of the frequency of the incident light, must be a straight line whose slope is independent of the nature of the emitting substance.[13]

As can be seen from Equation 3-21, the slope of V_0 versus f should equal h/e. At the time of this prediction there was no evidence that Planck's constant had anything to do with the photoelectric effect. There was also no evidence for the dependence of

Among the many applications of the photoelectric effect is the photomultiplier, a device that makes possible the accurate measurement of the energy of the light absorbed by a photosensitive surface. The SNO and Kamiokande neutrino observatories (see Chapter 12) use thousands of photomultipliers. Hundreds more are being deployed inside the Antarctic ice cap in the Ice Cube particle physics experiment.

STUDENTS-HUB.com Uploaded By: Malak Obaid

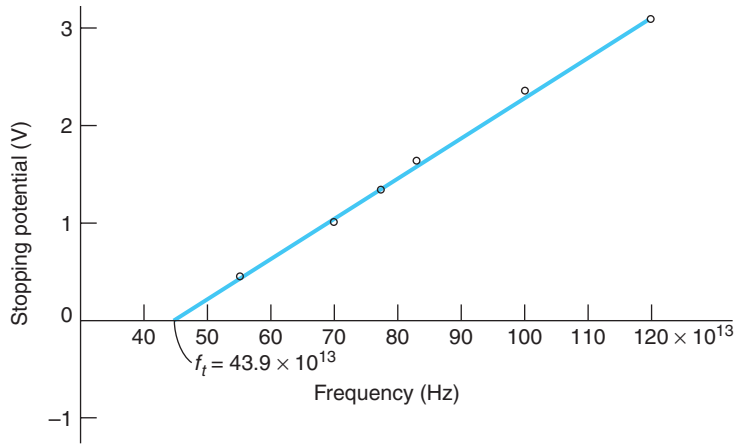

Figure 3-10 Millikan's data for stopping potential versus frequency for the photoelectric effect. The data fall on a straight line with slope h/e, as predicted by Einstein a decade before the experiment. The intercept on the stopping potential axis is $-\phi/e$. [*R. A. Millikan, Physical Review, 7, 362 (1915).*]

the stopping potential V_0 on the frequency. Careful experiments by Millikan, reported in 1914 and in more detail in 1916, showed that Equation 3-21 was correct and that measurements of h from it agreed with the value obtained by Planck. A plot taken from this work is shown in Figure 3-10.

The minimum, or threshold, frequency for the photoelectric effect, labeled f_t in this plot and in Figure 3-9*b*, and the corresponding threshold wavelength λ_t are related to the work function ϕ by setting $V_0 = 0$ in Equation 3-21:

$$\phi = hf_t = \frac{hc}{\lambda_t} \qquad \textbf{3-22}$$

Photons of frequencies lower than f_t (and therefore having wavelengths greater than λ_t) do not have enough energy to eject an electron from the metal. Work functions for metals are typically on the order of a few electron volts. The work functions for several elements are given in Table 3-1.

Table 3-1 Photoelectric work functions

Element	Work function (eV)
Na	2.28
C	4.81
Cd	4.07
Al	4.08
Ag	4.73
Pt	6.35
Mg	3.68
Ni	5.01
Se	5.11
Pb	4.14

STUDENTS-HUB.com Uploaded By: Malak Obaid

EXAMPLE 3-5 **Photoelectric Effect in Potassium** The threshold frequency of potassium is 558 nm. What is the work function for potassium? What is the stopping potential when light of 400 nm is incident on potassium?

SOLUTION

1. Both questions can be answered with the aid of Equation 3-21:

$$eV_0 = \left(\frac{1}{2}mv^2\right)_{\max} = hf - \phi$$

$$V_0 = \frac{hf}{e} - \frac{\phi}{e}$$

2. At the threshold wavelength the photoelectrons have just enough energy to overcome the work function barrier, so $\left(\frac{1}{2}mv^2\right)_{\max} = 0$, hence $V_0 = 0$, and

$$\frac{\phi}{e} = \frac{hf_{te}}{e} = \frac{hc}{e\lambda_t}$$

$$= \frac{1240 \text{ eV} \cdot \text{nm}}{558 \text{ nm}} = 2.22 \text{ eV}$$

3. When 400-nm light is used, V_0 is given by Equation 3-21:

$$V_0 = \frac{hf}{e} - \frac{\phi}{e} = \frac{hc}{e\lambda} - \frac{\phi}{e}$$

$$= \frac{1240 \text{ eV} \cdot \text{nm}}{400 \text{ nm}} - 2.22 \text{ eV}$$

$$= 3.10 \text{ eV} - 2.22 \text{ eV} = 0.88 \text{ V}$$

Another interesting feature of the photoelectric effect that is contrary to classical physics but is easily explained by the photon hypothesis is the lack of any time lag between the turning on of the light source and the appearance of photoelectrons. Classically, the incident energy is distributed uniformly over the illuminated surface; the time required for an area the size of an atom to acquire enough energy to allow the emission of an electron can be calculated from the intensity (power per unit area) of the incident radiation. Experimentally, the incident intensity can be adjusted so that the calculated time lag is several minutes or even hours. But no time lag is ever observed. The photon explanation of this result is that although the rate at which photons are incident on the metal is very small when the intensity is low, *each* photon has enough energy to eject an electron, and there is some chance that a photon will be absorbed immediately. The classical calculation gives the correct *average* number of photons absorbed per unit time.

EXAMPLE 3-6 **Classical Time Lag** Light of wavelength 400 nm and intensity 10^{-2} W/m^2 is incident on potassium. Estimate the time lag for the emission of photoelectrons expected classically.

SOLUTION

According to Example 3-5, the work function for potassium is 2.22 eV. If we assume $r = 10^{-10}$ m to be the typical radius of an atom, the total energy falling on the atom in time t is

$$E = (10^{-2} \text{ W/m}^2)(\pi r^2)t = (10^{-2} \text{ W/m}^2)(\pi 10^{-20} \text{ m}^2)t$$

$$= (3.14 \times 10^{-22} \text{ J/s})t$$

STUDENTS-HUB.com Uploaded By: Malak Obaid

Setting this energy equal to 2.22 eV gives

$$(3.14 \times 10^{-22}\ \text{J/s})t = (2.22\ \text{eV})(1.60 \times 10^{-19}\ \text{J/eV})$$

$$t = \frac{(2.22\ \text{eV})(1.60 \times 10^{-19}\ \text{J/eV})}{(3.14 \times 10^{-22}\ \text{J/s})} = 1.13 \times 10^{3}\ \text{s} = 18.8\ \text{min}$$

According to the classical prediction, no atom would be expected to emit an electron until 18.8 min after the light source was turned on. According to the photon model of light, each photon has enough energy to eject an electron immediately. Because of the low intensity, there are few photons incident per second, so the chance of any particular atom absorbing a photon and emitting an electron in any given time interval is small. However, there are so many atoms in the cathode that some emit electrons immediately.

EXAMPLE 3-7 Incident Photon Intensity In Example 3-6, how many photons are incident per second per square meter?

SOLUTION

The energy of each photon is

$$E = hf = hc/\lambda = (1240\ \text{eV} \cdot \text{nm})/(400\ \text{nm}) = (3.10\ \text{eV})(1.60 \times 10^{-19}\ \text{J/eV})$$

$$= 4.96 \times 10^{-19}\ \text{J}$$

Since the incident intensity is $10^{-2}\ \text{W/m}^2 = 10^{-2}\ \text{J/s} \cdot \text{m}^2$, the number of photons per second per square meter is

$$N = \frac{10^{-2}\ \text{J/s} \cdot \text{m}^2}{4.96 \times 10^{-19}\ \text{J/photon}}$$

$$= 2.02 \times 10^{16}\ \text{photons/s} \cdot \text{m}^2$$

This is, of course, a lot of photons, not a few; however, the number n per atom at the surface is quite small. $n = 2.02 \times 10^{16}\ \text{photons/s} \cdot \text{m}^2 \times \pi(10^{-10})^2\ \text{m}^2/\text{atom} = 6.3 \times 10^{-4}\ \text{photons/s} \cdot \text{atom}$, or about 1 photon for every 1000 atoms.

Questions

3. How is the result that the maximum photoelectric current is proportional to the intensity explained in the photon model of light?
4. What experimental features of the photoelectric effect can be explained by classical physics? What features cannot?

The photoemission of electrons has developed into a significant technique for investigating the detailed structure of molecules and solids, making possible discoveries far beyond anything that Hertz may have imagined. The use of x-ray sources (see Section 3-4) and precision detectors has made possible precise determination of valence electron configurations in chemical compounds, leading to detailed understanding of chemical bonding and the differences between the bulk and surface atoms of solids. Photoelectric-effect microscopes will show the chemical situation of each element in a specimen, a prospect of intriguing and crucial importance in molecular biology and microelectronics. And they are all based on a discovery that annoyed Hertz—at first.

STUDENTS-HUB.com Uploaded By: Malak Obaid

3-4 X Rays and the Compton Effect

Further evidence of the correctness of the photon concept was furnished by Arthur H. Compton, who measured the scattering of x rays by free electrons and, by his analysis of the data, resolved the last lingering doubts regarding special relativity (see Chapter 1). Before we examine Compton scattering in detail, we will briefly describe some of the early work with x rays since it provides a good conceptual understanding of x-ray spectra and scattering.

X Rays

The German physicist Wilhelm K. Roentgen discovered x rays in 1895 when he was working with a cathode-ray tube. Coming five years before Planck's explanation of the blackbody emission spectrum, Roentgen's discovery turned out to be the first significant development in quantum physics. He found that "rays" originating from the point where the cathode rays (electrons) hit the glass tube, or a target within the tube, could pass through materials opaque to light and activate a fluorescent screen or photographic film. He investigated this phenomenon extensively and found that all materials are transparent to these rays to some degree and that the transparency decreases with increasing density. This fact led to the medical use of x rays within months after the publication of Roentgen's first paper.[14]

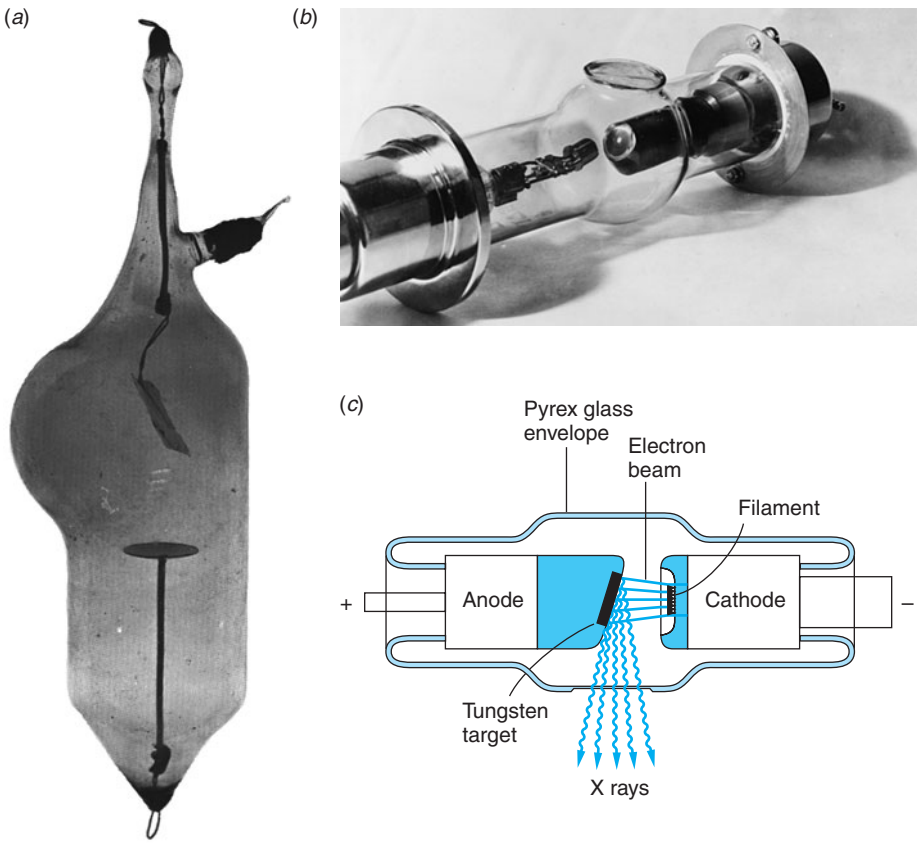

(*a*) Early x-ray tube. [*Courtesy of Cavendish Laboratory.*] (*b*) X-ray tubes became more compact over time. This tube was a design typical of the mid-twentieth century. [*Courtesy of Schenectady Museum, Hall of Electrical History, Schenectady, NY.*] (*c*) Diagram of the components of a modern x-ray tube. Design technology has advanced enormously, enabling very high operating voltages, beam currents, and x-ray intensities, but essential elements of the tubes remain unchanged.

STUDENTS-HUB.com Uploaded By: Malak Obaid

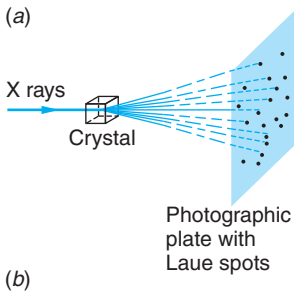

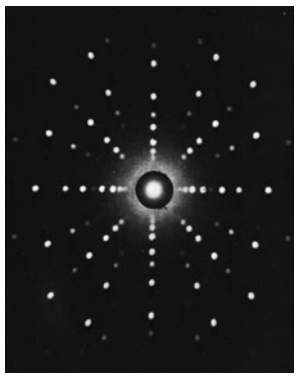

Figure 3-11 (*a*) Schematic sketch of a Laue experiment. The crystal acts as a three-dimensional grating, which diffracts the x-ray beam and produces a regular array of spots, called a *Laue pattern,* on photographic film or an x-ray-sensitive charge-coupled device (CCD) detector. (*b*) Laue x-ray diffraction pattern using a niobium boride crystal and 20-keV molybdenum x rays. [*General Electric Company.*]

An x ray of Mrs. Roentgen's hand taken by Roentgen shortly after his discovery.

Roentgen was unable to deflect these rays in a magnetic field, nor was he able to observe refraction or the interference phenomena associated with waves. He thus gave the rays the somewhat mysterious name of x rays. Since classical electromagnetic theory predicts that accelerated charges will radiate electromagnetic waves, it is natural to expect that x rays are electromagnetic waves produced by the acceleration of the electrons when they are deflected and stopped by the atoms of a target. Such radiation is called *bremsstrahlung,* German for "braking radiation." The slight diffraction broadening of an x-ray beam after passing through slits a few thousandths of a millimeter wide indicated the wavelength of x rays to be of the order of 10^{-10} m $= 0.1$ nm. In 1912 Max von Laue suggested that since the wavelengths of x rays were of the same order of magnitude as the spacing of atoms in a crystal, the regular array of atoms in a crystal might act as a three-dimensional grating for the diffraction of x rays. Experiments (Figure 3-11) soon confirmed that x rays are a form of electromagnetic radiation with wavelengths in the range of about 0.01 to 0.10 nm and that atoms in crystals are arranged in regular arrays.

W. L. Bragg, in 1912, proposed a simple and convenient way of analyzing the diffraction of x rays by crystals.[15] He examined the interference of x rays due to scattering from various sets of parallel planes of atoms, now called *Bragg planes.* Two sets of Bragg planes are illustrated in Figure 3-12 for NaCl, which has a cubic structure called *face-centered cubic.* Consider Figure 3-13. Waves scattered from the two successive atoms within a plane will be in phase and thus interfere constructively, independent of the wavelength, if the scattering angle equals the incident angle. (This condition is the same as for reflection.) Waves scattered at equal angles from atoms in two

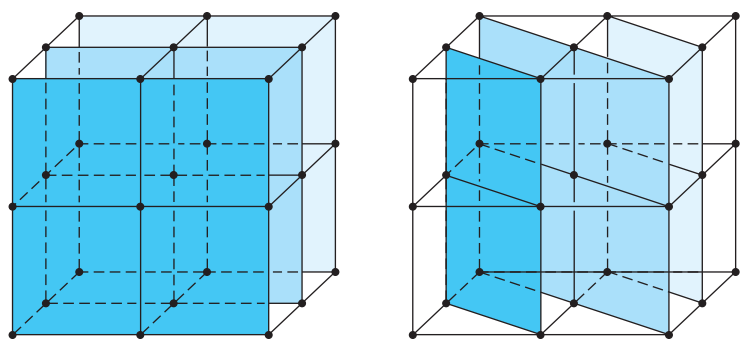

Figure 3-12 A crystal of NaCl showing two sets of Bragg planes.

STUDENTS-HUB.com Uploaded By: Malak Obaid

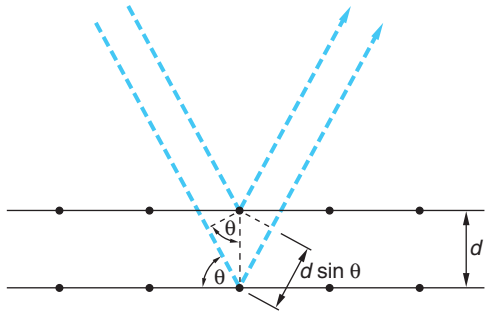

Figure 3-13 Bragg scattering from two successive planes. The waves from the two atoms shown have a path length difference of $2d \sin\theta$. They will be in phase if the Bragg condition $2d \sin\theta = m\lambda$ is met.

different planes will be in phase (constructive interference) only if the difference in path length is an integral number of wavelengths. From Figure 3-13 we see that this condition is satisfied if

$$2d \sin\theta = m\lambda \quad \text{where } m = \text{an integer} \qquad \textbf{3-23}$$

Equation 3-23 is called the *Bragg condition.*

Measurements of the spectral distribution of the intensity of x rays as a function of the wavelength using an experimental arrangement such as that shown in Figure 3-14 produces the x-ray spectrum and, for classical physics, some surprises. Figure 3-15*a* shows two typical x-ray spectra produced by accelerating electrons through two voltages V and bombarding a tungsten target mounted on the anode of the tube. In this figure $I(\lambda)$ is the intensity emitted within the wavelength interval $d\lambda$ for each value of λ. Figure 3-15*b* shows the short wavelength lines produced with a molybdenum target and 35-keV electrons. Three features of the spectra are of immediate interest, only one of which could be explained by classical physics. (1) The spectrum consists of a series of sharp lines, called the *characteristic spectrum,* superimposed on (2) the continuous

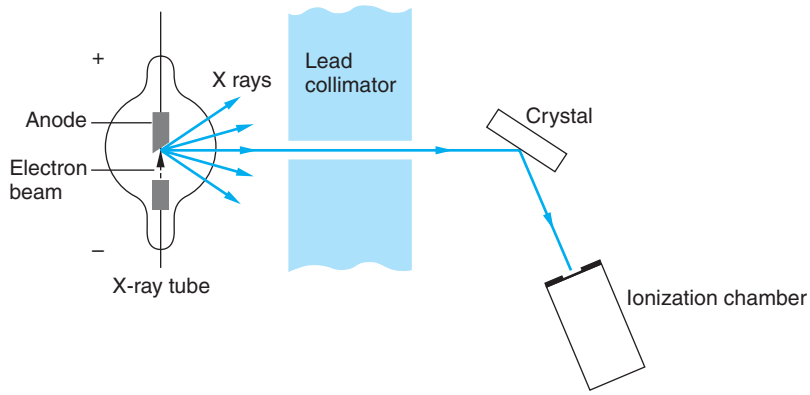

Figure 3-14 Schematic diagram of a Bragg crystal spectrometer. A collimated x-ray beam is incident on a crystal and scattered into an ionization chamber. The crystal and ionization chamber can be rotated to keep the angles of incidence and scattering equal as both are varied. By measuring the ionization in the chamber as a function of angle, the spectrum of the x rays can be determined using the Bragg condition $2d \sin\theta = m\lambda$, where d is the separation of the Bragg planes in the crystal. If the wavelength λ is known, the spacing d can be determined.

STUDENTS-HUB.com Uploaded By: Malak Obaid

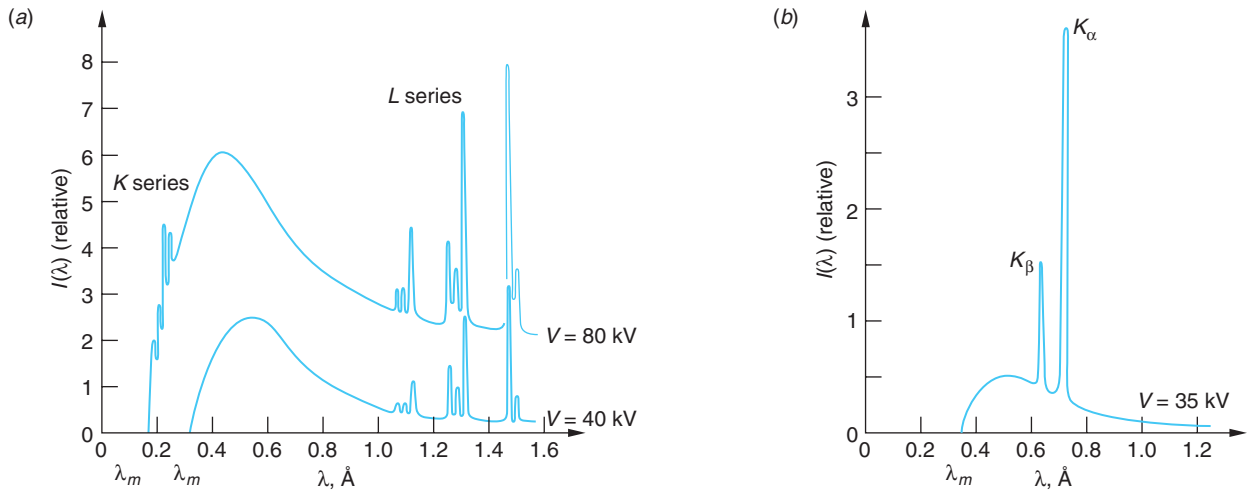

Figure 3-15 (*a*) X-ray spectra from tungsten at two accelerating voltages and (*b*) from molybdenum at one. The names of the line series (*K* and *L*) are historical and explained in Chapter 4. The *L*-series lines for molybdenum (not shown) are at about 0.5 nm. The cutoff wavelength λ_m is independent of the target element and is related to the voltage on the x-ray tube V by $\lambda_m = hc/eV$. The wavelengths of the lines are characteristic of the element.

bremsstrahlung spectrum. The line spectrum is characteristic of the target material and varies from element to element. (3) The continuous spectrum has a sharp cutoff wavelength, λ_m, which is independent of the target material but depends on the energy of the bombarding electrons. If the voltage on the x-ray tube is V volts, the cutoff wavelength is found empirically to be given by

$$\lambda_m = \frac{1.24 \times 10^3}{V} \text{ nm} \qquad \textbf{3-24}$$

Equation 3-24 is called the *Duane-Hunt rule,* after its discoverers. It was pointed out rather quickly by Einstein that x-ray production by electron bombardment was an inverse photoelectric effect and that Equation 3-21 should apply. The Duane-Hunt λ_m simply corresponds to a photon with the maximum energy of the electrons, that is, the photon emitted when the electron losses all of its kinetic energy in a single collision. Since the kinetic energy of the electrons in an x-ray tube is 20,000 eV or higher, the work function ϕ (a few eV) is negligible by comparison. That is, Equation 3-21 becomes $eV \approx hf = hc/\lambda_m$ or $\lambda_m = hc/eV = 1.2407 \times 10^{-6}\, V^{-1}$ m $= 1.24 \times 10^3\, V^{-1}$ nm. Thus, the Duane-Hunt rule is explained by Planck's quantum hypothesis. (Notice that the value of λ_m can be used to determine h/e.)

Well-known applications of x rays are medical and dental x rays (both diagnostic and treatment) and industrial x-ray inspection of welds and castings. Perhaps not so well known is the use of x rays in determining the structure of crystals, identifying black holes in the cosmos, and "seeing" the folded shapes of proteins in biological materials.

The continuous spectrum was understood as the result of the acceleration (i.e., "braking") of the bombarding electrons in the strong electric fields of the target atoms. Maxwell's equation predicted the continuous radiation. The real problem for classical physics was the sharp lines. The wavelengths of the sharp lines were a function of the target element, the set for each element being always the same. But the sharp lines never appeared if V was such that λ_m was larger than the particular line, as can be seen from Figure 3-15*a,* where the shortest-wavelength group disappears when V is reduced from 80 keV to 40 keV so that λ_m becomes larger. The origin of the sharp lines was a mystery that had to await the discovery of the nuclear atom. We will explain them in Chapter 4.

STUDENTS-HUB.com Uploaded By: Malak Obaid

Compton Effect

It had been observed that scattered x rays were "softer" than those in the incident beam, that is, were absorbed more readily. Compton[16] pointed out that if the scattering process were considered a "collision" between a photon of energy hf_1 (and momentum hf_1/c) and an electron, the recoiling electron would absorb part of the incident photon's energy. The energy hf_2 of the scattered photon would therefore be less than the incident one and thus of lower frequency f_2 and momentum hf_2/c. (The fact that electromagnetic radiation of energy E carried momentum E/c was known from classical theory and from the experiments of Nichols and Hull in 1903. This relation is also consistent with the relativistic expression $E^2 = p^2c^2 + (mc^2)^2$ for a particle with zero rest energy.) Compton applied the laws of conservation of momentum and energy in their relativistic form (see Chapter 2) to the collision of a photon with an isolated electron to obtain the change in the wavelength $\lambda_2 - \lambda_1$ of the photon as a function of the scattering angle θ. The result, called *Compton's equation* and derived in a More section on the home page, is

$$\lambda_2 - \lambda_1 = \frac{h}{mc}(1 - \cos\theta) \qquad \textbf{3-25}$$

The change in wavelength is thus predicted to be independent of the original wavelength. The quantity h/mc has the dimensions of length and is called the *Compton wavelength of the electron.* Its value is

$$\lambda_c = \frac{h}{mc} = \frac{hc}{mc^2} = \frac{1.24 \times 10^3 \text{ eV} \cdot \text{nm}}{5.11 \times 10^5 \text{ eV}} = 0.00243 \text{ nm}$$

Because $\lambda_2 - \lambda_1$ is small, it is difficult to observe unless λ_1 is very small so that the fractional change $(\lambda_2 - \lambda_1)/\lambda_1$ is appreciable. For this reason the Compton effect is generally only observed for x rays and gamma radiation.

Compton verified his result experimentally using the characteristic x-ray line of wavelength 0.0711 nm from molybdenum for the incident monochromatic photons and scattering these photons from electrons in graphite. The wavelength of the scattered photons was measured using a Bragg crystal spectrometer. His experimental arrangement is shown in Figure 3-16; Figure 3-17 shows his results. The first peak at

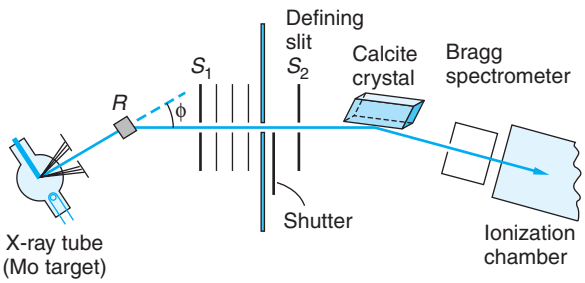

Figure 3-16 Schematic sketch of Compton's apparatus. X rays from the tube strike the carbon block R and are scattered into a Bragg-type crystal spectrometer. In this diagram, the scattering angle is 30°. The beam was defined by slits S_1 and S_2. Although the entire spectrum is being scattered by R, the spectrometer scanned the region around the K_α line of molybdenum.

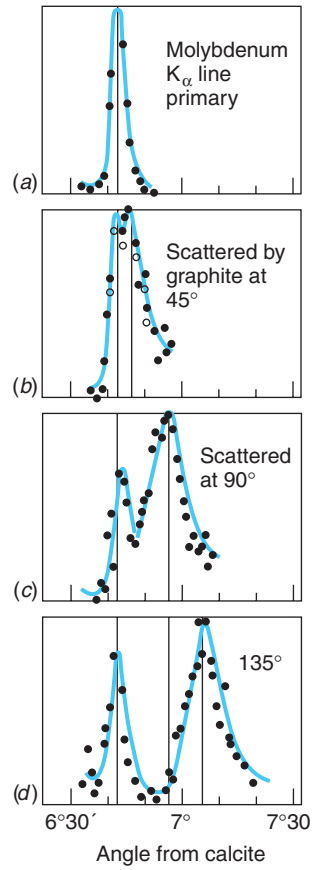

Figure 3-17 Intensity versus wavelength for Compton scattering at several angles. The left peak in each case results from photons of the original wavelength that are scattered by tightly bound electrons, which have an effective mass equal to that of the atom. The separation in wavelength of the peaks is given by Equation 3-25. The horizontal scale used by the Compton "angle from calcite" refers to the calcite analyzing crystal in Figure 3-16.

STUDENTS-HUB.com Uploaded By: Malak Obaid

Arthur Compton. After discovering the Compton effect, he became a world traveler seeking an explanation for cosmic rays. He ultimately showed that their intensity varied with latitude, indicating an interaction with Earth's magnetic field, and thus proved that they are charged particles. [*Courtesy of American Institute of Physics, Niels Bohr Library.*]

each scattering angle corresponds to scattering with no shift in the wavelength due to scattering by the inner electrons of carbon. Since these are tightly bound to the atom, it is the entire atom that recoils rather than the individual electrons. The expected shift in this case is given by Equation 3-25, with m being the mass of the atom, which is about 10^4 times that of the electron; thus, this shift is negligible. The variation of $\Delta\lambda = \lambda_2 - \lambda_1$ with θ was found to be that predicted by Equation 3-25.

We have seen in this section and the preceding two sections that the interaction of electromagnetic radiation with matter is a discrete interaction that occurs at the atomic level. It is perhaps curious that after so many years of debate about the nature of light, we now find that we must have both a particle (i.e., quantum) theory to describe in detail the energy exchange between electromagnetic radiation and matter and a wave theory to describe the interference and diffraction of electromagnetic radiation. We will discuss this so-called wave-particle duality in more detail in Chapter 5.

More

Derivation of Compton's Equation, applying conservation of energy and momentum to the relativistic collision of a photon and an electron, is included on the home page: www.whfreeman.com/tiplermodernphysics5e. See also Equations 3-26 and 3-27 and Figure 3-18 here.

Questions

5. Why is it extremely difficult to observe the Compton effect using visible light?
6. Why is the Compton effect unimportant in the transmission of television and radio waves? How many Compton scatterings would a typical FM signal have before its wavelengths were shifted by 0.01 percent?

STUDENTS-HUB.com Uploaded By: Malak Obaid

EXAMPLE 3-8 X Rays from TV The acceleration voltage of the electrons in a typical television picture tube is 25 keV. What is the minimum wavelength x ray produced when these electrons strike the inner front surface of the tube?

SOLUTION

From Equation 3-24, we have

$$\lambda_m = \frac{1.24 \times 10^3}{V}\text{ nm} = \frac{1.24 \times 10^3}{25{,}000} = 0.050\text{ nm}$$

These x rays penetrate matter very effectively. Manufacturers provide essential shields to protect against the hazard.

EXAMPLE 3-9 Compton Effect In a particular Compton scattering experiment it is found that the incident wavelength λ_1 is shifted by 1.5 percent when the scattering angle $\theta = 120°$. (*a*) What is the value of λ_1? (*b*) What will be the wavelength λ_2 of the shifted photon when the scattering angle is 75°?

SOLUTION

1. For question (*a*) , the value of λ_1 is found from Equation 3-25:

$$\begin{aligned}\lambda_2 - \lambda_1 = \Delta\lambda &= \frac{h}{mc}(1 - \cos\theta)\\ &= 0.00243(1 - \cos 120°)\end{aligned}$$

2. That the scattered wavelength λ_2 is shifted by 1.5 percent from λ_1 means that

$$\frac{\Delta\lambda}{\lambda_1} = 0.015$$

3. Combining these yields:

$$\begin{aligned}\lambda_1 &= \frac{\Delta\lambda}{0.015} = \frac{0.00243(1 - \cos 120)}{0.015}\\ &= 0.243\text{ nm}\end{aligned}$$

4. Question (*b*) is also solved with the aid of Equation 3-25, rearranged as

$$\lambda_2 = \lambda_1 + 0.00243(1 - \cos\theta)$$

5. Substituting $\theta = 75°$ and λ_1 from above yields

$$\begin{aligned}\lambda_2 &= 0.243 + 0.00243(1 - \cos 75)\\ &= 0.243 + 0.002\\ &= 0.245\text{ nm}\end{aligned}$$

A Final Comment

In this chapter, together with Section 2-4 of the previous chapter, we have introduced and discussed at some length the three primary ways by which photons interact with matter: (1) the photoelectric effect, (2) the Compton effect, and (3) pair production. As we proceed with our explorations of modern physics throughout the remainder of the book, we will have many occasions to apply what we have learned here to aid in our understanding of myriad phenomena, ranging from atomic structure to the fusion "furnaces" of stars.

STUDENTS-HUB.com Uploaded By: Malak Obaid

Summary

TOPIC	RELEVANT EQUATIONS AND REMARKS	
1. J. J. Thomson's experiment	Thomson's measurements with cathode rays showed that the same particle (the electron), with e/m about 2000 times that of ionized hydrogen, exists in all elements.	
2. Quantization of electric charge	$e = 1.60217653 \times 10^{-19}\ \text{C}$	
3. Blackbody radiation		
Stefan-Boltzmann law	$R = \sigma T^4$	**3-4**
Wein's displacement law	$\lambda_m T = 2.898 \times 10^{-3}\ \text{m} \cdot \text{K}$	**3-5**
Planck's radiation law	$u(\lambda) = \dfrac{8\pi hc\lambda^{-5}}{e^{hc/\lambda kT} - 1}$	**3-18**
Planck's constant	$h = 6.626 \times 10^{-34}\ \text{J} \cdot \text{s}$	**3-19**
4. Photoelectric effect	$eV_0 = hf - \phi$	**3-21**
5. Compton effect	$\lambda_2 - \lambda_1 = \dfrac{h}{mc}(1 - \cos\theta)$	**3-25**
6. Photon-matter interaction	The (1) photoelectric effect, (2) Compton effect, and (3) pair production are the three ways of interaction.	

General References

The following general references are written at a level appropriate for readers of this book.

Millikan, R. A., *Electrons (+ and −) Protons, Photons, Neutrons, Mesotrons, and Cosmic Rays,* 2d ed., University of Chicago Press, Chicago, 1947. This book on modern physics by one of the great experimentalists of his time contains fascinating, detailed descriptions of Millikan's oil drop experiment and his verification of the Einstein photoelectric-effect equation.

Mohr, P. J., and B. N. Taylor, "The Fundamental Physical Constants," *Physics Today* (August 2004). Also available at http://www.physicstoday.org/guide/fundcont.html.

Richtmyer, F. K., E. H. Kennard, and J. N. Cooper, *Introduction to Modern Physics,* 6th ed., McGraw-Hill, New York, 1969. This excellent text was originally published in 1928, intended as a survey course for graduate students.

Shamos, M. H. (ed.), *Great Experiments in Physics,* Holt, Rinehart, and Winston, New York, 1962. This book contains 25 original papers and extensive editorial comment. Of particular interest for this chapter are papers by Faraday, Hertz, Roentgen, J. J. Thomson, Einstein (photo electric effect), Millikan, Planck, and Compton.

Thomson, G. P., *J. J. Thomson, Discoverer of the Electron,* Doubleday/Anchor, Garden City, NY, 1964. An interesting study of J. J. Thomson by his son, also a physicist.

Virtual Laboratory (PEARL), Physics Academic Software, North Carolina State University, Raleigh, 1996. Computer simulation software allows the user to analyze blackbody radiation emitted over a wide range of temperatures and investigate the Compton effect in detail.

Weart, S. R., *Selected Papers of Great American Physicists,* American Institute of Physics, New York, 1976. The bicentennial commemorative volume of the American Physical Society.

STUDENTS-HUB.com Uploaded By: Malak Obaid

Notes

1. Democritus (about 470 B.C. to about 380 B.C.). Among his other modern-sounding ideas were the suggestions that the Milky Way is a vast conglomeration of stars and that the Moon, like Earth, has mountains and valleys.

2. G. J. Stoney (1826–1911). An Irish physicist who first called the fundamental unit of charge the electron. After Thomson discovered the particle that carried the charge, the name was transferred from the quantity of charge to the particle itself by Lorentz.

3. Joseph J. Thomson (1856–1940). English physicist and director for more than 30 years of the Cavendish Laboratory, the first laboratory in the world established expressly for research in physics. He was awarded the Nobel Prize in 1906 for his work on the electron. Seven of his research assistants also won Nobel Prizes.

4. Much early confusion existed about the nature of cathode rays due to the failure of Heinrich Hertz in 1883 to observe any deflection of the rays in an electric field. The failure was later found to be the result of ionization of the gas in the tube; the ions quickly neutralized the charges on the deflecting plates so that there was actually no electric field between the plates. With better vacuum technology in 1897, Thomson was able to work at lower pressure and observe electrostatic deflection.

5. R. A. Millikan, *Philosophical Magazine (6),* **19,** 209 (1910). Millikan, who held the first physics Ph.D. awarded by Columbia University, was one of the most accomplished experimentalists of his time. He received the Nobel Prize in 1923 for the measurement of the electron's charge. Also among his many contributions, he coined the phrase *cosmic rays* to describe radiation produced in outer space.

6. R. A. Millikan, *Physical Review,* **32,** 349 (1911).

7. Mohr, P. J., and B. N. Taylor, "The Fundamental Physical Constants," *Physics Today* (August 2004).

8. See pp. 135-137 of F. K. Richtmyer, E. H. Kennard, and J. N. Cooper (1969).

9. John W. S. Rayleigh (1842–1919). English physicist, almost invariably referred to by the title he inherited from his father. He was Maxwell's successor and Thomson's predecessor as director of the Cavendish Laboratory.

10. Max K. E. L. Planck (1858–1947). Most of his career was spent at the University of Berlin. In his later years his renown in the world of science was probably second only to that of Einstein.

11. Heinrich R. Hertz (1857–1894), German physicist, student of Helmholtz. He was the discoverer of electromagnetic "radio" waves, later developed for practical communication by Marconi.

12. H. Hertz, *Annalen der Physik,* **31,** 983 (1887).

13. A. Einstein, *Annalen der Physik,* **17,** 144 (1905).

14. A translation of this paper can be found in E. C. Watson, *American Journal of Physics,* **13,** 284 (1945), and in Shamos (1962). Roentgen (1845–1923) was honored in 1901 with the first Nobel Prize in Physics for his discovery of x rays.

15. William Lawrence Bragg (1890–1971), Australian-English physicist. An infant prodigy, his work on x-ray diffraction performed with his father, William Henry Bragg (1862–1942), earned for them both the Nobel Prize in Physics in 1915, the only father-son team to be so honored thus far. In 1938 W. L. Bragg became director of the Cavendish Laboratory, succeeding Rutherford.

16. Arthur H. Compton (1892–1962), American physicist. It was Compton who suggested the name *photon* for the light quantum. His discovery and explanation of the Compton effect earned him a share of the Nobel Prize in Physics in 1927.

Problems

Level I

Section 3-1 Quantization of Electric Charge

3-1. A beam of charged particles consisting of protons, electrons, deuterons, and singly ionized helium atoms and H_2 molecules all pass through a velocity selector, all emerging with speeds of 2.5×10^6 m/s. The beam then enters a region of uniform magnetic field $B = 0.40$ T directed perpendicular to their velocity. Compute the radius of curvature of the path of each type of particle.

3-2. Consider Thomson's experiment with the electric field turned "off." If the electrons enter a region of uniform magnetic field B and length l, show that the electrons are deflected through an angle $\theta \approx e\ell B/mu\ell$ for small values of θ. (Assume that the electrons are moving at nonrelativistic speeds.)

STUDENTS-HUB.com Uploaded By: Malak Obaid

3-3. Equation 3-3 suggests how a velocity selector for particles or mixtures of different particles all having the same charge can be made. Suppose you wish to make a velocity selector that allows undeflected passage for electrons whose kinetic energy is 5.0×10^4 eV. The electric field available to you is 2.0×10^5 V/m. What magnetic field will be needed?

3-4. A cosmic ray proton approaches Earth vertically at the equator, where the horizontal component of Earth's magnetic field is 3.5×10^{-5} T. If the proton is moving at 3.0×10^6 m/s, what is the ratio of the magnetic force to the gravitational force on the proton?

3-5. An electron of kinetic energy 45 keV moves in a circular orbit perpendicular to a magnetic field of 0.325 T. (*a*) Compute the radius of the orbit. (*b*) Find the period and frequency of the motion.

3-6. If electrons have kinetic energy of 2000 eV, find (*a*) their speed, (*b*) the time needed to traverse a distance of 5 cm between plates *D* and *E* in Figure 3-1, and (*c*) the vertical component of their velocity after passing between the plates if the electric field is 3.33×10^3 V/m.

3-7. In J. J. Thomson's first method (see Problem 3-44), the heat capacity of the beam stopper was about 5×10^{-3} cal/°C and the temperature increase was about 2°C. How many 2000-eV electrons struck the beam stopper?

3-8. On drop #16, Millikan measured the following total charges, among others, at different times:

25.41×10^{-19} C $\quad 17.47 \times 10^{-19}$ C $\quad 12.70 \times 10^{-19}$ C
20.64×10^{-19} C $\quad 19.06 \times 10^{-19}$ C $\quad 14.29 \times 10^{-19}$ C

What value of the fundamental quantized charge *e* do these numbers imply?

3-9. Show that the electric field needed to make the rise time of the oil drop equal to its field-free fall time is $\mathscr{E} = 2mg/q$.

3-10. One variation of the Millikan oil drop apparatus arranges the electric field horizontally, rather than vertically, giving charged droplets acceleration in the horizontal direction. The result is that the droplet falls in a straight line that makes an angle θ with the vertical. Show that

$$\sin\theta = q\mathscr{E}/bv_t'$$

where v_t' is the terminal speed along the angled path.

3-11. A charged oil droplet falls 5.0 mm in 20.0 s at terminal speed in the absence of an electric field. The specific gravity of air is 1.35×10^{-3} and that of oil is 0.75. The viscosity of air is 1.80×10^{-5} N · s/m^2. (*a*) What are the mass and radius of the drop? (*b*) If the droplet carries two units of electric charge and is in an electric field of 2.5×10^5 V/m, what is the ratio of the electric force to the gravitational force on the droplet?

Section 3-2 Blackbody Radiation

3-12. Find λ_m for blackbody radiation at (*a*) $T = 3$ K, (*b*) $T = 300$ K, and (*c*) $T = 3000$ K.

3-13. Use the result of Example 3-4 and Equations 3-4 and 3-6 to express Stefan's constant in terms of *h*, *c*, and *k*. Using the known values of these constants, calculate Stefan's constant.

3-14. Show that Planck's law, Equation 3-18, expressed in terms of the frequency *f*, is

$$u(f) = \frac{8\pi f^2}{c^3}\frac{hf}{e^{hf/kT} - 1}$$

3-15. As noted in the chapter, the cosmic microwave background radiation fits the Planck equation for a blackbody at 2.7 K. (*a*) What is the wavelength at the maximum intensity of the spectrum of the background radiation? (*b*) What is the frequency of the radiation at the maximum? (*c*) What is the total power incident on Earth from the background radiation?

3-16. Find the temperature of a blackbody if its spectrum has its peak at (*a*) $\lambda_m = 700$ nm (visible), (*b*) $\lambda_m = 3$ cm (microwave region), and (*c*) $\lambda_m = 3$ m (FM radio waves).

3-17. If the absolute temperature of a blackbody is doubled, by what factor is the total emitted power increased?

3-18. Calculate the average energy $\overline{E}$ per mode of oscillation for (*a*) a long wavelength $\lambda = 10\,hc/kT$, (*b*) a short wavelength $\lambda = 0.1\,hc/kT$, and compare your results with the classical prediction kT (see Equation 3-9). (The classical value comes from the equipartition theorem discussed in Chapter 8.)

STUDENTS-HUB.com Uploaded By: Malak Obaid

3-19. A particular radiating cavity has the maximum of its spectra distribution of radiated power at a wavelength of 27.0 μm (in the infrared region of the spectrum). The temperature is then changed so that the total power radiated by the cavity doubles. (*a*) Compute the new temperature. (*b*) At what wavelength does the new spectral distribution have its maximum value?
3-20. A certain very bright star has an effective surface temperature of 20,000 K. (*a*) Assuming that it radiates as a blackbody, what is the wavelength at which $u(\lambda)$ is maximum? (*b*) In what part of the electromagnetic spectrum does the maximum lie?
3-21. The energy reaching Earth from the Sun at the top of the atmosphere is 1.36×10^3 W/m^2, called the *solar constant.* Assuming that Earth radiates like a blackbody at uniform temperature, what do you conclude is the equilibrium temperature of Earth?
3-22. A 40-W incandescent bulb radiates from a tungsten filament operating at 3300 K. Assuming that the bulb radiates like a blackbody, (*a*) what are the frequency f_m and the wavelength λ_m at the maximum of the spectral distribution? (*b*) If f_m is a good approximation of the average frequency of the photons emitted by the bulb, about how many photons is the bulb radiating per second? (*c*) If you are looking at the bulb from 5 m away, how many photons enter your eye per second? (The diameter of your pupil is about 5.0 mm.)
3-23. Use Planck's law, Equation 3-18, to derive the constant in Wein's law, Equation 3-5.

Section 3-3 The Photoelectric Effect

3-24. The wavelengths of visible light range from about 380 nm to about 750 nm. (*a*) What is the range of photon energies (in eV) in visible light? (*b*) A typical FM radio station's broadcast frequency is about 100 MHz. What is the energy of an FM photon of the frequency?
3-25. The orbiting space shuttle moves around Earth well above 99 percent of the atmosphere, yet it still accumulates an electric charge on its skin due, in part, to the loss of electrons caused by the photoelectric effect with sunlight. Suppose the skin of the shuttle is coated with Ni, which has a relatively large work function $\phi = 4.87$ eV at the temperatures encountered in orbit. (*a*) What is the maximum wavelength in the solar spectrum that can result in the emission of photoelectrons from the shuttle's skin? (*b*) What is the maximum fraction of the total power falling on the shuttle that could potentially produce photoelectrons?
3-26. The work function for cesium is 1.9 eV, the lowest of any metal. (*a*) Find the threshold frequency and wavelength for the photoelectric effect. Find the stopping potential if the wavelength of the incident light is (*b*) 300 nm and (*c*) 400 nm.
3-27. (*a*) If 5 percent of the power of a 100-W bulb is radiated in the visible spectrum, how many visible photons are radiated per second? (*b*) If the bulb is a point source radiating equally in all directions, what is the flux of photons (number per unit time per unit area) at a distance of 2 m?
3-28. The work function of molybdenum is 4.22 eV. (*a*) What is the threshold frequency for the photoelectric effect in molybdenum? (*b*) Will yellow light of wavelength 560 nm cause ejection of photoelectrons from molybdenum? Prove your answer.
3-29. The NaCl molecule has a bond energy of 4.26 eV; that is, this energy must be supplied in order to dissociate the molecule into neutral Na and Cl atoms (see Chapter 9). (*a*) What are the minimum frequency and maximum wavelength of the photon necessary to dissociate the molecule? (*b*) In what part of the electromagnetic spectrum is this photon?
3-30. A photoelectric experiment with cesium yields stopping potentials for $\lambda = 435.8$ nm and $\lambda = 546.1$ nm to be 0.95 V and 0.38 V, respectively. Using these data only, find the threshold frequency and work function for cesium and the value of h.
3-31. Under optimum conditions, the eye will perceive a flash if about 60 photons arrive at the cornea. How much energy is this in joules if the wavelength of the light is 550 nm?
3-32. The longest wavelength of light that will cause emission of electrons from cesium is 653 nm. (*a*) Compute the work function for cesium. (*b*) If light of 300 nm (ultraviolet) were to shine on cesium, what would be the energy of the ejected electrons?

Section 3-4 X Rays and the Compton Effect

3-33. Use Compton's equation (Equation 3-25) to compute the value of $\Delta\lambda$ in Figure 3-17*d.* To what percent shift in the wavelength does this correspond?

STUDENTS-HUB.com Uploaded By: Malak Obaid

3-34. X-ray tubes currently used by dentists often have accelerating voltages of 80 kV. What is the minimum wavelength of the x rays they produce?
3-35. Find the momentum of a photon in eV/c and in kg · m/s if the wavelength is (*a*) 400 nm, (*b*) 1 Å = 0.1 nm, (*c*) 3 cm, and (*d*) 2 nm.
3-36. Gamma rays emitted by radioactive nuclei also exhibit measurable Compton scattering. Suppose a 0.511-MeV photon from a positron-electron annihilation scatters at 110° from a free electron. What are the energies of the scattered photon and the recoiling electron? Relative to the initial direction of the 0.511-MeV photon, what is the direction of the recoiling electron's velocity vector?
3-37. The wavelength of Compton-scattered photons is measured at $\theta = 90°$. If $\Delta\lambda/\lambda$ is to be 1 percent, what should the wavelength of the incident photon be?
3-38. Compton used photons of wavelength 0.0711 nm. (*a*) What is the energy of these photons? (*b*) What is the wavelength of the photons scattered at $\theta = 180°$? (*c*) What is the energy of the photons scattered at $\theta = 180°$? (*d*) What is the recoil energy of the electrons if $\theta = 180°$?
3-39. Compute $\Delta\lambda$ for photons scattered at 120° from (*a*) free protons, (*b*) free electrons, and (*c*) N_2 molecules in air.
3-40. Compton's equation (Equation 3-25) indicates that a graph of λ_2 versus $(1 - \cos\theta)$ should be a straight line whose slope h/mc allows a determination of h. Given that the wavelength of λ_1 in Figure 3-17 is 0.0711 nm, compute λ_2 for each scattering angle in the figure and graph the results versus $(1 - \cos\theta)$. What is the slope of the line?
3-41. (*a*) Compute the Compton wavelength of an electron and a proton. (*b*) What is the energy of a photon whose wavelength is equal to the Compton wavelength of (1) the electron and (2) the proton?

Level II

3-42. When light of wavelength 450 nm is incident on potassium, photoelectrons with stopping potential of 0.52 V are emitted. If the wavelength of the incident light is changed to 300 nm, the stopping potential is 1.90 V. Using *only* these numbers together with the values of the speed of light and the electron charge, (*a*) find the work function of potassium and (*b*) compute a value for Planck's constant.
3-43. Assuming that the difference between Thomson's calculated e/m in his second experiment (Figure 3-19) and the currently accepted value was due entirely to his neglecting the horizontal component of Earth's magnetic field outside the deflection plates, what value for that component does the difference imply? (Thomson's data: $B = 5.5 \times 10^{-4}$ T, $\mathscr{E} = 1.5 \times 10^4$ V/m, $x_1 = 5$ cm, $y_2/x_2 = 8/110$.)

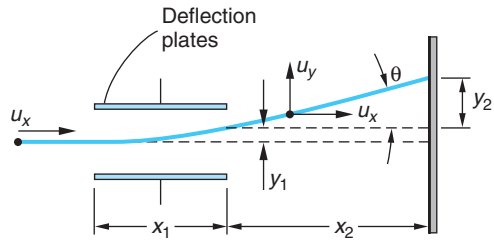

Figure 3-19 Deflection of the electron beam in Thomson's apparatus. The deflection plates are D and E in Figure 3-1. Deflection is shown with magnetic field off and the top plate positive. The magnetic field is applied perpendicular to the plane of the diagram and directed into the page.

3-44. In his first e/m experiment, Thomson determined the speed of electrons accelerated through a potential ΔV by collecting them in an insulated beam stopper and measuring both the total collected charge Q and the temperature rise ΔT of the beam stopper. (*a*) Show that with those measurements he could obtain an expression for e/m in terms of the speed of the electrons and the directly measured quantities. (*b*) Show that the expression obtained in (*a*) together with the result of Problem 3-2 enabled Thomson to compute e/m in terms of directly measured quantities.

STUDENTS-HUB.com Uploaded By: Malak Obaid

3-45. Data for stopping potential versus wavelength for the photoelectric effect using sodium are

λ, nm	200	300	400	500	600
V_0, V	4.20	2.06	1.05	0.41	0.03

Plot these data in such a way as to be able to obtain (*a*) the work function, (*b*) the threshold frequency, and (*c*) the ratio h/e.

3-46. Prove that the photoelectric effect cannot occur with a completely free electron, i.e., one not bound to an atom. (*Hint:* Consider the reference frame in which the total momentum if the electron and the incident photon is zero.)

3-47. When a beam of monochromatic x rays is incident on a particular NaCl crystal, Bragg reflection in the first order (i.e., with $m = 1$) occurs at $\theta = 20°$. The value of $d = 0.28$ nm. What is the minimum voltage at which the x-ray tube can be operating?

3-48. A 100-W beam of light is shone onto a blackbody of mass 2×10^{-3} kg for 10^4 s. The blackbody is initially at rest in a frictionless space. (*a*) Compute the total energy and momentum absorbed by the blackbody from the light beam, (*b*) calculate the blackbody's velocity at the end of the period of illumination, and (*c*) compute the final kinetic energy of the blackbody. Why is the latter less than the total energy of the absorbed photons?

3-49. Show that the maximum kinetic energy E_k, called the Compton edge, that a recoiling electron can carry away from a Compton scattering event is given by

$$E_k = \frac{hf}{1 + mc^2/2hf} = \frac{2E_\gamma^2}{2E_\gamma + mc^2}$$

3-50. The x-ray spectrometer on board a satellite measures the wavelength at the maximum intensity emitted by a particular star to be $\lambda_m = 82.8$ nm. Assuming that the star radiates like a blackbody, (*a*) compute the star's surface temperature. (*b*) What is the ratio of the intensity radiated at $\lambda = 70$ nm and at $\lambda = 100$ nm to that radiated at λ_m.

3-51. Determine the fraction of the energy radiated by the Sun in the visible region of the spectrum (350 nm to 700 nm). Assume that the Sun's surface temperature is 5800 K.

3-52. Millikan's data for the photoelectric effect in lithium are shown in the table:

Incident λ (nm)	253.5	312.5	365.0	404.7	433.9
Stopping voltage V_0 (V)	2.57	1.67	1.09	0.73	0.55

(*a*) Graph the data and determine the work function for lithium. (*b*) Find the value of Planck's constant directly from the graph in (*a*) . (*c*) The work function for lead is 4.14 eV. Which, if any, of the wavelengths in the table would not cause emission of photoelectrons from lead?

Level III

3-53. This problem is to derive the Wein displacement law, Equation 3-5. (*a*) Show that the energy density distribution function can be written $u = C\lambda^{-5}(e^{a/\lambda} - 1)^{-1}$, where C is a constant and $a = hc/kT$. (*b*) Show that the value of λ for which $du/d\lambda = 0$ satisfies the equation $5\lambda(1 - e^{-a/\lambda}) = a$. (*c*) This equation can be solved with a calculator by the trial-and-error method. Try $\lambda = \alpha a$ for various values of α until λ/a is determined to four significant figures. (*d*) Show that your solution in (*c*) implies $\lambda_m T =$ constant and calculate the value of the constant.

3-54. This problem is one of *estimating* the time lag (expected classically, but not observed) for the photoelectric effect. Assume that a point light source emits 1 W = 1 J/s of light energy. (*a*) Assuming uniform radiation in all directions, find the light intensity in $\text{eV/s} \cdot \text{m}^2$ at a distance of 1 m from the light source. (*b*) Assuming some reasonable size for an atom, find the energy per unit time incident on the atom for this intensity. (*c*) If the work function is 2 eV, how long does it take for this much energy to be absorbed, assuming that all of the energy hitting the atom is absorbed?

STUDENTS-HUB.com Uploaded By: Malak Obaid

3-55. A photon can be absorbed by a system that can have internal energy. Assume that a 15-MeV photon is absorbed by a carbon nucleus initially at rest. The recoil momentum of the carbon nucleus must be 15 MeV/c. (*a*) Calculate the kinetic energy of the carbon nucleus. What is the internal energy of the nucleus? (*b*) The carbon nucleus comes to rest and then loses its internal energy by emitting a photon. What is the energy of the photon?

3-56. The maximum kinetic energy given to the electron in a Compton scattering event plays a role in the measurement of gamma-ray spectra using scintillation detectors. The maximum is referred to as the *Compton edge.* Suppose that the Compton edge in a particular experiment is found to be 520 keV. What were the wavelength and energy of the incident gamma rays?

3-57. An electron accelerated to 50 keV in an x-ray tube has two successive collisions in being brought to rest in the target, emitting two bremsstrahlung photons in the process. The second photon emitted has a wavelength 0.095 nm longer than the first. (*a*) What are the wavelengths of the two photons? (*b*) What was the energy of the electron after emission of the first photon?

3-58. Derive Equation 3-17 from Equations 3-15 and 3-16.

STUDENTS-HUB.com Uploaded By: Malak Obaid

CHAPTER 4

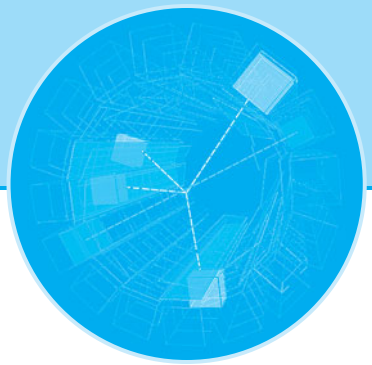

The Nuclear Atom

4-1 Atomic Spectra 148
4-2 Rutherford's Nuclear Model 150
4-3 The Bohr Model of the Hydrogen Atom 159
4-4 X-Ray Spectra 169
4-5 The Franck-Hertz Experiment 174

Among his many experiments, Newton found that sunlight passing through a small opening in a window shutter could be refracted by a glass prism so that it would fall on a screen. The white sunlight thus refracted was spread into a rainbow-colored band—a spectrum. He had discovered *dispersion*, and his experimental arrangement was the prototype of the modern *spectroscope* (Figure 4-1*a*). When, 150 years later, Fraunhofer[1] dispersed sunlight using an experimental setup similar to that shown in Figure 4-1*b* to test prisms made of glasses that he had developed, he found that the solar spectrum was crossed by more than 600 narrow, or sharp, dark lines.[2] Soon after, a number of scientists observed sharp *bright* lines in the spectra of light emitted by flames, arcs, and sparks. *Spectroscopy* quickly became an important area of research.

It soon became clear that chemical elements and compounds emit three general types of spectra. *Continuous* spectra, emitted mainly by incandescent solids, show no lines at all, bright or dark, in spectroscopes of the highest possible resolving power. *Band* spectra consist of very closely packed groups of lines that appear to be continuous in instruments of low resolving power. These are emitted when small pieces of solid materials are placed in the source flame or electrodes. The *line* spectra mentioned above arise when the source contains unbound chemical elements. The lines and bands turned out to be characteristic of individual elements and chemical compounds when excited under specific conditions. Indeed, the spectra could be (and are today) used as a highly sensitive test for the presence of elements and compounds.

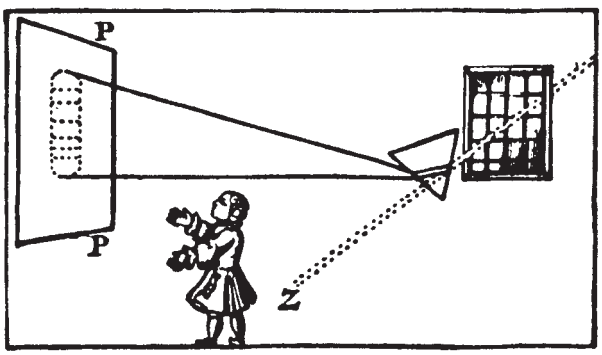

Voltaire's depiction of Newton's discovery of dispersion. [*Elémens de la Philosophie de Newton, Amsterdam, 1738.*]

STUDENTS-HUB.com
Uploaded By: Malak Obaid

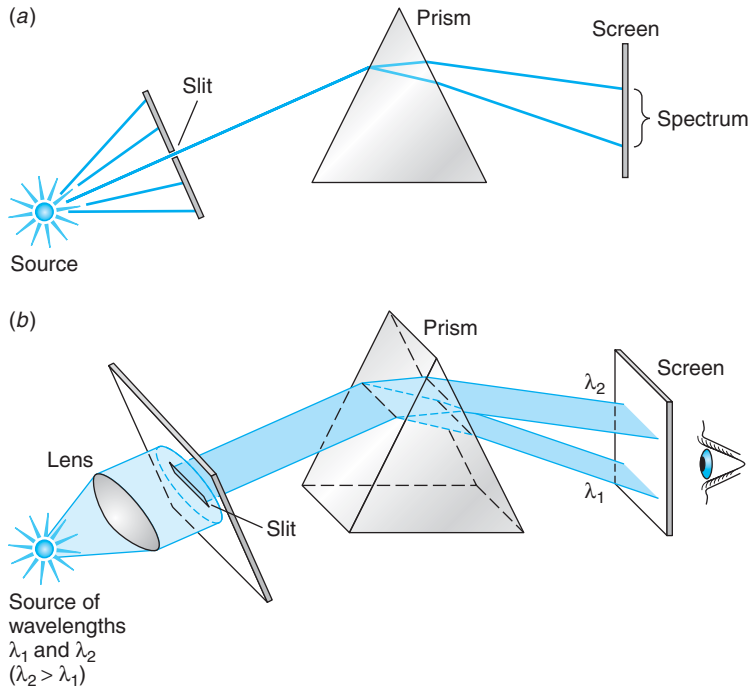

Figure 4-1 (*a*) Light from the source passes through a small hole or a narrow slit before falling on the prism. The purpose of the slit is to ensure that all the incident light strikes the prism face at the same angle so that the dispersion by the prism causes the various frequencies that may be present to strike the screen at different places with minimum overlap. (*b*) The source emits only two wavelengths, $\lambda_2 > \lambda_1$. The source is located at the focal point of the lens so that parallel light passes through the narrow slit, projecting a narrow line onto the face of the prism. Ordinary dispersion in the prism bends the shorter wavelength through the larger total angle, separating the two wavelengths at the screen. In this arrangement each wavelength appears on the screen (or on film replacing the screen) as a narrow line, which is an image of the slit. Such a spectrum was dubbed a "line spectrum" for that reason. Prisms have been almost entirely replaced in modern spectroscopes by diffraction gratings, which have much higher resolving power.

Line spectra raised an enormous theoretical problem: although classical physics could account for the existence of a continuous spectrum (if not its detailed shape, as we saw with blackbodies), it could in no way explain *why* sharp lines and bands should exist. Explaining the origin of the sharp lines and accounting for the primary features of the spectrum of hydrogen, the simplest element, was a major success of the so-called old quantum theory begun by Planck and Einstein and will be the main topic in this chapter. Full explanation of the lines and bands requires the later, more sophisticated quantum theory, which we will begin studying in Chapter 5.

4-1 Atomic Spectra

The characteristic radiation emitted by atoms of individual elements in a flame or in a gas excited by an electrical discharge was the subject of vigorous study during the late nineteenth and early twentieth centuries. When viewed or photographed through a spectroscope, this radiation appears as a set of discrete lines, each of a particular

STUDENTS-HUB.com Uploaded By: Malak Obaid

color or wavelength; the positions and intensities of the lines are characteristic of the element. The wavelengths of these lines could be determined with great precision, and much effort went into finding and interpreting regularities in the spectra. A major breakthrough was made in 1885 by a Swiss schoolteacher, Johann Balmer, who found that the lines in the visible and near ultraviolet spectrum of hydrogen could be represented by the empirical formula

$$\lambda_n = 364.6\frac{n^2}{n^2 - 4}\ \text{nm} \qquad \textbf{4-1}$$

where n is a variable integer that takes on the values $n = 3, 4, 5, \ldots$. Figure 4-2*a* shows the set of spectral lines of hydrogen (now known as the *Balmer series*) whose wavelengths are given by Balmer's formula. For example, the wavelength of the H_α line could be found by letting $n = 3$ in Equation 4-1 (try it!), and other integers each predicted a line that was found in the spectrum. Balmer suggested that his formula might be a special case of a more-general expression applicable to the spectra of other elements when ionized to a single electron, i.e., hydrogen-like elements.

The uniqueness of the line spectra of the elements has enabled astronomers to determine the composition of stars, chemists to identify unknown compounds, and theme parks and entertainers to have laser shows.

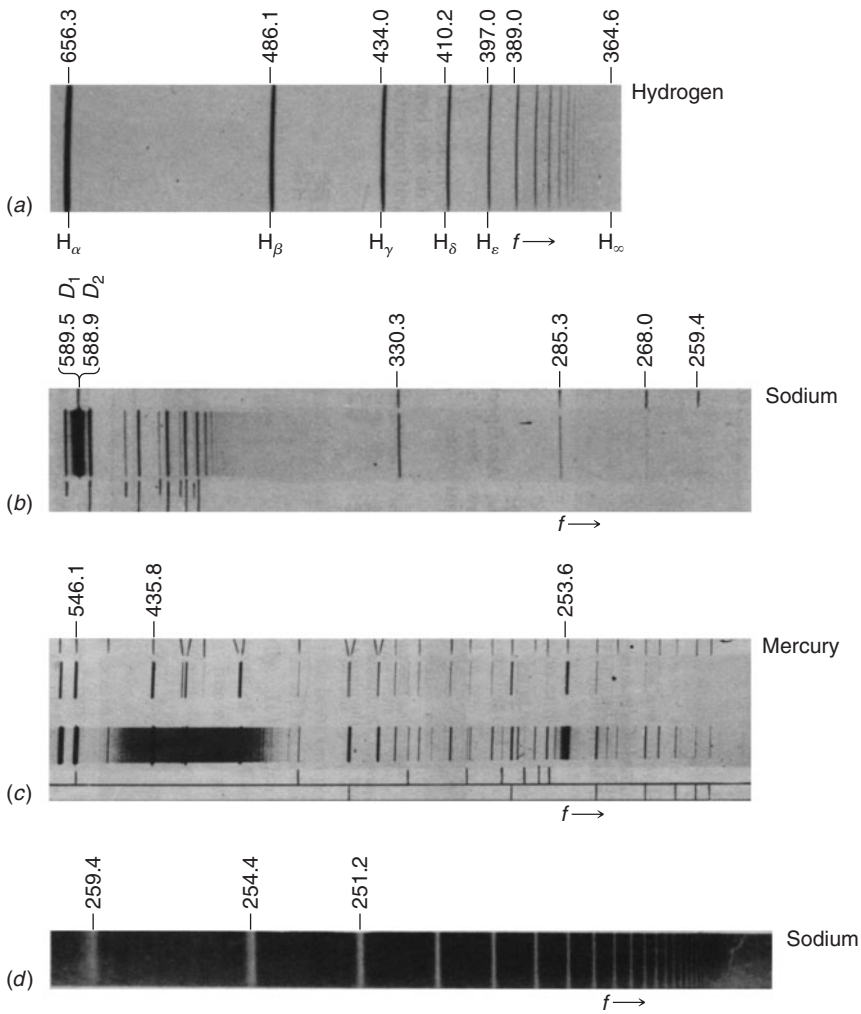

Figure 4-2 (*a*) Emission line spectrum of hydrogen in the visible and near ultraviolet. The lines appear dark because the spectrum was photographed; hence, the bright lines are exposed (dark) areas on the film. The names of the first five lines are shown, as is the point beyond which no lines appear, H_∞, called the *limit* of the series. (*b*) Part of the emission spectrum of sodium. The two very close bright lines at 589 nm are the D_1 and D_2 lines. They are the principal radiation from sodium street lighting. (*c*) Part of the emission spectrum of mercury. (*d*) Part of the dark line (absorption) spectrum of sodium. White light shining through sodium vapor is absorbed at certain wavelengths, resulting in no exposure of the film at those points. Note that the line at 259.4 nm is visible here in both the bright and dark line spectra. Note, too, that frequency increases toward the right, wavelength toward the left in the four spectra shown.

STUDENTS-HUB.com Uploaded By: Malak Obaid

Such an expression, found independently by J. R. Rydberg and W. Ritz and thus called the *Rydberg-Ritz formula*, gives the reciprocal wavelength[3] as

$$\frac{1}{\lambda_{mn}} = R\left(\frac{1}{m^2} - \frac{1}{n^2}\right) \qquad \text{for} \qquad n > m \tag{4-2}$$

where m and n are integers and R, the *Rydberg constant*, is the same for all series of spectral lines of the same element and varies only slightly, and in a regular way, from element to element. For hydrogen, the value of R is $R_H = 1.096776 \times 10^7\ \text{m}^{-1}$. For very heavy elements, R approaches the value of $R_\infty = 1.097373 \times 10^7\ \text{m}^{-1}$. Such empirical expressions were successful in predicting other series of spectral lines, such as other hydrogen lines outside the visible region.

EXAMPLE 4-1 **Hydrogen Spectral Series** The hydrogen Balmer series reciprocal wavelengths are those given by Equation 4-2, with $m = 2$ and $n = 3, 4, 5, \ldots$. For example, the first line of the series, H_α, would be for $m = 2$, $n = 3$:

$$\frac{1}{\lambda_{23}} = R\left(\frac{1}{2^2} - \frac{1}{3^2}\right) = \frac{5}{36}R = 1.523 \times 10^6\ \text{m}^{-1}$$

or

$$\lambda_{23} = 656.5\ \text{nm}$$

Other series of hydrogen spectral lines were found for $m = 1$ (by Theodore Lyman) and $m = 3$ (by Friedrich Paschen). Compute the wavelengths of the first lines of the Lyman and Paschen series.

SOLUTION

For the Lyman series ($m = 1$), the first line is for $m = 1$, $n = 2$:

$$\frac{1}{\lambda_{12}} = R\left(\frac{1}{1^2} - \frac{1}{2^2}\right) = \frac{3}{4}R = 8.22 \times 10^6\ \text{m}^{-1}$$

$$\lambda_{12} = 121.6\ \text{nm} \qquad \text{(in the ultraviolet)}$$

For the Paschen series ($m = 3$), the first line is for $m = 3$, $n = 4$:

$$\frac{1}{\lambda_{34}} = R\left(\frac{1}{3^2} - \frac{1}{4^2}\right) = \frac{7}{144}R = 5.332 \times 10^5\ \text{m}^{-1}$$

$$\lambda_{34} = 1876\ \text{nm} \qquad \text{(in the infrared)}$$

All of the lines predicted by the Rydberg-Ritz formula for the Lyman and Paschen series are found experimentally. Note that no lines are predicted to lie beyond $\lambda_\infty = 1/R = 91.2$ nm for the Lyman series and $\lambda_\infty = 9/R = 820.6$ nm for the Paschen series and none are found by experiments.

4-2 Rutherford's Nuclear Model

Many attempts were made to construct a model of the atom that yielded the Balmer and Rydberg-Ritz formulas. It was known that an atom was about 10^{-10} m in diameter (see Problem 4-6), that it contained electrons much lighter than the atom (see Section 3-1), and that it was electrically neutral. The most popular model was J. J. Thomson's model, already quite successful in explaining chemical reactions. Thomson

STUDENTS-HUB.com Uploaded By: Malak Obaid

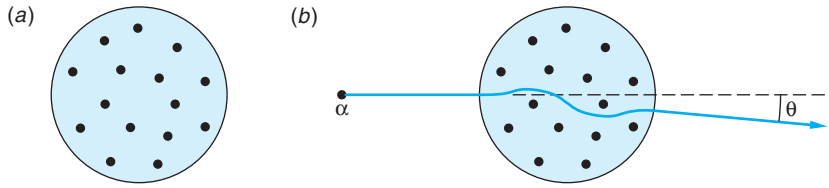

Figure 4-3 Thomson's model of the atom: (*a*) A sphere of positive charge with electrons embedded in it so that the net charge would normally be zero. The atom shown would have been phosphorus. (*b*) An α particle scattered by such an atom would have a scattering angle θ much smaller than 1°.

attempted various models consisting of electrons embedded in a fluid that contained most of the mass of the atom and had enough positive charge to make the atom electrically neutral. (See Figure 4-3*a*.) He then searched for configurations that were stable and had normal modes of vibration corresponding to the known frequencies of the spectral lines. One difficulty with all such models was that electrostatic forces alone cannot produce stable equilibrium. Thus, the charges were required to move and, if they stayed within the atom, to accelerate; however, the acceleration would result in continuous emission of radiation, which is not observed. Despite elaborate mathematical calculations, Thomson was unable to obtain from his model a set of frequencies of vibration that corresponded with the frequencies of observed spectra.

The Thomson model of the atom was replaced by one based on the results of a set of experiments conducted by Ernest Rutherford[4] and his students H. W. Geiger and E. Marsden. Rutherford was investigating radioactivity and had shown that the radiations from uranium consisted of at least two types, which he labeled α and β. He showed, by an experiment similar to that of Thomson, that q/m for the α was half that of the proton. Suspecting that the α particles were doubly ionized helium, Rutherford and his co-workers in a classic experiment let a radioactive substance α decay in a previously evacuated chamber; then, by spectroscopy, they detected the spectral lines of ordinary helium gas in the chamber. Realizing that this energetic, massive α particle would make an excellent probe for "feeling about" within the interiors of other atoms, Rutherford began a series of experiments with this purpose.

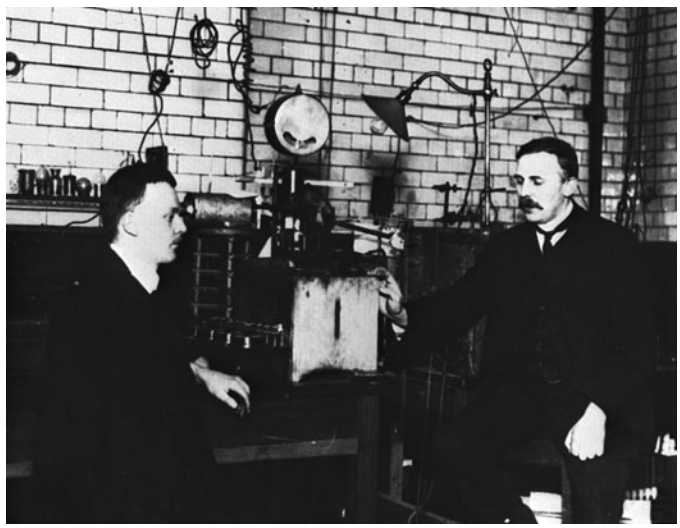

Hans Geiger and Ernest Rutherford in their Manchester Laboratory. [*Courtesy of University of Manchester.*]

STUDENTS-HUB.com Uploaded By: Malak Obaid

In these latter experiments, a narrow beam of α particles fell on a zinc sulfide screen, which emitted visible light scintillations when struck (Figure 4-4). The distribution of scintillations on the screen was observed when various thin metal foils were placed between it and the source. Most of the α particles were either undeflected or

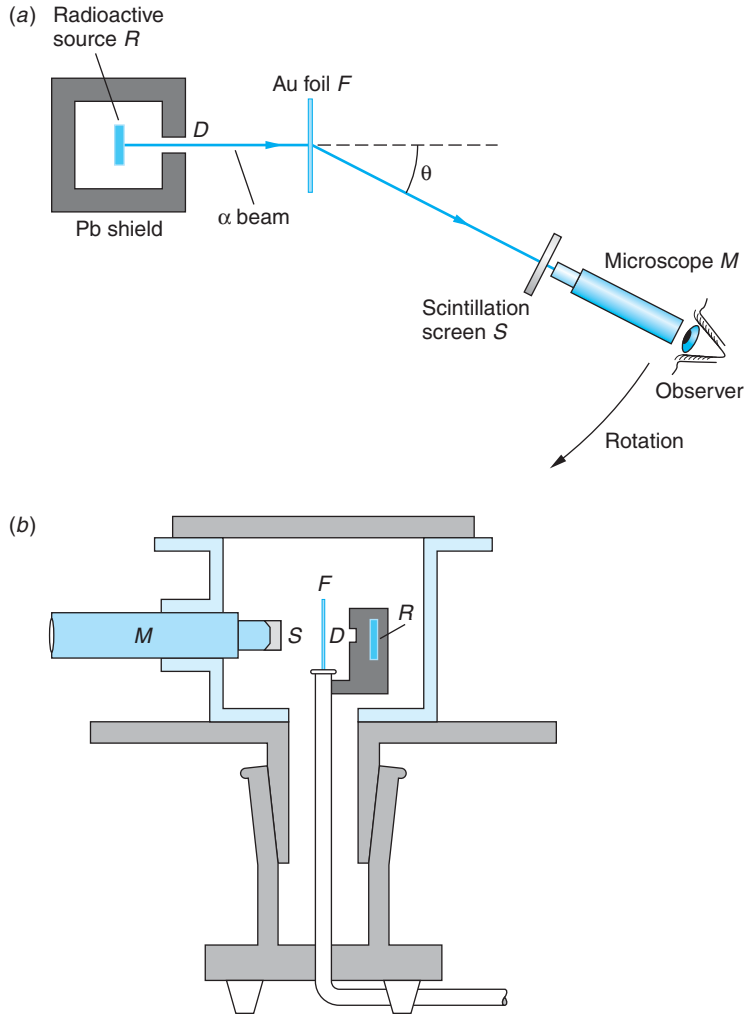

Figure 4-4 Schematic diagram of the apparatus used by Geiger and Marsden to test Rutherford's atomic model. (*a*) The beam of α particles is defined by the small hole *D* in the shield surrounding the radioactive source *R* of ^{214}Bi (called RaC in Rutherford's day). The α beam strikes an ultrathin gold foil *F* (about 2000 atoms thick), and the α particles are individually scattered through various angles. Those scattering at the angle θ shown strike a small screen *S* coated with a scintillator, i.e., a material that emits tiny flashes of light (scintillations) when struck by an α particle. The scintillations were viewed by the observer through a small microscope *M*. The scintillation screen–microscope combination could be rotated about the center of the foil. The region traversed by the α beam is evacuated. The experiment consisted of counting the number of scintillations as a function of θ. (*b*) A diagram of the actual apparatus as it appeared in Geiger and Marsden's paper describing the results. The letter key is the same as in (*a*). [*Part (b) from H. Geiger and E. Marsden, Philosophical Review,* ***25,*** *507 (1913).*]

STUDENTS-HUB.com Uploaded By: Malak Obaid

deflected through very small angles of the order of 1°. Quite unexpectedly, however, a few α particles were deflected through angles as large as 90° or more. If the atom consisted of a positively charged sphere of radius 10^{-10} m, containing electrons as in the Thomson model, only a very small deflection could result from a single encounter between an α particle and an atom, even if the α particle penetrated into the atom. Indeed, calculations showed that the Thomson atomic model could not possibly account for the number of large-angle scatterings that Rutherford saw. The unexpected scatterings at large angles were described by Rutherford with these words:

> It was quite the most incredible event that ever happened to me in my life. It was as incredible as if you fired a 15-inch shell at a piece of tissue paper and it came back and hit you.

Rutherford's Scattering Theory and the Nuclear Atom

The question is, then, Why would one obtain the large-angle scattering that Rutherford saw? The trouble with the Thomson atom is that it is too "soft"—the maximum force experienced by the α is too weak to give a large deflection. If the positive charge of the atom is concentrated in a more compact region, however, a much larger force will occur at near impacts. Rutherford concluded that the large-angle scattering obtained experimentally could result only from a single encounter of the α particle with a massive charge confined to a volume much smaller than that of the whole atom. Assuming this "nucleus" to be a point charge, he calculated the expected angular distribution for the scattered α particles. His predictions of the dependence of scattering probability on angle, nuclear charge, and kinetic energy were completely verified in a series of experiments carried out in his laboratory by Geiger and Marsden.

We will not go through Rutherford's derivation in detail, but merely outline the assumptions and conclusions. Figure 4-5 shows the geometry of an α particle being scattered by a nucleus, which we take to be a point charge Q at the origin. Initially, the α particle approaches with speed v along a line a distance b from a parallel line COA through the origin. The force on the α particle is $F = kq_\alpha Q/r^2$, given by

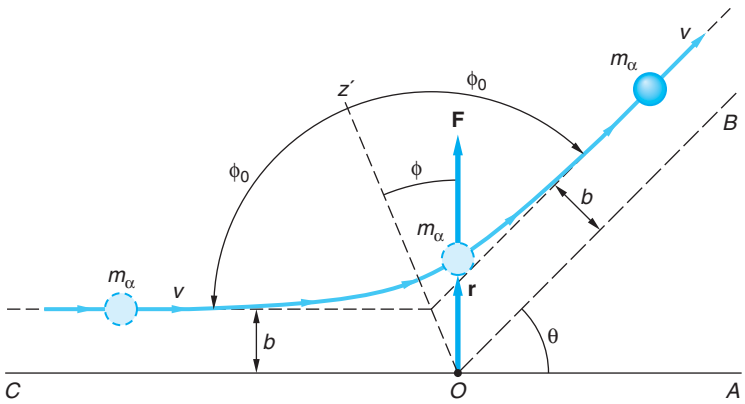

Figure 4-5 Rutherford scattering geometry. The nucleus is assumed to be a point charge Q at the origin O. At any distance r the α particle experiences a repulsive force $kq_\alpha Q/r^2$. The α particle travels along a hyperbolic path that is initially parallel to line COA a distance b from it and finally parallel to line OB, which makes an angle θ with OA. The scattering angle θ can be related to the impact parameter b by classical mechanics.

STUDENTS-HUB.com Uploaded By: Malak Obaid

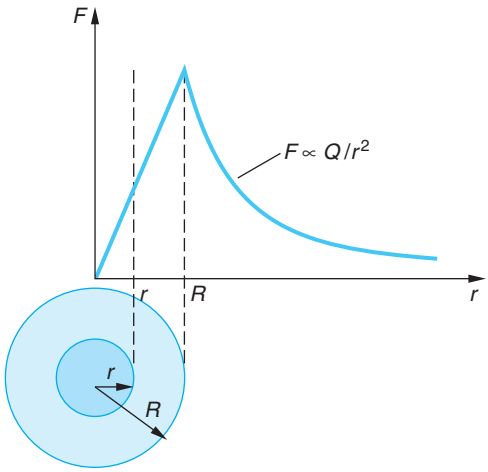

Figure 4-6 Force on a point charge versus distance r from the center of a uniformly charged sphere of radius R. Outside the sphere the force is proportional to Q/r^2, where Q is the total charge. Inside the sphere, the force is proportional to $q'/r^2 = QrR/R^3$, where $q' = Q(r/R)^3$ is the charge within a sphere of radius r. The maximum force occurs at $r = R$.

Coulomb's law (Figure 4-6). After scattering, when the α particle is again far from the nucleus, it is moving with the same speed v parallel to the line OB, which makes an angle θ with line COA. (Since the potential energy is again zero, the final speed must be equal to the initial speed by conservation of energy, assuming, as Rutherford did, that the massive nucleus remains fixed during the scattering.) The distance b is called the *impact parameter* and the angle θ, the *scattering angle*. The path of the α particle can be shown to be a hyperbola, and the scattering angle θ can be related to the impact parameter b from the laws of classical mechanics. The result is

$$b = \frac{kq_\alpha Q}{m_\alpha v^2} \cot \frac{\theta}{2} \qquad \textbf{4-3}$$

Of course, it is not possible to choose or know the impact parameter for any particular α particle, but when one recalls the values of the cotangent between 0° and 90°, all such particles with impact parameters less than or equal to a particular b will be scattered through an angle θ greater than or equal to that given by Equation 4-3; i.e., the smaller the impact parameter, the larger the scattering angle (Figure 4-7). Let the intensity of the incident α particle beam be I_0 particles per second per unit area. The number per second scattered by one nucleus through angles greater than θ equals the number per second that have impact parameters less than b (θ). This number is $\pi b^2 I_0$.

The quantity πb^2, which has the dimensions of an area, is called the *cross section* σ for scattering through angles greater than θ. *The cross section* σ *is thus defined as the number scattered per nucleus per unit time divided by the incident intensity.*

The particle-scattering technique devised by Rutherford to "look" at atoms now has wide application throughout physics. Scattering of high-energy electrons from protons and neutrons provided our first experimental hint of the existence of quarks. Rutherford back-scattering spectroscopy is widely used as a highly sensitive surface analysis technique.

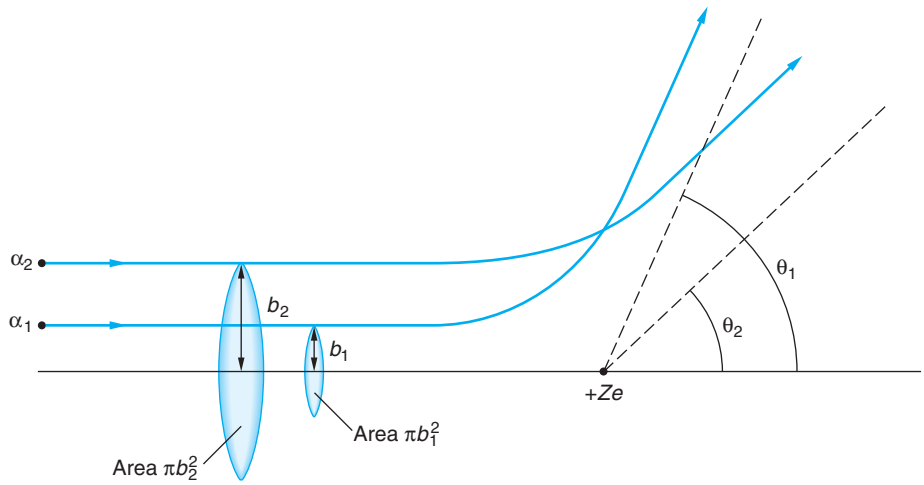

Figure 4-7 Two α particles with equal kinetic energies approach the positive charge $Q = +Ze$ with impact parameters b_1 and b_2, where $b_1 < b_2$. According to Equation 4-3, the angle θ_1 through which α_1 is scattered will be larger than θ_2. In general, all α particles with impact parameters smaller than a particular value of b will have scattering angles larger than the corresponding value of θ from Equation 4-3. The area πb^2 is called the cross section for scattering with angles greater than θ.

STUDENTS-HUB.com Uploaded By: Malak Obaid

The total number of particles scattered per second is obtained by multiplying $\pi b^2 I_0$ by the number of nuclei in the scattering foil (this assumes the foil to be thin enough to make the chance of overlap negligible). Let n be the number of nuclei per unit volume:

$$n = \frac{\rho(\text{g/cm}^3)N_A(\text{atoms/mol})}{M(\text{g/mol})} = \frac{\rho N_A}{M}\frac{\text{atoms}}{\text{cm}^3} \qquad \textbf{4-4}$$

For a foil of thickness t, the total number of nuclei "seen" by the beam is nAt, where A is the area of the beam (Figure 4-8). The total number scattered per second through angles greater than θ is thus $\pi b^2 I_0 nt A$. If we divide this by the number of α particles incident per second $I_0 A$, we get the fraction f scattered through angles greater than θ:

$$f = \pi b^2 nt \qquad \textbf{4-5}$$

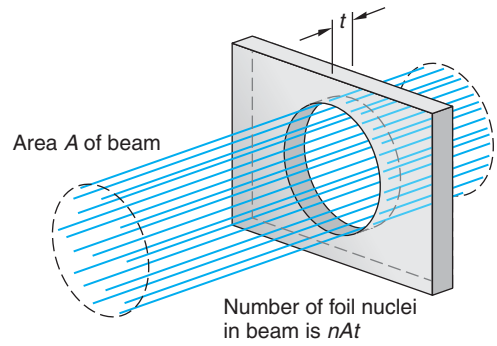

Figure 4-8 The total number of nuclei of foil atoms in the area covered by the beam is nAt, where n is the number of foil atoms per unit volume, A is the area of the beam, and t is the thickness of the foil.

EXAMPLE 4-2 Scattered Fraction f Calculate the fraction of an incident beam of α particles of kinetic energy 5 MeV that Geiger and Marsden expected to see for $\theta \geq 90°$ from a gold foil ($Z = 79$) 10^{-6} m thick.

SOLUTION

1. The fraction f is related to the impact parameter b, the number density of nuclei n, and the thickness t by Equation 4-5: $f = \pi b^2 nt$

2. The particle density n is given by Equation 4-4:
$$n = \frac{\rho N_A}{M} = \frac{(19.3\ \text{g/cm}^3)(6.02 \times 10^{23}\ \text{atoms/mol})}{197\ \text{gm/mol}}$$
$$= 5.90 \times 10^{22}\ \text{atoms/cm}^3 = 5.90 \times 10^{28}\ \text{atoms/m}^3$$

3. The impact parameter b is related to θ by Equation 4-3:
$$b = \frac{kq_\alpha Q}{m_\alpha v^2}\cot\frac{\theta}{2} = \frac{(2)(79)ke^2}{2K_\alpha}\cot\frac{90°}{2}$$
$$= \frac{(2)(79)(1.44\ \text{eV}\cdot\text{nm})}{(2)(5 \times 10^6\ \text{eV})} = 2.28 \times 10^{-5}\ \text{nm}$$
$$= 2.28 \times 10^{-14}\ \text{m}$$

4. Substituting these into Equation 4-5 yields f:
$$f = \pi(2.28 \times 10^{-14}\ \text{m})^2\left(5.9 \times 10^{28}\frac{\text{atoms}}{\text{m}^3}\right)(10^{-6}\ \text{m})$$
$$= 9.6 \times 10^{-5} \approx 10^{-4}$$

Remarks: This outcome is in good agreement with Geiger and Marsden's measurement of about 1 in 8000 in their first trial. Thus, the nuclear model is in good agreement with their results.

On the strength of the good agreement between the nuclear atomic model and the measured fraction of the incident α particles scattered at angles $\theta \geq 90°$, Rutherford derived an expression, based on the nuclear model, for the number of α particles ΔN that would be scattered at any angle θ. That number, which also depends on the atomic

STUDENTS-HUB.com Uploaded By: Malak Obaid

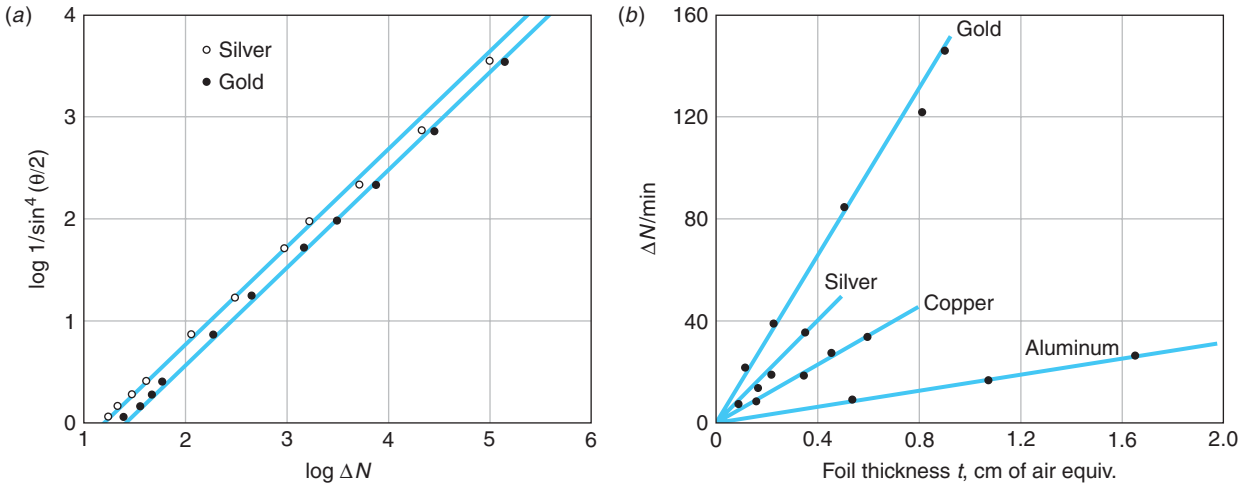

Figure 4-9 (*a*) Geiger and Marsden's data for α scattering from thin gold and silver foils. The graph is a log-log plot to show the data over several orders of magnitude. Note that scattering angle increases downward along the vertical axis. (*b*) Geiger and Marsden also measured the dependence of ΔN on t predicted by Equation 4-6 for foils made from a wide range of elements, this being an equally critical test. Results for four of the elements used are shown.

number Z and thickness t of the scattering foil, on the intensity I_0 of the incident α particles and their kinetic energy E_k, and on the geometry of the detector (A_{sc} is the detector area and r is the foil-detector distance), is given by

$$\Delta N = \left(\frac{I_0 A_{sc} n t}{r^2}\right)\left(\frac{kZe^2}{2E_k}\right)^2 \frac{1}{\sin^4 \frac{\theta}{2}} \qquad \textbf{4-6}$$

Within the uncertainties of their experiments, which involved visually observing several hundred thousand α particles, Geiger and Marsden verified every one of the predictions of Rutherford's formula over four orders of magnitude of ΔN. The excellent agreement of their data with Equation 4-6 firmly established the nuclear atomic model as the correct basis for further studies of atomic and nuclear phenomena. (See Figure 4-9.)

More

Rutherford's derivation of Equation 4-6 was based on his atomic model and the well-known Coulomb scattering process of charged particles. *Rutherford's Prediction and Geiger and Marsden's Results* are described on the home page: www.whfreeman.com/tiplermodernphysics5e. See also Equations 4-7 through 4-10 here, as well as Figures 4-10 through 4-12.

The Size of the Nucleus

The fact that the force law is shown to be correct, confirming Rutherford's model, does not imply that the nucleus is a mathematical point charge, however. The force law would be the same even if the nucleus were a ball of charge of some radius R_0 as long as the α particle did not penetrate the ball. (See Figures 4-6 and 4-13.) For a given scattering angle, the distance of closest approach of the α particle to the nucleus can be calculated from the geometry of the collision. For the largest angle, near 180°, the collision is nearly "head-on." The corresponding distance of closest approach r_d is thus an experimental

STUDENTS-HUB.com Uploaded By: Malak Obaid

upper limit on the size of the target nucleus. We can calculate the distance of closest approach for a head-on collision r_d by noting that conservation of energy requires the potential energy at this distance to equal the original kinetic energy:

$$(V + E_k)_{\text{large } r} = (V + E_k)_{r_d}$$

$$\left(0 + \frac{1}{2}m_\alpha v^2\right)_{\text{large } r} = \left(\frac{kq_\alpha Q}{r_d} + 0\right)_{r_d}$$

$$\frac{1}{2}m_\alpha v^2 = \frac{kq_\alpha Q}{r_d}$$

or

$$r_d = \frac{kq_\alpha Q}{\frac{1}{2}m_\alpha v^2} \qquad \textbf{4-11}$$

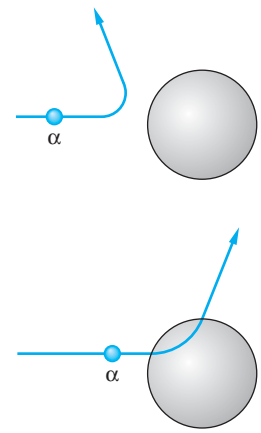

Figure 4-13 (*a*) If the α particle does not penetrate the nuclear charge, the nucleus can be considered a point charge located at the center. (*b*) If the particle has enough energy to penetrate the nucleus, the Rutherford scattering law does not hold but would require modification to account for that portion of the nuclear charge "behind" the penetrating α particle.

For the case of 7.7-MeV α particles, the distance of closest approach for a head-on collision is

$$r_d = \frac{(2)(79)(1.44\ \text{eV}\cdot\text{nm})}{7.7 \times 10^6\ \text{eV}} = 3 \times 10^{-5}\ \text{nm} = 3 \times 10^{-14}\ \text{m}$$

For other collisions, the distance of closest approach is somewhat greater, but for α particles scattered at large angles it is of the same order of magnitude. The excellent agreement of Geiger and Marsden's data at large angles with the prediction of Equation 4-6 thus indicates that the radius of the gold nucleus is no larger than about 3×10^{-14} m. If higher-energy particles could be used, the distance of closest approach would be smaller, and as the energy of the α particles increased, we might expect that eventually the particles would penetrate the nucleus. Since, in that event, the force law is no longer $F = kq_\alpha Q/r^2$, the data would not agree with the point-nucleus calculation. Rutherford did not have higher-energy α particles available, but he could reduce the distance of closest approach by using targets of lower atomic numbers.[9] For the case of aluminum, with $Z = 13$, when the most energetic α particles that he had available (7.7 MeV from ^{214}Bi) scattered at large angles, they did not follow the predictions of Equation 4-6. However, when the kinetic energy of the particles was reduced by passing the beam through thin mica sheets of various thicknesses, the data again followed the prediction of Equation 4-6. Rutherford's data are shown in Figure 4-14. The value of r_d (calculated from Equation 4-11) at which the data begin to deviate from the prediction can be thought of as the surface of the nucleus. From these data, Rutherford estimated the radius of the aluminum nucleus to be about 1.0×10^{-14} m. (The radius of the Al nucleus is actually about 3.6×10^{-15} m. See Chapter 11.)

A unit of length convenient for describing nuclear sizes is the fermi, or femtometer (fm), defined as 1 fm $= 10^{-15}$ m. As we will see in Chapter 11, the nuclear radius varies from about 1 to 10 fm from the lightest to the heaviest atoms.

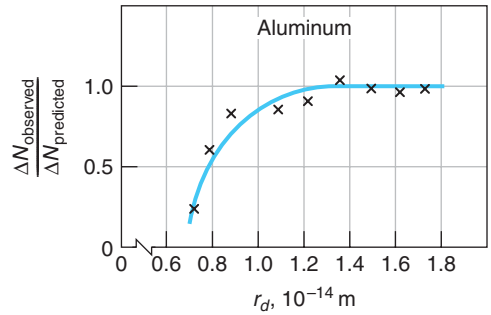

Figure 4-14 Data from Rutherford's group showing observed α scattering at a large fixed angle versus values of r_d computed from Equation 4-11 for various kinetic energies.

EXAMPLE 4-3 **Rutherford Scattering at Angle θ** In a particular experiment, α particles from ^{226}Ra are scattered at θ = 45° from a silver foil and 450 particles are counted each minute at the scintillation detector. If everything is kept the same except that the detector is moved to observe particles scattered at 90°, how many will be counted per minute?

STUDENTS-HUB.com Uploaded By: Malak Obaid

SOLUTION

Using Equation 4-6, we have that $\Delta N = 450$ when $\theta = 45°$, but we don't have any of the other parameters available. Letting all of the quantities in the parenthesis equal a constant C, we have that

$$\Delta N = 450 = C \sin^{-4}\frac{45°}{2}$$

or

$$C = 450 \sin^4\left(\frac{45°}{2}\right)$$

When the detector is moved to $\theta = 90°$, the value of C is unchanged, so

$$\Delta N = C \sin^{-4}\left(\frac{90°}{2}\right) = 450 \sin^4\left(\frac{45°}{2}\right) \sin^{-4}\left(\frac{90°}{2}\right)$$
$$= 38.6 \approx 39 \text{ particles/min}$$

EXAMPLE 4-4 **Alpha Scattering** A beam of α particles with $E_k = 6.0$ MeV impinges on a silver foil 1.0 μm thick. The beam current is 1.0 nA. How many α particles will be counted by a small scintillation detector of area equal to 5 mm^2 located 2.0 cm from the foil at an angle of 75°? (For silver $Z = 47$, $\rho = 10.5$ gm/cm^3, and $M = 108$.)

SOLUTION

1. The number counted ΔN is given by Equation 4-6:
$$\Delta N = \left(\frac{I_0 A_{sc} nt}{r^2}\right)\left(\frac{kZe^2}{2E_k}\right)^2 \frac{1}{\sin^4\frac{\theta}{2}}$$

2. Since each α particle has $q_\alpha = 2e$, I_0 is:
$$I_0 = (1.0 \times 10^{-9}\text{A})(2 \times 1.60 \times 10^{-19}\text{ C}/\alpha)^{-1}$$
$$= 3.12 \times 10^9\ \alpha/\text{s}$$

3. The kinetic energy of each α is
$$E_k = (6.0\text{ MeV})(1.60 \times 10^{-13}\text{ J/MeV})$$
$$= 9.60 \times 10^{-13}\text{ J}$$

4. For silver, n is given by
$$n = \rho N_A/M$$
$$= \frac{(10.5\text{ g/cm}^3)(6.02 \times 10^{23}\text{ atoms/mol})}{108\text{ g/mol}}$$
$$= 5.85 \times 10^{22}\text{ atoms/cm}^3 = 5.85 \times 10^{28}\text{ atoms/m}^3$$

5. Substituting the given values and computed results into Equation 4-6 gives ΔN:
$$\Delta N = \frac{(3.12 \times 10^9\ \alpha/\text{s})(5 \times 10^{-6}\text{ m}^2)(5.85 \times 10^{28}\text{ atoms/m}^3)(10^{-6}\text{ m})}{(2 \times 10^{-2})^2 \sin^4(75°/2)}$$
$$\times \left[\frac{(9 \times 10^9)(47)(1.60 \times 10^{-19})^2}{(2)(9.60 \times 10^{-13})}\right]^2$$
$$= 528\ \alpha/\text{s}$$

EXAMPLE 4-5 **Radius of the Au Nucleus** The radius of the gold (Au) nucleus has been measured by high-energy electron scattering as 6.6 fm. What kinetic energy α particles would Rutherford have needed so that for 180° scattering, the α particle would just reach the nuclear surface before reversing direction?

STUDENTS-HUB.com Uploaded By: Malak Obaid

SOLUTION

From Equation 4-11, we have

$$\frac{1}{2}mv^2 = \frac{kq_\alpha Q}{r_d} = \frac{(9 \times 10^9)(2)(79)(1.60 \times 10^{-19})^2}{6.6 \times 10^{-15}}$$
$$= 5.52 \times 10^{-12}\ \text{J} = 34.5\ \text{MeV}$$

Alpha particles of such energy are not emitted by naturally radioactive materials and so were not accessible to Rutherford. Thus, he could not have performed an experiment for Au equivalent to that for Al illustrated by Figure 4-14.

Questions

1. Why can't the impact parameter for a particular α particle be chosen?
2. Why is it necessary to use a very thin target foil?
3. Why could Rutherford place a lower limit on the radius of the Al nucleus but not on the Au nucleus?
4. How could you use the data in Figure 4-9*a* to determine the charge on a silver nucleus relative to that on a gold nucleus?
5. How would you expect the data (not the curve) to change in Figure 4-9 if the foil were so thick that an appreciable number of gold nuclei were hidden from the beam by being in the "shadow" of the other gold nuclei?

4-3 The Bohr Model of the Hydrogen Atom

In 1913, the Danish physicist Niels H. D. Bohr[10] proposed a model of the hydrogen atom that combined the work of Planck, Einstein, and Rutherford and was remarkably successful in predicting the observed spectrum of hydrogen. The Rutherford model assigned charge and mass to the nucleus but was silent regarding the distribution of the charge and mass of the electrons. Bohr, who had been working in Rutherford's laboratory during the experiments of Geiger and Marsden, made the assumption that the electron in the hydrogen atom moved in an orbit about the positive nucleus, bound by the electrostatic attraction of the nucleus. Classical mechanics allows circular or elliptical orbits in this system, just as in the case of the planets orbiting the Sun. For simplicity, Bohr chose to consider circular orbits.

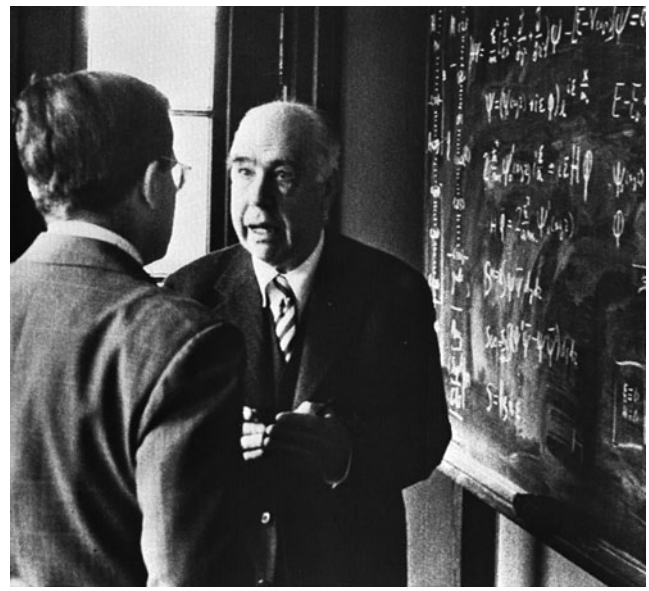

Niels Bohr explains a point in front of the blackboard (1956). [*American Institute of Physics, Niels Bohr Library, Margrethe Bohr Collection.*]

Such a model is mechanically stable because the Coulomb potential $V = -kZe^2/r$ provides the centripetal force

$$F = \frac{kZe^2}{r^2} = \frac{mv^2}{r} \qquad \textbf{4-12}$$

necessary for the electron to move in a circle of radius r at speed v, but it is electrically unstable because the electron is always accelerating toward the center of the circle.

STUDENTS-HUB.com Uploaded By: Malak Obaid

The laws of electrodynamics predict that such an accelerating charge will radiate light of frequency f equal to that of the periodic motion, which in this case is the frequency of revolution. Thus, classically,

$$f = \frac{v}{2\pi r} = \left(\frac{kZe^2}{rm}\right)^{1/2} \frac{1}{2\pi r} = \left(\frac{kZe^2}{4\pi^2 m}\right)^{1/2} \frac{1}{r^{3/2}} \sim \frac{1}{r^{3/2}} \qquad \textbf{4-13}$$

The total energy of the electron is the sum of the kinetic and the potential energies:

$$E = \frac{1}{2}mv^2 + \left(-\frac{kZe^2}{r}\right)$$

From Equation 4-12, we see that $\frac{1}{2}mv^2 = kZe^2/2r$ (a result that holds for circular motion in any inverse-square force field), so the total energy can be written as

$$E = \frac{kZe^2}{2r} - \frac{kZe^2}{r} = -\frac{kZe^2}{2r} \sim -\frac{1}{r} \qquad \textbf{4-14}$$

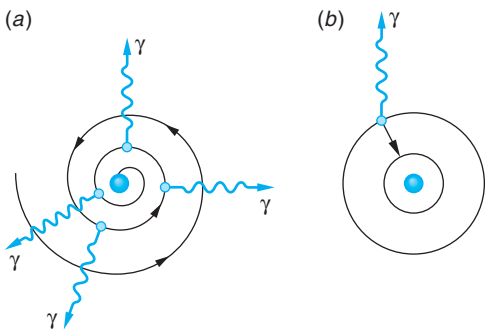

Figure 4-15 (*a*) In the classical orbital model, the electron orbits about the nucleus and spirals into the center because of the energy radiated. (*b*) In the Bohr model, the electron orbits without radiating until it jumps to another allowed radius of lower energy, at which time radiation is emitted.

Thus, classical physics predicts that, as energy is lost to radiation, the electron's orbit will become smaller and smaller while the frequency of the emitted radiation will become higher and higher, further increasing the rate at which energy is lost and ending when the electron reaches the nucleus. (See Figure 4-15*a*.) The time required for the electron to spiral into the nucleus can be calculated from classical mechanics and electrodynamics; it turns out to be less than a microsecond. Thus, at first sight, this model predicts that the atom will radiate a continuous spectrum (since the frequency of revolution changes continuously as the electron spirals in) and will collapse after a very short time, a result that fortunately does not occur. Unless excited by some external means, atoms do not radiate at all, and when excited atoms do radiate, a line spectrum is emitted, not a continuous one.

Bohr "solved" these formidable difficulties with two decidedly nonclassical postulates. His first postulate was that *electrons could move in certain orbits without radiating*. He called these orbits *stationary states*. His second postulate was to assume that *the atom radiates when the electron makes a transition from one stationary state to another* (Figure 4-15*b*) *and that the frequency f of the emitted radiation is not the frequency of motion in either stable orbit but is related to the energies of the orbits by Planck's theory*

$$hf = E_i - E_f \qquad \textbf{4-15}$$

where h is Planck's constant and E_i and E_f are the energies of the initial and final states. The second assumption, which is equivalent to that of energy conservation with the emission of a photon, is crucial because it deviated from classical theory, which requires the frequency of radiation to be that of the motion of the charged particle. Equation 4-15 is referred to as the Bohr *frequency condition*.

In order to determine the energies of the allowed, nonradiating orbits, Bohr made a third assumption, now known as the *correspondence principle*, which had profound implications:

> In the limit of large orbits and large energies, quantum calculations must agree with classical calculations.

STUDENTS-HUB.com Uploaded By: Malak Obaid

Thus, the correspondence principle says that whatever modifications of classical physics are made to describe matter at the submicroscopic level, when the results are extended to the macroscopic world, they must agree with those from the classical laws of physics that have been so abundantly verified in the everyday world. While Bohr's detailed model of the hydrogen atom has been supplanted by modern quantum theory, which we will discuss in later chapters, his frequency condition (Equation 4-15) and the correspondence principle remain as essential features of the new theory.

In his first paper,[11] in 1913, Bohr pointed out that his results implied that the angular momentum of the electron in the hydrogen atom can take on only values that are integral multiples of Planck's constant divided by 2π, in agreement with a discovery made a year earlier by J. W. Nicholson. That is, *angular momentum is quantized; it can assume only the values* $nh/2\pi$, *where n is an integer*. Rather than follow the intricacies of Bohr's derivation, we will use the fundamental conclusion of angular momentum quantization to find his expression for the observed spectra. The development that follows applies not only to hydrogen, but to any atom of nuclear charge $+Ze$ with a single orbital electron—e.g., singly ionized helium He^+ or doubly ionized lithium Li^{2+}.

If the nuclear charge is $+Ze$ and the electron charge $-e$, we have noted (Equation 4-12) that the centripetal force necessary to move the electron in a circular orbit is provided by the Coulomb force kZe^2/r^2. Solving Equation 4-12 for the speed of the orbiting electron yields

$$v = \left(\frac{kZe^2}{mr}\right)^{1/2} \qquad \textbf{4-16}$$

Bohr's quantization of the angular momentum L is

$$L = mvr = \frac{nh}{2\pi} = n\hbar \qquad n = 1, 2, 3, \ldots \qquad \textbf{4-17}$$

where the integer n is called a *quantum number* and $\hbar = h/2\pi$. (The constant $\hbar$, read "h-bar," is often more convenient to use than h itself, just as the angular frequency $\omega = 2\pi f$ is often more convenient than the frequency f.) Combining Equations 4-16 and 4-17 allows us to write for the circular orbits

$$r = \frac{n\hbar}{mv} = \frac{n\hbar}{m}\left(\frac{rm}{kZe^2}\right)^{1/2}$$

Squaring this relation gives

$$r^2 = \frac{n^2\hbar^2}{m^2}\left(\frac{rm}{kZe^2}\right)$$

and canceling common quantities yields

$$r_n = \frac{n^2\hbar^2}{mkZe^2} = \frac{n^2 a_0}{Z} \qquad \textbf{4-18}$$

where

$$a_0 = \frac{\hbar^2}{mke^2} = 0.529 \text{ Å} = 0.0529 \text{ nm} \qquad \textbf{4-19}$$

is called the *Bohr radius*. The Å, a unit commonly used in the early days of spectroscopy, equals 10^{-10} m or 10^{-1} nm. Thus, we find that the stationary orbits of Bohr's first postulate have quantized radii, denoted in Equation 4-18 by the subscript on r_n.

STUDENTS-HUB.com Uploaded By: Malak Obaid

Notice that the Bohr radius a_0 for hydrogen ($Z = 1$) corresponds to the orbit radius with $n = 1$, the smallest Bohr orbit possible for the electron in a hydrogen atom. Since $r_n \sim Z^{-1}$, the Bohr orbits for single-electron atoms with $Z > 1$ are closer to the nucleus than the corresponding ones for hydrogen.

The total energy of the electron (Equation 4-14) then becomes, upon substitution of r_n from Equation 4-18,

$$E_n = -\frac{kZe^2}{2r_n} = -\frac{kZe^2}{2}\left(\frac{mkZe^2}{n^2\hbar^2}\right)$$

$$E_n = -\frac{mk^2Z^2e^4}{2\hbar^2n^2} = -E_0\frac{Z^2}{n^2} \qquad n = 1, 2, 3, \ldots \qquad \textbf{4-20}$$

where $E_0 = mk^2e^4/2\hbar^2$. Thus, the energy of the electron is also quantized; i.e., the stationary states correspond to specific values of the total energy. This means that energies E_i and E_f that appear in the frequency condition of Bohr's second postulate must be from the allowed set E_n, and Equation 4-15 becomes

$$hf = E_{n_i} - E_{n_f} = -E_0\frac{Z^2}{n_i^2} - \left(-E_0\frac{Z^2}{n_f^2}\right)$$

or

$$f = \frac{E_0Z^2}{h}\left(\frac{1}{n_f^2} - \frac{1}{n_i^2}\right) \qquad \textbf{4-21}$$

which can be written in the form of the Rydberg-Ritz equation (Equation 4-2) by substituting $f = c/\lambda$ and dividing by c to obtain

$$\frac{1}{\lambda} = \frac{E_0Z^2}{hc}\left(\frac{1}{n_f^2} - \frac{1}{n_i^2}\right)$$

or

$$\frac{1}{\lambda} = Z^2R\left(\frac{1}{n_f^2} - \frac{1}{n_i^2}\right) \qquad \textbf{4-22}$$

where

$$R = \frac{E_0}{hc} = \frac{mk^2e^4}{4\pi c\hbar^3} \qquad \textbf{4-23}$$

is Bohr's prediction for the value of the Rydberg constant.

Using the values of m, e, c, and $\hbar$ known in 1913, Bohr calculated R and found his result to agree (within the limits of uncertainties of the constants) with the value obtained from spectroscopy, $1.097 \times 10^7\ \text{m}^{-1}$. Bohr noted in his original paper that this equation might be valuable in determining the best values for the constants e, m, and $\hbar$ because of the extreme precision possible in measuring R. This has indeed turned out to be the case.

The possible values of the energy of the hydrogen atom predicted by Bohr's model are given by Equation 4-20 with $Z = 1$:

$$E_n = -\frac{mk^2e^4}{2\hbar^2n^2} = -\frac{E_0}{n^2} \qquad \textbf{4-24}$$

where

$$E_0 = \frac{mk^2e^4}{2\hbar^2} = 2.18 \times 10^{-18}\ \text{J} = 13.6\ \text{eV}$$

STUDENTS-HUB.com Uploaded By: Malak Obaid

is the magnitude of E_n with $n = 1$. $E_1 (= -E_0)$ is called the *ground state*. It is convenient to plot these allowed energies of the stationary states as in Figure 4-16. Such a plot is called an *energy-level diagram*. Various series of transitions between the stationary states are indicated in this diagram by vertical arrows drawn between the levels. The frequency of light emitted in one of these transitions is the energy difference divided by h according to Bohr's frequency condition, Equation 4-15. The energy required to remove the electron from the atom, 13.6 eV, is called the *ionization energy*, or *binding energy*, of the electron.

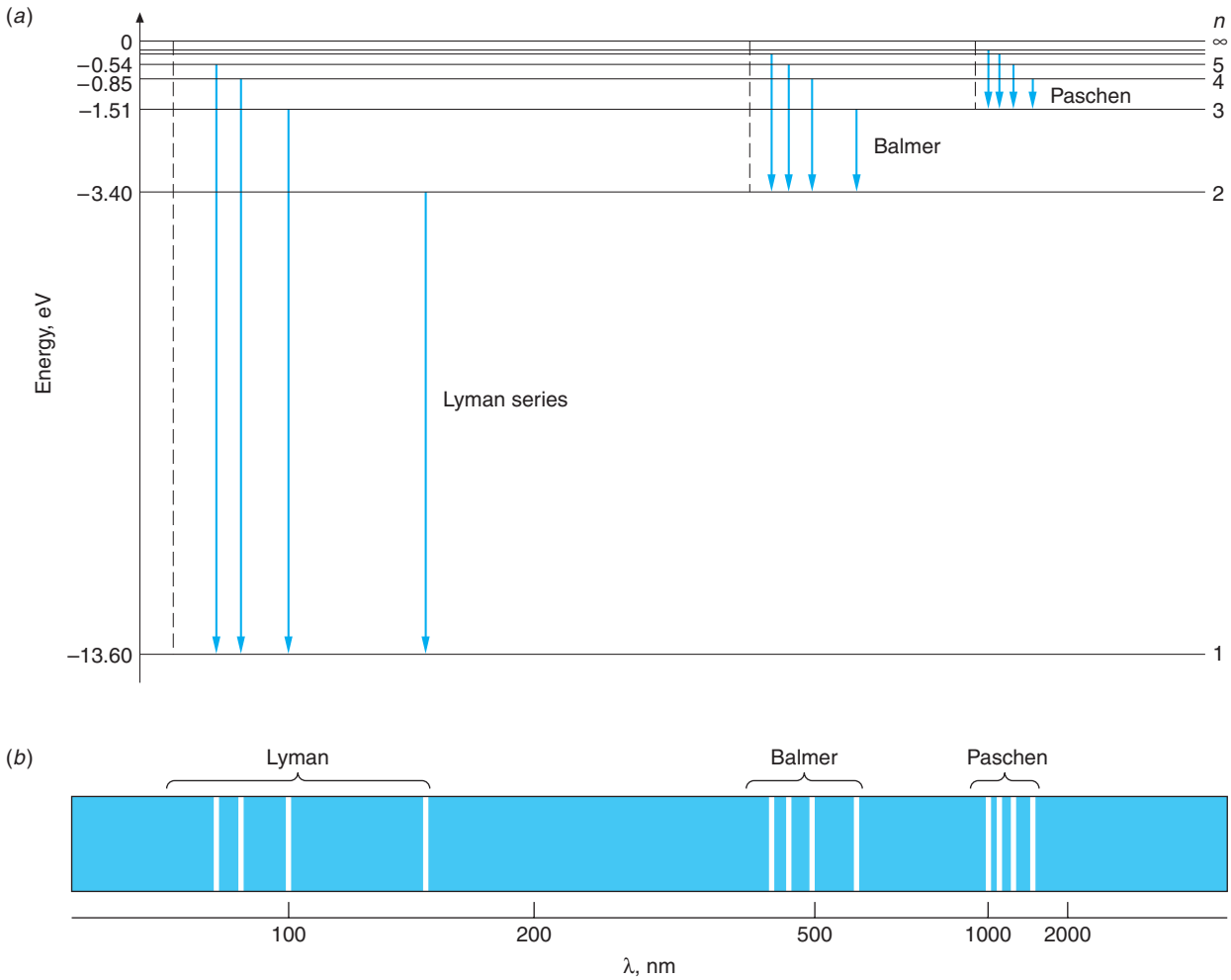

Figure 4-16 Energy-level diagram for hydrogen showing the seven lowest stationary states and the four lowest energy transitions each for the Lyman, Balmer, and Paschen series. There are an infinite number of levels. Their energies are given by $E_n = -13.6/n^2$ eV, where n is an integer. The dashed line shown for each series is the *series limit*, corresponding to the energy that would be radiated by an electron at rest far from the nucleus ($n \rightarrow \infty$) in a transition to the state with $n = n_f$ for that series. The horizontal spacing between the transitions shown for each series is proportional to the wavelength spacing between the lines of the spectrum. (*b*) The spectral lines corresponding to the transitions shown for the three series. Notice the regularities within each series, particularly the short-wavelength limit and the successively smaller separation between adjacent lines as the limit is approached. The wavelength scale in the diagram is not linear.

STUDENTS-HUB.com Uploaded By: Malak Obaid

A bit different sort of application, the Bohr/Rutherford model of the nuclear atom and electron orbits is the picture that, for millions of people, provides their link to the world of the atom and subatomic phenomena.

At the time Bohr's paper was published, there were two spectral series known for hydrogen: the Balmer series, corresponding to $n_f = 2$, $n_i = 3, 4, 5, \ldots$, and a series named after its discoverer, Paschen (1908), corresponding to $n_f = 3$, $n_i = 4, 5, 6, \ldots$. Equation 4-22 indicates that other series should exist for different values of n_f. In 1916 Lyman found the series corresponding to $n_f = 1$, and in 1922 and 1924 F. S. Brackett and A. H. Pfund, respectively, found series corresponding to $n_f = 4$ and $n_f = 5$. As can be easily determined by computing the wavelengths for these series, only the Balmer series lies primarily in the visible portion of the electromagnetic spectrum. The Lyman series is in the ultraviolet, the others in the infrared.

EXAMPLE 4-6 **Wavelength of the H_β Line** Compute the wavelength of the H_β spectral line, i.e., the second line of the Balmer series predicted by Bohr's model. The H_β line is emitted in the transition from $n_i = 4$ to $n_f = 2$.

SOLUTION

1. *Method 1:* The wavelength is given by Equation 4-22 with $Z = 1$:

$$\frac{1}{\lambda} = R\left(\frac{1}{n_f^2} - \frac{1}{n_i^2}\right)$$

2. Substituting $R = 1.097 \times 10^7\ \text{m}^{-1}$ and the values of n_i and n_f:

$$\frac{1}{\lambda} = (1.097 \times 10^7\ \text{m}^{-1})\left(\frac{1}{2^2} - \frac{1}{4^2}\right)$$

or

$$\lambda = 4.86 \times 10^{-7} = 486\ \text{nm}$$

3. *Method 2:* The wavelength may also be computed from Equation 4-15:

$$hf = hc/\lambda = E_i - E_f$$

or

$$\frac{1}{\lambda} = \frac{1}{hc}(E_i - E_f)$$

4. The values of E_i and E_f are given by Equation 4-24:

$$E_i = -\left(\frac{13.6\ \text{eV}}{n_i^2}\right) = -\left(\frac{13.6\ \text{eV}}{4^2}\right) = -0.85\ \text{eV}$$

$$E_f = -\left(\frac{13.6\ \text{eV}}{n_f^2}\right) = -\left(\frac{13.6\ \text{eV}}{2^2}\right) = -3.4\ \text{eV}$$

5. Substituting these into Equation 4-15 yields

$$\frac{1}{\lambda} = \frac{[-0.85\ \text{eV} - (-3.4\ \text{eV})](1.60 \times 10^{-19}\ \text{J/eV})}{(6.63 \times 10^{-34}\ \text{J}\cdot\text{s})(3.00 \times 10^8\ \text{m/s})}$$
$$= 2.051 \times 10^6\ \text{m}^{-1}$$

or

$$\lambda = 4.87 \times 10^{-7}\ \text{m} = 487\ \text{nm}$$

Remarks: *The difference in the two results is due to rounding of the Rydberg constant to three decimal places.*

STUDENTS-HUB.com Uploaded By: Malak Obaid

Reduced Mass Correction

The assumption by Bohr that the nucleus is fixed is equivalent to the assumption that it has infinite mass. In fact, the Rydberg constant in Equation 4-23 is normally written a R_∞, as we will do henceforth. If the nucleus has mass M, its kinetic energy will be $\frac{1}{2}Mv^2 = p^2/2M$, where $p = Mv$ is the momentum. If we assume that the total momentum of the atom is zero, conservation of momentum requires that the momenta of the nucleus and electron be equal in magnitude. The total kinetic energy is then

$$E_k = \frac{p^2}{2M} + \frac{p^2}{2m} = \frac{M + m}{2mM}p^2 = \frac{p^2}{2\mu}$$

where

$$\mu = \frac{mM}{m + M} = \frac{m}{1 + m/M} \qquad \textbf{4-25}$$

This is slightly different from the kinetic energy of the electron because μ, called the *reduced mass*, is slightly different from the electron mass. The results derived above for a nucleus of infinite mass can be applied directly for the case of a nucleus of mass M if we replace the electron mass in the equations by reduced mass μ, defined by Equation 4-25. (The validity of this procedure is proved in most intermediate and advanced mechanics books.) The Rydberg constant (Equation 4-23) is then written

$$R = \frac{\mu k^2 e^4}{4\pi c\hbar^3} = \frac{mk^2e^4}{4\pi c\hbar^3}\left(\frac{1}{1 + m/M}\right) = R_\infty\left(\frac{1}{1 + m/M}\right) \qquad \textbf{4-26}$$

This correction amounts to only 1 part in 2000 for the case of hydrogen and to even less for other nuclei; however, the predicted variation in the Rydberg constant from atom to atom is precisely that which is observed. For example, the spectrum of a singly ionized helium atom, which has one remaining electron, is just that predicted by Equation 4-22 and 4-26 with $Z = 2$ and the proper helium mass. The current value for the Rydberg constant R_∞ from precision spectroscopic measurements[12] is

$$R_\infty = 1.0973732 \times 10^7\ \text{m}^{-1} = 1.0973732 \times 10^{-2}\ \text{nm}^{-1} \qquad \textbf{4-27}$$

Urey[13] used the reduced mass correction to the spectral lines of the Balmer series to discover (in 1931) a second form of hydrogen whose atoms had twice the mass of ordinary hydrogen. The heavy form was called *deuterium*. The two forms, atoms with the same Z but different masses, are called *isotopes*.

EXAMPLE 4-7 Rydberg Constants for H and He^+ Compute the Rydberg constants for H and He^+ applying the reduced mass correction. ($m = 9.1094 \times 10^{-31}$ kg, $m_p = 1.6726 \times 10^{-27}$ kg, $m_\alpha = 5.0078 \times 10^{-27}$ kg)

SOLUTION

For hydrogen:

$$R_H = R_\infty\left(\frac{1}{1 + m/M_H}\right) = R_\infty\left(\frac{1}{1 + 9.1094 \times 10^{-31}/1.6726 \times 10^{-27}}\right)$$
$$= 1.09677 \times 10^7\ \text{m}^{-1}$$

STUDENTS-HUB.com Uploaded By: Malak Obaid

For helium: Since M in the reduced mass correction is the mass of the nucleus, for this calculation we use M equal to the α particle mass.

$$R_{\text{He}} = R_\infty\left(\frac{1}{1 + m/M_{\text{H}}}\right) = R_\infty\left(\frac{1}{1 + 9.1094 \times 10^{-31}/5.0078 \times 10^{-27}}\right)$$
$$= 1.09752 \times 10^7\ \text{m}^{-1}$$

Thus, the two Rydberg constants differ by about 0.04 percent.

Correspondence Principle

According to the correspondence principle, which applies also to modern quantum mechanics, when the energy levels are closely spaced, quantization should have little effect; classical and quantum calculations should give the same results. From the energy-level diagram of Figure 4-16, we see that the energy levels are close together when the quantum number n is large. This leads us to a slightly different statement of Bohr's correspondence principle: *In the region of very large quantum numbers (n in this case) quantum calculation and classical calculation must yield the same results*. To see that the Bohr model of the hydrogen atom does indeed obey the correspondence principle, let us compare the frequency of a transition between level $n_i = n$ and level $n_f = n - 1$ for large n with the classical frequency, which is the frequency of revolution of the electron. From Equation 4-22 we have

$$f = \frac{c}{\lambda} = \frac{Z^2mk^2e^4}{4\pi\hbar^3}\left[\frac{1}{(n-1)^2} - \frac{1}{n^2}\right] = \frac{Z^2mk^2e^4}{4\pi\hbar^3}\frac{2n-1}{n^2(n-1)^2}$$

For large n we can neglect the ones subtracted from n and $2n$ to obtain

$$f = \frac{Z^2mk^2e^4}{4\pi\hbar^3}\frac{2}{n^3} = \frac{Z^2mk^2e^4}{2\pi\hbar^3n^3} \qquad \textbf{4-28}$$

The classical frequency of revolution of the electron is (see Equation 4-13)

$$f_{\text{rev}} = \frac{v}{2\pi r}$$

Using $v = n\hbar/mr$ from Equation 4-17 and $r = n^2\hbar^2/mkZe^2$ from Equation 4-18, we obtain

$$f_{\text{rev}} = \frac{(n\hbar/mr)}{2\pi r} = \frac{n\hbar}{2\pi mr^2} = \frac{n\hbar}{2\pi m(n^2\hbar^2/mkZe^2)^2}$$
$$f_{\text{rev}} = \frac{m^2k^2Z^2e^4n\hbar}{2\pi mn^4\hbar^4} = \frac{mk^2Z^2e^4}{2\pi\hbar^3n^3} \qquad \textbf{4-29}$$

which is the same as Equation 4-28.

Fine Structure Constant

The demonstration of the correspondence principle for large n in the preceding paragraph was for $\Delta n = n_i - n_f = 1$; however, we have seen (see Figure 4-16) that transitions occur in the hydrogen atom for $\Delta n \geq 1$ when n is small, and such transitions should occur for large n too. If we allow $\Delta n = 2, 3, \ldots$ for large values of n, then the frequencies of the emitted radiation would be, according to Bohr's model, integer multiples of the frequency given in Equation 4-28. In that event, Equations 4-28 and 4-29 would not agree. This disagreement can be avoided by allowing elliptical orbits.[14] A result of Newtonian mechanics, familiar from planetary motion, is that in an inverse-square force

STUDENTS-HUB.com Uploaded By: Malak Obaid

field, the energy of an orbiting particle depends only on the major axis of the ellipse and not on its eccentricity. There is consequently no change in the energy at all unless the force differs from inverse square or unless Newtonian mechanics is modified. A. Sommerfeld considered the effect of special relativity on the mass of the electron in the Bohr model in an effort to explain the observed *fine structure* of the hydrogen spectral lines.[15] Since the relativistic corrections should be of the order of v^2/c^2 (see Chapter 2), it is likely that a highly eccentric orbit would have a larger correction because v becomes greater as the electron moves nearer the nucleus. The Sommerfeld calculations are quite complicated, but we can estimate the order of magnitude of the effect of special relativity by calculating v/c for the first Bohr orbit in hydrogen. For $n = 1$, we have from Equation 4-17 that $mvr_1 = \hbar$. Then, using $r_1 = a_0 = \hbar^2/mke^2$, we have

$$v = \frac{\hbar}{mr_1} = \frac{\hbar}{m(\hbar^2/mke^2)} = \frac{ke^2}{\hbar}$$

and

$$\frac{v}{c} = \frac{ke^2}{\hbar c} = \frac{1.44\ \text{eV}\cdot\text{nm}}{197.3\ \text{eV}\cdot\text{nm}} \approx \frac{1}{137} = \alpha \qquad \textbf{4-30}$$

where we have used another convenient combination

$$\hbar c = \frac{1.24 \times 10^3\ \text{eV}\cdot\text{nm}}{2\pi} = 197.3\ \text{eV}\cdot\text{nm} \qquad \textbf{4-31}$$

The dimensionless quantity $ke^2/\hbar c = \alpha$ is called the *fine-structure constant* because of its first appearance in Sommerfeld's theory, but as we will see, it has much more fundamental importance.

Though v^2/c^2 is very small, an effect of this magnitude is observable. In Sommerfeld's theory, the fine structure of the hydrogen spectrum is explained in the following way. For each allowed circular orbit of radius r_n and energy E_n, a set of n elliptical orbits is possible of equal major axes but different eccentricities. Since the velocity of a particle in an elliptical orbit depends on the eccentricity, so then will the mass and momentum, and therefore the different ellipses for a given n will have slightly different energies. Thus, the energy radiated when the electron changes orbit depends slightly on the eccentricities of the initial and final orbits as well as on their major axes. The splitting of the energy levels for a given n is called *fine-structure splitting*, and its value turns out to be of the order of $v^2/c^2 = \alpha^2$, just as Sommerfeld predicted. However, the agreement of Sommerfeld's prediction with the observed fine-structure splitting was quite accidental and led to considerable confusion in the early days of quantum theory. Although he had used the relativistic mass and momentum, he computed the energy using classical mechanics, leading to a correction much larger than that actually due only to relativistic effects. As we will see in Chapter 7, fine structure is associated with a completely nonclassical property of the electron called *spin*.

A lasting contribution of Sommerfeld's effort was the introduction of the fine-structure constant $\alpha = ke^2/\hbar c \approx 1/137$. With it we can write the Bohr radius a_0 and the quantized energies of the Bohr model in a particularly elegant form. Equations 4-24 and 4-19 for hydrogen become

$$E_n = -\frac{mk^2e^4}{2\hbar^2n^2}\frac{c^2}{c^2} = -\frac{mc^2}{2}\alpha^2\frac{1}{n^2} \qquad \textbf{4-32}$$

$$a_0 = \frac{\hbar^2}{mke^2}\frac{c}{c} = \frac{\hbar}{mc}\frac{1}{\alpha} \qquad \textbf{4-33}$$

STUDENTS-HUB.com Uploaded By: Malak Obaid

Since α is a dimensionless number formed of universal constants, *all* observers will measure the same value for it and find that energies and dimensions of atomic systems are proportional to α^2 and $1/\alpha$, respectively. We will return to the implications of this intriguing fact later in the book.

EXPLORING
Giant Atoms

Giant atoms called *Rydberg atoms*, long understood to be a theoretical possibility and first detected in interstellar space in 1965, are now being produced and studied in the laboratory. Rydberg atoms are huge! They are atoms that have one of the valence electrons in a state with a very large quantum number n. (See Figure 4-17.) Notice in Equation 4-18 that the radius of the electron orbit $r_n = n^2 a_0/Z \propto n^2$ and n can be any positive integer, so the diameter of a hydrogen atom (or any other atom, for that matter) could be very large, a millimeter or even a meter! What keeps such giant atoms from being common is that the energy difference between adjacent allowed energy states is extremely small when n is large and the allowed states are very near the $E_\infty = 0$ level where ionization occurs, because $E_n \propto 1/n^2$. For example, if $n = 1000$, the diameter of a hydrogen atom would be $r_{1000} = 0.1$ mm, but both E_{1000} and the difference in energy $\Delta E = E_{1001} - E_{1000}$ are about 10^{-5} eV! This energy is far below the average energy of thermal motion at ordinary temperatures (about 0.025 eV), so random collisions would quickly ionize an atom whose electron happened to get excited to a level with n equal to 20 or so with r still only about 10^{-8} m.

The advent of precisely tunable dye lasers in the 1970s made it possible to nudge electrons carefully into orbits with larger and larger n values. The largest Rydberg atoms made so far, typically using sodium or potassium, are 10,000 times the diameter of ordinary atoms, about 20 μm across or the size of a fine grain of sand, and exist for several milliseconds inside vacuum chambers. For hydrogen, this corresponds to quantum number $n \approx 600$. An electron moving so far from the nucleus is bound by a minuscule force. It also moves rather slowly since the classical period of $T = 1/f \propto n^3$ and follows an elliptical orbit. These characteristics of very large n orbits provide several intriguing possibilities. For example, very small electric fields might be studied, making possible the tracking of chemical reactions that proceed too quickly to be followed otherwise. More dramatic is the possibility of directly testing Bohr's correspondence principle by directly observing the slow (since $v \propto 1/n$) movement of the electron around the large n orbits—the transition from quantum mechanics to classical mechanics. Computer simulations of the classical motion of a Rydberg electron "wave" (see Chapter 5) in orbit around a nucleus are aiding the design of experiments to observe the correspondence principle.

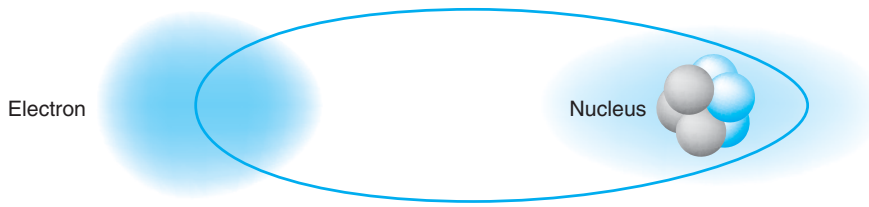

Figure 4-17 A lithium ($Z = 3$) Rydberg atom. The outer electron occupies a small volume and follows a nearly classical orbit with a large value of n. The two inner electrons are not shown.

STUDENTS-HUB.com Uploaded By: Malak Obaid

Questions

6. If the electron moves in an orbit of greater radius, does its total energy increase or decrease? Does its kinetic energy increase or decrease?
7. What is the energy of the shortest-wavelength photon that can be emitted by the hydrogen atom?
8. How would you characterize the motion and location of an electron with $E = 0$ and $n \rightarrow \infty$ in Figure 4-16?

4-4 X-Ray Spectra

The extension of the Bohr theory to atoms more complicated than hydrogen proved difficult. Quantitative calculations of the energy levels of atoms of more than one electron could not be made from the model, even for helium, the next element in the periodic table. However, experiments by H. Moseley in 1913 and J. Franck and G. Hertz in 1914 strongly supported the general Bohr-Rutherford picture of the atom as a positively charged core surrounded by electrons that moved in quantized energy states relatively far from the core. Moseley's analysis of x-ray spectra will be discussed in this section, and the Franck-Hertz measurement of the transmission of electrons through gases will be discussed in the chapter's concluding section.

Henry G.-J. Moseley. [*Courtesy of University of Manchester.*]

Using the methods of crystal spectrometry that had just been developed by W. H. Bragg and W. L. Bragg, Moseley[16] measured the wavelengths of the characteristic x-ray line spectra for about 40 different target elements. (Typical x-ray spectra are shown in Figure 3-15.) He noted that the x-ray line spectra varied in a regular way from element to element, unlike the irregular variations of optical spectra. He surmised that this regular variation occurred because characteristic x-ray spectra were due to transitions involving the innermost electrons of the atoms. (See Figure 4-18.) Because the inner electrons are

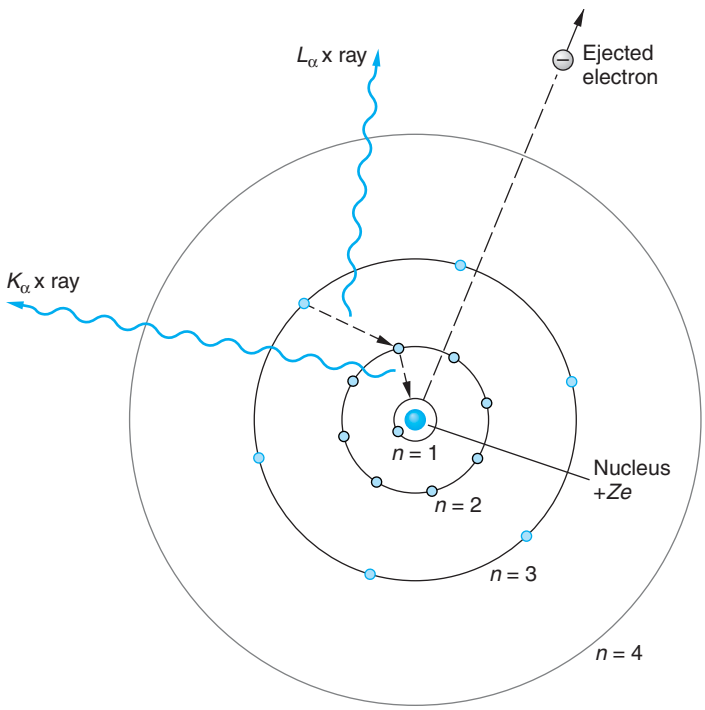

Figure 4-18 A stylized picture of the Bohr circular orbits for $n = 1$, 2, 3, and 4. The radii $r_n \sim n^2$. In a high-Z element (elements with $Z \geq 12$ emit x rays), electrons are distributed over all the orbits shown. If an electron in the $n = 1$ orbit is knocked from the atom, e.g., by being hit by a fast electron accelerated by the voltage across an x-ray tube, the vacancy thus produced is filled by an electron of higher energy (i.e., $n = 2$ or higher). The difference in energy between the two orbits is emitted as a photon, according to the Bohr frequency condition, whose wavelength will be in the x-ray region of the spectrum if Z is large enough.

STUDENTS-HUB.com Uploaded By: Malak Obaid

shielded from the outermost electrons by those in intermediate orbits, their energies do not depend on the complex interactions of the outer electrons, which are responsible for the complicated optical spectra. Furthermore, the inner electrons are well shielded from the interatomic forces that are responsible for the binding of atoms in solids.

According to the Bohr theory (published earlier the same year, 1913), the energy of an electron in the first Bohr orbit is proportional to the square of the nuclear charge (see Equation 4-20). Moseley reasoned that the energy, and therefore the frequency, of a characteristic x-ray photon should vary as the square of the atomic number of the target element. He therefore plotted the square root of the frequency of a particular characteristic line in the x-ray spectrum of various target elements versus the atomic number Z of the element. Such a plot, now called a *Moseley plot*, is shown in Figure 4-19.

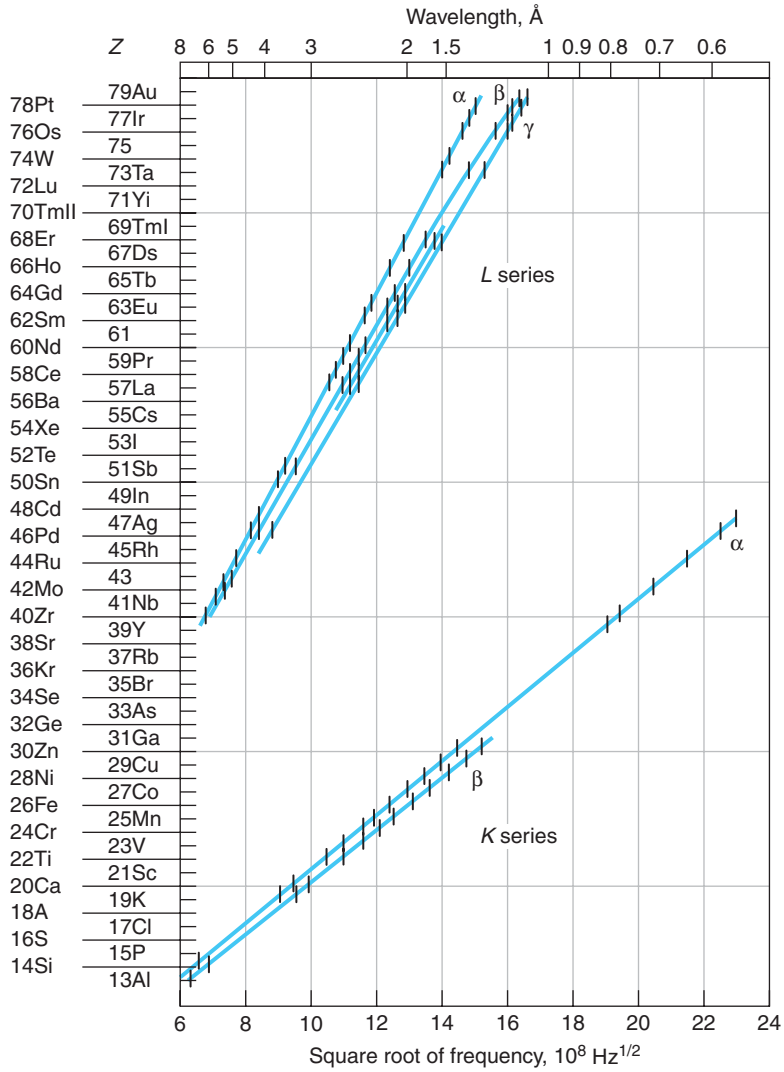

Figure 4-19 Moseley's plots of the square root of frequency versus Z for characteristic x rays. When an atom is bombarded by high-energy electrons, an inner atomic electron is sometimes knocked out, leaving a vacancy in the inner shell. The K-series x rays are produced by atomic transitions to vacancies in the $n = 1$ (K) shell, whereas the L series is produced by transitions to the vacancies in the $n = 2$ (L) shell. [*From H. Moseley, Philosophical Magazine (6), **27**, 713 (1914).*]

STUDENTS-HUB.com Uploaded By: Malak Obaid

These curves can be fitted by the empirical equation

$$f^{1/2} = A_n(Z - b) \qquad \textbf{4-34}$$

where A_n and b are constants for each characteristic x-ray line. One family of lines, called the *K series*, has $b = 1$ and slightly different values of A_n for each line in the graph. The other family shown in Figure 4-19, called the *L series*,[17] could be fitted by Equation 4-34 with $b = 7.4$.

If the bombarding electron in the x-ray tube causes ejection of an electron from the innermost orbit ($n = 1$) in a target atom completely out of the atom, photons will be emitted corresponding to transitions of electrons in other orbits ($n = 2, 3, \ldots$) to fill the vacancy in the $n = 1$ orbit. (See Figure 4-18.) (Since these lines are called the *K series*, the $n = 1$ orbit came to be called the *K shell*.) The lowest-frequency line corresponds to the lowest-energy transition ($n = 2 \rightarrow n = 1$). This line is called the K_α line. The transition $n = 3 \rightarrow n = 1$ is called the K_β line. It is of higher energy, and hence higher frequency, than the K_α line. A vacancy created in the $n = 2$ orbit by emission of a K_α x ray may then be filled by an electron of higher energy, e.g., one in the $n = 3$ orbit, resulting in the emission of a line in the *L* series, and so on. The multiple *L* lines in the Moseley plot (Figure 4-19) are due in part to the fact that there turn out to be small differences in the energies of electrons with a given n that are not predicted by the Bohr model. Moseley's work gave the first indication of these differences, but the explanation will have to await our discussion of more advanced quantum theory in Chapter 7.

Using the Bohr relation for a one-electron atom (Equation 4-21) with $n_f = 1$ and using $(Z - 1)$ in place of Z, we obtain for the frequencies of the *K* series

$$f = \frac{mk^2e^4}{4\pi\hbar^3}(Z - 1)^2\left(\frac{1}{1^2} - \frac{1}{n^2}\right) = cR_\infty(Z - 1)^2\left(1 - \frac{1}{n^2}\right) \qquad \textbf{4-35}$$

where R_∞ is the Rydberg constant. Comparing this with Equation 4-34, we see that A_n is given by

$$A_n^2 = cR_\infty\left(1 - \frac{1}{n^2}\right) \qquad \textbf{4-36}$$

The wavelengths of the lines in the *K* series are then given by

$$\lambda = \frac{c}{f} = \frac{c}{A_n^2(Z - 1)^2} = \frac{1}{R_\infty(Z - 1)^2\left(1 - \frac{1}{n^2}\right)} \qquad \textbf{4-37}$$

EXAMPLE 4-8 K_α **for Molybdenum** Calculate the wavelength of the K_α line of molybdenum ($Z = 42$), and compare the result with the value $\lambda = 0.0721$ nm measured by Moseley and with the spectrum in Figure 3-15*b*.

SOLUTION

Using $n = 2$, $R_\infty = 1.097 \times 10^7\ \text{m}^{-1}$, and $Z = 42$, we obtain

$$\lambda = \left[(1.097 \times 10^7\ \text{m}^{-1})(41)^2\left(1 - \frac{1}{4}\right)\right]^{-1} = 7.23 \times 10^{-11}\ \text{m} = 0.0723\ \text{nm}$$

This value is within 0.3 percent of Moseley's measurement and agrees well with that in Figure 3-15*b*.

STUDENTS-HUB.com Uploaded By: Malak Obaid

The fact that f is proportional to $(Z - 1)^2$ rather than to Z is explained by the partial shielding of the nuclear charge by the other electron remaining in the K shell as "seen" by electrons in the $n = 2$ (L) shell.[18] Using this reasoning, Moseley concluded that, since $b = 7.4$ for the L series, these lines involved electrons farther from the nucleus, which "saw" the nuclear charge shielded by more inner electrons. Assuming that the L series was due to transitions to the $n = 2$ shell, we see that the frequencies for this series are given by

$$f = cR_\infty\left(\frac{1}{2^2} - \frac{1}{n^2}\right)(Z - 7.4)^2 \qquad \textbf{4-38}$$

where $n = 3, 4, 5, \ldots$.

Before Moseley's work, the atomic number was merely the place number of the element in Mendeleev's periodic table of the elements arranged by weight. The experiments of Geiger and Marsden showed that the nuclear charge was approximately $A/2$, while x-ray scattering experiments by C. G. Barkla showed that the number of electrons in an atom was also approximately $A/2$. These two experiments are consistent since the atom as a whole must be electrically neutral. However, several discrepancies were found in the periodic table as arranged by weight. For example, the 18th element in order of weight is potassium (39.102), and the 19th is argon (39.948). Arrangement by weight, however, puts potassium in the column with the inert gases and argon with the active metals, the reverse of their known chemical properties. Moseley showed that for these elements to fall on the line $f^{1/2}$ versus Z, argon had to have $Z = 18$ and potassium $Z = 19$. Arranging the elements by the Z number obtained from the Moseley plot rather than by weight, gave a periodic chart in complete agreement with the chemical properties. Moseley also pointed out that there were gaps in the periodic table at $Z = 43$, 61, and 75, indicating the presence of undiscovered elements. All have subsequently been found. Figure 4-20 illustrates the discovery of promethium ($Z = 61$).

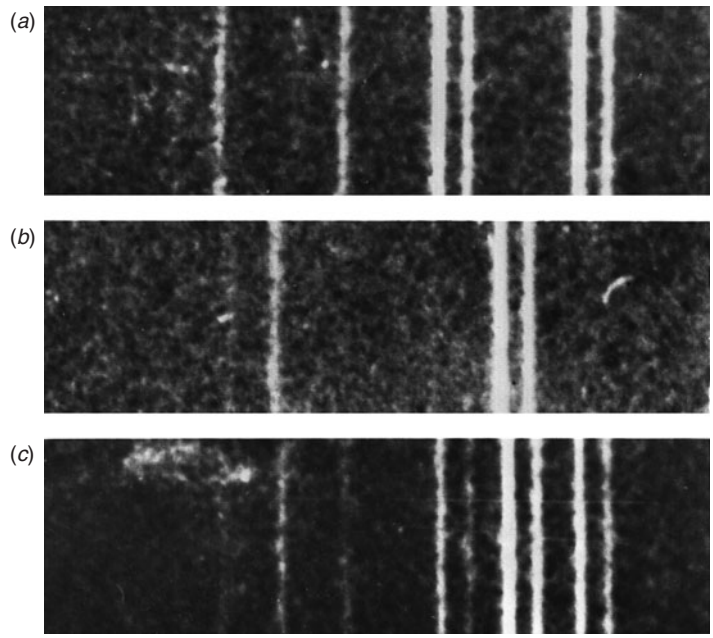

Figure 4-20 Characteristic x-ray spectra. (*a*) Part of the spectra of neodymium ($Z = 60$) and samarium ($Z = 62$). The two pairs of bright lines are the K_α and K_β lines. (*b*) Part of the spectrum of the artificially element promethium ($Z = 61$). This element was first positively identified in 1945 at the Clinton Laboratory (now Oak Ridge). Its K_α and K_β lines fall between those of neodymium and samarium, just as Moseley predicted. (*c*) Part of the spectra of all three of the elements neodymium, promethium, and samarium. [*Courtesy of J. A. Swartout, Oak Ridge National Laboratory.*]

STUDENTS-HUB.com Uploaded By: Malak Obaid

Auger Electrons

The process of producing x rays necessarily results in the ionization of the atom since an inner electron is ejected. The vacancy created is filled by an outer electron, producing the x rays studied by Moseley. In 1923 Pierre Auger discovered that, as an alternative to x-ray emission, the atom may eject a third electron from a higher-energy outer shell via a radiationless process called the *Auger effect*. In the Auger (pronounced oh-zhay) process, the energy difference $\Delta E = E_2 - E_1$ that could have resulted in the emission of a K_α x ray is removed from the atom by the third electron, e.g., one in the $n = 3$ shell. Since the magnitude of $E_3 < \Delta E$, the $n = 3$ electron would leave the atom with a characteristic kinetic energy $\Delta E - |E_3|$, which is determined by the stationary-state energies of the particular atom.[19] Thus, each element has a characteristic Auger electron spectrum. (See Figure 4-21*a*.) Measurement of the Auger electrons provides a simple and highly sensitive tool for identifying impurities on clean surfaces in electron microscope systems and investigating electron energy shifts associated with molecular bonding. (See Figure 4-21*b*.)

Question

9. Why did Moseley plot $f^{1/2}$ versus Z rather than f versus Z?

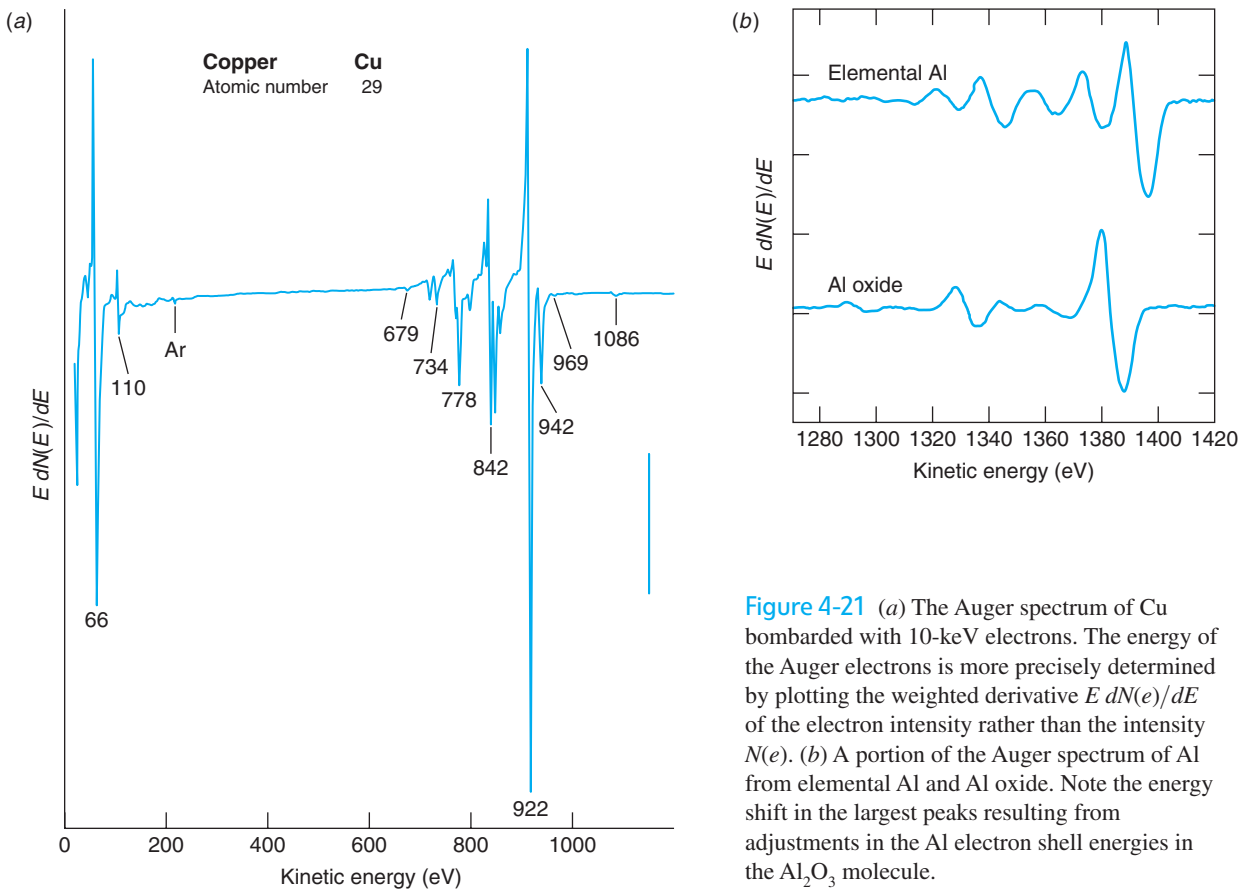

Figure 4-21 (*a*) The Auger spectrum of Cu bombarded with 10-keV electrons. The energy of the Auger electrons is more precisely determined by plotting the weighted derivative $E\,dN(e)/dE$ of the electron intensity rather than the intensity $N(e)$. (*b*) A portion of the Auger spectrum of Al from elemental Al and Al oxide. Note the energy shift in the largest peaks resulting from adjustments in the Al electron shell energies in the Al_2O_3 molecule.

STUDENTS-HUB.com Uploaded By: Malak Obaid

4-5 The Franck-Hertz Experiment

We conclude this chapter with discussion of an important experiment that provided strong support for the quantization of atomic energies, thus helping to pave the way for modern quantum mechanics. While investigating the inelastic scattering of electrons, J. Franck and G. Hertz[20] made a discovery that confirmed *by direct measurement* Bohr's hypothesis of energy quantization in atoms. First done in 1914, it is now a standard undergraduate laboratory experiment. Figure 4-22*a* is a schematic diagram of the apparatus. A small heater heats the cathode. Electrons are ejected from the heated cathode and accelerated toward a grid, which is at a positive potential V_0 relative to the cathode. Some electrons pass through the grid and reach the plate P, which is at a slightly lower potential $V_p = V_0 - \Delta V$. The tube is filled with a low-pressure gas of the element being investigated (mercury vapor, in Franck and Hertz's experiment). The experiment involves measuring the plate current as a function of V_0. As V_0 is increased from 0, the current increases until a critical value (about 4.9 V for Hg) is reached, at which point the current suddenly decreases. As V_0 is increased further, the current rises again.

The explanation of this result is a bit easier to visualize if we think for the moment of a tube filled with hydrogen atoms instead of mercury. (See Figure 4-22*b*.) Electrons accelerated by V_0 that collide with hydrogen electrons cannot transfer energy to the latter unless they have acquired kinetic energy $eV_0 = E_2 - E_1 = 10.2$ eV since the hydrogen electron according to Bohr's model cannot occupy states with energies intermediate between E_1 and E_2. Such a collision will thus be elastic; i.e., the incident electron's kinetic energy will be unchanged by the collision, and thus it can overcome the potential ΔV and contribute to the current I. However, if $eV_0 \geq 10.2$ eV,

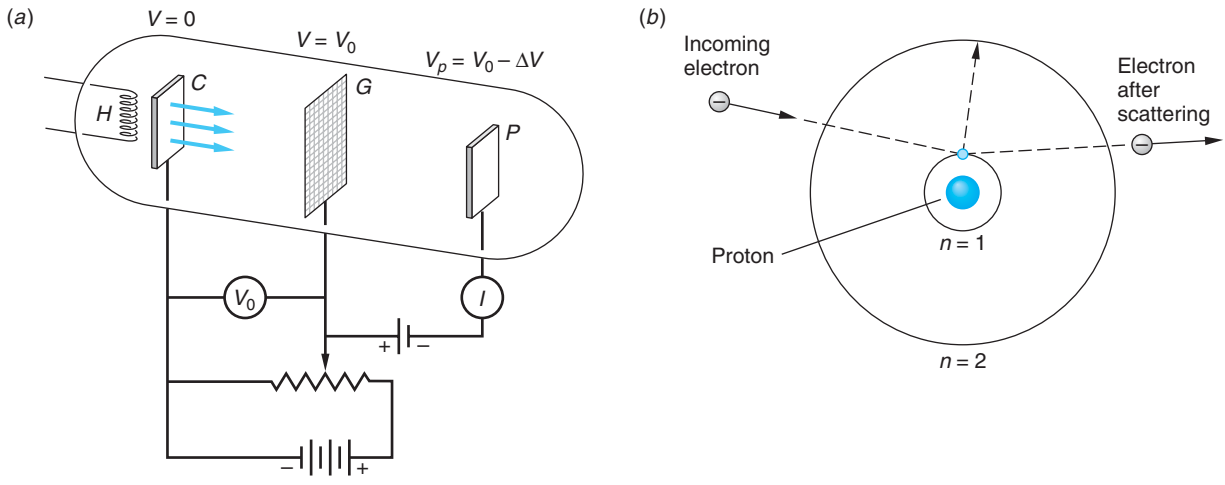

Figure 4-22 (*a*) Schematic diagram of the Franck-Hertz experiment. Electrons ejected from the heated cathode C at zero potential are drawn to the positive grid G. Those passing through the holes in the grid can reach the plate P and thereby contribute to the current I if they have sufficient kinetic energy to overcome the small back potential ΔV. The tube contains a low-pressure gas of the element being studied. (*b*) Results for hydrogen. If the incoming electron does not have sufficient energy to transfer $\Delta E = E_2 - E_1$ to the hydrogen electron in the $n = 1$ orbit (ground state), then the scattering will be elastic. If the incoming electron does have at least ΔE kinetic energy, then an inelastic collision can occur in which ΔE is transferred to the $n = 1$ electron, moving it to the $n = 2$ orbit. The excited electron will typically return to the ground state very quickly, emitting a photon of energy ΔE.

STUDENTS-HUB.com Uploaded By: Malak Obaid

then the incoming electron can transfer 10.2 eV to the hydrogen electron in the *ground state* ($n = 1$ orbit), putting it into the $n = 2$ orbit (called the *first excited state*). The incoming electron's energy is thus reduced by 10.2 eV; it has been inelastically scattered. With insufficient energy to overcome the small retarding potential ΔV, the incoming electrons can no longer contribute to the plate current I, and I drops sharply.

The situation with Hg in the tube is more complicated since Hg has 80 electrons. Although Bohr's theory cannot predict their individual energies, we still expect the energy to be quantized with a ground state, first excited state, and so on, for the atom. Thus, the explanation of the observed 4.9-V critical potential for Hg is that the first excited state is about 4.9 eV above the lowest level (ground state). Electrons with energy less than this cannot lose energy to the Hg atoms, but electrons with energy greater than 4.9 eV can have inelastic collisions and lose 4.9 eV. If this happens near the grid, these electrons cannot gain enough energy to overcome the small back voltage ΔV and reach the plate; the current therefore decreases. If this explanation is correct, the Hg atoms that are excited to an energy level of 4.9 eV above the ground state should return to the ground state by emitting light of wavelength

$$\lambda = \frac{c}{f} = \frac{hc}{hf} = \frac{hc}{eV_0} = 253 \text{ nm}$$

There is indeed a line of this wavelength in the mercury spectrum. When the tube is viewed with a spectroscope, this line is seen when V_0 is greater than 4.9 eV, while no lines are seen when V_0 is less than this amount. For further increases in V_0, additional sharp decreases in the current are observed, corresponding either to excitation of other levels in Hg (e.g., the second excited state of Hg is at 6.7 eV above the ground state) or to multiple excitations of the first excited state, i.e., due to an electron losing 4.9 eV more than once. In the usual setup, multiple excitations of the first level are observed and dips are seen every 4.9 V.[21] The probability of observing such multiple first-level excitations, or excitations of other levels, depends on the detailed variation of the potential of the tube. For example, a second decrease in the current at $V_0 = 2 \times 4.9 = 9.8$ V results when electrons have inelastic collisions with Hg atoms about halfway between the cathode and grid (see Figure 4-22*a*). They are reaccelerated, reaching 4.9 eV again in the vicinity of the grid. A plot of the data of Franck and Hertz is shown in Figure 4-23.

The Franck-Hertz experiment was an important confirmation of the idea that discrete optical spectra were due to the existence in atoms of discrete energy levels that could be excited by nonoptical methods. It is particularly gratifying to be able to detect the existence of discrete energy levels directly by measurements using only voltmeters and ammeters.

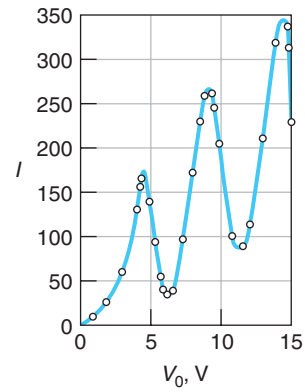

Figure 4-23 Current versus accelerating voltage in the Franck-Hertz experiment. The current decreases because many electrons lose energy due to inelastic collisions with mercury atoms in the tube and therefore cannot overcome the small back potential indicated in Figure 4-21*a*. The regular spacing of the peaks in this curve indicates that only a certain quantity of energy, 4.9 eV, can be lost to the mercury atoms. This interpretation is confirmed by the observation of radiation of photon energy 4.9 eV emitted by the mercury atoms, when V_0 is greater than this energy. [*From J. Franck and G. Hertz, Verband Deutscher Physiklischer Gesellschaften,* ***16****, 457 (1914).*]

Electron Energy Loss Spectroscopy

The Franck-Hertz experiment was the precursor of a highly sensitive technique for measuring the quantized energy states of atoms in both gases and solids. The technique, called *electron energy loss spectroscopy* (*EELS*), is particularly useful in solids, where it makes possible measurement of the energy of certain types of lattice vibrations and other processes. It works like this. Suppose that the electrons in an incident beam all have energy E_{inc}. They collide with the atoms of a material, causing them to undergo some process (e.g., vibration, lattice rearrangement, electron excitation) that requires energy E_1. Then, if a beam electron initiates a single such process, it will exit the material with energy $E_{inc} - E_1$ —i.e., it has been inelastically scattered.

STUDENTS-HUB.com Uploaded By: Malak Obaid

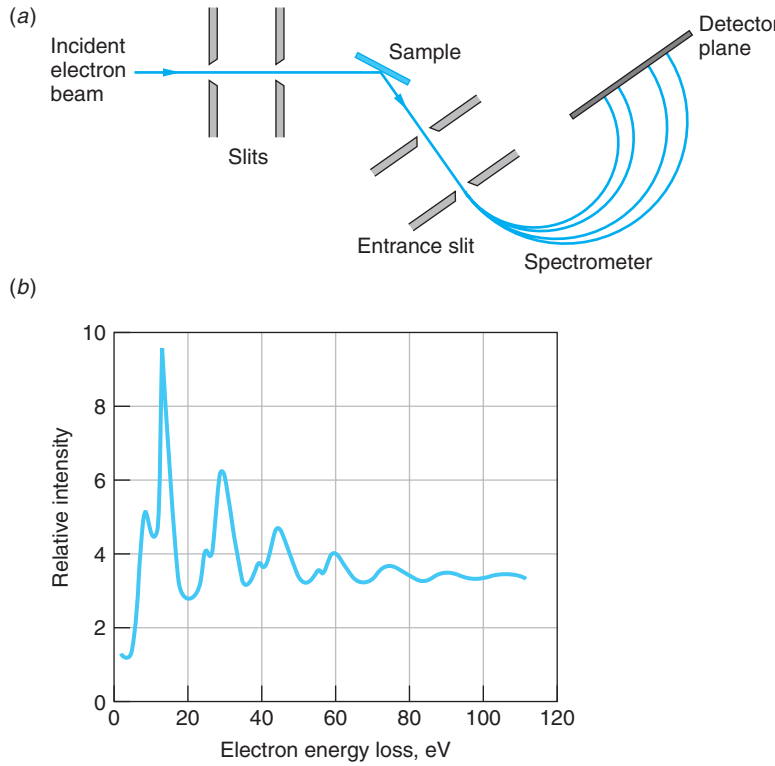

Figure 4-24 Energy-loss spectrum measurement. (*a*) A well-defined electron beam impinges upon the sample. Electrons inelastically scattered at a convenient angle enter the slit of the magnetic spectrometer, whose B field is directed out of the paper, and turn through radii R determined by their energy $E_{inc} - E_1$ via Equation 3-2 written in the form $R = [2m(E_{inc} - E_1)]^{1/2}/eB$. (*b*) An energy-loss spectrum for a thin Al film. [*From C. J. Powell and J. B. Swan, Physical Review,* ***115****, 869 (1954).*]

The exit energy can be measured very accurately with, e.g., a magnetic spectrometer designed for electrons.[22] Figure 4-24*a* illustrates a typical experimental arrangement for measuring an energy-loss spectrum.

As an example of its application, if an incident beam of electrons with $E_{inc} = 2$ keV is reflected from a thin Al film, the scattered electron energies measured in the magnetic spectrometer result in the energy-loss spectrum shown in Figure 4-24*b*, which directly represents the quantized energy levels of the target material. The loss peaks in this particular spectrum are due to the excitation of harmonic vibrations in the thin film sample, as well as some surface vibrations. The technique is also used to measure the vibrational energies of impurity atoms that may be absorbed on the surface and, with higher incident electron energies, to measure energy losses at the atomic inner levels, thus yielding information about bonding and other characteristics of absorbed atoms. Inelastic scattering techniques, including those using particles in addition to electrons, provide very powerful means for probing the energy structure of atomic, molecular, and nuclear systems. We will have occasion to refer to them many times throughout the rest of the book.

More

Here and in Chapter 3 we have discussed many phenomena that were "explained" by various ad hoc quantum assumptions. A *Critique of Bohr Theory and the "Old Quantum Mechanics"* contrasts some of its successes with some of its failures on the Web page: whfreeman.com/modphysics5e.

STUDENTS-HUB.com Uploaded By: Malak Obaid

Summary

TOPIC	RELEVANT EQUATIONS AND REMARKS	
1. Atomic spectra	$\frac{1}{\lambda_{mn}} = R\left(\frac{1}{m^2} - \frac{1}{n^2}\right) \qquad n > m$	**4-2**
	This empirical equation computes the correct wavelengths of observed spectral lines. The Rydberg constant R varies in a regular way from element to element.	
2. Rutherford scattering		
Impact parameter	$b = \frac{kq_\alpha Q}{m_\alpha v^2}\cot\frac{\theta}{2}$	**4-3**
Scattered fraction f	$f = \pi b^2 nt$	**4-5**
	for a scattering foil with n nuclei/unit volume and thickness t	
Number of scattered alphas observed	$\Delta N = \left(\frac{I_0 A_{sc} nt}{r^2}\right)\left(\frac{kZe^2}{2E_k}\right)^2 \frac{1}{\sin^4\frac{\theta}{2}}$	**4-6**
Size of nucleus	$r_d = \frac{kq_\alpha Q}{\frac{1}{2}m_\alpha v^2}$	**4-11**
3. Bohr model		
Bohr's postulates	1. Electrons occupy only certain nonradiating, stable, circular orbits selected by quantization of the angular momentum L.	
	$L = mvr = \frac{nh}{2\pi} = n\hbar \qquad$ for integer $\qquad n$	**4-17**
	2. Radiation of frequency f occurs when the electron jumps from an allowed orbit of energy E_i to one of lower energy E_f. f is given by the frequency condition	
	$hf = E_i - E_f$	**4-15**
Correspondence principle	In the region of very large quantum numbers classical and quantum calculations must yield the same results.	
Bohr radius	$a_0 = \frac{\hbar^2}{mke^2} = \frac{\hbar}{mc\alpha} = 0.0529 \text{ nm}$	**4-19**
Allowed energies	$E_n = -\frac{Z^2 E_0}{n^2} \qquad$ for $\qquad n = 1, 2, 3, \ldots$	**4-20**
	where $E_0 = mk^2e^2/2\hbar^2 = 13.6 \text{ eV}$	
Reduced mass	$\mu = \frac{mM}{m + M}$	**4-25**
Fine-structure constant	$\alpha = \frac{ke^2}{\hbar c} \approx 1/137$	**4-30**

STUDENTS-HUB.com Uploaded By: Malak Obaid

TOPIC	RELEVANT EQUATIONS AND REMARKS	
4. X-ray spectra Moseley equation	$f^{1/2} = A_n(Z - b)$	**4-34**
5. Franck-Hertz experiment	Supported Bohr's theory by verifying the quantization of atomic energies in absorption.	

General References

The following general references are written at a level appropriate for the readers of this book.

Boorse, H., and L. Motz (eds.), *The World of the Atom*, Basic Books, New York, 1966. This two-volume, 1873-page work is a collection of original papers, translated and edited. Much of the work referred to in this chapter and throughout this book can be found in these volumes.

Cline, B., *The Questioners: Physicists and the Quantum Theory*, Thomas Y. Crowell, New York, 1965.

Gamow, G., *Thirty Years That Shook Physics: The Story of the Quantum Theory*, Doubleday, Garden City, NY, 1965.

Herzberg, G., *Atomic Spectra and Atomic Structure*, Dover Publications, New York, 1944. This is without doubt one of the all-time classics of atomic physics.

Melissinos, A., and J. Napolitano, *Experiments in Modern Physics*, 2d ed., Academic Press, New York, 2003. Many of the classic experiments that are now undergraduate laboratory experiments are described in detail in this text.

Mohr, P. J., and B. N. Taylor, "The Fundamental Physical Constants," *Physics Today* (August 2004). Also available at http://physicstoday.org/guide/fundcont.html.

Shamos, M. H. (ed.), *Great Experiments in Physics*, Holt, Rinehart & Winston, New York, 1962.

Virtual Laboratory (PEARL), Physics Academic Software, North Carolina State University, Raleigh, 1996. Includes an interactive model of the Bohr atom.

Virtual Spectroscope, Physics Academic Software, North Carolina State University, Raleigh, 2003. Several sources can be viewed with a spectroscope to display the corresponding spectral lines.

Visual Quantum Mechanics, Kansas State University, Manhattan, 1996. The atomic spectra component of this software provides an interactive construction of the energy levels for several elements, including hydrogen and helium.

Notes

1. Joseph von Fraunhofer (1787–1826), German physicist. Although he was not the first to see the dark lines in the solar spectrum that bear his name (Wollaston had seen seven, 12 years earlier), he systematically measured their wavelengths, named the prominent ones, and showed that they always occurred at the same wavelength even if the sunlight were reflected from the moon or a planet.

2. To date, more than 10,000 Fraunhofer lines have been found in the solar spectrum.

3. Although experimentalists preferred to express their measurements in terms of wavelengths, it had been shown that the many empirical formulas being constructed to explain the observed regularities in the line spectra could be expressed in simpler form if the reciprocal wavelength, called the *wave number* and equal to the number of waves per unit length, was used instead. Since $c = f\lambda$, this was equivalent to expressing the formulas in terms of the frequency.

4. Ernest Rutherford (1871–1937), English physicist, an exceptional experimentalist and a student of J. J. Thomson. He was an early researcher in the field of radioactivity and received the Nobel Prize in 1908 for his work in the transmutation of elements. He bemoaned the fact that his prize was awarded in chemistry, not in physics, as work with the elements was considered chemistry in those days. He was Thomson's successor as director of the Cavendish Laboratory.

5. Alpha particles, like all charged particles, lose energy by exciting and ionizing the molecules of the materials through which they are moving. The energy lost per unit path length $(-dE/dx)$ is a function of the ionization potential of the molecules, the atomic number of the atoms, and the energy of the α particles. It can be computed (with some effort) and is relatively simple to measure experimentally.

6. Notice that $2\pi \sin\theta\, d\theta = d\Omega$, the differential solid angle subtended at the scattering nucleus by the surface in Figure 4-11. Since the cross section $\sigma = \pi b^2$, then $d\sigma = 2\pi b\, db$ and Equation 4-9 can be rewritten as

$$\frac{d\sigma}{d\Omega} = \left(\frac{kZe^2}{m_\alpha v^2}\right)^2 \frac{1}{\sin^4(\theta/2)}$$

$d\sigma/d\Omega$ is called the *differential cross section*.

7. H. Geiger and E. Marsden, *Philosophical Magazine* (6), **25**, 605 (1913).

STUDENTS-HUB.com Uploaded By: Malak Obaid

8. The value of Z could not be measured directly in this experiment; however, relative values for different foil materials could be found and all materials heavier than aluminum had Z approximately equal to half the atomic weight.

9. This also introduces a deviation from the predicted ΔN associated with Rutherford's assumption that the nuclear mass was much larger than the α particle mass. For lighter-atomic-weight elements that assumption is not valid. Correction for the nuclear mass effect can be made, however, and the data in Figure 4-9*b* reflect the correction.

10. Niels H. D. Bohr (1885–1962), Danish physicist and first-rate soccer player. He went to the Cavendish Laboratory to work with J. J. Thomson after receiving his Ph.D.; however, Thomson is reported to have been impatient with Bohr's soft, accented English. Happily, the occasion of Thomson's annual birthday banquet brought Bohr in contact with Rutherford, whom he promptly followed to the latter's laboratory at Manchester, where he learned of the nuclear atom. A giant of twentieth-century physics, Bohr was awarded the Nobel Prize in 1922 for his explanation of the hydrogen spectrum. On a visit to the United States in 1939, he brought the news that the fission of uranium atoms had been observed. The story of his life makes absolutely fascinating reading.

11. N. Bohr, *Philosophical Magazine* (6), **26**, 1 (1913).

12. P. J. Mohr and B. N. Taylor, "The Fundamental Physical Constants," *Physics Today* (August 2004). Only 8 of the 14 current significant figures are given in Equation 4-27. The relative uncertainty in the value is about 1 part in 10^{12}!

13. Harold C. Urey (1893–1981), American chemist. His work opened the way for the use of isotopic tracers in biological systems. He was recognized with the Nobel Prize in 1934.

14. The basic reason that elliptical orbits solve this problem is that the frequency of the radiation emitted classically depends on the acceleration of the charge. The acceleration is constant for a circular orbit but varies for elliptical orbits, being dependent on the instantaneous distance from the focus. The energy of a particle in a circular orbit of radius r is the same as that of a particle in an elliptical orbit with a semimajor axis of r, so one would expect the only allowed elliptical orbits to be those whose semimajor axis was equal to an allowed Bohr circular orbit radius.

15. Viewed with spectrographs of high resolution, the spectral lines of hydrogen in Figure 4-2*a*—and, indeed, most spectral lines of all elements—are found to consist of very closely spaced sets of lines, i.e., fine structure. We will discuss this topic in detail in Chapter 7.

16. Henry G.-J. Moseley (1887–1915), English physicist, considered by some the most brilliant of Rutherford's students. He would surely have been awarded the Nobel Prize had he not been killed in action in World War I. His father was a naturalist on the expedition of the HMS *Challenger*, the first vessel ever devoted to the exploration of the oceans.

17. The identifiers L and K were assigned by the English physicist C. G. Barkla, the discoverer of the characteristic x-ray lines, for which he received the Nobel Prize in 1917. He discovered two sets of x-ray lines for each of several elements, the *longer* wavelength of which he called the L series, the other the K series. The identifiers stuck and were subsequently used to label the atomic electron shells.

18. That the remaining K electron should result in $b = 1$, i.e., shielding of exactly $1e$, is perhaps a surprise. Actually it was a happy accident. It is the combined effect of the remaining K electron and the penetration of the electron waves of the outer L electrons that resulted in making $b = 1$, as we will see in Chapter 7.

19. Since in multielectron atoms the energies of the stationary states depend in part on the number of electrons in the atom (see Chapter 7), the energies E_n for a given atom change slightly when it is singly ionized, as in the production of characteristic x-ray lines, or doubly ionized, as in the Auger effect.

20. James Franck (1882–1964), German-American physicist; Gustav L. Hertz (1887–1975), German physicist. Franck won an Iron Cross as a soldier in World War I and later worked on the Manhattan Project. Hertz was a nephew of Heinrich Hertz, discoverer of the photoelectric effect. For their work on the inelastic scattering of electrons, Franck and Hertz shared the 1925 Nobel Prize in Physics.

21. We should note at this point that there is an energy state in the Hg atom at about 4.6 eV, slightly lower than the one found by Franck and Hertz. However, transitions from the ground state to the 4.6-eV level are not observed, and their absence is in accord with the prediction of more advanced quantum mechanics, as we will see in Chapter 7.

22. Since q/m for electrons is much larger than for ionized atoms, the radius for an electron magnetic spectrometer need not be as large as for a mass spectrometer, even for electron energies of several keV. (See Equation 3-2.)

Problems

Level I

Section 4-1 Atomic Spectra

4-1. Compute the wavelength and frequency of the series limit for the Lyman, Balmer, and Paschen spectral series of hydrogen.

4-2. The wavelength of a particular line in the Balmer series is measured to be 379.1 nm. What transition does it correspond to?

4-3. An astronomer finds a new absorption line with $\lambda = 164.1$ nm in the ultraviolet region of the Sun's continuous spectrum. He attributes the line to hydrogen's Lyman series. Is he right? Justify your answer.

STUDENTS-HUB.com Uploaded By: Malak Obaid

4-4. The series of hydrogen spectral lines with $m = 4$ is called Brackett's series. Compute the wavelengths of the first four lines of Brackett's series.
4-5. In a sample that contains hydrogen, among other things, four spectral lines are found in the infrared with wavelengths 7460 nm, 4654 nm, 4103 nm, and 3741 nm. Which one does not belong to a hydrogen spectral series?

Section 4-2 Rutherford's Nuclear Model

4-6. A gold foil of thickness 2.0 μm is used in a Rutherford experiment to scatter α particles with energy 7.0 MeV. (*a*) What fraction of the particles will be scattered at angles greater than 90°? (*b*) What fraction will be scattered at angles between 45° and 75°? (*c*) Use N_A, ρ, and M for gold to compute the approximate radius of a gold atom. (For gold, $\rho = 19.3\ \text{g/cm}^3$ and $M = 197\ \text{g/mol}$.)
4-7. (*a*) What is the ratio of the number of particles per unit area on the screen scattered at 10° to those at 1°? (*b*) What is the ratio of those scattered at 30° to those at 1°?
4-8. For α particles of 7.7 MeV (those used by Geiger and Marsden), what impact parameter will result in a deflection of 2° for a thin gold foil?
4-9. What will be the distance of closest approach r_d to a gold nucleus for an α particle of 5.0 MeV? 7.7 MeV? 12 MeV?
4-10. What energy α particle would be needed to just reach the surface of an Al nucleus if its radius is 4 fm?
4-11. If a particle is deflected by 0.01° in each collision, about how many collisions would be necessary to produce an rms deflection of 10°? (Use the result from the one-dimensional random walk problem in statistics stating that the rms deflection equals the magnitude of the individual deflections times the square root of the number of deflections.) Compare this result with the number of atomic layers in a gold foil of thickness 10^{-6} m, assuming that the thickness of each atom is 0.1 nm $= 10^{-10}$ m.
4-12. Consider the foil and α particle energy in Problem 4-6. Suppose that 1000 of those particles suffer a deflection of more than 25°. (*a*) How many of these are deflected by more than 45°? (*b*) How many are deflected between 25° and 45°? (*c*) How many are deflected between 75° and 90°?

Section 4-3 The Bohr Model of the Hydrogen Atom

4-13. The radius of the $n = 1$ orbit in the hydrogen atom is $a_0 = 0.053$ nm. (*a*) Compute the radius of the $n = 6$ orbit. (*b*) Compute the radius of the $n = 6$ orbit in singly ionized helium (He^+), which is hydrogen-like, i.e., it has only a single electron outside the nucleus.
4-14. Show that Equation 4-19 for the radius of the first Bohr orbit and Equation 4-20 for the magnitude of the lowest energy for the hydrogen atom can be written as

$$a_0 = \frac{hc}{\alpha mc^2} = \frac{\lambda_c}{2\pi\alpha} \qquad E_1 = \frac{1}{2}\alpha^2 mc^2$$

where $\lambda_c = h/mc$ is the Compton wavelength of the electron and $\alpha = ke^2/hc$ is the fine-structure constant. Use these expressions to check the numerical values of the constants a_0 and E_1.
4-15. Calculate the three longest wavelengths in the Lyman series ($n_f = 1$) in nm and indicate their position on a horizontal linear scale. Indicate the series limit (shortest wavelength) on this scale. Are any of these lines in the visible spectrum?
4-16. If the angular momentum of Earth in its motion around the Sun were quantized like a hydrogen electron according to Equation 4-17, what would Earth's quantum number be? How much energy would be released in a transition to the next lowest level? Would that energy release (presumably as a gravity wave) be detectable? What would be the radius of that orbit? (The radius of Earth's orbit is 1.50×10^{11} m.)
4-17. On average, a hydrogen atom will exist in an excited state for about 10^{-8} sec before making a transition to a lower energy state. About how many revolutions does an electron in the $n = 2$ state make in 10^{-8} sec?
4-18. An atom in an excited state will on average undergo a transition to a state of lower energy in about 10^{-8} seconds. If the electron in a doubly ionized lithium atom (Li^{+2}, which is hydrogenlike) is placed in the $n = 4$ state, about how many revolutions around the nucleus does it make before undergoing a transition to a lower energy state?

STUDENTS-HUB.com Uploaded By: Malak Obaid

4-19. It is possible for a muon to be captured by a proton to form a muonic atom. A muon is identical to an electron except for its mass, which is 105.7 MeV/c^2. (*a*) Calculate the radius of the first Bohr orbit of a muonic atom. (*b*) Calculate the magnitude of the lowest energy state. (*c*) What is the shortest wavelength in the Lyman series for this atom?

4-20. In the lithium atom ($Z = 3$) two electrons are in the $n = 1$ orbit and the third is in the $n = 2$ orbit. (Only two are allowed in the $n = 1$ orbit because of the exclusion principle, which will be discussed in Chapter 7.) The interaction of the inner electrons with the outer one can be approximated by writing the energy of the outer electron as

$$E = -Z'^2(E_1/n^2)$$

where $E_1 = 13.6$ eV, $n = 2$, and Z' is the effective nuclear charge, which is less than 3 because of the screening effect of the two inner electrons. Using the measured ionization energy of 5.39 eV, calculate Z'.

4-21. Draw to careful scale an energy-level diagram for hydrogen for levels with $n = 1, 2, 3, 4, \infty$. Show the following on the diagram: (*a*) the limit of the Lyman series, (*b*) the H_β line, (*c*) the transition between the state whose binding energy (= energy needed to remove the electron from the atom) is 1.51 eV and the state whose excitation energy is 10.2 eV, and (*d*) the longest wavelength line of the Paschen series.

4-22. A hydrogen atom at rest in the laboratory emits the Lyman α radiation. (*a*) Compute the recoil kinetic energy of the atom. (*b*) What fraction of the excitation energy of the $n = 2$ state is carried by the recoiling atom? (*Hint:* Use conservation of momentum.)

4-23. (a) Draw accurately to scale and label completely a partial energy-level diagram for C^{5+}, including at minimum the energy levels for $n = 1, 2, 3, 4, 5$, and ∞. (*b*) Compute the wavelength of the spectral line resulting from the $n = 3$ to the $n = 2$ transition, the $C^{5+}H_\alpha$ line. (*c*) In what part of the EM spectrum does this line lie?

4-24. The electron-positron pair that was discussed in Chapter 2 can form a hydrogenlike system called *positronium*. Calculate (*a*) the energies of the three lowest states and (*b*) the wavelength of the Lyman α and β lines. (Detection of those lines is a "signature" of positronium formation.)

4-25. With the aid of tunable lasers, Rydberg atoms of sodium have been produced with $n \approx 100$. The resulting atomic diameter would correspond in hydrogen to $n \approx 600$. (*a*) What would be the diameter of a hydrogen atom whose electron is in the $n \approx 600$ orbit? (*b*) What would be the speed of the electron in that orbit? (*c*) How does the result in (*b*) compare with the speed in the $n \approx 1$ orbit?

Section 4-4 X-Ray Spectra

4-26. (*a*) Calculate the next two longest wavelengths in the *K* series (after the K_α line) of molybdenum. (*b*) What is the wavelength of the shortest wavelength in this series?

4-27. The wavelength of the K_α x-ray line for an element is measured to be 0.0794 nm. What is the element?

4-28. Moseley pointed out that elements with atomic numbers 43, 61, and 75 should exist and (at that time) had not been found. (*a*) Using Figure 4-19, what frequencies would Moseley's graphical data have predicted for the K_α x ray for each of these elements? (*b*) Compute the wavelengths for these lines predicted by Equation 4-37.

4-29. What is the approximate radius of the $n = 1$ orbit of gold ($Z = 79$)? Compare this with the radius of the gold nucleus, about 7.1 fm.

4-30. An electron in the *K* shell of Fe is ejected by a high-energy electron in the target of an x-ray tube. The resulting hole in the $n = 1$ shell could be filled by an electron from the $n = 2$ shell, the *L* shell; however, instead of emitting the characteristic Fe K_α x ray, the atom ejects an Auger electron from the $n = 2$ shell. Using Bohr theory, compute the energy of the Auger electron.

4-31. In a particular x-ray tube, an electron approaches the target moving at 2.25×10^8 m/s. It slows down on being deflected by a nucleus of the target, emitting a photon of energy 32.5 keV. Ignoring the nuclear recoil, but not relativity, compute the final speed of the electron.

4-32. (*a*) Compute the energy of an electron in the $n = 1$ (*K* shell) of tungsten, using $Z - 1$ for the effective nuclear charge. (*b*) The experimental result for this energy is 69.5 keV. Assume that the effective nuclear charge is $Z - \sigma$, where σ is called the screening constant, and calculate σ from the experimental result.

STUDENTS-HUB.com Uploaded By: Malak Obaid

4-33. Construct a Moseley plot similar to Figure 4-19 for the K_β x rays of the elements listed below (the x-ray energies are given in keV):

Al 1.56	Ar 3.19	Sc 4.46	Fe 7.06
Ge 10.98	Kr 14.10	Zr 17.66	Ba 36.35

Determine the slope of your plot, and compare it with the K_β line in Figure 4-19.

Section 4-5 The Franck-Hertz Experiment

4-34. Suppose that, in a Franck-Hertz experiment, electrons of energy up to 13.0 eV can be produced in the tube. If the tube contained atomic hydrogen, (*a*) what is the shortest-wavelength spectral line that could be emitted from the tube? (*b*) List all of the hydrogen lines that can be emitted by this tube.

4-35. Using the data in Figure 4-24*b* and a good ruler, draw a carefully scaled energy-level diagram covering the range from 0 eV to 60 eV for the vibrational states of this solid. What approximate energy is typical of the transitions between adjacent levels corresponding to the larger of each pair of peaks?

4-36. The transition from the first excited state to the ground state in potassium results in the emission of a photon with $\lambda = 770$ nm If potassium vapor is used in a Franck-Hertz experiment, at what voltage would you expect to see the first decrease in current?

4-37. If we could somehow fill a Franck-Hertz tube with positronium, what cathode-grid voltage would be needed to reach the second current decrease in the positronium equivalent of Figure 4-23? (See Problem 4-24.)

4-38. Electrons in the Franck-Hertz tube can also have elastic collisions with the Hg atoms. If such a collision is a head-on, what fraction of its initial kinetic energy will an electron lose, assuming the Hg atom to be at rest? If the collision is not head-on, will the fractional loss be greater or less than this?

Level II

4-39. Derive Equation 4-8 along the lines indicated in the paragraph that immediately precedes it.

4-40. Geiger and Marsden used α particles with 7.7-MeV kinetic energy and found that when they were scattered from thin gold foil, the number observed to be scattered at all angles agreed with Rutherford's formula. Use this fact to compute an upper limit on the radius of the gold nucleus.

4-41. (*a*) The current i due to a charge q moving in a circle with frequency f_{rev} is qf_{rev}. Find the current due to the electron in the first Bohr orbit. (*b*) The magnetic moment of a current loop is iA, where A is the area of the loop. Find the magnetic moment of the electron in the first Bohr orbit in units A-m^2. This magnetic moment is called a *Bohr magneton*.

4-42. Use a spreadsheet to calculate the wavelengths (in nm) of the first five spectral lines of the Lyman, Balmer, Paschen, and Brackett series of hydrogen. Show the positions of these lines on a linear scale and indicate which ones lie in the visible.

4-43. Show that a small change in the reduced mass of the electron produces a small change in a spectral line given by $\Delta\lambda/\lambda = \Delta\mu/\mu$. Use this to calculate the difference $\Delta\lambda$ in the Balmer red line $\lambda = 656.3$ nm between hydrogen and deuterium, which has a nucleus with twice the mass of hydrogen.

4-44. Consider the Franck-Hertz experiment with Hg vapor in the tube and the voltage between the cathode and the grid equal to 4.0 V, i.e., not enough for the electrons to excite the Hg atom's first excited state. Therefore, the electron-Hg atom collisions are elastic. (*a*) If the kinetic energy of the electrons is E_k, show that the maximum kinetic energy that a recoiling Hg atom can have is approximately $4mE_k/M$, where M is the Hg atom mass. (*b*) What is the approximate maximum kinetic energy that can be lost by an electron with $E_k = 2.5$ eV?

4-45. The Li^{2+} ion is essentially identical to the H atom in Bohr's theory, aside from the effect of the different nuclear charges and masses. (*a*) What transitions in Li^{2+} will yield emission lines whose wavelengths are very nearly equal to the first two lines of the Lyman series in hydrogen?

STUDENTS-HUB.com Uploaded By: Malak Obaid

(*b*) Calculate the difference between the wavelength of the Lyman α line of hydrogen and the emission line from Li^{2+} that has very nearly the same wavelength.

4-46. In an α scattering experiment, the area of the α particle detector is 0.50 cm^2. The detector is located 10 cm from a 1.0-μm-thick silver foil. The incident beam carries a current of 1.0 nA, and the energy of each α particle is 6.0 MeV. How many α particles will be counted per second by the detector at (*a*) $\theta = 60°$? (*b*) $\theta = 120°$?

4-47. The K_α, L_α, and M_α x rays are emitted in the $n = 2 \rightarrow n = 1$, $n = 3 \rightarrow n = 2$, and $n = 4 \rightarrow n = 3$ transitions, respectively. For calcium ($Z = 20$) the energies of these transitions are 3.69 keV, 0.341 keV, and 0.024 keV, respectively. Suppose that energetic photons impinging on a calcium surface cause ejection of an electron from the *K* shell of the surface atoms. Compute the energies of the Auger electrons that may be emitted from the *L*, *M*, and *N* shells ($n = 2$, 3, and 4) of the sample atoms, in addition to the characteristic x rays.

4-48. Figure 3-15*b* shows the K_α and K_β characteristic x rays emitted by a molybdenum (Mo) target in an x-ray tube whose accelerating potential is 35 kV. The wavelengths are $K_\alpha = 0.071$ nm and $K_\beta = 0.063$ nm. (*a*) Compute the corresponding energies of these photons. (*b*) Suppose we wish to prepare a beam consisting primarily of K_α x rays by passing the molybdenum x rays through a material that absorbs K_β x rays more strongly than K_α x rays by photoelectric effect on *K*-shell electrons of the material. Which of the materials listed in the accompanying table with their *K*-shell binding energies would you choose? Explain your answer.

Element	Zr	Nb	Mo	Tc	Ru
Z	40	41	42	43	44
E_K (keV)	18.00	18.99	20.00	21.04	22.12

Level III

4-49. A small shot of negligible radius hits a stationary smooth, hard sphere of radius *R*, making an angle β with the normal to the sphere, as shown in Figure 4-25. It is reflected at an equal angle to the normal. The scattering angle is $\theta = 180° - 2\beta$, as shown. (*a*) Show by the geometry of the figure that the impact parameter *b* is related to θ by $b = R \cos \frac{1}{2}\theta$. (*b*) If the incoming intensity of the shot is I_0 particles/s · area, how many are scattered through angles greater than θ? (*c*) Show that the cross section for scattering through angles greater than 0° is πR^2. (*d*) Discuss the implication of the fact that the Rutherford cross section for scattering through angles greater than 0° is infinite.

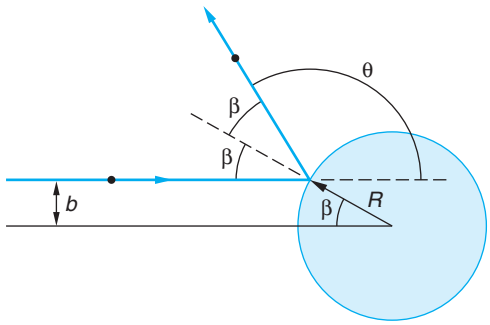

Figure 4-25 Small particle scattered by a hard sphere of radius *R*.

4-50. Singly ionized helium He^+ is hydrogenlike. (*a*) Construct a carefully scaled energy-level diagram for He^+ similar to that in Figure 4-16, showing the levels for $n = 1$, 2, 3, 4, 5, and ∞. (*b*) What is the ionization energy of He^+? (*c*) Compute the difference in wavelength between each of the first two lines of the Lyman series of hydrogen and the first two lines of the He^+ Balmer series. Be sure to include the reduced mass correction for both atoms. (*d*) Show that for every spectral line of hydrogen, He^+ has a spectral line of very nearly the same wavelength. (Mass of $He^+ = 6.65 \times 10^{-27}$ kg.)

STUDENTS-HUB.com Uploaded By: Malak Obaid

4-51. Listed in the table are the L_α x-ray wavelengths for several elements. Construct a Moseley plot from these data. Compare the slope with the appropriate one in Figure 4-19. Determine and interpret the intercept on your graph, using a suitably modified version of Equation 4-35.

Element	P	Ca	Co	Kr	Mo	I
Z	15	20	27	36	42	53
Wavelength (nm)	10.41	4.05	1.79	0.73	0.51	0.33

4-52. In this problem you are to obtain the Bohr results for the energy levels in hydrogen without using the quantization condition of Equation 4-17. In order to relate Equation 4-14 to the Balmer-Ritz formula, assume that the radii of allowed orbits are given by $r_n = n^2 r_0$, where n is an integer and r_0 is a constant to be determined. (*a*) Show that the frequency of radiation for a transition to $n_f = n - 1$ is given by $f \approx kZe^2/hr_0n^3$ for large n. (*b*) Show that the frequency of revolution is given by

$$f_{\text{rev}}^2 = \frac{kZe^2}{4\pi^2 m r_0^3 n^6}$$

(*c*) Use the correspondence principle to determine r_0 and compare with Equation 4-19.

4-53. Calculate the energies and speeds of electrons in circular Bohr orbits in a hydrogenlike atom using the relativistic expressions for kinetic energy and momentum.

4-54. (*a*) Write a computer program for your personal computer or programmable calculator that will provide you with the spectral series of H-like atoms. Inputs to be included are n_i, n_f, Z, and the nuclear mass M. Outputs are to be the wavelengths and frequencies of the first six lines and the series limit for the specified n_f, Z, and M. Include the reduced mass correction. (*b*) Use the program to compute the wavelengths and frequencies of the Balmer series. (*c*) Pick an $n_f > 100$, name the series the [your name] series, and use your program to compute the wavelengths and frequencies of the first three lines and the limit.

4-55. Figure 4-26 shows an energy loss spectrum for He measured in an apparatus such as that shown in Figure 4-24*a*. Use the spectrum to construct and draw carefully to scale an energy-level diagram for He.

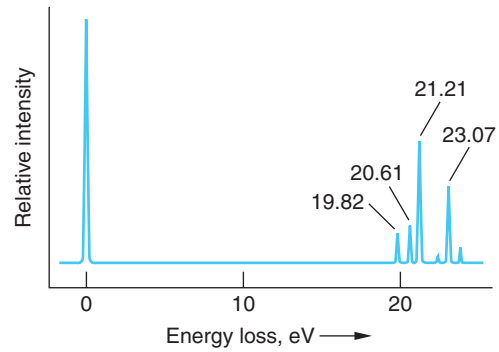

Figure 4-26 Energy-loss spectrum of helium. Incident electron energy was 34 eV. The elastically scattered electrons cause the peak at 0 eV.

4-56. If electric charge did not exist and electrons were bound to protons by the gravitational force to form hydrogen, derive the corresponding expressions for a_0 and E_n and compute the energy and frequency of the H_α line and the limit of the Balmer series. Compare these with the corresponding quantities for "real" hydrogen.

4-57. A sample of hydrogen atoms are all in the $n = 5$ state. If all the atoms return to the ground state, how many different photon energies will be emitted, assuming all possible transitions occur? If there are 500 atoms in the sample and assuming that from any state all possible downward transitions are equally probable, what is the total number of photons that will be emitted when all of the atoms have returned to the ground state?

4-58. Consider muonic atoms (see Problem 4-19). (*a*) Draw a correctly scaled and labeled partial energy level diagram including levels with $n = 1, 2, 3, 4, 5$, and ∞ for muonic hydrogen. (*b*) Compute the radius of the $n = 1$ muon orbit in muonic H, He^{1+}, Al^{12+}, and Au^{78+}. (*c*) Compare the results in (*b*) with the radii of these nuclei. (*d*) Compute the wavelength of the photon emitted in the $n = 2$ to $n = 1$ transition for each of these muonic atoms.

STUDENTS-HUB.com Uploaded By: Malak Obaid

CHAPTER 5

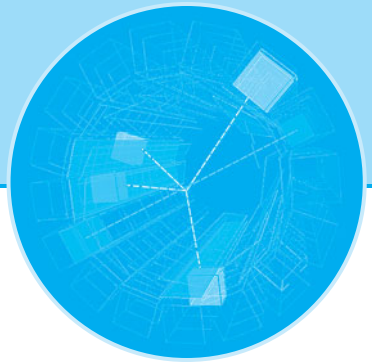

The Wavelike Properties of Particles

5-1 The de Broglie Hypothesis 185
5-2 Measurements of Particle Wavelengths 187
5-3 Wave Packets 196
5-4 The Probabilistic Interpretation of the Wave Function 202
5-5 The Uncertainty Principle 205
5-6 Some Consequences of the Uncertainty Principle 208
5-7 Wave-Particle Duality 212

In 1924, a French graduate student, Louis de Broglie,[1] proposed in his doctoral dissertation that the dual—i.e., wave-particle—behavior that was by then known to exist for radiation was also a characteristic of matter, in particular, electrons. This suggestion was highly speculative, since there was yet no experimental evidence whatsoever for any wave aspects of electrons or any other particles. What had led him to this seemingly strange idea? It was a "bolt out of the blue," like Einstein's "happy thought" that led to the principle of equivalence (see Chapter 2). De Broglie described it with these words:

> After the end of World War I, I gave a great deal of thought to the theory of quanta and to the wave-particle dualism. . . . It was then that I had a sudden inspiration. Einstein's wave-particle dualism was an absolutely general phenomenon extending to all physical nature.[2]

Since the visible universe consists entirely of matter and radiation, de Broglie's hypothesis is a fundamental statement about the grand symmetry of nature. (There is currently strong observational evidence that ordinary matter makes up only about 4 percent of the visible universe. About 22 percent is some unknown form of invisible "dark matter," and approximately 74 percent consists of some sort of equally mysterious "dark energy." See Chapter 13.)

5-1 The de Broglie Hypothesis

De Broglie stated his proposal mathematically with the following equations for the frequency and wavelength of the electron waves, which are referred to as the *de Broglie relations*:

$$f = \frac{E}{h} \qquad \textbf{5-1}$$

$$\lambda = \frac{h}{p} \qquad \textbf{5-2}$$

where E is the total energy, p is the momentum, and λ is called the *de Broglie wavelength* of the particle. For photons, these same equations result directly from

STUDENTS-HUB.com Uploaded By: Malak Obaid

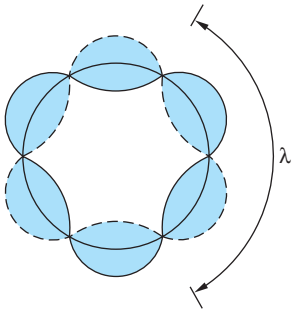

Figure 5-1 Standing waves around the circumference of a circle. In this case the circle is 3λ in circumference. If the vibrator were, for example, a steel ring that had been suitably tapped with a hammer, the shape of the ring would oscillate between the extreme positions represented by the solid and broken lines.

Einstein's quantization of radiation $E = hf$ and Equation 2-31 for a particle of zero rest energy $E = pc$ as follows:

$$E = pc = hf = \frac{hc}{\lambda}$$

By a more indirect approach using relativistic mechanics, de Broglie was able to demonstrate that Equations 5-1 and 5-2 also apply to particles with mass. He then pointed out that these equations lead to a physical interpretation of Bohr's quantization of the angular momentum of the electron in hydrogenlike atoms, namely, that the quantization is equivalent to a standing-wave condition. (See Figure 5-1.) We have

$$mvr = n\hbar = \frac{nh}{2\pi} \qquad \text{for} \qquad n = \text{integer}$$

$$2\pi r = \frac{nh}{mv} = \frac{nh}{p} = n\lambda = \text{circumference of orbit} \qquad \textbf{5-3}$$

The idea of explaining discrete energy states in matter by standing waves thus seemed quite promising.

De Broglie's ideas were expanded and developed into a complete theory by Erwin Schrödinger late in 1925. In 1927, C. J. Davisson and L. H. Germer verified the de Broglie hypothesis directly by observing interference patterns, a characteristic of waves, with electron beams. We will discuss both Schrödinger's theory and the Davisson-Germer experiment in later sections, but first we have to ask ourselves why wavelike behavior of matter had not been observed before de Broglie's work. We can understand why if we first recall that the wave properties of light were not noticed either until apertures or slits with dimensions of the order of the wavelength of light could be obtained. This is because the wave nature of light is not evident in experiments where the primary dimensions of the apparatus are large compared with the wavelength of the light used. For example, if A represents the diameter of a lens or the width of a slit, then diffraction effects[3] (a manifestation of wave properties) are limited to angles θ around the forward direction ($\theta = 0°$) where $\sin\theta = \lambda/A$. In geometric (ray) optics $\lambda/A \to 0$, so $\theta \approx \sin\theta \to 0$, too. However, if a characteristic

Louis V. de Broglie, who first suggested that electrons might have wave properties. [*Courtesy of Culver Pictures.*]

STUDENTS-HUB.com Uploaded By: Malak Obaid

dimension of the apparatus becomes of the order of (or smaller than) λ, the wavelength of light passing through the system, then $\lambda/A \rightarrow 1$. In that event $\theta \approx \lambda/A$ is readily observable, and the wavelike properties of light become apparent. Because Planck's constant is so small, the wavelength given by Equation 5-2 is extremely small for any macroscopic object. This point is among those illustrated in the following section.

5-2 Measurements of Particle Wavelengths

Although we now have diffraction systems of nuclear dimensions, the smallest-scale systems to which de Broglie's contemporaries had access were the spacings between the planes of atoms in crystalline solids, about 0.1 nm. This means that even for an extremely small macroscopic particle, such as a grain of dust ($m \approx 0.1$ mg) moving through air with the average kinetic energy of the atmospheric gas molecules, the smallest diffraction systems available would have resulted in diffraction angles τ only of the order of 10^{-10} radian, far below the limit of experimental detectability. The small magnitude of Planck's constant ensures that λ will be smaller than any readily accessible aperture, placing diffraction beyond the limits of experimental observation. For objects whose momenta are larger than that of the dust particle, the possibility of observing *particle*, or *matter waves*, is even less, as the following example illustrates.

EXAMPLE 5-1 De Broglie Wavelength of a Ping-Pong Ball What is the de Broglie wavelength of a Ping-Pong ball of mass 2.0 g after it is slammed across the table with speed 5 m/s?

SOLUTION

$$\lambda = \frac{h}{mv} = \frac{6.63 \times 10^{-34}\ \text{J}\cdot\text{s}}{(2.0 \times 10^{-3}\ \text{kg})(5\ \text{m/s})}$$
$$= 6.6 \times 10^{-32}\ \text{m} = 6.6 \times 10^{-23}\ \text{nm}$$

This is 17 orders of magnitude smaller than typical nuclear dimensions, far below the dimensions of any possible aperture.

The case is different for low-energy electrons, as de Broglie himself realized. At his *soutenance de thèse* (defense of the thesis), de Broglie was asked by Perrin[4] how his hypothesis could be verified, to which he replied that perhaps passing particles, such as electrons, through very small slits would reveal the waves. Consider an electron that has been accelerated through V_0 volts. Its kinetic energy (nonrelativistic) is then

$$E = \frac{p^2}{2m} = eV_0$$

Solving for p and substituting into Equation 5-2,

$$\lambda = \frac{h}{p} = \frac{hc}{pc} = \frac{hc}{(2mc^2eV_0)^{1/2}}$$

Using $hc = 1.24 \times 10^3\ \text{eV}\cdot\text{nm}$ and $mc^2 = 0.511 \times 10^6$ eV, we obtain

$$\lambda = \frac{1.226}{V_0^{1/2}}\text{nm} \qquad \text{for} \qquad eV_0 \sim mc^2 \qquad \textbf{5-4}$$

The following example computes an electron de Broglie wavelength, giving a measure of just how small the slit must be.

STUDENTS-HUB.com Uploaded By: Malak Obaid

EXAMPLE 5-2 **De Broglie Wavelength of a Slow Electron** Compute the de Broglie wavelength of an electron whose kinetic energy is 10 eV.

SOLUTION

1. The de Broglie wavelength is given by Equation 5-2:

$$\lambda = \frac{h}{p}$$

2. *Method 1:* Since a 10-eV electron is nonrelativistic, we can use the classical relation connecting the momentum and the kinetic energy:

$$E_k = \frac{p^2}{2m}$$

or

$$\begin{aligned} p &= \sqrt{2mE_k} \\ &= \sqrt{(2)(9.11 \times 10^{-31}\ \text{kg})(10\ \text{eV})(1.60 \times 10^{-19}\ \text{J/eV})} \\ &= 1.71 \times 10^{-24}\ \text{kg} \cdot \text{m/s} \end{aligned}$$

3. Substituting this result into Equation 5-2:

$$\begin{aligned} \lambda &= \frac{6.63 \times 10^{-34}\ \text{J} \cdot \text{s}}{1.71 \times 10^{-24}\ \text{kg} \cdot \text{m/s}} \\ &= 3.88 \times 10^{-10}\ \text{m} = 0.39\ \text{nm} \end{aligned}$$

4. *Method 2:* The electron's wavelength can also be computed from Equation 5-4 with $V_0 = 10$ V:

$$\begin{aligned} \lambda &= \frac{1.226}{V^{1/2}} = \frac{1.226}{\sqrt{10}} \\ &= 0.39\ \text{nm} \end{aligned}$$

Remarks: *Though this wavelength is small, it is just the order of magnitude of the size of an atom and of the spacing of atoms in a crystal.*

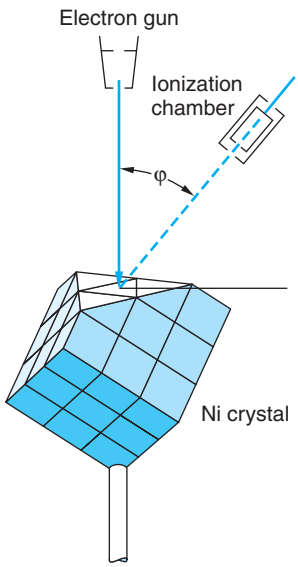

Figure 5-2 The Davisson-Germer experiment. Low-energy electrons scattered at angle φ from a nickel crystal are detected in an ionization chamber. The kinetic energy of the electrons could be varied by changing the accelerating voltage on the electron gun.

The Davisson-Germer Experiment

In a brief note in the August 14, 1925, issue of the journal *Naturwissenschaften*, Walter Elsasser, at the time a student of J. Franck's (of the Franck-Hertz experiment), proposed that the wave effects of low-velocity electrons might be detected by scattering them from single crystals. The first such measurements of the wavelengths of electrons were made in 1927 by C. J. Davisson[5] and L. H. Germer, who were studying electron reflection from a nickel target at Bell Telephone Laboratories, unaware of either Elsasser's suggestion or de Broglie's work. After heating their target to remove an oxide coating that had accumulated during an accidental break in their vacuum system, they found that the scattered electron intensity as a function of the scattering angle showed maxima and minima. The surface atoms of their nickel target had, in the process of cooling, formed relatively large single crystals, and they were observing electron diffraction. Recognizing the importance of their accidental discovery, they then prepared a target consisting of a single crystal of nickel and extensively investigated the scattering of electrons from it. Figure 5-2 illustrates their experimental arrangement. Their data for 54-eV electrons, shown in Figure 5-3, indicate a strong maximum of scattering at $\varphi = 50°$. Consider the scattering from a set of Bragg

STUDENTS-HUB.com Uploaded By: Malak Obaid

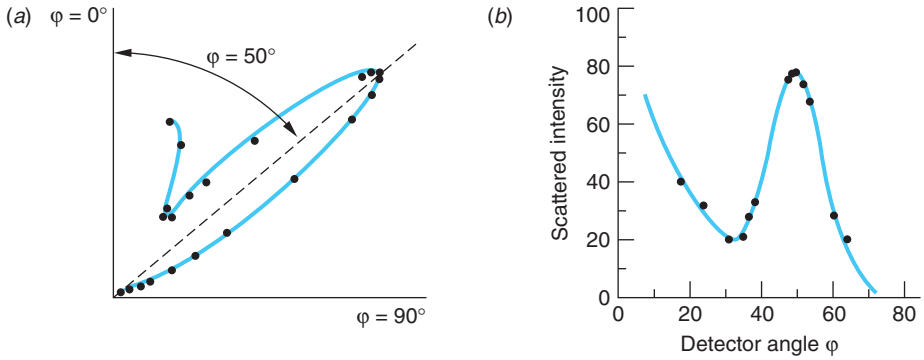

Figure 5-3 Scattered intensity vs. detector angle for 54-eV electrons. (*a*) Polar plot of the data. The intensity at each angle is indicated by the distance of the point from the origin. Scattering angle φ is plotted clockwise starting at the vertical axes. (*b*) The same data plotted on a Cartesian graph. The intensity scales are arbitrary but the same on both graphs. In each plot there is maximum intensity at $\varphi = 50°$, as predicted for Bragg scattering of waves having wavelength $\lambda = h/p$. [*From Nobel Prize Lectures: Physics (Amsterdam and New York: Elsevier, © Nobel Foundation, 1964).*]

planes, as shown in Figure 5-4. The Bragg condition for constructive interference is $n\lambda = 2d \sin\theta = 2d \cos\alpha$. The spacing of the Bragg planes d is related to the spacing of the atoms D by $d = D \sin\alpha$; thus

$$n\lambda = 2D \sin\alpha \cos\alpha = D \sin 2\alpha$$

or

$$n\lambda = D \sin\varphi \qquad \textbf{5-5}$$

where $\varphi = 2\alpha$ is the scattering angle.

The spacing D for Ni is known from x-ray diffraction to be 0.215 nm. The wavelength calculated from Equation 5-5 for the peak observed at $\varphi = 50°$ by Davisson and Germer is, for $n = 1$,

$$\lambda = 0.215 \sin 50° = 0.165 \text{ nm}$$

The value calculated from the de Broglie relation for 54-eV electrons is

$$\lambda = \frac{1.226}{(54)^{1/2}} = 0.167 \text{ nm}$$

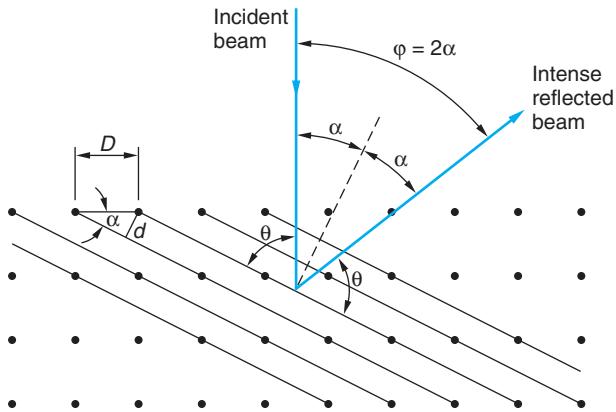

Figure 5-4 Scattering of electrons by a crystal. Electron waves are strongly scattered if the Bragg condition $n\lambda = 2d \sin\theta$ is met. This is equivalent to the condition $n\lambda = D \sin\varphi$.

STUDENTS-HUB.com Uploaded By: Malak Obaid

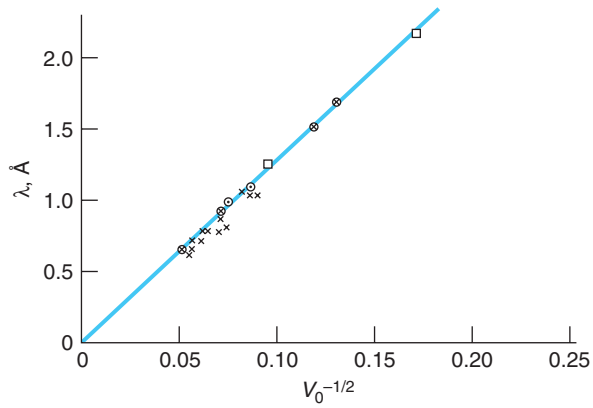

Figure 5-5 Test of the de Broglie formula $\lambda = h/p$. The wavelength is computed from a plot of the diffraction data plotted against $V_0^{-1/2}$, where V_0 is the accelerating voltage. The straight line is $1.226V_0^{-1/2}$ nm as predicted from $\lambda = h(2mE)^{-1/2}$. These are the data referred to in the quotation from Davisson's Nobel lecture. (× From observations with diffraction apparatus; ⊗ same, particularly reliable; □ same, grazing beams. ⊙ From observations with reflection apparatus.) [*From Nobel Prize Lectures: Physics (Amsterdam and New York: Elsevier, © Nobel Foundation, 1964).*]

The agreement with the experimental observation is excellent! With this spectacular result Davisson and Germer then conducted a systematic study to test the de Broglie relation using electrons up to about 400 eV and various experimental arrangements. Figure 5-5 shows a plot of measured wavelengths versus $V_0^{-1/2}$. The wavelengths measured by diffraction are slightly lower than the theoretical predictions because the refraction of the electron waves at the crystal surface has been neglected. We have seen from the photoelectric effect that it takes work of the order of several eV to remove an electron from a metal. Electrons entering a metal thus gain kinetic energy; therefore, their de Broglie wavelength is slightly less inside the crystal.[6]

A subtle point must be made here. Notice that the wavelength in Equation 5-5 depends only on D, the interatomic spacing of the crystal, whereas our derivation of that equation included the interplane spacing as well. The fact that the structure of the crystal really is essential shows up when the energy is varied, as was done in collecting the data for Figure 5-5. Equation 5-5 suggests that a change in λ, resulting from a change in the energy, would mean only that the diffraction maximum would occur at some other value of φ such that the equation remains satisfied. However, as can be seen from examination of Figure 5-4, the value of φ is determined by α, the angle of the planes determined by the crystal structure. Thus, if there are no crystal planes making an angle $\alpha = \varphi/2$ with the surface, then setting the detector at $\varphi = \sin^{-1}(\lambda/D)$ will not result in constructive interference and strong reflection for that value of λ, even though Equation 5-5 is satisfied. This is neatly illustrated by Figure 5-6, which shows a series of polar graphs (like Figure 5-3*a*) for electrons of energies from 36 eV through 68 eV. The building to a strong reflection at $\varphi = 50°$ is evident for $V_0 = 54$ V, as we have already seen. But Equation 5-5 by itself would also lead us to expect, for example, a strong reflection at $\varphi = 64°$ when $V_0 = 40$ V, which obviously does not occur.

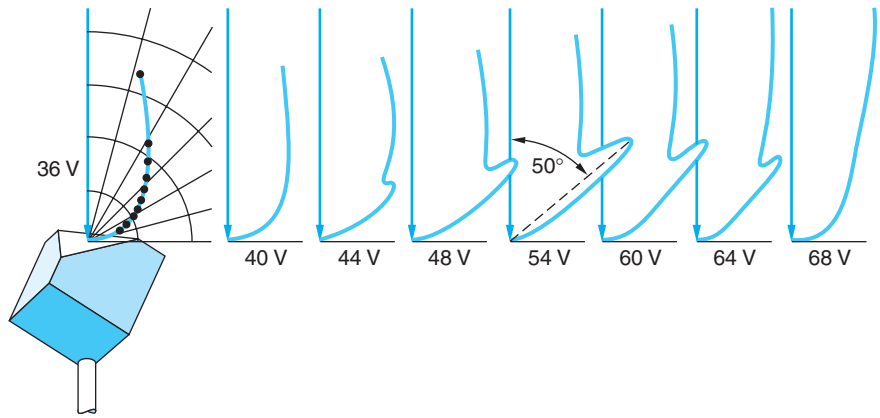

Figure 5-6 A series of polar graphs of Davisson and Germer's data at electron accelerating potentials from 36 V to 68 V. Note the development of the peak at $\varphi = 50°$ to a maximum when $V_0 = 54$ V.

STUDENTS-HUB.com Uploaded By: Malak Obaid

Clinton J. Davisson (left) and Lester H. Germer at Bell Laboratories, where electron diffraction was first observed. [*Bell Telephone Laboratories, Inc.*]

In order to show the dependence of the diffraction on the inner atomic layers, Davisson and Germer kept the detector angle φ fixed and varied the accelerating voltage rather than search for the correct angle for a given λ. Writing Equation 5-5 as

$$\lambda = \frac{D \sin \varphi}{n} = \frac{D \sin (2\alpha)}{n} \qquad \textbf{5-6}$$

and noting that $\lambda \propto V_0^{-1/2}$, a graph of intensity versus $V_0^{1/2} (\propto 1/\lambda)$ for a given angle φ should yield (1) a series of equally spaced peaks corresponding to successive values of the integer n, if $\alpha = \varphi/2$ is an existing angle for atomic planes, or (2) no diffraction peaks if $\varphi/2$ is not such an angle. Their measurements verified the dependence upon the interplane spacing, the agreement with the prediction being about ± 1 percent. Figure 5-7 illustrates the results for $\varphi = 50°$. Thus, Davisson and Germer showed conclusively that particles with mass moving at speeds $v \ll c$ do indeed have wavelike properties, as de Broglie had proposed.

The diffraction pattern formed by high-energy electron waves scattered from nuclei provides a means by which nuclear radii and the internal distribution of the nuclear charge (the protons) are measured. See Chapter 11.

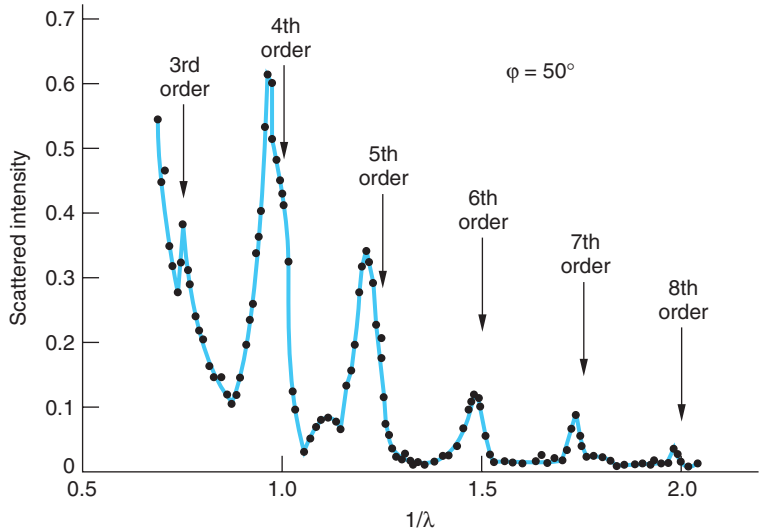

Figure 5-7 Variation of the scattered electron intensity with wavelength for constant φ. The incident beam in this case was 10° from the normal, the resulting refraction causing the measured peaks to be slightly shifted from the positions computed from Equation 5-5, as explained in note 6. [*After C. J. Davisson and L. H. Germer, Proceedings of the National Academy of Sciences,* ***14****, 619 (1928).*]

STUDENTS-HUB.com Uploaded By: Malak Obaid

Here is Davisson's account of the connection between de Broglie's predictions and their experimental verification:

> Perhaps no idea in physics has received so rapid or so intensive development as this one. De Broglie himself was in the van of this development, but the chief contributions were made by the older and more experienced Schrödinger. It would be pleasant to tell you that no sooner had Elsasser's suggestion appeared than the experiments were begun in New York which resulted in a demonstration of electron diffraction—pleasanter still to say that the work was begun the day after copies of de Broglie's thesis reached America. The true story contains less of perspicacity and more of chance. . . It was discovered, purely by accident, that the intensity of elastic scattering [of electrons] varies with the orientations of the scattering crystals. Out of this grew, quite naturally, an investigation of elastic scattering by a single crystal of predetermined orientation. . . Thus the New York experiment was not, at its inception, a test of wave theory. Only in the summer of 1926, after I had discussed the investigation in England with Richardson, Born, Franck and others, did it take on this character.[7]

A demonstration of the wave nature of relativistic electrons was provided in the same year by G. P. Thomson, who observed the transmission of electrons with energies in the range of 10 to 40 keV through thin metallic foils (G. P. Thomson, the son of J. J. Thomson, shared the Nobel Prize in 1937 with Davisson). The experimental arrangement (Figure 5-8*a*) was similar to that used to obtain Laue patterns with x rays (see Figure 3-11). Because the metal foil consists of many tiny crystals randomly oriented, the diffraction pattern consists of concentric rings. If a crystal is oriented at an angle θ with the incident beam, where θ satisfies the Bragg condition, this crystal will strongly scatter at an equal angle θ; thus there will be a scattered beam making an angle 2θ with the incident beam. Figure 5-8*b* and *c* show the similarities in patterns produced by x rays and electron waves.

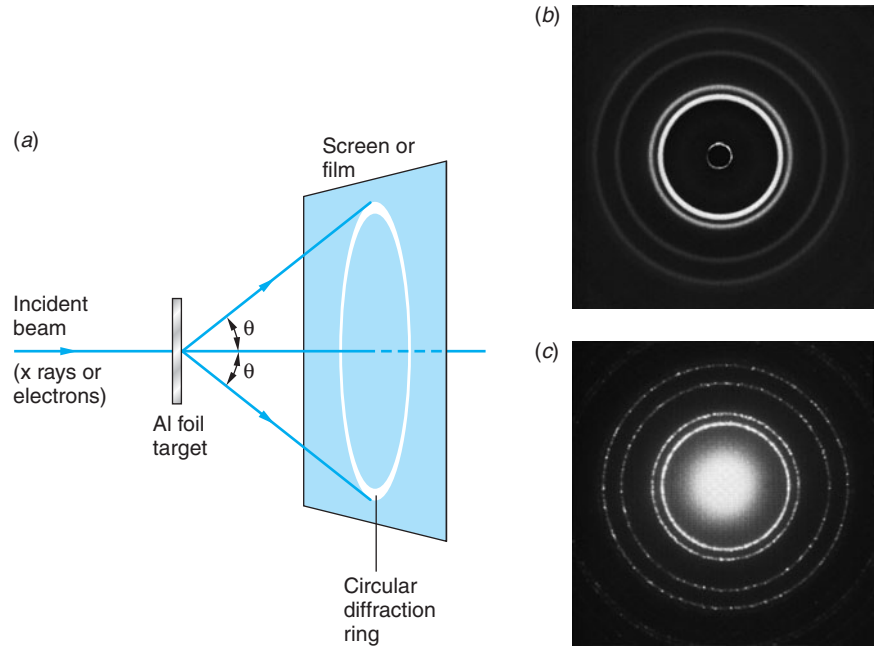

Figure 5-8 (*a*) Schematic arrangement used for producing a diffraction pattern from a polycrystalline aluminum target. (*b*) Diffraction pattern produced by x rays of wavelength 0.071 nm and an aluminum foil target. (*c*) Diffraction pattern produced by 600-eV electrons (de Broglie wavelength of about 0.05 nm) and an aluminum foil target. The pattern has been enlarged by 1.6 times to facilitate comparison with (*b*). [*Courtesy of Film Studio, Education Development Center.*]

STUDENTS-HUB.com Uploaded By: Malak Obaid

Diffraction of Other Particles

The wave properties of neutral atoms and molecules were first demonstrated by O. Stern and I. Estermann in 1930 with beams of helium atoms and hydrogen molecules diffracted from a lithium fluoride crystal. Since the particles are neutral, there is no possibility of accelerating them with electrostatic potentials. The energy of the molecules was that of their average thermal motion, about 0.03 eV, which implies a de Broglie wavelength of about 0.10 nm for these molecules, according to Equation 5-2. Because of their low energy, the scattering occurs just from the array of atoms on the surface of the crystal, in contrast to Davisson and Germer's experiment. Figure 5-9 illustrates the geometry of the surface scattering, the experimental arrangement, and the results. Figure 5-9*c* indicates clearly the diffraction of He atom waves.

The diffraction patterns formed by helium atom waves are used to study impurities and defects on the surfaces of crystals. Being a noble gas, helium does not react chemically with molecules on the surface nor "stick" to the surface.

Since then, diffraction of other atoms, of protons, and of neutrons has been observed (see Figures 5-10, 5-11, and 5-12 on page 194). In all cases the measured wavelengths agree with de Broglie's prediction. There is thus no doubt that all matter has wavelike, as well as particlelike, properties, in symmetry with electromagnetic radiation.

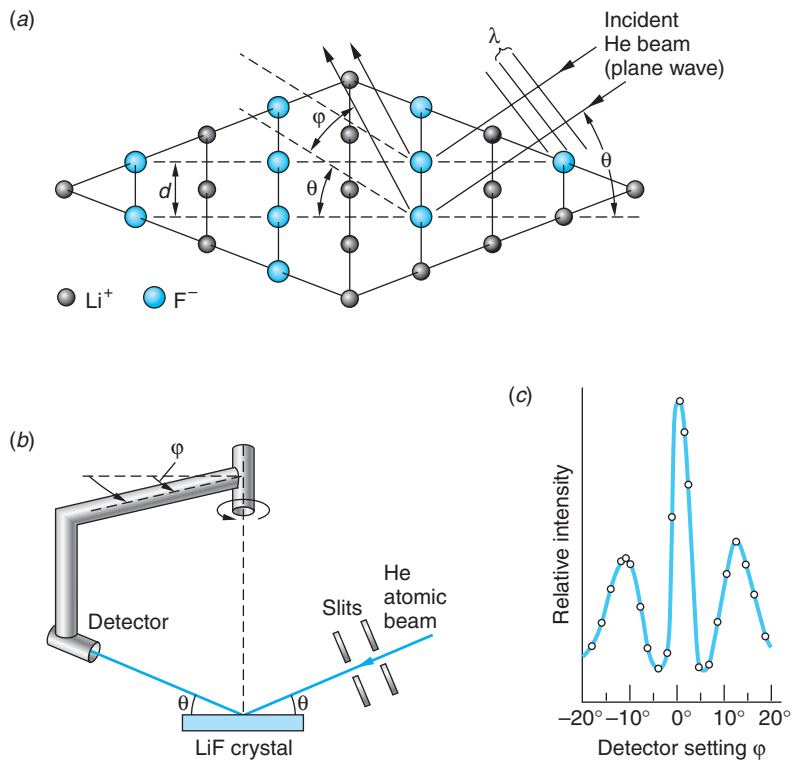

Figure 5-9 (*a*) He atoms impinge upon the surface of the LiF crystal at angle θ (θ = 18.5° in Estermann and Stern's experiment). The reflected beam also makes the same angle θ with the surface but is also scattered at azimuthal angles φ relative to an axis perpendicular to the surface. (*b*) The detector views the surface at angle θ but can scan through the angle φ. (*c*) At angle φ where the path difference ($d \sin\varphi$) between adjacent "rays" is $n\lambda$, constructive interference, i.e., a diffraction peak, occurs. The $n = 1$ peaks occur on either side of the $n = 0$ maximum.

STUDENTS-HUB.com Uploaded By: Malak Obaid

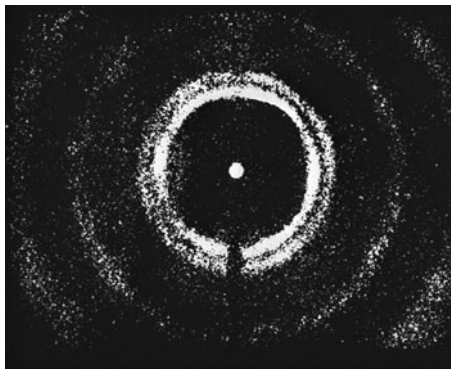

Figure 5-10 Diffraction pattern produced by 0.0568-eV neutrons (de Broglie wavelength of 0.120 nm) and a target of polycrystalline copper. Note the similarity in the patterns produced by x rays, electrons, and neutrons. [*Courtesy of C. G. Shull.*]

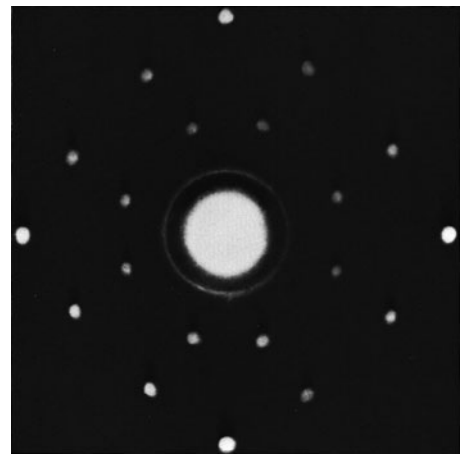

Figure 5-11 Neutron Laue pattern of NaCl. Compare this with the x-ray Laue pattern in Figure 3-14. [*Courtesy of E. O. Wollan and C. G. Shull.*]

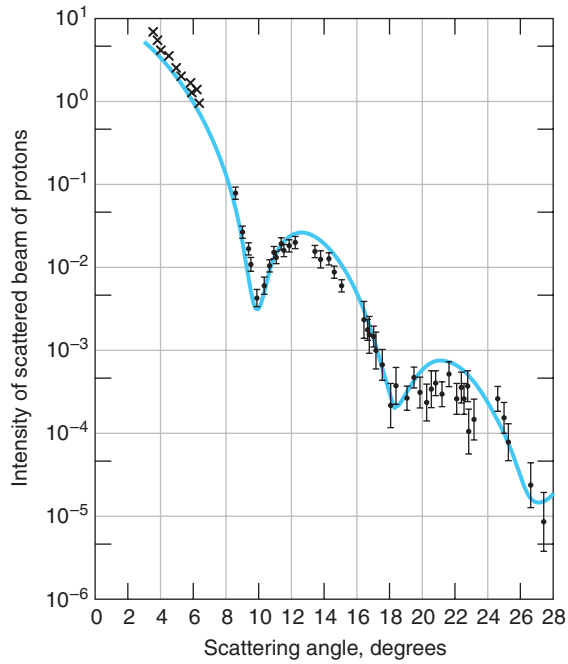

Figure 5-12 Nuclei provide scatterers whose dimensions are of the order of 10^{-15} m. Here the diffraction of 1-GeV protons from oxygen nuclei result in a pattern similar to that of a single slit.

An Easy Way to Determine de Broglie Wavelengths

It is frequently helpful to know the de Broglie wavelength for particles with a specific kinetic energy. For low energies where relativistic effects can be ignored, the equation leading to Equation 5-4 can be rewritten in terms of the kinetic energy as follows:

$$\lambda = \frac{h}{p} = \frac{h}{\sqrt{2mE_k}} \qquad \textbf{5-7}$$

STUDENTS-HUB.com Uploaded By: Malak Obaid

To find the equivalent expression that covers both relativistic and nonrelativistic speeds, we begin with the relativistic equation relating the total energy to the momentum:

$$E^2 = (pc)^2 + (mc^2)^2 \qquad \textbf{2-31}$$

Writing E_0 for the rest energy mc^2 of the particle for convenience, this becomes

$$E^2 = (pc)^2 + E_0^2 \qquad \textbf{5-8}$$

Since the total energy $E = E_0 + E_k$, Equation 5-8 becomes

$$(E_0 + E_k)^2 = (pc)^2 + E_0^2$$

that, when solved for p, yields

$$p = \frac{(2E_0E_k + E_k^2)^{1/2}}{c}$$

from which Equation 5-2 gives

$$\lambda = \frac{hc}{(2E_0E_k + E_k^2)^{1/2}} \qquad \textbf{5-9}$$

This can be written in a particularly useful way applicable to any particle of any energy by dividing the numerator and denominator by the rest energy $E_0 = mc^2$ as follows:

$$\lambda = \frac{hc/mc^2}{(2E_0E_k + E_k^2)^{1/2}/E_0} = \frac{h/mc}{[2(E_k/E_0) + (E_k/E_0)^2]^{1/2}}$$

Recognizing h/mc as the Compton wavelength λ_c of the particle of mass m (see Section 3-4), we have that, for any particle,

$$\lambda/\lambda_c = \frac{1}{[2(E_k/E_0) + (E_k/E_0)^2]^{1/2}} \qquad \textbf{5-10}$$

A log-log graph of λ/λ_c versus E_k/E_0 is shown in Figure 5-13. It has two sections of nearly constant slope, one for $E_k \ll mc^2$ and the other for $E_k \gg mc^2$, connected by a curved portion lying roughly between $0.1 < E_k/E_0 < 10$. The following example illustrates the use of Figure 5-13.

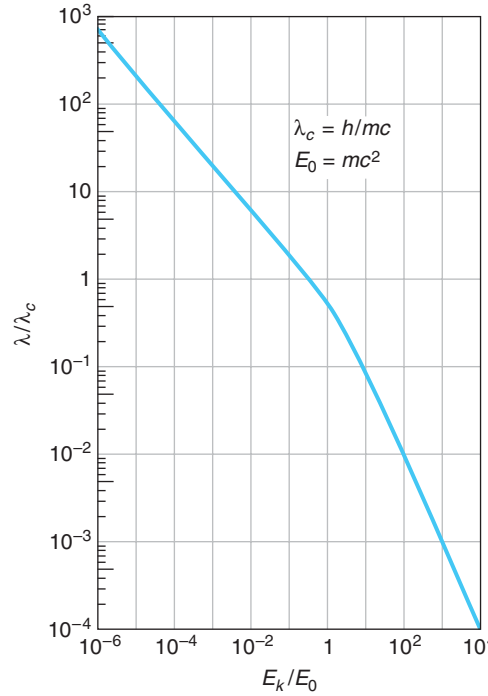

Figure 5-13 The de Broglie wavelength λ expressed in units of the Compton wavelength λ_c for a particle of mass m versus the kinetic energy of the particle E_k expressed in units of its rest energy $E_0 = mc^2$. For protons and neutrons $E_0 = 0.938$ GeV and $\lambda_c = 1.32$ fm. For electrons $E_0 = 0.511$ MeV and $\lambda_c = 0.00234$ nm.

EXAMPLE 5-3 The de Broglie Wavelength of a Cosmic Ray Proton Detectors on board a satellite measure the kinetic energy of a cosmic ray proton to be 150 GeV. What is the proton's de Broglie wavelength, as read from Figure 5-13?

SOLUTION

The rest energy of the proton is $mc^2 = 0.938$ GeV and the proton's mass is 1.67×10^{-27} kg. Thus, the ratio E_k/E_0 is

$$\frac{E_k}{E_0} = \frac{150 \text{ GeV}}{0.938 \text{ GeV}} = 160$$

STUDENTS-HUB.com Uploaded By: Malak Obaid

This value on the curve corresponds to about 6×10^{-3} on the λ/λ_c axis. The Compton wavelength of the proton is

$$\lambda_c = \frac{h}{mc} = \frac{6.63 \times 10^{-34}\ \text{J}\cdot\text{s}}{(1.67 \times 10^{-27}\ \text{kg})(3 \times 10^{8}\ \text{m/s})} = 1.32 \times 10^{-15}\ \text{m}$$

and we have then for the particle's de Broglie wavelength

$$\lambda = (6 \times 10^{-3})(1.32 \times 10^{-15}\ \text{m}) = 7.9 \times 10^{-18}\ \text{m} = 7.9 \times 10^{-3}\ \text{fm}$$

Questions

1. Since the electrons used by Davisson and Germer were low energy, they penetrated only a few atomic layers into the crystal, so it is rather surprising that the effects of the inner layers shows so clearly. What feature of the diffraction is most affected by the relatively shallow penetration?
2. How might the frequency of de Broglie waves be measured?
3. Why is it not reasonable to do crystallographic studies with protons?

5-3 Wave Packets

In any discussion of waves the question arises, "What's waving?" For some waves the answer is clear: for waves on the ocean, it is the water that "waves"; for sound waves in air, it is the molecules that make up the air; for light, it is the $\mathscr{E}$ and the **B**. So what is waving for matter waves? For matter waves as for light waves, there is no "ether." As will be developed in this section and the next, for matter it is the *probability of finding the particle* that waves.

Classical waves are solutions of the classical *wave equation*

$$\frac{\partial^2 y}{\partial x^2} = \frac{1}{v^2}\frac{\partial^2 y}{\partial t^2} \qquad \textbf{5-11}$$

Important among classical waves is the *harmonic wave* of amplitude y_0, frequency f, and period T, traveling in the $+x$ direction as written here:

$$y(x, t) = y_0 \cos(kx - \omega t) = y_0 \cos 2\pi\left(\frac{x}{\lambda} - \frac{t}{T}\right) = y_0 \cos\frac{2\pi}{\lambda}(x - vt) \qquad \textbf{5-12}$$

where the *angular frequency* ω and the *wave number*[8] k are defined by

$$\omega = 2\pi f = \frac{2\pi}{T} \qquad \textbf{5-13}\boldsymbol{a}$$

and

$$k = \frac{2\pi}{\lambda} \qquad \textbf{5-13}\boldsymbol{b}$$

and the velocity v of the wave, the so-called *wave* or *phase velocity* v_p, is given by

$$v_p = f\lambda \qquad \textbf{5-14}$$

STUDENTS-HUB.com Uploaded By: Malak Obaid

A familiar wave phenomenon that cannot be described by a single harmonic wave is a pulse, such as the flip of one end of a long string (Figure 5-14), a sudden noise, or the brief opening of a shutter in front of a light source. The main characteristic of a pulse is localization in time and space. A single harmonic wave is not localized in either time or space. The description of a pulse can be obtained by the superposition of a group of harmonic waves of different frequencies and wavelengths. Such a group is called a *wave packet*. The mathematics of representing arbitrarily shaped pulses by sums of sine or cosine functions involves Fourier series and Fourier integrals. We will illustrate the phenomenon of wave packets by considering some simple and somewhat artificial examples and discussing the general properties qualitatively. Wave groups are particularly important because a wave description of a particle must include the important property of localization.

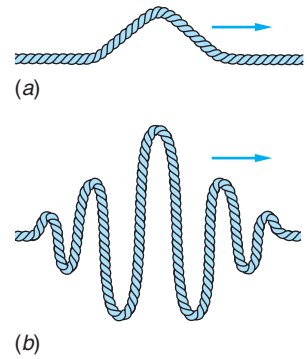

Figure 5-14 (*a*) Wave pulse moving along a string. A pulse has a beginning and an end; i.e., it is localized, unlike a pure harmonic wave, which goes on forever in space and time. (*b*) A wave packet formed by the superposition of harmonic waves.

Consider a simple group consisting of only two waves of equal amplitude and nearly equal frequencies and wavelengths. Such a group occurs in the phenomenon of beats and is described in most introductory textbooks. The quantities k, ω, and v are related to one another via Equations 5-13 and 5-14. Let the wave numbers be k_1 and k_2, the angular frequencies ω_1 and ω_2, and the speeds v_1 and v_2. The sum of the two waves is

$$y(x, t) = y_0 \cos(k_1 x - \omega_1 t) + y_0 \cos(k_2 x - \omega_2 t)$$

which, with the use of a bit of trigonometry, becomes

$$y(x, t) = 2y_0 \cos\left(\frac{\Delta k}{2} x - \frac{\Delta \omega}{2} t\right) \cos\left(\frac{k_1 + k_2}{2} x - \frac{\omega_1 + \omega_2}{2} t\right)$$

where $\Delta k = k_2 - k_1$ and $\Delta\omega = \omega_2 - \omega_1$. Since the two waves have nearly equal values of k and ω, we will write $\bar{k} = (k_1 + k_2)/2$ and $\bar{\omega} = (\omega_1 + \omega_2)/2$ for the mean values. The sum is then

$$y(x, t)) = 2y_0 \cos\left(\frac{1}{2}\Delta k x - \frac{1}{2}\Delta\omega t\right) \cos(\bar{k}x - \bar{\omega}t) \qquad \textbf{5-15}$$

Figure 5-15 shows a sketch of $y\ (x, t_0)$ versus x at some time t_0. The dashed curve is the envelope of the group of two waves, given by the first cosine term in Equation 5-15. The wave within the envelope moves with the speed $\bar{\omega}/\bar{k}$, the phase velocity v_p due to the second cosine term. If we write the first (amplitude-modulating) term as $\cos\{\frac{1}{2}\Delta k[x - (\Delta\omega/\Delta k)\, t]\}$, we see that the envelope moves with speed $\Delta\omega/\Delta k$. The speed of the envelope is called the *group velocity* v_g.

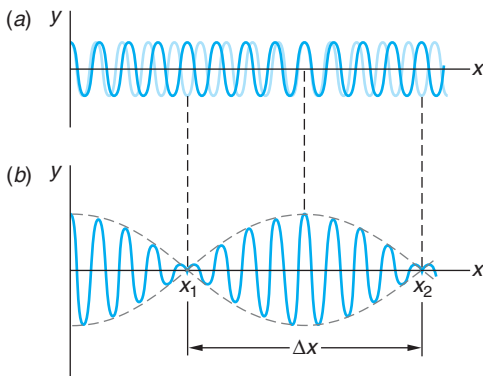

Figure 5-15 Two waves of slightly different wavelength and frequency produce beats. (*a*) Shows $y(x)$ at a given instant for each of the two waves. The waves are in phase at the origin, but because of the difference in wavelength, they become out of phase and then in phase again. (*b*) The sum of these waves. The spatial extent of the group Δx is inversely proportional to the difference in wave numbers Δk, where k is related to the wavelength by $k = 2\pi/\lambda$. Identical figures are obtained if y is plotted versus time t at a fixed point x. In that case the extent in time Δt is inversely proportional to the frequency difference $\Delta\omega$.

STUDENTS-HUB.com Uploaded By: Malak Obaid

A more general wave packet can be constructed if, instead of adding just two sinusoidal waves as in Figure 5-15, we superpose a larger, finite number with slightly different wavelengths and different amplitudes. For example, Figure 5-16*a* illustrates the superposing of seven cosines with wavelengths from $\lambda_9 = 1/9$ to $\lambda_{15} = 1/15$ (wave numbers from $k_9 = 18\pi$ to $k_{15} = 30\pi$) at time t_0. The waves are all in phase at $x = 0$ and again at $x = \pm 12, x = \pm 24, \ldots$. Their sum $y(x, t_0) = \sum_{i=9}^{15} y_i(x, t_0)$ oscillates with maxima at those values of x, decreasing and increasing at other values as a result of the changing phases of the waves (see Figure 5-16*b*). Now, if we superpose an infinite number of waves from the same range of wavelengths and wave numbers as in Figure 5-16 with infinitesimally different values of k, the central group around $x = 0$ will be essentially the same as in that figure. However, the additional groups will no longer be present since there is now no length along the x axis into which an exactly integral number of all of the infinite number of component waves can fit. Thus, we have formed a single wave packet throughout this (one-dimensional) space.

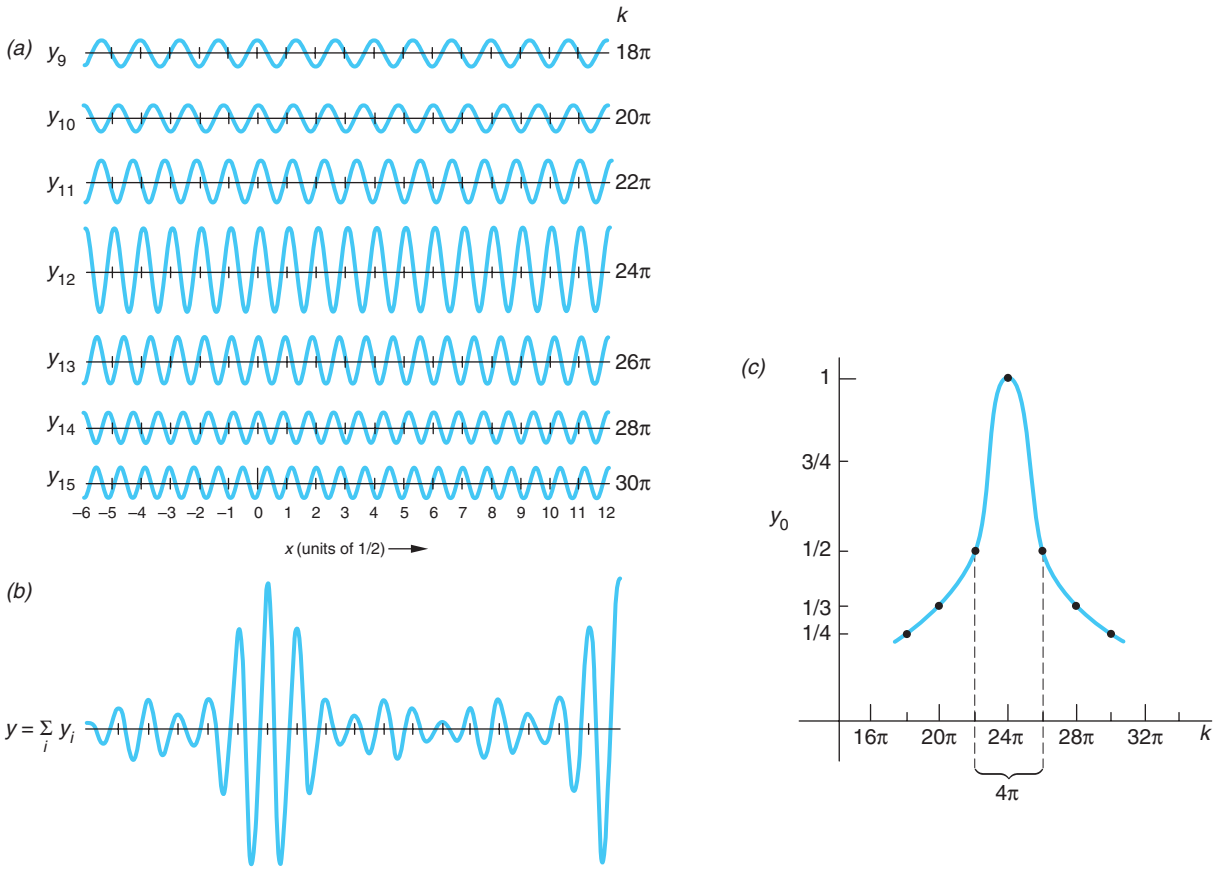

Figure 5-16 (*a*) Superposition of seven sinusoids $y_k(x, t) = y_{0k} \cos(kx - \omega t)$ with uniformly spaced wave numbers ranging from $k = (2\pi)9$ to $k = (2\pi)15$ with $t = 0$. The maximum amplitude is 1 at the center of the range ($k = (2\pi)12$), decreasing to 1/2, 1/3, and 1/4, respectively, for the waves on each side of the central wave. (*b*) The sum $y(x, 0) = \sum_{i=9}^{15} y_i(x, 0)$ is maximum at $x = 0$ with additional maxima equally spaced along the $\pm x$ axis. (*c*) Amplitudes of the sinusoids y_i versus wave number k.

STUDENTS-HUB.com Uploaded By: Malak Obaid

This packet moves at the group velocity $v_g = d\omega/dk$. The mathematics needed to demonstrate the above involves use of the Fourier integral described in the Classical Concept Review.

The phase velocities of the individual harmonic waves are given by Equation 5-14:

$$v_p = f\lambda = \left(\frac{\omega}{2\pi}\right)\left(\frac{2\pi}{k}\right) = \frac{\omega}{k}$$

Writing this as $\omega = kv_p$, the relation between the group and phase velocities is given by Equation 5-16:

$$v_g = \frac{d\omega}{dk} = v_p + k\frac{dv_p}{dk} \qquad \textbf{5-16}$$

If the phase velocity is the same for all frequencies and wavelengths, then $dv_p/dk = 0$, and the group velocity is the same as the phase velocity. A medium for which the phase velocity is the same for all frequencies is said to be *nondispersive*. Examples are waves on a perfectly flexible string, sound waves in air, and electromagnetic waves in a vacuum. An important characteristic of a nondispersive medium is that, since all the harmonic waves making up a packet move with the same speed, the packet maintains its shape as it moves; thus, it does not change its shape in time. Conversely, if the phase velocity is different for different frequencies, the shape of the pulse will change as it travels. In that case the group velocity and phase velocity are not the same. Such a medium is called a *dispersive* medium; examples are water waves, waves on a wire that is not perfectly flexible, light waves in a medium such as glass or water in which the index of refraction has a slight dependence on frequency, and electron waves. It is the speed of the packet, the group velocity v_g, that is normally seen by an observer.

Classical Uncertainty Relations

Notice that the width of the group[9] Δx of the superposition $y(x, t_0)$ in Figure 5-16*b* is just a bit larger than $1/12$. Similarly, the graph of the amplitude of these waves versus k has width $\Delta k = 4\pi$, which is a bit more than 12 (Figure 5-16*c*), so we see that

$$\Delta k \Delta x \sim 1 \qquad \textbf{5-17}$$

By a similar analysis, we would also conclude that

$$\Delta\omega\Delta t \sim 1 \qquad \textbf{5-18}$$

The range of wavelengths or frequencies of the harmonic waves needed to form a wave packet depends on the extent in space and duration in time of the pulse. In general, if the extent in space Δx is to be small, the range Δk of wave numbers must be large. Similarly, if the duration in time Δt is small, the range of frequencies $\Delta\omega$ must be large. We have written these as order-of-magnitude equations because the exact value of the products $\Delta k\Delta x$ and $\Delta\omega\Delta t$ depends on how these ranges are defined, as well as on the particular shape of the packets. Equation 5-18 is sometimes known as the *response time–bandwidth* relation, expressing the result that a circuit component such as an amplifier must have a large bandwidth ($\Delta\omega$) if it is to be able to respond to signals of short duration.

The classical uncertainty relations define the range of signal frequencies to which all kinds of communications equipment and computer systems must respond, from cell phones to supercomputers.

STUDENTS-HUB.com Uploaded By: Malak Obaid

There is a slight variation of Equation 5-17 that is also helpful in interpreting the relation between Δx and Δk. Differentiating the wave number in Equation 5-13*b* yields

$$dk = \frac{-2\pi d\lambda}{\lambda^2} \qquad \textbf{5-19}$$

Replacing the differentials by small intervals and concerning ourselves only with magnitudes, Equation 5-19 becomes

$$\Delta k = \frac{2\pi\Delta\lambda}{\lambda^2}$$

which when substituted into Equation 5-17 gives

$$\Delta x\Delta\lambda \approx \frac{\lambda^2}{2\pi} \qquad \textbf{5-20}$$

Equation 5-20 says that the product of the spatial extent of a classical wave Δx and the uncertainty (or "error") in the determination of its wavelength $\Delta\lambda$ will always be of the order of $\lambda^2/2\pi$. The following brief examples will illustrate the meaning of Equations 5-17 and 5-18, often referred to as the *classical uncertainty relations*, and Equation 5-20.

EXAMPLE 5-4 $\Delta\lambda$ for Ocean Waves Standing in the middle of a 20-m-long pier, you notice that at any given instant there are 15 wave crests between the two ends of the pier. Estimate the minimum uncertainty in the wavelength that could be computed from this information.

SOLUTION

1. The minimum uncertainty $\Delta\lambda$ in the wavelength is given by Equation 5-20:

$$\Delta x\Delta\lambda = \frac{\lambda^2}{2\pi}$$

2. The wavelength λ of the waves is

$$\lambda = \frac{20\text{ m}}{15\text{ waves}} = 1.3\text{ m}$$

3. The spatial extent of the waves used for this calculation is:

$$\Delta x = 20\text{ m}$$

4. Solving Equation 5-20 for $\Delta\lambda$ and substituting these values gives

$$\Delta\lambda = \frac{\lambda^2}{2\pi\Delta x} = \frac{(1.3)^2}{2\pi \times 20}$$
$$= 0.013\text{ m}$$
$$\Delta\lambda \approx 0.01\text{ m} = 1\text{ cm}$$

Remarks: *This is the minimum uncertainty. Any error that may exist in the measurement of the number of wave crests and the length of the pier would add further uncertainty to the determination of* λ.

STUDENTS-HUB.com Uploaded By: Malak Obaid

EXAMPLE 5-5 Frequency Control The frequency of the alternating voltage produced at electric generating stations is carefully maintained at 60.00 Hz. The frequency is monitored on a digital frequency meter in the control room. For how long must the frequency be measured and how often can the display be updated if the reading is to be accurate to within 0.01 Hz?

SOLUTION

Since $\omega = 2\pi f$, then $\Delta\omega = 2\pi\Delta f = 2\pi(0.01)$ rad/s and

$$\Delta t \sim 1/\Delta\omega = 1/2\pi(0.01)$$

$$\Delta t \sim 16 \text{ s}$$

Thus, the frequency must be measured for about 16 s if the reading is to be accurate to 0.01 Hz and the display cannot be updated more often than once every 16s.

Questions

4. Which is more important for communication, the group velocity or the phase velocity?
5. What are Δx and Δk for a purely harmonic wave of a single frequency and wavelength?

Particle Wave Packets

The quantity analogous to the displacement $y(x, t)$ for waves on a string, to the pressure $P(x, t)$ for a sound wave, or to the electric field $\mathscr{E}(x, t)$ for electromagnetic waves is called the *wave function for particles* and is usually designated $\Psi(x, t)$. It is $\Psi(x, t)$ that we will relate to the probability of finding the particle and, as we alerted you earlier, it is the probability that waves. Consider, for example, an electron wave consisting of a single frequency and wavelength; we could represent such a wave by any of the following, exactly as we did the classical wave: $\Psi(x, t) = A\cos(kx - \omega t)$, $\Psi(x, t) = A\sin(kx - \omega t)$, or $\Psi(x, t) = Ae^{i(kx-\omega t)}$.

The phase velocity for this wave is given by

$$v_p = f\lambda = (E/h)(h/p) = E/p$$

where we have used the de Broglie relations for the wavelength and frequency. Using the nonrelativistic expression for the energy of a particle moving in free space, i.e., no potential energy) with no forces acting upon it,

$$E = \frac{1}{2}mv^2 = \frac{p^2}{2m}$$

we see that the phase velocity is

$$v_p = E/p = (p^2/2m)/p = p/2m = v/2$$

i.e., the phase velocity of the wave is half the velocity of an electron with momentum p. The phase velocity does *not* equal the particle velocity. Moreover, a wave of a single frequency and wavelength is not localized but is spread throughout space, which makes it difficult to see how the particle and wave properties of the electron could be related.

STUDENTS-HUB.com Uploaded By: Malak Obaid

An application of phase and particle speeds by nature: produce a wave on a still pond (or in a bathtub) and watch the wavelets that make up the wave appear to "climb over" the wave crest at twice the speed of the wave.

Thus, for the electron to have the particle property of being localized, the matter waves of the electron must also be limited in spatial extent—i.e., realistically, $\Psi(x, t)$ must be a wave packet containing many more than one wave number k and frequency ω. It is the wave packet $\Psi(x, t)$ that we expect to move at a group velocity equal to the particle velocity, which we will show below is indeed the case. The particle, if observed, we will expect to find somewhere within the spatial extent of the wave packet $\Psi(x, t)$, precisely where within that space being the subject of the next section.

To illustrate the equality of the group velocity v_g and the particle velocity v, it is convenient to express de Broglie's relations in a slightly different form. Writing Equation 5-1 as follows,

$$E = hf = h\omega/2\pi \qquad \text{or} \qquad E = \hbar\omega \tag{5-21}$$

and Equation 5-2 as

$$p = \frac{h}{\lambda} = \frac{h}{2\pi/k} = \frac{hk}{2\pi} \qquad \text{or} \qquad p = \hbar k \tag{5-22}$$

The group velocity is then given by

$$v_g = d\omega/dk = (dE/\hbar)/(dp/\hbar) = dE/dp$$

Again using the nonrelativistic expression $E = p^2/2m$, we have that

$$v_g = dE/dp = p/m = v$$

and *the wave packet* $\Psi(x, t)$ *moves with the velocity of the electron*. This was, in fact, one of de Broglie's reasons for choosing Equations 5-1 and 5-2. (De Broglie used the relativistic expression relating energy and momentum, which also leads to the equality of the group velocity and particle velocity.)

5-4 The Probabilistic Interpretation of the Wave Function

Let us consider in more detail the relation between the wave function $\Psi(x, t)$ and the location of the electron. We can get a hint about this relation from the case of light. The wave equation that governs light is Equation 5-11, with $y = \mathscr{E}$, the electric field, as the wave function. The energy per unit volume in a light wave is proportional to $\mathscr{E}^2$, but the energy in a light wave is quantized in units of hf for each photon. We expect, therefore, that the number of photons in a unit volume is proportional to $\mathscr{E}^2$, a connection first pointed out by Einstein.

Consider the famous double-slit interference experiment (Figure 5-17). The pattern observed on the screen is determined by the interference of the waves from the slits. At a point on the screen where the wave from one slit is 180° out of phase with that from the other, the resultant electric field is zero; there is no light energy at this point, and this point on the screen is dark. If we reduce the intensity to a very low value, we can still observe the interference pattern if we replace the ordinary screen by a scintillation screen or a two-dimensional array of tiny photon detectors (e.g., a CCD camera) and wait a sufficient length of time.

STUDENTS-HUB.com Uploaded By: Malak Obaid

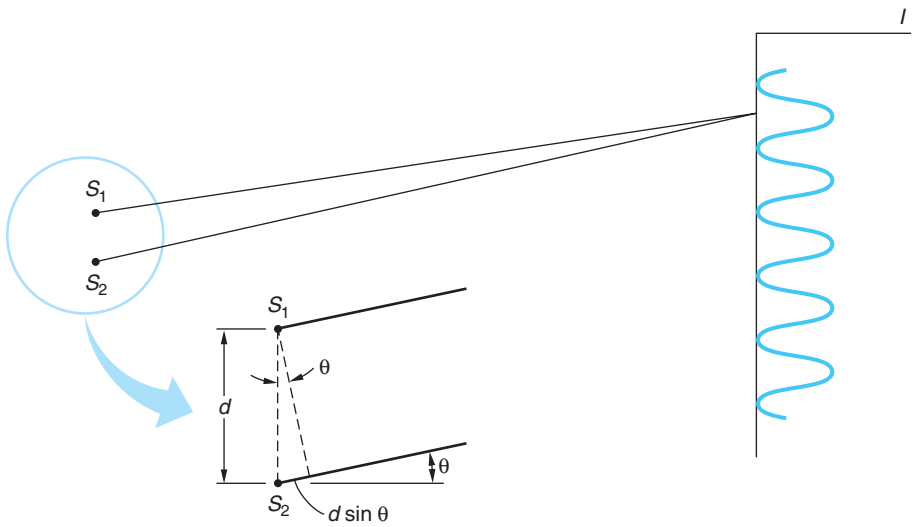

Figure 5-17 Two-source interference pattern. If the sources are coherent and in phase, the waves from the sources interfere constructively at points for which the path difference ($d \sin\theta$) is an integral number of wavelengths.

The interaction of light with the detector or scintillator is a quantum phenomenon. If we illuminate the scintillators or detectors for only a very short time with a low-intensity source, we do not see merely a weaker version of the high-intensity pattern; we see, instead, "dots" caused by the interactions of individual photons (Figure 5-18). At points where the waves from the slits interfere destructively, there are no dots, and at points where the waves interfere constructively, there are many dots. However,

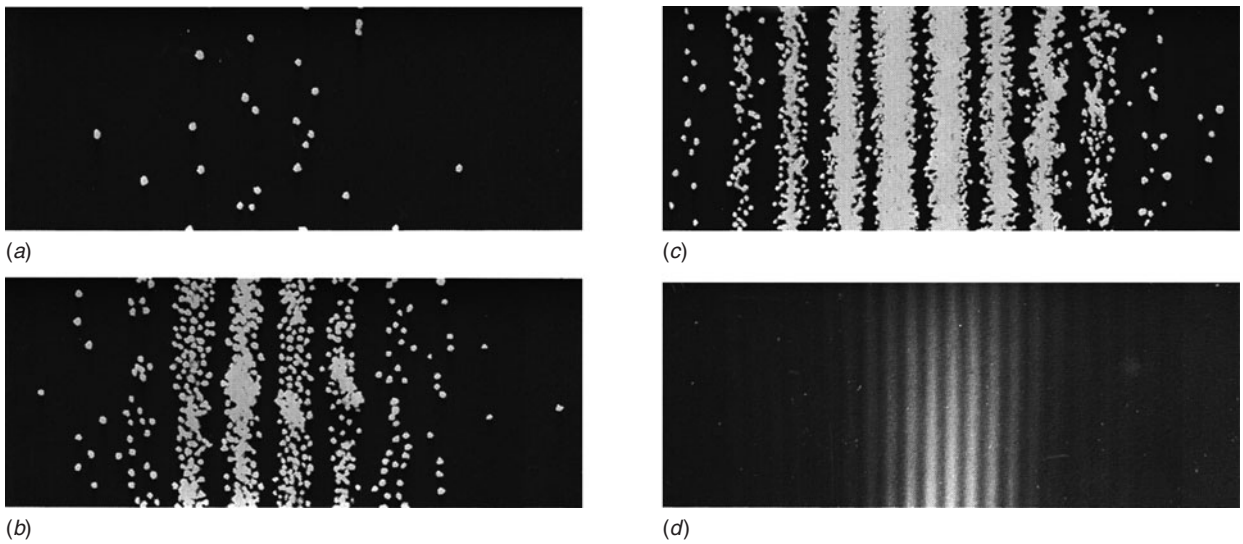

Figure 5-18 Growth of two-slit interference pattern. The photo (*d*) is an actual two-slit electron interference pattern in which the film was exposed to millions of electrons. The pattern is identical to that usually obtained with photons. If the film were to be observed at various stages, such as after being struck by 28 electrons, then after about 1000 electrons, and again after about 10,000 electrons, the patterns of individually exposed grains would be similar to those shown in (*a*), (*b*), and (*c*) except that the exposed dots would be smaller than the dots drawn here. Note that there are no dots in the region of the interference minima. The probability of any point of the film being exposed is determined by wave theory, whether the film is exposed by electrons or photons. [*Parts (a), (b), and (c) from E. R. Huggins, Physics 1, © by W. A. Benjamin, Inc., Menlo Park, California. Photo (d) courtesy of C. Jonsson.*]

STUDENTS-HUB.com Uploaded By: Malak Obaid

when the exposure is short and the source weak, random fluctuations from the average predictions of the wave theory are clearly evident. If the exposure is long enough that many photons reach the detector, the fluctuations average out and the quantum nature of light is not noticed. The interference pattern depends only on the total number of photons interacting with the detector and not on the rate. *Even when the intensity is so low that only one photon at a time reaches the detector, the wave theory predicts the correct average pattern.* For low intensities, we therefore interpret $\mathscr{E}^2$ as proportional to the *probability* of detecting a photon in a unit volume of space. At points on the detector where $\mathscr{E}^2$ is zero, photons are never observed, whereas they are most likely to be observed at points where $\mathscr{E}^2$ is large.

It is not necessary to use light waves to produce an interference pattern. Such patterns can be produced with electrons and other particles as well. In the wave theory of electrons the de Broglie wave of a *single* electron is described by a wave function Ψ. The amplitude of Ψ at any point is related to the probability of finding the particle at that point. In analogy with the foregoing interpretation of $\mathscr{E}^2$, *the quantity* $|\Psi|^2$ *is proportional to the probability of detecting an electron in a unit volume*, where $|\Psi|^2 \equiv \Psi^*\Psi$, the function Ψ^* being the complex conjugate of Ψ. In one dimension, $|\Psi|^2 dx$ is the probability of an electron being in the interval dx.[10] (See Figure 5-19.) If we call this probability $P(x)dx$, where $P(x)$ is the probability distribution function, we have

$$P(x)dx = |\Psi|^2 dx \qquad \textbf{5-23}$$

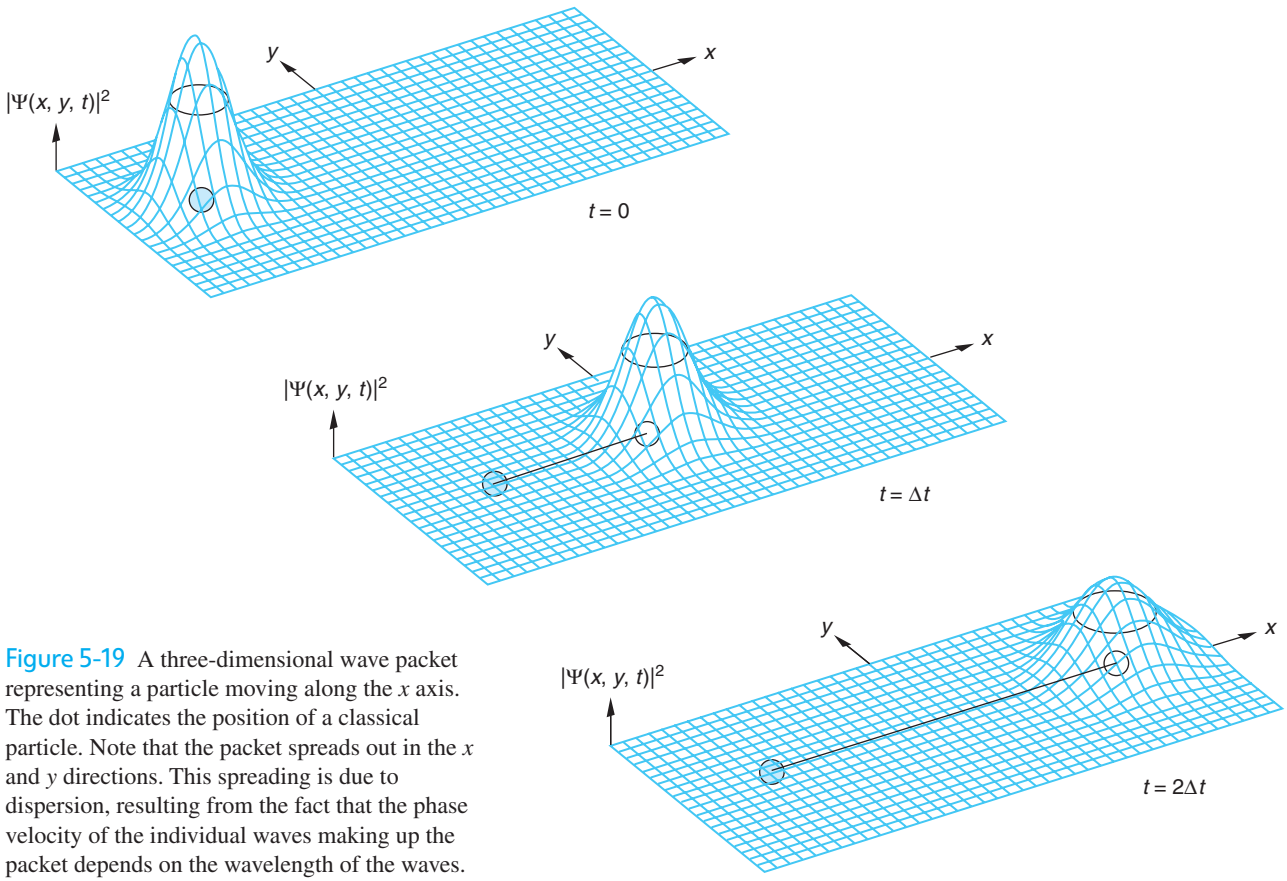

Figure 5-19 A three-dimensional wave packet representing a particle moving along the x axis. The dot indicates the position of a classical particle. Note that the packet spreads out in the x and y directions. This spreading is due to dispersion, resulting from the fact that the phase velocity of the individual waves making up the packet depends on the wavelength of the waves.

STUDENTS-HUB.com Uploaded By: Malak Obaid

In the next chapter we will more thoroughly discuss the amplitudes of matter waves associated with particles, in particular developing the mathematical system for computing the amplitudes and probabilities in various situations. The uneasiness that you may feel at this point regarding the fact that we have not given a precise physical interpretation to the amplitude of the de Broglie matter wave can be attributed in part to the complex nature of the wave amplitude; i.e., it is in general a complex function with a real part and an imaginary part, the latter proportional to $i = (-1)^{1/2}$. We cannot directly measure or physically interpret complex numbers in our world of real numbers. However, as we will see, defining the probability in terms of $|\Psi|^2$, which is always real, presents no difficulty in its physical interpretation. Thus, even though the amplitudes of the wave functions Ψ have no simple meaning, the waves themselves behave just as classical waves do, exhibiting the wave characteristics of reflection, refraction, interference, and diffraction and obeying the principles of superposition.

5-5 The Uncertainty Principle

The uncertainty relations for classical wave packets (Equations 5-17 and 5-18) have very important matter wave analogs.

Consider a wave packet $\Psi(x, t)$ representing an electron. The most probable position of the electron is the value of x for which $|\Psi(x, t)|^2$ is a maximum. Since $|\Psi(x, t)|^2$ is proportional to the probability that the electron is located at x and $|\Psi(x, t)|^2$ is nonzero for a range of values of x, there is an *uncertainty* in the position of the electron (see Figure 5-19). This means that if we make a number of position measurements on identical electrons—electrons with the same wave function—we will not always obtain the same result. In fact, the distribution function for the results of such measurements will be given by $|\Psi(x, t)|^2$. If the wave packet is very narrow, the uncertainty in position will be small. However, a narrow wave packet must contain a wide range of wave numbers k. Since the momentum is related to the wave number by $p = hk$, a wide range of k values means a wide range of momentum values. We have seen that for all wave packets the ranges Δx and Δk are related by

$$\Delta k \Delta x \sim 1 \qquad \textbf{5-17}$$

Similarly, a packet that is localized in time Δt must contain a range of frequencies $\Delta\omega$, where the ranges are related by

$$\Delta\omega \Delta t \sim 1 \qquad \textbf{5-18}$$

Equations 5-17 and 5-18 are inherent properties of waves. If we multiply these equations by $\hbar$ and use $p = \hbar k$ and $E = \hbar\omega$, we obtain

$$\Delta x \Delta p \sim \hbar \qquad \textbf{5-24}$$

and

$$\Delta E \Delta t \sim \hbar \qquad \textbf{5-25}$$

Equations 5-24 and 5-25 provide a statement of the *uncertainty principle* first enunciated in 1927 by Werner K. Heisenberg.[11] Equation 5-24 expresses the fact that the distribution functions for position and momentum cannot both be made arbitrarily narrow simultaneously (see Figure 5-16); thus, measurements of position and momentum will have similar uncertainties, which are related by Equation 5-24. Of course, because of

STUDENTS-HUB.com Uploaded By: Malak Obaid

Heisenberg's uncertainty principle is the key to the existence of *virtual particles* that hold the nuclei together (see Chapter 11) and is the root of quantum fluctuations that may have been the origin of the Big Bang (see Chapter 13).

inaccurate measurements, the product of Δx and Δp can be, and usually is, much larger than $\hbar$. The lower limit is not due to any technical problem in the design of measuring equipment that might be solved at some later time; it is instead due to the wave and particle nature of both matter and light.

If we define precisely what we mean by the uncertainty in the measurements of position and momentum, we can give a precise statement of the uncertainty principle. For example, if σ_x is the standard deviation for measurements of position and σ_k is the standard deviation for measurements of the wave number, the product $\sigma_x\sigma_k$ has its minimum value of $1/2$ when the distribution functions are Gaussian. If we define Δx and Δp to be the standard deviations, the minimum value of their product is $\hbar/2$. Thus,

$$\Delta x \Delta p \geq \frac{1}{2}\hbar \qquad \textbf{5-26}$$

Similarly,

$$\Delta E \Delta t \geq \frac{1}{2}\hbar \qquad \textbf{5-27}$$

Question

6. Does the uncertainty principle say that the momentum of a particle can never be precisely known?

EXPLORING
The Gamma-Ray Microscope

Let us see how one might attempt to make a measurement so accurate as to violate the uncertainty principle. A common way to measure the position of an object such as an electron is to look at it with light, i.e., scatter light from it and observe the diffraction pattern. The momentum can be obtained by looking at it again a short time later and computing what velocity it must have had the instant before the light scattered from it. Because of diffraction effects, we cannot hope to make measurements of length (position) that are smaller than the wavelength of the light used, so we will use the shortest-wavelength light that can be obtained, gamma rays. (There is, in principle, no limit to how short the wavelength of electromagnetic radiation can be.) We also know that light carries momentum and energy, so that when it scatters off the electron, the motion of the electron will be disturbed, affecting the momentum. We must, therefore, use the minimum intensity possible so as to disturb the electron as little as possible. Reducing the intensity decreases the number of photons, but we must scatter at least one photon to observe the electron. The minimum possible intensity, then, is that corresponding to one photon. The scattering of a photon by a free electron is, of course, a Compton scattering, which was discussed in Section 3-4. The momentum of the photon is $hf/c = h/\lambda$. The smaller λ that is used to measure the position, the more the photon will disturb the electron, but we can correct for that with a Compton-effect analysis, provided only that we know the photon's momentum and the scattering angles of the event.

Figure 5-20 illustrates the problem. (This illustration was first given as a gedanken-experiment, or thought experiment, by Heisenberg. Since a single photon doesn't form a diffraction pattern, think of the diffraction pattern as being built up by photons from

STUDENTS-HUB.com Uploaded By: Malak Obaid

many identical scattering experiments.) The position of the electron is to be determined by viewing it through a microscope. We will assume that only one photon is used. We can take for the uncertainty in position the minimum separation distance for which two objects can be resolved; this is[12]

$$\Delta x = \frac{\lambda}{2 \sin \theta}$$

where θ is the half angle subtended by the lens aperture, as shown in Figure 5-20*a* and *b*.

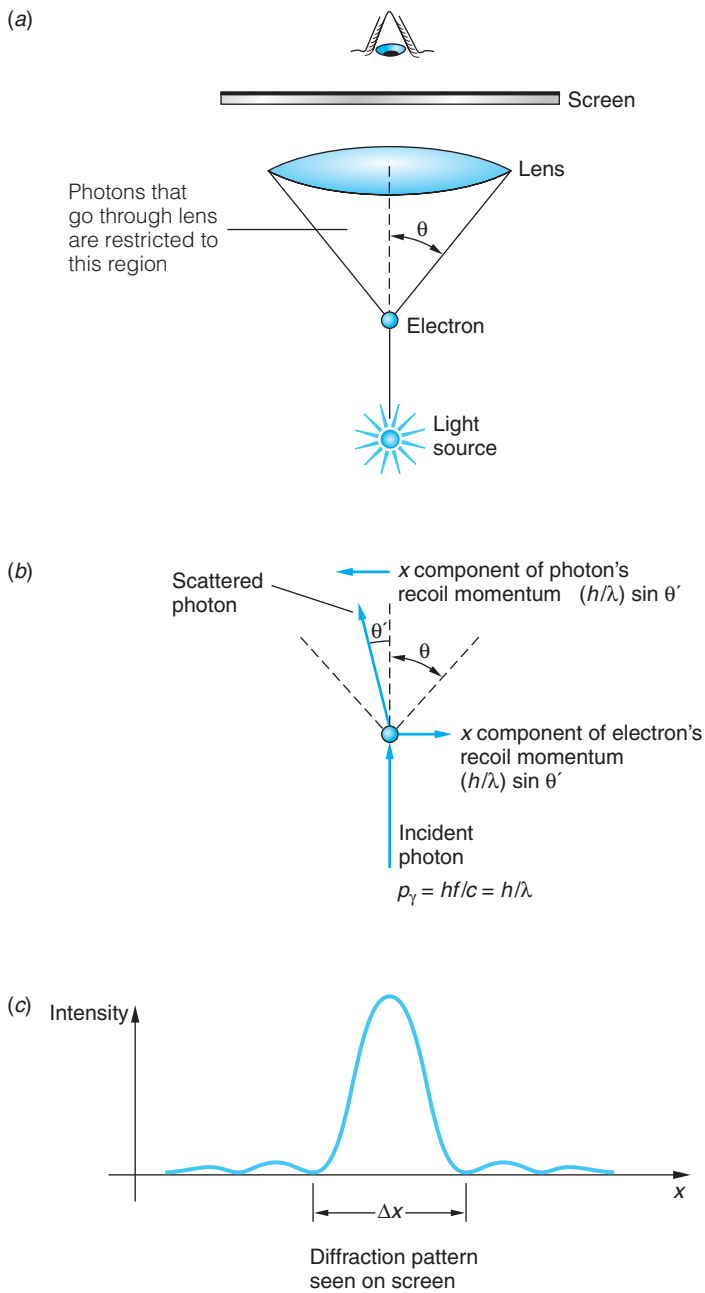

Figure 5-20 "Seeing an electron" with a gamma-ray microscope. (*b*) Because of the size of the lens, the momentum of the scattered photon is uncertain by $\Delta p_x \approx p \sin\theta = h \sin\theta/\lambda$. Thus the recoil momentum of the electron is also uncertain by at least this amount. (*c*) The position of the electron cannot be resolved better than the width of the central maximum of the diffraction pattern $\Delta x \approx \lambda/\sin\theta$. The product of the uncertainties $\Delta p_x \Delta x$ is therefore of the order of Planck's constant *h*.

STUDENTS-HUB.com Uploaded By: Malak Obaid

Let us assume that the x component of momentum of the incoming photon is known precisely from a previous measurement. To reach the screen and contribute to the diffraction pattern in Figure 5-20*c*, the scattered photon need only go through the lens aperture. Thus, the scattered photon can have any x component of momentum from 0 to $p_x = p \sin\theta$, where p is the total momentum of the scattered photon. By conservation of momentum, the uncertainty in the momentum of the electron after the scattering must be greater than or equal to that of the scattered photon (it would be equal, of course, if the electron's initial momentum were known precisely); therefore, we write

$$\Delta p_x \geq p \sin\theta = \frac{h}{\lambda}\sin\theta$$

and

$$\Delta x \Delta p_x \geq \frac{\lambda}{2\sin\theta}\frac{h\sin\theta}{\lambda} = \frac{1}{2}h$$

Thus, even though the electron prior to our observation may have had a definite position and momentum, our observation has unavoidably introduced an uncertainty in the measured values of those quantities. This illustrates the essential point of the uncertainty principle—that this product of uncertainties cannot be less than about *h in principle*, that is, even in an ideal situation. If electrons rather than photons were used to locate the object, the analysis would not change since the relation $\lambda = h/p$ is the same for both.

5-6 Some Consequences of the Uncertainty Principle

In the next chapter we will see that the Schrödinger wave equation provides a straightforward method of solving problems in atomic physics. However, the solution of the Schrödinger equation is often laborious and difficult. Much semiquantitative information about the behavior of atomic systems can be obtained from the uncertainty principle alone without a detailed solution of the problem. The general approach used in applying the uncertainty principle to such systems will first be illustrated by considering a particle moving in a box with rigid walls. We then use that analysis in several numerical examples and as a basis for discussing some additional consequences.

Minimum Energy of a Particle in a Box

An important consequence of the uncertainty principle is that a particle confined to a finite space cannot have zero kinetic energy. Let us consider the case of a one-dimensional "box" of length L. If we know that the particle is in the box, Δx is not larger than L. This implies that Δp is at least $\hbar/L$. (Since we are interested in orders of magnitude, we will ignore the $1/2$ in the minimum uncertainty product. In general, distributions are not Gaussian anyway, so $\Delta p \Delta x$ will be larger than $\hbar/2$.) Let us take the standard deviation as a measure of Δp,

$$(\Delta p)^2 = (p - \overline{p})^2_{\text{av}} = (p^2 - 2p\overline{p} + \overline{p}^2)_{\text{av}} = \overline{p^2} - \overline{p}^2$$

If the box is symmetric, $\overline{p}$ will be zero since the particle moves to the left as often as to the right. Then

$$(\Delta p)^2 = \overline{p^2} \geq \left(\frac{\hbar}{L}\right)^2$$

STUDENTS-HUB.com Uploaded By: Malak Obaid

and the average kinetic energy is

$$\overline{E} = \frac{\overline{p^2}}{2m} \geq \frac{\hbar^2}{2mL^2} \qquad \textbf{5-28}$$

Thus, we see that the uncertainty principle indicates that the minimum energy of a particle (*any* particle) in a "box" (*any* kind of "box") cannot be zero. This minimum energy given by Equation 5-28 for a particle in a one-dimensional box is called the *zero point energy*.

EXAMPLE 5-6 A Macroscopic Particle in a Box Consider a small but macroscopic particle of mass $m = 10^{-6}$ g confined to a one-dimensional box with $L = 10^{-6}$ m, e.g., a tiny bead on a very short wire. Compute the bead's minimum kinetic energy and the corresponding speed.

SOLUTION

1. The minimum kinetic energy is given by Equation 5-28:

$$\begin{aligned}\overline{E} &= \frac{\hbar^2}{2mL^2} = \frac{(1.055 \times 10^{-34}\ \text{J}\cdot\text{s})^2}{(2)(10^{-9}\ \text{kg})(10^{-6}\ \text{m})^2} \\ &= 5.57 \times 10^{-48}\ \text{J} \\ &= 3.47 \times 10^{-29}\ \text{eV}\end{aligned}$$

2. The speed corresponding to this kinetic energy is:

$$\begin{aligned}v &= \sqrt{\frac{2\overline{E}}{m}} = \sqrt{\frac{2(5.57 \times 10^{-48}\ \text{J})}{10^{-9}\ \text{kg}}} \\ &= 1.06 \times 10^{-19}\ \text{m/s}\end{aligned}$$

Remarks: *We can see from this calculation that the minimum kinetic energy implied by the uncertainty principle is certainly not observable for macroscopic objects even as small as 10^{-6} g.*

EXAMPLE 5-7 An Electron in an Atomic Box If the particle in a one-dimensional box of length $L = 0.1$ nm (about the diameter of an atom) is an electron, what will be its zero-point energy?

SOLUTION

Again using Equation 5-28, we find that

$$E = \frac{(\hbar c)^2}{2mc^2L^2} = \frac{(197.3\ \text{eV}\cdot\text{nm})^2}{2(0.511 \times 10^6\ \text{eV})(0.1\ \text{nm})^2} = 3.81\ \text{eV}$$

This is the correct order of magnitude for the kinetic energy of an electron in an atom.

Size of the Hydrogen Atom

The energy of an electron of momentum p a distance r from a proton is

$$E = \frac{p^2}{2m} - \frac{ke^2}{r}$$

STUDENTS-HUB.com Uploaded By: Malak Obaid

If we take for the order of magnitude of the position uncertainty $\Delta x = r$, we have

$$(\Delta p)^2 = \overline{p^2} \geq \frac{\hbar^2}{r^2}$$

The energy is then

$$E = \frac{\hbar^2}{2mr^2} - \frac{ke^2}{r}$$

There is a radius r_m at which E is minimum. Setting $dE/dr = 0$ yields r_m and E_m:

$$r_m = \frac{\hbar^2}{ke^2m} = a_0 = 0.0529 \text{ nm}$$

and

$$E_m = -\frac{k^2e^4m}{2\hbar^2} = -13.6 \text{ eV}$$

The fact that r_m came out to be exactly the radius of the first Bohr orbit is due to the judicious choice of $\Delta x = r$ rather than $2r$ or $r/2$, which are just as reasonable. It should be clear, however, that any reasonable choice for Δx gives the correct order of magnitude of the size of an atom.

Widths of Spectral Lines

Equation 5-27 implies that the energy of a system cannot be measured exactly unless an infinite amount of time is available for the measurement. If an atom is in an excited state, it does not remain in that state indefinitely but makes transitions to lower energy states until it reaches the ground state. The decay of an excited state is a statistical process.

We can take the mean time for decay τ, called the *lifetime*, to be a measure of the time available to determine the energy of the state. For atomic transitions, τ is of the order of 10^{-8} s. The uncertainty in the energy corresponding to this time is

$$\Delta E \geq \frac{\hbar}{\tau} = \frac{6.58 \times 10^{-16} \text{ eV} \cdot \text{s}}{10^{-8} \text{ s}} \approx 10^{-7} \text{ eV}$$

This uncertainty in energy causes a spread $\Delta\lambda$ in the wavelength of the light emitted. For transitions to the ground state, which has a perfectly certain energy E_0 because of its infinite lifetime, the percentage spread in wavelength can be calculated from

$$E - E_0 = \frac{hc}{\lambda}$$

$$dE = -hc\frac{d\lambda}{\lambda^2}$$

$$|\Delta E| \approx hc\frac{|\Delta\lambda|}{\lambda^2}$$

thus,

$$\frac{\Delta\lambda}{\lambda} \approx \frac{\Delta E}{E - E_0}$$

STUDENTS-HUB.com Uploaded By: Malak Obaid

The energy width $\Delta E = \hbar/\tau$ is called the *natural line width* and is represented by Γ_0. Other effects that cause broadening of spectral lines are the Doppler effect, the recoil of the emitting atom, and atomic collisions. For optical spectra in the eV energy range, the Doppler width D is about 10^{-6} eV at room temperature, i.e., roughly 10 times the natural width Γ_0, and the recoil width is negligible. For nuclear transitions in the MeV range, both the Doppler width and the recoil width are of the order of eV, much larger than the natural line width. We will see in Chapter 11 that in some special cases of atoms in solids at low temperatures, the Doppler and recoil widths are essentially zero and the width of the spectral line is just the natural width. This effect, called the *Mössbauer effect* after its discoverer, is extremely important since it provides photons of well-defined energy that are useful in experiments demanding extreme precision. For example, the 14.4-keV photon from ^{57}Fe has a natural width of the order of 10^{-11} of its energy.

Questions

7. What happens to the zero-point energy of a particle in a one-dimensional box as the length of the box $L \rightarrow \infty$?
8. Why is the uncertainty principle not apparent for macroscopic objects?

EXAMPLE 5-8 Emission of a Photon Most excited atomic states decay, i.e., emit a photon, within about $\tau = 10^{-8}$ s following excitation. What is the minimum uncertainty in the (1) energy and (2) frequency of the emitted photon?

SOLUTION

1. The minimum energy uncertainty is the natural line width $\Gamma_0 = \hbar/\tau$; therefore,

$$\Gamma_0 = \frac{6.63 \times 10^{-34}\ \text{J}\cdot\text{s}}{2\pi \times 10^{-8}\ \text{s}} = \frac{4.14 \times 10^{-15}\ \text{eV}\cdot\text{s}}{2\pi \times 10^{-8}\ \text{s}} = 6.6 \times 10^{-8}\ \text{eV}$$

2. From de Broglie's relation $E = \hbar\omega$ we have

$$\Delta E = \hbar\Delta\omega = \hbar(2\pi\Delta f) = h\Delta f$$

so that Equation 5-27 can be written as

$$\Delta E\Delta t = h\Delta f\Delta t \geq \hbar$$

and the minimum uncertainty in the frequency becomes

$$\Delta f \geq \frac{1}{2\pi\Delta t} = \frac{1}{2\pi \times 10^{-8}}$$

$$\Delta f \geq 1.6 \times 10^{7}\ \text{Hz}$$

Remarks: *The frequency of photons in the visible region of the spectrum is of the order of 10^{14} Hz.*

STUDENTS-HUB.com Uploaded By: Malak Obaid

5-7 Wave-Particle Duality

We have seen that electrons, which were once thought of as simply particles, exhibit the wave properties of diffraction and interference. In earlier chapters we saw that light, which we previously had thought of as a wave, also has particle properties in its interaction with matter, as in the photoelectric effect or the Compton effect. All phenomena—electrons, atoms, light, sound—have both particle and wave characteristics. It is sometimes said that an electron, for example, behaves both as a wave and a particle. This may seem confusing since, in classical physics, the concepts of waves and particles are mutually exclusive. A *classical particle* behaves like a pellet or BB shot from an air-powered rifle. It can be localized and scattered, it exchanges energy suddenly in a lump, and it obeys the laws of conservation of energy and momentum in collisions, but it does *not* exhibit interference and diffraction. A *classical wave* behaves like a water wave. It exhibits diffraction and interference patterns and has its energy spread out continuously in space and time, not quantized in lumps. Nothing, it was thought, could be both a classical particle and a classical wave.

We now see that the classical concepts do not adequately describe either waves or particles. Both matter and radiation have both particle and wave aspects. When emission and absorption are being studied, it is the particle aspects that are dominant. When matter and radiation propagate through space, wave aspects dominate. Notice that emission and absorption are events characterized by exchange of energy and discrete locations. For example, light strikes the retina of your eye and a photon is absorbed, transferring its energy to a particular rod or cone: an observation has occurred. This illustrates the point that *observations* of matter and radiation are described in terms of the particle aspects. On the other hand, predicting the intensity distribution of the light on your retina involves consideration of the amplitudes of waves that have propagated through space and been diffracted at the pupil. Thus, *predictions*, i.e., a priori statements about what may be observed, are described in terms of the wave aspects. Let's elaborate on this just a bit.

Every phenomenon is describable by a wave function that is the solution of a wave equation. The wave function for light is the electric field $\mathscr{E}(x, t)$ (in one space dimension), which is the solution of a wave equation like Equation 5-11. We have called the wave function for an electron $\Psi(x, t)$. We will study the wave equation of which Ψ is the solution, called the *Schrödinger equation*, in the next chapter. The magnitude squared of the wave function gives the probability per unit volume that the electron, if looked for, will be found in a given volume or region. The wave function exhibits the classical wave properties of interference and diffraction. In order to predict where an electron, or other particle, is likely to be, we must find the wave function by methods similar to those of classical wave theory. When the electron (or light) interacts and exchanges energy and momentum, the wave function is changed by the interaction. The interaction can be described by classical particle theory, as is done in the Compton effect. There are times when classical particle theory and classical wave theory give the same results. *If the wavelength is much smaller than any object or aperture, particle theory can be used as well as wave theory to describe wave propagation because diffraction and interference effects are too small to be observed.* Common examples are geometrical optics, which is really a particle theory, and the motion of baseballs and jet aircraft. If one is interested only in time averages of energy and momentum exchange, the wave theory works as well as the particle theory. For example, the wave theory of light correctly predicts that the total electron current in the photoelectric effect is proportional to the intensity of the light.

STUDENTS-HUB.com Uploaded By: Malak Obaid

More

That matter can exhibit wavelike characteristics as well as particlelike behavior can be a difficult concept to understand. A wonderfully clear discussion of wave-particle duality was given by R. P. Feynman, and we have used it as the basis of our explanation on the home page of the *Two-Slit Interference Pattern* for electrons: whfreeman.com/tiplermodernphysics5e/. See also Figures 5-21 and 5-22 and Equation 5-29 here.

Summary

TOPIC	RELEVANT EQUATIONS AND REMARKS	
1. De Broglie relations	$f = E/h$	**5-1**
	$\lambda = h/p$	**5-2**
	Electrons and all other particles exhibit the wave properties of interference and diffraction	
2. Detecting electron waves		
Davisson and Germer	Showed that electron waves diffracted from a single Ni crystal according to Bragg's equation	
	$n\lambda = D \sin\varphi$	**5-5**
3. Wave packets		
Wave equation	$\frac{d^2y}{dx^2} = \frac{1}{v^2}\frac{d^2y}{dt^2}$	**5-11**
Uncertainty relations	$\Delta k \Delta x \sim 1$	**5-17**
	$\Delta\omega\Delta t \sim 1$	**5-18**
Wave speed	$v_p = f\lambda = \omega/k$	
Group (packet) speed	$v_g = \frac{d\omega}{dk} = v_p + k\frac{dv_p}{dk}$	**5-16**
Matter waves	The wave packet moves with the particle speed; i.e., the particle speed is the group speed v_g.	
4. Probabilistic interpretation	The magnitude square of the wave function is proportional to the probability of observing a particle in the region dx at x and t.	
	$P(x)dx = \lvert\Psi\rvert^2 dx$	**5-23**
5. Heisenberg uncertainty principle	$\Delta x \Delta p \geq \frac{1}{2}\hbar$	**5-26**
	$\Delta E \Delta t \geq \frac{1}{2}\hbar$	**5-27**
	where each of the uncertainties is defined to be the standard deviation.	

STUDENTS-HUB.com Uploaded By: Malak Obaid

TOPIC	RELEVANT EQUATIONS AND REMARKS
Particle in a box	$\overline{E} \geq \frac{\hbar^2}{2mL^2}$ **5-28** The minimum energy of any particle in any "box" cannot be zero.
Energy of H atom	The Heisenberg principle predicts $E_{min} = -13.6$ eV in agreement with the Bohr model.

General References

The following general references are written at a level appropriate for the readers of this book.

De Broglie, L., *Matter and Light: The New Physics*, Dover, New York, 1939. In this collection of studies is de Broglie's lecture on the occasion of receiving the Nobel Prize, in which he describes his reasoning that led to the prediction of the wave nature of matter.

Feynman, R., "Probability and Uncertainty—The Quantum-Mechanical View of Nature," filmed lecture, available from Educational Services, Inc., Film Library, Newton, MA.

Feynman, R. P., R. B. Leighton, and M. Sands, *Lectures on Physics*, Addison-Wesley, Reading, MA, 1965.

Fowles, G. R., *Introduction to Modern Optics*, Holt, Rinehart & Winston, New York, 1968.

Hecht, E., *Optics,* 2d ed., Addison-Wesley, Reading, MA, 1987.

Jenkins, F. A., and H. E. White, *Fundamentals of Optics*, 4th ed., McGraw-Hill, New York, 1976.

Mehra, J., and H. Rechenberg, *The Historical Development of Quantum Theory*, Vol. 1, Springer-Verlag, New York, 1982.

Resnick, R., and D. Halliday, *Basic Concepts in Relativity and Early Quantum Theory,* 2d ed., Wiley, New York, 1992.

Tipler, P. A., and G. Mosca, *Physics for Scientists and Engineers*, 6th ed., W. H. Freeman and Co., New York, 2008. Chapters 15 and 16 include a complete discussion of classical waves.

Notes

1. Louis V. P. R. de Broglie (1892–1987), French physicist. Originally trained in history, he became interested in science after serving as a radio engineer in the French army (assigned to the Eiffel Tower) and through the work of his physicist brother Maurice. The subject of his doctoral dissertation received unusual attention because his professor, Paul Langevin (who discovered the principle on which sonar is based), brought it to the attention of Einstein, who described de Broglie's hypothesis to Lorentz as "the first feeble ray of light to illuminate . . . the worst of our physical riddles." He received the Nobel Prize in Physics in 1929, the first person so honored for work done for a doctoral thesis.

2. L. de Broglie, *New Perspectives in Physics*, Basic Books, New York, 1962.

3. See, e.g., Tipler, *Physics for Scientists and Engineers*, 5th ed. (New York: W. H. Freeman and Co., 2008), Section 35-5.

4. Jean-Baptiste Perrin (1870–1942), French physicist. He was the first to show that cathode rays are actually charged particles, setting the stage for J. J. Thomson's measurement of their q/m ratio. He was also the first to measure the approximate size of atoms and molecules and determined Avogadro's number. He received the Nobel Prize in Physics for that work in 1926.

5. Clinton J. Davisson (1881–1958), American physicist. He shared the 1937 Nobel Prize in Physics with G. P. Thomson for demonstrating the diffraction of particles. Davisson's Nobel Prize was the first ever awarded for work done somewhere other than at an academic institution. Germer was one of Davisson's assistants at Bell Telephone Laboratory.

6. Matter (electron) waves, like other waves, change their direction in passing from one medium (e.g., Ni crystal) into another (e.g., vacuum) in the manner described by Snell's law and the indices of refraction of the two media. For normal incidence Equation 5-5 is not affected, but for other incident angles it is altered a bit, and that change has not been taken into account in either Figure 5-6 or 5-7.

7. *Nobel Prize Lectures: Physics* (Amsterdam and New York: Elsevier, 1964).

8. In spectroscopy, the quantity $k = \lambda^{-1}$ is called the *wave number*. In the theory of waves, the term *wave number* is used for $k = 2\pi/\lambda$.

9. Following convention, the "width" is defined as the full width of the pulse or envelope measured at half the maximum amplitude.

STUDENTS-HUB.com Uploaded By: Malak Obaid

10. This interpretation of $|\Psi|^2$ was first developed by German physicist Max Born (1882–1970). One of his positions early in his career was at the University of Berlin, where he was to relieve Planck of his teaching duties. Born received the Nobel Prize in Physics in 1954, in part for his interpretation of $|\Psi|^2$.

11. Werner K. Heisenberg (1901–1976), German physicist. After obtaining his Ph.D. under Sommerfeld, he served as an assistant to Born and to Bohr. He was the director of research for Germany's atomic bomb project during World War II. His work on quantum theory earned him the Nobel Prize in Physics in 1932.

12. The resolving power of a microscope is discussed in some detail in Jenkins and White, *Fundamentals of Optics*, 4th ed. (New York: McGraw-Hill, 1976), pp. 332–334. The expression for Δx used here is determined by Rayleigh's criterion, which states that two points are just resolved if the central maximum of the diffraction pattern from one falls at the first minimum of the diffraction pattern of the other.

13. Richard P. Feynman (1918–1988), American physicist. This discussion is based upon one in his classic text *Lectures on Physics* (Reading, MA: Addison-Wesley, 1965). He shared the 1965 Nobel Prize in Physics for his development of quantum electrodynamics (QED). It was Feynman who, while a member of the commission on the *Challenger* disaster, pointed out that the booster stage O-rings were at fault. A genuine legend in American physics, he was also an accomplished bongo drummer and safecracker.

Problems

Level I

Section 5-1 The de Broglie Hypothesis

5-1. (*a*) What is the de Broglie wavelength of a 1-g mass moving at a speed of 1 m per year? (*b*) What should be the speed of such a mass if its de Broglie wavelength is to be 1 cm?

5-2. If the kinetic energy of a particle is much greater than its rest energy, the relativistic approximation $E \approx pc$ holds. Use this approximation to find the de Broglie wavelength of an electron of energy 100 MeV.

5-3. Electrons in an electron microscope are accelerated from rest through a potential difference V_0 so that their de Broglie wavelength is 0.04 nm. What is V_0?

5-4. Compute the de Broglie wavelengths of (*a*) an electron, (*b*) a proton, and (*c*) an alpha particle of 4.5-keV kinetic energy.

5-5. According to statistical mechanics, the average kinetic energy of a particle at temperature T is $3kT/2$, where k is the Boltzmann constant. What is the average de Broglie wavelength of nitrogen molecules at room temperature?

5-6. Find the de Broglie wavelength of a neutron of kinetic energy 0.02 eV (this is of the order of magnitude of kT at room temperature).

5-7. A free proton moves back and forth between rigid walls separated by a distance $L = 0.01$ nm. (*a*) If the proton is represented by a one-dimensional standing de Broglie wave with a node at each wall, show that the allowed values of the de Broglie wavelength are given by $\lambda = 2L/n$ where n is a positive integer. (*b*) Derive a general expression for the allowed kinetic energy of the proton and compute the values for $n = 1$ and 2.

5-8. What must be the kinetic energy of an electron if the ratio of its de Broglie wavelength to its Compton wavelength is (*a*) 10^2, (*b*) 0.2, and (*c*) 10^{-3}?

5-9. Compute the wavelength of a cosmic-ray proton whose kinetic energy is (*a*) 2 GeV and (*b*) 200 GeV.

Section 5-2 Measurements of Particle Wavelengths

5-10. What is the Bragg scattering angle φ for electrons scattered from a nickel crystal if their energy is (*a*) 75 eV, (*b*) 100 eV?

5-11. Compute the kinetic energy of a proton whose de Broglie wavelength is 0.25 nm. If a beam of such protons is reflected from a calcite crystal with crystal plane spacing of 0.304 nm, at what angle will the first-order Bragg maximum occur?

STUDENTS-HUB.com Uploaded By: Malak Obaid

5-12. (*a*) The scattering angle for 50-eV electrons from MgO is 55.6°. What is the crystal spacing D? (*b*) What would be the scattering angle for 100-eV electrons?

5-13. A certain crystal has a set of planes spaced 0.30 nm apart. A beam of neutrons strikes the crystal at normal incidence and the first maximum of the diffraction pattern occurs at $\varphi = 42°$. What are the de Broglie wavelength and kinetic energy of the neutrons?

5-14. Show that in Davisson and Germer's experiment with 54-eV electrons using the $D = 0.215$ nm planes, diffraction peaks with $n = 2$ and higher are not possible.

5-15. A beam of electrons with kinetic energy 350 eV is incident normal to the surface of a KCl crystal that has been cut so that the spacing D between adjacent atoms in the planes parallel to the surface is 0.315 nm. Calculate the angle φ at which diffraction peaks will occur for all orders possible.

Section 5-3 Wave Packets

5-16. Information is transmitted along a cable in the form of short electric pulses at 100,000 pulses/s. (*a*) What is the longest duration of the pulses such that they do not overlap? (*b*) What is the range of frequencies to which the receiving equipment must respond for this duration?

5-17. Two harmonic waves travel simultaneously along a long wire. Their wave functions are $y_1 = 0.002 \cos(8.0x - 400t)$ and $y_2 = 0.002 \cos(7.6x - 380t)$, where y and x are in meters and t in seconds. (*a*) Write the wave function for the resultant wave in the form of Equation 5-15. (*b*) What is the phase velocity of the resultant wave? (*c*) What is the group velocity? (*d*) Calculate the range Δx between successive zeros of the group and relate it to Δk.

5-18. (*a*) Starting from Equation 5-16, show that the group velocity can also be expressed as

$$v_g = v_p - \lambda(dv_p/d\lambda)$$

(*b*) The phase velocity of each wavelength of white light moving through ordinary glass is a function of the wavelength; i.e., glass is a dispersive medium. What is the general dependence of v_p on λ in glass? Is $dv_p/d\lambda$ positive or negative?

5-19. A radar transmitter used to measure the speed of pitched baseballs emits pulses of 2.0-cm wavelength that are 0.25 μs in duration. (*a*) What is the length of the wave packet produced? (*b*) To what frequency should the receiver be tuned? (*c*) What must be the minimum bandwidth of the receiver?

5-20. A certain standard tuning fork vibrates at 880 Hz. If the tuning fork is tapped, causing it to vibrate, then stopped a quarter of a second later, what is the approximate range of frequencies contained in the sound pulse that reached your ear?

5-21. If a phone line is capable of transmitting a range of frequencies $\Delta f = 5000$ Hz, what is the approximate duration of the shortest pulse that can be transmitted over the line?

5-22. (*a*) You are given the task of constructing a double slit experiment for 5-eV electrons. If you wish the first minimum of the diffraction pattern to occur at 5°, what must be the separation of the slits? (*b*) How far from the slits must the detector plane be located if the first minima on each side of the central maximum are to be separated by 1 cm?

Section 5-4 The Probabilistic Interpretation of the Wave Function

5-23. A 100-g rigid sphere of radius 1 cm has a kinetic energy of 2 J and is confined to move in a force-free region between two rigid walls separated by 50 cm. (*a*) What is the probability of finding the center of the sphere exactly midway between the two walls? (*b*) What is the probability of finding the center of the sphere between the 24.9- and 25.1-cm marks?

5-24. A particle moving in one dimension between rigid walls separated by a distance L has the wave function $\Psi(x) = A \sin(\pi x/L)$. Since the particle must remain between the walls, what must be the value of A?

STUDENTS-HUB.com Uploaded By: Malak Obaid

5-25. The wave function describing a state of an electron confined to move along the x axis is given at time zero by

$$\Psi(x, 0) = Ae^{-x^2/4\sigma^2}$$

Find the probability of finding the electron in a region dx centered at (*a*) $x = 0$, (*b*) $x = \sigma$, and (*c*) $x = 2\sigma$. (*d*) Where is the electron most likely to be found?

Section 5-5 The Uncertainty Principle

5-26. A tuning fork of frequency f_0 vibrates for a time Δt and sends out a waveform that looks like that in Figure 5-23. This wave function is similar to a harmonic wave except that it is confined to a time Δt and space $\Delta x = v\Delta t$, where v is the phase velocity. Let N be the approximate number of cycles of vibration. We can measure the frequency by counting the cycles and dividing by Δt. (*a*) The number of cycles is uncertain by approximately ± 1 cycle. Explain why (see the figure). What uncertainty does this introduce in the determination of the frequency f? (*b*) Write an expression for the wave number k in terms of Δx and N. Show that the uncertainty in N of ± 1 leads to an uncertainty in k of $\Delta k = 2\pi/\Delta x$.

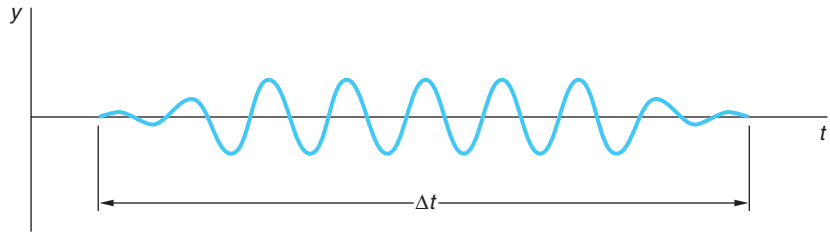

Figure 5-23

5-27. If an excited state of an atom is known to have a lifetime of 10^{-7} s, what is the uncertainty in the energy of photons emitted by such atoms in the spontaneous decay to the ground state?

5-28. A ladybug 5 mm in diameter with a mass of 1.0 mg being viewed through a low-power magnifier with a calibrated reticule is observed to be stationary with an uncertainty of 10^{-2} mm. How fast might the ladybug actually be walking?

5-29. ^{222}Rn decays by the emission of an α particle with a lifetime of 3.823 days. The kinetic energy of the α particle is measured to be 5.490 MeV. What is the uncertainty in this energy? Describe in one sentence how the finite lifetime of the excited state of the radon nucleus translates into an energy uncertainty for the emitted α particle.

5-30. If the uncertainty in the position of a wave packet representing the state of a quantum-system particle is equal to its de Broglie wavelength, how does the uncertainty in momentum compare with the value of the momentum of the particle?

5-31. In one of G. Gamow's Mr. Tompkins tales, the hero visits a "quantum jungle" where h is very large. Suppose that you are in such a place where $h = 50\ \text{J} \cdot \text{s}$. A cheetah runs past you a few meters away. The cheetah is 2 m long from nose to tail tip and its mass is 30 kg. It is moving at 40 m/s. What is the uncertainty in the location of the "midpoint" of the cheetah? Describe in one sentence how the cheetah would look different to you than when h has its actual value.

5-32. In order to locate a particle, e.g., an electron, to within 5×10^{-12} m using electromagnetic waves ("light"), the wavelength must be at least this small. Calculate the momentum and energy of a photon with $\lambda = 5 \times 10^{-12}$ m. If the particle is an electron with $\Delta x = 5 \times 10^{-12}$ m, what is the corresponding uncertainty in its momentum?

5-33. The decay of excited states in atoms and nuclei often leave the system in another, albeit lower-energy, excited state. (*a*) One example is the decay between two excited states of the nucleus of ^{48}Ti. The upper state has a lifetime of 1.4 ps, the lower state 3.0 ps. What is the fractional uncertainty $\Delta E/E$ in the energy of 1.3117-MeV gamma rays connecting the two states?

STUDENTS-HUB.com Uploaded By: Malak Obaid

(*a*) Another example is the H_α line of the hydrogen Balmer series. In this case the lifetime of both states is about the same, 10^{-8} s. What is the uncertainty in the energy of the H_α photon?

5-34. Laser pulses of femtosecond duration can be produced but for such brief pulses it makes no sense to speak of the pulse's color. To see this, compute the time duration of a laser pulse whose range of frequencies covers the entire visible spectrum (4.0×10^{14} Hz to 7.5×10^{14} Hz).

Section 5-6 Some Consequences of the Uncertainty Principle

5-35. A neutron has a kinetic energy of 10 MeV. What size object is necessary to observe neutron diffraction effects? Is there anything in nature of this size that could serve as a target to demonstrate the wave nature of 10-MeV neutrons?

5-36. Protons and neutrons in nuclei are bound to the nucleus by exchanging pions (π mesons) with each other (see Chapter 11). This is possible to do without violating energy conservation provided the pion is reabsorbed within a time consistent with the Heisenberg uncertainty relations. Consider the emission reaction $p \rightarrow p + \pi$ where $m_\pi = 135\ \text{MeV}/c^2$. (*a*) Ignoring kinetic energy, by how much is energy conservation violated in this reaction? (*b*) Within what time interval must the pion be reabsorbed in order to avoid violation of energy conservation?

5-37. Show that the relation $\Delta p_s \Delta s > \hbar$ can be written $\Delta L \Delta\varphi > \hbar$ for a particle moving in a circle about the z axis, where p_s is the linear momentum tangential to the circle, s is the arc length, and L is the angular momentum. How well can the angular position of the electron be specified in the Bohr atom?

5-38. An excited state of a certain nucleus has a half-life of 0.85 ns. Taking this to be the uncertainty Δt for emission of a photon, calculate the uncertainty in the frequency Δf, using Equation 5-25. If $\lambda = 0.01$ nm, find $\Delta f/f$.

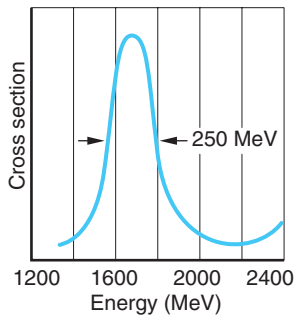

Figure 5-24

5-39. The lifetimes of so-called resonance particles cannot be measured directly but is computed from the energy width (or uncertainty) of the scattering cross section versus energy graph (see Chapter 12). For example, the scattering of a pion (π meson) and a proton can produce a short-lived Δ resonance particle with a mass of $1685\ \text{MeV}/c^2$ and an energy width of 250 MeV as shown in Figure 5-24: $\pi + p \rightarrow \Delta$. Compute the lifetime of the Δ.

Section 5-7 Wave-Particle Duality

There are no problems for this section.

Level II

5-40. Neutrons and protons in atomic nuclei are confined within a region whose diameter is about 10^{-15} m. (*a*) At any given instant, how fast might an individual proton or neutron be moving? (*b*) What is the approximate kinetic energy of a neutron that is localized to within such a region? (*c*) What would be the corresponding energy of an electron localized to within such a region?

5-41. Using the relativistic expression $E^2 = p^2c^2 + m^2c^4$, (*a*) show that the phase velocity of an electron wave is greater than c. (*b*) Show that the group velocity of an electron wave equals the particle velocity of the electron.

5-42. Show that if y_1 and y_2 are solutions of Equation 5-11, the function $y_3 = C_1y_1 + C_2y_2$ is also a solution for any values of the constants C_1 and C_2.

5-43. The London "Bobby" whistle has a frequency of 2500 Hz. If such a whistle is given a 3.0-s blast, (*a*) what is the uncertainty in the frequency? (*b*) How long is the wave train of this blast? (*c*) What would be the uncertainty in measuring the wavelength of this blast? (*d*) What is the wavelength of this blast?

5-44. A particle of mass m moves in a one-dimensional box of length L. (Take the potential energy of the particle in the box to be zero so that its total energy is its kinetic energy

STUDENTS-HUB.com Uploaded By: Malak Obaid

$p^2/2m$.) Its energy is quantized by the standing-wave condition $n(\lambda/2) = L$, where λ is the de Broglie wavelength of the particle and n is an integer. (*a*) Show that the allowed energies are given by $E_n = n^2E_1$ where $E_1 = h^2/8mL^2$. (*b*) Evaluate E_n for an electron in a box of size $L = 0.1$ nm and make an energy-level diagram for the state from $n = 1$ to $n = 5$. Use Bohr's second postulate $f = \Delta E/h$ to calculate the wavelength of electromagnetic radiation emitted when the electron makes a transition from (*c*) $n = 2$ to $n = 1$, (*d*) $n = 3$ to $n = 2$, and (*e*) $n = 5$ to $n = 1$.

5-45. (*a*) Use the results of Problem 5-44 to find the energy of the ground state ($n = 1$) and the first two excited states of a proton in a one-dimensional box of length $L = 10^{-15}$ m = 1 fm. (These are of the order of magnitude of nuclear energies.) Calculate the wavelength of electromagnetic radiation emitted when the proton makes a transition from (*b*) $n = 2$ to $n = 1$, (*c*) $n = 3$ to $n = 2$, and (*d*) $n = 3$ to $n = 1$.

5-46. (*a*) Suppose that a particle of mass m is constrained to move in a one-dimensional space between two infinitely high barriers located A apart. Using the uncertainty principle, find an expression for the zero-point (minimum) energy of the particle. (*b*) Using your result from (*a*) , compute the minimum energy of an electron in such a space if $A = 10^{-10}$ m and $A = 1$ cm. (*c*) Calculate the minimum energy for a 100-mg bead moving on a thin wire between two stops located 2 cm apart.

5-47. A proton and a 10-g bullet each move with a speed of 500 m/s, measured with an uncertainty of 0.01 percent. If measurements of their respective positions are made simultaneous with the speed measurements, what is the minimum uncertainty possible in the position measurements?

Level III

5-48. Show that Equation 5-11 is satisfied by $y = f(\varphi)$, where $\varphi = x - vt$ for any function f.

5-49. An electron and a positron are moving toward each other with equal speeds of 3×10^6 m/s. The two particles annihilate each other and produce two photons of equal energy. (*a*) What were the de Broglie wavelengths of the electron and positron? Find the (*b*) energy, (*c*) momentum, and (*d*) wavelength of each photon.

5-50. It is possible for some fundamental particles to "violate" conservation of energy by creating and quickly reabsorbing another particle. For example, a proton can emit a π^+ according to $p = n + \pi^+$ where the n represents a neutron. The π^+ has a mass of 140 MeV/c^2. The reabsorption must occur within a time Δt consistent with the uncertainty principle. (*a*) Considering the example shown, by how much ΔE is energy conservation violated? (Ignore kinetic energy.) (*b*) For how long Δt can the π^+ exist? (*c*) Assuming that the π^+ is moving at nearly the speed of light, how far from the nucleus could it get in the time Δt? (As we will discuss in Chapter 11, this is the approximate range of the strong nuclear force.) (*d*) Assuming that as soon as one pion is reabsorbed another is emitted, how many pions would be recorded by a "nucleon camera" with a shutter speed of 1 μs?

5-51. De Broglie developed Equation 5-2 initially for photons, assuming that they had a small but finite mass. His assumptions was that RF waves with $\lambda = 30$ m traveled at a speed of at least 99 percent of that of visible light with $\lambda = 500$ nm. Beginning with the relativistic expression $hf = \gamma mc^2$, verify de Broglie's calculation that the upper limit of the rest mass of a photon is 10^{-44} g. (*Hint*: Find an expression for v/c in terms of hf and mc^2, and then let $mc^2 \ll hf$) ($\gamma = 1/\sqrt{1 - v^2/c^2}$).

5-52. Suppose that you drop BBs onto a bull's-eye marked on the floor. According to the uncertainty principle, the BBs do not necessarily fall straight down from the release point to the center of the bull's-eye but are affected by the initial conditions. (*a*) If the location of the release point is uncertain by an amount Δx perpendicular to the vertical direction and the horizontal component of the speed is uncertain by Δv_x, derive an expression for the minimum spread ΔX

STUDENTS-HUB.com Uploaded By: Malak Obaid

of impacts at the bull's-eye if it is located a distance y_0 below the release point. (*b*) Modify your result in (*a*) to include the effect on ΔX of uncertainties Δy and Δv_y at the release point.

5-53. Using the first-order Doppler-shift formula $f' = f_0(1 + v/c)$, calculate the energy shift of a 1-eV photon emitted from an iron atom moving toward you with energy $(3/2)kT$ at $T = 300$ K. Compare this Doppler line broadening with the natural line width calculated in Example 5-8. Repeat the calculation for a 1-MeV photon from a nuclear transition.

5-54. Calculate the order of magnitude of the shift in energy of a (*a*) 1-eV photon and (*b*) 1-MeV photon resulting from the recoil of an iron nucleus. Do this by first calculating the momentum of the photon and then by calculating $p^2/2m$ for the nucleus using that value of momentum. Compare with the natural line width calculated in Example 5-8.

STUDENTS-HUB.com Uploaded By: Malak Obaid

CHAPTER 6

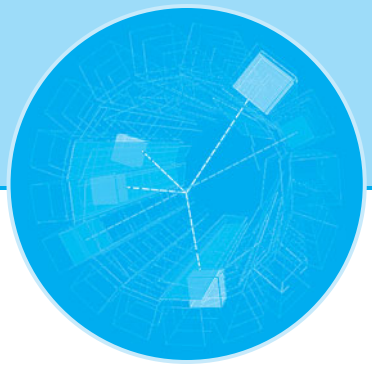

The Schrödinger Equation

The success of the de Broglie relations in predicting the diffraction of electrons and other particles, and the realization that classical standing waves lead to a discrete set of frequencies, prompted a search for a wave theory of electrons analogous to the wave theory of light. In this electron wave theory, classical mechanics should appear as the short-wavelength limit, just as geometric optics is the short-wavelength limit of the wave theory of light. The genesis of the correct theory went something like this, according to Felix Bloch,[1] who was present at the time:

> . . . in one of the next colloquia, Schrödinger gave a beautifully clear account of how de Broglie associated a wave with a particle and how he [i.e., de Broglie] could obtain the quantization rules . . . by demanding that an integer number of waves should be fitted along a stationary orbit. When he had finished Debye[2] casually remarked that he thought this way of talking was rather childish . . . [that to] deal properly with waves, one had to have a wave equation.

In 1926, Erwin Schrödinger[3] published his now-famous wave equation, which governs the propagation of matter waves, including those of electrons. A few months earlier, Werner Heisenberg had published a seemingly different theory to explain atomic phenomena. In the Heisenberg theory, only measurable quantities appear. Dynamical quantities such as energy, position, and momentum are represented by matrices, the diagonal elements of which are the possible results of measurement. Though the Schrödinger and Heisenberg theories appear to be different, it was eventually shown by Schrödinger himself that they were equivalent, in that each could be derived from the other. The resulting theory, now called *wave mechanics* or *quantum mechanics*, has been amazingly successful. Though its principles may seem strange to us, whose experiences are limited to the macroscopic world, and though the mathematics required to solve even the simplest problem is quite involved, there seems to be no alternative to describe correctly the experimental results in atomic and nuclear physics. In this book we will confine our study to the Schrödinger theory because it is easier to learn and is a little less abstract than the Heisenberg theory. We will begin by restricting our discussion to problems in one space dimension.

6-1 The Schrödinger Equation in One Dimension 222
6-2 The Infinite Square Well 229
6-3 The Finite Square Well 238
6-4 Expectation Values and Operators 242
6-5 The Simple Harmonic Oscillator 246
6-6 Reflection and Transmission of Waves 250

STUDENTS-HUB.com
Uploaded By: Malak Obaid

6-1 The Schrödinger Equation in One Dimension

The wave equation governing the motion of electrons and other particles with mass, which is analogous to the classical wave equation (Equation 5-11), was found by Schrödinger late in 1925 and is now known as the Schrödinger equation. Like the classical wave equation, the Schrödinger equation relates the time and space derivatives of the wave function. The reasoning followed by Schrödinger is somewhat difficult and not important for our purposes. In any case, it must be emphasized that we can't derive the Schrödinger equation just as we can't derive Newton's laws of motion. *Its validity, like that of any fundamental equation, lies in its agreement with experiment.* Just as Newton's second law is not relativistically correct, neither is Schrödinger's equation, which must ultimately yield to a relativistic wave equation. But, as you know, Newton's laws of motion are perfectly satisfactory for solving a vast array of nonrelativistic problems. So, too, will be Schrödinger's equation when applied to the equally extensive range of nonrelativistic problems in atomic, molecular, and solid-state physics. Schrödinger tried without success to develop a relativistic wave equation, a task accomplished in 1928 by Dirac.

Although it would be logical merely to postulate the Schrödinger equation, we can get some idea of what to expect by first considering the wave equation for photons, which is Equation 5-11 with speed $v = c$ and with $y(x, t)$ replaced by the electric field $\mathscr{E}(x, t)$.

$$\frac{\partial^2 \mathscr{E}}{\partial x^2} = \frac{1}{c^2}\frac{\partial^2 \mathscr{E}}{\partial t^2} \qquad \textbf{6-1}$$

As discussed in Chapter 5, a particularly important solution of this equation is the harmonic wave function $\mathscr{E}(x, t) = \mathscr{E}_0 \cos(kx - \omega t)$. Differentiating this function twice, we obtain

$$\frac{\partial^2 \mathscr{E}}{\partial t^2} = -\omega^2 \mathscr{E}_0 \cos(kx - \omega t) = -\omega^2 \mathscr{E}(x, t)$$

and

$$\frac{\partial^2 \mathscr{E}}{\partial x^2} = -k^2 \mathscr{E}(x, t)$$

Substitution into Equation 6-1 then gives

$$-k^2 = -\frac{\omega^2}{c^2}$$

or

$$\omega = kc \qquad \textbf{6-2}$$

Using $\omega = E/\hbar$ and $p = \hbar k$ for electromagnetic radiation, we have

$$E = pc \qquad \textbf{6-3}$$

which, as we saw earlier, is the relation between the energy and momentum of a photon.

STUDENTS-HUB.com Uploaded By: Malak Obaid

Erwin Schrödinger. [*Courtesy of the Niels Bohr Library, American Institute of Physics.*]

Now let us use the de Broglie relations for a particle such as an electron to find the relation between ω and k that is analogous to Equation 6-2 for photons. We can then use this relation to work backward and see how the wave equation for electrons must differ from Equation 6-1. The total energy (nonrelativistic) of a particle of mass m is

$$E = \frac{p^2}{2m} + V \qquad \textbf{6-4}$$

where V is the potential energy. Substituting the de Broglie relations (Equations 5-21 and 5-22) in Equation 6-4, we obtain

$$\hbar\omega = \frac{\hbar^2 k^2}{2m} + V \qquad \textbf{6-5}$$

This differs from Equation 6-2 for a photon because it contains the potential energy V and because the angular frequency ω does not vary linearly with k. Note that we get a factor of ω when we differentiate a harmonic wave function with respect to time and a factor of k when we differentiate with respect to position. We expect, therefore, that the wave equation that applies to electrons will relate the *first* time derivative to the *second* space derivative and will also involve the potential energy of the electron.

Finally, we require that the wave equation for electrons will be a differential equation that is linear in the wave function $\Psi(x, t)$, This ensures that, if $\Psi_1(x, t)$ and $\Psi_2(x, t)$ are both solutions of the wave equation for the same potential energy, then any arbitrary linear combination of these solutions is also a solution—i.e., $\Psi(x, t) = a_1\Psi_1(x, t) + a_2\Psi_2(x, t)$ is a solution, with a_1 and a_2 being arbitrary constants. Such a combination is called *linear* because both $\Psi_1(x, t)$ and $\Psi_2(x, t)$ appear only to the first power. Linearity guarantees that the wave functions will add together to produce constructive and destructive interference, which we have seen to be a characteristic of matter waves, as well as all other wave phenomena. Note, in particular, that (1) the linearity requirement means that *every* term in the wave equation must be linear in $\Psi(x, t)$ and (2) that *any* derivative of $\Psi(x, t)$ is linear in $\Psi(x, t)$.[4]

STUDENTS-HUB.com Uploaded By: Malak Obaid

The Schrödinger Equation

We are now ready to postulate the Schrödinger equation for a particle of mass m. In one dimension, it has the form

$$-\frac{\hbar^2}{2m}\frac{\partial^2\Psi(x,t)}{\partial x^2} + V(x,t)\Psi(x,t) = i\hbar\frac{\partial\Psi(x,t)}{\partial t} \qquad \textbf{6-6}$$

We will now show that this equation is satisfied by a harmonic wave function in the special case of a free particle, one on which no net force acts, so that the potential energy is constant, $V(x, t) = V_0$. First note that a function of the form $\cos(kx - \omega t)$ does not satisfy this equation because differentiation with respect to time changes the cosine to a sine, but the second derivative with respect to x gives back a cosine. Similar reasoning rules out the form $\sin(kx - \omega t)$. However, the exponential form of the harmonic wave function does satisfy the equation. Let

$$\begin{aligned}\Psi(x,t) &= Ae^{i(kx-\omega t)} \qquad \textbf{6-7}\\ &= A[\cos(kx-\omega t) + i\sin(kx-\omega t)]\end{aligned}$$

where A is a constant. Then

$$\frac{\partial\Psi}{\partial t} = -i\omega Ae^{i(kx-\omega t)} = -i\omega\Psi$$

and

$$\frac{\partial^2\Psi}{\partial x^2} = (ik)^2Ae^{i(kx-\omega t)} = -k^2\Psi$$

Substituting these derivatives into the Schrödinger equation with $V(x, t) = V_0$ gives

$$\frac{-\hbar^2}{2m}(-k^2\Psi) + V_0\Psi = i\hbar(-i\omega)\Psi$$

or

$$\frac{\hbar^2k^2}{2m} + V_0 = \hbar\omega$$

which is Equation 6-5.

An important difference between the Schrödinger equation and the classical wave equation is the explicit appearance[5] of the imaginary number $i = (-1)^{1/2}$. The wave functions that satisfy the Schrödinger equation are not necessarily real, as we see from the case of the free-particle wave function of Equation 6-7. Evidently the wave function $\Psi(x, t)$ which solves the Schrödinger equation is not a directly measurable function as the classical wave function $y(x, t)$ is since measurements always yield real numbers. However, as we discussed in Section 5-4, the probability of

STUDENTS-HUB.com Uploaded By: Malak Obaid

finding the electron in dx is certainly measurable, just as is the probability that a flipped coin will turn up heads. The probability $P(x)dx$ that the electron will be found in the volume dx was defined by Equation 5-23 to be equal to $|\Psi|^2\,dx$. This probabilistic interpretation of Ψ was developed by Max Born and was recognized, over the early and formidable objections of both Schrödinger and Einstein, as the appropriate way of relating solutions of the Schrödinger equation to the results of physical measurements. The probability that an electron is in the region dx, a real number, can be measured by counting the fraction of time it is found there in a very large number of identical trials. In recognition of the complex nature of $\Psi(x, t)$, we must modify slightly the interpretation of the wave function discussed in Chapter 5 to accommodate Born's interpretation so that the probability of finding the electron in dx is real. We take for the probability

$$P(x, t)\,dx = \Psi^*(x, t)\Psi(x, t)\,dx = |\Psi(x, t)|^2\,dx \qquad \textbf{6-8}$$

where Ψ^*, the complex conjugate of Ψ, is obtained from Ψ by replacing i with $-i$ wherever it appears.[6] The complex nature of Ψ serves to emphasize the fact that, in reality, we should not ask or try to answer the question, "What is waving in a matter wave?" or inquire as to what medium supports the motion of a matter wave. The wave function is a computational device with utility in Schrödinger's theory of wave mechanics. Physical significance is associated not with Ψ itself, but with the product $\Psi^*\Psi = |\Psi|^2$, which is the probability distribution *P(x, t)* or, as it is often called, the *probability density*. In keeping with the analogy with classical waves and wave functions, $\Psi(x, t)$ is also sometimes referred to as the *probability density amplitude*, or just the *probability amplitude*.

The probability of finding the electron in dx at x_1 or in dx at x_2 is the sum of separate probabilities, $P(x_1)\,dx + P(x_2)\,dx$. Since the electron must certainly be somewhere in space, the sum of the probabilities over all possible values of x must equal 1. That is[7]

$$\int_{-\infty}^{+\infty} \Psi^*\Psi\,dx = 1 \qquad \textbf{6-9}$$

Equation 6-9 is called the *normalization condition*. This condition plays an important role in quantum mechanics, for it places a restriction on the possible solutions of the Schrödinger equation. In particular, the wave function $\Psi(x, t)$ must approach zero sufficiently fast as $x \longrightarrow \pm\infty$ so that the integral in Equation 6-9 remains finite. If it does not, then the probability becomes unbounded. As we will see in Section 6-3, it is this restriction together with boundary conditions imposed at finite values of x that leads to energy quantization for bound particles.

In the chapters that follow, we are going to be concerned with solutions to the Schrödinger equation for a wide range of real physical systems, but in what follows in this chapter, our intent is to illustrate a few of the techniques of solving the equation and to discover the various, often surprising properties of the solutions. To this end we will focus our attention on one-dimensional problems, as noted earlier, and use some potential energy functions with unrealistic physical characteristics, e.g., infinitely rigid walls, which will enable us to illustrate various properties of the solutions without obscuring the discussion with overly complex mathematics.

STUDENTS-HUB.com Uploaded By: Malak Obaid

Separation of the Time and Space Dependencies of $\Psi(x, t)$

Schrödinger's first application of his wave equation was to problems such as the hydrogen atom (Bohr's work) and the simple harmonic oscillator (Planck's work), in which he showed that the energy quantization in those systems can be explained naturally in terms of standing waves. We referred to these in Chapter 4 as stationary states, meaning they did not change with time. Such states are also called *eigenstates*. For such problems that also have potential energy functions that are independent of time, the space and time dependence of the wave function can be separated, leading to a greatly simplified form of the Schrödinger equation.[8] The separation is accomplished by first assuming that $\Psi(x, t)$ can be written as a product of two functions, one of x and one of t, as

$$\Psi(x, t) = \psi(x)\phi(t) \tag{6-10}$$

If Equation 6-10 turns out to be incorrect, we will find that out soon enough, but it turns out that *if* the potential function is *not* an explicit function of time, i.e., if the potential is given by $V(x)$, our assumption turns out to be valid. That this is true can be seen as follows:

Substituting $\Psi(x, t)$ from Equation 6-10 into the general, time-dependent Schrödinger equation (Equation 6-6) yields

$$\frac{-\hbar^2}{2m}\frac{\partial^2\psi(x)\phi(t)}{\partial x^2} + V(x)\psi(x)\phi(t) = i\hbar\frac{\partial\psi(x)\phi(t)}{\partial t} \tag{6-11}$$

which is

$$\frac{-\hbar^2}{2m}\phi(t)\frac{d^2\psi(x)}{dx^2} + V(x)\psi(x)\phi(t) = i\hbar\psi(x)\frac{d\phi(t)}{dt} \tag{6-12}$$

where the derivatives are now ordinary rather than partial ones. Dividing Equation 6-12 by Ψ in the assumed product form $\psi\phi$ gives

$$\frac{-\hbar^2}{2m}\frac{1}{\psi(x)}\frac{d^2\psi(x)}{dx^2} + V(x) = i\hbar\frac{1}{\phi(t)}\frac{d\phi(t)}{dt} \tag{6-13}$$

Notice that each side of Equation 6-13 is a function of only one of the independent variables x and t. This means that, for example, changes in t cannot affect the value of the left side of Equation 6-13, and changes in x cannot affect the right side. Thus, both sides of the equation must be equal to the same constant C, called the *separation constant*, and we see that the assumption of Equation 6-10 is valid—the variables have been separated. We have thus replaced a partial differential equation containing two independent variables, Equation 6-6, with two ordinary differential equations each a function of only one of the independent variables:

$$\frac{-\hbar^2}{2m}\frac{1}{\psi(x)}\frac{d^2\psi(x)}{dx^2} + V(x) = C \tag{6-14}$$

$$i\hbar\frac{1}{\phi(t)}\frac{d\phi(t)}{dt} = C \tag{6-15}$$

STUDENTS-HUB.com Uploaded By: Malak Obaid

Let us solve Equation 6-15 first. The reason for doing so is twofold: (1) Equation 6-15 does not contain the potential $V(x)$; consequently, the time-dependent part $\phi(t)$ of *all* solutions $\Psi(x, t)$ to the Schrödinger equation will have the same form when the potential is not an explicit function of time, so we only have to do this once. (2) The separation constant C has particular significance that we want to discover before we tackle Equation 6-14. Writing Equation 6-15 as

$$\frac{d\phi(t)}{\phi(t)} = \frac{C}{i\hbar}\,dt = -\frac{iC}{\hbar}\,dt \qquad \textbf{6-16}$$

The general solution of Equation 6-16 is

$$\phi(t) = e^{-iCt/\hbar} \qquad \textbf{6-17}\boldsymbol{a}$$

which can also be written as

$$\phi(t) = e^{-iCt/\hbar} = \cos\left(\frac{Ct}{\hbar}\right) - i\sin\left(\frac{Ct}{\hbar}\right) = \cos\left(2\pi\frac{Ct}{h}\right) - i\sin\left(2\pi\frac{Ct}{h}\right) \qquad \textbf{6-17}\boldsymbol{b}$$

Thus, we see that $\phi(t)$, which describes the time variation of $\Psi(x, t)$, is an oscillatory function with frequency $f = C/h$, However, according to the de Broglie relation (Equation 5-1), the frequency of the wave represented by $\Psi(x, t)$ is $f = E/h$; therefore, we conclude that the separation constant $C = E$, the total energy of the particle, and we have

$$\phi(t) = e^{-iEt/\hbar} \qquad \textbf{6-17}\boldsymbol{c}$$

for all solutions to Equation 6-6 involving time-independent potentials. Equation 6-14 then becomes, on multiplication by $\psi(x)$,

$$\frac{-\hbar^2}{2m}\frac{d^2\psi(x)}{dx^2} + V(x)\psi(x) = E\psi(x) \qquad \textbf{6-18}$$

Equation 6-18 is referred to as the *time-independent Schrödinger equation*.

The time-independent Schrödinger equation in one dimension is an ordinary differential equation in one variable x and is therefore much easier to handle than the general form of Equation 6-6. The normalization condition of Equation 6-9 can be expressed in terms of $\psi(x)$, since the time dependence of the absolute square of the wave function cancels. We have

$$\Psi^*(x, t)\Psi(x, t) = \psi^*(x)e^{+iEt/\hbar}\psi(x)e^{-iEt/\hbar} = \psi^*(x)\psi(x) \qquad \textbf{6-19}$$

and Equation 6-9 then becomes

$$\int_{-\infty}^{+\infty} \psi^*(x)\psi(x)dx = 1 \qquad \textbf{6-20}$$

Conditions for Acceptable Wave Functions

The form of the wave function $\psi(x)$ that satisfies Equation 6-18 depends on the form of the potential energy function $V(x)$. In the next few sections we will study some simple but important problems in which $V(x)$ is specified. Our example potentials will be approximations to real physical potentials, simplified to make calculations easier.

STUDENTS-HUB.com Uploaded By: Malak Obaid

In some cases, the slope of the potential energy may be discontinuous, e.g., $V(x)$ may have one form in one region of space and another form in an adjacent region. (This is a useful mathematical approximation to real situations in which $V(x)$ varies rapidly over a small region of space, such as at the surface boundary of a metal.) The procedure in such cases is to solve the Schrödinger equation separately in each region of space and then require that the solutions join smoothly at the point of discontinuity.

Since the probability of finding a particle cannot vary discontinuously from point to point, the wave function $\psi(x)$ must be continuous.[9] Since the Schrödinger equation involves the second derivative $d^2\psi/dx^2 = \psi''$, the first derivative ψ' (which is the slope) must also be continuous. That is, the graph of $\psi(x)$ versus x must be smooth. (In a special case in which the potential energy becomes infinite, this restriction is relaxed. Since no particle can have infinite potential energy, $\psi(x)$ must be zero in regions where $V(x)$ is infinite. Then, at the boundary of such a region, ψ' may be discontinuous.)

If either $\psi(x)$ or $d\psi/dx$ were not finite or not single valued, the same would be true of $\Psi(x, t)$ and $d\Psi/dx$. As we will shortly see, the predictions of wave mechanics regarding the results of measurements involve both of those quantities and would thus not necessarily predict finite or definite values for real physical quantities. Such results would not be acceptable since measurable quantities, such as angular momentum and position, are never infinite or multiple valued. A final restriction on the form of the wave function $\psi(x)$ is that in order to obey the normalization condition, $\psi(x)$ must approach zero sufficiently fast as $x \longrightarrow \pm\infty$ so that normalization is preserved. For future reference, we may summarize the conditions that the wave function $\psi(x)$ must meet in order to be acceptable as follows:

1. $\psi(x)$ must exist and satisfy the Schrödinger equation.
2. $\psi(x)$ and $d\psi/dx$ must be continuous.
3. $\psi(x)$ and $d\psi/dx$ must be finite.
4. $\psi(x)$ and $d\psi/dx$ must be single valued.
5. $\psi(x) \longrightarrow 0$ fast enough as $x \longrightarrow \pm\infty$ so that the normalization integral, Equation 6-20, remains bounded.

Note that, given Equation 6-10, the acceptability conditions above ultimately apply to $\Psi(x, t)$.

Questions

1. Like the classical wave equation, the Schrödinger equation is linear. Why is this important?
2. There is no factor $i = (-1)^{1/2}$ in Equation 6-18. Does this mean that $\psi(x)$ must be real?
3. Why must the electric field $\mathscr{E}(x, t)$ be real? Is it possible to find a nonreal wave function that satisfies the classical wave equation?
4. Describe how the de Broglie hypothesis enters into the Schrödinger wave equation.
5. What would be the effect on the Schrödinger equation of adding a constant rest energy for a particle with mass to the total energy E in the de Broglie relation $f = E/h$?
6. Describe in words what is meant by normalization of the wave function.

STUDENTS-HUB.com Uploaded By: Malak Obaid

EXAMPLE 6-1 **A Solution to the Schrödinger Equation** Show that for a free particle of mass m moving in one dimension, the function $\psi(x) = A \sin kx + B \cos kx$ is a solution to the time-independent Schrödinger equation for any values of the constants A and B.

SOLUTION

A free particle has no net force acting upon it, e.g., $V(x) = 0$, in which case the kinetic energy equals the total energy. Thus, $p = \hbar k = (2mE)^{1/2}$. Differentiating $\psi(x)$ gives

$$\frac{d\psi}{dx} = kA \cos kx - kB \sin kx$$

and differentiating again,

$$\begin{aligned}\frac{d^2\psi}{dx^2} &= -k^2 A \sin kx - k^2 B \cos kx \\ &= -k^2(A \sin kx + B \cos kx) = -k^2\psi(x)\end{aligned}$$

Substituting into Equation 6-18,

$$\frac{-\hbar^2}{2m}[(-k^2)(A \sin kx + B \cos kx)] = E(A \sin kx + B \cos kx)$$

$$\frac{\hbar^2 k^2}{2m}\psi(x) = E\psi(x)$$

and, since $\hbar^2 k^2 = 2mE$, we have

$$E\psi(x) = E\psi(x)$$

and the given $\psi(x)$ is a solution of Equation 6-18.

6-2 The Infinite Square Well

A problem that provides several illustrations of the properties of wave functions and is also one of the easiest problems to solve using the time-independent, one-dimensional Schrödinger equation is that of the infinite square well, sometimes called the particle in a box. A macroscopic example is a bead moving on a frictionless wire between two massive stops clamped to the wire. We could also build such a "box" for an electron using electrodes and grids in an evacuated tube, as illustrated in Figure 6-1*a*. The walls of the box are provided by the increasing potential between the grids G and the electrode C as shown in Figures 6-1*b* and *c*. The walls can be made arbitrarily high and steep by increasing the potential V and reducing the separation between each grid-electrode pair. In the limit such a potential energy function looks like that in Figure 6-2, which is a graph of the potential energy of an infinite square well. For this problem the potential energy is of the form

$$\begin{aligned} V(x) &= 0 \qquad 0 < x < L \\ V(x) &= \infty \qquad x < 0 \quad \text{and} \quad x > L \end{aligned} \tag{6-21}$$

Although such a potential is clearly artificial, the problem is worth careful study for several reasons: (1) exact solutions to the Schrödinger equation can be obtained

STUDENTS-HUB.com Uploaded By: Malak Obaid

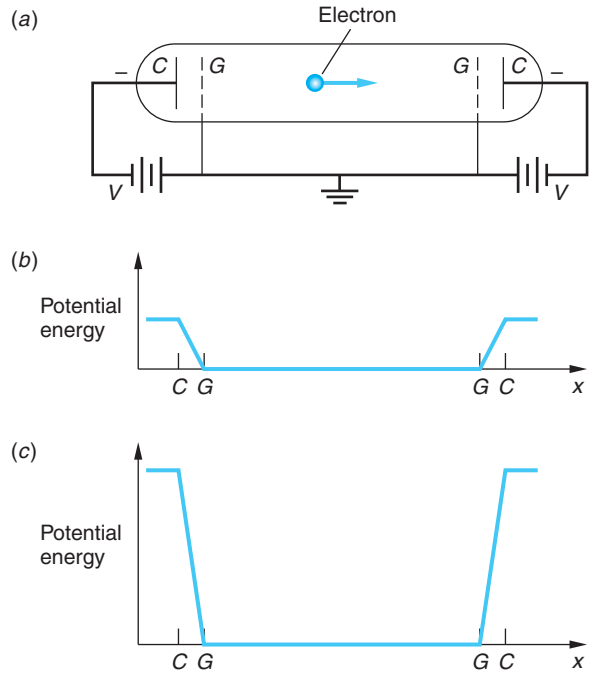

Figure 6-1 (*a*) The electron placed between the two sets of electrodes *C* and grids *G* experiences no force in the region between the grids, which are at ground potential. However, in the regions between each *C* and *G* is a repelling electric field whose strength depends upon the magnitude of *V*. (*b*) If *V* is small, then the electron's potential energy versus *x* has low, sloping "walls." (*c*) If *V* is large, the "walls" become very high and steep, becoming infinitely high for $V \rightarrow \infty$.

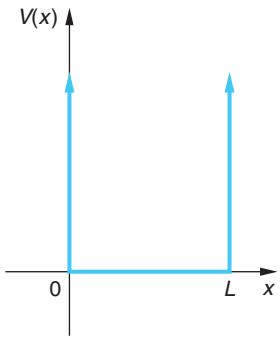

Figure 6-2 Infinite square well potential energy. For $0 < x < L$, the potential energy $V(x)$ is zero. Outside this region, $V(x)$ is infinite. The particle is confined to the region in the well $0 < x < L$.

without the difficult mathematics that usually accompanies its solution for more realistic potential functions, (2) the problem is closely related to the vibrating-string problem familiar in classical physics, (3) it illustrates many of the important features of all quantum-mechanical problems, and finally, (4) this potential is a relatively good approximation to some real situations; e.g., the motion of a free electron inside a metal.

Since the potential energy is infinite outside the well, the wave function is required to be zero there; that is, the particle must be inside the well. (As we proceed through this and other problems, keep in mind Born's interpretation: the probability density of the particle's position is proportional to $|\psi|^2$.) We then need only to solve Equation 6-18 for the region inside the well $0 < x < L$, subject to the condition that since the wave function must be continuous, $\psi(x)$ must be zero at $x = 0$ and $x = L$. Such a condition on the wave function at a boundary (here, the discontinuity of the potential energy function) is called a *boundary condition*. We will see that, mathematically, it is the boundary conditions together with the requirement that $\psi(x) \rightarrow 0$ as $x \rightarrow \pm\infty$ that lead to the quantization of energy. A classic example is the case of a vibrating string fixed at both ends. In that case the wave function $y(x, t)$ is the displacement of the string. If the string is fixed at $x = 0$ and $x = L$, we have the same boundary condition on the vibrating-string wave function: namely, that $y(x, t)$ be zero at $x = 0$ and $x = L$. These boundary conditions lead to discrete allowed frequencies of vibration of the string. It was this quantization of frequencies (which always occurs for standing waves in classical physics), along with de Broglie's hypothesis, that motivated Schrödinger to look for a wave equation for electrons.

The standing-wave condition for waves on a string of length *L* fixed at both ends is that *an integral number of half wavelengths fit into the length L.*

$$n\frac{\lambda}{2} = L \qquad n = 1, 2, 3, \ldots \qquad \textbf{6-22}$$

STUDENTS-HUB.com Uploaded By: Malak Obaid

We will show below that the same condition follows from the solution of the Schrödinger equation for a particle in an infinite square well. Since the wavelength is related to the momentum of the particle by the de Broglie relation $p = h/\lambda$ and the total energy of the particle in the well is just the kinetic energy $p^2/2m$ (see Figure 6-2), this quantum condition on the wavelength implies that the energy is quantized and the allowed values are given by

$$E = \frac{p^2}{2m} = \frac{h^2}{2m\lambda^2} = \frac{h^2}{2m(2L/n)^2} = n^2\frac{h^2}{8mL^2} \qquad \textbf{6-23}$$

Since the energy depends on the integer n, it is customary to label it E_n. In terms of $\hbar = h/2\pi$ the energy is given by

$$E_n = n^2\frac{\pi^2\hbar^2}{2mL^2} = n^2E_1 \qquad n = 1, 2, 3, \ldots \qquad \textbf{6-24}$$

where E_1 is the lowest allowed energy[10] and is given by

$$E_1 = \frac{\pi^2\hbar^2}{2mL^2} \qquad \textbf{6-25}$$

We now derive this result from the time-independent Schrödinger equation (Equation 6-18), which for $V(x) = 0$ is

$$-\frac{\hbar^2}{2m}\frac{d^2\psi(x)}{dx^2} = E\psi(x)$$

or

$$\psi''(x) = -\frac{2mE}{\hbar^2}\psi(x) = -k^2\psi(x) \qquad \textbf{6-26}$$

where we have substituted the square of the wave number k since

$$k^2 = \left(\frac{p}{\hbar}\right)^2 = \frac{2mE}{\hbar^2} \qquad \textbf{6-27}$$

and we have written $\psi''(x)$ for the second derivative $d^2\psi(x)/dx^2$. Equation 6-26 has solutions of the form

$$\psi(x) = A\sin kx \qquad \textbf{6-28}\boldsymbol{a}$$

and

$$\psi(x) = B\cos kx \qquad \textbf{6-28}\boldsymbol{b}$$

where A and B are constants. The boundary condition $\psi(x) = 0$ at $x = 0$ rules out the cosine solution (Equation 6-28*b*) because $\cos 0 = 1$, so B must equal zero. The boundary condition $\psi(x) = 0$ at $x = L$ gives

$$\psi(L) = A\sin kL = 0 \qquad \textbf{6-29}$$

STUDENTS-HUB.com Uploaded By: Malak Obaid

This condition is satisfied if kL is any integer times π, i.e., if k is restricted to the values k_n given by

$$k_n = n\frac{\pi}{L} \qquad n = 1, 2, 3, \ldots \tag{6-30}$$

If we write the wave number k in terms of the wavelength $\lambda = 2\pi/k$, we see that Equation 6-30 is the same as Equation 6-22 for standing waves on a string. The quantized energy values, or *energy eigenvalues*, are found from Equation 6-27, replacing k by k_n as given by Equation 6-30. We thus have

$$E_n = \frac{\hbar^2 k_n^2}{2m} = n^2 \frac{\hbar^2 \pi^2}{2mL^2} = n^2 E_1$$

which is the same as Equation 6-24. Figure 6-3 shows the energy level diagram and the potential energy function for the infinite square well potential.

The constant A in the wave function of Equation 6-28*a* is determined by the normalization condition:

$$\int_{-\infty}^{+\infty} \psi^*_n \psi_n \, dx = \int_0^L A_n^2 \sin^2\left(\frac{n\pi x}{L}\right) dx = 1 \tag{6-31}$$

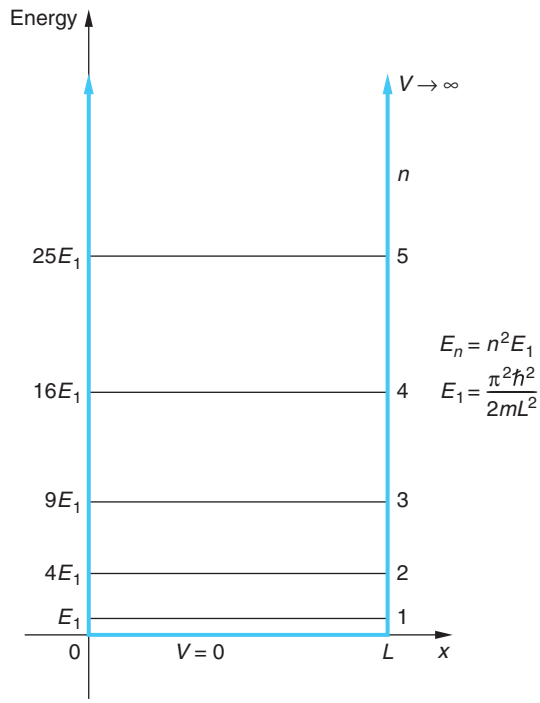

Figure 6-3 Graph of energy vs. x for a particle in an infinitely deep well. The potential energy $V(x)$ is shown with the colored lines. The set of allowed values for the particle's total energy E_n as given by Equation 6-24 form the energy-level diagram for the infinite square well potential. Classically, a particle can have any value of energy. Quantum mechanically, only the values given by $E_n = n^2(\hbar^2\pi^2/2mL^2)$ yield well-behaved solutions of the Schrödinger equation. As we become more familiar with energy-level diagrams, the x axis will be omitted.

STUDENTS-HUB.com Uploaded By: Malak Obaid

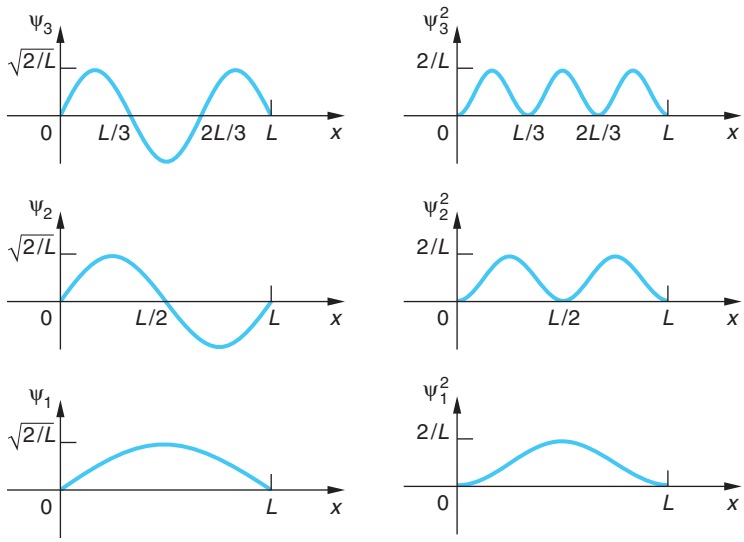

Figure 6-4 Wave functions $\psi_n(x)$ and probability densities $P_n(x) = \psi_n^2(x)$ for $n = 1, 2$, and 3 for the infinite square well potential. Though not shown, $\psi_n(x) = 0$ for $x < 0$ and $x > L$.

Since the wave function is zero in regions of space where the potential energy is infinite, the contributions to the integral from $-\infty$ to 0 and from L to $+\infty$ will both be zero. Thus, only the integral from 0 to L needs to be evaluated. Integrating, we obtain $A_n = (2/L)^{1/2}$ independent of n. The normalized wave function solutions for this problem, also called *eigenfunctions*, are then

$$\psi_n(x) = \sqrt{\frac{2}{L}} \sin \frac{n\pi x}{L} \qquad n = 1, 2, 3, \ldots \qquad \textbf{6-32}$$

These wave functions are exactly the same as the standing-wave functions $y_n(x)$ for the vibrating-string problem. The wave functions and the probability distribution functions $P_n(x)$ are sketched in Figure 6-4 for the lowest energy state $n = 1$, called the *ground state*, and for the first two *excited states*, $n = 2$ and $n = 3$. (Since these wave functions are real, $P_n(x) = \psi_n^* \psi_n = \psi_n^2$.) Notice in Figure 6-4 that the maximum amplitudes of each of the $\psi_n(x)$ are the same, $(2/L)^{1/2}$, as are those of $P_n(x)$, $2/L$. Note, too, that both $\psi_n(x)$ and $P_n(x)$ extend to $\pm\infty$. They just happen to be zero for $x < 0$ and $x > L$ in this case.

The number n in the equations above is called a *quantum number*. It specifies both the energy and the wave function. Given any value of n, we can immediately write down the wave function and the energy of the system. The quantum number n occurs because of the boundary conditions $\psi(x) = 0$ at $x = 0$ and $x = L$. We will see in Section 7-1 that for problems in three dimensions, three quantum numbers arise, one associated with boundary conditions on each coordinate.

Comparison with Classical Results

Let us compare our quantum-mechanical solution of this problem with the classical solution. In classical mechanics, if we know the potential energy function $V(x)$, we can find the force from $F_x = -dV/dx$ and thereby obtain the acceleration $a_x = d^2x/dt^2$ from Newton's second law. We can then find the position x as a function of time t if we know the initial position and velocity. In this problem there is no force when the

STUDENTS-HUB.com Uploaded By: Malak Obaid

particle is between the walls of the well because $V = 0$ there. The particle therefore moves with constant speed in the well. Near the edge of the well the potential energy rises discontinuously to infinity—we may describe this as a very large force that acts over a very short distance and turns the particle around at the wall so that it moves away with its initial speed. Any speed, and therefore any energy, is permitted classically. The classical description breaks down because, according to the uncertainty principle, we can never precisely specify both the position and momentum (and therefore velocity) at the same time. We can therefore never specify the initial conditions precisely and cannot assign a definite position and momentum to the particle. Of course, for a macroscopic particle moving in a macroscopic box, the energy is much larger than E_1 of Equation 6-25, and the minimum uncertainty of momentum, which is of the order of $\hbar/L$, is much less than the momentum and less than experimental uncertainties. Then the difference in energy between adjacent states will be a small fraction of the total energy, quantization will be unnoticed, and the classical description will be adequate.[11]

Let us also compare the classical prediction for the distribution of measurements of position with those from our quantum-mechanical solution. Classically, the probability of finding the particle in some region dx is proportional to the time spent in dx, which is dx/v, where v is the speed. Since the speed is constant, the classical distribution function is just a constant inside the well. The normalized classical distribution function is

$$P_C(x) = \frac{1}{L}$$

In Figure 6-4 we see that for the lowest energy states, the quantum distribution function is very different from this. According to Bohr's correspondence principle, the quantum distributions should approach the classical distribution when n is large, that is, at large energies. For any state n, the quantum distribution has n peaks. The distribution for $n = 10$ is shown in Figure 6-5. For very large n, the peaks are close together, and if there are many peaks in a small distance Δx, only the average value will be observed. But the average value of $\sin^2 k_n x$ over one or more cycles is $1/2$. Thus

$$\left[\psi_n^2(x)\right]_{\text{av}} = \left[\frac{2}{L}\sin^2 k_n x\right]_{\text{av}} = \frac{2}{L}\frac{1}{2} = \frac{1}{L}$$

which is the same as the classical distribution.

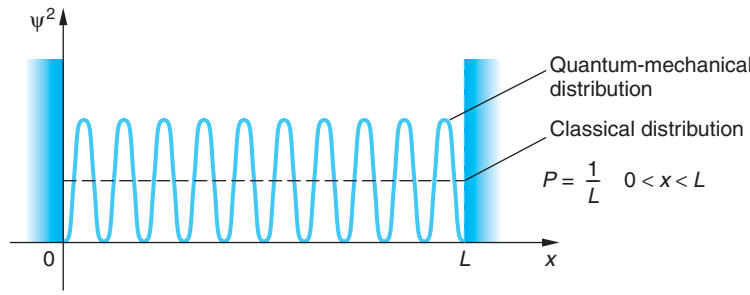

Figure 6-5 Probability distribution for $n = 10$ for the infinite square well potential. The dashed line is the classical probability density $P = 1/L$, which is equal to the quantum-mechanical distribution averaged over a region Δx containing several oscillations. A physical measurement with resolution Δx will yield the classical result if n is so large that $\psi^2(x)$ has many oscillations in Δx.

STUDENTS-HUB.com Uploaded By: Malak Obaid

The Complete Wave Function

The complete wave function, including its time dependence, is found by multiplying the space part by

$$e^{-i\omega t} = e^{-i(E_n/\hbar)t}$$

according to Equation 6-17*c*. As mentioned previously, a wave function corresponding to a single energy oscillates with angular frequency $\omega_n = E_n/\hbar$, but the probability distribution $|\Psi_n(x, t)|^2$ is independent of time. This is the wave-mechanical justification for calling such a state a stationary state or eigenstate, as we have done earlier. It is instructive to look at the complete wave function for a particular state n.

$$\Psi_n(x, t) = \sqrt{\frac{2}{L}} \sin k_n x \, e^{-i\omega_n t}$$

If we use the identity

$$\sin k_n x = \frac{(e^{ik_n x} - e^{-ik_n x})}{2i}$$

we can write this wave function as

$$\Psi_n(x, t) = \frac{1}{2i}\sqrt{\frac{2}{L}} [e^{i(k_n x - \omega_n t)} - e^{-i(k_n x + \omega_n t)}]$$

Just as in the case of the standing-wave function for the vibrating string, we can consider this stationary-state wave function to be the superposition of a wave traveling to the right and a wave of the same frequency and amplitude traveling to the left. Since measurable quantities are related to $P \propto |\Psi|^2$, the fact that Ψ is complex is not a problem.

EXAMPLE 6-2 **An Electron in a Wire** An electron moving in a thin metal wire is a reasonable approximation of a particle in a one-dimensional infinite well. The potential inside the wire is constant on average but rises sharply at each end. Suppose the electron is in a wire 1.0 cm long. (*a*) Compute the ground-state energy for the electron. (*b*) If the electron's energy is equal to the average kinetic energy of the molecules in a gas at $T = 300$ K, about 0.03 eV, what is the electron's quantum number n?

SOLUTION

1. For question (*a*), the ground-state energy is given by Equation 6-25:

$$\begin{aligned} E_1 &= \frac{\pi^2\hbar^2}{2mL^2} \\ &= \frac{\pi^2(1.055 \times 10^{-34}\ \text{J}\cdot\text{s})^2}{(2)(9.11 \times 10^{-31}\ \text{kg})(10^{-2}\ \text{m})^2} \\ &= 6.03 \times 10^{-34}\ \text{J} = 3.80 \times 10^{-15}\ \text{eV} \end{aligned}$$

2. For question (*b*), the electron's quantum number is given by Equation 6-24:

$$E_n = n^2 E_1$$

STUDENTS-HUB.com Uploaded By: Malak Obaid

3. Solving Equation 6-24 for n and substituting $E_n = 0.03$ eV and E_1 from above yields

$$n^2 = \frac{E_n}{E_1}$$

or

$$n = \sqrt{\frac{E_n}{E_1}} = \sqrt{\frac{0.03 \text{ eV}}{3.80 \times 10^{-15} \text{ eV}}}$$
$$= 2.81 \times 10^6$$

Remarks: The value of E_1 computed above is not only far below the limit of measurability, but also smaller than the uncertainty in the energy of an electron confined into 1 cm. For a value of n this large, the correspondence principle applies.

EXAMPLE 6-3 Calculating Probabilities Suppose that the electron in Example 6-2 could be measured while in its ground state. (*a*) What would be the probability of finding it somewhere in the region $0 < x < L/4$? (*b*) What would be the probability of finding it in a very narrow region $\Delta x = 0.01L$ wide centered at $x = 5L/8$?

SOLUTION

(*a*) The wave function for the $n = 1$ level, the ground state, is given by Equation 6-32 as

$$\psi_1(x) = \sqrt{\frac{2}{L}} \sin \frac{\pi x}{L}$$

The probability that the electron would be found in the region specified is

$$\int_0^{L/4} P_1(x)\, dx = \int_0^{L/4} \frac{2}{L} \sin^2\left(\frac{\pi x}{L}\right) dx$$

Letting $u = \pi x/L$, hence $dx = L\, du/\pi$, and noting the appropriate change in the limits on the integral, we have that

$$\int_0^{\pi/4} \frac{2}{\pi} \sin^2 u\, du = \frac{2}{\pi}\left(\frac{u}{2} - \frac{\sin 2u}{4}\right)\Bigg|_0^{\pi/4} = \frac{2}{\pi}\left(\frac{\pi}{8} - \frac{1}{4}\right) = 0.091$$

Thus, if one looked for the particle in a large number of identical searches, the electron would be found in the region $0 < x < 0.25$ cm about 9 percent of the time. This probability is illustrated by the shaded area on the left side in Figure 6-6.

(*b*) Since the region $\Delta x = 0.01L$ is very small compared with L, we do not need to integrate but can calculate the approximate probability as follows:

$$P = P(x)\, \Delta x = \frac{2}{L} \sin^2 \frac{\pi x}{L} \Delta x$$

Substituting $\Delta x = 0.01L$ and $x = 5L/8$, we obtain

$$P = \frac{2}{L} \sin^2 \frac{\pi(5L/8)}{L} (0.01L)$$
$$= \frac{2}{L}(0.854)(0.01L) = 0.017$$

STUDENTS-HUB.com Uploaded By: Malak Obaid

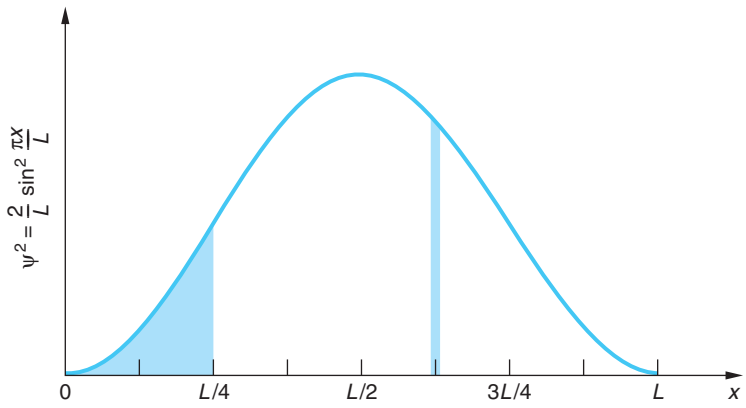

Figure 6-6 The probability density $\psi^2(x)$ versus x for a particle in the ground state of an infinite square well potential. The probability of finding the particle in the region $0 < x < L/4$ is represented by the larger shaded area. The narrow shaded band illustrates the probability of finding the particle within $\Delta x = 0.01L$ around the point where $x = 5L/8$.

This means that the probability of finding the electron within $0.01L$ around $x = 5L/8$ is about 1.7 percent. This is illustrated in Figure 6-6, where the area of the shaded narrow band at $x = 5L/8$ is 1.7 percent of the total area under the curve.

EXAMPLE 6-4 An Electron in an Atomic-Size Box (*a*) Find the energy in the ground state of an electron confined to a one-dimensional box of length $L = 0.1$ nm. (This box is roughly the size of an atom.) (*b*) Make an energy-level diagram and find the wavelengths of the photons emitted for all transitions beginning at state $n = 3$ or less and ending at a lower energy state.

SOLUTION

(*a*) The energy in the ground state is given by Equation 6-25. Multiplying the numerator and denominator by $c^2/4\pi^2$, we obtain an expression in terms of hc and mc^2, the energy equivalent of the electron mass (see Chapter 2):

$$E_1 = \frac{(hc)^2}{8mc^2L^2}$$

Substituting $hc = 1240 \text{ eV} \cdot \text{nm}$ and $mc^2 = 0.511$ MeV, we obtain

$$E_1 = \frac{(1240 \text{ eV} \cdot \text{nm})^2}{8(5.11 \times 10^5 \text{ eV})(0.1 \text{ nm})^2} = 37.6 \text{ eV}$$

This is of the same order of magnitude as the kinetic energy of the electron in the ground state of the hydrogen atom, which is 13.6 eV. In that case, the wavelength of the electron equals the circumference of a circle of radius 0.0529 nm, or about 0.33 nm, whereas for the electron in a one-dimensional box of length 0.1 nm, the wavelength in the ground state is $2L = 0.2$ nm.

(*b*) The energies of this system are given by

$$E_n = n^2E_1 = n^2(37.6 \text{ eV})$$

STUDENTS-HUB.com Uploaded By: Malak Obaid

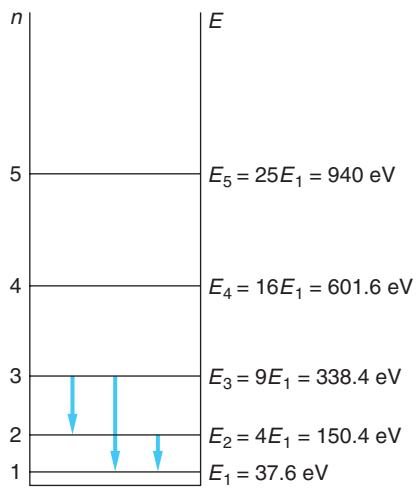

Figure 6-7 Energy-level diagram for Example 6-4. Transitions from the state $n = 3$ to the states $n = 2$ and $n = 1$, and from the state $n = 2$ to $n = 1$, are indicated by the vertical arrows.

Figure 6-7 shows these energies in an energy-level diagram. The energy of the first excited state is $E_2 = 4 \cdot (37.6 \text{ eV}) = 150.4 \text{ eV}$, and that of the second excited state is $E_3 = 9 \cdot (37.6 \text{ eV}) = 338.4 \text{ eV}$. The possible transitions from level 3 to level 2, from level 3 to level 1, and from level 2 to level 1 are indicated by the vertical arrows on the diagram. The energies of these transitions are

$$\Delta E_{3\to 2} = 338.4 \text{ eV} - 150.4 \text{ eV} = 188.0 \text{ eV}$$
$$\Delta E_{3\to 1} = 338.4 \text{ eV} - 37.6 \text{ eV} = 300.8 \text{ eV}$$
$$\Delta E_{2\to 1} = 150.4 \text{ eV} - 37.6 \text{ eV} = 112.8 \text{ eV}$$

The photon wavelengths for these transitions are

$$\lambda_{3\to 2} = \frac{hc}{\Delta E_{3\to 2}} = \frac{1240 \text{ eV} \cdot \text{nm}}{188.0 \text{ eV}} = 6.60 \text{ nm}$$
$$\lambda_{3\to 1} = \frac{hc}{\Delta E_{3\to 1}} = \frac{1240 \text{ eV} \cdot \text{nm}}{300.8 \text{ eV}} = 4.12 \text{ nm}$$
$$\lambda_{2\to 1} = \frac{hc}{\Delta E_{2\to 1}} = \frac{1240 \text{ eV} \cdot \text{nm}}{112.8 \text{ eV}} = 11.0 \text{ nm}$$

6-3 The Finite Square Well

The quantization of energy that we found for a particle in an infinite square well is a general result that follows from the solution of the Schrödinger equation for any particle confined in some region of space. We will illustrate this by considering the qualitative behavior of the wave function for a slightly more general potential energy function, the finite square well shown in Figure 6-8. The solutions of the Schrödinger equation for this type of potential energy are quite different, depending on whether the total energy E is greater or less than V_0. We will defer discussion of the case $E > V_0$ to Section 6-5 except to remark that in that case, the particle is not confined and any value of the energy is allowed; i.e., there is no energy quantization. Here we will assume that $E < V_0$.

STUDENTS-HUB.com Uploaded By: Malak Obaid

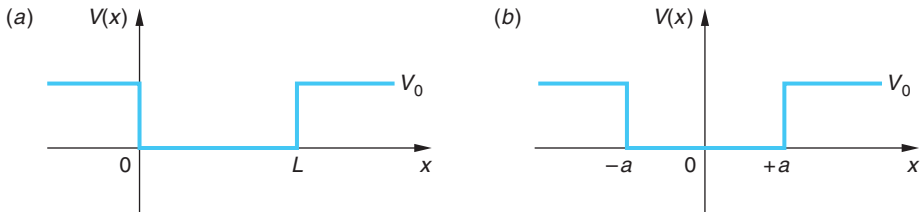

Figure 6-8 (*a*) The finite square well potential. (*b*) Region I is that with $x < -a$, II with $-a < x < +a$, and III with $x > +a$.

Inside the well, $V(x) = 0$ and the time-independent Schrödinger equation (Equation 6-18) becomes Equation 6-26, the same as for the infinite well:

$$\psi''(x) = -k^2\psi(x) \qquad k^2 = \frac{2mE}{\hbar^2}$$

The solutions are sines and cosines (Equation 6-28) except that now we do not require $\psi(x)$ to be zero at the well boundaries, but rather we require that $\psi(x)$ and $\psi'(x)$ be continuous at these points. Outside the well, i.e., for $0 > x > L$, Equation 6-18 becomes

$$\psi''(x) = \frac{2m}{\hbar^2}(V_0 - E)\psi(x) = \alpha^2\psi(x) \qquad \textbf{6-33}$$

where

$$\alpha^2 = \frac{2m}{\hbar^2}(V_0 - E) > 0 \qquad \textbf{6-34}$$

The straightforward method of finding the wave functions and allowed energies for this problem is to solve Equation 6-33 for $\psi(x)$ outside the well and then require that $\psi(x)$ and $\psi'(x)$ be continuous at the boundaries. The solution of Equation 6-33 is not difficult [it is of the form $\psi(x) = Ce^{-\alpha x}$ for positive x], but applying the boundary conditions involves a method that may be new to you; we describe it in the More section on the Graphical Solution of the Finite Square Well.

First, we will explain in words unencumbered by the mathematics how the conditions of continuity of ψ and ψ' at the boundaries and the need for $\psi \to 0$ as $x \to \pm\infty$ leads to the selection of only certain wave functions and quantized energies for values of E within the well; i.e., $0 < E < V_0$. The important feature of Equation 6-33 is that the second derivative ψ'', which is the curvature of the wave function, has the same sign as the wave function ψ. If ψ is positive, ψ'' is also positive and the wave function curves away from the axis, as shown in Figure 6-9*a*. Similarly, if ψ is negative, ψ'' is negative and, again, ψ curves away from the axis. This behavior is different from that inside the well, where $0 < x < L$. There, ψ *and* ψ'' *have opposite signs so that* ψ *always curves toward the axis like a sine or cosine function*. Because of this behavior outside the well,

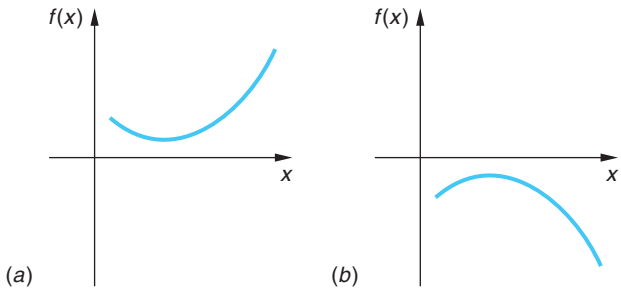

Figure 6-9 (*a*) Positive function with positive curvature; (*b*) negative function with negative curvature.

STUDENTS-HUB.com Uploaded By: Malak Obaid

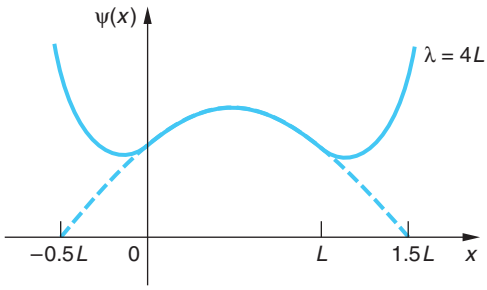

Figure 6-10 The function that satisfies the Schrödinger equation with $\lambda = 4L$ inside the well is not an acceptable wave function because it becomes infinite at large x. Although at $x = L$, the function is heading toward zero (slope is negative), the rate of increase of the slope ψ'' is so great that the slope becomes positive before the function becomes zero, and the function then increases. Since ψ'' has the same sign as ψ, the slope always increases and the function increases without bound. [*This computer-generated plot courtesy of Paul Doherty, The Exploratorium.*]

for most values of the energy the wave function becomes infinite as $x \rightarrow \pm\infty$; i.e., $\psi(x)$ is not well behaved. Such functions, though satisfying the Schrödinger equation, are not proper wave functions because they cannot be normalized.

Figure 6-10 shows the wave function for the energy $E = p^2/2m = h^2/2m\lambda^2$ for $\lambda = 4L$. Figure 6-11 shows a well-behaved wave function corresponding to wavelength $\lambda = \lambda_1$, which is the ground state wave function for the finite well, and the behavior of the wave functions for two nearby energies and wavelengths. The exact determination of the allowed energy levels in a finite square well can be obtained from a detailed solution of the problem. Figure 6-12 shows the wave functions and the probability distributions for the ground state and for the first two excited states. From this figure we see that the wavelengths inside the well are slightly longer than the corresponding wavelengths for the infinite well of the same width, so the corresponding energies are slightly less than those of the infinite well. Another feature of the finite well problem is that there are only a finite number of allowed energies, depending of the size of V_0. For very small V_0 there is only one allowed energy level; i.e., only one bound state can exist. This will be quite apparent in the detailed solution in the More section.

Note that, in contrast to the classical case, there is some probability of finding the particle outside the well, in the regions $x > L$ or $x < 0$. In these regions, the total energy is less than the potential energy, so it would seem that the kinetic energy must be negative. Since negative kinetic energy has no meaning in classical physics, it is interesting to speculate about the meaning of this penetration of wave function beyond the well boundary. Does quantum mechanics predict that we could measure a negative kinetic energy? If so, this would be a serious defect in the theory. Fortunately, we are saved by the uncertainty principle. We can understand

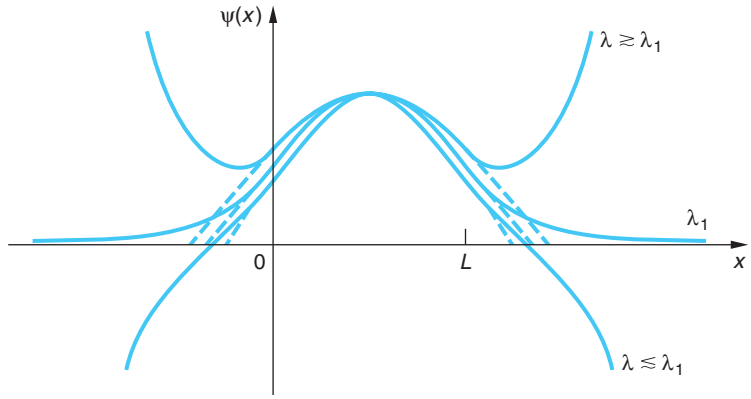

Figure 6-11 Functions satisfying the Schrödinger equation with wavelengths near the critical wavelength λ_1. If λ is slightly greater than λ_1, the function approaches infinity like that in Figure 6-10. At the wavelength λ_1, the function and its slope approach zero together. This is an acceptable wave function corresponding to the energy $E_1 = h^2/2m\lambda_1^2$. If λ is slightly less than λ_1, the function crosses the x axis while the slope is still negative. The slope becomes more negative because its rate of change ψ'' is now negative. This function approaches negative infinity at large x. [*This computer-generated plot courtesy of Paul Doherty, The Exploratorium.*]

STUDENTS-HUB.com Uploaded By: Malak Obaid

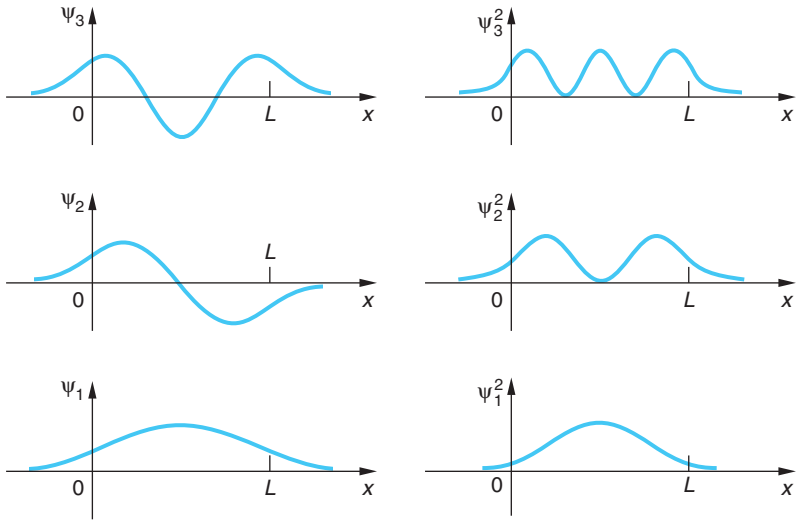

Figure 6-12 Wave functions $\psi_n(x)$ and probability distributions $\psi_n^2(x)$ for $n = 1$, 2, and 3 for the finite square well. Compare these with Figure 6-4 for the infinite square well, where the wave functions are zero at $x = 0$ and $x = L$. The wavelengths are slightly longer than the corresponding ones for the infinite well, so the allowed energies are somewhat smaller.

this qualitatively as follows (we will consider the region $x > L$ only). Since the wave function decreases as $e^{-\alpha x}$, with α given by Equation 6-34, the probability density $\psi^2 = e^{-2\alpha x}$ becomes very small in a distance of the order of $\Delta x \approx \alpha^{-1}$. If we consider $\psi(x)$ to be negligible beyond $x = L + \alpha^{-1}$, we can say that finding the particle in the region $x > L$ is roughly equivalent to localizing it in a region $\Delta x \approx \alpha^{-1}$. Such a measurement introduces an uncertainty in momentum of the order of $\Delta p \approx h/\Delta x = h\alpha$ and a minimum kinetic energy of the order of $(\Delta p)^2/2m = h^2\alpha^2/2m = V_0 - E$. This kinetic energy is just enough to prevent us from measuring a negative kinetic energy! The penetration of the wave function into a classically forbidden region does have important consequences in tunneling or barrier penetration, which we will discuss in Section 6-6.

Much of our discussion of the finite well problem applies to any problem in which $E > V(x)$ in some region and $E < V(x)$ outside that region. Consider, for example, the potential energy $V(x)$ shown in Figure 6-13. Inside the well, the Schrödinger equation is of the form

$$\psi''(x) = -k^2\psi(x) \qquad \textbf{6-35}$$

where $k^2 = 2m[E - V(x)]/\hbar^2$ now depends on x. The solutions of this equation are no longer simple sine or cosine functions because the wave number $k = 2\pi/\lambda$ varies with x, but since ψ'' and ψ have opposite signs, ψ will always curve toward the axis and the solutions will oscillate. Outside the well, ψ will curve away from the axis so there will be only certain values of E for which solutions exist that approach zero as x approaches infinity.

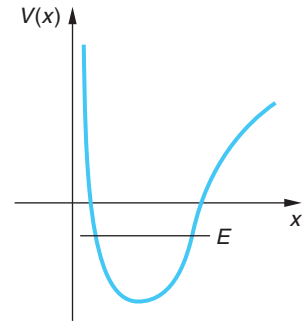

Figure 6-13 Arbitrary well-type potential with possible energy E. Inside the well $[E > V(x)]$, $\psi(x)$ and $\psi''(x)$ have opposite signs, and the wave function will oscillate. Outside the well, $\psi(x)$ and $\psi''(x)$ have the same sign and, except for certain values of E, the wave function will not be well behaved.

More

In most cases the solution of finite well problems involves transcendental equations and is very difficult. For some finite potentials, however, graphical solutions are relatively simple and provide both insights and numerical results. As an example, we have included the *Graphical Solution of the Finite Square Well* on the home page: www.whfreeman.com/tiplermodernphysics5e. See also Equations 6-36 through 6-43 and Figure 6-14 here.

STUDENTS-HUB.com Uploaded By: Malak Obaid

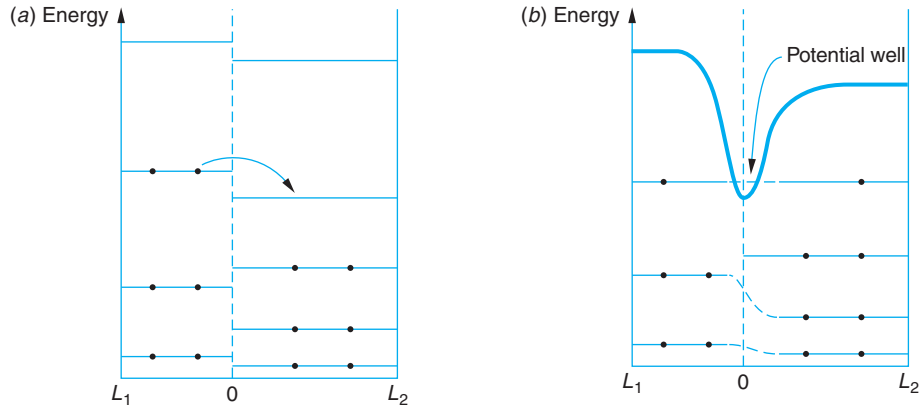

Figure 6-15 (*a*) Two infinite square wells of different widths L_1 and L_2, each containing the same number of electrons, are put together. An electron from well 1 moves to the lowest empty level of well 2. (*b*) The energies of the two highest electrons are equalized, but the unequal charge in the two wells distorts the energy-level structure. The distortion of the lowest empty levels in each well results in a potential well at the junction between the wells. The orientation of the newly formed well is perpendicular to the plane of the figure.

Quantum Wells

Development of techniques for fabricating devices whose dimensions are of the order of nanometers, called *nanostructures*, has made possible the construction of *quantum wells*. These are finite potential wells of one, two, and three dimensions that can channel electron movement in selected directions. A one-dimensional quantum well is a thin layer of material that confines particles to within the dimension perpendicular to the layer's surface but does not restrict motion in the other two dimensions. In the case of three-dimensional wells, called *quantum dots*, electrons are restricted entirely to quantized energy states within the well. A ubiquitous current application of quantum wells is the diode lasers that read CDs, DVDs, and bar codes. Quantum dots have potential applications in data storage and *quantum computers*, devices that may greatly enhance computing power and speed.

One-dimensional quantum wells, called *quantum wires*, offer the possibility of dramatically increasing the speed that electrons move through a device in selected directions. This in turn would increase the speed with which signals move between circuit elements in computer systems. Figure 6-15 is an outline of how such a well might be formed.

6-4 Expectation Values and Operators

Expectation Values

The objective of theory is to explain experimental observations. In classical mechanics the solution of a problem is typically specified by giving the position of a particle or particles as a function of time. As we have discussed, the wave nature of matter prevents us from doing this for microscopic systems. Instead, we find the wave function

STUDENTS-HUB.com Uploaded By: Malak Obaid

$\Psi(x, t)$ and the probability distribution function $|\Psi(x, t)|^2$. The most that we can know about a particle's position is the probability that a measurement will yield various values of x. The *expectation value* of x is defined as

$$\langle x \rangle = \int_{-\infty}^{+\infty} \Psi^*(x, t) x \Psi(x, t)\, dx \qquad \textbf{6-44}$$

The expectation value of x is the average value of x that we would expect to obtain from a measurement of the positions of a large number of particles with the same wave function $\Psi(x, t)$. As we have seen, for a particle in a state of definite energy, the probability distribution is independent of time. The expectation value of x is then given by

$$\langle x \rangle = \int_{-\infty}^{+\infty} \psi^*(x) x \psi(x)\, dx \qquad \textbf{6-45}$$

For example, for the infinite square well, we can see by symmetry (or by direct calculation) that $\langle x \rangle$ is $L/2$, the midpoint of the well.

In general, the expectation value of any function $f(x)$ is given by

$$\langle f(x) \rangle = \int_{-\infty}^{+\infty} \psi^* f(x) \psi\, dx \qquad \textbf{6-46}$$

For example, $\langle x^2 \rangle$ can be calculated as above, for the infinite square well of width L. It is left as an exercise (see Problem 6-56) to show that

$$\langle x^2 \rangle = \frac{L^2}{3} - \frac{L^2}{2n^2\pi^2} \qquad \textbf{6-47}$$

You may recognize the expectation values defined by Equations 6-45 and 6-46 as being weighted average calculations, borrowed by physics from probability and statistics. We should note that we don't necessarily expect to make a measurement whose result equals the expectation value. For example, for even n, the probability of measuring $x = L/2$ in some range dx around the midpoint of the well is zero because the wave function $\sin(n\pi x/L)$ is zero there. We get $\langle x \rangle = L/2$ because the probability density function $\psi^*\psi$ is symmetrical about that point. Remember that the expectation value is the average value that would result from many measurements.

Operators

If we knew the momentum p of a particle as a function of x, we could calculate the expectation value $\langle p \rangle$ from Equation 6-46. However, it is impossible in principle to find p as a function of x since, according to the uncertainty principle, both p and x cannot be determined at the same time. To find $\langle p \rangle$ we need to know the distribution function for momentum. If we know $\psi(x)$, it can be found by Fourier analysis. The $\langle p \rangle$ also can be found from Equation 6-48, where $\left(\frac{\hbar}{i}\frac{\partial}{\partial x}\right)$ is the mathematical operator acting on Ψ that produces the x component of the momentum (see also Equation 6-6).

$$\langle p \rangle = \int_{-\infty}^{+\infty} \Psi^* \left(\frac{\hbar}{i}\frac{\partial}{\partial x}\right) \Psi\, dx \qquad \textbf{6-48}$$

STUDENTS-HUB.com Uploaded By: Malak Obaid

Similarly, $\langle p^2 \rangle$ can be found from

$$\langle p^2 \rangle = \int_{-\infty}^{+\infty} \Psi^* \left(\frac{\hbar}{i} \frac{\partial}{\partial x} \right) \left(\frac{\hbar}{i} \frac{\partial}{\partial x} \right) \Psi \, dx$$

Notice that in computing the expectation value the operator representing the physical quantity operates on $\Psi(x, t)$, *not* on $\Psi^*(x, t)$; i.e., its correct position is between Ψ^* and Ψ. This is not important to the outcome when the operator is simply some $f(x)$, but it is critical when the operator includes a differentiation, as in the case of the momentum operator. Note that $\langle p^2 \rangle$ is simply $2mE$ since, for the infinite square well, $E = p^2/2m$. The quantity $\left(\frac{\hbar}{i} \frac{\partial}{\partial x} \right)$, which operates on the wave function in Equation 6-48, is called the *momentum operator* p_{op}:

$$p_{op} = \frac{\hbar}{i} \frac{\partial}{\partial x} \qquad \textbf{6-49}$$

EXAMPLE 6-5 Expectation Values for p and p^2 Find $\langle p \rangle$ and $\langle p^2 \rangle$ for the ground-state wave function of the infinite square well. (Before we calculate them, what do you think the results will be?)

SOLUTION

We can ignore the time dependence of Ψ, in which case we have

$$\langle p \rangle = \int_0^L \left(\sqrt{\frac{2}{L}} \sin \frac{nx}{L} \right) \left(\frac{\hbar}{i} \frac{\partial}{\partial x} \right) \left(\sqrt{\frac{2}{L}} \sin \frac{nx}{L} \right) dx$$

$$= \frac{\hbar}{i} \frac{2}{L} \frac{\pi}{L} \int_0^L \sin \frac{\pi x}{L} \cos \frac{\pi x}{L} dx = 0$$

The particle is equally as likely to be moving in the $-x$ as in the $+x$ direction, so its *average* momentum is zero.

Similarly, since

$$\frac{\hbar}{i} \frac{\partial}{\partial x} \left(\frac{\hbar}{i} \frac{\partial}{\partial x} \right) \psi = -\hbar^2 \frac{\partial^2 \psi}{\partial x^2} = -\hbar^2 \left(-\frac{\pi^2}{L^2} \sqrt{\frac{2}{L}} \sin \frac{\pi x}{L} \right)$$

$$= +\frac{\hbar^2 \pi^2}{L^2} \psi$$

we have

$$\langle p^2 \rangle = \frac{\hbar^2 \pi^2}{L^2} \int_0^L \psi^* \psi \, dx = \frac{\hbar^2 \pi^2}{L^2}$$

The time-independent Schrödinger equation (Equation 6-18) can now be written conveniently in terms of p_{op}:

$$\left(\frac{1}{2m} \right) p_{op}^2 \, \psi(x) + V(x) \psi(x) = E \psi(x) \qquad \textbf{6-50}$$

where

$$p_{op}^2 \, \psi(x) = \frac{\hbar}{i} \frac{\partial}{\partial x} \left[\frac{\hbar}{i} \frac{\partial}{\partial x} \psi(x) \right] = -\hbar^2 \frac{\partial^2 \psi}{\partial x^2}$$

STUDENTS-HUB.com Uploaded By: Malak Obaid

In classical mechanics, the total energy written in terms of the position and momentum variables is called the Hamiltonian function $H = p^2/2m + V$. If we replace the momentum by the momentum operator p_{op} and note that $V = V(x)$, we obtain the Hamiltonian operator H_{op}:

$$H_{op} = \frac{p_{op}^2}{2m} + V(x) \qquad \textbf{6-51}$$

The time-independent Schrödinger equation can then be written

$$H_{op}\psi = E\psi \qquad \textbf{6-52}$$

The advantage of writing the Schrödinger equation in this formal way is that it allows for easy generalization to more-complicated problems such as those with several particles moving in three dimensions. We simply write the total energy of the system in terms of position and momentum and replace the momentum variables by the appropriate operators to obtain the Hamiltonian operator for the system.

Table 6-1 summarizes the several operators representing physical quantities that we have discussed thus far and includes a few more that we will encounter later on.

Table 6-1 Some quantum-mechanical operators

Symbol	Physical quantity	Operator
$f(x)$	Any function of x—e.g., the position x, the potential energy $V(x)$, etc.	$f(x)$
p_x	x component of momentum	$\frac{\hbar}{i}\frac{\partial}{\partial x}$
p_y	y component of momentum	$\frac{\hbar}{i}\frac{\partial}{\partial y}$
p_z	z component of momentum	$\frac{\hbar}{i}\frac{\partial}{\partial z}$
E	Hamiltonian (time independent)	$\frac{p_{op}^2}{2m} + V(x)$
E	Hamiltonian (time dependent)	$i\hbar\frac{\partial}{\partial t}$
E_k	kinetic energy	$-\frac{\hbar^2}{2m}\frac{\partial^2}{\partial x^2}$
L_z	z component of angular momentum	$-i\hbar\frac{\partial}{\partial \phi}$

Questions

7. Explain (in words) why $\langle p \rangle$ and $\langle p^2 \rangle$ in Example 6-5 are not both zero.
8. Can $\langle x \rangle$ ever have a value that has zero probability of being measured?

STUDENTS-HUB.com Uploaded By: Malak Obaid

More

In order for interesting things to happen in systems with quantized energies, the probability density must change in time. Only in this way can energy be emitted or absorbed by the system. *Transitions Between Energy States* on the home page (www.whfreeman.com/tiplermodernphysics5e) describes the process and applies it to the emission of light from an atom. See also Equations 6-52*a–e* and Figure 6-16 here.

6-5 The Simple Harmonic Oscillator

One of the problems solved by Schrödinger in the second of his six famous papers was that of the simple harmonic oscillator potential, given by

$$V(x) = \frac{1}{2}Kx^2 = \frac{1}{2}m\omega^2x^2$$

where K is the force constant and ω the angular frequency of vibration defined by $\omega = (K/m)^{1/2} = 2\pi f$. The solution of the Schrödinger equation for this potential is particularly important, as it can be applied to such problems as the vibration of molecules in gases and solids. This potential energy function is shown in Figure 6-17, with a possible total energy E indicated.

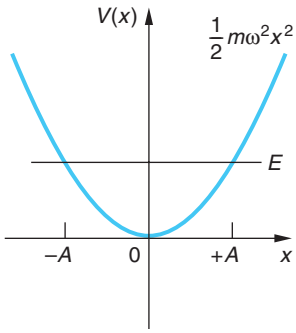

Figure 6-17 Potential energy function for a simple harmonic oscillator. Classically, the particle is confined between the "turning points" $-A$ and $+A$.

In classical mechanics, a particle in such a potential is in equilibrium at the origin $x = 0$, where $V(x)$ is minimum and the force $F_x = -dV/dx$ is zero. If disturbed, the particle will oscillate back and forth between $x = -A$ and $x = +A$, the points at which the kinetic energy is zero and the total energy is just equal to the potential energy. These points are called the classical turning points. The distance A is related to the total energy E by

$$E = \frac{1}{2}m\omega^2A^2 \qquad \textbf{6-53}$$

Classically, the probability of finding the particle in dx is proportional to the time spent in dx, which is dx/v. The speed of the particle can be obtained from the conservation of energy:

$$\frac{1}{2}mv^2 + \frac{1}{2}m\omega^2x^2 = E$$

The classical probability is thus

$$P_c(x)\,dx \propto \frac{dx}{v} = \frac{dx}{\sqrt{(2/m)\left(E - \frac{1}{2}m\omega^2x^2\right)}} \qquad \textbf{6-54}$$

Any value of the energy E is possible. The lowest energy is $E = 0$, in which case the particle is at rest at the origin.

The Schrödinger equation for this problem is

$$-\frac{\hbar^2}{2m}\frac{\partial^2\psi(x)}{\partial x^2} + \frac{1}{2}m\omega^2x^2\psi(x) = E\psi(x) \qquad \textbf{6-55}$$

STUDENTS-HUB.com Uploaded By: Malak Obaid

The mathematical techniques involved in solving this type of differential equation are standard in mathematical physics but unfamiliar to most students at this level. We will, therefore, discuss the problem qualitatively. We first note that since the potential is symmetric about the origin $x = 0$, we expect the probability distribution function $|\psi(x)|^2$ also to be symmetric about the origin, i.e., to have the same value at $-x$ as at $+x$.

$$|\psi(-x)|^2 = |\psi(x)|^2$$

The wave function $\psi(x)$ must then be either symmetric $\psi(-x) = +\psi(x)$ or antisymmetric $\psi(-x) = -\psi(x)$. We can therefore simplify our discussion by considering positive x only and find the solutions for negative x by symmetry. (The symmetry of Ψ is discussed further in the Exploring section, Parity; see page 250.)

Consider some value of total energy E. For x less than the classical turning point A defined by Equation 6-53, the potential energy $V(x)$ is less than the total energy E, whereas for $x > A$, $V(x)$ is greater than E. Our discussion in Section 6-3 applies directly to this problem. For $x < A$, the Schrödinger equation can be written

$$\psi''(x) = -k^2\psi(x)$$

where

$$k^2 = \frac{2m}{\hbar^2}[E - V(x)]$$

and $\psi(x)$ curves toward the axis and oscillates. For $x > A$, the Schrödinger equation becomes

$$\psi''(x) = +\alpha^2\psi(x)$$

with

$$\alpha^2 = \frac{2m}{\hbar^2}[V(x) - E]$$

and $\psi(x)$ curves away from the axis. Only certain values of E will lead to solutions that are well behaved, i.e., that approach zero as x approaches infinity. The allowed values of E for the simple harmonic oscillator must be determined by solving the Schrödinger equation; in this case they are given by

$$E_n = \left(n + \frac{1}{2}\right)\hbar\omega \qquad n = 0, 1, 2, \ldots \qquad \textbf{6-56}$$

Thus, the ground-state energy is $\frac{1}{2}\hbar\omega$ and the energy levels are equally spaced, each excited state being separated from the levels immediately adjacent by $\hbar\omega$.

The wave functions of the simple harmonic oscillator in the ground state and in the first two excited states ($n = 0$, $n = 1$, and $n = 2$) are sketched in Figure 6-18. The ground-state wave function has the shape of a Gaussian curve, and the lowest energy $E = \frac{1}{2}\hbar\omega$ is the minimum energy consistent with the uncertainty principle.

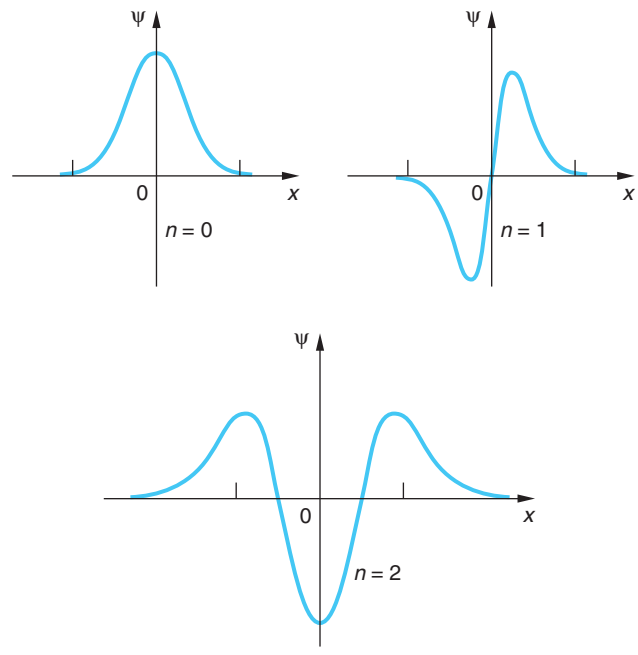

Figure 6-18 Wave functions for the ground state and the first two excited states of the simple harmonic oscillator potential, the states with $n = 0$, 1, and 2.

STUDENTS-HUB.com Uploaded By: Malak Obaid

The allowed solutions to the Schrödinger equation, the wave functions for the simple harmonic oscillator, can be written

$$\psi_n(x) = C_n e^{-m\omega x^2/2\hbar} H_n(x) \qquad \textbf{6-57}$$

where the constants C_n are determined by normalization and the functions $H_n(x)$ are polynomials of order n called the Hermite polynomials.[13] The solutions for $n = 0$, 1, and 2 (see Figure 6-18) are

$$\begin{aligned}
\psi_0(x) &= A_0 e^{-m\omega x^2/2\hbar} \\
\psi_1(x) &= A_1 \sqrt{\frac{m\omega}{\hbar}}\, x e^{-m\omega x^2/2\hbar} \qquad \textbf{6-58} \\
\psi_2(x) &= A_2 \left(1 - \frac{2m\omega x^2}{\hbar}\right) e^{-m\omega x^2/2\hbar}
\end{aligned}$$

Molecules vibrate as harmonic oscillators. Measuring vibration frequencies (see Chapter 9) enables determination of force constants, bond strengths, and properties of solids.

Notice that for even values of n, the wave functions are symmetric about the origin; for odd values of n, they are antisymmetric. In Figure 6-19 the probability distributions $\psi_n^2(x)$ are sketched for $n = 0$, 1, 2, 3, and 10 for comparison with the classical distribution.

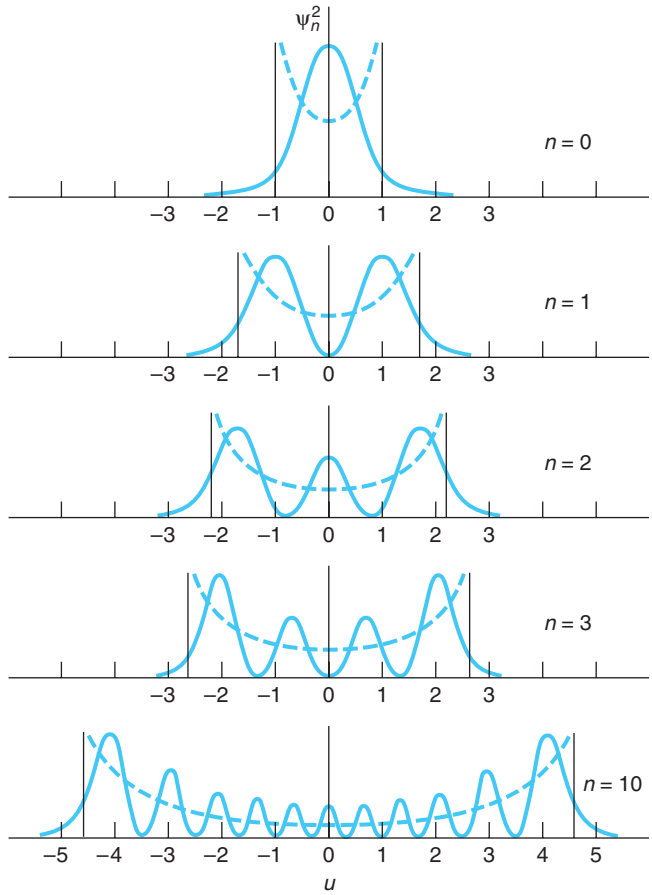

Figure 6-19 Probability density ψ_n^2 for the simple harmonic oscillator plotted against the dimensionless variable $u = (m\omega/\hbar)^{1/2}x$, for $n = 0$, 1, 2, 3, and 10. The dashed curves are the classical probability densities for the same energy, and the vertical lines indicate the classical turning points $x = \pm A$.

STUDENTS-HUB.com Uploaded By: Malak Obaid

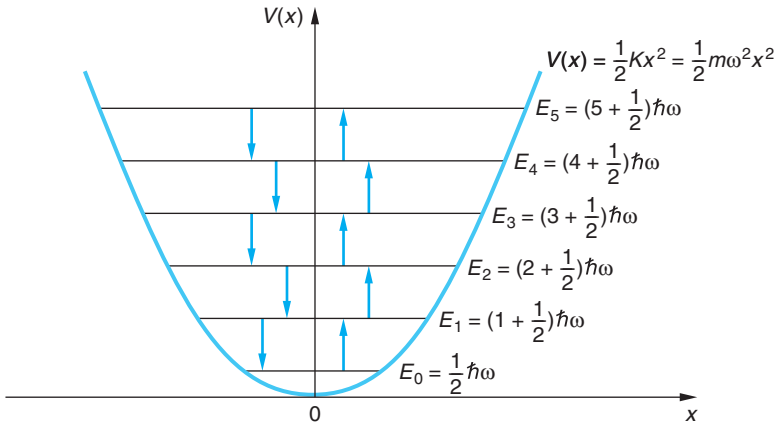

Figure 6-20 Energy levels in the simple harmonic oscillator potential. Transitions obeying the selection rule $\Delta n = \pm 1$ are indicated by the arrows (those pointing up indicate absorption). Since the levels have equal spacing, the same energy $\hbar\omega$ is emitted or absorbed in all allowed transitions. For this special potential, the frequency of the emitted or absorbed photon equals the frequency of oscillation, as predicted by classical theory.

A property of these wave functions that we will state without proof is that

$$\int_{-\infty}^{+\infty} \psi_n^* x \psi_m \, dx = 0 \quad \text{unless} \quad n = m \pm 1 \qquad \textbf{6-59}$$

This property places a condition on transitions that may occur between allowed states. This condition, called a *selection rule*, limits the amount by which n can change for (electric dipole) radiation emitted or absorbed by a simple harmonic oscillator:

The quantum number of the final state must be 1 less than or 1 greater than that of the initial state.

This selection rule is usually written

$$\Delta n = \pm 1 \qquad \textbf{6-60}$$

Since the difference in energy between two successive states is $\hbar\omega$, this is the energy of the photon emitted or absorbed in an electric dipole transition. The frequency of the photon is therefore equal to the classical frequency of the oscillator, as was assumed by Planck in his derivation of the blackbody radiation formula. Figure 6-20 shows an energy level diagram for the simple harmonic oscillator, with the allowed energy transitions indicated by vertical arrows.

More

Solution of the Schrödinger equation for the simple harmonic oscillator (Equation 6-55) involves some rather advanced differential equation techniques. However, a simpler exact solution is also possible using an approach invented by Schrödinger himself that we will call *Schrödinger's Trick*. With the authors' thanks to Wolfgang Lorenzon for bringing it to our attention, we include it on the home page www.whfreeman.com/tiplermodernphysics5e so that you, too, will know the trick.

STUDENTS-HUB.com Uploaded By: Malak Obaid

EXPLORING
Parity

We made a special point of arranging the simple harmonic oscillator potential symmetrically about $x = 0$ (see Figure 6-17), just as we had done with the finite square well in Figure 6-8*b* and will do with various other potentials in later discussions. The usual purpose in each case is to emphasize the symmetry of the physical situation and to simplify the mathematics. Notice that arranging the potential $V(x)$ symmetrically about the origin means that $V(x) = V(-x)$. This means that the Hamiltonian operator H_{op}, defined in Equation 6-51, is unchanged by a transformation that changes $x \longrightarrow -x$. Such a transformation is called a *parity operation* and is usually denoted by the operator P. Thus, if $\psi(x)$ is a solution of the Schrödinger equation

$$H_{op}\psi(x) = E\psi(x) \qquad \textbf{6-52}$$

then a parity operation P leads to

$$H_{op}\psi(-x) = E\psi(-x)$$

and $\psi(-x)$ is also a solution to the Schrödinger equation and corresponds to the same energy. When two (or more) wave functions are solutions corresponding to the same value of the energy E, that level is referred to as *degenerate*. In this case, where two wave functions, $\psi(x)$ and $\psi(-x)$, are both solutions with energy E, we call the energy level doubly degenerate.

It should be apparent from examining the two equations above that $\psi(x)$ and $\psi(-x)$ can differ at most by a multiplicative constant C; i.e.,

$$\psi(x) = C\psi(-x) \qquad \psi(-x) = C\psi(x)$$

or

$$\psi(x) = C\psi(-x) = C^2\psi(x)$$

from which it follows that $C = \pm 1$. If $C = 1$, $\psi(x)$ is an even function, i.e., $\psi(-x) = \psi(x)$. If $C = -1$, then $\psi(x)$ is an odd function, i.e., $\psi(-x) = -\psi(x)$. Parity is used in quantum mechanics to describe the symmetry properties of wave functions under a reflection of the *space* coordinates in the origin, i.e., under a parity operation. The terms even and odd parity describe the symmetry of the wave functions, not whether the quantum numbers are even or odd. We will have more on parity in Chapter 12.

6-6 Reflection and Transmission of Waves

Up to this point, we have been concerned with bound-state problems in which the potential energy is larger than the total energy for large values of x. In this section, we will consider some simple examples of unbound states for which E is greater than $V(x)$ as x gets larger in one or both directions. For these problems $d^2\psi(x)/dx^2$ and $\psi(x)$ have opposite signs for those regions of x where $E > V(x)$, so $\psi(x)$ in those regions curves toward the axis and does not become infinite at large values of $|x|$. Any value of E is allowed. Such wave functions are not normalizable since $\psi(x)$ does not approach zero as x goes to infinity in at least one direction and, as a consequence,

$$\int_{-\infty}^{+\infty} |\psi(x)|^2\, dx \longrightarrow \infty$$

STUDENTS-HUB.com Uploaded By: Malak Obaid

A complete solution involves combining infinite plane waves into a wave packet of finite width. The resulting finite packet is normalizable. However, for our purposes it is sufficient to note that the integral above is bounded between the limits a and b, provided only that $|b - a| < \infty$. Such wave functions are most frequently encountered, as we are about to do, in the scattering of beams of particles from potentials, so it is usual to normalize such wave functions in terms of the density of particles ρ in the beam. Thus,

$$\int_a^b |\psi(x)|^2\, dx = \int_a^b \rho\, dx = \int_a^b dN = N$$

where dN is the number of particles in the interval dx and N is the number of particles in the interval $(b - a)$.[14] The wave nature of the Schrödinger equation leads, even so, to some very interesting consequences.

Step Potential

Consider a region in which the potential energy is the step function

$$V(x) = 0 \quad \text{for} \quad x < 0$$
$$V(x) = V_0 \quad \text{for} \quad x > 0$$

as shown in Figure 6-21. We are interested in what happens when a beam of particles, each with the same total energy E, moving from left to right encounters the step.

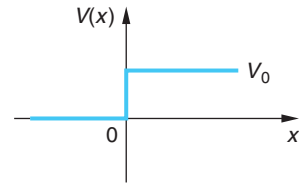

Figure 6-21 Step potential. A classical particle incident from the left, with total energy E greater than V_0, is always transmitted. The potential change at $x = 0$ merely provides an impulsive force that reduces the speed of the particle. However, a wave incident from the left is partially transmitted and partially reflected because the wavelength changes abruptly at $x = 0$.

The classical answer is simple. For $x < 0$, each particle moves with speed $v = (2E/m)^{1/2}$. At $x = 0$, an impulsive force acts on it. If the total energy E is less than V_0, the particle will be turned around and will move to the left at its original speed; that is, it will be reflected by the step. If E is greater than V_0, the particle will continue moving to the right but with reduced speed, given by $v = [2(E - V_0)/m]^{1/2}$. We might picture this classical problem as a ball rolling along a level surface and coming to a steep hill of height y_0, given by $mgy_0 = V_0$. If its original kinetic energy is less than V_0, the ball will roll partway up the hill and then back down and to the left along the level surface at its original speed. If E is greater than V_0, the ball will roll up the hill and proceed to the right at a smaller speed.

The quantum-mechanical result is similar to the classical one for $E < V_0$ but quite different when $E > V_0$, as in Figure 6-22*a*. The Schrödinger equation in each of the two space regions shown in the diagram is given by

Region I

$$(x < 0) \qquad \frac{d^2\psi(x)}{dx^2} = -k_1^2\psi(x) \qquad \textbf{6-61}$$

Region II

$$(x > 0) \qquad \frac{d^2\psi(x)}{dx^2} = -k_2^2\psi(x) \qquad \textbf{6-62}$$

$$k_1 = \frac{\sqrt{2mE}}{\hbar} \quad \text{and} \quad k_2 = \frac{\sqrt{2m(E - V_0)}}{\hbar}$$

STUDENTS-HUB.com Uploaded By: Malak Obaid

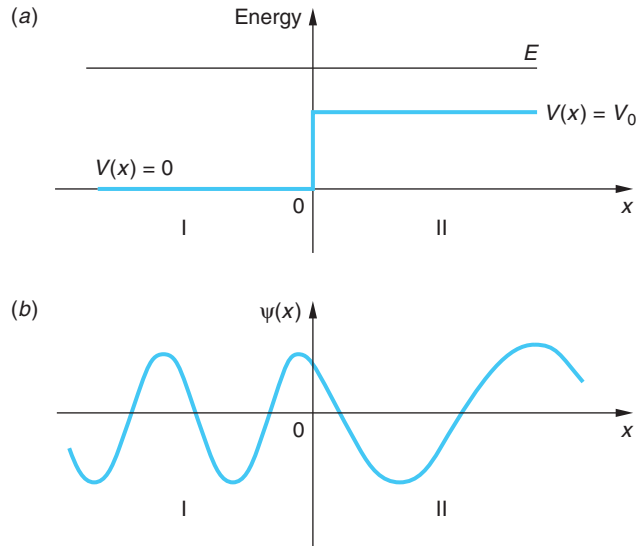

Figure 6-22 (*a*) A potential step. Particles are incident on the step from the left toward the right, each with total energy $E > V_0$. (*b*) The wavelength of the incident wave (Region I) is shorter than that of the transmitted wave (Region II). Since $k_2 < k_1$, $|C|^2 > |A|^2$; however, the transmission coefficient $T < 1$.

The general solutions are

Region I

$$(x < 0) \qquad \psi_I(x) = Ae^{ik_1x} + Be^{-ik_1x} \qquad \textbf{6-63}$$

Region II

$$(x > 0) \qquad \psi_{II}(x) = Ce^{ik_2x} + De^{-ik_2x} \qquad \textbf{6-64}$$

Specializing these solutions to our situation where we are assuming the incident beam of particles to be moving from left to right, we see that the first term in Equation 6-63 represents that beam since multiplying Ae^{ik_1x} by the time part of $\Psi(x, t)$, $e^{i\omega t}$, yields a plane wave (i.e., a beam of free particles) moving to the right. The second term, Be^{-ik_2x}, represents particles moving to the left in Region I. In Equation 6-64, $D = 0$ since that term represents particles incident on the potential step from the right and there are none. Thus, we have that the constant A is known or at least obtainable (determined by normalization of Ae^{ik_1x} in terms of the density of particles in the beam as explained above) and the constants B and C are yet to be found. We find them by applying the continuity condition on $\psi(x)$ and $d\psi(x)/dx$ at $x = 0$, i.e., by requiring that $\psi_I(0) = \psi_{II}(0)$ and $d\psi_I(0)/dx = d\psi_{II}(0)/dx$. Continuity of ψ at $x = 0$ yields

$$\psi_I(0) = A + B = \psi_{II}(0) = C$$

or

$$A + B = C \qquad \textbf{6-65}\boldsymbol{a}$$

Continuity of $d\psi/dx$ at $x = 0$ gives

$$k_1A - k_1B = k_2C \qquad \textbf{6-65}\boldsymbol{b}$$

STUDENTS-HUB.com Uploaded By: Malak Obaid

Solving Equations 6-65*a* and *b* for *B* and *C* in terms of *A* (see Problem 6-47), we have

$$B = \frac{k_1 - k_2}{k_1 + k_2} A = \frac{E^{1/2} - (E - V_0)^{1/2}}{E^{1/2} + (E - V_0)^{1/2}} A \qquad \textbf{6-66}$$

$$C = \frac{2k_1}{k_1 + k_2} A = \frac{2E^{1/2}}{E^{1/2} + (E - V_0)^{1/2}} A \qquad \textbf{6-67}$$

where Equations 6-66 and 6-67 give the relative amplitude of the reflected and transmitted waves, respectively. It is usual to define the coefficients of reflection R and transmission T, the relative *rates* at which particles are reflected and transmitted, in terms of the squares of the amplitudes A, B, and C as[15]

$$R = \frac{|B|^2}{|A|^2} = \left(\frac{k_1 - k_2}{k_1 + k_2}\right)^2 \qquad \textbf{6-68}$$

$$T = \frac{k_2}{k_1}\frac{|C|^2}{|A|^2} = \frac{4k_1k_2}{(k_1 + k_2)^2} \qquad \textbf{6-69}$$

from which it can be readily verified that

$$T + R = 1 \qquad \textbf{6-70}$$

Among the interesting consequences of the wave nature of the solutions to Schrödinger's equation, notice the following:

1. Even though $E > V_0$, R is *not* 0; i.e., in contrast to classical expectations, some of the particles are reflected from the step. (This is analogous to the internal reflection of electromagnetic waves at the interface of two media.)
2. The value of R depends on the difference between k_1 and k_2 but *not* on which is larger; i.e., a step down in the potential produces the same reflection as a step up of the same size.

Since $k = p/\hbar = 2\pi/\lambda$, the wavelength changes as the beam passes the step. We might also expect that the amplitude of ψ_{II} will be less than that of the incident wave; however, recall that the $|\psi|^2$ is proportional to the particle density. Since particles move more slowly in Region II ($k_2 < k_1$), $|\psi_{II}|^2$ may be larger than $|\psi_I|^2$. Figure 6-22*b* illustrates these points. Figure 6-23 shows the time development of a wave packet incident on a potential step for $E > V_0$.

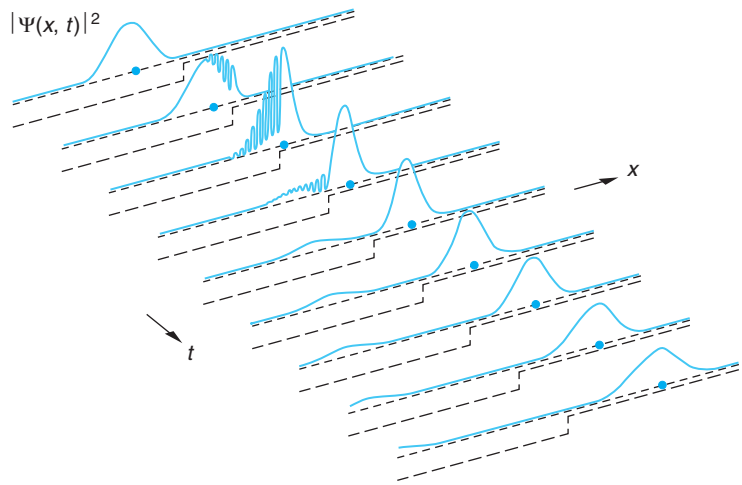

Figure 6-23 Time development of a one-dimensional wave packet representing a particle incident on a step potential for $E > V_0$. The position of a classical particle is indicated by the dot. Note that part of the packet is transmitted and part is reflected. The sharp spikes that appear are artifacts of the discontinuity in the slope of $V(x)$ at $x = 0$.

STUDENTS-HUB.com Uploaded By: Malak Obaid

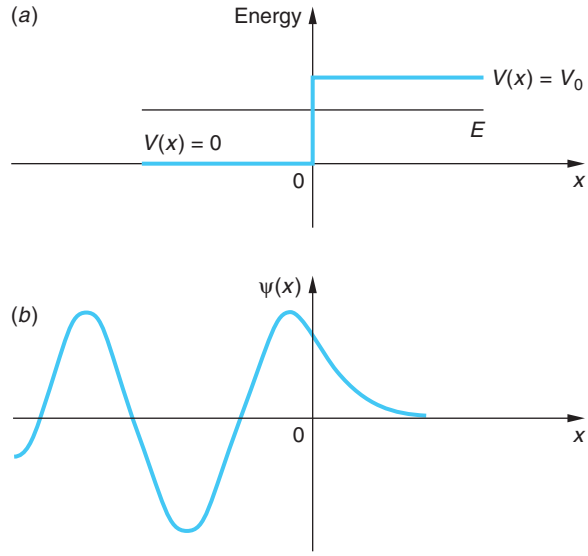

Figure 6-24 (*a*) A potential step. Particles are incident on the step from the left moving toward the right, each with total energy $E < V_0$. (*b*) The wave transmitted into region II is a decreasing exponential. However, the value of R in this case is 1 and no net energy is transmitted.

Now let us consider the case shown in Figure 6-24*a*, where $E < V_0$. Classically, we expect all particles to be reflected at $x = 0$; however, we note that k_2 in Equation 6-64 is now an imaginary number since $E < V_0$. Thus,

$$\psi_{II}(x) = Ce^{ik_2x} = Ce^{-\alpha x} \qquad \textbf{6-71}$$

is a *real* exponential function where $\alpha = \sqrt{2m(V_0 - E)}/\hbar$. (We choose the positive root so that $\psi_{II} \to 0$ as $x \to \infty$.) This means that the numerator and denominator of the right side of Equation 6-66 are complex conjugates of each other; hence $|B|^2 = |\mathbf{A}|^2$ and $R = 1$ and $T = 0$. Figure 6-25 is a graph of both R and T versus energy for a potential step. In agreement with the classical prediction, all of the particles (waves) are reflected back into Region I. However, another interesting result of our solution of Schrödinger's equation is that the particle waves do not all reflect at $x = 0$.

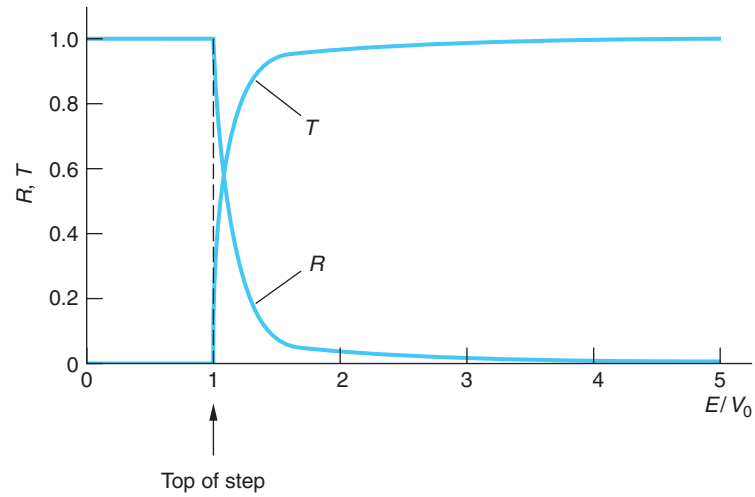

Figure 6-25 Reflection coefficient R and transmission coefficient T for a potential step V_0 high versus energy E (in units of V_0).

STUDENTS-HUB.com Uploaded By: Malak Obaid

Since ψ_{II} is an exponential decreasing toward the right, the particle density in Region II is proportional to

$$|\psi_{II}|^2 = |C|^2 e^{-2\alpha x} \qquad \textbf{6-72}$$

Figure 6-24*b* shows the wave function for the case $E < V_0$. The wave function does not go to zero at $x = 0$ but decays exponentially, as does the wave function for the bound state in a finite square well problem. The wave penetrates slightly into the classically forbidden region $x > 0$ but eventually is completely reflected. (As discussed in Section 6-3, there is no prediction that a negative kinetic energy will be *measured* in such a region because to locate the particle in such a region introduces an uncertainty in the momentum corresponding to a minimum kinetic energy greater than $V_0 - E$.) This situation is similar to that of total internal reflection in optics.

EXAMPLE 6-6 **Reflection from a Step with $E < V_0$** A beam of electrons, each with energy $E = 0.1\ V_0$, is incident on a potential step with $V_0 = 2$ eV. This is of the order of magnitude of the work function for electrons at the surface of metals. Graph the relative probability $|\psi|^2$ of particles penetrating the step up to a distance $x = 10^{-9}$ m, or roughly five atomic diameters.

SOLUTION

For $x > 0$, the wave function is given by Equation 6-71. The value of $|C|^2$ is, from Equation 6-67,

$$|C|^2 = \left| \frac{2(0.1\ V_0)^{1/2}}{(0.1\ V_0)^{1/2} + (-0.9\ V_0)^{1/2}} \right|^2 = 0.4$$

where we have taken $|A|^2 = 1$. Computing $e^{-2\alpha x}$ for several values of x from 0 to 10^{-9} m gives, with $2\alpha = 2[2m(0.9\ V_0)]^{1/2}/\hbar$, the first two columns of the Table 6-2. Taking $e^{-2\alpha x}$ and then multiplying by $|C|^2 = 0.4$ yields $|\psi|^2$, which is graphed in Figure 6-26.

Table 6-2 $|\psi|^2$

x (m)	$2\alpha x$	$\lvert\psi\rvert^2$
0	0	0.40
0.1×10^{-10}	0.137	0.349
1.0×10^{-10}	1.374	0.101
2.0×10^{-10}	2.748	0.026
5.0×10^{-10}	6.869	0.001
10.0×10^{-10}	13.74	≈ 0

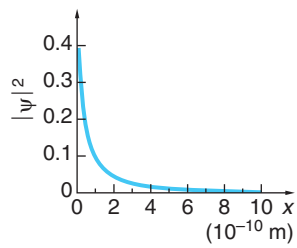

Figure 6-26

STUDENTS-HUB.com Uploaded By: Malak Obaid

Barrier Potential

Now let us consider one of the more interesting quantum-mechanical potentials, the barrier, illustrated by the example in Figure 6-27. The potential is

$$V(x) = \begin{cases} V_0 & \text{for} \quad 0 < x < a \\ 0 & \text{for} \quad 0 > x \quad \text{and} \quad x > a \end{cases} \tag{6-73}$$

Classical particles incident on the barrier from the left in Region I with $E > V_0$ will all be transmitted, slowing down while passing through Region II but moving at their original speed again in Region III. For classical particles with $E < V_0$ incident from the left, all are reflected back into Region I. The quantum-mechanical behavior of particles incident on the barrier in both energy ranges is *much* different!

First, let us see what happens when a beam of particles, all with the same energy $E < V_0$, as illustrated in Figure 6-27*a*, are incident from the left. The general solutions to the wave equation are, following the example of the potential step,

$$\begin{aligned} \psi_I(x) &= Ae^{ik_1x} + Be^{-ik_1x} && x < 0 \\ \psi_{II}(x) &= Ce^{-\alpha x} + De^{\alpha x} && 0 < x < \alpha \\ \psi_{III}(x) &= Fe^{ik_1x} + Ge^{-ik_1x} && x > a \end{aligned} \tag{6-74}$$

where, as before, $k_1 = \sqrt{2mE}/\hbar$ and $\alpha = \sqrt{2m(V_0 - E)}/\hbar$. Note that ψ_{II} involves real exponentials, whereas ψ_I and ψ_{III} contain complex exponentials. Since the particle beam is incident on the barrier from the left, we can set $G = 0$. Once again, the value of A is determined by the particle density in the beam and the four constants B, C, D, and F are found in terms of A by applying the continuity condition on ψ and $d\psi/dx$ at $x = 0$ and at $x = a$. The details of the calculation are not of concern to us here, but several of the more interesting results are.

As we discovered for the potential step with $E < V_0$, the wave function incident from the left does not decrease immediately to zero at the barrier but instead will decay exponentially in the region of the barrier. Upon reaching the far wall of the barrier, the wave function must join smoothly to a sinusoidal wave function to the right of the barrier, as shown in Figure 6-27*b*. This implies that there will be some probability of the particles represented by the wave function being found on the far right side of the

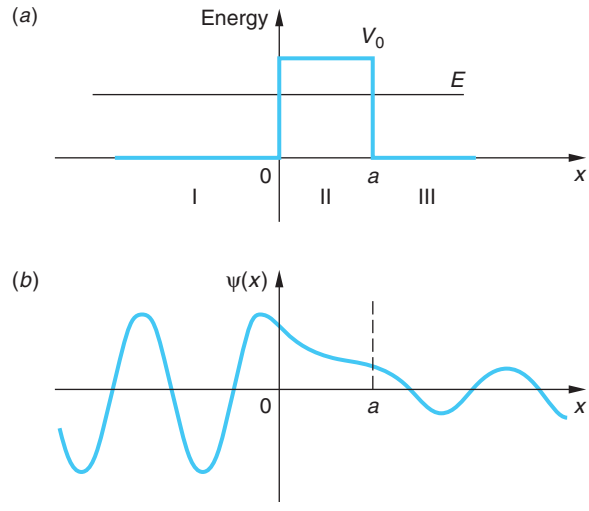

Figure 6-27 (*a*) Square barrier potential. (*b*) Penetration of the barrier by a wave with energy less than the barrier energy. Part of the wave is transmitted by the barrier even though, classically, the particle cannot enter the region $0 < x < a$ in which the potential energy is greater than the total energy.

STUDENTS-HUB.com Uploaded By: Malak Obaid

barrier, although classically they should never be able to get through; i.e., there is a probability that the particles approaching the barrier can penetrate it. This phenomenon is called *barrier penetration* or *tunneling* (see Figure 6-28). The relative probability of its occurrence in any given situation is given by the transmission coefficient.

The coefficient of transmission T from Region I into Region III is found to be (see Problem 6-64)

$$T = \frac{|F|^2}{|A|^2} = \left[1 + \frac{\sinh^2 \alpha a}{4\dfrac{E}{V_0}\left(1 - \dfrac{E}{V_0}\right)}\right]^{-1} \qquad \textbf{6-75}$$

If $\alpha a \gg 1$, Equation 6-75 takes on the somewhat simpler form to evaluate

$$T \approx 16\frac{E}{V_0}\left(1 - \frac{E}{V_0}\right)e^{-2\alpha a} \qquad \textbf{6-76}$$

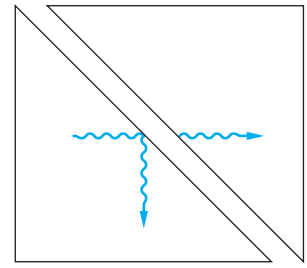

Figure 6-28 Optical barrier penetration, sometimes called frustrated total internal reflection. Because of the presence of the second prism, part of the wave penetrates the air barrier even though the angle of incidence in the first prism is greater than the critical angle. This effect can be demonstrated with two 45° prisms and a laser or a microwave beam and 45° prisms made of paraffin.

An important application of tunneling is the tunnel diode, a common component of electronic circuits. Another is *field emission*, tunneling of electrons facilitated by an electric field, now being used in wide-angle, flat-screen displays on some laptop computers.

Scanning Tunneling Microscope In the *scanning tunneling microscope* (STM), developed in the 1980s by G. Binnig and H. Rohrer, a narrow gap between a conducting specimen and the tip of a tiny probe acts as a potential barrier to electrons bound in the specimen, as illustrated in Figure 6-29. A small bias voltage applied between the probe and the specimen causes the electrons to tunnel through the barrier separating the two surfaces if the surfaces are close enough together. The tunneling current is extremely sensitive to the size of the gap, i.e., the width of the barrier, between the probe and specimen. A change of only 0.5 nm (about the diameter of one atom) in the width of the barrier can cause the tunneling current to change by as much as a factor of 10^4. As the probe scans the specimen, a constant tunneling current is maintained by a piezoelectric feedback system that keeps the gap constant. Thus, the surface of the specimen can be mapped out by the vertical motions of the probe. In this way, the surface features of a specimen can be measured by STMs with a resolution of the order of the size of a single atom (see Figure 6-29).

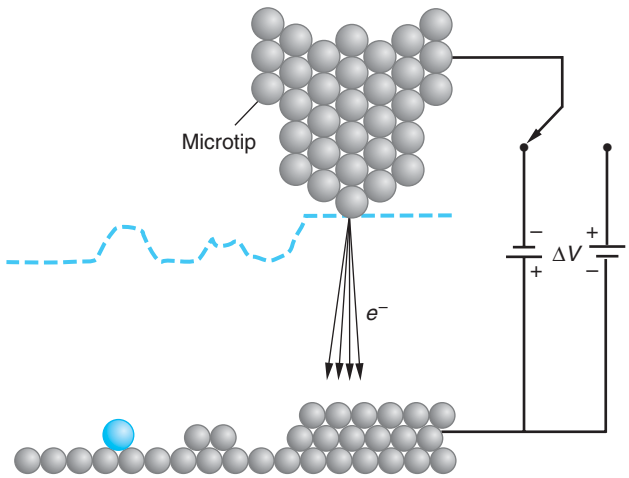

Figure 6-29 Schematic illustration of the path of the probe of an STM (dashed line) scanned across the surface of a sample while maintaining constant tunneling current. The probe has an extremely sharp microtip of atomic dimensions. Tunneling occurs over a small area across the narrow gap, allowing very small features (even individual atoms) to be imaged, as indicated by the dashed line.

STUDENTS-HUB.com Uploaded By: Malak Obaid

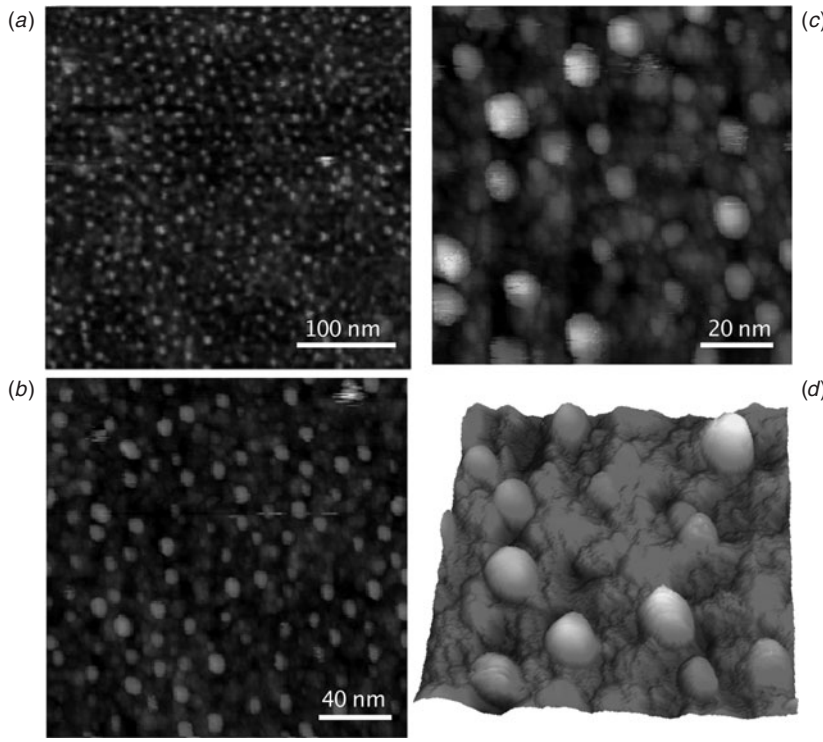

Room temperature UHV-STM images of gold (Au) nanoparticles supported on TiC after annealing at 500°C. Images are (*a*) 375 nm × 375 nm, (*b*) 200 × 200 nm, and (*c*) 100 × 100 nm. (*d*) A 3-D image of a 70 nm × 70 nm section of (*c*). [*The authors thank Beatriz Roldán Cuenya for permission to use these STM images.*]

EXPLORING
Alpha Decay

Barrier penetration was used by G. Gamow, E. U. Condon, and R. W. Gurney in 1928 to explain the enormous variation in the mean life for α decay of radioactive nuclei and the seemingly paradoxical very existence of α decay.[16] While radioactive α decay will be discussed more thoroughly in Chapter 11, in general, the smaller the energy of the emitted α particle, the larger the mean life. The energies of α particles from natural radioactive sources range from about 4 to 7 MeV, whereas the mean lifetimes range from about 10^{10} years to 10^{-6} s. Gamow represented the radioactive nucleus by a potential well containing an α particle, as shown in Figure 6-30*a*. For r less than the nuclear radius R, the α particle is attracted by the nuclear force. Without knowing much about this force, Gamow and his co-workers represented it by a square well. Outside the nucleus, the α particle is repelled by the Coulomb force. This is represented by the Coulomb potential energy $+kZze^2/r$, where $z = 2$ for the α particle and Ze is the remaining nuclear charge. The energy E is the measured kinetic energy of the emitted α particle, since when it is far from the nucleus its potential energy is zero. We see from the figure that a small increase in E reduces the relative height of the barrier $V - E$ and also reduces the thickness. Because the probability of transmission varies exponentially with the relative height and barrier thickness, as indicated by Equation 6-76, a small increase in E leads to a large increase in the probability of transmission and in turn to a shorter lifetime. Gamow and his co-workers were able to derive an expression for the α decay rate and the mean lifetime as a function of energy E that was in good agreement with experimental results as follows:

STUDENTS-HUB.com Uploaded By: Malak Obaid

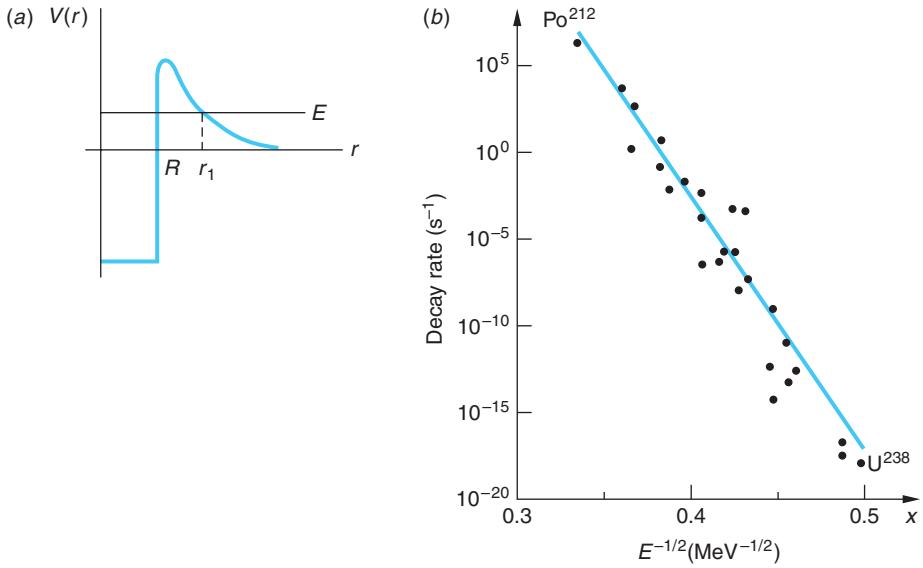

Figure 6-30 (*a*) Model of potential-energy function for an α particle and a nucleus. The strong attractive nuclear force for r less than the nuclear radius R can be approximately described by the potential well shown. Outside the nucleus the nuclear force is negligible, and the potential is given by Coulomb's law, $V(r) = +kZze^2/r$, where Ze is the nuclear charge and ze is the charge of the α particle. An α particle inside the nucleus oscillates back and forth, being reflected at the barrier at R. Because of its wave properties, when the α particle hits the barrier, there is a small chance that it will penetrate and appear outside the well at $r = r_1$. The wave function is similar to that shown in Figure 6-27*b*. (*b*) The decay rate for the emission of α particles from radioactive nuclei. The solid curve is the prediction of Equation 6-79; the points are experimental results.

The probability that an α particle will tunnel through the barrier in any one approach is given by T from Equation 6-76. In fact, in this case αa is so large that the exponential dominates the expression and

$$T \approx e^{-2\sqrt{2m(V_0 - E)}a/\hbar} \qquad \textbf{6-77}$$

which is a very small number; i.e., the α particle is usually reflected. The number of times per second N that the α particle approaches the barrier is given roughly by

$$N \approx \frac{v}{2R} \qquad \textbf{6-78}$$

where v equals the particle's speed inside the nucleus. Thus, the decay rate, or the probability per second that the nucleus will emit an α particle, which is also the reciprocal of the mean life τ, is given by

$$\text{decay rate} = \frac{1}{\tau} = \frac{v}{2R} e^{-2\sqrt{2m(V_0 - E)}a/\hbar} \qquad \textbf{6-79}$$

Figure 6-30*b* illustrates the good agreement between the barrier penetration calculation and experimental measurements.

In the event that $E/V_0 > 1$, there is no reflected wave for $\alpha a = \pi, 2\pi, \ldots$ as a result of destructive interference. For electrons incident on noble gas atoms the resulting 100 percent transmission is called Ramsauer-Townsend effect and is a way of measuring atomic diameters for those elements.

STUDENTS-HUB.com Uploaded By: Malak Obaid

EXPLORING
NH_3 Atomic Clock

Barrier penetration also takes place in the case of the periodic *inversion* of the ammonia molecule. The NH_3 molecule has two equilibrium configurations, as illustrated in Figure 6-31*a*. The three hydrogen atoms are arranged in a plane. The nitrogen atom oscillates between two equilibrium positions equidistant from each of the H atoms above and below the plane. The potential energy function $V(x)$ acting on the N atom has two minima located symmetrically about the center of the plane, as shown in Figure 6-31*b*. The N atom is bound to the molecule, so the energy is quantized and the lower states lie well below the central maximum of the potential. The central maximum presents a barrier to the N atoms in the lower states through which they slowly tunnel back and forth.[17] The oscillation frequency $f = 2.3786 \times 10^{10}$ Hz when the atom is in the state characterized by the energy E_1 in Figure 6-31*b*. This frequency is quite low compared with the frequencies of most molecular vibrations, a fact that allowed the N atom tunneling frequency in NH_3 to be used as the standard in the first *atomic clocks*, devices that now provide the world's standard for precision timekeeping.

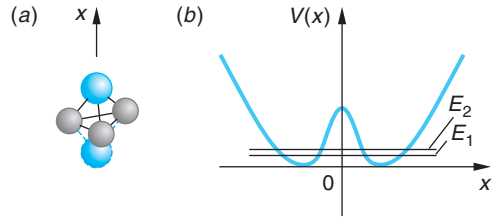

Figure 6-31 (*a*) The NH_3 molecule oscillates between the two equilibrium positions shown. The H atoms form a plane; the N atom is colored. (*b*) The potential energy of the N atom, where x is the distance above and below the plane of the H atoms. Several of the allowed energies, including the two lowest shown, lie below the top of the central barrier through which the N atom tunnels.

More

Quantum-mechanical tunneling involving two barriers is the basis for a number of devices such as the tunnel diode and the Josephson junction, both of which have a wide variety of useful applications. As an example of such systems, the *Tunnel Diode* is described on the home page: www.whfreeman.com/tiplermodernphysics5e. See also Equation 6-80 and Figure 6-32 here.

Summary

TOPIC	RELEVANT EQUATIONS AND REMARKS	
1. Schrödinger equation		
Time dependent, one space dimension	$-\frac{\hbar^2}{2m}\frac{\partial^2\psi(x,t)}{\partial x^2} + V(x,t)\psi(x,t) = i\hbar\frac{\partial\psi(x,t)}{\partial t}$	**6-6**

STUDENTS-HUB.com Uploaded By: Malak Obaid

TOPIC	RELEVANT EQUATIONS AND REMARKS	
Time independent, one space dimension	$\frac{-\hbar^2}{2m}\frac{d^2\psi(x)}{dx^2} + V(x)\psi(x) = E\psi(x)$	**6-18**
Normalization condition	$\int_{-\infty}^{+\infty} \Psi^*(x,t)\Psi(x,t)\,dx = 1$	**6-9**
	and	
	$\int_{-\infty}^{+\infty} \psi^*(x)\psi(x)\,dx = 1$	**6-20**
Acceptability conditions	1. $\psi(x)$ must exist and satisfy the Schrödinger equation. 2. $\psi(x)$ and $d\psi/dx$ must be continuous. 3. $\psi(x)$ and $d\psi/dx$ must be finite. 4. $\psi(x)$ and $d\psi/dx$ must be single valued. 5. $\psi(x) \longrightarrow 0$ fast enough as $x \longrightarrow \pm\infty$ so that the normalization integral, Equation 6-20, remains bounded.	
2. Infinite square well		
Allowed energies	$E_n = n^2\frac{\pi^2\hbar^2}{2mL^2} = n^2E_1 \qquad n = 1, 2, 3, \ldots$	**6-24**
Wave functions	$\psi_n(x) = \sqrt{\frac{2}{L}}\sin\frac{n\pi x}{L} \qquad n = 1, 2, 3, \ldots$	**6-32**
3. Finite square well	For a finite well of width L the allowed energies E_n in the well are lower than the corresponding levels for an infinite well. There is always at least one allowed energy (bound state) in a finite well.	
4. Expectation values and operators	The expectation or average value of a physical quantity represented by an operator, such as the momentum operator p_{op}, is given by	
	$\langle p\rangle = \int_{-\infty}^{+\infty} \psi^*\, p_{op}\psi\,dx = \int_{-\infty}^{+\infty} \psi^*\left(\frac{\hbar}{i}\frac{\partial}{\partial x}\right)\psi\,dx$	**6-48**
5. Simple harmonic oscillator		
Allowed energies	$E_n = \left(n + \frac{1}{2}\right)\hbar\omega \qquad n = 0, 1, 2, \ldots$	**6-56**
6. Reflection and transmission	When the potential changes abruptly in a distance small compared to the de Broglie wavelength, a particle may be reflected even though $E > V(x)$. A particle may also penetrate into a region where $E < V(x)$.	

STUDENTS-HUB.com Uploaded By: Malak Obaid

General References

The following general references are written at a level appropriate for the readers of this book.

Brandt, S., and H. D. Dahmen, *The Picture Book of Quantum Mechanics*, Wiley, New York, 1985.

Eisberg, R., and R. Resnick, *Quantum Physics*, 2d ed., Wiley, New York, 1985.

Feynman, R. P., R. B. Leighton, and M. Sands, *Lectures on Physics*, Addison-Wesley, Reading, MA, 1965.

Ford, K. W., *The Quantum World*, Harvard University Press, Cambridge, MA, 2004.

French, A. P., and E. F. Taylor, *An Introduction to Quantum Physics*, Norton, New York, 1978.

Mehra, J., and H. Rechenberg, *The Historical Development of Quantum Theory*, Vol. 1, Springer-Verlag, New York, 1982.

Park, D., *Introduction to the Quantum Theory*, 3d ed., McGraw-Hill, New York, 1992.

Visual Quantum Mechanics, Kansas State University, Manhattan, 1996. Computer simulation software allows the user to analyze a variety of one-dimensional potentials, including the square wells and harmonic oscillator discussed in this chapter.

Notes

1. Felix Bloch (1905–1983), Swiss American physicist. He was a student at the University of Zurich and attended the colloquium referred to. The quote is from an address before the American Physical Society in 1976. Bloch shared the 1952 Nobel Prize in Physics for measuring the magnetic moment of the neutron, using a method that he invented that led to the development of the analytical technique of nuclear magnetic resonance (NMR) spectroscopy.

2. Peter J. W. Debye (1884–1966), Dutch American physical chemist. He succeeded Einstein in the chair of theoretical physics at the University of Zurich and received the Nobel Prize in Chemistry in 1936.

3. Erwin R. J. A. Schrödinger (1887–1961), Austrian physicist. He succeeded Planck in the chair of theoretical physics at the University of Berlin in 1928 following Planck's retirement and two years after publishing in rapid succession six papers that set forth the theory of wave mechanics. For that work he shared the Nobel Prize in Physics with P. A. M. Dirac in 1933. He left Nazi-controlled Europe in 1940, moving his household to Ireland.

4. To see that this is indeed the case, consider the effect on $\partial^2\Psi(x,t)/\partial x^2$ of multiplying $\Psi(x,t)$ by a factor C. Then $\partial^2 C\Psi(x,t)/\partial x^2 = C\partial^2\Psi(x,t)/\partial x^2$, and the derivative is increased by the same factor. Thus, the derivative is proportional to the first power of the function; i.e., it is linear in $\Psi(x,t)$.

5. The imaginary i appears because the Schrödinger equation relates a *first* time derivative to a *second* space derivative as a consequence of the fact that the total energy is related to the *square* of the momentum. This is unlike the classical wave equation (Equation 5-11), which relates two second derivatives. The implication of this is that, in general, the $\Psi(x,t)$ will be complex functions, whereas the $y(x,t)$ are real.

6. The fact that Ψ is in general complex does not mean that its imaginary part doesn't contribute to the values of measurements, which are real. Every complex number can be written in the form $z = a + bi$, where a and b are real numbers and $i = (-1)^{1/2}$. The magnitude or absolute value of z is defined as $(a^2 + b^2)^{1/2}$. The complex conjugate of z is $z^* = a - bi$, so $z^*z = (a - bi)(a + bi) = a^2 + b^2 = |z|^2$; thus, the value of $|\Psi|^2$ will contain a contribution from its imaginary part.

7. Here we are using the convention of probability and statistics that certainty is represented by a probability of 1.

8. This method for solving partial differential equations is called *separation of variables*, for obvious reasons. Since most potentials in quantum mechanics, as in classical mechanics, are time independent, the method may be applied to the Schrödinger equation in numerous situations.

9. We should note that there is an exception to this in the quantum theory of measurement.

10. $E = 0$ corresponding to $n=0$ is not a possible energy for a particle in a box. As discussed in Section 5-6, the uncertainty principle limits the minimum energy for such a particle to values $> \hbar^2/2mL^2$.

11. Recalling that linear combinations of solutions to Schrödinger's equation will also be solutions, we should note here that simulation of the classical behavior of a macroscopic particle in a macroscopic box requires wave functions that are the superpositions of many stationary states. Thus, the classical particle never has definite energy in the quantum mechanical sense.

12. To simplify the notation in this section, we will sometimes omit the functional dependence and merely write ψ_n for $\psi_n(x)$ and Ψ_n for $\Psi_n(x,t)$.

13. The Hermite polynomials are known functions that are tabulated in most books on quantum mechanics.

14. It is straightforward to show that the only difference between a $\psi(x)$ normalized in terms of the particle density and one for which $|\psi(x)|^2$ is the probability density is a multiplicative constant.

STUDENTS-HUB.com Uploaded By: Malak Obaid

15. T and R are derived in terms of the particle currents, i.e., particles/unit time, in most introductory quantum mechanics books.

16. Rutherford had shown that the scattering of 8.8-MeV α particles from the decay of ^{212}Po obeyed the Coulomb force law down to distances of the order of 3×10^{-14} m, i.e., down to about nuclear dimensions. Thus, the Coulomb barrier at that distance was at least 8.8 MeV high; however, the energy of α particles emitted by ^{238}U is only 4.2 MeV, less than half the barrier height. How that could be possible presented classical physics with a paradox.

17. Since the molecule's center of mass is fixed in an inertial reference frame, the plane of H atoms also oscillates back and forth in the opposite direction to the N atom; however, their mass being smaller than that of the N atom, the amplitude of the plane's motion is actually larger than that of the N atom. It is the relative motion that is important.

18. See, for example, F. Capasso and S. Datta, "Quantum Electron Devices," *Physics Today*, **43**, 74 (1990). Leo Esaki was awarded the Nobel Prize in Physics in 1973 for inventing the resonant tunnel diode.

Problems

Level I

Section 6-1 The Schrödinger Equation in One Dimension

6-1. Show that the wave function $\Psi(x, t) = Ae^{kx - \omega t}$ does not satisfy the time-dependent Schrödinger equation.

6-2. Show that $\Psi(x, t) = Ae^{i(kx - \omega t)}$ satisfies both the time-dependent Schrödinger equation and the classical wave equation (Equation 6-1).

6-3. In a region of space, a particle has a wave function given by $\psi(x) = Ae^{-x^2/2L^2}$ and energy $\hbar^2/2mL^2$, where L is some length. (*a*) Find the potential energy as a function of x, and sketch V versus x. (*b*) What is the classical potential that has this dependence?

6-4. (*a*) For Problem 6-3, find the kinetic energy as a function of x. (*b*) Show that $x = L$ is the classical turning point. (*c*) The potential energy of a simple harmonic oscillator in terms of its angular frequency ω is given by $V(x) = \frac{1}{2} m \omega^2 x^2$. Compare this with your answer to part (*a*) of Problem 6-3, and show that the total energy for this wave function can be written $E = \frac{1}{2} h\omega$.

6-5. (*a*) Show that the wave function $\Psi(x, t) = A \sin(kx - \omega t)$ does *not* satisfy the time-dependent Schrödinger equation. (*b*) Show that $\Psi(x, t) = A \cos(kx - \omega t) + iA \sin(kx - \omega t)$ does satisfy this equation.

6-6. The wave function for a free electron, i.e., one on which no net force acts, is given by $\psi(x) = A \sin(2.5 \times 10^{10} x)$, where x is in meters. Compute the electron's (*a*) momentum, (*b*) total energy, and (*c*) de Broglie wavelength.

6-7. A particle with mass m and total energy zero is in a particular region of space where its wave function is $\psi(x) = Ce^{-x^2/L^2}$. (*a*) Find the potential energy $V(x)$ versus x and (*b*) make a sketch of $V(x)$ versus x.

6-8. Normalize the wave function in Problem 6-2 between $-a$ and $+a$. Why can't that wave function be normalized between $-\infty$ and $+\infty$?

Section 6-2 The Infinite Square Well

6-9. A particle is in an infinite square well of width L. Calculate the ground-state energy if (*a*) the particle is a proton and $L = 0.1$ nm, a typical size for a molecule; (*b*) the particle is a proton and $L = 1$ fm, a typical size for a nucleus.

6-10. A particle is in the ground state of an infinite square well potential given by Equation 6-21. Find the probability of finding the particle in the interval $\Delta x = 0.002\ L$ at (*a*) $x = L/2$, (*b*) $x = 2L/3$, and (*c*) $x = L$. (Since Δx is very small, you need not do any integration.)

6-11. Do Problem 6-10 for a particle in the second excited state ($n = 3$) of an infinite square well potential.

6-12. A mass of 10^{-6} g is moving with a speed of about 10^{-1} cm/s in a box of length 1 cm. Treating this as a one-dimensional infinite square well, calculate the approximate value of the quantum number n.

STUDENTS-HUB.com Uploaded By: Malak Obaid

6-13. (*a*) For the classical particle of Problem 6-12, find Δx and Δp, assuming that $\Delta x/L = 0.01$ percent and $\Delta p/p = 0.01$ percent. (*b*) What is $(\Delta x \Delta p)/\hbar$?

6-14. A particle of mass m is confined to a tube of length L. (*a*) Use the uncertainty relationship to estimate the smallest possible energy. (*b*) Assume that the inside of the tube is a force-free region and that the particle makes elastic reflections at the tube ends. Use Schrödinger's equation to find the ground-state energy for the particle in the tube. Compare the answer to that of part (*a*).

6-15. (*a*) What is the wavelength associated with the particle of Problem 6-14 if the particle is in its ground state? (*b*) What is the wavelength if the particle is in its second excited state (quantum number $n = 3$)? (*c*) Use de Broglie's relationship to find the magnitude for the momentum of the particle in its ground state. (*d*) Show that $p^2/2m$ gives the correct energy for the ground state of this particle in the box.

6-16. The wavelength of light emitted by a ruby laser is 694.3 nm. Assuming that the emission of a photon of this wavelength accompanies the transition of an electron from the $n = 2$ level to the $n = 1$ level of an infinite square well, compute L for the well.

6-17. The allowed energies for a particle of mass m in a one-dimensional infinite square well are given by Equation 6-24. Show that a level with $n = 0$ violates the Heisenberg uncertainty principle.

6-18. Suppose a macroscopic bead with a mass of 2.0 g is constrained to move on a straight frictionless wire between two heavy stops clamped firmly to the wire 10 cm apart. If the bead is moving at a speed of 20 nm/y (i.e., to all appearances it is at rest), what is the value of its quantum number n?

6-19. An electron moving in a one-dimensional infinite square well is trapped in the $n = 5$ state. (*a*) Show that the probability of finding the electron between $x = 0.2\ L$ and $x = 0.4\ L$ is 1/5. (*b*) Compute the probability of finding the electron within the "volume" $\Delta x = 0.01\ L$ at $x = L/2$.

6-20. In the early days of nuclear physics before the neutron was discovered, it was thought that the nucleus contained only electrons and protons. If we consider the nucleus to be a one-dimensional infinite well with $L = 10$ fm and ignore relativity, compute the ground-state energy for (*a*) an electron and (*b*) a proton in the nucleus. (*c*) Compute the energy difference between the ground state and the first excited state for each particle. (Differences between energy levels in nuclei are found to be typically of the order of 1 MeV.)

6-21. An electron is in the ground state with energy E_n of a one-dimensional infinite well with $L = 10^{-10}$ m. Compute the force that the electron exerts on the wall during an impact on either wall. (*Hint:* $F = -dE_n/dL$. Why?) How does this result compare with the weight of an electron at the surface of Earth?

6-22. The wave functions of a particle in a one-dimensional infinite square well are given by Equation 6-32. Show that for these functions $\int \psi_n(x)\psi_m(x)\,dx = 0$, i.e., that $\psi_n(x)$ and $\psi_m(x)$ are orthogonal.

Section 6-3 The Finite Square Well

6-23. Sketch (*a*) the wave function and (*b*) the probability distribution for the $n = 4$ state for the finite square well potential.

6-24. A finite square well 1.0 fm wide contains one neutron. How deep must the well be if there are only two allowed energy levels for the neutron?

6-25. An electron is confined to a finite square well whose "walls" are 8.0 eV high. If the ground-state energy is 0.5 eV, estimate the width of the well.

6-26. Using arguments concerning curvature, wavelength, and amplitude, sketch very carefully the wave function corresponding to a particle with energy E in the finite potential well shown in Figure 6-33.

STUDENTS-HUB.com Uploaded By: Malak Obaid

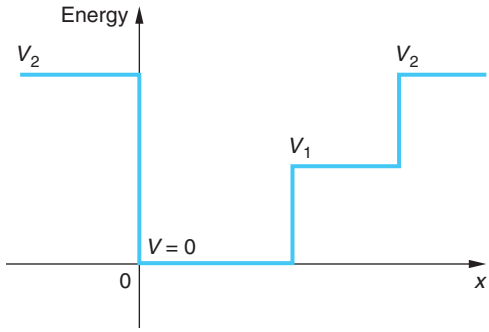

Figure 6-33 Problem 6-26.

6-27. For a finite square well potential that has six quantized levels, if $a = 10$ nm (*a*) sketch the finite well, (*b*) sketch the wave function from $x = -2a$ to $x = +2a$ for $n = 3$, and (*c*) sketch the probability density for the same range of x.

Section 6-4 Expectation Values and Operators

6-28. Compute the expectation value of the x component of the momentum of a particle of mass m in the $n = 3$ level of a one-dimensional infinite square well of width L. Reconcile your answer with the fact that the kinetic energy of the particle in this level is $9\pi^2\hbar^2/2mL^2$.

6-29. Find (*a*) $\langle x \rangle$ and (*b*) $\langle x^2 \rangle$ for the second excited state ($n = 3$) in an infinite square well potential.

6-30. (*a*) Show that the classical probability distribution function for a particle in a one-dimensional infinite square well potential of length L is given by $P(x) = 1/L$. (*b*) Use your result in (*a*) to find $\langle x \rangle$ and $\langle x^2 \rangle$ for a classical particle in such a well.

6-31. Show directly from the time-independent Schrödinger equation that $\langle p^2 \rangle = \langle 2m[E - V(x)] \rangle$ in general and that $\langle p^2 \rangle = \langle 2mE \rangle$ for the infinite square well. Use this result to compute $\langle p^2 \rangle$ for the ground state of the infinite square well.

6-32. Find $\sigma_x = \sqrt{\langle x^2 \rangle - \langle x \rangle^2}$, $\sigma_p = \sqrt{\langle p^2 \rangle - \langle p \rangle^2}$, and $\sigma_x \sigma_p$ for the ground-state wave function of an infinite square well. (Use the fact that $\langle p \rangle = 0$ by symmetry and $\langle p^2 \rangle = \langle 2mE \rangle$ from Problem 6-31.)

6-33. Compute $\langle x \rangle$ and $\langle x^2 \rangle$ for the ground state of a harmonic oscillator (Equation 6-58). Use $A_0 = (m\omega/\hbar\pi)^{1/4}$.

6-34. Use conservation of energy to obtain an expression connecting x^2 and p^2 for a harmonic oscillator, then use it along with the result from Problem 6-33 to compute $\langle p^2 \rangle$ for the harmonic oscillator ground state.

6-35. (*a*) Using A_0 from Problem 6-33, write down the total wave function $\Psi_0(x, t)$ for the ground state of a harmonic oscillator. (*b*) Use the operator for p_x from Table 6-1 to compute $\langle p^2 \rangle$.

Section 6-5 The Simple Harmonic Oscillator

6-36. For the harmonic oscillator ground state $n = 0$ the Hermite polynomial $H_n(x)$ in Equation 6-57 is given by $H_0 = 1$. Find (*a*) the normalization constant C_0, (*b*) $\langle x^2 \rangle$, and (*c*) $\langle V(x) \rangle$ for this state. (*Hint:* Use the Probability Integral in Appendix B1 to compute the needed integrals.)

6-37. For the first excited state, $H_1(x) = x$. Find (*a*) the normalization constant C_1, (*b*) $\langle x \rangle$, (*c*) $\langle x^2 \rangle$, (*d*) $\langle V(x) \rangle$ for this state (see Problem 6-36).

6-38. A quantum harmonic oscillator of mass m is in the ground state with classical turning points at $\pm A$. (*a*) With the mass confined to the region $\Delta x \approx 2A$, compute Δp for this state. (*b*) Compare the kinetic energy implied by Δp with (1) the ground-state total energy and (2) the expectation value of the kinetic energy.

STUDENTS-HUB.com Uploaded By: Malak Obaid

6-39. Compute the spacing between adjacent energy levels per unit energy, i.e., $\Delta E_n/E_n$, for the quantum harmonic oscillator and show that the result agrees with Bohr's correspondence principle (see Section 4-3) by letting $n \rightarrow \infty$.
6-40. Compute $\langle x \rangle$ and $\langle x^2 \rangle$ for (*a*) the ground state and (*b*) the first excited state of the harmonic oscillator.
6-41. The period of a macroscopic pendulum made with a mass of 10 g suspended from a massless cord 50 cm long is 1.42 s. (*a*) Compute the ground-state (zero-point) energy. (*b*) If the pendulum is set into motion so that the mass raises 0.1 mm above its equilibrium position, what will be the quantum number of the state? (*c*) What is the frequency of the motion in (*b*)?
6-42. Show that the wave functions for the ground state and the first excited state of the simple harmonic oscillator, given in Equation 6-58, are orthogonal; that is, show that $\int \psi_0(x)\psi_1(x)\,dx = 0$.

Section 6-6 Reflection and Transmission of Waves

6-43. A free particle of mass m with wave number k_1 is traveling to the right. At $x = 0$, the potential jumps from zero to V_0 and remains at this value for positive x. (*a*) If the total energy is $E = \hbar^2 k_1^2/2m = 2V_0$, what is the wave number k_2 in the region $x > 0$? Express your answer in terms of k_1 and V_0. (*b*) Calculate the reflection coefficient R at the potential step. (*c*) What is the transmission coefficient T? (*d*) If one million particles with wave number k_1 are incident upon the potential step, how many particles are expected to continue along in the positive x direction? How does this compare with the classical prediction?
6-44. In Problem 6-43, suppose that the potential jumps from zero to $-V_0$ at $x = 0$ so that the free particle speeds up instead of slowing down. The wave number for the incident particle is again k_1, and the total energy is $2V_0$. (*a*) What is the wave number for the particle in the region of positive x? (*b*) Calculate the reflection coefficient R at the potential step. (*c*) What is the transmission coefficient T? (*d*) If one million particles with wave number k_1 are incident upon the potential step, how many particles are expected to continue along in the positive x direction? How does this compare with the classical prediction?
6-45. In a particular semiconductor device an oxide layer forms a barrier 0.6 nm wide and 9 V high between two conducting wires. Electrons accelerated through 4 V approach the barrier. (*a*) What fraction of the incident electrons will tunnel through the barrier? (*b*) Through what potential difference should the electrons be accelerated in order to increase the tunneling fraction by a factor of 2?
6-46. For particles incident on a step potential with $E < V_0$, show that $T = 0$ using Equation 6-70.
6-47. Derive Equations 6-66 and 6-67 from those that immediately precede them.
6-48. A beam of electrons, each with kinetic energy $E = 2.0$ eV, is incident on a potential barrier with $V_0 = 6.5$ eV and width 5.0×10^{-10} m. (See Figure 6-26.) What fraction of the electrons in the beam will be transmitted through the barrier?
6-49. A beam of protons, each with kinetic energy 40 MeV, approaches a step potential of 30 MeV. (*a*) What fraction of the beam is reflected and transmitted? (*b*) Does your answer change if the particles are electrons?

Level II

6-50. A proton is in an infinite square well potential given by Equation 6-21 with $L = 1$ fm. (*a*) Find the ground-state energy in MeV. (*b*) Make an energy-level diagram for this system. Calculate the wavelength of the photon emitted for the transitions (*c*) $n = 2$ to $n = 1$, (*d*) $n = 3$ to $n = 2$, and (*e*) $n = 3$ to $n = 1$.
6-51. A particle is in the ground state of an infinite square well potential given by Equation 6-21. Calculate the probability that the particle will be found in the region (*a*) $0 < x < \frac{1}{2}L$, (*b*) $0 < x < \frac{1}{3}L$, and (*c*) $0 < x < \frac{3}{4}L$.
6-52. (*a*) Show that for large n, the fractional difference in energy between state n and state $n + 1$ for a particle in an infinite square well is given approximately by

$$\frac{E_{n+1} - E_n}{E_n} \approx \frac{2}{n}$$

(*b*) What is the approximate percentage energy difference between the states $n_1 = 1000$ and $n_2 = 1001$? (*c*) Comment on how this result is related to Bohr's correspondence principle.

STUDENTS-HUB.com Uploaded By: Malak Obaid

6-53. Compute the expectation value of the kinetic energy of a particle of mass m moving in the $n = 2$ level of a one-dimensional infinite square well of width L.

6-54. A particle of mass m is in an infinite square well potential given by

$$V = \infty \qquad x < -L/2$$
$$V = 0 \qquad -L/2 < x < +L/2$$
$$V = \infty \qquad +L/2 < x$$

Since this potential is symmetric about the origin, the probability density $|\psi(x)|^2$ must also be symmetric. (*a*) Show that this implies that either $\psi(-x) = \psi(x)$ or $\psi(-x) = -\psi(x)$. (*b*) Show that the proper solutions of the time-independent Schrödinger equation can be written

$$\psi(x) = \sqrt{\frac{2}{L}} \cos \frac{n\pi x}{L} \qquad n = 1, 3, 5, 7, \ldots$$

and

$$\psi(x) = \sqrt{\frac{2}{L}} \sin \frac{n\pi x}{L} \qquad n = 2, 4, 6, 8, \ldots$$

(*c*) Show that the allowed energies are the same as those for the infinite square well given by Equation 6-24.

6-55. The wave function $\psi_0(x) = Ae^{-x^2/2L^2}$ represents the ground-state energy of a harmonic oscillator. (*a*) Show that $\psi_1(x) = L\, d\psi_0(x)/dx$ is also a solution of Schrödinger's equation. (*b*) What is the energy of this new state? (*c*) From a look at the nodes of this wave function, how would you classify this excited state?

6-56. For the wave functions

$$\psi(x) = \sqrt{\frac{2}{L}} \sin \frac{n\pi x}{L} \qquad n = 1, 2, 3, \ldots$$

corresponding to an infinite square well of width L, show that

$$\langle x^2 \rangle = \frac{L^2}{3} - \frac{L^2}{2n^2\pi^2}$$

6-57. A 10-eV electron is incident on a potential barrier of height 25 eV and width 1 nm. (*a*) Use Equation 6-76 to calculate the order of magnitude of the probability that the electron will tunnel through the barrier. (*b*) Repeat your calculation for a width of 0.1 nm.

6-58. A particle of mass m moves in a region in which the potential energy is constant $V = V_0$. (*a*) Show that neither $\Psi(x, t) = A \sin(kx - \omega t)$ nor $\Psi(x, t) = A \cos(kx - \omega t)$ satisfies the time-dependent Schrödinger equation. (*Hint:* If $C_1 \sin\phi + C_2 \cos\phi = 0$ for all values of ϕ, then C_1 and C_2 must be zero.) (*b*) Show that $\Psi(x, t) = A[\cos(kx - \omega t) + i \sin(kx - \omega t)] = Ae^{i(kx - \omega t)}$ does satisfy the time-independent Schrödinger equation providing that k, V_0, and ω are related by Equation 6-5.

Level III

6-59. A particle of mass m on a table at $z = 0$ can be described by the potential energy

$$V = mgz \quad \text{for} \quad z > 0$$
$$V = \infty \quad \text{for} \quad z < 0$$

For some positive value of total energy E, indicate the classically allowed region on a sketch of $V(z)$ versus z. Sketch also the kinetic energy versus z. The Schrödinger equation for this problem is quite difficult to solve. Using arguments similar to those in Section 6-3 about the curvature of a wave function as given by the Schrödinger equation, sketch your "educated guesses" for the shape of the wave function for the ground state and the first two excited states.

STUDENTS-HUB.com Uploaded By: Malak Obaid

6-60. Use the Schrödinger equation to show that the expectation value of the kinetic energy of a particle is given by

$$\langle E_k \rangle = \int_{-\infty}^{+\infty} \psi(x) \left(-\frac{\hbar^2}{2m} \frac{d^2\psi(x)}{dx^2} \right) dx$$

6-61. An electron in an infinite square well with $L = 10^{-12}$ m is moving at relativistic speed; hence, the momentum is *not* given by $p = (2mE)^{1/2}$. (*a*) Use the uncertainty principle to verify that the speed is relativistic. (*b*) Derive an expression for the electron's allowed energy levels and (*c*) compute E_1. (*d*) By what fraction does E_1 computed in (*c*) differ from the nonrelativistic E_1?

6-62. (*a*) Derive Equation 6-75. (*b*) Show that, if $\alpha x \gg 1$, Equation 6-76 follows from Equation 6-75 as an approximation.

6-63. A beam of protons, each with energy $E = 20$ MeV, is incident on a potential step 40 MeV high. Graph the relative probability of finding protons at values of $x > 0$ from $x = 0$ to $x = 5$ fm. (*Hint:* Take $|A|^2 = 1$ and refer to Example 6-6.)

STUDENTS-HUB.com Uploaded By: Malak Obaid

CHAPTER 7

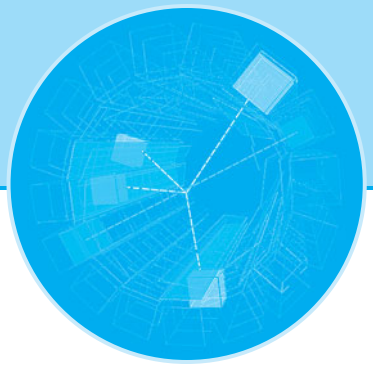

Atomic Physics

In this chapter we will apply quantum theory to atomic systems. For all neutral atoms except hydrogen, the Schrödinger equation cannot be solved exactly. Despite this, it is in the realm of atomic physics that the Schrödinger equation has had its greatest success because the electromagnetic interaction of the electrons with one another and with the atomic nucleus is well understood. With powerful approximation methods and high-speed computers, many features of complex atoms, such as their energy levels and the wavelengths and intensities of their spectra, can be calculated, often to whatever accuracy is desired. The Schrödinger equation for the hydrogen atom was first solved in Schrödinger's first paper on quantum mechanics, published in 1926. This problem is of considerable importance not only because the Schrödinger equation can be solved exactly in this case, but also because the solutions obtained form the basis for the approximate solutions for other atoms. We will therefore discuss this problem in some detail. Although the mathematics that arises in solving the Schrödinger equation is a bit difficult in a few places, we will be as quantitative as possible, presenting results without proof and discussing important features of these results qualitatively only when necessary. Whenever possible, we will give simple physical arguments to make important results plausible.

7-1 The Schrödinger Equation in Three Dimensions 269
7-2 Quantization of Angular Momentum and Energy in the Hydrogen Atom 272
7-3 The Hydrogen Atom Wave Functions 281
7-4 Electron Spin 285
7-5 Total Angular Momentum and the Spin-Orbit Effect 291
7-6 The Schrödinger Equation for Two (or More) Particles 295
7-7 Ground States of Atoms: The Periodic Table 297
7-8 Excited States and Spectra of Atoms 301

7-1 The Schrödinger Equation in Three Dimensions

In Chapter 6 we considered motion in just one dimension, but of course the real world is three-dimensional. Although in many cases the one-dimensional form brings out the essential physical features, there are some considerations introduced in three-dimensional problems that we want to examine. In rectangular coordinates, the time-independent Schrödinger equation is

$$-\frac{\hbar^2}{2m}\left(\frac{\partial^2\psi}{\partial x^2}+\frac{\partial^2\psi}{\partial y^2}+\frac{\partial^2\psi}{\partial z^2}\right)+V\psi=E\psi \qquad \textbf{7-1}$$

The wave function and the potential energy are generally functions of all three coordinates x, y, and z.

STUDENTS-HUB.com
Uploaded By: Malak Obaid

Infinite Square Well in Three Dimensions

Let us consider the three-dimensional version of a particle in a cubical box. The potential energy function $V(x, y, z) = 0$ for $0 < x < L$, $0 < y < L$, and $0 < z < L$. V is infinite outside this region. For this problem, the wave function must be zero at the walls of the box and will be a sine function inside the box. In fact, if we consider just one coordinate such as x, the solution will be the same as in the one-dimensional box discussed in Section 6-2. That is, the x dependence of the wave function will be of the form $\sin k_1 x$ with the restriction $k_1 L = n_1 \pi$, where n_1 is an integer. The complete wave function $\psi(x, y, z)$ can be written as a product of a function of x only, a function of y only, and a function of z only.

$$\psi(x, y, z) = \psi_1(x)\psi_2(y)\psi_3(z) \qquad \textbf{7-2}$$

where each of the functions ψ_n is a sine function as in the one-dimensional problem. For example, if we try the solution

$$\psi(x, y, z) = A \sin k_1 x \sin k_2 y \sin k_3 z \qquad \textbf{7-3}$$

we find by inserting this function into Equation 7-1 that the energy is given by

$$E = \frac{\hbar^2}{2m}(k_1^2 + k_2^2 + k_3^2)$$

which is equivalent to

$$E = \frac{(p_x^2 + p_y^2 + p_z^2)}{2m}$$

with $p_x = \hbar k_1$ and so forth. Using the restrictions on the wave numbers $k_i = n_i \pi / L$ from the boundary condition that the wave function be zero at the walls, we obtain for the total energy

$$E_{n_1 n_2 n_3} = \frac{\hbar^2 \pi^2}{2mL^2}(n_1^2 + n_2^2 + n_3^2) \qquad \textbf{7-4}$$

where n_1, n_2, and n_3 are integers greater than zero, as in Equation 6-24.

Notice that *the energy and wave function are characterized by three quantum numbers, each arising from a boundary condition on one of the coordinates*. In this case the quantum numbers are independent of one another, but in more-general problems the value of one quantum number may affect the possible values of the others. For example, as we will see in a moment, in problems such as the hydrogen atom that have a spherical symmetry, the Schrödinger equation is most readily solved in spherical coordinates r, θ, and φ. The quantum numbers associated with the boundary conditions on these coordinates are interdependent.

The lowest energy state, the ground state for the cubical box, is given by Equation 7-4 with $n_1 = n_2 = n_3 = 1$. The first excited energy level can be obtained in three different ways: either $n_1 = 2, n_2 = n_3 = 1$ or $n_2 = 2, n_1 = n_3 = 1$ or $n_3 = 2, n_1 = n_2 = 1$ since we see from Equation 7-4 that $E_{211} = E_{121} = E_{112}$. Each has a different wave function.

STUDENTS-HUB.com Uploaded By: Malak Obaid

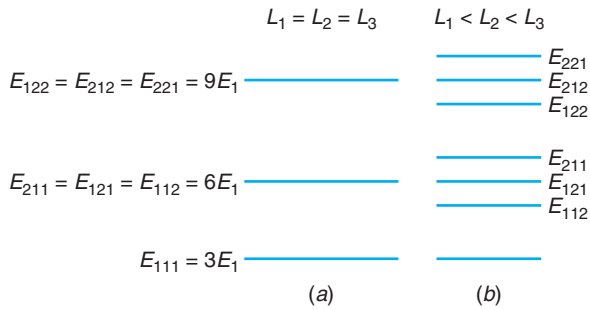

Figure 7-1 Energy-level diagram for (*a*) cubic infinite square well potential and (*b*) noncubic infinite square well. In the cubic well, the energy levels above the ground state are threefold degenerate; i.e., there are three wave functions having the same energy. The degeneracy is removed when the symmetry of the potential is removed, as in (*b*). The diagram is only schematic, and none of the levels in (*b*) necessarily has the same value of the energy as any level in (*a*).

For example, the wave function for $n_1 = 2$ and $n_2 = n_3 = 1$ is of the form

$$\psi_{211} = A \sin\frac{2\pi x}{L} \sin\frac{\pi y}{L} \sin\frac{\pi z}{L}$$

An energy level that has more than one wave function associated with it is said to be *degenerate*. In this case there is threefold degeneracy because there are three wave functions $\psi(x, y, z)$ corresponding to the same energy. The degeneracy is related to the symmetry of the problem, and anything that destroys or breaks the symmetry will also destroy or remove the degeneracy.[1] If, for example, we considered a noncubical box $V = 0$ for $0 < x < L_1$, $0 < y < L_2$, and $0 < z < L_3$, the boundary condition at the walls would lead to the quantum conditions $k_1 L_1 = n_1\pi$, $k_2 L_2 = n_2\pi$, and $k_3 L_3 = n_3\pi$, and the total energy would be

$$E_{n_1 n_2 n_3} = \frac{\hbar^2\pi^2}{2m}\left(\frac{n_1^2}{L_1^2} + \frac{n_2^2}{L_2^2} + \frac{n_3^2}{L_3^2}\right) \qquad \textbf{7-5}$$

Figure 7-1 shows the energy levels for the ground state and first two excited states when $L_1 = L_2 = L_3$, for which the excited states are degenerate, and when L_1, L_2, and L_3 are slightly different, in which case the excited levels are slightly split apart and the degeneracy is removed.

The Schrödinger Equation in Spherical Coordinates

In the next section we are going to consider another, different potential, that of a real atom. Assuming the proton to be at rest, we can treat the hydrogen atom as a single particle, an electron moving with kinetic energy $p^2/2m_e$ and a potential energy $V(r)$ due to the electrostatic attraction of the proton:

$$V(r) = -\frac{Zke^2}{r} \qquad \textbf{7-6}$$

As in the Bohr theory, we include the atomic number Z, which is 1 for hydrogen, so we can apply our results to other similar systems, such as ionized helium He^+, where $Z = 2$. We also note that we can account for the motion of the nucleus by replacing

STUDENTS-HUB.com Uploaded By: Malak Obaid

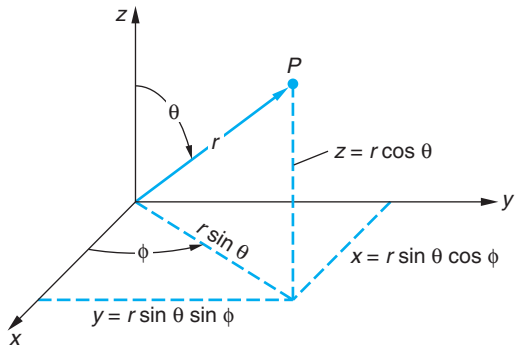

Range of variables
Cartesian
$x, y, z: -\infty \rightarrow +\infty$
Spherical
$r: 0 \rightarrow +\infty$
$\theta: 0 \rightarrow \pi$
$\phi: 0 \rightarrow 2\pi$

Figure 7-2 Geometric relations between spherical (polar) and rectangular coordinates.

Hydrogenlike atoms, those with a single electron, have been produced from elements up to and including U^{91+}. Highly ionized atomic beams are used to further our understanding of relativistic effects and atomic structure. Collision of two completely ionized Au atoms, each moving at nearly the speed of light, produced the "star" of thousands of particles reproduced on page 562 in Chapter 12.

the electron mass m_e by the reduced mass $\mu = m_e/(1 + m_e/M_N)$, where M_N is the mass of the nucleus. The time-independent Schrödinger equation for a particle of mass μ moving in three dimensions is Equation 7-1, with m replaced by μ:

$$-\frac{\hbar^2}{2\mu}\left(\frac{\partial^2\psi}{\partial x^2}+\frac{\partial^2\psi}{\partial y^2}+\frac{\partial^2\psi}{\partial z^2}\right)+V\psi=E\psi \qquad \textbf{7-7}$$

Since the potential energy $V(r)$ depends only on the radial distance $r = (x^2 + y^2 + z^2)^{1/2}$, the problem is most conveniently treated in spherical coordinates r, θ, and ϕ. These are related to x, y, and z by

$$\begin{aligned} x &= r\sin\theta\cos\phi \\ y &= r\sin\theta\sin\phi \\ z &= r\cos\theta \end{aligned} \qquad \textbf{7-8}$$

These relations are shown in Figure 7-2. The transformation of the three-dimensional Schrödinger equation into spherical coordinates is straightforward but involves much tedious calculation, which we will omit. The result is

$$-\frac{\hbar^2}{2\mu}\frac{1}{r^2}\frac{\partial}{\partial r}\left(r^2\frac{\partial\psi}{\partial r}\right)-\frac{\hbar^2}{2\mu r^2}\left[\frac{1}{\sin\theta}\frac{\partial}{\partial\theta}\left(\sin\theta\frac{\partial\psi}{\partial\theta}\right)+\frac{1}{\sin^2\theta}\frac{\partial^2\psi}{\partial\phi^2}\right]+V(r)\psi=E\psi \qquad \textbf{7-9}$$

Despite the formidable appearance of this equation, it was not difficult for Schrödinger to solve because it is similar to other partial differential equations that arise in classical physics, and such equations had been thoroughly studied. We will present the solution of this equation in detail, taking care to point out the origin of the quantum number associated with each dimension. As was the case with the three-dimensional square well, the new quantum numbers will arise as a result of boundary conditions on the solution of the wave equation, Equation 7-9 in this case.

7-2 Quantization of Angular Momentum and Energy in the Hydrogen Atom

In this section we will solve the time-independent Schrödinger equation for hydrogen and hydrogenlike atoms. We will see how the quantization of both the energy and the angular momentum arise as natural consequences of the acceptability conditions on the wave function (see Section 6-1) and discover the origin and physical meaning of the quantum numbers n, ℓ, and m.

STUDENTS-HUB.com Uploaded By: Malak Obaid

The first step in the solution of a partial differential equation such as Equation 7-9 is to search for separable solutions by writing the wave function $\psi(r, \theta, \phi)$ as a product of functions of each single variable. We write

$$\psi(r, \theta, \phi) = R(r)f(\theta)g(\phi) \qquad \textbf{7-10}$$

where R depends only on the radial coordinate r, f depends only on θ, and g depends only on ϕ. When this form of $\psi(r, \theta, \phi)$ is substituted into Equation 7-9, the partial differential equation can be transformed into three ordinary differential equations, one for $R(r)$, one for $f(\theta)$, and one for $g(\phi)$. Most of the solutions of Equation 7-9 are, of course, not of this separable product form; however, if enough product solutions of the form of Equation 7-10 can be found,[2] all solutions can be expressed as superpositions of them. Even so, the separable solutions given by Equation 7-10 turn out to be the most important ones physically because they correspond to definite values (*eigenvalues*) of energy and angular momentum. When Equation 7-10 is substituted into Equation 7-9 and the indicated differentiations are performed, we obtain

$$-\frac{\hbar^2}{2\mu}fg\frac{1}{r^2}\frac{d}{dr}\left(r^2\frac{dR}{dr}\right) - \frac{\hbar^2}{2\mu r^2}Rg\frac{1}{\sin\theta}\frac{d}{d\theta}\left(\sin\theta\frac{df}{d\theta}\right) - \frac{\hbar^2}{2\mu r^2}\frac{Rf}{\sin^2\theta}\frac{d^2g}{d\phi^2} + VRfg = ERfg \qquad \textbf{7-11}$$

since derivatives with respect to r do not affect $f(\theta)$ and g(ϕ), derivatives with respect to θ do not affect $R(r)$ and g(ϕ), and those with respect to ϕ do not affect $R(r)$ and $f(\theta)$. Separation of the r-dependent functions from the θ- and ϕ -dependent ones is accomplished by multiplying Equation 7-11 by $-2\mu r^2/(\hbar^2 Rfg)$ and rearranging slightly to obtain

$$\frac{1}{R(r)}\frac{d}{dr}\left(r^2\frac{dR(r)}{dr}\right) + \frac{2\mu r^2}{\hbar^2}\left[E - V(r)\right] = -\left[\frac{1}{f(\theta)\sin\theta}\frac{d}{d\theta}\left(\sin\theta\frac{df(\theta)}{d\theta}\right) + \frac{1}{g(\phi)\sin^2\theta}\frac{d^2g(\phi)}{d\phi^2}\right] \qquad \textbf{7-12}$$

Note two points about Equation 7-12: (1) The left side contains only terms that are functions of r, while the right side has only terms depending on θ and ϕ. Since the variables are independent, changes in r cannot change the value of the right side of the equation, nor can changes in θ and ϕ have any effect on the left side. Thus, the two sides of the equation must be equal to the same constant, which we will call, with foresight, $\ell(\ell + 1)$. (2) The potential is a function only of r so the solution of the right side, the angular part, of Equation 7-12 will be the same for *all* potentials that are only functions[3] of r.

In view of the second point above, we will first solve the angular equation so that its results will be available to us as we consider solutions to the r-dependent equation, referred to usually as the *radial equation*, for various $V(r)$. Setting the right side of Equation 7-12 equal to $\ell(\ell + 1)$, multiplying by $\sin^2\theta$, and rearranging slightly, we obtain

$$\frac{1}{g(\phi)}\frac{d^2g(\phi)}{d\phi^2} = -\ell(\ell + 1)\sin^2\theta - \frac{\sin\theta}{f(\theta)}\frac{d}{d\theta}\left[\sin\theta\frac{df(\theta)}{d\theta}\right] \qquad \textbf{7-13}$$

Once again we see that the two sides of the relation, Equation 7-13, are each a function of only one of the independent variables hence both sides must be equal to the same constant, which we will, again with foresight, call $-m^2$. Setting the left side of Equation 7-13 equal to $-m^2$ and solving for g(ϕ) yields

$$g_m(\phi) = e^{im\phi} \qquad \textbf{7-14}$$

STUDENTS-HUB.com Uploaded By: Malak Obaid

The single valued condition on ψ (see Section 6-1) implies that $g(\phi + 2\pi) = g(\phi)$, which in turn requires that m be a positive or negative integer or zero.

Now letting the right side of Equation 7-13 equal $-m^2$ and solving for $f(\theta)$, we obtain (not intended to be obvious; for the detailed solution see Weber and Arfken, Chapter 11):

$$f_{\ell m}(\theta) = \frac{(\sin\theta)^{|m|}}{2^{\ell}\ell!}\left[\frac{d}{d(\cos\theta)}\right]^{\ell+|m|}(\cos^2\theta - 1)^{\ell} \qquad \textbf{7-15}$$

The condition that ψ be finite requires that $f(\theta)$ be finite at $\theta = 0$ and $\theta = \pi$, which restricts the values of ℓ to zero and positive integers and limits $m \leq \ell$. The notation reflects the link between ℓ and m, namely, that each value of ℓ has associated values of m ranging from 0 up to $\pm\ell$. The functions $f_{\ell m}(\theta)$, given by Equation 7-15, are called the *associated Legendre functions*. The subset of those with $m = 0$ is referred to as the *Legendre polynomials*.

The product of $f_{\ell m}(\theta)$ and $g_m(\phi)$, which describes the angular dependence of $\psi(r, \theta, \phi)$ for *all* spherically symmetric potentials, forms an often-encountered family of functions $Y_{\ell m}(\theta, \phi)$,

$$Y_{\ell m}(\theta, \phi) = f_{\ell m}(\theta)g_m(\phi) \qquad \textbf{7-16}$$

called the *spherical harmonics*. The first few of these functions, which give the combined angular dependence of the motion of the electron in the hydrogen atom, are given in Table 7-1. The associated Legendre functions and the Legendre polynomials ($m = 0$) can, if needed, be easily taken from the same table. (Extended tables of both functions can be found in Weber and Arfken.) In the following section we will discover the physical significance of ℓ and m.

Table 7-1 Spherical harmonics

$\ell = 0$	$m = 0$	$Y_{00} = \sqrt{\frac{1}{4\pi}}$
$\ell = 1$	$m = 1$	$Y_{11} = -\sqrt{\frac{3}{8\pi}}\sin\theta\, e^{i\phi}$
	$m = 0$	$Y_{10} = \sqrt{\frac{3}{4\pi}}\cos\theta$
	$m = -1$	$Y_{1-1} = \sqrt{\frac{3}{8\pi}}\sin\theta\, e^{-i\phi}$
$\ell = 2$	$m = 2$	$Y_{22} = \sqrt{\frac{15}{32\pi}}\sin^2\theta\, e^{2i\phi}$
	$m = 1$	$Y_{21} = -\sqrt{\frac{15}{8\pi}}\sin\theta\cos\theta\, e^{i\phi}$
	$m = 0$	$Y_{20} = \sqrt{\frac{5}{16\pi}}(3\cos^2\theta - 1)$
	$m = -1$	$Y_{2-1} = \sqrt{\frac{15}{8\pi}}\sin\theta\cos\theta\, e^{-i\phi}$
	$m = -2$	$Y_{2-2} = \sqrt{\frac{15}{32\pi}}\sin^2\theta\, e^{-2i\phi}$

STUDENTS-HUB.com Uploaded By: Malak Obaid

Quantization of the Angular Momentum

The definition of the angular momentum **L** of a mass m moving with velocity **v**, hence momentum **p**, at some location **r** relative to the origin, given in most introductory physics textbooks, is

$$\mathbf{L} = \mathbf{r} \times \mathbf{p}$$

where the momentum $\mathbf{p} = m(d\mathbf{r}/dt)$. In cases where $V = \mathrm{V}(r)$, such as the electron in the hydrogen atom, **L** is conserved (see Problem 7-15) and the classical motion of the mass m lies in a fixed plane perpendicular to **L**, which contains the coordinate origin. The momentum **p** has components (in that plane) $\mathbf{p}_r$ along **r** and $\mathbf{p}_t$ perpendicular to **r**, as illustrated in Figure 7-3, whose magnitudes are given by

$$p_r = \mu\left(\frac{dr}{dt}\right) \quad \text{and} \quad p_t = \mu r\left(\frac{dA}{dt}\right)$$

and the magnitude of the conserved (i.e., constant) vector **L** is

$$L = rp \sin A = rp_t$$

The kinetic energy can be written in terms of these components as

$$\frac{p^2}{2\mu} = \frac{p_r^2 + p_t^2}{2\mu} = \frac{p_r^2}{2\mu} + \frac{L^2}{2\mu r^2}$$

from which the classical total energy E is given by

$$\frac{p_r^2}{2\mu} + \frac{L^2}{2\mu r^2} + V(r) = E \qquad \textbf{7-17}$$

Rewriting Equation 7-17 in terms of the "effective" potential $V_{\text{eff}}(r) = L^2/2\mu r^2 + V(r)$, as is often done, we obtain

$$\frac{p_r^2}{2\mu} + V_{\text{eff}}(r) = E \qquad \textbf{7-18}$$

which is identical in form to Equation 6-4, which we used as a basis for our introduction to the Schrödinger equation.

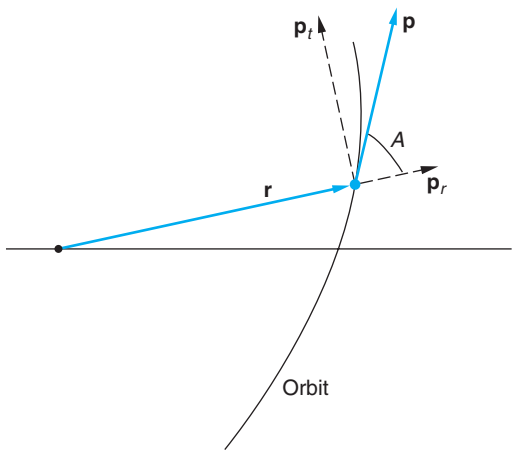

Figure 7-3 The orbit of a classical particle with $V = V(r)$ lies in a plane perpendicular to **L**. The components of the momentum **p** parallel and perpendicular to **r** are $\mathbf{p}_r$ and $\mathbf{p}_t$, respectively. The momentum **p** makes an angle A with the displacement **r**.

STUDENTS-HUB.com Uploaded By: Malak Obaid

Equation 7-17 can be used to write the Schrödinger equation, just as we did in Chapter 6 by inserting de Broglie's relation and the appropriate differential operators in spherical coordinates for p_r^2 and L^2. Doing so is a lengthy though not particularly difficult exercise whose details we will omit here. For p_r^2 the operator turns out to be

$$(p_r^2)_{\text{op}} = -\hbar^2 \frac{1}{r^2} \frac{\partial}{\partial r}\left(r^2 \frac{\partial}{\partial r}\right) \qquad \textbf{7-19}$$

which, divided by 2μ and operating on ψ, you recognize as the first term (kinetic energy) of the Schrödinger equation in spherical coordinates (Equation 7-9). Similarly, the operator for L^2 turns out to be

$$(L^2)_{\text{op}} = -\hbar^2\left[\frac{1}{\sin\theta}\frac{\partial}{\partial\theta}\left(\sin\theta\frac{\partial}{\partial\theta}\right) + \frac{1}{\sin^2\theta}\frac{\partial^2}{\partial\phi^2}\right] \qquad \textbf{7-20}$$

which, divided by $2\mu r^2$ and operating on ψ, is the second term of the Schrödinger equation in spherical coordinates (Equation 7-9). The right side of Equation 7-12, which equals $\ell(\ell + 1)$, can now be written as follows when multiplied by $\hbar^2 f(\theta)g(\phi)$, remembering that $f_{\ell m}(\theta)g_m(\phi) = Y_{\ell m}(\theta, \phi)$:

$$-\hbar^2\left[\frac{1}{\sin\theta}\frac{\partial}{\partial\theta}\left(\sin\theta\frac{\partial}{\partial\theta}\right) + \frac{1}{\sin^2\theta}\frac{\partial^2}{\partial\phi^2}\right]Y_{\ell m}(\theta, \phi) = \ell(\ell + 1)\hbar^2 Y_{\ell m}(\theta, \phi) \qquad \textbf{7-21}\boldsymbol{a}$$

or

$$(L^2)_{op}Y_{\ell m}(\theta, \phi) = \ell(\ell + 1)\hbar^2 Y_{\ell m}(\theta, \phi) \qquad \textbf{7-21}\boldsymbol{b}$$

or, since $\psi(r, \theta, \phi) = R(r)Y(\theta, \phi)$,

$$(L^2)_{\text{op}}\psi(r, \theta, \phi) = \ell(\ell + 1)\hbar^2\psi(r, \theta, \phi) \qquad \textbf{7-21}\boldsymbol{c}$$

Thus, we have the very important result that, for all potentials where $V = V(r)$, *the angular momentum is quantized* and its allowed magnitudes (eigenvalues) are given by

$$|\mathbf{L}| = L = \sqrt{\ell(\ell + 1)}\hbar \quad \text{for} \quad \ell = 0, 1, 2, 3, \ldots \qquad \textbf{7-22}$$

where ℓ is referred to as the *angular momentum quantum number* or the *orbital quantum number*.

In addition, if we use the same substitution method on L_z, the z component of $\mathbf{L}$, we find that *the z component of the angular momentum is also quantized* and its allowed values are given by

$$L_z = m\hbar \quad \text{for} \quad m = 0, \pm 1, \pm 2, \ldots, \pm\ell \qquad \textbf{7-23}$$

The physical significance of Equation 7-23 is that the angular momentum $\mathbf{L}$, whose magnitude is quantized with values $\sqrt{\ell(\ell + 1)}\hbar$, can only point in those directions *in space* such that the projection of $\mathbf{L}$ on the z axis is one or another of the values given by $m\hbar$. Thus, $\mathbf{L}$ is also *space quantized*. The quantum number m is referred to as the *magnetic quantum number*. (Why "magnetic"? See Section 7-4.)

STUDENTS-HUB.com Uploaded By: Malak Obaid

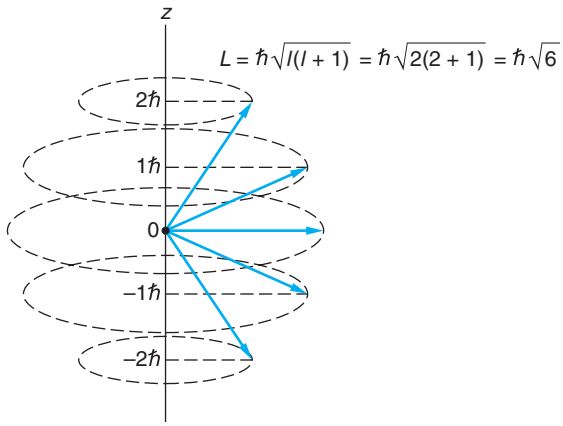

Figure 7-4 Vector model illustrating the possible orientations of **L** in space and the possible values of L_z for the case where $\ell = 2$.

Figure 7-4 shows a diagram, called the *vector model* of the atom, illustrating the possible orientations of the angular momentum vector. Note the perhaps unexpected result that the angular momentum vector never points in the z direction, since the maximum z component $m\hbar$ is always less than the magnitude $\sqrt{\ell(\ell+1)}\hbar$. This is a consequence of the uncertainty principle for angular momentum (which we will not derive) that implies that no two components of angular momentum can be precisely known simultaneously,[4] except in the case of zero angular momentum. It is worth noting that *for a given value of ℓ there are $2\ell + 1$ possible values of m, ranging from $-\ell$ to $+\ell$ in integral steps*. Operators for L_x and L_y can also be obtained by the substitution method; however, operating with them on ψ does not produce eigenvalues. This is mainly because specifying rotation about the x and y axes requires measurement of both θ and ϕ.

EXAMPLE 7-1 Quantized Values of L If a system has angular momentum characterized by the quantum number $\ell = 2$, what are the possible values of L_z, what is the magnitude L, and what is the smallest possible angle between **L** and the z axis?

SOLUTION

1. The possible values of L_z are given by Equation 7-23: $L_z = m\hbar$
2. The values of m for $\ell = 2$ are $m = 0, \pm 1, \pm 2$
3. Thus, allowed values of L_z are $L_z = -2\hbar, -1\hbar, 0, \hbar, 2\hbar$
4. The magnitude of **L** is given by Equation 7-22. For $\ell = 2$ $|\mathbf{L}| = \sqrt{\ell(\ell+1)}\hbar = \sqrt{6}\hbar = 2.45\hbar$
5. From Figure 7-4 the angle θ between **L** and the z axis is given by: $\cos\theta = \dfrac{L_z}{L} = \dfrac{m\hbar}{\sqrt{\ell(\ell+1)}\hbar} = \dfrac{m}{\sqrt{\ell(\ell+1)}}$
6. The smallest possible angle θ between **L** and the z axis is that for $m = \pm\ell$, which for $\ell = 2$ gives $\cos\theta = \dfrac{2}{\sqrt{6}} = 0.816$ or $\theta = 35.5^\circ$

STUDENTS-HUB.com Uploaded By: Malak Obaid

Quantization of the Energy

The results discussed so far apply to any system that is spherically symmetric, that is, one for which the potential energy depends on r only. The solution of the radial equation for $R(r)$, on the other hand, depends on the detailed form of $V(r)$. The new quantum number associated with the coordinate r is called the *principal quantum number* n. This quantum number, as we will see, is related to the energy in the hydrogen atom. Figure 7-5 shows a sketch of the potential energy function of Equation 7-6. If the total energy is positive, the electron is not bound to the atom. We are interested here only in bound-state solutions, for which the values of E are negative. For this case, the potential energy function becomes greater than E for large r, as shown in the figure. As we have discussed previously, for bound systems only certain values of the energy E lead to well-behaved solutions. These values are found by solving the radial equation, which is formed by equating the left side of Equation 7-12 to the constant $\ell(\ell + 1)$. For $V(r)$ of the hydrogen atom, given by Equation 7-6, the radial equation is

$$-\frac{\hbar^2}{2\mu r^2}\frac{\partial}{\partial r}\left(r^2\frac{\partial R(r)}{\partial r}\right) + \left[-\frac{kZe^2}{r} + \frac{\hbar^2\ell(\ell+1)}{2\mu r^2}\right]R(r) = ER(r) \qquad \textbf{7-24}$$

The radial equation can be solved using standard methods of differential equations whose details we will omit here, except to note that (1) we expect a link to appear between the principal quantum number n and the angular momentum quantum number ℓ (since the latter already appears in Equation 7-24) and (2) in order that the solutions of Equation 7-24 be well behaved, only certain values of the energy are allowed, just as we discovered for the square well and the harmonic oscillator. The allowed values of E are given by

$$E_n = -\left(\frac{kZe^2}{\hbar}\right)^2\frac{\mu}{2n^2} = -\frac{Z^2E_1}{n^2} \qquad \textbf{7-25}$$

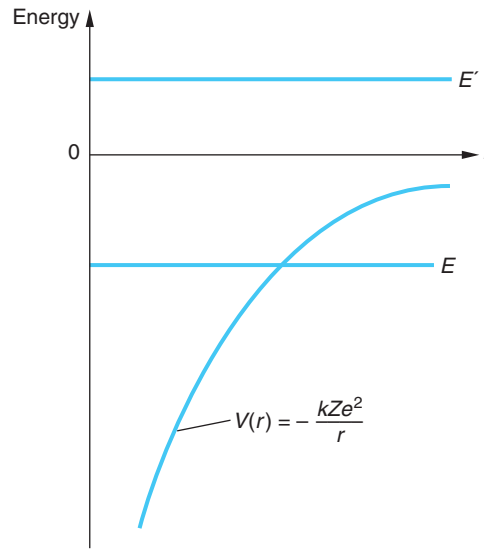

Figure 7-5 Potential energy of an electron in a hydrogen atom. If the total energy is greater than zero, as E', the electron is not bound and the energy is not quantized. If the total energy is less than zero, as E, the electron is bound. Then, as in one-dimensional problems, only certain discrete values of the total energy lead to well-behaved wave functions.

STUDENTS-HUB.com Uploaded By: Malak Obaid

Table 7-2 Radial functions for hydrogen

$n = 1$	$\ell = 0$	$R_{10} = \frac{2}{\sqrt{a_0^3}} e^{-r/a_0}$
$n = 2$	$\ell = 0$	$R_{20} = \frac{1}{\sqrt{2a_0^3}}\left(1 - \frac{r}{2a_0}\right) e^{-r/2a_0}$
	$\ell = 1$	$R_{21} = \frac{1}{2\sqrt{6a_0^3}} \frac{r}{a_0} e^{-r/2a_0}$
$n = 3$	$\ell = 0$	$R_{30} = \frac{2}{3\sqrt{3a_0^3}}\left(1 - \frac{2r}{3a_0} + \frac{2r^2}{27a_0^2}\right) e^{-r/3a_0}$
	$\ell = 1$	$R_{31} = \frac{8}{27\sqrt{6a_0^3}} \frac{r}{a_0}\left(1 - \frac{r}{6a_0}\right) e^{-r/3a_0}$
	$\ell = 2$	$R_{32} = \frac{4}{81\sqrt{30a_0^3}} \frac{r^2}{a_0^2} e^{-r/3a_0}$

where $E_1 = (1/2)(ke^2/\hbar)^2\mu \approx 13.6$ eV and the principal quantum number n can take on the values $n = 1, 2, 3, \ldots$, with the further restriction that n must be greater than ℓ. *These energy values are identical to those found from the Bohr model.* The radial functions resulting from the solution of Equation 7-24 for hydrogen are given by Equation 7-26, where the $\mathcal{L}_{n\ell}(r/a_0)$ are standard functions called Laguerre polynomials.

$$R_{n\ell}(r) = A_{n\ell}\, e^{-r/a_0 n} r^{\ell}\, \mathcal{L}_{n\ell}(r/a_0) \qquad \textbf{7-26}$$

and the Bohr radius $a_0 = \hbar^2/(ke^2\mu)$. The radial functions $R_{n\ell}(r)$ for $n = 1$, 2, and 3 are given in Table 7-2. (For a detailed solution of Equation 7-24 and an extended table of Laguerre polynomials, see Weber and Arfken, Chapter 13.)

Summary of the Quantum Numbers

The allowed values of and restrictions on the quantum numbers n, ℓ, and m associated with the variables r, θ, and ϕ are summarized as follows:

$$\begin{aligned} n &= 1, 2, 3, \ldots \\ \ell &= 0, 1, 2, \ldots, (n-1) \\ m &= -\ell, (-\ell+1), \ldots, 0, 1, 2, \ldots, +\ell \end{aligned} \qquad \textbf{7-27}$$

The fact that the energy of the hydrogen atom depends only on the principal quantum number n and not on ℓ is a peculiarity of the inverse-square force. It is related to the result in classical mechanics that the energy of a mass moving in an elliptical orbit in an inverse-square force field depends only on the major axis of the orbit and not on the eccentricity. The largest value of angular momentum ($\ell = n - 1$) corresponds most nearly to a circular orbit, whereas a small value of ℓ corresponds to a highly eccentric orbit. (Zero angular momentum corresponds to oscillation along a line through the force center, i.e., through the nucleus, in the case of the hydrogen atom.) For central forces that do not obey an inverse-square law, the energy does depend on the angular momentum (both classically and quantum mechanically) and thus depends on both n and ℓ.

STUDENTS-HUB.com Uploaded By: Malak Obaid

The quantum number m is related to the z component of angular momentum. Since there is no preferred direction for the z axis for any central force, the energy cannot depend on m. We will see later that if we place an atom in an external magnetic field, there is a preferred direction in space (the direction of the field) and the energy then does depend on the value of m. (This effect, called the Zeeman effect, is discussed in a More section on the Web site. See page 303.)

Figure 7-6 shows an energy-level diagram for hydrogen. This diagram is similar to Figure 4-16*a* except that states with the same n but different ℓ are shown separately. These states are referred to by giving the value of n along with a code letter: S stands for $\ell = 0$, P for $\ell = 1$, D for $\ell = 2$, and F for $\ell = 3$. These code letters are remnants of the spectroscopist's descriptions of various series of spectral lines as *S*harp, *P*rincipal, *D*iffuse, and *F*undamental. (For values of ℓ greater than 3, the letters follow alphabetically; thus G for $\ell = 4$, etc.) The allowed electric dipole transitions between energy levels obey the *selection rules*

$$\Delta m = 0 \quad \text{or} \quad \pm 1$$
$$\Delta \ell = \pm 1 \qquad \textbf{7-28}$$

That the quantum number ℓ of the atom must change by ± 1 when the atom emits or absorbs a photon results from conservation of angular momentum and the fact that the photon itself has an intrinsic angular momentum of 1 $\hbar$. For the principal quantum number, Δn is unrestricted.

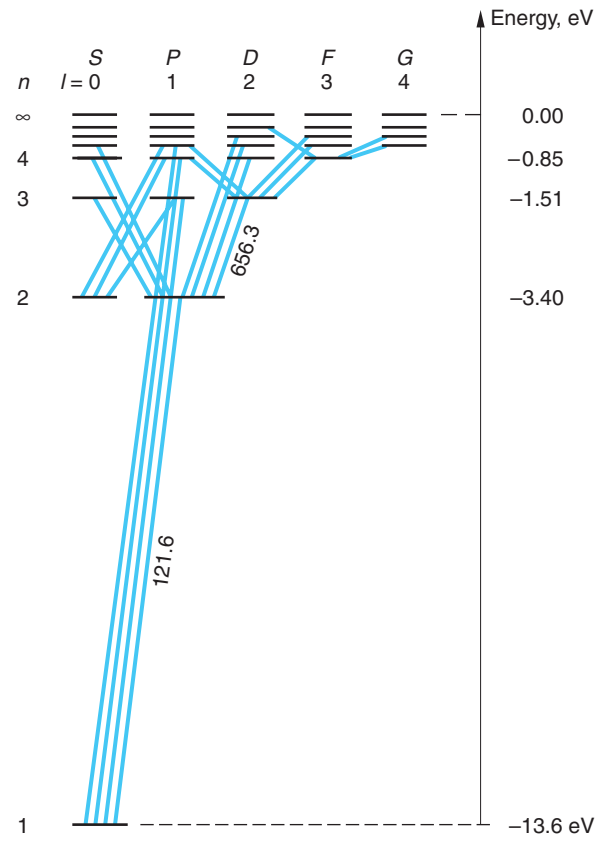

Figure 7-6 Energy-level diagram for the hydrogen atom, showing transitions obeying the selection rule $\Delta \ell = \pm 1$. States with the same n value but different ℓ value have the same energy, $-E_1/n^2$, where $E_1 = 13.6$ eV, as in the Bohr theory. The wavelengths of the Lyman $\alpha(n = 2 \rightarrow n = 1)$ and Balmer $\alpha(n = 3 \rightarrow n = 2)$ lines are shown in nm. Note that the latter has two possible transitions due to the ℓ degeneracy.

STUDENTS-HUB.com Uploaded By: Malak Obaid

Questions

1. Why wasn't quantization of angular momentum noticed in classical physics?
2. What are the similarities and differences between the quantization of angular momentum in the Schrödinger theory and in the Bohr model?
3. Why doesn't the energy of the hydrogen atom depend on ℓ ? Why doesn't it depend on m?

7-3 The Hydrogen Atom Wave Functions

The wave functions $\psi_{n\ell m}(r, \theta, \phi)$ satisfying the Schrödinger equation for the hydrogen atom are rather complicated functions of r, θ, and ϕ. In this section we will write some of these functions and display some of their more important features graphically.

As we have seen, the ϕ dependence of the wave function, given by Equation 7-14, is simply $e^{im\phi}$. The θ dependence is described by the associated Legendre functions $f_{\ell m}(\theta)$ given by Equation 7-15. The complete angular dependence is then given by the spherical harmonic functions $Y_{\ell m}(\theta, \phi)$, the product of $g_m(\phi)$ and $f_{\ell m}(\theta)$ as indicated by Equation 7-16 and, for the first few, tabulated in Table 7-1. The solutions to the radial equation $R_{n\ell}(r)$ are of the form indicated by Equation 7-26 and are listed in Table 7-2 for the three lowest values of the principal quantum number n. Referring to Equation 7-10, our assumed product solutions of the time-independent Schrödinger equation, we have that the complete wave function of the hydrogen atom is

$$\psi_{n\ell m}(r, \theta, \phi) = C_{n\ell m} R_{n\ell}(r) f_{\ell m}(\theta) g_m(\phi) \qquad \textbf{7-29}$$

where $C_{n\ell m}$ is a constant determined by the normalization condition.

We see from the form of this expression that the complete wave function depends on the quantum numbers n, ℓ, and m that arose because of the boundary conditions on $R(r)$, $f(\theta)$, and $g(\phi)$. The energy, however, depends only on the value of n. From Equation 7-27 we see that for any value of n, there are n possible values of ℓ ($\ell = 0, 1, 2, \ldots, n - 1$), and for each value of ℓ, there are $2\ell + 1$ possible values of m ($m = -\ell, -\ell + 1, \ldots, +\ell$). Except for the lowest energy level (for which $n = 1$ and therefore ℓ and m can only be zero) there are generally many different wave functions corresponding to the same energy. As discussed in the previous section, the origins of this degeneracy are the $1/r$ dependence of the potential energy and the fact that there is no preferred direction in space.

The Ground State

Let us examine the wave functions for several particular states beginning with the lowest-energy level, the ground state, which has $n = 1$. Then ℓ and m must both be zero. The Laguerre polynomial $\mathscr{L}_{10}$ in Equation 7-26 is equal to 1, and the wave function is

$$\psi_{100} = C_{100} e^{-Zr/a_0} \qquad \textbf{7-30}$$

STUDENTS-HUB.com Uploaded By: Malak Obaid

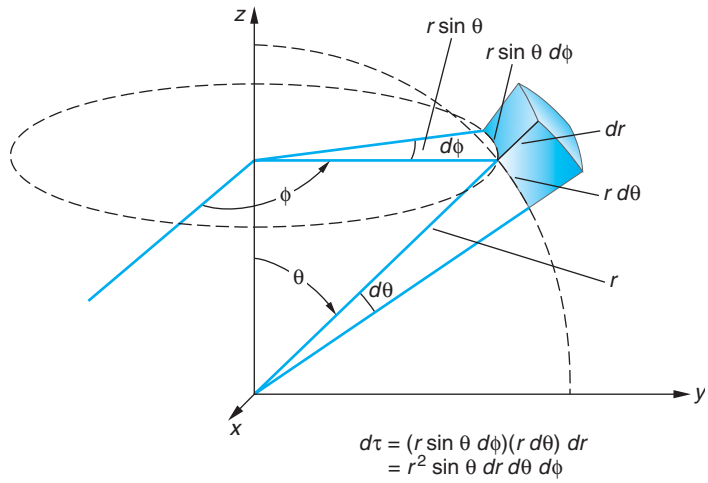

Figure 7-7 Volume element $d\tau$ in spherical coordinates.

The constant C_{100} is determined by normalization:

$$\int \psi^* \psi d\tau = \int_0^{\infty} \int_0^{\pi} \int_0^{2\pi} \psi^* \psi r^2 \sin\theta \, d\phi \, d\theta \, dr = 1$$

using for the volume element in spherical coordinates (see Figure 7-7)

$$d\tau = (r \sin\theta \, d\phi)(r \, d\theta)(dr)$$

Because $\psi^*\psi$ for this state is spherically symmetric, the integration over angles gives 4π. Carrying out the integration over r gives[5]

$$C_{100} = \frac{1}{\sqrt{\pi}} \left(\frac{Z}{a_0} \right)^{3/2} = \frac{1}{\sqrt{\pi}} \left(\frac{1}{a_0} \right)^{3/2} \quad \text{for} \quad Z = 1 \qquad \textbf{7-31}$$

The probability of finding the electron in the volume $d\tau$ is $\psi^*\psi d\tau$.

The probability density $\psi^*\psi$ is illustrated in Figure 7-8. The probability density for the ground state is maximum at the origin. It is often of more interest to determine the probability of finding the electron in a spherical shell between r and $r + dr$. This probability, $P(r)dr$, is just the probability density $\psi^*\psi$ times the volume of the spherical shell of thickness dr:

The angular dependence of the electron probability distributions is critical to our understanding of the bonding of atoms into molecules and solids (see Chapters 9 and 10).

$$P(r) \, dr = \psi^* \psi \, 4\pi r^2 \, dr = 4\pi r^2 C_{100}^2 e^{-2Zr/a_0} \, dr \qquad \textbf{7-32}$$

Figure 7-9 shows a sketch of $P(r)$ versus r/a_0. It is left as a problem (see Problem 7-21) to show that $P(r)$ has its maximum value at $r = a_0/Z$. In contrast to the Bohr model for hydrogen, in which the electron stays in a well-defined orbit at $r = a_0$, we see that it is *possible* for the electron to be found at any distance from the nucleus.

STUDENTS-HUB.com Uploaded By: Malak Obaid

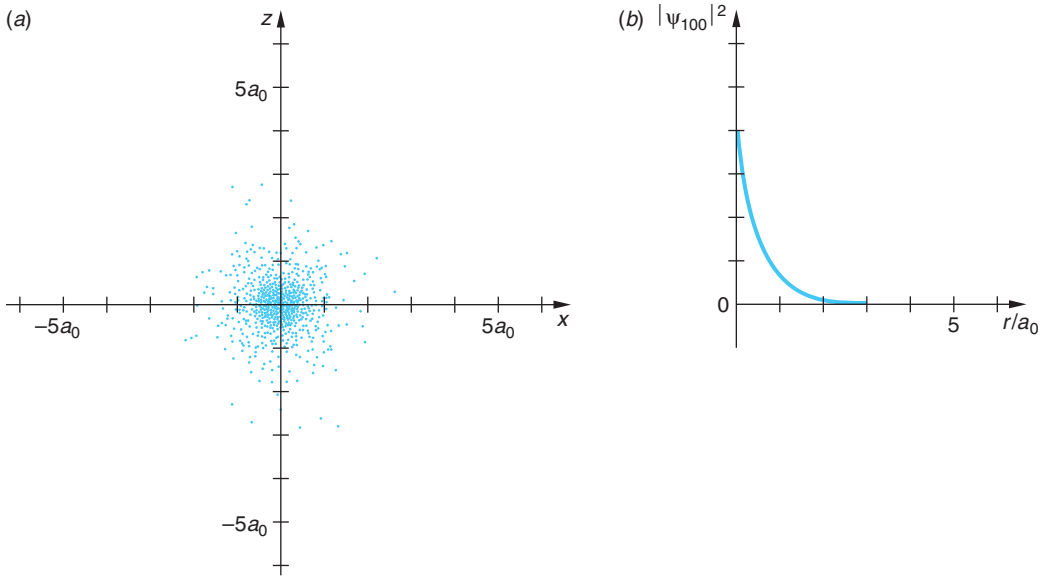

Figure 7-8 Probability density $\psi^*\psi$ for the ground state in hydrogen. The quantity $e\psi^*\psi$ can be thought of as the electron charge density in the atom. (*a*) The density is spherically symmetric, is greatest at the origin, and decreases exponentially with r. This computer-generated plot was made by making hundreds of "searches" for the hydrogen electron in the x-z plane (i.e., for $\phi = 0$), recording each finding with a dot. (*b*) The more conventional graph of the probability density $|\psi_{100}|^2$ vs. r/a_0. Compare the two graphs carefully. [*This computer-generated plot courtesy of Paul Doherty, The Exploratorium.*]

However, the most probable distance is a_0, and the chance of finding the electron at a much different distance is small. It is useful to think of the electron as a charged cloud of charge density $\rho = e\psi^*\psi$. (We must remember, though, that the electron is always *observed* as one charge.) Note that the angular momentum in the ground state is zero, contrary to the Bohr model assumption of 1 $\hbar$.

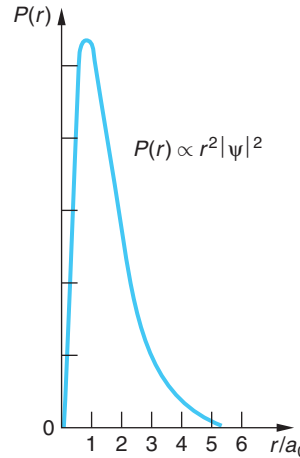

Figure 7-9 Radial probability density $P(r)$ versus r/a_0 for the ground state of the hydrogen atom. $P(r)$ is proportional to $r^2|\psi_{100}|^2$. The most probable distance r is the Bohr radius a_0.

The Excited States

In the first excited state, $n = 2$ and ℓ can be either 0 or 1. For $\ell = 0$, $m = 0$, and again we have a spherically symmetric wave function, given by

$$\psi_{200} = C_{200}\left(2 - \frac{Zr}{a_0}\right)e^{-Zr/2a_0} \qquad \textbf{7-33}$$

For $\ell = 1$, m can be $+1$, 0, or -1. The corresponding wave functions are (see Tables 7-1 and 7-2)

$$\psi_{210} = C_{210}\frac{Zr}{a_0}e^{-Zr/2a_0}\cos\theta \qquad \textbf{7-34}$$

$$\psi_{21\pm1} = C_{21\pm1}\frac{Zr}{a_0}e^{-Zr/2a_0}\sin\theta\, e^{\pm i\phi} \qquad \textbf{7-35}$$

STUDENTS-HUB.com Uploaded By: Malak Obaid

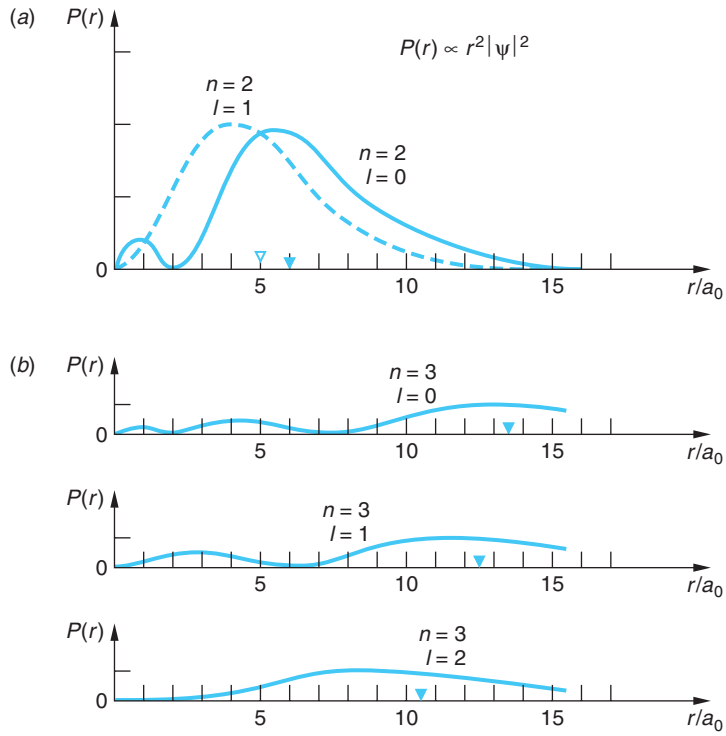

Figure 7-10 (*a*) Radial probability density $P(r)$ vs. r/a_0 for the $n = 2$ states in hydrogen. $P(r)$ for $\ell = 1$ has a maximum at the Bohr value 2^2a_0. For $\ell = 0$, there is a maximum near this value and a smaller submaximum near the origin. The markers on the r/a_0 axis denote the values of $\langle r/a_0 \rangle$. (*b*) $P(r)$ vs. r/a_0 for the $n = 3$ states in hydrogen.

Figure 7-10*a* shows $P(r)$ for these wave functions. The distribution for $n = 2$, $\ell = 1$ is maximum at the radius of the second Bohr orbit,

$$r_{\text{max}} = 2^2a_0$$

while for $n = 2$ and $\ell = 0$, $P(r)$ has two maxima, the larger of which is near this radius.

Radial probability distributions can be obtained in the same way for the other excited states of hydrogen. For example, those for the second excited state $n = 3$ are shown in Figure 7-10*b*. The main radial dependence of $P(r)$ is contained in the factor e^{-Zr/na_0}, except near the origin. A detailed examination of the Laguerre polynomials shows that $\psi \rightarrow r^\ell$ as $r \rightarrow 0$. Thus, *for a given n,* $\psi_{n\ell m}$ *is greatest near the origin when* ℓ *is small.*

An important feature of these wave functions is that for $\ell = 0$, the probability densities are spherically symmetric, whereas for $\ell \neq 0$, they depend on the angle θ. The probability density plots of Figure 7-11 illustrate this result for the first excited state $n = 2$. These angular distributions of the electron charge density depend only on the value of ℓ and not on the radial part of the wave function. Similar charge distributions for the valence electrons in more complicated atoms play an important role in the chemistry of molecular bonding.

Question

4. At what value of r is $\psi^*\psi$ maximum for the ground state of hydrogen? Why is $P(r)$ maximum at a different value of r?

STUDENTS-HUB.com Uploaded By: Malak Obaid

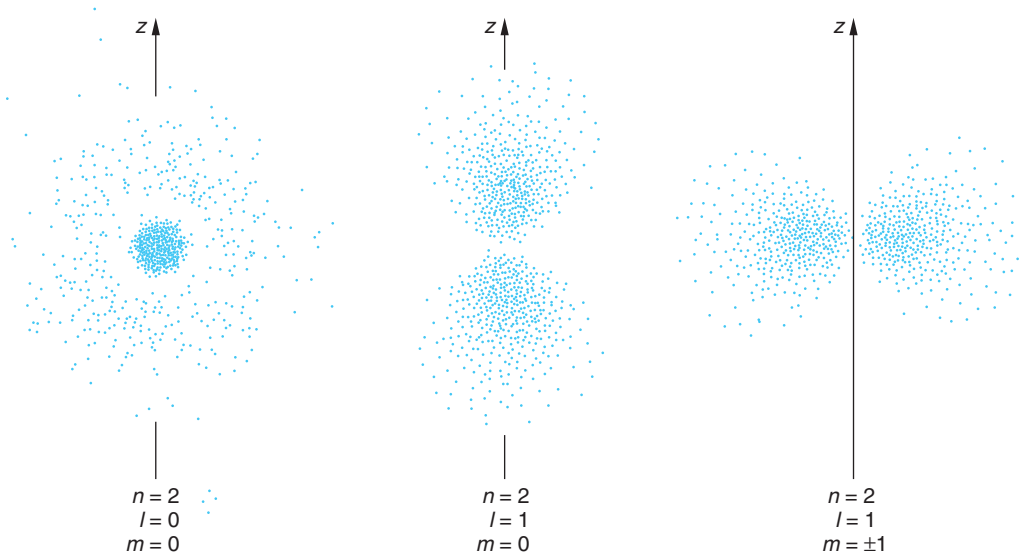

Figure 7-11 Probability densities $\psi^*\psi$ for the $n = 2$ states in hydrogen. The probability is spherically symmetric for $\ell = 0$. It is proportional to $\cos^2\theta$ for $\ell = 1$, $m = 0$, and to $\sin^2\theta$ for $\ell = 1$, $m = \pm 1$. The probability densities have rotational symmetry about the z axis. Thus, the three-dimensional charge density for the $\ell = 1$, $m = 0$ state is shaped roughly like a dumbbell, while that for the $\ell = 1$, $m = \pm 1$ states resembles a doughnut, or toroid. The shapes of these distributions are typical for all atoms in S states ($\ell = 0$) and P states ($\ell = 1$) and play an important role in molecular bonding. [*This computer-generated plot courtesy of Paul Doherty, The Exploratorium.*]

7-4 Electron Spin

As was mentioned in Chapter 4, when a spectral line of hydrogen or other atoms is viewed with high resolution, it shows a *fine structure*; that is, it is seen to consist of two or more closely spaced lines. As we noted then, Sommerfeld's relativistic calculation based on the Bohr model agrees with the experimental measurements of this fine structure for hydrogen, but the agreement turned out to be accidental since his calculation predicts fewer lines than are seen for other atoms. In order to explain fine structure and to clear up a major difficulty with the quantum-mechanical explanation of the periodic table (Section 7-6), W. Pauli[6] in 1925 suggested that in addition to the quantum numbers n, ℓ, and m, the electron has a fourth quantum number, which could take on just two values.

As we have seen, quantum numbers arise from boundary conditions on some coordinate (see Equations 7-14 and 7-15). Pauli originally expected that the fourth quantum number would be associated with the time coordinate in a relativistic theory, but this idea was not pursued. In the same year, S. Goudsmit and G. Uhlenbeck,[7] graduate students at Leiden, suggested that this fourth quantum number was the z component, m_s, of an intrinsic angular momentum of the electron, euphemistically called *spin*. They represented the spin vector $\mathbf{S}$ with the same form that Schrödinger's wave mechanics gave for $\mathbf{L}$:

$$|\mathbf{S}| = S = \sqrt{s(s+1)}\hbar \qquad \textbf{7-36}$$

STUDENTS-HUB.com Uploaded By: Malak Obaid

Since this intrinsic spin angular momentum **S** is described by a quantum number s like the orbital angular momentum quantum number ℓ, we expect $2s + 1$ possible values of the z component just as there are $2\ell + 1$ possible z components of the orbital angular momentum **L**. If m_s is to have only two values, as Pauli had suggested, then s could only be $\frac{1}{2}$ and m_s only $\pm\frac{1}{2}$. In addition to explaining fine structure and the periodic table, this proposal of electron spin explained the unexpected results of an interesting experiment that had been preformed by O. Stern and W. Gerlach in 1922, which is described briefly in an Exploring section later on (see pages 288–289). To understand why the electron spin results in the splitting of the energy levels needed to account for the fine structure, we must consider the connection between the angular momentum and the magnetic moment of any charged particle system.

Magnetic Moment

If a system of charged particles is rotating, it has a *magnetic moment* proportional to its angular momentum. This result is sometimes known as the *Larmor theorem*. Consider a particle of mass M and charge q moving in a circle of radius r with speed v and frequency $f = v/2\pi r$; this constitutes a current loop. The angular momentum of the particle is $L = Mvr$. The magnetic moment of the current loop is the product of the current and the area of the loop. For a circulating charge, the current is the charge times the frequency,

$$i = qf = \frac{qv}{2\pi r} \tag{7-37}$$

and the magnetic moment μ is[8]

$$\mu = iA = q\left(\frac{v}{2\pi r}\right)(\pi r^2) = \frac{1}{2}q\left(\frac{L}{M}\right) \tag{7-38}$$

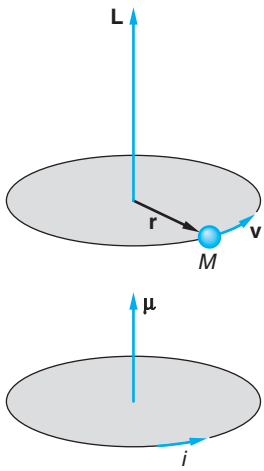

Figure 7-12 A particle moving in a circle has angular momentum **L**. If the particle has a positive charge, the magnetic moment due to the current is parallel to **L**.

From Figure 7-12 we see that, if q is positive, the magnetic moment is in the same direction as the angular momentum. If q is negative, $\boldsymbol{\mu}$ and **L** point in opposite directions; i.e., they are antiparallel. This enables us to write Equation 7-38 as a vector equation:

$$\boldsymbol{\mu} = \frac{q}{2M}\mathbf{L} \tag{7-39}$$

Equation 7-39, which we have derived for a single particle moving in a circle, also holds for a system of particles in any type of motion if the charge-to-mass ratio q/M is the same for each particle in the system.

Applying this result to the *orbital* motion of the electron in the hydrogen atom and substituting the magnitude of **L** from Equation 7-22, we have for the magnitude of $\boldsymbol{\mu}$

$$\mu = \frac{e}{2m_e}L = \frac{e\hbar}{2m_e}\sqrt{\ell(\ell+1)} = \sqrt{\ell(\ell+1)}\,\mu_B \tag{7-40}$$

and, from Equation 7-23, a z component of

$$\mu_z = -\frac{e\hbar}{2m_e}m = -m\mu_B \tag{7-41}$$

STUDENTS-HUB.com Uploaded By: Malak Obaid

where m_e is the mass of the electron, $m\hbar$ is the z component of the angular momentum, and μ_B is a natural unit of magnetic moment called the *Bohr magneton*, which has the value

$$\mu_B = \frac{e\hbar}{2m_e} = 9.27 \times 10^{-24}\ \text{joule/tesla}$$
$$= 5.79 \times 10^{-9}\ \text{eV/gauss} = 5.79 \times 10^{-5}\ \text{eV/tesla} \qquad \textbf{7-42}$$

The orbital motion and spin of the electrons are the origin of magnetism in metals, such as iron, cobalt, and nickel (see Chapter 10). Devices ranging from giant electricity transformers to decorative refrigerator magnets rely on these quantum properties of electrons.

The proportionality between $\boldsymbol{\mu}$ and $\mathbf{L}$ is a general property of rotating charge distributions; however, the particular relation expressed by Equation 7-39 is for a single charge q rotating in a circle. To allow the same mathematical form to be used for other, more complicated situations, it is customary to express the magnetic moment in terms of μ_B and a dimensionless quantity g called the *gyromagnetic ratio*, or simply the g *factor*, where the value of g is determined by the details of the charge distribution. In the case of the orbital angular momentum $\mathbf{L}$ of the electron, $g_L = 1$ and Equation 7-39 would be written

$$\boldsymbol{\mu} = \frac{-g_L \mu_B \mathbf{L}}{\hbar} \qquad \textbf{7-43}$$

and Equations 7-40 and 7-41 as

$$\mu = \sqrt{\ell(\ell+1)}\, g_L \mu_B \qquad \textbf{7-44}$$
$$\mu_z = -m g_L \mu_B \qquad \textbf{7-45}$$

There are minus signs in Equations 7-43 and 7-45 because the electron has a negative charge. The magnetic moment and the angular momentum vectors associated with the orbital motion are therefore oppositely directed, and we see that *quantization of angular momentum implies quantization of magnetic moments*. Other magnetic moments and g factors that we will encounter will have the same form.

Finally, the behavior of a system with a magnetic moment in a magnetic field can be visualized by considering a small bar magnet (Figure 7-13). When placed in an external magnetic field $\mathbf{B}$ there is a torque $\boldsymbol{\tau} = \boldsymbol{\mu} \times \mathbf{B}$ that tends to align the magnet with the field $\mathbf{B}$. If the magnet is spinning about its axis, the effect of the torque is to make the spin axis precess about the direction of the external field, just as a spinning top or gyroscope precesses about the direction of the gravitational field.

To change the orientation of the magnet relative to the applied field direction (whether or not it is spinning), work must be done on it. If it moves through angle $d\theta$, the work required is

$$dW = \tau d\theta = \mu B \sin\theta\, d\theta = d(-\mu B \cos\theta) = d(-\boldsymbol{\mu}\cdot\mathbf{B})$$

The potential energy of the magnetic moment $\boldsymbol{\mu}$ in the magnetic field $\mathbf{B}$ can thus be written

$$U = -\boldsymbol{\mu}\cdot\mathbf{B} \qquad \textbf{7-46}$$

If $\mathbf{B}$ is in the z direction, the potential energy is

$$U = -\mu_z B \qquad \textbf{7-47}$$

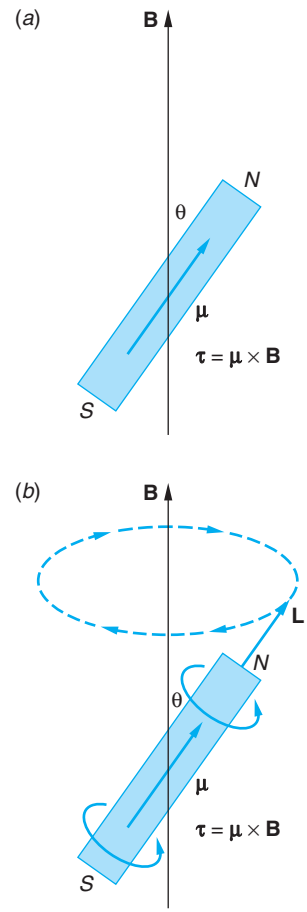

Figure 7-13 Bar-magnet model of magnetic moment. (*a*) In an external magnetic field, the moment experiences a torque that tends to align it with the field. If the magnet is spinning (*b*), the torque causes the system to precess around the external field.

STUDENTS-HUB.com Uploaded By: Malak Obaid

Applying these arguments to the *intrinsic spin* of the electron results in the predictions (with $s = \frac{1}{2}$)

$$\mu = \sqrt{s(s+1)}\mu_B = \sqrt{\tfrac{3}{4}}\,\mu_B \quad \text{and} \quad \mu_z = m_s\mu_B = \pm\tfrac{1}{2}\mu_B \qquad \textbf{7-48}$$

Since the atomic electron is in a magnetic field arising from the apparent motion of the nuclear charge around the electron, the two values of m_s correspond to two different energies, according to Equation 7-47. *It is this splitting of the energy levels that results in the fine structure of the spectral lines.*

The restriction of the spin, and hence the intrinsic magnetic moment, to two orientations in space with $m_s = \pm\frac{1}{2}$ is another example of space quantization. The magnitude of the magnetic moment due to the spin angular momentum can be determined from quantitative measurement of the deflection of the beam in a Stern-Gerlach experiment. The result is *not* $\frac{1}{2}$ Bohr magneton, as predicted by Equation 7-41 with $m = m_s = \frac{1}{2}$, but twice this value. (This type of experiment is not an accurate way to measure magnetic moments, although the measurement of angular momentum this way is accurate because that involves simply counting the number of lines.) The g factor for the electron, g_s in Equation 7-49, has been precisely measured to be $g_s = 2.002319$.

$$\mu_z = -m_s g_s \mu_B \qquad \textbf{7-49}$$

This result, and the fact that s is a half integer rather than an integer like the orbital quantum number ℓ, makes it clear that the classical model of the electron as a spinning ball is not to be taken literally. Like the Bohr model of the atom, the classical picture is useful in describing results of quantum-mechanical calculations, and it often gives useful guidelines as to what to expect from an experiment. The phenomenon of spin, while not a part of Schrödinger's wave mechanics, is included in the relativistic wave mechanics formulated by Dirac. In its nonrelativistic limit, Dirac's wave equation predicts $g_s = 2$, which is approximately correct. The exact value of g_s is correctly predicted by *quantum electrodynamics* (QED), the relativistic quantum theory that describes the interaction of electrons with electromagnetic fields. Although beyond the scope of our discussions, QED is arguably the most precisely tested theory in physics.

EXPLORING
Stern-Gerlach Experiment

If a magnetic moment $\boldsymbol{\mu}$ is placed in an *inhomogeneous* external magnetic field $\mathbf{B}$, the $\boldsymbol{\mu}$ will feel an external force that depends on μ_z and the gradient of $\mathbf{B}$. This is because the force $\mathbf{F}$ is the negative gradient of the potential, so

$$F = -\nabla U = -\nabla(-\boldsymbol{\mu}\cdot\mathbf{B}) \qquad \textbf{7-50}$$

from Equation 7-46. If we arrange the inhomogeneous $\mathbf{B}$ field so that it is homogeneous in the x and y directions, then the gradient has only $\partial B/\partial z \neq 0$ and $\mathbf{F}$ has only a z component, i.e.,

$$F_z = \mu_z(dB/dz) = -mg_L\mu_B(dB/dz) \qquad \textbf{7-51}$$

STUDENTS-HUB.com Uploaded By: Malak Obaid

This effect was used by Stern and Gerlach[9] in 1922 (before spin) to measure the possible orientations in space, i.e., the space quantization, of the magnetic moments of silver atoms. The experiment was repeated in 1927 (after spin) by Phipps and Taylor using hydrogen atoms.

The experimental setup is shown in Figure 7-14. Atoms from an oven are collimated and sent through a magnet whose poles are shaped so that the magnetic field B_z increases slightly with z, while B_x and B_y are constant in the x and y directions, respectively. The atoms then strike a collector plate. Figure 7-15 illustrates the effect of the dB/dz on several magnetic moments of different orientations. In addition to the torque, which merely causes the magnetic moment to precess about the field direction, there is the force F_z in the positive or negative z direction, depending on whether μ_z is positive or negative, since dB/dz is always positive. This force deflects the magnetic moment up or down by an amount that depends on the magnitudes of both dB/dz and the z component of the magnetic moment μ_z. Classically, one would expect a continuum of possible orientations of the magnetic moments. However, since the magnetic moment is proportional to $\mathbf{L}$, which is quantized, quantum mechanics predicts that μ_z also can have only the $2\ell + 1$ values corresponding to the $2\ell + 1$ possible values of m. We therefore expect $2\ell + 1$ deflections (counting 0 as a deflection). For example, for $\ell = 0$ there should be one line on the collector plate corresponding to no deflection, and for $\ell = 1$ there should be three lines corresponding to the three values $m = -1$, $m = 0$, and $m = +1$. The $\ell = 1$ case is illustrated in Figure 7-15.

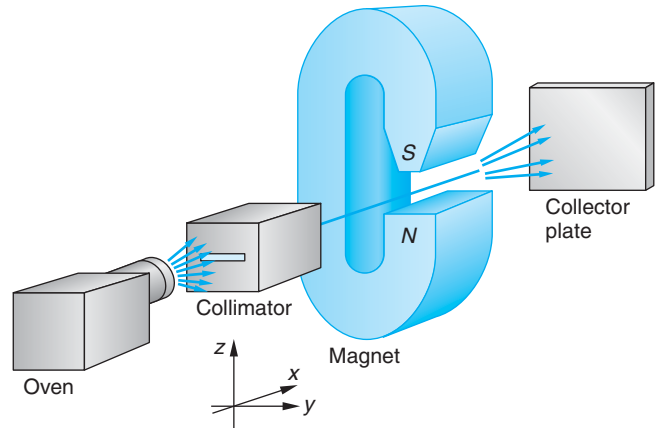

Figure 7-14 In the Stern-Gerlach experiment, atoms from an oven are collimated, passed through an inhomogeneous magnetic field, and detected on a collector plate.

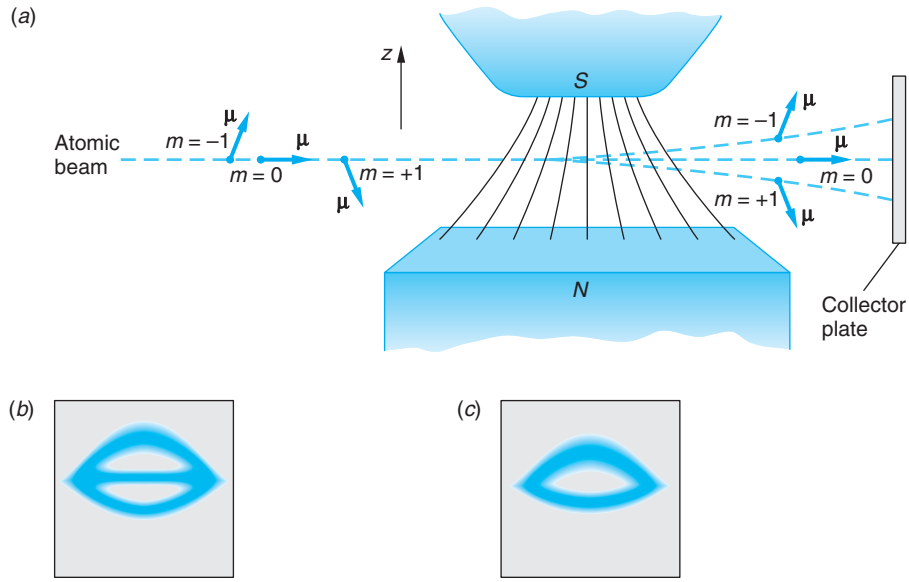

Figure 7-15 (*a*) In an inhomogeneous magnetic field the magnetic moment μ experiences a force F_z whose direction depends on the direction of the z component μ_z of μ and whose magnitude depends on those of μ_z and dB/dz. The beam from an oven (not shown) is collimated into a horizontal line. (*b*) The pattern for the $\ell = 1$ case illustrated in (*a*). The three images join at the edges and have different detailed shapes due to differences in the field inhomogeneity. (*c*) The pattern observed for silver and hydrogen.

STUDENTS-HUB.com Uploaded By: Malak Obaid

Using neutral silver atoms, Stern and Gerlach expected to see only a single line, the middle line in Figure 7-15*b*, because the ground state of silver was known to be an $\ell = 0$ state; therefore, $m = 0$ and $\mu = 0$. The force F_z would then be zero, and no deflection of the atomic beam should occur. However, when the experiment was done with either silver or hydrogen atoms, there were *two* lines, as shown in Figure 7-15*c*. Since the ground state of hydrogen also has $\ell = 0$, we should again expect only one line, were it not for the electron spin. If the electron has spin angular momentum of magnitude $|S| = \sqrt{s(s+1)}\hbar$, where $s = \frac{1}{2}$, the z component can be either $+\hbar/2$ or $-\hbar/2$. Since the orbital angular momentum is zero, the total internal angular momentum of the atom is simply the spin[10] and two lines would be expected. Stern and Gerlach had made the first direct observation of electron spin and space quantization.

The Complete Hydrogen Atom Wave Functions

Our description of the hydrogen atom wave functions in Section 7-3 is not complete because we did not include the spin of the electron. The hydrogen atom wave functions are also characterized by the spin quantum number m_s, which can be $+\frac{1}{2}$ or $-\frac{1}{2}$. (We need not include the quantum number s because it always has the value $s = \frac{1}{2}$.) A general wave function is then written $\psi_{n\ell m_\ell m_s}$, where we have included the subscript ℓ on m_ℓ to distinguish it from m_s. There are now two wave functions for the ground state of the hydrogen atom, $\psi_{100+1/2}$ and $\psi_{100-1/2}$, corresponding to an atom with its electron spin "parallel" or "antiparallel" to the z axis (as defined, for example, by a external magnetic field). In general, the ground state of a hydrogen atom is a linear combination of these wave functions:

$$\psi = C_1\psi_{100+1/2} + C_2\psi_{100-1/2}$$

The probability of measuring $m_s = +\frac{1}{2}$ (for example, by observing to which spot the atom goes in the Stern-Gerlach experiment) is $|C_1|^2$. Unless atoms have been preselected in some way (such as by passing them through a previous inhomogeneous magnetic field or by their having recently emitted a photon), $|C_1|^2$ and $|C_2|^2$ will each be $\frac{1}{2}$, so that measuring the spin "up" ($m_s = +\frac{1}{2}$) and measuring the spin "down" ($m_s = -\frac{1}{2}$) are equally likely.

Questions

5. Does a system have to have a net charge to have a magnetic moment?
6. Consider the two beams of hydrogen atoms emerging from the magnetic field in the Stern-Gerlach experiment. How does the wave function for an atom in one beam differ from that of an atom in the other beam? How does it differ from the wave function for an atom in the incoming beam before passing through the magnetic field?

(*a*)

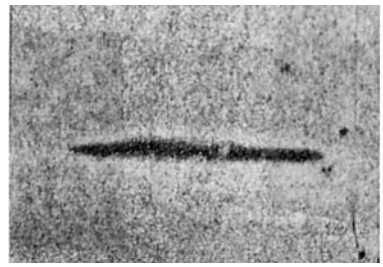

(*b*)

Photographs made by Stern and Gerlach with an atomic beam of silver atoms. (*a*) When the magnetic field is zero, all atoms strike in a single, undeviated line. (*b*) When the magnetic field is nonzero, the atoms strike in upper and lower lines, curved due to differing inhomogeneities. [*From O. Stern and W. Gerlach, Zeitschr. f. Physik* **9**, *349 (1922).*]

STUDENTS-HUB.com Uploaded By: Malak Obaid

7-5 Total Angular Momentum and the Spin-Orbit Effect

In general, an electron in an atom has both orbital angular momentum characterized by the quantum number ℓ and spin angular momentum characterized by the quantum number s. Analogous classical systems that have two kinds of angular momentum are Earth, which is spinning about its axis of rotation in addition to revolving about the Sun, or a precessing gyroscope, which has angular momentum of precession in addition to its spin. Classically the total angular momentum

$$\mathbf{J} = \mathbf{L} + \mathbf{S} \qquad \textbf{7-52}$$

is an important quantity because the resultant torque on a system equals the rate of change of the total angular momentum, and in the case of central forces, the total angular momentum is conserved. For a classical system, the magnitude of the total angular momentum J can have any value between $L + \mathrm{S}$ and $|L - S|$. We have already seen that in quantum mechanics, angular momentum is more complicated: both **L** and **S** are quantized and their relative directions are restricted. The quantum-mechanical rules for combining orbital and spin angular momenta or any two angular momenta (such as for two particles) are somewhat difficult to derive, but they are not difficult to understand. For the case of orbital and spin angular momenta, the magnitude of the total angular momentum **J** is given by

$$|\mathbf{J}| = \sqrt{j(j+1)}\hbar \qquad \textbf{7-53}$$

where the *total angular momentum quantum number* j can be either

$$j = \ell + s \quad \text{or} \quad j = |\ell - s| \qquad \textbf{7-54}$$

and the z component of **J** is given by

$$J_z = m_j\hbar \quad \text{where} \quad m_j = -j, -j+1, \ldots, j-1, j \qquad \textbf{7-55}$$

(If $\ell = 0$, the total angular momentum is simply the spin, and $j = \mathrm{s}$.) Figure 7-16*a* is a simplified vector model illustrating the two possible combinations $j = 1 + \frac{1}{2} = \frac{3}{2}$ and $j = 1 - \frac{1}{2} = \frac{1}{2}$ for the case of an electron with $\ell = 1$. The lengths of the vectors are proportional to $[\ell(\ell+1)]^{1/2}$, $[s(s+1)]^{1/2}$, and $[j(j+1)]^{1/2}$. The spin and orbital angular momentum vectors are said to be "parallel" when $j = \ell + s$ and "antiparallel" when $j = |\ell - s|$. A quantum mechanically more accurate vector addition is shown in Figure 7-16*b*. The quantum number m_j can take on $2j + 1$ possible values in integer steps between $-j$ and $+j$, as indicated by Equation 7-55. Equation 7-55 also implies that $m_j = \mathrm{m}_\ell + \mathrm{m}_\mathrm{s}$ since $J_z = L_z + S_z$.

Equation 7-54 is a special case of a more-general rule for combining two angular momenta that is useful when dealing with more than one particle. For example, there are two electrons in the helium atom, each with spin, orbital, and total angular momentum. The general rule is

If $\mathbf{J}_1$ is one angular momentum (orbital, spin, or a combination) and $\mathbf{J}_2$ is another, the resulting total angular momentum $\mathbf{J} = \mathbf{J}_1 + \mathbf{J}_2$ has the value $[j(j+1)]^{1/2}\hbar$ for its magnitude, where j can be any of the values

$$j_1 + j_2, j_1 + j_2 - 1, \ldots, |j_1 - j_2|$$

STUDENTS-HUB.com Uploaded By: Malak Obaid

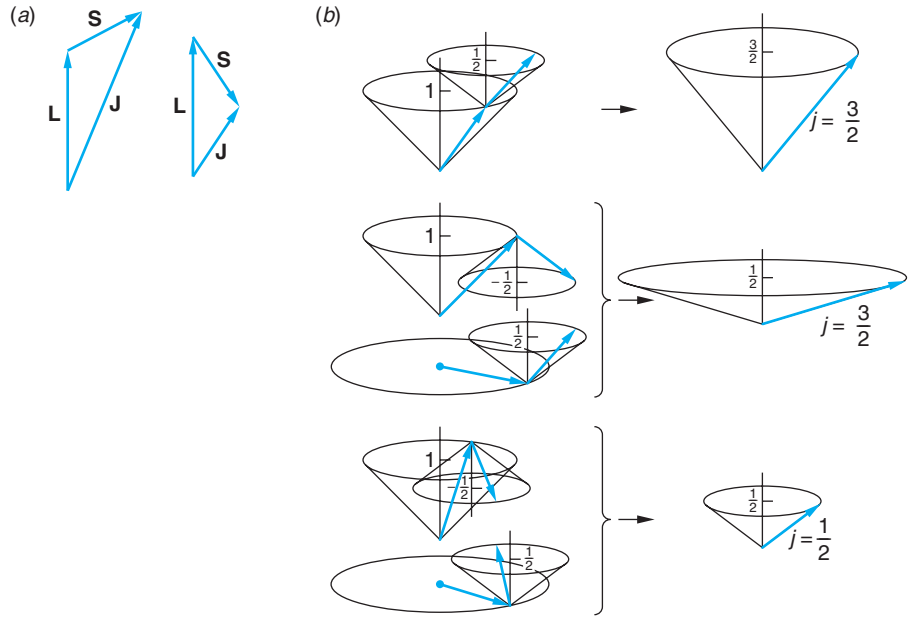

Figure 7-16 (*a*) Simplified vector model illustrating the addition of orbital and spin angular momenta. The case shown is for $\ell = 1$ and $s = \frac{1}{2}$. There are two possible values of the quantum number for the total angular momentum: $j = \ell + s = \frac{3}{2}$ and $j = \ell - s = \frac{1}{2}$. (*b*) Vector addition of the orbital and spin angular momenta, also for the case $\ell = 1$ and $s = \frac{1}{2}$. According to the uncertainty principle, the vectors can lie anywhere on the cones, corresponding to the definite values of their z components. Note in the middle sketch that there are two ways of forming the states with $j = \frac{3}{2}$, $m_j = \frac{1}{2}$ and $j = \frac{1}{2}$, $m_j = \frac{1}{2}$.

EXAMPLE 7-2 **Addition of Angular Momenta I** Two electrons each have zero orbital angular momentum. What are the possible quantum numbers for the total angular momentum of the two-electron system? (For example, these could be the He atom electrons in any of the S states.)

SOLUTION

In this case $j_1 = j_2 = \frac{1}{2}$. The general rule then gives two possible results, $j = 1$ and $j = 0$. These combinations are commonly called parallel and antiparallel, respectively.

EXAMPLE 7-3 **Addition of Angular Momenta II** An electron in an atom has orbital angular momentum $\mathbf{L_1}$ with quantum number $\ell_1 = 2$, and a second electron has orbital angular momentum $\mathbf{L_2}$ with quantum number $\ell_2 = 3$. What are the possible quantum numbers for the total orbital angular momentum $\mathbf{L} = \mathbf{L_1} + \mathbf{L_2}$?

SOLUTION

Since $\ell_1 + \ell_2 = 5$ and $|\ell_1 - \ell_2| = 1$, the possible values of ℓ are 5, 4, 3, 2, and 1.

Spectroscopic Notation

Spectroscopic notation, a kind of shorthand developed in the early days of spectroscopy to condense information and simplify the description of transitions between states, has since been adopted for general use in atomic, molecular, nuclear, and

STUDENTS-HUB.com Uploaded By: Malak Obaid

particle physics. The notation code appears to be arbitrary,[11] but it is easy to learn and, as you will discover, convenient to use. For single electrons we have:

1. For single-electron states the letter code *s p d f g h* . . . is used in one-to-one correspondence with the values of the orbital angular momentum quantum number ℓ : 0 1 2 3 4 5. . . . For example, an electron with $\ell = 2$ is said to be a *d* electron or in a *d* state.
2. The single-electron (Bohr) energy levels are called *shells*, labeled *K L M N O* . . . in one-to-one correspondence with the values of the principal quantum number n: 1 2 3 4 5. . . . For example, an electron with $n = 3$ in an atom is said to be in the *M* shell. (This notation is less commonly used.)

For atomic states that may contain one or more electrons, the notation includes the principal quantum number and the angular momenta quantum numbers. The total orbital angular momentum quantum number is denoted by a capital letter in the same sequence as in rule 1 above, i.e., *S P D F* . . . correspond to ℓ values 0 1 2 3. . . . The value of n is written as a prefix and the value of the total angular momentum quantum number j by a subscript. The magnitude of the total spin quantum number s appears as a left superscript in the form $2s + 1$.[12] Thus, a state with $\ell = 1$, a *P* state, would be written as

$$n^{2s+1}P_j$$

For example, the ground state of the hydrogen atom ($n = 1$, $\ell = 0$, $s = 1/2$) is written $1^2\,S_{1/2}$, read "one doublet S one-half." The $n = 2$ state can have $\ell = 0$ or $\ell = 1$, so the spectroscopic notation for these states is $2^2\,S_{1/2}$, $2^2\,P_{3/2}$, and $2^2P_{1/2}$. (The principal quantum number and spin superscript are sometimes not included if they are not needed in specific situations.)

Spin-Orbit Coupling

Atomic states with the same n and ℓ values but different j values have slightly different energies because of the interaction of the spin of the electron with its orbital motion. This is called the *spin-orbit effect*. The resulting splitting of the spectral lines such as the one that results from the splitting of the $2P$ level in the transition $2P \rightarrow 1S$ in hydrogen is called *fine-structure splitting*. We can understand the spin-orbit effect qualitatively from a simple Bohr model picture, as shown in Figure 7-17. In this picture, the electron moves in a circular orbit with speed v around a fixed proton. In the figure, the orbital angular momentum **L** is up. In the frame of reference of the electron, the proton moves in a circle around it, thus constituting a circular loop current that produces a magnetic field **B** at the position of the electron. The direction of **B** is also up, parallel to **L**. Recall that the potential energy of a magnetic moment in a magnetic field depends on its orientation relative to the field direction and is given by

$$U = -\boldsymbol{\mu} \cdot \mathbf{B} = -\mu_z B \qquad \textbf{7-56}$$

The potential energy is lowest when the magnetic moment is parallel to **B** and highest when it is antiparallel. Since the intrinsic magnetic moment of the electron is directed opposite to its spin (because the electron has a negative charge), the spin-orbit energy is highest when the spin is parallel to **B** and thus to **L**. The energy of the $2P_{3/2}$ state in

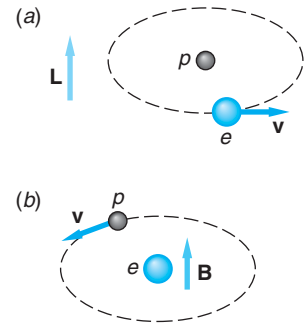

Figure 7-17 (*a*) An electron moving about a proton with angular momentum **L** up. (*b*) The magnetic field **B** seen by the electron due to the apparent (relative) motion of the proton is also up. When the electron spin is parallel to **L**, the magnetic moment is antiparallel to **L** and **B**, so the spin-orbit energy has its largest value.

STUDENTS-HUB.com Uploaded By: Malak Obaid

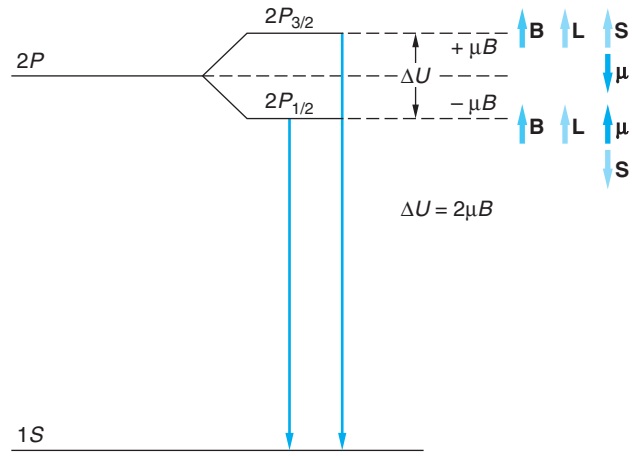

Figure 7-18 Fine-structure energy-level diagram. On the left, the levels in the absence of a magnetic field are shown. The effect of the magnetic field due to the relative motion of the nucleus is shown on the right. Because of the spin-orbit interaction, the magnetic field splits the $2P$ level into two energy levels, with the $j = \frac{3}{2}$ level having slightly greater energy than the $j = \frac{1}{2}$ level. The spectral line due to the transition $2P \longrightarrow 1S$ is therefore split into two lines of slightly different wavelengths. (Diagram is not to scale.)

hydrogen, in which **L** and **S** are parallel, is therefore slightly higher than the $2P_{1/2}$ state, in which **L** and **S** are antiparallel (Figure 7-18).[13] The measured splitting is about 4.5×10^{-5} eV for the $2P_{1/2}$ and $2P_{3/2}$ levels in hydrogen. For other atoms, the fine-structure splitting is larger than this. For example, for sodium it is about 2×10^{-3} eV, as will be discussed in Section 7-7. Recalling that transitions resulting in spectral lines in the visible region are of the order of 1.5 to 3.0 eV, you can see that the fine-structure splitting is quite small.

EXAMPLE 7-4 **Fine-Structure Splitting** The fine-structure splitting of the $2P_{3/2}$ and $2P_{1/2}$ levels in hydrogen is 4.5×10^{-5} eV. From this, estimate the magnetic field that the $2p$ electron in hydrogen experiences. Assume **B** is parallel to the z axis.

SOLUTION

1. The energy of the $2p$ electrons is shifted in the presence of a magnetic field by an amount given by Equation 7-56: $U = -\boldsymbol{\mu} \cdot \mathbf{B} = -\mu_z B$

2. U is positive or negative depending on the relative orientation of $\boldsymbol{\mu}$ and **B**, so the total energy difference ΔE between the two levels is: $\Delta E = 2U = 2\mu_z B$

3. Since the magnetic moment of the electron is μ_B, $\mu_z \approx \mu_B$ and $\Delta E \approx 2\mu_B B$

4. Solving this for B substituting for μ_B and the energy splitting ΔE gives
$$B \approx \frac{\Delta E}{2\mu_B} \approx \frac{4.5 \times 10^{-5}\ \text{eV}}{(2)(5.79 \times 10^{-5}\ \text{eV/T})} \approx 0.39\ \text{T}$$

Remarks: This is a substantial magnetic field, nearly 10,000 times Earth's average magnetic field.

STUDENTS-HUB.com Uploaded By: Malak Obaid

When an atom is placed in an *external* magnetic field **B**, the total angular momentum **J** is quantized in space relative to the direction of **B** and the energy of the atomic state characterized by the angular momentum quantum number j is split into $2j + 1$ energy levels corresponding to the $2j + 1$ possible values of the z component of **J** and therefore to the $2j + 1$ possible values of the z component of the total magnetic moment. This splitting of the energy levels in the atom gives rise to a splitting of the spectral lines emitted by the atom. The splitting of the spectral lines of an atom placed in an external magnetic field was discovered by P. Zeeman and is known as the *Zeeman effect*. (See the second More section on page 303 and Section 3-1.) Zeeman and Lorentz shared the Nobel Prize in Physics for the discovery and explanation of the Zeeman effect.

7-6 The Schrödinger Equation for Two (or More) Particles

Our discussion of quantum mechanics so far has been limited to situations in which a single particle moves in some force field characterized by a potential energy function V. The most important physical problem of this type is the hydrogen atom, in which a single electron moves in the Coulomb potential of the proton nucleus. This problem is actually a two-body problem, as the proton also moves in the Coulomb potential of the electron. However, as in classical mechanics, we can treat this as a one-body problem by considering the proton to be at rest and replacing the electron mass with the reduced mass. When we consider more complicated atoms we must face the problem of applying quantum mechanics to two or more electrons moving in an external field. Such problems are complicated by the interaction of the electrons with each other and also by the fact that the electrons are identical.

The interaction of the electrons with each other is electromagnetic and essentially the same as that expected classically for two charged particles. The Schrödinger equation for an atom with two or more electrons cannot be solved exactly, and approximation methods must be used. This is not very different from the situation in classical problems with three or more particles. The complication arising from the identity of electrons is purely quantum mechanical and has no classical counterpart.

The indistinguishability of identical particles has important consequences related to the *Pauli exclusion principle*. We will illustrate the origin of this important principle in this section by considering the simple case of two noninteracting identical particles in a one-dimensional infinite square well.

The time-independent Schrödinger equation for two particles of mass m is

$$-\frac{\hbar^2}{2m}\frac{\partial^2\psi(x_1, x_2)}{\partial x_1^2} - \frac{\hbar^2}{2m}\frac{\partial^2\psi(x_1, x_2)}{\partial x_2^2} + V\psi(x_1, x_2) = E\psi(x_1, x_2) \qquad \textbf{7-57}$$

where x_1 and x_2 are the coordinates of the two particles. If the particles are interacting, the potential energy V contains terms with both x_1 and x_2, which cannot usually be separated. For example, if the particles are charged, their mutual electrostatic potential energy (in one dimension) is $+ke^2/|x_2 - x_1|$. If they do not interact, however, we can write V as $V_1(x_1) + V_2(x_2)$. For the case of an infinite square well potential, we need solve the Schrödinger equation only inside the well where $V = 0$ and require the wave function to be zero at the walls of the well. Solutions of Equation 7-57 can be written as products of single-particle solutions and linear combinations of such solutions.

STUDENTS-HUB.com Uploaded By: Malak Obaid

The single-particle product solutions are

$$\psi_{nm}(x_1, x_2) = \psi_n(x_1)\psi_m(x_2) \tag{7-58}$$

where $\psi_n(x_1)$ and $\psi_m(x_2)$ are the single-particle wave functions for an infinite square well given by Equation 6-32. Thus, for $n = 1$ and $m = 2$,

$$\psi_{12} = C \sin \frac{\pi x_1}{L} \sin \frac{2\pi x_2}{L} \tag{7-59}$$

The probability of finding particle 1 in dx_1 and particle 2 in dx_2 is $|\psi(x_1, x_2)|^2\, dx_1\, dx_2$, which is just the product of the separate probabilities $|\psi(x_1)|^2\, dx_1$ and $|\psi(x_2)|^2\, dx_2$. However, even though we have labeled the particles 1 and 2, if they are identical, we cannot distinguish which is in dx_1 and which is in dx_2. For identical particles, therefore, we must construct the wave function so that the probability density is the same if we interchange the labels:

$$|\psi(x_1, x_2)|^2 = |\psi(x_2, x_1)|^2 \tag{7-60}$$

Equation 7-60 holds if $\psi(x_1, x_2)$ is either symmetric or antisymmetric on exchange of particles—that is,

$$\psi(x_2, x_1) = +\psi(x_1, x_2) \quad \text{symmetric}$$

$$\psi(x_2, x_1) = -\psi(x_1, x_2) \quad \text{antisymmetric}$$

We note that the general wave function of the form of Equation 7-58 and the example (Equation 7-59) are neither symmetric nor antisymmetric. If we interchange x_1 and x_2, we get a different wave function, implying that the particles can be distinguished. These forms are thus *not* consistent with the indistinguishability of identical particles. However, from among all of the possible linear combination solutions of the single product functions, we see that, if ψ_{nm} and ψ_{mn} are added or subtracted, we form symmetric or antisymmetric wave functions necessary to preserve the indistinguishability of the two particles:

$$\psi_S = C\left[\psi_n(x_1)\psi_m(x_2) + \psi_n(x_2)\psi_m(x_1)\right] \quad \text{symmetric}$$

$$\psi_A = C\left[\psi_n(x_1)\psi_m(x_2) - \psi_n(x_2)\psi_m(x_1)\right] \quad \text{antisymmetric}$$

Pauli Exclusion Principle

There is an important difference between the antisymmetric and symmetric combinations. If $n = \mathrm{m}$, the antisymmetric wave function is identically zero for all x_1 and x_2, whereas the symmetric function is not. More generally, it is found that electrons (and many other particles, including protons and neutrons) can only have antisymmetric *total* wave functions, that is

$$\Psi_{n\ell m_\ell m_s} = R_{n\ell} Y_{\ell m_\ell} X_{m_s} \tag{7-61}$$

where $R_{n\ell}$ is the radial wave function, $Y_{\ell m_\ell}$ is the spherical harmonic, and X_{m_s} is the spin wave function. Thus, single-particle wave functions such as $\psi_n(x_1)$ and $\psi_m(x_1)$ for two such particles cannot have exactly the same set of values for the quantum numbers.

STUDENTS-HUB.com Uploaded By: Malak Obaid

This is an example of the *Pauli exclusion principle*. For the case of electrons in atoms and molecules, four quantum numbers describe the state of each electron, one for each space coordinate and one associated with spin. The Pauli exclusion principle for electrons states that

> No more than one electron may occupy a given quantum state specified by a particular set of single-particle quantum numbers n, ℓ, m_ℓ, m_s.

The effect of the exclusion principle is to exclude certain states in the many-electron system. It is an additional quantum condition imposed on solutions of the Schrödinger equation. It will be applied to the development of the periodic table in the following section. Particles such as α particles, deuterons, photons, and mesons have symmetric wave functions and do not obey the exclusion principle.

7-7 Ground States of Atoms: The Periodic Table

We now consider qualitatively the wave functions and energy levels for atoms more complicated than hydrogen. As we have mentioned, the Schrödinger equations for atoms other than hydrogen cannot be solved exactly because of the interaction of the electrons with one another, so approximate methods must be used. We will discuss the energies and wave functions for the ground states of atoms in this section and consider the excited states and spectra for some of the less complicated cases in the following section. We can describe the wave function for a complex atom in terms of single-particle wave functions. By neglecting the interaction energy of the electrons, that description can be simplified to products of the single-particle wave functions. These wave functions are similar to those of the hydrogen atom and are characterized by the quantum numbers n, ℓ, m_ℓ, m_s. The energy of an electron is determined mainly by the quantum numbers n (which is related to the radial part of the wave function) and ℓ (which characterizes the orbital angular momentum). Generally, the lower the value of n and ℓ, the lower the energy of the state. (See Figure 7-19.) The specification of n and ℓ for each electron in an atom is called the *electron configuration*. Customarily, the value of ℓ and the various electron shells are specified with the same code defined in the subsection "Spectroscopic Notation" (page 292) in Section 7-5. The electron configurations of the atomic ground states are given in Appendix C.

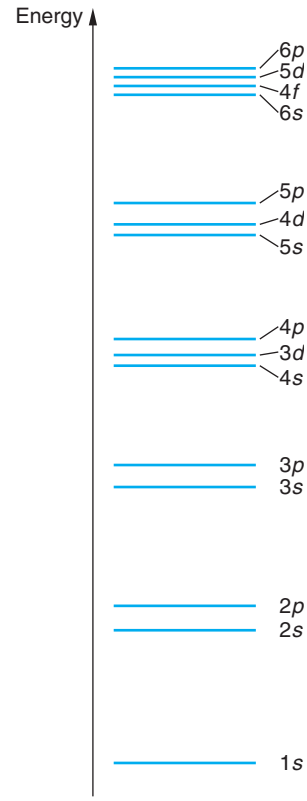

Figure 7-19 Relative energies of the atomic shells and subshells.

The Ground States of the Atoms

Helium ($Z = 2$) The energy of the two electrons in the helium atom consists of the kinetic energy of each electron, a potential energy of the form $-kZe^2/r_i$ for each electron corresponding to its attraction to the nucleus, and a potential energy of interaction V_{int} corresponding to the mutual repulsion of the two electrons. If $\mathbf{r}_1$ and $\mathbf{r}_2$ are the position vectors for the two electrons, V_{int} is given by

$$V_{\text{int}} = +\frac{ke^2}{|\mathbf{r}_2 - \mathbf{r}_1|} \qquad \textbf{7-62}$$

Because this interaction term contains the position variables of the two electrons, its presence in the Schrödinger equation prevents the separation of the equation into separate equations for each electron. If we neglect the interaction term, however, the

STUDENTS-HUB.com Uploaded By: Malak Obaid

Schrödinger equation can be separated and solved exactly. We then obtain separate equations for each electron, with each equation identical to that for the hydrogen atom except that $Z = 2$. The allowed energies are then given by

$$E = -\frac{Z^2 E_0}{n_1^2} - \frac{Z^2 E_0}{n_2^2} \quad \text{where} \quad E_0 = 13.6 \text{ eV} \tag{7-63}$$

The lowest energy, $E_1 = -2(2)^2 E_0 \approx -108.8$ eV, occurs for $n_1 = n_2 = 1$. For this case, $\ell_1 = \ell_2 = 0$. The total wave function, neglecting the spin of the electrons, is of the form

$$\psi = \psi_{100}(r_1, \theta_1, \phi_1)\psi_{100}(r_2, \theta_2, \phi_2) \tag{7-64}$$

The quantum numbers n, ℓ, and m_ℓ can be the same for the two electrons only if the fourth quantum number m_s is different, i.e., if one electron has $m_s = +\frac{1}{2}$ and the other has $m_s = -\frac{1}{2}$. The resulting total spin of the two electrons must therefore be zero.

We can obtain a first-order correction to the ground-state energy by using the approximate wave function of Equation 7-64 to calculate the average value of the interaction energy V_{int}, which is simply the expectation value $\langle V_{\text{int}} \rangle$. The result of this calculation is

$$\langle V_{\text{int}} \rangle = +34 \text{ eV} \tag{7-65}$$

With this correction, the ground-state energy is

$$E \approx -108.8 + 34 = -74.8 \text{ eV} \tag{7-66}$$

This approximation method, in which we neglect the interaction of the electrons to find an approximate wave function and then use this wave function to calculate the interaction energy, is called *first-order perturbation theory*. The approximation can be continued to higher orders: for example, the next step is to use the new ground-state energy to find a correction to the ground-state wave function. This approximation method is similar to that used in classical mechanics to calculate the orbits of the planets about the Sun. In the first approximation the interaction of the planets is neglected and the elliptical orbits are found for each planet. Then, using this result for the position of each planet, the perturbing effects of the nearby planets can be calculated.

The experimental value of the energy needed to remove both electrons from the helium atom is about 79 eV. The discrepancy between this result and the value 74.8 eV is due to the inaccuracy of the approximation used to calculate $\langle V_{\text{int}} \rangle$, as indicated by the rather large value of the correction (about 30 percent). (It should be pointed out that there are better methods of calculating the interaction energy for helium that give much closer agreement with experiment.) The helium *ion* He^+, formed by removing one electron, is identical to the hydrogen atom except that $Z = 2$; so the ground-state energy is

$$-Z^2(13.6) = -54.4 \text{ eV}$$

The energy needed to remove the first electron from the helium atom is 24.6 eV. The corresponding potential, 24.6 V, is called the *first ionization potential* of the atom. The ionization energies are given in Appendix C.

The configuration of the ground state of the helium atom is written $1s^2$. The 1 signifies $n = 1$, the s signifies $\ell = 0$, and the 2 signifies that there are two electrons in this state. Since ℓ can only be zero for $n = 1$, the two electrons fill the K shell ($n = 1$).

STUDENTS-HUB.com Uploaded By: Malak Obaid

Lithium ($Z = 3$) Lithium has three electrons. Two are in the K shell ($n = 1$), but the third cannot have $n = 1$ because of the exclusion principle. The next-lowest energy state for this electron has $n = 2$. The possible ℓ values are $\ell = 1$ or $\ell = 0$.

In the hydrogen atom, these ℓ values have the same energy because of the degeneracy associated with the inverse-square nature of the force. This is not true in lithium and other atoms because the charge "seen" by the outer electron is not a point charge.[14] The positive charge of the nucleus $+Ze$ can be considered to be approximately a point charge, but the negative charge of the K shell electrons $-2e$ is spread out in space over a volume whose radius is of the order of a_0/Z. We can in fact take for the charge density of each inner electron $\rho = -e|\psi|^2$, where ψ is a hydrogenlike $1s$ wave function (neglecting the interaction of the two electrons in the K shell). The probability distribution for the outer electron in the $2s$ or $2p$ states is similar to that shown in Figure 7-10. We see that the probability distribution in both cases has a large maximum well outside the inner K-shell electrons but that the $2s$ distribution also has a small bump near the origin. We could describe this by saying that the electron in the $2p$ state is nearly always outside the shielding of the two $1s$ electrons in the K shell so that it sees an effective central charge of $Z_{\text{eff}} \approx 1$, whereas in the $2s$ state the electron penetrates this "shielding" more often and therefore sees a slightly larger effective positive central charge. The energy of the outer electron is therefore lower in the $2s$ state than in the $2p$ state, and the lowest energy configuration of the lithium atom is $1s^2 2s$.

George Gamow and Wolfgang Pauli in Switzerland in 1930. [*Courtesy of George Gamow.*]

The total angular momentum of the electrons in this atom is $\frac{1}{2}\hbar$ due to the spin of the outer electron since each of the electrons has zero orbital angular momentum and the inner K-shell electrons are paired to give zero spin. The first ionization potential for lithium is only 5.39 V. We can use this result to calculate the effective positive charge seen by the $2s$ electron. For $Z = Z_{\text{eff}}$ and $n = 2$, we have

$$E = \frac{Z^2 E_0}{n^2} = \frac{Z_{\text{eff}}^2 (13.6 \text{ eV})}{2^2} = 5.39 \text{ eV}$$

which gives $Z_{\text{eff}} \approx 1.3$. It is generally true that the smaller the value of ℓ, the greater the penetration of the wave function into the inner shielding cloud of electrons: The result is that in a multielectron atom, *for given n, the energy of the electron increases with increasing* ℓ. (See Figure 7-19.)

Beryllium ($Z = 4$) The fourth electron has the least energy in the $2s$ state. The exclusion principle requires that its spin be antiparallel to the other electron in this state so that the total angular momentum of the four electrons in this atom is zero. The electron configuration of beryllium is $1s^2 2s^2$. The first ionization potential is 9.32 V. This is greater than that for lithium because of the greater value of Z.

Boron to Neon ($Z = 5$ to $Z = 10$) Since the $2s$ subshell is filled, the fifth electron must go into the $2p$ subshell; that is, $n = 2$ and $\ell = 1$. Since there are three possible values of m_ℓ ($+1$, 0, and -1) and two values of m_s for each, there can be up to six electrons in this subshell. The electron configuration for boron is $1s^2 2s^2 2p$. Although it might be expected that boron would have a greater ionization potential than beryllium because of the greater Z, the $2p$ wave function penetrates the shielding of the core electrons to a lesser extent and the ionization potential of boron is actually about 8.3 V, slightly less than that of beryllium. The electron configuration of the elements carbon ($Z = 6$) to neon ($Z = 10$) differs from boron only by the number of electrons in the $2p$ subshell. The ionization potential increases slightly with Z for these elements, reaching the value of 21.6 V for the last element in the group, neon. Neon has the

STUDENTS-HUB.com Uploaded By: Malak Obaid

maximum number of electrons allowed in the $n = 2$ shell. The electron configuration of neon is $1s^2 2s^2 2p^6$. Because of its very high ionization potential, neon, like helium, is chemically inert. The element just before this, fluorine, has a "hole" in this shell; that is, it has room for one more electron. It readily combines with elements such as lithium, which has one outer electron that is donated to the fluorine atom to make an F^- ion and a Li^+ ion, which bond together. This is an example of ionic bonding, to be discussed in Chapter 9.

Sodium to Argon ($Z = 11$ to $Z = 18$) The eleventh electron must go into the $n = 3$ shell. Since this electron is weakly bound in the Na atom, Na combines readily with atoms such as F. The ionization potential for sodium is only 5.14 V. Because of the lowering of the energy due to penetration of the electronic shield formed by the other 10 electrons—similar to that discussed for Li—the $3s$ state is lower than the $3p$ or $3d$ states. (With $n = 3$, ℓ can have the values 0, 1, or 2.) This energy difference between subshells of the same n value becomes greater as the number of electrons increases. The configuration of Na is thus $1s^2 2s^2 2p^6 3s$. As we move to higher-Z elements, the $3s$ subshell and then the $3p$ subshell begin to fill up. These two subshells can accommodate $2 + 6 = 8$ electrons. The configuration of argon ($Z = 18$) is $1s^2 2s^2 2p^6 3s^2 3p^6$. There is another large energy difference between the eighteenth and nineteenth electrons, and argon, with its full $3p$ subshell, is stable and inert.

Atoms with $Z > 18$ One might expect that the nineteenth electron would go into the $3d$ subshell, but the shielding or penetration effect is now so strong that the energy is lower in the $4s$ shell than in the $3d$ shell. The nineteenth electron in potassium ($Z = 19$) and the twentieth electron in calcium ($Z = 20$) go into the $4s$ rather than the $3d$ subshell. The electron configurations of the next 10 elements, scandium ($Z = 21$) through zinc ($Z = 30$), differ only in the number of electrons in the $3d$ subshell except for chromium ($Z = 24$) and copper ($Z = 29$), each of which has only one $4s$ electron. These elements are called *transition elements*. Since their chemical properties are mainly due to their $4s$ electrons, they are quite similar chemically.

Figure 7-20 shows a plot of the first ionization potential of an atom versus Z up to $Z = 90$. The sudden decrease in ionization potential after the Z numbers 2, 10, 18, 36, and 54 marks the closing of a shell or subshell. A corresponding sudden increase occurs in the atomic radii, as illustrated in Figure 7-21. The ground-state electron configurations of the elements are tabulated in Appendix C.

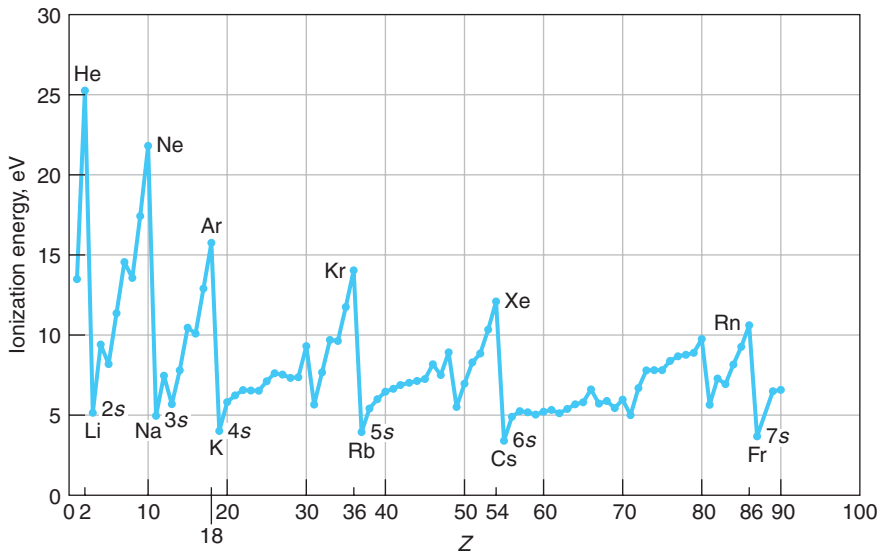

Figure 7-20 First ionization energy vs. Z up to $Z = 90$. The energy is the binding energy of the last electron in the atom. This energy increases with Z until a shell is closed at Z values of 2, 10, 18, 36, 54, and 86. The next electron must go into the next higher shell and hence is farther from the center of core charge and thus less tightly bound. The ionization potential (in volts) is numerically equal to the ionization energy (in eV).

STUDENTS-HUB.com Uploaded By: Malak Obaid

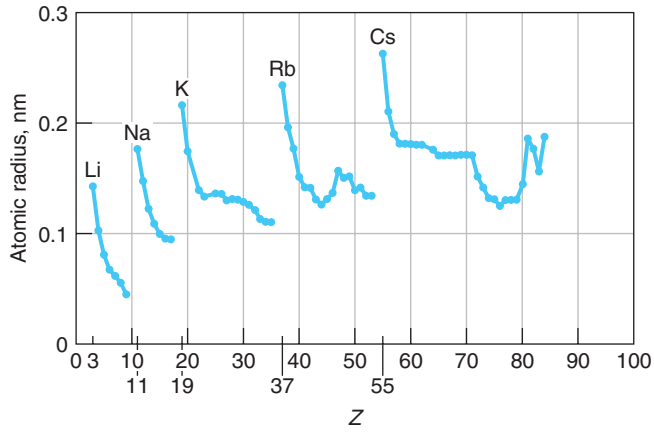

Figure 7-21 The atomic radii versus Z shows a sharp rise following the completion of a shell as the next electron must have the next larger n. The radii then decline with increasing Z, reflecting the penetration of wave functions of the electrons in the developing shell. The recurring patterns here and in Figure 7-20 are examples of the behavior of many atomic properties that give the periodic table its name.

Questions

7. Why is the energy of the 3s state considerably lower than that of the 3p state for sodium, whereas in hydrogen these states have essentially the same energy?
8. Discuss the evidence from the periodic table of the need for a fourth quantum number. How would the properties of He differ if there were only three quantum numbers, n, ℓ, and m?

The concept of shell structure for the electrons in the atomic systems was a significant aid to the later understanding of molecular bonding (see Chapter 9) and the complex structure of the atomic nuclei (see Chapter 11).

7-8 Excited States and Spectra of Atoms

Alkali Atoms

In order to understand atomic spectra, we need to understand the excited states of atoms. The situation for an atom with many electrons is, in general, much more complicated than that of hydrogen. An excited state of the atom usually involves a change in the state of one of the electrons or more rarely two or even more electrons. Even in the case of the excitation of only one electron, the change in state of this electron changes the energies of the others. Fortunately, there are many cases in which this effect is negligible, and the energy levels can be calculated accurately from a relatively simple model of one electron plus a stable core. This model works particularly well for the alkali metals: Li, Na, K, Rb, and Cs. These elements are in the first column of the periodic table. The optical spectra of these elements are similar in many ways to the spectrum of hydrogen.

Another simplification is possible because of the wide difference between excitation energy of a core electron and the excitation energy of an outer electron. Consider the case of sodium, which has a neon core (except $Z = 11$ rather than $Z = 10$) and an outer 3s electron. If this electron did not penetrate the core, it would see an effective nuclear charge of $Z_{\text{eff}} = 1$ resulting from the $+11e$ nuclear charge and the $-10e$ of the completed electron shells. The ionization energy would be the same as the energy of the $n = 3$ electron in hydrogen, about 1.5 eV. Penetration into the core increases Z_{eff} and so lowers the energy of the outer electron, i.e., binds it more tightly, thereby increasing the ionization energy. The measured ionization energy of sodium is about 5 eV. The energy needed to remove one of the outermost core electrons, a 2p electron, is about 31 eV, whereas that needed to remove one of the 1s electrons is about 1041 eV.

STUDENTS-HUB.com Uploaded By: Malak Obaid

Among the many applications of atomic spectra is their use in answering questions about the composition of stars and the evolution of the universe (see Chapter 13).

An electron in the inner core cannot be excited to any of the filled $n = 2$ states because of the exclusion principle. Thus, the minimum excitation of an $n = 1$ electron is to the $n = 3$ shell, which requires an energy only slightly less than that needed to remove this electron completely from the atom. Since the energies of photons in the visible range (about 400 to 800 nm) vary only from about 1.5 to 3 eV, *the optical (i.e., visible) spectrum of sodium must be due to transitions involving only the outer electron*. Transitions involving the core electrons produce line spectra in the ultraviolet and x-ray regions of the electromagnetic spectrum.

Figure 7-22 shows an energy-level diagram for the optical transitions in sodium. Since the spin angular momentum of the neon core adds up to zero, the spin of each state in sodium is $\frac{1}{2}$. Because of the spin-orbit effect, the states with $j = \ell - \frac{1}{2}$ have a slightly lower energy than those with $j = \ell + \frac{1}{2}$. Each state is therefore a doublet (except for the S states). The doublet splitting is very small and is not evident on the energy scale of Figure 7-22 but is shown in Figure 7-18. The states are labeled by the usual spectroscopic notation, with the superscript 2 before the letter indicating that the state is a doublet. Thus, $^2P_{3/2}$, read as "doublet P three-halves," denotes a state

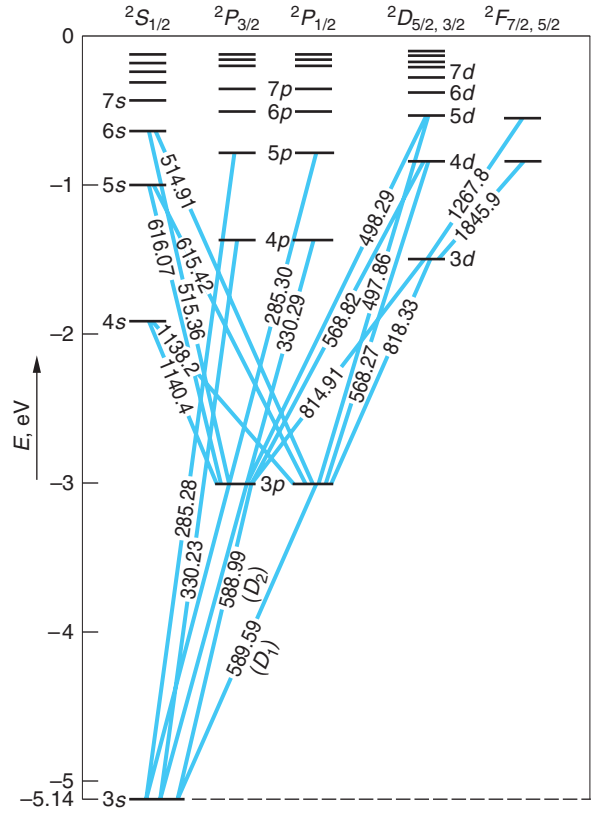

Figure 7-22 Energy-level diagram for sodium (Na) with some transitions indicated. Wavelengths shown are in nanometers. The spectral lines labeled D_1 and D_2 are very intense and are responsible for the yellow color of lamps containing sodium. The energy splittings of the D and F levels, also doublets, are not shown.

STUDENTS-HUB.com Uploaded By: Malak Obaid

in which $\ell = 1$ and $j = \frac{3}{2}$. (The S states are customarily labeled as if they were doublets even though they are not. This is done because they belong to the set of levels with $S = \frac{1}{2}$ but, unlike the others, have $\ell = 0$ and are thus not split. The number indicating the n value of the electron is often omitted.) In the first excited state, the outer electron is excited from the $3s$ level to the $3p$ level, which is about 2.1 eV above the ground state. The spin-orbit energy difference between the $P_{3/2}$ and $P_{1/2}$ states due to the spin-orbit effect is about 0.002 eV. Transitions from these states to the ground state give the familiar sodium yellow doublet

$$3p(^2P_{1/2}) \longrightarrow 3s(^2S_{1/2}) \qquad \lambda = 589.6 \text{ nm}$$

$$3p(^2P_{3/2}) \longrightarrow 3s(^2S_{1/2}) \qquad \lambda = 589.0 \text{ nm}$$

The energy levels and spectra of other alkali atoms are similar to those for sodium.

It is important to distinguish between doublet energy states and doublet spectral lines. All transitions beginning or ending on an S state give double lines because they involve one doublet state and one singlet state (the selection rule $\Delta\ell = \pm 1$ rules out transitions between two S states). There are four possible energy differences between two doublet states. One of these is ruled out by a selection rule on j, which is[15]

$$\Delta j = \pm 1 \text{ or } 0 \qquad (\text{but no } j = 0 \longrightarrow j = 0) \qquad \textbf{7-67}$$

Transitions between pairs of doublet energy states therefore result in three spectral lines, i.e., a triplet. Under relatively low resolution the three lines look like two, as illustrated in Figure 7-23, because two of them are very close together. For this reason, they are often referred to as a *compound doublet* to preserve the verbal hint that they involve doublet energy states.

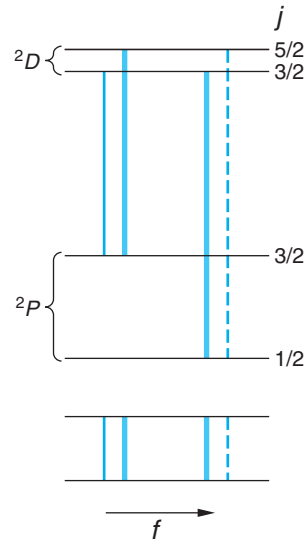

Figure 7-23 The transitions between a pair of doublet energy states in singly ionized calcium. The transition represented by the dotted line is forbidden by the $\Delta j = \pm 1, 0$ selection rule. The darkness of the lines indicates relative intensity. Under low resolution the faint line on the left of the spectrum at the bottom merges with its neighbor and the compound doublet (or triplet) looks like a doublet.

More

Atoms with more than one electron in the outer shell have more complicated energy-level structures. Additional total spin possibilities exist for the atom, resulting in multiple sets of nearly independent energy states and multiple sets of spectral lines. *Multielectron Atoms* and their spectra are described on the home page: www.whfreeman.com/tiplermodernphysics5e. See also Equations 7-68 and 7-69 and Figures 7-24 through 7-27 here.

More

Tradition tells us that Mrs. Bohr encountered an obviously sad young Wolfgang Pauli sitting in the garden of Bohr's Institute for Theoretical Physics in Copenhagen and asked considerately if he was unhappy. His reply was, "Of course I'm unhappy! I don't understand the anomalous Zeeman effect!" On the home page we explain *The Zeeman Effect* so you, too, won't be unhappy: www.whfreeman.com/tiplermodernphysics5e. See also Equations 7-70 through 7-74 and Figures 7-28 through 7-31 here.

STUDENTS-HUB.com Uploaded By: Malak Obaid

EXPLORING
Frozen Light

Using the quantum properties of atomic energy states, tunable lasers, and a Bose-Einstein (BE) condensate of sodium atoms (see Chapter 8), physicists have been able to slow a light pulse to a dead stop, then regenerate it some time later and send it on its way. Here is how it's done.

Consider the 3*s* and 3*p* energy levels of sodium in Figure 7-22. L-S coupling does not cause splitting of the 3*s* state because the orbital angular momentum of that state is zero; however, we will discover in Chapter 11 (see also Problem 7-72) that protons and neutrons also have intrinsic spins and magnetic moments, resulting in a *nuclear* spin and magnetic moment. Although the latter is smaller than the electron's magnetic moment by a factor of about 1000, it causes a very small splitting of the 3*s* level exactly analogous to that due to L-S coupling in states with nonzero orbital angular momenta. Called *hyperfine structure* (because it's smaller than the fine-structure splitting discussed earlier), the 3*s* level is split into two levels spaced about 3.5×10^{-6} eV above and below the original 3*s* state.

Producing the BE condensate results in a cigar-shaped "cloud" about one centimeter long suspended by a magnetic field in a vacuum chamber. The cloud contains several million sodium atoms *all with their spins aligned and all in the lower of the two 3s hyperfine levels*, the new ground state. (See Figure 7-32*a*.) The light pulse that we wish to slow (the probe beam) is provided by a laser precisely tuned to the energy difference between the lower of the 3*s* hyperfine levels (the new ground state) and the 3*p* state. A second laser (the coupling beam) is precisely tuned to the energy difference between the higher of the 3*s* hyperfine levels and the 3*p* state and illuminates the BE condensate perpendicular to the probe beam.

If the probe beam alone were to enter the sample, all of the atoms would be excited to the 3*p* level, absorbing the beam completely. As the atoms relaxed back to the ground state, sodium yellow light would be emitted randomly in all directions. If the coupling beam alone entered the sample, no excitation of the 3*p* level would result because the coupling beam photons do not have enough energy to excite electrons from the ground state to the 3*p* state. However, if the coupling beam is illuminating the sample with all atoms in the ground state and the probe beam is turned on, as the leading edge of the probe pulse enters the sample (Figure 7-32*b*), the two beams together shift the sodium atoms into a quantum superposition of both states, meaning that in that region of the sample *each* atom is in *both* hyperfine states (Figure 7-32*c*). Instead of both beams now being able to excite those atoms to the 3*p* level, the two processes cancel, a phenomenon called *quantum interference*, and the BE condensate becomes transparent to the probe beam, as in Figure 7-32*c*. A similar cancellation causes the index of refraction of the sample to change very steeply over the narrow frequency range of the probe pulse, slowing the leading edge from 3×10^8 m/s to about 15 m/s. As the rest of the probe pulse (still moving at 3×10^8 m/s) enters the sample and slows, it piles up behind the leading edge, dramatically compressing the pulse to about 0.05 mm in length, which fits easily within the sample. Over the region occupied by the compressed pulse, the quantum superposition shifts the atomic spins in synchrony with the superposition, as illustrated in Figure 7-32*d*.

At this point the coupling beam is turned off. The BE condensate immediately becomes opaque to the probe beam; the pulse comes to a stop and turns off. The light has "frozen"! The information imprinted on the pulse is now imprinted like a hologram on the spins of the atoms in the superposition states. (See Figure 7-32*e*.) When the coupling pulse is again turned on, the sample again becomes transparent to the probe pulse.

STUDENTS-HUB.com Uploaded By: Malak Obaid

The "frozen" probe pulse is regenerated carrying the original information, moves slowly to the edge of the sample, then zooms away at 3×10^8 m/s. (See Figure 7-32*f*.)

The ability to slow and stop light raises new opportunities in many areas. For example, it may make possible the development of quantum communications that cannot be eavesdropped upon. Building large-scale quantum computers may depend upon the ultra-high-speed switching potential of quantum superpositions in slow light systems. Astrophysicists may be able to use BE condensates in vortex states, already achieved experimentally, with slow light to simulate in the laboratory the dragging of light into black holes. Stay tuned!

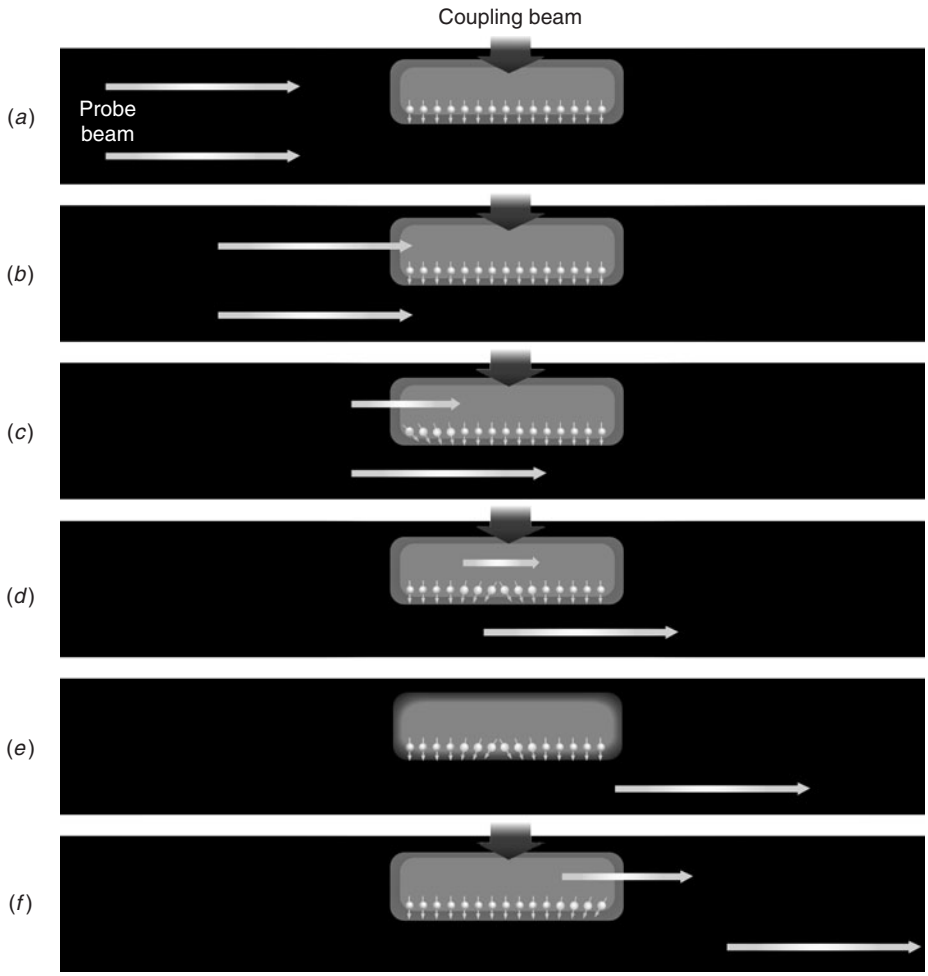

Figure 7-32 (*a*) The coupling beam illuminates the sodium Bose-Einstein condensate, whose atoms are in the ground state with spins aligned. (*b*) The leading edge of the probe beam pulse enters the sample. (*c*) Quantum superposition shifts the spins, and the rapidly changing refractive index dramatically slows and shortens the probe beam inside the condensate. (*d*) Now completely contained inside the sample, the speed of the probe pulse is about 15 m/s. (*e*) The coupling beam is turned off and the probe pulse stops, its information stored in the shifted spins of the atoms. (*f*) The coupling beam is turned back on and the probe pulse regenerates, moves slowly to the edge of the sample, then leaves at 3×10^8 m/s. [*Courtesy of Samuel Velasco.*]

STUDENTS-HUB.com Uploaded By: Malak Obaid

Summary

TOPIC	RELEVANT EQUATIONS AND REMARKS
1. Schrödinger equation in three dimensions	The equation is solved for the hydrogen atom by separating it into three ordinary differential equations, one for each coordinate r, θ, ϕ. The quantum numbers n, ℓ, and m arise from the boundary conditions to the solutions of these equations.
2. Quantization	
Angular momentum	$\lvert\mathbf{L}\rvert = \sqrt{\ell(\ell+1)}\hbar \quad \text{for} \quad \ell = 0, 1, 2, 3, \ldots$ **7-22**
z component of $\mathbf{L}$	$L_z = m\hbar \quad \text{for} \quad m = 0, \pm 1, \pm 2, \ldots, \pm\ell$ **7-23**
Energy	$E_n = -\left(\frac{kZe^2}{\hbar}\right)^2 \frac{\mu}{2n^2} = -13.6\frac{Z^2}{n^2}\,\text{eV}$ **7-24**
3. Hydrogen wave functions	$\Psi_{n\ell m} = C_{n\ell m} R_{n\ell}(r) Y_{n\ell m}(\theta, \phi)$ where $C_{n\ell m}$ are normalization constants, $R_{n\ell}$ are the radial functions, and $Y_{\ell m}$ are the spherical harmonics.
4. Electron spin	The electron spin is not included in Schrödinger's wave equation.
Magnitude of $\mathbf{S}$	$\lvert\mathbf{S}\rvert = \sqrt{s(s+1)}\hbar \quad s = \frac{1}{2}$ **7-36**
z component of $\mathbf{S}$	$S_z = m_s\hbar \quad m_s = \pm\frac{1}{2}$
Stern-Gerlach experiment	This was the first direct observation of the electron spin.
5. Spin-orbit coupling	$\mathbf{L}$ and $\mathbf{S}$ add to give the total angular momentum $\mathbf{J} = \mathbf{L} + \mathbf{S}$, whose magnitude is given by $\lvert\mathbf{J}\rvert = \sqrt{j(j+1)}\hbar$ **7-53** where $j = \ell + s$ or $\lvert\ell - s\rvert$. This interaction leads to the fine-structure splitting of the energy levels.
6. Exclusion principle	No more than one electron can occupy a given quantum state specified by a particular set of the single-particle quantum numbers n, ℓ, m_ℓ, and m_s.

General References

The following general references are written at a level appropriate for the readers of this book.

Brehm, J. J., and W. J. Mullin, *Introduction to the Structure of Matter*, Wiley, New York, 1989.

Eisberg, R., and R. Resnick, *Quantum Physics,* 2d ed., Wiley, New York, 1985.

Herzberg, G., *Atomic Spectra and Atomic Structure*, Dover, New York, 1944.

Kuhn, H. G., *Atomic Spectra*, Academic Press, New York, 1962.

Mehra, J., and H. Rechenberg, *The Historical Development of Quantum Theory*, Vol. 1, Springer-Verlag, New York, 1982.

Pauling, L., and S. Goudsmit, *The Structure of Line Spectra*, McGraw-Hill, New York, 1930.

Weber, H. J., and G. B. Arfken, *Essential Mathematical Methods for Physicists*, Elsevier Academic Press, New York, 2004.

STUDENTS-HUB.com Uploaded By: Malak Obaid

Notes

1. Degeneracy may arise because of a particular symmetry of the physical system, such as the symmetry of the potential energy described here. Degeneracy may also arise for completely different reasons and can certainly occur for nonproduct wave functions. The latter are sometimes called accidental degeneracies, and both types can exist in the same system.

2. "Enough" means a complete set in the mathematical sense.

3. Such potentials are called central field or, sometimes, conservative potentials. The Coulomb potential and the gravitational potential are the most frequently encountered examples.

4. $L_z = |\mathbf{L}|$ would mean that $L_x = L_y = 0$. All three components of $\mathbf{L}$ would then be known exactly, a violation of the uncertainty principle.

5. The functions $Y_{\ell m}$ and $R_{n\ell}$ listed in Tables 7-1 and 7-2 are normalized. The $C_{n\ell m}$ are simply the products of those corresponding normalization constants.

6. Wolfgang Pauli (1900–1958), Austrian physicist. A bona fide child prodigy, while a graduate student at Munich he wrote a paper on general relativity that earned Einstein's interest and admiration. Pauli was 18 at the time. A brilliant theoretician, he became the conscience of the quantum physicists, assaulting "bad physics" with an often devastatingly sharp tongue, one of his oft-quoted dismissals of a certain poor paper being, "It isn't even wrong." He belatedly won the Nobel Prize in Physics in 1945 for his discovery of the exclusion principle.

7. Samuel A. Goudsmit (1902–78) and George E. Uhlenbeck (1900–88), Dutch-American physicists. While graduate students at Leiden, they proposed the idea of electron spin to their thesis adviser Paul Ehrenfest, who suggested that they ask H. A. Lorentz his opinion. After some delay, Lorentz pointed out that an electron spin of the magnitude necessary to explain the fine structure was inconsistent with special relativity. Returning to Ehrenfest with this disturbing news, they found that he had already sent their paper to a journal for publication.

8. Since the same symbol μ is used for both the reduced mass and the magnetic moment, some care is needed to keep these unrelated concepts clear. The symbol m is sometimes used to designate the magnetic moment, but there is confusion enough between the symbol m of the quantum number for the z component of angular momentum and m_e as the electron mass.

9. Otto Stern (1888–1969), German-American physicist, and Walther Gerlach (1899–1979), German physicist. After working as Einstein's assistant for two years, Stern developed the atomic/molecular beam techniques that enabled him and Gerlach, an excellent experimentalist, to show the existence of space quantization in silver. Stern received the 1943 Nobel Prize in Physics for his pioneering molecular beam work.

10. The nucleus of an atom also has angular momentum and therefore a magnetic moment, but the mass of the nucleus is about 2000 times that of the electron for hydrogen and greater still for other atoms. From Equation 7-39 we expect the magnetic moment of the nucleus to be on the order of $1/2000$ of a Bohr magneton since M is now m_p rather than m_e. This small effect does not show up in the Stern-Gerlach experiment.

11. The letters first used, *s, p, d, f*, weren't really arbitrary. They described the visual appearance of certain groups of spectral lines. After improved instrumentation vastly increased the number of measurable lines, the letters went on alphabetically. As we noted in Chapter 4, the *K*, *L*, etc., notation was assigned by Barkla.

12. This particular form for writing the total spin was chosen because it also corresponded to the number of lines in the fine structure of the spectrum; e.g., hydrogen lines were doublets and $s = \frac{1}{2}$, so $2s + 1 = 2$.

13. A more precise interpretation is that the electron, possessing an intrinsic magnetic moment due to its spin, carries with it a dipole magnetic field. This field varies in time due to the orbital motion of the electron, thus generating a time-varying electric field at the (stationary) proton, which produces the energy shift.

14. Actually, it's not quite true for hydrogen either. W. Lamb showed that the $2S$ and $2P$ levels of hydrogen differ slightly in energy. That difference together with the spin-orbit splitting of the $2P$ state puts the $2^2P_{1/2}$ level 4.4×10^{-6} eV below the $2^2S_{1/2}$ level, an energy difference called the Lamb shift. It enables the $2^2S_{1/2}$ state, which would otherwise have been metastable due to the $\Delta\ell = \pm 1$ selection rule, to deactivate to the $1^2S_{1/2}$ ground state via a transition to the $2^2P_{1/2}$ level. The Lamb shift is accounted for by relativistic quantum theory.

15. We can think of this rule in terms of the conservation of angular momentum. The intrinsic spin angular momentum of a photon has the quantum number $s = 1$. For electric dipole radiation, the photon spin is its total angular momentum relative to the center of mass of the atom. If the initial angular momentum quantum number of the atom is j_1 and the final is j_2, the rules for combining angular momenta imply that $j_2 = j_1 + 1, j_1$, or $j_1 - 1$, if $j_1 \neq 0$. If $j_1 = 0, j_2$ must be 1.

16. This is true for nearly all two-electron atoms, such as He, Be, Mg, and Ca, except for the triplet P states in the very heavy atom mercury, where fine-structure splitting is of about the same order of magnitude as the singlet-triplet splitting.

17. Pieter Zeeman (1865–1943), Dutch physicist. His discovery of the Zeeman effect, which so enlightened our understanding of atomic structure, was largely ignored until its importance was pointed out by Lord Kelvin. Zeeman shared the 1902 Nobel Prize in Physics with his professor H. A. Lorentz for its discovery.

18. The terminology is historical, arising from the fact that the effect in transitions between singlet states could be explained by Lorentz's classical electron theory and hence was "normal," while the effects in other transitions could not and were thus mysterious or "anomalous."

19. This calculation can be found in Herzberg (1944).

20. After Alfred Landé (1888–1975), German physicist. His collaborations with Born and Heisenberg led to the correct interpretation of the anomalous Zeeman effect.

STUDENTS-HUB.com Uploaded By: Malak Obaid

Problems

Level I

Section 7-1 The Schrödinger Equation in Three Dimensions

7-1. Find the energies E_{311}, E_{222}, and E_{321} and construct an energy-level diagram for the three-dimensional cubic well that includes the third, fourth, and fifth excited states. Which of the states on your diagram are degenerate?

7-2. A particle is confined to a three-dimensional box that has sides L_1, $L_2 = 2L_1$, and $L_3 = 3L_1$. Give the sets of quantum numbers n_1, n_2, and n_3 that correspond to the lowest 10 energy levels of this box.

7-3. A particle moves in a potential well given by $V(x, y, z) = 0$ for $-L/2 < x < L/2$, $0 < y < L$, and $0 < z < L$ and $V = \infty$ outside these ranges. (*a*) Write an expression for the ground-state wave function for this particle. (*b*) How do the allowed energies compare with those for a box having $V = 0$ for $0 < x < L$ rather than for $-L/2 < x < L/2$?

7-4. Write down the wave functions for the 5 lowest energy levels of the particle in Problem 7-2.

7-5. (*a*) Repeat Problem 7-2 for the case $L_2 = 2L_1$ and $L_3 = 4L_1$. (*b*) What sets of quantum numbers correspond to degenerate energy levels?

7-6. Write down the wave functions for the lowest 10 quantized energy states for the particle in Problem 7-5.

7-7. Suppose the particle in Problem 7-1 is an electron and $L = 0.10$ nm. Compute the energy of the transitions from each of the third, fourth, and fifth excited states to the ground state.

7-8. Consider a particle moving in a two-dimensional space defined by $V = 0$ for $0 < x < L$ and $0 < y < L$ and $V = \infty$ elsewhere. (*a*) Write down the wave functions for the particle in this well. (*b*) Find the expression for the corresponding energies. (*c*) What are the sets of quantum numbers for the lowest-energy degenerate state?

Section 7-2 Quantization of Angular Momentum and Energy in the Hydrogen Atom

7-9. If $n = 3$, (*a*) what are the possible values of ℓ ? (*b*) For each value of ℓ in (*a*), list the possible values of m. (*c*) Using the fact that there are two quantum states for each combination of values of ℓ and m because of electron spin, find the total number of electron states with $n = 3$.

7-10. Determine the minimum angle that $\mathbf{L}$ can make with the z axis when the angular momentum quantum number is (*a*) $\ell = 4$ and (*b*) $\ell = 2$.

7-11. The moment of inertia of a compact disc is about 10^{-5} kg · m^2. (*a*) Find the angular momentum $L = I\omega$ when the disc rotates at $\omega/2\pi = 735$ rev/min and (*b*) find the approximate value of the quantum number ℓ.

7-12. Draw an accurately scaled vector model diagram illustrating the possible orientations of the angular momentum vector $\mathbf{L}$ for (*a*) $\ell = 1$, (*b*) $\ell = 2$, (*c*) $\ell = 4$. (*d*) Compute the magnitude of $\mathbf{L}$ in each case.

7-13. For $\ell = 2$, (*a*) what is the minimum value of $L_x^2 = L_y^2$? (*b*) What is the maximum value of $L_x^2 = L_y^2$? (*c*) What is $L_x^2 = L_y^2$ for $\ell = 2$ and $m = 1$? Can either L_x or L_y be determined from this? (*d*) What is the minimum value of n that this state can have?

7-14. For $\ell = 1$, find (*a*) the magnitude of the angular momentum L and (*b*) the possible values of m. (*c*) Draw to scale a vector diagram showing the possible orientations of $\mathbf{L}$ with the z axis. (*d*) Repeat the above for $\ell = 3$.

7-15. Show that, if V is a function only of r, then $d\mathbf{L}/dt = 0$, i.e., that $\mathbf{L}$ is conserved.

7-16. What are the possible values of n and m if (*a*) $\ell = 3$, and (*b*) $\ell = 4$, and (*c*) $\ell = 0$? (*d*) Compute the minimum possible energy for each case.

7-17. A hydrogen atom electron is in the 6*f* state. (*a*) What are the values of n and ℓ? (*b*) Compute the energy of the electron. (*c*) Compute the magnitude of $\mathbf{L}$. (*d*) Compute the possible values of L_z in this situation.

7-18. At what values of r/a_0 is the radial function R_{30} equal to zero? (See Table 7-2.)

STUDENTS-HUB.com Uploaded By: Malak Obaid

Section 7-3 The Hydrogen Atom Wave Functions

7-19. For the ground state of the hydrogen atom, find the values of (*a*) ψ, (*b*) ψ^2, and (*c*) the radial probability density $P(r)$ at $r = a_0$. Give your answers in terms of a_0.

7-20. For the ground state of the hydrogen atom, find the probability of finding the electron in the range $\Delta r = 0.03a_0$ at (*a*) $r = a_0$ and at (*b*) $r = 2a_0$.

7-21. The radial probability distribution function for the hydrogens ground state can be written $P(r) = Cr^2e^{-2Zr/a_0}$, where C is a constant. Show that $P(r)$ has its maximum value at $r = a_0/Z$.

7-22. Compute the normalization constant C_{210} in Equation 7-34.

7-23. Find the probability of finding the electron in the range $\Delta r = 0.02a_0$ at (*a*) $r = a_0$ and (*b*) $r = 2a_0$ for the state $n = 2, \ell = 0, m = 0$ in hydrogen. (See Problem 7-25 for the value of C_{200}.)

7-24. Show that the radial probability density for the $n = 2$, $\ell = 1$, $m = 0$ state of a one-electron atom can be written as

$$P(r) = A \cos^2\theta\, r^2 e^{-Zr/a_0}$$

where A is a constant.

7-25. The value of the constant C_{200} in Equation 7-33 is

$$C_{200} = \frac{1}{\sqrt{2\pi}}\left(\frac{Z}{a_0}\right)^{3/2}$$

Find the values of (*a*) ψ, (*b*) ψ^2, and (*c*) the radial probability density $P(r)$ at $r = a_0$ for the state $n = 2, \ell = 0, m = 0$ in hydrogen. Give your answers in terms of a_0.

7-26. Show that an electron in the $n = 2$, $\ell = 1$ state of hydrogen is most likely to be found at $r = 4a_0$.

7-27. Write down the wave function for the hydrogen atom when the electron's quantum numbers are $n = 3$, $\ell = 2$, and $m_\ell = -1$. Check to be sure that the wave function is normalized.

7-28. Verify that the wave function ψ_{100} is a solution of the time-independent Schrödinger equation, Equation 7-9.

Section 7-4 Electron Spin

7-29. If a classical system does not have a constant charge-to-mass ratio throughout the system, the magnetic moment can be written

$$\mu = g\frac{Q}{2M}L$$

where Q is the total charge, M is the total mass, and $g \neq 1$. (*a*) Show that $g = 2$ for a solid cylinder ($I = \frac{1}{2}MR^2$) that spins about its axis and has a uniform charge on its cylindrical surface. (*b*) Show that $g = 2.5$ for a solid sphere ($I = 2MR^2/5$) that has a ring of charge on the surface at the equator, as shown in Figure 7-33.

7-30. Assuming the electron to be a classical particle, a sphere of radius 10^{-15} m and a uniform mass density, use the magnitude of the spin angular momentum $|\mathbf{S}| = s(s +]1)]^{1/2}\hbar = (3/4)^{1/2}\hbar$ to compute the speed of rotation at the electron's equator. How does your result compare with the speed of light?

7-31. How many lines would be expected on the detector plate of a Stern-Gerlach experiment (see Figure 7-15) if we use a beam of (*a*) potassium atoms, (*b*) calcium atoms, (*c*) oxygen atoms, and (*d*) tin atoms?

7-32. The force on a magnetic moment with z component μ_z moving in an inhomogeneous magnetic field is given by Equation 7-51. If the silver atoms in the Stern-Gerlach experiment traveled horizontally 1 m through the magnet and 1 m in a field-free region at a speed of 250 m/s, what must have been the gradient of B_z, dB_z/dz in order that the beams each be deflected a maximum of 0.5 mm from the central, or no-field, position?

7-33. (*a*) The angular momentum of the yttrium atom in the ground state is characterized by the quantum number $j = 3/2$. How many lines would you expect to see if you could do a Stern-Gerlach experiment with yttrium atoms? (*b*) How many lines would you expect to see if the beam consisted of atoms with zero spin but $\ell = 1$?

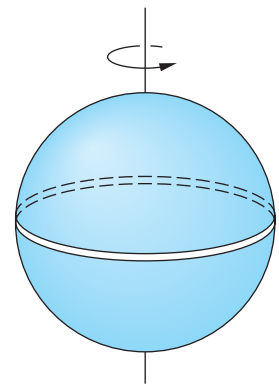

Figure 7-33 Solid sphere with charge Q uniformly distributed on ring.

STUDENTS-HUB.com Uploaded By: Malak Obaid

Section 7-5 Total Angular Momentum and the Spin-Orbit Effect

7-34. The spin-orbit effect removes a symmetry in the hydrogen atom potential, splitting the energy levels. (*a*) Considering the state with $n = 4$, write down in spectroscopic notation the identification of each state and list them in order of increasing energy. (*b*) If a weak external magnetic field is applied to the atoms, into how many levels will each state in (*a*) be split?

7-35. Suppose the outer electron in a potassium atom is in a state with $\ell = 2$. Compute the magnitude of $\mathbf{L}$. What are the possible values of j and the possible magnitudes of $\mathbf{J}$?

7-36. A hydrogen atom is in the 3*D* state ($n = 3$, $\ell = 2$). (*a*) What are the possible values of j? (*b*) What are the possible values of the magnitude of the total angular momentum? (*c*) What are the possible z components of the total angular momentum?

7-37. Compute the angle between $\mathbf{L}$ and $\mathbf{S}$ in (*a*) the $d_{5/2}$ and (*b*) the $d_{3/2}$ states of atomic hydrogen.

7-38. Write down all possible sets of quantum numbers for an electron in a (*a*) 4*f*, (*b*) 3*d*, and (*c*) 2*p* subshell.

7-39. Consider a system of two electrons, each with $\ell = 1$ and $s = \frac{1}{2}$. (*a*) What are the possible values of the quantum number for the total orbital angular momentum $\mathbf{L} = \mathbf{L_1} + \mathbf{L_2}$? (*b*) What are the possible values of the quantum number S for the total spin $\mathbf{S} = \mathbf{S_1} + \mathbf{S_2}$? (*c*) Using the results of parts (*a*) and (*b*), find the possible quantum numbers j for the combination $\mathbf{J} = \mathbf{L} + \mathbf{S}$. (*d*) What are the possible quantum numbers j_1 and j_2 for the total angular momentum of each particle? (*e*) Use the results of part (*d*) to calculate the possible values of j from the combinations of j_1 and j_2. Are these the same as in part (*c*)?

7-40. The prominent yellow doublet lines in the spectrum of sodium result from transitions from the $3P_{3/2}$ and $3P_{1/2}$ states to the ground state. The wavelengths of these two lines are 589.0 nm and 589.6 nm. (*a*) Calculate the energies in eV of the photons corresponding to these wavelengths. (*b*) The difference in energy of these photons equals the difference in energy ΔE of the $3P_{3/2}$ and $3P_{1/2}$ states. This energy difference is due to the spin-orbit effect. Calculate ΔE. (*c*) If the 3*p* electron in sodium sees an internal magnetic field B, the spin-orbit energy splitting will be of the order of $\Delta E = 2\mu_B B$, where μ_B is the Bohr magneton. Estimate B from the energy difference ΔE found in part (*b*).

Section 7-6 The Schrödinger Equation for Two (or More) Particles

7-41. Show that the wave function of Equation 7-59 satisfies the Schrödinger equation (Equation 7-57) with $V = 0$ and find the energy of this state.

7-42. Two neutrons are in an infinite square well with $L = 2.0$ fm. What is the minimum total energy that the system can have? (Neutrons, like electrons, have antisymmetric wave functions. Ignore spin.)

7-43. Five identical noninteracting particles are placed in an infinite square well with $L = 1.0$ nm. Compare the slowest total energy for the system if the particles are (*a*) electrons and (*b*) pions. Pions have symmetric wave functions and their mass is 264 m_e.

Section 7-7 Ground States of Atoms: The Periodic Table

7-44. Write the electron configuration of (*a*) carbon, (*b*) oxygen, and (*c*) argon.

7-45. Using Figure 7-34, determine the ground-state electron configurations of tin (Sn, $Z = 50$), neodymium (Nd, $Z = 60$), and ytterbium (Yb, $Z = 70$). Check your answers with Appendix C. Are there any disagreements? If so, which one(s)?

7-46. In Figure 7-20 there are small dips in the ionization potential curve at $Z = 31$ (gallium), $Z = 49$ (indium), and $Z = 81$ (thallium) that are not labeled in the figure. Explain these dips, using the electron configuration of these atoms given in Appendix C.

7-47. Which of the following atoms would you expect to have its ground state split by the spin-orbit interaction: Li, B, Na, Al, K, Ag, Cu, Ga? (*Hint:* Use Appendix C to see which elements have $\ell = 0$ in their ground state and which do not.)

STUDENTS-HUB.com Uploaded By: Malak Obaid

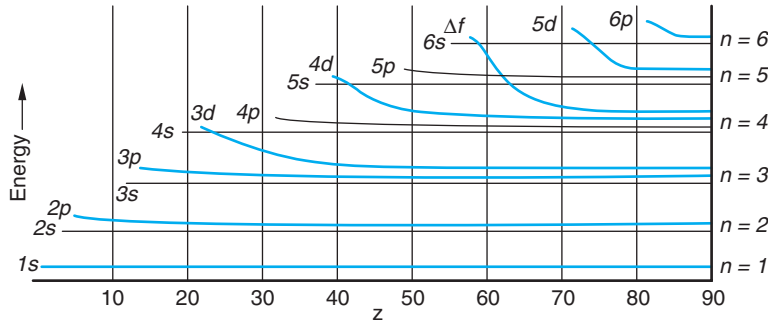

Figure 7-34 Energy of electron ground-state configurations versus Z.

7-48. If the 3s electron in sodium did not penetrate the inner core its energy would be $-13.6\ \text{eV}/3^2 = -1.51$ eV. Because it does penetrate, it sees a higher effective Z and its energy is lower. Use the measured ionization potential of 5.14 V to calculate Z_{eff} for the 3s electron in sodium.

7-49. What elements have these ground-state electron configurations? (*a*) $1s^2 2s^2 2p^6 3s^2 3p^2$ and (*b*) $1s^2 2s^2 2p^6 3s^2 3p^6 4s^2$?

7-50. Give the possible values of the z component of the orbital angular momentum of (*a*) a d electron, (*b*) an f electron, and (*c*) an s electron.

Section 7-8 Excited States and Spectra of Atoms

7-51. Which of the following elements should have an energy-level diagram similar to that of sodium and which should be similar to mercury: Li, He, Ca, Ti, Rb, Ag, Cd, Mg, Cs, Ba, Fr, Ra?

7-52. The optical spectra of atoms with two electrons in the same outer shell are similar, but they are quite different from the spectra of atoms with just one outer electron because of the interaction of the two electrons. Separate the following elements into two groups such that those in each group have similar spectra: lithium, beryllium, sodium, magnesium, potassium, calcium, chromium, nickel, cesium, and barium.

7-53. Which of the following elements should have optical spectra similar to that of hydrogen and which should have optical spectra similar to that of helium: Li, Ca, Ti, Rb, Ag, Cd, Ba, Hg, Fr, Ra?

7-54. The quantum numbers n, ℓ, and j for the outer electron in potassium have the values 4, 0, and $\frac{1}{2}$, respectively, in the ground state; 4, 1, and $\frac{1}{2}$ in the first excited state; and 4, 1, and $\frac{3}{2}$ in the second excited state. Make a table giving the n, ℓ, and j values for the 12 lowest-energy states in potassium (see Figure 7-24).

7-55. Which of the following transitions in sodium do not occur as electric dipole transitions? (Give the selection rule that is violated.)

$$4S_{1/2} \rightarrow 3S_{1/2} \qquad 4S_{1/2} \rightarrow 3P_{3/2} \qquad 4P_{3/2} \rightarrow 3S_{1/2} \qquad 4D_{5/2} \rightarrow 3P_{1/2}$$
$$4D_{3/2} \rightarrow 3P_{1/2} \qquad 4D_{3/2} \rightarrow 3S_{1/2} \qquad 5D_{3/2} \rightarrow 4S_{1/2} \qquad 5P_{1/2} \rightarrow 3S_{1/2}$$

7-56. Transitions between the inner electron levels of heavier atoms result in the emission of characteristic x rays, as was discussed in Section 4-4. (*a*) Calculate the energy of the electron in the K shell for tungsten using $Z - 1$ for the effective nuclear charge. (*b*) The experimental result for this energy is 69.5 keV. Assume that the effective nuclear charge is $(Z - \sigma)$, where σ is called the screening constant, and calculate σ from the experimental result for the energy.

7-57. Since the P states and the D states of sodium are all doublets, there are four possible energies for transitions between these states. Indicate which three transitions are allowed and which one is not allowed by the selection rule of Equation 7-67.

STUDENTS-HUB.com Uploaded By: Malak Obaid

7-58. The relative penetration of the inner-core electrons by the outer electron in sodium can be described by the calculation of Z_{eff} from $E = -\left[Z_{\text{eff}}^2(13.6)\text{ eV}\right]/n^2$ and comparing with $E = -13.6\text{ eV}/n^2$ for no penetration (see Problem 7-45). (*a*) Find the energies of the outer electron in the 3*s*, 3*p*, and 3*d* states from Figure 7-22. (*Hint:* An accurate method is to use -5.14 eV for the ground state as given and find the energy of the 3*p* and 3*d* states from the photon energies of the indicated transitions.) (*b*) Find Z_{eff} for the 3*p* and 3*d* states. (*c*) Is the approximation $-13.6\text{ eV}/n^2$ good for any of these states?

7-59. A hydrogen atom in the ground state is placed in a magnetic field of strength $B_z = 0.55$ T. (*a*) Compute the energy splitting of the spin states. (*b*) Which state has the higher energy? (*c*) If you wish to excite the atom from the lower to the higher energy state with a photon, what frequency must the photon have? In what part of the electromagnetic spectrum does this lie?

7-60. Show that the change in wavelength $\Delta\lambda$ of a transition due to a small change in energy is

$$\Delta\lambda \approx -\frac{\lambda^2}{hc}\Delta E$$

(*Hint:* Differentiate $E = hc/\lambda$.)

7-61. (*a*) Find the normal Zeeman energy shift $\Delta E = e\hbar B/2m_e$ for a magnetic field of strength $B = 0.05$ T. (*b*) Use the result of Problem 7-57 to calculate the wavelength changes for the singlet transition in mercury of wavelength $\lambda = 579.07$ nm. (*c*) If the smallest wavelength change that can be measured in a spectrometer is 0.01 nm, what is the strength of the magnetic field needed to observe the Zeeman effect in this transition?

Level II

7-62. If the outer electron in lithium moves in the $n = 2$ Bohr orbit, the effective nuclear charge would be $Z_{\text{eff}}e = 1e$ and the energy of the electron would be $-13.6\text{ eV}/2^2 = -3.4$ eV. However, the ionization energy of lithium is 5.39 eV, not 3.4 eV. Use this fact to calculate the effective nuclear charge Z_{eff} seen by the outer electron in lithium. Assume that $r = 4a_0$ for the outer electron.

7-63. Show that the expectation value of *r* for the electron in the ground state of a one-electron atom is $\langle r\rangle = (3/2)a_0/Z$.

7-64. If a rigid body has moment of inertia *I* and angular velocity ω, its kinetic energy is

$$E = \frac{1}{2}I\omega^2 = \frac{(I\omega)^2}{2I} = \frac{L^2}{2I}$$

where *L* is the angular momentum. The solution of the Schrödinger equation for this problem leads to quantized energy values given by

$$E_\ell = \frac{\ell(\ell+1)\hbar^2}{2I}$$

(*a*) Make an energy-level diagram of these energies, and indicate the transitions that obey the selection rule $\Delta\ell = \pm 1$. (*b*) Show that the allowed transition energies are E_1, $2E_1$, $3E_1$, $4E_1$, etc., where $E_1 = \hbar^2/I$. (*c*) The moment of inertia of the H_2 molecule is $I = \frac{1}{2}m_p r^2$, where m_p is the mass of the proton and $r \approx 0.074$ nm is the distance between the protons. Find the energy of the first excited state $\ell = 1$ for H_2, assuming it is a rigid rotor. (*d*) What is the wavelength of the radiation emitted in the transition $\ell = 1$ to $\ell = 0$ for the H_2 molecule?

7-65. In a Stern-Gerlach experiment hydrogen atoms in their ground state move with speed $v_x = 14.5$ km/s. The magnetic field is in the *z* direction, and its maximum gradient is given by $dB_z/dz = 600$ T/m. (*a*) Find the maximum acceleration of the hydrogen atoms. (*b*) If the region of the magnetic field extends over a distance $\Delta x = 75$ cm and there is an additional 1.25 m from the edge of the field to the detector, find the maximum distance between the two lines on the detector.

7-66. Find the minimum value of the angle between the angular momentum **L** and the *z* axis for a general value of ℓ, and show that for large values of ℓ, $\theta_{\text{min}} \approx 1/\ell^{1/2}$.

STUDENTS-HUB.com Uploaded By: Malak Obaid

7-67. The wavelengths of the photons emitted by potassium corresponding to transitions from the $4P_{3/2}$ and $4P_{1/2}$ states to the ground state are 766.41 nm and 769.90 nm. (*a*) Calculate the energies of these photons in electron volts. (*b*) The difference in energies of these photons equals the difference in energy ΔE between the $4P_{3/2}$ and $4P_{1/2}$ states in potassium. Calculate ΔE. (*c*) Estimate the magnetic field that the $4p$ electron in potassium experiences.

7-68. The radius of the proton is about $R_0 = 10^{-15}$ m. The probability that the electron is inside the volume occupied by the proton is given by

$$P = \int_0^{R_0} P(r)\, dr$$

where $P(r)$ is the radial probability density. Compute P for the hydrogen ground state. (*Hint:* Show that $e^{-2r/a_0} \approx 1$ for $r \ll a_0$ is valid for this calculation.)

7-69. (*a*) Calculate the Landé g factor (Equation 7-74) for the $^2P_{1/2}$ and $^2S_{1/2}$ levels in a one-electron atom and show that there are four different energies for the transition between these levels in a magnetic field. (*b*) Calculate the Landé g factor for the $^2P_{3/2}$ level and show that there are six different energies for the transition $^2P_{3/2} \rightarrow {}^2S_{1/2}$ in a magnetic field.

7-70. (*a*) Show that the function

$$\psi = A\frac{r}{a_0}e^{-r/2a_0}\cos\theta$$

is a solution of Equation 7-9, where A is a constant and a_0 is the Bohr radius. (*b*) Find the constant A.

Level III

7-71. Consider a hypothetical hydrogen atom in which the electron is replaced by a K^- particle. The K^- is a meson with spin 0, hence, no intrinsic magnetic moment. The only magnetic moment for this atom is that given by Equation 7-43. If this atom is placed in a magnetic field with $B_z = 1.0$ T, (*a*) what is the effect on the $1s$ and $2p$ states? (*b*) Into how many lines does the $2p \rightarrow 1s$ spectral line split? (*c*) What is the fractional separation $\Delta\lambda/\lambda$ between adjacent lines? (See Problem 7-57.) The mass of the K^- is 493.7 MeV/c^2.

7-72. If relativistic effects are ignored, the $n = 3$ level for one-electron atoms consists of the $3^2S_{1/2}$, $3^2P_{1/2}$, $3^2P_{3/2}$, $3^2D_{3/2}$, and $3^2D_{5/2}$ states. Compute the spin-orbit-effect splittings of $3P$ and $3D$ states for hydrogen.

7-73. In the anomalous Zeeman effect, the external magnetic field is much weaker than the internal field seen by the electron as a result of its orbital motion. In the vector model (Figure 7-30) the vectors $\mathbf{L}$ and $\mathbf{S}$ precess rapidly around $\mathbf{J}$ because of the internal field and $\mathbf{J}$ precesses slowly around the external field. The energy splitting is found by first calculating the component of the magnetic moment μ_J in the direction of $\mathbf{J}$ and then finding the component of $\boldsymbol{\mu}_z$ in the direction of $\mathbf{B}$. (*a*) Show that $\mu_J = \dfrac{\boldsymbol{\mu}\cdot\mathbf{J}}{J}$ can be written

$$\mu_J = -\frac{\mu_B}{\hbar J}(L^2 + 2S^2 + 3\mathbf{S}\cdot\mathbf{L})$$

(*b*) From $J^2 = (\mathbf{L} + \mathbf{S})\cdot(\mathbf{L} + \mathbf{S})$ show that $\mathbf{S}\cdot\mathbf{L} = \frac{1}{2}(J^2 - L^2 - S^2)$. (*c*) Substitute your result in part (*b*) into that of part (*a*) to obtain

$$\mu_J = -\frac{\mu_B}{2\hbar J}(3J^2 + S^2 - L^2)$$

(*d*) Multiply your result by J_z/J to obtain

$$\mu_z = -\mu_B\left(1 + \frac{J^2 + S^2 - L^2}{2J^2}\right)\frac{J_z}{\hbar}$$

STUDENTS-HUB.com Uploaded By: Malak Obaid

7-74. If the angular momentum of the nucleus is $\mathbf{I}$ and that of the atomic electrons is $\mathbf{J}$, the total angular momentum of the atom is $\mathbf{F} = \mathbf{I} + \mathbf{J}$, and the total angular momentum quantum number f ranges from $I + J$ to $|I - J|$. Show that the number of possible f values is $2I + 1$ if $I < J$ or $2J + 1$ if $J < I$. (If you can't find a general proof, show it for enough special cases to convince yourself of its validity.) (Because of the very small interaction of the nuclear magnetic moment with that of the electrons, a hyperfine splitting of the spectral lines is observed. When $I < J$, the value of I can be determined by counting the number of lines.)

7-75. Because of the spin and magnetic moment of the proton, there is a very small splitting of the ground state of the hydrogen atom called *hyperfine splitting*. The splitting can be thought of as caused by the interaction of the electron magnetic moment with the magnetic field due to the magnetic moment of the proton, or vice versa. The magnetic moment of the proton is parallel to its spin and is about $2.8\mu_N$, where $\mu_N = e\hbar/2m_p$ is called the *nuclear magneton*. (*a*) The magnetic field at a distance r from a magnetic moment varies with angle, but it is of the order of $B \sim 2k_m\boldsymbol{\mu}/r^3$, where $k_m = 10^{-7}$ in SI units. Find B at $r = a_0$ if $\boldsymbol{\mu} = 2.8\boldsymbol{\mu}_N$. (*b*) Calculate the order of magnitude of the hyperfine splitting energy $\Delta E \approx 2\boldsymbol{\mu}_B B$, where $\boldsymbol{\mu}_B$ is the Bohr magneton and B is your result from part (*a*). (*c*) Calculate the order of magnitude of the wavelength of radiation emitted if a hydrogen atom makes a "spin flip" transition between the hyperfine levels of the ground state. [Your result is greater than the actual wavelength of this transition, 21.22 cm, because $\langle r^{-3} \rangle$ is appreciably smaller than a_0^{-3}, making the energy ΔE found in part (*b*) greater. The detection of this radiation from hydrogen atoms in interstellar space is an important part of radio astronomy.]

STUDENTS-HUB.com Uploaded By: Malak Obaid

CHAPTER 8

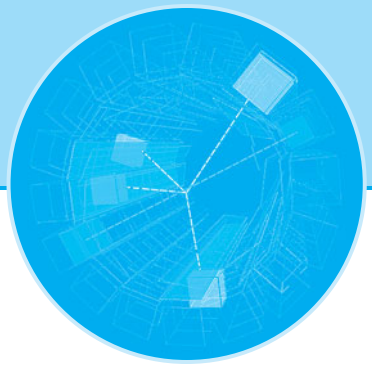

Statistical Physics

8-1 Classical Statistics: A Review 316
8-2 Quantum Statistics 328
8-3 The Bose-Einstein Condensation 335
8-4 The Photon Gas: An Application of Bose-Einstein Statistics 344
8-5 Properties of a Fermion Gas 351

The physical world that we experience with our senses consists entirely of *macroscopic* objects, i.e., systems that are large compared with atomic dimensions and thus are assembled from very large numbers of atoms. As we proceed to the description of such systems from our starting point of studying single-electron atoms, then multielectron atoms and molecules, we expect to encounter increasing complexity and difficulty in correctly explaining their observed properties. Classically, the behavior of any macroscopic system could, in principle, be predicted in detail from the solution of the equation of motion for each constituent particle, given its state of motion at some particular time; however, the obvious problems with such an approach soon become intractable. For example, consider the difficulties that would accompany the task of accounting for the measured properties of a standard liter of any gas by simultaneously solving the equations of motion for all of the 10^{22} molecules of which the system is composed. Fortunately, we can predict the values of the measurable properties of macroscopic systems without the need to track the motions of each individual particle. This remarkable shortcut is made possible by the fact that we can apply general principles of physics, such as conservation of energy and momentum, to large ensembles of particles, ignoring their individual motions, and determine the *probable* behavior of the system from *statistical* considerations. We then use the fact that there is a relation between the calculated probable behavior and the observed properties of the system. This successful, so-called microscopic approach to explaining the behavior of large systems is called *statistical mechanics*. It depends critically on the system containing a sufficiently large number of particles so that ordinary statistical theory is valid.[1]

In this chapter we will investigate how this statistical approach can be applied to predict the way in which a given amount of energy will most likely be distributed among the particles of a system. You may have already encountered kinetic theory, the first successful such microscopic approach, in introductory physics. Since the assumptions, definitions, and basic results of kinetic theory form the foundation of classical statistical physics, we have included a brief review of kinetic theory in the Classical Concept Review. We will see how, in an isolated system of particles in thermal equilibrium, the particles must be able to exchange energy, one result of which is that the energy of any individual particle may sometimes be larger and sometimes smaller than the average value for a particle in the system. Classical statistical mechanics requires

STUDENTS-HUB.com
Uploaded By: Malak Obaid

that the values of the energy taken on by an individual particle over time, or the values of the energy assumed by all of the particles in the system at any particular time, be determined by a specific probability distribution, the *Boltzmann distribution*. In the first section of the chapter we will briefly review the principal concepts of classical statistical physics, noting some of the successful applications and some of the serious failures. We will then see how quantum considerations require modification of the procedures used for classical particles, obtaining in the process the quantum-mechanical *Fermi-Dirac distribution* for particles with antisymmetric wave functions, such as electrons, and the *Bose-Einstein distribution* for particles with symmetric wave functions, such as helium atoms. Finally, we will apply the distributions to several physical systems, comparing our predictions with experimental observations and gaining an understanding of such important phenomena as superfluidity and the specific heat of solids.

8-1 Classical Statistics: A Review

Statistical physics, whether classical or quantum, is concerned with the distribution of a fixed amount of energy among a large number of particles, from which the observable properties of the system may then be deduced. Classically, the system consists of a large ensemble of identical but distinguishable particles. That is, the particles are all exactly alike, but in principle they can be individually tracked during interactions. Boltzmann[2] derived a distribution relation that made possible prediction of the probable numbers of particles that will occupy each of the available energy states in such a system in thermal equilibrium.

Boltzmann Distribution

The *Boltzmann's distribution* $f_B(E)$ given by Equation 8-1 is the fundamental distribution function of classical statistical physics:

$$f_B(E) = Ae^{-E/kT} \qquad \textbf{8-1}$$

where A is a normalization constant whose value depends on the particular system being considered, $e^{-E/kT}$ is called the *Boltzmann factor*, and k is the *Boltzmann constant*:

$$k = 1.381 \times 10^{-23}\ \text{J/K} = 8.617 \times 10^{-5}\ \text{eV/K}$$

Boltzmann's derivation was done to establish the fundamental properties of a distribution function for the velocities of molecules in a gas in thermal equilibrium that had been obtained by Maxwell a few years before and to show that the velocity distribution for a gas that was not in thermal equilibrium would evolve toward Maxwell's distribution over time. Boltzmann's derivation is more complex than is appropriate for our discussions, but in the Classical Concept Review we present a straightforward numerical derivation that results in an approximation of the correct distribution and then show by a simple mathematical argument that the form obtained is exact and is the only one possible. Here we will illustrate application of the Boltzmann distribution with some examples by way of providing a basis for comparing classical and quantum statistical physics later in the chapter.

The number of particles with energy E is given by

$$n(E) = g(E)f_B(E) = A\,g(E)e^{-E/kT} \qquad \textbf{8-2}$$

where $g(E)$ is the statistical weight (degeneracy) of the state with energy E.

STUDENTS-HUB.com Uploaded By: Malak Obaid

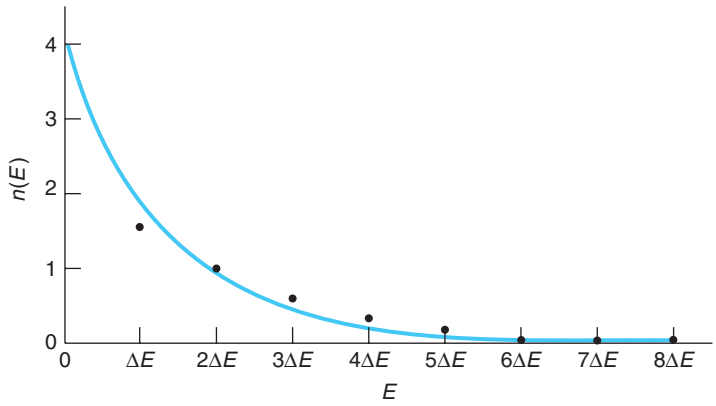

Figure 8-1 $n(E)$ versus E for data from Table 1 in the CCR Boltzmann distribution derivation. The solid curve is the exponential $n(E) = Be^{-E/E_c}$, where the constants B and E_c have been adjusted to give the best fit to the data points.

Classically, the energy E is a continuous function and so is $n(E)$ (Figure 8-1). Consequently, $g(E)$ and $f_B(E)$ are also continuous functions, in which case $g(E)$ in Equation 8-2 is referred to as the *density of states*, meaning that $g(E)dE$ is the number of states with energy between E and $E+dE$. The next two examples illustrate how to apply the Boltzmann distribution and how the results explain observations of physical systems.

EXAMPLE 8-1 The Law of Atmospheres Consider an ideal gas in a uniform gravitational field. (*a*) Find how the density of the gas depends upon the height above ground. (*b*) Assuming that air is an ideal gas with molecular weight 28.6, compute the density of air 1 km above the ground when $T = 300$ K. (The density at the ground is 1.292 kg/m^3 at 300 K.)

SOLUTION

(*a*) Let the force of gravity be in the negative z direction and consider a column of gas of cross-sectional area A. The energy of a gas molecule is then

$$E = \frac{p_x^2}{2m} + \frac{p_y^2}{2m} + \frac{p_z^2}{2m} + mgz = \frac{p^2}{2m} + mgz$$

where $p^2 = p_x^2 + p_y^2 + p_z^2$ and mgz is the potential energy of a molecule at height z above the ground. The density ρ is proportional to f_B since ρ is proportional to N, the number of molecules in a unit volume at height z, and N is proportional to f_B.

From Equation 8-1 we have

$$f_B = Ae^{-p^2/2mkT}e^{-mgz/kT}$$

Since we are interested only in the dependence on z, we can integrate over the other variables p_x, p_y, and p_z. The integration merely gives a new normalization constant A'; i.e., the result is equivalent to ignoring these variables. The fraction of the molecules between z and $z + dz$ is then

$$f_B(z)\,dz = A'e^{-mgz/kT}\,dz \qquad \textbf{8-3}$$

The constant A' is obtained from the normalization condition $\int_0^\infty f_B(z)\,dz = 1$. The result is $A' = mg/kT$. The density, therefore, also decreases exponentially with the distance above the ground. Equation 8-3 is known as the *law of atmospheres*.

STUDENTS-HUB.com Uploaded By: Malak Obaid

(*b*) The ratio of the density at $z = 1000$ m to that at $z = 0$ m is the same as $f_B(1000)/f_B(0)$, where $f_B(z)$ is given by Equation 8-3. Thus,

$$\frac{\rho(1000)}{\rho(0)} = \frac{f_B(1000)}{f_B(0)} = \frac{e^{-mg(1000)/k(300)}}{e^{-mg(0)/k(300)}} = e^{-mg(1000)/k(300)}$$

Substituting $m = 28.6 \times 1.67 \times 10^{-27}$ kg and $g = 9.8$ m/s^2 yields

$$\rho(1000) = \rho(0)e^{-0.113} = 1.292 \times 0.893 = 1.154 \text{ kg/m}^3$$

EXAMPLE 8-2 **H Atoms in the First Excited State** The first excited state E_2 of the hydrogen atom is 10.2 eV above the ground state E_1. What is the ratio of the number of atoms in the first excited state to the number in the ground state at (*a*) $T = 300$ K and (*b*) $T = 5800$ K? The latter is the temperature at the surface of the Sun.

SOLUTION

1. The number of atoms in a state with energy E is given by Equation 8-2:
$$n(E) = g(E)f_B(E) = A\, g(E)e^{-E/kT}$$

2. The ratio of the number in the first excited state to the number in the ground state is then
$$\frac{n_2}{n_1} = \frac{Ag_2e^{-E_2/kT}}{Ag_1e^{-E_1/kT}} = \frac{g_2}{g_1}e^{-(E_2-E_1)/kT}$$

3. The statistical weight (= degeneracy) of the ground state g_1, including spin, is 2; the degeneracy of the first excited state g_2 is 8 (one $\ell = 0$ and three $\ell = 1$ states, each with two spin states). Therefore:
$$\frac{g_2}{g_1} = \frac{8}{2} = 4$$
and
$$\frac{n_2}{n_1} = 4e^{-(E_2-E_1)/kT}$$

4. For question (*a*), at $T = 300$ K, $kT \approx 0.026$ eV. Substituting this and $E_2 - E_1 = 10.2$ eV from above gives
$$\frac{n_2}{n_1} = 4e^{-(10.2)/(0.026)} = 4e^{-392} \approx 10^{-171} \approx 0$$

5. For question (*b*), at the surface of the Sun where $T = 5800$ K, $kT \approx 0.500$. Substituting this and $E_2 - E_1 = 10.2$ eV gives
$$\frac{n_2}{n_1} = 4e^{-(10.2)/(0.500)} = 4e^{-20.4}$$
$$\approx e^{-19} \approx 10^{-8}$$

Remarks: *The result in step 4 illustrates that, because of the large energy difference between the two states compared with kT, very few atoms are in the first excited state. Even fewer would be in the higher excited states, which explains why a container of hydrogen sitting undisturbed at room temperature does not spontaneously emit the visible Balmer series. At the surface of the Sun (step 5 above) about 10^{15} atoms of every mole of atomic hydrogen are in the first excited state at any given time.*

STUDENTS-HUB.com Uploaded By: Malak Obaid

More

In learning about systems containing large numbers of particles, the meaning of the *temperature* needs to be more carefully defined. It is closely related to another descriptor of such systems, the *entropy*. To help you understand both concepts better, we have included *Temperature and Entropy* on the home page: www.whfreeman.com/tiplermodernphysics5e. See also Equations 8-4 *a*, *b*, *c*, and *d* here.

Maxwell Distribution of Molecular Speeds

The Boltzmann distribution is a very fundamental relation from which many properties of classical systems, both gases and condensed matter, can be derived. Two of the most important are Maxwell's distribution of the speeds of molecules in a gas and the equipartition theorem. Considering the first of these, Maxwell derived the velocity and speed distributions of gases in 1859, some five years before Boltzmann derived Equation 8-1. As with the Boltzmann distribution, we will present the results here, illustrating their application with examples and including fuller descriptions and derivations in the Classical Concept Review. Maxwell obtained the velocity distribution, $F(v_x, v_y, v_z)$, which can also be used to obtain the speed distribution, by assuming that the components v_x, v_y, and v_z of the velocity were independent and that therefore the probability of a molecule having a certain v_x, v_y, v_z could be factored into the product of the separate probabilities of its having v_x, v_y, and v_z. He also assumed that the distribution could depend only on the speed; i.e., the velocity components could occur only in the combination $v_x^2 + v_y^2 + v_z^2$. He thus wrote for the distribution function for v_x

$$f(v_x) = Ce^{-mv_x^2/2kT} \qquad \textbf{8-5}$$

where $f(v_x)$ is the distribution function for v_x only; i.e., $f(v_x)dv_x$ is the fraction of the total number of molecules that have their x component of velocity between v_x and $v_x + dv_x$.[3] Similar expressions can be written for $f(v_y)$ and $f(v_z)$. The constant C is determined by the normalization condition. The complete normalized velocity distribution is

$$F(v_x, v_y, v_z) = f(v_x)f(v_y)f(v_z) = \left(\frac{m}{2\pi kT}\right)^{3/2} e^{-m(v_x^2+v_y^2+v_z^2)/2kT} \qquad \textbf{8-6}$$

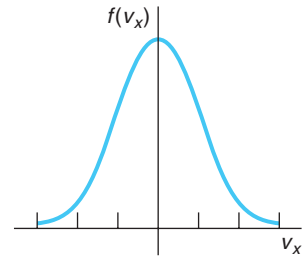

Figure 8-2 The distribution function $f(v_x)$ for the x component of velocity. This is a Gaussian curve symmetric about the origin.

The utility of distribution functions is that they make possible the calculation of average or expectation values of physical quantities; i.e., they allow us to make predictions regarding the physical properties of systems. For example, the observation from Figure 8-2 that the average value of v_x is zero can be verified by computing $\langle v_x \rangle$ as indicated by Equation 8-7.

$$\langle v_x \rangle = \int_{-\infty}^{+\infty} v_x f(v_x)\, dv_x = \int_{-\infty}^{+\infty} v_x \left(\frac{m}{2\pi kT}\right)^{1/2} e^{-mv_x^2/2kT}\, dv_x \qquad \textbf{8-7}$$

Writing $\lambda = m/2kT$, we have

$$\langle v_x \rangle = (\lambda/\pi) \int_{-\infty}^{+\infty} v_x e^{-\lambda v_x^2}\, dv_x$$

STUDENTS-HUB.com Uploaded By: Malak Obaid

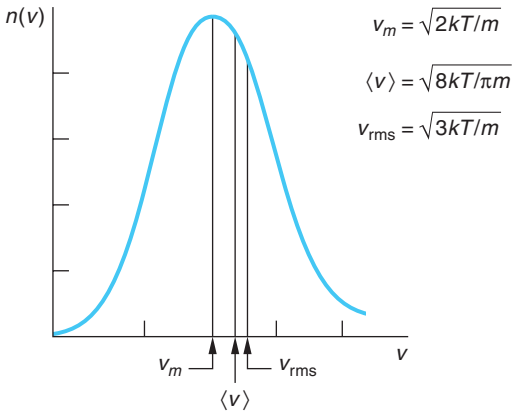

Figure 8-3 Maxwell speed distribution function $n(v)$. The most probable speed v_m, the average speed $\langle v \rangle$, and the rms speed v_{rms} are indicated.

From Table B1-1 we see that the value of the integral is zero, so $\langle v_x \rangle = 0$, as expected.

The probability distribution function for the speeds of the molecules in a classical ideal gas can be derived from the Boltzmann distribution. The result is the famous *Maxwell distribution of molecular speeds*:

$$n(v)\,dv = 4\pi N\left(\frac{m}{2\pi kT}\right)^{3/2} v^2 e^{-mv^2/2kT}\,dv \qquad \textbf{8-8}$$

The distribution of speeds is shown graphically in Figure 8-3. The most probable speed v_m, the average speed $\langle v \rangle$, and the rms speed v_{rms} are indicated in the figure. Although the velocity distribution function F (see Equation 8-6 and Figures 8-4 and 8-5) is a maximum at the origin (where $v_x = v_y = v_z = 0$), the speed distribution function $n(v)$ approaches zero as $v \to 0$ because the latter is proportional to the volume of the spherical shell $4\pi v^2\,dv$ (see Equation 8-8), which approaches zero. At very high speeds, the speed distribution function again approaches zero because of the exponential factor $e^{-mv^2/2kT}$.

The most probable speed v_m is that where $n(v)$ has its maximum value. It is left as an exercise (see Problem 8-9) to show that its value is

$$v_m = \left(\frac{2kT}{m}\right)^{1/2} \qquad \textbf{8-9}$$

The average speed $\langle v \rangle$ is obtained in general and for a specific situation in the next example.

One of the ways used to separate ^{235}U from the far more abundant ^{238}U isotope is to react the uranium metal with fluorine, forming UF_6, a gas. ^{235}UF diffuses through a membrane just a bit faster than ^{238}UF since both molecules have the same average kinetic energy. After several stages of diffusion, the concentration of ^{235}U is high enough for making nuclear reactor fuel (see Chapter 11).

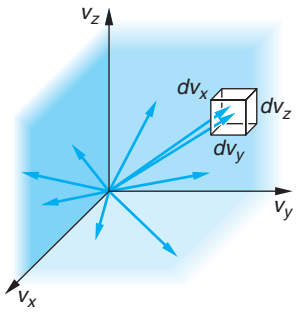

Figure 8-4 Velocity vectors in velocity space. The velocity distribution function gives the fraction of molecular velocities whose vectors end in a cell of volume $dv_x dv_y dv_z$.

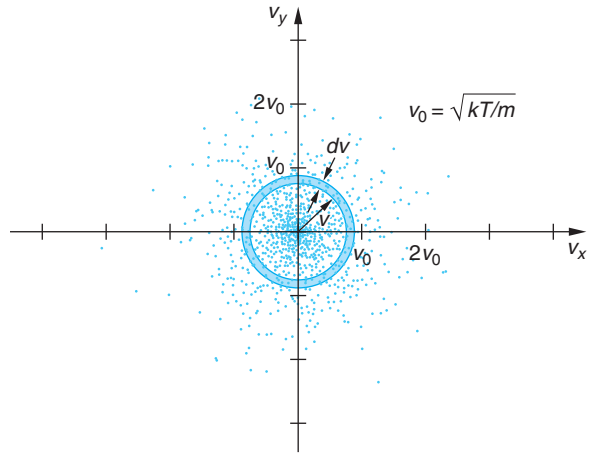

Figure 8-5 Two-dimensional representation of velocity distribution in velocity space. Each molecular velocity with components v_x, v_y, and v_z is represented by a point in velocity space. The velocity distribution function is the density of points in this space. The density is maximum at the origin. The speed distribution is found by multiplying the density times the volume of the spherical shell $4\pi v^2\,dv$. [*This computer-generated plot courtesy of Paul Doherty, The Exploratorium.*]

STUDENTS-HUB.com Uploaded By: Malak Obaid

EXAMPLE 8-3 **Average Speed of N_2 Molecules** Obtain the average speed $\langle v \rangle$ of the Maxwell distribution and use it to compute the average speed of nitrogen molecules at 300 K. The mass of the N_2 molecule is 4.68×10^{-26} kg.

SOLUTION

1. The average speed $\langle v \rangle$ is found by multiplying the distribution of speeds (Equation 8-8) by v, integrating over all possible speeds, and dividing by the total number of molecules N:

$$\langle v \rangle = \frac{1}{N} \int_0^\infty v n(v)\, dv = \int_0^\infty A v^3 e^{-\lambda v^2}\, dv$$

where $\lambda = m/2kT$ and $A = 4\pi(m/2kT)^{3/2}$.

2. Writing this as

$$\langle v \rangle = A I_3$$

where

$$I_3 = \int_0^\infty v^3 e^{-\lambda v^2}\, dv$$

3. Using Table B1-1 for evaluating I_3, we have

$$\begin{aligned} \langle v \rangle &= A\lambda^{-2}/2 \\ &= \frac{4\pi}{2}\left(\frac{m}{2\pi kT}\right)^{3/2}\left(\frac{2kT}{m}\right)^2 \\ &= \left(\frac{8kT}{\pi m}\right)^{1/2} \end{aligned} \qquad \textbf{8-10}$$

4. The $\langle v \rangle$ found in step 3 can now be used to find the average speed of nitrogen molecules at $T = 300$ K. Substituting the mass of a nitrogen molecule into Equation 8-10 yields

$$\begin{aligned} \langle v \rangle &= \left[\frac{8 \times 1.38 \times 10^{-23} \times 300}{\pi \times 4.68 \times 10^{-26}}\right]^{1/2} \\ &= 475 \text{ m/s} \\ &= 1700 \text{ km/h} \end{aligned}$$

The average speed is about 8 percent less than $v_{rms} = (3kT/m)^{1/2}$, as indicated in Figure 8-3. The rms speed can be computed from the speed distribution following the same procedure as in Example 8-3 or, as we will see below, from the equipartition theorem. Figure 8-6, a plot of Equation 8-8 for H_2 and O_2 molecules at 300 K, illustrates the effect of mass on the speed distribution.

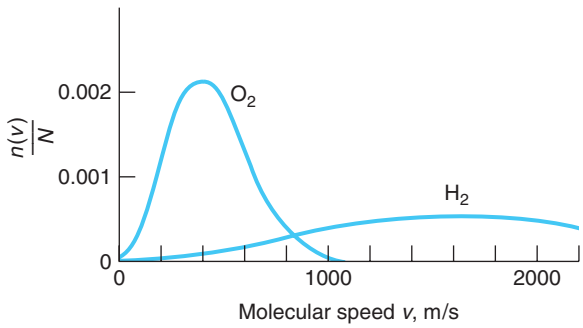

Figure 8-6 Graph of $n(v)/N$ versus v from Equation 8-8 for O_2 and H_2 molecules, both at $T = 300$ K.

STUDENTS-HUB.com Uploaded By: Malak Obaid

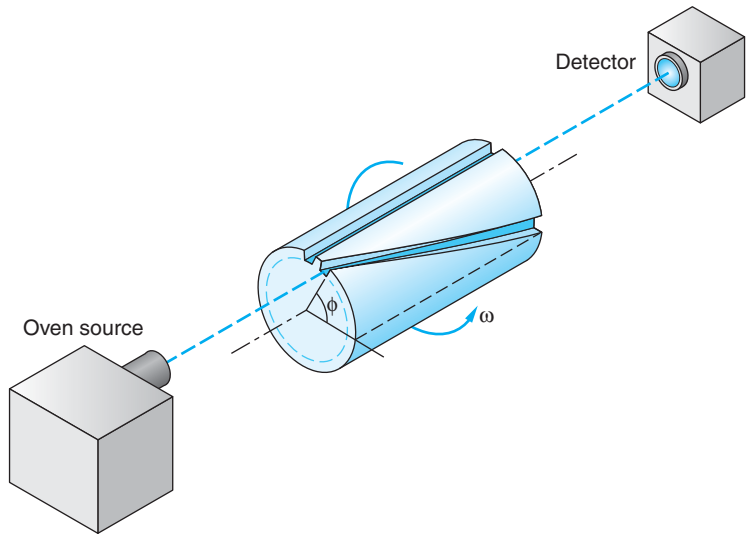

Figure 8-7 Schematic sketch of apparatus of Miller and Kusch for measuring the speed distribution of molecules. Only one of the 720 helical slits in the cylinder is shown. For a given angular velocity ω only molecules of a certain speed from the oven pass through the helical slits to the detector. The straight slit is used to align the apparatus. [*From R. C. Miller and P. Kusch, Physical Review,* **99**, *1314 (1955).*]

Evaporation is a cooling process, even at very low temperatures! The sample from which a BE condensate will form, confined at about 1 mK, is cooled further by allowing the atoms in the high-speed "tail" of the Maxwell distribution to "leak" from the sample, taking kinetic energy with them and thus reducing the temperature (see Section 8-3).

Maxwell's speed distribution has been precisely verified by many experiments, so there is little incentive to perform additional measurements. One of the more recent experiments, that of R. C. Miller and P. Kusch, illustrated in Figures 8-7 and 8-8, is applicable to the measurement of any sort of molecular speed distribution, and variations of it are used to measure the speeds in jet or nozzle molecular beams.

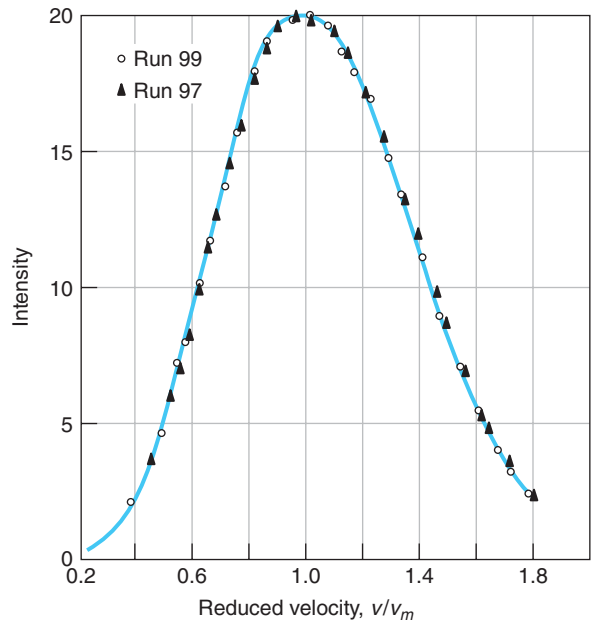

Figure 8-8 Data of Miller and Kusch showing the distribution of speed of thallium atoms from an oven at 870 K. The data have been corrected to give the distribution inside the oven since the faster molecules approach the exit slit more frequently and skew the external distribution slightly. The measured value for v_m at 870 K is 376 m/s. The solid curve is that predicted by the Maxwell speed distribution. [*From R. C. Miller and P. Kusch, Physical Review,* **99**, *1314 (1955).*]

Questions

1. How does v_{rms} for H_2 molecules compare with v_{rms} for O_2 molecules under standard conditions?

STUDENTS-HUB.com Uploaded By: Malak Obaid

Maxwell Distribution of Kinetic Energy

Maxwell's distribution of molecular speeds also provides, as a bonus, the distribution of the molecular translational kinetic energy and the average kinetic energy of a molecule. These can also be determined from Equation 8-2. Since $E = \frac{1}{2}mv^2$, $v^2 = 2E/m$, and $dv = (2mE)^{1/2}\,dE$, $g(E)\,dE$ is

$$g(E)\,dE = 4\pi C(2E/m)(2mE)^{-1/2}\,dE \qquad \textbf{8-11}$$

Substituting the above into Equation 8-2, we have

$$n(E)\,dE = 4\pi A'(2/m^3)^{1/2}E^{1/2}e^{E/kT}\,dE \qquad \textbf{8-12}$$

Evaluating A' using the fact that $\int_0^\infty n(E)\,dE = N$, the total number of particles, allows us to write *Maxwell's distribution of kinetic energy* as

$$n(E)\,dE = \frac{2\pi N}{(\pi kT)^{3/2}}E^{1/2}e^{-E/kT}\,dE \qquad \textbf{8-13}$$

The kinetic energy distribution is sketched in Figure 8-9. The average kinetic energy is computed in the same manner as the average speed; i.e., the distribution is multiplied by E (the quantity being averaged), and the result is integrated[4] over all values of E (from $0 \rightarrow \infty$) and divided by the number of molecules N:

$$\langle E\rangle = \frac{1}{N}\int_0^\infty E\,n(E)\,dE = \frac{2\pi}{(\pi kT)^{3/2}}\int_0^\infty E^{3/2}e^{-E/kT}\,dE = \frac{3}{2}kT \qquad \textbf{8-14}$$

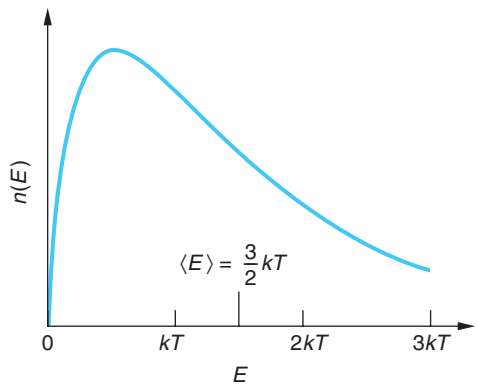

Figure 8-9 Maxwell distribution of kinetic energies for the molecules of an ideal gas. The average energy $\langle E\rangle = 3kT/2$ is shown.

EXAMPLE 8-4 **Escape of H_2 from Earth's Atmosphere** A rule of thumb used by astrophysicists is that a gas will escape from a planet's atmosphere in 10^8 years if the average speed of its molecules is one-sixth of the escape velocity. Compute the average speed from the average kinetic energy and show that the absence of hydrogen in Earth's atmosphere suggests that Earth must be older than 10^8 years (mass of H_2 molecules $= 3.34 \times 10^{-27}$ kg).

STUDENTS-HUB.com Uploaded By: Malak Obaid

SOLUTION

The escape speed at the bottom of the atmosphere, i.e., Earth's surface, is 11.2 km/s, and one-sixth of that value is 1.86 km/s. If we assume $T = 300$ K, the average energy of a hydrogen molecule (or any other molecule since $\langle E \rangle$ is independent of mass) is

$$\langle E \rangle = \frac{3}{2}kT = \frac{3 \times 1.38 \times 10^{-23} \times 300}{2} = 6.21 \times 10^{-21}\ \text{J}$$

Thus,

$$\tfrac{1}{2}mv^2 = 6.21 \times 10^{-21}\ \text{J}$$

or, for hydrogen molecules,

$$v^2 = \frac{2 \times 6.21 \times 10^{-21}}{3.34 \times 10^{-27}} = 3.72 \times 10^6\ \text{m}^2/\text{s}^2$$

Therefore,

$$v = 1.93\ \text{km/s}$$

Remarks: *Since $v > (1/6)v_{esc} = 1.86$ km/s, the absence of hydrogen in the atmosphere suggests that the age of Earth is greater than 10^8 years.*

Questions

2. How does $\langle E_k \rangle$ for He molecules compare with $\langle E_k \rangle$ for Kr molecules under standard conditions?
3. H_2 molecules can escape so freely from Earth's gravitational field that H_2 is not found in Earth's atmosphere. (See Example 8-4.) Yet the average speed of H_2 molecules at ordinary atmospheric temperatures is much less than the escape speed. How, then, can all of the H_2 molecules escape?
4. Why wouldn't you expect all molecules in a gas to have the same speed?

Heat Capacities of Gases and Solids

The second important property of classical systems derivable from the Boltzmann distribution is one that applies to both gases and solids. Called the *equipartition theorem*, it states that

> In equilibrium, each degree of freedom contributes $\frac{1}{2}kT$ to the average energy per molecule.

A *degree of freedom* is a coordinate or a velocity component that appears squared in the expression for the total energy of a molecule. For example, the one-dimensional harmonic oscillator has two degrees of freedom, x and v_x; a monatomic gas molecule has three degrees of freedom, v_x, v_y, and v_z.

More

That each degree of freedom in a classical material should have the same average energy per molecule is not at all obvious. On the home page we have included *A Derivation of the Equipartition Theorem* for a special case, the harmonic oscillator, to illustrate how the more general result arises: www.whfreeman.com/tiplermodernphysics5e. See also Equations 8-15 through 8-23 here.

STUDENTS-HUB.com Uploaded By: Malak Obaid

C_V for Gases

The power of the equipartition theorem is its ability to accurately predict the heat capacities of gases and solids, but therein is also found its most dramatic failures. As an example, consider a rigid-dumbbell model of a diatomic molecule (Figure 8-10*a*) that can translate in the x, y, and z directions and can rotate about axes x' and y' through the center of mass and perpendicular to the z' axis along the line joining the two atoms.[5] The total energy for this rigid-dumbbell model molecule is then

$$E = \tfrac{1}{2}mv_x^2 + \tfrac{1}{2}mv_y^2 + \tfrac{1}{2}mv_z^2 + \tfrac{1}{2}I_{x'}\omega_{x'}^2 + \tfrac{1}{2}I_{y'}\omega_{y'}^2$$

where $I_{x'}$ and $I_{y'}$ are the moments of inertia about the x' and y' axes. Since this molecule has 5 degrees of freedom, 3 translational and 2 rotational, the equipartition theorem predicts the average energy to be $(5/2)kT$ per molecule. The energy per mole U is then $(5/2)N_Akt = (5/2)RT$ and the molar heat capacity at constant volume $C_V = (\partial U/\partial T)_V$ is $(5/2)R$. The observation that C_V for both nitrogen and oxygen is about $(5/2)R$ enabled Rudolf Clausius to speculate (in about 1880) that these gases must be diatomic gases, which can rotate about two axes as well as translate. (See Table 8-1.)

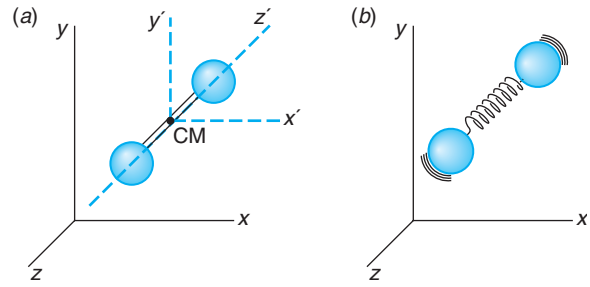

Figure 8-10 (*a*) Rigid-dumbbell model of a diatomic gas molecule that can translate along the x, y, or z axis and rotate about the x' or y' axis fixed to the center of mass. If the spheres are smooth or are points, rotation about the z' axis can be neglected. (*b*) Nonrigid-dumbbell model of a diatomic gas molecule that can translate, rotate, and vibrate.

Table 8-1 C_V for some gases at 15°C and 1 atm

Gas	C_V (cal/mol-deg)	C_V/R
Ar	2.98	1.50
He	2.98	1.50
CO	4.94	2.49
H_2	4.87	2.45
HCl	5.11	2.57
N_2	4.93	2.49
NO	5.00	2.51
O_2	5.04	2.54
Cl_2	5.93	2.98
CO_2	6.75	3.40
CS_2	9.77	4.92
H_2S	6.08	3.06
N_2O	6.81	3.42
SO_2	7.49	3.76
$R = 1.987$ cal/mol-deg		

From J. R. Partington and W. G. Shilling, *The Specific Heats of Gases* (London: Ernest Benn, Ltd., 1924).

STUDENTS-HUB.com Uploaded By: Malak Obaid

If a diatomic molecule is not rigid, the atoms can also vibrate along the line joining them (Figure 8-10*b*). Then, in addition to the translational energy of the center of mass and rotational energy, there can be vibrational energy. The vibration, a simple harmonic motion, adds two more squared terms to the energy, one for the potential energy and one for kinetic energy. For a diatomic molecule that is translating, rotating, and vibrating, the equipartition theorem thus predicts a molar heat capacity of $(3 + 2 + 2)\frac{1}{2}R$, or $(7/2)R$. However, measured values of C_V for diatomic molecules (see Table 8-1) show no contribution from the vibrational degrees of freedom. The equipartition theorem provides no explanation for their absence.

Experimental values of C_V for several diatomic gases are included in Table 8-1. For all of these except Cl_2, the data are consistent with the equipartition theorem prediction, assuming a rigid, nonvibrating molecule. The value for Cl_2 is about halfway between that predicted for a rigid molecule and that predicted for a vibrating molecule. The situation for molecules with three or more atoms, several of which are also listed in Table 8-1, is more complicated and will not be examined in detail here.

The equipartition theorem in conjunction with the point-atom, rigid-dumbbell model was so successful in predicting the molar heat capacity for most diatomic molecules that it was difficult to understand why it did not do so for all of them. Why should some diatomic molecules vibrate and not others? Since the atoms are not points, the moment of inertia about the line joining the atoms, while small, is not zero, and there are three terms for rotational energy rather than two. Assuming no vibration, C_V should then be $(6/2)R$. This agrees with the measured value for Cl_2 but not for the other diatomic gases. Furthermore, monatomic molecules would have three terms for rotational energy if the atoms were not points, and C_V should also be $(6/2)R$ for these atoms rather than the $(3/2)R$ that is observed. Since the average energy is calculated by *counting* terms, it should not matter how small the atoms are as long as they are not merely points. In addition to these difficulties, it is found experimentally that the molar heat capacity depends on temperature, contrary to the predictions from the equipartition theorem. The most spectacular case is that of H_2, shown in Figure 8-11. It seems as if at very low temperatures, below about 60 K, H_2 behaves like a monatomic molecule and does not rotate. It seems to undergo a transition, and between about 250 K and 700 K it has $C_V = (5/2)R$, thus behaving like a rotating rigid

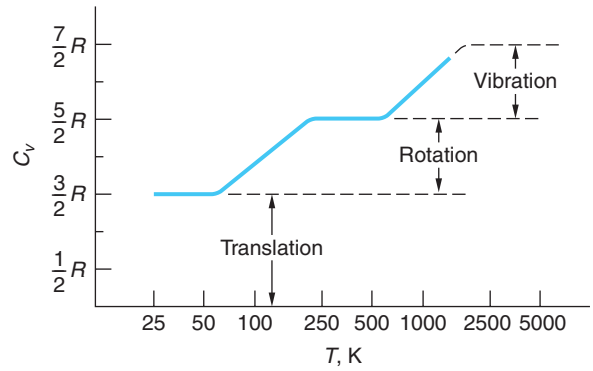

Figure 8-11 Temperature dependence of molar heat capacity of H_2. Between about 250 and 750 K, C_V is $(5/2)R$, as predicted by the rigid-dumbbell model. At low temperatures, C_V is only $(3/2)R$, as predicted for a nonrotating molecule. At high temperatures C_V seems to be approaching $(7/2)R$, as predicted for a dumbbell model that rotates and vibrates, but the molecule dissociates before this plateau is reached.

STUDENTS-HUB.com Uploaded By: Malak Obaid

dumbbell. At very high temperatures H_2 begins to vibrate, but the molecule dissociates before C_V reaches $(7/2)R$. Other diatomic gases show similar behavior except that at low temperatures they liquefy before C_V reaches $(3/2)R$. The failure of the equipartition theorem to account for these observations occurs because classical mechanics itself fails when applied to atoms and molecules. As we will see, it must be replaced by quantum mechanics.

C_V for Solids

The equipartition theorem is also useful in understanding the heat capacity of solids. In 1819 P. Dulong and A. Petit pointed out that the molar heat capacity of most solids was very nearly equal to 6 cal/K-mol $\approx 3R$. This result was used by them to obtain unknown molecular weights from the experimentally determined heat capacities. The empirical *Dulong-Petit law* is easily derived from the equipartition theorem by assuming that the internal energy of a solid consists entirely of the vibrational energy of the molecules (see Figure 8-12). If the force constants in the x, y, and z directions are κ_1, κ_2, and κ_3, respectively, the vibrational energy of each molecule is

$$E = \tfrac{1}{2}mv_x^2 + \tfrac{1}{2}mv_y^2 + \tfrac{1}{2}mv_z^2 + \tfrac{1}{2}\kappa_1 x^2 + \tfrac{1}{2}\kappa_2 y^2 + \tfrac{1}{2}\kappa_3 z^2$$

Since there are six squared terms, the average energy per molecule is $6(\frac{1}{2}\,kT)$, and the total energy of 1 mole is $3N_A kT = 3RT$, giving $C_V = 3R$.

At high temperatures, all solids obey the Dulong-Petit law. For temperatures below some critical value, C_V drops appreciably below the value of $3R$ and approaches zero as T approaches zero. The critical temperature is a characteristic of the solid. It is lower for soft solids such as lead than for hard solids such as diamond. The temperature dependence of C_V for several solids is shown in Figure 8-13.

The fact that C_V for metals is not appreciably different from that for insulators is puzzling. The classical model of a metal is moderately successful in describing the conduction of electricity and heat. It assumes that approximately one electron per atom is free to move about the metal, colliding with the atoms much as the molecules do in a gas. According to the equipartition theorem, this "electron gas" should have an average kinetic energy of $(3/2)kT$ per electron; thus, the molar heat capacity should be about $(3/2)R$ greater for a conductor than for an insulator. Although the molar heat capacity for metals is slightly greater than $3R$ at very high temperatures, the difference is much less than the $(3/2)R$ predicted for the contribution of the electron gas.

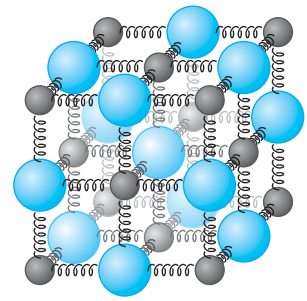

Figure 8-12 Simple model of a solid consisting of atoms connected to each other by springs. The internal energy of the solid then consists of kinetic and potential vibrational energy.

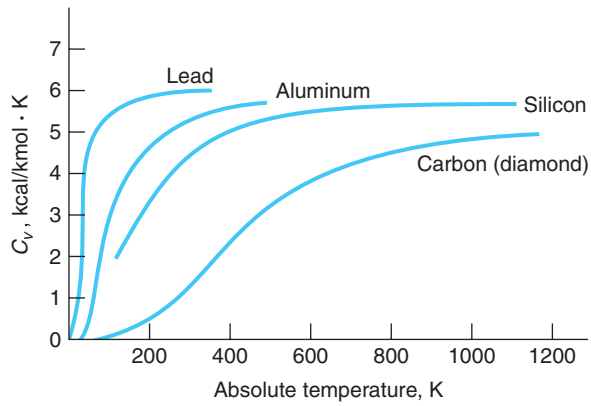

Figure 8-13 Temperature dependence of molar heat capacity of several solids. At high temperatures C_V is $3R$, as predicted by the equipartition theorem. However, at low temperatures C_V approaches zero. The critical temperature at which C_V becomes nearly $3R$ is different for different solids.

STUDENTS-HUB.com Uploaded By: Malak Obaid

The Boltzmann distribution and statistical mechanics were enormously successful in predicting the observed thermal properties of physical systems; however, the failure of the theory to account correctly for the heat capacities of gases and solids was a serious problem for classical physics, constituting as it did a failure of classical mechanics itself. The search for an understanding of specific heats was instrumental in the discovery of energy quantization in the early years of the twentieth century. The following sections show how quantum mechanics provides a basis for the complete understanding of the experimental observations.

EXAMPLE 8-5 **Broadening of Spectral Lines** In Chapter 5 we saw that spectral lines emitted by atoms had a certain natural width due to the uncertainty principle. However, in luminous gases, such as sodium and mercury vapor lamps and the visible surface of the Sun, the atoms are moving with the Maxwell velocity distribution. The velocity distribution results in a Doppler effect that Rayleigh showed was proportional to the Boltzmann factor and led to a broadening Δ of spectral lines equal to

$$\Delta = 0.72 \times 10^{-6} \lambda \sqrt{T/M}$$

where λ is the wavelength of the line, T is the absolute temperature, and M is the molecular weight. From this, compute the velocity (Doppler) broadening of the hydrogen H_α line emitted by H atoms at the surface of the Sun, where $T = 5800$ K.

SOLUTION

The wavelength of the H_α line is 656.3 nm and the atomic weight of H is 1, so

$$\Delta = 0.72 \times 10^{-6} \times 656.3 \sqrt{5800/1} = 0.036 \text{ nm}$$

For comparison, the natural width of the H_α line is about 0.0005 nm. Note that the effect of the pressure of the gas in causing spectral line broadening via collisions is also an important factor and, in fact, at high pressures, is the dominant cause. Collisions reduce the level lifetime, hence broaden the energy width (uncertainty principle). This is the reason that the Sun's visible spectrum is a continuous one.

8-2 Quantum Statistics

Bose-Einstein and Fermi-Dirac Distributions

The classical systems that were the subject of Section 8-1 consisted of identical but distinguishable particles. They were treated like billiard balls: exactly the same as one another but with numbers painted on their sides. Indeed, that was the point of the first assumption on the first page of the kinetic theory review in the Classical Concept Review on the Web site. However, the wave nature of particles in quantum mechanics prevents identical particles from being distinguished from one another. The finite extent and the overlap of wave functions makes identical particles indistinguishable. Thus, if two identical particles 1 and 2 pass within a de Broglie wavelength of each other in some event, we cannot tell which of the emerging particles is 1 and which is 2—i.e., we cannot distinguish between the several possible depictions of the event in Figure 8-14. The treatment of classical particles that led to the Boltzmann distribution can be extended to systems containing large numbers of identical indistinguishable particles.

STUDENTS-HUB.com Uploaded By: Malak Obaid

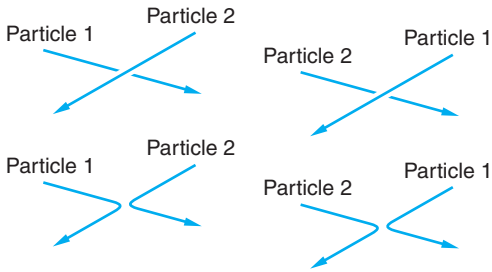

Figure 8-14 The wave nature of quantum-mechanical particles prevents us from determining which of the four possibilities shown actually occurred when the two identical, indistinguishable particles passed within a de Broglie wavelength of each other.

The first such theoretical treatment for particles with zero or integer spins—i.e., those that do not obey the exclusion principle, such as helium atoms (spin 0) and photons (spin 1), was done by Bose[6] in 1924, when he realized that the Boltzmann distribution did not adequately account for the behavior of photons. Bose's new statistical distribution for photons was generalized to massive particles by Einstein shortly thereafter. The resulting distribution function, called the *Bose-Einstein distribution* $f_{BE}(E)$, is given by

$$f_{BE}(E) = \frac{1}{e^{\alpha}e^{E/kT} - 1} \qquad \textbf{8-24}$$

where e^{α} is a system-dependent normalization constant. Particles whose statistical distributions are given by Equation 8-24 are called *bosons*.

Following the discovery of electron spin and Dirac's development of relativistic wave mechanics for spin-$\frac{1}{2}$ particles, Fermi[7] and Dirac[8] completed the statistical mechanics for quantum mechanical particles by deriving the probability distribution for large ensembles of identical indistinguishable particles that obey the exclusion principle. The result is called the *Fermi-Dirac distribution* $f_{FD}(E)$ and is given by

$$f_{FD}(E) = \frac{1}{e^{\alpha}e^{E/kT} + 1} \qquad \textbf{8-25}$$

where, again, e^{α} is a system-dependent normalization constant. Particles whose behavior is described by Equation 8-25 are called *fermions* or *Fermi-Dirac particles*.

Comparison of the Distribution Functions

We can write the Boltzmann distribution (Equation 8-1) in the form

$$f_B(E) = \frac{1}{e^{\alpha}e^{E/kT}} \qquad \textbf{8-26}$$

where the normalization constant A in Equation 8-1 is replaced by $e^{-\alpha}$. After doing so, one is immediately struck by the very close resemblance between the three distributions (Equations 8-24, 8-25, and 8-26), the Fermi-Dirac and Bose-Einstein probability functions differing from that of Boltzmann only by the ± 1 in the denominator. The question immediately arises as to the significance of this seemingly small difference. In particular, since integrals of the form $\int_0^{\infty} F(E)f_{BE}(E)\,dE$ and $\int_0^{\infty} F(E)f_{FD}(E)\,dE$ require the use of numerical methods for their solutions, it would be helpful to know if and under what conditions the Boltzmann distribution can be used for indistinguishable quantum-mechanical particles.

Enrico Fermi on a picnic in Michigan in July 1935. The bandage covers a cut on his forehead received when he accidentally hit himself with his racket while playing tennis.

STUDENTS-HUB.com Uploaded By: Malak Obaid

Let us first examine the physical meaning of the difference between the distributions. Consider a system of two identical particles, 1 and 2, one of which is in state n and the other in state m. As we discussed in Section 7-6, there are two possible single-particle-product solutions to the Schrödinger equation. They are

$$\psi_{nm}(1, 2) = \psi_n(1)\psi_m(2) \qquad \textbf{8-27}a$$

$$\psi_{nm}(2, 1) = \psi_n(2)\psi_m(1) \qquad \textbf{8-27}b$$

where the numbers 1 and 2 represent the space coordinates of the two particles. If the two identical particles are distinguishable from each other, i.e., if they are classical particles, then we can tell the difference between the two states represented by Equations 8-27a and 8-27b. However, for indistinguishable particles we have seen that the solutions must be the symmetric or antisymmetric combinations given in Section 7-6:

$$\psi_S = \frac{1}{\sqrt{2}}[\psi_n(1)\psi_m(2) + \psi_n(2)\psi_m(1)] \qquad \textbf{8-28}a$$

$$\psi_A = \frac{1}{\sqrt{2}}[\psi_n(1)\psi_m(2) - \psi_n(2)\psi_m(1)] \qquad \textbf{8-28}b$$

The factor $1/\sqrt{2}$ is the normalization constant. As we have discussed earlier (see Section 7-6), the antisymmetric function ψ_A describes particles that obey the exclusion principle, i.e., fermions. The symmetric function ψ_S describes indistinguishable particles that do not obey the exclusion principle, i.e., bosons.

Writing $\psi_A \equiv \psi_{FD}$ and $\psi_S \equiv \psi_{BE}$ to keep us reminded of the probability distributions followed by the fermions and bosons, respectively, let us now consider the probability that, if we look for the two particles, we will find them *both* in the same state, say state n. For two distinguishable particles Equations 8-27a and 8-27b both become

$$\psi_{nn}(1, 2) = \psi_{nn}(2, 1) = \psi_n(1)\psi_n(2) = \psi_n(2)\psi_n(1) = \psi_B \qquad \textbf{8-29}$$

where we have written $\psi_{nn}(1, 2) \equiv \psi_B$ to remind us that distinguishable particles follow the Boltzmann distribution. Thus, the probability density of finding both distinguishable particles in state n is

$$\psi_B^*\psi_B = \psi_n^*(1)\psi_n^*(2)\psi_n(1)\psi_n(2) \qquad \textbf{8-30}$$

Turning to indistinguishable particles, the wave function for two bosons both occupying state n is, from Equation 8-28a,

$$\psi_{BE} = \frac{1}{\sqrt{2}}[\psi_n(1)\psi_n(2) + \psi_n(2)\psi_n(1)] = \frac{2}{\sqrt{2}}\psi_n(1)\psi_n(2) \qquad \textbf{8-31}$$

and the probability density of finding both bosons in state n is then

$$\psi_{BE}^*\psi_{BE} = 2\psi_n^*(1)\psi_n^*(2)\psi_n(1)\psi_n(2) = 2\psi_B^*\psi_B \qquad \textbf{8-32}$$

Thus, the probability that both bosons would be found by an experiment to be occupying the same state is *twice* as large as for a pair of classical particles. This surprising discovery can be generalized to large ensembles of bosons as follows:

> The presence of a boson in a particular quantum state *enhances* the probability that other identical bosons will be found in the same state.

It is as if the presence of the boson attracts other identical bosons. Thus, the -1 that appears in the denominator of Equation 8-24 results physically in an increased

STUDENTS-HUB.com Uploaded By: Malak Obaid

probability that multiple bosons will occupy a given state, compared with the probability for classical particles in the same circumstances. The laser is the most common example of this phenomenon (see Chapter 9). We will consider another result of this intriguing behavior in Section 8-3.

If the two indistinguishable particles are fermions, the wave function for both occupying the same state is, as we have previously discussed in Section 7-6,

$$\psi_{FD} = \frac{1}{\sqrt{2}}[\psi_n(1)\psi_n(2) - \psi_n(2)\psi_n(1)] = 0 \qquad \textbf{8-33}$$

And, of course, the probability density $\psi^*_{FD}\psi_{FD} = 0$, also. This result, too, can be generalized to large ensembles of fermions as follows:

> The presence of a fermion in a particular quantum state *prevents* any other identical fermions from occupying the same state.

It is as if identical fermions actually repel one another. The $+1$ in the denominator of Equation 8-25 is thus due to the exclusion principle. We will consider consequences of this peculiar property of fermions further in Chapter 10. Figure 8-15 compares the distributions of bosons and fermions.

With the physical discussion above in mind, now let's compare the three functions. Figure 8-16 shows a comparison of the three distributions for $\alpha = 0$ over the energy range from zero up to $5kT$. Notice that for any given energy the f_{BE} curve for bosons lies above that for f_B for classical particles, reflecting the enhanced probability pointed out by Equation 8-32. Similarly, the f_{FD} curve for fermions lies below those for both f_{BE} and f_B, a consequence of the exclusion of identical fermions from states that are already occupied. Notice that Equations 8-24 and 8-25 both approach the Boltzmann distribution when $e^{\alpha} \gg e^{E/kT}$. For this situation $f_{BE}(E) \approx f_B(E) \ll 1$ and $f_{FD}(E) \approx f_B(E) \ll 1$. Thus, $f_{BE}(E)$ and $f_{FD}(E)$ both approach the classical Boltzmann distribution when the probability that a particle occupies the state with energy E is much less than 1. The same is also clearly the case when, for a given α, $E \gg kT$, as Figure 8-16 illustrates.

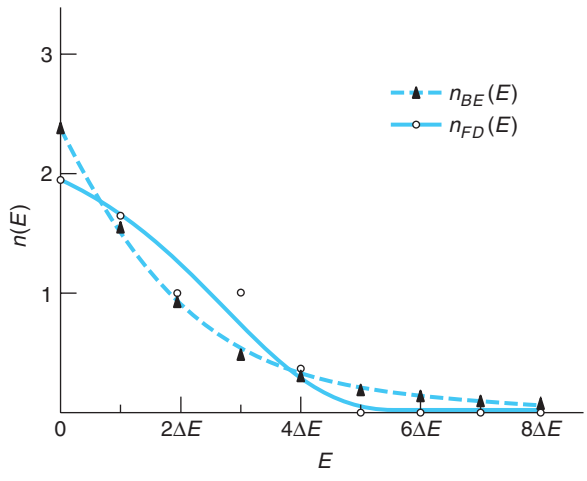

Figure 8-15 $n(E)$ versus E for a system of six identical, indistinguishable particles. $n_{BE}(E)$ is for particles with zero or integer spin (bosons). $n_{FD}(E)$ is for particles with $\frac{1}{2}$-integer spin (fermions). Compare with Figure 8-1.

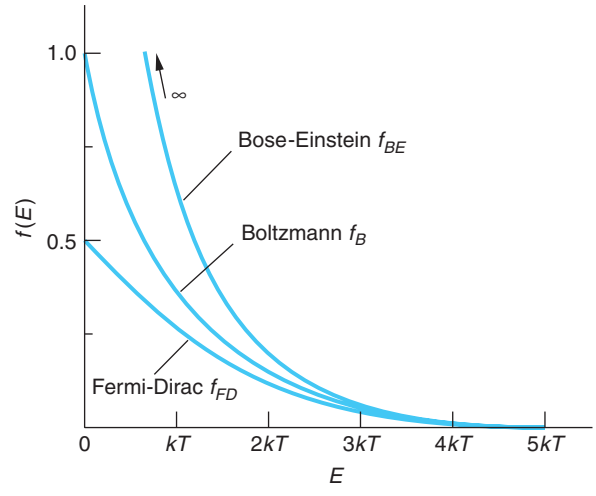

Figure 8-16 Graph of the distributions f_B, f_{BE}, and f_{FD} versus energy for the value $\alpha = 0$. f_{BE} always lies above f_B, which in turn is always above f_{FD}. All three distributions are approximately equal for energies larger than about 5 kT.

STUDENTS-HUB.com Uploaded By: Malak Obaid

At the beginning of this section we noted that identical quantum particles were rendered indistinguishable from one another by the overlap of their de Broglie waves. This provides another means of determining for a given system when the Boltzmann distribution may be used that can be shown to be equivalent to the $f_B(E) \ll 1$ condition above but that is sometimes easier to apply. If the de Broglie wavelength λ is much smaller than the average separation $\langle d \rangle$ of the particles, then we can neglect the overlap of the de Broglie waves, in which case the particles can be treated as if they were distinguishable:

$$\lambda \ll \langle d \rangle \qquad \textbf{8-34}$$

where

$$\lambda = \frac{h}{p} = \frac{h}{\sqrt{2mE_k}} = \frac{h}{\sqrt{2m(3kT/2)}} = \frac{h}{\sqrt{3mkT}} \qquad \textbf{8-35}$$

The average separation of the particles is $\langle d \rangle = (V/N)^{1/3}$, where N/V is the number of particles per unit volume in the system. Thus, the condition stated by Equation 8-34 becomes

$$\frac{h}{\sqrt{3mkT}} \ll \left(\frac{V}{N}\right)^{1/3}$$

which when cubed and rearranged becomes

$$\left(\frac{N}{V}\right)\frac{h^3}{(3mkT)^{3/2}} \ll 1 \qquad \textbf{8-36}$$

Equation 8-36 gives the condition under which the Boltzmann distribution can be used. Note that in general the condition requires low particle densities and high temperatures for particles of a given mass. The next example illustrates the application of the condition.

EXAMPLE 8-6 **Statistical Distribution of He in the Atmosphere** He atoms have spin 0 and hence are bosons. He makes up 5.24×10^{-6} of the molecules in the atmosphere. (*a*) Can the Boltzmann distribution be used to predict the thermal properties of atmospheric helium at $T = 273$ K? (*b*) Can it be used for liquid helium at $T = 4.2$ K?

SOLUTION

(*a*) N_A atoms of air occupy 2.24×10^{-2} m^3 at standard conditions. The number of He atoms per unit volume is then

$$\frac{N_A}{V} = \frac{6.02 \times 10^{23} \times 5.24 \times 10^{-6}}{2.24 \times 10^{-2}\ \text{m}^3} = 1.41 \times 10^{20}\ \text{molecules He/m}^3$$

The left side of Equation 8-36 is then

$$\frac{(1.41 \times 10^{20})(6.63 \times 10^{-34})^3}{(3 \times 1.66 \times 10^{-27} \times 4 \times 1.38 \times 10^{-23} \times 273)^{3/2}} = 6.3 \times 10^{-11} \ll 1$$

The behavior of the helium in the atmosphere can therefore be described by the Boltzmann distribution.

STUDENTS-HUB.com Uploaded By: Malak Obaid

(*b*) The density of liquid helium at its boiling point $T = 4.2$ K is 0.124 g/cm^3. The particle density N/V is then

$$\frac{N}{V} = \frac{N_A \text{ molecules}}{4 \text{ g}} \times (0.124 \text{ g/cm}^3) \times (10^2 \text{ cm/m})^3 = 1.87 \times 10^{28} \text{ He atoms/m}^3$$

The left side of Equation 8-36 is then

$$\frac{(1.87 \times 10^{28})(6.63 \times 10^{-34})^3}{(3 \times 1.66 \times 10^{-27} \times 4 \times 1.38 \times 10^{-23} \times 4.2)^{3/2}} = 4.39$$

which is *not* $\ll 1$. Therefore, the Boltzmann distribution does not adequately describe the behavior of liquid helium, so the Bose-Einstein distribution must be used.

Using the Distribution: Finding $n(E)$

In order to find the actual number of particles $n(E)$ with energy E, each of the three distribution functions given by Equations 8-24, 8-25, and 8-26 must be multiplied by the density of states, as indicated by Equation 8-2.

$$n_B(E) = g_B(E) f_B(E) \qquad \textbf{8-37}a$$

$$n_{BE}(E) = g_{BE}(E) f_{BE}(E) \qquad \textbf{8-37}b$$

$$n_{FD}(E) = g_{FD}(E) f_{FD}(E) \qquad \textbf{8-37}c$$

Finding $g(E)$ enables the constant e^{α} to be determined for particular systems from the normalization condition that we have used several times, namely, the total number of particles $N = \int_0^\infty n(E)\, dE$.

Density of States

As an example of determining $g(E)$, consider an equilibrium system of N classical particles confined in a cubical volume of side L. Treating the cube as a three-dimensional infinite square well, in Chapter 7 we found the energy of a particle in such a well to be

$$E_{n_1 n_2 n_3} = \frac{\hbar^2 \pi^2}{2mL^2}(n_1^2 + n_2^2 + n_3^2) \qquad \textbf{7-4}$$

which we will for the convenience of our present discussion write as

$$E_n = E_0(n_x^2 + n_y^2 + n_z^2) \qquad \textbf{8-38}$$

where x, y, and z replace 1, 2, and 3 and $E_0 = \hbar^2\pi^2/2mL^2$. The three quantum numbers n_x, n_y, and n_z specify the particular quantum state of the system. Recalling that $g(E)$ is the number of states with energy between E and $(E + dE)$, our task is to find an expression for the total number of states from zero energy up to E, then differentiate that result to find the number within the shell dE. This is made quite straightforward by (1) observing that Equation 8-38 is the equation of a sphere of radius $R = (E/E_0)^{1/2}$ in $n_x\, n_y\, n_z$ "space" and (2) recalling that the quantum numbers must be integers, each combination of which represents a particular energy and corresponds to a point in the "space." (See Figure 8-17.) Since the quantum numbers must all be positive, the "space" is confined to that octant of the sphere, as Figure 8-17 shows.

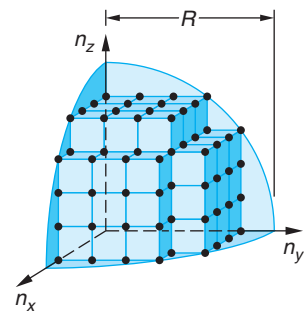

Figure 8-17 A representation of the allowed quantum states for a system of particles confined in a three-dimensional infinite square well. The radius $R \propto E^{1/2}$.

STUDENTS-HUB.com Uploaded By: Malak Obaid

The number of states N within radius R (equal to the number of different combinations of the quantum numbers) in the volume is given by

$$N = \left(\frac{1}{8}\right)\left(\frac{4\pi R^3}{3}\right) = \frac{\pi}{6}\left(\frac{E}{E_0}\right)^{3/2} \qquad \textbf{8-39}$$

The density of states in $n_x\, n_y\, n_z$ "space" is

$$g(E) = \frac{dN}{dE} = \frac{\pi}{4}E_0^{-3/2}E^{1/2} = \frac{(2m)^{3/2}L^3}{4\pi^2\hbar^3}E^{1/2} \qquad \textbf{8-40}$$

or

$$g(E) = \frac{(2m)^{3/2}V}{4\pi^2\hbar^3}E^{1/2} = \frac{2\pi(2m)^{3/2}V}{h^3}E^{1/2} \qquad \textbf{8-41}$$

where the volume $V = L^3$. If the particles were electrons, then each state could accommodate two (one with spin up and one with spin down) and the density of states $g_e(E)$ would be twice that given by Equation 8-41, or

$$g_e(E) = \frac{4\pi(2m_e)^{3/2}V}{h^3}E^{1/2} \qquad \textbf{8-42}$$

We can compute the constant e^{α} in the Boltzmann distribution for these two cases from the normalization condition

$$N = \int_0^\infty n_B(E)\,dE = \int_0^\infty g_B(E)f_B(E)\,dE = \int_0^\infty g_B(E)e^{-\alpha}e^{-E/kT}\,dE \qquad \textbf{8-43}$$

If the distinguishable particles are electrons, $g_B(E) = g_e(E)$ and we have that

$$N = e^{-\alpha}\frac{4\pi(2m_e)^{3/2}V}{h^3}\int_0^\infty E^{1/2}e^{-E/kT}\,dE$$

which, when evaluated, yields

$$N = \frac{2(2\pi m_e kT)^{3/2}V}{h^3}e^{-\alpha}$$

or

$$e^{-\alpha} = \frac{Nh^3}{2(2\pi m_e kT)^{3/2}V} \quad \text{or} \quad e^{\alpha} = \frac{2(2\pi m_e kT)^{3/2}V}{Nh^3} \qquad \textbf{8-44}$$

For particles that do not obey the exclusion principle, the 2 multiplying the parentheses in Equation 8-44 is not present. Note that $e^{-\alpha}$ depends upon the number density of particles N/V. Note too that $e^{-\alpha}$ is essentially the quantity on the left side of Equation 8-36, which was obtained from de Broglie's relation for classical particles. Thus, the test for when the Boltzmann distribution may be used given by Equation 8-36 is equivalent to the condition that $e^{-\alpha} \ll 1$.

STUDENTS-HUB.com Uploaded By: Malak Obaid

Questions

5. How can identical particles also be distinguishable classically?
6. What are the physical conditions under which the Boltzmann distribution holds for a system of particles?
7. Do the opposite spins of two electrons in the same state make them distinguishable from each other?
8. How would you characterize a boson? A fermion?

8-3 The Bose-Einstein Condensation

We saw in Section 8-2 that, for ordinary gases, the Bose-Einstein distribution differs very little from the classical Boltzmann distribution, basically because there are many quantum states per particle due to the low density of gases and the large mass of the particles. However, for liquid helium, there is approximately one particle per quantum state at very low temperatures, and the classical distribution is invalid, as was illustrated in Example 8-6. The somewhat daring idea that liquid helium can be treated as an ideal gas obeying the Bose-Einstein distribution was suggested in 1938 by F. London in an attempt to understand the amazing properties of helium at low temperatures. When liquid helium is cooled, several remarkable changes take place in its properties at a temperature of 2.17 K. In 1924, H. Kamerlingh Onnes and J. Boks measured the density of liquid helium as a function of temperature and discovered a cusp in the curve at that temperature, as illustrated in Figure 8-18. In 1928, W. H. Keesom and M. Wolfke suggested that this discontinuity in the slope of the curve was an indication of a phase transition. They used the terms "helium I" for the liquid above 2.17 K, called the *lambda point* (see Figure 8-19), and "helium II" for the liquid below that temperature. In London's theory, called the two-fluid model, helium II is imagined to consist of two parts, a normal fluid with properties similar to helium I and a superfluid (i.e., a fluid with viscosity ≈ 0) with quite different properties. The density of liquid helium II is the sum of the densities of the normal fluid and the superfluid:

$$\rho = \rho_s + \rho_n \qquad \textbf{8-45}$$

As the temperature is lowered from the lambda point, the fraction consisting of the superfluid increases and that of the normal fluid decreases until, at absolute zero, only the superfluid remains. The superfluid corresponds to the helium atoms being in the lowest possible quantum state, the ground state. These atoms are not excited to higher states, so the superfluid cannot contribute to viscosity. When the viscosity of helium II is measured by the rotating disk method (a standard technique for measuring the viscosity of liquids), only the normal-fluid component exerts a viscous force on the disk. As the

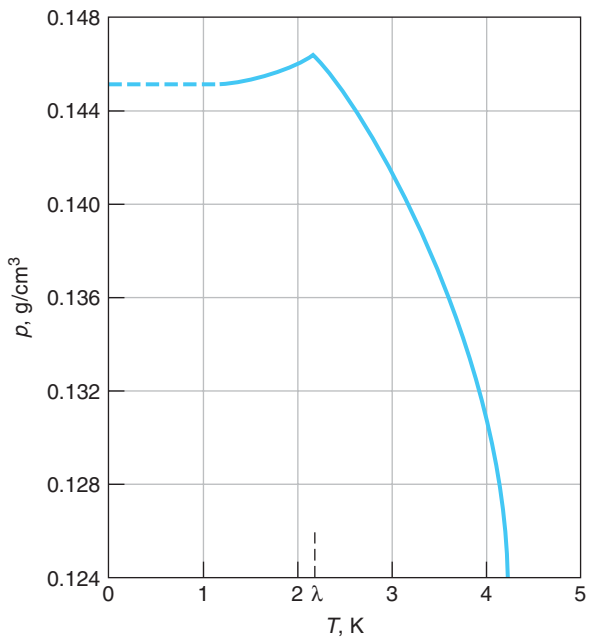

Figure 8-18 Plot of density of liquid helium versus temperature, by Kamerlingh Onnes and Boks. Note the discontinuity at 2.17 K. [*From F. London, Superfluids (New York: Dover Publications, Inc., 1964). Reprinted by permission of the publisher.*]

STUDENTS-HUB.com Uploaded By: Malak Obaid

temperature is lowered, the fraction of helium in the normal component decreases from 100 percent at the lambda point to 0 percent at $T = 0$ K; thus, the viscosity decreases rapidly with temperature in agreement with experiment.

It is not at all obvious that liquid helium should behave like an ideal gas, because the atoms do exert forces on each other. However, these are weak van der Waals forces (to be discussed in Chapter 9), and the fairly low density of liquid helium (0.145 g/cm^3 near the lambda point) indicates that the atoms are relatively far apart. The ideal gas model is therefore a reasonable first approximation. It is used mainly because it is relatively simple and because it yields qualitative insight into the behavior of this interesting fluid.

EXPLORING
Liquid Helium

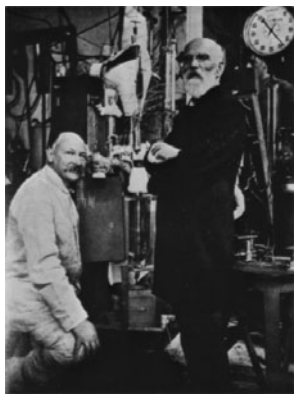

H. Kamerlingh Onnes and J. D. Van der Waals by the helium liquefier in the Kamerlingh Onnes Laboratory in Leiden in 1911. [*Courtesy of the Kamerlingh Onnes Laboratory.*]

Liquid helium, because of its extremely low boiling temperature, is the standard coolant for superconducting magnets throughout the world. Medical diagnostic MRI systems use such magnets. The large particle accelerators at, e.g., CERN and Fermilab use hundreds of them (see Chapter 11).

In a classic experiment conducted in 1908, H. Kamerlingh Onnes[9] succeeded in liquefying helium, condensing the last element that had steadfastly remained in gaseous form and culminating a determined effort that had consumed nearly a quarter of a century of his life. Even then, he nearly missed seeing it. After several hours of cooling, the temperature of the helium sample, being measured by a constant-volume helium gas thermometer, refused to fall any further. The liquid hydrogen being used to precool the system was gone, and it appeared that the experiment had failed when one of the several interested visitors gathered in Kamerlingh Onnes's lab suggested that perhaps the temperature was steady because the thermometer was immersed in boiling liquid that was so completely transparent as to be very hard to see. At the visitor's suggestion, a light was shined from below onto the glass sample vessel and the gas-liquid interface became clearly visible! Condensation to the very low-density, transparent liquid had occurred at 4.2 K.

The liquid helium must have been boiling vigorously. Soon afterward Kamerlingh Onnes was able to reduce the temperature further, passing below 2.17 K, at which point the vigorous boiling abruptly ceased. He must have observed the sudden cessation of the violent boiling, yet he made no mention of it then or in the reports of any of his many later experiments. Indeed, it was another quarter century before any mention of this behavior would appear in the literature,[10] even though many investigators must have surely seen it. The abrupt halt in boiling at 2.17 K signaled a phase transition in which helium changed from a normal fluid to a *superfluid*, that is, bulk matter that flows essentially without resistance (viscosity ≈ 0). Of all the elements, only the two naturally occurring isotopes of helium exhibit this property. The transition to the superfluid phase in ^{4}He occurs at 2.17 K. In ^{3}He, which accounts for only 1.3×10^{-4} percent of natural helium, the transition occurs at about 2 mK. This transition should not be interpreted as due in some way to a peculiarity in the structure of helium. Liquid phases of other bosons do not become superfluids because all other such systems solidify at temperatures well above the critical temperature for Bose-Einstein condensation. Only helium remains liquid under its vapor pressure at temperatures approaching absolute zero.[11] The fundamental reason that it does not solidify is that the interaction potential energy (see Section 9-3) between helium molecules is quite weak. Since helium atoms have small mass, their zero-point motion (i.e., their motion in the lowest-allowed energy level—see Section 5-6) is large, in fact, so large that its kinetic energy exceeds the interaction potential energy, thus melting the solid at low pressure. It is the superfluid phase of ^{4}He that we will be referring to throughout the remainder of this section. It turns out that ^{3}He becomes a superfluid for a different reason. (*Hint:* ^{4}He has spin 0, hence is a boson; ^{3}He has spin $\frac{1}{2}$ and is thus a fermion.)

STUDENTS-HUB.com Uploaded By: Malak Obaid

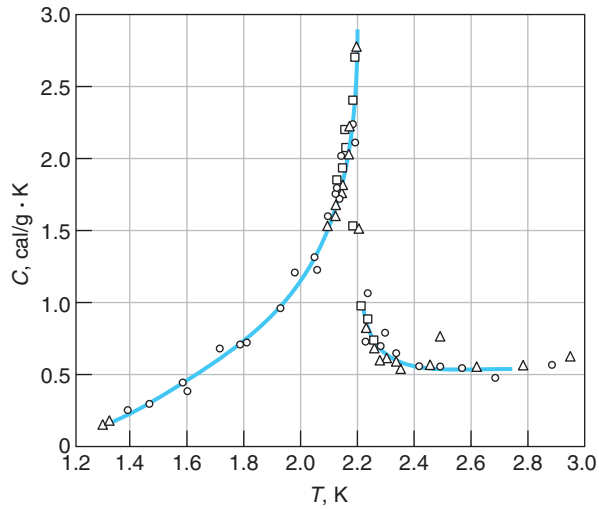

Figure 8-19 Specific heat of liquid helium versus temperature. Because of the resemblance of this curve to the Greek letter λ, the transition point is called the lambda point. [*From F. London, Superfluids (New York: Dover Publications, Inc., 1964). Reprinted by permission of the publisher.*]

Experimental Characteristics of Superfluid ^{4}He

In 1932 W. Keesom and K. Clusius measured the specific heat as a function of temperature and made a dramatic discovery of an enormous discontinuity, obtaining the curve shown in Figure 8-19. Because of the similarity of this curve to the Greek letter λ, the transition temperature 2.17 K is called the *lambda point*. Figure 8-20 shows this same curve measured with much greater resolution. Just above the lambda point, He boils vigorously as it evaporates. The bubbling immediately ceases at the lambda point, although evaporation continues. This effect is due to the sudden large increase in the thermal conductivity at the lambda point. In normal liquid helium, like other liquids, the development of local hot spots causes local vaporization, resulting in the formation of bubbles. Below the lambda point the thermal conductivity becomes so large, dissipating heat so rapidly, that local hot spots cannot form. Measurements of thermal conductivity show that helium II conducts heat better than helium I by a factor of more than a million; in fact, helium II is a better heat conductor than any metal, exceeding that of copper at room temperature by a factor of 2000. This conduction process is different from ordinary heat conduction, for the rate of conduction is not proportional to the temperature difference. Bubble formation ceases (even though evaporation continues) because all parts of the fluid are at exactly the same temperature.

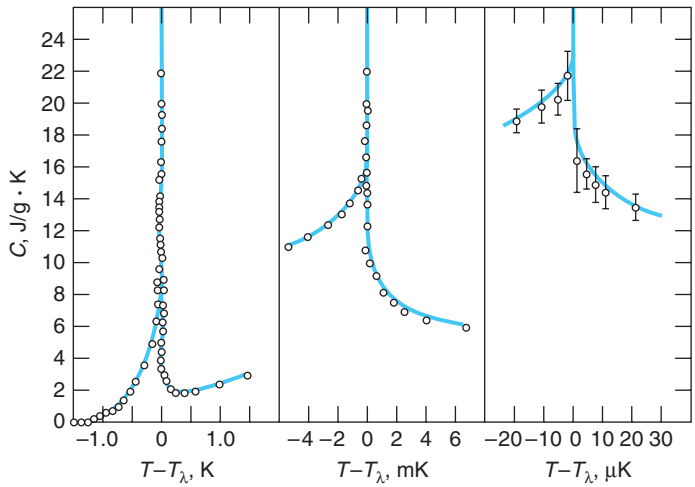

Figure 8-20 The lambda point with high resolution. The specific heat curve maintains its shape as the scale is expanded. [*From M. J. Buckingham and W. M. Fairbank, "The Nature of the λ-Transition," Progress in Low Temperature Physics, edited by C. J. Gorter, Vol. III, (Amsterdam: North-Holland Publishing Company, 1961).*]

STUDENTS-HUB.com Uploaded By: Malak Obaid

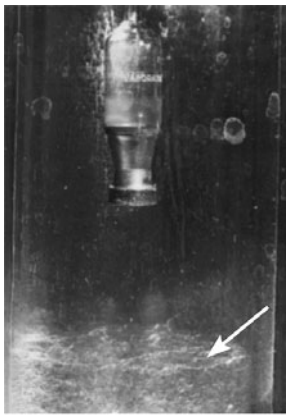

(*a*)

(*b*)

Figure 8-21 (*a*) Liquid helium being cooled by evaporation just above the lambda point boils vigorously. (*b*) Below the lambda point the boiling ceases and the superfluid runs out through the fine pores in the bottom of the vessel suspended above the helium bath. [*Courtesy of Clarendon Laboratory. From K. Mendelssohn, The Quest for Absolute Zero: The Meaning of Low Temperature Physics, World University Library (New York: McGraw-Hill Book Company, 1966).*]

This lambda-point transition is clearly visible on the surface of the liquid shown in Figures 8-21*a* and *b*, which also illustrates the phenomenon largely responsible for applying the name *superfluid* to helium II. The small container of liquid helium suspended above the surface has a bottom made of tightly packed, ultrafine powder (fine emery powder or jeweler's rouge). The microscopic channels through the powder are too small for the ordinary liquid to pass through, but when the temperature drops below the lambda point, the superfluid flows through essentially unimpeded, the viscosity suddenly dropping at that point by a factor of about one million.[12]

Figures 8-22*a* and *b* illustrate the *creeping film* effect. A container containing liquid helium has a thin film (several atomic layers thick) of helium vapor coating the walls, just as is the case with any other enclosed liquid. However, if the level of liquid helium in the container is raised above the general level in the reservoir, such as the cup in the photo of Figure 8-22*a*, the superfluid film on the walls creeps up the inner walls, over the top, and down the outside and returns to the reservoir until both surfaces are level or the cup is empty! In the *thermomechanical effect*, which involves two containers of liquid helium II connected by a superleak, if heat is added to one side, e.g., by a small heater as illustrated in Figure 8-23*a*, the superfluid on the other side migrates *toward* the heated side, where the level of liquid (still superfluid) rises. If the system is suitably arranged, as in Figure 8-23*b*, the rising liquid can jet out a fine capillary in the so-called *fountain effect*.[13]

Superfluid ^{3}He

Physicists thought for a long time that ^{3}He could not form a superfluid since its nucleus consists of two protons and a neutron. It thus has $\frac{1}{2}$-integer spin and obeys Fermi-Dirac statistics, which prohibits such particles from sharing the same energy state. However, early in the 1970s D. M. Lee, D. D. Osheroff, and R. C. Richardson showed that when cooled to 2.7 mK, the spins of *pairs* of ^{3}He atoms can align parallel, creating, in effect, a boson of spin 1 and allowing the liquid to condense to a superfluid state. Two additional superfluid states were subsequently discovered, a spin-0 state (antiparallel spins) at 1.8 mK and a second spin-1 state that is created when an external magnetic field aligns the spins of the ^{3}He pairs. The three scientists received the 1996 Nobel Prize for their discovery.

(*a*)

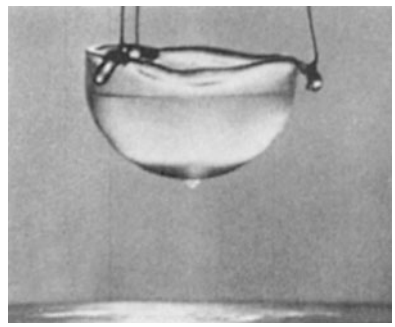

(*b*)

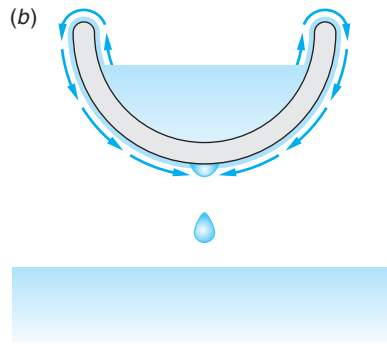

Figure 8-22 (*a*) The creeping film. The liquid helium in the dish is at a temperature of about 1.6 K. A thin film creeps up the sides of the dish, over the edge, and down the outside to form the drop shown, which then falls into the reservoir below. [*Courtesy of A. Leitner, Rensselaer Polytechnic Institute.*] (*b*) Diagram of creeping film. If the dish is lowered until partially submerged in the reservoir, the superfluid creeps out until the levels in the dish and reservoir are the same. If the level in the cup is initially lower than that of the reservoir, superfluid creeps into the dish.

STUDENTS-HUB.com Uploaded By: Malak Obaid

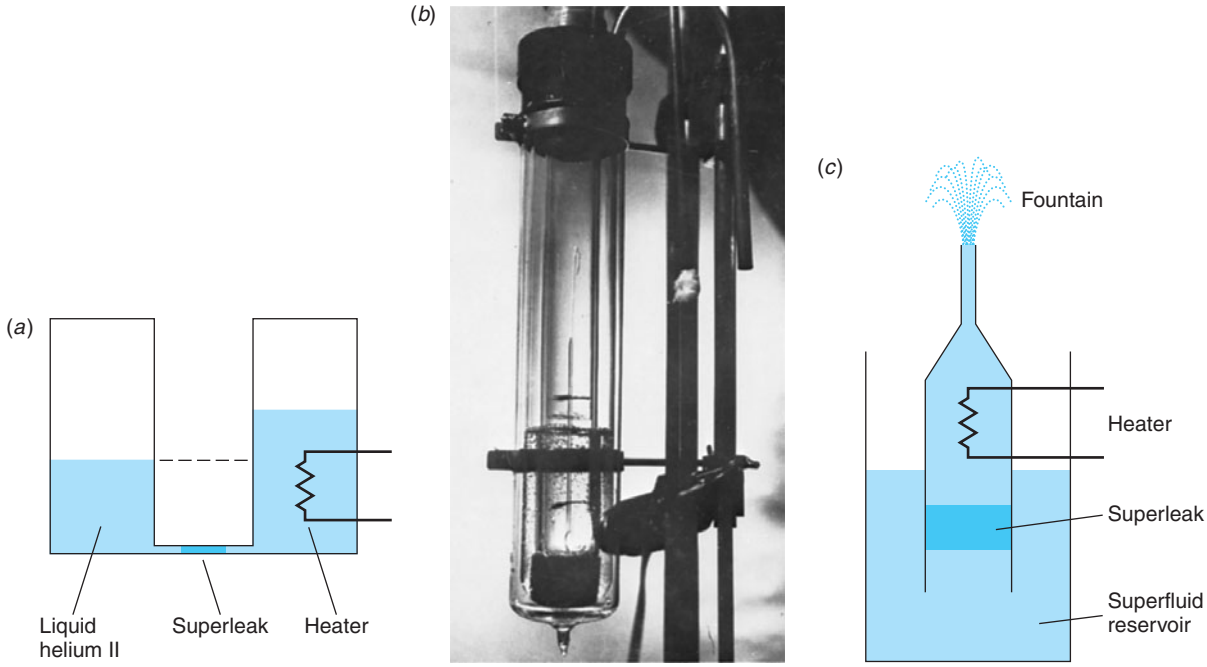

Figure 8-23 (*a*) Diagram of the thermomechanical effect. The level of the fluid rises in the container where the heat is being added. (*b*) A bulb containing liquid helium is in a cold bath of liquid helium II at 1.6 K. When light containing infrared radiation is focused on the bulb, liquid helium rises above the ambient level. The height of the level depends on the narrowness of the tube. If the tube is packed with powder and the top drawn out into a fine capillary, the superfluid spurts out in a jet as shown, hence the name "fountain effect." (*c*) Diagram showing the components in the photograph in (*b*). [*Photo courtesy of Helix Technology Corporation.*]

In the Bose-Einstein distribution the number of particles in the energy range dE is given by $n(E)dE$, where we have from Equation 8-37*b*

$$n(E) = \frac{g(E)}{e^{\alpha}e^{E/kT} - 1} \qquad \textbf{8-46}$$

where $g(E)$ is given by Equation 8-41. The constant α, which is determined by normalization, cannot be negative, for if it were, $n(E)$ would be negative for low values of E. This situation would make no sense physically since, if α were negative for small energies (i.e., $|\alpha| > E/kT$), then $f_{BE}(E)$ would be negative. But $f_{BE}(E)$ is the number of particles in the state with energy E, and a negative value would be meaningless. The normalization condition is

$$N = \int_0^{\infty} n(E)\,dE = \frac{2\pi V}{h^3}(2m)^{3/2}\int_0^{\infty}\frac{E^{1/2}\,dE}{e^{\alpha}e^{E/kT} - 1} = \frac{2\pi V}{h^3}(2mkT)^{3/2}\int_0^{\infty}\frac{x^{1/2}\,dx}{e^{\alpha+x} - 1} \qquad \textbf{8-47}$$

where $x = E/kT$ and the integral in this equation is a function of α.

The usual justification for using a continuous energy distribution to describe a quantum system with discrete energies is that the energy levels are numerous and closely spaced. In this case, as we have already seen, for a gas of N particles in a macroscopic box of volume V (the container), this condition holds, as you can demonstrate for yourself by computing the spacing using Equation 7-4 for a three-dimensional box.

STUDENTS-HUB.com Uploaded By: Malak Obaid

However, in replacing the discrete distribution of energy states by a continuous distribution, we ignore the ground state. This is apparent from Equation 8-41, where we see that $g(E) \propto E^{1/2}$ therefore, if $E = 0$, $g(E) = 0$ also. This has little effect for a gas consisting of Fermi-Dirac particles since there can be only two particles in any single state, and ignoring two particles out of 10^{22} causes no difficulty. In a Bose-Einstein gas, however, there can be any number of particles in a single state. If we ignore the ground state, as we have up to now, the normalization condition expressed by Equation 8-47 cannot be satisfied below some minimum critical temperature T_c corresponding to the minimum possible value of α, $\alpha = 0$. This implies that at very low temperatures there are a significant number of particles in the ground state.

The critical temperature T_c can be found by evaluating Equation 8-47 numerically. The integral has a maximum value of 2.315 when α has its minimum value of 0. This results in a maximum value for N/V given by

$$\frac{N}{V} \leq \frac{2\pi}{h^3}(2mkT)^{3/2}(2.315)$$

Since N/V is determined by the density of liquid helium, this implies a value for the critical temperature, given by

$$T \geq \frac{h^2}{2mk}\left[\frac{N}{2\pi(2.315)V}\right]^{2/3} = T_c \qquad \textbf{8-48}$$

Inserting the known constants and the density of helium, we find for the critical temperature

$$T_c = 3.1 \text{ K} \qquad \textbf{8-49}$$

For temperatures below 3.1 K the normalization Equation 8-47 cannot be satisfied for any value of α. Evidently at these temperatures there are a significant number of particles in the ground state, which we have not included.

We can specifically include the ground state by replacing Equation 8-47 with

$$N = N_0 + \frac{2\pi V}{h^3}(2mkT)^{3/2}\int_0^\infty \frac{x^{1/2}\,dx}{e^{\alpha+x} - 1} \qquad \textbf{8-50}$$

where N_0 is the number in the ground state. If we choose $E_0 = 0$ for the energy of the ground state, this number is

$$N_0 = \frac{g_0}{e^\alpha e^{E_0/kT} - 1} = \frac{1}{e^\alpha - 1} \qquad \textbf{8-51}$$

where g_0, the density of states or statistical weight, is 1 for a single state. We see that N_0 becomes large as α becomes small. With the inclusion of N_0, which depends on α, the normalization condition (Equation 8-50) can be met and α can be computed numerically for any temperature and density. For temperatures below the critical temperature T_c we see from Equation 8-51 that $e^\alpha = 1 + 1/N_0$. Expanding e^α for small α yields $e^\alpha = 1 + \alpha + \ldots$, and we thus conclude that α is of the order of N_0^{-1} and that the fraction of molecules in the ground state is given approximately by

$$\frac{N_0}{N} \approx 1 - \left(\frac{T}{T_c}\right)^{3/2} \qquad \textbf{8-52}$$

STUDENTS-HUB.com Uploaded By: Malak Obaid

In the London two-fluid model the N_0 atoms that we added in Equation 8-50 have condensed to the ground state. These particles in the ground state constitute the superfluid. The remaining $(N - N_0)$ atoms are the normal fluid. That fraction of the fluid that is superfluid for $T \leq T_c$ is shown in Figure 8-24.

The value $T_c = 3.1$ K is not very different from the observed lambda-point temperature $T = 2.17$ K, especially considering that our calculation is based on the assumption that the liquid helium is an ideal gas. The process of atoms dropping into the ground state as the temperature is lowered below T_c is called *Bose-Einstein condensation*. Such an occurrence was predicted by Einstein in 1924, before there was any evidence that such a process could occur in nature.

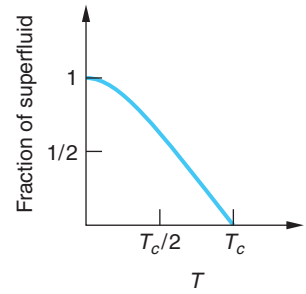

Figure 8-24 Graph of the fraction of superfluid in a sample of liquid helium as a function of temperature.

The Bose-Einstein Condensate

Like all atoms, the constituents of ^{4}He (protons, neutrons, and electrons) are fermions; however, they are assembled in such a way that the total spin of the ground state is integer (zero), so that the ^{4}He *atom* is a boson. Indeed, a review of the periodic table shows that, although atoms can be either fermions or bosons, the ground-state spins are mostly integer, so in their lowest energy state most atoms are bosons. This fact is of no great consequence in determining the properties of a gas in a macroscopic container because the spacing between the quantized energies is extremely small, so the probability that any particular level is occupied by an atom is also small. For example, the spacing between adjacent levels in a cubical box with a volume of 1 cm^3 containing sodium gas is about 10^{-20} eV (see Equation 8-38), so even at relatively low temperatures the atoms in a sample of a few billion would be widely spread among the allowed levels, as in Figure 8-25*a*. In addition, the average distance between atoms in the box would be about $(10^{-6}\ \text{m}^3/10^9\ \text{atoms})^{1/3} = 10^{-5}$ m, or tens of thousands of atomic diameters, so the interactions between the atoms are minuscule.

If our goal is to form a Bose-Einstein condensate (BEC) from the widely separated atomic bosons of the gas sample in the box, the obvious approach is that used to condense any gas; that is, the sample is cooled and the density is increased until the gas liquefies. However, this approach presents us with a formidable problem: as the gas liquefies, the atoms get very close together, the density approximating that of the solid. The atoms now interact strongly, mainly via their outer electrons, and thus all begin to act like fermions! (This is essentially what happens in liquid helium II, where even at very low temperatures the fraction of the atoms in the ground state [superfluid phase] is only about 10 percent or so.)

This problem was solved by C. E. Wieman and E. Cornell in 1995, more than 70 years after Einstein's prediction. They did it by forming the BEC directly from a supersaturated vapor, cooling the sample but never allowing it to reach ordinary thermal equilibrium.[14] This was done with standard cooling methods and a very neat "trick." First, a sample of rubidium vapor at room temperature was illuminated by the beams from six small diode

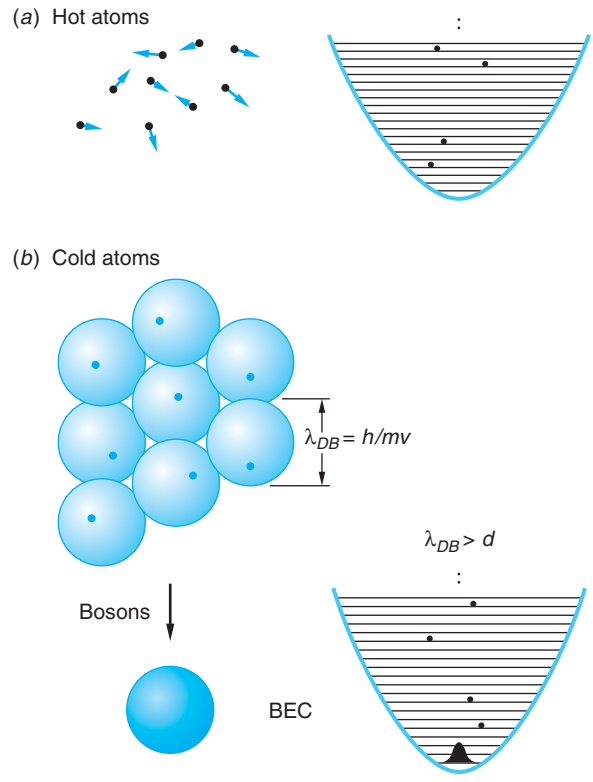

Figure 8-25 (*a*) The atoms in a sample of dilute gas in any macroscopic container are distributed over a very large number of levels, making the probability of any one level being occupied quite small. (*b*) Cooled to the point where the de Broglie wavelength becomes larger than the interatomic spacing, atoms fall into the ground state, all occupying the same region of space.

STUDENTS-HUB.com Uploaded By: Malak Obaid

lasers of appropriate frequency. Collisions of the laser photons with atoms in the low-speed tail of the Maxwell distribution (see Figure 8-3) slowed those atoms, and within a second or two a sample of about 10^7 atoms collected in the volume defined by the intersecting laser beams, about 1.5 cm in diameter. The temperature of this laser-cooled sample was about 1 mK. Then a special magnetic trap (i.e., a magnetic field shaped so as to confine the atoms) was used to "squeeze" the cooled sample, whose atomic spins ($= 2\hbar$) had been polarized in the $m = 2$ direction. (Polarizing the spins was the "trick" referred to above. Equilibrium is reached in the spin-polarized vapor very rapidly, long before the true thermal equilibrium state—the solid—can form, thus maintaining the sample as a supersaturated vapor.) The warmer atoms on the high-speed tail of the Maxwell distribution of the trapped atoms are allowed to escape through a "leak" in the magnetic trap, taking with them a substantial amount of the kinetic energy and evaporatively cooling the remaining few thousand atoms to less than 100 nK, just as water molecules evaporating from the surface of a cup of hot coffee cool that which remains in the cup. These remaining cold atoms fall into the ground state of the confining potential and have, within the experimental uncertainties, reached absolute zero. They are the condensate. The BEC is illustrated in Figure 8-25*b*. The condensate, if left undisturbed in the dark, lives for 15 to 20 seconds, its destruction eventually resulting from collisions with impurity atoms in the vacuum that are also colliding with the hot (room temperature) walls of the experimental cell. The peak in Figure 8-26 is a *macroscopic quantum wave function* of the condensate.

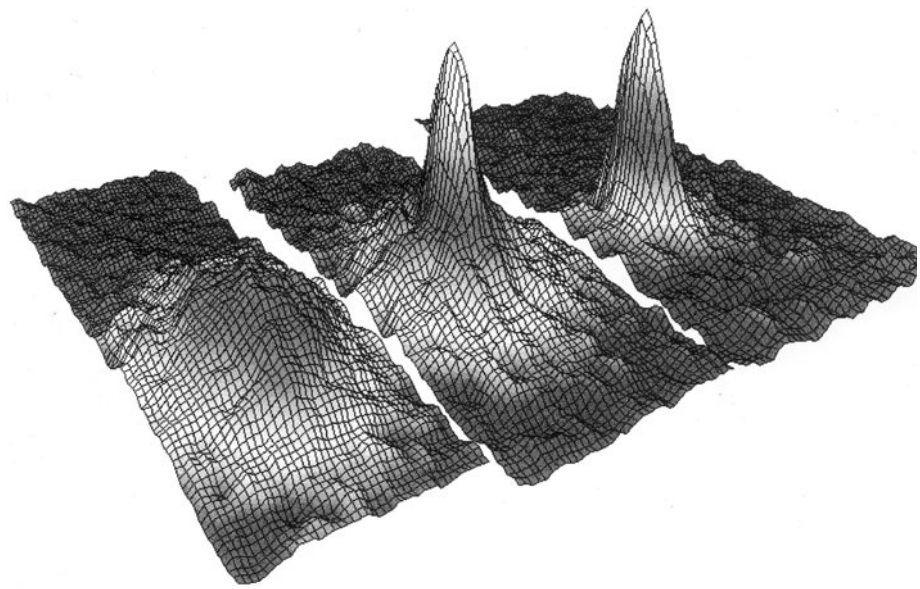

Figure 8-26 Two-dimensional velocity distributions of the trapped cloud for three experimental runs with different amounts of cooling. The axes are the x and z velocities, and the third axis is the number density of atoms per unit velocity-space volume. This density is extracted from the measured optical thickness of the shadow. The distribution on the left shows a gentle hill and corresponds to a temperature of about 200 nK. The middle picture is about 100 nK and shows the central condensate spire on the top of the noncondensed background hill. In the picture on the right, only condensed atoms are visible, indicating that the sample is at absolute zero, to within experimental uncertainty. The gray bands around the peaks are an artifact left over from the conversion of false-color contour lines into the present black and white. [*From C. E. Wieman, American Journal of Physics* ***64*** *(7), 853 (1996).*]

STUDENTS-HUB.com Uploaded By: Malak Obaid

Since the discovery by Wieman and Cornell, several other physicists have produced Bose-Einstein condensates. One of the largest produced (by W. Ketterle and co-workers) contained 9×10^7 sodium atoms, was about a millimeter long, and lived for half a minute. Its direct photograph is shown in Figure 8-27. As of this writing, the largest condensates are made of hydrogen and contain about 10^9 atoms.

Does this discovery have any potential use? The answer is, probably many that we can't even imagine yet, but here is one possibility. The BEC can form the basis of an *atomic laser*. This was demonstrated in late 1996, also by Ketterle and his colleagues, and is illustrated in Figure 8-28. The condensate is coherent matter, just as the laser beam is coherent light. It could place atoms on substrates with extraordinary precision, conceivably replacing microlithography in the production of microcircuitry. Here is another potential use for the BEC: It could form the basis for atomic interferometers, making possible measurements far more precise than those made with visible lasers since the de Broglie wavelengths are much shorter than those of light. Ketterle, Cornell, and Wieman shared the 2001 Nobel Prize in Physics for their work.

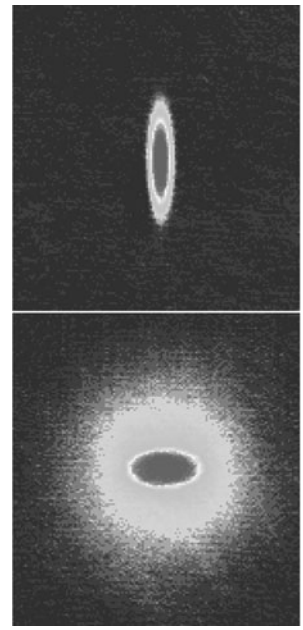

Figure 8-27 Successive images show shadow of a millimeter-long cloud of atoms containing Bose-Einstein condensate as it expands from its initial cigar shape (top). [*From D. S. Durfee, Science* ***272****, 1587 (1996).*]

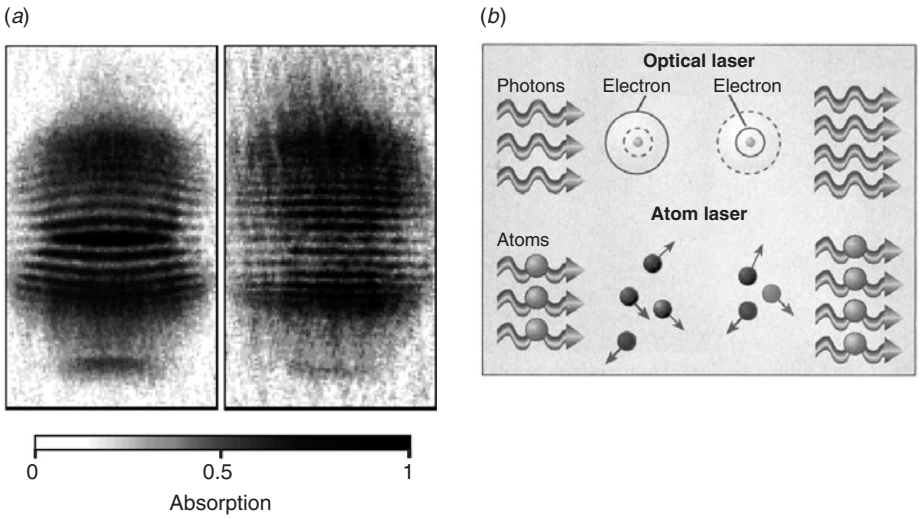

Figure 8-28 (*a*) When the two identical condensates of sodium atoms, each containing about 5×10^6 atoms, were allowed to expand freely and overlapped, phase contrast imagery revealed interference fringes, the "signature" of coherent waves—the first atomic laser. (*b*) Optical lasers amplify light by stimulating atoms to emit photons. Atom lasers amplify by stimulating more atoms to join the "beam." [(*a*) *From D. S. Durfee, Science* ***275****, 639 (1997).* (*b*) *From Science* ***279****, 986 (1998). Courtesy of L. Carroll.*]

Questions

9. Explain how the escaping "hot" rubidium atoms cool those remaining in the sample.
10. What is Bose-Einstein condensation?
11. Would you expect a gas or liquid of ^{3}He atoms to be much different from one of ^{4}He atoms? Why or why not?

STUDENTS-HUB.com Uploaded By: Malak Obaid

8-4 The Photon Gas: An Application of Bose-Einstein Statistics

Photon Gas

Planck's empirical expression for the energy spectrum of the blackbody radiation in a cavity (Equation 3-18) can now be derived by treating the photons in the cavity as a gas consisting of bosons. The distribution is then given by

$$f_{BE}(E) = \frac{1}{e^{\alpha}e^{E/kT} - 1} \qquad \textbf{8-24}$$

As we saw in Section 8-2 and in particular in the discussion of Equation 8-44, the value of α is determined by the total number of particles that the system contains. However, in the case of photons contained in a cavity, which we are discussing, that seems to present a problem since the total number of photons is not constant. Photons are continually being created (emitted by the oscillators in the cavity walls) and destroyed (absorbed by the oscillators). Even so, this does indeed specify the value of α: it tells us that Equation 8-24 *for photons* cannot be a function of e^{α}; i.e.,

$$f_{\text{ph}}(E) = \frac{1}{e^{E/kT} - 1} \qquad \textbf{8-53}$$

The fact that the total number of photons is not constant makes it necessary that $\alpha = 0$ so that $e^{\alpha} = 1$. We will see in a moment that this must be true.

The number of photons with energy E is found by substituting Equation 8-53 into Equation 8-37*b*, which yields

$$n_{\text{ph}}(E) = g_{\text{ph}}(E)f_{\text{ph}}(E)$$

or

$$n_{\text{ph}}(E) = \frac{g_{\text{ph}}(E)}{e^{E/kT} - 1} \qquad \textbf{8-54}$$

The density of states $g_{\text{ph}}(E)$ is derived in the same manner as it was for massive particles in Section 8-2. The result, which we first encountered as $n(\lambda) = 8\pi\lambda^{-4}$ in our discussion of Planck's derivation of the blackbody spectrum, is given in terms of the photon frequency f as

$$g_{\text{ph}}(E)\,dE = \frac{8\pi V f^2\,df}{c^3} = \frac{8\pi V E^2\,dE}{c^3h^3} \qquad \textbf{8-55}$$

where V is the volume of the cavity. The energy density $u(E)dE$ in the energy interval between E and $E + dE$ is then given by

$$u(E)\,dE = \frac{Eg_{\text{ph}}(E)f_{\text{ph}}(E)\,dE}{V} = \frac{8\pi E^3\,dE}{c^3h^3(e^{E/kT} - 1)} \qquad \textbf{8-56}$$

or, in terms of the photon frequency f, using $E = hf$ for the conversion, we have

$$u(f)\,df = \frac{8\pi f^2}{c^3}\frac{hf\,df}{e^{hf/kT} - 1} \qquad \textbf{8-57}$$

STUDENTS-HUB.com Uploaded By: Malak Obaid

Equation 8-57 is identical to Equation 3-18 when the latter is converted from wavelength λ to frequency f as the variable using $c = f\lambda$. We saw in Chapter 3 that Equation 3-18 is in precise agreement with experimental observations. This agreement serves as justification for the Bose-Einstein distribution function for photons given by Equation 8-53, which resulted from our argument that $\alpha = 0$ for photons. Notice that Planck's derivation presented in Chapter 3, in which the radiation in the blackbody cavity was treated as a set of distinguishable standing electromagnetic waves to which he (correctly) applied the Boltzmann distribution, agrees exactly with the derivation presented here, in which the radiation is treated as indistinguishable particles to which the Bose-Einstein distribution must be applied. This is an example of the wave-particle duality of photons.

EXAMPLE 8-7 **Photon Density of the Universe** The high temperature of the early universe implied a thermal (i.e., blackbody) electromagnetic radiation field which has, over aeons, cooled to the present 2.7 K. This cosmic background radiation was discovered in 1965. (See Chapter 13.) Compute the number of these photons per unit volume in the universe.

SOLUTION

1. The number of photons with energy E is given by Equation 8-54:
$$n_{ph}(E) = \frac{g_{ph}(E)}{e^{E/kT} - 1}$$

2. The total number per unit volume N/V is then given by
$$\frac{N}{V} = \frac{1}{V}\int_0^\infty n_{ph}(E)\,dE = \frac{1}{V}\int_0^\infty \frac{g_{ph}(E)\,dE}{e^{E/kT} - 1}$$

3. Substituting the density of states $g_{ph}(E)$ from Equation 8-55 yields
$$\frac{N}{V} = \int_0^\infty \frac{8\pi E^2\,dE}{(ch)^3(e^{E/kT} - 1)} = \frac{8\pi(kT)^3}{(ch)^3}\int_0^\infty \frac{(E/kT)^2(dE/kT)}{e^{E/kT} - 1}$$

4. Letting $x = E/kT$, this can be written
$$\frac{N}{V} = 8\pi\left(\frac{kT}{ch}\right)^3\int_0^\infty \frac{x^2\,dx}{e^x - 1}$$

5. Evaluating the integral from standard tables:
$$\int_0^\infty \frac{x^2\,dx}{e^x - 1} \approx 2.40$$

6. Substituting values into the expression for N/V in step 4 yields
$$\frac{N}{V} = 8\pi\left(\frac{1.38 \times 10^{-23}\ \text{J/K} \times 2.7\ \text{K}}{3.00 \times 10^8\ \text{m/s} \times 6.63 \times 10^{-34}\ \text{J}\cdot\text{s}}\right)^3 (2.40)$$
$$= 3.97 \times 10^8\ \text{photons/m}^3$$

STUDENTS-HUB.com Uploaded By: Malak Obaid

Quantization of the Energy States of Matter

We pointed out earlier that the molar heat capacity C_V for solids falls appreciably below the classical Dulong-Petit value of $3R$ when the temperature falls below some critical value. In 1908 Einstein showed that the failure of the equipartition theorem in predicting the specific heats of solids at low temperatures could be understood if it were assumed that the atoms of the solid could have only certain discrete energy values. Einstein's calculation is closely related to Planck's calculation of the average energy of a harmonic oscillator, assuming the oscillator can take on only a discrete set of energies. The calculation itself presents no real problem, as we have seen in Chapter 3. Einstein's most important contribution in this area was the extension of the idea of quantization to any oscillating system, including matter. We will see in this subsection how the idea of quantized energy states for matter also explains the puzzling behavior of the heat capacities of diatomic gases that was pointed out in Section 8-1. In particular, we will be able to understand why the H_2 molecule seems to have only 3 degrees of freedom (corresponding to translation) at low temperatures, 5 degrees of freedom at intermediate temperatures (corresponding to translation and rotation), and 7 degrees of freedom at high temperature (corresponding to translation, rotation, and vibration).

Consider 1 mole of a solid consisting of N_A molecules, each free to vibrate in three dimensions about a fixed center. For simplicity, Einstein assumed that all the molecules oscillate at the same frequency f in each direction. The problem is then equivalent to $3N_A$ distinguishable one-dimensional oscillators, each with frequency f. The classical distribution function for the energy of a set of one-dimensional oscillators is the Boltzmann distribution, given by Equation 8-1. Following Planck, Einstein assumed that the energy of each oscillator could take on only the values given by

$$E_n = nhf \tag{8-58}$$

where $n = 0,1,2,\ldots$, rather than have an average value of kT as predicted by the equipartition theorem. He then used the Boltzmann distribution[15] to compute the average energy $\langle E \rangle$ for the distinguishable oscillators, just as we have done previously, from

$$\langle E \rangle = \int_0^\infty E n_B(E)\, dE \tag{8-59}$$

obtaining

$$\langle E \rangle = \frac{hf}{e^{hf/kT} - 1} \tag{8-60}$$

which is, of course, the same as Equation 3-17. We can expand the exponential, using $e^x \approx 1 + x + (x^2/2!) + \ldots$ for $x \ll 1$, where $x = hf/kT$ (see Appendix B2). At high temperatures the quantity $hf/kT \ll 1$ and then, keeping only the first two terms of the expansion,

$$e^{hf/kT} - 1 \approx \left(1 + \frac{hf}{kT} + \ldots\right) - 1 \approx \frac{hf}{kT}$$

and $\langle E \rangle$ approaches kT, in agreement with the equipartition theorem from classical statistics (see Equation 8-14).

STUDENTS-HUB.com Uploaded By: Malak Obaid

The total energy for $3N_A$ oscillators is now

$$U = 3N_A\langle E\rangle = \frac{3N_A hf}{e^{hf/kT} - 1} \qquad \textbf{8-61}$$

and the heat capacity is

$$C_V = \frac{dU}{dT} = 3N_A k\left(\frac{hf}{kT}\right)^2 \frac{e^{hf/kT}}{(e^{hf/kT} - 1)^2} \qquad \textbf{8-62}$$

It is left as an exercise (see Problem 8-29) to show directly from Equation 8-62 that $C_v \to 0$ as $T \to 0$ and $C_v \to 3N_A k = 3R$ as $T \to \infty$.

By comparing the Einstein calculation of the average energy per molecule, Equation 8-60, with the classical one, we can gain some insight into the problem of when the classical theory will work and when it will fail. Let us define the critical temperature,

$$T_E = \frac{hf}{k} \qquad \textbf{8-63}$$

called the *Einstein temperature*. The energy distribution in terms of this temperature is

$$f_B(E_n) = Ae^{-E_n/kT} = Ae^{-nhf/kT} = Ae^{-nT_E/T}$$

For temperatures T much higher than T_E, small changes in n have little effect on the exponential in the distribution; that is $f_B(E_n) \approx f_B(E_{n+1})$. Then E can be treated as a continuous variable. However, for temperatures much lower than T_E, even the smallest possible change in n, $\Delta n = 1$, results in a significant change in $e^{-nT_E/T}$, and we would expect that the discontinuity of possible energy values becomes significant. Since hard solids have stronger binding forces than soft ones, their frequencies of molecular oscillation and therefore their Einstein temperatures are higher. For lead and gold, T_E is of the order of 50 to 100 K; ordinary temperatures of around 300 K are "high" for these metals, and they obey the classical Dulong-Petit law at these temperatures. For diamond, T_E is well over 1000 K; in this case 300 K is a "low" temperature, and C_v is much less than the Dulong-Petit value of $3R$ at this temperature.

The agreement between Equation 8-62 and experimental measurements justifies Einstein's approach to understanding the molar heat capacity of solids. Figure 8-29 shows a comparison of this equation with experiments. The curve fits the experimental points well except at very low temperatures, where the data fall slightly above the curve.

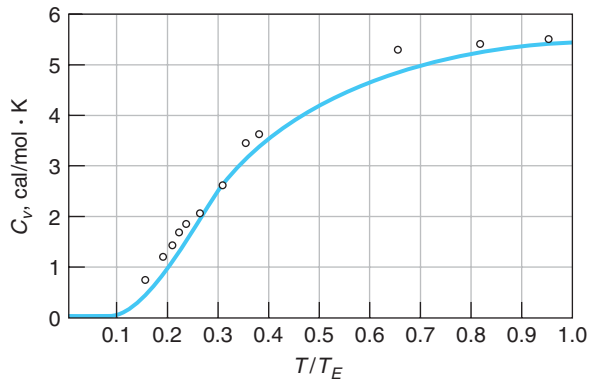

Figure 8-29 Molar heat capacity of diamond versus reduced temperature T/T_E. The solid curve is that predicted by Einstein. [*From Einstein's original paper, Annalen der Physik* ***22*** *(4), 180 (1907).*]

STUDENTS-HUB.com Uploaded By: Malak Obaid

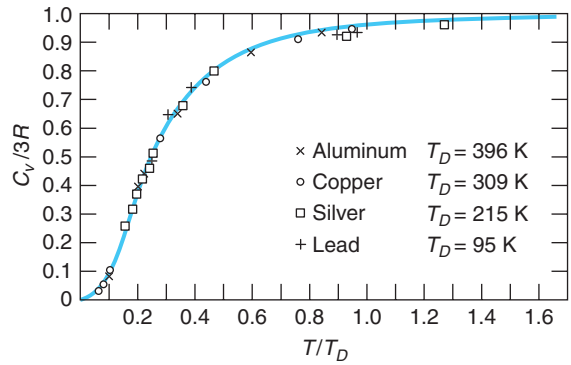

Figure 8-30 Molar heat capacity of several solids versus reduced temperature T/T_D, where T_D is the Debye temperature, defined as $T_D = hf_D/k$. The solid curve is that predicted by Debye. The data are taken from Debye's original paper. $C_v/3R = 1$ is the Dulong-Petit value. [*From Annalen der Physik* ***39*** *(4), 789 (1912), as adapted by David MacDonald, Introductory Statistical Mechanics for Physicists (New York: John Wiley & Sons, Inc., 1963); by permission.*]

The lack of detailed agreement of the curve with the data at low T is due to the oversimplification of the model. A refinement of this model was made by P. Debye, who gave up the assumption that all molecules vibrate at the same frequency. He allowed for the possibility that the motion of one molecule could be affected by that of the others and treated the solid as a system of coupled oscillators. The effect was to allow a range of vibrational frequencies from $f = 0$ up to a maximum f_D, called the *Debye frequency*, used to define the *Debye temperature* $T_D = hf_D/k$. This contrasts with the infinite range of oscillation modes in the blackbody cavity. Debye's argument was that the number of vibrational modes or frequencies cannot exceed the number of degrees of freedom of the atoms that make up the solid. Calculations with the Debye model are somewhat more involved and will not be considered here. The improvement of the Debye model over the Einstein model is shown by Figure 8-30. Note that *all* solids fall on the same curve.

Understanding Specific Heats of Gases

Let us now see if we can understand the specific heats of diatomic gases on the basis of discrete, or quantized, energies. In Section 8-1 we wrote the energy of a diatomic molecule as the sum of translational, rotational, and vibrational energies. If f is the frequency of vibration and the vibrational energy is quantized by $E_{\text{vib}} = nhf$, as we assumed for solids, we know from the previous calculation (see Equation 8-62) that for low temperatures, the average energy of vibration approaches zero and vibration will not contribute to C_V. We can define a critical temperature for vibration of a diatomic gas molecule by

$$T_v = \frac{hf}{k} \qquad \textbf{8-64}$$

where f is the frequency of vibration. Apparently $T_v > 15°$ C for all the diatomic gases listed in Table 8-1 except for Cl_2. From Figure 8-11 we can see that T_v is of the order of 1000 to 5000 K for H_2.

STUDENTS-HUB.com Uploaded By: Malak Obaid

The rotational energy of a diatomic molecule is

$$E_R = \tfrac{1}{2} I\omega^2$$

where I is the moment of inertia and ω is the angular velocity of rotation. It is not obvious how the rotational energy is quantized or even if it is; however, let us make use of a result from Section 7-2, where we learned that the angular momentum is quantized. If L is the angular momentum of a diatomic molecule, $L = I\omega$, and we can write the energy as

$$E_R = \frac{L^2}{2I}$$

Equation 7-22 tells us that $L^2 = \ell(\ell + 1)\hbar^2$, where $\ell = 0,1,2,\ldots$. Thus, the rotational energy becomes

$$E_R = \ell(\ell + 1)\frac{h^2}{8\pi^2 I} \qquad \textbf{8-65}$$

The energy distribution function will contain the factor

$$e^{-E_R/kT} = e^{-\ell(\ell+1)h^2/8\pi^2 IkT}$$

and we can define a critical temperature for rotation similar to that for vibration as

$$T_R = \frac{E_R}{k} = \frac{h^2}{8\pi^2 Ik} \qquad \textbf{8-66}$$

If this procedure is correct, we expect that for temperatures $T \gg T_R$, i.e., $E_R \gg kT$, the equipartition theorem will hold for rotation and the average energy of rotation will approach $(\frac{1}{2})kT$ for each axis of rotation, while for low temperatures, $T \ll T_R$, the average energy of rotation will approach 0. Let us examine T_R for some cases of interest:

1. H_2. For rotation about the x or y axis as in Figure 8-10*a*, taking the z axis as the line joining the atoms, the moments of inertia I_x and I_y through the center of mass are

   $$I_x = I_y = \tfrac{1}{2}MR^2$$

   The separation of the atoms is about $R \approx 0.08$ nm. The mass of the H atom is about $M \approx 940 \times 10^6\ \text{eV}/c^2$. We first calculate kT_R:

   $$kT_R = \frac{h^2}{8\pi^2 I} = \frac{(hc)^2}{4\pi^2 Mc^2 R^2} = \frac{(1.24 \times 10^3\ \text{eV}\cdot\text{nm})^2}{4\pi^2(940 \times 10^6\ \text{eV})(0.08\ \text{nm})^2} \approx 6.4 \times 10^{-3}\ \text{eV}$$

   Using $k \approx 2.6 \times 10^{-2}\ \text{eV}/300\ \text{K}$, we obtain

   $$T_R = \frac{6.4 \times 10^{-3}}{2.6 \times 10^{-2}} 300\ \text{K} \approx 74\ \text{K}$$

   As can be seen from Figure 8-11, this is indeed the temperature region below which the rotational energy does not contribute to the heat capacity.

2. O_2. Since the mass of the oxygen atom is 16 times that of the hydrogen atom and the separation is roughly the same, the critical temperature for rotation will be $T_R \approx (74/16) \approx 4.6$ K. For all temperatures at which O_2 exists as a gas, $T \gg T_R$.

STUDENTS-HUB.com Uploaded By: Malak Obaid

3. A monatomic gas, or rotation of diatomic gas about the z axis. We will take the H atom for calculation. The moment of inertia of the atom is mainly due to the electron since the radius of the nucleus is extremely small (about 10^{-15} m). The distance from the nucleus to the electron is about the same as the separation of atoms in the H_2 molecule. Since the mass of the electron is about 2000 times smaller than that of the atom, we have

$$I_H \approx \frac{1}{2000} I_{H_2}$$

and

$$T_R \approx 2000 \times 74 \text{ K} \approx 1.5 \times 10^5 \text{ K}$$

This is much higher than the dissociation temperature for any diatomic gas. Thus, $\langle E_R \rangle \approx 0$ for monatomic gases and for rotation of diatomic gases about the line joining the atoms for all attainable temperatures.

We see that energy quantization explains, at least qualitatively, the temperature dependence of the specific heats of gases and solids.

EXAMPLE 8-8 **Average Vibrational Energy** What is the average energy of vibration of the molecules in a solid if the temperature is (*a*) $T = hf/2k$, (*b*) $T = 4hf/k$?

SOLUTION

(*a*) This is lower than the critical temperature for vibration hf/k given by Equation 8-64, so we expect a result considerably lower than the high temperature limit of kT given by the equipartition theorem. From Equation 8-60 we have

$$\langle E \rangle = \frac{hf}{e^{hf/kT} - 1} = \frac{2kT}{e^2 - 1} = 0.31\, kT$$

(*b*) This temperature is four times the critical temperature, so we expect a result near the high temperature limit of kT. Using $hf/kT = 1/4$ in Equation 8-60, we have

$$\langle E \rangle = \frac{0.25kT}{e^{0.25} - 1} = 0.880\, kT$$

EXAMPLE 8-9 **Number of Oscillators** At the "low" and "high" temperatures of Example 8-8, find the ratio of the number of oscillators with energy $E_1 = hf$ to the number with $E_0 = 0$.

SOLUTION

At any temperature T, the Boltzmann distribution for the fraction of oscillators with energy $E_n = nhf$ is $f_B(E_n) = Ae^{-E_n/kT} = Ae^{-nhf/kT}$. For $n = 0$, this gives $f_0 = Ae^0 = A$. The ratio f_n/f_0 is then $f_n/f_0 = e^{-nhf/kT}$.

(*a*) For $n = 1$ and $kT = \frac{1}{2}hf$, we have $f_1/f_0 = e^{-hf/kT} = e^{-2} = 0.135$. Most of the oscillators are in the lowest energy state $E_0 = 0$.

(*b*) For the higher temperature $kT = 4hf$, we get $f_1/f_0 = e^{-hf/kT} = e^{-0.25} = 0.779$. At the higher temperature the states are more nearly equally populated and the average energy is larger.

STUDENTS-HUB.com Uploaded By: Malak Obaid

EXAMPLE 8-10 **Debye Frequency** Note from Figure 8-30 that the Debye temperature of silver is 215 K. Compute the Debye frequency for silver and predict the Debye temperature for gold. Silver and gold have identical crystal structures and similar physical properties.

SOLUTION

1. From the definition of the Debye temperature T_D, the Debye frequency f_D for silver can be computed:

$$T_D = \frac{hf_D}{k}$$

or

$$f_D = \frac{kT_D}{h} = \frac{1.38 \times 10^{-23}\ \text{J/K} \times 215\ \text{K}}{6.63 \times 10^{-34}\ \text{J} \cdot \text{s}} = 4.48 \times 10^{12}\ \text{Hz}$$

2. We would expect the interatomic forces of silver and gold to be roughly the same, hence their vibrational frequencies to be in inverse ratio to the square root of their atomic masses:

$$\frac{f_D(\text{Ag})}{f_D(\text{Au})} = \sqrt{\frac{M(\text{Au})}{M(\text{Ag})}} = \frac{kT_D(\text{Ag})/h}{kT_D(\text{Au})/h} = \frac{T_D(\text{Ag})}{T_D(\text{Au})}$$

3. Solving this for $T_D(\text{Au})$ yields

$$T_D(\text{Au}) = T_D(\text{Ag})\sqrt{\frac{M(\text{Au})}{M(\text{Ag})}} = 215\sqrt{\frac{108}{197}}$$

$$= 159\ \text{K}$$

Remarks: This estimate is in reasonable agreement with the measured value of 164 K.

8-5 Properties of a Fermion Gas

The fact that metals conduct electricity so well led to the conclusion that they must contain electrons free to move about through a lattice of more or less fixed positive metal ions. Indeed, this conclusion had led to the development of a free-electron theory to explain the properties of metals within three years after the electron's discovery by Thomson and long before wave mechanics was even a glimmer in Schrödinger's eye. The free-electron theory of metals was quite successful in explaining a number of metallic properties, as we will discuss further in Chapter 10; however, it also suffered a few dramatic failures. For example, in a conductor at temperature T the lattice ions have average energy $3kT$ consisting, as we have seen, of $3kT/2$ of kinetic energy and $3kT/2$ of potential energy, leading to a molar heat capacity $C_V = 3R$ (rule of Dulong-Petit). Interactions (i.e., collisions) between the free electrons and lattice ions would be expected to provide the electrons with an average translational kinetic energy of $3kT/2$ at thermal equilibrium, resulting in a total internal energy U for metals of $3kT + 3kT/2 = 9kT/2$. Thus, metals should have $C_V = 4.5R$. In fact, they do not. The heat capacity of conductors is essentially the same as that of other solids, except for a slight temperature-dependent increase that is much smaller than $3R/2$. The problems with the classical free-electron theory are due mainly to the fact that electrons are indistinguishable particles that obey the exclusion principle, and as a

STUDENTS-HUB.com Uploaded By: Malak Obaid

consequence they have the Fermi-Dirac distribution of energies rather than the Boltzmann distribution. In this section we will investigate the general characteristics of systems made up of fermions. In Chapter 10 we will see how the absence of a significant electron contribution to the heat capacity of conductors is explained.

In the Fermi-Dirac distribution given by

$$f_{FD}(E) = \frac{1}{e^{\alpha}e^{E/kT} + 1} \qquad \textbf{8-25}$$

it is convenient to write α as

$$\alpha = \frac{-E_F}{kT} \qquad \textbf{8-67}$$

where E_F is called the *Fermi energy*. Doing so allows Equation 8-25 to be written as

$$f_{FD}(E) = \frac{1}{e^{(E-E_F)/kT} + 1} \qquad \textbf{8-68}$$

The Fermi energy is an important quantity in systems of fermions, such as the electron gas in metals (discussed in Chapter 10) and the neutron gas in a neutron star. Notice in particular that for $E = E_F$ the quantity $e^{(E-E_F)/kT} = 1$ for all values of the temperature greater than zero and hence $f_{FD}(E_F) = \frac{1}{2}$. If we consider a system of fermions at $T = 0$ K, we find that

For $E < E_F$:

$$f_{FD}(E) = \frac{1}{e^{(E-E_F)/kT} + 1} = 1$$

and

For $E > E_F$:

$$f_{FD}(E) = \frac{1}{e^{\infty} + 1} = 0$$

In other words, at absolute zero all energy states from the ground state up to the Fermi energy are occupied and all energy states above the Fermi energy are empty. This is in sharp contrast with a system of bosons, such as the rubidium BE condensate, where all particles condense to the ground state at $T = 0$ K. This situation is illustrated in Figure 8-31*a*. If the system contains N fermions, we can find its Fermi energy by filling the energy states in increasing order starting with the ground state.

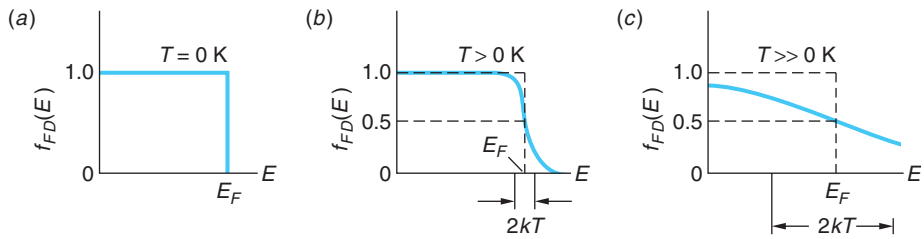

Figure 8-31 Fermi-Dirac distribution function $f_{FD}(E)$ for three different temperatures. (*a*) At $T = 0$ K, all levels above E_F are unoccupied. (*b*) For $T > 0$ K with $kT < E_F$, some particles near the Fermi energy can move to levels within about kT above E_F. (*c*) For high temperatures where $kT > E_F$, even particles in the lower energy states may move to higher levels so that $f_{FD}(0) < 1$.

STUDENTS-HUB.com Uploaded By: Malak Obaid

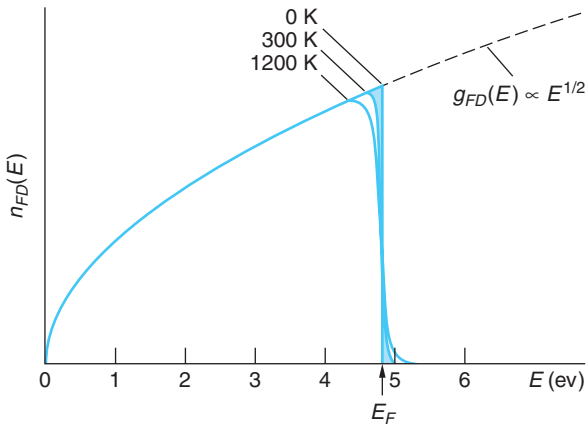

Figure 8-32 The distribution of fermion energies at three different temperatures for a material whose Fermi energy is 4.8 eV. Curves are plots of Equation 8-69 for the indicated values of temperature. (See text for explanation of shaded area.)

The energy state occupied by the Nth particle will be the Fermi energy. We can find the total energy of the system simply by adding up the energies of all N particles and their average energy by dividing that total by N. Each of these calculations will be done for electrons in Section 10-3.

If the temperature of the system is increased to some temperature $T > 0$ K but with kT remaining smaller than E_F, fermions within about kT of the Fermi energy could now move to previously unoccupied levels lying within about kT above the Fermi energy in response to collisions with the lattice ions. However, fermions occupying levels much lower than kT below E_F would not be able to move since the additional kT of energy that they might acquire in a collision would not be enough to move them past levels occupied by other fermions in order to reach the unoccupied levels near or above E_F. Figure 8-31*b* illustrates this situation. At temperatures so high that $kT > E_F$, fermions in even the very low-lying energy states will be able to move to higher states. Only then can $f_{FD}(0)$ drop below 1, as shown in Figure 8-31*c*. This latter situation also corresponds to the lowest curve in Figure 8-16.

The number $n_{FD}(E)$ of fermions with energy E is given by Equation 8-37*c*. The density of states was computed for fermions in Section 8-3 and is given by Equation 8-42, so we have for fermions that

$$n_{FD}(E) = \frac{\pi}{2}\left(\frac{8m}{h^2}\right)^{3/2} \frac{VE^{1/2}}{e^{(E-E_F)/kT} + 1} \qquad \textbf{8-69}$$

Figure 8-32 is a graph of Equation 8-69 for three different temperatures. The $T = 0$ K curve is the result of multiplying $f_{FD}(E)$ in Figure 8-31*a* by the $g_{FD}(E)$ function, which increases as $E^{1/2}$. The curves for $T = 300$ K and $T = 1200$ K result from multiplying $g_{FD}(E)$ by appropriate versions of Figure 8-31*b*. The shaded areas for $T > 0$ K represent those electrons near the Fermi energy, a very small number, that are able to move into the empty states above E_F at each temperature.

Quantum Degenerate Fermion Gas

Since fermions have half-integer spins, the Pauli exclusion principle prohibits two identical fermions from occupying the same quantum state. Thus, a system of half-integer-spin atoms cannot all occupy the ground state to form a fermion version of the Bose-Einstein condensate as is possible for integer-spin bosons. The fermion analog of

STUDENTS-HUB.com Uploaded By: Malak Obaid

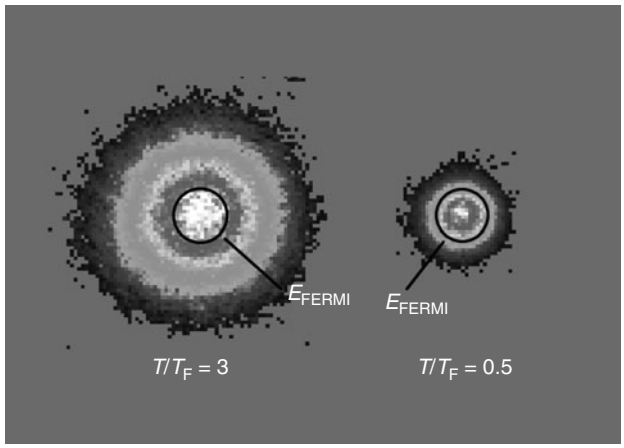

Figure 8-33 Quantum degenerate state of a Fermi gas. The images show that more of the atoms of the ultracold gas lie below the Fermi energy (black circles) than above it in the right sample than in the left one. The colder cloud on the right contains 0.78 million ^{40}K atoms at $T = 0.29\ \mu K$. The cloud on the left contains 2.5 million atoms at $T = 2.4\ \mu K$.

the BEC occurs when the atoms fill all of the energy states from the ground state up to the Fermi energy. The transition to this quantum degenerate state for a gas of fermions is a gradual one, quite unlike the sudden phase transition to the BEC. This makes it harder to detect, in addition to which the exclusion principle makes evaporative cooling that is so important in producing the BEC much less effective as the temperature of the fermion gas decreases. In 1999 these problems were solved by Deborah Jin and Brian DeMarco, four years after the first BEC was produced. They loaded a magnetic trap with ^{40}K (total atomic spin = 9/2), dividing the atoms between two magnetic substates to solve the evaporative cooling problem. One of several ways used to detect the quantum degenerate state of the ^{40}K atoms was to determine the total energy (from the momentum distribution) of the approximately 8×10^5 atoms in the sample (Figure 8-33). Classically, the total energy $(3/2)N_A kT \rightarrow 0$ as $T \rightarrow 0$. Quantum mechanically, however, the total energy should be higher than expected classically as T decreases and remain finite as $T \rightarrow 0$. This is exactly what Jin and DeMarco observed. High on the list of new things their discovery may make possible is the study of Cooper pairs (see Section 10-8) as they condense into a superconductor.

More recently, scientists have been successful in forming Bose-Einstein condensates from paired fermions using ^{6}Li and ^{40}K. The very loosely bonded ^{6}Li-^{6}Li and ^{40}K-^{40}K are bosons and dropped into their respective ground states when the temperature reached about 50×10^{-9} K.

Questions

12. Why does the exclusion principle make evaporative cooling less effective as T decreases for fermions in a single-spin state?
13. Why does the total energy of the fermion gas not approach zero as T $\rightarrow$ 0?

Summary

TOPIC	RELEVANT EQUATIONS AND REMARKS	
1. Boltzmann distribution	$f_B(E) = Ae^{-E/kT}$ where the distribution $f_B(E)$ is the probability that the state with energy E will be occupied.	**8-1**
Boltzmann's constant	$k = 1.381 \times 10^{-23}$ J/K $= 8.617 \times 10^{-5}$ eV/K	

STUDENTS-HUB.com Uploaded By: Malak Obaid

TOPIC	RELEVANT EQUATIONS AND REMARKS	
Maxwell distribution of molecular speeds	$n(v)\,dv = 4\pi N\left(\frac{m}{2\pi kT}\right)^{3/2} v^2 e^{-mv^2/2kT}\,dv$	**8-8**
Equipartition theorem	In equilibrium, each degree of freedom contributes $\frac{1}{2}kT$ to the average energy per molecule.	
Average kinetic energy	$\langle E\rangle = \frac{3}{2}kT$	**8-14**
	where $\langle E\rangle$ is the average *translational* kinetic energy per molecule.	
Dulong-Petit law	$C_V = 3R$	
2. Quantum statistics		
Bose-Einstein distribution	$f_{BE}(E) = \frac{1}{e^{\alpha}e^{E/kT} - 1}$	**8-24**
Fermi-Dirac distribution	$f_{FD}(E) = \frac{1}{e^{\alpha}e^{E/kT} + 1}$	**8-25**
	In all three distributions f_B, f_{BE}, and f_{FD}, e^{α} is a normalization constant that depends on the particle density. The FD distribution applies to particles with $\frac{1}{2}$ -integral spin, the BE distribution to particles with zero or integral spin. At high energies both f_{BE} and f_{FD} approach f_B.	
	The Boltzmann distribution will be a good approximation of either f_{BE} or f_{FD} if $e^{\alpha} \ll 1$.	
3. Applications		
Liquid helium	^{4}He becomes a superfluid at 2.17 K, called the lambda point. ^{3}He, the only other naturally occurring isotope that has this property, becomes superfluid at about 2 mK.	
Bose-Einstein condensate	Bosons undergo a phase transition, condensing to the lowest quantum state.	
Degenerate Fermi gas	Fermions condensed to states from the ground state to the Fermi energy.	

General References

The following general references are written at a level appropriate for the readers of this book.

Blatt, F. J., *Modern Physics*, McGraw-Hill, New York, 1992.

Brehm, J. J., and W. J. Mullin, *Introduction to the Structure of Matter*, Wiley, New York, 1989.

Eisberg, R., and R. Resnick, *Quantum Physics of Atoms, Molecules, Solids, Nuclei, and Particles*, 2d ed., Wiley, New York, 1985. An excellent but somewhat more advanced discussion of quantum statistics can be found in Chapter 11 of this book.

Ford, K. W., *The Quantum World*, Harvard University Press, Cambridge, MA, 2005.

Kittel, C., and H. Kroemer, *Thermal Physics*, W. H. Freeman and Co., New York, 1995.

Leitner, A., *Liquid Helium II: The Superfluid*, Michigan State University, East Lansing, 1963. This 39-minute film is an excellent introduction to the subject of liquid helium II.

London, F., *Superfluids*, Vol. II:*Macroscopic Theory of Superfluid Helium*, 2d rev. ed., Dover, New York, 1954.

Mandel, F., *Statistical Physics*, Wiley, New York, 1988.

Mendelssohn, K., *The Quest for Absolute Zero: The Meaning of Low Temperature Physics*, World University Library, McGraw-Hill, New York, 1966.

STUDENTS-HUB.com Uploaded By: Malak Obaid

Notes

1. The statistical approach may also be used as an approximation in systems where the number of particles is not particularly large. For example, in Chapter 11 we will discuss briefly a statistical model of the atomic nucleus, a system containing only of the order of 100 particles.

2. Ludwig E. Boltzmann (1844–1906), Austrian physicist. His pioneering statistical interpretation of the second law of thermodynamics earned for him recognition as the founder of statistical mechanics. He explained theoretically the experimental observations of Stefan, whom he served as an assistant while in college, that the quantity of radiation increased with the fourth power of the temperature. He eventually succeeded Josef Stefan in the chair of physics at Vienna. A strong proponent of the atomic theory of matter, his suicide was apparently motivated in part by opposition to his views by others.

3. To avoid having to repeat this rather long phrase frequently, which will occur for E as well as v, we will hereafter use the expression "the number in dv_x at v_x" or simply "the number in dv_x."

4. Or refer to a table of integrals.

5. Historically, rotation about the z' axis of the dumbbell was ruled out by assuming either that the atoms are points and the moment of inertia about this axis is therefore zero (not true) or that the atoms are hard smooth spheres, in which case rotation about this axis cannot be changed by collisions and therefore does not participate in the exchange of energy (also not true). Either of these assumptions also rules out the possibility of rotation of a monatomic molecule.

6. Satyendra Nath Bose (1894–1974), Indian physicist. Following publication of his paper on the statistics of indistinguishable particles, which was translated into German for publication by Einstein himself, Bose spent two years in Europe, then returned to India to devote himself to teaching. Lacking a Ph.D., he was denied a professorship until a one-sentence postcard from Einstein was received at Dacca University in his support.

7. Enrico Fermi (1901–1954), Italian-American physicist. An exceedingly prolific scientist and intrepid amateur tennis player whose work encompassed solid-state, nuclear, and particle physics, he is perhaps best known as the "father" of the nuclear reactor. He was awarded the Nobel Prize in Physics in 1938 for his work in nuclear physics.

8. Paul A. M. Dirac (1902–1984), English physicist. His development of relativistic wave mechanics for spin-$\frac{1}{2}$ particles led to his prediction in 1930 of the existence of the positron. Its discovery by Anderson two years later resulted in Dirac's being awarded (along with Schrödinger) the 1933 Nobel Prize in Physics. From 1932 until his retirement he occupied the Lucasian Chair of Mathematics at Cambridge University, which had been held 250 years earlier by Newton and is currently held by Stephen Hawking.

9. Heike Kamerlingh Onnes (1853–1926), Dutch physicist. His success in liquefying helium enabled him to investigate the properties of other materials at liquid helium temperatures. This in turn led to his discovery of superconductivity in 1911. His work on the behavior of materials at low temperatures earned him the Nobel Prize in Physics in 1913.

10. J. C. McLennan, H. D. Smith, and J. O. Wilhelm, *Philosophical Magazine*, **14,** 161 (1932).

11. At very low temperatures liquid ^{4}He does solidify at a pressure of about 25 atm, liquid ^{3}He at about 30 atm.

12. Narrow channels that permit only the superfluid to pass are, of course, called *superleaks*.

13. These and many other properties are elegantly displayed in the film *Liquid Helium II: The Superfluid*, available from the Instructional Media Center, Michigan State University, East Lansing, Michigan 48824.

14. In the thermodynamic equilibrium state their sample, rubidium, is a solid metal at room temperature.

15. Einstein used the Boltzmann distribution in its discrete form $f_B(E) = \sum_{n=0}^{\infty} Ae^{-E_n/kT}$.

Problems

Level I

Section 8-1. Classical Statistics: A Review

8-1. (*a*) Calculate v_{rms} for H_2 at $T = 300$ K. (*b*) Calculate the temperature T for which v_{rms} for H_2 equals the escape speed of 11.2 km/s.

8-2. (*a*) The ionization energy for hydrogen atoms is 13.6 eV. At what temperature is the average kinetic energy of translation equal to 13.6 eV? (*b*) What is the average kinetic energy of translation of hydrogen atoms at $T = 10^7$ K, a typical temperature in the interior of the Sun?

8-3. The molar mass of oxygen gas (O_2) is about 32 g/mol and that of hydrogen gas (H_2) about 2 g/mol. Compute (*a*) the rms speed of O_2 and (*b*) the rms speed of H_2 when the temperature is 0°C.

8-4. Show that the SI units of $(3RT/M)^{1/2}$ are m/s.

STUDENTS-HUB.com Uploaded By: Malak Obaid

8-5. (*a*) Find the total kinetic energy of translation of 1 mole of N_2 molecules at $T = 273$ K. (*b*) Would your answer be the same, greater, or less for 1 mole of He atoms at the same temperature? Justify your answer.

8-6. Use the Maxwell distribution of molecular speeds to calculate $\langle v^2 \rangle$ for the molecules of a gas.

8-7. Neutrons in a nuclear reactor have a Maxwell speed distribution when they are in thermal equilibrium. Find $\langle v \rangle$ and v_m for neutrons in thermal equilibrium at 300 K. Show that $n(v)$ (Equation 8-8) has its maximum value at $v = v_m = (2kT/m)^{1/2}$.

8-8. A container holds 128 identical molecules whose speeds are distributed as follows:

No. of molecules	4	12	20	24	20	16	12	8	6	4
Speed range (m/s)	0.0–1.0	1.0–2.0	2.0–3.0	3.0–4.0	4.0–5.0	5.0–6.0	6.0–7.0	7.0–8.0	8.0–9.0	9.0–10.0

Graph these data and indicate on the graph v_m, $\langle v \rangle$, and v_{rms}.

8-9. Show that the most probable speed v_m of the Maxwell distribution of speeds is given by Equation 8-9.

8-10. Compute the total translational kinetic energy of one liter of oxygen held at a pressure of one atmosphere and a temperature of 20°C.

8-11. From the absorption spectrum it is determined that about one out of 10^6 hydrogen atoms in a certain star is in the first excited state, 10.2 eV above the ground state (other excited states can be neglected). What is the temperature of the star? (Take the ratio of statistical weights to be 4, as in Example 8-2.)

8-12. The first excited rotational energy state of the H_2 molecule ($g_2 = 3$) is about 4×10^{-3} eV above the lowest energy state ($g_1 = 1$). What is the ratio of the numbers of molecules in these two states at room temperature (300 K)?

8-13. A monatomic gas is confined to move in two dimensions so that the energy of an atom is $E_k = \frac{1}{2}mv_x^2 + \frac{1}{2}mv_y^2$. What are C_V, C_P, and γ for this gas? (C_P, the heat capacity at constant pressure, is equal to $C_V + nR$ and $\gamma = C_P/C_V$.)

8-14. Use the Dulong-Petit law that $C_V = 3R$ for solids to calculate the specific heat $c_V = C_V/M$ in cal/g for (*a*) aluminum, $M = 27.0$ g/mol, (*b*) copper, $M = 63.5$ g/mol, and (*c*) lead, $M = 207$ g/mol, and compare your results with the values given in a handbook. (Include the reference in your answer.)

8-15. Calculate the most probable kinetic energy E_m from the Maxwell distribution of kinetic energies (Equation 8-13).

8-16. (*a*) Show that the speed distribution function can be written $n(v) = 4\pi^{-1/2}(v/v_m)^2 v_m^{-1} e^{-(v/v_m)^2}$, where v_m is the most probable speed. Consider 1 mole of molecules and approximate dv by $\Delta v = 0.01\ v_m$. Find the number of molecules with speeds in dv at (*b*) $v = 0$, (*c*) $v = v_m$, (*d*) $v = 2\ v_m$, and (*e*) $v = 8\ v_m$.

8-17. Consider a sample containing hydrogen atoms at 300 K. (*a*) Compute the number of atoms in the first ($n = 2$) and second ($n = 3$) excited states compared to those in the ground state ($n = 1$). Include the effects of degeneracy in your calculations. (*b*) At what temperature would one percent of the atoms be in the $n = 2$ state? (*c*) At the temperature found in (*b*), what fraction of the atoms will be in the $n = 3$ state?

8-18. Consider a sample of noninteracting lithium atoms (Li, $Z = 3$) with the third (outer) electron in the $3p$ state in a uniform 4.0 T magnetic field. (*a*) Determine the fraction of the atom in the $m_\ell = +1, 0$, and -1 states at 300 K. (*b*) In the $3p \rightarrow 2s$ transition, what will be the relative intensities of the three lines of the Zeeman effect?

Section 8-2 Quantum Statistics

8-19. Find the number density N/V for electrons such that (*a*) $e^{-\alpha} = 1$ and (*b*) $e^{-\alpha} = 10^{-6}$.

8-20. (*a*) Compute $e^{-\alpha}\sqrt{b^2 - 4ac}$ from Equation 8-44 for O_2 gas at standard conditions. (*b*) At what temperature is $e^{-\alpha} = 1$ for O_2?

8-21. Given three containers all at the same temperature, one filled with a gas of classical molecules, one with a fermion gas, and one with a boson gas, which will have the highest pressure? Which will have the lowest pressure? Support your answer.

STUDENTS-HUB.com Uploaded By: Malak Obaid

8-22. (*a*) For $T = 5800$ K, at what energy will the Bose-Einstein distribution function $f_{BE}(E)$ equal 1 (for $\alpha = 0$)? (*b*) Still with $\alpha = 0$, to what value must the temperature change if $f_{BE}(E) = 0.5$ for the energy in part (*a*)?
8-23. A container at 300 K contains H_2 gas at a pressure of one atmosphere. At this temperature H_2 obeys the Boltzmann distribution. To what temperature must the H_2 gas be cooled before quantum effects become important and the use of the Boltzmann distribution is no longer appropriate? (*Hint:* Equate the de Broglie wavelength at the average energy to the average spacing between molecules, using the ideal gas law to compute the density.)

Section 8-3 The Bose-Einstein Condensation

8-24. Compute N_0/N from Equation 8-52 for (*a*) $T = 3T_c/4$, (*b*) $T = \frac{1}{2}T_c$, (*c*) $T = T_c/4$, and (*d*) $T = T_c/8$.
8-25. Show that $N_0 \approx 1/\alpha$ for small values of α as asserted in the paragraph above Equation 8-52.
8-26. Like ^{4}He, the most common form of neon, ^{20}Ne, is a rare gas and the ^{20}Ne atoms have zero spin and hence are bosons. But unlike helium, neon does not become superfluid at low temperatures. Show that this is to be expected by computing neon's critical temperature and comparing it with the element's freezing point of 24.5 K.

Section 8-4 The Photon Gas: An Application of Bose-Einstein Statistics

8-27. If the Sun were to become cooler (without changing its radius), the energy density at the surface would decrease according to Equation 8-56. Suppose the Sun's temperature were to decrease by 5 percent. Compute the fractional change in the rate at which solar energy arrives at Earth. (Assume that the Sun's surface is in equilibrium and radiates as a blackbody.)
8-28. Find the average energy of an oscillator at (*a*) $T = 10hf/k$, (*b*) $T = hf/k$, and (*c*) $T = 0.1hf/k$ and compare your results with those from the equipartition theorem.
8-29. (*a*) Show that the rule of Dulong-Petit follows directly from Einstein's specific heat formula (Equation 8-62) as $T \rightarrow \infty$. (*b*) Show that $C_V \rightarrow 0$ as $T \rightarrow 0$.
8-30. Using Figure 8-13, compute the (approximate) frequency of atomic oscillations in silicon and in aluminum at 200 K.
8-31. Use Equation 8-62 to calculate the value of C_V for a solid at the Einstein temperature $T_E = hf/k$.

Section 8-5 Properties of a Fermion Gas

8-32. Use Equation 8-69 to plot an accurate graph of $n_{FD}(E)/V$ for electrons whose Fermi energy is 4.8 eV from $E = 4.5$ eV to $E = 5.1$ eV at $T = 300$ K. Determine from the graph the number of electrons per unit volume just below the Fermi energy that can move to states just above the Fermi energy.
8-33. Consider a gas of electrons (fermions) and a gas of photons (bosons). Which has more states available at $T = 1$ K? Explain why.

Level II

8-34. The molar heat capacity data given in Table 8-2 are taken from *AIP Handbook*, 2d ed. (McGraw-Hill, New York, 1963). Plot the data for these solids all on one graph and sketch in the curves C_V versus T. Estimate the Einstein temperature for each of the solids using the result of Problem 8-31.
8-35. Recalling that the Fermi-Dirac distribution function applies to all fermions, including protons and neutrons, each of which have spin $\frac{1}{2}$, consider a nucleus of ^{22}Ne consisting of 10 protons and 12 neutrons. Protons are distinguishable from neutrons, so two of each particle (spin up, spin down) can be put into each energy state. Assuming that the radius of the ^{22}Ne nucleus is 3.1×10^{-15} m, estimate the Fermi energy and the average energy of the nucleus in ^{22}Ne. Express your results in MeV. Do the results seem reasonable?

STUDENTS-HUB.com Uploaded By: Malak Obaid

Table 8-2 Heat capacities in cal/mole • K for Au, diamond, Al, and Be

T, K	Au	Diamond	Al	Be
20	0.77	0.00	0.05	0.003
50	3.41	0.005	0.91	0.04
70	4.39	0.016	1.85	0.12
100	5.12	0.059	3.12	0.43
150	5.62	0.24	4.43	1.36
200	5.84	0.56	5.16	2.41
250	5.96	0.99	5.56	3.30
300	6.07	1.46	5.82	3.93
400	6.18	2.45	6.13	4.77
500	6.28	3.24	6.42	5.26
600	6.40	3.85	6.72	5.59
800	6.65	4.66	7.31	6.07
1000	6.90	5.16	7.00	6.51

8-36. What is the ground-state energy of 10 noninteracting bosons in a one-dimensional box of length L?

8-37. Make a plot of $f_{FD}(E)$ versus E for (*a*) $T = 0.1T_F$, and (*b*) $T = 0.5T_F$, where $T_F = E_F/k$.

8-38. Compute the fraction of helium atoms in the superfluid state at (*a*) $T = T_c/2$ and (*b*) $T = T_c/4$.

8-39. The depth of the potential well for free electrons in a metal can be accurately determined by observing that the photoelectric work function is the energy necessary to remove an electron at the top of the occupied states from the metal; an electron in such a state has the Fermi energy. Assuming each atom provides one free electron to the gas, compute the depth of the well for the free electrons in gold. The work function for gold is 4.8 eV.

8-40. An early method testing Maxwell's theoretical prediction for the distribution of molecular speeds is shown in Figure 8-34. In 1925 Otto Stern used a beam of Bi_2 molecules emitted from an oven at 850 K. The beam defined by slit S_1 was admitted into the interior of a rotating drum via slit S_2 in the drum wall. The identical bunches of molecules thus formed struck and

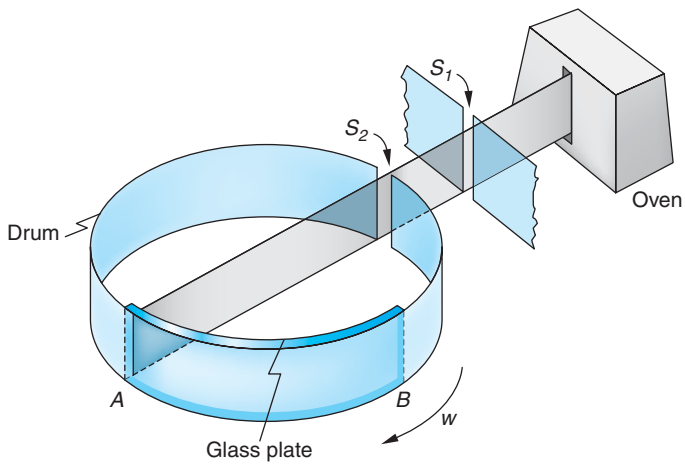

Figure 8-34

STUDENTS-HUB.com Uploaded By: Malak Obaid

adhered to a curved glass plate fixed to the interior drum wall, the fastest molecules striking near A, which was opposite S_2, the slowest near B, and the others in between depending on their speeds. The density of the molecular deposits along the glass plate were measured with a densitometer. The density (proportional to the number of molecules) plotted against distance along the glass plate (dependent on v) made possible determination of the speed distribution. If the drum is 10 cm in diameter and is rotating at 6250 rpm, (*a*) find the distance from A where molecules traveling at v_m,$\langle v\rangle$, and v_{rms} will strike. (*b*) The plot in (*a*) must be corrected slightly in order to be compared with Maxwell's distribution equation. Why? (*c*) Would N_2 molecules work as well as Bi_2 molecules in this experiment? Why or why not?

8-41. The speed distribution of molecules in a container is the Maxwell distribution $f(v) \propto v^2 e^{-mv^2/2kT}$. The number with speed v that hit the wall in a given time is proportional to the speed v and to $f(v)$. Thus, if there is a very small hole in the wall (too small to have much effect on the distribution inside), the speed distribution of those that escape is $F(v) \propto vf(v) \propto v^3 e^{-mv^2/2kT}$. Show that the mean energy of those that escape is $2kT$.

Level III

8-42. This problem is related to the equipartition theorem. Consider a system in which the energy of a particle is given by $E = Au^2$, where A is a constant and u is any coordinate or momentum that can vary from $-\infty$ to $+\infty$. (*a*) Write the probability of the particle having u in the range du and calculate the normalization constant C in terms of A. (*b*) Calculate the average energy $\langle E\rangle = \langle Au^2\rangle$ and show that $\langle E\rangle = \frac{1}{2}kT$.

8-43. Calculate the average value of the magnitude of v_x from the Maxwell distribution.

8-44. Show that $f_{FD}(E) \rightarrow f_B(E)$ for $E \gg E_F$.

8-45. Carry out the integration indicated in Equation 8-43 to show that α is given by Equation 8-44.

8-46. Consider a system of N particles that has only two possible energy states, $E_1 = 0$ and $E_2 = \epsilon$. The distribution function is $f_i = Ce^{-E_i/kT}$. (*a*) What is C for this case? (*b*) Compute the average energy $\langle E\rangle$ and show that $\langle E\rangle \rightarrow 0$ as $T \rightarrow 0$ and $\langle E\rangle \rightarrow \epsilon/2$ as $T \rightarrow \infty$. (*c*) Show that the heat capacity is

$$C_V = Nk\left(\frac{\epsilon}{kT}\right)^2 \frac{e^{-\epsilon/kT}}{(1 + e^{-\epsilon/kT})^2}$$

(*d*) Sketch C_V versus T.

8-47. If the assumptions leading to the Bose-Einstein distribution are modified so that the number of particles is not assumed constant, the resulting distribution has $e^{\alpha} = 1$. This distribution can be applied to a "gas" of photons. Consider the photons to be in a cubic box of side L. The momentum components of a photon are quantized by the standing-wave conditions $k_x = n_1\pi/L$, $k_y = n_2\pi/L$, and $k_z = n_3\pi/L$, where $p = \hbar(k_x^2 + k_y^2 + k_z^2)^{1/2}$ is the magnitude of the momentum. (*a*) Show that the energy of a photon can be written $E = N(\hbar c\pi/L)$, where $N^2 = n_1^2 + n_2^2 + n_3^2$. (*b*) Assuming two photons per space state because of the two possible polarizations, show that the number of states between N and $N + dN$ is $\pi N^2\, dN$. (*c*) Find the density of states and show that the number of photons in the energy interval dE is

$$n(E)\, dE = \frac{8\pi(L/hc)^3 E^2\, dE}{e^{E/kT} - 1}$$

(*d*) The energy density in dE is given by $u(E)\, dE = En(E)\, dE/L^3$. Use this to obtain the Planck blackbody radiation formula for the energy density in $d\lambda$, where λ is the wavelength:

$$u(\lambda) = \frac{8\pi hc\lambda^{-5}}{e^{hc/\lambda kT} - 1}$$

STUDENTS-HUB.com Uploaded By: Malak Obaid

PART 2

Applications of Quantum Mechanics and Relativity

Part 1 introduced the principles of the special and general relativity theories and illustrated how they led to profound alterations of our classical views of space and time. We then saw how the ideas and methods of quantum mechanics developed and how their application to atomic physics provides us with an understanding of atomic structure and spectra that is in excellent accord with our observations. In Part 2 we extend the applications of quantum theory and relativity to a wider variety of physical systems and phenomena that are, like atomic physics, of great interest to engineers, chemists, and physicists.

The topics we will discuss form the foundation of a broad range of theoretical and experimental research by physicists, chemists, and mathematicians and provide the basic understanding of the principles underlying many practical devices developed by engineers. They include molecular bonding and spectra (Chapter 9); the structure of solids and their thermal and electrical properties (Chapter 10); superconductors (Chapter 10); nuclear structure, radioactivity, and nuclear reactions (Chapter 11); and elementary particles, the quarks and leptons, that are the constituents of all visible matter (Chapter 12). Practical applications include the study of lasers (Chapter 9); semiconductors, semiconductor junctions, and transistors (Chapter 10), and radioactive dating and elemental analysis, nuclear fission and fusion, and reactors (Chapter 11). Many of these applications have revolutionized contemporary society. Part 2 concludes with a look outward into the cosmos from our solar system to the Big Bang, the realm of astrophysics and cosmology (Chapter 13), topics that stimulate the imagination of everyone. These chapters are independent of one another and can be studied in any order.

STUDENTS-HUB.com
Uploaded By: Malak Obaid

This page intentionally left blank

STUDENTS-HUB.com Uploaded By: Malak Obaid

CHAPTER 9

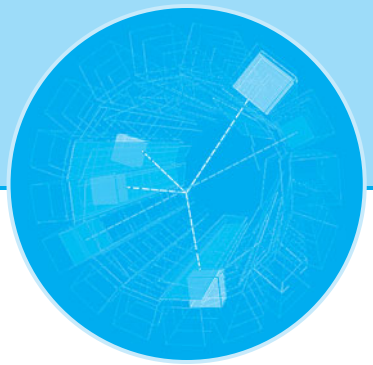

Molecular Structure and Spectra

9-1 The Ionic Bond 364
9-2 The Covalent Bond 369
9-3 Other Bonding Mechanisms 375
9-4 Energy Levels and Spectra of Diatomic Molecules 379
9-5 Scattering, Absorption, and Stimulated Emission 390
9-6 Lasers and Masers 396

In this chapter we will study the bonding of molecules—systems of two or more atoms. Properly, a molecule is the smallest constituent of a substance that retains its chemical properties. The study of the properties of molecules forms the basis for theoretical chemistry. The application of quantum mechanics to molecular physics has been spectacularly successful in explaining the structure of molecules and the complexity of their spectra and in answering such puzzling questions as why two H atoms join together to form a molecule but three H atoms do not. As in atomic physics, the detailed quantum-mechanical calculations are often difficult. When the difficulty would tend to obscure understanding of the physics, we will, as before, make our discussions semiquantitative or qualitative. In the final sections we will discuss the interaction of electromagnetic radiation with molecules, concluding with a discussion of the common general types of lasers.

There are essentially two extreme views we can take of a molecule. Consider, for example, H_2. We can think of it either as two H atoms somehow joined together or as a quantum-mechanical system of two protons and two electrons. The latter picture is more fruitful in this case because neither of the electrons in the H_2 molecule can be considered as belonging to either proton. Instead, the wave function for each electron is spread out in space about the whole molecule. For more complicated molecules, however, an intermediate picture is useful. Consider the N_2 molecule as an example. We need not consider the complicated problem of 2 nuclei and 14 electrons. The electron configuration of an N atom in the ground state is $1s^2 2s^2 2p^3$. Of the three electrons in the $2p$ state, two are in an $m_\ell = -1$ state with their spins paired (that is, with spins antiparallel so that the resultant spin for those two is zero). The third one is in an $m_\ell = 0$ level and its spin is, of course, unpaired. Only the electron with the unpaired spin is free to take part in the bonding of the N_2 molecule. We therefore can consider this molecule as two N^+ ions and two electrons that belong to the molecule as a whole. The molecular wave functions for these bonding electrons are called *molecular orbitals*. In many cases these molecular wave functions can be constructed from linear combinations of the atomic wave functions with which we are familiar.

Another type of bonding involves the transfer of one or more electrons between atoms, the bond resulting from Coulomb attraction between the ions, an example being NaCl. Again in this case, as in all four types of molecular bonding, it is the wave properties of the spin-$\frac{1}{2}$ electrons that are the key to understanding.

STUDENTS-HUB.com
Uploaded By: Malak Obaid

9-1 The Ionic Bond

The two principal types of bonds that join two or more atoms together to form a molecule are called *ionic* and *covalent* bonds. Other types of bonds that are important in the bonding of liquids and solids are *dipole-dipole* bonds and *metallic* bonds. In many cases the bonding is a mixture of these mechanisms. We will discuss all of these in this chapter and the next, but it is important to recognize that all types of molecular bonding arise for the same fundamental reasons: the total energy of the stable bound molecule is lower than the total energy of the constituent atoms when they are widely separated, and there is a net attractive force between constituent atoms when their separation becomes larger than some equilibrium value. The bonding mechanisms are primarily due to electrostatic forces between the atoms or ions of the system together with the wave properties of electrons and the fact that they obey the exclusion principle. The complete description of molecular bonding is in most cases quite complex, involving as it does the mutual interactions of many electrons and nuclei; consequently, we will discuss each type using simplified models consisting of two or a few atoms, then illustrate qualitatively the extension of the results to more complex molecules.

The easiest type of bond to understand is the ionic bond, typically the strongest of the bonds and the one found in most salts. Consider KCl as an example. For the molecule to be stable, we must be able to show that $E(\text{KCl}) < E(\text{K}) + E(\text{Cl})$ when the K and Cl atoms are far apart and at rest. Let us define the energy of the system to be zero when the neutral atoms are widely separated. (See Figure 9-1.) The potassium atom has one 4*s* electron outside an argon core, $1s^2 2s^2 2p^6 3s^2 3p^6$. The ionization energy for K is low, as it is for all the alkali metals; for K only 4.34 eV is required to remove the outer electron from the atom. (See Table 9-1.) The removal of one electron from K leaves a positive ion with a spherically symmetric, closed-shell core. Chlorine, on the other hand, is only one electron short of having a closed argon core. The energy released by the acquisition of one electron is called the *electron affinity*, which in the case of Cl is 3.62 eV. Energy is released because the wave function of the "extra" electron penetrates the outer shell to a degree (see Figure 7-10*b*) and thus sees a net positive charge. The acquisition of one electron by chlorine results in a negative

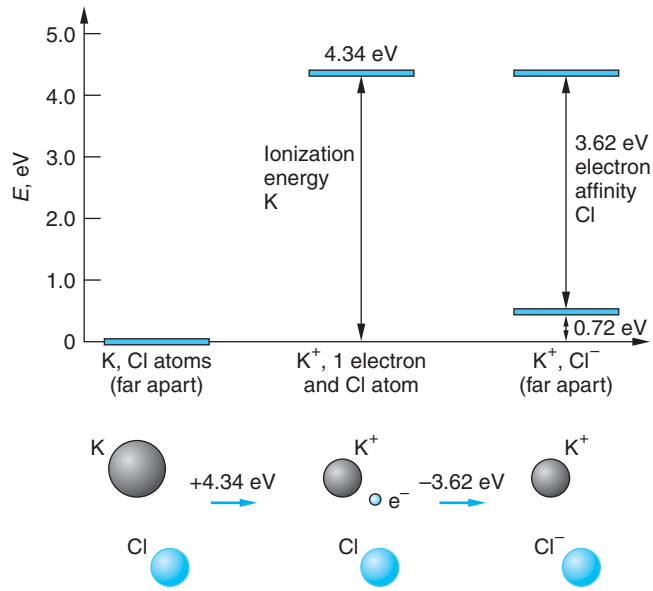

Figure 9-1 Net energy required to ionize a K and a Cl atom. An addition of 4.34 eV is required to remove the 4*s* electron from the neutral K atom, forming K^+ and a free electron. That electron (or some electron) can then occupy the vacancy in the 3*p* shell of the Cl atom forming a Cl^- ion. The electron is positively bound, with the release of 3.62 eV. Formation of the widely separated K^+ and Cl^- ions thus requires a net addition of 0.72 eV.

STUDENTS-HUB.com Uploaded By: Malak Obaid

Table 9-1 Ionization energies of alkali metal atoms and electron affinities of halogen atoms

Alkali metal	Ionization energy (eV)	Halogen	Electron affinity (eV)
Li	5.39	F	3.40
Na	5.14	Cl	3.61
K	4.34	Br	3.36
Rb	4.18	I	3.06
Cs	3.89	At	2.8
Fr	4.07		

Source: Data from *Handbook of Chemistry and Physics,* 85th ed. (New York: Chemical Rubber Co., 2004).

ion with a spherically symmetric, closed-shell electron core. Thus, the formation of a K^+ ion and a Cl^- ion by the donation of one electron of K to Cl requires just $4.34-3.62 = 0.72$ eV. If this were the whole story, the KCl molecule would not form; however, the electrostatic potential energy of the two ions separated by a distance r is $-ke^2/r$. When the separation of the ions is less than about 2.8 nm, the negative potential energy of attraction is of greater magnitude than the energy needed to create the ions, and the ions move toward each other.

Since the electrostatic attraction increases as the ions get closer, it would seem that equilibrium could not exist. For very small separation of the ions, however, the wave function of the $3p$ electrons in the K^+ ion and the $3p$ electrons in the Cl^- ion begin to overlap. Since the $3p$ shells in each ion contain electrons with sets of quantum numbers identical to those in the other, a strong repulsion develops due to the exclusion principle. This "exclusion-principle repulsion" is primarily responsible for the repulsion of the atoms in all molecules (except H_2), no matter which type of bonding occurs. When the ions are very far apart, the wave function for a core electron of one ion does not overlap that of the other ion. We can distinguish the electrons by the ion to which they belong, and the electrons of one ion can have the same quantum numbers as in the other ion. However, when the ions are close, the wave functions of their core electrons begin to overlap, and some of the electrons must go into higher-energy quantum states because of the exclusion principle, thus increasing the total energy of the system. This is not a sudden process: the energy states of the electrons are gradually changed as the ions move closer together. The total potential energy U of the KCl system can be expressed in terms of the separation r of the ion centers as the sum of the electrostatic potential, the exclusion-principle repulsion, and net ionization energy.

$$U(r) = -\frac{ke^2}{r} + E_{ex} + E_{ion} \qquad \textbf{9-1}$$

where $E_{ion} = 0.72$ eV for K^+ and Cl^-, as was found above. The exclusion-principle repulsion E_{ex} can be written as

$$E_{ex} = \frac{A}{r^n} \qquad \textbf{9-2}$$

STUDENTS-HUB.com Uploaded By: Malak Obaid

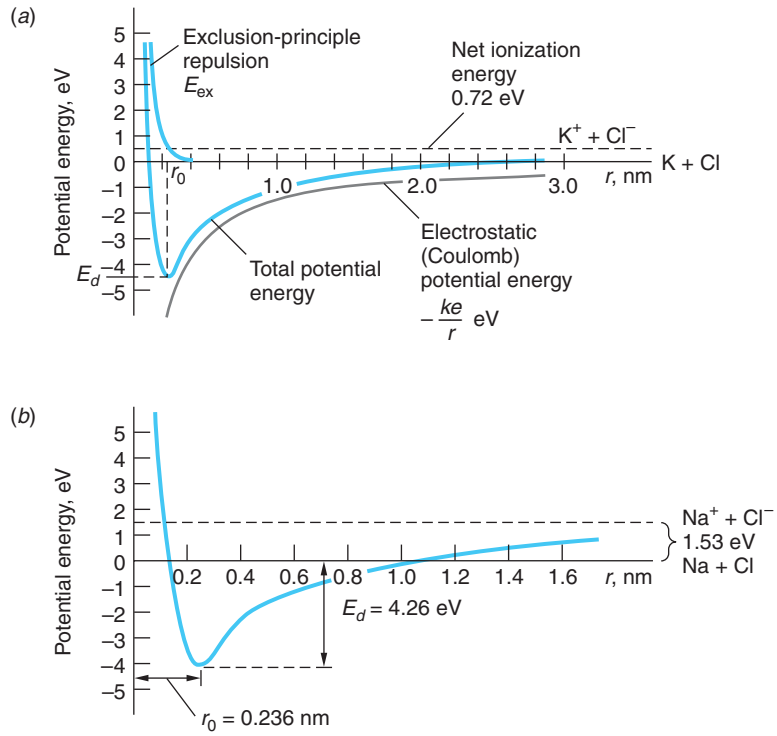

Figure 9-2 (*a*) Potential energy for K^+ and Cl^- ions as a function of separation distance *r*. The energy at infinite separation was chosen to be 0.72 eV, corresponding to the energy needed to form the ions from neutral atoms. The minimum energy for this curve is at the equilibrium separation $r_0 = 0.27$ nm for the ions in the molecule. (*b*) Potential energy for Na^+ and Cl^- ions as a function of *r*. Differences between the two similar molecules are due to the higher ionization potential and smaller core of Na.

where *A* and *n* are constants for each ionic molecule. Figure 9-2*a* is a sketch of the potential energy of the K^+ and Cl^- ions versus their separation. The energy is lowest at an equilibrium separation r_0 of about 0.27 nm. At smaller separations, the energy rises steeply as a result of the exclusion principle. The energy E_d required to separate the ions and form K and Cl *atoms*, called the *dissociation energy*, is about 4.40 eV. Figure 9-2*b* shows the total potential energy of another ionically bonded molecule, NaCl. Note the differences between the two total potential energy curves, which are due to the higher ionization potential and smaller closed-shell core of Na compared to K. Example 9-1 illustrates calculations used to construct curves like those in the diagram. Example 9-2 describes how the constants *A* and *n* in Equation 9-2 are found.

EXAMPLE 9-1 **Ionic Bonding in NaF** The ionization potential of sodium is 5.14 eV, the electron affinity of fluorine is 3.40 eV, and the equilibrium separation of sodium fluoride (NaF) is 0.193 nm. (*a*) How much energy is needed to form Na^+ and F^- ions from neutral sodium and fluorine atoms? (*b*) What is the electrostatic potential energy of the Na^+ and F^- ions at their equilibrium separation? (*c*) The dissociation energy of NaF is 4.99 eV. What is the energy due to repulsion of the ions at the equilibrium separation?

SOLUTION

(*a*) Since the energy needed to ionize sodium is 5.14 eV and the electron affinity of F is 3.40 eV, the energy needed to form Na^+ and F^- ions from neutral sodium and fluorine atoms is 5.14 eV − 3.40 eV = 1.74 eV = E_{ion}.

(*b*) The electrostatic potential energy of the Na^+ and F^- ions at their equilibrium separation (with $-ke^2/r = 0$ at infinite separation) is

STUDENTS-HUB.com Uploaded By: Malak Obaid

$$-\frac{ke^2}{r_0} = -\frac{(8.99 \times 10^9\ \text{N} \cdot \text{m}^2/C^2)(1.60 \times 10^{-19} C)^2}{1.93 \times 10^{-10}\ \text{m}}$$
$$= -1.19 \times 10^{-18}\ \text{J} = -7.45\ \text{eV}$$

(*c*) Choosing the total potential energy at infinity to be 1.74 eV (the net ionization energy needed to form Na^+ and F^- from the neutral atoms), the net electrostatic (Coulomb) potential U_C is

$$U_C = -\frac{ke^2}{r} + 1.74\ \text{eV}$$

At the equilibrium separation r_0, this energy is $U_C = -7.45\ \text{eV} + 1.74\ \text{eV} = -5.71\ \text{eV}$. Since the measured dissociation energy is 4.99 eV, the potential energy due to exclusion-principle repulsion E_{ex} of the Na^+ and F^- at equilibrium separation, from Equation 9-1, must be $5.71\ \text{eV} - 4.99\ \text{eV} = 0.72\ \text{eV}$.

EXAMPLE 9-2 Contribution from Exclusion-Principle Repulsion Find the values of A and n in Equation 9-2 for NaF.

SOLUTION

From Example 9-1 we have that the potential energy due to exclusion-principle repulsion at equilibrium separation of the ions is

$$E_{ex}(r_0) = \frac{A}{r_0^n} = \frac{A}{(0.193\ \text{nm})^n} = 0.72\ \text{eV}$$

At $r = r_0$ the net force on each ion must be zero because the potential energy has its minimum value at that point. This means that at $r = r_0$, the net Coulomb force F_C is equal in magnitude and opposite in sign to the exclusion-principle repulsive force, i.e.,

$$F_C = -\left(\frac{dU_C}{dr}\right)_{r=r_0} = \left(\frac{nA}{r^{n+1}}\right)_{r=r_0}$$

At $r = r_0$

$$F_C = \frac{U_C(r_0)}{r_0} = \frac{ke^2}{r_0^2} = 38.7\ \text{eV/nm}$$

Thus, we have that

$$\frac{nA}{r_0^{n+1}} = \frac{n}{r_0}\frac{A}{r_0^n} = \frac{n}{r_0}(0.72\ \text{eV}) = 38.7\ \text{eV/nm}$$

or

$$n = \frac{38.7\ \text{eV/nm}}{0.72\ \text{eV}} \times (0.193\ \text{nm}) = 10.4 \approx 10$$

and, therefore, $A = 5.4 \times 10^{-8}\ \text{eV} \cdot \text{nm}^{10}$. Finally, for NaF, E_{ex} is given by

$$E_{ex} = \frac{(5.4 \times 10^{-8}\ \text{eV} \cdot \text{nm}^{10})}{r^{10}}$$

STUDENTS-HUB.com Uploaded By: Malak Obaid

It should be emphasized that our discussion of ionic bonding and, in particular, the graphs of potential energy in Figure 9-2 apply to the *ground states* of the molecules. The outer (valence) electrons of molecules may occupy excited states, just as they do in atoms. Since the electron wave functions of the excited states tend to extend farther from the ions than do those of the ground state, the potential energy curve is broader and shallower than for the ground state, resulting in a slightly weaker bond and a larger equilibrium separation of the ions. In our discussion we have ignored two additional contributions to the total energy of the molecule: (1) the zero-point energy (see Section 5-6), which decreases the magnitude of E_d, and (2) the van der Waals attraction, which increases the magnitude of E_d. Both are small and tend to partially offset each other. The latter, which arises from induced dipole moments, is the only form of bonding available for certain molecules and will be discussed later in this chapter.

The KCl equilibrium separation of 0.27 nm noted earlier is for gaseous diatomic KCl (which can be obtained by evaporation of solid KCl). Normally, KCl exists in a cubic crystal structure, with K^+ and Cl^- at alternate corners of a cube. The separation of the ions in a crystal is somewhat larger—about 0.32 nm. Because of the presence of neighboring ions of opposite charge, the Coulomb energy per ion pair is lower when the ions are in a crystal. This energy is usually expressed as $\alpha ke^2/r_0$, where r_0 is the equilibrium separation distance or *bond length* and α, called the *Madelung constant*, depends on the crystal structure, as will be discussed further in Chapter 10. For KCl, α is about 1.75. The values of E_d and r_0 listed in Table 9-2 are for several ionically bonded (gaseous) molecules.

Table 9-2 Dissociation energies E_d and equilibrium separations r_0 for several ionic molecules* in the gaseous state

Molecule	Dissociation energy (eV)	Equilibrium separation (nm)
NaCl	4.27	0.236
NaF	5.34	0.193
NaH	1.92	0.189
NaBr	3.81	0.250
LiCl	4.86	0.202
LiH	2.47	0.159
LiI	3.58	0.239
KCl	4.49	0.267
KBr	3.94	0.282
RbF	5.12	0.227
RbCl	4.43	0.279
CsI	3.50	0.332

*The two entries of molecules formed by an alkali atom and a hydrogen atom may seem odd, but hydrogen atoms, like those of a number of other elements, may form molecules as either positive or negative ions. The ionization energy of H is, of course, 13.6 eV; its electron affinity is 0.75 eV.

Source: Data from *Handbook of Chemistry and Physics,* 85th ed. (New York: Chemical Rubber Co., 2004).

STUDENTS-HUB.com Uploaded By: Malak Obaid

One final comment concerning ionic bonding: Few of the molecules in Table 9-2 are bonded exclusively by the ionic mechanism. As we will see in the next section, they may also be covalently bonded.

9-2 The Covalent Bond

A completely different mechanism is responsible for the bonding of such molecules as H_2, N_2, H_2O, and CO and also leads to bonding of many of the molecules in Table 9-2. If we calculate the energy needed to form the ions H^+ and H^- by the transfer of an electron from one atom to the other, we find the net ionization energy to be more than 12 eV. Adding this energy to the electrostatic energy (including the repulsion of the protons), we find that there is no separation distance for which the total energy is negative. The bond of H_2 thus cannot be ionic. The attraction of two hydrogen atoms is instead an entirely quantum-mechanical effect. The decrease in energy when two hydrogen atoms approach each other is due to the sharing of the two electrons by both atoms and is intimately connected with the symmetry properties of the electron wave functions. We can gain some insight into this phenomenon by first studying a simple one-dimensional quantum-mechanics problem—that of two finite square wells each of width L.

Consider first a single electron that is equally likely to be in either well. Since the wells are identical, symmetry requires that $|\Psi|^2$ be symmetric about the midpoint of the wells. Then Ψ must be either symmetric or antisymmetric about that point. These two possibilities for the ground state are shown in Figure 9-3. Previously, we did not distinguish between these two possibilities when superimposing (i.e., adding) wave functions because the energies $\pi^2\hbar^2/2mL^2$ and the probability densities Ψ^2 for both of these wave functions are the same when the wells are far apart. Figure 9-4 shows the symmetric and antisymmetric wave functions when the wells are very close together. Now the parts of the wave function describing the electron in one well or the other overlap, and the symmetric and antisymmetric resultant wave functions are quite different. Notice that for the symmetric wave functions the probability of the electron being found in the region between the wells is much larger than for the antisymmetric wave function. In the limiting case of no separation, the symmetric wave function Ψ_S approaches the ground-state wave function for a particle in a well

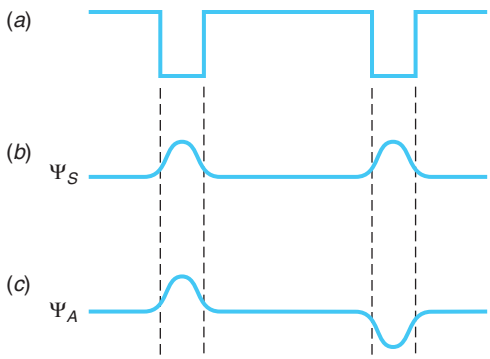

Figure 9-3 (*a*) Two square wells far apart. The electron wave function can be either (*b*) symmetric or (*c*) antisymmetric. The probability distributions and energies are the same for the two wave functions when the wells are far apart.

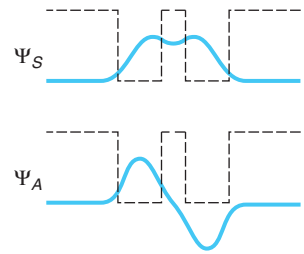

Figure 9-4 Symmetric and antisymmetric space wave functions for two square wells close together. The probability distributions and energies are not the same for the two wave functions in this case. The symmetric space wave function (and therefore the probability density) is larger between the wells than the antisymmetric space wave function.

STUDENTS-HUB.com Uploaded By: Malak Obaid

of size $2L$ and the antisymmetric wave function Ψ_A approaches that for the first excited state in such a well; thus Ψ_S is a lower energy state than Ψ_A. This discussion has two important results:

1. The originally equal energies for Ψ_A and Ψ_S are split into two different energies as the wells become close.
2. The wave function for the symmetric state is large in the region between the wells, whereas that for the antisymmetric state is small.

Now consider adding a second electron to the two wells. The *total* wave function for the two electrons must be antisymmetric on exchange of the electrons since they obey the Pauli exclusion principle. Note that exchanging the electrons in the wells is the same as exchanging the wells; i.e., for a two-particle system, exchange symmetry is the same as space symmetry. The two electrons can therefore be in the space-symmetric state if the spins are antiparallel ($S = 0$) or in the space-antisymmetric state if their spins are parallel ($S = 1$).

H_2^+ Molecule

Now let us consider a real physical system with one electron, the hydrogen molecule ion H_2^+. For a one-dimensional model, the double potential well formed by the two protons is illustrated in Figure 9-5. The Hamiltonian (total energy) operator for this system is (see Equation 6-51 and Figure 9-5*b*)

$$H_{\text{op}} = \frac{p_{\text{op}}^2}{2m} + ke^2\left(-\frac{1}{r_1} - \frac{1}{r_2} + \frac{1}{r_0}\right)$$

In the ground state, the hydrogen atom wave function is proportional to e^{-r/a_0}. For our one-dimensional model, we will write this as $e^{-|x|/a_0}$. The symmetric and antisymmetric combinations for two values of the distance between the protons are shown in Figure 9-6. In general,

$$\Psi_S = \left(\frac{1}{\sqrt{2}}\right)(\Psi_{100}(r_1) + \Psi_{100}(r_2))$$

and

$$\Psi_A = \left(\frac{1}{\sqrt{2}}\right)(\Psi_{100}(r_1) - \Psi_{100}(r_2))$$

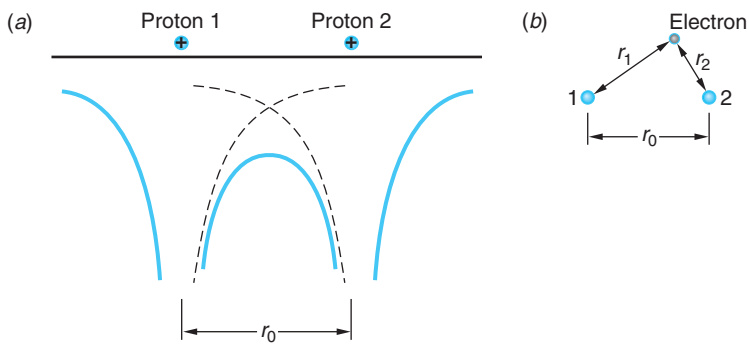

Figure 9-5 Coulomb potential for an electron resulting from two protons separated by a distance r_0. The solid line is the total potential for a one-dimensional model. The circled plus signs mark the locations of the protons.

STUDENTS-HUB.com Uploaded By: Malak Obaid

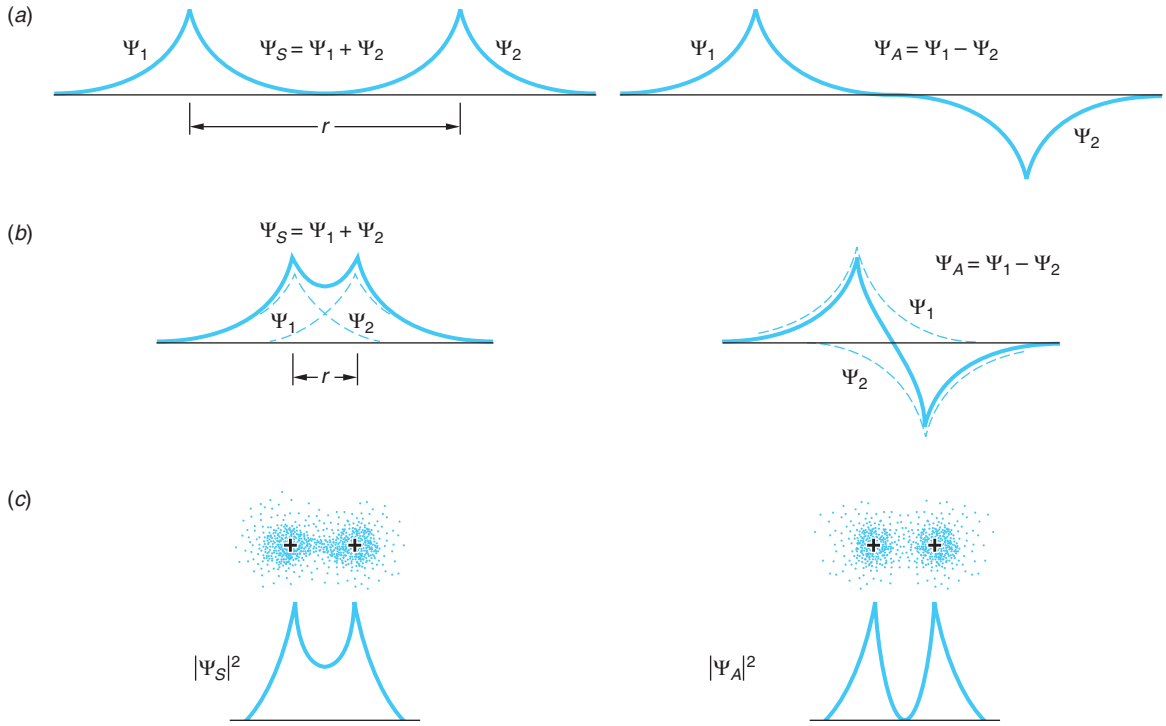

Figure 9-6 One-dimensional symmetric and antisymmetric electron space wave functions for (*a*) two protons far apart and (*b*) two protons close together. (*c*) Probability distributions for wave functions in (*b*). Computer-drawn electron density around the protons is shown above the probability densities.

The results are similar to the square-well case: Ψ_S is large in the region between the protons, while Ψ_A is small in that region. Only in the case where the electron wave function and, hence, the probability density is large near the center of the molecule do we expect a stable molecular bond to form. This concentration of negative charge between the protons for Ψ_S holds the protons together. Similarly, we would not expect Ψ_A to result in a stable molecule. The justification of this conclusion would be the solution of the Schrödinger equation and calculation of $|\Psi|^2$ for H_2^+.

The solution and calculation are quite difficult, so we will simply state the results for the energy of the molecule as a function of the separation r of the protons, describing in the process how, in general, the potential energy function arises. Referring first to Figure 9-6*a*, when the protons are far apart, the electron's energy is −13.6 eV. The potential energy U_p (repulsion) of the protons is negligibly small for large r and, since there is only a single electron in the system, there is no exclusion-principle repulsion. As the two protons are brought closer together as in Figure 9-6*b*, U_p increases and the energy of the electron decreases since the electron experiences a greater Coulomb force and becomes more tightly bound. Consider what is happening to the energy of the electron as the separation r of the protons is reduced. As $r \rightarrow 0$, the electron's wave function is approaching that of an atom with $Z = 2$. The symmetric wave function Ψ_S has a maximum at $r = 0$ and thus corresponds to the 1*s* (ground) state of the $Z = 2$ atom. As we have already seen (Equation 7-25), its energy is $E_1 = -13.6\ Z^2/n^2 = -54.4$ eV. For our discussion here, let us call the electron's energy E_S for the wave function Ψ_S.

STUDENTS-HUB.com Uploaded By: Malak Obaid

Thus, $E_S = -13.6$ eV for $r \to \infty$ and $E_S = -54.4$ eV for $r \to 0$. The antisymmetric wave function Ψ_A is zero at $r = 0$ and thus corresponds to the $2p$ (first excited) state of the $Z = 2$ atom, this state being the lowest energy state with a wave function that vanishes at $r = 0$. (See Equation 7-26 and Table 7-2.) The energy of this state is $E_2 = -13.6\ Z^2/n^2 = -13.6$ eV. As above, if we call E_A the energy of the electron for the wave function Ψ_A, then $E_A = -13.6$ eV for $r \to \infty$ (where $|\Psi_S|^2$ and $|\Psi_A|^2$ are the same) and $E_A = -13.6$ eV for $r \to 0$. Recall that the smaller average slope of Ψ_S compared to Ψ_A as $r \to 0$ implies a smaller energy for the symmetric state. The variation of both E_S and E_A are shown in Figure 9-7.

The potential energy U_p of the protons as a function of their separation is, of course, $U_p = ke^2/r$, and the total energy of the H_2^+ molecule is then $U_p + E_S$ or $U_p + E_A$, depending on which of the electronic wave functions happens to exist. As can be seen in Figure 9-7, only one of the total energy functions has a minimum and therefore can result in bonding of the H_2^+ molecule. The potential energy function $E_{\text{total}} = U_p + E_S$ has a minimum at $r = 0.106$ nm. This tells us that the H_2^+ molecule is stable, with equilibrium separation $r_0 = 0.106$ nm and binding energy $= E_{\text{total}}(r \to \infty) - E_{\text{total}}(r_0) = -13.6 - (-16.3) = 2.7$ eV. In contrast, the potential energy function $E_{\text{total}} = U_p + E_A$ has no minimum; therefore, the antisymmetric wave function does not result in a stable molecule, as we expected at the outset of this discussion. Note that the H_2^+-type bond will tend to be unstable unless the nuclei have the same Z.

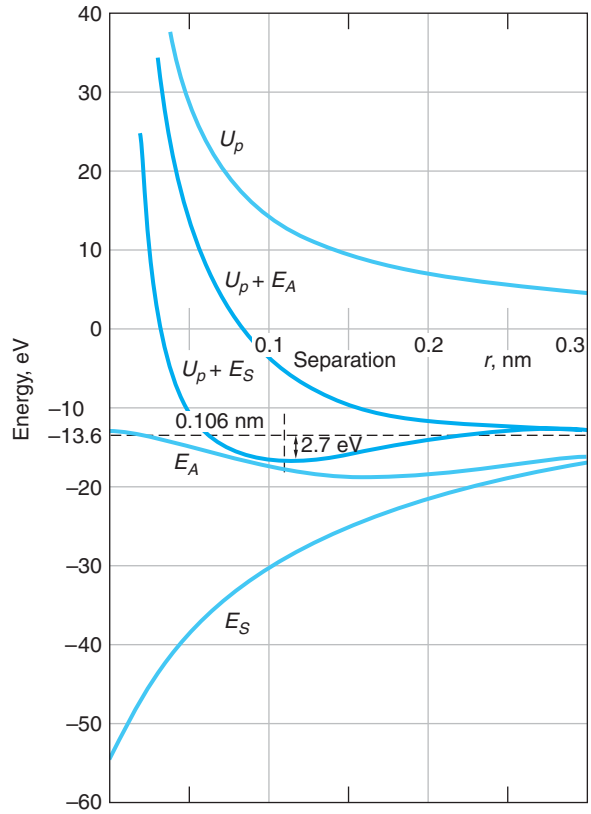

Figure 9-7 Dependence of the molecular potential energy on the separation of the protons and on the symmetry of the electron wave function for the H_2^+ system.

STUDENTS-HUB.com Uploaded By: Malak Obaid

H_2 Molecule

Formation of the H_2 molecule is very similar to that of H_2^+. We can think of it as two H atoms in their ground states, initially far apart. Each has a 1*s* electronic *orbital*,[1] i.e., an electron the space part of whose wave function is Ψ_{100}, with an energy of -13.6 eV. Thus, the total energy of the H_2 system for large r (i.e., $r \rightarrow \infty$) is -27.2 eV. As the two atoms approach each other, the wave functions begin to overlap, again as illustrated by Figure 9-6*a* and *b*, so that the two atoms (protons) share both electrons. Just as was discussed above, the two wave functions may add to produce a symmetric total wave function Ψ_S that results in a stable bound H_2 molecule or an antisymmetric one Ψ_A, which does not lead to a stable molecule. Since the *total* wave function Ψ must always be antisymmetric to an exchange of the electrons, the *space* wave function $\Psi_S (= R_{n\ell} Y_{\ell m})$ must be associated with an antisymmetric *spin* function χ_A (see Section 7-6). Thus, Ψ_S is a singlet state ($S = 0$) and Ψ_A is a triplet state ($S = 1$).

There is a difference between the H_2 molecule and the H_2^+ molecule that needs explanation. Just as H_2^+, the H_2 molecule has two *molecular* states whose total energy at large r is, as we have seen, -27.2 eV. As r gets smaller, the molecule still has two states, but their energies separate, as sketched in Figure 9-8*a*. The lower energy E_S is, as before, associated with Ψ_S, the electronic wave function of the stable molecule, known also as the *bonding orbital*. The wave function Ψ_A associated with the energy E_A that does not result in bonding is also called the *antibonding orbital*. The difference is that there are now two electrons whose probability density is large in the region between the protons, both in the Ψ_S molecular orbital. Since electrons obey the exclusion principle, their spins must be antiparallel ($S = 0$). Thus, a molecular orbital, just like an atomic orbital, can be occupied by no more than two electrons. For H_2 both electrons can occupy the bonding orbital. Both electrons being in *s* states, H_2 is referred to as being *s-bonded*.

Figure 9-8*b* illustrates the potential energy functions for H_2. The energy corresponding to Ψ_S, the bonding orbital, has a minimum of $E = -31.7$ eV at $r = 0.074$ nm—i.e., the equilibrium separation $r_0 = 0.074$ nm—and the binding

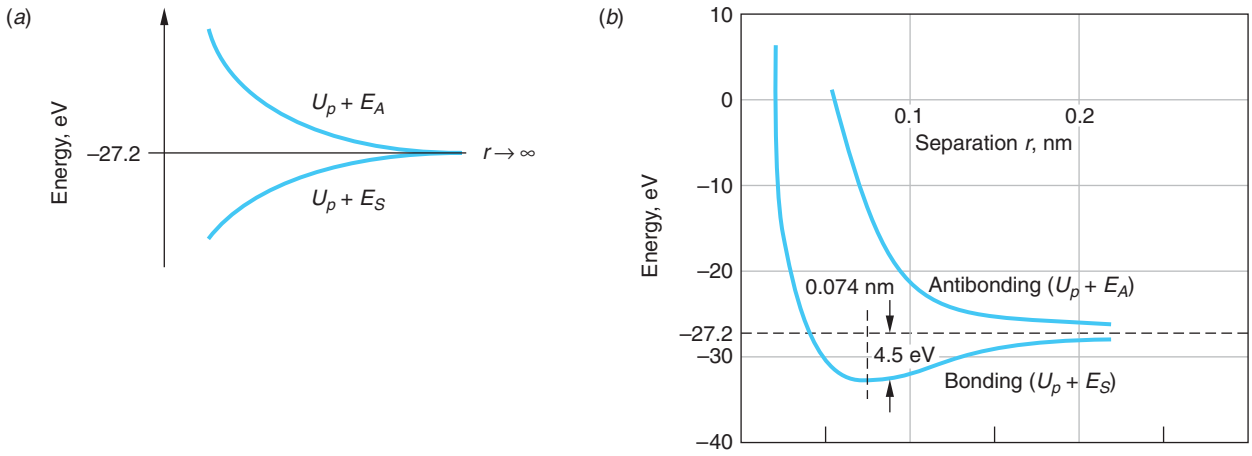

Figure 9-8 (*a*) The two levels of the H_2 system, which have the same energy for $r \rightarrow \infty$, have different energies as the atoms approach each other. (*b*) Potential energy versus separation for two hydrogen atoms. $U_p + E_S$ is for the symmetric (bonding) space wave function, and $U_p + E_A$ is for the antisymmetric (antibonding) space wave function. As the separation approaches zero, both curves approach $+\infty$.

STUDENTS-HUB.com Uploaded By: Malak Obaid

energy is $E(r \rightarrow \infty) - E(r_0) = -27.2 - (-31.7) = 4.5$ eV. The effect of adding the second electron to H_2^+ to form H_2 is evident from a comparison of Figure 9-7 and Figure 9-8*b*. The increased charge concentration between the protons binds them more tightly, the binding energy increasing from 2.7 eV to 4.5 eV and the equilibrium separation decreasing by 30 percent. The sharing of the outer, or valence, electrons in a molecule, as in our H_2 example, is the mechanism of the *covalent* molecular bond. The basic requirement for covalent bonding is that the wave functions of the valence electrons of the participating atoms overlap as much as possible. Unlike the H_2^+ case, the covalent bond is just as strong for nonidentical nuclei as it is for identical nuclei.[2]

We can now see why three H atoms do not bond to form H_3. If a third H atom is brought near an H_2 molecule, the third electron cannot be in a 1*s* state and have its spin antiparallel to both the other electrons. It must therefore occupy the higher-energy, antibonding orbital. If it is in an antisymmetric state with respect to exchange with one of the electrons, the repulsion of this atom is greater than the attraction of the other. Thus, as the three atoms are pushed together, the third electron is in effect forced into a higher quantum state by the exclusion principle. The bond between two H atoms is called a *saturated bond* because there is no room for another electron. The two electrons being shared essentially fill the 1*s* states of both atoms. This is basically the reason why covalent bonds involving three (or more) electrons are typically unstable. However, be aware that the H_3^+ ion *is* stable. Discovered by J. J. Thomson in 1911, this simplest of all polyatomic molecules provides important cosmic spectral lines for astrophysicists and a calculation benchmark for quantum chemists.

Although the H_3 molecule is not bound, the H_3^+ ion is! Discovered by J. J. Thomson in 1911, and lacking a stable excited state, H_3^+ is used as a probe in Jupiter's atmosphere and serves as the benchmark for quantum chemistry calculations for polyatomic molecules.

It should also be clear now why He atoms do not bond together to form He_2. There are no valence electrons that can be shared. As two He atoms approach each other, the bonding and antibonding molecular orbitals form, just as they do for H_2; however, each orbital can accommodate only two electrons (with spins antiparallel), so two of the four electrons in the He_2 system cannot remain in the 1*s* atomic states but must be in the antibonding orbital. The net effect is that He_2 does not form as a stable bond. At low temperatures or high pressures, He atoms do bond together, but the bonds are very weak and are due to van der Waals forces, which we will discuss in Section 9-3. The bonding is so weak that at atmospheric pressure, He boils at 4.2 K, and it does not form a solid at any temperature unless the pressure is greater than about 20 atm.

Covalent or Ionic?

Covalently bonded fullerene molecules have been assembled into nanotubes, i.e., tubes with diameters in the nanometer range. Adding a few impurity atoms per molecule turns it into a superconductor. (See Section 10-8.)

When two identical atoms bond, as in homonuclear diatomic molecules such as O_2 or N_2, the bonding is purely covalent. Since the wave functions of the two atoms are exactly alike, neither atom dominates and the electrons are completely shared between them. However, the bonding of two dissimilar atoms is often a mixture of covalent and ionic bonding. Even in NaCl, the electron donated by sodium to chlorine has some probability of being at the sodium atom because its wave function does not suddenly fall to zero. Thus, this electron is partially shared in a covalent bond, although this bonding is only a small part of the total bond, which is mainly ionic.

A measure of the degree to which a bond is ionic or covalent can be obtained from the electric dipole moment of the molecule. For example, if the bonding in NaCl were purely ionic, the center of positive charge would be at the Na^+ ion and the center of negative charge would be at the Cl^- ion. The electric dipole moment would have the magnitude

$$p_{\text{ionic}} = er_0 \qquad \textbf{9-3}$$

STUDENTS-HUB.com Uploaded By: Malak Obaid

where r_0 is the equilibrium separation of the ions. Thus, the dipole moment of NaCl would be

$$p_{\text{ionic}} = er_0 = (1.60 \times 10^{-19}\,\text{C})(2.36 \times 10^{-10}\,\text{m}) = 3.78 \times 10^{-29}\,\text{C}\cdot\text{m}$$

The actual measured electric dipole moment of NaCl is

$$p_{\text{measured}} = 3.00 \times 10^{-29}\,\text{C}\cdot\text{m}$$

A purely covalent molecule would be expected to have an electric dipole moment of zero. We can define the ratio of p_{measured} to p_{ionic} as the fractional amount of ionic bonding. For NaCl, this ratio is 3.00/3.78 = 0.79. Thus, the bonding in NaCl is about 79 percent ionic and 21 percent covalent.

EXAMPLE 9-3 Bonding in LiH The measured electric dipole moment of LiH is $1.96 \times 10^{-29}\,\text{C}\cdot\text{m}$. This molecule is among those listed in Table 9-3 (on the home page) as being covalently *s*-bonded. What portion of the LiH bond is covalent?

SOLUTION

The equilibrium separation of LiH from the table is 0.159 nm. If it were a purely ionically bonded molecule, its dipole moment p_{ionic} would be

$$p_{\text{ionic}} = (1.60 \times 10^{-19}\,\text{C})(0.159 \times 10^{-9}\,\text{m}) = 2.54 \times 10^{-29}\,\text{C}\cdot\text{m}$$

The fractional amount of the bond that is ionic is 1.96/2.54 = 0.77. Thus, LiH is only about 23 percent covalently *s*-bonded.

More

In addition to the *s*-bonded H_2 molecule, there are many other covalently bonded molecules involving shared pairs of *s* electrons, *s* and *p* electrons, and *p* electrons. Important among these are the *s*-*p* bonds involving carbon that are the basis for the vast array of hydrocarbon molecules and compounds. Several examples, including the remarkable fullerenes, are discussed in *Other Covalent Bonds* on the home page: www.whfreeman.com/tiplermodernphysics5e See also Equations 9-4 and 9-5 here, as well as Tables 9-3 through 9-6 and Figures 9-9 through 9-17.

EXPLORING

9-3 Other Bonding Mechanisms

The two bonding mechanisms that we have discussed thus far, ionic and covalent, account for a large fraction of the cases in which atoms combine to form molecules. As is described in Chapter 10, when atoms combine on a larger scale to form solids, these exact same mechanisms are responsible for the bonding in many solids. In addition to these types of bonding, two other types occur in solids. One of these, *molecular bonding*, or *dipole-dipole bonding*, also occurs in the formation of many large molecules from smaller molecules and will be discussed in this section. The second type, *metallic bonding*, is responsible for the structure of metals in the solid state and has no single-molecule version or counterpart. For that reason, our discussion of metallic bonding will be deferred to Chapter 10.

STUDENTS-HUB.com Uploaded By: Malak Obaid

Dipole-Dipole Bonding

It was first suggested by J. D. van der Waals[5] in 1873 that any two separated molecules will be attracted toward each other by electrostatic forces. Similarly, atoms that do not otherwise form ionic or covalent bonds will be attracted to each other by the same sort of weak electrostatic bonds. The practical result of this is that at temperatures low enough so that the disruptive effects of thermal agitation are negligible, all substances will condense into a liquid and then a solid form. (Recall that helium is the only element that does not solidify at any temperature under its own vapor pressure.) The relatively weak electrostatic forces responsible for this sort of intermolecular attraction arise because of the electrostatic attraction of electric dipoles.

The electric field due to an electric dipole is illustrated in Figure 9-18*a*. The electric field $\mathbf{E}_d$ at point A due to the dipole is given by

$$\mathbf{E}_d = k\left[\frac{\mathbf{p}}{r^3} - \frac{3(\mathbf{p}\cdot\mathbf{r})}{r^5}\mathbf{r}\right] \qquad \textbf{9-6}$$

whose magnitude for $r \gg a$ is

$$E_d = \frac{kqa}{r^3} = \frac{kp_1}{r^3} \qquad \textbf{9-7}$$

where $|\mathbf{p}_1| = qa$ is the dipole moment.[6] Thus, the electric field of the dipole, and hence the electric force on a charge, falls off as $1/r^3$. This result, which is correct even if the point A is not on the perpendicular, is to be compared with the $1/r^2$ dependence of the Coulomb force that occurs in the covalent and ionic bonds: the force on a test charge due to the dipole qa is weaker at a distance r than that due to a charge q. A second dipole $\mathbf{p}_2$ that happens into the vicinity of $\mathbf{p}_1$ will then orient itself along the $\mathbf{E}_d$ field lines, as illustrated in Figure 9-18*b*, as a result of the electric force on the charges.

The potential energy of the second dipole $\mathbf{p}_2$ in the field of $\mathbf{p}_1$ is given by

$$U = -\mathbf{p}_2\cdot\mathbf{E}_d \qquad \textbf{9-8}$$

and, since $\mathbf{E}_d$ falls off like $1/r^3$, the electric force $\mathbf{F}$ $(= -\partial U/\partial r)$ between two *permanent* dipoles falls off as $1/r^4$. Thus, it is attractive ($\mathbf{F}$ is negative), relatively weak, and of short range.

Polar Molecules

It is then not hard to see physically why molecules with permanent electric dipole moments—so-called *polar molecules* such as H_2O and NaCl—will attract other polar molecules. Consider the H_2O molecule as an example. Although the molecule is electrically neutral, its bonding is partially ionic, so the electrons tend to be concentrated nearer the oxygen atom, making it look like the negative end of a dipole. The two protons then look like the positive end of the dipole. There will then be a mutual

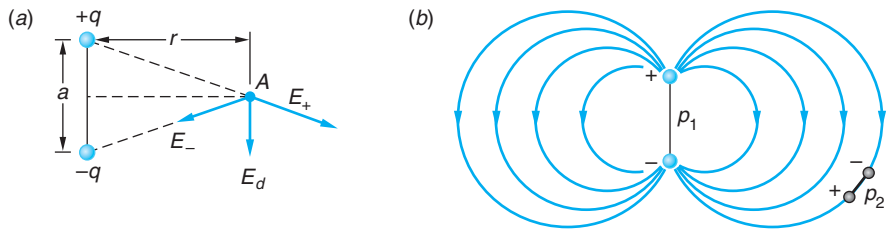

Figure 9-18 (*a*) The electric field $\mathbf{E}_d$ at a point A on a line perpendicular to the axis of an electric dipole $p_1 = qa$. (*b*) The field of $\mathbf{E}_d$ acts on a second dipole p_2 to orient it along the field lines. The force on a charge due to p_1 is $\propto 1/r^3$.

STUDENTS-HUB.com Uploaded By: Malak Obaid

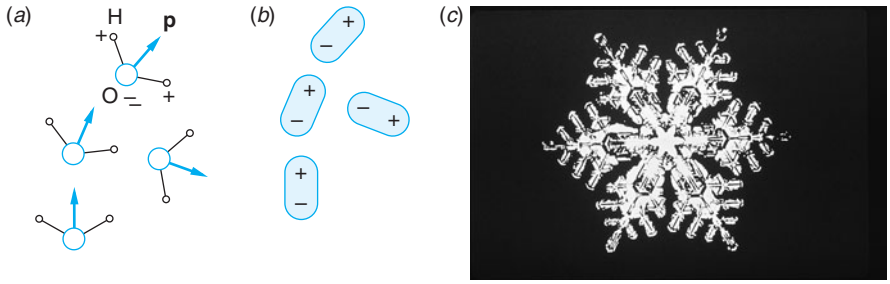

Figure 9-19 (*a*) Schematic of four H_2O molecules. The water molecules' permanent dipole moments are shown by the vectors **p**. (*b*) The four polar water molecules represented as electric dipoles. Notice that the attractive dipole-dipole force tends to align the dipoles so that the nearest neighbors of each charge are charges of the opposite sign. (*c*) A snowflake—one result of dipole-dipole bonding.

attraction between the molecule and other nearby molecules with potential energy given by Equation 9-8. (See Figure 9-19.) Pairs of polar molecules will thus move closer to each other, decreasing their potential energy, until the combined effects of the increasing nuclear repulsion and the exclusion principle produce a minimum in the total potential energy similar to the minima in Figures 9-2 and 9-8*b*. For H_2O the resulting bonding energy is about 0.5 eV per molecule. Although this is only about 10 percent of the strength of the H—OH bond in the water molecule, it is this dipole-dipole force that bonds H_2O molecules to each other to form ice and is responsible in part for the beautiful hexagonal patterns that we see in snowflakes (Figure 9-19*c*).

When dipole-dipole bonds between molecules with permanent dipole moments involve hydrogen, as is the case for water, the bond is referred to as a *hydrogen bond*. The hydrogen bond is of enormous importance since it is the bonding mechanism responsible for the cross-linking that allows giant biological molecules and polymers to hold their fixed shape. For example, it is the hydrogen bond that forms the linkage between the two strands of the double helix DNA molecule. It is the weakness of the hydrogen bonds relative to the covalent/ionic bonds along each strand that allows the two strands to unwind from each other in the DNA molecular replication process. Notice that the hydrogen bond can be viewed as the sharing of a proton by two negatively charged atoms, oxygen atoms in the case of water. (See Figure 9-19.) In this way it is similar to the sharing of electrons that is responsible for the covalent bond. Hydrogen bonding is facilitated by the small mass of the proton and the absence of inner-core electrons.

Nonpolar Molecules

A nonpolar molecule will be polarized by the field of a polar molecule and thus have an induced dipole moment and be attracted to the polar molecule. If $\mathbf{p}_2$ in Figure 9-18*b* is an induced dipole, then

$$\mathbf{p}_2 = \alpha \mathbf{E}_d \qquad \textbf{9-9}$$

where α is a constant characteristic of the nonpolar molecule called the *polarizability*. In this case we expect the potential energy of the interaction to fall off as $1/r^6$ since we have from Equations 9-8 and 9-9 that

$$U = -\mathbf{p}_2 \cdot \mathbf{E}_d = -\alpha E_d^2 = -\alpha k^2 p_1^2 / r^6 \qquad \textbf{9-10}$$

Once again, the energy is negative, signifying that the force between the dipoles is attractive. The force $F = -\partial U/\partial r$ is thus proportional to $1/r^7$, i.e., the force is very short range, dropping rapidly with increasing r. Indeed, increasing the separation of the molecules by a factor of 2 reduces the attractive force between them to only 0.008 of its original value.

STUDENTS-HUB.com Uploaded By: Malak Obaid

Perhaps surprisingly, two molecules, neither of which has a permanent dipole moment, can also attract each other via the mechanism just described. It is somewhat harder to see why an attractive force exists between two nonpolar molecules. Though the *average* dipole moment $\overline{\mathbf{p}}$ of a nonpolar molecule is zero, the *average square* dipole moment $\overline{p^2}$ is not because the electrons are in constant motion and at any given instant there will be an excess or deficiency of them in one part or another of the molecule. A measurement that we might do in the laboratory reveals the average value (zero), not the instantaneous value. The instantaneous dipole moment of a nonpolar molecule is, in general, not zero. When two nonpolar molecules are nearby, the fluctuations in the instantaneous dipole moments tend to be correlated so as to produce attraction, as illustrated in Figure 9-20. The potential energy is again given approximately by Equation 9-10, so that the potential energy is proportional to $1/r^6$ and the attractive force is proportional to $1/r^7$. This attractive force between nonpolar molecules is called the *van der Waals force*[7] or, occasionally, the *London dispersion force*, after Fritz London, the German physicist who in 1930 first explained the physical origin of the interaction.

As van der Waals first suggested, dipole-dipole forces act between all molecules and, in addition, between all atoms. They are the only forces that occur between rare gas atoms, without which the atoms of these elements would not condense into liquids or form solids. (The single exception to the latter is He, whose quantum-mechanical zero-point energy exceeds the minimum of the potential energy resulting from Equation 9-10 and core repulsion.) The dipole-dipole forces between molecules, although relatively weak, are also responsible for the physical phenomena of surface tension and friction.

Scientists have recently succeeded in trapping a sample of *molecules* in a single quantum level at a temperature in the millikelvin range. This ability raises the possibilities for, among other things, high-precision molecular spectroscopy and producing a molecular Bose-Einstein condensate.

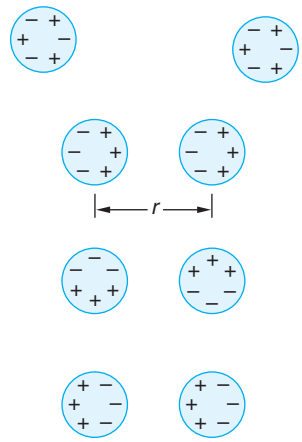

Figure 9-20 Nonpolar molecules have, on average, symmetric charge distributions, as illustrated by the pair of molecules at the top of the figure. However, instantaneous fluctuations in the electron distribution are asymmetric and tend to be correlated with those of nearby molecules, as shown in the other three examples. The correlated distributions lead to an attractive force proportional to $1/r^7$ that draws the molecules closer to each other as shown.

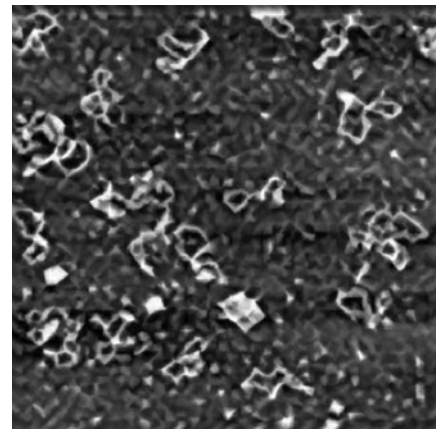

The 2-nm height of DNA molecules is readily imaged by an atomic force microscope (AFM). [*Taken from www.di.com, Digital Instruments, Veeco metrology Group, Santa Barbara, CA.*]

STUDENTS-HUB.com Uploaded By: Malak Obaid

Questions

1. Why would you expect the separation distance between the two protons to be larger in the H_2^+ ion than in the H_2 molecule?
2. Would you expect the NaCl molecule to be polar or nonpolar?
3. Would you expect the N_2 molecule to be polar or nonpolar?
4. Does neon occur naturally as Ne or Ne_2? Why?

9-4 Energy Levels and Spectra of Diatomic Molecules

As is the case with an atom, a molecule often emits electromagnetic radiation when it makes a transition from an excited energy state to a state of lower energy. Conversely, a molecule can absorb radiation and make a transition from a lower energy state to a higher energy state. The study of molecular emission and absorption spectra thus provides us with information about the energy states of molecules. For simplicity, we will consider only diatomic molecules here.

As might be expected, the energy levels of molecular systems are even more complex than those of atoms. The energy of a molecule can be conveniently separated into three parts: electronic, due to the excitation of its electrons; vibrational, due to the oscillations of the atoms of the molecule; and rotational, due to the rotation of the molecule about an axis through its center of mass. Fortunately, the magnitudes of these energies are sufficiently different that they can be treated separately. Electrons in molecules can be excited to higher states, just as those in atoms. For example, a 1*s* electron in the H_2 molecule can be excited to a 2*p* level, emitting a photon as it returns to the ground state. The energies due to the electronic excitations of a molecule are of the order of magnitude of 1 eV, the same as for the excitation of atoms. We have already discussed such transitions and will not consider them further in this section. The energies of vibration and rotation are about 1/100 to 1/1000 times smaller and will be the focus of our attention.

Rotational Energy Levels

Classically, the kinetic energy of rotation is

$$E = \frac{1}{2}I\omega^2 = \frac{(I\omega)^2}{2I} = \frac{L^2}{2I} \qquad \textbf{9-11}$$

where I is the moment of inertia, ω the angular velocity of rotation, and $L = I\omega$ the angular momentum. The solution of the Schrödinger equation for the rotation of a rigid body leads to the quantization of the angular momentum, with values given by

$$L^2 = \ell(\ell + 1)\hbar^2 \qquad \ell = 0, 1, 2, \ldots \qquad \textbf{9-12}$$

where ℓ is the *rotational quantum number*. This is the same quantum condition on angular momentum that holds for the orbital angular momentum of an electron in an atom.

STUDENTS-HUB.com Uploaded By: Malak Obaid

Note, however, that L in Equation 9-11 refers to the angular momentum of the entire molecule rotating about an axis through its center of mass. The energy levels of a rotating molecule are therefore given by

$$E = \frac{\ell(\ell + 1)\hbar^2}{2I} = \ell(\ell + 1)E_{0r} \quad \ell = 0, 1, 2, \ldots \tag{9-13}$$

where E_{0r} is the *characteristic rotational energy* of a particular molecule, which is inversely proportional to its moment of inertia:

$$E_{0r} = \frac{\hbar^2}{2I} \tag{9-14}$$

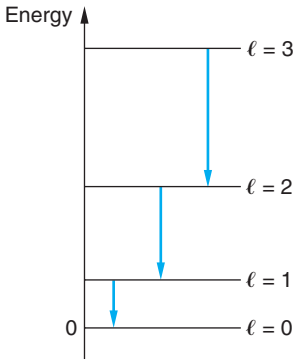

Figure 9-21 Energy levels and allowed transitions for a rotating rigid body as given by Equation 9-13.

The rotational-energy level scheme is shown in Figure 9-21. Transitions between these levels produce the *pure rotational spectrum* of a molecule. While all diatomic molecules have rotational energy levels, those without permanent dipole moments (symmetric molecules such as H_2, Cl_2, or CO_2) cannot emit or absorb electric dipole radiation by only changing the rotational quantum state and thus do not have a pure rotational spectrum. For molecules that do have dipole moments and emit pure rotational spectra, the quantum number ℓ is subject to the selection rule $\Delta\ell = \pm 1$, just as it was for the atomic electrons. Thus, the energy separation between adjacent rotation states is given by

$$\Delta E_{\ell,\,\ell+1} = \frac{[(\ell + 1)(\ell + 2) - \ell(\ell + 1)]\hbar^2}{2I} = \frac{(\ell + 1)\hbar^2}{I} \tag{9-15}$$

A measurement of the rotational energy of a molecule from its rotational spectrum can be used to determine the moment of inertia of the molecule, which can then be used to find the equilibrium separation of the atoms in the molecule, i.e., the bond length. The moment of inertia about an axis through the center of mass of a diatomic molecule (see Figure 9-22) is

$$I = m_1 r_1^2 + m_2 r_2^2$$

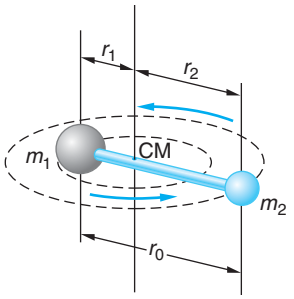

Figure 9-22 Diatomic molecule rotating about an axis through its center of mass.

Using $m_1 r_1 = m_2 r_2$, which relates the distances r_1 and r_2 from the atoms to the center of mass, and $r_0 = r_1 + r_2$ for the separation of the atoms, we can write the moment of inertia as

$$I = \mu r_0^2 \tag{9-16}$$

where μ, the reduced mass, is

$$\mu = \frac{m_1 m_2}{m_1 + m_2} \tag{9-17}$$

If the masses are equal ($m_1 = m_2$), as in H_2 and O_2, the reduced mass $\mu = m/2$ and

$$I = \frac{1}{2} m r_0^2 \tag{9-18}$$

A unit of mass convenient for discussing atomic and molecular masses is the *unified mass unit* u, which is defined as one-twelfth of the mass of a neutral carbon-12 (^{12}C) atom.

STUDENTS-HUB.com Uploaded By: Malak Obaid

The mass of one ^{12}C atom is thus 12 u. The mass of an atom in unified mass units is therefore numerically equal to the molar mass of the atom in grams. The unified mass unit is related to the gram and kilogram by

$$1\text{ u} = \frac{1g}{N_A} = \frac{10^{-3}\text{ kg}}{6.0221 \times 10^{23}} = 1.6605 \times 10^{-27}\text{ kg} = 931.4940 \times 10^{6}\text{ eV}/c^2 \qquad \textbf{9-19}$$

where N_A is Avogadro's number.

EXAMPLE 9-4 The Reduced Mass of HCl Compute the reduced mass of the HCl molecule.

SOLUTION

1. The reduced mass μ is given by Equation 9-17:
$$\mu = \frac{m_1 m_2}{m_1 + m_2}$$
2. From the periodic table on the inside back cover of this book, the mass of the hydrogen atom is 1.01 u and that of the chlorine atom is 35.5 u. Substituting these gives
$$\mu = \frac{(1.01\text{ u})(35.5\text{ u})}{1.01\text{ u} + 35.5\text{ u}} = 0.98\text{ u}$$

Remarks: *Note that the reduced mass of the HCl molecule is less than that of a single hydrogen atom.*

EXAMPLE 9-5 Equilibrium Separation in CO The energy difference ΔE between the $\ell = 0$ and $\ell = 1$ rotational levels in the CO molecule is found experimentally from measurement of the wavelength $\lambda = 2.6$ mm of the corresponding transition. For CO, ΔE is equal to 4.77×10^{-4} eV. Find the equilibrium separation, or bond length r_0, of the CO molecule.

SOLUTION

1. The bond length r_0 is given in terms of the moment of inertia I of the molecule by Equation 9-16:
$$I = \mu r_0^2 \quad \text{or} \quad r_0 = \sqrt{\frac{I}{\mu}}$$
2. I in terms of ΔE is given by Equation 9-15:
$$\Delta E_{\ell,\,\ell+1} = \frac{(\ell + 1)\hbar^2}{I} \quad \text{or} \quad I = \frac{(\ell + 1)\hbar^2}{\Delta E_{\ell,\,\ell+1}}$$
3. Substituting $\ell = 0$ and $\Delta E = 4.77 \times 10^{-4}$ eV into step 2 gives
$$I = \frac{\hbar^2}{4.77 \times 10^{-4}\text{ eV}}$$
4. The reduced mass of the CO molecule is computed from Equation 9-17 using atomic mass values from the periodic table:
$$\mu = \frac{m_1 m_2}{m_1 + m_2} = \frac{(12\text{ u})(16\text{ u})}{12\text{ u} + 16\text{ u}} = 6.86\text{ u}$$

STUDENTS-HUB.com Uploaded By: Malak Obaid

5. Substituting these results into step 1 gives

$$r_0 = \left(\frac{\hbar^2}{4.77 \times 10^{-4}\,\text{eV} \times 6.86\,\text{u}}\right)^{1/2}$$

$$= \frac{1.055 \times 10^{-34}}{[(4.77 \times 10^{-4}\,\text{eV})(1.60 \times 10^{-19}\,\text{J/eV})(6.86\,\text{u})(1.66 \times 10^{-27}\,\text{kg/u})]^{1/2}}$$

$$= 0.133\,\text{nm}$$

The rotational energy levels are several orders of magnitude smaller than those due to electron excitation, which have energies of the order of 1 eV or higher. For example, the characteristic rotational energy of the O_2 molecule, whose equilibrium separation is about 0.1 nm, is 2.59×10^{-4} eV, calculated from Equation 9-14. Transitions within a given set of rotational energy levels yield photons in the far infrared region of the electromagnetic spectrum. Notice that the rotational energies are also small compared with the typical thermal energy kT at normal temperatures. For $T = 300$ K, for example, kT is about 2.6×10^{-2} eV. Thus, at ordinary temperatures, a molecule can easily be excited to the lower rotational energy levels by collisions with other molecules. But such collisions cannot excite the molecule to electronic energy levels above the ground state.

Vibrational Energy Levels

The molecular vibrational energies are a bit harder to estimate than were the rotational energies. Our discussion is aided by the fact that the molecular potential energy functions of Figures 9-2, 9-7, and 9-8*b* can be closely approximated by parabolas in the vicinity of the equilibrium point. (See Figure 9-23*b*.) Thus, we can use the

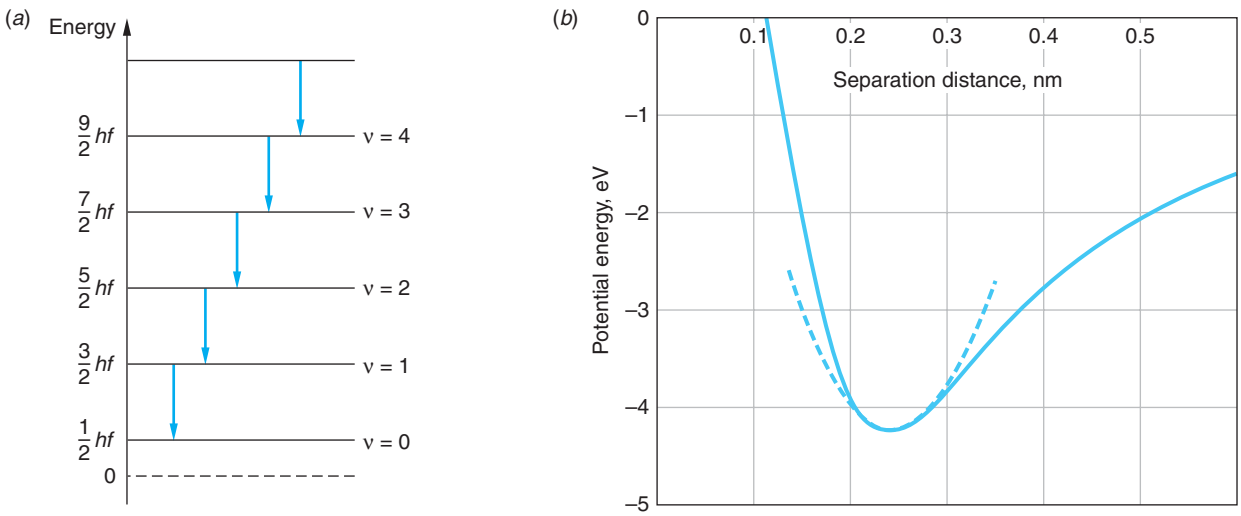

Figure 9-23 (*a*) The energy levels of the molecular vibrations are equally spaced in the vicinity of the equilibrium spacing of the atoms. (*b*) A harmonic oscillator potential fitted to the actual potential energy function of the NaCl molecule shown in Figure 9-2*b*.

STUDENTS-HUB.com Uploaded By: Malak Obaid

results of our study of the simple harmonic oscillator in Chapter 6. The energy levels are given by

$$E_v = (v + 1/2)hf \qquad v = 0, 1, 2, 3, \ldots \tag{9-20}$$

where f is the frequency of the vibration and v is the *vibrational quantum number*.[8] An interesting feature of this result is that the energy levels are equally spaced with intervals $\Delta E_{v,\,v+1} = hf$, as shown in Figure 9-23*a*. The frequency of vibration of a diatomic molecule can be related to the force exerted by one atom on the other. Consider two objects of mass m_1 and m_2 connected by a spring of force constant K. The frequency of oscillation of this system is (see Section 6-5)

$$f = \frac{1}{2\pi}\sqrt{\frac{K}{\mu}} \tag{9-21}$$

where μ is the reduced mass given by Equation 9-17. The effective force constant of a diatomic molecule can thus be determined from a measurement of the frequency of oscillation of the molecule.

We could get a good estimate of f by fitting the one-dimensional parabolic harmonic oscillator potential energy function for the molecule as illustrated in Figure 9-23*b*, but for simplicity we can get a rough idea of the order of magnitude of the vibrational energies by observing that the energy of an atom of mass m in a square well of width r_0 is (Figure 9-24)

$$E_n = n^2\frac{h^2}{8mr_0^2} = n^2\frac{4\pi^2\hbar^2}{8mr_0^2} = n^2\frac{\pi^2}{2}\frac{\hbar^2}{mr_0^2}$$

Except for the factor $\pi^2/2 \approx 5$ (and the n^2), this expression is the same as the characteristic rotational energy E_{0r}; thus we expect the vibrational energies to be somewhat larger than the rotational energies.

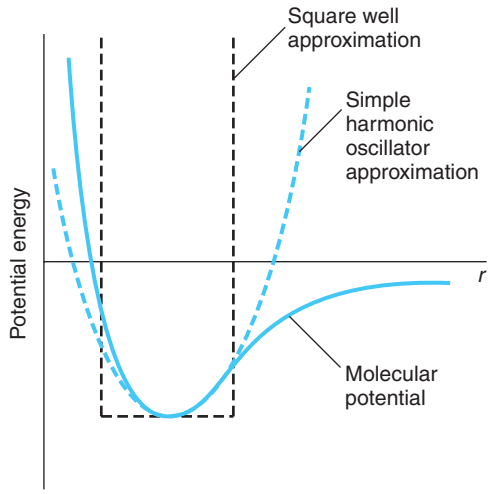

Figure 9-24 Molecular potential. The simple harmonic oscillator approximation, used to calculate the energy levels, and a square well approximation, used to estimate the order of magnitude of the energy levels, are each indicated by dashed curves.

STUDENTS-HUB.com Uploaded By: Malak Obaid

The selection rule for transitions between vibrational states (of the same electronic state) requires that v change only by ± 1, so the energy of a photon emitted by such a transition is hf and the frequency is the same as the frequency of vibration. A typical measured frequency of a transition between vibrational states is 5×10^{13} Hz, which gives for the order of magnitude of vibrational energies

$$E \sim hf = (4.14 \times 10^{-15}\ \text{eV} \cdot \text{s})(5 \times 10^{13}\ \text{s}^{-1}) = 0.2\ \text{eV}$$

Thus, a typical vibrational energy is actually about 1000 times greater than the typical rotational energy E_{0r} of the O_2 molecule we noted above and about 8 times greater than the typical thermal energy $kT = 0.026$ eV at $T = 300$ K. In contrast with the rotational levels, the molecular vibrational states are not readily excited by collisions between molecules at ordinary temperatures.

EXAMPLE 9-6 **Force Constant of CO** The observed vibrational frequency of the CO molecule is 6.42×10^{13} Hz. What is the effective force constant for this molecule?

SOLUTION

1. The force constant K is given in terms of the vibrational frequency f by Equation 9-21: $$f = \frac{1}{2\pi}\sqrt{\frac{K}{\mu}}$$
2. The reduced mass μ of the CO molecule was computed in step 4 of Example 9-5: $$\mu = 6.86\ \text{u}$$
3. Solving Equation 9-21 for K and substituting the values of f and μ gives

$$\begin{aligned} K &= (2\pi f)^2\mu \\ &= (2\pi \times 6.42 \times 10^{13}\ \text{Hz})^2(6.86\ \text{u})(1.66 \times 10^{-27}\ \text{kg/u}) \\ &= 1.86 \times 10^{3}\ \text{N/m} \end{aligned}$$

Emission Spectra

Figure 9-25 shows schematically some electronic, vibrational, and rotational energy levels of a diatomic molecule. The vibrational levels are labeled with the quantum number v and the rotational levels with the quantum number ℓ. The lower vibrational levels are evenly spaced, with $\Delta E = hf$. For higher vibrational levels, the approximation that the vibration is simple harmonic is not valid and the levels are not quite evenly spaced. The actual potential spreads somewhat more rapidly, as can be seen in Figure 9-24, and the spacing of the vibrational levels becomes closer for large values of the quantum number v. Notice in Figure 9-25 that the potential energy curves representing the force between the two atoms in the molecule do not have exactly the same shape for the electronic ground and excited states. This implies that the fundamental frequency of vibration f is different for different electronic states. For transitions between vibrational states of different electronic states, the selection rule $\Delta v = \pm 1$ does not hold. Such transitions result in the emission of photons of wavelength in or near the visible spectrum.

STUDENTS-HUB.com Uploaded By: Malak Obaid

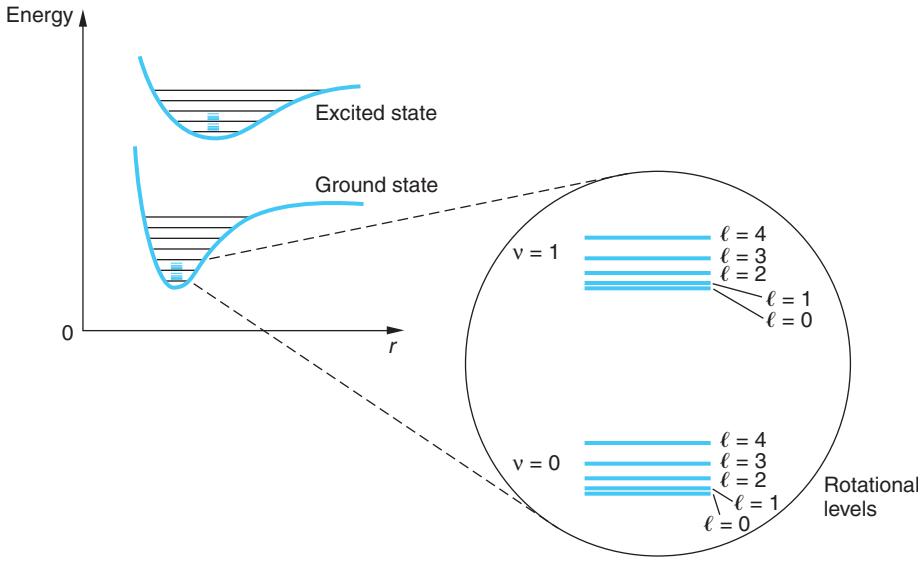

Figure 9-25 Electronic, vibrational, and rotational energy levels of a diatomic molecule. The rotational levels are shown in an enlargement of the $v = 0$ and $v = 1$ vibrational levels of the electronic ground state.

The spacing of the rotational levels increases with increasing values of ℓ. Since the energies of rotation are so much smaller than those of vibrational or electronic excitations of a molecule, molecular rotation shows up in molecular spectra as a fine-structure splitting of the spectral lines. When the fine structure is not resolved, the spectrum appears as bands, as shown in Figure 9-26*a* (page 386). Close inspection of these bands reveals that they have a fine structure due to the rotational energy levels, as shown in the enlargement in Figure 9-26*b*.

Absorption Spectra

Much molecular spectroscopy is done using infrared absorption techniques in which only the vibrational and rotational energy levels of the ground-state electronic level are excited. Consequently, we will now direct our attention to what is called the *vibration-rotation spectrum*. For ordinary temperatures, the vibrational energies are sufficiently large in comparison with the thermal energy kT that most of the molecules are in the lowest vibrational state $v = 0$, for which the energy is $E_0 = \frac{1}{2}hf$. The transition from $v = 0$ to $v = 1$ is the predominant transition in absorption. The rotational energies, however, are sufficiently smaller than kT that the molecules are distributed among several rotational energy states, the relative number in each state being determined by the Boltzmann factor. If the molecule is originally in a rotational state characterized by the quantum number ℓ, its initial energy, in addition to that of the electronic state, is

$$E_\ell = \tfrac{1}{2}hf + \ell(\ell + 1)E_{0r} \qquad \textbf{9-22}$$

where E_{0r} is given by Equation 9-14. From this state, two transitions are permitted by the selection rules. For a transition to the next highest vibrational state $v = 1$ and a rotational state characterized by $\ell + 1$, the final energy is

$$E_{\ell+1} = \tfrac{3}{2}hf + (\ell + 1)(\ell + 2)E_{0r} \qquad \textbf{9-23}$$

STUDENTS-HUB.com Uploaded By: Malak Obaid

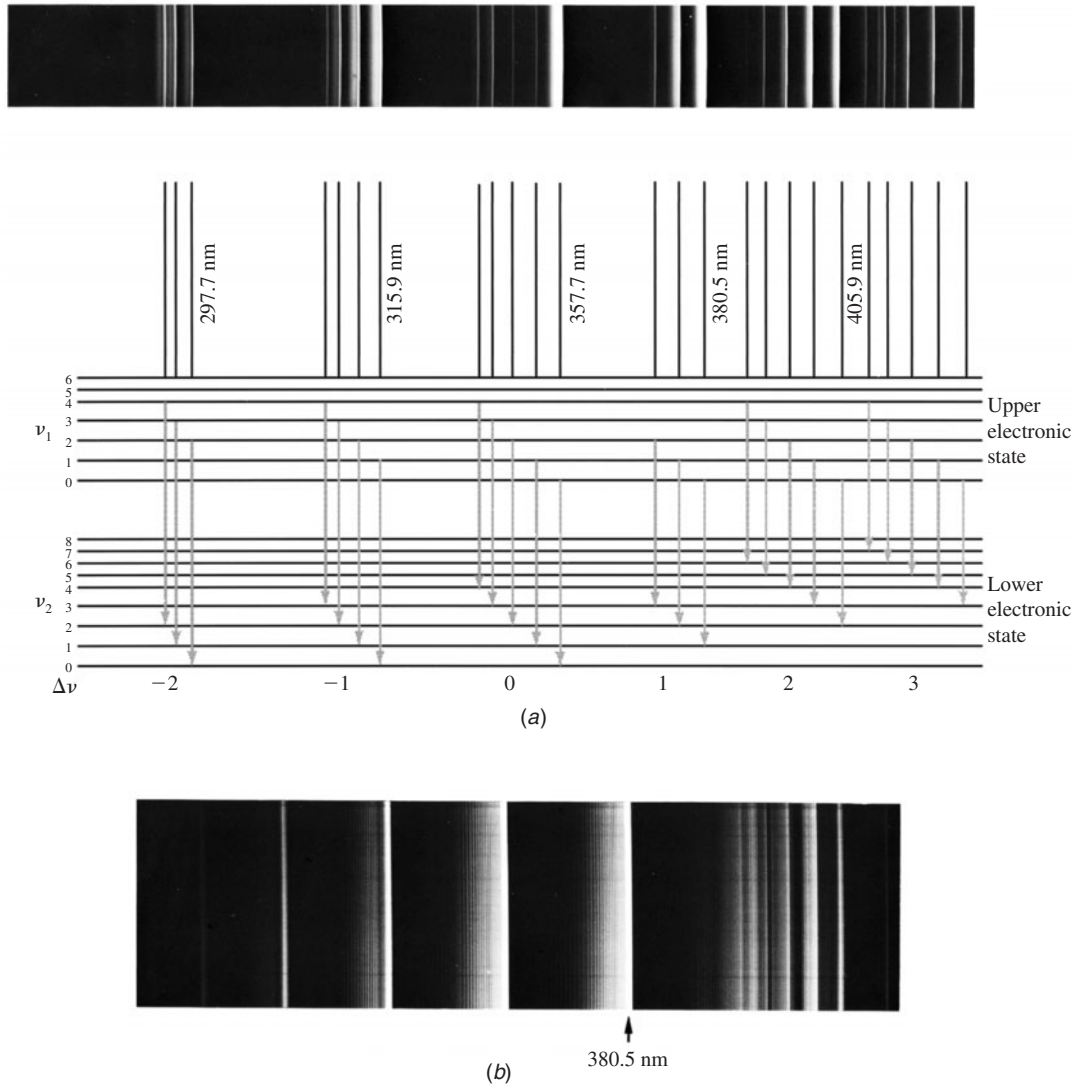

Figure 9-26 Part of the emission spectrum of N_2. (*a*) These components of the band are due to transitions between the vibrational levels of two electronic states, as indicated in the diagram. (*b*) An enlargement of part of (*a*) shows that the apparent lines in (*a*) are in fact band heads with structure caused by rotational levels. [*Courtesy of J. A. Marquisee.*]

For a transition to the next highest vibrational state and to a rotational state characterized by $\ell - 1$, the final energy is

$$E_{\ell-1} = \tfrac{3}{2}hf + (\ell - 1)\ell E_{0r} \qquad \textbf{9-24}$$

The energy differences are

$$\Delta E_{\ell \to \ell+1} = E_{\ell+1} - E_{\ell} = hf + 2(\ell + 1)E_{0r} \qquad \textbf{9-25}$$

where $\ell = 0, 1, 2, \ldots$, and

STUDENTS-HUB.com Uploaded By: Malak Obaid

$$\Delta E_{\ell \to \ell - 1} = E_{\ell - 1} - E_{\ell} = hf - 2\ell E_{0r} \qquad \textbf{9-26}$$

where $\ell = 1, 2, 3, \ldots$. (In Equation 9-26, ℓ begins at $\ell = 1$ because from $\ell = 0$ only the transition $\ell \to \ell + 1$ is possible.) Figure 9-27 illustrates these transitions. The frequencies of these transitions are given by

$$f_{\ell \to \ell + 1} = \frac{\Delta E_{\ell \to \ell + 1}}{h} = f + \frac{2(\ell + 1)E_{0r}}{h} \qquad \ell = 0, 1, 2, \ldots \qquad \textbf{9-27}$$

and

$$f_{\ell \to \ell - 1} = \frac{\Delta E_{\ell \to \ell - 1}}{h} = f - \frac{2\ell E_{0r}}{h} \qquad \ell = 1, 2, 3, \ldots \qquad \textbf{9-28}$$

The frequencies for the transitions $\ell = \ell + 1$ are thus, $f + 2(E_{0r}/h)$, $f + 4(E_{0r}/h)$, $f + 6(E_{0r}/h)$, and so forth; those corresponding to the transition $\ell \to \ell - 1$ are $f - 2(E_{0r}/h)$, $f - 4(E_{0r}/h)$, $f - 6(E_{0r}/h)$, and so forth. We thus expect the absorption spectrum to contain frequencies equally spaced by $2E_{0r}/h$ except for a gap of $4E_{0r}/h$ at the vibrational frequency f, as shown in Figure 9-28. A measurement of the position of the gap gives f and a measurement of the spacing of the absorption peaks gives E_{0r}, which is inversely proportional to the moment of inertia of the molecule.

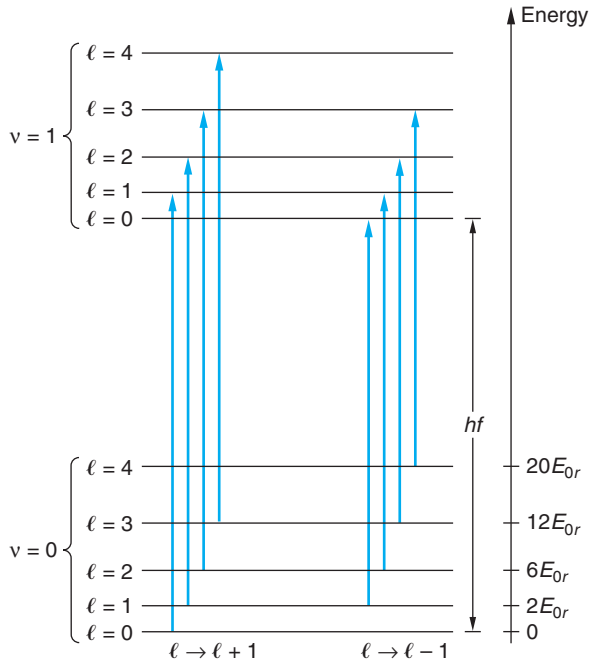

Figure 9-27 Absorptive transitions between the lowest vibrational states $v = 0$ and $v = 1$ in a diatomic molecule. These transitions obey the selection rule $\Delta\ell = \pm 1$ and fall into two bands. The energies of the $\ell \to \ell + 1$ band are $hf + 2E_{0r}$, $hf + 4E_{0r}$, $hf + 6E_{0r}$, and so forth, whereas the energies of the $\ell \to \ell - 1$ band are $hf - 2E_{0r}$, $hf - 4E_{0r}$, $hf - 6E_{0r}$, and so forth.

STUDENTS-HUB.com Uploaded By: Malak Obaid

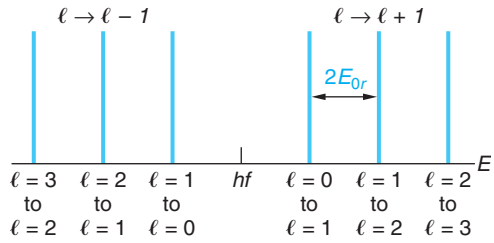

Figure 9-28 Expected absorption spectrum of a diatomic molecule. The right branch corresponds to the transitions $\ell \rightarrow \ell + 1$ and the left branch to the transitions $\ell \rightarrow \ell - 1$. The lines are equally spaced by $2E_{0r}$. The energy midway between the branches is hf, where f is the frequency of vibration of the molecule.

Figure 9-29 shows the absorption spectrum of HCl. The double-peak structure results from the fact that chlorine occurs naturally in two isotopes, ^{35}Cl and ^{37}Cl, which results in slightly different moments of inertia. If all of the rotational levels were equally populated initially, we would expect the intensities of each absorption line to be equal. However, the population $n(E_\ell)$ of a rotational level ℓ is proportional to the density of states $g(E_\ell)$, which equals the degeneracy of the level in this case, that is, the number of states with the same value of ℓ, which is $2\ell + 1$, and to the Boltzmann factor $e^{-E_\ell/kT}$,where E_ℓ is the energy of the state:

$$n(E_\ell) = g(E_\ell)e^{-E_\ell/kT} \qquad \textbf{9-29}$$

or

$$n(E_\ell) = (2\ell + 1)e^{-[\frac{1}{2}hf + \ell(\ell+1)E_{0r}]/kT} \qquad \textbf{9-30}$$

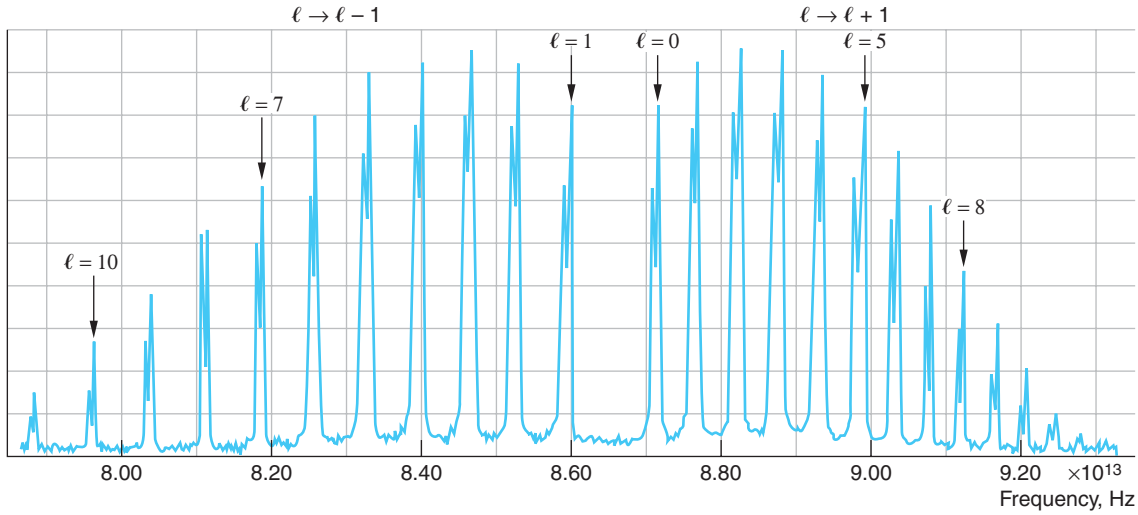

Figure 9-29 Absorption spectrum of the diatomic molecule HCl. The double-peak structure results from the two isotopes of chlorine, ^{35}Cl (abundance 75.5 percent) and ^{37}Cl (abundance 24.5 percent). The intensities of the peaks vary because the population of the initial state depends on ℓ.

STUDENTS-HUB.com Uploaded By: Malak Obaid

The $(2\ell + 1)$-fold degeneracy of the rotational state with angular momentum $\ell\hbar$ makes the thermal equilibrium population proportional to $(2\ell + 1) \exp [-\ell(\ell + 1)\hbar^2/2\, IkT]$. Therefore, the $\ell = 0$ state is usually not the most densely populated state at room temperature. For low values of ℓ, the population increases slightly because of the degeneracy factor, whereas for higher values of ℓ, the population decreases because of the Boltzmann factor. The intensities of the absorption lines therefore increase with ℓ for low values of ℓ and then decrease with ℓ for high values of ℓ, as can be seen from the figure. We can find out where the maximum population of the rotational states is located and hence which lines will be the most intense by differentiating Equation 9-30 with respect to ℓ and setting $dn/d\ell$ equal to zero. The result is

$$\ell_{\max} = \frac{1}{2}\left[\sqrt{\frac{4kT}{h^2/mr^2}} - 1\right] \qquad \textbf{9-31}$$

For a measurement made at room temperature, $kT = 0.026$ eV and thus $\ell_{\max} \approx 3$. This, too, can be seen in Figure 9-29.

Notice also in Figure 9-29 that the spacing between adjacent peaks, which we expected to be constant and equal to $2E_{0r}$ on the basis of our calculation above, is in fact not constant. The reason for this is our assumption that the moment of inertia of the molecule is constant. The rotation of the molecule tends to increase the separation of the atoms and hence increase the moment of inertia and decrease the rotational energy. As might be expected and the figure also shows, this effect becomes larger as ℓ increases.

As mentioned above, the gap in the spectrum in Figure 9-29 is due to the absence of a transition beginning on the $\ell = 0$ level in the $\ell \rightarrow \ell - 1$ group of peaks. The center of the gap is at the characteristic oscillation frequency f of the molecule given by Equation 9-21. From the figure we see that f for HCl is about 8.56×10^{13} Hz, or about 0.36 eV, corresponding to a force constant K of about 476 N/m. Table 9-7 lists the rotational and vibrational constants for several diatomic molecules. All diatomic

Table 9-7 Rotational and vibrational constants for selected diatomic molecules

Molecule	Equilibrium separation r_0 (nm)	Frequency f (Hz)	E_{0r} (eV)
H_2	0.074	1.32×10^{14}	7.56×10^{-3}
Li_2	0.267	1.05×10^{13}	8.39×10^{-5}
O_2	0.121	4.74×10^{13}	1.78×10^{-4}
LiH	0.160	4.22×10^{13}	9.27×10^{-4}
HCl^{35}	0.127	8.97×10^{13}	1.32×10^{-3}
$NaCl^{35}$	0.251	1.14×10^{13}	2.36×10^{-5}
KCl^{35}	0.279	8.40×10^{12}	1.43×10^{-5}
KBr^{79}	0.294	6.93×10^{12}	9.1×10^{-6}

Symmetric molecules such as H_2 or O_2 have no electric dipole moment. The vibration or rotation of these molecules does not involve a changing dipole moment, and there is no vibrational-rotational electric dipole absorption or radiation for these molecules.

STUDENTS-HUB.com Uploaded By: Malak Obaid

molecules[9] have a gap at f in their vibration-rotation spectra; however, many polyatomic molecules have more complex vibrations and rotations, one result of which is that $\Delta\ell = 0$ may be allowed, i.e., vibrational energy may change without an accompanying rotational transition. In that event, a line will occur in the vibration-rotation spectrum at the frequency f. Such lines are given the rather enigmatic name of *Q branch*.[10]

9-5 Scattering, Absorption, and Stimulated Emission

Scattering

In the interactions between radiation incident on atomic or molecular systems, photons may also be scattered both elastically and inelastically. The process by which photons scatter elastically, i.e., without a change in their frequency, is called *elastic* or *Rayleigh scattering* since it was first described adequately by a classical scattering theory derived by Rayleigh in about 1900. Rayleigh scattering is illustrated in Figure 9-30*d*. In the classical theory, the oscillating electric field of the incident radiation produces an oscillating acceleration of the atomic electrons, causing them to radiate electromagnetic waves of the same frequency as and in phase with the incident wave. Thus, the electrons of the target atoms and molecules absorb energy from the incident wave and re-emit, or scatter it, in all directions without changing its frequency. The intensity of the scattered radiation is proportional to f^4. Rayleigh scattering is the origin of the unmodified line in our discussion of the Compton scattering of x rays in Section 3-4. (See Figure 3-17.) We saw there that if the incident wavelength λ_1 was large compared with the Compton shift λ_2—λ_1, i.e., visible wavelengths or larger, then the scattered wave always included a wavelength equal to the incident wavelength to within experimental accuracy regardless of whether the electron mass or atomic mass is used in Equation 3-25. So as $\lambda \rightarrow \infty$, the quantum explanation of Chapter 3 and Rayleigh's classical explanation of elastic scattering agree. However, for incident wavelengths in the x-ray and gamma-ray regions of the spectrum, Compton scattering, shown in Figure 9-30*e*, becomes increasingly important for low-Z atoms whose electron binding energies are not large. In the gamma-ray region as $\lambda \rightarrow 0$, the photon energy becomes so large that even the most tightly bound electrons are freed in the process and Compton effect becomes the dominant process.

The incident and scattered photons are also correlated in the *inelastic* scattering process illustrated in Figure 9-30*f*. Such scattering of light from molecules was first observed by physicist C. V. Raman[11] and is known as *Raman scattering*, or sometimes as the *Raman effect*. The scattered photon may have less energy than the incident photon or it may have greater energy if the molecule is initially in an excited vibrational or rotational energy state. Both possibilities are illustrated in Figure 9-30*f*. Thus, the scattered frequency is not the same as the incident frequency, nor is it related to a characteristic frequency of the molecule. It is found that for incident monochromatic radiation of frequency f the scattered radiation contains not only the frequency f (Rayleigh scattering; see Figure 9-31), but also much weaker lines on either side of the Rayleigh line, with frequencies given by

$$f' = f \pm \Delta f \qquad \textbf{9-32}$$

STUDENTS-HUB.com Uploaded By: Malak Obaid

These are the Raman lines illustrated in Figure 9-31. If the incident frequency is varied, the Raman lines are observed to move along the frequency axis at the same rate so that the *difference* Δf between f and f' remains constant. It is this difference Δf that corresponds to characteristic transitions of the scattering molecule.

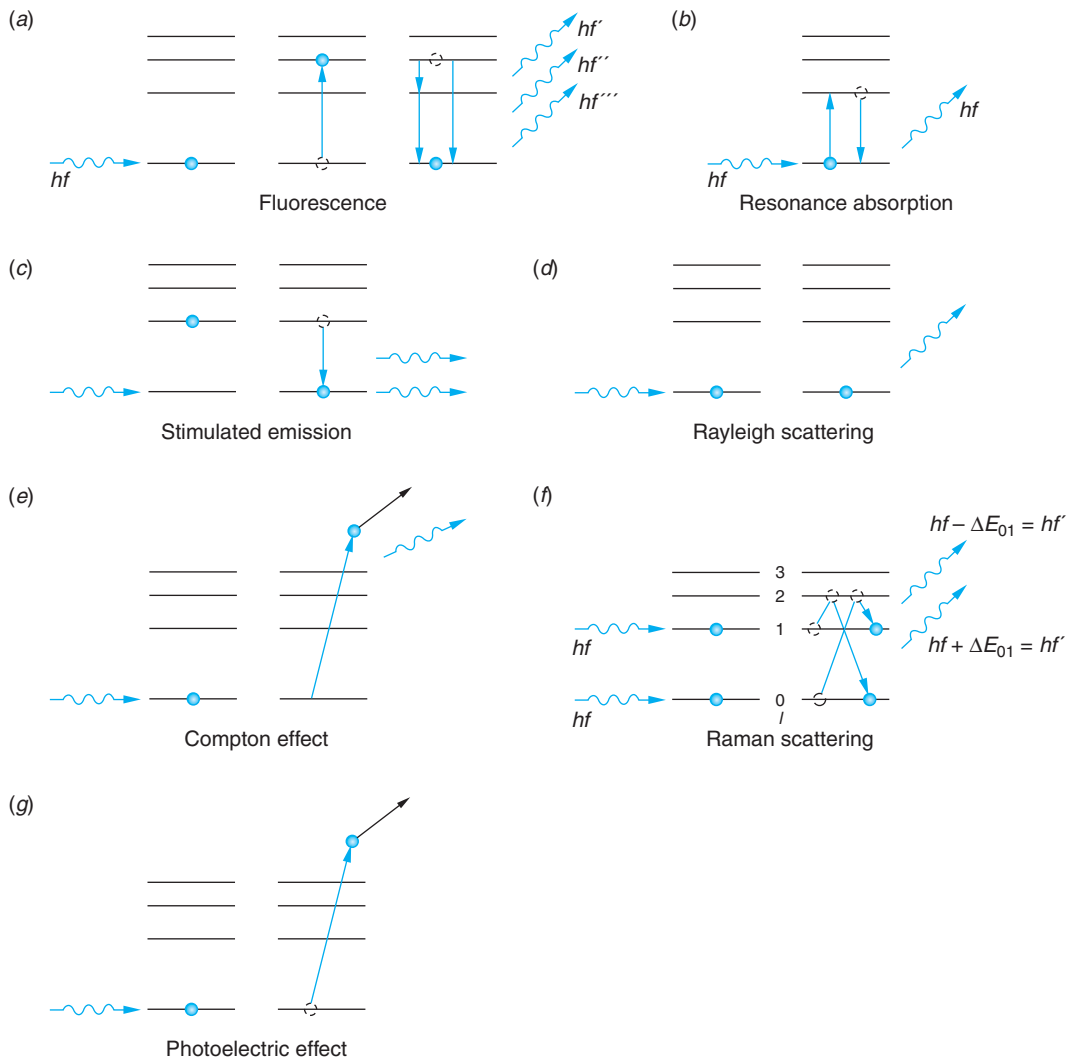

Figure 9-30 Description of photon interactions with an atom. (*a*) The photon is absorbed and the atom, in an excited state, later emits one or more photons as it decays to a state of lower energy. This is a two-step process called *fluorescence*, and the emitted photons are uncorrelated with the incident photon. (*b*) If the energy of the incident photon matches one of the excitation energies of the atom, resonance radiation results. (*c*) The atom, in an excited state, is stimulated to make a transition to a lower state by an incident photon of just the right energy. The emitted and incident photons have the same energy and are coherent. The Rayleigh scattering process (*d*) and Raman scattering (*f*) differ from (*a*) and (*b*) in that they are single-step processes and there is a correlation between the incident and emitted photons. Parts (*e*) and (*g*) illustrate Compton scattering and the photoelectric effect discussed in Chapter 3.

STUDENTS-HUB.com Uploaded By: Malak Obaid

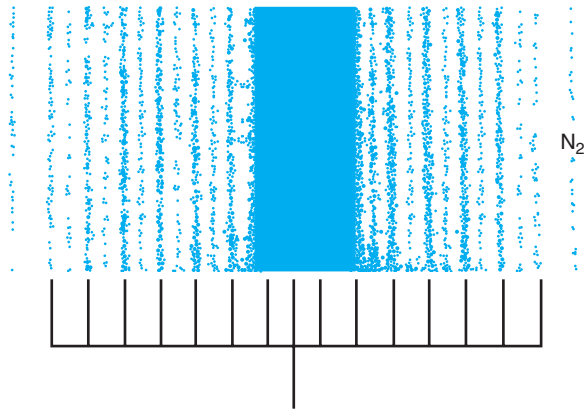

Figure 9-31 The rotational Raman spectrum of N_2. The alternating intensities, determined by the nuclear spins, are in the ratio of 1/2, corresponding with the $I = 1$ spin of the nitrogen nucleus. The dark central area is the result of the much more intense Rayleigh-scattered portion of the incident wave. [*R. Eisberg and R. Resnick, Quantum Physics, 2d ed. (New York: Wiley, 1985), p. 436.*]

Although the measurements of Δf for each line in the Raman spectrum makes possible construction of the rotational levels for a given molecule,[12] its quantum-mechanical explanation is different from that of the rotational spectrum. In particular, the selection rule for the rotational quantum number in the Raman effect is $\Delta\ell = 0, \pm 2$. The $\Delta\ell = 0$ value yields Rayleigh scattering, while $\Delta\ell = \pm 2$ yields the Raman lines. One can see how this comes about physically by studying the transitions shown in Figure 9-30*f*. An electron initially in the $\ell = 0$ state absorbs energy $\Delta E_{01} + \Delta E_{12}$ from the incident photon of frequency f and emits energy ΔE_{12}. Thus, the energy of the scattered photon is

$$hf' = hf - (\Delta E_{01} + \Delta E_{12}) + \Delta E_{12} = hf - \Delta E_{01} \qquad \textbf{9-33}$$

or

$$f' = f - \Delta f$$

where $\Delta f = \Delta E_{01}/h$. If the electron is initially in the $\ell = 1$ state, then it absorbs ΔE_{12} from the incident photon and emits $\Delta E_{12} + \Delta E_{01}$. Thus, the scattered photon has energy

$$hf' = hf - \Delta E_{12} + (\Delta E_{12} + \Delta E_{01}) = hf + \Delta E_{01} \qquad \textbf{9-34}$$

or

$$f' = f + \Delta f$$

Many Raman spectra have been studied. They provide a valuable source of information regarding molecular quantum states, including, as was pointed out earlier, the structure of the rotational levels for homonuclear diatomic molecules. For example, the detailed understanding of the complex vibrations and rotations of the ammonia molecule referred to in Section 6-6 that enabled the development of the first atomic clocks was made possible by studies of the Raman rotational-vibrational spectrum of the NH_3 molecule, the so-called *ammonia inversion spectrum*. Finally, Figure 9-30*g* illustrates the photoelectric effect, the final example of the interaction of radiation with matter, in which the absorption of the photon ionizes the atom or molecule. Like Compton scattering, this effect was discussed in Chapter 3 and will not be considered further here.

STUDENTS-HUB.com Uploaded By: Malak Obaid

Absorption

Information about the energy levels of an atom or molecule is usually obtained from the radiation emitted when the atom or molecule makes a transition from an excited state to a state of lower energy. As mentioned in Section 9-4, we can also obtain information about such energy levels from the absorption spectrum. When atoms and molecules are irradiated with a continuous spectrum of radiation, the transmitted radiation shows dark lines corresponding to absorption of light at discrete wavelengths. Absorption spectra of atoms were the first line spectra observed. Fraunhofer in 1817 labeled the most prominent absorption lines in the spectrum of sunlight; it is for this reason that the two intense yellow lines in the spectrum of sodium are called the *Fraunhofer D lines*. Since at normal temperatures atoms and molecules are in their ground states or in low-lying excited states, the absorption spectra are usually simpler than the emission spectra. For example, only those lines corresponding to the Lyman emission series are seen in the absorption spectrum of atomic hydrogen because nearly all the atoms are originally in their ground states. In the Chapter 6 MORE section "Transitions Between Energy States," we described how transitions between quantum states in an atomic system occur as a result of interaction with oscillating electromagnetic fields. In particular, if the frequency greater than f_{12} is present in radiation incident on an atom whose ground-state and an excited-state energies are respectively E_1 and E_2, then there is a probability that the atom will undergo a transition from the lower energy state E_1, absorbing the energy $hf_{12} = E_2 - E_1$ from the radiation. This absorption of energy resulting from the interaction between the electric field of the radiation oscillating at f_{12} and the charge on the atomic electrons was first described quantum mechanically by Einstein, who expressed the probability of absorption per atom per unit time as $B_{12}u(f)$, where $u(f)$ is the energy density of the radiation per unit frequency and B_{12} is Einstein's coefficient of absorption.

In addition to absorption, several other interesting phenomena occur when electromagnetic radiation—i.e., photons—is incident on atoms or molecules. These are illustrated in Figure 9-30. In Figure 9-30*a* a photon of energy hf is absorbed and the system makes a transition to the excited state. Later, the system makes a transition to a lower state and/or back to the ground state with the *spontaneous emission* of one or more photons via the mechanism described on the home page in the Chapter 6 MORE section "Transitions Between Energy States." The radiation thus emitted is called *fluorescence*. If state 2 happens to be the first excited state, then this two-step process is called *resonance absorption* and the photon emitted is called *resonance radiation*, as shown in Figure 9-30*b*. As a result of motions that occur while the system is in state 2, there is no correlation in direction or phase between the incident and emitted photons. While in state 2 the system has definite probabilities of making spontaneous transitions to each of the lower states as determined by the probability density given by Equation 6-52*d* in the MORE section. For example, the probability per atom per unit time of returning to state 1 with the spontaneous emission of a photon can be expressed by the quantity A_{21} (transitions per unit time). Notice that the reciprocal $1/A_{21}$ has the units of time per transition; i.e., it is a measure of how long the system stays in state 2 before returning to state 1. This is t_s, the mean lifetime of the state, defined as $t_s = 1/A_{21}$. For most atomic (electric dipole) transitions this characteristic lifetime is of the order of 10^{-8} s. A_{21} is called Einstein's coefficient of spontaneous emission.

STUDENTS-HUB.com Uploaded By: Malak Obaid

Stimulated Emission

In addition to the spontaneous emission of fluorescent and resonant radiation with probability A_{21}, which is independent of the energy density $u(f)$ of the incident radiation, emission can also be induced to occur by the oscillating electromagnetic field of the incident radiation. Called *stimulated emission*, its probability does depend upon $u(f)$. This phenomenon, like absorption and spontaneous emission, was first analyzed by Einstein, in 1917. The probability of stimulated emission per atom per unit time (transition rate) can be written as $B_{21}u(f)$, where B_{21} is called Einstein's coefficient of stimulated emission. In this process the electric field of an incident photon with energy hf equal to the energy difference $E_2 - E_1$ in Figure 9-30*c* stimulates the atom or molecule in state 2 to emit a photon with energy $E_2 - E_1 = hf$, which is propagated in the same direction and with the same phase as the incident photon. Such photons (or radiation) are said to be *coherent*.

The relation between the three Einstein coefficients can be found as follows. Consider a system of atoms and radiation in thermal equilibrium at temperature T. Let N_1 and N_2 be the number of atoms occupying the states with energies E_1 and E_2. The ratio N_2/N_1 is determined by the Boltzmann factor, given by Equation 8-2, assuming the two states have the same degeneracy:

$$\frac{N_2}{N_1} = e^{-(E_2 - E_1)/kT} = e^{-hf/kT} \tag{9-35}$$

This ratio represents a dynamic equilibrium in which the number of absorption transitions ($E_1 \rightarrow E_2$) per unit time equals the sum of the number of spontaneous and stimulated emissions ($E_2 \rightarrow E_1$) per unit time. Since the number of atoms making a transition (of any type) is proportional to the population of the state on which the transition begins and to the probability, we can express the dynamic equilibrium as

$$N_1 B_{12} u(f) = N_2(A_{21} + B_{21}u(f)) \tag{9-36}$$

Solving Equation 9-36 for the energy density $u(f)$ of the radiation yields

$$u(f) = \frac{\dfrac{A_{21}}{B_{21}}}{\dfrac{N_1}{N_2}\dfrac{B_{12}}{B_{21}} - 1} \tag{9-37}$$

Inserting N_1/N_2 from Equation 9-35, we have that

$$u(f) = \frac{\dfrac{A_{21}}{B_{21}}}{\dfrac{B_{12}}{B_{21}}e^{hf/kT} - 1} \tag{9-38}$$

This expression for the energy density of radiation of frequency f in thermal equilibrium at temperature T with atoms of energies E_1 and E_2 must be consistent with Planck's law for a blackbody spectrum at temperature T given by Equation 8-57:

$$u(f) = \frac{8\pi h f^3}{c^3}\left(\frac{1}{e^{hf/kT} - 1}\right) \tag{9-39}$$

STUDENTS-HUB.com Uploaded By: Malak Obaid

Comparing Equation 9-38 and 9-39, we conclude that

$$\frac{B_{12}}{B_{21}} = 1 \qquad \textbf{9-40}$$

and that

$$\frac{A_{21}}{B_{21}} = \frac{8\pi hf^3}{c^3} \qquad \textbf{9-41}$$

Although this analysis gives us only the ratios of the coefficients, A_{21} can be computed from quantum mechanics, as was discussed in the home page MORE section "Transitions Between Energy States" in Chapter 6, and the other coefficients may then be computed from the result.

There are several points of interest in these equations. For instance, Equation 9-40 tells us that the coefficients for absorption and stimulated emission are the same for the same pair of states. Notice, too, that Equation 9-41 says that the ratio of the spontaneous emission coefficient to that for stimulated emission is proportional to f^3. This means that the larger $\Delta E = E_2 - E_1$, the more likely spontaneous emission will be comparable to stimulated emission. Rewriting Equation 9-39 as

$$\frac{A_{21}}{B_{21}u(f)} = e^{hf/kT} - 1 \qquad \textbf{9-42}$$

yields the result that, in equilibrium situations, spontaneous emission is far more probable than stimulated emission for $hf \gg kT$. Since this is usually the case for electronic transitions in both atoms and molecules, de-excitation of excited electronic states by stimulated emission is normally ignored in these transitions. Stimulated emission does become important when $hf \approx kT$ and may dominate de-excitation of excited states when $hf \ll kT$. This latter condition exists for ordinary temperatures in the microwave region of the spectrum. We will return to these matters in Section 9-6 in connection with the discussion of lasers and masers.

EXAMPLE 9-7 Spontaneous versus Stimulated Emission Compare the relative probabilities of spontaneous and stimulated emission in an equilibrium system at room temperature ($T = 300$ K) for transitions that occur in (*a*) the visible and (*b*) the microwave regions of the spectrum.

SOLUTION

Equation 9-42 gives the ratio of the probability for spontaneous emission A_{21} to that for stimulated emission $B_{21}u(f)$. At $T = 300$ K, $kT = 0.026$ eV.

(*a*) In the visible region of the spectrum, $hf \approx 2$ eV, so $hf/kT = 2/0.026 = 77$. Therefore,

$$\frac{A_{21}}{B_{21}u(f)} = e^{77} - 1$$

Clearly, under these conditions spontaneous emission is favored over stimulated emission by an enormous factor.

(*b*) In the microwave region of the spectrum, $hf \approx 10^{-4}$ eV, so $hf/kT = 10^{-4}/0.026 = 0.0038 \approx 1/260$ and stimulated emission is rather heavily favored.

STUDENTS-HUB.com Uploaded By: Malak Obaid

Questions

5. How does Rayleigh scattering differ from resonance absorption?
6. How does the photoelectric effect differ from all the other processes illustrated in Figure 9-30?
7. Why is stimulated emission usually not observed?

9-6 Lasers and Masers

The *laser* (*l*ight *a*mplification by *s*timulated *e*mission of *r*adiation) is a device that produces a strong beam of coherent photons by stimulated emission. The *maser*, where *m*icrowave replaces *l*ight in the definition from which the acronym is formed, was the laser's predecessor. Both devices depend on stimulated emission for their operation. We will discuss it more fully here because of its application to these important devices. Stimulated emission occurs if the atom is initially in an excited state and if the energy of the photon incident on the atom is just $E_2 - E_1$, where E_2 is the excited energy of the atom and E_1 is the energy of a lower state or the ground state. In this case, the oscillating electromagnetic field of the incident photon accelerates the electron(s) at a rate that matches the photon's frequency and thus, we say, stimulates the excited atom, which may then emit a photon in the same direction as the incident photon and with the same phase. We have seen that the relative probabilities of stimulated emission and absorption B_{21} and B_{12} are equal (Equation 9-40). Ordinarily, at normal temperatures, nearly all atoms will initially be in the ground state, so absorption will be the main effect. That is, $N_1 \gg N_2$, so

$$N_1 u(f) B_{12} \gg N_2 u(f) B_{21}$$

where N_1 and N_2 are the populations of the two states. To produce more stimulated emission transitions than absorption transitions, we must arrange to have more atoms in the excited state than in the ground state ($N_2 > N_1$). This condition is called *population inversion*. It can be achieved if the excited state E_2 is a metastable state. Once population inversion is achieved, any light emitted by a spontaneous $E_2 \rightarrow E_1$ transition is amplified by stimulated emission from the excited atoms that it encounters. Population inversion is often obtained by a method called *optical pumping*, in which atoms are "pumped" up to energy levels greater than E_2 by the absorption of an intense auxiliary radiation. The atoms then decay down to the metastable state E_2 by either spontaneous emission or by nonradiative transitions such as those due to collisions.

The maser was the first of these devices to be constructed, an accomplishment of Charles Townes and his co-workers in 1953. Currently, the most important type of maser is the hydrogen maser, which is used as an atomic-frequency standard, one type of atomic clock. The hydrogen transition used in these masers is that between the hyperfine levels of the ground state, the same transition used to map hydrogen clouds in interstellar space (see Chapter 13). This transition between the $\Psi_{100+\frac{1}{2}}$ and $\Psi_{100-\frac{1}{2}}$ states is shown in Figure 9-32*a*. Townes shared the 1964 Nobel Prize in Physics for his contributions to the development of masers and lasers.

STUDENTS-HUB.com Uploaded By: Malak Obaid

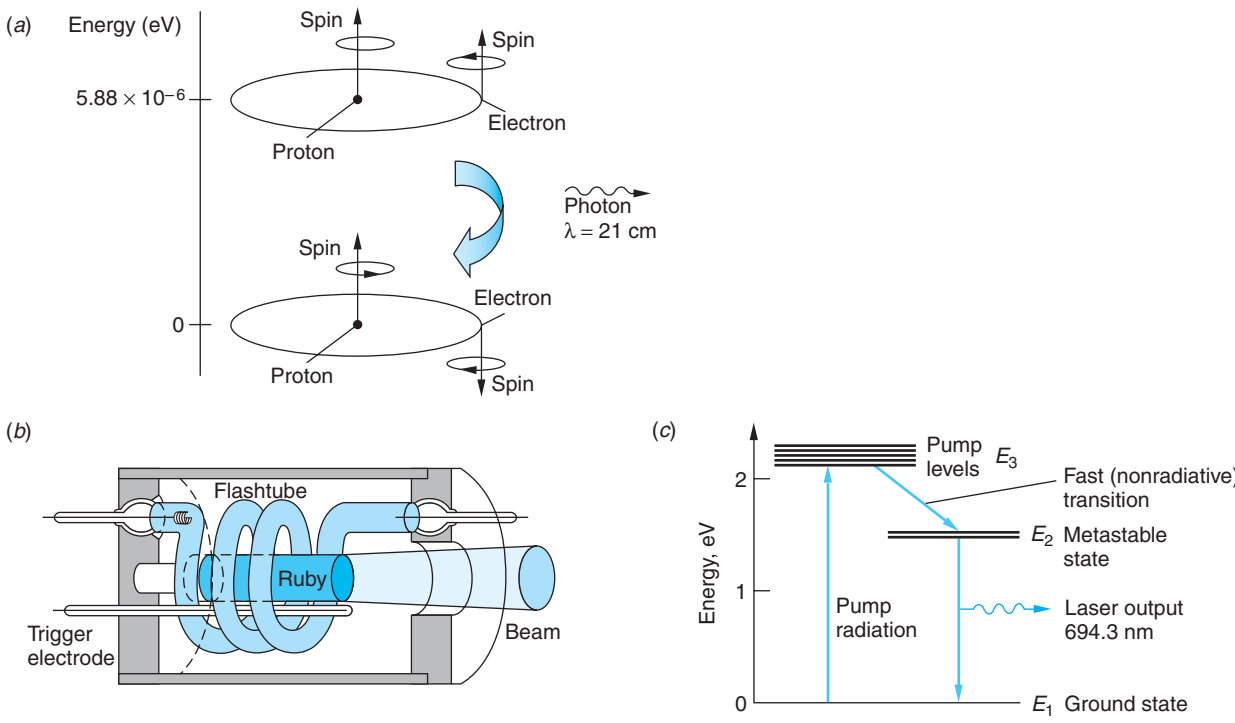

Figure 9-32 (*a*) Hyperfine levels used in the hydrogen maser. (*b*) Schematic diagram of the first ruby laser. (*c*) Energy levels of chromium in ruby, Al_2O_3.

The Ruby Laser

Figure 9-32*b* shows a schematic diagram of the first laser, a ruby laser built by Theodore Maiman in 1960.[13] It consists of a small rod of ruby (a few centimeters long) surrounded by a helical gaseous flashtube. The ends of the ruby rod are flat and perpendicular to the axis of the rod. Ruby is a transparent crystal of Al_2O_3 containing a small amount (about 0.05 percent) of chromium. It appears red because the chromium ions (Cr^{3+}) have strong absorption bands in the blue and green regions of the visible spectrum. The energy levels of chromium that are important for the operation of a ruby laser are shown in Figure 9-32*c*.

When the mercury- or xenon-filled flashtube is fired, there is an intense burst of light lasting a few milliseconds. Absorption excites many of the chromium ions to the bands of energy levels called *pump levels* in Figure 9-32*c*. The excited chromium ions give up their energy to the crystal in nonradiative transitions and drop down to a pair of metastable states labeled E_2 in the figure. These metastable states are about 1.79 eV above the ground state. If the flash is intense enough, more atoms will make the transition to the states E_2 than remain in the ground state. As a result, the populations of the ground state and the metastable states become inverted. When some of the atoms in the states E_2 decay to the ground state by spontaneous emission, they emit photons of energy 1.79 eV and wavelength 694.3 nm. Some of these photons then stimulate other excited atoms to emit photons of the same energy and wavelength, moving in the same direction with the same phase.

STUDENTS-HUB.com Uploaded By: Malak Obaid

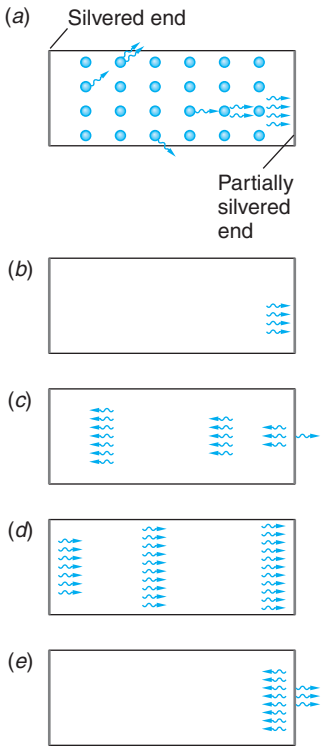

Figure 9-34 Buildup of photon beam in a laser. (*a*) Some of the atoms spontaneously emit photons, some of which travel to the right and stimulate other atoms to emit photons parallel to the axis of the crystal. The others are absorbed, transmitted through the walls, or otherwise lost to the lasing process. (*b*) Four photons strike the partially silvered right face of the laser. (*c*) One photon has been transmitted and the others have been reflected. As these photons traverse the laser crystal, they stimulate other excited atoms to emit photons and the beam intensity increases. By the time the beam reaches the right face again (*d*), it comprises many photons. (*e*) Some of these photons are transmitted to become part of the external laser beam and the rest are reflected to sustain the process.

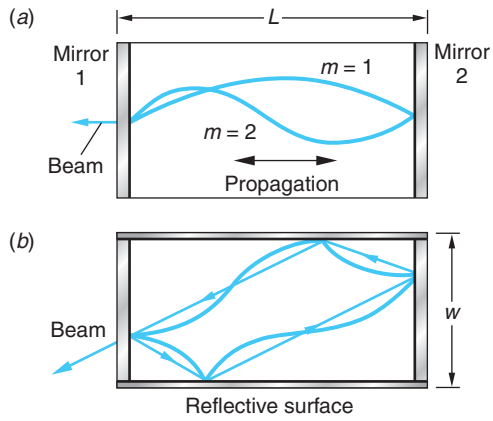

Figure 9-33 Laser as a resonating optical cavity. If mirror 1 is the partially reflecting end, then (*a*) illustrates the longitudinal standing-wave modes, for which $L = m\lambda/2$, where λ is the laser wavelength and m is integral. If the sides of the cavity are also reflective, as in (*b*), then standing-wave modes transverse to the long axis are also possible. Notice that the exit beam for these modes is not parallel to the long axis of the laser.

The ruby laser, like other conventional lasers, acts as a resonating optical cavity. In the ruby laser, both ends of the crystal are silvered such that one end is almost totally reflecting (about 99.9 percent) and the other end is only partially reflecting (about 99 percent) so that some of the beam is transmitted through that slightly transparent end. If the ends are parallel, standing waves are set up, as shown in Figure 9-33, and an intense beam of coherent light emerges through the partially silvered end. Figure 9-34 illustrates the buildup of the beam inside the laser. When photons traveling parallel to the axis of the crystal strike the silvered ends, all are reflected from the back face and most are reflected from the front face, with a few escaping through the partially silvered front face. During each pass through the crystal, the photons stimulate more and more atoms so that an intense photon beam is developed.

Modern ruby lasers generate intense light beams with energies ranging from 50 J to 100 J in pulses lasting a few milliseconds. This pulse length is approximately equal to that of the flash tube, whose output excites atoms into the pump levels shown in Figure 9-32*c*. The output of the laser during that time is actually a series of very short pulses, each of the order of a microsecond long, as illustrated in Figure 9-35. This is because the pump levels depopulate quickly compared to the pump rate. Therefore, the flash requires some time to reestablish the population inversion that generates the next short pulse.

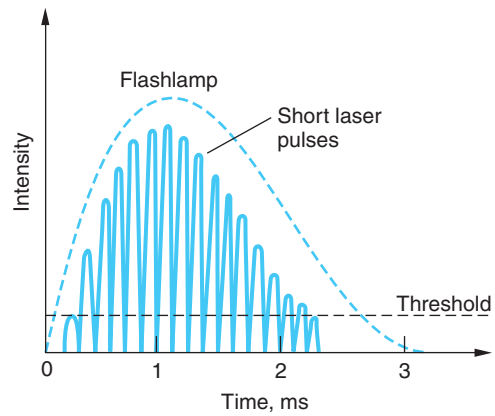

Figure 9-35 A single output pulse from a ruby laser. The pulse actually consists of a series of very short pulses each about 1 μs long. Flashlamp intensities below the threshold do not produce a sufficient population inversion to initiate lasing. Not shown is a weak background of incoherent spontaneous emission that accompanies the coherent laser light.

STUDENTS-HUB.com Uploaded By: Malak Obaid

Notice in Figure 9-35 that the first of the very brief laser pulses, or "spikes," begins very soon after the population inversion $N_2 > N_1$ occurs and ends when N_2 falls back to N_1 due to stimulated emissions. Extremely intense spikes can be generated via a technique called *Q-switching*, whereby the resonating property of the cavity is temporarily destroyed in order to sharply reduce the stimulated emissions so as to allow the pumping radiation to make $N_2 \ggg N_1$. The resonant status is then suddenly restored and an extremely intense laser pulse results. This is how the very high-energy pulses mentioned above are typically produced. The Q in *Q-switching* refers to the cavity's *quality factor*, or its ability to maintain the intensity of the reverberating wave. If the end mirrors are low loss and the medium very transparent to the laser frequency, then the wave will die out slowly and the cavity is of high quality, or high Q. If Q is low, then substantial light is lost in each pass and the wave will die out quickly. If Q is too low, lasing will not occur at all. Q can be made very low, for example, by replacing the totally reflecting end mirror with an external one of equal reflectivity that rotates. When the rotating mirror is not parallel to the one on the other end of the cavity, Q is very low and little stimulated emission occurs as the pumping flash builds the population of state E_2 so that $N_2 \ggg N_1$. When the rotating mirror becomes parallel to the other, Q suddenly becomes very high (hence the name Q-switch) and the extremely intense laser pulse is generated as E_2 depopulates.

Sustaining laser action requires that the increase in the number of coherent photons produced by stimulated emission per round trip through the resonating cavity to be greater than or equal to the decrease resulting from all losses, such as transmission through the partially reflecting end mirror and scattering. Although its a bit difficult, we have information to calculate the population inversion density necessary for lasing with the aid of the Einstein coefficients from Section 9-5, so let's try it. To begin, let's combine all of the various ways by which photons may be lost into a single characteristic time t_p. That is, the intensity of radiation I of a particular frequency f in the resonant cavity will decay due to the losses according to

$$I = I_0 e^{-t/t_p} \tag{9-43}$$

where I_0 is the intensity at $t = 0$. Thus, the rate at which intensity is lost is given by

$$\left(\frac{dI}{dt}\right)_{\text{loss}} = -\frac{I_0}{t_p} e^{-t/t_p} = -\frac{I}{t_p} \tag{9-44}$$

The net rate at which the intensity of the frequency f gains due to the difference between the gain from stimulated emissions $E_2 \longrightarrow E_1$ and the offsetting loss from absorptions $E_1 \longrightarrow E_2$ is equal to the difference in the populations $(N_2 - N_1)$ times the intensity per photon times the transition probability $u(f)B_{21}$. The transition probability $u(f)B_{21}$ must be corrected for the width Δf of the spectral line emitted in the $E_2 \longrightarrow E_1$ transition arising from the finite width of the level E_2, as described in Chapter 5.[14] The correction is a multiplicative factor approximately equal to $2/\pi\Delta f$. Taking these together, we obtain

$$\left(\frac{dI}{dt}\right)_{\text{gain}} = (N_2 - N_1)\frac{hfc}{V}\frac{2}{\pi\Delta f}u(f)B_{21} \tag{9-45}$$

where V is the volume of the resonant cavity and hfc/V is the intensity per photon.

STUDENTS-HUB.com Uploaded By: Malak Obaid

Using Equation 9-38 and the fact that A_{21} is the reciprocal of the lifetime for spontaneous emission t_s, Equation 9-45 can be written as

$$\left(\frac{dI}{dt}\right)_{\text{gain}} = \frac{(N_2 - N_1)}{V}(hfc)\left[\frac{u(f)c^3}{4\pi^2 hf^3 \Delta f\, t_s}\right] \qquad \textbf{9-46}$$

or

$$\left(\frac{dI}{dt}\right)_{\text{gain}} = (n_2 - n_1)\frac{c^3 I}{4\pi^2 f^2 \Delta f\, t_s} \qquad \textbf{9-47}$$

where $n_2 = N_2/V$ and $n_1 = N_1/V$ are the *population densities* of the states and $cu(f) = I$, the intensity.[15] If the density of states (degeneracies) $g(E)$ of E_2 and E_1 are not equal, then Equation 9-47 must be modified to

$$\left(\frac{dI}{dt}\right)_{\text{gain}} = \left[n_2 - n_1\left(\frac{g(E_2)}{g(E_1)}\right)\right]\frac{c^3 I}{4\pi^2 f^2 \Delta f\, t_s} \qquad \textbf{9-48}$$

Thus, the condition for laser action becomes

$$\left(\frac{dI}{dt}\right)_{\text{gain}} \geq \left(\frac{dI}{dt}\right)_{\text{loss}} \qquad \textbf{9-49}$$

or

$$\left[n_2 - n_1\left(\frac{g(E_2)}{g(E_1)}\right)\right]\frac{c^3 I}{4\pi^2 f^2 \Delta f\, t_s} \geq \frac{I}{t_p} \qquad \textbf{9-50}$$

The equal sign provides the threshold condition for the initiation of lasing. The greater-than sign represents sustained laser action. Solving the threshold condition yields the *critical population inversion density* Δn_c:

$$\Delta n_c = \frac{4\pi^2 f^2 \Delta f\, t_s}{c^3 t_p} \qquad \textbf{9-51}$$

where

$$n_2 - n_1\left(\frac{g(E_2)}{g(E_1)}\right) = \Delta n_c$$

Equation 9-51 describes the population inversion that must be established if laser action is to be achieved for a given frequency and spontaneous emission lifetime. It also points out that the only property of the cavity that affects Δn_c is its characteristic decay lifetime t_p.

The ruby laser is an example of a three-level laser, referring to the energy levels in Figure 9-32*c*. Such lasers have a practical disadvantage for many applications in that more than half of the atoms must be pumped from $E_1 \rightarrow E_3$ in order to obtain the necessary population inversion between levels E_2 and E_1. In addition, the source of the excitation energy, the flashlamp, produces light over a broad range of frequencies, most of which do not contribute to exciting the level E_3 and are thus wasted. The large pumping requirement and relatively low excitation efficiency mean that substantial energy must be dissipated as heat, so three-level solid-state lasers such as the ruby laser must be pulsed in order to allow the system time to cool periodically. A more advantageous

STUDENTS-HUB.com Uploaded By: Malak Obaid

system is one that does not require such a large fraction of the atoms to be excited at any one time and avoids the excess heat produced by optical pumping. Such lasers provide continuous output and are called *continuous wave*, or *cw*, lasers.

Helium-Neon Lasers

In 1961, the first successful operation of a cw laser, a continuous helium-neon gas laser, was announced by Ali Javan, W. R. Bennet, Jr., and D. R. Herriott.[16] Figure 9-36 shows a schematic diagram of the type of helium-neon laser commonly used for physics demonstrations and laser pointers and by land surveyors and carpenters. It consists of a gas tube containing 15 percent helium gas and 85 percent neon gas. A totally reflecting flat mirror is mounted on one end of the gas tube and a partially reflecting concave mirror is placed at the other end. The concave mirror focuses parallel light at the flat mirror and also acts as a lens that transmits part of the light so that it emerges as a parallel beam.

Population inversion is achieved somewhat differently in the helium-neon laser than in the ruby laser. Figure 9-37 shows the energy levels of helium and neon that are important for operation of the laser. (The complete energy-level diagrams for helium and neon are considerably more complicated.) Helium has excited states, the 2^3S and 2^1S levels that lie 19.72 eV and 20.61 eV, respectively, above the 1^1S ground state. Both are metastable because of the $\Delta\ell = \pm 1$ selection rule, the 2^3S level being more strongly forbidden due to the $\Delta S = 0$ selection rule, discussed in the Chapter 7 home page MORE section "Multielectron Atoms," that prohibits intercombination lines. Helium atoms are excited to these states by an electrical discharge. Neon has closely spaced groups of excited states at 19.83 eV and 20.66 eV above its ground state—the energies of these neon states almost exactly match the excited states of helium. The neon atoms are excited to these levels by collisions with excited helium atoms. The kinetic energy of the helium atoms provides the extra energy, about 0.05 eV, needed to excite the neon atoms. There is another excited state of neon that is 18.70 eV above its ground state and 1.96 eV below the 20.66 eV state. Since this state is normally unoccupied, population inversion between these states is obtained immediately. The stimulated emission that occurs between these states results in photons of energy 1.96 eV and wavelength 632.8 nm, which produces a bright red light. After stimulated emission, the atoms in the 18.70 eV state decay to the ground state by spontaneous emission of a photon with a wavelength of about 600 nm followed by a nonradiative de-excitation, typically collision with the cavity wall. The collisions are an important part of the laser process since if the diameter of the tube (see Figure 9-36) is too large, the probability of collision with the wall decreases and the 600-nm radiation may re-excite the 18.70 eV level. This reduces the population inversion and decreases the laser gain. Stimulated emission also occurs from the state at 19.83 eV to the 18.70 eV level, producing laser light with a wavelength of 1100 nm (infrared).

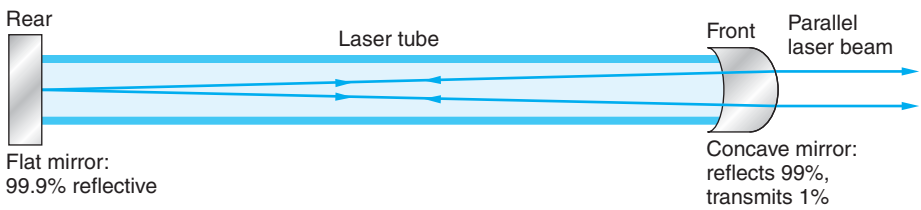

Figure 9-36 Schematic drawing of a helium-neon laser. The use of a concave mirror rather than a second plane mirror makes the alignment of the mirrors less critical than it is for the ruby laser. The concave mirror on the right also serves as a lens that focuses the emitted light into a parallel beam.

STUDENTS-HUB.com Uploaded By: Malak Obaid

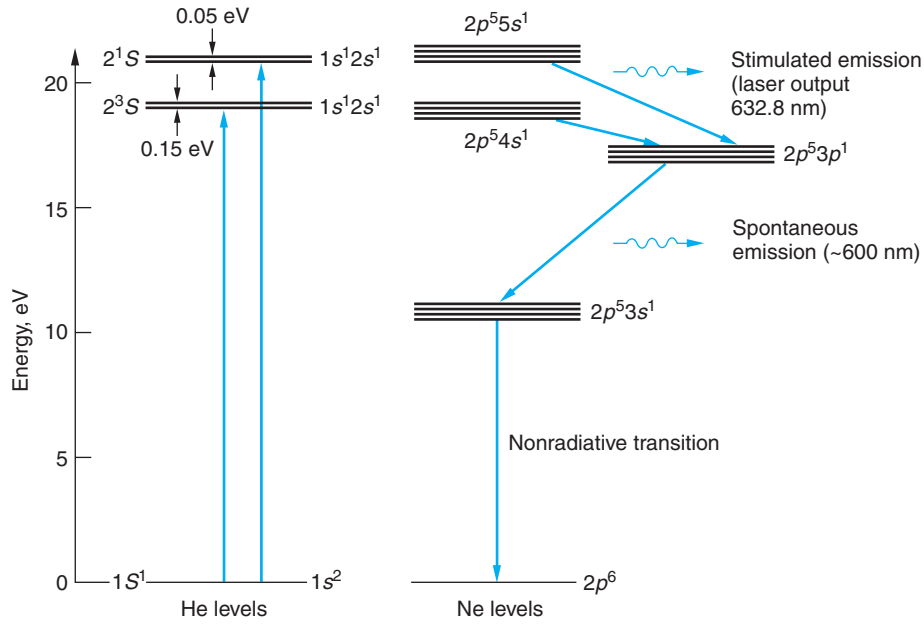

Figure 9-37 Energy levels of helium and neon that are important for the helium-neon laser. The helium atoms are excited by electrical discharge to energy states 19.72 eV and 20.61 eV above the ground state. They collide with neon atoms, exciting some neon atoms to energy states 19.83 eV and 20.66 eV above the ground state. Population inversion is thus achieved between these levels and one at 18.70 eV above the ground state. The spontaneous emission of photons of energy 1.96 eV from the upper state stimulates other atoms in the upper state to emit photons of energy 1.96 eV, producing the characteristic He-Ne red laser light. Emission from the 19.83 eV neon state to the 18.70 eV level also produces laser output at about 1100 nm.

Helium-neon lasers have recently been developed that lase at a number of other visible and infrared wavelengths. The several possible laser wavelengths are not present simultaneously since each device is designed to operate at a particular wavelength.

Note that there are four energy levels involved in producing the 632.8-nm helium-neon laser line, whereas the ruby laser involved only three levels. In a three-level laser, population inversion is difficult to achieve because more than half the atoms in the ground state must be excited, i.e., $N_2 > N_1/2$ in Equation 9-46. In a four-level laser, population inversion is easily achieved because the state after stimulated emission is not the ground state but an excited state that is normally unpopulated, so that $N_1 \approx 0$.

New Lasers and Applications

A laser beam is coherent, very narrow, and intense. Its coherence makes the laser beam useful in the production of holograms, such as those used on credit cards and "heads-up" displays; i.e., transparent data displays that don't obstruct the user's view. The precise direction and small angular spread of the beam make it useful as a surgical tool for destroying cancer cells or reattaching a detached retina. Lasers are also used by land surveyors and carpenters to ensure precise alignment over large distances. Distances can be accurately measured by reflecting a laser pulse from a mirror and measuring the time the pulse takes to travel to the mirror and back. The distance to the Moon is currently measured to within a few millimeters using corner reflectors placed on the Moon by Apollo astronauts for that purpose. Laser beams are also used in fusion research.

STUDENTS-HUB.com Uploaded By: Malak Obaid

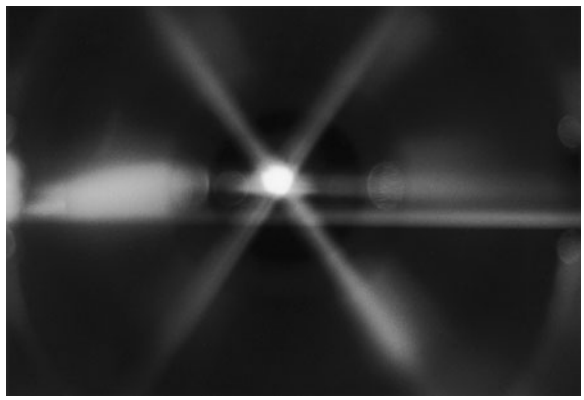

Three counterpropagating pairs of orthogonal laser beams illuminate about 100 million sodium atoms at their intersection. The pressure of the laser light cools the atoms, slowing them to rms velocities comparable to those resulting from recoil due to emission or absorption of a single photon. Systems incorporating laser cooling of sodium atoms have achieved a record low temperature of 450 pK. [*National Institute of Science and Technology.*]

An intense laser pulse is focused on tiny pellets of deuterium-tritium in a combustion chamber. The beam heats the pellets to temperatures of the order of 10^8 K in a very short time, causing the deuterium and tritium to fuse and release energy. (See Section 11-8.) At the other end of the temperature scale, using advanced cooling techniques that included the focusing of three orthogonal pairs of lasers (optical tweezers) on a sample containing 2500 cesium atoms, in 2003 W. Ketterle and his group achieved a record low temperature of 450 pK.[17] (See the photo above.) Orthogonal pairs of laser beams, called *optical traps*, capable of cooling samples containing millions of atoms down to the submicrokelvin range, are used in creating Bose-Einstein condensates and the degenerate Fermi gas, discussed in Chapter 8, and antihydrogen atoms, described in Chapter 12.

While cw lasers are the lasers of choice for many applications, many others require pulsed lasers, particularly those where very high power levels are important or even essential. For these applications the current state of the art is *chirped pulse amplification*. With this technique, invented in the 1980s by Gérhard Mourou, an input ultrashort pulse is stretched out (in time) by dispersing the wavelengths (frequencies) of the pulse with a suitable arrangement of gratings or prisms together with mirrors. After passing through the optical stretcher, the pulse duration is up to 10^5 times longer than the original pulse and the intensity has been correspondingly lowered as a result to avoid nonlinear effects that would damage or destroy the amplification medium. The laser pulse, amplified by a factor of 10^6 or more, is recompressed by an optical system that is essentially the reverse of the stretcher. Off-the-shelf chirped pulse lasers are available with peak power in the 10- to 100-gigawatt range. Several major research facilities operate chirped lasers with peak power in the petawatt range.

Long-range fiber optic communication lines will be enhanced by the recent development of the erbium-doped fiber optic amplifier. Light from a diode laser "pumps up" a segment of erbium-doped optical fiber in the line. A signal moving down the line stimulates emission from the erbium atoms, resulting in amplification of the signal.

Laser technology is advancing so fast that it is possible to mention only a few recent developments. In addition to the ruby laser, there are many other solid-state lasers with output wavelengths ranging from about 18 nm (soft x rays) to about 3900 nm (infrared). Lasers that generate more than 1 kW of continuous power have been constructed, and pulsed lasers can now deliver nanosecond pulses of power exceeding 10^9 W. Various gas lasers produce wavelengths ranging from the far infrared to the ultraviolet. Semiconductor lasers (also known as diode lasers or junction lasers; these will be discussed further in Chapter 10) the size of a pinhead can develop 200 mW of power.

STUDENTS-HUB.com Uploaded By: Malak Obaid

In addition to the ubiquitous diode lasers used in supermarket checkout counters, compact disc players, copiers, and computer printers, through very recent developments in materials physicists have constructed reliable diode lasers that emit in the blue to ultraviolet region of the spectrum. These lasers should make possible significantly increased high-density optical storage on digital versatile discs (DVDs). Liquid lasers using chemical dyes can be tuned over a range of wavelengths (about 70 nm for continuous lasers and more than 170 nm for pulsed lasers). The free-electron laser extracts light energy from a beam of free electrons moving through a spatially varying magnetic field. It has the potential for very high power and high efficiency and can be tuned over a large range of wavelengths. The variety and uses of modern lasers seem limitless.

Questions

8. What are the advantages of a four-level laser over a three-level laser?
9. Why is helium needed in a helium-neon laser? Why not just use neon?

EXAMPLE 9-8 **Critical Population Inversion Comparison** Compare the critical population inversion necessary for laser action in the ruby and He-Ne lasers. Compute the corresponding power requirements.

SOLUTION

The critical population density Δn_c is given by Equation 9-51. The typical parameters of these systems are as follows:

Parameter	Ruby laser	He-Ne laser
λ	694.3 nm	632.8 nm
f	$4.32 \times 10^{14}\ s^{-1}$	$4.74 \times 10^{14}\ s^{-1}$
n (refractive index)	1.76	1.00
t_s	3×10^{-3} s	10^{-7} s
t_p	2.9×10^{-8} s	3.3×10^{-7} s
Δf	$3.3 \times 10^{11}\ s^{-1}$	$9 \times 10^{8}\ s^{-1}$
N (Cr^{3+} concentration)	$2 \times 10^{19}/cm^3$	—

For ruby laser:

$$\Delta n_c = \frac{4\pi^2 f^2 \Delta f\, t_s}{c^3 t_p} = \frac{4\pi^2(4.32 \times 10^{14})^2(3.3 \times 10^{11})(3 \times 10^{-3})}{(3.00 \times 10^8/1.76)^3(2.9 \times 10^{-8})}$$

$$\Delta n_c = 5.08 \times 10^{22}\ \text{atoms/m}^3 = 5.08 \times 10^{16}\ \text{atoms/cm}^3$$

For He-Ne laser:

$$\Delta n_c = \frac{4\pi^2 f^2 \Delta f\, t_s}{c^3 t_p} = \frac{4\pi^2(4.74 \times 10^{14})^2(9 \times 10^{8})(10^{-7})}{(3.00 \times 10^8)^3(3.3 \times 10^{-7})}$$

$$\Delta n_c = 8.96 \times 10^{13}\ \text{atoms/m}^3 = 8.96 \times 10^{7}\ \text{atoms/cm}^3$$

Thus, the critical population density is far smaller for the He-Ne laser.

STUDENTS-HUB.com Uploaded By: Malak Obaid

The minimum power input P needed to maintain the laser action in the helium-neon system is approximately equal to $\Delta n_c(hf/t_s)$ since $N_1 \approx 0$, or

$$P(\text{He-Ne}) \approx \Delta n_c(hf/t_s) \approx \frac{(8.96 \times 10^7)(6.63 \times 10^{-34})(4.74 \times 10^{14})}{10^{-7}} \approx 2.8 \times 10^{-4}\ \text{W/cm}^3$$

For the ruby laser, about one-half of the Cr^{3+} ions must be in the pumped level E_3 in Figure 9-32*c*, and the power per unit volume necessary to maintain that population is approximately

$$P(\text{ruby}) \approx \frac{N}{2}\left(\frac{hf}{t_s}\right) \approx \frac{(2 \times 10^{19})(6.63 \times 10^{-34})(4.32 \times 10^{14})}{2 \times 3 \times 10^{-3}} \approx 955\ \text{W/cm}^3$$

Summary

TOPIC	RELEVANT EQUATIONS AND REMARKS
1. The ionic bond	The bonding mechanism typical of most salts, it involves the transfer of one or more electrons to form ions that are attracted by the Coulomb force. The exclusion principle limits the close approach of the ions, resulting in a minimum in the potential energy $U(r)$. For a diatomic molecule, $U(r) = -\frac{ke^2}{r} + E_{ex} + E_{ion}$ **9-1** where E_{ion} is the net ionization energy and E_{ex} is the exclusion-principle energy. The latter is given by $E_{ex} = \frac{A}{r^n}$ **9-2** where A and n are constants.
2. The covalent bond	This bond is a quantum-mechanical effect arising from the sharing of one or more electrons by identical or similar atoms. The symmetry of the molecular wave functions resulting from their superposition of electron orbitals determines whether bonding will occur. The wave function for the symmetric state Ψ_S is large between the atomic potential wells, resulting in minimum potential energy and bonding. The antisymmetric wave function Ψ_A is small in that region. Bonding of two nonidentical atoms is often a mixture of ionic and covalent bonding.
Other covalent bonds	Covalent bonds differ in detail, depending upon which electrons are shared. For example, H_2 with only *s* electrons, is *s*-bonded. O_2 is *p*-*p* bonded. There are also *s*-*p* bonds, of which H_2O is one example.
3. Dipole-dipole bonds	Bonding between atoms and molecules may arise due to interactions between dipole moments. The interaction may involve molecules with either permanent electric dipole moments (polar molecules) or induced dipole moments (nonpolar molecules). The potential energy U of a dipole $\mathbf{p}_2$ in the electric field $\mathbf{E}_d$ of dipole $\mathbf{p}_1$ is given by $U = -\mathbf{p}_2 \cdot \mathbf{E}_d$ **9-8** The force between permanent dipoles decreases as $1/r^4$. If one or both of the dipoles is an induced dipole, the force between them decreases as $1/r^7$.

STUDENTS-HUB.com Uploaded By: Malak Obaid

TOPIC	RELEVANT EQUATIONS AND REMARKS
4. Molecular spectra	The energy states of diatomic molecules consist of rotational bands superimposed on more widely spaced vibrational levels, which are in turn superimposed on the much more widely spaced atomic electron levels.
Rotational energies	The rotational energies of a diatomic molecule are $E = \frac{\ell(\ell+1)\hbar^2}{2I} = \ell(\ell+1)E_{0r} \qquad \ell = 0, 1, 2, \ldots$ **9-13** where I is the moment of inertia, $E_{0r} = \hbar^2/2I$ is the characteristic rotational energy, and ℓ is the rotational quantum number, which obeys the selection rule $\Delta\ell = \pm 1$.
Vibrational energies	The vibrational energies of a diatomic molecule are $E_v = (v + 1/2)hf \qquad v = 0, 1, 2, \ldots$ **9-20** where f is the vibrational frequency and v is the vibrational quantum number, which obeys the selection rule $\Delta v = \pm 1$.
5. Scattering, absorption, and stimulated emission	A photon incident on an atom can be absorbed, producing fluorescence or resonance radiation, or scattered elastically (Rayleigh scattering) or inelastically (Raman scattering). If the photon energy is greater than the ionization energy of the atom, Compton scattering or the photoelectric effect can occur. If the atom is initially in an excited state, an incident photon of the proper energy can stimulate emission of another photon of the same energy. The incident and emitted photons are in phase and travel parallel to each other. In an equilibrium system the probabilities (Einstein coefficients) for absorption and for stimulated emission between two states are equal.
6. Lasers and masers	Lasers and masers are important applications of stimulated emission, differing only in the wavelengths of their outputs. Amplification by stimulated emission depends on the possibility of obtaining population inversion, in which there are more atoms in an excited state than in the ground state or another excited state of lower energy. Population inversion is usually obtained by optical pumping and is produced more readily in four-level systems than in three-level systems.

General References

The following general references are written at a level appropriate for the readers of this book.

Brehm, J. J., and W. J. Mullin, *Introduction to the Structure of Matter*, Wiley, New York, 1989.

Eisberg, R., and R. Resnick, *Quantum Physics of Atoms, Molecules, Solids, Nuclei, and Particles*, 2d ed., Wiley, New York, 1985.

Herzberg, G., *Atomic Spectra & Atomic Structure*, Dover, New York, 1944.

Pauling, L., *The Chemical Bond*, Cornell University Press, Ithaca, NY, 1967.

Schawlow, A. L., "Laser Light," *Scientific American*, September 1968. This article and several other excellent articles on lasers and masers are reprinted in *Lasers and Light*, W. H. Freeman and Co., New York, 1969.

Serway, R. A., C. J. Moses, and Curt A. Moyer, *Modern Physics*, 3d ed., Thomson, Belmont, CA, 2005.

Zeilinger, A., "Quantum Teleportation," *Scientific American*, April 2000.

STUDENTS-HUB.com Uploaded By: Malak Obaid

Notes

1. The term *orbital* is frequently used in molecular physics and in chemistry to refer to the space part of the electron wave functions, that is, the quantum numbers n, ℓ, and m_ℓ. In molecular physics the electrons of interest are usually the outermost (valence) ones of the constituent atoms, which become associated with the entire molecule rather than their original atoms, so we speak of "molecular orbitals" as well as "atomic orbitals."

2. Molecules whose atoms are identical, such as H_2, are sometimes called *homopolar* or *homonuclear*. Those whose atoms are not identical are called *heteropolar* or *heteronuclear*.

3. C_{60} and the other fullerenes are named after the philosopher and engineer R. Buckminster Fuller, who invented the architectural geodesic dome structure. Such domes, as Fuller pointed out, can be considered as networks of pentagons and hexagons.

4. Leonhard Euler (1707–1783), Swiss mathematician. Arguably the most prolific mathematician of all time, he published 866 papers during his lifetime and, despite having lost his sight in 1766 (in part due to his earlier observations of the Sun), he left so many manuscripts at his death that it took another 35 years to get them all published. He introduced the symbol e as the base of the natural logarithms and i as the square root of -1.

5. Johannes D. van der Waals (1837–1923), Dutch physicist. Largely self-taught, he became interested in the fact that the ideal gas law derived from kinetic theory does not hold exactly for real gases. This led him to question the assumption that no forces act between individual gas molecules except during collisions, which resulted in his development of an equation, the van der Waals equation, which more accurately describes real gases. He was awarded the 1910 Nobel Prize in Physics for his work.

6. This result is derived in most introductory physics books. See, e.g., P. A. Tipler and G. Mosca, *Physics for Scientists and Engineers,* 6th ed., W. H. Freeman and Co., New York, 2008, p. 671.

7. Terminology concerning the dipole-dipole forces is a bit confused. Some textbooks use *van der Waals* to describe all three types of dipole-dipole forces. We will follow the more common (and traditional) use, reserving *van der Waals* for the attractive force between induced dipoles only.

8. We use v (the Greek letter nu) here rather than n so as not to confuse the vibrational quantum number with the principal quantum number n for electronic energy levels.

9. The nitric oxide (NO) molecule is an exception due to its odd electron.

10. Also, the $\ell \rightarrow \ell - 1$ group of lines are called the *P branch* and the $\ell \rightarrow \ell + 1$ group the *R branch*.

11. Chandrasekhara V. Raman (1888–1970), Indian physicist. Graduating from college at the age of 16, like Einstein he became a civil servant and worked at science in his spare time. He had predicted that visible light should be inelastically scattered even before Heisenberg had predicted and Compton had found the effect for x rays. He was awarded the 1930 Nobel Prize in Physics for his work, becoming the first Asian to be so recognized in the sciences.

12. There is also a Raman effect for the vibrational and electronic levels of molecules.

13. T. H. Maiman, "Stimulated Optical Radiation in Ruby," *Nature*, **187**, 493 (1960).

14. The correction essentially accounts for the fact that, due to the finite line width, the energy density $u(f)$ in the transition probability must include a narrow range of frequencies Δf rather than just the single frequency f.

15. Recall that the energy per unit volume $u(f)$ times c is the intensity, e.g., W/m^2 in SI units.

16. A. Javan, W. B. Bennet, Jr., and D. R. Herriott, *Physical Review Letters*, **6**, 106 (1961).

17. W. Ketterle et al., *Science*, **301**, 1513 (2003).

Problems

Level I

Section 9-1 The Ionic Bond

9-1. The dissociation energy is sometimes expressed in kilocalories per mole. (*a*) Find the relation between electron volts per molecule and kilocalories per mole. (*b*) Find the dissociation energy of molecular NaCl in kilocalories per mole. (*c*) The dissociation energy of the Li_2 molecule is 106 kJ/mole. Find the value in eV per molecule.

STUDENTS-HUB.com Uploaded By: Malak Obaid

9-2. The dissociation energy of Cl_2 is 2.48 eV. Consider the formation of an NaCl molecule by the reaction

$$Na + \tfrac{1}{2}Cl_2 \longrightarrow NaCl$$

Is this reaction endothermic (requiring energy) or exothermic (giving off energy)? How much energy per molecule is required or given off?

9-3. Using the data in Table 9-1, compute the net energy required to transfer an electron between the following pairs of atoms: Cs to F, Li to I, and Rb to Br.

9-4. Using the data in Tables 9-1 and 9-2, estimate the dissociation energy of the three ionically bonded molecules CsI, NaF, and LiI. Your results are probably all higher than those in Table 9-2. Explain why.

9-5. The equilibrium separation of the Rb^+ and Cl^- ions in RbCl is about 0.267 nm. (*a*) Calculate the potential energy of attraction of the ions, assuming them to be point charges. (*b*) The ionization energy of rubidium is 4.18 eV, and the electron affinity of Cl is 3.62 eV. Find the dissociation energy, neglecting the energy of repulsion. (*c*) The measured dissociation energy is 4.37 eV. What is the energy due to repulsion of the ions?

9-6. Compute the Coulomb energy of the KBr molecule at the equilibrium separation. Use that result to compute the exclusion-principle repulsion at r_0.

9-7. If the exclusion-principle repulsion in Problem 9-6 is given by Equation 9-2, compute the coefficient A and the exponent n.

9-8. Compute the dissociation energy of molecular NaBr in kilocalories per mole.

9-9. Note in Table 9-2 that the equilibrium separations of the KBr and RbCl molecules are very nearly equal. Compute the exclusion-principle repulsion for these molecules.

Section 9-2 The Covalent Bond

9-10. Hydrogen can bond covalently with many atoms besides those listed in Tables 9-3 and 9-5, including sulfur, tellurium, phosphorus, and antimony. What would you expect to be the chemical formula of the resulting molecules? (*Hint:* Use the table of electron configurations in Appendix C.)

9-11. What kind of bonding mechanism would you expect for (*a*) the KCl molecule, (*b*) the O_2 molecule, and (*c*) the CH_4 molecule?

9-12. The equilibrium separation of the atoms in the HF molecule is 0.0917 nm, and its measured electric dipole moment is 6.40×10^{-30} C · m. What percentage of the bonding is ionic?

9-13. The equilibrium separation of CsF is 0.2345 nm. If its bonding is 70 percent ionic, what should its measured electric dipole moment be?

9-14. Ionic bonding in the BaO molecule involves the transfer of two electrons from the Ba atom. If the equilibrium separation is 0.193 nm and the measured electric dipole moment is 26.7×10^{-30} C · m, to what extent is the bond actually ionic?

Section 9-3 Other Bonding Mechanisms

9-15. Find three other elements with the same subshell electron configuration in the two outermost orbits as carbon. Would you expect the same kind of hybrid bonding for these elements as for carbon? Support your answer.

9-16. The dipole moment $\mathbf{p}$ of the water molecule, illustrated in Figure 9-19, is actually the vector sum of two equal dipoles $\mathbf{p}_1$ and $\mathbf{p}_2$ directed from the oxygen atom to each of the hydrogen atoms. The measured value of the angle between the two hydrogen atoms is 104.5°, the O–H bond length is 0.0956 nm, and the magnitude of $\mathbf{p}$ is 6.46×10^{-30} C · m. Compute the fraction of the electron charge that is transferred from each hydrogen to the oxygen.

9-17. The polarizability of Ne is 1.1×10^{-37} m · C^2/N. (*a*) At what separation would the dipole-dipole energy between a molecule of H_2O and an atom of Ne in the atmosphere be sufficient to withstand collision with an N_2 molecule moving with the average kinetic energy for $T = 300$ K? (*b*) At what separation does this energy occur for a typically bonded molecule? (*c*) On the basis of these results, do you expect H_2O–Ne bonds to be very likely? Explain your answer.

STUDENTS-HUB.com Uploaded By: Malak Obaid

9-18. The hydrogen bonds linking the two helical strands of DNA have bond strengths of about 0.3 eV, or approximately 15 percent of the strengths of the ionic/covalent bonds along the strands. (*a*) What is the wavelength of a photon with sufficient energy to break this bond? (*b*) In what part of the spectrum does this wavelength lie? (*c*) Since a significant intensity exists at this wavelength in the environment, why haven't all the DNA hydrogen bonds long since broken?

9-19. Would you expect the following molecules to be polar or nonpolar? Explain your answer in each case. (*a*) NaCl; (*b*) O_2.

Section 9-4 Molecular Spectra

9-20. The characteristic rotational energy E_{0r} for N_2 molecules is 2.48×10^{-4} eV. From this, find the separation distance of the nitrogen atoms in N_2.

9-21. For the O_2 molecule, the separation of the atoms is 0.121 nm. Calculate the characteristic rotational energy $E_{0r} = \hbar^2/2I$ in eV.

9-22. The CO molecule undergoes a transition from the $v = 1$ vibrational state to the $v = 0$ state. (*a*) What is the wavelength of the emitted photon? (*b*) At what temperature would 1 percent of the CO molecules be in the $v = 1$ vibrational state?

9-23. Using data from Table 9-7, (*a*) compute the vibrational energy of the LiH molecule in its lowest vibrational state. (*b*) Compute the reduced mass of LiH. (*c*) Determine the force constant for LiH. (*d*) From those results, compute an estimate of the LiH bond length and compare your result with the value in the table.

9-24. Calculate the reduced mass in unified mass units for (*a*) H_2, (*b*) N_2, (*c*) CO, and (*d*) HCl.

9-25. The characteristic rotational energy $E_{0r} = \hbar^2/2I$ for KCl is 1.43×10^{-5} eV. (*a*) Find the reduced mass for the KCl molecule. (*b*) Find the separation distance of the K^+ and Cl^- ions.

9-26. Use the data from Table 9-7 to find the force constant for (*a*) the $H^{35}Cl$ and (*b*) the $K^{79}Br$ molecules.

9-27. The equilibrium separation of HBr is 0.141 nm. Treating the Br atom as fixed, compute the four lowest rotational energies of the HBr molecule and show them in a carefully sketched energy-level diagram.

9-28. The vibrational spectrum of Li_2 consists of a series of equally spaced lines in the microwave region 1.05×10^{13} Hz apart. Compute the equilibrium separation for Li_2.

9-29. Compute the difference in the rotational energy E_{0r} for $K^{35}Cl$ and $K^{37}Cl$.

9-30. What type of bonding mechanism would you expect for (*a*) NaF, (*b*) KBr, (*c*) N_2, and (*d*) Ne?

9-31. For NaCl compute (*a*) the energy in eV necessary to excite the first rotational state and (b) the wavelength and frequency of the photon emitted in the transition back to the ground state. (Assume that the molecule is in the electronic and vibrational ground states.)

Section 9-5 Scattering, Absorption, and Stimulated Emission

9-32. The five lowest levels of a certain monatomic gas have the values $E_1 = 0$, $E_2 = 3.80$ eV, $E_3 = 4.30$ eV, $E_4 = 7.2$ eV, and $E_5 = 7.5$ eV. (*a*) If the temperature is high enough that all levels are occupied and the gas is illuminated with light of wavelength 2400 nm, what transitions can occur? (*b*) Which of those found in part (*a*) will still occur if the temperature is so low that only the state E_1 is occupied? (*c*) Repeat (*a*) and (*b*) for light of 250 nm wavelength. (*d*) What wavelength of the incident light would stimulate emission from state E_4?

9-33. A hydrogen discharge tube is operated at about 300 K in the laboratory in order to produce the Balmer series. Compute the ratio of the probability for spontaneous emission of the H_α line to that for stimulated emission.

9-34. Determine the ratio of the number of molecules in the $v = 1$ state to the number in the $v = 0$ state for a sample of O_2 molecules at 273 K. Repeat the calculation for 77 K. (Ignore rotational motion.)

STUDENTS-HUB.com Uploaded By: Malak Obaid

9-35. The nuclei in the F_2 molecule are separated by 0.14 nm. (*a*) Compute the energy separations and sketch an energy-level diagram for the lowest four rotational levels with $v = 0$. (*b*) What are the wavelengths of possible transitions between these levels?

Section 9-6 Lasers and Masers

9-36. A pulse from a ruby laser has an average power of 10 MW and lasts 1.5 ns. (*a*) What is the total energy of the pulse? (*b*) How many photons are emitted in this pulse?

9-37. A helium-neon laser emits light of wavelength 632.8 nm and has a power output of 4 mW. How many photons are emitted per second by this laser?

9-38. A laser beam is aimed at the Moon, a distance 3.84×10^8 m away. The angular spread of the beam is given by the diffraction formula (Rayleigh's criterion), $\sin\theta = 1.22\,\lambda/D$, where D is the diameter of the laser tube or rod. (a) Calculate the size of the beam on the Moon for $D = 10$ cm and $\lambda = 600$ nm. (*b*) Repeat the calculation if the laser beam is projected toward the Moon through a 1.0-m-diameter telescope.

9-39. A particular atom has two energy levels with a transition wavelength of 420 nm. At 297 K there are 2.5×10^{21} atoms in the lower state. (*a*) How many atoms are in the upper state? (*b*) Suppose that 1.8×10^{21} of the atoms in the lower state are pumped to the upper state. How much energy could this system release in a single laser pulse?

Level II

9-40. (*a*) Calculate the electrostatic potential energy of Na^+ and Cl^- ions at their equilibrium separation distance of 0.24 nm, assuming the ions to be point charges. (*b*) What is the energy of repulsion at this separation? (*c*) Assume that the energy of repulsion is given by Equation 9-2. From Figure 9-2*b*, this energy equals ke^2/r at about $r = 0.14$ nm. Use this and your answer to part (*b*) to calculate n and A. (Although this calculation is not very accurate, the energy of repulsion does vary much more rapidly with r than does the energy of attraction.)

9-41. The angular width of a ruby laser beam is determined by Rayleigh's criterion (see Problem 9-38). For this laser the diameter of the ruby rod is 1.0 cm and $\lambda = 694.3$ nm. (*a*) What is the diameter of the spot projected by the ruby laser at a distance of 1.0 km? (*b*) If the laser is emitting 10^{18} photons/s, what is the power deposited per square centimeter on the target at 1.0 km?

9-42. The equilibrium separation of the K^+ and Cl^- ions in KCl is about 0.267 nm. (*a*) Calculate the potential energy of attraction of the ions assuming them to be point charges at this separation. (*b*) The ionization energy of potassium is 4.34 eV and the electron affinity of chlorine is 3.62 eV. Find the dissociation energy for KCl, neglecting any energy of repulsion (see Figure 9-2*a*). (*c*) The measured dissociation energy is 4.40 eV. What is the energy due to repulsion of the ions at the equilibrium separation?

9-43. Use the equilibrium separation for the K^+ and Cl^- ions given in Problem 9-42 and the reduced mass of KCl to calculate the characteristic rotational energy E_{0r} of KCl.

9-44. In this problem, you are to find how the van der Waals force between a polar and a nonpolar molecule depends on the distance between the molecules. Let the dipole moment of the polar molecule be in the x direction and the nonpolar molecule be a distance x away. (*a*) How does the electric field due to an electric dipole depend on the distance x? (*b*) Use the facts that the potential energy of an electric dipole of moment $\mathbf{p}$ in an electric field $\mathbf{E}$ is $U = -\mathbf{p} \cdot \mathbf{E}$ and that the induced dipole moment of the nonpolar molecule is proportional to $\mathbf{E}$ to find how the potential energy of interaction of the two molecules depends on separation distance. (*c*) Using $F_x = -dU/dx$, find the x dependence of the force between the two molecules.

9-45. The microwave spectrum of CO has lines at 0.86 mm, 1.29 mm, and 2.59 mm. (*a*) Compute the photon energies and carefully sketch the energy level diagram that corresponds. What molecular motion produces these lines? (*b*) Compute the equilibrium separation (bond length) of CO.

STUDENTS-HUB.com Uploaded By: Malak Obaid

9-46. Carefully draw a potential energy curve for a diatomic molecule (like Figure 9-2*b*) and indicate the mean values of r for two vibrational levels. Show that because of the asymmetry of the curve, r_{av} increases with increasing vibrational energy and therefore solids expand when heated.

9-47. A sample of HCl is illuminated with light of wavelength 435.8 nm. (*a*) Compute the wavelengths of the four lines in the rotational Raman spectrum that are closest to that of the incident light. (*b*) Compare the difference in their frequencies with the corresponding lines in Figure 9-29.

9-48. Use data from Table 9-7 to compute the first excited vibrational and the first excited rotational states of (*a*) the Li_2 and (*b*) the $K^{79}Br$ molecules.

9-49. Calculate the effective force constant for HCl from its reduced mass and the fundamental vibrational frequency obtained from Figure 9-29.

9-50. Notice in Figure 9-32*c* that the level E_2 in Cr^{3+} is a doublet, the pair of states being separated by only 0.0036 eV. (*a*) Assume that all of the Cr^{3+} ions in a certain laser are in the three states E_1 and E_2 (doublet) and compute the relative populations of these levels. (*b*) If only the lower state of the E_2 doublet can produce laser light but both levels must be pumped together, determine the pumping power necessary for laser action to occur. The density of states (degeneracy) of level E_1 is 4 and for *each* of the E_2 levels is 2.

9-51. The central frequency for the absorption band of HCl shown in Figure 9-29 is at $f = 8.66 \times 10^{13}$ Hz, and the absorption peaks are separated by about $\Delta f = 6 \times 10^6$ Hz. Using this information, find (*a*) the lowest (zero-point) vibrational energy for HCl, (*b*) the moment of inertia of HCl, and (*c*) the equilibrium separation of the atoms.

Level III

9-52. The potential energy between two atoms in a molecule can often be described rather well by the Lenard-Jones potential, which can be written

$$U(r) = U_0\left[\left(\frac{a}{r}\right)^{12} - 2\left(\frac{a}{r}\right)^{6}\right]$$

where U_0 and a are constants. (*a*) Find the interatomic separation r_0 in terms of a for which the potential energy is minimum. (*b*) Find the corresponding value of U_{min}. (*c*) Use Figure 9-8*b* to obtain numerical values for r_0 and U_0 for the H_2 molecule. Express your answer in nanometers and electron volts. (*d*) Make a plot of the potential energy $U(r)$ versus the internuclear separation r for the H_2 molecule. Plot each term separately, together with the total $U(r)$.

9-53. (*a*) Find the exclusion-principle repulsion for NaCl. (*b*) Use Equation 9-2 to find A and n.

9-54. Show that the H^+–H^- system cannot be ionically bonded. (*Hint:* Show that $U(r)$ has no negative minimum.)

9-55. (*a*) Calculate the fractional difference $\Delta\mu/\mu$ for the reduced masses of the $H^{35}Cl$ and $H^{37}Cl$ molecules. (*b*) Show that the mixture of isotopes in HCl leads to a fractional difference in the frequency of a transition from one rotational state to another given by $\Delta f/f = -\Delta\mu/\mu$. (*c*) Compute $\Delta f/f$ and compare your result with Figure 9-29.

9-56. For a molecule such as CO, which has a permanent electric dipole moment, radiative transitions obeying the selection rule $\Delta\ell = \pm 1$ between two rotational energy levels of the same vibrational energy state are allowed. (That is, the selection rule $\Delta v = \pm 1$ does not hold.) (*a*) Find the moment of inertia of CO for which $r_0 = 0.113$ nm, and calculate the characteristic rotational energy E_{0r} in electron volts. (*b*) Make an energy-level diagram for the rotational levels for $\ell = 0$ to $\ell = 5$ for some vibrational level. Label the energies in electron

STUDENTS-HUB.com Uploaded By: Malak Obaid

volts, starting with $E = 0$ for $\ell = 0$. (*c*) Indicate on your diagram transitions that obey $\Delta\ell = -1$ and calculate the energy of the photons emitted. (*d*) Find the wavelength of the photon emitted for each transition in (*c*). In what region of the electromagnetic spectrum are these photons?

9-57. An H_2 molecule in its ground electronic, vibrational, and rotational state absorbs a photon of frequency 1.356×10^{14} Hz, undergoing a transition to the $v = 1$, $\ell = 1$ state while remaining in the electronic ground state. It then undergoes a transition to the $v = 0$, $\ell = 2$ state, emitting a photon of frequency 1.246×10^{14} Hz. (*a*) Compute the moment of inertia of the H_2 molecule about an axis through the center of mass. (*b*) Determine the vibrational frequency and r_0 for H_2 and compare these with the values in Table 9-7.

STUDENTS-HUB.com Uploaded By: Malak Obaid

CHAPTER 10

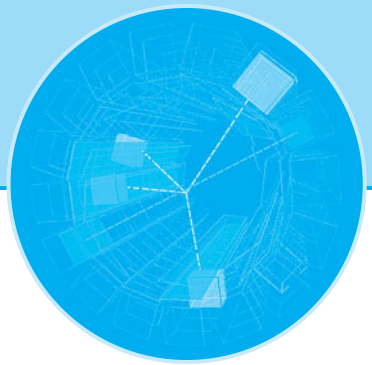

Solid State Physics

The many and varied properties of solids have intrigued us for centuries. Technological developments involving metals and alloys have shaped the courses of civilizations, and the symmetry and beauty of naturally occurring, large single crystals have consistently captured our imaginations. However, the origins of the physical properties of solids were not understood even in rudimentary form until the development of quantum mechanics. The application of quantum mechanics to solids has provided the basis for much of the technological progress of modern times. We will study briefly some aspects of the structure of solids in Section 10-1 and then concentrate on the electrical and magnetic properties of solids.

10-1 The Structure of Solids 413
10-2 Classical Theory of Conduction 422
10-3 Free-Electron Gas in Metals 426
10-4 Quantum Theory of Conduction 430
10-5 Magnetism in Solids 434
10-6 Band Theory of Solids 438
10-7 Impurity Semiconductors 445
10-8 Semiconductor Junctions and Devices 452
10-9 Superconductivity 458

10-1 The Structure of Solids

In our everyday world we see matter in three phases: gases, liquids, and solids. In a gas the average distance between two atoms or molecules is large compared with the size of an atom or molecule. The molecules have little influence on one another except during their frequent but brief collisions. In a liquid or solid the atoms or molecules are close together and exert forces on one another comparable to the forces that bind atoms into molecules. (There is a fourth phase of matter, plasma, which occurs when the matter consists largely—or entirely—of ions and free electrons. Usually this condition exists only at very high temperatures, such as inside stars, in intense electrical discharges—e.g., lightning—and in the laboratory. The properties of a plasma are very different from those of an ordinary gas because of the long-range electrical and magnetic effects arising from the charges of the particles. The recently discovered low-temperature gas phase of matter, the Bose-Einstein condensate, was discussed in Chapter 8.) In a liquid, the molecules form temporary short-range bonds that are continually broken and re-formed as the result of the thermal kinetic energy of the molecules. The strength of the bonds depends on the type of molecule. For example, as we discussed in Section 9-3, the bonds between helium atoms are very weak van der Waals bonds, and He does not liquefy at atmospheric pressure until the very low temperature of 4.2 K is reached.

STUDENTS-HUB.com
Uploaded By: Malak Obaid

If a liquid is slowly cooled, the kinetic energy of its molecules is reduced and the molecules will arrange themselves in a regular crystalline array, producing the maximum number of bonds and leading to a minimum potential energy. However, if the liquid is cooled rapidly so that its internal energy is removed before the molecules have a chance to arrange themselves, a solid is often formed that is not crystalline but resembles a "snapshot" of a liquid. Such a solid is called *amorphous*; it displays short-range order but not the long-range order (over many atomic diameters) characteristic of a crystal. Glass is a typical amorphous solid. A characteristic of the long-range ordering of a crystal is that it has a well-defined melting point, whereas an amorphous solid merely softens as its temperature is increased. Many materials may solidify in either an amorphous or a crystalline state, depending on how they are prepared. Others exist only in one form or the other. Most common solids are polycrystalline—i.e., they are collections of single crystals. The size of such single crystals is typically a fraction of a millimeter; however, large single crystals occur naturally and can be produced artificially (Figure 10-1). We will discuss only simple crystalline solids in this chapter.

The most important property of a single crystal is its symmetry and regularity of structure: it can be thought of as a single unit structure repeated throughout the solid.

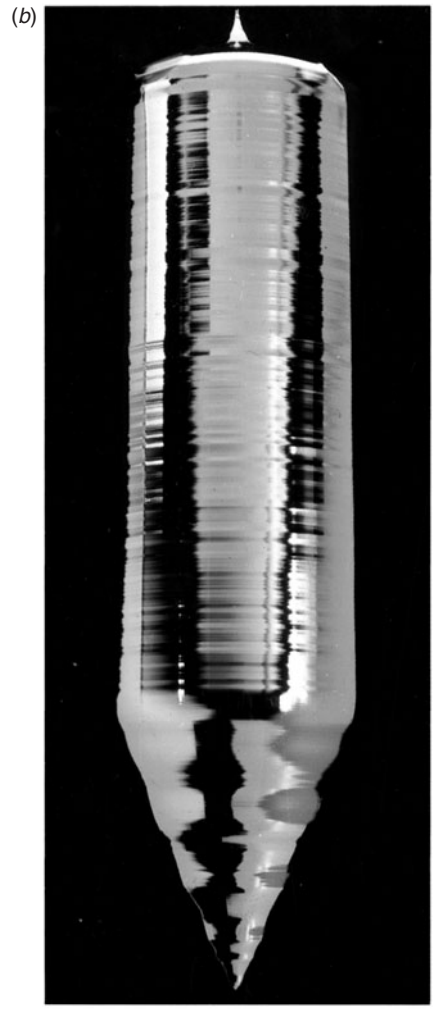

Figure 10-1 (*a*) A single crystal of quartz, one of several naturally occurring crystalline forms of SiO_2. [*Courtesy of Sawyer Research Products, Inc.*] (*b*) A synthetic silicon crystal is created beginning with a raw material containing silicon (for instance, common beach sand), purifying out the silicon, and melting it. From a seed crystal, the molten silicon grows into a cylindrical crystal, such as the one shown here. The crystals (typically about 1.3 m long) are formed under highly controlled conditions to ensure that they are flawless and sliced into thousands of thin wafers, onto which the layers of an integrated circuit are etched. [*Courtesy of the Museum of Modern Art, New York City.*]

STUDENTS-HUB.com Uploaded By: Malak Obaid

The smallest unit of a crystal is called the *unit cell*. The structure of the unit cell depends on the type of bonding between the atoms, ions, or molecules in the crystal. If more than one kind of atom is present, the structure will also depend on their relative size. The structure may also change in response to changes in pressure and/or temperature. The bonding mechanisms are those discussed in Chapter 9: ionic, covalent, and dipole-dipole, the latter including the hydrogen and van der Waals bonds. In addition, a quantum-mechanical mechanism responsible for bonding metals in the solid state, *metallic bonding*, will be described later in this section.

Ionic and Covalent Solids

Figure 10-2 shows the structure of the ionic crystal NaCl. The Na^+ and Cl^- ions are spherically symmetric (see Section 9-1) with the Cl^- ions approximately twice as large as the Na^+ ions. The minimum potential energy of this crystal occurs when an ion of either kind has six nearest neighbors of the other kind. This structure is called *face-centered-cubic* (*fcc*) because the unit cell is a cube and an ion, in this case Cl^-, occupies the center of each face. Note that the Na^+ and Cl^- ions are *not* paired into NaCl molecules in solid NaCl.

The net attractive part of the potential energy of an ion in a crystal can be written

$$U_{\text{att}} = -\alpha\frac{ke^2}{r} \qquad \textbf{10-1}$$

where r is the separation distance between neighboring ions (which is 0.282 nm for the Na^+ and Cl^- ions in crystalline NaCl) and α, called the *Madelung constant*, depends on the geometry of the crystal. If only the six nearest neighbors of each ion were important, α would be 6. However, in addition to the six neighbors of opposite charge at a distance r there are 12 ions of the same charge at a distance $2^{1/2}r$, 8 ions of opposite charge at distance $3^{1/2}r$, and so on. The Madelung constant is thus an infinite sum:

$$\alpha = 6 - \frac{12}{\sqrt{2}} + \frac{8}{\sqrt{3}} - \frac{6}{2} + \frac{20}{\sqrt{5}} - \cdots \qquad \textbf{10-2}$$

Unfortunately, the sum in Equation 10-2 does not converge! We are saved by the fact that NaCl crystals are not spherical, as the analysis above implies. A better physical approach is to use cubic shells rather than spherical ones; then the cubic-shell equivalent

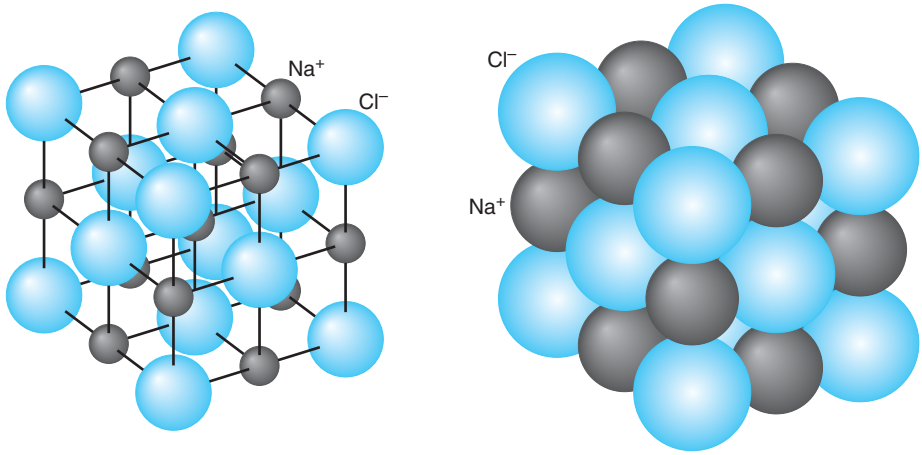

Figure 10-2 Structure of the face-centered-cubic (fcc) NaCl crystal.

STUDENTS-HUB.com Uploaded By: Malak Obaid

Table 10-1 Properties of selected crystalline solids

Solid	Bonding	Equilibrium separation (nm)	Crystal symmetry	Madelung constant	Cohesive energy (eV/atom)	Melting point (K)
NaCl	ionic	0.282	fcc	1.7476	3.19	1074
LiBr	ionic	0.275	fcc	1.7476	3.10	823
KCl	ionic	0.315	fcc	1.7476	3.24	1043
RbF	ionic	0.282	fcc	1.7476	3.55	1068
CsCl	ionic	0.348	sc	1.7627	3.27	918
ZnO	ionic	0.222	hcp	1.4985	7.22	2248
Li	metallic	0.302	bcc	—	1.63	454
Fe	metallic	0.248	bcc	—	4.28	1811
Au	metallic	0.288	fcc	—	3.81	1338
Zn	metallic	0.266	hcp	—	1.35	693
C	covalent	0.154	fcc	—	7.37	†
Si	covalent	0.235	fcc	—	4.63	1687
Ge	covalent	0.245	fcc	—	3.85	1211
H_2O	dipole-dipole	0.367	hcp	—	0.52*	273
C_{60}	dipole-dipole	1.00	fcc	—	1.5*	?
Ne	dipole-dipole	0.313	fcc	—	0.020	24

* eV/molecule.

† Diamond transforms to graphite at high temperature. The latter then sublimes at about 3800 K.

of Equation 10-2 does converge, albeit slowly. The result for face-centered-cubic structures such as NaCl is $\alpha = 1.7476$. The geometric details of other ionic arrangements results in slightly different values for α. (See Table 10-1.)

When Na^+ and Cl^- ions are very close together, they repel each other because of the overlap of the wave functions of their electrons and the exclusion principle repulsion discussed in Section 9-1. A simple empirical expression for the potential energy associated with this repulsion that works fairly well is

$$U_{\text{rep}} = \frac{A}{r^n}$$

where A and n are constants.[1] The total potential energy of an ion is then

$$U = -\alpha\frac{ke^2}{r} + \frac{A}{r^n} \qquad \textbf{10-3}$$

The equilibrium separation $r = r_0$ is that at which the force $F = -dU/dr$ is zero. Differentiating Equation 10-3 and setting $dU/dr = 0$ at $r = r_0$, we obtain

$$A = \frac{\alpha k e^2 r_0^{n-1}}{n} \qquad \textbf{10-4}$$

STUDENTS-HUB.com Uploaded By: Malak Obaid

The total potential energy of an ion in the crystal can thus be written

$$U = -\alpha \frac{ke^2}{r_0}\left[\frac{r_0}{r} - \frac{1}{n}\left(\frac{r_0}{r}\right)^n\right] \qquad \textbf{10-5}$$

At $r = r_0$, we have

$$U(r_0) = -\alpha \frac{ke^2}{r_0}\left[1 - \frac{1}{n}\right] \qquad \textbf{10-6}$$

If we know the equilibrium separation r_0, which can be found from x-ray diffraction experiments or computed from the crystal density, the value of n can be found approximately from the *dissociation energy* or *lattice energy* of the ionic crystal, which is the energy needed to break up the crystal into its constituent ions. In the case of NaCl the measured dissociation energy is 770 kJ/mol. Using 1 eV $= 1.602 \times 10^{-19}$ J and the fact that 1 mol of NaCl contains N_A pairs of ions, we can express the dissociation energy in electron volts per ion pair, which makes possible an easier comparison with, e.g., the binding energy per molecule. The conversion between electron volts per ion pair and kilojoules per mole is

$$1\frac{\text{eV}}{\text{ion pair}} \times \frac{6.022 \times 10^{23}\ \text{ion pairs}}{\text{mol}} \times \frac{1.602 \times 10^{-19}\ \text{J}}{1\ \text{eV}} = 96.47\frac{\text{kJ}}{\text{mol}} \qquad \textbf{10-7}$$

Thus, 770 kJ/mol = 7.98 eV per ion pair. Substituting −7.98 eV for $U(r_0)$, 0.282 nm for r_0 (see Example 10-1), and 1.75 for α in Equation 10-6, we can solve for n. The result is $n = 9.35 \approx 9$.

The dissociation energy is also used to compute the *cohesive energy* of a crystal, which is the potential energy per atom or per atomic pair rather than per ion pair and is the term used for all crystalline bonding mechanisms. For the NaCl illustration above, 7.98 eV is the energy needed to remove an Na^+ and Cl^- pair from the crystal. Forming Cl from Cl^- requires the input of 3.62 eV, and forming Na from Na^+ releases 5.14 eV. Therefore, the energy necessary to remove the neutral Na and Cl pair from the crystal is 7.98 eV + 3.62 eV − 5.14 eV = 6.46 eV, and the cohesive energy of NaCl is 6.46 eV per Na and Cl pair. This result is in good agreement with the observed value of 3.19 eV/atom in Table 10-1. A large cohesive energy implies a high melting point and vice versa.

EXAMPLE 10-1 **Equilibrium Spacing r_0 in an NaCl Crystal** Calculate the equilibrium spacing r_0 for NaCl from the measured density of NaCl, which is $\rho = 2.16\ \text{g/cm}^3$.

SOLUTION

We consider each ion to occupy a cubic volume of side r_0. The mass of 1 mol of NaCl is 58.4 g, which is the sum of the atomic masses of sodium and chlorine. The ions occupy a volume of $2N_A r_0^3$, where $N_A = 6.02 \times 10^{23}$ is Avogadro's number. The density is thus related to r_0 by

$$\rho = \frac{m}{V} = \frac{m}{2N_A r_0^3}$$

Then

$$r_0^3 = \frac{m}{2N_A\rho} = \frac{58.4\ \text{g}}{2(6.02 \times 10^{23})(2.16\ \text{g/cm}^3)} = 2.24 \times 10^{-23}\ \text{cm}^3$$

$$r_0 = 2.82 \times 10^{-8}\ \text{cm} = 0.282\ \text{nm}$$

STUDENTS-HUB.com Uploaded By: Malak Obaid

EXAMPLE 10-2 **Measuring r_0 from X-Ray Diffraction** Molybdenum K_α x rays ($\lambda = 0.071$ nm) strike the diagonal Bragg planes of the NaCl crystal shown on the right in Figure 3-15 such that a diffraction maximum (a bright Laue spot) is observed for $\theta = 10.25°$. Determine the value of r_0.

SOLUTION

1. Since NaCl is a cubic crystal, the distance d between the diagonal Bragg planes is related to the equilibrium separation r_0 by

$$d = \frac{r_0}{\sqrt{2}}$$

2. The x-ray diffraction maxima satisfy the Bragg condition, Equation 3-23:

$$2d \sin\theta = m\lambda$$

3. For $m = 1$ and substituting d from above:

$$2\left(\frac{r_0}{\sqrt{2}}\right)\sin\theta = \lambda$$

4. Solving this for r_0 and substituting values from above gives

$$r_0 = \frac{\sqrt{2}\,\lambda}{2\sin\theta} = \frac{(\sqrt{2})(0.071\text{ nm})}{(2)(\sin 10.25°)} = 0.282\text{ nm}$$

Remarks: *This result agrees with the value calculated from the density of NaCl in Example 10-1.*

Most ionic crystals, such as LiF, KF, KCl, KI, AgCl, and others formed by molecules in Table 9-2, have a face-centered-cubic structure. Some elemental solids that also have this structure are Ag, Al, Au, Ca, Cu, Ni, and Pb.

Figure 10-3 illustrates the structure of another ionic crystal, CsCl, which is called *simple cubic* (*sc*) because it can be considered as two interpenetrating cubic structures, one of Cs^+ ions and the other of Cl^- ions. In this structure, each ion has eight nearest-neighbor ions of the opposite charge. The Madelung constant for ionic crystals with simple cubic structure is 1.7627. Other crystals with this structure include CsI, TlI, TlBr, LiHg, and NH_4Cl. Some elemental solids, such as Ba, Cs, Fe, K, Li, Mo, and Na, also crystallize with the structure shown in Figure 10-3; when the atoms are the same at the vertices and in the center of the cube, the structure is called *body-centered-cubic* (*bcc*).

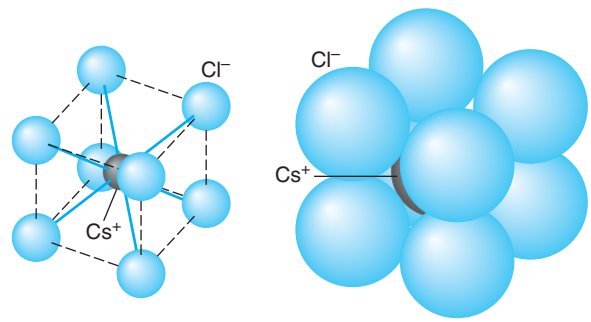

Figure 10-3 Structure of the simple cubic (sc) crystal CsCl.

STUDENTS-HUB.com Uploaded By: Malak Obaid

Figure 10-4 illustrates another important crystal structure, called *hexagonal close-packed* (*hcp*). This is the structure obtained by stacking identical spheres such as Ping-Pong balls. In one layer, each ball touches six others; hence the name *hexagonal*. In the next layer, each ball fits into the triangular depressions of the first layer. In the third layer, each ball fits into a triangular depression of the second layer such that it lies directly over a ball in the first layer. Elements with a hexagonal close-packed crystal structure include Be, Cd, Ce, Mg, Os, Zn, and Zr. There are a total of 14 different types of three-dimensional crystal lattice structures, of which we have discussed only a few of the most common ones. (See Appendix B3.)

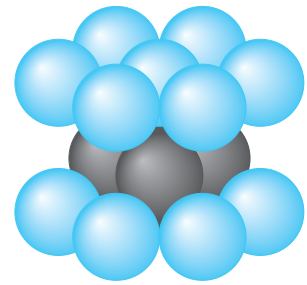

Figure 10-4 Hexagonal close-packed (hcp) crystal structure.

EXAMPLE 10-3 **Madelung Constant for a Two-Dimensional Crystal** Calculate out to four terms in the series the Madelung constant for the hypothetical univalent, two-dimensional ionic crystal shown in Figure 10-5.

SOLUTION

The net attractive potential is given by Equation 10-1. When the negative ion at the origin of Figure 10-5 is considered, there are four positive ions located a distance r away, as indicated by circle A in the diagram. There are four negative ions lying on circle B, whose radius is $2^{1/2}r$. Four negative ions are located on circle C, whose distance from the ion at the origin is $2r$, and finally, eight positive ions lie on circle D at $5^{1/2}r$ from the origin. Therefore, to four terms the net attractive potential is

$$U_{\text{att}} = -ke^2\left(\frac{4}{r} - \frac{4}{\sqrt{2}\,r} - \frac{4}{2r} + \frac{8}{\sqrt{5}\,r}\right)$$

or

$$U_{\text{att}} = -\frac{ke^2}{r}\left(4 - \frac{4}{\sqrt{2}} - 2 + \frac{8}{\sqrt{5}}\right)$$

The quantity in parentheses is the Madelung constant α correct to four terms in the infinite expansion; thus we have that $\alpha \approx 2.749$.

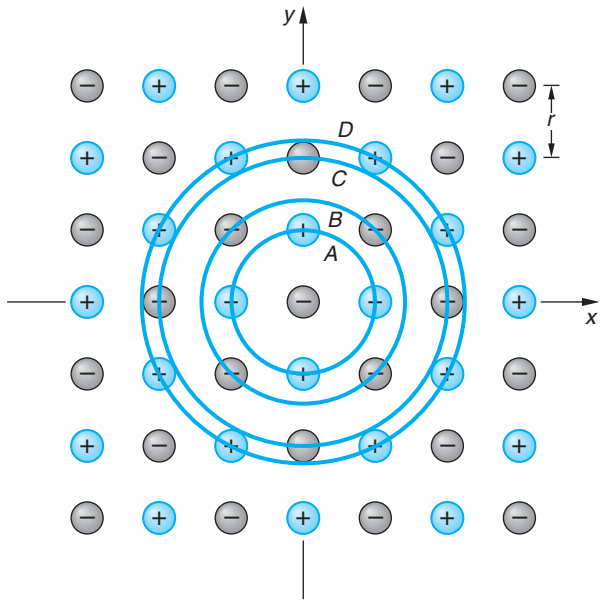

Figure 10-5 A hypothetical univalent two-dimensional ionic crystal (Example 10-3).

STUDENTS-HUB.com Uploaded By: Malak Obaid

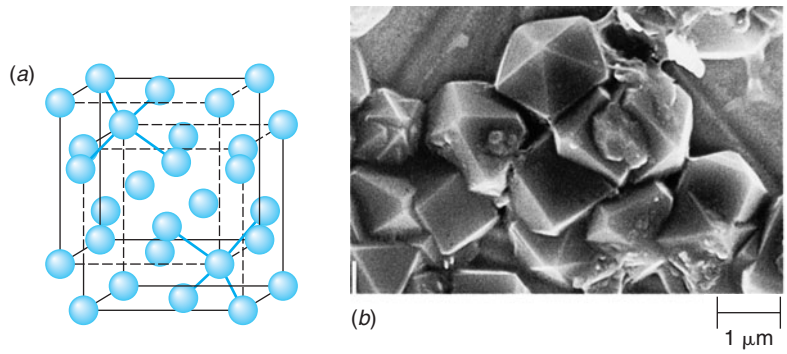

Figure 10-6 (*a*) Diamond crystal structure showing how this structure can be considered to be a combination of two interpenetrating face-centered-cubic structures. (*b*) Synthetic diamonds magnified about 50,000 times. In diamond, each carbon atom is at the center of a tetrahedron formed by four other carbon atoms. [*Courtesy of Chris Kovach/Discover Publications.*]

In covalently bonded crystals the nature of the individual bonds is just like that in covalently bonded molecules, as was described in Section 9-2. The electron-sharing character of the bond enhances its effectiveness in crystals, for example, enabling tetravalent carbon atoms to form bonds with as many as four other carbon atoms. The crystal structure is determined by the directional nature of the bonds. Figure 10-6 illustrates the diamond structure of carbon (which is also the structure of Ge and Si), in which each atom is bonded to four others located at the vertices of a regular tetrahedron as a result of the sp^3 hybridization discussed in the Chapter 9 MORE section *Other Covalent Bonds* on the home page. The diamond structure can be considered to be two interpenetrating face-centered-cubic structures. This arrangement with equal bond angles is particularly tightly bound and results in the carbon diamond structure having one of the largest atomic cohesive energies of all solids, about 7.37 eV per carbon atom. Carbon has two other well-defined crystalline structures, graphite and solid fullerenes,[2] both the result of carbon orbitals hybridized in the sp^2 configuration. In graphite, illustrated in Figure 10-7*a*, three of the valence electrons link each atom to

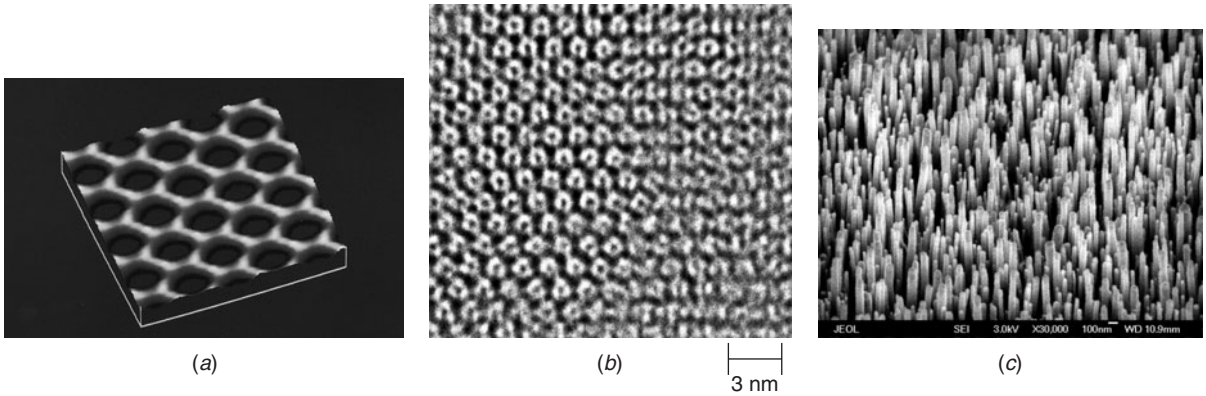

Figure 10-7 (*a*) An atomic-force micrograph of graphite. The brighter spots at each vertex are single carbon atoms. In graphite, carbon atoms are arranged in sheets, each sheet made up of atoms in hexagonal rings. The sheets slide easily across one another, a property that allows graphite to function as a lubricant. [*Courtesy of Srinivas Manne, University of California at Santa Barbara.*] (*b*) This high-resolution transmission electron micrograph shows clearly the close-packed fcc arrangement of the C_{60} molecules in the solid fullerene. [*Courtesy of P. R. Buseck, Science,* ***257****, 215 (1992).*] (*c*) Carbon nanotubes grown on a titanium substrate. The nanotubes are perpendicular to the substrate and range between 40 nm and 100 nm in diameter. [*Courtesy of Z. F. Ren et al., Boston College.*]

STUDENTS-HUB.com Uploaded By: Malak Obaid

three near neighbors via directed bonds, forming a planar hexagonal structure. The planes thus formed are connected by much weaker dipole-dipole forces. This results in a structure consisting of strong sheets that can be readily separated from one another. The structure of the fullerenes, using solid C_{60} as an example, is quite different from that of both diamond and graphite. As described in Section 9-2, the C_{60} molecule achieves its spheroid shape by incorporating 12 pentagons into the hexagonal structure, thus distorting the graphite planes into the soccer-ball configuration. The C_{60} molecules are then bonded to each other by dipole-dipole forces, just as are the sheets of graphite. As a result, the cohesive energy per atom is quite high, about 7.4 eV, or nearly equal to that of diamond, but the cohesive energy per molecule is low, only 1.5 eV. The C_{60} crystal, shown in Figure 10-7*b*, is face-centered-cubic. The equilibrium separation between the molecules is 1.00 nm. The nanotubes shown in Figure 10-7*c* are a remarkable example of carbon's possible bonding configurations.

Racing bicycles and Formula 1 race cars are constructed from woven carbon fibers. They absorb shock extremely well and are lighter and stronger than older bikes and race cars made of steel or aluminum.

Metallic Bonding in Solids

All solid metals, formed from the metal elements that make up more than half of the periodic table, are bonded by the *metallic bond*, which, as was noted earlier, has no single-molecule counterpart. It is somewhat analogous to the covalent bond, in which the atoms of the molecule share one or more electrons. In the metallic bond one or two of the valence electrons of each atom are free to move throughout the solid, and *all* of the atoms share all of those electrons. Thus, the metallic crystal can be pictured as a lattice of fixed, positive ions immersed in an electron gas. It is the attraction between the positively charged lattice and the negatively charged electron gas that results in bonding of the solid.[3]

To see how metallic bonding occurs, let us consider a specific simple example, the bonding of solid lithium. The electron structure of the lithium atom is $1s^2 2s$, and the radial wave function of the $2s$ electron, which "sees" a hydrogenlike core consisting of the nucleus and the completed $1s$ shell, is

$$\psi_{20} = C_{20}\left(2 - \frac{r}{a_0}\right)e^{-r/2a_0} \qquad \textbf{10-8}$$

where C_{20} is a normalization constant and a_0 is the Bohr radius. The probability density corresponding to this wave function for a single lithium atom located at $r = 0$ is shown in one dimension in Figure 10-8*a*. The probability density decays exponentially to zero as r approaches $\pm\infty$. Figure 10-8*b* illustrates the probability density of the electrons in the metal, which must be the same around each Li ion core. The peaks of the probability density are now closer to the positive Li ion core than was the case for the isolated atom. Thus, the potential energy of the electrons has been reduced. However, the effect of assembling the atoms into a lattice has also been to effectively confine the electrons to within about ± 0.3 nm of the ion core rather than the larger volume of the isolated atom. The uncertainty principle then implies an increase in the momentum, hence kinetic energy, of the electrons. The metallic bond is stable because the rise in kinetic energy is more than offset by the decrease in the potential energy, thus lowering the total energy of the system of atoms. The net effect is greatest when the difference in size between the atom and the core is large (so that the magnitude of the potential energy reduction is large) and when the number of valence electrons is small (so that the increase in kinetic energy is as small as possible). These conditions are increasingly satisfied as one moves toward the left across the periodic table.

Even hydrogen becomes a metal under ultrahigh pressure. The pressure reduces the conduction-valence band gap (see Section 10-6) from about 15 eV to 0.3 eV. Understanding metallic hydrogen will be of significant benefit to fusion energy research (see Section 11-8).

STUDENTS-HUB.com Uploaded By: Malak Obaid

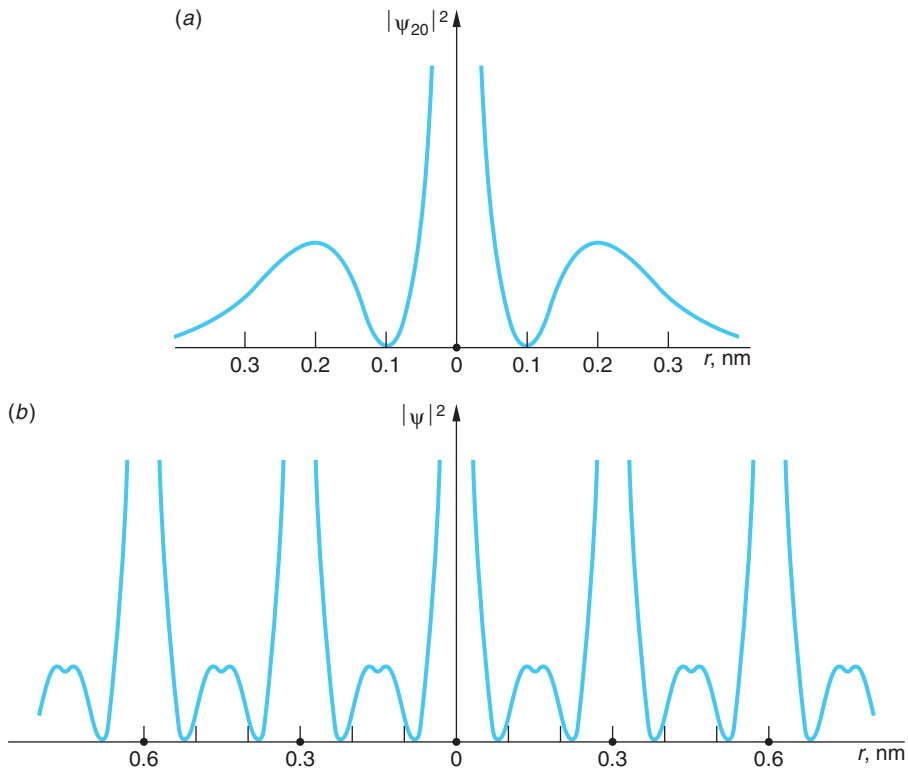

Figure 10-8 (*a*) Probability density for the 2*s* electron in an isolated Li atom. (*b*) Probability density for the 2*s* electrons in a (one-dimensional) Li crystal. The large dots on the *r* axis represent Li nuclei. Note that $|\psi|^2$ is compressed relative to that of the single atom and that an electron is, on the average, confined to within about ± 0.3 nm of a Li nucleus rather than between $\pm\infty$.

Questions

1. Why is r_0 different for solid NaCl than for the diatomic molecule?
2. Why would you not expect NaCl to have an hcp structure?
3. How can you account for the difference in the Madelung constants of NaCl and CsCl?
4. Although it is in the same column of the periodic table as Li, why is solid hydrogen not metallically bonded?

10-2 Classical Theory of Conduction

Because metals conduct electricity so readily, there must be charges in metals that are relatively free to move. The idea that metals contain electrons free to move about through a lattice of relatively fixed positive ions was proposed by the German physicist Paul Drude around 1900, just three years after Thomson's discovery of the electron, and was developed by H. A. Lorentz in about 1909. This microscopic model, now called the *classical model of electrical conduction*, successfully predicts Ohm's law and relates electrical conduction and heat conduction to the motion of free electrons in conductors. However, the model gives the wrong temperature dependence for electrical conductivity, and it predicts that the heat capacity of metals should be greater than that of insulators by $(3/2)R$ per mole, which is not observed. Despite these failures, the classical free-electron theory is a good starting point for a more sophisticated treatment

STUDENTS-HUB.com Uploaded By: Malak Obaid

of metals based on quantum mechanics. For that reason, a discussion of the classical theory is included in the Classical Concept Review on the Web page. In this section we will briefly outline those predictions from classical theory that are pertinent to our subsequent discussion of the quantum mechanical theory of conduction. As we will see, the main defects in the classical theory are the use of the classical Maxwell-Boltzmann distribution function for electrons in a conductor and the treatment of the scattering of electrons by the lattice as a classical particle scattering.

Electrical Conduction

The classical model of a metal is a regular three-dimensional array of atoms or ions with a large number of electrons free to move throughout the entire metal. In the absence of an applied electric field the average speed of these electrons is quite high. For example, at $T = 300$ K, their average speed is

$$\langle v \rangle = \sqrt{\frac{8kT}{\pi m_e}} = \sqrt{\frac{8(1.38 \times 10^{-23}\ \text{J/K})(300\ \text{K})}{\pi(9.11 \times 10^{-31}\ \text{kg})}} = 1.08 \times 10^5\ \text{m/s} \qquad \textbf{10-9}$$

Applying an electric field $\mathscr{E}$ superimposes a *drift velocity* $\mathbf{v}_d$ on the free electrons that is opposite to the field direction. For n electrons per unit volume, the resulting current I in the conductor, the charge ΔQ through a cross-sectional area A per unit time (see Figure 10-9), is

$$I = \frac{\Delta Q}{\Delta t} = neAv_d \qquad \textbf{10-10}$$

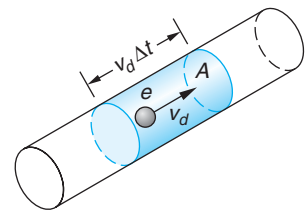

Figure 10-9 In time Δt, all the charges in the shaded volume pass through A. If there are n charge carriers per unit volume, each with charge e, the total charge in this volume is $\Delta Q = nev_dA\ \Delta t$, where v_d is the drift velocity of the charge carriers. The total current is then $I = \Delta Q/\Delta t = nev_dA$.

In contrast to the average speed of the electrons due to their thermal motion, the drift velocity is quite low, as Example 10-4 illustrates for copper.

EXAMPLE 10-4 Drift Velocity of Electrons in Copper What is the magnitude of the drift velocity of electrons in a typical copper wire of radius 0.815 mm carrying a current of 1 A?

SOLUTION

If we assume one free electron per copper atom, the density of free electrons is the same as the density of atoms n_a, which is related to the mass density ρ, Avogadro's number N_A, and the molar mass M by

$$n_a = \frac{\rho N_A}{M}$$

For copper $\rho = 8.92\ \text{g/cm}^3$ and $M = 63.5$ g/mol. Then

$$n_a = \frac{(8.93\ \text{g/cm}^3)(6.02 \times 10^{23}\ \text{atoms/mol})}{63.5\ \text{g/mol}} = 8.47 \times 10^{22}\ \text{atoms/cm}^3$$

The density of electrons is then

$$8.47 \times 10^{22}\ \text{electrons/cm}^3 = 8.47 \times 10^{28}\ \text{electrons/m}^3$$

The magnitude of the drift velocity is therefore

$$v_d = \frac{I}{Ane} = \frac{1\ \text{C/s}}{\pi(0.000815\ \text{m})^2(8.47 \times 10^{28}\ \text{m}^{-3})(1.60 \times 10^{-19}\ \text{C})} \approx 3.54 \times 10^{-5}\ \text{m/s}$$

STUDENTS-HUB.com Uploaded By: Malak Obaid

We see that typical drift velocities are of the order of 0.01 mm/s, which is quite small. Notice in particular that the magnitude of the drift velocity is very small compared with the average speed of the electrons due to their thermal energy as given by Equation 10-9. Indeed, the difference is approximately 10 orders of magnitude.

According to Ohm's law, the current in a conducting wire segment is proportional to the voltage drop across the segment $I \propto V$. The constant of proportionality is $1/R$, so that $I = V/R$. The resistance R of the wire is independent of both I and V, being proportional to the length of the wire L divided by its cross-sectional area A: $R = \rho L/A$. The constant of proportionality ρ is called the *resistivity* of the conductor material. Combining these two expressions and recalling that the electric field in the wire is $\mathscr{E} = V/L$, Equation 10-10 enables us to write

$$v_d = \frac{j}{ne} \qquad \textbf{10-11}$$

where $j = I/A$ is the *current density*. For materials that obey Ohm's law, the resistivity and, of course, its reciprocal the *conductivity* σ must be independent of $\mathscr{E}$.

Mean Free Path λ

The objective of the classical theory of conduction is to find an expression for ρ in terms of the properties of the conductor, a task that is aided by a consideration of the average distance an electron travels in the conductor between collisions, called the *mean free path* λ. It is the product of the average speed $\langle v \rangle$ and the average time between collisions τ, called the *relaxation time*:

$$\lambda = \langle v \rangle \tau = 1/n_a \pi r^2 \qquad \textbf{10-12}$$

where n_a is the number of ions per unit volume and r is the ion radius. As an example, λ for copper is about 0.38 nm. In terms of λ the resistivity and conductivity are given by

$$\rho = \frac{m_e \langle v \rangle}{ne^2 \lambda} \quad \text{and} \quad \sigma = \frac{ne^2 \lambda}{m_e \langle v \rangle} \qquad \textbf{10-13}$$

In Example 10-5 we compute the classical values for the resistivity and conductivity for copper, which illustrates a basic defect in the classical theory of conduction.

EXAMPLE 10-5 Conductivity and Resistivity of Copper Calculate the values of the resistivity and the conductivity of copper at 300 K.

SOLUTION

Using Equations 10-12 and 10-13, we have

$$\tau = \lambda/\langle v \rangle = (0.38 \times 10^{-9}\,\text{m})/(1.08 \times 10^{5}\,\text{m/s}) = 3.52 \times 10^{-15}\,\text{s}$$

and then

$$\begin{aligned} \rho &= \frac{m_e \langle v \rangle}{ne^2 \lambda} = \frac{m_e}{ne^2 \tau} \\ &= \frac{9.11 \times 10^{-31}\,\text{kg}}{(8.47 \times 10^{28}\,\text{electrons/m}^3)(1.60 \times 10^{-19}\,\text{C})^2(3.52 \times 10^{-15}\,\text{s})} \\ &= 1.19 \times 10^{-7}\,\Omega \cdot \text{m} \end{aligned}$$

STUDENTS-HUB.com Uploaded By: Malak Obaid

and $\sigma = 1/\rho = 8.33 \times 10^6\,(\Omega \cdot \mathrm{m})^{-1}$

Remarks: *This value for the resistivity is about 7 times greater than the measured value of* $1.7 \times 10^{-8}\ \Omega \cdot m$.

Defects in the Classical Theory

At first glance it is surprising that any material obeys Ohm's law since in the presence of an electric field, a free electron experiences a force of magnitude $e\mathscr{E}$. If this were the only force acting on the electron, it would have acceleration $e\mathscr{E}/m_e$ and its velocity would steadily increase. However, the agreement of Ohm's law with experiment implies that there is a steady-state situation in which the drift velocity of the electron is proportional to the field $\mathscr{E}$ because the current I is proportional to both $\mathscr{E}$ and v_d, i.e., $v_d = j/ne = \sigma\mathscr{E}/ne$. In the classical model, it is assumed that a free electron is accelerated for a short time and then collides with a lattice ion. After the collision, the velocity of the electron is assumed to be completely unrelated to that before the collision. The justification for this assumption is that, as we have seen, the drift velocity is very small compared to the average thermal velocity. With the average speed given by Equation 10-9 and the mean free path by Equation 10-12, the resistivity has been expressed in terms of the properties of metals, which was the objective of the classical theory of conduction. According to Ohm's law, the resistivity is independent of the electric field $\mathscr{E}$. The only quantities in Equation 10-13 that might depend on the electric field are the average speed $\langle v \rangle$ and the mean free path λ. As we have seen, the drift velocity, a result of the applied electric field, is very much smaller than the average thermal speed of the electrons in equilibrium with the lattice ions. Thus, the electric field has essentially no effect on the average speed of the electrons. The mean free path of the electrons depends on the size of the lattice ions and on the density of the ions, neither of which depends on the electric field $\mathscr{E}$. Thus the classical model predicts Ohm's law with the resistivity as given by Equation 10-13.

Although successful in predicting Ohm's law, the classical theory of conduction has several defects. We saw from Example 10-5 that the magnitude of the resistivity of copper calculated from Equation 10-13 is about 7 times the measured value at $T = 300$ K. The temperature dependence of ρ is also not correct. Experimentally, the resistivity varies linearly with temperature over a wide range of temperatures. The temperature dependence of resistivity in Equation 10-13 is given completely by the speed $\langle v \rangle$, which according to Equation 10-9 is proportional to $T^{1/2}$. Thus, this calculation does not give a linear dependence on temperature. Finally, the classical model says nothing about why some materials are conductors, others insulators, and still others semiconductors.

In the quantum-mechanical theory of electrical conduction, which is discussed in Section 10-4, the resistivity is again given by Equation 10-13, but the average speed and the mean free path are interpreted in terms of quantum theory. We discovered in Section 8-5 that the average energy of the electrons, hence their average speed, is not proportional to $T^{1/2}$, but is approximately independent of T because electrons do not obey the Boltzmann distribution law, but instead obey the Fermi-Dirac distribution. Also, in the quantum-mechanical calculation of the mean free path the wave nature of the electron is important and must be taken into account.

STUDENTS-HUB.com Uploaded By: Malak Obaid

Heat Capacity

If the electron gas in metals were a classical ensemble of identical distinguishable particles, it would obey Boltzmann statistics (see Chapter 8) and have the Maxwell distribution of speeds. It should then have an average kinetic energy $(3/2)kT$, and we would expect the molar heat capacity of a metal to be $(3/2)R$ greater than that of an insulator—that is, $3R$ from the lattice vibrations (rule of Dulong and Petit—see Section 8-1) and $(3/2)R$ from the electron gas:

$$C_v = (3R)_{\text{lattice vibrations}} + (3/2)R_{\text{electron gas}} = (9/2)R$$

As was noted in Section 8-5, this is not observed. The molar heat capacity of metals is very nearly $3R$. At higher temperatures it is slightly greater, but the increase is nowhere near the value of $(3/2)R$ predicted by the classical theory. The increase is, in fact, proportional to temperature, and at $T = 300$ K, it is only about $0.02R$.

10-3 Free-Electron Gas in Metals

Classically, at $T = 0$, all the electrons in a metal would have zero kinetic energy. As a conductor is heated, the lattice ions acquire an average kinetic energy of $(3/2)kT$, which is imparted to the electron gas by interactions of the lattice with the electrons. The electrons classically would be expected to have a mean kinetic energy of $(3/2)kT$ in equilibrium. Quantum mechanically, however, since the electrons are confined to the space occupied by the metal, it is clear from the uncertainty principle that even at $T = 0$, an electron cannot have zero kinetic energy. Furthermore, the exclusion principle prevents more than two electrons (with opposite spins) from being in the lowest energy level. At $T = 0$, we expect the electrons to have the lowest energies consistent with the exclusion principle. This is illustrated clearly by first considering a one-dimensional model that provides us with the foundation needed for the quantum theory of conduction in Section 10-4.

One-Dimensional Model

To simplify visualization, let us first consider N electrons in a one-dimensional infinite square well of width L. The physical analog of such a model could be a long, thin metal wire. As we have seen previously, the allowed energies are given by

$$E_n = \frac{n^2h^2}{8mL^2} = n^2E_1 \qquad \textbf{10-14}$$

where m is the electron mass and $E_1 = h^2/8mL^2$ is the energy of the ground state. Since two electrons can be put in the $n = 1$ level, two in the $n = 2$ level, etc., at $T = 0$, the N electrons in the system will fill $N/2$ levels, i.e., from the $n = 1$ to the $n = N/2$ state. (See Figure 10-10*a*.) The energy of the last filled level (or half-filled level, if N happens to be odd) is the Fermi energy, which for our one-dimensional system is

$$E_F = E_{N/2} = \frac{(N/2)^2h^2}{8mL^2} = \frac{h^2}{32m}\left(\frac{N}{L}\right)^2 \qquad \textbf{10-15}$$

STUDENTS-HUB.com Uploaded By: Malak Obaid

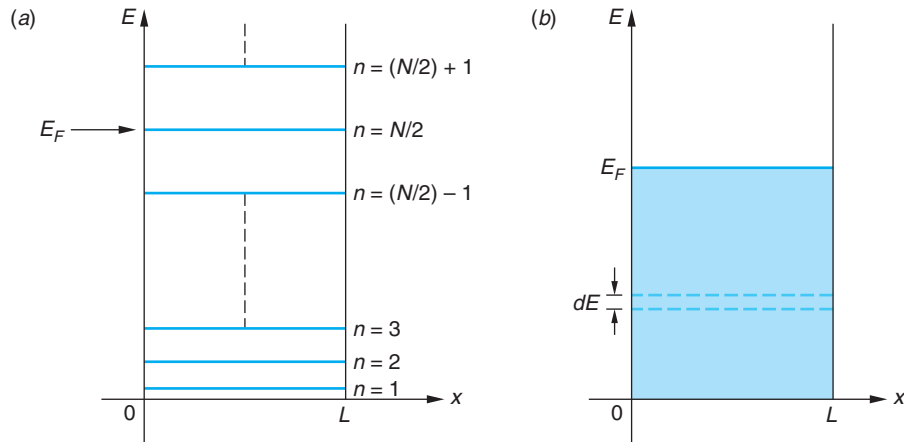

Figure 10-10 (*a*) A one-dimensional infinite square well for N electrons at $T = 0$ K. Two electrons, one with spin up and one with spin down, occupy each level. The Fermi energy is the energy of the level with $n = N/2$, the highest occupied level. (*b*) The levels are so closely spaced, they can be assumed to be continuous. The density of states $g(E)$ is the number of states between E and $E + dE$ divided by dE.

We see that the Fermi energy is a function of the number of electrons per unit length, which is the *number density* or number per unit volume in one dimension. The number density of electrons in copper, computed in Example 10-4, is $8.47 \times 10^{28}/\text{m}^3$. In one dimension this corresponds to

$$\frac{N}{L} = (8.47 \times 10^{28}/\text{m}^3)^{1/3} = 4.40 \times 10^9/\text{m} = 0.440/\text{Å} = 4.40/\text{nm}$$

Using this value, we see that the Fermi energy for a one-dimensional copper system, such as a wire, is

$$E_F = \frac{(hc)^2}{32mc^2}\left(\frac{N}{L}\right)^2 = \frac{(1240\ \text{eV} \cdot \text{nm})^2(4.40/\text{nm})^2}{(32)(5.11 \times 10^5\ \text{eV})} = 1.82\ \text{eV}$$

This value is much larger than the room temperature value of kT, which is about 0.026 eV. The average energy of the electrons is the total energy divided by N:

$$\langle E \rangle = \frac{1}{N}\sum_{n=1}^{N/2} 2n^2 E_1$$

where the factor of 2 accounts for the two electrons in each energy state. Since $N/2 \gg 1$, the summation can be replaced by an integral, so we have that

$$\langle E \rangle = \frac{E_1}{N}\int_0^{N/2} 2n^2\, dn = \frac{E_1}{N}\frac{2}{3}\left(\frac{N}{2}\right)^3 = \frac{h^2}{8mL^2}\frac{2}{3N}\left(\frac{N}{2}\right)^3 = \frac{1}{3}E_F \qquad \textbf{10-16}$$

Our one-dimensional calculation thus gives an average energy for copper's free electrons of about 0.6 eV at $T = 0$. This is 15 times the room-temperature average kinetic energy of molecules in the atmosphere. The temperature at which the average energy would be 0.6 eV for a one-dimensional Boltzmann distribution is about 14,000 K, obtained from $\frac{1}{2}kT = 0.6$ eV.

STUDENTS-HUB.com Uploaded By: Malak Obaid

The expression for the number $n(E)$ of electrons with energy E in the one-dimensional system follows from Equation 8-37*c*:

$$n(E)\,dE = g(E)f_{FD}(E)\,dE$$

where $f_{FD}(E) = 1$ for $T = 0$ K and $E < E_F$ and $f_{FD}(E) = 0$ for $T = 0$ K and $E > E_F$. The density of states $g(E)$ is the number dn of states between E and $E + dE$ divided by dE and multiplied by 2 to account for the two spin states per space state (see Figure 10-10*b*):

$$g(E) = 2\frac{dn}{dE}$$

Since $E = n^2E_1$, then $dE = 2E_1 n\,dn = 2E_1^{1/2}E^{1/2}\,dn$ and we have that

$$g(E) = E_1^{-1/2}E^{-1/2}$$

The number of electrons with energy E at $T = 0$ K in the one-dimensional conductor is then

$$n(E) = \begin{cases} E_1^{-1/2}E^{-1/2} & \text{for} \quad E < E_F \\ 0 & \text{for} \quad E > E_F \end{cases} \qquad \textbf{10-17}$$

Three-Dimensional Electron Gas

Now let us extend the discussion to three-dimensional systems. The Fermi energy can be computed from the general expression for the number of fermions $n_{FD}(E)$ given by Equation 8-37*c*. The number density N/V of electrons in three dimensions, where V is the volume of the metal, is

$$\frac{N}{V} = \frac{1}{V}\int_0^\infty n_{FD}(E)\,dE = \frac{\pi}{2}\left(\frac{8m}{h^2}\right)^{3/2}\int_0^\infty \frac{E^{1/2}\,dE}{e^{(E-E_F)/kT}+1} \qquad \textbf{10-18}$$

For arbitrary values of T, Equation 10-18 must be evaluated numerically, but for $T = 0$ K, the solution is straightforward since, as noted above, $f_{FD}(E) = 0$ or 1 as E is greater than or less than E_F. In that event, we have that

$$\frac{N}{V} = \frac{\pi}{2}\left(\frac{8m}{h^2}\right)^{3/2}\int_0^{E_F} E^{1/2}\,dE = \frac{\pi}{2}\left(\frac{8m}{h^2}\right)^{3/2}\frac{2}{3}E_F^{3/2} \qquad \textbf{10-19}$$

Solving for E_F we have for $T = 0$ K that

$$E_F = \frac{h^2}{2m}\left(\frac{3N}{8\pi V}\right)^{2/3} \qquad \textbf{10-20}$$

Table 10-3 lists the number density of free electrons for several elements. Notice that E_F increases slowly with N/V, as would be expected at $T = 0$ K since all states up to E_F are being filled and an increasing N/V requires more states to be filled, i.e., a larger value of E_F. The number $n(E)$ of electrons with energy E is then given by

$$n(E) = \frac{\pi}{2}\left(\frac{8m}{h^2}\right)^{3/2}VE^{1/2} = \frac{3N}{2}E_F^{-3/2}E^{1/2} \qquad \textbf{10-21}$$

STUDENTS-HUB.com Uploaded By: Malak Obaid

Table 10-3 Free-electron number densities, Fermi energies, and Fermi temperatures for selected elements

Element	$N/V(\times 10^{28}\ \mathrm{m}^{-3})$	Fermi energy (eV)	Fermi temperature ($\times 10^4$ K)
Al	18.1	11.7	13.6
Ag	5.86	5.53	6.41
Au	5.90	5.55	6.43
Cu	8.47	7.06	8.19
Fe	17.0	11.2	13.0
K	1.40	2.13	2.47
Li	4.70	4.77	5.53
Mg	8.61	7.14	8.28
Mn	16.5	11.0	12.8
Na	2.65	3.26	3.78
Sn	14.8	10.3	11.9
Zn	13.2	9.50	11.0

and the average energy of an electron at $T = 0$ K by

$$\langle E\rangle = \frac{1}{N}\int_0^{E_F} E\,n(E)\,dE = \frac{3}{2}E_F^{-3/2}\int_0^{E_F} E^{3/2}\,dE = \frac{3}{5}E_F \qquad \textbf{10-22}$$

At temperatures greater than zero, some electrons will gain energy and occupy higher energy states. However, electrons cannot move to a higher or lower energy state unless the state is unoccupied. Since the kinetic energy of the lattice ions is of the order of kT, electrons cannot gain much more energy than kT in collisions with the lattice; therefore, only those electrons with energies within about kT of the Fermi energy can gain energy as the temperature is increased.

At $T = 300$ K, kT is only 0.026 eV, so the exclusion principle prevents all but a very few electrons near the top of the energy distribution from gaining energy by random collisions. Figure 10-11 shows the small fraction of the free electrons that move at $T = 300$ K (shaded rectangle at the Fermi energy of the $T = 0$ K curve). *Even for temperatures as high as several thousand degrees, the energy distribution of an electron gas does not differ very much from that at* $T = 0$ K.

For values of $T > 0$, we must remember that the Fermi energy is defined by Equation 8-68, since for $T > 0$, there is no state below which all states are full and above which all states are empty. Equation 8-68 defines the Fermi energy as that energy for which $f_{FD}(E) = \frac{1}{2}$. For all but extremely high temperatures, the difference between the Fermi energy at temperature T, $E_F(T)$ and that at $T = 0$ K, $E_F(0)$ is essentially negligible. As is clear from Equation 8-68 and Figure 8-31*b*, the value of $f_{FD}(E)$ at arbitrary T differs from that at $T = 0$ K only for those energies within about kT of the Fermi energy.

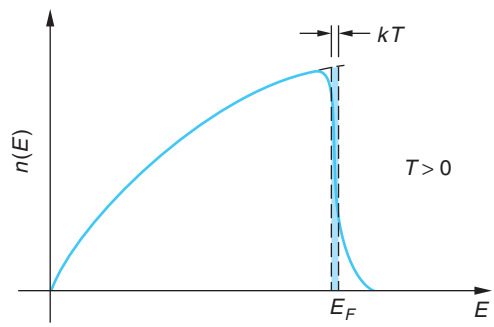

Figure 10-11 The fraction of the N electrons in the metal that contribute to C_v is the ratio of the shaded rectangle to the total area under the $n(E)$ versus E curve.

STUDENTS-HUB.com Uploaded By: Malak Obaid

Fermi Temperature

It is convenient to define the *Fermi temperature* T_F by

$$E_F = kT_F \tag{10-23}$$

For temperatures much lower than the Fermi temperature, the average energy of the lattice ions will be much less than the Fermi energy; thus the electron energy distribution will not differ greatly from that at $T = 0$. The Fermi temperature corresponding to $E_F = 7.0$ eV for copper is about 81,900 K. Table 10-3 lists the Fermi temperatures for several elements. At temperatures much larger than the Fermi temperature (i.e., much larger than 81,900 K for copper) $f_{FD}(E)$ approaches $e^{-E/kT}$ and the Fermi-Dirac distribution approaches the Boltzmann distribution. This result is not very important for the understanding of the behavior of conductors since there are no conductors that remain as solids or even liquids at such extreme temperatures.

EXAMPLE 10-6 **Fermi Energy and Temperature of Silver** Compute (*a*) the Fermi energy and (*b*) the Fermi temperature for silver at 0 K.

SOLUTION

The density of silver is 10.50 gm/cm^3, and its molecular weight is 107.9 gm/mol. If each silver atom is assumed to contribute one electron to the Fermi gas, the number density N/V is computed as follows:

$$\frac{N}{V} = (10.50 \text{ g/cm}^3)(1/107.9 \text{ g/mol})(6.02 \times 10^{23} \text{ electrons/mol})$$
$$= 5.86 \times 10^{22} \text{ electrons/cm}^3 = 5.86 \times 10^{28} \text{ electrons/m}^3$$

which agrees with the entry in Table 10-3.

(*a*) The Fermi energy is then, from Equation 10-20,

$$E_F = \frac{(6.63 \times 10^{-34} \text{ J} \cdot \text{s})^2}{2(9.11 \times 10^{-31} \text{ kg})} \left(\frac{3 \times 5.86 \times 10^{28}}{8\pi} \right)^{2/3}$$
$$= 8.84 \times 10^{-19} \text{ J} = 5.53 \text{ eV}$$

in agreement with the entry for Ag in Table 10-3.

(*b*) The Fermi temperature is then

$$T_F = \frac{E_F}{k} = \frac{8.84 \times 10^{-19} \text{ J}}{1.38 \times 10^{-23} \text{ J/K}} = 6.41 \times 10^4 \text{ K}$$

again, in agreement with Table 10-3.

10-4 Quantum Theory of Conduction

With two relatively simple but important quantum-mechanical modifications of the classical free-electron theory, we can understand the electrical conductivity, heat capacity, and thermal conductivity of metals. First, we must replace the classical Boltzmann distribution with the Fermi distribution of energies in the electron gas, as was discussed in Section 8-5. Second, we must consider the effect of the wave properties of the electrons on their scattering by the lattice ions. We will discuss the latter modification qualitatively.

STUDENTS-HUB.com Uploaded By: Malak Obaid

Electrical Conduction

We might expect that most of the electrons would not participate in the conduction of electricity because of the exclusion principle, but this is not the case because the electric field accelerates all the electrons together. Figure 10-12 shows the Fermi-Dirac distribution function versus velocity for some temperature T that is small compared with T_F (such as $T = 300$ K). The function is approximately 1 for $-u_F < v_x < +u_F$, where the *Fermi speed* u_F is the speed corresponding to the Fermi energy:

$$u_F = \left(\frac{2E_F}{m_e}\right)^{1/2} \qquad \textbf{10-24}$$

EXAMPLE 10-7 Fermi Speed in Al Compute the Fermi speed of electrons in aluminum.

SOLUTION

From Table 10-3, the Fermi energy E_F of Al is 11.7 eV. Thus,

$$u_F(\text{Al}) = \left(\frac{2 \times 11.7 \text{ eV} \times 1.60 \times 10^{-19} \text{ J/eV}}{9.11 \times 10^{-31} \text{ kg}}\right)^{1/2} = 2.03 \times 10^6 \text{ m/s}$$

The dashed curve in Figure 10-12 shows the Fermi distribution after the electric field has been acting for some time t. Although all of the electrons have been shifted to higher velocities, the net effect is equivalent to shifting only the electrons near the Fermi level; therefore, we can use the classical equations for the resistivity and conductivity (Equations 10-13) if we use the Fermi speed u_F in place of $\langle v \rangle$:

$$\rho = \frac{1}{\sigma} = \frac{m_e u_F}{ne^2\lambda} \qquad \textbf{10-25}$$

We now have two problems. First, since u_F is independent of temperature (to a very good approximation), the above expression for σ and ρ is independent of temperature unless the mean free path depends on it. The second problem concerns the magnitudes. We saw in Example 10-5 that the classical expression for σ yielded a result that was too small by a factor of 7, using $\langle v \rangle$ calculated from the Maxwell-Boltzmann distribution. Since u_F is about 19 times the value of $\langle v \rangle$, the magnitude of σ predicted from Equation 10-25 will be even smaller by another factor of 19 and the magnitude of ρ will, correspondingly, be larger than the observed value by the same factor.

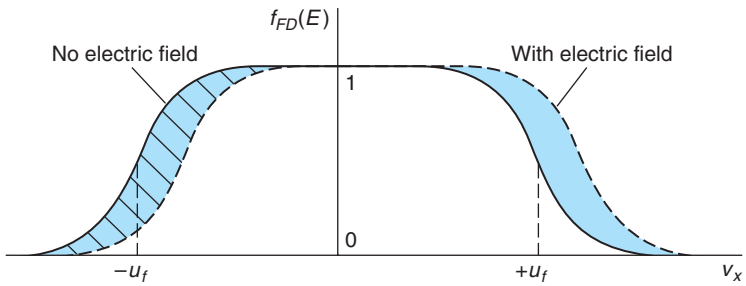

Figure 10-12 Occupation probability $f_{FD}(E)$ versus velocity in one dimension, with no electric field and with an electric field in the $+x$ direction. The difference is greatly exaggerated.

STUDENTS-HUB.com Uploaded By: Malak Obaid

The resolution of both of these problems lies in the way that the value of the mean free path is calculated. If we use u_F from Equation 10-24 and the experimental value $\rho \approx 1.7 \times 10^{-8}\ \Omega \cdot \text{m}$ for copper in Equation 10-25, we obtain for the mean free path $\lambda \approx 39$ nm, about 100 times the value of 0.38 nm, which was noted in Section 10-2 for Cu ions.

We shouldn't be too surprised that the mean free path of electrons in the copper lattice is not given correctly by classical kinetic theory. The reason for this large discrepancy between the classical calculation of the mean free path and the "experimental" result calculated from Equation 10-25 is that the wave nature of the electron must be taken into account. The collision of an electron with a lattice ion is not similar to the collision of a baseball and a tree. Instead, it involves the scattering of the electron wave by the regularly spaced ions of the lattice. If the wavelength is long compared with the crystal spacing, as is approximately the case here (see Problem 10-55), Bragg scattering cannot occur. Detailed calculations of the scattering of electron waves by a *perfectly* ordered crystal of infinite extent show that there is *no scattering*, and the mean free path is infinite. *Thus, the scattering of electron waves must arise from imperfections in the crystal lattice.* The most common imperfections are due to impurities and to thermal vibrations of the lattice ions.

In Equation 10-12, for the classical mean free path, the quantity πr^2 can be thought of as the cross-sectional area of the lattice ions as seen by the electron, where r is the ion radius. Figure 10-13*a* depicts the classical picture in which the lattice ions have area πr^2. According to quantum mechanics applied to the scattering of electron waves, however, the "area" of the ion's cross section seen by the electron wave has nothing to do with the size of the ion. Instead, it depends upon the *deviations* of the lattice ions from a perfectly ordered array. We can estimate the magnitude of the deviations and thus compute a more accurate value for the mean free path in the following way.

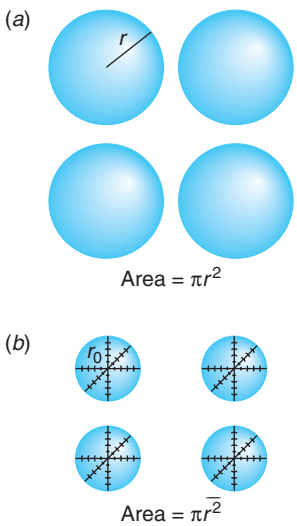

Figure 10-13 (*a*) Classical picture of the lattice ions as spherical balls of radius r that present an area πr^2 to the electrons. (*b*) Quantum-mechanical picture of the lattice ions as points that are vibrating in three dimensions. The area presented to the electrons is $\pi \overline{r_0^2}$, where r_0 is the amplitude of oscillation of the ions.

Let us assume that the lattice ions are *points* that are vibrating because of their thermal energy. (See Figure 10-13*b*.) We will take for the scattering cross section $\pi \overline{r^2}$, where $\overline{r^2} = \overline{x^2} + \overline{y^2}$ is the mean-square displacement of the point atom in a plane perpendicular to the direction of the electron's motion and represents a measure of the deviation of the ion from its equilibrium location. We can calculate $\overline{r^2}$ from the equipartition theorem. We have

$$\frac{1}{2}K\overline{r^2} = \frac{1}{2}M\omega^2\overline{r^2} = kT \qquad \textbf{10-26}$$

where K is the force constant, M is the mass of the ion, and $\omega = (K/M)^{1/2}$ is the angular frequency of vibration. The mean free path is then

$$\lambda = \frac{1}{n\pi\overline{r^2}} = \frac{M\omega^2}{2\pi nk}\frac{1}{T} \qquad \textbf{10-27}$$

We thus see that this argument gives the correct temperature dependence for σ and ρ; that is, $\rho \propto 1/\lambda$ (Equation 10-25), and so $\rho \propto T$ rather than $\rho \propto T^{1/2}$, as was obtained from the classical calculation.

We can then calculate the magnitude of $\overline{r^2}$, and therefore λ, using the Einstein model of a solid, which is fairly accurate except at very low temperatures. In the Einstein model (see Section 8-4) all the atoms vibrate with the same frequency. The Einstein temperature was defined by Equation 8-63 as

$$kT_E = hf = \hbar\omega$$

STUDENTS-HUB.com Uploaded By: Malak Obaid

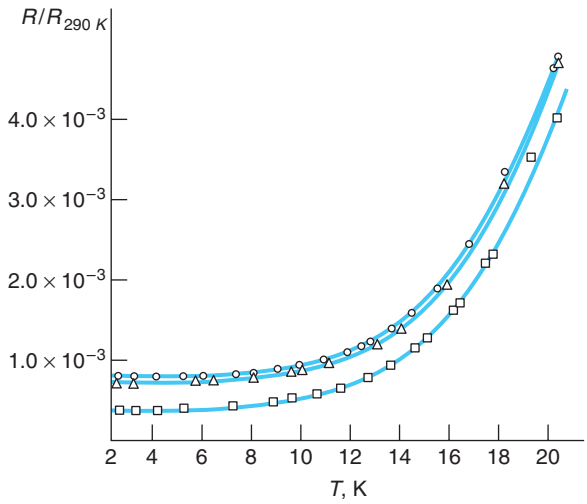

Figure 10-14 Relative resistance versus temperature for three samples of sodium. The three curves have the same temperature dependence but have different magnitudes because of differing amounts of impurities in the samples. [*From D. MacDonald and K. Mendelssohn, Proceedings of the Royal Society, A202, 103 (1950).*]

Using this for ω, we have

$$\overline{r^2} = \frac{2kT}{M\omega^2} = \frac{2T\hbar^2}{MkT_E^2} = \frac{2(\hbar c)^2}{Mc^2kT_E}\frac{T}{T_E} \qquad \textbf{10-28}$$

The Einstein temperature for copper is about 200 K, corresponding to an energy of $kT_E = 0.0172$ eV. Using this and $Mc^2 = 63.5 \times 931$ MeV for the mass of a copper ion, the value of $\overline{r^2}$ at $T = 300$ K is

$$\overline{r^2} = \frac{2(197.3 \text{ eV} \cdot \text{nm})^2}{(63.5 \times 931 \times 10^6 \text{ eV})(0.0172 \text{ eV})}\frac{300 \text{ K}}{200 \text{ K}} = 1.14 \times 10^{-4} \text{ nm}^2$$

Since this is about 100 times smaller than the area presented by a copper ion of radius 0.1 nm, the mean free path is about 100 times larger than that calculated from the classical model, in agreement with that calculated from the measured value of the conductivity. We see, therefore, that *the free-electron model of metals gives a good account of electrical conduction if the classical average speed is replaced by the Fermi speed u_F and if collisions are interpreted in terms of the scattering of electron waves for which only deviations from a perfectly ordered lattice are important.*

The presence of impurities in a metal also causes deviations from perfect regularity in the crystal. The effects of impurities on resistivity are approximately independent of temperature. The resistivity of a metal containing impurities can be written $\rho = \rho_t + \rho_I$, where ρ_t is due to the thermal motion of the lattice and ρ_I is due to impurities. Figure 10-14 shows a typical resistance versus temperature curve for a metal with impurities. As the temperature approaches zero, ρ_t approaches zero and the resistivity approaches the constant ρ_I.

Heat Capacity

Next, let's estimate the contribution of the electron gas to the molar heat capacity. At $T = 0$, the average energy of the electron, given by Equation 10-22, is $(3/5)E_F$, so the total energy for N electrons is $U = (3/5)NE_F$. At a temperature T, only those electrons near the Fermi level can be excited by random collisions with the lattice ions, which have

STUDENTS-HUB.com Uploaded By: Malak Obaid

an average energy of the order of kT. The fraction of the electrons that are excited is of the order kT/E_F, and their energy is increased from that at $T = 0$ by an amount of the order of kT. We can thus write for the energy of the N electrons at temperature T,

$$U = \frac{3}{5}NE_F + \alpha N\frac{kT}{E_F}kT \qquad \textbf{10-29}$$

where α is some constant, which we expect to be of the order of 1 if our reasoning is correct. The calculation of α requires the use of the complete Fermi electron distribution at an arbitrary temperature T and is quite difficult. Such a calculation, first carried out by A. A. Sommerfeld, shows that this equation is correct with $\alpha = \pi^2/4$. Using this result, the contribution of the electrons to the molar heat capacity is

$$C_v(\text{electrons}) = \frac{dU}{dT} = 2\alpha Nk\frac{kT}{E_F} = \frac{\pi^2}{2}R\frac{T}{T_F} \qquad \textbf{10-30}$$

Understanding quantum theory of heat conduction and heat capacity has made possible such devices as "high-tech" frozen yogurt/ice cream makers for consumers. Using specially designed working fluids, they are replacing the old salt/ice-in-a-bucket freezers because of their convenience.

where $Nk = R$ for 1 mole and $T_F = E_F/k$ is the Fermi temperature. We see that because of the large value of T_F, the contribution of the electron gas is a small fraction of R at ordinary temperatures. Using $T_F = 81{,}900$ K for copper, the molar heat capacity of the electron gas at $T = 300$ K is

$$C_v = \frac{\pi^2}{2}\left(\frac{300}{81{,}900}\right)R = 0.018R$$

which is in reasonable agreement with the value estimated from the small fraction of electrons with energies greater than E_F in Figure 10-11 and in good agreement with experiment.

More

Quantum theory readily accounts for heat conduction, predicting results in good agreement with observations. *Thermal Conduction—The Quantum Model* is outlined briefly on the home page: www.whfreeman.com/tiplermodernphysics5e. See also Equations 10-31 and 10-32 here.

Questions

5. When the temperature is lowered from 300 K to 4 K, the resistivity of pure copper drops by a much greater factor than that of brass. Why?
6. Explain why, physically, you would expect the mean free path of electrons in a metal to decrease as the temperature increases.

10-5 Magnetism in Solids

Electron spins with their associated magnetic moments are the origin of magnetism in solids. If the atoms of the solid have unpaired spins, the solid itself may have a net magnetic moment. Since the atoms are effectively fixed in one or another of the several crystalline structures, the interactions between them may have a substantial effect on the magnetism exhibited by the solid. Several types of magnetism are observed in solids, *ferromagnetism* being perhaps the most familiar, though hardly the most common, among elements and compounds. In this section we will describe each of the several types.

STUDENTS-HUB.com Uploaded By: Malak Obaid

Paramagnetism

Consider a solid consisting of atoms that each have an unpaired electron spin; that is, each atom has a net spin of $\frac{1}{2}$ (actually $\sqrt{3/4}\hbar$, of course) and the atoms do not interact magnetically. Examples of such solids are the rare earth elements and many of the transition elements. In that event, the only magnetic energy the system may have results from interaction with an applied external field **B**. Such a solid, one with no net magnetic moment in the absence of an applied external field, is called *paramagnetic*.

The magnetic moment of each atom is thus that of the unpaired electron $\mu = g_s \mu_s \mathbf{s}/\hbar$. Its z component is given by Equation 7-49:

$$\mu_z = -m_s g_s \mu_B \qquad \textbf{7-49}$$

where g_s is the g factor for the electron and μ_B is the Bohr magneton. In an applied field **B**, whose direction provides the atom with an external z axis, the possible energies of the magnetic moment are

$$U = -\mu_z B \qquad \textbf{7-47}$$

or

$$U = m_s g_s \mu_B B \qquad \textbf{10-33}$$

Since $m_s = \pm 1/2$, the $m_s = -1/2$ orientation of **s** (called "spin down" because **s** is antiparallel to **B**) is of lower energy than the $m_s = +1/2$ orientation (called "spin up," of course). Thus, in a thermal distribution the spin-down states will contain more atoms than the spin-up states and the solid will have a net magnetic moment per unit volume **M** whose magnitude is given by

$$M = \mu(\rho_+ - \rho_-)$$

where ρ_+ and ρ_- are the densities of electrons with spin-up and spin-down, respectively. Since $\rho_- > \rho_+$ and μ is negative, M is positive. For sufficiently small fields **M** is proportional to **B**:

$$\mu_0 \mathbf{M} = \chi \mathbf{B} \qquad \textbf{10-34}$$

where χ is called the *magnetic susceptibility*. For high temperatures such that $\mu B \ll kT$, it can be shown that (see Problem 10-60)

$$\chi = \frac{\mu_0 M}{B} = \frac{\rho \mu^2}{kT} \qquad \textbf{10-35}$$

where $\rho = (\rho_+ + \rho_-)$ is the total electron density. Equation 10-35 is known as *Curie's law*, after Pierre Curie. Thus, as T increases, the ability of the magnetic field to align the spins decreases. Many solids exhibit Curie's law behavior. For low temperatures where $\mu B \gg kT$, $M \rightarrow \mu\rho$ as $T \rightarrow 0$, corresponding to the alignment of all the magnetic moments with the field.

Equation 10-35 does not apply to the magnetism arising from electrons in metals. The reason is that $T \ll T_F$, since $T_F = 10^4 - 10^5$ K for metals. Thus, the electrons are highly degenerate, with each allowed level containing two with paired spins. When an external **B** field is applied, spins cannot just "flip" to align with the field since doing so would violate the exclusion principle. A spin flip must be accompanied by raising that electron to a higher, unoccupied energy state. Thus, even at $T = 0$ K, metals have a finite susceptibility. This type of magnetic behavior is called *Pauli paramagnetism*.

STUDENTS-HUB.com Uploaded By: Malak Obaid

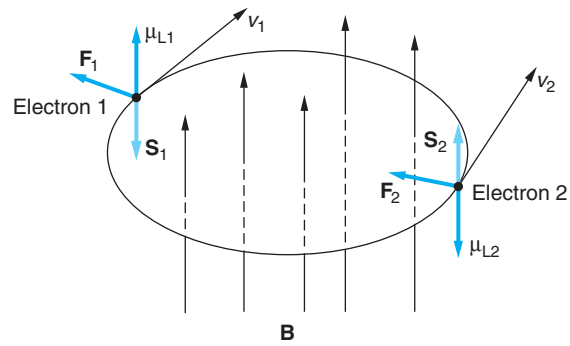

Figure 10-15 Electrons 1 and 2 orbit the atomic core (not shown) in opposite directions. The magnetic field **B** is perpendicular to the plane of the orbits. The magnetic forces $\mathbf{F}_1$ and $\mathbf{F}_2$ increase the orbital magnetic moment of electron 2 and decrease that of electron 1, resulting in a net moment opposite to **B**.

Diamagnetism

Recall that a free electron moving perpendicular to a magnetic field experiences a magnetic force $\mathbf{F} = -e(\mathbf{v} \times \mathbf{B})$. The resulting circular motion produces a current loop with a magnetic moment *opposite* to the direction of the applied field. (To see this, use the right-hand rule.) Now consider two electrons with paired spins orbiting in opposite directions in an atom. (See Figure 10-15.) If an external **B** field perpendicular to the plane of the orbits is turned on, the net force ($\mathbf{F}_{\text{Coulomb}} - \mathbf{F}_{\text{magnetic}}$) on electron 1 is reduced, reducing its *orbital* magnetic moment, which is parallel to **B**. The net force on electron 2 is increased, increasing its magnetic moment. The result is a net magnetic moment opposite to the direction of the applied field. This magnetic behavior is called *diamagnetism*. The diamagnetic effect is seen only in solids consisting of atoms whose electron spins are all paired. As we will see in Section 10-9, the "test" of superconductivity is that the material exhibit perfect diamagnetism.

Ferromagnetism

The first magnetic effect discovered, a result of its existence in iron that led to its early use as a compass, *ferromagnetism* is the consequence of a phase transition in certain materials. At high temperatures a piece of iron is unmagnetized, the spin directions of the atoms having rotational symmetry—all spin directions are equally probable. (In an applied **B** field iron is paramagnetic at high temperatures.) As the temperature decreases, at a certain temperature T_C, called the *Curie temperature*, the magnetic interaction between the atoms exceeds the randomizing effect of thermal agitation, spontaneously breaking the rotational symmetry and causing a phase transition in the solid that tends to align the spins parallel to each other, converting the sample into a permanent magnet. Only four elements besides iron exhibit ferromagnetism: nickel, cobalt, gadolinium, and dysprosium. There are also several ferromagnetic compounds, including some that contain none of the ferromagnetic elements.

In certain compounds the magnetic interaction between the atoms tends to align the spins on adjacent atoms antiparallel below a certain temperature, analogous to the Curie temperature, called the *Neel temperature* T_N. Such materials are called *antiferromagnetic*. Examples are FeO, $NiCl_2$, MnO, and MnS. In a few other materials the spins on adjacent sites are antiparallel below T_N, but because they contain two different types of positive ions, the spins do not exactly cancel and the material is left with a small net magnetization. Such materials are called *ferrimagnetic*. The most common example is the iron ore magnetite, $FeO \cdot Fe_2O_3$.

STUDENTS-HUB.com Uploaded By: Malak Obaid

EXPLORING
Spintronics

A relatively new field of research with almost immediate applications, s*pintronics*, or *spin electronics*, is the manipulation of electron spin currents rather than charge currents. N. F. Mott was the first to suggest the possibility of spin-polarized currents in ferromagnetic materials more than 30 years ago. Utilization of spin currents was first realized with the discovery of the giant magnetoresistance (GMR) of magnetic multilayers in 1988. A magnetic multilayer film consists of a stack of alternate ferromagnetic and nonmagnetic layers. The resistance to current flow is low when the electron spins, hence magnetic moments, of the ferromagnetic layers are aligned parallel. The resistance is high when the spins of the ferromagnetic layers are aligned antiparallel, a result of spin-dependent scattering. The resulting relative resistance change can be as large as 200 percent (although 10–20 percent is more typical); hence the name *giant* magnetoresistance. Depending on the design of the layers, the direction of the spins (magnetic moments) can be changed very quickly by an applied magnetic field of only about 10^{-6} tesla. These so-called *spin valves* can detect very small magnetic fields, such as those of the magnetic bits on CDs and DVDs.

Spin valves, the first spintronic devices, form the read/write heads on the hard drives of essentially all modern computers. In addition, recent commercial development of magnetoresistive random access memory (MRAM) chips have read/write speeds much faster than flash memory and, like the latter, do not degrade over time.

Another spintronic device with enormous potential applications is the *magnetic tunnel junction*. In these devices the ferromagnetic layers are separated by very thin insulating layers, typically aluminum oxide (see Figure 10-16). Electrons can tunnel through the insulating layer (see Sections 6-6 and 10-8) and, since the tunneling probability from a ferromagnetic layer depends on the spin direction, the resistance of the junction is different by as much as 75 percent between the parallel and antiparallel configurations. Extremely small junctions can be mass-produced making possible random access memory for portable permanent computer memory with write speeds three orders of magnitude faster than current flash memory devices. The magnetic tunnel junction was also the key element in the recent direct electrical detection of the potential due to the *spin Hall effect* (see page 452), opening opportunities for controlling spin currents with electric fields.

Yet another intriguing future possibility is the application of spintronic devices to the development of quantum computers. The use of electron charge states for information storage is currently a barrier to their development since such states are readily destroyed by scattering. Spin states, on the other hand, have very long relaxation times.

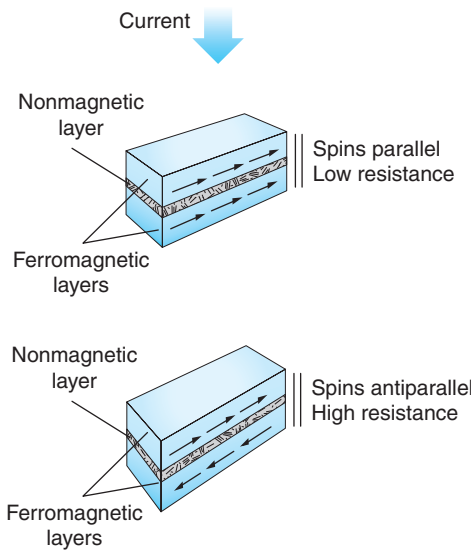

Figure 10-16 A magnetic tunnel junction consists of two ferromagnetic layers separated by a very thin nonmagnetic insulating layer. (*a*) The probability of electrons tunneling through the barrier layer is dependent on the spin direction, being highest when the spins, hence the magnetic moments, of the electrons in the ferromagnetic layers are parallel. This is the configuration of low resistance. (*b*) The tunneling probability is low when the spins are antiparallel, resulting in high resistance. Thus, each junction can store one bit of data, (*a*) representing, e.g., "0" and (*b*) representing "1."

STUDENTS-HUB.com Uploaded By: Malak Obaid

10-6 Band Theory of Solids

We have seen that, if the electron gas is treated as a Fermi gas and the electron-lattice collisions treated as the scattering of electron waves, the free-electron model gives a good account of the electrical and thermal properties of conductors. This simple model, however, gives no indication why one material is a good conductor and another is an insulator. The conductivity (and its reciprocal, the resistivity) vary enormously from the best insulators to the best conductors. For example, the resistivity of a typical insulator (such as quartz) is of the order of $10^{16}\ \Omega \cdot \text{m}$, whereas that of a typical conductor (most metals) is of the order of $10^{-8}\ \Omega \cdot \text{m}$ and that of a superconductor is less than $10^{-19}\ \Omega \cdot \text{m}$.

To understand why some materials conduct and others do not, we must refine the free-electron model and consider the effect of the lattice on the electron energy levels. There are two standard approaches to this problem of determining the energy levels of electrons in a crystal. One is to consider the problem of an electron moving in a periodic potential and to determine the possible energies by solving the Schrödinger equation. The other is to determine the energy levels of the electrons in a solid by following the behavior of the energy levels of individual atoms as they are brought together to form the solid, in much the same way that we did in Section 9-2 in the explanation of the covalent bonding in the H_2 molecule. Both approaches lead to the result that the energy levels are grouped into allowed and forbidden bands. The details of the band structure of a particular material determine whether that material is a conductor, an insulator, or a semiconductor. Qualitative discussion of the first of these methods is given in this section. The second is described in the MORE section *Energy Bands in Solids—An Alternate Approach* on the home page.

Kronig-Penney Model

Consider first the problem of an electron moving in a periodic potential. Figure 10-17*a* shows a one-dimensional sketch of the potential energy function for a lattice of positive ions. The most important feature of this potential is not the shape, but the fact that it is periodic. A simpler periodic potential consisting of finite square wells is shown in Figure 10-17*b*. The model based on this potential is called the *Kronig-Penney model*. It has the important feature of periodicity and is easier to treat mathematically; however, even for this model the mathematical solution of the Schrödinger equation is

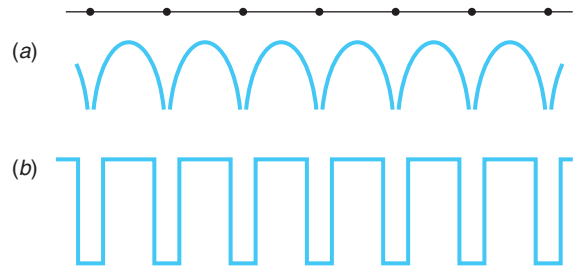

Figure 10-17 (*a*) One-dimensional potential energy of an electron in a crystal. $U(x)$ approaches $\pm\infty$ at the atom sites. (*b*) Simplified (Kronig-Penney) model of potential energy of an electron in a crystal.

STUDENTS-HUB.com Uploaded By: Malak Obaid

quite involved, and we will only outline it here. For both potential functions shown in Figure 10-17, for certain ranges of energy traveling-wave-type solutions of the Schrödinger equation exist. This result is based on an important discovery made by Felix Bloch[4] that solutions to the Schrödinger equation for periodic potentials must be of the form (in one dimension)

$$\psi(x) = u_k(x)e^{ikx} \qquad \textbf{10-36}$$

where $u_k(x) = u_k(x + L) = u_k(x + nL)$, L is the periodic spacing of the potential wells, and n is an integer. The function e^{ikx} is a plane wave, i.e., a free electron (see Section 6-6) with wave number $k = 2\pi/\lambda$. As Bloch himself described it:

> I felt that the main problem was to explain how the electrons could sneak by all the ions in a metal. . . . I found to my delight the wave differed from the plane wave of free electrons only by a periodic modulation.

Thus, we require that the solutions of the Schrödinger equation

$$-\frac{\hbar^2}{2m}\frac{d^2\psi(x)}{dx^2} + U(x)\psi(x) = E\psi(x) \qquad \textbf{10-37}$$

where $U(x)$ is the Kronig-Penney potential of periodic square wells and $\psi(x)$ has the form of the *Bloch function* given by Equation 10-36. The solution for the region $0 < x < a$ in Figure 10-18 is

$$\psi(x) = A_1e^{ik'x} + A_2e^{-ik'x} \qquad \textbf{10-38}$$

where $k' = 2\pi/\lambda = (2mE)^{1/2}/\hbar^2$. In the region $-b < x < 0$, the solutions are of the form

$$\psi(x) = B_1e^{\alpha x} + B_2e^{-\alpha x} \qquad \textbf{10-39}$$

where $\alpha = [2m(U_0 - E)]^{1/2}/\hbar^2$. The requirement that $\psi(x)$ have the form of Equation 10-36 means that

$$\begin{aligned}\psi(x + a + b) &= u_k(x + a + b)e^{ik(x+a+b)}\\ \psi(x + a + b) &= u_k(x)e^{ikx}e^{ik(a+b)}\\ \psi(x + a + b) &= \psi(x)e^{ik(a+b)}\end{aligned} \qquad \textbf{10-40}\boldsymbol{a}$$

where $a + b$ is the periodic spacing of the wells. In general,

$$\psi(x + n(a + b)) = \psi(x)e^{ikn(a+b)} \qquad \textbf{10-40}\boldsymbol{b}$$

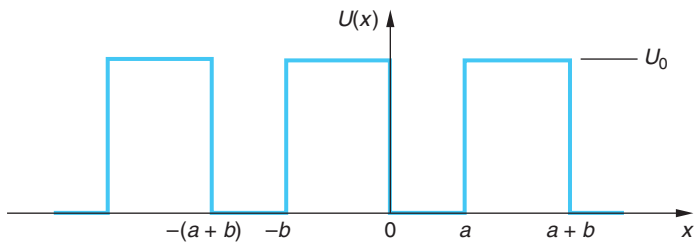

Figure 10-18 A portion of the Kronig-Penney potential of Figure 10-17*b* showing the width of the square wells a and their periodic spacing $(a + b)$.

STUDENTS-HUB.com Uploaded By: Malak Obaid

As was done in Section 6-3 for solving the finite one-dimensional square well, the constants A_1, A_2, B_1, and B_2 are chosen so as to make $\psi(x)$ and $d\psi/dx$ continuous at $x = 0$ and $x = a$. Obtaining the constants is beyond the scope of our discussion here, but as in Chapter 6, doing so yields a conditional equation connecting k, k', and α with a and b, the parameters of the lattice. The result is that, in order to satisfy the requirement of Equation 10-40, only certain ranges of electron energies are allowed. These energy ranges, called *bands*, are separated by forbidden energy regions called *energy gaps*, in which no traveling wave can exist. Figure 10-19*a* shows the energy versus the wave number k for a completely free electron. This is, of course, merely a sketch of $E = \hbar^2 k^2/2m$. Figure 10-19*b* shows E versus k for an electron in the periodic potential of Figure 10-18. The energy gaps occur at

$$ka = \pm n\pi \qquad \textbf{10-41}$$

where n is an integer and a is the lattice spacing.[5] We can understand this result in terms of the Bragg reflection of the electron waves. Consider E to be small (near zero in Figure 10-19*b*) so that k is small; hence λ is large. As E increases, k eventually becomes large enough so that λ becomes small enough to suffer a Bragg reflection (constructive interference) from the lattice. (See Section 3-4.) Bragg reflection is governed by the Bragg condition (Equation 3-23):

$$n\lambda = 2a \sin\theta$$

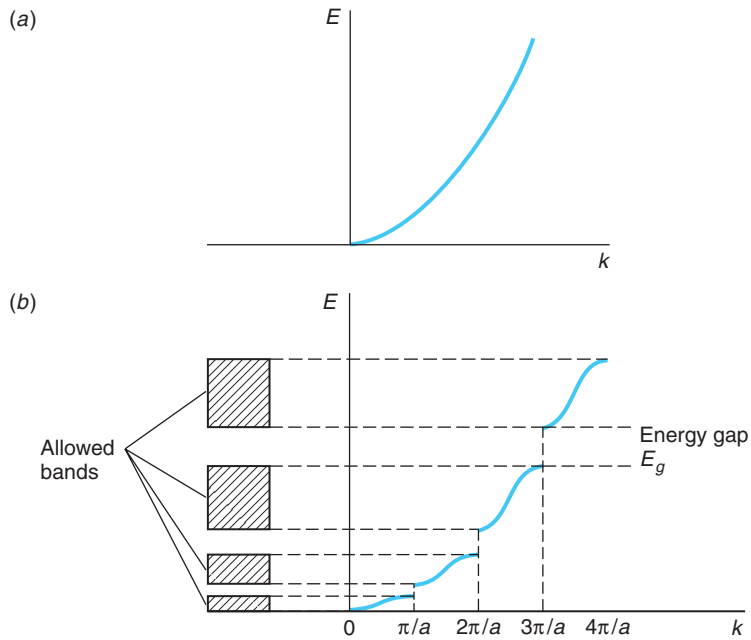

Figure 10-19 (*a*) Energy versus k for a free electron. (*b*) Energy versus k for a nearly free electron in the one-dimensional periodic potential of Figure 10-18 with $b = 0$ and $U_0 \rightarrow \infty$. Energy gaps occur at the k values which satisfy the Bragg scattering condition. In each case only the portions with $k > 0$ are shown. The complete curves are symmetric about $k = 0$.

STUDENTS-HUB.com Uploaded By: Malak Obaid

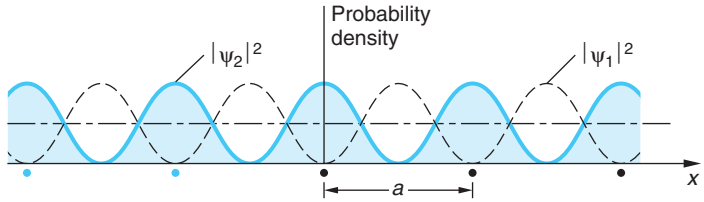

Figure 10-20 Probability density (proportional to the charge distribution) for standing waves of wave number $k = \pi/a$ in a one-dimensional crystal. The solid curve $|\psi_2|^2$ is a maximum at the lattice ion sites and has a lower potential energy than the dashed curve $|\psi_1|^2$.

In a one-dimensional system such as we are considering here, reflection means $\theta = 90°$. Since $k = 2\pi/\lambda$, Equation 10-41 becomes the condition for Bragg reflection. The reason that traveling waves cannot exist for these wave numbers is that the amplitude of the reflection from one atom in the chain becomes equal to and in phase with the forward electron wave from the preceding atom, so that standing waves are set up. Figure 10-20 shows a sketch of the electron probability density $|\psi|^2$ for the two types of standing waves for the lowest energy gap, where the value $k = \pi/a$:

$$\psi_1 = \sin kx = \sin\frac{\pi x}{a} \qquad \psi_2 = \cos kx = \cos\frac{\pi x}{a}$$

Since ψ_2 gives a higher concentration of electron charge density near the ion sites than ψ_1, the potential energy is less for ψ_2 than for ψ_1. The difference in the potential energies corresponds to the magnitude of the energy gap. Within the allowed energy bands, the energy has a continuous range if the number of atoms in the chain is infinite; for N atoms, there are N allowed energy levels in each band. Since the number of atoms is very large in a macroscopic solid, the energy bands can be considered continuous. Calculations in three dimensions are more difficult, of course, but the results are similar. The allowed ranges of the wave vector **k** are called *Brillouin zones*. Referring to Figure 10-19*a*, the first Brillouin zone has $-\pi/a < k < +\pi/a$, the second has $-2\pi/a < k < -\pi/a$ and $\pi/a < k < 2\pi/a$, and so on.

Conductors, Insulators, and Semiconductors

Conductors We can now understand why some solids are conductors and others are insulators. Consider sodium. There is room for two electrons in the 3*s* state of each atom, but each sodium atom has only one 3*s* electron. Therefore, when N sodium atoms are bound in a solid, the 3*s* energy band is only half filled. In addition, the empty 3*p* band overlaps the 3*s* band. The allowed energy bands of sodium are shown schematically in Figure 10-21. We can see that many allowed energy states are available immediately above the filled lower half of the 3*s* band, so the valence electrons can easily be raised to a higher energy state by an electric field. Accordingly, sodium is a good conductor. Magnesium, on the other hand, has two 3*s* electrons, so the 3*s* band is filled. However, like sodium, the empty 3*p* band overlaps the 3*s* band, so magnesium is also a conductor. The band occupied by the outer, or valence electrons, is called the *valence band*. The next (higher) allowed band is called the *conduction band*.

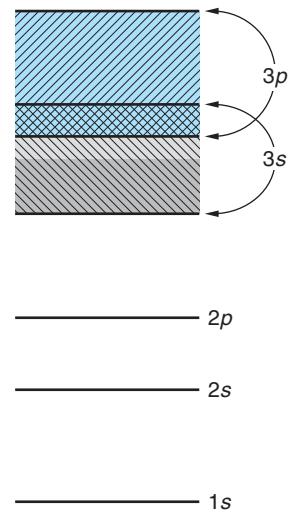

Figure 10-21 Energy-band structure of sodium. The empty 3*p* band overlaps the half-filled 3*s* band. Just above the filled states are many empty states into which electrons can be excited by an electric field, so sodium is a conductor.

STUDENTS-HUB.com Uploaded By: Malak Obaid

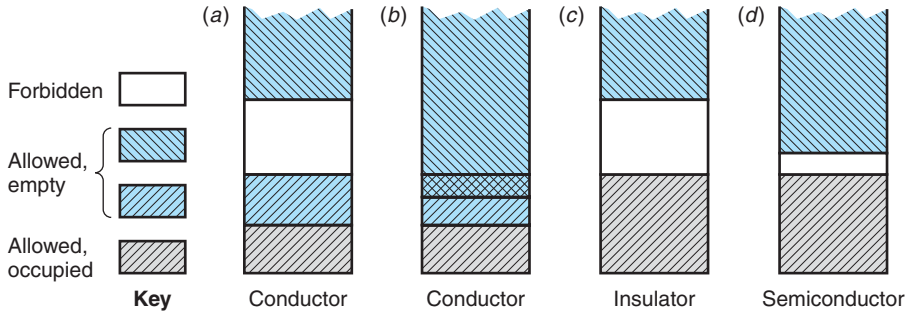

Figure 10-22 Four possible band structures for a solid. (*a*) The allowed band is only partially full, so electrons can be excited to nearby energy states. At 0 K the Fermi level is at the top of the filled states. (*a*) is a conductor. (*b*) is a conductor because the allowed bands overlap. In (*c*) there is a forbidden band with a large energy gap between the filled band and the next allowed band; this is an insulator. (*d*) The energy gap between the filled band and the next allowed band is very small, so some electrons are excited to the conduction band at normal temperatures, leaving holes in the valence band. The Fermi level is approximately in the middle of the gap. (*d*) is a semiconductor.

Thus, a conductor is a solid whose valence band is only partly filled or whose conduction band overlaps its valence band. There are a few elements, notably antimony, arsenic, and bismuth, whose conduction band overlaps the valence band only very slightly, limiting the number of available empty states. These materials are called *semimetals*. (See Figures 10-22*a* and *b*.)

Insulators A solid that has a completely filled valence band is an insulator if the energy gap between the valence band and the empty conduction band is larger than about 2eV, as illustrated in Figure 10-22*c*. For example, ionic crystals are insulators. The band structure of an ionic crystal, such as NaCl, is quite different from that of a metal. The energy bands arise from the energy levels of the Na^+ and Cl^- ions. Both of these ions have a closed-shell configuration, so the highest occupied band in NaCl is completely full. The next allowed band, which is empty, arises from the excited states of Na^+ and Cl^-. There is a large energy gap between the filled band and this empty band. Typical electric fields applied to NaCl will be too weak to excite an electron from the upper energy levels of the filled valence band across the large gap into the lower energy levels of the empty conduction band, so NaCl is an insulator. When an applied electric field is sufficiently strong to cause an electron to be excited to the empty band, the phenomenon called *dielectric breakdown* occurs.

Intrinsic Semiconductors If the gap between a filled valence band and an empty conduction band is small, the solid is a semiconductor. Consider carbon, which has two 2*s* electrons and two 2*p* electrons. We might expect carbon to be a conductor because of the four unfilled 2*p* states. However, the 2*s* and 2*p* levels mix when carbon forms covalent bonds.[6] Figure 10-23 shows the splitting of the eight $2s - 2p$ levels when carbon bonds in the diamond structure. This splitting is due to the nature of the covalent bond and is similar to the splitting of the 1*s* levels in hydrogen discussed in Section 9-2. The energy of the levels corresponding to the four space-symmetric wave functions (one for the 2*s* levels and three for the 2*p* levels) is lowered while the energy of the other four levels (one 2*s* and three 2*p*) is raised. The valence band therefore contains four levels per atom that are filled, and the conduction band is empty.

STUDENTS-HUB.com Uploaded By: Malak Obaid

At the diamond lattice spacing of about 0.154 nm, the energy gap between the filled valence band and the empty conduction band is about 7 eV. Since this gap is large compared to the energy that an electron might receive by thermal excitation due to scattering from the lattice ions, which on the average is of the order of $kT \approx 0.026$ eV at $T = 300$ K, very few electrons can reach the conduction band. Thus, diamond is an insulator. The band structure is similar for silicon, which has two 3*s* and two 3*p* electrons, and for germanium, which has two 4*s* and two 4*p* electrons. At the silicon lattice spacing of 0.235 nm the energy gap is about 1 eV; at the germanium lattice spacing of 0.243 nm the energy gap is only about 0.7 eV. For these gaps, at ordinary temperatures there are an appreciable number of electrons in the conduction band due to thermal excitation, although the number is still small compared with the number in a typical conductor. Solids such as these are called *intrinsic semiconductors*. Figure 10-22*d* illustrates the band structure of intrinsic semiconductors.

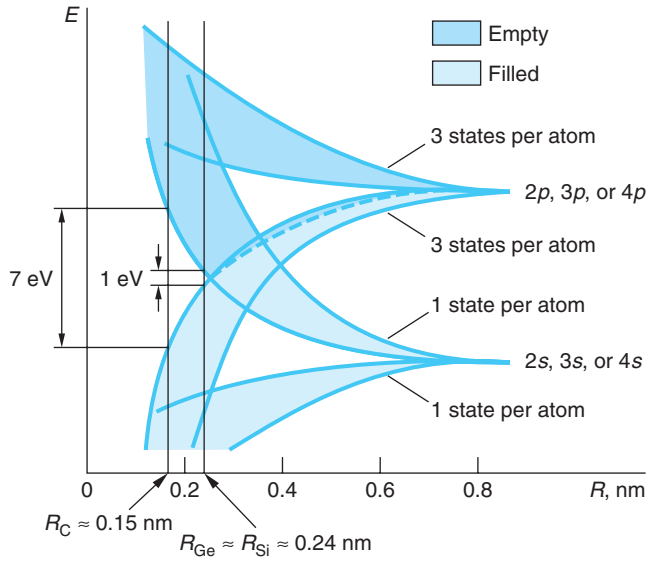

Figure 10-23 Splitting of the 2*s* and 2*p* states of carbon, the 3*s* and 3*p* states of silicon, or the 4*s* and 4*p* states of germanium versus separation of the atoms. The energy gap between the four filled states in the valence band and the empty states in the conduction band is 7 eV for the diamond-lattice spacing, $R_C = 0.154$ nm. For the silicon spacing $R_{Si} = 0.235$ nm, the energy gap is 1.09 eV. The splitting is similar for the 4*s* and 4*p* levels in germanium, which has an atom spacing of 0.243 nm, giving an energy gap of only 0.7 eV.

In the presence of an electric field, the electrons in the conduction band of an intrinsic semiconductor can be accelerated because there are empty states nearby. Also, for each electron that has been excited to the conduction band there is a vacancy, or hole, in the nearby filled valence band. In the presence of an electric field, other electrons in this band can be excited to the vacant energy level, thus filling that hole but creating another hole. This contributes to the electric current and is most easily described as the motion of a hole in the direction of the field and opposite to the motion of the electrons. The hole thus acts like a positive charge. An analogy of a two-lane, one-way road with one lane full of parked cars and the other empty may help in visualizing the conduction of holes. If a car moves out of the filled lane into the empty lane, it can move ahead freely. As the other cars move up to occupy the space left, the empty space propagates backward in the direction opposite to the motion of the cars. Both the forward motion of the car in the nearby empty lane and the backward propagation of the empty space contribute to a net forward propagation of the cars.

An interesting characteristic of semiconductors is that the conductivity increases (and the resistivity decreases) as the temperature increases, which is contrary to the case for normal conductors. The reason is that as the temperature is increased, the number of free electrons is increased because there are more electrons in the conduction band. The number of holes in the valence band is also increased, of course. In semiconductors, the effect of the increase in the number of charge carriers, both electrons and holes, exceeds the effect of the increase in resistivity due to the increased scattering of the electrons by the lattice ions due to thermal vibrations. Semiconductors therefore have negative temperature coefficients of resistivity.

Whether a solid with a filled valence band will be a semiconductor or an insulator depends critically on the width of the energy gap E_g, as Figure 10-23 suggests. A comparison of the relative numbers of electrons with various energies that *could* be

STUDENTS-HUB.com Uploaded By: Malak Obaid

Table 10-4 Values of $f_{FD}(E)$ for $T = 293$ K

$E - E_F$ (eV)	0.05	0.10	0.25	1.0	2.5	7.5
Multiple of kT	2	4	10	40	100	300
$f_{FD}(E)$	1.2×10^{-1}	1.8×10^{-2}	5.1×10^{-5}	6.5×10^{-18}	1.1×10^{-43}	1.3×10^{-129}

above the Fermi level (located at the center of the band gap) at ordinary temperatures illustrates why this is true. Those numbers are given by the Fermi-Dirac distribution $f_{FD}(E)$ given by Equation 8-68:

$$f_{FD}(E) = \frac{1}{E^{(E-E_F)/kT} + 1} \qquad \textbf{8-68}$$

At $T = 293$ K, $kT = 0.025$ eV. Recall that for $E = E_F$, $f_{FD}(E) = 1/2$ (see Section 8-5). For $(E - E_F) = 0.10$, or $4(kT)$, we have

$$f_{FD}(E) = \frac{1}{e^{0.10/0.025} + 1} = 0.018$$

Repeating this calculation for several additional values of $(E - E_F)$ yields the relative numbers of electrons in Table 10-4. From the numbers in the table we see that, if a certain material has an energy gap E_g between the valence and conduction bands of 0.25 eV, for example, then approximately 10^{-5} of the electrons within kT of the Fermi level would be excited to the conduction band and thus able to participate in the conduction of electricity. This is a sizable number, given the numbers of electrons near the Fermi level, so we expect this material to have a higher electrical conductivity than materials with larger values of E_g.

For a gap of 1.0 eV, just four times that of the previous example, the relative number of electrons excited to the conduction band decreases by more than 12 orders of magnitude, illustrating the sharp decline of $f_{FD}(E)$ as the energy gap increases. The calculation of $f_{FD}(E)$ above also illustrates the increased conductivity of semiconductors as the temperature increases described earlier. If the temperature of a material with an energy gap of 1.0 eV is increased to 393 K from 293 K, as in Table 10-4, $f_{FD}(E)$ increases to 1.5×10^{-13}, thus increasing the relative number of electrons in the conduction band by nearly four orders of magnitude. Table 10-5 lists the energy gaps for several semiconducting elements and compounds. Notice that the energy gap is slightly temperature dependent.

A concept that is helpful in understanding a number of characteristics of semiconductors is that of *effective mass*. As pointed out above, Figure 10-19*a* is a graph of $E = \hbar^2 k^2/2m_e$, the energy of a free electron of wavelength $\lambda = 2\pi/k$. The curvature of the E versus k graph is given by $d^2E/dk^2 = \hbar^2/m_e$, and we may say that the curvature is determined by $1/m_e$, the reciprocal mass. In Figure 10-19*a* $1/m_e$ is of course constant; however, in regions near the energy gaps in Figure 10-19*b* the curvature is much higher than that for the free electron. Since the behavior of electrons near the band/gap boundary is of considerable interest, particularly in the discussion of impurity semiconductors and devices in Section 10-7, it is helpful to continue to describe the curvature of the E versus k curve near the boundary in terms of a reciprocal mass. Accordingly, we define the effective mass m^* as

$$\frac{1}{m^*} = \frac{1}{\hbar^2}\frac{d^2E}{dk^2} \qquad \textbf{10-42}$$

STUDENTS-HUB.com Uploaded By: Malak Obaid

Table 10-5 Energy gap E_g and dielectric constant κ for selected semiconductors

Material	E_g (eV) 0 K	E_g (eV) 293 K	κ	Material	E_g (eV) 0 K	E_g (eV) 293 K	κ
Si	1.15	1.11	11.8	CdTe	1.56	1.44	10.2
Ge	0.74	0.67	15.9	PbS	0.28	0.37	17.0
Te	—	0.33	—	InP	1.41	1.27	12.4
GaAs	1.53	1.35	13.1	CdSe	1.85	1.74	10.1
InSb	0.23	0.16	17.8	GaP	2.40	2.24	11.1
ZnS	—	3.54	5.2	PbTe	0.19	0.25	30.1

Then, as in the case of the free electron, the curvature of E versus k for electrons bound in the crystal energy bands is also described in terms of a reciprocal mass, $1/m^*$. For a free electron $m^* = m_e$, as is also the case for electrons that are not close to the boundaries in Figure 10-19*b*. Close to the band/gap boundaries, however, is a different matter. Starting from $k = 0$ in the figure, the curvature is initially constant and equal to that of a free electron, thus $m^* = m_e$, but near the boundary where $k = \pi/a$, the curvature becomes large and, very close to the boundary, negative; hence m^* becomes smaller than m_e and also eventually negative! Just above the gap, the curvature is large and positive, so $m^* < m_e$ and positive. For the situation where E_g is small compared to the width of the band, the values of the effective mass are typically of the order of $0.01-0.1$ of the mass of a free electron. We will make further use of the effective mass in Section 10-7.

Questions

7. How does the change in resistivity of copper compare with that of silicon when the temperature increases?
8. Suppose an electron is excited from the valence band of a semiconductor to a state several levels above the lower edge of the conduction band. Devise an explanation for why it will quickly "decay" to a level at the bottom of the conduction band.

More

An alternative to the Kronig-Penny model of a solid is based on the molecular bonding model discussed in Section 9-2 for hydrogen. *Energy Bands in Solids—An Alternate Approach* is described briefly on the home page: www.whfreeman.com/tiplermodernphysics5e. See also Figures 10-24 and 10-25 here.

10-7 Impurity Semiconductors

Most semiconductor devices, such as the semiconductor diode and the transistor, make use of *impurity semiconductors*, which are created through the controlled addition of certain impurities to intrinsic semiconductors. This process is called *doping*.

STUDENTS-HUB.com Uploaded By: Malak Obaid

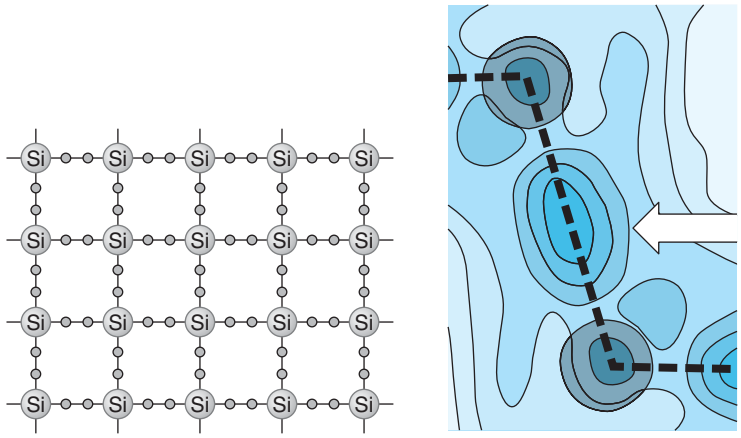

Figure 10-26 (a) A two-dimensional schematic illustration of solid silicon. Each atom forms a covalent bond with four neighbors, sharing one of its four valence electrons with each neighbor. (*b*) X-ray scattering measurement of electron density in the vicinity of two atoms in an Si crystal. The arrow points to the high electron density of the covalent bond. [*Adapted from Y. W. Yang, P. Coppens, Solid State Comm., 15, 1555 (1974).*]

Figure 10-26*a* illustrates the lattice structure of pure silicon, and Figure 10-27*a* is a schematic illustration of silicon doped with a small amount of arsenic such that arsenic atoms replace a few of the silicon atoms in the crystal lattice. Arsenic has five valence electrons in the $n = 4$ shell, whereas silicon has four valence electrons in the $n = 3$ shell. Four of the five arsenic electrons take part in covalent bonds with the four neighboring silicon atoms, and the fifth electron is very loosely bound to the atom. This extra electron occupies an energy level that is just slightly below the conduction band in the solid and is easily excited into the conduction band, where it can contribute to electrical conduction. The fifth arsenic valence electron and the arsenic ion core form a hydrogenlike system. Thus, Bohr theory (see Section 4-3) can be used to calculate the approximate values of the energies available to it, provided only that we make allowance for the fact that the electron-arsenic ion system is embedded in the semiconductor crystal rather than being isolated from other atoms. First, the crystal is a medium with a high dielectric constant; thus the potential energy function in the Schrödinger equation for a hydrogenlike atom (Equation 7-6) becomes[7] $V(r) = (-Zke^2/R)(1/\kappa)$ where κ is the dielectric constant of the material and $k = 1/4\pi\epsilon_0$. Second, the electron mass in the Schrödinger equation must be replaced by the effective mass m^*, which accounts for the fact that the electron "sees" a three-dimensional version of the periodic potential of Figure 10-17. With these two modifications the solution of the Schrödinger equation is carried out just as in Chapter 7. The results for the allowed energies and average values of the radii of the Bohr orbits for the fifth arsenic electron are given by

$$E_n = -\frac{1}{2}\left(\frac{ke^2}{\hbar}\right)^2 \frac{m_e}{n^2} \times \frac{m^*}{m_e} \times \frac{1}{\kappa^2} = -\frac{1}{2}\left(\frac{ke^2}{\hbar}\right)^2 \frac{m^*}{\kappa^2}\frac{1}{n^2} \qquad \textbf{10-43}$$

$$\langle r_n \rangle = a_0 n^2 \times \frac{m_e}{m^*} \times \kappa \qquad \textbf{10-44}$$

where a_0 is the Bohr radius, equal to 0.0529 nm (see Equation 4-19), and n is the principal quantum number.

To understand where these energy levels lie relative to the bands and gap of the silicon, consider that when the arsenic atom is ionized by removing the fifth electron, that electron is then free to move about and to participate in electrical conduction; i.e., it is then in the conduction band. Thus, we conclude that $E_\infty = 0$ is at the bottom edge of the conduction band and the other E_n hydrogenlike levels lie below it in the gap. The energy of the ground state E_1 can be calculated from the experimentally determined value of the electron's effective mass in silicon, about 0.2 m_e, and the dielectric constant of silicon given in Table 10-5. Substituting these into Equation 10-43 yields $E_1 = -0.020$ eV below the conduction band, which is substantially smaller than the -13.6-eV ground state for hydrogen. Similarly, substitution into Equation 10-44 yields $\langle r_1 \rangle = 3.1$ nm, or about 60 times the ground-state radius of hydrogen.[8]

STUDENTS-HUB.com Uploaded By: Malak Obaid

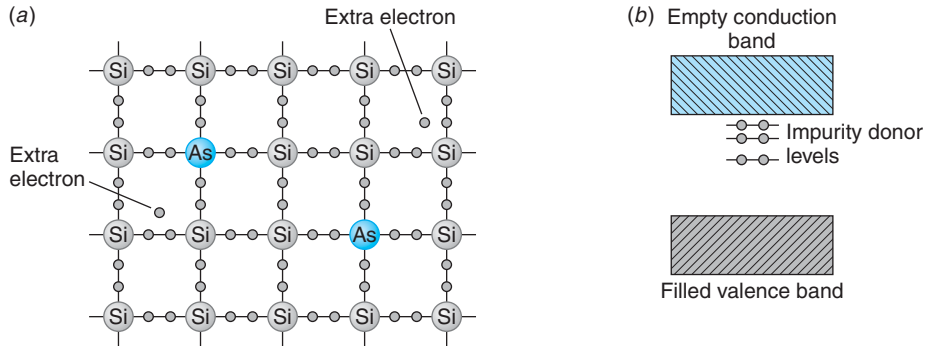

Figure 10-27 (*a*) A two-dimensional schematic illustration of silicon doped with arsenic. Because arsenic has five valence electrons, there is an extra, weakly bound electron that is easily excited to the conduction band, where it can contribute to electrical conduction. (*b*) Band structure of an *n*-type semiconductor such as silicon doped with arsenic. The impurity atoms provide filled energy levels that are just below the conduction band. These levels donate electrons to the conduction band.

These energies are quite close to the conduction band, as illustrated in Figure 10-27*b*; thus these electrons can be easily excited to the conduction band since their ionization energy is comparable to kT at room temperature.

These hydrogenlike levels just below the conduction band are called *donor levels* because they donate electrons to the conduction band without leaving holes in the valence band. Such a semiconductor is called an *n-type semiconductor* because the major charge carriers are *negative* electrons. The conductivity of a doped semiconductor can be controlled by controlling the amount of impurity added. The addition of just one part per million can increase the conductivity by several orders of magnitude.

Another type of impurity semiconductor can be made by replacing a silicon atom in the crystal lattice with a gallium atom, which has three electrons in its valence level rather than four (see Figure 10-28*a*). The gallium atom accepts electrons from the valence band of the silicon in order to complete its four covalent bonds, thus creating a hole in the valence band. The effect on the band structure of silicon achieved by doping it with

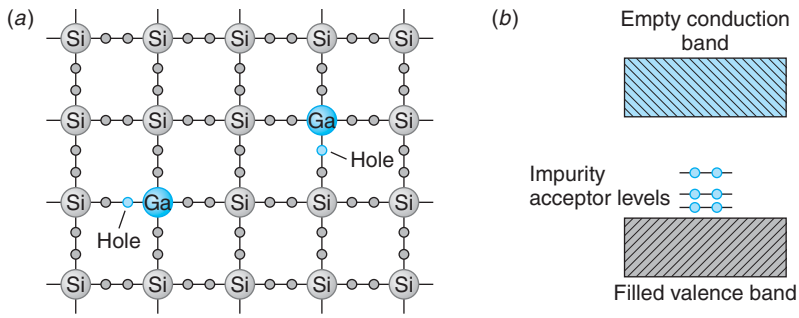

Figure 10-28 (*a*) Two-dimensional schematic illustration of silicon doped with gallium. Because gallium has only three valence electrons, there is a hole in one of its bonds. As electrons move into the hole, the hole moves about, contributing to the conduction of electric current. (*b*) Band structure of a *p*-type semiconductor such as silicon doped with gallium. The impurity atoms provide empty energy levels just above the filled valence band that accept electrons from the valence band.

STUDENTS-HUB.com Uploaded By: Malak Obaid

gallium is shown in Figure 10-28*b*. The empty levels shown just above the valence band are due to the holes resulting from the ionization of the gallium atoms. These levels are called *acceptor levels* because they accept electrons from the filled valence band when these electrons are thermally excited to a higher energy state. They arise because the holes, which act like positive charges, may be bound to the negative gallium core much like the fifth electron was bound to the positive arsenic core. Thus, the hole-gallium ion system also forms a hydrogenlike system and the energy levels of the hole can also be calculated approximately using the Bohr model with results similar to Equation 10-43. Since the energy-band diagrams like Figure 10-27*b* and 10-28*b* are drawn with electron energy increasing upward, hole energy in those diagrams increases downward. Ionizing the hole-gallium system means returning the hole to the valence band; hence these levels are just above the top of the valence band, as shown in Figure 10-28*b*, and their magnitudes are of the same order as those of the donor levels discussed previously. Increasing the energy of holes is equivalent to promoting electrons from the valence band into the acceptor levels. This creates holes in the valence band that are free to propagate in the direction of an electric field. Such a semiconductor is called a *p-type semiconductor* because the charge carriers are *positive* holes. The fact that conduction is due to the motion of holes can be verified by the Hall effect, described in the Exploring section on page 449.

EXAMPLE 10-8 **Donor Ionization Energy in Ge** If phosphorus is used to dope germanium to form an *n*-type semiconductor, what is the ionization energy of the levels? What is the radius of the electron's orbit? Phosphorus has five valence electrons. (The effective mass for electrons in germanium is about 0.1 m_e.)

SOLUTION

1. The magnitude of the ionization energy is computed from Equation 10-43 with $n = 1$:
$$E_1 = \frac{1}{2}\left(\frac{ke^2}{\hbar}\right)^2 \frac{m^*}{\kappa^2}$$

2. The dielectric constant κ for germanium is given in Table 10-5:
$$\kappa = 15.9$$

3. Substituting values into Equation 10-43 gives
$$E_1 = \frac{1}{2}\left(\frac{9 \times 10^9\ \text{N} \cdot \text{m}^2/\text{C}^2 \times (1.60 \times 10^{-19}\ \text{C})^2}{1.055 \times 10^{-34}\ \text{J} \cdot \text{s}}\right)^2 \frac{(0.1 \times 9.11 \times 10^{-31}\ \text{kg})}{(15.9)^2}$$
$$= 8.6 \times 10^{-22}\ \text{J} = 5.4 \times 10^{-3}\ \text{eV}$$

4. The orbit radius $\langle r_1 \rangle$ of the fifth phosphorus electron is computed from Equation 10-44 with $n = 1$:
$$\langle r_1 \rangle = a_0 \frac{m_e}{m^*} \kappa$$

5. Substituting values, where the Bohr radius $a_0 = 0.0529$ nm, gives
$$\langle r_1 \rangle = 0.0529 \times \frac{m_e}{0.1 m_e} \times 15.9$$
$$= 8.4\ \text{nm}$$

Remarks: *The value computed above for E_1 is very close to the experimental value of 12.0×10^{-3} eV, even though our calculation is a Bohr model approximation.*

STUDENTS-HUB.com Uploaded By: Malak Obaid

EXPLORING
Hall Effect

The number of donated electrons in a doped *n*-type semiconductor, or holes in a doped *p*-type semiconductor, is typically much greater than the intrinsic number of electron-hole pairs created by thermal excitation of electrons from the valence band to the conduction band. In an electric field, the current will therefore consist of both majority carriers (electrons in an *n*-type or holes in a *p*-type semiconductor) and minority carriers. The reality of conduction by motion of positive holes is clearly evident in the Hall effect, illustrated in Figure 10-29*a*. In this figure a thin strip of a doped semiconductor is connected to a battery (not shown), so that there is a current to the right. A uniform magnetic field B is applied perpendicular to the current. For the direction of the current and magnetic field shown, the magnetic force on a moving charged particle $q\,\mathbf{v}_d \times \mathbf{B}$ is upward (where $\mathbf{v}_d$ is the drift velocity) independent of whether the current is due to a positive charge moving to the right or a negative charge moving to the left. Let us assume for the moment that the charge carriers are electrons, as in Figure 10-29*b*. The magnetic force will then cause the electrons to drift up to the top of the strip, leaving the bottom of the strip with an excess positive charge. This will continue until the electrostatic field $\mathscr{E}$ caused by the charge separation produces an electric force on the charge carriers just balancing the magnetic force. The condition for balance is $q\mathscr{E} = qv_dB$. If w is the width of the strip, there will be a potential difference called the Hall voltage

$$V_H = \mathscr{E}w = v_dBw \qquad \textbf{10-45}$$

between the top and bottom of the strip. This potential difference can be measured with a high-resistance voltmeter. A measurement of the sign of the potential difference (i.e., whether the top of the strip is at a higher potential due to positive charge or lower potential due to negative charge) determines the sign of the majority carriers. Such measurements reveal that, indeed, the charge carriers are negative in *n*-type and positive in *p*-type semiconductors. The value of the Hall voltage provides a measurement of the drift velocity v_d. Since the current density $j = nqv_d$ can be easily measured from the total current and cross-sectional area of the strip, measurement of the drift velocity determines n, the number of charge carriers per unit volume.

Hall-effect probes are frequently used to measure magnetic field strengths. A current is established in a calibrated metal strip. Measuring the Hall voltage then yields the value of B (see Equation 10-46).

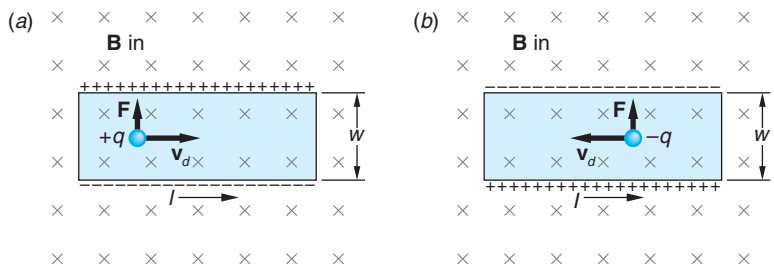

Figure 10-29 The Hall effect. The force on the charge carriers is up whether the carriers are positive charges moving to the right (*a*) or negative charges moving to the left (*b*). The sign of the charge carriers can be determined by the sign of the potential difference between the top and bottom of the strip, and the drift velocity can be determined by the magnitude of this potential difference. The thickness t of the strip is not shown.

STUDENTS-HUB.com Uploaded By: Malak Obaid

EXAMPLE 10-9 **Hall Effect in Aluminum** A strip of aluminum of width $w = 1.5$ cm and thickness $t = 250$ μm is placed in a uniform magnetic field of 0.55 T oriented perpendicular to the plane of the strip. When a current of 25 A is established in the strip, a voltage of 1.64 μV is measured across the width of the strip. What is the density of charge carriers in aluminum and how many charge carriers are provided, on average, by each atom?

SOLUTION

Substituting for the drift velocity v_d in terms of the current density (Equation 10-11) in Equation 10-45 yields

$$V_H = v_d Bw = \frac{jBw}{nq} = \frac{iB}{qnt} \qquad \textbf{10-46}$$

since $j = i/wt$. The density of the charge carriers in aluminum is then given by

$$n = \frac{iB}{qtV_H} = \frac{(25\text{ A})(0.55\text{ T})}{(1.60 \times 10^{-19}\text{ C})(250 \times 10^{-6}\text{ m})(1.64 \times 10^{-6}\text{ V})}$$

$$= 2.10 \times 10^{29}\text{ carriers/m}^3$$

The density of atoms N in aluminum is given by the following, where the density $\rho(\text{Al}) = 2.72 \times 10^3\text{ kg/m}^3$ and the molar mass $M = 26.98$ kg/mol:

$$N = \frac{N_A \rho}{M} = \frac{(6.02 \times 10^{26}\text{ atoms/mol})(2.702 \times 10^3\text{ kg/m}^3)}{26.98\text{ kg/mol}}$$

$$= 6.02 \times 10^{28}\text{ atoms/m}^3$$

Thus, each aluminum atom contributes on average $n/N = 3.5$ charge carriers.

The Quantum Hall Effect

According to Equation 10-46, the Hall voltage should increase linearly with the magnetic field B for a given current. In 1980, while studying the Hall effect in thin semiconductors at very low temperatures and very large magnetic fields, Klaus von Klitzing[9] discovered that a plot of V_H versus B was *not* linear, but included a series of plateaus, as shown in Figure 10-30*a*. That is, the Hall voltage is quantized. More specifically, if we define the Hall resistance $R_H = V_H/i$, it is the Hall resistance that is quantized, taking on only the values

$$R_H = \frac{V_H}{i} = \frac{R_K}{n} \qquad \textbf{10-47}$$

where R_K, called the *von Klitzing constant*, is related to the fundamental electron charge e and Planck's constant h by

$$R_K = \frac{h}{e^2} = \frac{6.626 \times 10^{-34}\text{ J} \cdot \text{s}}{(1.602 \times 10^{-19}\text{ C})^2} = 25{,}813\ \Omega \qquad \textbf{10-48}$$

STUDENTS-HUB.com Uploaded By: Malak Obaid

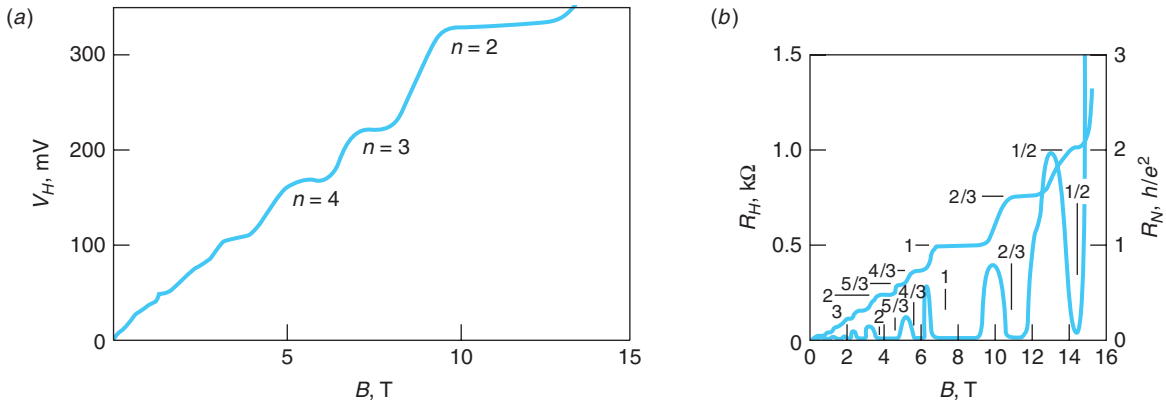

Figure 10-30 (*a*) A plot of the Hall voltage versus applied magnetic field shows plateaus, indicating that the Hall voltage is quantized. These data were taken at a temperature of 1.39 K with the current i held fixed at 25.52 μA. (*b*) The fractional quantum Hall effect. The Hall resistance R_H (the curve with the plateaus) is read on the left vertical axis, the normal resistance R_N (the curve with the peaks) on the right vertical axis. [*Data collected by Y. W. Suen and co-workers at Princeton University.*]

The values of n found by von Klitzing were small positive integers ($n = 1, 2, 3, \ldots$), as indicated in Figure 10-30*a*. Then, in 1982, Daniel Tsui and his co-workers,[10] while investigating the quantum Hall effect in ultrapure semiconductors, discovered quantized values of the Hall resistance for values of ν that were series of rational fractions formed from small integers. Values of R_H have been found thus far for more than 30 values of ν where $\nu = a, b$, where a and b are integers with no common factors. Several of these are seen in Figure 10-30*b*.

Von Klitzing's discovery is referred to as the integral quantized Hall effect (IQHE) and that of Tsui and his colleagues as the fractional quantized Hall effect (FQHE). The theoretical models that have been developed to explain these phenomena are as yet incomplete and, in any case, beyond the scope of our discussion here; however, we can give a brief qualitative description of the IQHE. In the "normal" Hall effect the material carries a current i due to an applied electric field $\mathscr{E}$. The electric field is perpendicular to the applied magnetic field $\mathbf{B}$, and as a result, the charge carriers move in a circular path, or orbit, of radius $r = m^*v/qB$. The fact that electrons obey the Pauli exclusion principle prevents the orbits from overlapping and determines how closely the electrons can group together on the negative side of the sample. Recalling that the orbital motion of electrons is quantized with only certain radii being allowed—namely those for which the orbit circumference equals an integral number of de Broglie wavelengths—we see that increasing the magnetic field decreases the orbit radius, but such decreases must occur suddenly and result in another, smaller allowed radius. Thus, more electron orbits can fit without overlapping in a given area and the density of charge carriers increases on the edges of the semiconductor sample. This increases the frequency of collisions and hence the Hall resistance. Since the orbit radii change only in quantized steps, so must the Hall resistance. Surprisingly, when the Hall resistance is on one of the plateaus, the ordinary resistance $R = V/i$ falls to zero, as illustrated by the multiple peaked curve in Figure 10-30*b*. The additional plateaus that occur in the FQHE are due to electron-electron spin interactions.

Because the von Klitzing constant can be measured with a precision of better than 1 part in 10^{10}, the quantum Hall effect is now used to define the standard of resistance. The ohm is now defined so that R_K has the value 25,812.807 Ω exactly.

STUDENTS-HUB.com Uploaded By: Malak Obaid

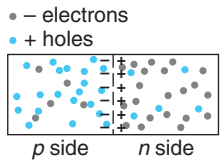

Figure 10-31 A *pn* junction. Because of the difference in their concentrations, holes diffuse from the *p* side to the *n* side and electrons diffuse from the *n* side to the *p* side. As a result, there is a double layer of charge at the junction, with the *p* side negative and the *n* side positive.

Spin Hall Effect

A new vista for spintronics was opened in 2004 with the observation of the spin Hall effect in GeAs at 20 K by David Awschalom and his group. In the spin Hall effect the electrons of a charge current flow in a nonmagnetic material in the absence of an external magnetic field but with an applied external electric field separate perpendicular to the conventional current direction into spin-up and spin-down populations that accumulate on opposite sides of the conducting material. The same phenomenon was detected at 295 K (room temperature) in ZnSe in 2006 by the same researchers. Although the effect is small, the potential useful applications, e.g., injecting spin-polarized electrons into semiconductor devices, would be enormous if current experiments to improve the size of the effect are successful.

10-8 Semiconductor Junctions and Devices

Semiconductor devices such as diodes and transistors make use of *n*-type and *p*-type semiconductors joined together as shown in Figure 10-31. In practice, the two types of semiconductors are often a single silicon crystal doped with donor impurities on one side and acceptor impurities on the other. The region in which the semiconductor changes from a *p*-type to an *n*-type is called a *junction*.

When an *n*-type and *p*-type semiconductor are placed in contact, the initially unequal concentrations of electrons and holes result in the diffusion of electrons across the junction from the *n* side to the *p* side until equilibrium is established. The result of this diffusion is a net transport of positive charge from the *p* side to the *n* side. Unlike the case when two different metals are in contact, there are fewer electrons available to participate in this diffusion because the semiconductor is not a particularly good conductor. The diffusion of electrons and holes creates a double layer of charge at the junction similar to that on a parallel-plate capacitor. There is thus a potential difference V across the junction, which tends to inhibit further diffusion. In equilibrium, the *n* side with its net positive charge will be at a higher potential than the *p* side with its net negative charge. In the junction region, there will be very few charge carriers of either type, so the junction region has a high resistance. Figure 10-32 shows the energy-level diagram for a *pn* junction. The junction region is also called the *depletion region* because it has been depleted of charge carriers.

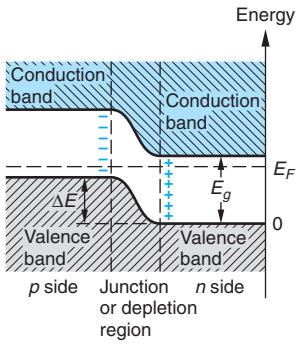

Figure 10-32 Electron energy levels for an unbiased *pn* junction.

Diodes

A semiconductor with a *pn* junction can be used as a simple diode rectifier. In Figure 10-33, an external potential difference has been applied across the junction by connecting a battery and resistor to the semiconductor. When the positive terminal of the battery is connected to the *p* side of the junction, as shown in Figure 10-33*a*, the diode is said to be *forward biased*. Forward biasing lowers the potential across the junction. The diffusion of electrons and holes is thereby increased as they attempt to reestablish equilibrium, resulting in a current in the circuit. If the positive terminal of the battery is connected to the *n* side of the junction, as shown in Figure 10-33*b*, the diode is said to be

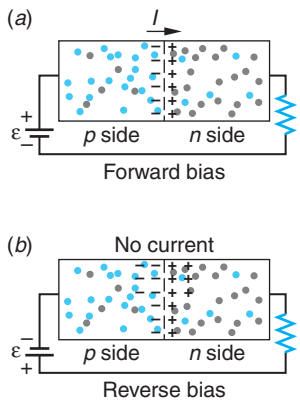

Figure 10-33 A *pn*-junction diode. (*a*) Forward-biased *pn* junction. The applied potential difference enhances the diffusion of holes from the *p* side to the *n* side and electrons from the *n* side to the *p* side, resulting in a current I. (*b*) Reverse-biased *pn* junction. The applied potential difference inhibits the further diffusion of holes and electrons, so there is no current.

STUDENTS-HUB.com Uploaded By: Malak Obaid

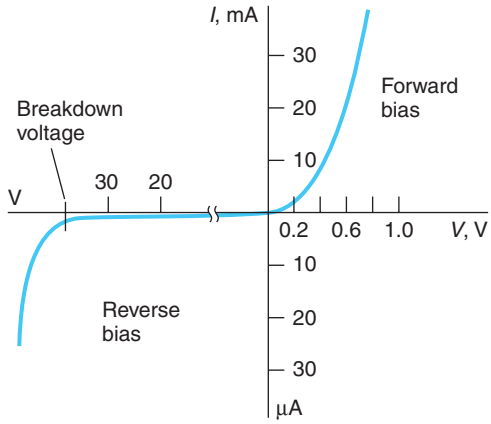

Figure 10-34 Current versus applied voltage across a *pn* junction. Note the different scales for the forward- and reverse-bias conditions.

reverse biased. Reverse biasing tends to increase the potential difference across the junction, thereby further inhibiting diffusion. Figure 10-34 shows a plot of current versus voltage for a typical semiconductor junction. Essentially, the junction conducts only in one direction, the same as a vacuum-tube diode. Junction diodes have replaced vacuum diodes in nearly all applications except when a very high current is required.

We can get an idea of how the current depends on applied voltage quantitatively if we note that the electrons and holes, being at the high energy end of the distribution, are approximately described by the Maxwell-Boltzmann distribution. Let N_e be the number of conduction electrons in the n region. With no external voltage, only a small fraction given by $N_e e^{-eV/kT}$ will have enough energy to diffuse across the contact potential difference. When a forward bias V_b is applied, the number that can cross the barrier becomes

$$N_e e^{-e(V-V_b)/kT} = (N_e e^{-eV/kT}) e^{+eV_b/kT}$$

The current due to the majority electron carriers in the n region will be

$$I = I_0 e^{+eV_b/kT}$$

where I_0 is the current with no bias. The current due to the minority carriers, the holes from the n side, will be merely I_0, the same as with no bias. (The minority carriers are swept across the junction by the contact potential V with or without a bias voltage.) The net current due to carriers from the n side will therefore be

$$I_{\text{net}} = I_0(e^{+eV_b/kT} - 1) \qquad \textbf{10-49}$$

If we now consider the current due to the majority and minority carriers from the p side, we obtain the same results. We can use Equation 10-49 for the total current if we interpret I_0 as the total current due to both kinds of minority carriers, holes in the n region and electrons in the p region. For positive V_b the exponential quickly dominates. For $V_b = 0$, the current is 0, and for V_b less than zero, the current saturates at $-I_0$, due to the flow of minority carriers. Note that the current in Figure 10-35 suddenly increases in magnitude at extreme values of reverse bias. In such large electric fields, two things can happen: either electrons are stripped from their atomic bonds or the few free electrons that exist in a reversed-biased junction are accelerated across the junction and gain enough energy to cause others to break loose. The first effect is

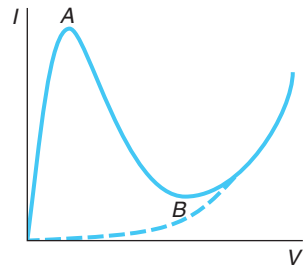

Figure 10-35 Current versus applied voltage for a tunnel diode. Up to point A, an increase in the bias voltage enhances tunneling. Between points A and B, an increase in the bias voltage inhibits tunneling, i.e., the diode acts as if it has negative resistance. After point B, the tunneling is negligible, and the diode behaves like an ordinary *pn*-junction diode, shown by the dashed line.

STUDENTS-HUB.com Uploaded By: Malak Obaid

called *Zener breakdown*; the second, *avalanche breakdown*. Although such a breakdown can be disastrous in a circuit where it is not intended, the fact that it occurs at a sharp voltage value makes it of use in a special voltage reference standard known as a *Zener diode*.

An interesting effect that we can discuss only qualitatively occurs if both the *n* side and the *p* side of a *pn*-junction diode are so heavily doped that the bottom of the conduction band lies below the top of the valence band. Figure 10-36*a* shows the energy-level diagram for this situation. Since there are states on the *p* side with the same energy as states on the *n* side and the depletion region is now so narrow, electrons can tunnel across the potential barrier (see Section 6-6). This flow of electrons is called *tunneling current*, and such a heavily doped diode is called a *tunnel diode*.

At equilibrium with no bias, there is an equal tunneling current in each direction. When a small bias voltage is applied across the junction, the energy-level diagram is as shown in Figure 10-36*b* and the tunneling of electrons from the *n* to the *p* side is increased, whereas that in the opposite direction is decreased. This tunneling current in addition to the usual current due to diffusion results in a considerable net current. When the bias voltage is increased slightly, the tunneling current decreases because there are fewer states on the *p* side with the same energy as states on the *n* side. Although the diffusion current is increased, the net current is decreased. At large bias voltages the energy-level diagram is as shown in Figure 10-36*c*, the tunneling current is completely negligible, and the total current increases with increasing bias voltage due to diffusion as in an ordinary *pn*-junction diode. Figure 10-35 shows the current versus voltage curve for a tunnel diode. Such diodes are used in electric circuits because of their very fast response time. When operated near the peak in the current versus voltage curve, a small change in bias voltage results in a large change in the current.

Among the many applications of semiconductors with *pn* junctions are particle detectors called *surface-barrier detectors*. These consist of a *pn*-junction semiconductor with a large reverse bias so that there is ordinarily no current. When a high-energy particle, such as an electron, passes through the semiconductor, it excites electrons into the conduction band, creating many electron-hole pairs as it loses energy. The intrinsic electric field sweeps the electrons toward the positive (*n*) side of the junction and the holes toward the negative (*p*) side. The resulting current pulse signals the passage of the particles and records the energy lost by the particle in the detector. The pulses are of short duration ($10^{-8} - 10^{-7}$ seconds), making possible high-energy-resolution measurements.

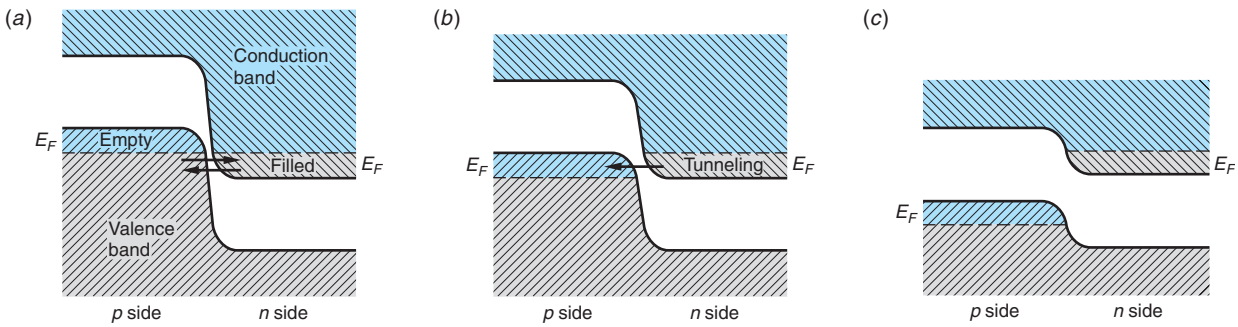

Figure 10-36 Electron energy levels for a heavily doped *pn*-junction tunnel diode. (*a*) With no bias voltage, some electrons tunnel in each direction. (*b*) With a small bias voltage, the tunneling current is enhanced in one direction, making a sizable contribution to the net current. (*c*) With further increases in the bias voltage, the tunneling current decreases dramatically.

STUDENTS-HUB.com Uploaded By: Malak Obaid

Light-emitting and light-absorbing *pn*-junction semiconductors function similar to gaseous atoms emitting and absorbing light, with the conduction and valence bands analogous to the atomic energy levels. The light-absorbing *pn*-junction semiconductor diode, or *solar cell*, is illustrated schematically in Figure 10-37*a*. When photons with energy greater than the gap energy (1.1 eV in silicon) strike the *pn*-junction, they can excite electrons from the valence band into the conduction band, leaving holes in the valence band. This region is already rich in holes. Some of the electrons created by the photons will recombine with holes, but some will migrate to the junction. From there they are accelerated into the *n*-type region by the intrinsic electric field between the double layers of charge. This creates an excess negative charge in the *n*-type region and excess positive charge in the *p*-type region. The result is a potential difference, a *photovoltage*, between the two regions, which in practice is about 0.6 V. If a load resistance is connected across the two regions, a charge flows through the resistance. Some of the incident light energy is thus converted into electrical energy. The current in the resistor is proportional to the number of incident photons, which is in turn proportional to the intensity of the incident light.

Light-emitting diodes (*LEDs*) are *pn*-junction semiconductors with a large forward bias that produces a large excess concentration of electrons on the *p* side and holes on the *n* side of the junction. (See Figure 10-37*b*.) Under these conditions, the diode emits light as the electrons and holes recombine. This is essentially the reverse of the process that occurs in a solar cell. Following the first practical demonstration of an LED (in 1962), the performance of LEDs has steadily improved. (See Figure 10-38.) They can be fabricated in all of the primary colors and, more recently, white light as well, portending them as a common source of white light in the future. LEDs already provide a viable alternative to filtered incandescent lighting in applications requiring monochromatic light. They are used, for example, as indicator lamps in appliances,

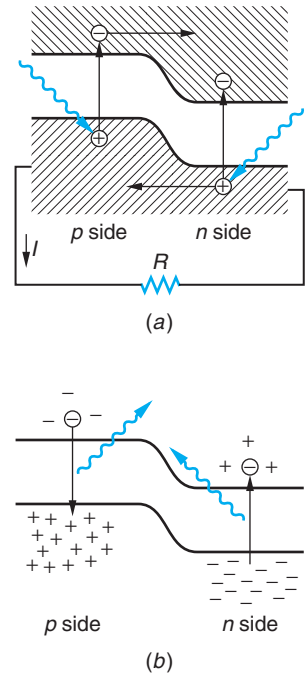

Figure 10-37 (*a*) A *pn* junction as a solar cell. Radiation striking the junction produces electrons and holes. The electrons are swept from the *p* side and holes from the *n* side by the intrinsic electric field. The accumulated charge results in a potential difference that produces a current through an external load. (*b*) A *pn* junction as an LED. Large forward bias produces current of electrons moving to the left and holes moving to the right. When they recombine, radiation is emitted.

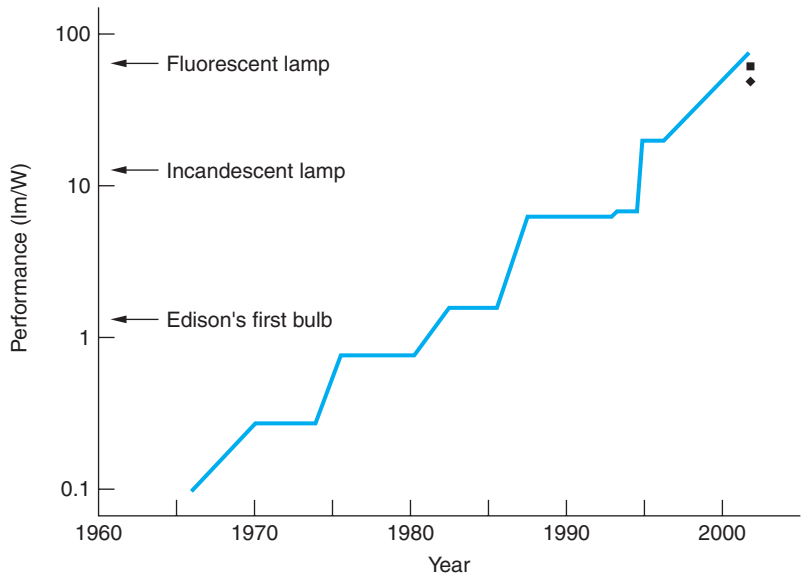

Figure 10-38 Summary of the performance improvements in LEDs over the span of their existence. The ■ marks the current performance of small-molecule OLEDs; the ◆ marks that of the polymer OLEDs. A few performance benchmarks are indicated on the vertical axis.

STUDENTS-HUB.com Uploaded By: Malak Obaid

The development of InGaAlP HB LEDs in the early 1990s led to their rapid application to automotive rear lighting. The recent development of high-powered, large area, white GaN HB LEDs makes automobile headlights using these LEDs a possibility for the near future.

electronic equipment, calculators, and digital watches. In automobiles they are used in instrument panel lighting, and high-brightness (HB) LEDs are now often used for rear, stop, and turn lights. In traffic signals the red, amber, and green LED arrays now in common use require only 10 percent of the power consumed by the standard 140-W incandescent lamps, are brighter, and have a much longer lifetime. Rapid development of organic semiconductor light-emitting diodes (OLEDs) in the 1990s was catalyzed by worldwide efforts to construct large, full-color, flat-screen displays. Fabricated from small organic molecules and various polymers, OLEDs have an advantage over LEDs in that they can be produced on a large scale at very low cost. In LEDs high forward currents result in a very large population inversion, i.e., electrons on the *p* side and holes on the *n* side, so that stimulated emission dominates the light emission process and lasing results. By appropriate construction of the diode, a resonant cavity can be formed, leading to the production of a coherent beam of laser light in a selected direction (see Figure 10-39).

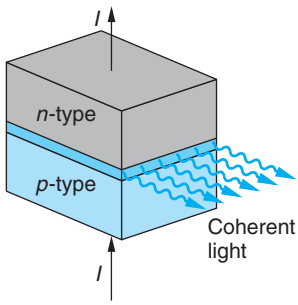

Figure 10-39 The resonant cavity is formed by cleaving the ends of the diode crystal parallel to one another and with the proper separation. Gallium arsenide and similar compounds, which have much higher photon-production efficiency than silicon, are typically used as diode laser semiconductors. Their light-energy-out to electrical-energy-in ratios are greater than 50 percent.

Transistors

The transistor, invented in 1948 by William Shockley, John Bardeen, and Walter Brattain,[11] has revolutionized the electronics industry and our everyday world. A simple junction transistor consists of three distinct semiconductor regions called the *emitter*, the *base*, and the *collector*. The base is a very thin region of one type of semiconductor sandwiched between two regions of the opposite type. The emitter semiconductor is much more heavily doped than either the base or the collector. In an *npn* transistor, the emitter and collector are *n*-type semiconductors and the base is a *p*-type semiconductor; in a *pnp* transistor, the base is an *n*-type semiconductor and the emitter and collector are *p*-type semiconductors. In a *pnp* transistor holes are emitted by the emitter; in an *npn* transistor electrons are emitted.

Figures 10-40 and 10-41 show, respectively, a *pnp* transistor and an *npn* transistor with the symbols used to represent each transistor in circuit diagrams. Notice that a transistor consists of two *pn* junctions. The operation of a *pnp* transistor is described in the MORE section *How Transistors Work*. The operation of an *npn* transistor is similar.

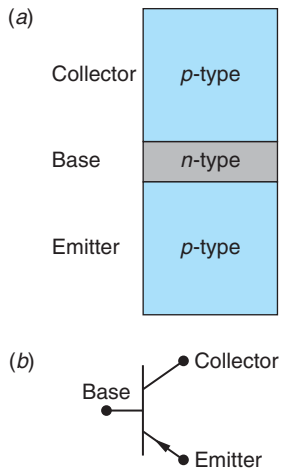

Figure 10-40 (*a*) A *pnp* transistor. The heavily doped emitter emits holes that pass through the thin base to the collector. (*b*) Symbol for a *pnp* transistor in a circuit. The arrow points in the direction of the conventional current, which is the same as that of the emitted holes.

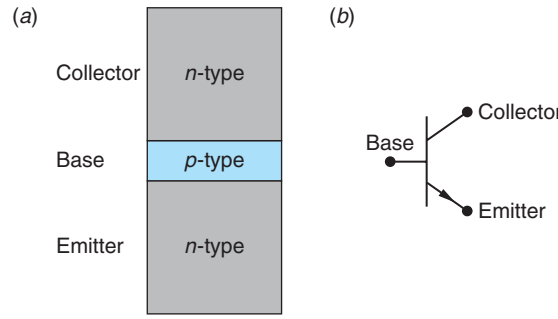

Figure 10-41 (*a*) An *npn* transistor. The heavily doped emitter emits electrons that pass through the thin base to the collector. (*b*) Symbol for an *npn* transistor. The arrow points in the direction of the conventional current, which is opposite the direction of the emitted electrons.

STUDENTS-HUB.com Uploaded By: Malak Obaid

(*a*)

(*a*) LED traffic lights use 10 percent of the power of the old 140-W signal lamps, last far longer, and are collectively brighter. (*b*) Automobile LED rear lighting and brake lights have become ubiquitous, as have LED traffic signals. Pictured here are examples of the scores of different colors, shapes, and sizes of vehicle clearance and safety LED lights one sees every day on the streets and highways. [*Photos by Francisco Roman.*]

(*b*)

More

How Transistors Work, on the home page at www.whfreeman.com/tiplermodernphysics5e, describes the way transistors function in electrical circuits. Also located here are Equations 10-50 through 10-54, Example 10-10, and Figures 10-42 and 10-43.

Questions

9. Why is a semiconductor diode less effective at high temperatures?
10. Explain why adding impurities to metals decreases their conductivity but adding impurities to semiconductors increases their conductivity.
11. What would you expect to be the effect on the conductivity when impurities are added to an insulator?

STUDENTS-HUB.com Uploaded By: Malak Obaid

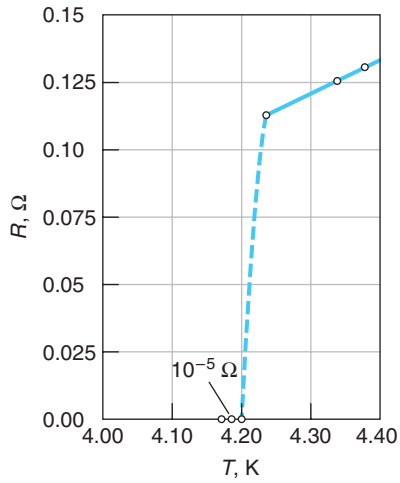

Figure 10-44 Plot by Kamerlingh Onnes of the resistance of mercury versus temperature, showing sudden decrease at the critical temperature $T = 4.2$ K signifying the onset of superconductivity.

10-9 Superconductivity

In 1911, just a few years after he had succeeded in liquefying helium and while he was investigating the properties of materials at liquid helium temperatures, the Dutch physicist H. Kamerlingh Onnes discovered that for some materials a certain temperature exists, called the *critical temperature* T_c, below which the resistivity is zero and the conductivity $\sigma = 1/\rho \rightarrow \infty$. He called this phenomenon *superconductivity*. Figure 10-44 shows the plot Kamerlingh Onnes obtained of the resistance of mercury versus temperature. The critical temperature for mercury is 4.2 K. The critical temperature varies from material to material, but below this temperature the electrical resistance of the material is zero. Critical temperatures for other superconducting elements range from less than 0.1 K for hafnium and iridium to 9.2 K for niobium. The critical temperatures of several superconducting materials are given in Table 10-6. In the presence of a magnetic field B, the critical temperature is lower than it is when there is no field. As the magnetic field increases, the critical temperature decreases, as illustrated in Figure 10-45. If the magnetic field is greater than some critical field B_c, superconductivity does not exist at any temperature. The values of T_c in the table are for $B = 0$.

Many metallic compounds are also superconductors. For example, the superconducting alloy Nb_3Ge, discovered in 1973, has a critical temperature of 23.2 K, which was the highest known until 1986, when the first of the complex high-T_c cuprate ceramic superconductors was discovered. More recently, in 2001 Jun Akimitsu discovered that the metal compound MgB_2, available "off the shelf" for about \$2/g, became superconducting at 39 K, as of this writing the highest T_c yet for a conventional superconductor. (See Table 10-6.) Despite the cost and inconvenience of refrigeration with expensive liquid helium, which boils at 4.2 K, many superconducting magnets have been built using such materials.

Electromagnets wound with superconducting wire are used in applications ranging from medical diagnostic MRI systems to beam-focusing and beam-bending magnets at large particle accelerators worldwide.

Table 10-6 T_c and B_c values for some type I and type II superconductors

Type I element	T_c (K)	B_c (at 0 K; T)	Type II compound	T_c (K)	B_{c2} (at 0 K; T)
Al	1.175	0.0105	Nb_3Sn	18.1	24.5
Cd	0.517	0.0028	Nb_3Ge	23.2	34.0
Hg	4.154	0.0411	NbN	16.0	15.3
In	3.408	0.0282	V_3Ga	16.5	35.0
Nb	9.25	0.2060	V_3Si	17.1	15.6
Os	0.66	0.0070	PbMoS	14.4	6.0
Pb	7.196	0.0803	CNb	8.0	1.7
Sn	3.722	0.0305	MgB_2	39.0	16
Tl	2.38	0.0178	Rb_3C_{60}	29.0	?
Zn	0.85	0.0054	Cs_2RbC_{60}	33.0	?

STUDENTS-HUB.com Uploaded By: Malak Obaid

The conductivity of a superconductor cannot be defined since its resistance is zero. There can be a current in a superconductor even when the electric field in the superconductor is zero. Such currents are called *supercurrents*. Indeed, steady currents have been observed to persist for years without apparent loss in superconducting rings in which there was no electric field.

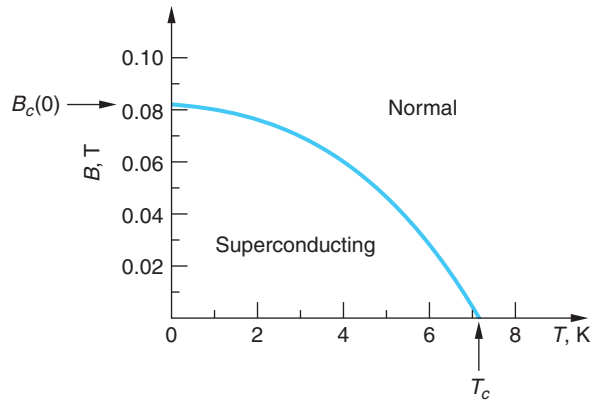

Figure 10-45 Variation of the critical temperature with magnetic field for lead. Note that B_c approaches zero as T approaches T_c.

Meissner Effect

Consider a superconducting material that is originally at a temperature greater than the critical temperature and is in the presence of a small external magnetic field $B < B_c$. We now cool the material below the critical temperature so that it becomes superconducting. Since the resistance is now zero, there can be no emf in the superconductor. Thus, from Faraday's law, the magnetic field in the superconductor cannot change. We therefore expect from classical physics that the magnetic field in the superconductor will remain constant. However, it is observed experimentally that when a superconductor is cooled below the critical temperature in an external magnetic field, the magnetic field lines are expelled from the superconductor and thus the magnetic field inside the superconductor is zero. (See Figure 10-46.) This effect was discovered by H. W. Meissner

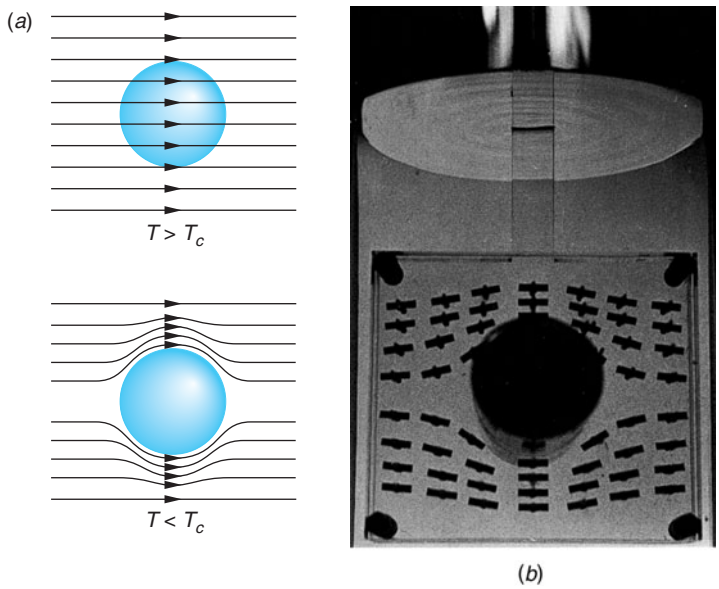

Figure 10-46 (*a*) The Meissner effect in a superconducting sphere cooled in a constant applied magnetic field. As the temperature drops below the critical temperature T_c, the magnetic field lines are expelled from the sphere. (*b*) Demonstration of the Meissner effect. A superconducting tin cylinder is situated with its axis perpendicular to a horizontal magnetic field. The directions of the field lines near the cylinder are indicated by weakly magnetized compass needles mounted in a Lucite sandwich so that they are free to turn. [*Courtesy of A. Leitner, Rensselaer Polytechnic Institute.*]

STUDENTS-HUB.com Uploaded By: Malak Obaid

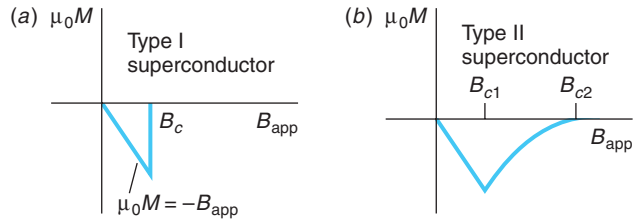

Figure 10-47 Plots of μ_0 times the magnetization M versus applied magnetic field for type I and type II superconductors. (*a*) In a type I superconductor, the resultant magnetic field is zero below a critical applied field B_c because the field due to induced currents on the surface of the superconductor exactly cancels the applied field. Above the critical field, the material is a normal conductor and the magnetization is too small to be seen on this scale. (*b*) In a type II superconductor, the magnetic field starts to penetrate the superconductor at a field B_{c1}, but the material remains superconducting up to the field B_{c2}, after which it becomes a normal conductor.

and R. Ochsenfeld in 1933 and is now known as the *Meissner effect*. It, not zero resistance, is the criterion that determines if a material is a superconductor. The mechanism by which the magnetic field lines are expelled or, more specifically, canceled within the bulk of the superconductor is that a supercurrent (called a screening current) is induced on the surface in such a direction as to exactly cancel the external field within the material.[12] Thus, the superconductor exhibits perfect diamagnetism. Establishing the supercurrent "costs" the superconductor an amount of energy per unit volume equal to $B^2/2\mu_0$, where μ_0 is the permeability of the vacuum. When the field B becomes larger than B_c, there is insufficient energy available and the material reverts to its "normal" resistive state. The magnetic levitation shown in the photograph below results from the repulsion between the permanent magnet producing the external field and the magnetic field produced by the currents induced in the superconductor.

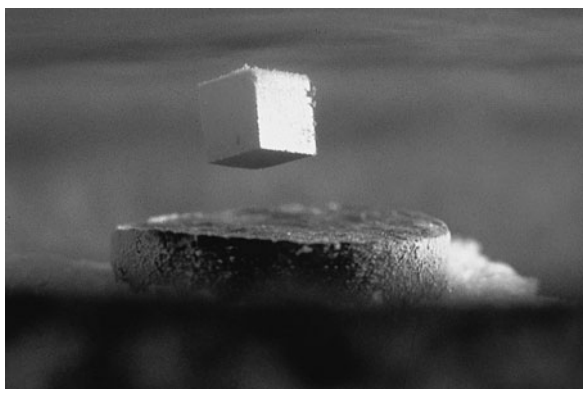

A small, cubicle permanent magnet levitates above a disk of the superconductor yttrium-barium-copper oxide, cooled by liquid nitrogen to 77 K. At temperatures below 92 K, the disk becomes superconducting. The magnetic field of the cube sets up circulating electric supercurrents in the superconducting disk, such that the resultant magnetic field in the superconductor is zero. These currents produce a magnetic field opposite to that of the cube, and thus the cube is repelled. [*Courtesy of IBM Research.*]

Only certain superconductors called *type I*, or *"soft,"* superconductors exhibit the complete Meissner effect. Type I superconductors are primarily very pure metal elements. Figure 10-47*a* shows a plot of the magnetization M times μ_0 versus the applied magnetic field B_{app} for a type I superconductor. For a magnetic field less than the critical field B_c, the magnetic field $\mu_0 M$ induced in the superconductor is equal and opposite to the external magnetic field; that is, the superconductor is a perfect diamagnet. The values of B_c for type I superconductors are all too small for such materials to be useful in the coils of a superconducting magnet. (See Table 10-6.)

Other materials, known as *type II*, or *"hard," superconductors*, have a magnetization curve similar to that in Figure 10-47*b*. Such materials are usually alloys or metals that have large resistivities in the normal state. Type II superconductors exhibit *two* critical magnetic fields, B_{c1} and B_{c2}, as shown in Figure 10-48 for tantalum. Applied fields less than B_{c1} result in the Meissner effect of total magnetic flux cancellation and the entire sample is superconducting, as in type I superconductors. Applied fields greater than B_{c2} result in complete penetration of the magnetic field throughout the sample, and the resistivity of

STUDENTS-HUB.com Uploaded By: Malak Obaid

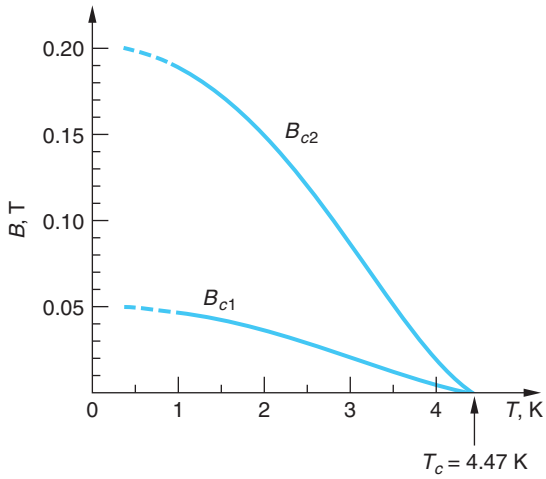

Figure 10-48 Critical magnetic fields B_{c1} and B_{c2} for Ta (99.95 percent) as a function of temperature. Below the B_{c1} curve Ta exhibits the Meissner effect. Between the two curves is a mixed, or vortex, state with filaments of normal Ta penetrating the superconducting state. Above the B_{c2} curve there is complete magnetic field penetration and the entire sample has normal resistivity.

the material returns to normal. However, in the region between B_{c1} and B_{c2} there is partial penetration of the magnetic field, the field lines being confined to *flux tubes*, also called *vortices*, in which the material has normal resistivity. The surrounding material remains field free and superconducting, as illustrated schematically in Figure 10-49. Each flux tube contains one quantized unit of magnetic flux, as will be described later in this section. For many type II superconductors the critical field B_{c2} may be several hundred times larger than the typical values of critical fields for type I superconductors (see Table 10-6). For example, the alloy Nb_3Ge has a critical field $B_{c2} = 34$ T. Such materials can be used to construct high-field superconducting magnets.

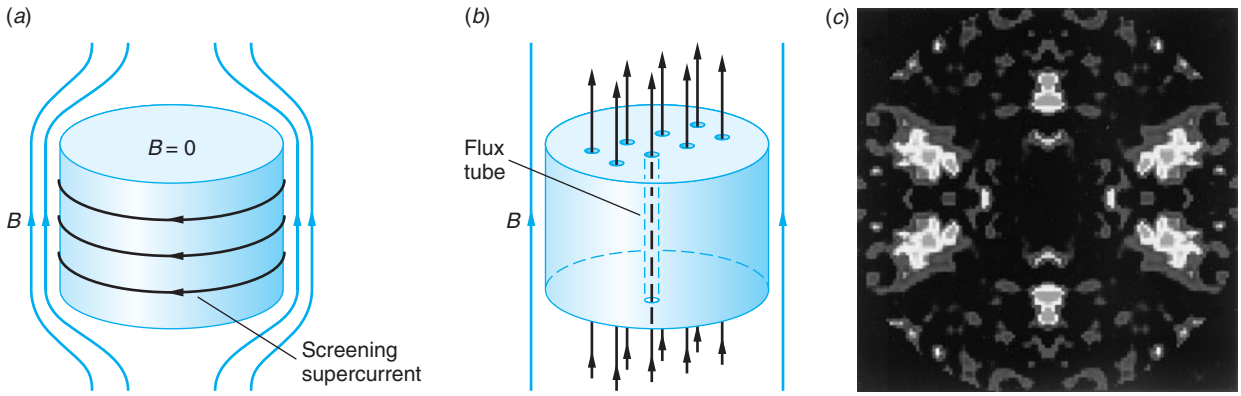

Figure 10-49 (*a*) Below B_{c1} the type II material shows the Meissner effect. For temperatures below T_c the material is superconducting and $B = 0$ throughout the volume. (*b*) For $B_{c1} < B < B_{c2}$, magnetic field lines penetrate the material but are confined to flux tubes of normally resistive material that form the so-called vortex lattice. For a given $T < T_c$, as the applied field B approaches B_{c2}, the size of the superconducting region shrinks as more flux tubes occupy the volume. When $B > B_{c2}$, the entire material has normal resistivity. (*c*) The lattice of magnetic vortices in UPt_3, a strongly type II superconductor, is shown clearly by neutron diffraction.

STUDENTS-HUB.com Uploaded By: Malak Obaid

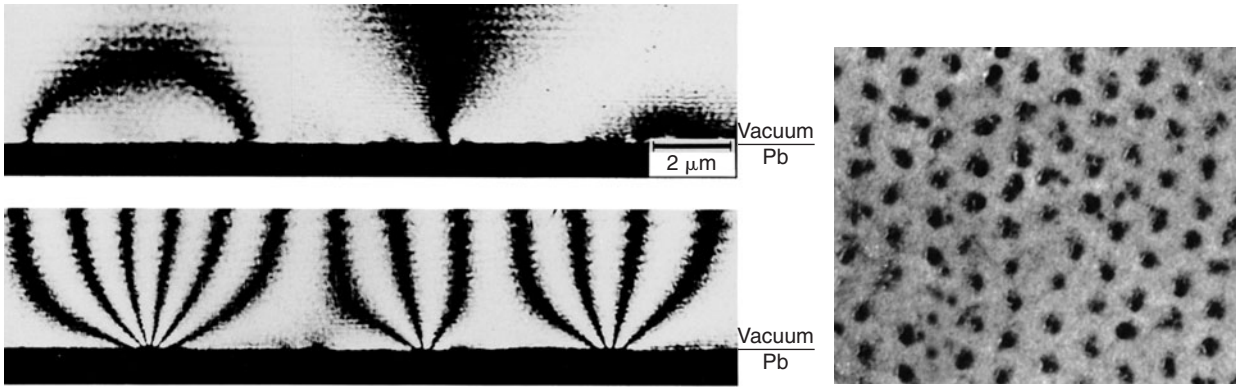

(*a*) (*b*)

Fluxoids penetrating a superconducting film. The image has been formed by the technique of electron holography, in which coherent electron beams are used in place of coherent light beams to create a hologram. Electrons passing by a magnetic field are phase-shifted; i.e., the phase term in their wave function changes. (The shift arises from a phenomenon known as the Aharonov-Bohm effect.) By superposing such a phase-shifted beam with an unshifted reference beam, an interference pattern is created that can be interpreted as an image of the magnetic field. For the upper images, a magnetic field was applied perpendicular to a thin superconducting lead film. When the field was weak, it was expelled by the Meissner effect. A stronger field, however, penetrated the film. The fluxoids shown arose from vortices of current set up in the superconductor—not from the applied field directly. In the upper right is an isolated fluxoid; in the upper left is an antiparallel pair of fluxoids. The lower micrograph, in which the lead film is thicker, shows penetration by bundles of fluxoids. [*Courtesy of Akira Tonomura, Hitachi Ltd., Saitama, Japan.*] (*b*) A lattice of fluxoid vortices penetrating the surface of a superconductor. They were made visible for the photograph by a dusting of fine ferromagnetic particles. [*Courtesy of U. Essmann.*]

EXPLORING
Flux Quantization

Consider a superconducting loop of area A carrying a current. There can be a magnetic flux $\phi_m = B_n A$ through the loop due to the current in the loop. According to Faraday's law of induction, if the flux changes, an emf will be induced in the loop that is proportional to the rate of change of the flux. But for a superconductor there can be no emf in the loop because there is no resistance. Therefore, the flux through the ring is frozen and cannot change. Indeed, the quantum-mechanical treatment of superconductivity reveals that the total flux through the loop is quantized and is given by

$$\phi_m = n\frac{h}{2e} \qquad n = 1, 2, 3, \ldots$$

The quantum of flux, called a *fluxoid*, is

$$\phi_0 = \frac{h}{2e} = 2.0678 \times 10^{-15}\ \mathrm{T \cdot m^2}$$

Each flux tube in a type II superconductor with $B_{c1} < B < B_{c2}$ contains one quantum of flux.

STUDENTS-HUB.com Uploaded By: Malak Obaid

BCS Theory

Our discussion of the classical free-electron theory in Section 10-2 considered the ions of the crystal lattice to be fixed. Resistivity was due to the interactions of the electrons with the ions of the lattice, and both electron-electron interactions and the effects of lattice vibrations, i.e., electron-phonon interactions, were ignored. In the quantum theory of conduction, lattice vibrations were explicitly taken into account (see Equations 10-41 to 10-43). Lattice vibrations are also responsible for the *isotope effect*[13] in superconductivity, discovered in 1950. This experimental observation revealed that the critical temperature depended on the isotopic mass of the crystal according to

$$M^{\alpha}T_c = \text{constant} \qquad \textbf{10-55}$$

where M is the average isotopic mass and α varies from material to material. For example, for mercury $\alpha = 0.50$ and $T_c = 4.185$ K for samples of average isotopic mass $M = 199.5$ u, whereas $T_c = 4.146$ K for samples with $M = 203.4$ u. Table 10-7 lists experimental values for α for a few superconductors.

The importance of the discovery represented by Equation 10-55 is to tell us that the lattice vibrations, hence the electron-phonon interactions, cannot be ignored. The assumption of fixed lattice ions is equivalent to assuming that $M \rightarrow \infty$ for electron-lattice ion interactions. But if $M \rightarrow \infty$, then T_c would be zero for all materials.

It had been recognized for some time that superconductivity is due to a collective behavior of the conducting electrons, and discovery of the isotope effect pointed to the crucial interaction as being with the phonons. In 1957, John Bardeen, Leon Cooper, and Bob Schrieffer published a successful theory of superconductivity now known as the *BCS theory*.[14] According to this theory, the electrons in a superconductor are coupled in pairs at low temperatures. The coupling comes about because of the interaction between electrons and the crystal lattice. An electron moving through the lattice of positive ions interacts with and perturbs it, as illustrated in Figure 10-50. The electron attracts the positive ions nearby, displacing them slightly, resulting in a region of increased positive charge density. Because the ions are bound to the lattice by elastic forces, this region of increased charge density propagates through the material as a vibrational wave in the lattice, i.e., a *phonon*. The momentum of the phonon has been provided by the electron, and we can think of the electron as having emitted a phonon.

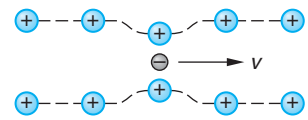

Figure 10-50 An electron traveling through the lattice of positive ions generates a wave of increased charge density, shown in two dimensions by the dashed lines. The momentum of the wave comes at the expense of the electron's momentum. A second electron may encounter the wave and absorb its momentum. The net effect is an attraction between the two electrons and the production, for $T < T_c$, of a Cooper pair.

Table 10-7 Experimental values of α for a few superconductors

Material	α	Material	α
Cd	0.32	Nb_3Sn	0.08
Hg	0.50	Os	0.15
Pb	0.49	Zn	0.45

Data from C. Kittel, *Introduction to Solid State Physics,* 8th ed. (New York: Wiley, 2005).

STUDENTS-HUB.com Uploaded By: Malak Obaid

A second electron that encounters the wave of increased positive charge concentration is attracted toward it by the Coulomb interaction and can absorb the momentum carried by the wave; i.e., it may absorb the phonon. Thus, the two electrons can interact via the phonon and (very important) the interaction is an attractive one since both electrons experience an attractive force toward the region of increased positive charge density. At low temperatures ($T < T_c$) the attraction between the two electrons can exceed the Coulomb repulsion between them. Then the electrons can form a bound state called a *Cooper pair*, provided the temperature is low enough so that the number and energy of randomly generated thermal phonons will not disrupt its formation. The electrons in a Cooper pair have opposite spins and equal and opposite linear momenta. Thus, they form a system with zero spin and zero momentum. Each Cooper pair may be considered as a single particle with zero spin. Such a particle does not obey the Pauli exclusion principle, so any number of Cooper pairs may be in the same quantum state with the same energy.[15] In the ground state of a superconductor (at $T = 0$), all the electrons are in Cooper pairs and all the Cooper pairs are in the same energy state. In the superconducting state, the Cooper pairs are correlated, so that they all act together. In order for the electrons in a superconducting state to absorb or emit energy, the binding of the Cooper pairs must be broken. The energy needed to break up a Cooper pair is analogous to that needed to break up a molecule into its constituent atoms. This energy is called the *superconducting energy gap* E_g. In the BCS theory, this energy at absolute zero is predicted to be

$$E_g = 3.5kT_c \qquad \textbf{10-56}$$

In agreement with experimental observations, BCS theory also predicts the flux quantization described in the Exploring section on page 462 and the temperature dependence of B_c.

$$B_c(T)/B_c(0) = 1 - (T/T_c)^2$$

EXAMPLE 10-11 **Energy Gap of Cadmium** (*a*) Calculate the superconducting energy gap at $T = 0$ K predicted by the BCS theory for cadmium and compare the result with the measured result of 1.50×10^{-4} eV. (*b*) Compute the wavelength of a photon whose energy is just sufficient to break up a Cooper pair in cadmium.

SOLUTION

(*a*) From Table 10-6, we have that $T_c = 0.517$ K for cadmium. The BCS prediction of the energy gap is then

$$E_g = 3.5kT_c = \frac{3.5(1.38 \times 10^{-23}\ J/K)(0.517\ \text{K})}{(1.60 \times 10^{-19}\ \text{J/eV})} = 1.56 \times 10^{-4}\ \text{eV}$$

This differs from the measured values of 1.50×10^{-4} eV by about 4 percent.

(*b*) $E_g = hf = hc/\lambda$, or we have that

$$\lambda = hc/E_g = \frac{(6.63 \times 10^{-34}\ \text{J} \cdot \text{s})(3.00 \times 10^8\ \text{m/s})}{(1.56 \times 10^{-4}\ \text{eV})(1.60 \times 10^{-19}\ \text{J/eV})} = 7.97 \times 10^{-3}\ \text{m}$$

Remarks: This wavelength is in the short-wavelength microwave region of the electromagnetic spectrum.

Note that the energy gap for a typical superconductor is much smaller than the energy gap for a typical semiconductor, which is of the order of 1 eV. As the temperature is increased from $T = 0$, some of the Cooper pairs are broken. The resulting individual (unpaired) electrons interact with the remaining Cooper pairs, reducing the energy gap until at $T = T_c$ the energy gap is zero (see Figure 10-51). Notice, too, that the gap

STUDENTS-HUB.com Uploaded By: Malak Obaid

energy is typically larger than that available from the thermal energy of the system. For example, for $T = 0.5\,T_c$, $E_g(T) = (0.95)\,E_g(0) \approx (3.3)\,kT_c$, whereas the thermal energy $kT = (0.5)kT_c$.

The Cooper pairs that we have discussed so far have zero momentum, so there are as many electrons traveling in one direction as the other and there is no current. Cooper pairs can also be formed with a net momentum **p** rather than zero momentum, but all the pairs have the same momentum. In this state, current is carried by the Cooper pairs. In ordinary conductors, resistance is present because the current carriers can be scattered with a change in momentum. As we have discussed, this scattering may be due to impurity atoms or thermal vibrations of the lattice ions. In a superconductor, the Cooper pairs are constantly scattering each other, but since the total momentum remains constant in this process, there is no change in the current. A Cooper pair cannot be scattered by a lattice ion because all the pairs act together. The only way that the current can be decreased by scattering is if a pair is broken up, which requires energy greater than or equal to the energy gap E_g. At reasonably low currents, scattering events in which the total momentum of a Cooper pair is changed are completely prohibited, so there is no resistance.

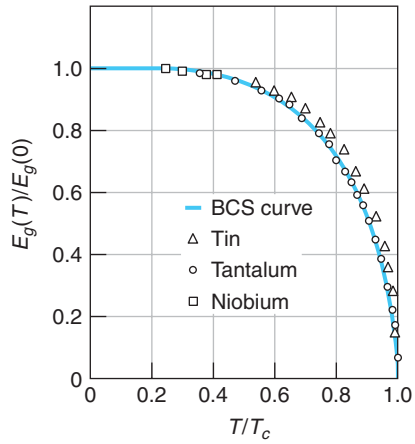

Figure 10-51 Ratio of the energy gap at temperature T to that at $T = 0$ as a function of the relative temperature T/T_c. The solid curve is that predicted by the BCS theory.

EXAMPLE 10-12 How Big Is a Cooper Pair? Calculate an estimate of the separation Δx of the electrons forming a Cooper pair, assuming that the binding energy of the pair equals the gap energy E_g and that, like semiconductors, the gap is centered on the Fermi energy E_F.

SOLUTION

The energy of either electron is, with the aid of the de Broglie relation, given by

$$E = \frac{p^2}{2m^*} = \frac{\hbar^2 k^2}{2m^*}$$

and

$$\Delta E = \frac{2k\hbar^2\,\Delta k}{2m^*}$$

If we associate E with the Fermi energy and ΔE with the gap, then

$$\frac{\Delta E}{E} \approx \frac{E_g}{E_F} \approx \frac{2k\hbar^2\,\Delta k}{2m^*} \times \frac{2m^*}{\hbar^2 k^2} \approx \frac{2\,\Delta k}{k}$$

Since the Fermi energy is typically of the order of 1 eV and the gap of the order 10^{-4} eV, as computed in Example 10-12, then $E_g/E_F \approx 10^{-4}$ and

$$\Delta k \approx 0.5 \times 10^{-4} k$$

where k refers to the value at the Fermi level. As was discussed in Section 10-6 and illustrated in Figure 10-19, $k = \pi/a$ at the top of the first allowed band, where the energy is approximately E_F. The lattice spacing $a \approx 0.1$ nm, so we have that $k \approx \pi/0.1\ \text{nm}^{-1}$ and $\Delta k = 10^{-3}\ \text{nm}^{-1}$. From the uncertainty relation (Equation 5-17), we then have that the uncertainty in the location of either electron, i.e., the extent of their wave functions in space, is

$$\Delta x = \frac{1}{\Delta k} = 10^3\ \text{nm}$$

or roughly equal to 10,000 atomic diameters and approximately equal to the wavelength of visible light.

STUDENTS-HUB.com Uploaded By: Malak Obaid

High-Temperature Superconductivity

For many years, the highest known critical temperature for a superconductor was 23.2 K for the alloy Nb_3Ge. Then in 1986 J. G. Bednorz and K. A. Müller found that an oxide of lanthanum, barium, and copper became superconducting at 30 K. Soon afterward, in 1987, superconductivity with a critical temperature of 92 K was found in a ceramic of copper oxide containing yttrium and barium ($YBa_2Cu_3O_7$). Since then, several copper oxides have been found with critical temperatures as high as 164 K. Table 10-8 lists some of the high-temperature superconductors along with their critical temperatures. These discoveries have revolutionized the study of superconductivity because relatively inexpensive liquid nitrogen, which boils at 77 K, can be used for a coolant. However, there are many problems, such as the brittleness of ceramics, that thus far make these new superconductors difficult to use. High-temperature superconductors are all type II superconductors with very high upper critical fields. For some, B_{c2} is estimated to be as high as 100 T. Although the BCS theory appears to be the correct starting place for understanding these new superconductors, they have many features that are not clearly understood, and the theoretical explanation of the phenomenon is not yet in hand. Thus, there is much work, both experimental and theoretical, to be done.

Table 10-8 Critical temperatures of some high T_c superconductors

Material	T_c, K
LaBaCuO	30
La_2CuO_4	40
$YBa_2Cu_3O_7$	92
$DyBa_2Cu_3O_7$	92.5
$C_{60}(CHBr_3)$	117
BiSrCaCuO	120
$Tl_2Ba_2Ca_2Cu_3O_{10}$	120
$Hg_{.8}Tl_{.2}Ba_2Ca_2Cu_3O_{8.33}$	138

EXPLORING
Josephson Junction

In Section 6-6, we discussed barrier penetration—the tunneling of a single particle through a potential barrier. The tunneling of electrons from one metal to another can be observed by separating the two metals with a thin layer only a few nanometers thick of an insulating material such as aluminum oxide. When both metals are normal metals (not superconductors), the current resulting from the tunneling of

STUDENTS-HUB.com Uploaded By: Malak Obaid

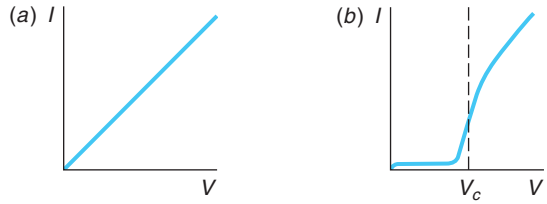

Figure 10-52 Tunneling current versus voltage for a junction of two metals separated by a thin oxide layer. (*a*) When both metals are normal metals, the current is proportional to the voltage as predicted by Ohm's law. (*b*) When one metal is a normal metal and one is a superconductor, the current is approximately zero until the applied voltage exceeds the critical voltage $V_c = E_g/2e$.

electrons through the insulating layer obeys Ohm's law for low applied voltages (see Figure 10-52*a*). When one of the metals is a normal metal and the other is a superconductor, there is no current (at absolute zero) unless the applied voltage V is greater than a critical voltage $V_c = E_g/2e$, where E_g is the superconductor energy gap. Figure 10-52*b* shows the plot of current versus voltage for this situation. The current jumps abruptly when V is great enough to break up a Cooper pair. (At temperatures above absolute zero, there is a small current because some of the electrons in the superconductor are thermally excited above the energy gap and therefore are not paired.) The superconducting energy gap can thus be accurately measured by measuring the critical voltage V_c.

In 1962, Brian Josephson[16] proposed that when two superconductors form a junction, now called a *Josephson junction*, Cooper pairs could tunnel from one superconductor to the other with no resistance. The current is observed with no voltage applied across the junction and is given by

$$I = I_{\max} \sin(\phi_2 - \phi_1) \qquad \textbf{10-57}$$

where $I_{\max}$ is the maximum current, which depends on the thickness of the barrier, ϕ_1 is the phase of the wave function for the Cooper pairs in one of the superconductors, and ϕ_2 is the phase of the corresponding wave function in the other superconductor. (The phase of a wave function is the exponent $Et/\hbar = \omega t$ of the time part of the total wave function. See Section 6-1.) This result has been observed experimentally and is known as the *dc Josephson effect*.

Josephson also predicted that if a dc voltage were applied across a Josephson junction, there would be a current that alternates with frequency f given by

$$f = \frac{2eV}{h} \qquad \textbf{10-58}$$

This result, known as the *ac Josephson effect*, has also been observed experimentally, and careful measurement of the frequency allows a precise determination of the ratio e/h. Because frequency can be measured so accurately, the ac Josephson effect is also used to establish precise voltage standards. The inverse effect, in which the application of an alternating voltage across a Josephson junction results in a dc current, has also been observed.

STUDENTS-HUB.com Uploaded By: Malak Obaid

EXAMPLE 10-13 **AC Josephson Effect** Using $e = 1.602 \times 10^{-19}$ C and $h = 6.626 \times 10^{-34}$ J · s, calculate the frequency of the Josephson current if the applied voltage is 1 μV.

SOLUTION

From Equation 10-58, we obtain

$$f = \frac{2eV}{h} = \left(\frac{2(1.602 \times 10^{-19}\ \text{C})(10^{-6}\ \text{V})}{6.616 \times 10^{-34}\ \text{J} \cdot \text{s}}\right) = 4.836 \times 10^{8}\ \text{Hz}$$
$$= 483.6\ \text{MHz}$$

There is a third effect observed with Josephson junctions. When a dc magnetic field is applied through a superconducting ring containing two Josephson junctions, the total supercurrent shows interference effects that depend on the intensity of the magnetic field (Figure 10-53). This effect can be used to measure very weak magnetic fields. It is the basis for a device called a *SQUID* (for *S*uperconducting *Qu*antum *I*nterference *D*evice) that can detect magnetic fields as low as 10^{-14} T. Such a device can detect the magnetic fields produced by the tiny currents flowing in the heart and brain.

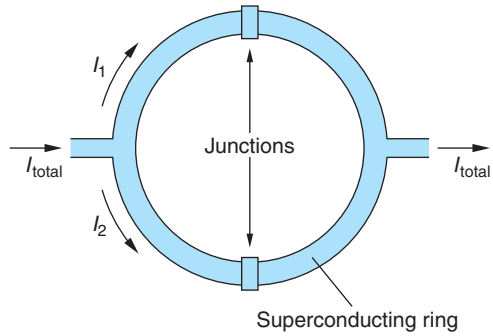

Figure 10-53 A superconducting ring with two Josephson junctions. When there is no applied magnetic field through the ring, the currents I_1 and I_2 are in phase. A very small applied magnetic field produces a phase difference in the two currents that produces interference in the total current exiting the ring.

Summary

TOPIC	RELEVANT EQUATIONS AND REMARKS
1. Structure of solids	Solids are often found in crystalline form, in which a small structure called the *unit cell* is repeated over and over. The structure of the unit cell depends on the type of bonding between the atoms, ions, or molecules forming the crystal.
Ionic and covalent solids	The attractive part of the potential energy of an ion in an ionic crystal is $U_{att} = -\alpha\frac{ke^2}{r}$ **10-1** where r is the separation between neighboring ions and α is the Madelung constant, which depends on the crystal geometry. The constant α is 1.7476 for face-centered-cubic crystals.

STUDENTS-HUB.com Uploaded By: Malak Obaid

TOPIC	RELEVANT EQUATIONS AND REMARKS
	In covalently bonded crystals the individual bonds are just like those in covalently bonded molecules. The metallic bond has no single-molecule counterpart. One or more valence electrons are free to move throughout the solid, and *all* of the atoms share all of the free electrons, making this bond roughly analogous to the covalent bond.
2. Classical free-electron theory	Electrical resistivity ρ and conductivity σ are given by $\rho = \frac{m_e\langle v\rangle}{ne^2\lambda}$ and $\sigma = \frac{ne^2\lambda}{m_e\langle v\rangle}$ **10-13** where $\langle v\rangle$ is the mean speed of the electrons and λ is the mean free path between collisions. The latter is given by $\lambda = \frac{1}{n_a\pi r^2}$ **10-12** where n_a is the ion density. These yield Ohm's law correctly but result in the wrong temperature dependence of the resistivity.
3. Electron gas in metals	The average energy of the electrons at ordinary temperatures is much larger than kT: $\langle E\rangle = \frac{3}{5}E_F$ **10-22** where typical values of the Fermi energy E_F are 1 to 2 eV.
4. Quantum theory of conduction	This theory results from making two important corrections to the classical free-electron theory. First, the Fermi-Dirac distribution of electron energies is used rather than the Maxwell-Boltzmann distribution. Second, the effect of the wave characteristics of the electrons is considered in their scattering from the lattice ions. The resulting theory is in good agreement with observations.
5. Magnetism in solids	The origin of magnetism in solids is the electron spins and their associated magnetic moments.
6. Band theory of solids	When many atoms are brought together to form a solid, the individual energy levels are split into bands of allowed energies. The splitting depends on the type of bonding and the lattice separation. In a conductor, the uppermost band containing electrons is only partially full, so there are many available states for excited electrons. In an insulator, the uppermost band containing electrons, the valence band, is completely full and there is a large energy gap between it and the next allowed band, the conduction band. In a semiconductor, the energy gap between the filled valence band and the empty conduction band is small, so at ordinary temperatures an appreciable number of electrons are thermally excited into the conduction band.
Kronig-Penney model	The solid is modeled as a periodic potential. The wave functions are then $\psi(x) = u_k(x)e^{ikx}$ **10-36** where the function $u_k(x)$ is periodic with a period equal to that of the spacing of the potential wells and e^{ikx} is a free electron, i.e., a plane wave. The energy gaps occur at $ka = \pm n\pi$ **10-41** for integer n and a equal to the lattice spacing.

STUDENTS-HUB.com Uploaded By: Malak Obaid

TOPIC	RELEVANT EQUATIONS AND REMARKS
7. Impurity semiconductors	The conductivity of a semiconductor can be greatly increasing by doping. In an *n*-type semiconductor, the doping adds electrons just below the conduction band. In a *p*-type semiconductor, holes are added just above the valence band. A junction between an *n*-type and *p*-type semiconductors has applications in many devices, such as diodes, solar cells, and light-emitting diodes. A transistor consists of a very thin semiconductor of one type sandwiched between two semiconductors of the opposite type. Transistors are used in amplifiers because a small variation in the base current results in a large variation in the collector current.
8. Superconductivity	In a superconductor the resistance drops suddenly to zero below a critical temperature T_c. Magnetic field lines are expelled and $B = 0$ inside a type I semiconductor, a phenomenon called the Meissner effect. Superconductivity at low temperatures is described by BCS theory, in which free electrons form Cooper pairs. Recently discovered high-temperature semiconductors are only partially understood in terms of BCS theory.

General References

The following general references are written at a level appropriate for the readers of this book.

Anderson, B., *Fundamentals of Semiconductor Devices*, McGraw-Hill, New York, 2005.

Blatt, F., *Modern Physics*, McGraw-Hill, New York, 1992.

Burns, G., *Solid State Physics*, Academic Press, Orlando, FL, 1985.

Eisberg, R., and R. Resnick, *Quantum Physics of Atoms, Molecules, Solids, Nuclei, and Particles,* 2d ed., Wiley, New York, 1985.

Fermi, E., *Molecules, Crystals, and Quantum Statistics* (trans. M. Ferro-Luzzi), W. A. Benjamin, New York, 1966.

Holden, A., *The Nature of Solids*, Columbia University Press, 1968. An excellent nonmathematical treatment of the properties of solids.

Kittel, C., *Introduction to Solid State Physics*, 8th ed., Wiley, New York, 2005.

Leitner, A., *Introduction to Superconductivity*, Michigan State University, East Lansing, 1965. This excellent film, running 48 minutes, is probably one of the best introductions to superconductivity available.

Shockley, W., *Electrons and Holes in Semiconductors*, Van Nostrand, Princeton, NJ, 1950.

Notes

1. The constant n is often called the Born exponent.

2. Carbon also has a fourth solid form, charcoal, which has no well-defined crystalline structure.

3. Notice that this view of the metal fits the definition of a plasma set forth in the opening paragraph of the chapter. Though not usually thought of in that way, metals are indeed low-temperature plasmas.

4. Felix Bloch (1905–1983), Swiss American physicist. He devised a method for measuring atomic magnetic fields in liquids and solids that led to the development of nuclear magnetic resonance (NMR) spectroscopy and earned for him a share (with E. M. Purcell) of the 1952 Nobel Prize in Physics. He was the first director-general of CERN, the European Center for Nuclear Research.

5. The graph of the energy bands and gaps of Figure 10-19*b* results from a simplified version of the conditional equation connecting k, k', and α in which $b \rightarrow 0$ and $U_0 \rightarrow \infty$. In that limit the lattice spacing is a, rather than $a + b$, as in Figure 10-18.

6. This mixing, called hybridization, was discussed in Section 9-2.

7. See, e.g., Section 25-5 in P. Tipler and G. Mosca, *Physics for Scientists and Engineers*, 6th ed. (W. H. Freeman and Co., New York, 2008).

8. The fact that the radius of the bound electron is several times the equilibrium spacing of the atoms helps justify our tacit assumption that the fifth electron sees a uniform dielectric constant in the crystal.

STUDENTS-HUB.com Uploaded By: Malak Obaid

9. Klaus von Klitzing (b. 1943), German physicist. He received the 1985 Nobel Prize in Physics for this discovery.
10. Daniel C. Tsui (b. 1939), Chinese American physicist. He received the 1998 Nobel Prize in Physics with H. L. Stormer and R. B. Laughlin for their discovery.
11. William B. Shockley (1910–1989), John Bardeen (1908–1991), and Walter H. Brattain (1902–1987), American physicists. Shockley discovered that doped germanium crystals were excellent rectifiers, and subsequently the three Bell Laboratories colleagues discovered that two such "solid-state rectifiers" combined would amplify current. The discovery of this device, the transistor, earned them the 1956 Nobel Prize in Physics.
12. Actually, the field decreases exponentially across the surface, reaching zero at a depth of about 10 nm.
13. Isotopes are atoms with the same atomic number Z but different atomic mass numbers A. Isotopes will be discussed in Chapter 11.
14. John Bardeen (1908–1991), Leon N. Cooper (b. 1930), and J. Robert Schrieffer (b. 1931), American physicists. Developed at the University of Illinois, the BCS theory earned the collaborators the 1972 Nobel Prize in Physics, and Bardeen became the only person thus far to win two physics Nobel Prizes (see note 11).
15. This may make it seem like the Cooper pair is a boson and superconductivity another example of Bose-Einstein condensation (see Section 8-3); however, the large size of the Cooper pair (see Example 10-12) means many pairs overlap and that the symmetry of the pair with respect to an exchange of electrons must also take into account exchanges involving electrons in different pairs. The result is that the Cooper pair is neither a pure boson nor a pure fermion.
16. Brian D. Josephson (b. 1940), Welsh physicist. For this discovery, made while he was still a graduate student, he shared the 1973 Nobel Prize in Physics with L. Esaki and I. Giaever. Bardeen had strongly opposed Josephson's tunneling prediction until experiments, led by those of Giaever (also done while he was a graduate student), confirmed tunneling by Cooper pairs.

Problems

Level I

Section 10-1 The Structure of Solids

10-1. Find the value of n in Equation 10-6 that gives the measured dissociation energy of 741 kJ/mol for LiCl, which has the same structure as NaCl and for which $r_0 = 0.257$ nm.
10-2. Calculate the distance r_0 between the K^+ and Cl^- ions in KCl, assuming that each ion occupies a cubic volume of side r_0. The molar mass of KCl is 74.55 g/mol and its density is 1.984 g/cm^3.
10-3. The distance between the Li^+ and Cl^- ions in LiCl is 0.257 nm. Use this and the molecular mass of LiCl (42.4 g/mol) to compute the density of LiCl.
10-4. The crystal structure of KCl is the same as that of NaCl. (*a*) Calculate the electrostatic potential energy of attraction of KCl, assuming that r_0 is 0.314 nm. (*b*) Assuming that $n = 9$ in Equation 10-6, calculate the dissociation energy in eV per ion pair and in kcal/mol. (*c*) The measured dissociation energy is 165.5 kcal/mol. Use this to determine n in Equation 10-6.
10-5. The observed dissociation energy of solid LiBr is 788 kJ/mol. Compute the cohesive energy of LiBr and compare the result with the value in Table 10-1. (Ionization energies for Li and Br are in Table 9-1.)
10-6. The density of NaCl (an fcc crystal) is 2.16 g/cm^3. Find the distance between ions that are nearest neighbors.
10-7. The separation of nearest neighbor ions in the KCl crystal (an fcc structure) is 0.315 nm. Use this information to determine the density of KCl.
10-8. Using the data for ionic and metallic crystals from Table 10-1, (*a*) graph cohesive energy versus melting point and put the best straight line through the points. (*b*) Determine the cohesive energies of cobalt, silver, and sodium, whose melting temperatures are 1495°C, 962°C, and 98°C, respectively. (The measured values are cobalt 4.43 eV, silver 2.97 eV, and sodium 1.13 eV.)
10-9. Figure 10-54 shows a one-dimensional ionic lattice consisting of doubly charged positive ions and twice as many singly charged negative ions. Compute the Madelung constant for this "crystal" to within 1 percent.

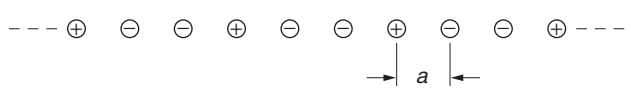

Figure 10-54

STUDENTS-HUB.com Uploaded By: Malak Obaid

Section 10-2 Classical Theory of Conduction

10-10. (*a*) Given a mean free path $\lambda = 0.4$ nm and a mean speed $\langle v \rangle = 1.17 \times 10^5$ m/s for the current flow in copper at a temperature of 300 K, calculate the classical value for the resistivity ρ of copper. (*b*) The classical model suggests that the mean free path is temperature independent and that $\langle v \rangle$ depends on temperature. From this model, what would ρ be at 100 K?

10-11. Find (*a*) the current density and (*b*) the drift velocity if there is a current of 1 mA in a No. 14 copper wire. (The diameter of No. 14 wire, which is often used in household wiring, is 0.064 in = 0.163 cm.)

10-12. A measure of the density of the free-electron gas in a metal is the distance r_s, which is defined as the radius of the sphere whose volume equals the volume per conduction electron. (*a*) Show that $r_s = (3/4\pi n_a)$, where n_a is the free-electron number density. (*b*) Calculate r_s for copper in nanometers.

10-13. Calculate the number density of free electrons in (*a*) Ag ($\rho = 10.5$ g/cm^3) and (*b*) Au ($\rho = 19.3$ g/cm^3), assuming one free electron per atom, and compare your results with the values listed in Table10-3.

10-14. Calculate the number density of free electrons for (*a*) Mg ($\rho = 1.74$ g/cm^3) and (*b*) Zn ($\rho = 7.1$ g/cm^3), assuming two free electrons per atom, and compare your results with the values listed in Table 10-3.

10-15. (*a*) Using $\lambda = 0.37$ nm and $\langle v \rangle = 1.08 \times 10^5$ m/s at $T = 300$ K, calculate σ and ρ for copper from Equations 10-13. Using the same value of λ, find σ and ρ at (*b*) $T = 200$ K and (*c*) $T = 100$ K.

Section 10-3 Free-Electron Gas in Metals

10-16. Find the average energy of the electrons at $T = 0$ K in (*a*) copper ($E_F = 7.06$ eV) and (*b*) Li ($E_F = 4.77$ eV).

10-17. Calculate the Fermi energy for magnesium in a long, very thin wire.

10-18. Compute (*a*) the Fermi energy and (*b*) the Fermi temperature for silver and for iron and compare your results with the corresponding values in Table 10-3.

10-19. Show that for $T = 300$ K about 0.1 percent of the free electrons in metallic silver have an energy greater than E_F.

Section 10-4 Quantum Theory of Conduction

10-20. What is the Fermi speed, i.e., the speed of a conduction electron whose energy is equal to the Fermi energy E_F, for (*a*) Na, (*b*) Au, and (*c*) Sn? (See Table 10-3.)

10-21. The resistivities of Na, Au, and Sn at $T = 273$ K are 4.2 $\mu\Omega \cdot$cm, 2.04 $\mu\Omega \cdot$cm, and 10.6 $\mu\Omega \cdot$cm, respectively. Use these values and the Fermi speeds calculated in Problem 10-20 to find the mean free paths λ for the conduction electrons in these elements.

10-22. At what temperature is the heat capacity due to the electron gas in copper equal to 10 percent of that due to lattice vibrations?

10-23. Use Equation 10-29 with $\alpha = \pi^2/4$ to calculate the average energy of an electron in copper at $T = 300$ K. Compare your result with the average energy at $T = 0$ and the classical result of $(3/2)kT$.

10-24. Compute the maximum fractional contribution to the heat capacity of solid iron that can be made by the electrons.

Section 10-5 Magnetism in Solids

10-25. The magnetic polarization P of any material is defined as $P = (\rho_+ - \rho_-)/\rho$. Compute the high-temperature polarization of a paramagnetic solid at $T = 200$ K in a magnetic field of 2.0 T.

10-26. Show that the magnetic susceptibility χ is a dimensionless quantity.

STUDENTS-HUB.com Uploaded By: Malak Obaid

Section 10-6 Band Theory of Solids

10-27. (*a*) The energy gap between the valence band and the conduction band in silicon is 1.14 eV at room temperature. What is the wavelength of a photon that will excite an electron from the top of the valence band to the bottom of the conduction band? Do the same calculation for (*b*) germanium, for which the energy gap is 0.72 eV, and (*c*) for diamond, for which the energy gap is 7.0 eV.

10-28. (*a*) The energy band gap in germanium is 0.72 eV. What wavelength range of visible light will be transmitted by a germanium crystal? (Think about it carefully!) (*b*) Now consider a crystal of an insulator whose energy band gap is 3.6 eV. What wavelength range of visible light will this crystal transmit? (*c*) Justify each of your answers to (*a*) and (*b*).

10-29. A photon of wavelength 3.35 μm has just enough energy to raise an electron from the valence band to the conduction band in a lead sulfide crystal. (*a*) Find the energy gap between these bands in lead sulfide. (*b*) Find the temperature T for which kT equals this energy gap.

10-30. Consider a small silicon crystal measuring 100 nm on each side. (*a*) Compute the total number N of silicon atoms in the crystal. (The density of silicon is 2.33 g/cm^3.) (*b*) If the conduction band in silicon is 13 eV wide and recalling that there are $4N$ states in this band, compute an approximate value for the energy spacing between adjacent conduction band states for the crystal.

Section 10-7 Impurity Semiconductors

10-31. Arsenic has five valence electrons. If arsenic is used as a dopant in silicon, compute (*a*) the ionization energy and (*b*) the orbit radius of the fifth arsenic electron. The effective mass for electrons in silicon is 0.2 m_e. (*c*) What is the ratio of the ionization energy of the fifth electron to the energy gap in silicon?

10-32. Gallium has three valence electrons. If gallium is used to dope germanium, compute (*a*) the ionization energy of the hole and (*b*) the orbit radius of the hole. The effective mass of holes in germanium is 0.34 m_e.

10-33. What type of semiconductor is obtained if silicon is doped with (*a*) aluminum and (*b*) phosphorus? (See Appendix C for the electron configurations of these elements.)

10-34. The donor energy levels in an *n*-type semiconductor are 0.01 eV below the conduction band. Find the temperature for which $kT = 0.01$ eV.

10-35. A strip of tin is 10 mm wide and 0.2 mm thick. When a current of 20 A is established in the strip and a uniform magnetic field of 0.25 T is oriented perpendicular to the plane of the strip, a Hall voltage of 2.20 μV is measured across the width of the strip. Compute (*a*) the density of charge carriers in tin and (*b*) the average number of charge carriers contributed by each tin atom. The density of tin is 5.75×10^3 kg/m^3 and its molecular mass is 118.7.

Section 10-8 Semiconductor Junctions and Devices

10-36. For a temperature of 300 K, use Equation 10-49 to find the bias voltage V_b for which the exponential term has the value (*a*) 10 and (*b*) 0.1.

10-37. For what value of bias voltage V_b does the exponential in Equation 10-49 have the value (*a*) 5, and (*b*) 0.5 for $T = 200$ K?

10-38. Compute the fractional change in the current through a *pn* junction diode when the forward bias is changed from +0.1 V to +0.2 V.

10-39. For $T = 300$ K, use Equation 10-49 to find the bias voltage V_b for which the exponential term had the value (*a*) 10 and (*b*) 0.1.

10-40. When light of wavelength no larger than 484 nm illuminates a CdS solar cell, the cell produces electric current. Determine the energy gap in CdS.

Section 10-9 Superconductivity

10-41. Three naturally occurring isotopes of lead are ^{206}Pb, ^{207}Pb, and ^{208}Pb. Using the value of α from Table 10-7 and the isotopic masses from Appendix A, compute the critical temperatures of these isotopes.

STUDENTS-HUB.com Uploaded By: Malak Obaid

10-42. Compute (*a*) the superconducting energy gap for indium and (*b*) the wavelength of a photon that could just break up a Cooper pair in indium at $T = 0$ K.

10-43. (*a*) Use Equation 10-56 to calculate the superconducting energy gap for tin and compare your result with the measured value of 6×10^{-4} eV. (*b*) Use the measured value to calculate the wavelength of a photon having sufficient energy to break up a Cooper pair in tin at $T = 0$ K.

10-44. Use the BCS curve in Figure 10-51 to estimate the energy gaps in (*a*) tin, (*b*) niobium, (*c*) aluminum, and (*d*) zinc, all at $T = 0.5T_c$.

10-45. Expressing the temperature T as a fraction of the critical temperature T_c, according to BCS theory at what temperature is (*a*) $B_c = 0.1B_c(0)$, (*b*) $B_c = 0.5B_c(0)$, (*c*) $B_c = 0.9B_c(0)$?

Level II

10-46. Estimate the fraction of free electrons in copper that are in excited states above the Fermi energy at (*a*) room temperature of 300 K and (*b*) 1000 K.

10-47. A one-dimensional model of an ionic crystal consists of a line of alternating positive and negative ions with distance r_0 between adjacent ions. (*a*) Show that the potential energy of attraction of one ion in the line is

$$V = -\frac{2ke^2}{r_0}\left(1 - \frac{1}{2} + \frac{1}{3} - \frac{1}{4} + \frac{1}{5} - \ldots\right)$$

(*b*) Using the result that

$$\ln(1 + x) = x - \frac{x^2}{2} + \frac{x^3}{3} - \frac{x^4}{4} + \ldots$$

show that the Madelung constant for this one-dimensional model is $\alpha = 2 \ln 2 = 1.386$.

10-48. Estimate the Fermi energy of zinc from its electronic molar heat capacity of $(3.74 \times 10^{-4}\ \text{J/mol} \cdot \text{K})T$.

10-49. The density of the electron states in a metal can be written $g(E) = AE^{1/2}$, where A is a constant and E is measured from the bottom of the conduction band. (*a*) Show that the total number of states is $(2/3)A(E_F)^{3/2}$. (*b*) About what fraction of the conduction electrons are within kT of the Fermi energy? (*c*) Evaluate this fraction for copper at $T = 300$ K.

10-50. High-purity germanium (HPGe) crystals are used as detectors for x rays and gamma rays. On interacting with the crystal, incoming photons produce electron-hole pairs, exciting many electrons across the 0.72-eV energy gap into the conduction band. The decay of the radioisotope ^{60}Co results in the emission of two gamma rays with energies 1.17 MeV and 1.33 MeV (see Chapter 11). (*a*) Compute the numbers of electrons N_1 and N_2 excited across the energy gap by each of the two gamma rays. (*b*) The numbers N_1 and N_2 are subject to statistical fluctuations of $\pm\sqrt{N_1}$ and $\pm\sqrt{N_2}$. Compute the fractional uncertainties in N_1 and N_2. (*c*) Compute the corresponding fractional uncertainties in the energies of the two gamma rays. This is a measure of the energy resolution of the HPGe crystal.

10-51. A doped *n*-type silicon sample with 10^{16} electrons per cubic centimeter in the conduction band has a resistivity of $5 \times 10^{-3}\ \Omega \cdot \text{m}$ at 300 K. Find the mean free path of the electrons. Use $0.2\ m_e$ for the effective mass of the electron. Compare your result with the mean free path of electrons in copper at 300 K.

10-52. A "good" silicon diode has a current-voltage characteristic given by

$$I = I_0(e^{eV_b/kT} - 1)$$

Let $kT = 0.025$ eV (room temperature) and the saturation current $I_0 = 1$ nA. (*a*) Show that for small reverse-bias voltages, the resistance is 25 MΩ. (*Hint:* Do a Taylor expansion of the exponential function or use your calculator and enter small values for V_b.) (*b*) Find the dc resistance for a reverse bias of 0.5 V. (*c*) Find the dc resistance for a 0.5-V forward bias. What is the current in this case? (*d*) Calculate the ac resistance dV/dI for a 0.5-V forward bias.

STUDENTS-HUB.com Uploaded By: Malak Obaid

10-53. The relative binding of the extra electron in the arsenic atom that replaces an atom in silicon or germanium can be understood from a calculation of the first Bohr orbit of this electron in these materials. Four of arsenic's outer electrons form covalent bonds, so the fifth electron sees a singularly charged center of attraction. This model is a modified hydrogen atom. In the Bohr model of the hydrogen atom, the electron moves in free space at a radius a_0 given by

$$a_0 = \frac{\epsilon_0 h^2}{\pi m_e e^2}$$

When an electron moves in a crystal, we can approximate the effect of the other atoms by replacing ϵ_0 with $\kappa\epsilon_0$ and m_e with an effective mass for the electron. For silicon κ is 12 and the effective mass is about $0.2m_e$, and for germanium κ is 16 and the effective mass is about $0.1m_e$. Estimate the Bohr radii for the outer electron as it orbits the impurity arsenic atom in silicon and germanium.

10-54. InSb is a semiconductor. The energy gap E_g between its valence and conduction bands is 0.23 eV, and its dielectric constant $\kappa = 18$. In the InSb crystal the electron's effective mass $m^* = 0.015m_e$. (*a*) Compute the ionization energy for an electron donor in InSb. (*b*) What is the radius of the ground-state orbit? (*c*) At approximately what donor concentration will the orbits of adjacent donor atoms begin to overlap?

10-55. The mean free path of an electron in a metal depends on both the lattice oscillations of the metal ions and those of any impurity ions according to $1/\lambda = 1/\lambda_m + 1/\lambda_i$. The resistivity of pure copper is increased by about $1.2 \times 10^{-8}\ \Omega \cdot \text{m}$ by the addition of 1 percent (by number of atoms) of a certain impurity dispersed evenly throughout the metal. (*a*) Estimate λ_i from this information. (*b*) The impurity atoms are "seen" by the electrons to have an effective diameter d. Estimate the scattering cross section d^2 from Equation 10-12, where $d = 2r$.

Level III

10-56. When arsenic is used to dope silicon, the fifth arsenic electron and the As^+ ion act like a hydrogen atom system except that the potential function $V(r)$ and the electron mass must be modified as described in Section 10-7 to account for the crystal lattice. With these modifications, (*a*) solve the Schrödinger equation, using the solution in Chapter 7 as a guide. (*b*) Obtain Equation 10-43, and (*c*) sketch a properly scaled energy-level diagram for the fifth electron for $n = 1$ through 5.

10-57. The quantity K is the force constant for a "spring" consisting of a line of alternating positive and negative ions. If these ions are displaced slightly from their equilibrium separation r_0, they will vibrate with a frequency

$$f = \frac{1}{2\pi}\sqrt{\frac{K}{m}}$$

(*a*) Use the values of α, n, and r_0 for NaCl and the reduced mass for the NaCl molecule to calculate this frequency. (*b*) Calculate the wavelength of electromagnetic radiation corresponding to this frequency, and compare your result with the characteristic strong infrared absorption bands in the region of about $\lambda = 61\ \mu\text{m}$ that are observed for NaCl.

10-58. Consider a model for a metal in which the lattice of positive ions forms a container for a classical electron gas with n electrons per unit volume. In equilibrium, the average electron velocity is zero, but the application of an electric field produces an acceleration of the electrons. If we use a relaxation time τ to account for the electron-lattice collisions, then we have the equation

$$m\frac{dv}{dt} + \frac{m}{\tau}v = -eE$$

(*a*) Solve the equation for the drift velocity in the direction of the applied electric field. (*b*) Verify that Ohm's law is valid, and find the resistivity as a function of n, e, m, and the relaxation time τ.

STUDENTS-HUB.com Uploaded By: Malak Obaid

10-59. Imagine a cubic crystal like NaCl, with a negative charge at the center of a Cartesian coordinate system with scale units equal to the interatomic distance (*a*) Show that an ion at a position r units along the x axis, s units along the y axis, and t units along the z axis has a charge of $e(-1)^r \cdot (-1)^s \cdot (-1)^t = e(-1)^{r+s+t}$, where e is the electron charge. (*b*) Using Equation 10-2 as a guide, calculate the Madelung constant for a cube 2 units on a side. Do the same for cubes of sides 4, 6, 8, 10, 12, 16, and 20 units (You will probably want to use a computer spreadsheet to write a program to do the calculations for the larger cubes). Are your answers approaching the value $\alpha = 1.7476$?

10-60. (*a*) Show that for a paramagnetic solid with electron energies given by Equation 10-33 the magnetization per unit volume M is given by

$$M = \mu\rho \tanh (\mu B/kT)$$

(*b*) For $\mu B \ll kT$ show that the susceptibility is given by Equation 10-35.

STUDENTS-HUB.com Uploaded By: Malak Obaid

CHAPTER 11

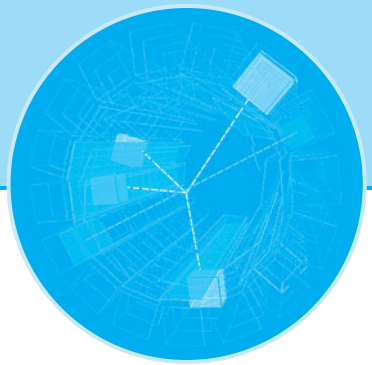

Nuclear Physics

11-1 The Composition of the Nucleus 478
11-2 Ground-State Properties of Nuclei 480
11-3 Radioactivity 492
11-4 Alpha, Beta, and Gamma Decay 495
11-5 The Nuclear Force 506
11-6 The Shell Model 513
11-7 Nuclear Reactions 516
11-8 Fission and Fusion 526
11-9 Applications 537

The first information about the atomic nucleus came with the discovery of radioactivity by A. H. Becquerel[1] in 1896. Intrigued by Roentgen's discovery of x rays the previous year, Becquerel was investigating the possibility that minerals that exhibit fluorescence after exposure to sunlight might also be emitting x rays. He used the simple technique of placing a sample of such a mineral, potassium uranyl sulfate, on top of a photographic plate wrapped in black paper lying in the sunlight on a window ledge. Sure enough, an image of the sample appeared on the developed plate, and Becquerel concluded that x rays had indeed been emitted. But when a similar sample lying on a wrapped photographic plate in a drawer without exposure to sunlight during a period of cloudy weather produced an image just as dark, he investigated further and found that the sample was spontaneously emitting a previously unknown penetrating radiation. He had discovered radioactivity.[2]

The rays emitted by radioactive nuclei were first classified by Rutherford as α, β, and γ, according to their ability to penetrate matter and to ionize air: α radiation penetrates the least and produces the most ionization, γ radiation penetrates the most with the least ionization, and β radiation is intermediate between them. In a classic experiment, Rutherford soon found that α rays are ^{4}He nuclei. It was also quickly discovered that β rays are electrons and γ rays are very short-wavelength electromagnetic radiation. Geiger and Marsden's α-particle-scattering experiments in 1911 (see Section 4-2) and the successes of the Bohr model of the atom led to the modern view of an atom as consisting of a tiny, massive nucleus with a radius of 1 to 10 femtometer (fm; 1 fm $= 10^{-15}$ m) surrounded by a cloud of electrons at a relatively great distance, of the order of 0.1 nm ($=$ 100,000 fm) from the nucleus.

In 1928, the correct explanation of α radioactivity as a quantum-mechanical, barrier-penetration phenomenon was given by G. Gamow, R. W. Gurney, and E. U. Condon. Then, in rapid succession in 1932, the *neutron* was discovered by J. Chadwick and the *positron* by C. D. Anderson, and the first nuclear reaction using artificially accelerated particles (protons) was observed by J. D. Cockcroft and E. T. S. Walton.[3] Thus, it is quite reasonable to mark that year as the beginning of modern nuclear physics. Much of the information about nuclei is obtained by bombarding them with various particles and observing the results. The advent of particle accelerators, the Van de Graaff electrostatic generator in 1931 and the cyclotron in 1932,

STUDENTS-HUB.com
Uploaded By: Malak Obaid

made many experimental studies possible without the severe limitations on particle type and energy imposed by naturally radioactive sources. Since then, an enormous technology has been developed for accelerating and detecting particles, and many nuclear reactions and fundamental particle interactions have been studied.

Among the myriad nuclear reactions that have been investigated are two types of special interest: *fission* and *fusion*. Both are processes by which nuclear mass is converted into other forms of energy, such as thermal energy, just as some atomic mass is converted in chemical reactions such as oxidation. Fission reactions currently provide a significant, albeit controversial, means of producing electrical energy in 30 countries, accounting for 6.0 percent of the world's total consumption of energy in 2005.[4] The similar potential of fusion reactions has not yet been realized at a practical level; however, of far more intrinsic importance is the role of fusion in the production of energy in stars. The grim reality that both fission and fusion are also the basis for weapons of enormous destructive power means that this application of nuclear reactions influences political debate to a greater degree than has perhaps any other scientific discovery in history.

In this chapter we will discuss some of the general properties of atomic nuclei and the important features of radioactivity. While our discussions will of necessity be only semiquantitative, we will consider the nature of the nuclear force as it is currently understood and describe one of the most useful models in terms of which many nuclear properties may be explained. The applications of radioactivity and nuclear reactions are by no means limited to fission and fusion. The radiations emitted by radioisotopes have long been used in medical diagnosis and treatment. These contributions were measurably enhanced with the development of *computer assisted tomography*[5] (CAT) in the 1970s, which made possible not only x-ray CAT scans, but also the more recent development of *positron emission tomography*, called PET. Neutron-induced nuclear reactions provide an extremely sensitive technique, called *neutron activation analysis* (NAA), for measuring trace amounts of certain isotopes for most elements in the periodic table. These and many other applications will be discussed in this chapter.

11-1 The Composition of the Nucleus

The experiments of Moseley (see Section 4-4) showed that the nuclear charge is Z times the proton charge, where Z is the *atomic number*, which is about half the *atomic mass number* A (except for hydrogen, for which $Z = A$). Thus, the nucleus has a mass about equal to that of A protons but a charge of only $Z \approx \frac{1}{2}A$ protons. Before the discovery of the neutron, it was difficult to understand this unless there were A–Z electrons in the nucleus to balance the charge without changing the mass very much. The idea that the nucleus contained electrons was supported by the observation of β decay, in which electrons are ejected by certain radioactive nuclei. However, there were serious difficulties with this model. A relatively simple calculation from the uncertainty principle (see Problem 11-2) shows that an electron has a minimum kinetic energy of about 100 MeV if it is confined in the region of $r < 10^{-14}$ m; however, the energies of the electrons emitted in β decay are only of the order of 1 or 2 MeV. In addition, there is no evidence for such a strong attractive force between nuclei and electrons as would be implied by a negative potential energy of 50 to 100 MeV inside the nucleus. Furthermore, since the electrostatic potential energy of the electron and nucleus is negative, there is no barrier to be overcome, as there is in α decay (Figure 11-1). If the electron's total energy were positive, as required for β decay, the electron should escape from the nucleus immediately and most naturally occurring β emitters should

STUDENTS-HUB.com Uploaded By: Malak Obaid

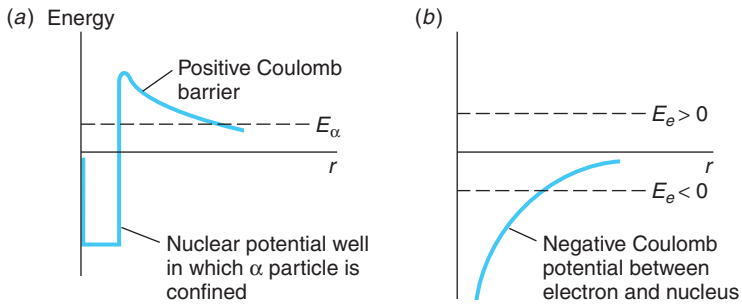

Figure 11-1 (*a*) Potential barrier for an α particle compared with (*b*), potential for a negative electron. Because there is no barrier for the electron, it will not be bound at all unless the total energy is negative, in which case it can never escape. The very narrow steep rise to the potential in (*a*) as $r \rightarrow 0$ represents the "hard core" of the nucleus.

have long since disappeared. A further difficulty is the observation that the magnetic moments of nuclei are of the order of nuclear magnetons, $\mu_N = e\hbar/2m_p$, about 2000 times smaller than a Bohr magneton $\mu_B = e\hbar/2m_e$, which would be expected if there were electrons inside the nucleus.

A further convincing argument against electrons existing in the nucleus concerns angular momentum. Protons and neutrons are fermions with spins of 1/2 and as such both obey the exclusion principle. The angular momentum of the nitrogen nucleus has a quantum number of 1, which can be inferred from a very small splitting of atomic spectral lines called *hyperfine structure* (see Section 11-2). It is also known (from molecular spectra—see Section 9-4) that the nitrogen nucleus obeys Bose-Einstein rather than Fermi-Dirac statistics. If ^{14}N contained 14 protons and 7 electrons, each with spin 1/2, the resultant angular momentum would have to be 1/2, 3/2, 5/2, etc., and the nucleus would obey Fermi-Dirac statistics.

In 1920 Rutherford suggested that there might be a neutral particle, possibly a proton and an electron tightly bound together, which he called a *neutron*. When such a particle was found by Chadwick in 1932, the idea that electrons were permanent constituents of nuclei was abandoned. Instead, the nucleus was assumed to contain N neutrons and Z protons, a total of $A = N + Z$ particles. N is referred to as the *neutron number*. The notion of the neutron being a proton and electron bound together has also been abandoned since the spin of the neutron is 1/2. Thus, the nucleus is composed of protons and neutrons, the *nucleons*, which collectively occupy a volume whose radius is of the order of 1 to 10 fm. All of the large variety of nuclei with their broad diversity of properties are assembled from various numbers of these two particles. The fundamental properties of the individual nucleons are given in Table 11-1. We should note at this point that the nucleons are not fundamental particles. Each of the two types of nucleons is composed of a set of three *quarks*, fundamental particles that interact with each other via the strong force, which accounts for the fact that the nucleons also feel that force. Quarks and their interactions will be discussed in Chapter 12.

Table 11-1 Fundamental properties of atomic constituents

Particle	Charge	Mass (u)	Mass (kg)	Spin	Magnetic moment
Proton	$+e$	1.007276	1.6726×10^{-27}	1/2	$2.79285\ \mu_N$
Neutron	0	1.008665	1.6749×10^{-27}	1/2	$-1.91304\ \mu_N$
Deuteron	$+e$	2.013553	3.3436×10^{-27}	1	$0.85744\ \mu_N$
Electron	$-e$	5.4858×10^{-4}	9.1094×10^{-31}	1/2	$1.00116\ \mu_B$

STUDENTS-HUB.com Uploaded By: Malak Obaid

11-2 Ground-State Properties of Nuclei

Understanding nuclei, like atoms, requires the application of quantum theory. It was the study of nuclear spectra, the energy and particles emitted spontaneously by radioactive nuclei, that provided the first indication of the existence of quantized energy levels, angular momenta, and magnetic moments in nuclei, just as the regularities in atomic spectra had earlier pointed the way to Bohr's theory and, ultimately, to wave mechanics. Interpreting the nuclear studies presents more complex problems due to the existence of two nucleons, the possible emission of several different particles in addition to photons from excited energy states, and our incomplete knowledge of the nuclear potential function.

In this section we will discuss some of the properties of nuclei in the ground state and mention a few methods of determining these properties. In Section 11-3 we will study radioactivity, which provides information about the excited states of nuclei. Several of the general references at the end of this chapter contain good discussions of the experimental methods used in measuring nuclear properties. We will use the following standard terminology: the letter N stands for the number of neutrons in a nucleus and Z for the number of protons (the atomic number); $A = N + Z$ is the total number of nucleons, the mass number. The mass number is an integer approximately equal to the atomic weight. A particular nuclear species is called a *nuclide*. Nuclides are denoted by the chemical symbol with a presuperscript giving the value of A, such as ^{16}O or ^{15}O. Sometimes Z is given as a pre-subscript, such as $^{15}_{8}O$, although this is not necessary because each element (Z number) has a unique chemical symbol. Occasionally, N is also given as a subscript, such as $^{15}_{8}O_7$, although this, too, is unnecessary since $N = A - Z$. Nuclides with the same Z, such as ^{15}O and ^{16}O, are called *isotopes*. Nuclides with the same N, such as $^{13}_{6}C_7$ and $^{14}_{7}N_7$, are called *isotones*, while nuclides with the same A, such as ^{14}C and ^{14}N, are called *isobars*.

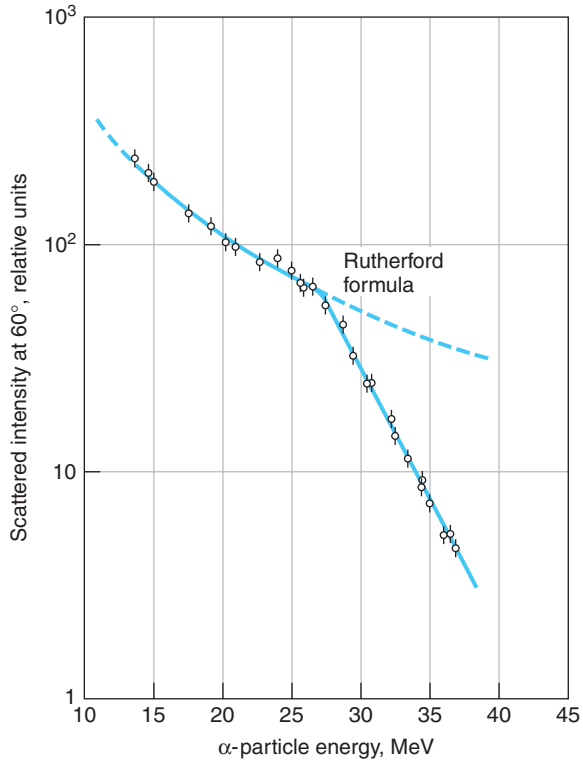

Figure 11-2 Rutherford's α-scattering formula (Equation 4-6) is shown by the dashed line. α particles of increasing energy incident on the nuclei of a Pb target scattered as would be expected by the Rutherford formula until their energy reached about 27 MeV. At greater energies the α particles approach the Pb nuclei closely enough so that the nucleons of the α and the Pb interact via the attractive nuclear force and the scattered intensity falls below that predicted by the Rutherford equation. [*Data from R. M. Eisberg and C. E. Porter, Rev. Mod. Phys., 33, 190 (1961).*]

Size and Shape of Nuclei

Nuclear Radii All of the methods for measuring nuclear radii agree that the radii are proportional to the cube root of the mass number. The nuclear radius can be determined by scattering experiments similar to the first ones of Rutherford or in some cases from measurements of radioactivity. Indeed, as we discussed in Section 4-2 and as illustrated in Figure 11-2, Rutherford's original α-particle-scattering experiment furnished the first measurement of the nuclear radius. An interesting, nearly classical method of determining the nuclear radius involves the measurement of the energy of β decay between *mirror nuclides*, which are nuclides whose Z and N numbers are interchanged (Figure 11-3). For example, ^{15}O, with eight protons and seven neutrons, and ^{15}N, with

STUDENTS-HUB.com Uploaded By: Malak Obaid

eight neutrons and seven protons, are mirror nuclides. If one assumes that the nuclear force between nucleons is independent of the kind of nucleons, the only difference in energy between ^{15}O and ^{15}N is electrostatic. The electrostatic energy of a ball of uniform charge is given by

$$U = \frac{3}{5}\frac{1}{4\pi\epsilon_0}\frac{q^2}{R} \qquad \textbf{11-1}$$

where q is the charge and R is the radius. ^{15}O is radioactive and, as we will discuss further in a later section, decays to ^{15}N by emitting a positron and a neutrino. The energy difference between ^{15}O and ^{15}N, the beta-decay energy, is then

$$\Delta U = \frac{3}{5}\frac{1}{4\pi\epsilon_0}\frac{e^2}{R}\left[Z^2 - (Z-1)^2\right] \qquad \textbf{11-2}$$

with $Z = 8$. A measurement of the energy of decay, equal to ΔU, thus gives a measurement of R. If one assumes a uniform charge distribution, measurements of the positron-decay energies (see Section 11-4) for 18 pairs of mirror nuclides give for the nuclear radius

$$R = R_0 A^{1/3} \quad \text{with} \quad R_0 = 1.2 \pm 0.2 \text{ fm} \qquad \textbf{11-3}$$

where A is the atomic mass number. The value of R_0 in Equation 11-3 includes the effect of a quantum-mechanical correction using a charge distribution calculated from the nuclear shell model discussed in Section 11-6. The consistency of these results with other methods of determining R is a strong indication that the nuclear part of the potential energy is the same for each pair of mirror nuclei.

The most extensive measurements of nuclear radii were carried out by Robert Hofstadter and his co-workers in a series of experiments begun in 1953.[6] In these experiments at the Stanford Linear Accelerator (SLAC), nuclei were bombarded with electrons having energies of about 200 to 500 MeV. The wavelength of a 500-MeV electron is about 2.5 fm, which is smaller than the radius of heavy nuclei. It is thus possible to learn something about the detailed structure of the charge distribution of nuclei by analyzing the diffraction pattern that results from the scattering of these electrons. The analysis is fairly complicated because the electrons are relativistic. Figure 11-4 shows the diffraction pattern of high-energy electrons scattered by ^{16}O and ^{12}C nuclei. If we consider the incoming electron beam to be a plane wave of wavelength λ, the scattering process is similar to the diffraction of light from a circular hole of radius R, discussed in most introductory physics textbooks, where R in this case is the nuclear radius. The first minimum of the diffraction pattern is then given approximately by

$$\sin\theta = 0.16\lambda/R \qquad \textbf{11-4}$$

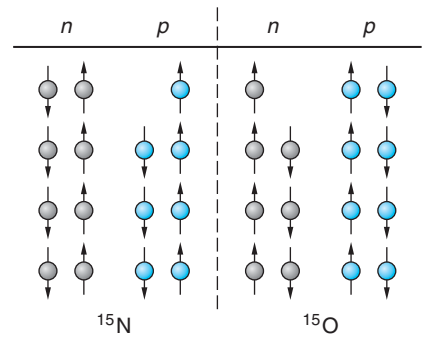

Figure 11-3 Mirror nuclides. If all the neutrons are changed to protons and all the protons are changed to neutrons, ^{15}N becomes its mirror, ^{15}O. The ground-state energy of mirror pairs differs only in the electrostatic energy.

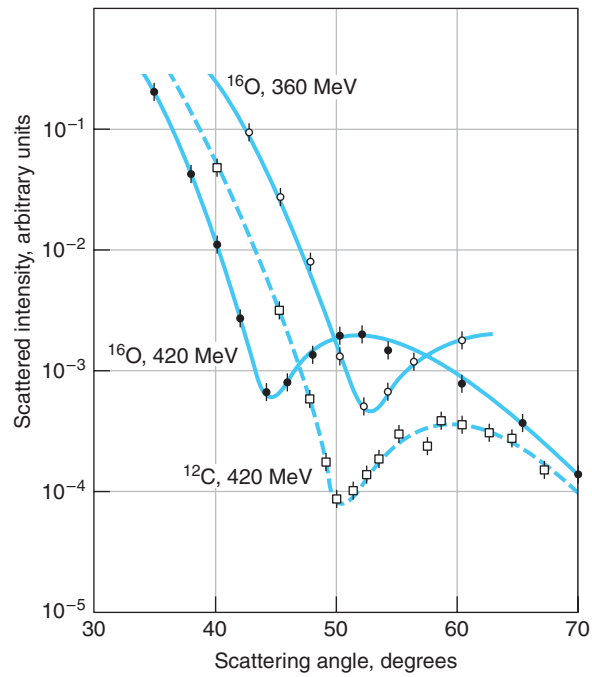

Figure 11-4 Diffraction pattern of high-energy electrons scattered by ^{16}O and ^{12}C. The angle at which the minimum occurs in each pattern is given by Equation 11-4.

STUDENTS-HUB.com Uploaded By: Malak Obaid

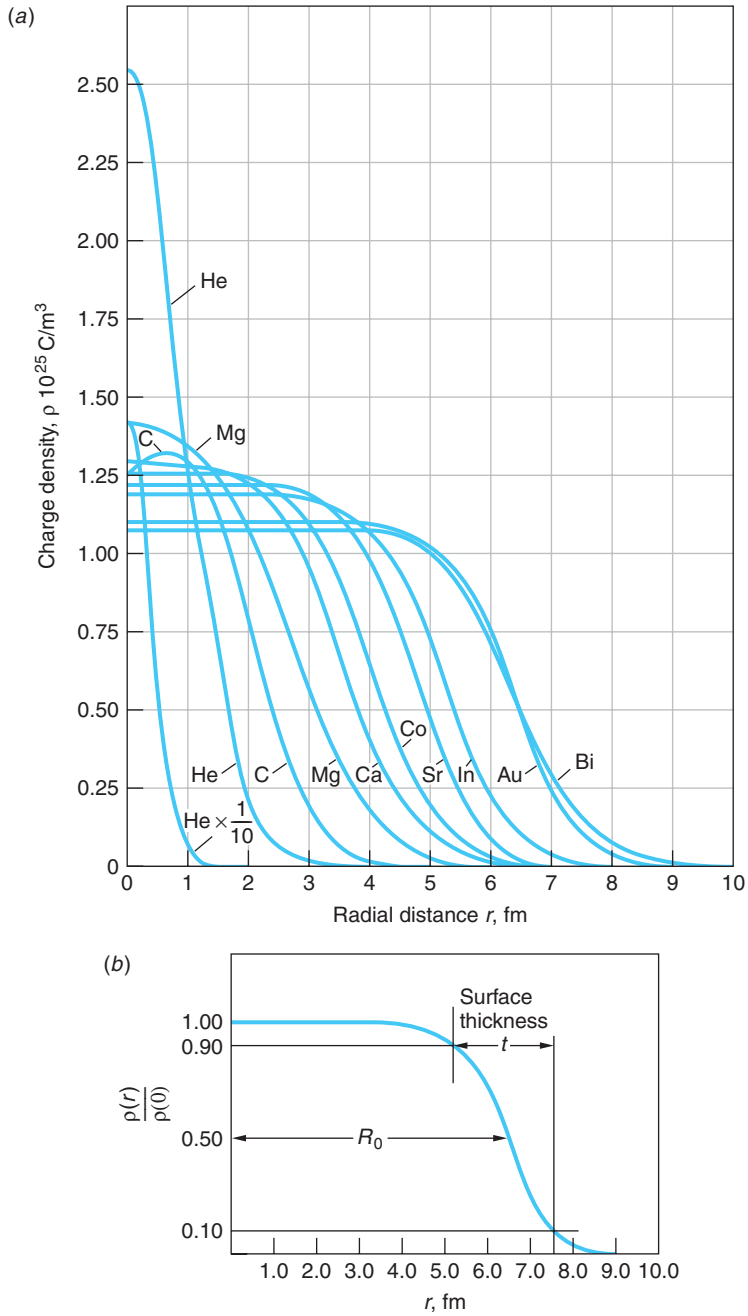

Figure 11-5 (*a*) Charge density versus distance for several nuclei as determined by high-energy electron scattering experiments. (*b*) Definitions of parameters R_0 and t used to describe nuclear charge density. The skin thickness t is measured from 10 percent to 90 percent of the central core density. [*From R. Hofstadter, Annual Review of Nuclear Science, 7, 231 (1957).*]

Example 11-2 shows how the nuclear radius can be calculated from Equation 11-4 with the aid of Figure 11-4. Figure 11-5*a* shows some charge distributions obtained from detailed analysis of these experiments. The mean electromagnetic radius R and the surface thickness t, defined in Figure 11-5*b*, are given by

$$R = (1.07 \pm 0.02)A^{1/3} \text{ fm}$$
$$t = 2.4 \pm 0.3 \text{ fm} \qquad \textbf{11-5}$$

These results are consistent with those obtained from the β-decay studies of mirror nuclides.

STUDENTS-HUB.com Uploaded By: Malak Obaid

EXAMPLE 11-1 Nuclear Radii of ^{4}He and ^{238}U Use Equation 11-3 to compute the radii of ^{4}He and ^{238}U.

SOLUTION

For ^{4}He: $R_{He} = 1.2(4)^{1/3} = 1.90$ fm

For ^{238}U: $R_U = 1.2(238)^{1/3} = 7.42$ fm

Thus, the nuclear radius varies only by a factor of about 4 from the lightest nuclides to the heaviest.

EXAMPLE 11-2 Nuclear Radius of ^{16}O Using the data for 420-MeV electrons scattered from ^{16}O in Figure 11-4, compute a value for the radius of the ^{16}O nucleus.

SOLUTION

1. The radius R of the ^{16}O nucleus is computed from Equation 11-4:
$$\sin\theta = \frac{0.61\lambda}{R} \quad \text{or} \quad R = \frac{0.61\lambda}{\sin\theta}$$

2. The angle θ in Equation 11-4 is the first minimum of the diffraction pattern. From Figure 11-4 we see that the first minimum occurs at about:
$$\theta = 44^\circ$$

3. The de Broglie wavelength λ of the electrons is
$$\lambda = \frac{h}{p}$$

4. The momentum p of the 420-MeV electrons is computed from the relativistic expression, Equation 2-32:
$$p^2c^2 = E^2 - (mc^2)^2$$
$$= (420)^2 - (0.511)^2$$
$$\approx (420 \text{ MeV})^2$$
or
$$p = 420 \text{ MeV}/c = 2.24 \times 10^{-19} \text{ kg} \cdot \text{m/s}$$

5. Substituting this value in λ from step 3 gives
$$\lambda = \frac{6.63 \times 10^{-34} \text{ J} \cdot \text{s}}{2.24 \times 10^{-19} \text{ kg} \cdot \text{m/s}}$$
$$= 2.96 \times 10^{-15} \text{ m} = 2.96 \text{ fm}$$

6. The radius R is computed by substituting the values for θ and λ into Equation 11-4:
$$R = \frac{(0.61)(2.96 \text{ fm})}{\sin 44^\circ} = 2.60 \text{ fm}$$

Remarks: This result agrees well with the values of R_0 for the low-Z nuclei in Figure 11-5a.

STUDENTS-HUB.com Uploaded By: Malak Obaid

A different kind of measurement of the nuclear radius can be made using the attenuation of a beam of fast neutrons as it moves through a sample. The total cross section for attenuation can be shown to be

$$\sigma = 2\pi\left(R + \frac{\lambda}{2\pi}\right)^2 \qquad \textbf{11-6}$$

where R is the nuclear radius and λ is the de Broglie wavelength of the neutron. The neutrons must be fast enough so that $\lambda/2\pi < R$ in order to gain information about R from measurement of σ. These experiments do not measure the charge distribution but instead measure the "radius" of the nuclear force between a neutron and the nucleus. The results of these measurements are

$$R = R_0 A^{1/3} \quad \text{with} \quad R_0 = 1.4 \text{ fm} \qquad \textbf{11-7}$$

These different types of experiments thus give comparable but not identical results, depending on whether the particular experiment measures the nuclear force radius (neutrons) or the nuclear charge radius (electrons). The fact that the radius is proportional to $A^{1/3}$ implies that the volume of the nucleus is proportional to A. Since the mass of the nucleus is also approximately proportional to A, the densities of all nuclei are approximately the same. A drop of liquid also has a constant density independent of its size, and this fact has led to a model in which the nucleus is viewed as analogous to a liquid drop. This model has been helpful in computing nuclear masses and in understanding certain types of nuclear behavior, particularly the fission of heavy elements. The numerical value of the nuclear density is about 10^{17} kg/m^3. This fantastically high density, compared with 10^3 kg/m^3 for atoms, is a consequence of the fact that nearly all the mass of the atom is concentrated in a region whose radius is only about 10^{-5} that of the atom. A cubic millimeter of nuclear matter has a mass of about 200,000 metric tons, or about the same mass as a supertanker filled with petroleum!

EXAMPLE 11-3 Radius of a Neutron Star In certain supernova events, the outer layer of the star is blown away, leaving a core consisting entirely of neutrons. This stellar remnant is called a *neutron star*, and its density is approximately the same as that of atomic nuclei. Compute the radius of a neutron star whose mass is equal to that of the Sun, 1.99×10^{30} kg.

SOLUTION

The mass of the neutron star is $M = \rho V$, where V is the volume and the density ρ is approximately 10^{17} kg/m^3. Assuming the neutron star to be a sphere, we have that

$$M = 1.99 \times 10^{30} \text{ kg} = \rho V = (10^{17} \text{ kg/m}^3)(4\pi R^3/3)$$

where R is the radius of the star in meters. Solving for R^3 yields

$$R^3 = \frac{(3)(1.99 \times 10^{30} \text{ kg})}{(4\pi)(10^{17} \text{ kg/m}^3)} = 4.75 \times 10^{12} \text{ m}^3$$

and taking the cube root

$$R = 1.68 \times 10^4 \text{ m} = 16.8 \text{ km}$$

Remarks: *By way of comparison, the mean diameter of the Sun is* 1.39×10^6 km.

STUDENTS-HUB.com Uploaded By: Malak Obaid

Nuclear Shape With a few exceptions, nuclei are nearly spherical. Most of the exceptions occur in the rare earth elements (the transition region in the periodic table, $Z = 57$ to $Z = 71$), in which the shape is ellipsoidal, with the major axis differing from the minor axis by about 20 percent or less. In these heavy nuclides, the inner atomic electron wave functions penetrate the nucleus, and deviations from spherical shape, which correspond to deviations in the nuclear charge distributions, show up as small changes in the atomic energy levels. In direct analogy with the fact that the potential at points outside a static distribution of charges is determined by the dimensions of the distribution[7] and, conversely, that measuring the potential yields information about the distribution, measuring these small changes in the atomic energy levels yields information about the nuclear charge distribution, even though it can't be measured directly. If the nucleus is shaped like a watermelon (Figure 11-6*a*), with the extent of the distribution larger along the z axis than along the x and y axes, the average value of z^2 is larger than the average values of x^2 and y^2. In this case the *electric quadrupole moment* Q, which is proportional to $3(z^2)_{av} - (x^2 + y^2 + z^2)_{av}$, is positive. This is the most common case for nonspherical nuclei. Nuclei with negative quadrupole moments are shaped more like flattened pumpkins, with the two equal axes longer than the third axis, as in Figure 11-6*b*. The average value of the electric quadrupole moment is given by

$$\langle Q \rangle = Z \int \psi^* \left[3(z^2)_{av} - (x^2 + y^2 + z^2)_{av} \right] \psi \, dV \qquad \textbf{11-8}$$

> 0 for $z^2 > x^2, y^2$ (Figure 11-6*a*)

$= 0$ for $z^2 = x^2 = y^2$ (spherical)

< 0 for $z^2 < x^2, y^2$ (Figure 11-6*b*)

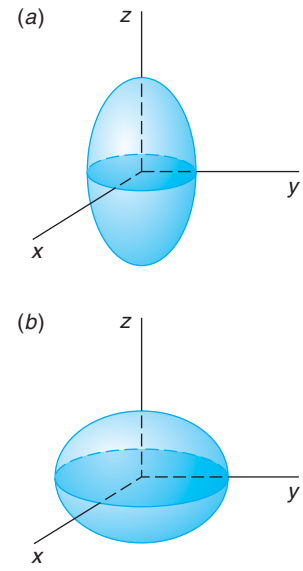

Figure 11-6 Nonspherical nuclear shapes. Nuclei with positive quadrupole moments have $(z^2)_{av}$ greater than $(x^2)_{av}$ or $(y^2)_{av}$ and are of watermelon shape, as in (*a*). Nuclei with negative quadrupole moments have $(z^2)_{av}$ less than $(x^2)_{av}$ or $(y^2)_{av}$ and are shaped like flattened pumpkins, as in (*b*).

Figure 11-7 shows the measured values of the electric quadrupole moment for the odd A nuclei, i.e., those for which either Z or N is odd. Equation 11-8 is evaluated for wave functions corresponding to the nuclear charge distributions of various theoretical models of the nucleus and compared with the values in Figure 11-7. As you might imagine, the calculations are formidable!

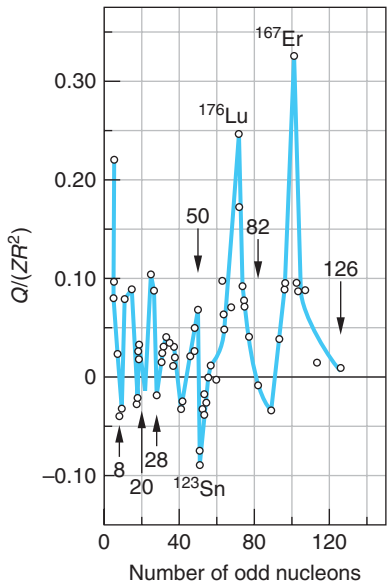

Figure 11-7 The electric quadrupole moment Q divided by Z and R^2, where R is the average nuclear radius, is plotted versus the number of nucleons of the odd type (Z or N). The arrows indicate the points where $Q/ZR^2 = 0$, corresponding to spherical shape.

STUDENTS-HUB.com Uploaded By: Malak Obaid

Nuclear Stability

Among the more than 3000 known nuclides, there are only 266 whose ground states are stable. All of the rest have unstable ground states, which eventually undergo radioactive decay, that is, transition to some lower-energy state of a different element. Figure 11-8

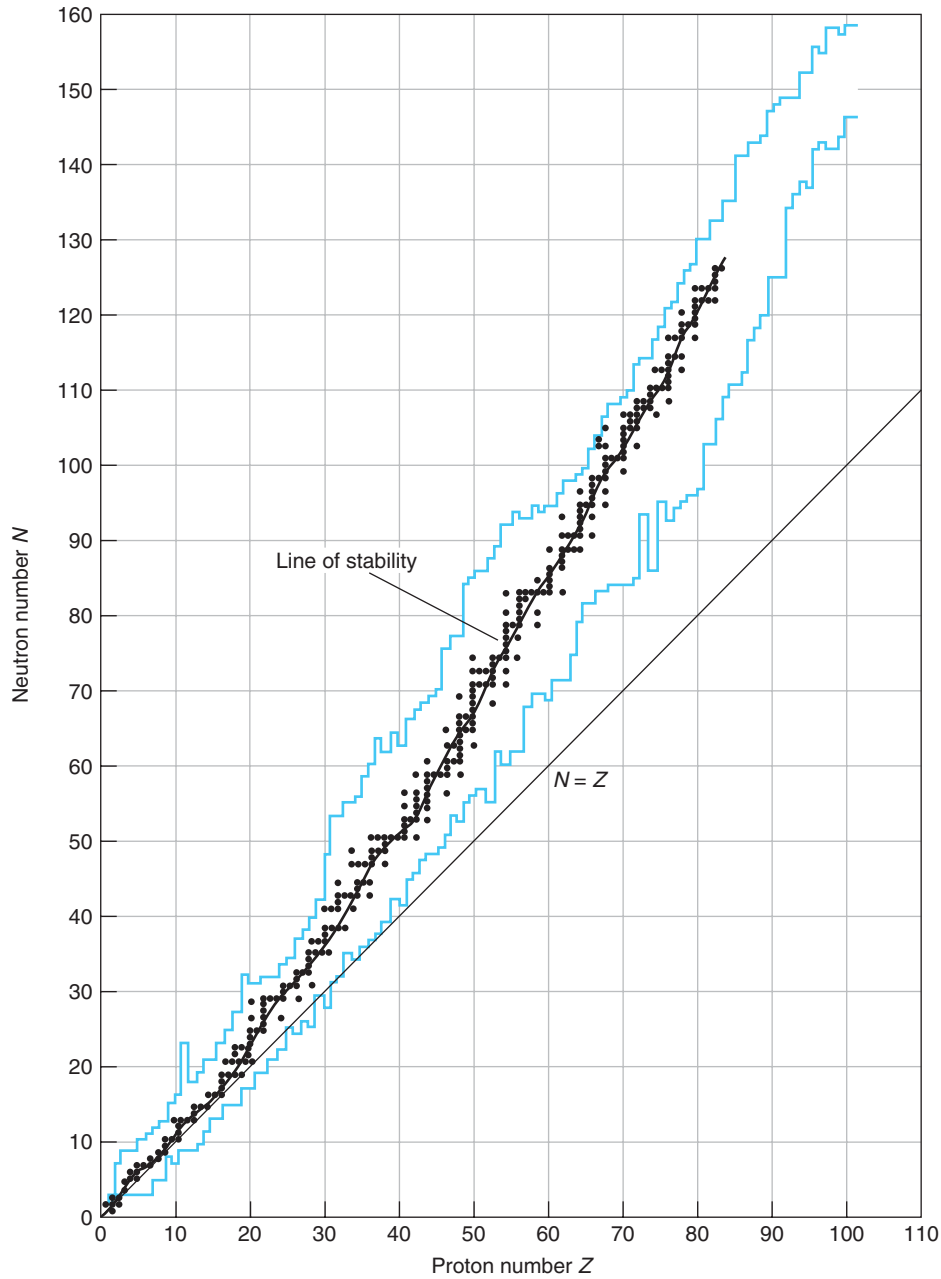

Figure 11-8 Plot of neutron number N versus proton number Z for the known nuclides. The 266 stable nuclides are indicated by the black dots. The area between the irregular colored lines represents the known unstable, or radioactive, nuclides whose lifetimes are longer than about a millisecond. The curved line through the stable nuclides is called the *line of stability*.

STUDENTS-HUB.com Uploaded By: Malak Obaid

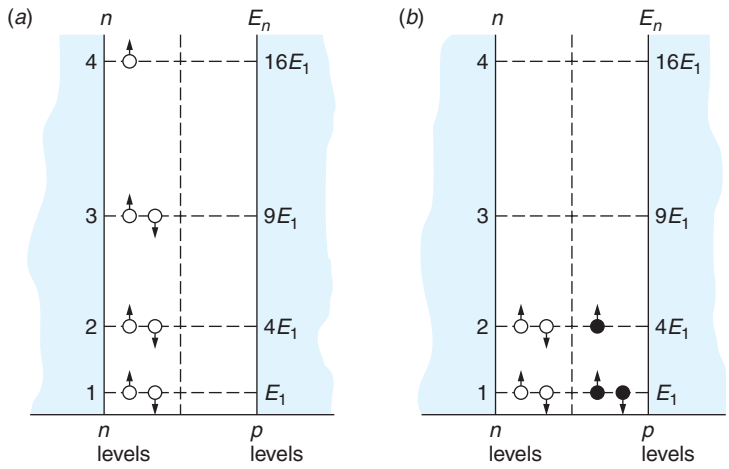

Figure 11-9 (*a*) Seven neutrons in an infinite square well. In accordance with the exclusion principle, only two neutrons can be in a given space state. The total energy is $16E_1 + (2 \times 9E_1) + (2 \times 4E_1) + (2 \times 1E_1) = 44E_1$. (*b*) Four neutrons and three protons in the same infinite square well. Because protons and neutrons are not identical, four particles (two neutrons and two protons) can be in the state $n = 1$. The total energy is $(3 \times 4E_1) + (4 \times 1E_1) = 16E_1$. This is much less than in (*a*). The integers on the left of each well are infinite square well principal quantum numbers.

shows a plot of the neutron number N versus the proton number Z for the stable nuclides and the known unstable ones whose lifetimes are longer than about a millisecond. The straight line is $N = Z$. The general shape of the *line of stability*, shown by the light curve tracing through the stable nuclides in Figure 11-8, can be understood in terms of the exclusion principle and the electrostatic energy of the protons. Consider the kinetic energy of A particles in a one-dimensional square well, which is an adequate model for demonstrating this point. The energy is smallest if $A/2$ are neutrons and $A/2$ are protons and greatest if all the particles are of one type (Figure 11-9). Hence there is a tendency, due to the exclusion principle, for N and Z to be equal. If we include the electrostatic energy of repulsion of the protons, the result is changed somewhat. This potential energy is proportional to Z^2. At large A, the energy is increased less by adding two neutrons than by adding one neutron and one proton, and so the difference $N - Z$ increases with increasing Z.

There is also a tendency for nucleons to pair with other identical nucleons. Of the 266 nuclides whose ground states are stable, 159 have even Z and even N, 50 have odd Z and even N, 53 have even Z and odd N, and only 4 have both odd N and Z. (See Table 11-2.)

Table 11-2 *N* versus *Z* for stable isotopes

	Z	
N	Even	Odd
Even	159	50
Odd	53	4

STUDENTS-HUB.com Uploaded By: Malak Obaid

Since there are about 100 different elements and about 270 stable nuclides, there is an average of about 2.7 stable isotopes per element. There is a larger than the average number of stable isotopes for nuclei with Z equal to 20, 28, 50, and 82. For example, tin, with $Z = 50$, has 10 stable isotopes. Similarly, nuclides with these same numbers of neutrons have a larger than average number of isotones. These numbers, called *magic numbers*, are a manifestation of shell structure in very much the same way that the atomic "magic numbers" 2, 10, 18, and 36 correspond to closed-electron-shell structure. As we will discuss further in Section 11-6, the nuclear magic numbers, which also include 2, 8, and 126, represent configurations of particular stability. An *island of stability* is hypothesized to exist around $Z = 126$. In the search for it thus far, a few atoms with atomic numbers up to 118 have been created in that region. (Atoms with atomic number 117 have not yet been synthesized.)

Nuclides that fall between the irregular colored lines in Figure 11-8, except those marked by the black dots, are radioactive. We will discuss radioactivity in Section 11-3.

Masses and Binding Energies

The mass of an atom can be accurately measured in a mass spectrometer, which measures q/M for ions by bending them in a magnetic field.[8] The mass of an atom is slightly smaller than the mass of the nucleus plus the mass of the electrons because of the binding energy of the electrons. The binding energy of the electrons is defined by

$$B_{\text{atomic}} = M_N c^2 + Z m_e c^2 - M_A c^2 = \Delta m c^2 \qquad \textbf{11-9}$$

where M_N is the mass of the nucleus, M_A is the mass of the atom, m_e is the mass of an electron, and Δm is the mass equivalent of B_{atomic}. (See Section 2-3.) Because the binding energies of atoms are only of the order of keV, compared with nuclear binding energies of many MeV, atomic binding energies are usually neglected in nuclear physics. The binding energy of a nucleus with Z protons and N neutrons is defined as

$$B_{\text{nuclear}} = Z m_p c^2 + N m_n c^2 - M_A c^2 \qquad \textbf{11-10}$$

where m_p is the mass of a proton, m_n the mass of a neutron, and M_A the mass of the nucleus of mass number A. Since the mass of an atom is very nearly equal to the mass of the nucleus plus the mass of the electrons (neglecting the atomic binding energy), the nuclear binding energy can be accurately computed from

$$B_{\text{nuclear}} = Z M_{\text{H}} c^2 + N m_n c^2 - M_A c^2 \qquad \textbf{11-11}$$

where M_A is the atomic mass and M_{H} is the mass of a hydrogen atom. Note that the masses of the Z electrons cancel out. This expression is more convenient to use because it is the mass of the atom that is usually measured in mass spectrometers. The atomic masses of all stable nuclides and of many unstable ones are listed in Appendix A.

Once the mass of a nucleus or atom is determined, the binding energy can be computed from Equation 11-10 or 11-11. The binding energy per nucleon B/A is plotted against A for the most stable isotope of each element in Figure 11-10. The mean value is about 8.3 MeV/nucleon. The fact that this curve is approximately constant (for $A > 16$) indicates that the nuclear force is a *saturated* force. This is partially explained by the short range of the nuclear force (see Section 11-5). If each nucleon interacted with every other nucleon, there would be $A - 1$ interactions for each nucleon, and the binding energy per nucleon would be proportional to $A - 1$ rather than constant.

STUDENTS-HUB.com Uploaded By: Malak Obaid

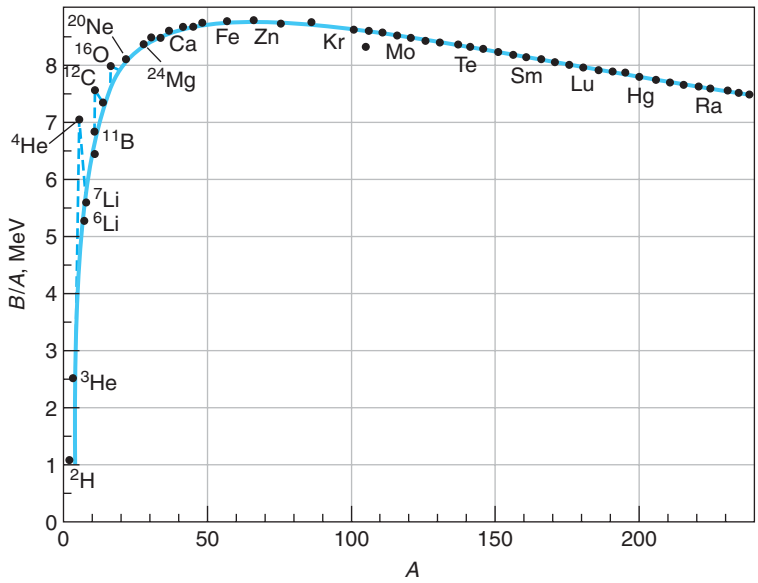

Figure 11-10 The binding energy per nucleon versus atomic mass number A. The solid curve represents the Weizsächer semiempirical binding-energy formula, Equation 11-12.

Figure 11-10 indicates that instead there is a fixed number of interactions per nucleon, as would be the case if each nucleon were attracted only to its nearest neighbors. Such a situation also leads to a constant nuclear density, consistent with the radius measurements. If the binding energy per nucleon were instead proportional to the number of nucleons, then the nuclear radius would be approximately constant, as is the case for the atomic radii.

More

Of the several models of the nucleus physicists have developed, the liquid-drop model has been one of the most useful. It has been successful in describing the fission process and nuclear reactions and, in particular, predicting the binding energies (i.e., masses) of isotopes and individual nucleons within the nucleus. These topics are discussed in *Liquid-Drop Model and the Semiempirical Mass Formula* on the home page: www.whfreeman.com/tiplermodernphysics5e. See also Equations 11-12 through 11-14 and Table 11-3 here, as well as Examples 11-4 through 11-6.

Nuclear Angular Momenta and Magnetic Moments

The spin quantum number of both the neutron and the proton is 1/2, which means that the nucleons are fermions. The angular momentum of the nucleus is a combination of the spin angular momenta of the nucleons plus any orbital angular momentum due to the motion of the nucleons. This resultant angular momentum is usually called *nuclear spin* and designated by the symbol **I**. The nucleons individually have magnetic moments, which also combine to produce the *nuclear magnetic moment*. Evidence for nuclear spin and magnetic moment was first found in atomic spectra. The nuclear spin adds to the angular momentum $\mathbf{J} = \mathbf{L} + \mathbf{S}$ of the electrons to form a total angular momentum **F**:

$$\mathbf{F} = \mathbf{I} + \mathbf{J} \qquad \textbf{11-15}$$

STUDENTS-HUB.com Uploaded By: Malak Obaid

The possible quantum numbers for F are $(I + J), (I + J - 1), \ldots, |I - J|$, according to the usual rule for combining angular momenta. F obeys the selection rule $\Delta F = \pm 1, 0$, but no $F = 0 \rightarrow F = 0$. The number of possible values of F is $(2J + 1)$ or $(2I + 1)$, whichever is smaller. Because of the energy of the interaction between the electronic magnetic moment and the nuclear magnetic moment associated with I, each atomic spectral line is split into $(2J + 1)$ or $(2I + 1)$ components. This splitting is one of several effects that are the result of interactions of the nuclear spins and moments with the environment of the nucleus, including its own atomic electrons, collectively called *hyperfine structure*.[10] The hyperfine splitting of the spectral lines associated with the nuclear magnetic moment occurs for a reason that is exactly analogous to the spin-orbit coupling discussed in Section 7-5 that is the origin of the fine structure of the atomic spectral lines. The coupling between $\mathbf{I}$ and $\mathbf{J}$ expressed by Equation 11-15 results in a splitting of the *atomic* energy levels by an amount ΔE, in addition to the spin-orbit splitting of Equation 7-68, given by the analogous relation

$$\Delta E = g_N m_I \mu_N B_e \qquad \textbf{11-16}$$

where g_N is the nuclear Landé factor, m_I is the magnetic quantum number of the z component of $\mathbf{I}$, $\mu_N = e\hbar/2m_p$ is the nuclear magneton, and B_e is the magnetic field at the nucleus produced by the electrons (Table 11-4). The product $g_N m_I \mu_N$ is the nuclear magnetic moment. Except for μ_N, the quantities on the right side of Equation 11-16 are all of the same order of magnitude as the corresponding ones in Equation 7-68; however, the ratio $\mu_N/\mu_B \approx 10^{-3}$. Thus, the hyperfine splitting for a given atom is very small, about 10^{-3} times the fine-structure splitting. Using as an example the sodium doublet levels $^2P_{1/2}$, $^2P_{3/2}$, and $^2S_{1/2}$ shown in Figure 7-30, which produce the yellow D lines, Figure 11-11 illustrates the hyperfine splitting of these levels resulting from $I - J$ coupling. It can be observed only with extremely high resolution. The use of tunable dye lasers and atomic beam fluorescence spectroscopy has made high precision measurements of these extremely small energy splittings possible in recent years.

For the case $I \leq J$, there are $(2I + 1)$ different F states; thus the nuclear spin can be determined by counting the number of lines in the hyperfine splitting. The spin of all even-even nuclides (those with even Z and even N) is zero in the ground state.

Table 11-4 Magnetic field B_e at the nucleus due to electron for selected alkali elements

Element	n	B_e, $^2S_{1/2}$(T)	B_e, $^2P_{1/2}$(T)	B_e, $^2P_{3/2}$(T)
H	1	17	—	—
Li	2	13	—	—
Na	3	44	4.2	2.5
K	4	63	7.9	4.6
Rb	5	130	16	8.6
Cs	6	210	28	13

Source: Data are from E. Segrè, *Nuclei and Particles*, 2d ed. (Menlo Park, CA: Benjamin/Cummings 1977), p. 259.

STUDENTS-HUB.com Uploaded By: Malak Obaid

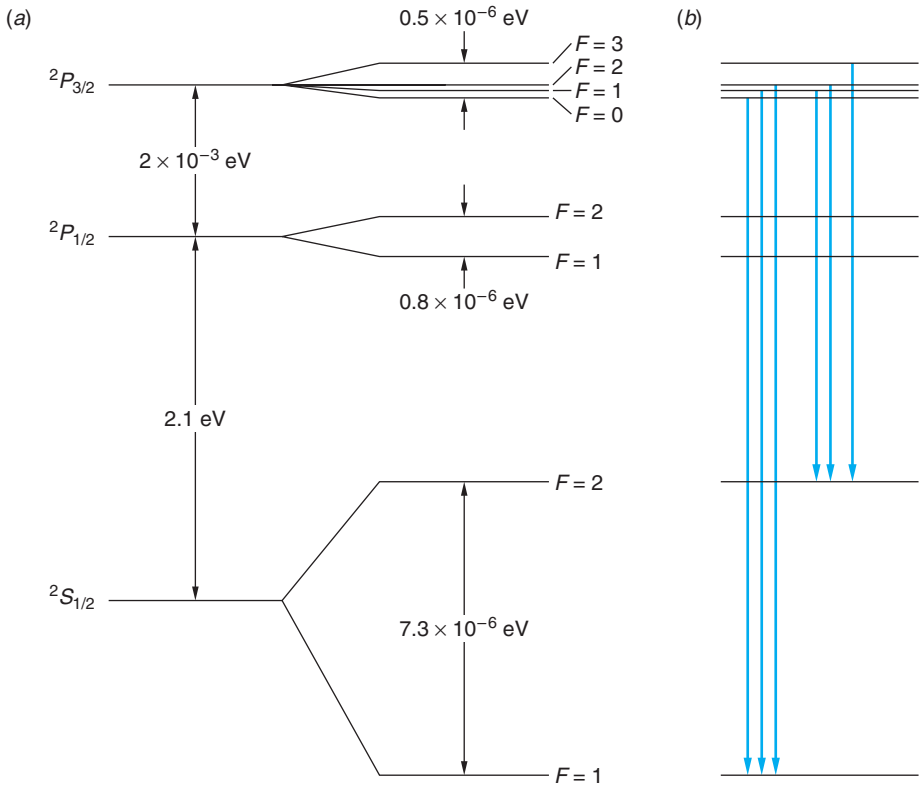

Figure 11-11 (*a*) Transitions between the sodium doublet levels produce the yellow *D* lines, $^2P_{1/2} \rightarrow {}^2S_{1/2}$ being D_1 and $^2P_{3/2} \rightarrow {}^2S_{1/2}$ being D_2. Coupling between the atomic angular momentum J and the nuclear spin $I = 3/2$ results in the hyperfine splitting, each level having total angular momentum $\mathbf{F} = \mathbf{I} + \mathbf{J}$. Note that the hyperfine splitting of each of the doublet levels is about 10^{-3} times that of the fine-structure splitting of the ^2P level. (*b*) The selection rule $\Delta F = \pm 1, 0$ leads to the D_2 line being split into six components. The D_1 line is correspondingly split into four components (not shown).

Evidently the nucleons couple together in such a way that their angular momenta add to zero in pairs, as is often the case for electrons in atoms. There is no such simple rule for other nuclides with either odd N or odd Z or both. Some of the successes of the shell model to be discussed in Section 11-6 are the correct prediction of nuclear spins for many nuclei.

The magnetic moment of the nucleus $g_N m_I \mu_N$ is of the order of the nuclear magneton, $\mu_N = e\hbar/2m_p$, since the magnitude of g_N is typically between 1 and 5 and the maximum value of $|m_I| = I$. The exact value is difficult to predict because it depends on the detailed motion of the nucleons. If the proton and neutron obeyed the Dirac relativistic wave equation, as does the electron, the magnetic moment due to spin would be 1 nuclear magneton for the proton because its charge is $+e$ and 0 for the neutron because it has no charge.[11] The experimentally determined moments of the nucleons are

$$(\mu_p)_z = +2.79285\ \mu_N$$
$$(\mu_n)_z = -1.91304\ \mu_N$$

As we will see in Chapter 12, the proton and neutron are more complex particles than the electron. It is interesting that the deviations of these moments from those predicted by the Dirac equation are about the same magnitude, 1.91 for the neutron and 1.79 for the proton. The reason that the magnetic moments of the nucleons have these particular values is not yet completely understood; the current theoretical predictions of μ_p and μ_n agree with high-precision, experimentally measured values only to within about 1 percent.

The degeneracy of the hyperfine levels in nuclei with nonzero spins, e.g., the proton in ^{1}H, is removed by an external **B** field, a nuclear analog of the Zeeman effect. Transitions between these levels, separated (in ^{1}H) by $2\mu_p B$, oscillate at the spin precession rate. Detection of the resulting absorption or emission of radiation allows "mapping" of the hydrogen-containing soft tissue, the basis for medical *magnetic resonance imaging* (MRI).

STUDENTS-HUB.com Uploaded By: Malak Obaid

EXAMPLE 11-7 **Nuclear Spin of Thallium-205** High-resolution spectroscopic study of the spectrum of ^{205}Tl reveals that each component of the doublet $^2P_{1/2} \rightarrow {}^2S_{1/2}$ (377.7 nm), $^2P_{3/2} \rightarrow {}^2S_{1/2}$ (535.2 nm) consists of three hyperfine components. This requires that there be two hyperfine levels for each J. Determine the spin of the ^{205}Tl nucleus.

SOLUTION

If $I \leq J$, then there are $(2I + 1)$ different F levels, and if $I > J$, there are $(2J + 1)$ different F levels. Since the hyperfine spectrum indicates that there are two levels for each J, then for the $^2P_{3/2}$ level either

$$2I + 1 = 2 \quad \text{or} \quad 2J + 1 = 2$$

But we already know that $J = (3/2)$, so $(2J + 1)$ cannot equal 2; therefore $(2I + 1) = 2$ and the spin of the ^{205}Tl nucleus (in its ground state) must be $1/2$.

Note that for the $^2P_{1/2}$ and $^2S_{1/2}$ levels both of the equations above are satisfied since in these two cases $I = J$.

Questions

1. Why is N approximately equal to Z for stable nuclei? Why is N greater than Z for heavy nuclei?
2. Why are there no stable isotopes with $Z > 83$?
3. The mass of ^{12}C, which contains 6 protons and 6 neutrons, is exactly 12.000 u by the definition of the unified mass unit. Why isn't the mass of ^{16}O, which contains 8 protons and 8 neutrons, exactly 16.000 u?

11-3 Radioactivity

Of the more than 3000 nuclides known, only 266 are stable. All of the rest are radioactive; that is, they decay into other nuclides by emitting radiation. The term *radiation* here refers to particles as well as electromagnetic radiation. In 1900 Rutherford discovered that the rate of emission of radiation from a substance was not constant but decreased exponentially with time. This exponential time dependence is characteristic of all radioactivity and indicates that it is a statistical process. Because each nucleus is well shielded from others by the atomic electrons, pressure and temperature changes have no effect on nuclear properties.[12]

For a statistical decay (in which the decay of any individual nucleus is a random event), the number of nuclei decaying in a time interval dt is proportional to dt and to the number of nuclei present. If $N(t)$ is the number of radioactive nuclei at time t and $-dN$ is the number that decay in dt (the minus sign is necessary because N decreases), we have

$$-dN = \lambda N\, dt \qquad \textbf{11-17}$$

where the constant of proportionality, λ, is called the *decay constant*. λ is the probability per unit time of the decay of any given nucleus. The solution of this equation is

$$N(t) = N_0 e^{-\lambda t} \qquad \textbf{11-18}$$

STUDENTS-HUB.com Uploaded By: Malak Obaid

where N_0 is the number of nuclei present at time $t = 0$. The decay rate is

$$R = -\frac{dN}{dt} = \lambda N_0 e^{-\lambda t} = R_0 e^{-\lambda t} \qquad \textbf{11-19}$$

Note that *both the number of nuclei and the rate of decay decrease exponentially with time*. It is the decrease in the rate of decay that is determined experimentally. Figure 11-12 shows N versus t. If we multiply the numbers on the N axis by λ, this becomes a graph of R versus t.

We can calculate the *mean lifetime* from Equation 11-18. The number of nuclei with lifetimes between t and $t + dt$ is the number that decay in dt, which is $\lambda N\, dt$; thus the fraction with lifetimes in dt is

$$f(t)\, dt = \frac{\lambda N\, dt}{N_0} = \lambda e^{-\lambda t}\, dt \qquad \textbf{11-20}$$

When we use this distribution function, the mean lifetime τ is

$$\tau = \int_0^\infty t f(t)\, dt = \int_0^\infty t\lambda e^{-\lambda t}\, dt = \frac{1}{\lambda} \qquad \textbf{11-21}$$

which is the reciprocal of the decay constant λ. The *half-life* $t_{1/2}$ is defined as the time after which the number of radioactive nuclei has decreased to half its original value. From Equation 11-18,

$$\frac{1}{2}N_0 = N_0 e^{-\lambda t_{1/2}} \quad \text{or} \quad e^{\lambda t_{1/2}} = 2$$

$$t_{1/2} = \frac{\ln 2}{\lambda} = (\ln 2)\tau = \frac{0.693}{\lambda} = 0.693\,\tau \qquad \textbf{11-22}$$

After each time interval of one half-life, the number of nuclei left in a given sample and the decay rate have both decreased to half of their previous values. For example, if the decay rate is R_0 initially, it will be $(1/2)R_0$ after one half-life, $(1/2)(1/2)R_0$ after two half-lives, and so forth. During one mean lifetime, the number of nuclei remaining in the sample and the decay rate have decreased to $1/e$ of their previous values. Thus, if the initial decay rate is R_0, it will be $(1/e)R_0$ after time τ has elapsed, $(1/e)(1/e)R_0$ after time 2τ, and so on. The SI unit of radioactivity is the *becquerel* (Bq), which is defined as one decay per second:

$$1\ \text{Bq} = 1\ \text{decay/s} \qquad \textbf{11-23}$$

A historical unit of activity, the *curie* (Ci), is also frequently used. The curie is defined as

$$1\ \text{Ci} = 3.7 \times 10^{10}\ \text{decay/s} = 3.7 \times 10^{10}\ \text{Bq} \qquad \textbf{11-24}$$

The curie is the disintegration rate of 1 g of radium. Since this is a very large unit, the millicurie (mCi), microcurie (μCi), and picocurie (pCi) are also often used.

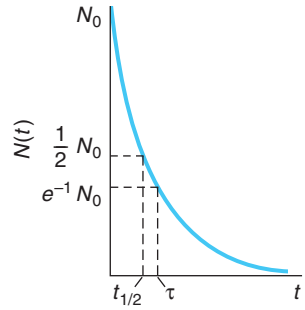

Figure 11-12 Exponential radioactive decay law. The number of nuclei remaining at time t decreases exponentially with time t. The half-life $t_{1/2}$ and the mean life $\tau = 1/\lambda$ are indicated. The decay rate $R(t) = \lambda N(t)$ has the same time dependence.

STUDENTS-HUB.com Uploaded By: Malak Obaid

EXAMPLE 11-8 **Counting Rate of a Radioactive Sample** A radioactive source has a half-life of 1 minute. At time $t = 0$ it is placed near a detector and the counting rate (the number of decay particles detected per unit time) is observed to be 2000 counts/s. (*a*) Find the mean life and the decay constant. (*b*) Find the counting rate at times $t = 1$ min, 2 min, 3 min, and 10 min.

SOLUTION

1. For question (*a*), the mean life τ is related to the half-life $t_{1/2}$ by Equation 11-22:

$$t_{1/2} = (\ln 2)\tau$$

or

$$\tau = \frac{t_{1/2}}{\ln 2} = \frac{1 \text{ min}}{0.693} = 1.44 \text{ min} = 86.6 \text{ s}$$

2. From Equation 11-21, the decay constant is given by

$$\lambda = \frac{1}{\tau} = \frac{1}{86.6 \text{ s}} = 1.16 \times 10^{-2} \text{ s}^{-1}$$

3. *Method 1.* For question (*b*), the counting rate is proportional to the decay rate R in Equation 11-19. The counting rate at $t = 0$ has the same proportionality to R_0, so we can write the counting rate as R, substituting values for λ and for $t_{1/2}$:

$$R = 2000\, e^{-\lambda t} = 2000\, e^{-(1.16\times 10^{-2})t}$$
$$= 2000\, e^{-(\ln 2)t/t_{1/2}}$$
$$= 2000\, e^{-(0.693)t}$$

where t is now expressed in minutes

4. The counting rate R can now be computed for each of the times $t = 1$ min, 2 min, 3 min, and 10 min as follows:

$$R(1 \text{ min}) = 2000\, e^{-(0.693)(1)} = 2000 \times 0.50 = 1000 \text{ counts/s}$$
$$R(2 \text{ min}) = 2000\, e^{-(0.693)(2)} = 500 \text{ counts/s}$$

and similarly

$$R(3 \text{ min}) = 250 \text{ counts/s}$$
$$R(10 \text{ min}) = 1.95 \text{ counts/s}$$

5. *Method 2.* Since the half-life is 1 min, the counting rate at $t = 1$ min will be half that at $t = 0$; at $t = 2$ min it will be half of that at $t = 1$ min, and so on. In general, at $t = n$ min the count rate will be

$$R = (1/2)^n R_0$$

and again

$$R(1 \text{ min}) = (1/2)^1 2000 = 1000 \text{ counts/s}$$

and

$$R(10 \text{ min}) = (1/2)^{10} 2000$$
$$= (0.0010)(2000) = 1.95 \text{ counts/s}$$

STUDENTS-HUB.com Uploaded By: Malak Obaid

More

Very often the decay of a radioactive nucleus results in a new nucleus that is also radioactive and that, in general, has a different decay constant. In some cases such sequential decays may result in a dozen or more different radioactive isotopes. *Production and Sequential Decays*, on the home page (www.whfreeman.com/tiplermodernphysics5e), describes the way to calculate the total activity and the net rate at which new isotopes are produced. See Equations 11-25 through 11-29 and Figures 11-13 and 11-14 here, as well as Examples 11-9 and 11-10 and Questions 4 and 5.

11-4 Alpha, Beta, and Gamma Decay

From the time when Becquerel's discovery of radioactivity gave the first hint of the existence of the nucleus, much of what physicists have learned about nuclear structure has resulted from studies of radioactive nuclides, that is, by studying the transitions of nuclei from one quantum state to another of lower energy. As noted earlier, of the approximately 3000 known isotopes, all but 266 are radioactive. In addition, nearly all of a theoretically estimated 2000 more possible isotopes that have yet to be created are radioactive. The radioisotopes decay by one or another of at least nine different modes; however, most decays occur via one or sometimes two of the most common modes: alpha, beta, and gamma. Others occur by more unusual routes, such as emission of a proton or neutron or spontaneous fission. A few may decay by modes that are exceedingly rare, such as a double beta decay, which is the focus of considerable current theoretical and experimental interest. The fundamental purpose of the studies of radioactive nuclei is to obtain information about nuclear structure, the nature of the strong nuclear force, and the properties of elementary particles.

In the subsections that follow we will discuss the three most common types of decay in some detail, touching on certain of the others when pertinent. In these discussions it will be helpful to keep two points in mind. The first of these is that the line of stability in Figure 11-8 is the floor of an energy valley formed by plotting the binding energy for each isotope on an energy scale perpendicular to the N and Z axes, as illustrated in Figure 11-15*a*. In Figure 11-15*a* the energy is artificially truncated; however, there are theoretical limitations placed on the numbers of protons and neutrons that can be assembled into a nucleus, even a highly unstable one. These limits, given the whimsical name *driplines*, are shown in Figure 11-15*b* and define the N-Z boundaries within which lie the 5000 or so isotopes that may, in principle, exist. The limits are set by the energies at which the nuclei will spontaneously emit a proton or neutron.

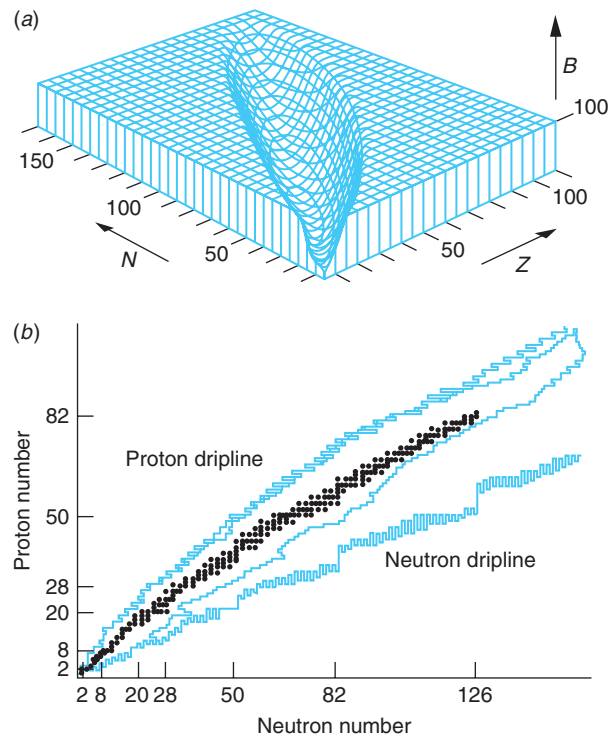

Figure 11-15 (*a*) The graph of Z versus N with the nuclear binding energy B (in MeV) plotted upward. The surface thus formed is truncated at 100 MeV to make the energy valley more clearly visible. (*b*) More than 5000 theoretically predicted nuclei lie between the proton and neutron driplines. Only about 3000 (those between the inner irregular colored lines) are found in nature or have been created in the laboratory, and only 266 of those are stable (black dots). The edges of the truncation in (*a*) are analogous to artificial driplines.

STUDENTS-HUB.com Uploaded By: Malak Obaid

The second point to bear in mind is that radioactive-decay processes conform to the same conservation laws that are obeyed by all physical processes. In particular, (1) relativistic mass-energy, (2) electric charge, (3) linear momentum, (4) angular momentum, (5) nucleon number, and (6) lepton number[13] are all conserved quantities. The first four of these are already familiar to you from your previous study of physics. The last two relate specifically to the interactions and decays of fundamental particles and will be discussed in Chapter 12. As we discuss the three most common modes of radioactive decay, consequences of each of the conservation laws will be illustrated.

Alpha Decay

The α particles emitted by a tiny amount of ^{241}Am are used to ionize the air inside smoke detectors. When smoke is present, the ionized air molecules stick to the smoke particles, reducing a trickle current maintained in the ionized air, thereby triggering an alarm. Ionization-type smoke detectors are considerably more sensitive than those using photoelectric sensors.

In order for a radioactive substance to be found in nature, either it must have a half-life that is not much shorter than the age of Earth (about 4.5×10^9 years) or it must be continually produced by the decay of another radioactive substance or by a nuclear reaction. For a nucleus to be radioactive at all, its mass must be greater than the sum of the masses of the decay products. Many heavy nuclei are unstable to α decay. Because the Coulomb barrier inhibits the decay process (the α particle must "tunnel" through a region in which its energy is less than the potential energy, as shown in Figure 11-1*a*), the half-life for α decay can be very long if the decay energy is small, that is, if the width of the barrier to be tunneled through is large. Indeed, the relation between the half-life of an α emitter and the energy of the α particle is so striking that it was first noticed by two research assistants in Rutherford's laboratory, Geiger and Nuttall, in 1911, the same year that Rutherford discovered the nucleus. The general relation, called the Geiger-Nuttall rule, is illustrated in Figure 11-16 and given by Equation 11-30.

$$\log t_{1/2} = AE_\alpha^{-1/2} + B \qquad \textbf{11-30}$$

where E_α is the kinetic energy of the emitted α particle and A and B are experimentally determined constants.

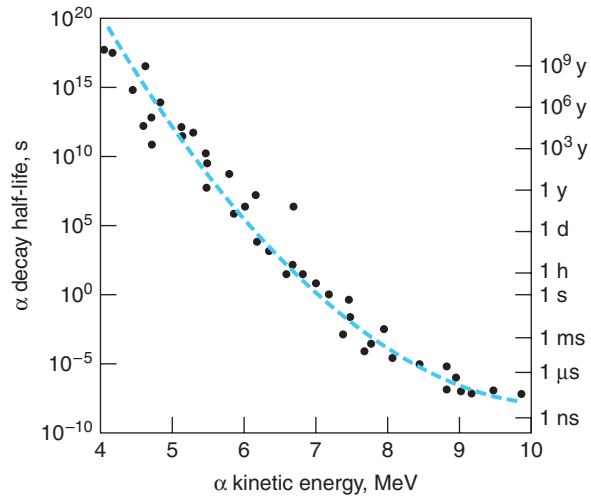

Figure 11-16 The Geiger-Nuttall relation is illustrated by the semilogarithmic graph of the α decay half-life versus the kinetic energy of the emitted α particle for the naturally occurring α emitters. The broken line represents the empirical Geiger-Nuttall rule given by Equation 11-30.

STUDENTS-HUB.com Uploaded By: Malak Obaid

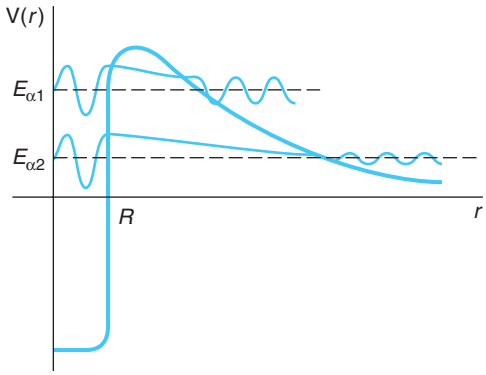

Figure 11-17 Schematic representations of the wave functions of two α particles with energies $E_{\alpha 1}$ and $E_{\alpha 2}$ within the nuclear potential well. The probability of α1 penetrating the barrier is larger than that for α2 since the barrier is narrower at $E_{\alpha 1}$. Thus, the amplitude of $\psi(\alpha 1)$ is larger outside the nucleus than that of $\psi(\alpha 2)$. Hence, $\lambda(\alpha 1) > \lambda(\alpha 2)$ and therefore $t_{1/2}(\alpha 1) < t_{1/2}(\alpha 2)$.

Subsequently, an expression for the half-life of an α emitter was derived from the Schrödinger equation treating α decay as a barrier penetration phenomenon. Its good agreement with experimental results was one of the earliest successful applications of wave mechanics. Briefly, the derivation considered an α particle confined within the nucleus with energy E_α as was shown in Figure 11-1. The wave functions for two such particles are illustrated in Figure 11-17. The potential for $r > R$ is taken to be the Coulomb function $V(r) = zZe^2/4\pi\epsilon_0 r$ where $z = 2$ for the α particle, with a smooth transition to the nuclear potential. The probability that the α particle will penetrate the barrier on any one approach is the transmission coefficient T that was derived in Section 6-6, Equations 6-75 and 6-76. The decay constant $\lambda = 1/\tau = 0.693/t_{1/2}$ is then given by the product of the transmission coefficient T and the frequency with which the nuclear α particle approaches the barrier. The latter, given by Equation 6-78, depends on the α particle's speed v, determined by its kinetic energy for $r < R$ in Figure 11-17 and the value of the nuclear radius. Thus,

$$\lambda = \frac{Tv}{2R} \qquad \textbf{11-31}$$

The result of the wave mechanical derivation, done by B. Taagepera and M. Nurmia, is

$$\log t_{1/2} = 1.61(ZE_\alpha^{-1/2} - Z^{2/3}) - 28.9 \qquad \textbf{11-32}$$

where $t_{1/2}$ is in years, E_α is in MeV, and Z refers to the daughter nucleus. Notice that the dependence of $t_{1/2}$ on the nuclear radius provides a method of measuring nuclear radii that is independent of the methods mentioned in Section 11-2.

Alpha-Decay Chains All very heavy nuclei ($Z > 83$) are theoretically unstable to α decay because the mass of the parent radioactive nucleus is greater than the sum of the masses of the decay products—the daughter nucleus and an α particle. When a nucleus emits an α particle, both N and Z decrease by 2, and A decreases by 4. There are four possible α-decay chains or sequences, depending on whether A equals $4n$, $(4n + 1)$, $(4n + 2)$, or $(4n + 3)$, where n is an integer. For the longest-lived nucleus in each sequence, $n = 58$ for the first and fourth and $n = 59$ for the second and third. All but one of these series are found in nature. The $(4n + 1)$ series is not, because its longest-lived member (other than the stable end product ^{209}Bi), ^{237}Np, has a half-life of only 2×10^6 years, which is much shorter than the age of Earth; hence ^{237}Np present when Earth was formed has long since decayed away.

STUDENTS-HUB.com Uploaded By: Malak Obaid

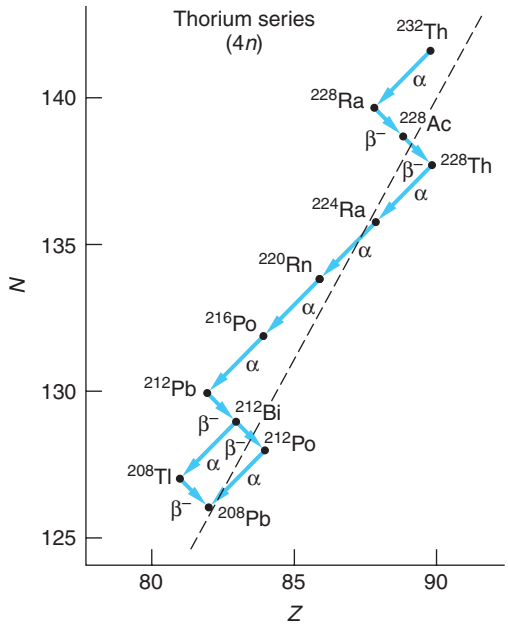

Figure 11-18 The thorium ($4n$) α-decay series. The broken line is the line of stability (floor of the energy valley) shown in Figures 11-8 and 11-15.

Figure 11-18 illustrates the thorium series, which has $A = 4n$ and begins with an α decay from ^{232}Th to ^{228}Ra. Decreasing n successively by 1 generates A for possible daughter nuclides until a stable one is reached. The daughter nuclide of an α decay is on the left, or neutron-rich, side of the stability curve (dashed line), so it often decays by β^- decay, in which one neutron changes to a proton by emitting an electron. In Figure 11-18 ^{228}Ra decays by β^- decay to ^{228}Ac, which in turn decays to ^{228}Th. There are then four α decays to ^{212}Pb, which β^- decays to ^{212}Bi. There is a branch point at ^{212}Bi, which decays either by α decay to ^{208}Tl or by β^- decay to ^{212}Po. The branches meet at the stable lead isotope ^{208}Pb. The $(4n + 2)$ series begins with ^{238}U and ends with ^{206}Pb. The $(4n + 3)$ series starts with ^{235}U and ends with ^{209}Pb. Figure 11-19 shows a typical α-decay spectrum.

More

The energy spectrum of the alpha particles emitted by a heavy nucleus such as ^{232}Th shows a number of sharp peaks with energies less than the decay energy Q. The highest energy of these corresponds to the transition from the parent's ground state to that of the daughter. The others are the result of alpha transitions to excited states of the daughter. In *Energetics of Alpha Decay*, on the home page (www.whfreeman.com/tiplermodernphysics5e), we describe how they can be used to construct the excited levels of the daughter nucleus. See also Figures 11-19 and 11-20, Equations 11-33 through 11-36, and Example 11-11 here.

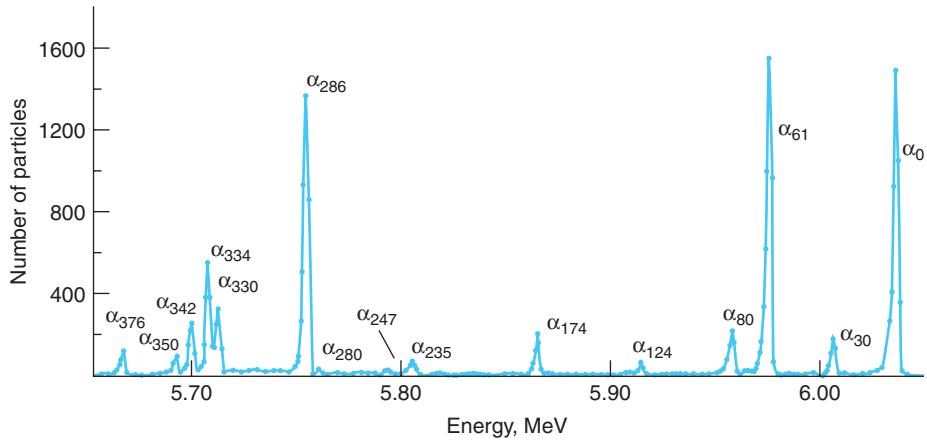

Figure 11-19 Alpha-particle spectrum from ^{227}Th. The highest-energy α particles correspond to decay to the ground state of ^{223}Ra with a transition energy of $Q = 6.04$ MeV. The next highest energy particles, α_{30}, result from transitions to the first excited state of ^{223}Ra, 30 keV above the ground state. The energy levels of the daughter nucleus, ^{223}Ra, can be determined by measurement of the α-particle energies.

STUDENTS-HUB.com Uploaded By: Malak Obaid

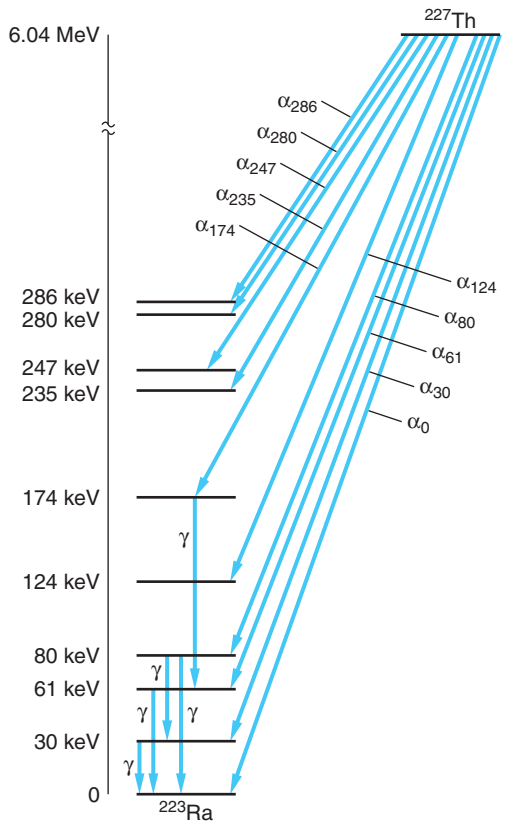

Figure 11-20 Energy levels of ^{223}Ra determined by measurement of α-particle energies from ^{227}Th, as shown in Figure 11-19. Only the lowest-lying levels and some of the γ-ray transitions are shown.

Beta Decay

There are three radioactive-decay processes in which the mass number A remains unchanged while Z and N change by ± 1. These are β^- decay, in which a neutron inside a nucleus changes into a proton with the emission of an electron; β^+ decay, in which a proton inside a nucleus changes into a neutron with the emission of a positron; and electron capture (EC), in which a proton in a nucleus changes to a neutron by capturing an atomic electron, usually a 1s electron from the K shell since these have the highest probability density in the vicinity of the nucleus. Those nuclei on the neutron-rich side of the energy valley in Figure 11-15 will tend to decay by β^- emission, while those on the proton-rich side will most probably decay by β^+ emission or electron capture. We will discuss each of these processes briefly.

β^- Decay The simplest example of β^- decay is that of the free neutron, which decays into a proton plus an electron with a half-life of about 10.8 minutes. The energy of decay is 0.78 MeV, which is the difference between the rest energy of the neutron (939.57 MeV) and that of the proton plus electron (938.28 + 0.511 MeV). More generally, in β^- decay, a nucleus of mass number A, atomic number Z, and neutron number N changes into one with mass number A, atomic number $Z' = Z + 1$, and neutron number $N' = N - 1$, conserving charge with the emission of an electron.

STUDENTS-HUB.com Uploaded By: Malak Obaid

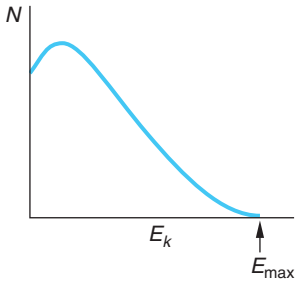

Figure 11-21 Energy spectrum of electrons emitted in β decay. The number of electrons per unit energy interval N is plotted versus kinetic energy. The fact that all the electrons do not have the same kinetic energy E_{max} suggests that there is another particle emitted that shares the energy available for decay.

The energy of decay Q is c^2 times the difference between the mass of the parent nucleus and that of the decay products. If we add the mass of Z electrons to both the parent nucleus and the decay products, we can write Q in terms of the *atomic* masses of the parent and daughter atoms:

$$\frac{Q}{c^2} = M_P - M_D \qquad \textbf{11-37}$$

Another way of understanding this result is to note that in β^- decay an electron of mass m_e leaves the atom, which is now a daughter *ion* of nuclear charge $(Z + 1)$ and Z atomic electrons. To obtain the mass of the *neutral* daughter atom, we must add the mass of an electron m_e so the total mass change is just the difference in mass between the parent and daughter *atoms*. If the decay energy Q were shared only by the daughter atom and the emitted electron, the energy of the electron would be uniquely determined by conservation of energy and momentum, just as in α decay. Experimentally, however, the energies of the electrons emitted in β decay are observed to vary from zero to the maximum energy available E_{max}. A typical energy spectrum is shown in Figure 11-21; compare this with the discrete spectrum of α-particle energies of Figure 11-19. Thus, in a particular decay event in which the electron carried away less than the energy E_{max}, it would appear that energy was not conserved since in that decay $Q/c^2 < M_P - M_D$. A moment of reflection will persuade you that linear momentum would not be conserved either and, recalling that the neutron, proton, and electron are all spin $1/2$ particles, neither would the angular momentum.

A solution to this apparent multiple failure of conservation laws was first suggested by Wolfgang Pauli in 1930. He proposed that a third particle was emitted in β decay that carried the energy, linear momentum, and angular momentum needed to conserve these quantities in each individual decay. It would carry no electric charge since charge was already conserved in β decay. Its mass would be much less than that of the electron since the maximum energy of electrons emitted in β decay is observed to be very nearly equal to the value of Q, the total energy available for the decay. In 1933 Enrico Fermi developed a highly successful quantum theory of β decay that incorporated Pauli's proposed particle, which Fermi called the *neutrino* ("little neutral one" in Italian) to distinguish it from the massive neutron that had been discovered by Chadwick earlier that same year. It was not until 1956, in an experiment performed by Clyde Cowan and Frederick Reines, that neutrinos were first observed in the laboratory. It is now known that there are six kinds of neutrinos, one (ν_e) associated with electrons, one (ν_μ) associated with muons, one (ν_τ) associated with the tau particle, and the *antiparticles* of each of those, written $\bar{\nu}_e$, $\bar{\nu}_\mu$, and $\bar{\nu}_\tau$. The electrons, muons, and taus together with the neutrinos constitute a family of particles called *leptons*, which will be discussed further in Chapter 12. The decay of the free neutron is then expressed by

$$n \longrightarrow p + \beta^- + \bar{\nu}_e \qquad \textbf{11-38}$$

and that of ^{198}Au, a more or less typical β^- emitter, by

$$^{198}\text{Au} \longrightarrow {}^{198}\text{Hg} + \beta^- + \bar{\nu}_e \qquad \textbf{11-39}$$

where the lepton conservation law (see Section 12-3) dictates the emission of an electron antineutrino to accompany a β^- decay. Presently the subject of intense experimental and theoretical research, current results place the upper limit of the electron neutrino's mass at about 2.2 eV/c^2, or no more than about 4×10^{-6} times the mass of the electron.

STUDENTS-HUB.com Uploaded By: Malak Obaid

β^+ Decay In β^+ decay, a proton changes into a neutron with the emission of a positron and a neutrino. A free proton cannot decay by positron emission because of conservation of energy (the rest energy of the neutron is greater than that of the proton), but because of binding energy effects, a proton inside a nucleus may emit a positron. A typical β^+ decay is

$$^{13}_{7}\mathrm{N} \longrightarrow {}^{13}_{6}\mathrm{C} + \beta^+ + \nu_e \qquad \textbf{11-40}$$

The only naturally occurring positron emitter known to exist is ^{40}K, which also may decay by β^- emission or electron capture! The β^+-decay equation is

$$^{40}_{19}\mathrm{K} \longrightarrow {}^{40}_{18}\mathrm{Ar} + \beta^+ + \nu_e \qquad \textbf{11-41}$$

As in all nuclear transformations, the decay energy Q is related to the difference in mass between the parent nucleus and the decay products. Note that if we add the mass of Z electrons to the nuclear masses ($Z = 7$ in the case of Equation 11-40 and $Z = 19$ in Equation 11-41), we obtain on the right side of each equation the mass of the daughter atom plus two extra electron masses (the positron and electron have identical mass). The decay energy for β^+ decay is thus related to the atomic mass of the parent and daughter atoms by

$$\frac{Q}{c^2} = M_P - (M_D + 2m_e) \qquad \textbf{11-42}$$

Again, we can understand this by noting that in β^+ decay, a positron of mass m_e leaves the system, which is now a negative daughter ion of nuclear charge $(Z - 1)$ and Z atomic electrons. To obtain the mass of the neutral daughter atom, we must subtract the mass of another electron, giving a net change of $2m_e$ in addition to the difference in mass of the parent and daughter atoms. Thus, β^+ decay cannot occur unless that energy difference is at least $2m_ec^2 = 1.022$ MeV.

As we have mentioned, neither electrons nor positrons exist inside the nucleus prior to the decay. They are created in the process of decay by the conversion of energy to mass, just as photons are created when an atom makes a transition from a higher to a lower energy state. In this regard β decay differs from α decay. There is, however, a fundamental difference between the emission of electrons (and neutrinos) that de-excite the bound states of nucleons that compose a nucleus and the emission of photons accompanying the de-excitation of the electrons bound to a nucleus. The latter bonding is due to the electromagnetic interaction, whereas the nucleons are bound by the strong nuclear force. However, electrons and neutrinos are not affected by the strong nuclear force and, since the neutron is uncharged, the electromagnetic interaction is not involved in its decay. Thus, in order to explain β decay, we must invoke a new interaction. Since β-decay lifetimes are typically quite long compared to the characteristic nuclear time scale ($\approx 10^{-23}$ s, the time for a particle moving at near the speed of light to cross the nucleus), the new interaction must act for a long (nuclear) time in order to generate the decay. In other words, it is weaker than the strong attractive force between the nucleons and is therefore called the *weak interaction* or the *weak force*. So we now have two nuclear forces, a strong one and a weak one. Like the strong nuclear force, the weak nuclear force also has a short range.

PET scanners used in medical diagnosis detect photons emitted in electron-positron annihilation following β^+ decay.

STUDENTS-HUB.com Uploaded By: Malak Obaid

Electron Capture In electron capture, a proton inside a nucleus captures an atomic electron and changes into a neutron with the emission of a neutrino; thus the effect on the atomic number is the same as in β^+ decay. The energy available for this process is given by

$$\frac{Q}{c^2} = M_P - M_D \qquad \textbf{11-43}$$

Whenever the mass of an atom of atomic number Z is greater than that of the adjacent atom with atomic number $(Z - 1)$, electron capture is possible. If the mass difference is greater than $2m_e$, β^+ decay is also possible, and these two processes compete. The probability of electron capture is negligible unless the atomic electron is in the immediate vicinity of the nucleus. This probability is proportional to the square of the electron wave function integrated over the volume of the nucleus. It is significant only for the $1s$ electrons of the K shell or, with much lower probability, the $2s$ electrons of the L shell. A typical example of electron capture is

$$^{51}_{24}\text{Cr} \longrightarrow {}^{51}_{23}\text{V} + \nu_e \qquad \textbf{11-44}$$

which has $Q = 0.751$ MeV. Note that the emission of the neutrino conserves leptons since the captured electron has disappeared.

Further understanding of the β-decay processes can be gained by considering their relation to the energy valley of the N versus Z graphs shown in Figure 11-15, with the energy scale computed from the Weizsäcker formula (Equation 11-14). Cuts through Figure 11-15*a* at constant mass number A yield parabolas since Equation 11-14 is quadratic in Z, one parabola for $a_5 = 0$ (odd A) and two parabolas for $a_5 = \pm 12$ MeV/c^2 (even A). Figure 11-22 illustrates an example of each case. The β decays always proceed down the sides of the energy valley toward the lowest-energy, stable isotope on the valley floor. Notice in Figure 11-22*b* the possible double β decay from ^{60}Fe to ^{60}Ni.

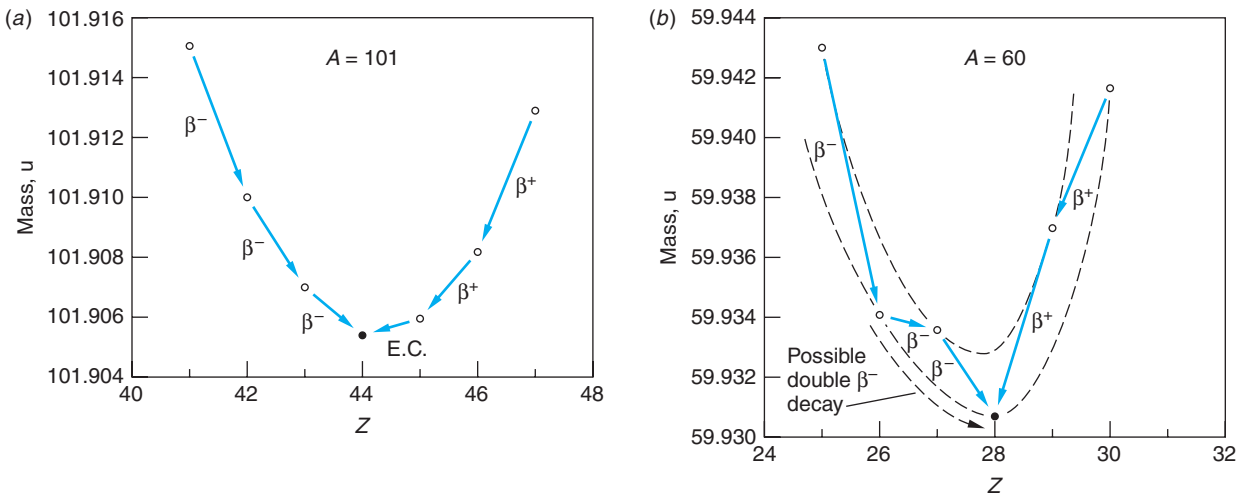

Figure 11-22 Profiles of constant atomic mass show the cross section of the energy valley of the N versus Z graph. The energy axes are expressed in mass units as computed from the Weizsächer mass formula. (*a*) Odd-A nuclei, such as $A = 101$ shown, have Z and N odd-even or even-odd and $a_5 = 0$. (*b*) Even-A nuclei are either even-even with $a_5 = 12$ MeV/c^2 or odd-odd with $a_5 = -12$ MeV/c^2. The even-even parabola lies below the odd-odd one.

STUDENTS-HUB.com Uploaded By: Malak Obaid

Since β decay proceeds via the weak interaction, the probability of the weak force producing two β^- particles simultaneously is indeed small, as you might imagine. Prior to 1985 its existence had been inferred only indirectly by abundance measurements on decay products in geologic materials. In 1985 Steven Elliott and his co-workers made the first direct observation of double beta decay using ^{82}Se as the source. The decay equation is

$$^{82}_{34}\text{Se} \longrightarrow {}^{82}_{36}\text{Kr} + \beta^- + \beta^- + \bar{\nu}_e + \bar{\nu}_e \qquad \textbf{11-45}$$

The half-life for the double β decay measured by Elliott is 1.1×10^{20} years! Double beta decay has subsequently been observed in several other nuclides. Since recent experiments show that the neutrino has a very small mass, current theory (the Standard Model—see Chapter 12) would allow the decay in Equation 11-45 to proceed without the emission of neutrinos, albeit with an even lower probability. The implications of a neutrinoless double beta decay are profound for both particle physics and cosmology. Although active searches are currently under way, no such decays have yet been observed.

EXAMPLE 11-12 **Maximum β^+ Energy from ^{40}K** We noted earlier that one of the decay modes of ^{40}K is positron emission, shown in Equation 11-41. What is the maximum energy of the positrons?

SOLUTION

1. The maximum energy Q of the positrons is given by Equation 11-42, where ^{40}K is the parent and ^{40}Ar is the daughter:
$$\frac{Q}{c^2} = M_P - (M_D + 2m_e)$$

2. The atomic masses are given in Appendix A:
$$M(^{40}\text{K}) = 39.964000\ \text{u}$$
$$M(^{40}\text{Ar}) = 39.962384\ \text{u}$$
$$m_e = 5.4858 \times 10^{-4}\ \text{u}$$

3. Substituting these into Equation 11-42 yields
$$\frac{Q}{c^2} = 39.964000\ \text{u} - [39.962384 + 2 \times 3.4858 \times 10^{-4}]\ \text{u}$$
$$= 0.000519\ \text{u} \times 931.5\ \text{MeV}/c^2 \cdot u$$
$$= 0.483\ \text{MeV}/c^2$$

Remarks: *Neglecting the recoil of the Ar nucleus, the decay energy $Q = 0.483$ MeV is the maximum energy of the emitted positrons.*

EXAMPLE 11-13 **The Decay of $^{233}_{93}$Np** Determine which decay mode or modes among α decay and the three types of β decay are allowed for $^{233}_{93}$Np.

SOLUTION

The four decays whose possibility of occurrence we are to find are

$$\alpha \text{ decay:} \quad {}^{233}_{93}\text{Np} \longrightarrow {}^{229}_{91}\text{Pa} + \alpha$$
$$\beta^- \text{ decay:} \quad {}^{233}_{93}\text{Np} \longrightarrow {}^{233}_{94}\text{Pu} + \beta^- + \bar{\nu}_e$$
$$\beta^+ \text{ decay:} \quad {}^{233}_{93}\text{Np} \longrightarrow {}^{233}_{92}\text{U} + \beta^+ + \nu_e$$
$$\text{electron capture:} \quad {}^{233}_{93}\text{Np} \longrightarrow {}^{233}_{92}\text{U} + \nu_e$$

STUDENTS-HUB.com Uploaded By: Malak Obaid

The decay energy Q for each of these is computed as follows:

α decay (Equation 11-34):

$$\frac{Q}{c^2} = 233.040805 - (229.032085 + 4.002603)$$
$$= 0.006117 \text{ u} = 5.70 \text{ MeV}/c^2$$

which is greater than zero; therefore, α decay is allowed.

β^- decay (Equation 11-37):

$$\frac{Q}{c^2} = 233.040805 - 233.042963$$
$$= -0.002158 \text{ u} = -2.01 \text{ MeV}/c^2$$

β^- decay is forbidden.

β^+ decay (Equation 11-42):

$$\frac{Q}{c^2} = 233.040805 - (233.039630 + 2 \times 5.4858 \times 10^{-4})$$
$$= 0.000078 \text{ u} = 0.073 \text{ MeV}/c^2$$

β^+ decay is allowed.

Electron capture (Equation 11-43):

$$\frac{Q}{c^2} = 233.040805 - 233.039630$$
$$= 0.001175 \text{ u} = 1.09 \text{ MeV}/c^2$$

Electron capture is allowed.

Thus, the available decay energy would allow α decay, β^+ decay, and electron capture, although the energy for β^+ decay is very small. β^- decay is forbidden. Experimentally, ^{233}Np decays more than 99 percent of the time by electron capture and about 0.3 percent of the time by α decay. β^+ decay has not been observed.

Gamma Decay

In γ decay, a nucleus in an excited state decays to a lower energy state of the same isotope by the emission of a photon. This decay is the nuclear analog of the emission of light by atoms. Since the spacing of the nuclear energy levels is of the order of MeV (as compared with eV in atoms), the wavelength of the emitted photons are of the order of

$$\lambda = \frac{hc}{E} \approx \frac{1240 \text{ eV} \cdot \text{nm}}{1 \text{ MeV}} = 1.24 \times 10^{-3} \text{ nm}$$

Gamma-ray emission usually follows beta decay or alpha decay. For example, if a radioactive parent nucleus decays by beta decay to an excited state of the daughter nucleus, the daughter nucleus often decays to its ground state by emission of one or more γ rays. The mean life for γ decay is usually very short. Direct measurements of mean lives as short as 10^{-11} s are possible. Measurements of lifetimes smaller than 10^{-11} s are difficult but can sometimes be accomplished by determining the natural line width Γ and using the uncertainty relation $\tau = \hbar/\Gamma$. A few γ emitters have very

STUDENTS-HUB.com Uploaded By: Malak Obaid

long lifetimes, of the order of hours and even, in a few cases, years. Nuclear energy states with such long lifetimes are called *isomers* or *metastable states*. The differences in γ-ray lifetimes are a consequence of the quantum-mechanical selection rules that govern transitions between the energy levels of nuclei, just as they do between atomic energy levels. For example, large angular momentum (spin) changes are forbidden for γ transitions; that is, they have very low probability. This is the major reason that, for instance, the first excited state of ^{93}Nb, an isomer, decays to the ground state with a half-life of 13.6 years. The spin of the isomeric state is 1/2, while that of the ground state is 9/2. The decay requires the γ ray to carry away $4\hbar$ of angular momentum, a very unlikely occurrence that accounts for the long half-life.

The energy hf of a gamma-ray photon is the difference in energy of the states between which the transition occurs. That is,

$$hf = E_{\text{high}} - E_{\text{low}} \qquad \textbf{11-46}$$

where E_{high} is the energy of the upper level and E_{low} is that of the lower level. Several gamma decays are shown in Figure 11-20 between some of the excited states of ^{223}Ra that resulted from the α decay of ^{227}Th. For example, a γ ray is emitted from the 174-keV level of ^{223}Ra, reducing the excitation energy of that nucleus to 61 keV above the ground state. From Equation 11-46, the energy of that γ ray is equal to 174 keV − 61 keV = 113 keV. To be more precise, conservation of momentum requires that the ^{223}Ra nucleus carry a small part of this energy as it recoils from the emission of the photon. (See Figure 11-23.) The energy of the nuclear recoil E_r is given by

$$E_r = \frac{p^2}{2M} = \frac{(hf)^2}{2Mc^2} \qquad \textbf{11-47}$$

where M is the nuclear mass. All gamma-ray energies are small compared with atomic and nuclear rest energies; that is, $hf \ll Mc^2$ or $hf/Mc^2 \ll 1$; therefore, $E_r \ll hf$. Thus, Equation 11-46 is an excellent approximation of the gamma ray's energy.

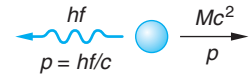

Figure 11-23 A nucleus of rest energy Mc^2 emits a photon of energy hf and momentum $p = hf/c$. Conservation of momentum requires that the nucleus also recoil with momentum p.

Internal Conversion An important alternative to gamma-ray emission for the de-excitation of an excited nuclear state, particularly low-lying states rather than being emitted as a photon, is the process of internal conversion. In this process the excitation energy of the state is transferred to an orbital electron, which is ejected from the atom. Those electrons with the highest probabilities of being close to the nucleus, the K and L electrons, are the ones most likely to be emitted. The ejected electron has kinetic energy equal to the nuclear transition energy minus the electron's binding energy. Since the latter are accurately known for nearly all elements, measuring the kinetic energies of the *conversion electrons* makes possible determination of many nuclear excited states. While internal conversion is quantum mechanically a one-step process, it was initially pictured as the emission of a photon followed by a photoelectric-effect interaction with an orbital electron of the same atom, hence the name *internal conversion*.

More

In 1958 Rudolf Mössbauer[14] observed a remarkable feature of gamma decay, the recoilless emission of gamma rays from ^{191}Ir. A discovery made while he was still a graduate student, it made possible high-precision-frequency measurements, leading to a host of applications. It is described in the section *The Mössbauer Effect* on the home page: www.whfreeman.com/tiplermodernphysics5e. See Figures 11-24 through 11-26 here.

The exceptional precision of frequency measurements made possible by the Mössbauer effect has applications in a broad range of areas, such as measurements of gravitational red shift, impurities and imperfections in crystalline solids, and the transverse Doppler effect (see Section 1-5), to name just three.

STUDENTS-HUB.com Uploaded By: Malak Obaid

Questions

6. De-excitation of the first excited state of ^{93}Nb requires the gamma ray to carry away $4\hbar$ of angular momentum. Since the gamma ray's intrinsic angular momentum is $1\hbar$, how could it carry away $4\hbar$?
7. Why is the decay series $A = (4n + 1)$ not found in nature?
8. A decay by α emission is often followed by a β decay. When this occurs, it is usually a β^- decay. Why?
7. How can the application of very high pressure affect the lifetime of a sample that decays by electron capture? Why are other types of decay not affected?

11-5 The Nuclear Force

The study of nuclear physics is quite different from that of atomic physics. The simplest atom, the hydrogen atom, can be completely understood by solving the Schrödinger equation using the known potential energy of interaction between the electron and proton, $V(r) = -ke^2/r$ (though, as we have seen, the mathematics needed is fairly complicated). The simplest nucleus (other than a single proton) is the deuteron, consisting of a proton and a neutron. We cannot solve the Schrödinger equation for this problem and then compare with the experiment because, although many of its characteristics have been determined, the exact mathematical form of the potential energy of interaction V is not known. There is no macroscopic way to measure the force between a neutron and a proton. It is clear from the fact that many nuclei are stable that there are other forces much stronger than electromagnetic or gravitational forces between nucleons. Considering ^{4}He as an example, we see that the electrostatic potential energy of two protons separated by 1 fm is

$$V = \frac{ke^2}{r} = \frac{1.44 \text{ MeV} \cdot \text{fm}}{1 \text{ fm}} = 1.44 \text{ MeV}$$

and note that it is positive—i.e., the electrostatic force between the protons is, of course, repulsive. However, the energy needed to remove a proton or neutron from ^{4}He is about 20 MeV. The force responsible for such a large binding energy must be attractive and significantly stronger than the electrostatic force. This must certainly be the case since the neutrons are electrically neutral and hence do not feel the Coulomb force and the protons are all positively charged and thus feel a repulsive electrostatic force. Nor can we appeal to the gravitational attractive force between the protons to offset their Coulomb repulsion since, as Example 11-14 illustrates, the gravitational force between pairs of protons in the nucleus is insignificantly small compared to their Coulomb repulsion. Thus, the attractive force that holds the nucleons together must be strong, stronger even than the electromagnetic interaction. It is called the *nuclear* or *hadronic force* or often simply the *strong force*.

Determination of the characteristics of the nuclear force is one of the central problems of nuclear physics. Much information about this force can be and has been obtained from scattering experiments involving protons, neutrons, and other particles. Although the results of a scattering experiment can be predicted unambiguously from knowledge of the force law, the force law cannot be completely determined from the results of such experiments. The results of scattering experiments do indicate that

STUDENTS-HUB.com Uploaded By: Malak Obaid

(1) the nuclear force has the same strength between any two nucleons—that is, *n*-*n*, *p*-*p*, or *n*-*p*; (2) the force is strong when the particles are close together and drops rapidly to zero when the particles are separated by a few fm; and (3) it is a saturated force. The potential energy of the nucleon-nucleus interaction can be roughly represented by a square well of about 40 MeV depth and a few fm width.

EXAMPLE 11-14 **Ratio of F_{grav}/F_{Coul} Between Protons** Compare the gravitational attractive force between two protons in an atomic nucleus (or anywhere else, for that matter) with the electrostatic repulsion between them.

SOLUTION

The electrostatic repulsion for two protons separated by a distance r is

$$F_{\text{Coul}} = \frac{1}{4\pi\epsilon_0}\frac{e^2}{r^2} = \frac{(1.60 \times 10^{-19}\ \text{C})^2}{4\pi\epsilon_0 r^2}$$

and the gravitational attraction between them is

$$F_{\text{Grav}} = G\frac{m_p^2}{r^2} = \frac{G(1.67 \times 10^{-27}\ \text{kg})^2}{r^2}$$

The ratio is independent of r and equal to

$$\frac{F_{\text{grav}}}{F_{\text{Coul}}} = \frac{Gm_p^2}{(1/4\pi\epsilon_0)e^2} = \frac{(6.67 \times 10^{-11}\ \text{N}\cdot\text{m}^2/\text{kg}^2)(1.67 \times 10^{-27}\ \text{kg})^2}{(8.99 \times 10^{9}\ \text{N}\cdot\text{m}^2/\text{C}^2)(1.60 \times 10^{-19})^2}$$

$$\frac{F_{\text{grav}}}{F_{\text{Coul}}} = 8.1 \times 10^{-37} \approx 10^{-36}$$

Solution of the nuclear-wave equation presents all of the mathematical complexities of our earlier studies of atomic and molecular systems plus some truly monumental new ones. Like the atomic and molecular systems, the nucleus (except for ^{1}H and ^{2}H) is a many-body system with all of the accompanying computational difficulties. In addition, the nuclear interaction is far more complex than the electromagnetic interaction and, even worse, it is not yet known how the nuclear interaction can be expressed in closed, analytic form; that is, we do not know the nuclear force law equivalent of Coulomb's law for the electrostatic force. This means that we cannot yet write down the exact form of the nuclear potential function that must be included in the wave equation in order to solve for the nuclear-wave functions and allowed energies.

Substantial progress has been made in recent years toward obtaining the analytic expression for the interaction. For instance, an estimate of the depth of the nuclear potential can be made by assuming its shape to be approximated by a square well and computing the ground-state energy of a nucleon, based on a reasonable assumption of the well width. Using 2 fm as a typical width for light nuclei (see Figure 11-5), the potential $-V$ for a nucleon is approximately

$$-V \approx E_1 \approx \frac{h^2}{8ma^2} = \frac{(6.63 \times 10^{-34}\ \text{J}\cdot\text{s})^2}{(8)(1.67 \times 10^{-27}\ \text{kg})(2 \times 10^{-15}\ \text{m})^2(1.60 \times 10^{-13}\ \text{J/MeV})}$$

$$V \approx -50\ \text{MeV}$$

STUDENTS-HUB.com Uploaded By: Malak Obaid

Two protons separated by that same distance experience an electrostatic Coulomb repulsive potential given by

$$V_{\text{Coulomb}} = \frac{1}{4\pi\epsilon_0}\frac{e^2}{a} = \frac{(9 \times 10^9\ \text{N}\cdot\text{m}^2/\text{C}^2)(1.60 \times 10^{-19}\ \text{C})^2}{(2 \times 10^{-15}\ \text{m})(1.60 \times 10^{-13}\ \text{J/MeV})}$$

$$V_{\text{Coulomb}} = 0.72\ \text{MeV}$$

Thus, our square well approximation suggests that at 2 fm, the attractive nuclear potential exceeds the Coulomb repulsion experienced by a proton by nearly two orders of magnitude.[15]

More detailed understanding of the nature of the nuclear force and the shape and depth of the potential is provided by two types of experiments. First, just as atomic spectroscopy yielded information that made possible the determination of such things as the energies, spins, and magnetic moments of the electronic structure of the atoms, nuclear spectroscopy—i.e., the study of the emission and absorption of particles and radiation by the nuclei—yields valuable information concerning the ground and excited states of nuclei, including energies, magnetic moments, electric quadrupole moments, and spins. The second source of our detailed information comes from the analysis of scattering experiments. These are experiments in which particles that feel the nuclear force, such as protons or alpha particles, are used as projectiles "fired" at target nuclei. The de Broglie wavelength of projectile protons with kinetic energies of 20 MeV (or more) are of the order of nuclear dimensions:

$$\lambda = \frac{h}{p} = \frac{h}{\sqrt{2mE}} = \frac{6.63 \times 10^{-34}\ \text{J}\cdot\text{s}}{\sqrt{2 \times 1.67 \times 10^{-27}\ \text{kg} \times 20\ \text{MeV} \times 1.60 \times 10^{-13}\ \text{J/MeV}}}$$

$$\lambda = 6 \times 10^{-15}\ \text{m} = 6\ \text{fm}$$

Thus, such protons will experience considerable diffraction in collisions with the target nuclei. Analysis of the resulting diffraction pattern yields detailed information concerning the interaction between the particles. Many such experiments, particularly protons scattered from protons, called *p-p* scattering, and neutrons scattered from protons, or *n-p* scattering, reveal that the nuclear potential for proton-proton pairs and neutron-proton pairs are of the form sketched in Figure 11-27. Although the

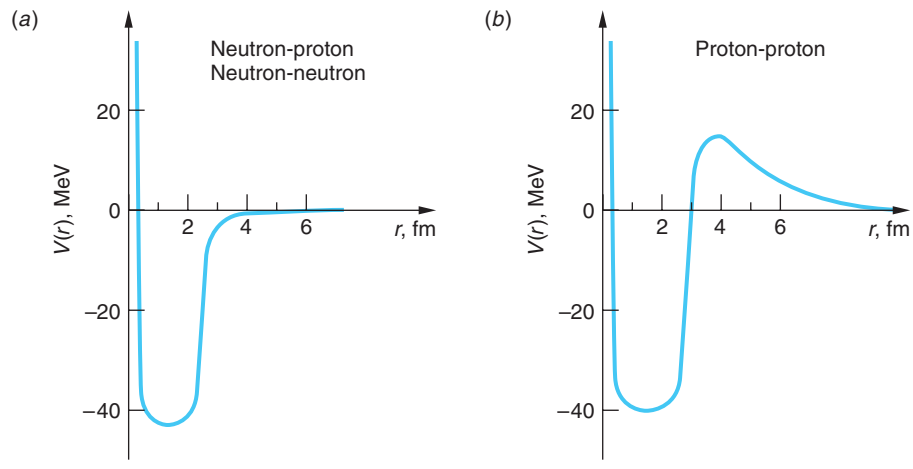

Figure 11-27 (*a*) The approximate shape of the potential between *n-p* and *n-n* pairs. The hard core suggested by the nearly constant central density of the nucleus has a radius of about 0.5 fm. (*b*) The *p-p* potential differs from those in (*a*) by the added Coulomb repulsion, which dominates beyond about 3 fm. Notice the *n-p* and *n-n* potential well is slightly deeper than the *p-p* potential due to the absence of the Coulomb repulsion.

STUDENTS-HUB.com Uploaded By: Malak Obaid

shape of the potential for neutron-neutron pairs can only be determined indirectly since free neutrons are radioactive and we do not know how to make targets consisting only of neutrons (such as the matter of neutron stars), it appears to be identical to that of *n-p* pairs. In fact, when the Coulomb repulsion component of the *p-p* pair potential in Figure 11-27*b* is subtracted from the total potential $V(r)$, the remaining nuclear *p-p* potential is also the same as those for *n-p* and *n-n* pairs. This leads to the very important conclusion that *the nuclear force is independent of the charge of the nucleons*. This suggests that the proton and neutron can be considered as different charge states of the same particle, the nucleon. We will pursue this suggestion further in Chapter 12.

As described in Section 11-2, the charge radius of the proton is about 1 fm. The neutron is approximately the same size. As Figure 11-27 illustrates, two nucleons experience the attractive nuclear force as long as they are within about 2.5 fm of each other, but the force diminishes rapidly over the next 1/2 fm of separation and is essentially zero beyond 3 fm. Thus, we also conclude that *the nuclear force is a short-range force*. Nucleon pairs also experience an extremely strong repulsive component of the nuclear force when they approach within about 0.5 fm. This *hard core* is consistent with the observation that the central density is nearly the same for all nuclei (see Figure 11-27). That is, as more and more nucleons are added, the size of the nucleus increases in such a way that the density remains approximately constant, so something must prevent the nucleons from crowding too closely together. The short range of the nuclear force together with the repulsion of the hard core means that, as the size of the nucleus increases beyond the 2.5- to 3-fm range of the force, an individual nucleon will be able to interact with only a limited number of the other particles in the nucleus, namely its nearby neighbors that are within range of its force. This is analogous to the limited number of bonds associated with each atom in the covalent bonding of solids. For example, each carbon atom in diamond bonds with only four of its nearest neighbors, and we could describe the carbon covalent bond as being a saturated bond. Similarly, *the nuclear force is a saturated force*.

The Nuclear Exchange Force

Without knowing the analytic form of the nuclear potential function, we have been able to conclude that the nuclear force is a short-range, saturated, charge-independent, spin-dependent force with a hard core and a small noncentral component and is about two orders of magnitude stronger than the electrostatic force. What could be the origin or mechanism for such a force was first suggested by H. Yukawa[16] in 1935.

Yukawa proposed that the nuclear force resulted from an exchange of particles between the nucleons. He based his theory on an analogy with the quantum-mechanical explanation of the electrostatic interaction, one of two exchange mechanisms that you have previously studied, though perhaps not by that name. Classically, any distribution of charges produces an electric field $\mathscr{E}$ and the force felt by another charge q located in the field is the product $q\mathscr{E}$. Any change in the charge distribution changes $\mathscr{E}$; however, the information that a change has occurred does not appear instantaneously throughout the field but is propagated outward at the speed of light. Time-dependent changes in the charge distribution create time-dependent changes in $\mathscr{E}$, that is, electromagnetic radiation, or waves.[17] We have seen that the particle representation of the electromagnetic radiation is the photon. Quantum mechanically, every charge is continually emitting and absorbing photons, even when it is not moving. They are called *virtual photons*, meaning that they are not directly observable.

STUDENTS-HUB.com Uploaded By: Malak Obaid

A charge can emit a virtual photon of energy hf without changing its energy or recoiling, i.e., without violating conservation of energy and momentum, provided that the photon exists for no longer than $\Delta t = \hbar/\Delta E$, where $\Delta E = hf$, as required by the uncertainty principle. The distance that the virtual photon can travel during the time Δt, called the range R, is given by

$$R = c\,\Delta t = c\hbar/\Delta E \qquad \textbf{11-48}$$

and substituting for ΔE,

$$R = c\hbar/hf = c/2\pi f = \lambda/2\pi \qquad \textbf{11-49}$$

A second charge located up to a distance R from the first can absorb the photon and a similar photon emitted by the second charge may be absorbed by the first, all without violating energy and momentum conservation. It is this exchange of virtual photons that results in the electrostatic Coulomb force between the two stationary charges in quantum mechanics. Note that there is no limit to the wavelength of the photon in Equation 11-49 since the energy of the photon may be arbitrarily small, the photon having no rest mass. Thus, the distance separating the two charges, the range R of the Coulomb force, may also be infinite, as you have already learned.

An exchange mechanism was also used in BCS theory to account for the attractive force between the electrons of the Cooper pairs. (See Section 10-8.) In that case, the exchange particles were the phonons and the range of the force was not infinite but determined by the fact that $\Delta E \approx$ the energy gap.

Yukawa proposed that the nuclear force could also be explained in terms of the exchange of virtual particles by the nucleons. These particles, which he called *mesons*, were pictured as the analogs of the virtual photons in the electromagnetic interaction and established the *meson field* in analogy with the electromagnetic field. The mechanism for the nuclear force was proposed to be an exchange of a meson between a pair of nucleons, as illustrated by Figure 11-28. Yukawa accounted for the observed short range of the nuclear force by assigning mass to the meson. Thus, the energy uncertainty ΔE in Equation 11-48 would be

$$\Delta E \geq mc^2$$

where m is the mass of the meson and mc^2 is its rest energy. The range R of the meson and therefore the nuclear force that it mediates cannot be larger than

$$R = c\,\Delta t = c\hbar/\Delta E = \hbar/mc \qquad \textbf{11-50}$$

since the speed of the meson must be less than the speed of light. Recall that h/mc is the Compton wavelength λ_c of the particle whose mass is m, so $R = \lambda_c/2\pi$. The range of the nuclear force was known to be about 1 fm, which allowed an approximation of the meson's expected mass from Equation 11-50:

$$m \approx 3.5 \times 10^{-28}\ \text{kg} \approx 380\ m_e \approx 200\ \text{MeV}/c^2$$

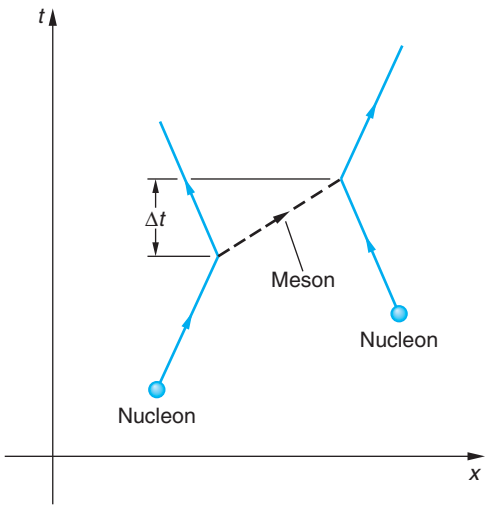

Figure 11-28 Schematic representation of the exchange of a meson by a pair of nucleons. The meson is emitted by the nucleon on the left, which recoils as a result and is absorbed after a time Δt by the nucleon on the right, which also recoils. The effect on the nucleons is as if they had interacted with each other. This kind of spacetime diagram of the interaction of fundamental particles is called a Feynman diagram (see Section 12-1). The x and t axes are normally omitted.

STUDENTS-HUB.com Uploaded By: Malak Obaid

The observed charge independence of the nuclear force was incorporated by Yukawa into the theory by allowing the mesons to carry $+e$, 0, or $-e$ charge. Thus, the exchange of a neutral meson would leave both of the nucleons with their original charge, while the exchange of a charged meson would interchange their charges (see Figure 11-28). Note that $m = 0$ for photons in Equation 11-50 implies the infinite range of the electromagnetic force.

If the nucleon that emits the meson happens to interact with another particle (or nucleus) that has sufficient kinetic energy in the emitting nucleon's rest system to supply the meson's rest energy and also provide the recoil momentum to the emitting nucleon, thus conserving both energy and momentum, the virtual meson can become real and be observable in the laboratory. Such a situation is shown schematically in Figure 11-29. Note the analogy to the emission of photons (bremsstrahlung) by accelerated electrons in an x-ray tube (see Section 3-4). It was interactions such as shown in Figure 11-29 in which Yukawa's mesons, now called π *mesons* or *pions*, were first seen in cosmic rays in 1947, more than a decade after they were proposed.[18] The mass measured for the pions is 140 MeV/c^2, in quite good agreement with Yukawa's predicted approximate value of about 200 MeV/c^2, and all three charge versions were subsequently discovered, providing beautiful confirmation of Yukawa's theory. Since then additional mesons have been discovered and our understanding of the nuclear force has been modified to include the effect of their being exchanged by nucleons as well, but the pions remain as the dominant carrier of the force between nucleons and the cornerstone of our understanding of it. As we will discuss further in Chapter 12, the Standard Model of particle physics describes the nucleons and the mesons as composites of other, more fundamental particles, called *quarks*. The interaction between quarks to form these particles is mediated by a field particle, the *gluon*, carrying the strong force between quark pairs in analogy with our discussion above.

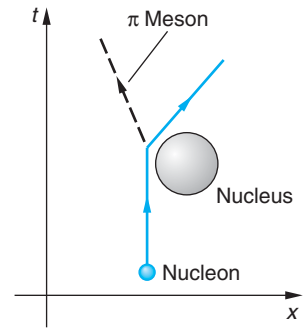

Figure 11-29 A Feynman-like diagram of a nucleon emitting a virtual pion in the vicinity of a nucleus. If the nucleus can provide at least the pion's rest energy and participate in the conservation of momentum, the pion may become real, i.e., visible in the laboratory.

EXAMPLE 11-15 **Range of the Nuclear Force** Using the experimentally measured mass of the pion, 140 MeV/c^2, estimate the range of the nuclear force.

SOLUTION

The range R cannot be larger than $\hbar c/mc^2$ according to Equation 11-50. We then have that

$$R = \frac{\hbar c}{mc^2} = \frac{(1.06 \times 10^{-34}\ \text{J} \cdot \text{s})(3.00 \times 10^{8}\ \text{m/s})}{(140\ \text{MeV}/c^2)(c^2)(1.60 \times 10^{-13}\ \text{J/MeV})}$$

$$R = 1.4 \times 10^{-15}\ \text{m} = 1.4\ \text{fm}$$

Questions

10. What property of the nuclear force is indicated by the fact that all nuclei have about the same density?
11. How does the nuclear force differ from the electromagnetic force?
12. Mesons that have been discovered in recent years are all more massive than the pion. What does that mean regarding the range of the force that they mediate?

STUDENTS-HUB.com Uploaded By: Malak Obaid

EXPLORING
Probability Density of the Exchange Mesons

A nucleon continually emits and absorbs virtual mesons. The time Δt during which a virtual meson exists can be estimated from Equation 11-50:

$$\Delta t = \frac{\hbar}{mc^2} = \frac{(1.055 \times 10^{-34}\ \text{J} \cdot \text{s})}{(140\ \text{MeV}/c^2)(c^2)(1.60 \times 10^{-13}\ \text{J/MeV})}$$

$$\Delta t = 5 \times 10^{-24}\ \text{s}$$

This is not a very long time! Thus, a 10^{-20}-second time-exposure "snapshot" of a nucleon would show a cloud consisting of more than 10,000 mesons surrounding the nucleon! The probability density of the mesons can be determined using the results that we obtained from relativity and wave mechanics in Chapters 2 and 6, respectively. The relativistic expression connecting the total energy E and momentum p, the magnitude of the energy/momentum four-vector, is

$$(mc^2)^2 = E^2 - (pc)^2 \qquad \textbf{2-32}$$

With the appropriate operator substitutions from Table 6-1,

$$E \longrightarrow i\hbar\frac{\partial}{\partial t} \qquad p^2 \longrightarrow -\hbar^2\nabla^2 \qquad \textbf{11-51}$$

Equation 2-32 can be written as

$$\nabla^2\Phi(\mathbf{r}, t) - \frac{1}{c^2}\frac{\partial^2\Phi(\mathbf{r}, t)}{\partial t^2} = \left(\frac{mc}{\hbar}\right)^2\Phi(\mathbf{r},t) \qquad \textbf{11-52}$$

where $\Phi(\mathbf{r},t)$ is the wave function of the meson. Equation 11-52 is a relativistic wave equation. It was first obtained by Oskar Klein and Walter Gordon in 1926, the same year that Schrödinger developed his nonrelativistic wave equation.

That the extent of the meson field is related to the range of the nuclear force given by Equation 11-50 can be illustrated by computing the probability density of the meson $|\Phi|^2$ for a static, or time-independent, distribution. This is roughly analogous to the virtual photon distribution, or the electric field intensity, for a stationary charge. In this case, the time derivative of Φ vanishes and Equation 11-52 can be written as

$$\nabla^2\Phi(\mathbf{r}) = \left(\frac{mc}{\hbar}\right)^2\Phi(\mathbf{r}) = \frac{1}{R}\Phi(\mathbf{r}) \qquad \textbf{11-53}$$

whose solution is

$$\Phi(\mathbf{r}) = \frac{Ae^{-r/R}}{\mathbf{r}} \qquad \textbf{11-54}$$

where A is a factor determined by the normalization condition. The probability density is then

$$|\Phi(\mathbf{r})|^2 = \frac{|A|^2 e^{-2r/R}}{\mathbf{r}^2} \qquad \textbf{11-55}$$

and we see that the probability density of the mesons falls off exponentially at a rate determined by R. In other words, R determines the range of the exchange mesons as we had interpreted it in Equation 11-50. Figure 11-30 illustrates the probability distribution function $P(r) = |\Phi|^2 r^2$ for the virtual mesons. For values of r greater than about $0.5R$,

STUDENTS-HUB.com Uploaded By: Malak Obaid

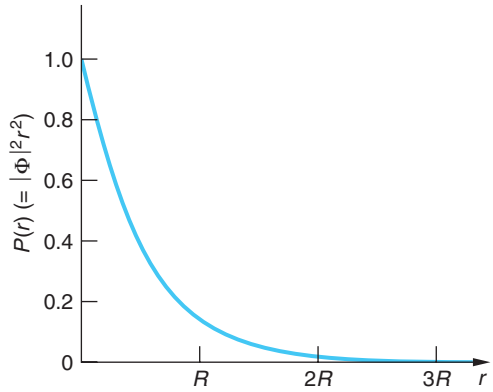

Figure 11-30 Probability $P(r)$, equal to $|\Phi|^2 r^2$, for the virtual mesons emitted by a nucleon, and the range $R = \hbar/mc$, the Compton wavelength of the mesons divided by 2π. There are essentially no mesons beyond about $3R$.

the curve agrees well with experimental results; however, for small values of r the measured meson density is much lower than Figure 11-30 would suggest. Indeed, if the predicted values at very small r values actually existed, they would lead to some quite unusual nuclear properties that are, in fact, not observed. Nuclear theorists conclude that the number of pions at very small r is somehow suppressed, likely as a result of the quark-gluon interaction mentioned above. This is an area of active current research.

11-6 The Shell Model

Existence of 126 as a magic number has prompted searches for unusually stable (but still radioactive) isotopes with Z in the vicinity of 126. Finding them will strengthen our understanding of nuclear structure. Thus far, the highest Z discovered is 118.

Although the general features of the binding energy of nuclei are well accounted for by the semiempirical mass formula that was based on modeling the nucleus as a liquid drop, the binding energy and other properties do not vary with perfect smoothness from nucleus to nucleus. It is not surprising that the smooth curve predicted by Equation 11-12 does not fit the data for very small A, for which the addition of a single proton or a neutron makes a drastic difference. However, even for medium and large A there are some substantial fluctuations of nuclear properties in neighboring nuclei. Consider the binding energy of the last neutron in a nucleus. (Note that this is not the same as the average binding energy per nucleon.) We can calculate this from the semiempirical mass formula by computing the difference in mass $M[(A-1), Z] + m_n - M(A, Z)$. Figure 11-31 shows a plot of the difference between the experimentally measured binding energy and that calculated from Equation 11-12 as a function of the neutron number N. There are large fluctuations near $N = 20$, 28, 50, 82, and 126. These are also the neutron numbers of the nuclei that have an unusually large number of isotones. Nuclei with these proton numbers (except that no element with $Z = 126$ has been observed) have an unusually large number of isotopes.

These numbers are the "magic numbers" that were referred to in Section 11-2. In the regions between these magic numbers, the binding energy of the last neutron is predicted quite accurately by the semiempirical mass

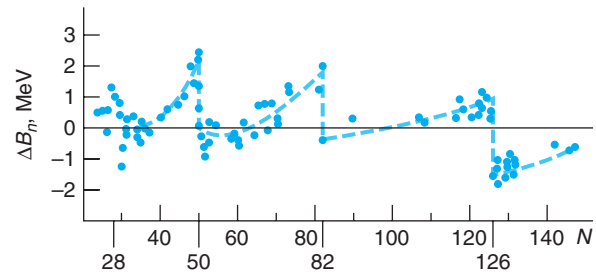

Figure 11-31 Difference in the measured binding energy of the last neutron and that calculated from mass formula versus neutron number. Note the similarity of this curve and the ionization energy of atoms versus Z (Figure 7-20). The neutron numbers 28, 50, 82, and 126 correspond to closed shells. These data show that the neutron with N = magic number $+1$ is much less tightly bound than that with N = magic number.

STUDENTS-HUB.com Uploaded By: Malak Obaid

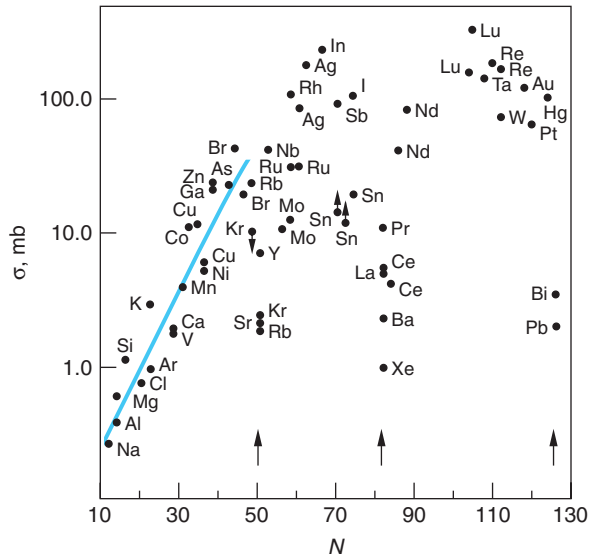

Figure 11-32 The capture cross section measures the probability that a neutron approaching a nucleus will be captured, or bound to the nucleus. The solid line traces the average value. Notice the sharp drop in capture probability of nearly two orders of magnitude at $N = 50$, 82, and 126.

formula. Figure 11-31 should be compared with Figure 7-20, which shows the binding energy of the last electron in an atom as a function of the atomic number Z. The similarity of these two figures suggests a shell structure of the nucleus analogous to the shell structure of atoms. There is considerable additional evidence for these magic numbers, such as the electric quadrupole moments (see Figure 11-7), the neutron capture cross sections illustrated in Figure 11-32, and the binding energies of the last neutron for isotopes of a given Z as shown in Figure 11-33. Additional evidence of nuclear shell structure is discussed in Mayer and Jensen (1955).

Although the unusual stability of the nuclei with N or Z equal to one of the magic numbers was noticed in the 1930s, there was no successful explanation in terms of shell structure until 1949. In the discussion of atoms in Chapter 7, we started with a fixed positive charge $+Ze$ and computed the energies of individual electrons, assuming first that each electron was independent of the others as long as the exclusion principle was not violated. The interaction of the outer electrons with the inner core could be taken care of by assuming an effective nuclear charge that is less than Z because of the screening of the nuclear charge by the inner electrons. This works quite well since the electrons are fairly far from each other in an atom. We could therefore use the individual electron quantum states of the hydrogen atom described by n, l, m_l, and m_s as a first approximation for the electrons in complex atoms. The atomic magic numbers come about naturally due to the large energy difference between one shell or subshell and the next. The actual calculations of atomic-wave functions and atomic energies require powerful approximation or numerical techniques, but they can be done reliably because the forces involved are well known.

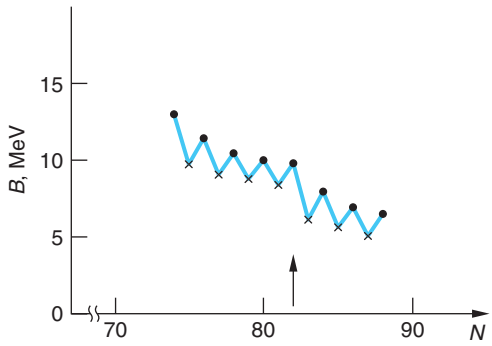

Figure 11-33 Binding energy B for the last neutron of the isotopes of Ce ($Z = 58$). These data are typical of nuclei with $Z > 20$. B decreases sharply (about 2 MeV) for $N = 82 + 1$. This graph also shows the pairing energy associated with a_5 in the Weizsächer formula (see Section 11-2), where the last neutron is more tightly bound if N is even than if N is odd.

The situation is not the same for the nuclear-shell model. In the first place, there is no central potential analogous to the fixed positive charge of the atom. The interaction of the nucleons with one another is the only interaction present. In addition to being noncentral, the situation is further complicated by the fact that we know little about the strong force between nucleons beyond what we have

STUDENTS-HUB.com Uploaded By: Malak Obaid

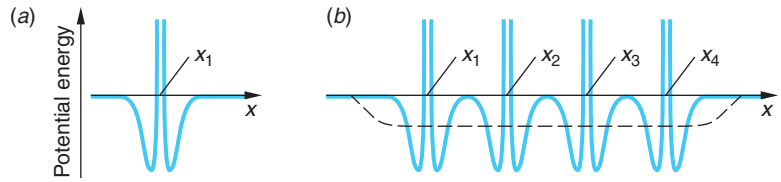

Figure 11-34 (*a*) A single nucleon moving in one dimension sees the potential due to a second nucleon located at x_1. (*b*) The potential seen by the single nucleon due to four other nucleons located along the x axis fluctuates rapidly; however, the average of the four potentials can be reasonably well approximated by the dashed curve, a finite well with sloping sides.

discussed: that it is saturated, has a short range, is charge independent, and is spin dependent. At first sight, it is difficult to imagine a neutron or proton moving almost freely in a well-defined orbit when there are $A - 1$ particles nearby exerting very strong forces on it. Despite these difficulties, the observed properties, such as are illustrated in Figures 11-7, 11-31, 11-32, and 11-33, give strong motivation to try a model in which each nucleon moves about more or less freely in an average potential field produced by the other nucleons. Figure 11-34 shows how such an average potential could be produced. The assumption that the nucleon can move in an orbit without making many collisions can be rationalized by using the exclusion principle. Consider N neutrons in some potential well. In the ground state, the N lowest energy levels will be filled. A collision between two neutrons that does not result in their merely exchanging states is forbidden by the exclusion principle if there are no accessible unfilled states. A collision involving the exchange of identical particles has no effect. Thus, only those nucleons in the highest filled levels, where there are empty states available nearby, can collide with one another. This is analogous to the result that most of the free electrons in a metal cannot absorb energy in random collisions with the lattice because all the nearby energy levels are full. Like the electrons, the nucleons also have a Fermi level.

The first shell-model calculations attempted to use a square well about 40 MeV deep to fit the nuclear energy levels, but they failed to produce the correct magic numbers. In 1949, M. Mayer and J. H. D. Jensen [19] independently showed that, with a modification in these calculations, the magic numbers do follow directly from a relatively simple shell model. Mayer and Jensen resolved the problem by proposing that the spin dependence of the nuclear force results in a very strong spin-orbit interaction, coupling the spin of each nucleon to its own orbital angular momentum. Thus, the nuclear spin-orbit effect depends on *j-j* coupling[20] rather than *L-S* coupling that characterizes the electron spin-orbit interaction (see Section 7-5). This strong spin-orbit interaction results in a decrease in the energy if the spin and the orbital angular momentum of the nucleon are parallel and an increase if they are antiparallel. Figure 11-35 illustrates the nuclear-shell model of Mayer and Jensen that yields the correct magic numbers. Depending on the details of the spin-orbit interaction in the superheavy elements, the island of stability may begin to

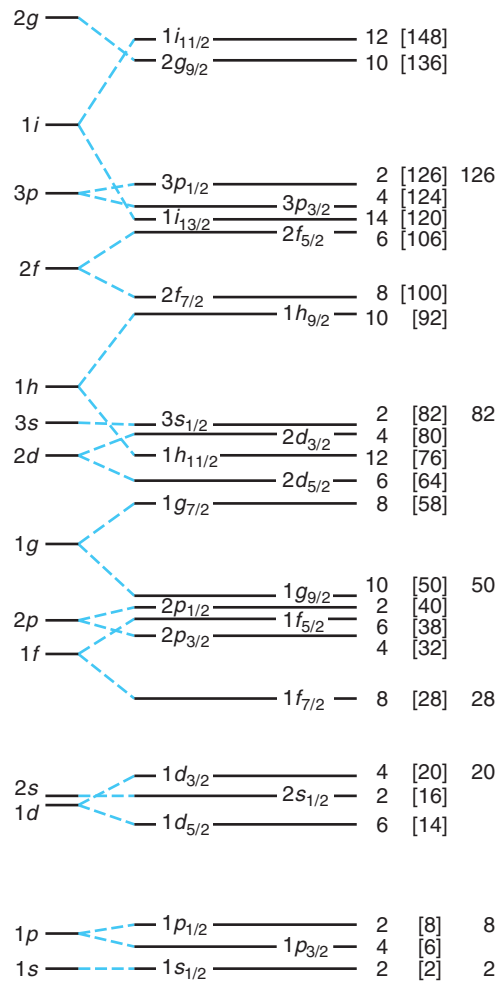

Figure 11-35 Energy levels for a single particle in a nuclear well, including spin-orbit splitting. The maximum number of particles in each level is given at the right, followed by the total number through that level in brackets. The total numbers just before the large energy gaps are the magic numbers. The spacing shown here is for protons; the spacing for neutrons is slightly different (lower).

STUDENTS-HUB.com Uploaded By: Malak Obaid

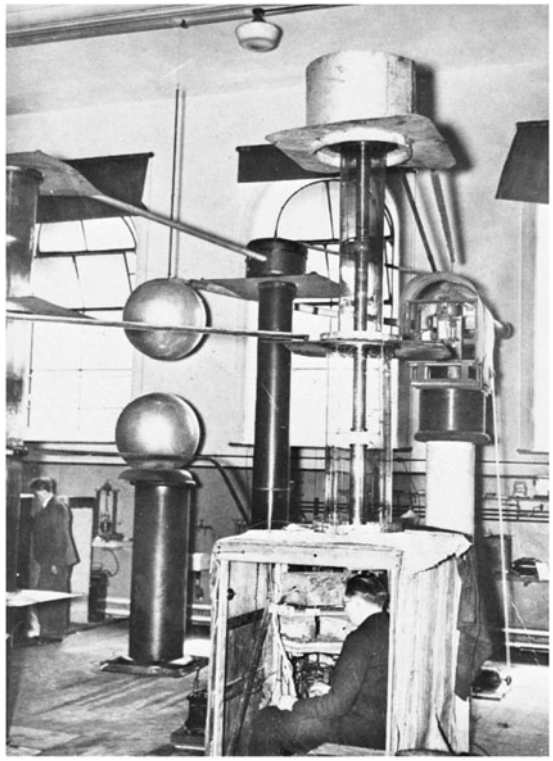

(*a*)

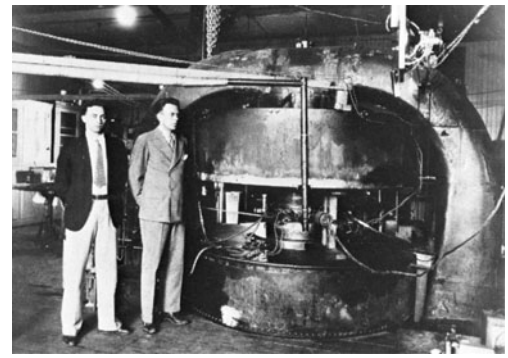

(*b*)

(*a*) The Cockcroft-Walton accelerator. Walton is sitting in the shielded enclosure in the foreground. J. D. Cockcroft and E. T. S. Walton produced the first transmutation of nuclei with artificially accelerated particles in 1932, for which they received the Nobel Prize (1951). (*b*) M. S. Livingston and E. O. Lawrence standing in front of their 27-in. cyclotron in 1934. Lawrence won the Nobel Prize (1939) for the invention of the cyclotron. [*(a) Courtesy of Cavendish Laboratory. (b) Courtesy of Lawrence Radiation Laboratory, University of California, Berkeley.*]

be evident at $Z = 114$ or 120 with metastable states whose lifetimes may be as long as hours or days. In the MORE section on the Web site we consider some of the more detailed qualitative aspects of the nuclear-shell model. Detailed calculations of energies and wave functions require many approximations, the understanding of which is a major area of continuing study in nuclear physics.

More

Finding the "Correct" Shell Model describes some of the qualitative aspects of the several approaches to developing the nuclear-shell model and its successes (and some failures) in predicting nuclear spins and magnetic moments. It is on the home page: www.whfreeman.com/tiplermodernphysics5e. See also Equations 11-56 and 11-57 and Figures 11-36 through 11-38.

11-7 Nuclear Reactions

When a particle is incident on a nucleus, any of several different things can happen. The particle may be scattered elastically or inelastically (in which case the nucleus is left in an excited state and decays by emitting photons or other particles) or the original particle may be absorbed and another particle or particles emitted.

Figure 11-39 illustrates schematically the several possible stages of a nuclear reaction. *Elastic scattering* refers to the reflection of the incident particle's wave at the edge of the nuclear potential well. This is the kind of scattering for α particles that

STUDENTS-HUB.com Uploaded By: Malak Obaid

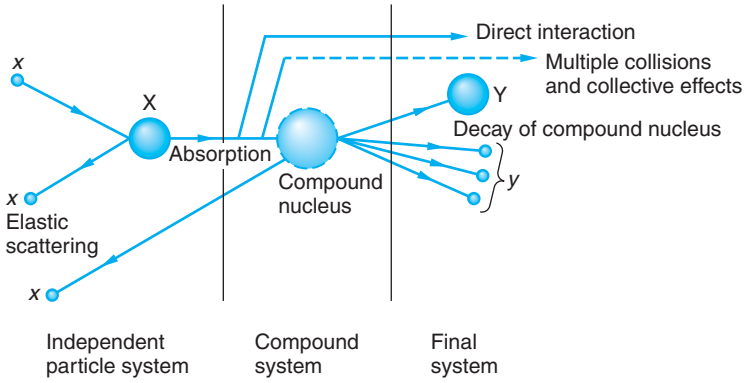

Figure 11-39 Schematic representation of the several possible stages of the nuclear reaction X (x, y) Y, according to the theory developed by V. Weisskopf and H. Feshbach.

was described by Rutherford's theory in Section 4-2. If the incident particle interacts with a single nucleon in the nucleus so that the nucleon leaves the nucleus, the reaction is called a *direct interaction*. Direct interactions are more probable at high energies since the incident particle can penetrate deeper into the nucleus. If the nucleon does not leave the nucleus but interacts with several other nucleons, complicated excited states can be formed in the nucleus. In such a case, when the energy carried by the incident particle is shared by many nucleons, the excited nucleus is called a *compound nucleus*. The compound nucleus can decay by emitting a particle identical to the incident particle and with the same kinetic energy (also elastic scattering) or by emission of one or more other particles (including photons). The decay of the compound nucleus can be treated as a statistical process independent of the detailed manner of formation, just as in the case of a radioactive nucleus.

In this section we will examine some of the systematics of nuclear reactions and some typical reactions produced by incident neutrons, protons, or deuterons. We will limit the discussion to energies of less than 140 MeV. At higher energies, mesons and other particles can be created. The study of higher-energy reactions is generally undertaken to reveal the properties of fundamental particles and of the nuclear force rather than the structure of the nucleus and will be discussed further in Chapter 12.

Energy Conservation

Consider a general reaction of particle x incident on nucleus X resulting in nucleus Y and particle y. The reaction may be written

$$x + \mathrm{X} \longrightarrow \mathrm{Y} + y + Q$$

or, as we will usually write it, X(x, y)Y. The quantity Q, defined by

$$Q = (m_x + m_{\mathrm{X}} - m_y - m_{\mathrm{Y}})c^2 \qquad \textbf{11-58}$$

is the energy released in the reaction and is called the Q *value* of the reaction.

When energy is released by a nuclear reaction, the reaction is said to be *exothermic*. In an exothermic reaction, the total mass of the initial particles is greater than that of the final particles and the Q value is positive. If the total mass of the initial particles is

STUDENTS-HUB.com Uploaded By: Malak Obaid

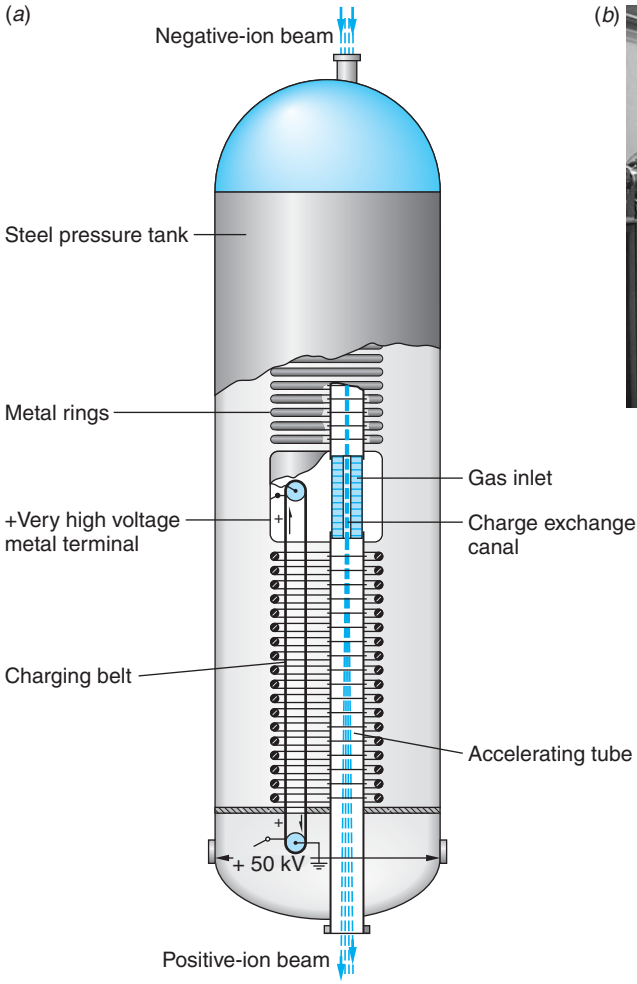

(*a*) Schematic diagram of a two-stage, or tandem, Van de Graaff accelerator. Negative ions at ground potential (atoms of a large fraction of the elements in the periodic table form stable negative ions) enter the beam tube at the top and are accelerated to the positive high-voltage terminal in the center, acquiring eV of kinetic energy. In the charge exchange canal, electrons are stripped from the negative ions in collisions with gas molecules, producing positive ions with charges up to $+Ze$. The positive ions are accelerated back to ground potential, acquiring an additional kinetic energy as large as ZeV. Large Van de Graaff accelerators have terminal voltages V over 16 million volts. Thus, for example, oxygen atoms stripped of all their electrons may be accelerated to energies of 100 MeV or more. (*b*) A portion of the tandem Van de Graaff laboratory at Purdue University. The high-voltage terminal is in the tank at the right rear, insulated from the surroundings by inert gas under high pressure. The beam travels in the tube and is deflected to experimental areas by the bending magnets. The Purdue accelerator is used extensively in accelerator mass spectrometry. [*Courtesy of David Elmore, Purdue University.*]

less than that of the final particles, the Q value is negative and energy is required for the reaction to take place. The reaction is then *endothermic*.

Examples are

$$n + {}^1\text{H} \longrightarrow {}^2\text{H} + \gamma + 2.22\ \text{MeV} \quad \text{(exothermic)}$$

$$\gamma + {}^2\text{H} \longrightarrow {}^1\text{H} + n - 2.22\ \text{MeV} \quad \text{(endothermic)}$$

Thus, an endothermic reaction cannot take place unless a certain threshold energy is supplied to the system. In the reference frame in which the total momentum is zero (the center-of-mass frame), the threshold energy is just $|Q|$. However, many reactions occur with nucleus X at rest relative to the laboratory. In this frame, called the *laboratory frame*, the incident particle x must have energy greater than $|Q|$ because, by conservation of momentum, the kinetic energy of y and Y cannot be zero. Consider the nonrelativistic case of x, of mass m, incident on X, of mass M (Figure 11-40).

STUDENTS-HUB.com Uploaded By: Malak Obaid

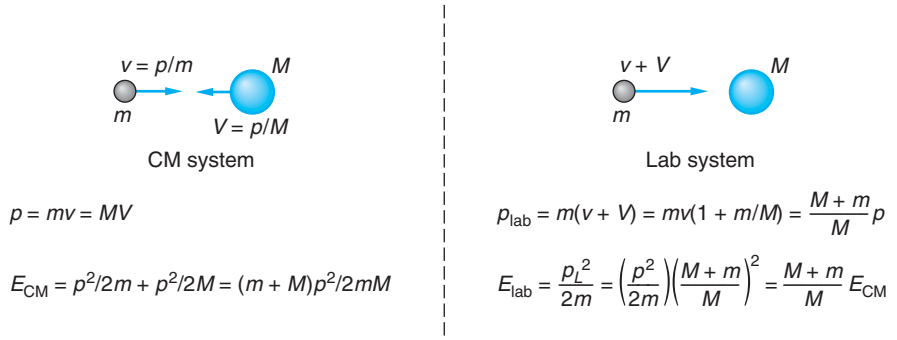

Figure 11-40 Energetics of nuclear reaction in center-of-mass system and laboratory system. The energies are related by $E_{lab} = [(M + m)/M]E_{CM}$.

In the center-of-mass frame, both particles have momenta of equal magnitude and the total kinetic energy is

$$E_{CM} = \frac{p^2}{2m} + \frac{p^2}{2M} = \frac{1}{2}p^2\left(\frac{m + M}{mM}\right) \qquad \textbf{11-59}$$

where $p = mv = MV$. We transform to the lab frame by adding V to each velocity so that M is at rest and m has velocity $v + V$. The momentum of m in the lab frame is then

$$p_{lab} = m(v + V) = mv\left(1 + \frac{m}{M}\right) = p\left(\frac{m + M}{M}\right)$$

and its energy is

$$E_{lab} = \frac{p_{lab}^2}{2m} = \frac{p^2}{2m}\left(\frac{m + M}{M}\right)^2 = \frac{m + M}{M}E_{CM} \qquad \textbf{11-60}$$

The threshold for an endothermic reaction in the lab frame is thus

$$E_{th} = \frac{m + M}{M}|Q| \qquad \textbf{11-61}$$

(If the incident particle is a photon, the Lorentz transformation must be used. For low energies, the momentum of a photon is small and approximate methods can be used. For a photon, $pc = E$, whereas for a proton or neutron, $pc = (2mc^2E)^{1/2} \gg E$ for $E \ll 140$ MeV.)

EXAMPLE 11-16 Q Value of a Nuclear Reaction Find the Q value of the reaction

$$p + {}^7\text{Li} \longrightarrow {}^4\text{He} + {}^4\text{He}$$

and state whether the reaction is exothermic or endothermic. The atomic mass of ^{7}Li is 7.016003 u.

STUDENTS-HUB.com Uploaded By: Malak Obaid

SOLUTION

Using 1.007825 u for the mass of ^{1}H and 4.002602 u for the mass of ^{4}He from Appendix A, we have for the total mass of the initial particles

$$m_i = 1.007825 \text{ u} + 7.016003 \text{ u} = 8.023828 \text{ u}$$

and for the total mass of the final particles

$$m_f = 2(4.002602 \text{ u}) = 8.005204 \text{ u}$$

Since the initial mass is greater than the final mass by

$$\Delta m = m_i - m_f = 8.023828 \text{ u} - 8.005204 \text{ u} = 0.018624 \text{ u}$$

mass is converted into energy and the reaction is exothermic. The Q value is positive and given by

$$Q = (\Delta m)c^2 = (0.018624 \text{ u})c^2(931.5 \text{ MeV/u} \cdot c^2) = 17.35 \text{ MeV}$$

Note that we used the mass of atomic hydrogen rather than that of the proton and the atomic masses of the ^{7}Li and ^{4}He atoms rather than the masses of the individual nuclei so that the masses of the four electrons on each side of the reaction cancel.

EXAMPLE 11-17 Threshold Energy in Lab Frame Compute the minimum kinetic energy of protons incident on ^{13}C nuclei at rest in the laboratory that will produce the endothermic reaction $^{13}\text{C}(p, n)^{13}\text{N}$.

SOLUTION

1. The minimum, or threshold, energy of the incident protons in the lab frame is given by Equation 11-61:

$$E_{\text{th}} = \frac{m + M}{M}|Q|$$

2. The magnitude of the Q value of the reaction is

$$\frac{|Q|}{c^2} = m_{\text{final}} - m_{\text{initial}}$$
$$= [M(^{13}\text{N}) + m_n] - [M(^{13}\text{C}) + M(^1\text{H})]$$

3. The masses of the particles involved are tabulated in Appendix A:

$$M(^{13}\text{C}) = 13.003355 \text{ u} \quad M(^1\text{H}) = 1.007825 \text{ u}$$
$$M(^{13}\text{N}) = 13.005738 \text{ u} \quad m_n = 1.008665 \text{ u}$$

4. Substituting these into the expression for $|Q|$ gives

$$|Q| = (14.014403 - 14.011180) \text{ u} \cdot c^2$$
$$= 0.003223 \text{ u} \cdot c^2 \times 931.5 \text{ MeV/u} \cdot c^2$$
$$= 3.00 \text{ MeV}$$

5. Substituting this value, $m = M(^1\text{H})$, and $M = M(^{13}\text{C})$ into Equation 11-61 gives

$$E_{\text{th}} = \frac{1.007825 + 13.003355}{13.003355} \times 3.00$$
$$= 3.23 \text{ MeV}$$

STUDENTS-HUB.com Uploaded By: Malak Obaid

Cross Section

The probability that a particle incident on a nucleus will scatter or induce a reaction depends on the particle's energy and what particular particle and nucleus are involved. It is as if different kinds of particles approaching a given nucleus "see" targets of different sizes. Similarly, identical particles with different energies "see" the same target nucleus larger or smaller than actual size. This effect is a consequence of the detailed arrangement of the allowed energy states of the target nucleus. A useful measure of the effective size of a nucleus for a particular scattering or nuclear reaction is the *cross section* σ. If I is the number of particles incident per unit time per unit area (the incident intensity) and R is the number of reactions per unit time per nucleus, the cross section is defined as

$$\sigma = \frac{R}{I} \qquad \textbf{11-62}$$

Consider, for example, the bombardment of ^{13}C by protons. A number of reactions might occur. Elastic scattering is written $^{13}C(p, p)^{13}C$; the first p indicates an incident proton, the second indicates that the particle that leaves is also a proton. If the scattering is inelastic, the outgoing proton is indicated by p' and the nucleus in the resulting excited state by $^{13}C^*$ and one writes $^{13}C(p, p')^{13}C^*$. Some other possible reactions are

(p, n)	$^{13}C(p, n)^{13}N$
capture	$^{13}C(p, \gamma)^{14}N$
(p, α)	$^{13}C(p, \alpha)^{10}B$

Each possible scattering or reaction has its own cross section, called the *partial cross section*. The partial cross section is also defined by Equation 11-62 with R equal to the number of events of the specific kind per unit time per nucleus. The total cross section is the sum of the partial cross sections:

$$\sigma = \sigma_{p,p} + \sigma_{p,p'} + \sigma_{p,n} + \sigma_{p,\gamma} + \sigma_{p,\alpha} + \ldots$$

Cross sections have the dimensions of area. Since nuclear cross sections are of the order of the square of the nuclear radius, that is, $(10^{-14}\ \text{m})^2$, a convenient unit for them is the *barn*, defined by

$$1\ \text{barn} = 10^{-24}\ \text{cm}^2 = 10^{-28}\ \text{m}^2 \qquad \textbf{11-63}$$

The cross section for a particular reaction is a function of energy. For an endothermic reaction, it is zero for energies below the threshold.

Compound Nucleus

In 1936, Niels Bohr pointed out that many low-energy reactions could be described as two-stage processes—the formation of a compound nucleus and its subsequent decay. In this description, the incident particle is absorbed by the target nucleus and the energy is shared by all the nucleons of the compound nucleus. After a time that is long compared with the time necessary for the incident particle to cross the nucleus, enough of the excitation energy of the compound nucleus becomes concentrated in one particle for it to escape. The emission of a particle is a statistical process that depends only on the state of the compound nucleus and not on how it was produced.

STUDENTS-HUB.com Uploaded By: Malak Obaid

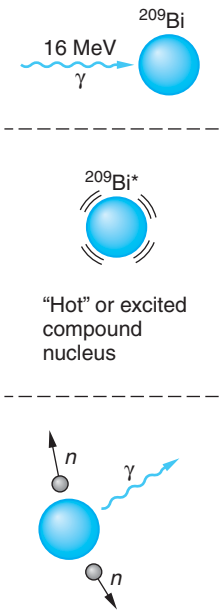

Figure 11-41 Nuclear reaction via formation of compound nucleus. The 16-MeV photon is absorbed by the ^{209}Bi nucleus, producing an excited nucleus that lives so long that excitation energy is shared by many nucleons. The excited nucleus then decays by emitting neutrons and photons, each with energy of the order of a few MeV.

An incident 1-MeV proton has a speed of about 10^7 m/s, so that it takes time $R/v \approx 10^{-14}/10^7 = 10^{-21}$ s to cross a nucleus. The lifetime of a compound nucleus can be inferred to be about 10^{-16} s. This is too short to be measured directly, but it is so long compared with 10^{-21} s that it is reasonable to assume that the decay is independent of how it was formed.

The compound nucleus for the reactions on ^{13}C shown above is ^{14}N*. This nucleus can be formed by many other reactions, such as

$$\begin{aligned} {}^{10}\text{B} + \alpha &\longrightarrow {}^{14}\text{N}^* \longrightarrow {}^{12}\text{C} + d \\ {}^{13}\text{N} + n &\longrightarrow {}^{14}\text{N}^* \longrightarrow {}^{10}\text{B} + \alpha \\ {}^{14}\text{N} + \gamma &\longrightarrow {}^{14}\text{N}^* \longrightarrow {}^{14}\text{N} + \gamma \\ {}^{12}\text{C} + d &\longrightarrow {}^{14}\text{N}^* \longrightarrow {}^{13}\text{N} + n \end{aligned} \qquad \textbf{11-64}$$

The reactions on the left are called the *entrance channels* and the decays on the right are called the *exit channels*.

Since the decay of ^{14}N* is independent of the formation, we can write the cross section for a particular reaction such as $^{13}\text{C}(p, n)^{13}\text{N}$ as the product of the cross section for the formation of the compound nucleus, σ_c, and the relative probability of decay by neutron emission, P_n:

$$\sigma_{p,n} = \sigma_c P_n \qquad \textbf{11-65}$$

An illustration of the statistical decay of the compound nucleus is afforded by the energy distribution of neutrons from reactions such as (Figure 11-41)

$$\gamma + {}^{209}\text{Bi} \longrightarrow {}^{208}\text{Bi} + n$$

where σ shows a broad peak at 14 to 20 MeV and neutrons "evaporate" as ^{209}Bi decays to the ground state.

Excited States of Nuclei from Nuclear Reactions

The excited states of a nucleus can be determined in two ways from nuclear reactions. A peak in the cross section $\sigma(E)$ as a function of energy indicates an excited state of the compound nucleus, corresponding to the relatively large probability of the incident particle giving up all its energy in the single event of exciting an allowed energy level. (Think of the Franck-Hertz experiment as an analogy.) Information about the lifetimes τ of the excited states of the compound nucleus is obtained by measuring the energy width Γ of these peaks, or *resonances*, and using the uncertainty principle $\tau\Gamma \approx \hbar$. Figure 11-42 shows the cross section for formation of ^{14}N by the reaction $^{10}\text{B} + \alpha \rightarrow {}^{14}\text{N}^*$ as a function of the α-particle energy. The peaks in this curve indicate energy levels in the ^{14}N nucleus. The Q value for this reaction is $M(^{10}\text{B})c^2 + M(\alpha)c^2 - M(^{14}\text{N})c^2 = 11.61$ MeV. The Q value is the binding energy of the incident particle in the compound nucleus, which is always of the order of 6 to 10 MeV; thus levels with energy less than 6 MeV cannot be reached in the compound nucleus.

The kinetic energy in the center-of-mass frame is related to the lab energy of the α particle by

$$E_{\text{CM}} = \frac{M}{M+m}E_{\text{lab}} = \frac{10}{14}E_{\text{lab}}$$

STUDENTS-HUB.com Uploaded By: Malak Obaid

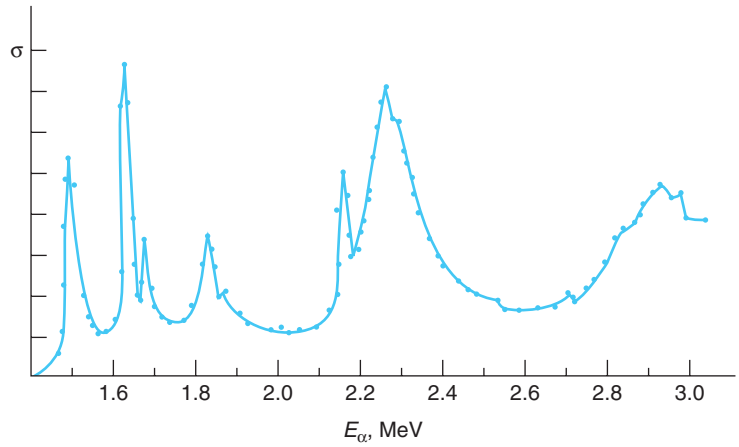

Figure 11-42 Cross section for the reaction $^{10}B + \alpha \rightarrow {}^{14}N^*$ versus energy. The resonances indicate energy levels in the compound nucleus $^{14}N^*$.

The peak in Figure 11-42 at $E_{lab} = 1.63$ MeV corresponds to an excited state in ^{14}N of energy $E = 11.61 + (10/14)(1.63) = 12.77$ MeV. The same level can be excited by the reaction $^{12}C + {}^2H \rightarrow {}^{14}N^*$. For this case, the Q value is 10.26 MeV. Thus, the deuteron energy in the lab must be

$$E_d = \left(\frac{14}{12}\right)(12.77 - 10.26) = 2.93 \text{ MeV}$$

A second way to determine the energy levels in a nucleus is to observe the energies of particles scattered inelastically. In this case, the energy levels of the target nucleus are determined. Figure 11-43 shows the energy spectrum of protons from the reaction $p + {}^{14}N \rightarrow {}^{14}N^* + p'$ using 6.92-MeV protons. (The horizontal scale in this figure is proportional to the momentum of the protons since this is what is measured experimentally.) The two peaks in the curve correspond to energy losses of 2.31 and 3.75 MeV, which indicated energy levels in ^{14}N of 2.31 and 3.75 MeV. The excited product nucleus decays from these states by γ emission. The method of inelastic scattering can determine energy levels of the target nucleus lying relatively close to the ground state, whereas the levels excited in the compound nucleus must be much higher because of the Q values for formation of the compound nucleus.

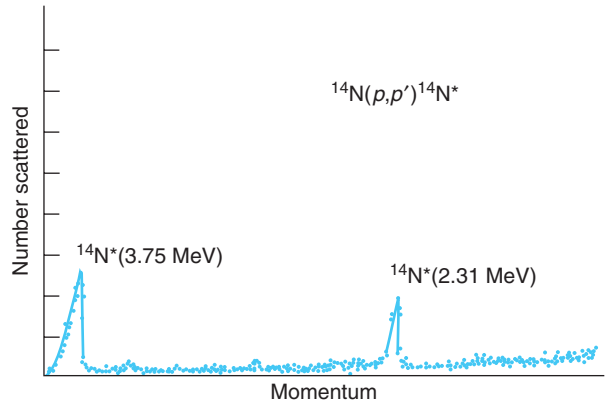

Figure 11-43 Spectrum of protons scattered from ^{14}N, indicating energy levels in ^{14}N.

STUDENTS-HUB.com Uploaded By: Malak Obaid

Reactions with Neutrons

Neutrons are used to dope silicon with phosphorus more uniformly than the conventional diffusion method. Irradiating Si with neutrons produces the P dopant via the reaction and subsequent decay $n + {}^{30}\text{Si} \rightarrow {}^{31}\text{Si} \rightarrow {}^{31}\text{P} + \beta^- + \bar{\nu}$. Silicon doped with P this way can operate at higher power levels in rectifier applications than diffusion-doped silicon.

Nuclear reactions involving neutrons are important for understanding the elemental analytical technique of neutron activation analysis and the operation of nuclear reactors. The most likely reaction with a nucleus for a neutron of more than about 1 MeV is scattering. However, even if the scattering is elastic, the neutron loses some energy to the nucleus because conservation of momentum requires that the nucleus recoil. If a neutron is scattered many times in a material, its energy decreases until it is of the order of the energy of thermal motion kT, where k is the Boltzmann constant and T is the absolute temperature. (At ordinary room temperatures, kT is about 0.025 eV.) The neutron is then equally likely to gain or lose energy from a nucleus when it is elastically scattered. A neutron with energy of the order of kT is called a *thermal neutron*.

At low energies, a neutron is more likely to be captured, with the emission of a γ ray from the excited nucleus:

$$n + {}^{A}_{Z}\text{M} \longrightarrow {}^{A+1}_{Z}\text{M} + \gamma$$

For example,

$$n + {}^{107}_{47}\text{Ag} \longrightarrow {}^{108}_{47}\text{Ag} + \gamma$$

Since the binding energy of a neutron is of the order of 6 to 10 MeV and the kinetic energy of the neutron is negligible by comparison, the excitation energy of the compound nucleus is from 6 to 10 MeV, and γ rays of this energy are emitted. Figure 11-44 shows the neutron capture cross section for silver as a function of the energy of the neutron. Except for the resonances, the cross section $\sigma(n, \gamma)$ varies smoothly with energy, decreasing with increasing energy approximately as $1/v$, where v is the speed of the neutron. This energy dependence can be understood as follows. Consider a neutron moving with speed v near a nucleus of diameter $2R$. The time it takes the neutron to pass the nucleus is $2R/v$. Thus, the neutron capture cross section is proportional to the time spent by the neutron in the vicinity of the nucleus. The dashed line in Figure 11-44 indicates this $1/v$ dependence.[21] At the maximum of the large resonance, the value of the cross section is very large ($\sigma > 5000$ barns) compared with a value of only about 10 barns just past the resonance. Many elements show similar resonances in the neutron capture cross sections. For example, the maximum cross section for ^{113}Cd is about 57,000 barns. Thus, ^{113}Cd is a strong absorber, which makes it very useful as a shield against low-energy neutrons.[22]

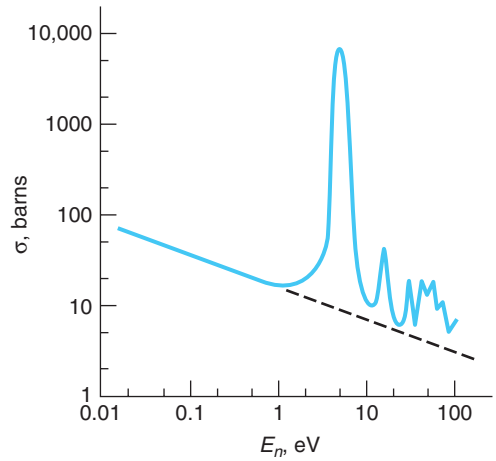

Figure 11-44 Neutron capture cross section for Ag versus energy. The dashed-line extension would be expected if there were no resonances and the cross section were merely proportional to the time spent near the nucleus, i.e., proportional to $1/v$. The resonance widths of a few eV indicate states with lifetimes of the order of $h/\Gamma \approx 10^{-16}$ s.

STUDENTS-HUB.com Uploaded By: Malak Obaid

Questions

13. What is meant by the cross section for a nuclear reaction? Why is that term used to describe it?
14. Why is the neutron capture cross section (excluding resonances) proportional to $1/v$?
15. What is meant by the Q value of a reaction? Why is the reaction threshold not equal to Q?
16. Why can't low-lying energy levels (1 to 2 MeV above the ground state) be studied using neutron capture?

EXAMPLE 11-18 Determination of Reaction Rates The cross section for the reaction $^{91}Zr(n,\gamma)^{92}Zr$ is 900 millibarns for thermal neutrons. This reaction is produced in the so-called thermal column of a reactor where the *flux* of thermal neutrons is 6.5×10^{12} neutrons/cm$^2 \cdot s$. The sample of natural Zr is a circular foil 1.0 cm in diameter and 20.0 μm thick. The density of Zr is 6.506 g/cm^3, and ^{91}Zr makes up 11.27 percent of natural Zr. Compute the rate of this reaction.

SOLUTION

First we need to compute the number of ^{91}Zr atoms in the sample. This number is given by

$$N(^{91}\text{Zr}) = \frac{N_A V \rho_{\text{Zr}}}{M_{\text{Zr}}} \times 0.1127$$

where the volume of the sample $V = 2.00 \times 10^{-3} \times (\pi/4)\text{cm}^3$ and the molecular weight of Zr, $M_{\text{Zr}} = 91.22$ g/mol. Thus,

$$N(^{91}\text{Zr}) = \frac{(6.02 \times 10^{23} \text{ atoms/mol})\left(2.00 \times 10^{-3} \times \frac{\pi}{4} \text{ cm}^3\right) \times 6.506 \text{ g/cm}^3}{91.22 \text{ gm/mol}}$$

$$N(^{91}\text{Zr}) = 1.04 \times 10^{19} \text{ atoms}$$

From the definition of the cross section given by Equation 11-62, the number of (n, γ) reactions per unit time per ^{91}Zr nucleus is

$$R = \sigma I = (900 \times 10^{-3} \text{ barns} \times 10^{-24} \text{ cm}^2/\text{barn}) \times 6.5 \times 10^{12} \text{ neutrons/cm}^2 \cdot \text{s}$$

$$R = 5.85 \times 10^{-12} \text{ s}^{-1} \text{ per } ^{91}\text{Zr nucleus}$$

The rate $\mathcal{R}$ at which the reaction $^{91}Zr(n, \gamma)^{92}Zr$ proceeds is then

$$\mathcal{R} = N(^{91}\text{Zr})R = (1.04 \times 10^{19} \, ^{91}\text{Zr nuclei})(5.85 \times 10^{-12} \text{ s}^{-1} \text{ per } ^{91}\text{Zr nucleus})$$

$$\mathcal{R} = 6.08 \times 10^{7} \text{ s}^{-1}$$

Remarks: *This is a low reaction rate, given the high neutron flux. It is the result of the low neutron capture cross section of ^{91}Zr and the other naturally occurring Zr isotopes. This is the principal reason why zirconium is used to enclose nuclear reactor fuel elements.*

STUDENTS-HUB.com Uploaded By: Malak Obaid

11-8 Fission and Fusion

Two nuclear reactions, fission and fusion, are of particular importance. In the fission of ^{235}U, for example, the uranium nucleus is excited by the capture of a neutron and splits into two nuclei, each with very roughly half of the original total mass. A typical fission reaction is

$$^{235}U + n \longrightarrow {}^{92}Kr + {}^{142}Ba + 2n + 179.4\ \text{MeV} \qquad \textbf{11-66}$$

The Coulomb force of repulsion drives the fission fragments apart, giving them very large kinetic energies. As a result of collisions with other atoms, this energy eventually shows up as thermal energy. In fusion, two light nuclei such as those of deuterium and tritium (^2H and ^3H) fuse together to form a heavier nucleus (in this case ^4He plus a neutron). A typical reaction is

$$^2H + {}^3H \longrightarrow {}^4He + n + 17.6\ \text{MeV} \qquad \textbf{11-67}$$

Figure 11-45 shows a plot of the mass difference per nucleon $(M - Zm_p - Nm_n)/A$ versus A in units of MeV/c^2. This curve is just the negative of the binding energy curve of Figure 11-10. From Figure 11-45 we see that the rest energy per particle for both very heavy nuclides ($A \approx 200$) and very light nuclides ($A \leq 20$) is more than that for nuclides of intermediate mass. Thus, in both fission and fusion the total mass decreases and energy is released. Since for $A = 200$ the rest energy is about 1 MeV per nucleon greater than for $A = 100$, about 200 MeV is released in the fission of a heavy nucleus. The energy release in fusion depends on the particular reaction. For the $^2H + {}^3H$ reaction in Equation 11-67, 17.6 MeV is released. Although this is less than the energy released in a single fission, it is a greater amount of energy per unit mass, as Example 11-19 illustrates. In this section, we will look at some of the features of fission and fusion that are important for their application in reactors to generate electricity.

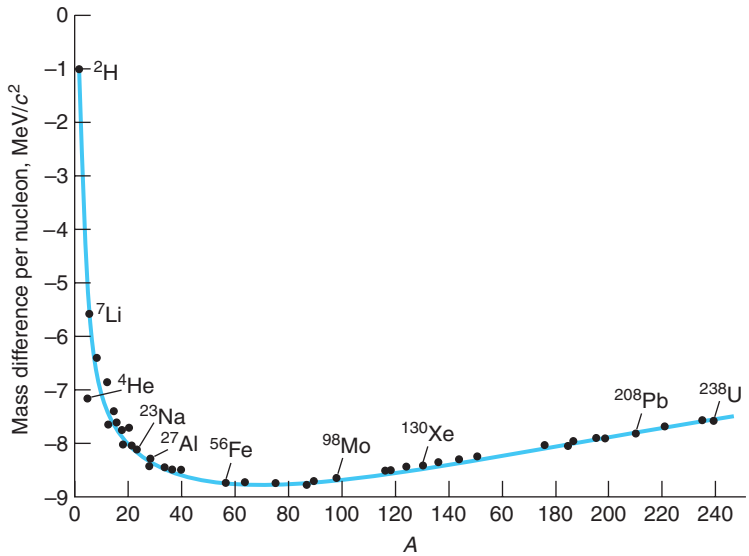

Figure 11-45 Plot of mass difference per nucleon $(M - Zm_p - Nm_n)/A$ in units of MeV/c^2 versus A. The rest energy per nucleon is smaller for intermediate-mass nuclei than for either very light or very heavy nuclei.

STUDENTS-HUB.com Uploaded By: Malak Obaid

EXAMPLE 11-19 **Energy Release in Fission and Fusion** Compare the energy release per unit mass in the fusion of deuterium and tritium (Equation 11-67) with that of a typical fission reaction, such as that of ^{235}U given by Equation 11-66.

SOLUTION

(*a*) A quick approximate comparison can be made by noting that the energy difference per nucleon between ^{235}U and its fission products is about 1.0 MeV. In the fusion of $^{2}H + {}^{3}H$, it is 17.6 MeV/5 nucleons = 3.5, or about 3.5 times larger. Thus, the energy released per kilogram will also be about 3.5 times larger in the fusion reaction.

(*b*) The mass differences per nucleon for ^{235}U and the two fission products in Equation 11-66 can be estimated from Figure 11-45. A more accurate calculation of the total binding energy can be made with the aid of Equation 11-12 and used to compute the total mass differences as follows:

$$^{235}U: \quad -7.6\ \text{MeV}/c^2 \text{ per nucleon} \longrightarrow -1797.1\ \text{MeV}/c^2 \text{ per nucleus}$$

$$^{92}Kr: \quad -8.7\ \text{MeV}/c^2 \text{ per nucleon} \longrightarrow -800.9\ \text{MeV}/c^2 \text{ per nucleus}$$

$$^{142}Ba: \quad -8.4\ \text{MeV}/c^2 \text{ per nucleon} \longrightarrow -1189.5\ \text{MeV}/c^2 \text{ per nucleus}$$

The difference between the mass of ^{235}U and the sum of masses for the fission products is 193.3 MeV/c^2. Thus, the energy release per fission event (with these particular products) is 193.3 MeV. The mass of ^{235}U (see Appendix A) is 235.043924 u = 3.9030×10^{-25} kg. Therefore, the energy release per kilogram in the fission of ^{235}U is

$$\frac{\left(\dfrac{193.3\ \text{MeV}}{^{235}\text{U}}\right)}{\left(\dfrac{3.903 \times 10^{-25}\ \text{kg}}{^{235}\text{U}}\right)} = 4.95 \times 10^{26}\ \text{MeV/kg}$$

The energy release in the deuterium/tritium fusion reaction is

$$\frac{17.6\ \text{MeV}}{M_d + M_t} = \frac{17.6\ \text{MeV}}{8.353 \times 10^{-27}\ \text{kg}} = 2.11 \times 10^{27}\ \text{MeV/kg}$$

Thus, the fusion reaction releases about 4.3 times the energy/kg released by the fission reaction.

Fission

The fission of uranium was discovered in 1938 by O. Hahn and F. Strassmann,[23] who found, by careful chemical analysis, that medium-mass elements (in particular, barium) were produced in the bombardment of uranium with neutrons. The discovery that several neutrons are emitted in the fission process led to speculation concerning the possibility of using these neutrons to cause further fissions, thereby producing a chain reaction. When ^{235}U captures a thermal neutron, the resulting ^{236}U nucleus undergoes fission about 85 percent of the time and emits gamma rays as it de-excites to the ground state about 15 percent of the time. The fission process is somewhat analogous to the oscillation of a liquid drop, as shown in Figure 11-46. If the oscillations are violent enough, the drop splits in two. Using the liquid-drop model, A. Bohr and J. Wheeler calculated the critical energy E_c needed by the ^{236}U nucleus to undergo fission. (^{236}U is the compound nucleus formed by the capture of a neutron by ^{235}U.)

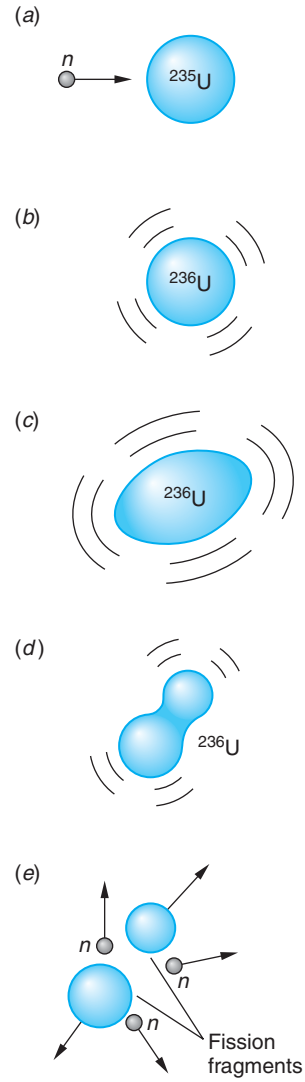

Figure 11-46 Schematic illustration of nuclear fission. (*a*) The absorption of a neutron by ^{235}U leads to (*b*) ^{236}U in an excited state. (*c*) Oscillation deforms the excited ^{236}U nucleus. (*d*) The oscillation of ^{236}U has become unstable. (*e*) The nucleus splits apart into two nuclei of medium mass and emits several neutrons that can produce fission in other nuclei.

STUDENTS-HUB.com Uploaded By: Malak Obaid

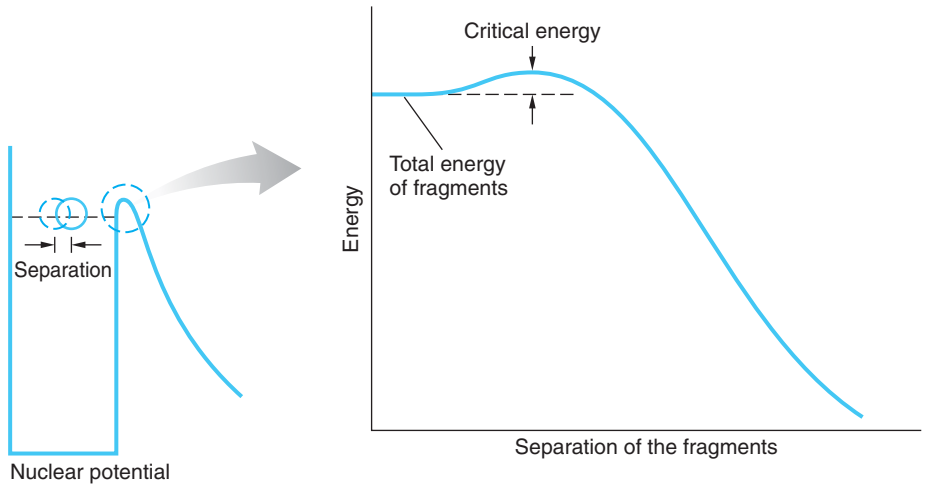

Figure 11-47 The nucleus may exist instantaneously as two fragments as shown on the left; however, the Coulomb potential barrier prevents their fission. To overcome the barrier, energy equal to the critical energy must be provided.

The critical energy is the magnitude of the Coulomb barrier seen by the fragments, as illustrated in Figure 11-47. For this nucleus, the critical energy is about 6.2 MeV, which is less than the 6.5 MeV of excitation energy produced when ^{235}U captures a neutron. The capture of a neutron by ^{235}U therefore produces an excited state of the ^{236}U nucleus that has more than enough energy to break apart. On the other hand, the critical energy for the fission of the ^{239}U nucleus is 5.9 MeV. The capture of a neutron by a ^{238}U nucleus produces an excitation energy of only 5.2 MeV. Therefore, when a thermal neutron is captured by ^{238}U to form ^{239}U, the excitation energy is not great enough for fission to occur. In this case the excited ^{239}U nucleus de-excites by γ or α emission. Nuclides that may fission upon capturing a slow neutron are called *fissile*.

We noted earlier that all nuclei with $Z > 83$ are radioactive. Among the possible decay modes of the very heavy nuclei ($Z > 90$) is that of spontaneous fission. These nuclei may break apart into two nuclei even if left to themselves without absorbing a neutron. We can also understand spontaneous fission using the analogy of a liquid drop of positive charges. If the drop is not too large, surface tension can overcome the repulsive forces of the charges and hold the drop together. There is, however, a certain maximum size beyond which the drop will be unstable and will spontaneously break apart since the repulsive force is proportional to the number of protons, which is proportional to the volume, hence to R^3, whereas the surface tension is proportional to the surface area and so increases only as R^2. (See Section 11-2.) Spontaneous fission puts an upper limit on the size of a nucleus and therefore on the number of elements that are possible. It should be noted that the probability for spontaneous fission in naturally occurring nuclides is quite low compared with the other possible decay modes. For example, the half-life of ^{238}U for α decay is 4.5×10^9 years, while that for spontaneous fission is about 10^{16} years. The reason is that fission, like α decay, is inhibited by the Coulomb barrier. Even though the process is energetically possible, the large positively charged fission fragments have a very low probability of tunneling through the Coulomb barrier part of the nuclear potential.

A fissioning nucleus can break into two medium-mass fragments in many different ways, as shown in Figure 11-48. Depending on the particular reaction, one, two, or three neutrons may be emitted. The average number of neutrons emitted in the thermal-neutron-induced fission of ^{235}U is about 2.4. Equation 11-66 is a typical fission reaction. The reason that several neutrons are emitted is that the fission fragments are typically neutron rich and far off the line of stability, as shown in Figure 11-49.

STUDENTS-HUB.com Uploaded By: Malak Obaid

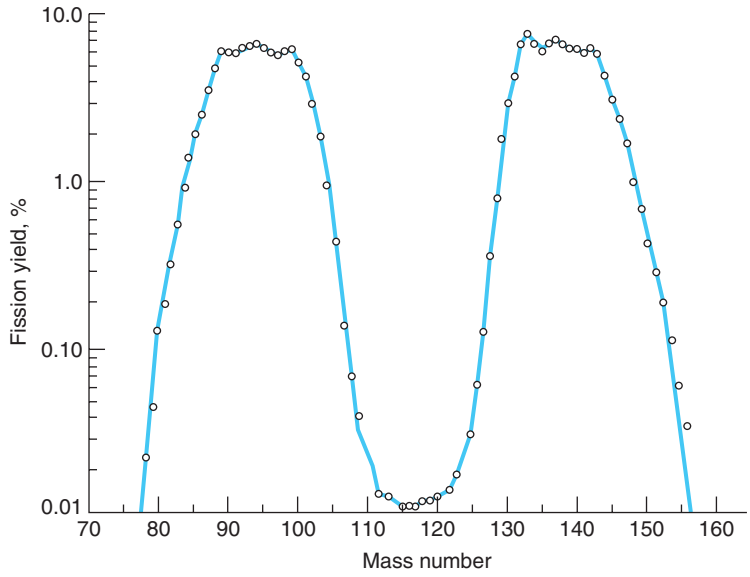

Figure 11-48 Distribution of fission fragments from the thermal-neutron-induced fission of ^{235}U. Symmetric fission, in which the uranium nucleus splits into two nuclei of nearly equal mass, is much less probable than asymmetric fission, in which the fragments have unequal masses. Note the symmetry of the light and heavy lobes of the distribution, including the small variations in the tops of the peaks and the convex outer edges. [*Data from G. J. Dilorio, Direct Physical Measurement of Mass Yields in Thermal Fission of Uranium-235, Garland, New York, 1979.*]

As a result, neutrons are spontaneously emitted during fission and the fragments β^- decay toward stability. The Coulomb force of repulsion drives the fission fragments apart with very large kinetic energies. This energy is transferred to other nearby atoms via collisions, eventually showing up as thermal energy of the surroundings. We have seen that about 200 MeV per nucleus is released in such a fission, a large amount of energy. By contrast, in the chemical combustion reaction, only about 4 eV is released per molecule of oxygen consumed.

The fission fragments and their decay products that build up in reactors are the source of many radioisotopes used in medical diagnosis, treatment, and research. Important among these is ^{99}Mo, the source of ^{99}Tc, the most widely used radioisotope in nuclear medicine.

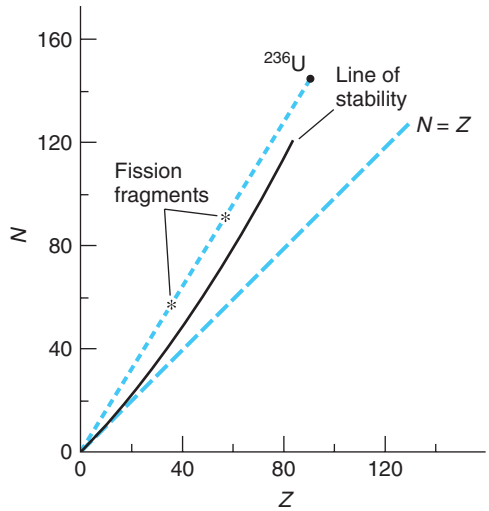

Figure 11-49 Fission of ^{236}U ($^{235}U + n$) produces fragments that are neutron-rich and well to the left of the line of stability. As a result, the fission is accompanied by the prompt emission of one or more of the excess neutrons followed by β^- decay of the fission fragments to further reduce their neutron numbers.

STUDENTS-HUB.com Uploaded By: Malak Obaid

EXAMPLE 11-20 Kilowatt-hours from ^{235}U Calculate the total energy in kilowatt-hours released in the fission of 1 g of ^{235}U, assuming that 200 MeV is released per fission.

SOLUTION

Since 1 mol of ^{235}U has a mass of 235 g and contains $N_A = 6.02 \times 10^{23}$ nuclei, the number of ^{235}U nuclei in 1 g is

$$N = \frac{6.02 \times 10^{23} \text{ nuclei/mol}}{235 \text{ g/mol}} = 2.56 \times 10^{21} \text{ nuclei/g}$$

The energy released per gram is then

$$\frac{200 \text{ MeV}}{\text{nucleus}} \times \frac{2.56 \times 10^{21} \text{ nuclei}}{1 \text{ g}} \times \frac{1.6 \times 10^{-19} \text{ J}}{1 \text{ eV}} \times \frac{1 \text{ h}}{3600 \text{ s}} \times \frac{1 \text{ kW}}{1000 \text{ J/s}} = 2.28 \times 10^4 \text{ kW} \cdot \text{h/g}$$

Remark: *This is approximately equal to the amount of electrical energy used by a typical U.S. household in 15 months.*

The discovery that several neutrons were emitted in the fission process led to speculation concerning the possibility of using these neutrons to initiate other fissions, thereby producing a *chain reaction*. On December 2, 1942, less than four years after Hahn and Strassmann's discovery of fission, a group led by Enrico Fermi produced the first self-sustaining chain reaction in a nuclear reactor that they had constructed at the University of Chicago.[24]

The application of both fission and fusion to the development of nuclear weapons has had a profound effect on our lives for more than 60 years. The peaceful application of these reactions to the development of energy resources may well have an even greater effect in the future, provided that satisfactory solutions are found to problems concerning safety, environmental protection, and the spread of nuclear weapons technology. Indeed, as world demand for energy increases, the diminishing finite reserves of fossil fuels will undoubtedly result in increasing use of nuclear reactors to provide the primary energy for the generation of electricity. The MORE section *Nuclear Power* is a comprehensive primer on fission reactors and closely related issues.

More

Nuclear fission reactors provided 6.0 percent of the energy consumed worldwide in 2005. *Nuclear Power*, on the home page at www.whfreeman.com/tiplermodernphysics5e, is a thorough review of existing and possible future types of fission reactors, the nuclear fuel cycle, reactor control, and safety issues. See also Equations 11-68 through 11-70 here, as well as Tables 11-5 and 11-6, Figures 11-50 through 11-54, and Examples 11-21 through 11-23.

STUDENTS-HUB.com Uploaded By: Malak Obaid

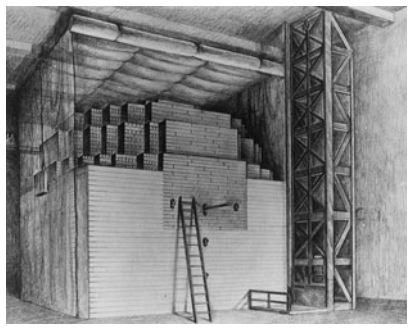

(*a*)

(*b*)

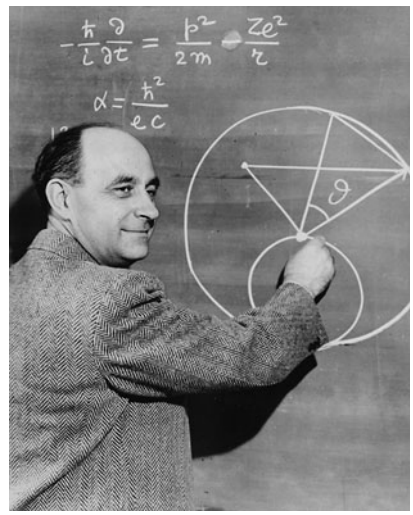

(*c*)

(*a*) A sketch of the world's first nuclear reactor, the CP-1 (for Chicago Pile number 1). Projecting from the near face next to the top of the ladder is one of the cadmium-plated rods used to control the chain reaction by absorbing neutrons. The cubical balloon surrounding the reactor, open on the near side, was to contain neutron-activated radioactive air. News of the reactor's successful test was transmitted by A. H. Compton, one of those present, to President Franklin Delano Roosevelt's adviser (and Harvard University president) J. B. Conant in a phone call thus: "The Italian navigator [i.e., Fermi] has landed in the New World," said Compton. "How were the natives?" asked Conant. "Very friendly," was Compton's reply. (*b*) The only photograph of CP-1 known to exist, taken during addition of the 19th layer of graphite. Alternate layers of graphite, containing uranium metal and/or uranium oxide, were separated by layers of solid-graphite blocks. Layer 18, almost covered, contained uranium oxide. (*c*) Enrico Fermi, leader of the group of scientists who succeeded in initiating the first man-made nuclear chain reaction, on December 2, 1942. [*(a) and (b) American Institute of Physics, Emilio Segrè Visual Archives; courtesy of Argonne National Laboratory, University of Chicago. (c) Courtesy of Argonne National Laboratory.*]

Fusion

The production of power from the fusion of light nuclei has the potential for future use because of the relative abundance of the fuel and the absence of some of the hazards presented by fission reactors. In fusion, two light nuclei such as deuterium (^{2}H) and tritium (^{3}H) fuse together to form a heavier nucleus. A typical fusion reaction is

$$^2\text{H} + {}^3\text{H} \longrightarrow {}^4\text{He} + n + 17.6\ \text{MeV} \qquad \textbf{11-71}$$

As was shown in Example 11-19, the energy released in this fusion reaction is (17.6 MeV)/(5 nucleons) = 3.52 MeV per nucleon, or about 3.5 times as great as the 1 MeV per nucleon released in fission. The technology necessary to make fusion a practical source of energy has not yet been developed. We will consider the fusion reaction of Equation 11-71; other reactions present similar problems.

STUDENTS-HUB.com Uploaded By: Malak Obaid

Because of the Coulomb repulsion between the ^{2}H and ^{3}H nuclei, very large kinetic energies, of the order of 1 MeV, are needed to get the nuclei close enough together for the attractive nuclear forces to become effective and cause fusion. Such energies can be obtained in an accelerator, but since the scattering of one nucleus by the other is much more probable than fusion, the bombardment of one nucleus by the other in an accelerator requires the input of more energy than is recovered. Therefore, to obtain energy from fusion, the particles must be heated to a temperature great enough for the fusion reaction to occur as the result of random thermal collisions. Because a significant number of particles have kinetic energies greater than the mean kinetic energy $(3/2)kT$ and because some particles can tunnel through the Coulomb barrier, a temperature T corresponding to $kT \approx 10$ keV is adequate to ensure that a reasonable number of fusion reactions will occur if the density of particles is sufficiently high. The temperature corresponding to $kT = 10$ keV is of the order of 10^8 K. Such temperatures occur in the interiors of stars, where such reactions are common. At these temperatures, a gas consists of positive ions and negative electrons called a *plasma* (see Chapter 10). One of the problems arising in attempts to produce controlled fusion reactions is that of confining the plasma long enough for the reactions to take place. In the interior of the Sun the plasma is confined by the enormous gravitational field of the Sun. In a laboratory on Earth, confinement is a difficult problem.

The energy required to heat a plasma is proportional to the density of its ions n, whereas the fusion rate is proportional to n^2, the square of the density (since the rate is the product of the Maxwell energy distribution and the fusion cross section, both of which are proportional to n). If τ is the confinement time, the output energy is thus proportional to $n^2\tau$. If the output energy is to exceed the input energy, we must have

$$C_1 n^2 \tau > C_2 n$$

where C_1 and C_2 are constants. In 1957, the British physicist J. D. Lawson evaluated these constants from estimates of the efficiencies of various hypothetical fusion reactors and derived the following relation between density and confinement time, known as *Lawson's criterion*:

$$n\tau > 10^{20}\ \text{s} \cdot \text{particles/m}^3 \qquad \textbf{11-72}$$

If Lawson's criterion is met and the thermal energy of the ions is great enough ($kT \approx 10$ keV), the energy released by a fusion reactor will just equal the energy input; that is, the reactor will just break even. For the reactor to be practical, much more energy must be released.

Two schemes for achieving Lawson's criterion are currently under investigation. In one scheme, *magnetic confinement*, a magnetic field is used to confine the plasma.[25] In the most common arrangement, first developed in Russia and called the *tokamak*, the plasma is confined in a large toroid. The magnetic field is a combination of the doughnut-shaped magnetic field due to the current in the windings of the toroid and the self-field due to the current of the circulating plasma. An international consortium of nations is currently constructing the International Thermonuclear Experimental Reactor (ITER) tokamak in France. Production of the first plasma is scheduled for 2016. The Chinese Experimental Advanced Superconducting Tokamak (EAST) which uses superconducting windings recognized as essential for continuous energy production, began operation late in 2006. The break-even point using magnetic confinement was achieved a few years ago, but we are still a long way from building a practical fusion reactor.

STUDENTS-HUB.com Uploaded By: Malak Obaid

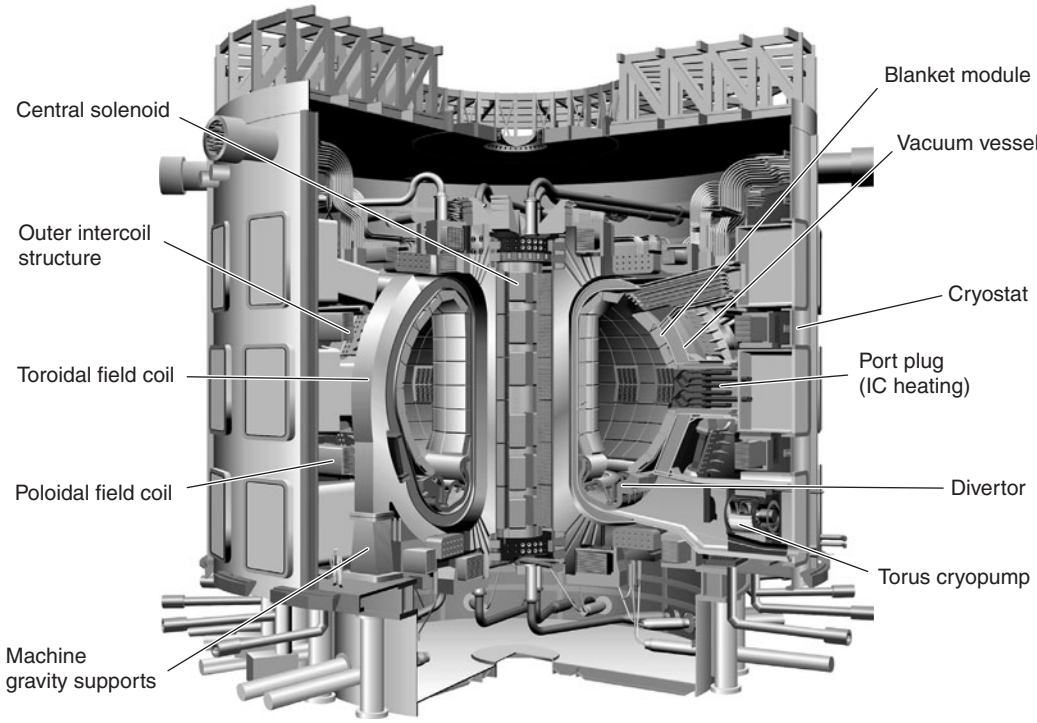

Schematic of the ITER tokamak experimental fusion reactor. The toroidal field coils, encircling the 6.2-m maximum diameter doughnut-shaped tritium-deuterium plasma contained in the vacuum vessel, are designed to conduct current for 300 s up to, eventually, steady state. The design plasma current is 15×10^6 A, producing a magnetic field of 5.3 T. This field is the principal means of confining the deuterium-tritium plasma that circulates within the vacuum vessel. Sets of poloidal field coils, perpendicular to the toroidal coils, carry an oscillating current that generates a current through the confined plasma itself, heating it ohmically. Additional poloidal fields help stabilize the confined plasma. Design total fusion power is 15 MW. ITER's first plasma is expected to be produced in 2016. Follow the development of ITER at *www.iter.org*. [*ITER Organization.*]

In a second scheme, called *inertial confinement*, a pellet of frozen-solid deuterium and tritium is bombarded from all sides by intense pulsed laser beams of energies of the order of 10^6 J lasting about 10^{-8} s. (Intense ion and electron beams are also used.) Computer simulation studies indicate the momentum absorbed by the hydrogen nuclei from the beams should compress the pellet to about 10^4 times its normal density and heat it to a temperature greater than 10^8 K. This should produce about 10^6 J of fusion energy in 10^{-10} s, which is so brief that confinement is achieved by inertia alone. (See Figure 11-55*a* and *b*.) In theory, after this burst of fusion energy is radiated away from the site to be absorbed by a heat-transfer fluid, such as liquid lithium, another pellet is injected at the confluence of the beams and the process repeats.

Because the break-even point has barely been achieved in magnetic confinement fusion and because the building of a fusion reactor involves many practical problems that have not yet been solved, for example, activation of the reactor walls, the availability of fusion to meet world energy needs is not expected for several decades.

STUDENTS-HUB.com Uploaded By: Malak Obaid

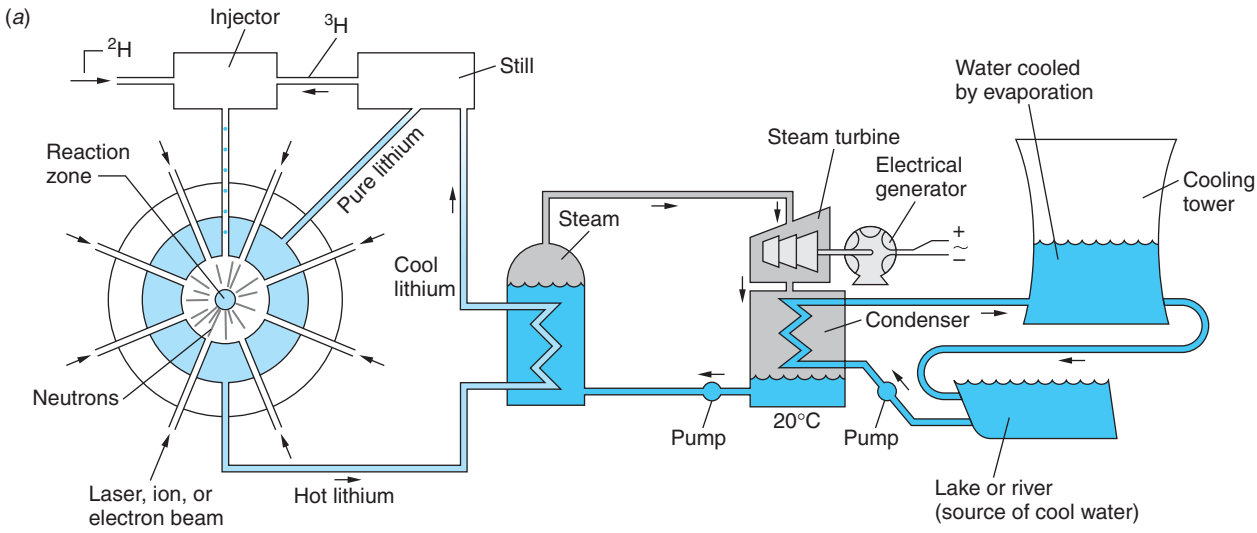

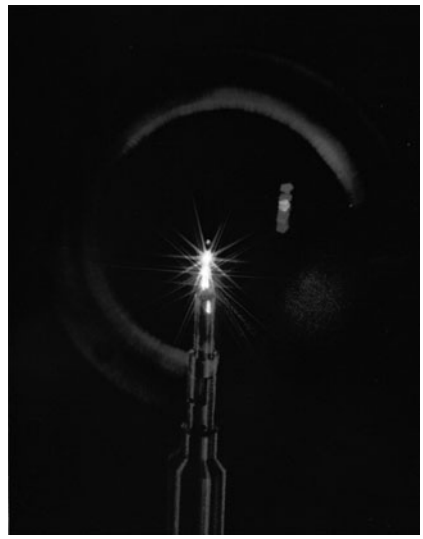

(b)

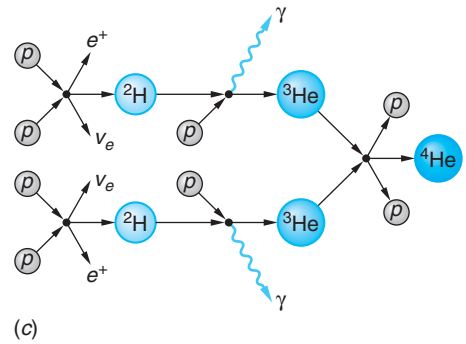

Figure 11-55 (*a*) Schematic diagram of a possible fusion reactor using inertial confinement and the $^2H + {}^3H \rightarrow {}^4He + n$ reaction. This reaction produces 17.6 MeV per fusion, and the neutron produced reacts with either ^{6}Li (slow neutron) or ^{7}Li (fast neutron) to produce the ^{3}H needed for the reaction. The latter reaction produces an additional slow neutron; thus, every two neutrons produced by fusion have the potential for generating three ^{3}H nuclei; that is, this system may also be a tritium breeder. (*b*) The Nova inertial confinement fusion reactor uses 10 powerful laser beams focused on a hydrogen-containing pellet 0.5 mm in diameter. The resulting fusion reaction, visible here as a tiny bright star, lasts 10^{-10} s and releases 10^{13} neutrons. (*c*) The proton-proton reaction is the primary source of the Sun's energy. The neutrino produced in the initial reaction escapes from the core. The net energy produced per cycle is about 26.7 MeV. [*(b) Courtesy of Lawrence Livermore National Laboratory, U.S. Department of Energy.*]

STUDENTS-HUB.com Uploaded By: Malak Obaid

EXAMPLE 11-24 **Fusion Temperature for $^1H + {}^1H \rightarrow {}^2H + e^+ + \nu$** The fusion of two protons requires that two particles be separated by no more than about 10^{-14} m in order for the attractive force of the nuclear potential to overcome the repulsive force of the Coulomb potential. Compute (*a*) the minimum temperature of a hydrogen plasma that will enable a proton with the average energy of those in the plasma to overcome the Coulomb barrier and (*b*) the energy released in the fusion.

SOLUTION

(*a*) The height of the potential energy barrier seen by the protons is given by

$$U = \frac{1}{4\pi\epsilon_0}\frac{e^2}{r} = \frac{(9 \times 10^9\ \text{N}\cdot\text{m}^2/\text{C}^2)(1.60 \times 10^{-19}\ \text{C})^2}{3.0 \times 10^{-15}\ \text{m}}$$

$$U = 7.68 \times 10^{-14}\ \text{J} = 0.48\ \text{MeV}$$

In order to overcome this barrier, the average energy of the protons in the plasma, $(3/2)kT$, must equal at least half this amount; that is, each of the two fusing protons must have 3.84×10^{-14} J.

$$(3/2)kT = 3.84 \times 10^{-14}\ \text{J}$$

where k is Boltzmann's constant. Thus,

$$T = \frac{2 \times 3.84 \times 10^{-14}\ \text{J}}{3 \times 1.38 \times 10^{-23}\ \text{J/K}} = 1.9 \times 10^9\ \text{K}$$

(*b*) The energy released, equal to the Q value of the fusion reaction, is

$$Q = [2m(^1\text{H}) - m(^2\text{H}) - 2m_e]c^2$$

$$= [2 \times 1.007825\ \text{u} - 2.014102\ \text{u} - 0.001097\ \text{u}]c^2$$

$$= 0.000451\ \text{u}\cdot c^2 \times 931.5\ \text{MeV/u}\cdot c^2 = 0.42\ \text{MeV}$$

where the atomic mass values are given in Appendix A. Thus, the energy release per $^1H + {}^1H$ fusion is 0.42 MeV. That of the $^2H + {}^3H$ fusion illustrated in Figure 11-55*a* is 17.6 MeV, which explains why the latter reaction is used in controlled fusion experiments.

The Source of the Sun's Energy The present energy content of the Sun as calculated from thermodynamics would be radiated away in about 3×10^7 years. Since life has existed on Earth for approximately 100 times that long, we can conclude that the Sun has been radiating at close to its present rate for at least 3×10^9 years. Therefore, the Sun must have a supply of energy far larger than that represented by the hot plasma and the observed radiation field. The source of the Sun's energy is nuclear fusion. Current theory proposes that, as the young Sun contracted, its temperature rose. Eventually the temperature of the core reached about 1.5×10^7 K, which is high enough for the hydrogen nuclei (protons) in the plasma to have sufficient energy on the average (about 1 keV) to fuse into helium nuclei. This reaction, actually a chain of reactions, was first proposed by H. A. Bethe and is referred to as the *proton-proton cycle*. The first reaction in the chain is (see Example 11-24)

$$^1\text{H} + {}^1\text{H} \longrightarrow {}^2\text{H} + e^+ + \nu_e + 0.42\ \text{MeV}$$

STUDENTS-HUB.com Uploaded By: Malak Obaid

The probability for this reaction is very low except for those protons in the high-energy tail of the Maxwell-Boltzmann distribution. This sets a limit on the rate at which the Sun can produce energy and thus ensures a long lifetime for the Sun and similar stars. This limit is sometimes called the "bottleneck" of the solar fusion cycle. Once ^{2}H (deuterium) is formed, the following reaction becomes very probable:

$$^2\text{H} + {}^1\text{H} \longrightarrow {}^3\text{He} + \gamma + 5.49\ \text{MeV}$$

It is followed by:

$$^3\text{He} + {}^3\text{He} \longrightarrow {}^4\text{He} + 2\ {}^1\text{H} + \gamma + 12.86\ \text{MeV}$$

This process by which hydrogen nuclei are "burned" to helium nuclei is shown schematically in Figure 11-55*c*. There are other possible reactions for converting ^{3}He to ^{4}He, all of which have the same net Q value. Their rates, however, differ depending on the composition and temperature of the interior.

The neutrinos produced in the proton-proton cycle escape from the core, providing our only means for direct observation of the Sun's interior. The measured value of the total power radiated by the Sun and the known total Q value of the proton-proton cycle allow a calculation of the total reaction rate. In addition, the alternative reactions for ^{4}He have different neutrino energy spectra, thus providing a way of determining the relative contributions of each reaction and gaining information about the composition and temperature of the core. However, the measured rate at which solar neutrinos arrive at Earth is less than half that predicted by theoretical calculations based on the standard solar model. This discrepancy is referred to as the *solar-neutrino problem*. Solving this problem was the focus of a recent major international research effort. Results from the Sudbury (Canada) and Super-Kamiokande (Japan) neutrino observatories show that neutrinos have a small mass and may transform from one type to another, leading to the observed discrepancy. (See Section 12-5.)

Questions

17. Explain why water is more effective than lead in slowing down fast neutrons.
18. What happens to the neutrons produced in fission that do not produce another fission?
19. Why does fusion occur spontaneously in the Sun but not on Earth?

More

The *Interaction of Particles and Matter* is of central importance in understanding the biological effects of ionizing radiation, in the development and use of nuclear radiation detectors, and in protecting the environment from potential radiation hazards. This topic is discussed for charged particles, neutrons, and photons on the home page: www.whfreeman.com/tiplermodernphysics5e. See also Equations 11-73 through 11-83 here, as well as Figures 11-56 through 11-61 and Example 11-25.

STUDENTS-HUB.com Uploaded By: Malak Obaid

11-9 Applications

Certainly among the most important of the applications of nuclear reactions and interactions have been those developed in the field of nuclear medicine, particularly in the area of diagnosis, but also including the treatment of cancer and certain other diseases. State-of-the-art detectors and computer-based data analysis have made critical contributions to these developments. Also important to a broad spectrum of disciplines ranging from art through chemistry and geology to zoology are the precision isotope-specific analytical techniques of *accelerator mass spectrometry* and *neutron activation analysis*. Anthropologists, archeologists, and geologists routinely rely on the decay properties of a number of radioisotopes to determine the age of artifacts and samples. Examples of these applications will be discussed briefly in this concluding section of the chapter.

Neutron Activation Analysis

This isotope-specific analytical method for elements is capable of very high sensitivity and accuracy. While some elements are more readily analyzed by activation analysis than others, it is particularly useful for the many elements that cannot be conveniently assayed by the more standard chemical methods of trace analysis. It has a wide range of applications from identifying trace pollutants in the environment through semiconductor processing and materials science to the analysis and authentication of works of art.

Potential oil- and gas-bearing regions in exploratory oil wells are identified by lowering an intense source of neutrons (usually a mixture of ^{239}Pu and ^{9}Be or ^{241}Am and ^{9}Be) into the well along with a gamma-ray detector. The neutrons produce gamma rays via $X(n, \gamma)Y$ reactions in the surrounding rock. Analysis of the gamma-ray spectra identifies elements in the rock that are typical indicators of the presence of oil and natural gas.

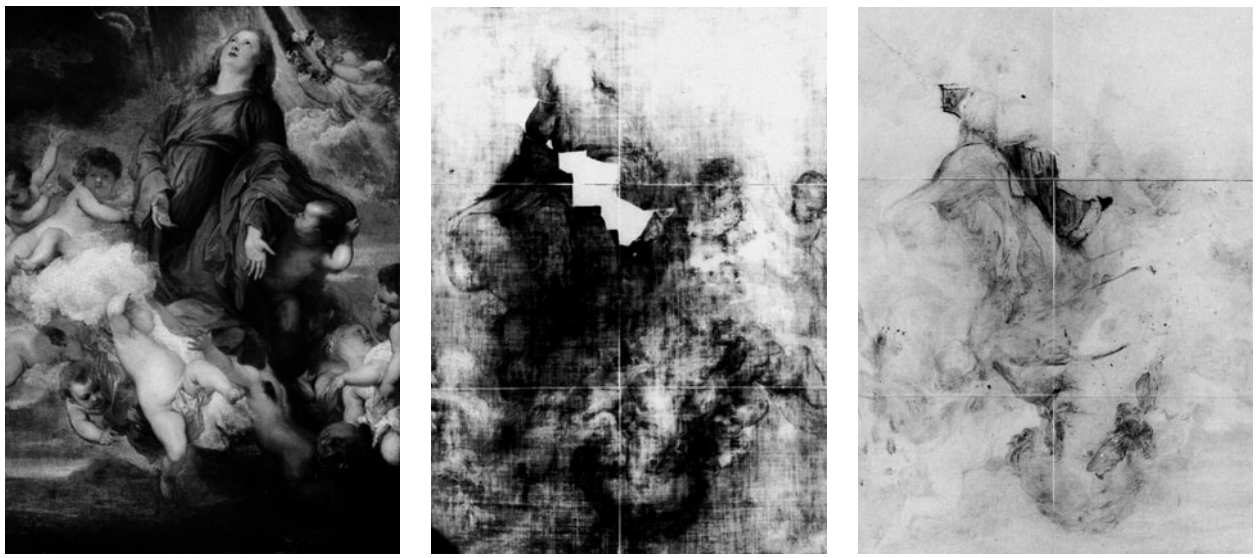

(*a*) (*b*) (*c*)

An application of neutron activation analysis. Hidden layers in paintings are analyzed by bombarding the painting with neutrons and observing the radiative emissions from nuclei that have captured a neutron. Different elements used in the painting have different half-lives. (*a*) Van Dyck's painting *Saint Rosalie Interceding for the Plague-Stricken of Palermo*. The black-and-white images in (*b*) and (*c*) were formed using a special film sensitive to electrons emitted by the radioactively decaying elements. Image (*b*), taken a few hours after the neutron irradiation, reveals the presence of manganese, found in umber, a dark earth pigment used for the painting's base layer. (Blank areas show where modern repairs, free of manganese, have been made.) The image in (*c*) was taken four days later, after the umber emissions had died away and when phosphorus, found in charcoal and boneblack, was the main radiating element. Upside down is revealed a sketch of Van Dyck himself. The self-portrait, executed in charcoal, had been overpainted by the artist. (See Problem 11-83.) [*(a) Courtesy of Metropolitan Museum of Art, New York City. (b) and (c) Courtesy of Paintings Conservation Department, Metropolitan Museum of Art, New York City.*]

STUDENTS-HUB.com Uploaded By: Malak Obaid

The method consists of exposing the sample to be analyzed to a high flux of slow neutrons. Isotope ${}^{A}_{Z}\mathrm{M}$ of the element of interest undergoes the reaction ${}^{A}_{Z}\mathrm{M}(n, \gamma){}^{A+1}_{Z}\mathrm{M}$, as described in Section 11-7, where ${}^{A+1}_{Z}\mathrm{M}$ is radioactive. ${}^{A+1}_{Z}\mathrm{M}$ can be identified by its half-life and the energy of its beta- and gamma-ray emissions. The activity $R(t)$ after the beginning of the neutron irradiation is given by

$$R(t) = \lambda N(t) = R_0(1 - e^{-\lambda t}) \qquad \textbf{11-84}$$

where λ is the decay constant of ${}^{A+1}_{Z}\mathrm{M}$ and R_0 is the constant production rate of that isotope. $R(t)$ is measured and R_0 is computed from Equation 11-62 since $R_0 = N_0 R$, where N_0 is the number of ${}^{A}_{Z}\mathrm{M}$ nuclei in the sample. Thus,

$$R_0 = N_0 R = N_0 \sigma I \qquad \textbf{11-85}$$

where σ is the cross section for the reaction ${}^{A}_{Z}\mathrm{M}(n, \gamma)\ {}^{A+1}_{Z}\mathrm{M}$ in cm^2 and I is the neutron flux in neutrons/$\mathrm{s} \cdot \mathrm{cm}^2$. Equation 11-84 can then be written

$$R(t) = N_0 \sigma I(1 - e^{-\lambda t}) \qquad \textbf{11-86}$$

When the half-life is short enough, irradiation is usually continued to saturation, that is, until $R(t) = R(\infty) = N_0 \sigma I$. Table 11-7 gives saturation activities per μg for a few isotopes. The number of atoms of ${}^{A}_{Z}\mathrm{M}$ in the sample is, at the saturation activity,

$$N_0 = \frac{R(\infty)}{\sigma I}$$

and the mass of ${}^{A}_{Z}\mathrm{M}$ in the sample is

$$m({}^{A}_{Z}\mathrm{M}) = \frac{N_0 W}{N_A} = \frac{R(\infty) W}{N_A \sigma I} \qquad \textbf{11-87}$$

where W is the atomic weight of the element and N_A is Avogadro's number.

Table 11-7 Selected saturation activities ($I = 10^{12}$ neutrons/$\mathrm{min} \cdot \mathrm{cm}^2$)

${}^{A}_{Z}\mathrm{M}$	${}^{A+1}_{Z}\mathrm{M}$	Saturation activity $R(\infty)$ decays/$\mathrm{m} \cdot \mu\mathrm{g}$
${}^{55}\mathrm{Mn}$	${}^{56}\mathrm{Mn}$	8.8×10^6
${}^{63}\mathrm{Cu}$	${}^{64}\mathrm{Cu}$	1.7×10^6
${}^{127}\mathrm{I}$	${}^{128}\mathrm{I}$	1.6×10^6
${}^{197}\mathrm{Au}$	${}^{198}\mathrm{Au}$	1.7×10^7

STUDENTS-HUB.com Uploaded By: Malak Obaid

EXAMPLE 11-26 **The "Gold" Chain** After buying a chain advertised as 10 percent pure gold, the suspicious purchaser irradiates one 25-mg link in a constant neutron flux of 10^{10} neutrons/s · cm^2 for a time long enough for any gold activity to saturate. She then measures the activity of the link to be 7.5×10^4 decays/s with a detector whose efficiency is 12 percent. What is the percent by weight of gold in the link? (σ for ^{197}Au is 98.8 barns.)

SOLUTION

Since the detector efficiency is 12 percent, the actual value of $R(\infty)$ is

$$R(\infty) = \frac{7.5 \times 10^4 \text{ decays/s}}{0.12} = 6.3 \times 10^5 \text{ decays/s}$$

From Equation 11-87 we can then compute

$$m(^{197}\text{Au}) = \frac{(6.3 \times 10^5 \text{ decays/s})(197 \text{ g/mol})}{(6.02 \times 10^{23} \text{ atoms/mol})(98.8 \times 10^{-24} \text{ cm}^2)(10^{10} \text{ neutrons/s/cm}^2)}$$

$$m(^{197}\text{Au}) = 2.1 \times 10^{-4} \text{ g}$$

The weight percent of gold in the link is then

$$\%\text{Au} = \left(\frac{2.1 \times 10^{-4} \text{ g}}{25 \times 10^{-3} \text{ g}}\right) \times 100 = 0.8\%$$

or less than 1/10 of the advertised amount.

Nuclear Magnetic Resonance

In Section 7-7, we saw that the energy levels of the atom were split in the presence of an external magnetic field (the Zeeman effect) because of the interaction of the atomic magnetic moment and the field. Since nuclei also have magnetic moments, the energy levels of a nucleus is also split in the presence of a magnetic field. We can readily understand this by considering the simplest case, the hydrogen atom, for which the nucleus is a single proton.

The potential energy of a magnetic moment μ in an external magnetic field **B** is given by

$$U = -\mu \cdot \mathbf{B} \qquad \textbf{11-88}$$

The potential energy is lowest when the magnetic moment is aligned with the field and highest when it is in the opposite direction. Since the spin quantum number of the proton is 1/2, the proton's magnetic moment has two possible orientations in an external magnetic field: parallel to the field (spin up) or antiparallel to the field (spin down). The difference in energy of these two orientations (Figure 11-62) is

$$\Delta E = 2(\mu_z)_p B \qquad \textbf{11-89}$$

When hydrogen atoms are irradiated with photons of energy ΔE, some of the nuclei are induced to make transitions from the lower state to the upper state by resonance absorption. These nuclei then decay back to the lower state, emitting photons of energy ΔE. The frequency of the photons absorbed and emitted is found from

$$hf = \Delta E = 2(\mu_z)_p B$$

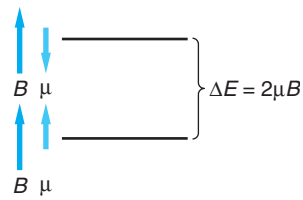

Figure 11-62 A proton has two energy states in the presence of a magnetic field, corresponding to whether the magnetic moment of the proton is aligned parallel or antiparallel to the field.

STUDENTS-HUB.com Uploaded By: Malak Obaid

In a magnetic field of 1 T, this energy is

$$\begin{aligned}\Delta E &= 2(\mu_z)_p B \\ &= 2(2.79\mu_N)\left(\frac{3.15 \times 10^{-8}\ \text{eV/T}}{1\ \mu_N}\right)(1\ \text{T}) \\ &= 1.76 \times 10^{-7}\ \text{eV}\end{aligned}$$

and the frequency of the photons is

$$\begin{aligned}f &= \frac{\Delta E}{\hbar} = \frac{1.76 \times 10^{-7}\ \text{eV}}{4.14 \times 10^{-15}\ \text{eV} \cdot \text{s}} \\ &= 4.25 \times 10^{7}\ \text{Hz} = 42.5\ \text{MHz}\end{aligned}$$

This frequency is in the radio band of the electromagnetic spectrum; hence the radiation is called *RF* (radio-frequency) *radiation*. The measurement of this resonance frequency for free protons can be used to determine the magnetic moment of the proton.

When a hydrogen atom is in a molecule, the magnetic field at the proton is the sum of the external magnetic field and the local magnetic field due to the electrons and nuclei of the surrounding material. Since the resonance frequency is proportional to the total magnetic field seen by the proton, a measurement of this frequency can give information about the internal magnetic field seen in the molecule. This is called *nuclear magnetic resonance*. It is a sensitive tool for probing the internal magnetic structure of materials.

Nuclear magnetic resonance is also used as an alternative to x rays or ultrasound for medical imaging, in which case it is called *m*agnetic *r*esonance *i*maging (MRI). A patient can be placed in a magnetic field (provided by superconducting magnets) that is constant in time but not in space. When the patient is irradiated by a broadband RF source, the resonance frequency of the absorbed and emitted RF photons is then dependent on the value of the magnetic field, which can be related to specific positions in the body of the patient. Since the energy of the photons is much less than the energy of molecular bonds and the intensity used is low enough so that it produces negligible heating, the RF photons produce little, if any, biological damage. Diagnosis with MRI requires no surgical procedure and is more sensitive than other methods in detecting tumors in soft tissue.

Computer-Assisted Tomography

Wilhelm Roentgen received the first physics Nobel Prize in 1901 for his discovery of x rays in 1895, an event that also marked the beginning of *radiography*, the use of radiation and particle beams to produce images that are otherwise inaccessible. For half a century x rays were the probing beam of medical imaging. Then in the late 1940s the introduction of radioisotopes into a patient's body made it possible for physicians to target particular organs and produce images that recorded their behavior, a technique now a part of the specialty of nuclear medicine. The isotopes used are typically relatively short-lived gamma emitters since α and β particles have ranges in biological tissue that are too short to be useful. The detector normally employed is a collimated (to provide directional information) scintillation crystal viewed by a photomultiplier. (See Figure 11-63.) The image is then constructed by a computer from the output of the photomultiplier.

STUDENTS-HUB.com Uploaded By: Malak Obaid

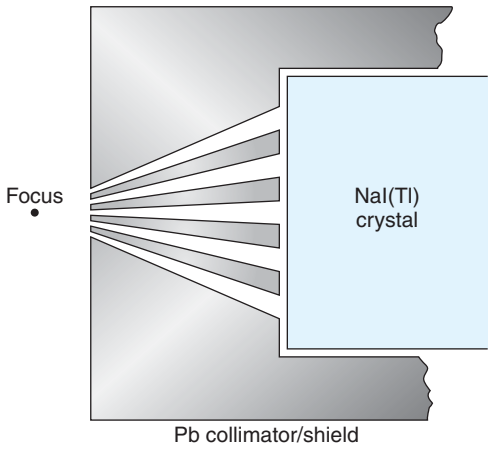

Figure 11-63 Schematic drawing of a scintillation crystal with a Pb collimator to define a focus, a gamma camera. As the detector is moved around the patient, the intensity of the gamma radiation yields information about the location and concentration of the source radioisotope in the body, which can be used by a computer to produce an image of the distribution. Actual gamma cameras incorporate collimators with hundreds or even thousands of tiny channels for the gamma rays to reach the crystal.

Just as with ordinary x-ray radiographs, the images formed by the gamma camera are two-dimensional projections of a three-dimensional distribution. Thus, radiographs provide no depth information, a very serious disadvantage. G. Hounsfield and A. Cormack solved this problem in 1972 with the invention of the computer-assisted tomography (CT or CAT) scanner.[26] A fan-shaped x-ray beam collimated to a thickness of a few millimeters is rotated about the patient and the transmitted fan beam is recorded by an arc of detectors opposite the source, as illustrated in Figure 11-64. The measurements are then reconstructed into an image of a two-dimensional image (*not* a projection) of a transverse slice of the body—a tomograph. By simultaneously making a series of two-dimensional projections with a gamma camera and combining the results with the CT scan, the distribution of the trace radioisotopes in two-dimensional transverse sections can be constructed. The combination system is called *single-photon emission computer tomography*, or SPECT.

It had been recognized early on that the collimators that were essential to the operation of CT scanners and gamma cameras placed a serious restriction on their sensitivity. It was also recognized that the collimators could be eliminated and the sensitivity

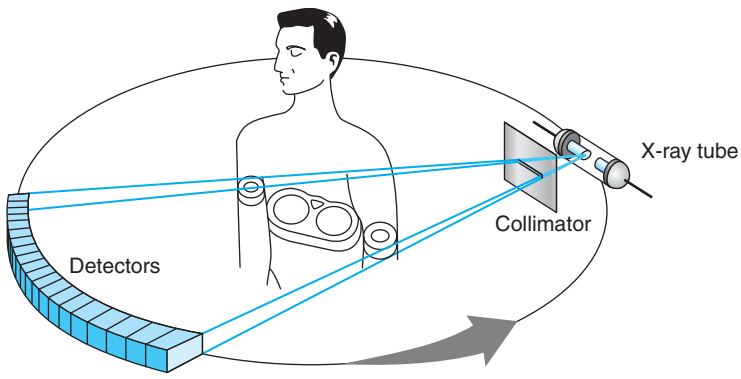

Figure 11-64 Sections of the patient's body transverse to the long axis are imaged by the CT scanner. The fan-shaped x-ray beam, a few millimeters thick, and the bank of detectors, typically proportional or wire counters, rotate about the long axis to produce each complete image. The patient is moved slowly along the axis while the scanner produces successive images, their sum constituting a full three-dimensional composite.

STUDENTS-HUB.com Uploaded By: Malak Obaid

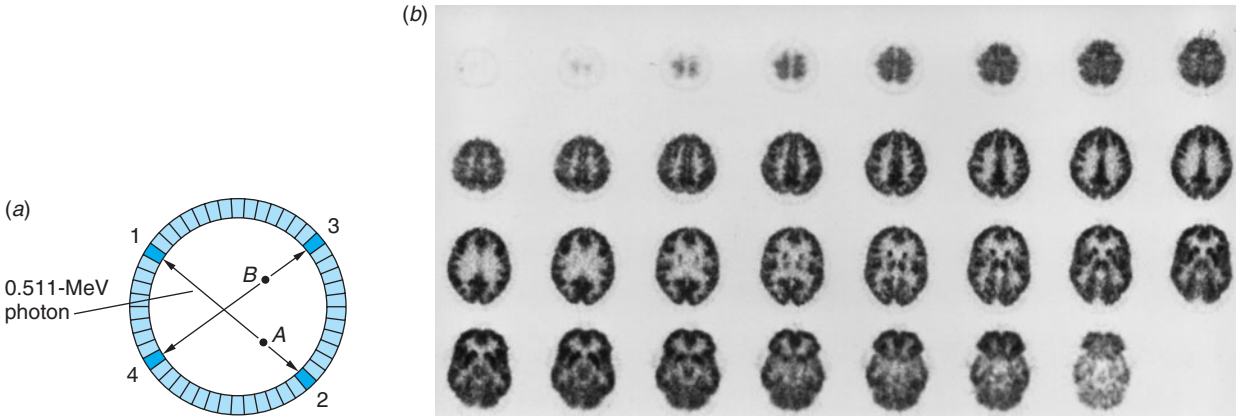

Figure 11-65 (*a*) Nuclei emit positrons at *A* and *B*. The oppositely directed 0.511-MeV photons from each annihilation are detected by a pair of BGO crystal detectors in the annular ring around the subject (not shown). Electronic coincidence circuits establish the line along which each pair of photons traveled. (*b*) The pattern of coincidence measurements is used by a computer to construct an image of the distribution of the radioisotope in the plane of the detector ring. This sequence of PET scans shows the utilization of glucose in the brain, traced by 7 mCi of a positron emitter. The sequence begins in the upper left. [*Courtesy of D. W. Townsend, Division of Nuclear Medicine, University Hospital of Geneva, Geneva, Switzerland.*]

significantly enhanced if the trace radioisotope employed was a positron emitter. The reason is that the positron is stopped within a few millimeters in the tissue and its subsequent annihilation results in two 0.511-MeV photons emitted in opposite directions. Detection of the photons by counters 180° apart whose outputs are analyzed by a time-of-flight coincidence spectrometer yields a precise location for the decay. (See Figure 11-65.) However, this idea did not find its way into a useful diagnostic scanner until the mid-1980s because of the absence of detectors with good efficiency for the 0.511-MeV photons and small enough to localize the incident photons to within a millimeter or so. This problem was solved with the invention by C. Thompson and his co-workers of the bismuth germanate (BGO) crystal. Currently, nearly all commercial positron emission tomography (PET) scanners rely on detector rings made of BGO crystals, as illustrated in Figure 11-65*a*. A PET scan of brain activity made with BGO detectors is shown in Figure 11-65*b*. The availability of PET scans is limited to locations in the proximity of cyclotron facilities because most biologically useful positron emitters, those that readily participate in reactions in the body, are ^{11}C, ^{13}N, ^{15}O, and ^{18}F. They have short half-lives of 20 min, 10 min, 2 min, and 110 min, respectively, and supplies must be regularly replenished by nuclear reactions.

Technetium ($Z = 43$) does not occur in nature. Predicted by Moseley in 1914 and first produced by Segrè in 1937, ^{99}Tc is by far the most widely used radioisotope in nuclear medicine research and diagnosis. Its decay produces a 140-keV gamma ray easily detected by scintillation and germanium detectors.

Radioactive Dating

Radioactivity occurs in nature as a result of (1) decays within the three decay chains originating with long-lived α emitters discussed in Section 11-4, (2) the existence of isolated long-lived primordial radioisotopes such as ^{40}K ($t_{1/2} = 1.25 \times 10^9$ y), and (3) the production of isolated radioisotopes due to reactions between cosmic ray protons and neutrons and nuclei in the atmosphere. Each of these provides a means by which the age of materials, such as rocks and archeological artifacts, can be measured. As one might guess, the very long-lived isotopes, such as ^{40}K and ^{232}Th ($t_{1/2} = 1.24 \times 10^{10}$ y), are used in determining the ages of "old" rocks, while shorter-lived isotopes are employed in determining the ages of "younger" rocks, other inorganic materials, and archeological samples containing carbon, such as charcoal.

STUDENTS-HUB.com Uploaded By: Malak Obaid

Table 11-8 Selected naturally occurring isolated radioactive nuclides

Nuclide	$t_{1/2}$ (y)	Abundance (%)	Daughter
^{14}C	5730	1.35×10^{-10}	^{14}N
^{40}K	1.25×10^{9}	0.0117	^{40}A
^{87}Rb	4.88×10^{10}	27.83	^{87}Sr
^{147}Sm	1.06×10^{11}	15.0	^{143}Nd
^{176}Lu	3.59×10^{10}	2.59	^{176}Hf
^{187}Re	4.30×10^{10}	62.60	^{187}Os

The general technique used in determining the age of a sample by radioactive dating is to measure the present abundance ratio of two isotopes, at least one of which is either radioactive or the stable end product of a radioactive decay, relative to the abundance ratio that is known (or assumed) to have existed at the time when the material was formed. Table 11-8 lists the present isotopic abundances of a few of the naturally occurring isolated radioisotopes used in dating.

^{14}C Dating An important example, used in dating archeological materials containing carbon such as bone and charcoal, measures the abundance ratio $^{14}C/^{12}C$. Radioactive ^{14}C is continuously produced in the atmosphere by the reaction $^{14}N(n, p)^{14}C$. The neutrons are produced by cosmic rays. ^{14}C is a β^- emitter that decays back to ^{14}N via the reaction

$$^{14}C \longrightarrow {}^{14}N + \beta^- + \bar{\nu}_e \qquad \textbf{11-90}$$

with $t_{1/2} = 5730$ years.[27]

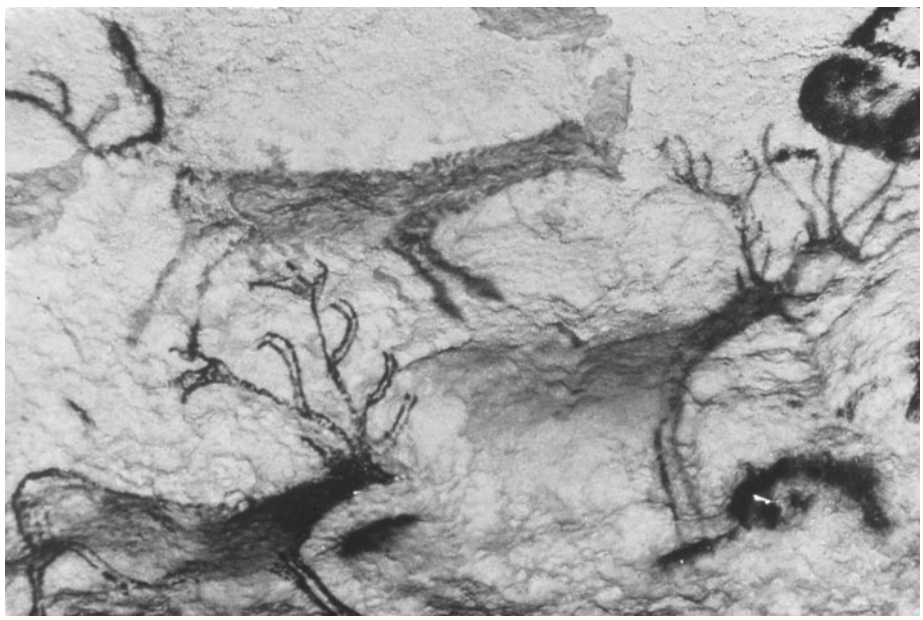

"Group of Stags" from the Lascaux Caves in France. Prehistoric paintings such as this are ^{14}C-dated, the oldest found so far having been painted 33,000 to 38,000 B.C., depending on the $^{14}C/^{12}C$ ratio used for that period. [*Art Resource.*]

STUDENTS-HUB.com Uploaded By: Malak Obaid

The chemical behavior of ^{14}C atoms is the same as that of ordinary ^{12}C atoms. For example, atoms with ^{14}C nuclei combine with oxygen to form CO_2 molecules. Since living organisms continually exchange CO_2 with the atmosphere, the ratio of ^{14}C to ^{12}C in a living organism is the same as the equilibrium ratio in the atmosphere, which is presently about 1.35×10^{-12}. When an organism dies, it no longer absorbs ^{14}C from the atmosphere. The ratio $^{14}C/^{12}C$ in a dead sample continually decreases due to the radioactive decay of ^{14}C. A measurement of the decay rate per gram of carbon thus allows the calculation of the time of death of the organism, as illustrated by Example 11-28.

EXAMPLE 11-27 ^{14}C Decay Rate in Living Organisms Calculate the decay rate of ^{14}C per gram of carbon in a living organism, assuming the ratio $^{14}C/^{12}C = 1.35 \times 10^{-12}$. The half-life of ^{14}C is 5730 years.

SOLUTION

1. Combining Equation 11-19 with Equation 11-22, the decay rate R can be written in terms of the half-life and the number of radioactive atoms N as

$$R = -\frac{dN}{dt} = \lambda N = \frac{0.693}{t_{1/2}} N$$

2. N is computed from the $^{14}C/^{12}C$ ratio by first computing the number of ^{12}C in a unit mass, e.g., in 1 g:

$$N_{^{12}C} = \frac{N_A}{M} = \frac{6.02 \times 10^{23} \text{ atoms/mol}}{12 \text{ g/mol}} = 5.02 \times 10^{22} \text{ nuclei/g}$$

3. The number N of ^{14}C nuclei per gram is then given by

$$N_{^{14}C} = 1.35 \times 10^{-12} N_{^{12}C} = (1.35 \times 10^{-12})(5.02 \times 10^{22}) = 6.78 \times 10^{10} \text{ nuclei/g}$$

4. The decay rate is then

$$R = \frac{(0.693)(6.78 \times 10^{10} \text{ g}^{-1})(60 \text{ s/min})}{(5730 \text{ y})(3.16 \times 10^{7} \text{ s/y})} = 15.6 \text{ decays/min} \cdot \text{g}$$

Remarks: *Thus, the decay rate for a living organism is 15.6 decays per minute per gram of carbon.*

EXAMPLE 11-28 Age of a Bone Fragment A bone fragment found in central Mexico was thought to be associated with the army of Hernán Cortés, who conquered the Aztecs in the early 1500s. The fragment contains 200 g of carbon and has a β-decay rate of 400 decays/min. Could the sample have come from a person who died during the 16th century?

SOLUTION

First we obtain a rough estimate. If the bone were from a living organism, we would expect the decay rate to be 200 g × 15.6 decays/min · g = 3120 decays/min.

STUDENTS-HUB.com Uploaded By: Malak Obaid

Since 400/3120 is roughly $1/8 = 1/2^3$ (actually 1/7.8), the sample must have decayed for about 3 half-lives, or be about 3×5730 years old. To find the age more accurately, we note that after n half-lives, the decay rate has decreased by a factor of $(1/2)^n$. We therefore find n from

$$\left(\frac{1}{2}\right)^n = \frac{400}{3120}$$

or

$$2^n = \frac{3120}{400} = 7.8$$

$$n \ln 2 = \ln 7.8$$

$$n = \frac{\ln 7.8}{\ln 2} = 2.96$$

The age is therefore $t = nt_{1/2} = 2.96(5730 \text{ years}) = 16{,}980$ years. Thus, the bone fragment is much older than 500 years and cannot be related to Cortés's conquests. Instead, it places early humans in Mesoamerica at least 17,000 years ago.

Note that the calculation in Example 11-28 assumes that the ^{14}N concentration in the atmosphere and the cosmic ray intensity 17,000 years ago were essentially the same as they are today. Actually, neither has remained unchanged over that period. Accurate ^{14}C measurements must include corrections for (1) the variations of Earth's magnetic field, which affects the cosmic ray intensity, and (2) the changing composition of the atmosphere, which depends on global geological and chemical activity and on the average temperature of the atmosphere. For example, current evidence suggests that just prior to 9000 years ago, the $^{14}C/^{12}C$ ratio was about 1.5 times as large as the current value. The ratio has also been significantly altered over the past century by the burning of fossil fuels, which adds ^{14}C-free carbon to the atmosphere, and by atmospheric testing of hydrogen weapons, which added ^{14}C during the 1950s. Accelerator mass spectrometry, which was originally developed for just this purpose, makes possible determination of the $^{14}C/^{12}C$ ratio with sufficient accuracy to extend the applicability of ^{14}C dating back 50,000 years before the present with samples as small as a few milligrams. Calibration of the ratio for earlier periods requires cross-dating with other methods, such as U-Th dating.

Dating Ancient Rocks Starting with Equation 11-18, a useful relation can be derived for the age of a sample that initially contains N_0 radioactive parent nuclei that decay to a stable daughter with a half-life $t_{1/2}$. Assuming there are no daughter nuclei present initially, after a time t has elapsed, there will be N_P parent nuclei and N_D daughter nuclei in the sample. From Equation 11-18,

$$t = \frac{1}{\lambda} \ln\left(\frac{N_0}{N_P}\right) = \frac{t_{1/2}}{\ln 2} \ln\left(\frac{N_0}{N_P}\right) \qquad \textbf{11-91}$$

Since $N_P + N_D = N_0$ at any time, Equation 11-91 can be written as

$$t = \frac{t_{1/2}}{\ln 2} \ln\left(1 + \frac{N_D}{N_P}\right) \qquad \textbf{11-92}$$

where N_D/N_P is the isotopic ratio at age t.

STUDENTS-HUB.com Uploaded By: Malak Obaid

Several isotopic abundance ratios are used as "rock clocks" for samples of geologic age. These include $^{238}U/^{206}Pb$, $^{87}Rb/^{87}Sr$, $^{40}K/^{40}Ar$, and the dual ratio $^{238}U/^{234}U/^{230}Th$. These have been used to determine the age of Earth rocks, Moon rocks, meteorites, and, by inference, the solar system itself. The oldest rocks on Earth have been dated at about 4.5×10^9 years. At that time the molten surface froze, fixing the isotopic ratios, which thereafter changed only as a result of decay. Surprisingly, perhaps, all meteorites turn out to be about the same age, 4.5×10^9 years, regardless of their composition or when they collided with Earth. This suggests that they originated in or are the debris of other bodies within the solar system that formed at the same time as Earth. This value for the age of Earth is supported by a number of independent ratio measurements, initially the relative abundances of ^{238}U and ^{235}U and the $^{238}U/^{206}Pb$ ratio and corroborated more recently by measurements of the $^{40}K/^{40}Ar$ and $^{87}Rb/^{87}Sr$ ratios.

EXAMPLE 11-29 $^{87}Rb/^{87}Sr$ **Dating** The $^{87}Rb/^{87}Sr$ ratio for a particular rock is found to be 40.0. How old is the rock?

SOLUTION

Note first that in Equation 11-92, the radioactive parent appears in the denominator of the ratio; therefore, in this case $N_D/N_P = 1/(^{87}Rb/^{87}Sr) = 1/40.0 = 0.025$. Substituting this value and the half-life of ^{87}Rb from Table 11-8 into Equation 11-92, we have

$$t = \frac{4.88 \times 10^{10}\ \text{y}}{\ln 2} \ln(1 + 0.025) = \frac{4.88 \times 10^{10}\ \text{y}}{0.693} \times 0.0247 = 1.74 \times 10^8\ \text{y}$$

This is a young rock, considerably younger than the 4.5×10^9 y age of Earth.

Rocks found on Earth's surface have a range of ages from zero up to 3.7×10^9 years. None are older. In contrast, rocks brought back from the surface of the Moon by Apollo astronauts have ages ranging from 3.1 to 4.5×10^9 years; none are younger. The implications of these results from radioactive dating are (1) Earth surface rocks older than 3.7×10^9 years have weathered, eroded, and been recycled into other rocks or into the mantle and (2) the Moon's internal heat source (gravity and radioactivity) cooled sufficiently to solidify all its material and fix the initial isotopic ratios about 1.5×10^9 years after it was formed. The Earth's internal heat source has not yet reached that point.

Accelerator Mass Spectrometry

Originally developed to extend the usable time span and improve the accuracy of ^{14}C dating of archeological materials, accelerator mass spectrometry (AMS) is an ultrasensitive analytical technique in which the atoms of interest in a sample are counted directly rather than irradiating the sample with slow neutrons, then counting the gamma rays emitted by the radioactive daughter produced or measuring the radiations emitted by long-lived, naturally occurring radionuclides. To understand how AMS works, we will use its application to ^{14}C dating as an illustration. At the present time the $^{14}C/^{12}C$ ratio in living organic material is about 10^{-12}. Thus, a 1-g sample of carbon contains about 5×10^{10} ^{14}C atoms. Since the half-life of ^{14}C is 5730 y, a 1.0-g sample of 20,000-year-old charcoal would emit about one β^- per minute. To record 10,000 decays (the number needed for a statistical accuracy of 1 percent) would require counting for one week and involve only 2×10^{-6} of the ^{14}C atoms present in the sample, a very inefficient method.

STUDENTS-HUB.com Uploaded By: Malak Obaid

Table 11-9 Radioisotopes measurable with AMS

Nuclide	Half-life (y)	Stable isobar	Sensitivity
^{3}H	12.3	^{3}He	10^{-14}
^{10}Be	1.5×10^{6}	^{10}B	10^{-15}
^{14}C	5.730×10^{3}	^{14}N	2×10^{-15}
^{26}Al	7.40×10^{5}	^{26}Mg	10^{-15}
^{36}Cl	3.01×10^{5}	^{36}S	2×10^{-15}
^{41}Ca	1.0×10^{5}	^{41}K	10^{-15}
^{129}I	1.6×10^{7}	^{129}Xe	10^{-14}

Mass spectrometry, which records *every* atom in the sample, provides a possible alternative (see Section 3-1). However, conventional mass spectrometers do not have the capability of measuring isotope ratios at the level of $^{14}C/^{12}C$ (or the other radioisotopes listed in Table 11-9) due to the presence of isobars and molecules with nearly the same mass. In the case of ^{14}C these include ^{14}N from residual air within the spectrometer and $^{12}CH_2$ and ^{13}CH, both from the sample itself or contamination. AMS works in part like a conventional mass spectrometer but reduces background due to mass ambiguities by taking advantage of the operational characteristics of medium-energy accelerators, particularly cyclotrons and tandem van de Graaffs. Using the latter as the basis of our discussion and referring to the photograph and diagram on page 518 and to Figure 11-66, the positive high-voltage terminal is in the middle of the accelerator with the two ends of the beam tube essentially at ground potential. The atoms of the sample are converted to negative ions in the ion source. The atoms of most elements can form stable negative ions, a notable exception being nitrogen. Thus, AMS immediately removes background due to ^{14}N. A bending magnet deflects the ions according to their radii of curvature. The negative ions are accelerated to the positive terminal, where a stripper removes several electrons, forming positive ions. If more than three electrons are removed, most molecules break apart. The ions are then accelerated further (to 50–100 MeV), emerging from the machine into another bending magnet, which effectively removes the molecular fragments that in general do not have the same radii of curvature as do the atomic ions. After passing through another 90° bending magnet that cleans the beam of any residual molecular fragments, the high-energy beam enters the detector, a so-called E-ΔE counting telescope (see

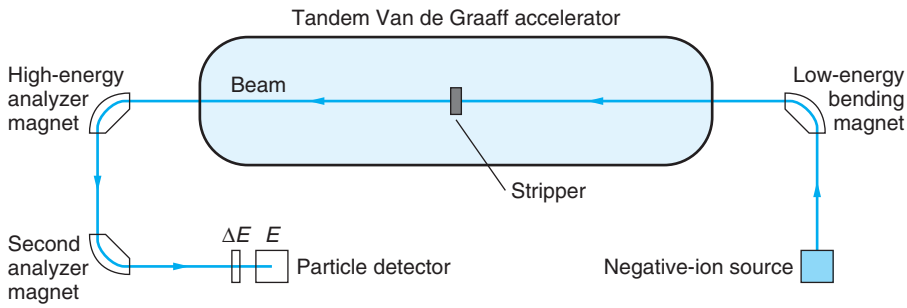

Figure 11-66 Schematic drawing of a tandem Van de Graaff accelerator configured as an accelerator mass spectrometer.

STUDENTS-HUB.com Uploaded By: Malak Obaid

The perfectly preserved mummy of Ötzi the Iceman was found in the Tyrolean Alps in 1991. Accelerator mass spectrometry places his date of death between 3300 and 3200 years B.C. Recent (2003) measurements of oxygen isotopic ratios in his teeth and bones have pinpointed the area where he lived. [© *South Tyrol Museum of Archeology, Italy. www.iceman.it.*]

Figure 11-66). The very thin ΔE detector measures the energy loss by the atoms, which for particles with the same energy is approximately proportional to Z^2, thus rejecting atoms with a different atomic number than that of interest. The high-energy ions are then stopped in the E detector, which measures the energy of each one. The product $E \times \Delta E$ for each atom is approximately proportional to mZ^2. Thus, requiring sample masses of only a few milligrams, AMS measures the mass and atomic number of each atom, and it does so with very high precision and extremely low background.

Table 11-9 lists several long-lived radioisotopes that can be effectively assayed with AMS. For example, the technique has been used to time the migration of surface water into deep aquifers by measuring the concentration of ^{36}Cl, produced by cosmic ray bombardment of argon in the atmosphere. Using only a few strands, AMS ^{14}C-dated the famous Shroud of Turin as having been made in the Middle Ages, around 1300. Ötzi (the Iceman) discovered in 1991 in the Tyrolean Alps, was found to have lived during the late Neolithic age, about 5200 years ago. Some meteorites have been found to contain relatively short-lived ^{26}Al in excess of the concentration attributable to cosmic ray production, raising the intriguing question of its origin in the cosmos.

Particle-Induced X-ray Emission

An elemental analysis technique similar to neutron activation analysis (NAA), particle-induced x-ray emission (PIXE) involves bombarding the material of interest with low-energy (a few MeV) ions, such as protons or alpha particles. Coulomb interaction between the ions and the target atoms ionize the latter by ejecting K- or L-shell electrons. Since the interactions occur over atomic dimensions, the cross sections are quite high, as much as 1000 b for low-Z atoms, decreasing smoothly to about 1 b at $Z = 82$ (Pb). The vacancies produced are quickly filled by electrons from higher-energy shells, emitting K and L x rays or Auger electrons in the process that are characteristic of the elements in the target (see Section 4-4). Since the bombarding particles are relatively low energy, they do not penetrate far into matter, so the interactions occur near the surface. That fact, together with the low energy of the emitted x rays, 10 to 100 keV, dictates the use of thin samples. Figure 11-67*a* is a schematic of a typical PIXE experimental arrangement. The sensitivity of PIXE is comparable to NAA and has the advantage of being applicable to all elements above $Z = 20$, whereas NAA is restricted to those nuclides with sufficiently large thermal neutron absorption cross sections. The main disadvantage of PIXE is x-ray energy ambiguities. For example, the energy of the L_α x ray from Pb is 10.55 keV, while that of the K_α line of As is 10.54 keV. The resolution of the cooled Si(Li) detectors used for x rays is about 100 eV, insufficient to resolve the two lines. Figure 11-67*b* shows a typical PIXE spectrum.

STUDENTS-HUB.com Uploaded By: Malak Obaid

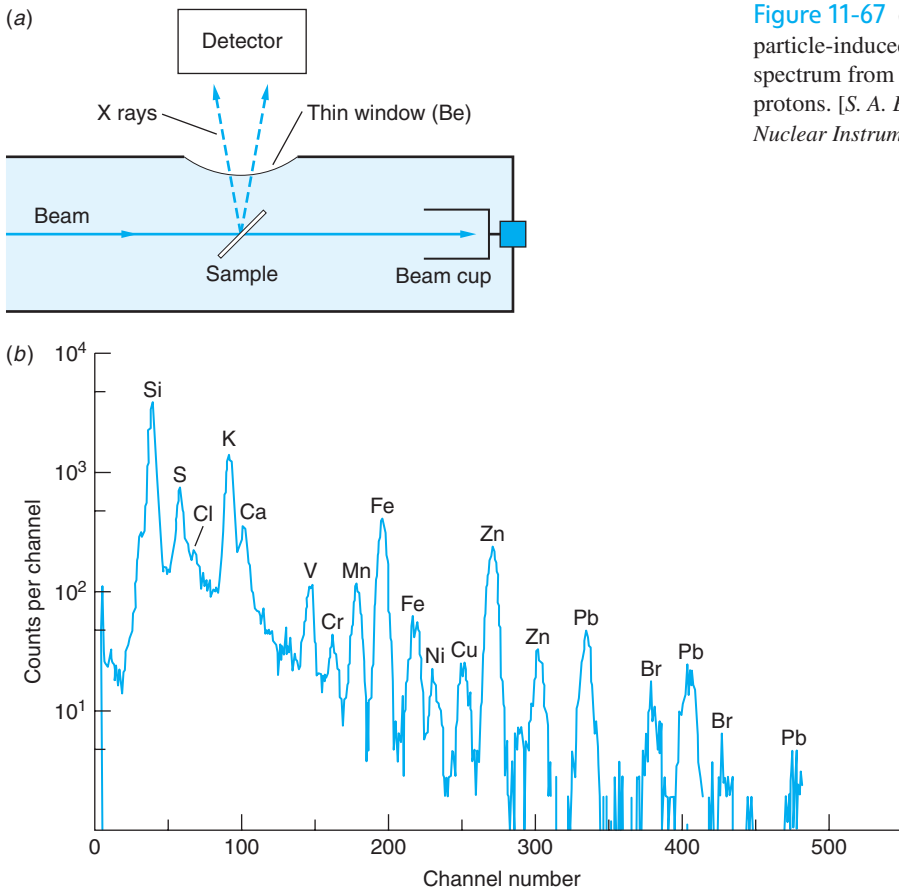

Figure 11-67 (*a*) Schematic drawing of a typical particle-induced x-ray emission system. (*b*) PIXE spectrum from an aerosol bombarded with 2-MeV protons. [*S. A. E. Johansson and T. B. Johansson, Nuclear Instruments and Methods, 137, 473, 1976.*]

Questions

20. If the $^{14}C/^{12}C$ ratio was 1.5 times larger than that used in Example 11-28, is the calculated age too large or too small? Explain.
21. Some meteorites are found to contain measurable amounts of ^{26}Al, whose $t_{1/2}$ is only 7.4×10^5 years. Devise a scenario that would account for its presence.
22. ^{40}Ar is a gas at ordinary temperatures. Explain why solid rocks can be accurately dated using the $^{40}K/^{40}Ar$ ratio in spite of that fact.
23. Explain why accelerator mass spectrometry can achieve reliable results using samples of only 1 mg.

More

The biological effects of ionizing radiation were largely unknown in the early days of atomic and nuclear physics. It took such things as the plight of the radium-watch dial painters, x-ray crystallographers with missing fingertips, and young cyclotron physicists with cataracts to focus scientific attention on the risks that attend exposure to ionizing radiation in the home, the workplace, and the environment. Questions of *Radiation Dosage*, its definition, origin, and effects, are discussed on the home page: www.whfreeman.com/tiplermodernphysics5e. See also Equations 11-93 through 11-95 here, as well as Tables 11-10 through 11-13.

STUDENTS-HUB.com Uploaded By: Malak Obaid

Summary

TOPIC	RELEVANT EQUATIONS AND REMARKS
1. The composition of the nuclei	Nuclei have Z protons, N neutrons, and mass number $A = Z + N$. Nuclei with the same Z but different N (and A) are called isotopes. The nucleons are Fermi-Dirac (spin 1/2) particles and both have intrinsic magnetic moments.
2. Ground-state properties of nuclei	
Size and shape	The mean radius of the nuclear charge distribution is $R = (1.07 \pm 0.02)A^{1/3}$ fm **11-5** The radii thus vary from about 1 fm for the proton to about 10 fm for the heaviest nuclei. With few exceptions, nuclei are nearly spherical.
Binding energy and mass	The binding energy of the nucleus is given by $B_{\text{nuclear}} = ZM_{\text{H}}c^2 + Nm_nc^2 - M_Ac^2$ **11-11**
Magnetic moments	The moments of the proton and neutron are $(\mu_p)_z = +2.79285\ \mu_N$ $(\mu_n)_z = -1.91304\ \mu_N$ where $\mu_N = e\hbar/2m_p$ is the nuclear magneton.
3. Radioactivity	The decay rate R of radioactive nuclei is $R = -\frac{dN}{dt} = \lambda N_0 e^{-\lambda t} = R_0 e^{-\lambda t}$ **11-19** where λ is the decay constant. N_0 and R_0 are the number of nuclei present and the decay rate at $t = 0$.
Half-life	$t_{1/2} = \frac{\ln 2}{\lambda} = 0.693\tau$ **11-22** where $\tau = 1/\lambda$ is the mean life.
Units	1 decay/s = 1 becquerel = 1 Bq **11-23**
4. Alpha, beta, and gamma decay	These are the three most common forms of radioactive decay. Alpha particles are ^{4}He nuclei, beta particles are electrons and positrons, and gamma rays are very short wavelength electromagnetic radiation.
5. The nuclear force	The nuclear force is (*a*) About 10^2 stronger than the Coulomb force (*b*) Short-range (≈ 0 beyond 3 fm) (*c*) Charge independent (*d*) Saturated (*e*) Dependent on spin orientation The nuclear force is considered to be an exchange force in which the attraction between a pair of nucleons is due to an exchange of virtual pions. The range R of the force, determined by the uncertainty principle, is $R = c\,\Delta t = c\hbar/\Delta E = \hbar/mc$ **11-50** where m is the mass of the virtual pion.

STUDENTS-HUB.com Uploaded By: Malak Obaid

TOPIC	RELEVANT EQUATIONS AND REMARKS
6. The shell model	An independent particle model, similar to that used for assigning energy states to the atomic electrons, but one that makes use of a strong spin-orbit coupling for each nucleon accounts for the shell-like structure of the protons and neutrons. It explains the magic numbers 2, 8, 20, 28, 50, 82, and 126 in terms of the completion of the shells. Shell-model calculations are relatively successful in predicting nuclear spins and magnetic moments, particularly in the vicinity of closed shells.
7. Nuclear reactions	The Q value of a reaction X(x, y)Y determines if energy is released or must be supplied. Q is given by $$Q = (m_x + m_X - m_y - m_Y)c^2 \quad \textbf{11-58}$$
Cross section	The cross section σ measures the effective size of a nucleus for a particular nuclear reaction. $$\sigma = \frac{R}{I} \quad \textbf{11-62}$$ where R is the number of reactions per unit time per nucleus and I is the incident particle intensity.
8. Fission and fusion	Fission is the process by which heavy elements such as ^{235}U and ^{239}Pu capture a neutron and split into two medium-mass nuclei. Each event releases about 1 MeV/nucleon. Fusion is the reaction in which two light nuclei, such as ^{2}H and ^{3}H, fuse together to produce a heavier nucleus. Each event releases 1 to 4 MeV/nucleon.
9. Applications	The applications of nuclear reactions in medicine include the use of nuclear radiation in the treatment of diseases and the use of nuclear-based imaging techniques in diagnosis and research. Nuclear magnetic resonance imaging (MRI) is an alternative to x-ray imaging with the advantage that the RF photons involved produce little damage to biological tissue. Computer-assisted tomography using short-lived positron emitters (PET) provides rapid, three-dimensional images. Radioactive dating employs a number of naturally occurring radioisotopes to determine the age of rocks and artifacts. Accelerator mass spectrometry and neutron activation analysis are highly sensitive means of measuring the concentration of particular isotopes of nearly every element in the periodic table.

General References

The following general references are written at a level appropriate for the readers of this book.

Beyer, R. (ed.), *Foundations of Nuclear Physics*, Dover, New York, 1949. This paperback contains 13 original papers, eight in English—by Anderson, Chadwick, Cockroft and Walton, Fermi, Lawrence and Livingston, Rutherford (two papers), and Yukawa—the others are in German or French.

Biological Effects of Ionizing Radiation (*BEIR III*), National Academy of Sciences/National Research Council, Washington, D.C., 1988.

Das, A., and T. Ferbil, *Introduction to Nuclear and Particle Physics*, Wiley, New York, 1994.

Fermi, E., *Nuclear Physics*, rev. ed., University of Chicago Press, Chicago, 1974.

Frauenfelder, H., *The Mössbauer Effect*, W. A. Benjamin, New York, 1962.

STUDENTS-HUB.com Uploaded By: Malak Obaid

Frauenfelder, H., and E. M. Henley, *Subatomic Physics*, 2d ed., Prentice-Hall, Englewood Cliffs, N.J., 1991.

Krane, K. S., *Introductory Nuclear Physics*, Wiley, New York, 1987.

Lilley, J., *Nuclear Physics: Principles and Applications*, Wiley, Chichester, UK, 2001.

Mayer, M., and J. H. D. Jensen, *Elementary Theory of Nuclear Shell Structure*, Wiley, New York, 1955.

Nero, A. V., Jr., *A Guidebook to Nuclear Reactors*, University of California Press, Berkeley, 1979.

Priest, J., *Energy: Principles, Problems, and Alternatives*, 5th ed., Kendall/Hunt, Dubuque, Iowa, 2000.

Segrè, E., *Nuclei and Particles,* 2d ed., Benjamin Cummings, Menlo Park, Calif., 1977.

Walecka, J. D., *Theoretical Nuclear and Subnuclear Physics*, 2d ed., Imperial College Press/World Scientific, London, 2004. Part 1 is appropriate reading for this chapter.

Notes

1. Antoine Henri Becquerel (1852–1908), French physicist. He held the scientific post at the Museum of Natural History in Paris that had been held by his father and grandfather before him, and his research on the fluorescence of potassium uranyl sulfate was a continuation of work that his father had begun. His discovery of radioactivity, which revolutionized existing theories of atomic structure, earned him a share of the 1903 Nobel Prize in Physics, together with Marie and Pierre Curie.

2. The phenomenon was named *radioactivity* by Marie Curie in 1898.

3. These accomplishments were of such importance to the development of nuclear physics that all four men were subsequently awarded the Nobel Prize, James Chadwick in 1935, Carl Anderson in 1936 (shared with Victor Hess, the discoverer of cosmic rays), and John Cockcroft and Ernest Walton in 1951.

4. The United States produced about 30 percent of the world's nuclear-generated electric power in 2005.

5. The term *tomography* is from the Greek *tomos*, meaning "slice," and *graphé*, meaning "picture." Thus, a tomograph is the pictorial representation of a slice through the object or body being studied.

6. Robert Hofstadter (1915–1990), American physicist. His electron-scattering measurements also revealed that the proton and neutron possessed internal structure, opening the way to a more fundamental understanding of the structure of matter. For his work he shared the 1961 Nobel Prize in Physics with Rudolf Mössbauer.

7. See, for example, Section 23-2 in P. A. Tipler and G. Mosca, *Physics for Scientists and Engineers*, 6th ed., W. H. Freeman and Co., New York, 2008.

8. See, for example, Section 26-2 in P. A. Tipler and G. Mosca, *Physics for Scientists and Engineers*, 6th ed., W. H. Freeman and Co., New York, 2008.

9. See P. A. Seeger, *Nuclear Physics*, **25**, 1 (1961).

10. The electric quadrupole moment of the nucleus, discussed earlier in this section, also causes hyperfine splitting, as do externally applied magnetic and electric fields. The effect of the reduced mass (isotope effect) mentioned in Chapter 4 is also considered a hyperfine effect.

11. Actually, the electron's magnetic moment deviates slightly from that predicted by the Dirac wave equation, one Bohr magneton. Quantum electrodynamics is able to account for the small deviation observed experimentally with an error of less than 1 part in 10^8, one of the most remarkable agreements between quantum theory and experiment in physics.

12. This statement requires a small qualification. An alternative to β^+ decay, discussed in Section 11-4, is electron capture, in which an orbital electron may be captured by the nucleus. The probability of its occurrence depends on the probability density of the electrons, which can be affected slightly by very high external pressures.

13. Leptons include the electrons and neutrinos that are emitted in β decay. (See Chapter 12.)

14. Rudolf Ludwig Mössbauer (b. 1929), German physicist. His discovery of the recoilless emission and absorption of gamma rays, made while he was a graduate student in Munich, made possible the verification (by R. V. Pound and G. A. Rebka in 1960) of the gravitational red shift predicted by general relativity. Mössbauer shared the 1961 Nobel Prize in Physics with Robert Hofstadter.

15. Note that this electrostatic potential corresponds to a force of nearly 60 N, or the weight of a 6-kg mass! It is acting not on 6 kg, however, but on only 1.67×10^{-27} kg.

16. Hideki Yukawa (1907–1981), Japanese physicist. His paper presenting the exchange meson theory of the nuclear force was his first publication. He was awarded the 1949 Nobel Prize in Physics for the discovery.

17. See, for example, Section 30-3 in P. A. Tipler and G. Mosca, *Physics for Scientists and Engineers*, 6th ed., W. H. Freeman and Co., New York, 2008.

18. Previously unknown particles had been observed in cosmic rays at about the same time that Yukawa proposed the meson exchange theory. He sent an article to the journal *Nature* in 1937 suggesting that they might be the mesons, but the journal rejected the article. Those particles were later found to be muons, a product of the decay of Yukawa's pi mesons.

19. Maria Goeppert-Mayer (1906–1972), German-American physicist, and Johannes Hans Daniel Jensen (1907–1973), German physicist. Goeppert-Mayer's antecedents for many generations had been university professors, while Jensen was the son of a gardener. They co-authored a famous (among physicists, at least) book explaining their nuclear-shell model and for that work shared the 1963 Nobel Prize in Physics with Eugene Wigner.

STUDENTS-HUB.com Uploaded By: Malak Obaid

20. In *j-j* coupling the spin and orbital angular momentum of each particle add to give a total angular momentum **j** for that particle, and then **J** equals the sum of the individual *j* vectors. In L-S coupling the spins of all the particles and the orbital angular momenta of all the particles add to yield total **S** and total **L**, which then add to yield **J**.

21. This dependence, which occurs only for (n, γ) reactions with relatively low-energy neutrons, was first measured by Emilio Segrè in 1935.

22. The first such resonance was observed unexpectedly in the results of a neutron irradiation of silver conducted by Edoardo Amaldi and others on the morning of October 22, 1934. By 3:00 p.m. that day, Enrico Fermi had developed the correct explanation of the strange phenomenon. The paper describing the discovery was written that evening and delivered to the scientific journal *Ricerca Scientifica* the next morning, less than 24 hours after the discovery!

23. Otto Hahn (1879–1968), German physical chemist, and Fritz Stassmann (1902–1980), German chemist. Hahn recognized that uranium nuclei bombarded with neutrons were breaking apart but carefully avoided characterizing the event as fission since no such thing had been recorded before. He received the 1944 Nobel Prize in Chemistry for the discovery.

24. Actually, Fermi's reactor was the first *constructed* fission reactor. About 2 billion years ago several deposits of natural uranium located in what is now Gabon, West Africa, began chain reactions that continued for 150 million years at an average power of 100 kW before naturally shutting themselves off. The evidence that verified the discovery of the first of these, a fascinating example of scientific detective work, can be found in G. A. Cowan, "A Natural Fission Reactor," *Scientific American*, July 1976. The sites are being mined, and efforts to preserve one of the natural reactors as an international historic site are currently under way.

25. An elementary discussion of a magnetic bottle can be found in Section 26-2 in P. A. Tipler and G. Mosca, *Physics for Scientists and Engineers*, 6th ed., W. H. Freeman and Co., New York, 2008.

26. Godfrey Hounsfield (1919–2004), English engineer, and Allan Cormack (1924–1998), American physicist. They shared the 1979 Nobel Prize in Medicine for the invention of the CT scanner.

27. The radiocarbon-dating technique was developed by Willard F. Libby (1908–1980), an American chemist. He received the 1960 Nobel Prize in Chemistry for his work.

Problems

Level I

Section 11-1 The Composition of the Nucleus

11-1. What are the number of protons and the number of neutrons in each of the following isotopes? ^{18}F, ^{25}Na, ^{51}V, ^{84}Kr, ^{120}Te, ^{148}Dy, ^{175}W, and ^{222}Rn.

11-2. Electrons emitted in β decay have energies of the order of 1 MeV or smaller. Use this fact and the uncertainty principle to show that electrons cannot exist inside the nucleus.

11-3. The spin of the ground state of ^{6}Li, which constitutes 7.5 percent of natural lithium, is zero. Show that this value is not compatible with a model of the nucleus that consists of protons and electrons.

11-4. The magnetic moment of ^{14}N is 0.4035 μ_N. Show that this value is not compatible with a model of the nucleus that consists of protons and electrons.

11-5. Suppose that the deuteron really did consist of two protons and one electron. (It doesn't!) Compute the spin and magnetic moment of such a deuteron's ground state and compare the results with the values in Table 11-1.

Section 11-2 Ground-State Properties of Nuclei

11-6. Give the symbols for at least two isotopes and two isotones of each of the following nuclides: (*a*) ^{18}F, (*b*) ^{208}Pb, and (*c*) ^{120}Sn.

11-7. Give the symbols for at least two isobars and one isotope of each of the following nuclides: (*a*) ^{14}O, (*b*) ^{63}Ni, and (*c*) ^{236}Np.

11-8. Approximating the mass of a nucleus with mass number A as $A \times$ u and using Equation 11-3, compute the nuclear density in SI units.

11-9. Use the masses in the table in Appendix A to compute the total binding energy and the binding energy per nucleon of the following nuclides: (*a*) ^{9}Be, (*b*) ^{13}C, and (*c*) ^{57}Fe.

11-10. Use Equation 11-3 to compute the radii of the following nuclei: (*a*) ^{16}O, (*b*) ^{56}Fe, (*c*) ^{197}Au, and (*d*) ^{238}U.

STUDENTS-HUB.com Uploaded By: Malak Obaid

11-11. Find the energy needed to remove a neutron from (*a*) ^{4}He, (*b*) ^{7}Li, and (*c*) ^{14}N.
11-12. Use the Weizsäcker formula to compute the mass of ^{23}Na. Compute the percent difference between the result and the value in the table in Appendix A.
11-13. Compute the "charge distribution radius" from Equation 11-5 and the "nuclear force radius" from Equation 11-7 for the following nuclides: (*a*) ^{16}O, (*b*) ^{63}Cu, and (*c*) ^{208}Pb.
11-14. ^{39}Ca and ^{39}K are a mirror pair, ^{39}Ca decaying into ^{39}K. Use Equations 11-1 and 11-2 to compute the radius of ^{40}Ca.

Section 11-3 Radioactivity

11-15. The counting rate from a radioactive source is 4000 counts per second at time $t = 0$. After 10 s, the counting rate is 1000 counts per second. (*a*) What is the half-life? (*b*) What is the counting rate after 20 s?
11-16. A certain source gives 2000 counts per second at time $t = 0$. Its half-life is 2 min. (*a*) What is the counting rate after 4 min? (*b*) After 6 min? (*c*) After 8 min?
11-17. A sample of a radioactive isotope is found to have an activity of 115.0 Bq immediately after it is pulled from the reactor that formed it. Its activity 2 h 15 min later is measured to be 85.2 Bq. (*a*) Calculate the decay constant and the half-life of the sample. (*b*) How many radioactive nuclei were there in the sample initially?
11-18. The half-life of radium is 1620 years. (*a*) Calculate the number of disintegrations per second of 1 g of radium and show that the disintegration rate is approximately 1 Ci. (*b*) Calculate the approximate energy of the α particle in the decay $^{226}\text{Ra} \rightarrow {}^{222}\text{Rn} + \alpha$, assuming the energy of recoil of the Rn nucleus is negligible. (Use the mass table of Appendix A.)
11-19. The counting rate from a radioactive source is 8000 counts per second at time $t = 0$. Ten minutes later the rate is 1000 counts per second. (*a*) What is the half-life? (*b*) What is the decay constant? (*c*) What was the counting rate after 1 minute?
11-20. The counting rate from a radioactive source is measured every minute. The resulting numbers of counts per second are 1000, 820, 673, 552, 453, 371, 305, 250, . . . (*a*) Plot the counting rate versus time and (*b*) use your graph to estimate the half-life. (*c*) What would be the approximate result of the next measurement after the 250 counts per second?
11-21. ^{62}Cu is produced at a constant rate [e.g., by the (γ, n) reaction on ^{63}Cu placed in a high-energy x-ray beam] and decays by β^+ decay with a half-life of about 10 min. How long does it take to produce 90 percent of the equilibrium value of ^{62}Cu?
11-22. The decay constant of ^{235}U is 9.8×10^{-10} y^{-1}. (*a*) Compute the half-life. (*b*) How many decays occur each second in a 1.0-μg sample of ^{235}U? (*c*) How many ^{235}U atoms will remain in the 1.0-μg sample after 10^6 years?
11-23. The decay constant of ^{22}Na is 0.266 y^{-1}. (*a*) Compute the half-life. (*b*) What is the activity of a sample containing 1.0 g of ^{22}Na? (*c*) What is the activity of the sample after 3.5 years have passed? (*d*) How many ^{22}Na atoms remain in the sample at the time?

Section 11-4 Alpha, Beta, and Gamma Decay

11-24. The stable isotope of sodium is ^{23}Na. What kind of radioactivity would you expect of (*a*) ^{22}Na and (*b*) ^{24}Na?
11-25. Using Figure 11-16, find the parameters A and B in Equation 11-30.
11-26. Make a diagram like Figure 11-18 for the $(4n + 1)$ decay chain that begins with ^{237}Np, a nuclide that is no longer present in nature. (Use Appendix A.)
11-27. Show that the α particle emitted in the decay of ^{232}Th carries away 4.01 MeV, or 98 percent, of the total decay energy.
11-28. ^{7}Be decays exclusively by electron capture to ^{7}Li with a half-life of 53.3 d. Would the characteristics of the decay be altered and, if so, how if (*a*) a sample of ^{7}Be were placed under very high pressure or (*b*) all four electrons were stripped from each ^{7}Be atom in the sample?
11-29. Compute the energy carried by the neutrino in the electron capture decay of ^{67}Ga to the ground state of ^{67}Zn.
11-30. Compute the maximum energy of the β^- particle emitted in the decay of ^{72}Zn.
11-31. In Example 11-13 we saw that ^{233}Np could decay by emitting an α particle. Show that decay by emission of a nucleon of either type is forbidden for this nuclide.

STUDENTS-HUB.com Uploaded By: Malak Obaid

11-32. With the aid of Figures 11-19 and 11-20, list the energies of all of the possible γ rays that may be emitted by ^{223}Ra following the α decay of ^{227}Th.
11-33. ^{8}Be is very unusual among low-Z nuclides; it decays by emitting two α particles. Show why ^{8}Be is unstable toward α decay.
11-34. ^{80}Br can undergo all three types of β decay. (*a*) Write down the decay equation in each case. (*b*) Compute the decay energy for each case.

Section 11-5 The Nuclear Force

11-35. Assuming that the average separation between two protons in ^{12}C is equal to the nuclear diameter, compute the Coulomb force of repulsion and the gravitational force of attraction between the protons. If the nuclear potential seen by the protons is 50 MeV for separations up to 3 fm, compare the nuclear force to the other two forces.
11-36. Suppose the range of the nuclear force was 5 fm. Compute the mass (in MeV/c^2) of an exchange particle that might mediate such a force.
11-37. The repulsive force that results in the "hard core" of the nucleus might be due to the exchange of a particle, just as the strong attractive force is. Compute the mass of such an exchange particle if the range of the repulsive force equals about 0.25 fm, the radius of the core.

Section 11-6 The Shell Model

11-38. The nuclei listed below have filled j shells plus or minus one nucleon. (For example, $^{29}_{14}$Si has the $1d_{5/2}$ shell filled for both neutrons and protons, plus one neutron in the $2s_{5/2}$ shell.) Use the shell model to predict the orbital and total angular momentum of these nuclei:

$$^{29}_{14}\text{Si} \quad ^{37}_{17}\text{Cl} \quad ^{71}_{31}\text{Ga} \quad ^{59}_{27}\text{Co} \quad ^{73}_{32}\text{Ge} \quad ^{33}_{16}\text{S} \quad ^{87}_{38}\text{Sr}$$

11-39. Use the shell model to predict the nuclear magnetic moments of the isotopes listed in Problem 11-38.
11-40. The atomic spectral lines of ^{14}N exhibit a hyperfine structure, indicating that the ground state is split into three closely spaced levels. What must be the spin of the ^{14}N ground state?
11-41. Which of the following nuclei have closed neutron shells: ^{36}S, ^{50}V, ^{50}Ca, ^{53}Mn, ^{61}Ni, ^{82}Ge, ^{88}Sr, ^{93}Ru, ^{94}Ru, ^{131}In, and ^{145}Eu?
11-42. Sketch diagrams like Figure 11-9 for the ground states of ^{3}H, ^{3}He, ^{14}N, ^{14}C, ^{15}N, ^{15}O, and ^{16}O.
11-43. Which of the following nuclei have closed proton shells: ^{3}He, ^{19}F, ^{12}C, ^{40}Ca, ^{50}Ti, ^{56}Fe, ^{60}Ni, ^{60}Cu, ^{90}Zr, ^{124}Sn, ^{166}Yb, and ^{204}Pb?
11-44. (*a*) Use Figure 11-35 to draw a diagram like Figure 11-9 for ^{13}N. (*b*) What value would you predict for the value of j? (*c*) What value would you predict for j for the first excited state? (*d*) Draw a diagram like Figure 11-9 for the first excited state. (Is there only one possible?)
11-45. Use Figure 11-35 to predict the values of j for the ground states of ^{30}Si, ^{37}Cl, ^{55}Co, ^{90}Zr, and ^{107}In.

Section 11-7 Nuclear Reactions

11-46. Using data from Appendix A, find the Q values for the following reactions: (*a*) $^{2}\text{H} + {}^{2}\text{H} \rightarrow {}^{3}\text{H} + {}^{1}\text{H} + Q$, (*b*) $^{3}\text{He}(d,p)^{4}\text{He}$, and (*c*) $^{6}\text{Li} + n \rightarrow {}^{3}\text{H} + {}^{4}\text{He} + Q$.
11-47. (*a*) Find the Q value for the reaction $^{3}\text{H} + {}^{1}\text{H} \rightarrow {}^{3}\text{He} + n + Q$. (*b*) Find the threshold for this reaction if stationary ^{1}H nuclei are bombarded with ^{3}H nuclei from an accelerator. (*c*) Find the threshold for this reaction if stationary ^{3}H nuclei are bombarded with ^{1}H nuclei from an accelerator.
11-48. What is the compound nucleus for the reaction of deuterons on ^{14}N? What are the possible product nuclei and particles for this reaction?
11-49. Using data from Appendix A, compute the Q value for the reaction (*a*) $^{12}\text{C}(\alpha,p)^{15}\text{N}$, and (*b*) $^{16}\text{O}(p,d)^{17}\text{O}$.
11-50. The cross section for the reaction $^{75}\text{As}(n,\gamma)^{76}\text{As}$ is 4.5 b for thermal neutrons. A sample of natural As in the form of a crystal 1 cm × 2 cm that is 30 μm thick is exposed to a thermal neutron flux of 0.95×10^{13} neutrons/cm$^2 \cdot$s. Compute the rate at which this reaction proceeds. (Natural arsenic is 100% ^{75}As. Its density is 5.73 g/cm^3.)

STUDENTS-HUB.com Uploaded By: Malak Obaid

11-51. Write three different reactions that could produce the products (*a*) $n + {}^{23}\text{Na}$, (*b*) $p + {}^{14}\text{C}$, and (*c*) $d + {}^{31}\text{P}$.

11-52. Write down the correct symbol for the particle or nuclide represented by the x in the following reactions: (*a*) ${}^{14}\text{N}(n, p)\,x$; (*b*) ${}^{208}\text{Pb}\,(n, x){}^{208}\text{Pb}$; (*c*) $x(\alpha, p){}^{61}\text{Cu}$; (*d*) ${}^{9}\text{Be}(x, n){}^{12}\text{C}$; (*e*) ${}^{16}\text{O}(d, \alpha)x$; (*f*) ${}^{162}\text{Dy}(\alpha, 6n)x$; (*g*) $x(d, n){}^{4}\text{He}$; (*h*) ${}^{90}\text{Zr}(d, x){}^{91}\text{Zr}$.

Section 11-8 Fission and Fusion

11-53. A few minutes after the Big Bang the first fusion reaction occurred in the early universe. It was $n + p \rightarrow d + \gamma$. Compute the Q for this reaction.

11-54. Assuming an average energy release of 200 MeV per fission, calculate the number of fissions per second needed for a 500-MW reactor.

11-55. If the reproduction factor of a reactor is $k = 1.1$, find the number of generations needed for the power level to (*a*) double, (*b*) increase by a factor of 10, and (*c*) increase by a factor of 100. Find the time needed in each case if (*d*) there are no delayed neutrons, so the time between generations is 1 ms, and (*e*) there are delayed neutrons that make the average time between generations 100 ms.

11-56. Write down the several reactions possible when ${}^{235}\text{U}$ captures a thermal neutron and $1n$, $2n$, $3n$, or $4n$ is produced.

11-57. Assuming an average energy release of 17.6 MeV/fusion, calculate the rate at which ${}^{2}\text{H}$ must be supplied to a 500-MW fusion reactor.

11-58. From Figure 11-52, the cross section for the capture of 1.0-MeV neutrons by ${}^{238}\text{U}$ is 0.02 b. A 5-gm sample of ${}^{238}\text{U}$ is exposed to a total flux of 1.0-MeV neutrons of 5.0×10^{11} per m^2. Compute the number of ${}^{239}\text{U}$ atoms produced.

11-59. Compute the total energy released in the following set of fusion reactions. This is the proton-proton cycle, the primary source of the sun's energy.

$$
\begin{aligned}
{}^{1}\text{H} + {}^{1}\text{H} &\longrightarrow {}^{2}\text{H} + e^{+} + \nu_e \\
{}^{2}\text{H} + {}^{1}\text{H} &\longrightarrow {}^{3}\text{He} + \gamma \\
{}^{3}\text{He} + {}^{3}\text{He} &\longrightarrow {}^{4}\text{He} + 2\,{}^{1}\text{H} + \gamma
\end{aligned}
$$

11-60. A particular nuclear power reactor operates at 1000 MWe (megawatts electric) with an overall efficiency in converting fission energy to electrical energy of 30 percent. What mass of ${}^{235}\text{U}$ must fission in order for the power plant to operate for (*a*) one day, (*b*) one year? (*c*) If the energy were provided by burning coal instead of ${}^{235}\text{U}$, what would be the answers to (*a*) and (*b*)? (Burning coal produces approximately 3.15×10^7 J/kg.)

11-61. (*a*) Assuming that the natural abundance of deuterium given in Appendix A is reflected in the formation of water molecules, compute the energy that would be released if all the deuterons in 1.0 m^3 of water were fused via the reaction ${}^{2}\text{H} + {}^{1}\text{H} \rightarrow {}^{3}\text{He} + \gamma$. (*b*) Given that the world's 5.9×10^9 people used 3.58×10^{20} J in 1999, how long (in hours) would the result in part (*a*) have lasted a "typical" person?

11-62. Consider the possible fission reaction

$$n + {}^{235}_{92}\text{U} \longrightarrow {}^{120}_{48}\text{Cd} + {}^{112}_{44}\text{Ru} + 3n$$

(*a*) Compute the energy released in the reaction. (*b*) Is this reaction likely to occur? Explain.

Section 11-9 Applications

11-63. A bone claimed to be 10,000 years old contains 15 g of carbon. What should the decay rate of ${}^{14}\text{C}$ be for this bone?

11-64. A sample of animal bone unearthed at an archeological site is found to contain 175 g of carbon, and the decay rate of ${}^{14}\text{C}$ in the sample is measured to be 8.1 Bq. How old is the bone?

11-65. The ${}^{87}\text{Rb}/{}^{87}\text{Sr}$ ratio for a particular rock is measured to be 36.5. How old is the rock?

11-66. In a PIXE experiment, an element with $A = 80$ forms 0.001 percent by weight of a thin foil whose mass is 0.35 mg/cm^2. The foil is bombarded with a 250 nA proton beam for 15 minutes. The cross section for exciting the L shell is 650 b. If the probability that the excited atom will emit an L x ray is 0.60 and the overall efficiency of the x-ray detector is 0.0035, how many counts will the detector record during the 15-minute bombardment?

STUDENTS-HUB.com Uploaded By: Malak Obaid

11-67. The naturally occurring $A = 4n$ decay series begins with ^{232}Th and eventually ends on ^{208}Pb. (See Figure 11-18.) A particular rock is measured to contain 4.11 g of ^{232}Th and 0.88 g of ^{208}Pb. Compute the age of the rock.

11-68. Compute the resonance frequency of free protons in a magnetic field of (*a*) 0.5×10^{-4} T (approximate strength of Earth's field), (*b*) 0.25 T, and (*c*) 0.5 T.

11-69. A small piece of papyrus is to be ^{14}C-dated using AMS. During a 10-minute run with the system set to record ^{14}C, 1500 ions are counted. With the system set to transmit $^{12}C^{+3}$ ions, the beam current is 12 μA. (*a*) Compute the $^{14}C/^{12}C$ ratio, assuming both isotopes are transmitted with the same efficiency. (*b*) If the entire sample is consumed in 75 minutes, what was the mass of ^{12}C it contained? (Assume a constant consumption rate and an efficiency of 0.015. (*c*) How old is the sample?

11-70. A wooden spear found in the mountains of southeastern Spain was found to have ^{14}C activity of 2.05 disintegrations per minute per gram. How old is it? (The ^{14}C activity of live wood is 15.6 disintegrations per minute per gram.)

Level II

11-71. Using Equation 11-14 and the constants in Table 11-3, find the Z for which $dM/dZ = 0$, i.e., the minimum of curves like Figure 11-22*a* for (*a*) A = 27, (*b*) A = 65, and (*c*) A = 139. Do these calculations give the correct stable isobars ^{27}Al, ^{65}Cu, and ^{139}La?

11-72. An empirical expression for distance that α particles can travel in air, called the *range*, is $R(\text{cm}) = (0.31)E^{3/2}$ for E in MeV and $4 < E < 7$ MeV. (*a*) What is the range in air of a 5-MeV α particle? (*b*) Express this range in g/cm^2, using $\rho = 1.29 \times 10^{-3}$ g/cm^3 for air. (*c*) Assuming the range in g/cm^2 is the same as that of aluminum ($\rho = 2.70$ g/cm^3), find the range in aluminum in cm for a 5-MeV α particle.

11-73. Show that the average electrostatic energy of a proton-proton pair is about $6ke^2/5R$, where R is the separation of the pair and $k = 1/4\pi\epsilon_0$.

11-74. A sample of ^{114}Nd has a mass of 0.05394 kg and emits an average of 2.36 α particles per second. Determine the decay constant and the half-life.

11-75. A sample of radioactive material is found initially to have an activity of 115.0 decays/minute. After 4 d 5 h, its activity is measured to be 73.5 decays/minute. (*a*) Calculate the half-life of this material. (*b*) How long (after $t = 0$) will it take for the sample to reach an activity of 10.0 decays/minute? (*c*) How long after the time in (*b*) will it take for the activity to reach 2.5 decays/minute?

11-76. The half-life of ^{227}Th is 18.72 days. It decays by α emission to ^{223}Ra, an α emitter whose half-life is 11.43 days. A particular sample contains 10^6 atoms of ^{227}Th and no ^{223}Ra at time $t = 0$. (*a*) How many atoms of each type will be in the sample at $t = 15$ days? (*b*) At what time will the number of atoms of each type be equal?

11-77. The Mössbauer effect was discovered using the decay of the 0.12939-MeV second excited state of ^{191}Ir. The lifetime of this isomer is 0.13 ns. (*a*) Compute the width Γ of this level. (*b*) Compute the recoil energy of a free ^{191}Ir atom that emits the 0.12939-MeV photon. (*c*) Resonant (recoilless) absorption occurs when ^{191}Ir is bound into a lattice. If a Doppler shift equal to Γ destroys the resonance absorption, show that the Doppler velocity v necessary is given by

$$v \approx \frac{c\Gamma}{e}$$

11-78. ^{3}He and ^{3}H are a pair of mirror nuclei. Compute the difference in total binding energy between the two nuclides and compare the result to the electrostatic repulsion of the protons in ^{3}He. Let the protons be separated by the radius of the helium nucleus.

11-79. Use the masses in Appendix A to compute the energy necessary to separate a neutron from ^{47}Ca and ^{48}Ca. From those results determine a value for a_5 in the Weizsäcker formula (Equation 11-14) and compare it with the value in Table 11-3.

11-80. The centripetal force of a nucleus with $I \neq 0$ makes it more stable toward α decay. Use Figure 11-1*a* and a (classical) argument to show why this is the case.

11-81. (*a*) Calculate the radii of $^{141}_{56}$Ba and $^{92}_{36}$Kr from Equation 11-4. (*b*) Assume that after the fission of ^{235}U into ^{141}Ba and ^{92}Kr, the two nuclei are momentarily separated by a distance r equal to the sum of the radii found in (*a*), and calculate the electrostatic potential energy for these two nuclei at this separation. Compare your result with the measured fission energy of 175 MeV.

STUDENTS-HUB.com Uploaded By: Malak Obaid

11-82. Consider a neutron of mass m moving with speed v_L and colliding head-on with a nucleus of mass M. (*a*) Show that the speed of the center of mass in the lab frame is $V = mv_L/(m + \mathrm{M})$. (*b*) What is the speed of the nucleus in the center-of-mass frame before the collision? After the collision? (*c*) What is the speed of the nucleus in the original lab frame after the collision? (*d*) Show that the energy of the nucleus after the collision is

$$\frac{1}{2}M(2V)^2 = \left[\frac{4mM}{(m + M)^2}\right]\frac{1}{2}mv_L^2$$

and use this to obtain Equation 11-82.

11-83. Suppose that the Van Dyck painting shown in the photographs on page 537 was irradiated with a thermal neutron flux of 10^{12} neutrons/cm$^2 \cdot$ s for 2 h. In terms of the numbers of manganese and phosphorus atoms initially present, determine the activity (*a*) 2 hours and (*b*) 2 days after the irradiation stopped. The (n, γ) cross section for ^{31}P is 0.180 b and for ^{55}Mn is 13.3 b. (Both isotopes are 100 percent of the naturally occurring elements.)

11-84. The total energy consumed in the United States in 1 y is about 7.0×10^{19} J. How many kilograms of ^{235}U would be needed to provide this amount of energy if we assume that 200 MeV of energy is released by each fissioning uranium nucleus, that 3 percent of the uranium atoms undergo fission, and that all of the energy-conversion mechanisms used are 25 percent efficient?

11-85. The rubidium isotope ^{87}Rb is a β emitter with a half-life of 4.9×10^{10} y that decays into ^{87}Sr. It is used to determine the age of rocks and fossils. Rocks containing the fossils of early animals contain a ratio of ^{87}Sr to ^{87}Rb of 0.010. Assuming that there were no ^{87}Sr present when the rocks were formed, calculate the age of these fossils.

11-86. In 1989, researchers claimed to have achieved fusion in an electrochemical cell at room temperature. They claimed a power output of 4 W from deuterium fusion reactions in the palladium electrode of their apparatus. (*a*) If the two most likely reactions are

$$^2\mathrm{H} + {}^2\mathrm{H} \longrightarrow {}^3\mathrm{He} + n + 3.27\ \mathrm{MeV}$$

and

$$^2\mathrm{H} + {}^2\mathrm{H} \longrightarrow {}^3\mathrm{H} + {}^1\mathrm{H} + 4.03\ \mathrm{MeV}$$

with 50 percent of the reactions going by each branch, how many neutrons per second would we expect to be emitted in the generation of 4 W of power? (*b*) If 1/10th of these neutrons were absorbed by the body of an 80.0-kg worker near the device, and if each absorbed neutron carries an average energy of 0.5 MeV with an RBE of 4, to what radiation dose rate in rems per hour would this correspond? (*c*) How long would it take for a person to receive a total dose of 500 rems? (This is the dose that is usually lethal to half of those receiving it.)

11-87. Neutron activation analysis is used to study a small sample of automotive enamel found at the scene of a hit-and-run collision. The sample was exposed to a thermal neutron flux of 3.5×10^{12} neutrons/cm$^2 \cdot$ s for 2.0 minutes. Placed immediately in a gamma-ray detector, it was found to have an activity of 35 Bq due to ^{60}Co and 115 Bq due to ^{51}Ti. Compute the total amount of each metal in the original sample. (The cross section for ^{59}Co is 19 b; that for ^{50}Ti is 0.15 b.)

11-88. A fusion reactor using only deuterium for fuel would have the following two reactions taking place in it:

$$^2\mathrm{H} + {}^2\mathrm{H} \longrightarrow {}^3\mathrm{He} + n + 3.27\ \mathrm{MeV}$$

and

$$^2\mathrm{H} + {}^2\mathrm{H} \longrightarrow {}^3\mathrm{H} + {}^1\mathrm{H} + 4.03\ \mathrm{MeV}$$

The ^{3}H produced in the second reaction reacts immediately with another ^{2}H to produce

$$^3\mathrm{H} + {}^2\mathrm{H} \longrightarrow {}^4\mathrm{He} + n + 17.7\ \mathrm{MeV}$$

The ratio of ^{2}H to ^{1}H atoms in naturally occurring hydrogen is 1.5×10^{-4}. How much energy would be produced from 4 liters of water if all of the ^{2}H nuclei undergo fusion?

11-89. (*a*) Using the Compton-scattering result that the maximum change in wavelength is $\Delta\lambda = 2hc/Mc^2$ and the approximation $\Delta E \approx hc\,\Delta\lambda/\lambda^2$, show that for a photon to lose an amount of energy E_p to a proton, the energy of the photon must be at least $E = [(1/2)Mc^2E_p]^{1/2}$.

STUDENTS-HUB.com Uploaded By: Malak Obaid

(*b*) Calculate the photon energy needed to produce a 5.7-MeV proton by Compton scattering. (*c*) Calculate the energy given a ^{14}N nucleus in a head-on collision with a 5.7-MeV neutron. (*d*) Calculate the photon energy needed to give a ^{14}N nucleus this energy by Compton scattering.

11-90. A photon of energy E is incident on a deuteron at rest. In the center-of-mass reference frame, both the photon and the deuteron have momentum p. Prove that the approximation $p \approx E/c$ is good by showing that the deuteron with this momentum has energy much less than E. If the binding energy of the deuteron is 2.22 MeV, what is the threshold energy in the lab for photodisintegration?

Level III

11-91. (*a*) Compute the binding-energy differences between the two nuclides of the mirror pairs (^{7}Li, ^{7}Be), (^{11}B, ^{11}C), and (^{15}N, ^{15}O). (*b*) From each value computed in (*a*), determine a value of the constant a_3 in Equation 11-14. Compare each value and their average with the value given in Table 11-3.

11-92. (*a*) Differentiate the Weizsäcker empirical mass formula with respect to Z, as in Problem 11-71, and show that the minima of the constant A curves that result, i.e., Z values for the most stable isotopes, are given by

$$Z = \frac{A}{2}\left[\frac{1 + \dfrac{(m_n - m_p)c^2}{4a_4}}{1 + \dfrac{a_3 A^{2/3}}{4a_4}}\right]$$

(*a*) Determine the atomic number for the most stable nuclides for $A = 29$, 59, 78, 119, and 140. (*c*) Compare the results in (*b*) with the data in Appendix A and discuss any differences.

11-93. (*a*) Use Figure 11-35 to make a diagram like Figure 11-9 for the ground state of ^{11}B. What do you predict for the value of j for this state? (*b*) The first excited state of ^{11}B involves excitation of a proton. Draw the diagram for this state and predict its j value. (*c*) The j value for the second excited state is $5/2$. Draw a diagram of the nucleons like Figure 11-9 that could account for that value. (*d*) Repeat parts (*a*) and (*b*) for ^{17}O, where the excitation of the first excited state involves a neutron. (*e*) The j value for the second excited state of ^{17}O is $1/2$. Draw a diagram like Figure 11-9 that would explain that value.

11-94. Approximately 2000 nuclides remain to be discovered between the proton and neutron driplines in Figure 11-15*b*. Consider those that lie on the energy parabola (see Figure 11-22*a*) for $A = 151$, whose only stable isotope is ^{151}Eu. (*a*) From the data in Appendix A, draw an accurate diagram of the $A = 151$ parabola showing known nuclides *and* those yet to be discovered between $Z = 50$ and $Z = 71$. (*b*) Determine where the edges of the driplines lie for $A = 151$, i.e., the lowest mass isotopes for which spontaneous proton or neutron emission becomes possible.

11-95. There are theoretical reasons to expect that a cluster of relatively long-lived nuclides will exist in the neighborhood of the doubly magic nucleus with $Z = 126$ and $N = 184$, the latter being the next magic number beyond 126 predicted by the shell model. (*a*) Compute the mass of this exotic nucleus using Equation 11-14. (*b*) Computing the necessary masses of the nearby nuclei, predict the decay modes that would be available to the doubly magic nucleus.

11-96. Assume that a neutron decays into a proton plus an electron without the emission of a neutrino. The energy shared by the proton and electron is then 0.782 MeV. In the rest frame of the neutron, the total momentum is zero, so the momentum of the proton must be equal and opposite that of the electron. This determines the relative energies of the two particles, but because the electron is relativistic, the exact calculation of these relative energies is somewhat difficult. (*a*) Assume that the kinetic energy of the electron is 0.782 MeV and calculate the momentum p of the electron in units of MeV/c. (*Hint:* Use Equation 2-32.) (*b*) From your result for (*a*), calculate the kinetic energy $p^2/2m_p$ of the proton. (*c*) Since the total energy of the electron plus proton is 0.782 MeV, the calculation in (*b*) gives a correction to the assumption that the energy of the electron is 0.782 MeV. What percentage of 0.782 MeV is this correction?

STUDENTS-HUB.com Uploaded By: Malak Obaid

11-97. Radioactive nuclei with a decay constant of λ are produced in an accelerator at a constant rate R_p. The number of radioactive nuclei N then obeys the equation $dN/dt = R_p - \lambda N$. (*a*) If N is zero at $t = 0$, sketch N versus t for this situation. (*b*) The isotope ^{62}Cu is produced at a rate of 100 per second by placing ordinary copper (^{63}Cu) in a beam of high-energy photons. The reaction is

$$\gamma + {}^{63}\text{Cu} \longrightarrow {}^{62}\text{Cu} + n$$

^{62}Cu decays by β decay with a half-life of 10 minutes. After a time long enough so that $dN/dt \approx 0$, how many ^{62}Cu nuclei are there?

11-98. The $(4n + 3)$ decay chain begins with ^{235}U and ends on ^{207}Pb. (*a*) How many α decays are there in the chain? (*b*) How many β decays are there? (*c*) Compute the total energy released when one ^{235}U atom decays through the complete chain. (*d*) Assuming no energy escapes, determine the approximate temperature rise of 1 kg of ^{235}U metal over the period of 1 year.

11-99. Energy is generated in the Sun and other stars by fusion. One of the fusion cycles, the proton-proton cycle, consists of the following reactions:

$$^1\text{H} + {}^1\text{H} \longrightarrow {}^2\text{H} + \beta^+ + \nu_e$$

$$^1\text{H} + {}^2\text{H} \longrightarrow {}^3\text{He} + \gamma$$

followed by either

$$^3\text{He} + {}^3\text{He} \longrightarrow {}^4\text{He} + {}^1\text{H} + {}^1\text{H}$$

or

$$^1\text{H} + {}^3\text{He} \longrightarrow {}^4\text{He} + \beta^+ + \nu_e$$

(*a*) Show that the net effect of these reactions is

$$4\,{}^1\text{H} \longrightarrow {}^4\text{He} + 2\beta^+ + 2\nu_e + \gamma$$

(*b*) Show that the rest mass energy of 24.7 MeV is released in this cycle, not counting the 2×0.511 MeV released when each positron meets an electron and is annihilated according to $e^+ + e^- \rightarrow 2\gamma$. (*c*) The Sun radiates energy at the rate of about 4×10^{26} W. Assuming that this is due to the conversion of four protons into helium plus γ rays and neutrinos, which releases 26.7 MeV, what is the rate of proton consumption in the Sun? How long will the Sun last if it continues to radiate at its present level? (Assume that protons constitute about half the total mass of the Sun, which is about 2×10^{30} kg.)

11-100. The fusion reaction between ^{2}H and ^{3}H is

$$^3\text{H} + {}^2\text{H} \longrightarrow {}^4\text{He} + n + 17.7\ \text{MeV}$$

Using the conservation of momentum and the given Q value, find the final energies of both the ^{4}He nucleus and the neutron, assuming that the initial momentum of the system is zero.

11-101. (*a*) A particular light-water ^{235}U-fueled reactor had a reproduction factor of 1.005 and an average neutron lifetime of 0.08 s. By what percentage will the rate of energy production by the reactor increase in 5 s? (*b*) By what fraction must the neutron flux in the reactor be reduced in order to reduce the reproduction factor to 1.000?

11-102. Compute the reproduction factor for uranium enriched to (*a*) 5 percent and (*b*) 95 percent in ^{235}U. Compute the corresponding fission rate doubling time in each case. Assuming no loss of neutrons and the release of 200 MeV/fission, at what rate will energy be produced in each case 1.0 s after the first fission occurs?

STUDENTS-HUB.com Uploaded By: Malak Obaid

CHAPTER 12

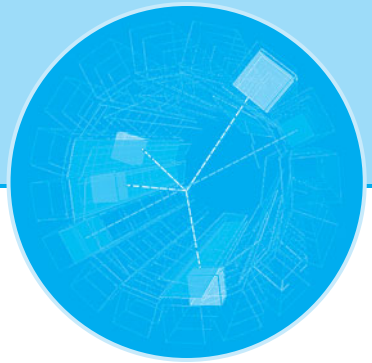

Particle Physics

12-1 Basic Concepts 562
12-2 Fundamental Interactions and the Force Carriers 570
12-3 Conservation Laws and Symmetries 580
12-4 The Standard Model 591
12-5 Beyond the Standard Model 605

Notwithstanding the speculations of the ancient Greek natural philosopher Democritus (about 450 BC) and Dalton's atomic theory of matter (1808),[1] the story of particle physics really began with the discovery of the *electron* by Thomson in 1897 (see Section 3-1). That event was followed in 1913 by Rutherford's discovery of the atomic nucleus whose lightest example, that of hydrogen, he named the *proton* (see Section 4-2). As one moved upward through the periodic table of the elements, a dilemma arose, caused by the more-rapid increase of the atomic mass compared to that of the nuclear charge, even though both were presumably due to the protons bound together in the nucleus. That problem was solved in 1932 by Chadwick's discovery of the *neutron* (see Section 11-1). In the meantime Einstein had proposed (in 1905) that Planck's quantization of blackbody radiation was in fact a quite general property of the electromagnetic field (see Sections 3-2 and 3-3). Einstein's suggestion was not widely accepted until, over the next 20 years, Millikan's thorough experimental investigation of the photoelectric effect and Compton's discovery and explanation of the Compton effect provided incontrovertible evidence for the quantization of electromagnetic radiation, the field quantum being a particle we now call the *photon*. For a brief time, it was thought these four were the "elementary" particles from which all matter was formed. But then Anderson discovered the positron, or antielectron, later in 1932. Shortly thereafter, the muon, pion, and many other particles were discovered in searches that have intensified and continued down to the present.

During the past 50 years several nations and international consortia have constructed increasingly larger and more sophisticated particle accelerators capable of producing greater and greater energies with the goals of testing the predictions of current theories and searching for additional particles predicted by them. Initially, an important consideration in such complex experiments, which often involve hundreds of scientists from many nations, was the question of how to tell if a particle is truly elementary or composed of a combination of other particles. For example, both the proton and the neutron were once thought to be elementary, but probing with high-energy (short-wavelength) electron beams revealed that the nucleons have internal structure, just as do atoms and nuclei. Each of the nucleons was found to be a composite particle consisting of three, still more fundamental particles called *quarks*. Several hundred particles have at one time or another been considered to be elementary, but a series of

STUDENTS-HUB.com
Uploaded By: Malak Obaid

The construction of large particle accelerators in various countries has, over the years, been an impetus for developing bigger and better superconducting electromagnets. The LHC at CERN has 1232 large, superconducting dipole magnets. High-field, efficient superconducting magnets are used in applications ranging from medical diagnostic magnetic resonance imaging (MRI) systems to magnetically levitated (maglev) trains.

brilliant theoretical achievements over that same 50-year period vastly expanded our understanding of the "particle zoo." The culmination of these achievements is the *Standard Model*, which has been spectacularly successful in explaining and predicting the properties and interactions of particles by describing them in terms of a relatively small number of truly (for now, at least) elementary particles. Research at universities and at the giant accelerator laboratories around the world continues to strengthen our understanding of the structure of matter. In addition to the usual particle properties of mass, charge, and spin, research has unveiled new properties that have no classical analogs, some given whimsical names such as strangeness, charm, and color. Coincident with the construction of the large accelerators has been the development and deployment of larger and more sensitive particle detectors at the big machines and, for neutrinos, detectors deep underground, in the oceans, and buried in the polar ice cap.

In this chapter, we will first look at a few basic concepts that will enable us to classify and describe particles. We will then consider the fundamental interactions between particles and the conservation laws that apply to them. Central to our discussions will be the current theory of elementary particles, the Standard Model, in which all matter in nature—from the most exotic particles produced in the giant accelerator laboratories to ordinary grains of sand—is constructed from just three groups of elementary particles: leptons, quarks, and the particles that mediate interactions between them.

12-1 Basic Concepts

Antiparticles

The Positron In the same year that the neutron was discovered, the positron was discovered (and named) by Carl Anderson.[2] This particle has the same mass and intrinsic angular momentum as the electron but has positive charge; therefore, its intrinsic magnetic moment is parallel, rather than antiparallel, to its spin. It is the antiparticle of the electron and is represented by the symbol e^+, or sometimes in radioactive decay equations by β^+. The existence of the positron had been predicted by Dirac from his relativistic wave equation,[3] though there was some difficulty about the interpretation of this prediction. (See Section 2-4.)

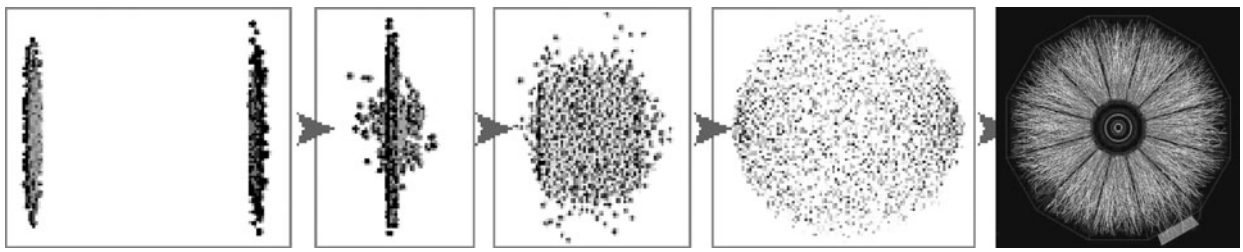

The Relativistic Heavy Ion Collider (RHIC) at Brookhaven National Laboratory began colliding gold nuclei (fully ionized gold atoms) late in 2000, with each of the ions moving at 99.99 percent of the speed of light. (*a*) through (*d*) are simulations of the accelerating Au nuclei at several stages. (*a*) Two Lorentz-contracted ions approach each other. (*b*) The collision "melts" the protons and neutrons and (*c*) for an instant releases the quarks and gluons from which the nucleons were formed. (*d*) From the enormous energy of the collision thousands more are created, creating in turn thousands of particles. (*e*) Computer construction of the tracks of the thousands of particles created in a single collision of two gold ions. [*Courtesy Brookhaven National Laboratory, STAR experiment.*]

STUDENTS-HUB.com Uploaded By: Malak Obaid

Air view of the European Laboratory for Particle Physics (CERN) just outside of Geneva, Switzerland. The large circle shows the Large Hadron Collider (LHC) tunnel, which is 27 kilometers in circumference. The irregular dashed line is the border between France and Switzerland (in the foreground). The LHC occupies the tunnel formerly used by the Large Electron-Positron (LEP) collider, which was retired in 2000. The LHC began operations in 2008. [*CERN.*]

The energy of a relativistic particle is given by Equation 2-31:

$$E^2 = (pc)^2 + (mc^2)^2 \qquad \textbf{2-31}$$

from which we can write

$$E = \pm[(pc)^2 + (mc^2)^2]^{1/2} \qquad \textbf{12-1}$$

Though we can usually choose the plus sign and ignore the negative-energy solution with a "physical argument," the mathematics of the Dirac equation requires the existence of wave functions corresponding to these negative-energy states. Dirac postulated that all the negative-energy states were filled with electrons. Electrons in the negative-energy states would exert no net force on anything and thus would not be observable. Dirac invoked the exclusion principle to suggest that only holes in this "infinite sea" of negative-energy states would be observable. The holes would act as positive charges with positive energy. Anderson's discovery of a particle with mass identical to that of the electron but with positive charge seemed to indicate that this interpretation was reasonable, since the positron is produced simultaneously with an electron in pair production (see Figure 12-1).

Antiparticles The notion that we are immersed in an infinite sea of negative-energy electrons is an unsettling one, however. It was rendered unnecessary with the development of quantum electrodynamics (QED) by Feynman[4] and others in the late 1940s. The negative energy solutions of the Dirac equation were re-expressed as positive energy solutions of a *new* particle—the positron. And the need for the invisible "sea" of electrons with its mysterious "holes" vanished. However, Dirac's prediction of an antielectron turned out to be farsighted. QED, whose predictions have been verified to the highest precision of any physical theory, requires that *every* particle must have a corresponding antiparticle with the same mass but opposite electric charge. For example, the theory predicts that protons and neutrons, which are both spin-1/2 particles whose wave functions are solutions of the Dirac equation, should have antiparticles.

STUDENTS-HUB.com Uploaded By: Malak Obaid

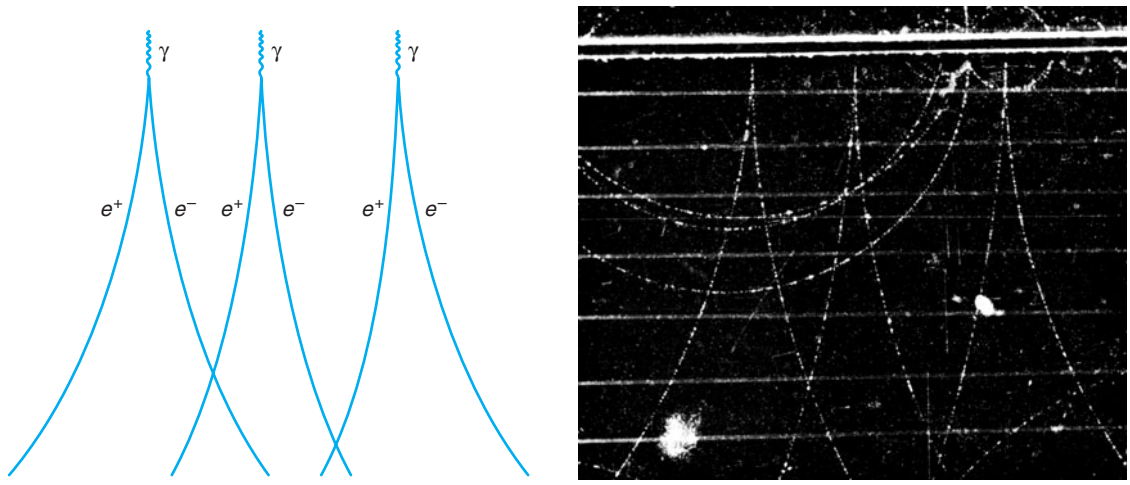

Figure 12-1 Tracks of electron-positron pairs produced by 300-MeV synchrotron x rays at the Lawrence Livermore Laboratory. The magnetic field in the chamber points out of the page. [*Photo courtesy of Lawrence Radiation Laboratory, University of California, Berkeley.*]

The creation of a proton-antiproton pair requires at least $2m_pc^2 = 1877$ MeV, which was not available except in cosmic rays until the development of high-energy accelerators in the 1950s. The antiproton (designated $\overline{p}$) was discovered by Segrè[5] and Chamberlain at Berkeley in 1955 using a beam of protons with kinetic energy 6.2-GeV from the Bevatron particle accelerator. (See Figure 12-2.) The antineutron ($\overline{n}$) (a particle with the same mass as the neutron but with a positive magnetic moment) was discovered two years later. (The standard notation for an antiparticle is the overbar; however, in many cases it is customary to specify the charge instead, as we did for the positron.)

Particles with integral spin, whose wave functions are not solutions of the Dirac equation, also have antiparticles. For example, those with zero spin, which are described by the Klein-Gordon relativistic wave equation (see Equation 11-52), include the pions, thought in the early days (circa 1940) to be the mediating exchange particle, or force carrier, of the nuclear force. In general, an antiparticle has exactly the same mass as the particle but with electric charge, *baryon number*, and *strangeness* (see Section 12-4) opposite in sign to that of the particle.

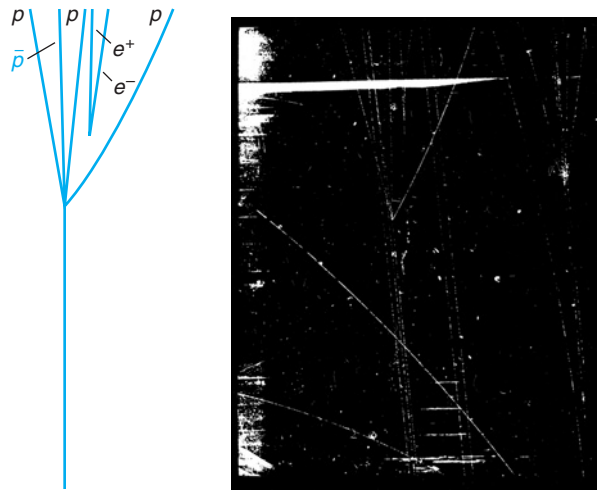

Figure 12-2 Bubble chamber tracks showing creation of proton-antiproton pair in the collision of an incident 25-GeV proton from the Brookhaven Alternating Gradient Synchrotron with a liquid hydrogen nucleus (stationary proton). The reaction is $p + p \rightarrow p + p + p + \overline{p}$. The energy necessary to create the pair is $2m_pc^2 = 1.877$ GeV in the center of mass system. A relativistic calculation in the laboratory frame shows that the beam protons must have at least $6m_pc^2 \approx 5.6$ GeV to reach the reaction threshold. [*Photo courtesy of R. Ehrlich.*]

STUDENTS-HUB.com Uploaded By: Malak Obaid

The tunnel of the proton-antiproton collider at CERN. The same bending magnets and focusing can be used for protons or antiprotons moving in opposite directions. The rectangular box in the foreground is a focusing magnet; the next four boxes are bending magnets. [*CERN.*]

Although the positron is stable, it has only a short-term existence in our universe because of the large supply of electrons in matter. The fate of the positron is annihilation according to the reaction

$$e^+ + e^- \longrightarrow \gamma + \gamma \quad \text{or} \quad e^+ + e^- \longrightarrow \gamma + \gamma + \gamma \qquad \textbf{12-2}$$

Whether bound (as positronium—see Section 2-4) or unbound, annihilation occurs from S states (zero orbital angular momentum), the antiparallel spins ^1S state producing two quanta as on the left in Equation 12-2, the parallel spins ^3S state producing three photons. The fact that we call electrons *particles* and positrons *antiparticles* does not imply that positrons are less fundamental than electrons, but was initially merely an arbitrary choice reflecting the nature of our part of the universe. If our matter were made up of negative protons, positive electrons, and neutrons with positive magnetic moments, then particles such as positive protons, negative electrons, and neutrons with negative magnetic moments would suffer quick annihilation and would probably be called the antiparticles. Antihydrogen atoms (an antiproton and a positron) were first produced "hot" in the antiproton beam at the European Center for Nuclear Research (CERN) in 1995. Subsequently, the CERN ATHENA project has produced substantial amounts of "cold" (slow) antihydrogen and is conducting definitive comparisons of its physical properties with those of hydrogen. The cover of this book illustrates the annihilation of an antihydrogen atom recorded by the ATHENA project. The matter-antimatter asymmetry of the universe, that is, why our universe consists of matter with essentially no antimatter despite the prediction of QED and the symmetry of the relativistic wave equation, is a question we will return to later in this chapter and in Chapter 13.

EXAMPLE 12-1 **Proton-Antiproton Annihilation** A proton and an antiproton at rest annihilate according to the reaction (standard particle physics notation typically omits the + signs in reaction equations):

$$p\bar{p} \longrightarrow \gamma\gamma$$

Find the energies and wavelengths of the photons.

SOLUTION

Since the proton and the antiproton are at rest, conservation of momentum requires that the two photons created in their annihilation have equal and opposite momenta

STUDENTS-HUB.com Uploaded By: Malak Obaid

and therefore equal energies. Since the total energy on the left side of the reaction is $2m_pc^2$, the energy of each photon is

$$E_\gamma = m_pc^2 = 938 \text{ MeV}$$

The wavelength is

$$\lambda = \frac{c}{f} = \frac{hc}{hf} = \frac{hc}{E_\gamma} = \frac{1240 \text{ eV} \cdot \text{nm}}{9.38 \times 10^8 \text{ eV}} = 1.32 \times 10^{-15}\text{m} = 1.32 \text{ fm}$$

Feynman Diagrams

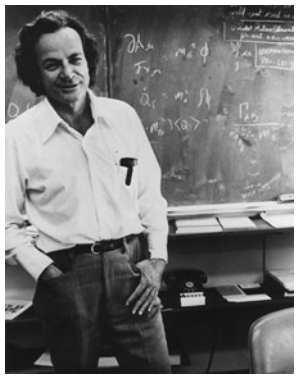

Richard Feynman, who called himself a "curious character," shared the 1965 Nobel Prize in Physics for his contributions to the development of quantum electrodynamics. [*American Institute of Physics, Emilio Segrè Visual Archives, Physics Today Collection.*]

As a part of quantum electrodynamics Feynman developed a wonderfully clear yet powerful technique for describing all electromagnetic phenomena. Like QED itself, the technique of *Feynman diagrams* is so good that it is used as a model by other quantum field theories, notably quantum chromodynamics (QCD), which we will discuss in Section 12-4. The detailed rules for drawing Feynman diagrams are directly related to the equations of QED and are beyond the scope of our discussions here; however, a brief description of a simplified version of the diagrams and a few basic rules will be ample for our use in illustrating the phenomena of interest in this chapter. (For a more complete discussion of Feynman diagrams refer to D. J. Griffith, Chapter 2, cited in the General References section.)

Feynman diagrams are spacetime diagrams, that is, *ct* versus *x* graphs, similar to those developed and used in Chapters 1 and 2. In particle physics Feynman diagrams are used to describe interactions at the level of quarks, leptons, and the mediators of the interactions and to compute lifetimes and cross sections for events. As noted in Figure 11-28, where a Feynman-like diagram was used to illustrate the early view of the π meson as the mediator of the nuclear force, the *ct* and *x* axes are normally not drawn. In this chapter, as in the earlier relativity chapters, time (*ct*) is positive upward. (Particle physicists often draw the diagrams with time flowing horizontally toward the right; there is no convention.) Particles are represented by straight lines with an arrow. A particle line whose arrow points backward in time is interpreted as the corresponding antiparticle moving forward in time. The arrows allow us to omit the overbars in the diagrams. The lines are symbolic and do *not* represent the particle trajectories. The rules for analyzing the diagrams, the details of which are beyond the scope of our discussions, force conservation of energy and momentum at each vertex. It is the *interactions* that we are interested in describing. Particles that are their own antiparticles, like the photon, have no arrows and are represented by wiggly or broken lines of various sorts. All electromagnetic phenomena can be represented by combinations of the process illustrated in Figure 12-3, called the *primitive vertex*. Interactions occur at the vertices. This diagram is read as follows: a moving charged particle enters, emits (or absorbs) a photon, and leaves. The primitive vertex is not itself a complete Feynman diagram, but rather the basic unit from which complete diagrams are constructed.

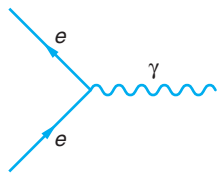

Figure 12-3 The primitive vertex of the Feynman diagram. The particle, shown as an electron, could be a proton or any other particle that feels the electromagnetic force. Note that the photon line has no arrow. The primitive vertex should be thought of as a "building block," combinations of which form complete Feynman diagrams.

Let's examine the Feynman diagrams for a few familiar events. In Figure 12-4*a*, two electrons enter, exchange a photon, and then leave. That is Coulomb repulsion of like charges.[6] Figure 12-4*b* represents Coulomb attraction of opposite charges. These serve to illustrate one more rule: Particle lines that both begin and end within the diagram are *virtual particles*, that is, like Yukawa's exchange pion in Section 11-5, they are not, indeed, cannot be observed in the laboratory. Note that a virtual particle need not have the same mass as the corresponding real particle; it is energy and momentum that are conserved at vertices, not mass. Only lines that enter or leave the diagram represent real, observable particles, and these do, of course, have the proper mass. The diagram makes clear why we say that the electromagnetic force is *mediated* by photons.

STUDENTS-HUB.com Uploaded By: Malak Obaid

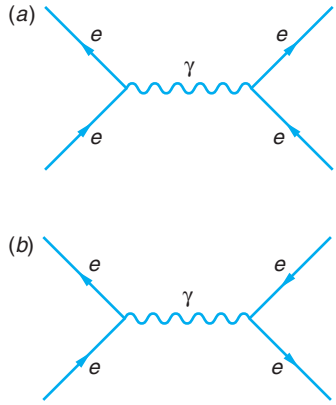

Figure 12-4 Feynman diagrams describing (*a*) Coulomb repulsion of charges of the same sign and (*b*) Coulomb attraction between charges of opposite signs.

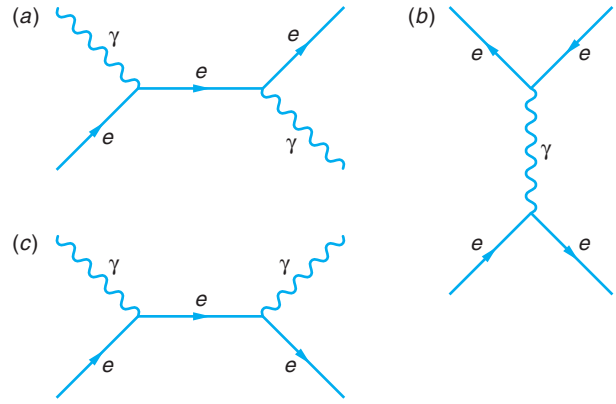

Figure 12-5 (*a*) The Compton effect. A photon enters and is absorbed by an electron, which then emits a photon and leaves. (Note that time, *ct*, is positive to the right in this diagram.) (*b*) At the lower vertex an electron and a positron enter and annihilate, producing a photon. At the upper vertex the photon creates a particle-antiparticle pair. (*c*) Another possible pair annihilation process.

Figure 12-5*a* illustrates Compton scattering. Figure 12-5*b* is another diagram that describes electron-positron scattering (Coulomb attraction) and includes both pair production (upper part) and pair annihilation (lower part). This points up the fact that there may be many diagrams representing any given reaction.[7] For example, Figure 12-5*c* is also a possible pair annihilation. With this introduction we will now use simple Feynman diagrams throughout the remainder of this chapter to visualize interactions that might otherwise be very difficult to understand.

EXAMPLE 12-2 Feynman Diagram of Particle-Antiparticle Creation In Section 2-4 we described the production of an electron-positron pair. Construct a Feynman diagram that illustrates this process.

SOLUTION

Consider the primitive vertex as an electron-photon interaction as below, left. Using the rules outlined above and noting that the now virtual electron exists for too short a time to be measured, we draw its line horizontal, i.e., with $\Delta(ct) = 0$. The positron interacts with a photon at the second primitive vertex. Together the two diagrams depict the creation of an electron-positron pair.

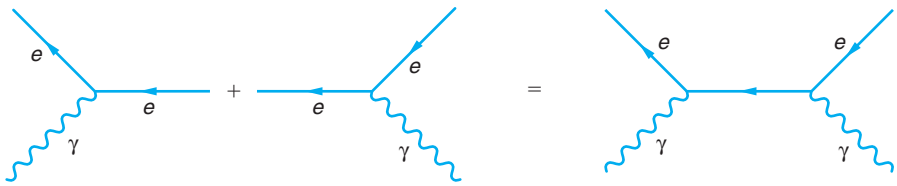

Other, so-called higher-order diagrams representing pair production are also possible. Can you draw one?

STUDENTS-HUB.com Uploaded By: Malak Obaid

Questions

1. What problem might arise in using Dirac's filled infinite sea of negative energy states to explain the existence of particle-antiparticle pairs of pions, whose spins are zero?
2. Why do electron-positron pairs annihilate mainly from *S* states?

Leptons and Quarks

Since Thomson discovered the electron, theoretical and experimental research in particle physics has revealed the existence of 62 fundamental particles and antiparticles, fundamental in the sense that they have no internal structure, as far as we can tell with current technology. This is not to say that this is all that exist. In fact, an important task of CERN's Large Hadron Collider is to search for the predicted Higgs boson, which may be the key to explaining the origin of mass, and to test current theoretical predictions of supersymmetry (SUSY) that suggest the existence of a "superpartner" for each of the known fundamental particles (see Section 12-5).

Many particles with electric charge were first "seen" in the particle detectors of experimental searches. The existence of many electrically neutral particles was deduced indirectly by applying conservation laws, particularly energy and momentum, to interactions that included charged particles recorded by particle detectors. Still others, both charged and neutral, remain unseen directly or indirectly. These are the *quarks* and the force carriers that bind them together, the *gluons*. Nevertheless, we are confident of their existence because their properties and interactions are so successfully explained by the Standard Model of particle physics, which is second only to QED in the precision of its predictions. We will be discussing the Standard Model and its relation to the fundamental interactions and conservation laws throughout the rest of this chapter. In this section we will introduce the classifications of the quarks and leptons in *generations* (or *families*) and *flavors* and list a few of their physical properties. Once you are familiar with general characteristics, we will discuss their properties and interactions more thoroughly.

Leptons There are three generations of leptons,[8] each consisting of a charged lepton and its related neutrino, as shown in Table 12-1. The electron is the most familiar of the charged leptons and the only one that is stable. Each charged lepton has a distinct antiparticle. The Standard Model assigns each lepton a *weak isospin* T_z, the z component of a quantum-mechanical property represented by the vector $\mathbf{T}$ that is loosely analogous to spin (see Section 12-3). For each neutrino there is also an antineutrino, although at this point in time it is possible that the two are not distinct; that is, each neutrino may be its own antiparticle (a so-called Majorana neutrino), much as the photon is its own antiparticle. Investigating that possibility is an active area of current research. Unlike the quarks, as we will see, there are no lepton-lepton bound states. We also refer to leptons as having three flavors: electron, muon, and tau. We will use this terminology in Section 12-5 in a discussion of neutrino mass.

Quarks As with leptons, there are six quarks grouped into three generations. All have fractional electric charge and distinct antiparticles. As we will learn in the following sections, it is the quarks and antiquarks that bind together in a multitude of ways to form more than 200 particles, accounting for the vast majority of the visible mass of the universe. The bound states of the quarks and antiquarks are called *hadrons* (from

STUDENTS-HUB.com Uploaded By: Malak Obaid

Table 12-1 The leptons

	Lepton l	Symbol	Charge (*e*)	Weak isospin T_z	Mass (MeV/c^2)	Lifetime (*s*)	Spin ($\hbar$)
1st generation	electron	e	−1	−1/2	0.5110	stable	1/2
	electron neutrino	ν_e	0	1/2	≤2.2 eV/c^2	stable	1/2
2nd generation	muon	μ	−1	−1/2	105.659	2.197×10^{-6}	1/2
	muon neutrino	ν_μ	0	1/2	≤3.5 eV/c^2	stable	1/2
3rd generation	tau	τ	−1	−1/2	1,784	3.3×10^{-13}	1/2
	tau neutrino	ν_τ	0	1/2	≤8.4 eV/c^2	stable	1/2

the Greek *hadros*, meaning "robust"). There are two subgroups of hadrons. Three-quark combinations are called *baryons* (from the Greek *barys*, meaning "heavy"), of which the proton and neutron are the two most common examples. Quark-antiquark pairs form the *mesons*. The term *meson*, derived from the Greek *mesos*, meaning "middle," was chosen because the first mesons discovered (the pions) had masses intermediate between those of the electron and the proton; however, many mesons heavier than the proton were subsequently discovered, so the name is no longer an indicator of the masses of these hadrons. For reasons we will discuss in Section 12-4, single, or "free" quarks have not been nor seem likely to be observed. The recently reported five-quark combination has not been independently confirmed. Table 12-2 records basic descriptions of the quarks.

Each quark in the table also has an additional property, analogous to electric charge, called *color*, or *color charge*. Color has three possible values: *red*, *blue*, and *green*. So, for example, there are three different *u* quarks: u_r, u_b, and u_g. The antiquarks have anti-color, just as they have opposite electric charge, so the three anti-*u* quarks are the $\overline{u}_{\bar{r}}$, $\overline{u}_{\bar{b}}$, and $\overline{u}_{\bar{g}}$. Of course, these terms have nothing to do with the usual meanings of the words *color*, *red*, *blue*, and *green*. They are simply labels that are used to describe a particular

Table 12-2 The quarks

	Quark (*q*)	Symbol	Charge (*e*)	Weak isospin T_z	Mass (MeV/c^2)	Spin ($\hbar$)	Baryon number
1st generation	up	u	2/3	1/2	336	1/2	1/3
	down	d	−1/3	−1/2	338	1/2	1/3
2nd generation	charm	c	2/3	1/2	1,500	1/2	1/3
	strange	s	−1/3	−1/2	540	1/2	1/3
3rd generation	top	t	2/3	1/2	170,900	1/2	1/3
	bottom	b	−1/3	−1/2	5,000	1/2	1/3

STUDENTS-HUB.com Uploaded By: Malak Obaid

quantum-mechanical property of the particles, a choice that will turn out, perhaps unexpectedly, to be very convenient (see Section 12-4). Like electric charge, color charge is conserved. Quarks with $2e/3$ electric charge (see Table 12-2) are *up-type quarks* (up, charm, and top), and those with $-e/3$ are referred to as *down-type quarks* (down, strange, and bottom). As with the leptons, the Standard Model also assigns each quark a weak isospin T_z. The up-type quarks have $T_z = 1/2$; the down-type quarks have $T_z = -1/2$. Notice in Table 12-2 that each of the quark generations is an isospin doublet. The Standard Model provides for an equal number of lepton and quark generations, as you see are contained in Tables 12-1 and 12-2. We refer to the quarks as having six flavors; e.g., the down quark and antiquark are of the "down flavor." Altogether, Table 12-2 represents 36 quarks and antiquarks. Like the leptons, the quarks are all fermions.

12-2 Fundamental Interactions and the Force Carriers

All the different forces observed in nature, from ordinary friction to the tremendous forces involved in supernova explosions, can be understood in terms of the four basic interactions that occur among elementary particles. In order of decreasing strength, these are

1. The strong interaction
2. The electromagnetic interaction
3. The weak interaction
4. The gravitational interaction

Molecular forces and most of the everyday forces that we observe between macroscopic objects (for example, friction, contact forces, and forces exerted by springs and strings) are complex manifestations of the electromagnetic interaction, which occurs between all particles that carry electric charge. Although gravity, the interaction between all particles with mass, plays an important role in our lives, it is so weak compared with other forces that its role in the interactions between elementary particles is essentially negligible. The weak interaction acts between particles that carry *weak charge* and describes, among others, the interaction between electrons or positrons and nucleons that results in beta decay, which we discussed in Chapter 11. The strong interaction acts between particles that carry color charge and describes, for example, the force between nucleons that holds nuclei together. Some particles participate in all four interactions, whereas others participate in only some of them.

In 1979, S. L. Glashow, A. Salam, and S. Weinberg shared the Nobel Prize in Physics for development of the *electroweak theory*, successfully unifying theories of the electromagnetic and the weak interactions. This event, which came exactly 100 years after Maxwell had accomplished unification of the theories of electricity and magnetism, was a major advance toward achieving unification of the theoretical descriptions of the four basic interactions. Developing such a unified field theory has been a goal of physics for a long time, one that was vigorously sought without success by Einstein, among many others. As we will discuss in Section 12-4, the electroweak unification occurs only at high particle energies. Current efforts to unify the electroweak, strong, and gravitational interaction will be discussed in Section 12-5.

The term "strength" of the interactions refers specifically to the relative magnitudes of the dimensionless *coupling constants*[9] that multiply the fundamental space-dependent part of the potential energy function whose gradient determines the particular force.

STUDENTS-HUB.com Uploaded By: Malak Obaid

The relative strengths stated in the paragraphs below and in Table 12-4 are only approximate as there is no unambiguous method of comparison, particularly for the weak interaction. As an example, the electric (Coulomb) potential energy of two charges is $U(r) = -(1/4\pi\epsilon_0)e^2/r$. The multiplier of the space-dependent function $1/r$ is made dimensionless by dividing both sides of the equation by the quantity $\hbar c$:

$$V(r) = U(r)/\hbar c = -\frac{e^2}{4\pi\epsilon_0 \hbar c}\frac{1}{r} \qquad \textbf{12-3}$$

where $V(r)$ is in m^{-1}. The quantity $(e^2/4\pi\epsilon_0\hbar c)$ you will recognize as the fine-structure constant $\alpha \approx 1/137$, first encountered in our discussion of Bohr's model of the hydrogen atom (see Section 4-3). The fine-structure constant is thus the coupling constant of the electromagnetic interaction. As we discovered in Chapter 4, energies resulting from this interaction are proportional to α^2 and characteristic dimensions (e.g., the Bohr radius a_0) are proportional to $1/\alpha$. (See Equations 4-32 and 4-33.) Moreover, the probability densities for atomic phenomena discussed in Chapter 7 are all directly dependent on the value of α. (See Equation 7-32.)

Just as Yukawa postulated the pion as the mediator, or carrier, of the force between nucleons (see Section 11-5), the Standard Model postulates one or more particles as the force carrier, or mediator, of each fundamental interaction. Each of these mediators, all of which the theory requires to be bosons, will be introduced in the following paragraphs, concerned with each of the interactions.

Strong Interaction

All hadrons interact via the strong interaction. Of the two subgroups of hadrons, baryons (the three-quark combinations) have 1/2-integral spins (1/2, 3/2, 5/2, etc.). Mesons (the two-quark combinations) have zero or integral spins. The range of the strong force is about 10^{-15} m, or one fm. (See Chapter 11.) The coupling constant α_s of the strong interaction is approximately 1, or about 10^2 larger than the fine-structure constant α of the electromagnetic force. Within the framework of the Standard Model, the strong force is due to color charge, analogous to the electromagnetic force being due to electric charge. The mediator of the strong force is the *gluon*. Like the quarks, the gluons carry color charge, but with a difference. Each quark carries one unit of one of the three color charges, but each gluon carries one unit of one of the three color charges *and* one unit of one of the three anticolor charges. Since there are nine possible combinations of r, b, and g with $\bar{r}$, $\bar{b}$, and $\bar{g}$, we expect nine different gluons; however, a technicality reduces that number to eight. One consequence of color-charged gluons is that the emission of a gluon by a quark can change the color (but not the flavor) of the quark. Another is that gluons can couple to other gluons (see Section 12-3). Since leptons don't carry color charge, they don't participate in the strong interaction. Note, too, that the photon, the electromagnetic interaction's counterpart to the gluon, does not carry electric charge.

The characteristic *interaction time* of the strong interaction is extremely short, only about 10^{-23} s, meaning that an event caused by this interaction "happens" in this length of time. Thus, if the probability is to be high that two particles will interact via the strong force by exchanging a virtual particle, the two must remain within the range of the force for at least 10^{-23} s. Similarly, particles that change into another particle or particles, that is, decay due to the action of the strong force, do so within about 10^{-23} s. This is about the time it takes light to travel a distance equal to the diameter of a nucleus.

STUDENTS-HUB.com Uploaded By: Malak Obaid

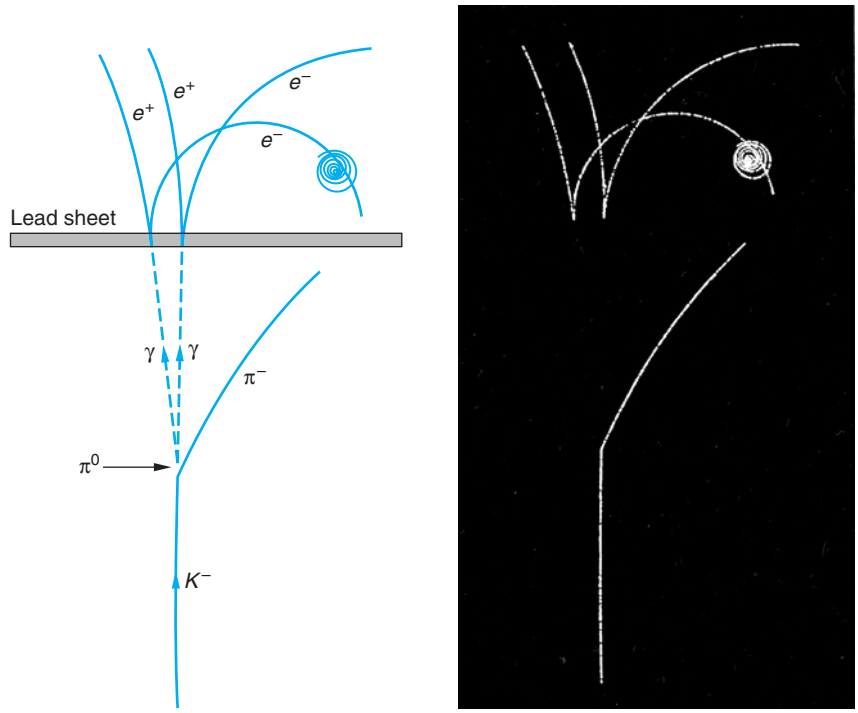

A negative kaon (K^-) enters a bubble chamber from the bottom and decays into a π^-, which moves off to the right, and a π^0, which immediately decays into two photons, whose paths are indicated by the dashed lines in the drawing. Each photon interacts in the lead sheet, producing an electron-positron pair. The spiral at the right is an electron that has been knocked out of an atom in the chamber. (Other, extraneous tracks have been removed from the photograph.)

Table 12-3 lists some of the properties of the hadrons that are stable against decay via the strong interaction, that is, those with lifetimes significantly longer than 10^{-23} s. Those that decay via the electromagnetic and weak interactions have much longer lifetimes, typically of the order of 10^{-18} s and 10^{-10} s, respectively. Note that all baryons ultimately decay to a proton. Note, too, that the baryons cluster into "charge multiplets" of about the same mass: the nucleons (n and p) of mass about 939 MeV, the Λ of mass about 1116 MeV, the Σ particles of mass about 1190 MeV, the Ξ particles of mass about 1315 MeV, and the Ω of mass 1672 MeV. The differences in masses within multiplets (such as between the neutron and proton) are due primarily to differences in the masses of the constituent quarks (see Section 12-4). The energy of the electromagnetic field also makes a contribution to the mass differences. There are six mesons in Table 12-3: three pions, two kaons, and the eta particle. The mesons also cluster into charge multiplets. As with the baryons, the mass differences within each multiplet are due primarily to the mass differences of the constituent quarks. Note that the mass of the π^+ is exactly equal to that of the π^-, as it must be since these particles are antiparticles of each other.

Being complex particles composed of other, more fundamental particles (quarks), the hadrons each have a ground state and a set of quantized excited states directly analogous to the allowed energy levels of atoms and nuclei, which are of course also complex particles composed of other, more fundamental particles. These excited hadron states usually decay via the strong interaction and thus have large energy widths, as

STUDENTS-HUB.com Uploaded By: Malak Obaid

Table 12-3 Hadrons that are stable against decay via the strong interaction

Name	Symbol	Mass (MeV/c^2)	Spin ($\hbar$)	Charge (e)	Antiparticle	Mean lifetime(s)	Typical decay products†
Baryons							
Nucleon	p (proton) or N^+	938.3	1/2	+1	p^-	$>10^{32}$ y	
	n (neutron) or N^0	939.6	1/2	0	$\overline{n}$	930	$p + e^- + \overline{\nu}_e$
Lambda	Λ^0	1116	1/2	0	$\overline{\Lambda}^0$	2.5×10^{-10}	$p + \pi^-$
Sigma	Σ^+	1189	1/2	+1	$\overline{\Sigma}^-$	0.8×10^{-10}	$n + \pi^+$
	Σ^0	1193	1/2	0	$\overline{\Sigma}^0$	10^{-20}	$\Lambda^0 + \gamma$
	Σ^-	1197	1/2	−1	$\overline{\Sigma}^+$	1.7×10^{-10}	$n + \pi^-$
Xi*	Ξ^0	1315	1/2	0	$\overline{\Xi}^0$	3.0×10^{-10}	$\Lambda^0 + \pi^0$
	Ξ^-	1321	1/2	−1	$\overline{\Xi}^+$	1.7×10^{-10}	$\Lambda^0 + \pi^-$
Omega	Ω^-	1672	3/2	−1	Ω^+	1.3×10^{-10}	$\Xi^0 + \pi^-$
Charmed lambda	Λ_c^+	2285	1/2	+1	$\overline{\Lambda}_c^-$	1.8×10^{-13}	$p + K^- + \Lambda^+$
Mesons							
Pion	π^+	139.6	0	+1	π^-	2.6×10^{-8}	$\mu^+ + \nu_\mu$
	π^0	135	0	0	self	0.8×10^{-16}	$\gamma + \gamma$
	π^-	139.6	0	−1	π^+	2.6×10^{-8}	$\mu^- + \overline{\nu}_\mu$
Kaon	K^+	493.7	0	+1	K^-	1.24×10^{-8}	$\pi^+ + \pi^0$
	K^0	497.7	0	0	$\overline{K}^0$	0.88×10^{-10} and 5.2×10^{-8}‡	$\pi^+ + \pi^-$ and $\pi^+ + e^- + \overline{\nu}_e$
Eta	η^0	549	0	0	self	2×10^{-19}	$\gamma + \gamma$

† Other decay modes also occur for most particles.
‡ The K^0 has two distinct lifetimes, sometimes referred to as K^0_{short} and K^0_{long}. All other particles have a unique lifetime.
* The Ξ particle is sometimes called the cascade.

required by the uncertainty principle ($\Delta E \approx \hbar/\Delta t$) and in contrast to the much slower atomic transitions and nuclear decays. Excited hadron states are usually observed as resonances in the cross section for scattering of one hadron on another and are therefore also called *resonance particles*. We describe resonance particles more thoroughly on the home page (see page 591).

STUDENTS-HUB.com Uploaded By: Malak Obaid

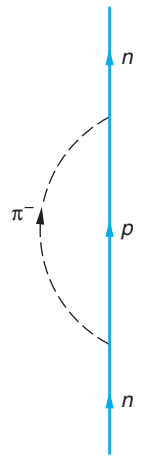

Figure 12-6 A neutron emits a virtual π^-. During the time Δt that the positive proton and the π^- exist, they can interact with other charged particles. After time Δt the π^- is reabsorbed by the proton.

The need to transfer rapidly enormous volumes of data collected by detectors at the major particle physics laboratories throughout the world to the thousands of collaborating scientists in many countries led to the development of the World Wide Web at CERN.

Electromagnetic Interaction

This is the dominant interaction at scales larger than subatomic, the realm of the strong interaction, and smaller than astronomical, where the gravitational interaction rules. All particles that carry electric charge or have a magnetic moment participate in the electromagnetic interaction. In addition, neutral particles without magnetic moments may also participate in the interaction if the emission of virtual particles results in charged particles. A neutron emitting and reabsorbing a virtual π^- as shown in Figure 12-6 is an example of a neutral particle involved in an electromagnetic interaction. The range of the electromagnetic force is infinite, and its strength is about $1/137$ times that of the strong interaction, as we discussed earlier. Its characteristic interaction time is about 10^{-18} s. According to QED, the mediator of the electromagnetic force is the photon. In contrast to the gluon, the photon does not carry electric charge. Decays via the electromagnetic interaction generally result in the emission of one or more photons, although there are a few exceptions, e.g., $\pi^0 \longrightarrow e^+e^-$. Notice in Table 12-3 that the Σ^0, π^0, and η^0 decay via the electromagnetic interaction.

Weak Interaction

All quarks and leptons participate in the weak interaction. The range of the weak force is about 10^{-18} m or about 10^{-3} fm, considerably smaller than that of the strong force. Example 12-3 shows how the range of the weak force is determined. Its characteristic interaction time varies from about 10^{-16} s to about 10^{-10} s. No particular name is given to the source of the weak force, although it is occasionally called the *weak charge* or *flavor charge*, in analogy with electric charge. The strength of the weak interaction relative to the strong interaction is about 10^{-5}. The weak force is carried by three particles, the *charged weak force* by the W^+ and W^- (W for "weak") and the *neutral weak force* by the Z^0 (Z for "zero"). All three have spin 1 and thus are bosons. A very important aspect of the weak force is that interactions mediated by the $W^\pm$ turn one quark flavor into another. The weak interaction does not, however, change the lepton flavor. The mediation of three typical weak interactions, the scattering of a muon neutrino by an electron, the scattering of an electron neutrino and a muon, and the inverse beta decay of a proton are illustrated in Figure 12-7.

The mediators of the weak interaction were all discovered in 1983 by C. Rubbia and a large international team of co-workers after a long search using the $p\overline{p}$ collider

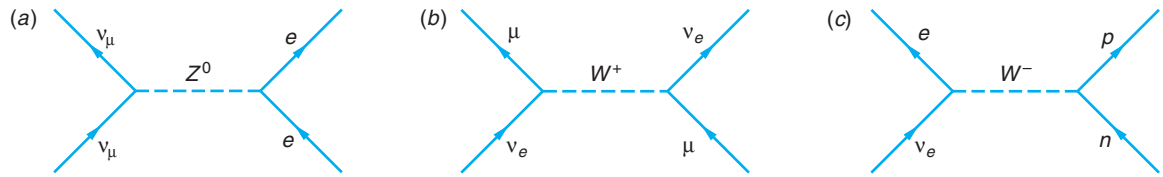

Figure 12-7 (*a*) The scattering of a muon neutrino from an electron involves the exchange of a Z^0. Such an exchange is called a *neutral current* interaction. The interaction does not convert the electron into a muon neutrino. (*b*) The scattering of an electron neutrino from a muon may also occur via a neutral current interaction as in (*a*), but a *charged current* interaction in which a charged W is exchanged is also possible, and both would contribute to the cross section. Measuring the cross sections thus provides a means of testing the standard model. (*c*) Inverse beta decay also proceeds via a *charged current* interaction.

STUDENTS-HUB.com Uploaded By: Malak Obaid

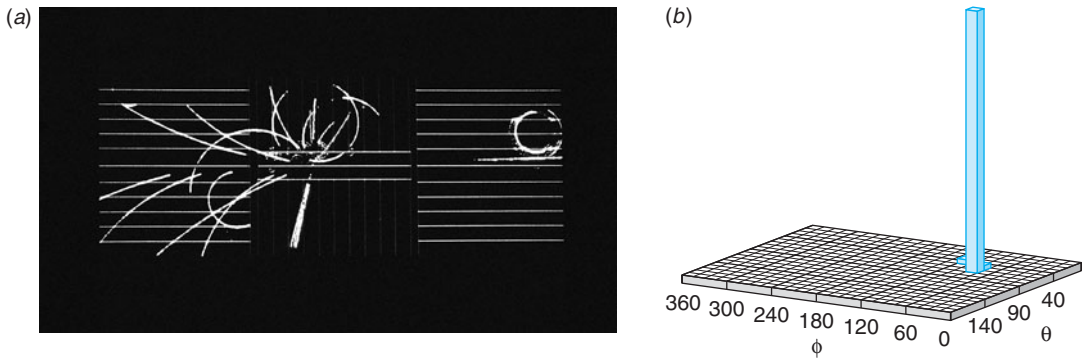

Figure 12-8 (*a*) The production and subsequent decay of one of the first *W* bosons ever detected was recorded by the UA1 detector at the CERN $S\bar{p}\bar{p}S$ proton-antiproton collider. A $p\bar{p}$ collision occurs at the center. A W^+ is produced, which decays by $W^+ \rightarrow \tau^+ + \nu_\tau$. The tau decays into charged particles clearly seen as the thicker pencil-jet in the central detector directed nearly vertically downward. Conservation of energy and momentum for all particle tracks produced yields results consistent with a missing ν_τ from the decay. [*CERN.*] (*b*) The UA1's energy detectors surrounding the beam pipe recorded the energetic τ^+ and its angular position relative to the decay event. Energy is plotted vertically upward.

at CERN[10] that was specifically designed for the task. (See Figures 12-8 and 12-9.) The Z^0 is the second-heaviest elementary particle known, with a mass of 91 GeV/c^2 or nearly 100 times that of the proton. The $W^\pm$, with masses of 80 GeV/c^2, are the next heaviest.

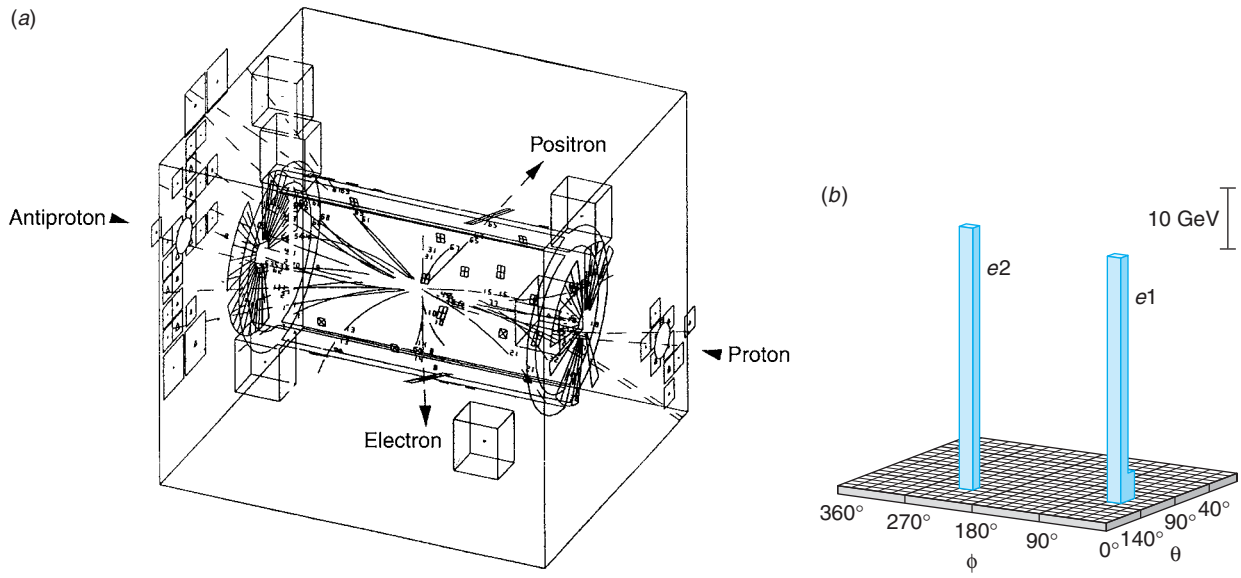

Figure 12-9 (*a*) This computer reconstruction of the CERN UA1 detector shows the first Z^0 decay ever recorded, obtained by Rubbia's group in 1983. Millions more such events have since been seen. [CERN Courier, ***33***, *4 (1993).*] (*b*) The energy plot of the electron-positron pair from the $Z^0 \rightarrow e^+ + e^-$ decay. Energy, plotted vertically, is measured by individual detectors that "wrap around" the central cylinder of the UA1. The angular locations of the recorded electron and positron are measured relative to the position of the Z^0. Graphs like this are called "Lego plots."

STUDENTS-HUB.com Uploaded By: Malak Obaid

EXAMPLE 12-3 **Range of the Weak Interaction** The mass of the Z^0 has been accurately measured to be 91.16 GeV/c^2. What range does that value imply for the neutral current weak interaction mediated by the Z^0?

SOLUTION

1. The range, the distance R traveled in time $t = \hbar/\Delta E$ by a particle moving at about c, is given by Equation 11-50:
$$R = \frac{\hbar}{mc} = \frac{\hbar c}{mc^2}$$

2. Substituting the mass of the Z^0 into this expression for R gives
$$R = \frac{(1.055 \times 10^{-34}\ \text{J}\cdot\text{s})(3.00 \times 10^{8}\ \text{m/s})}{(91.16\ \text{GeV}/c^2)(1.60 \times 10^{-10}\ \text{J/GeV})}$$
$$= 2.17 \times 10^{-18}\ \text{m} = 2.17 \times 10^{-3}\ \text{fm}$$

3. An alternate calculation of R:
$$R = \frac{(197.3\ \text{eV}\cdot\text{nm})}{(91.16\ \text{GeV})(10^7\ \text{eV/GeV})(10^9\ \text{nm/m})}$$
$$= 2.17 \times 10^{-3}\ \text{fm}$$

Gravitational Interaction

All particles participate in the gravitational interaction, but this interaction is so weak as to be unimportant in the discussion of elementary particles. As we have seen previously, its strength relative to the strong interactions is about 10^{-38}. The interaction has infinite range, with the force decreasing as $1/r^2$, as does the electrostatic force. The mediating particle for this force is the *graviton*, which is expected to be uncharged, massless, and have spin 2. This particle has not yet been observed, nor does the experimental capability to do so yet exist. Experiments with the objective of detecting gravity waves are currently under way. (See Section 2-5.) The gravitational interaction is produced by mass, which is the "gravitational charge" corresponding to the color charge, electric charge, and weak charge of the strong, electromagnetic, and weak interactions, respectively. Table 12-4 summarizes the characteristics of the four fundamental interactions.

Table 12-4 Characteristics of the fundamental interactions

Interaction	Force carrier	Mass (GeV/c^2)	Spin ($\hbar$)	Source	Particles carrying charge	Range (m)	Interaction time (s)	Coupling constant
Strong	gluon	0	1	color charge	q, g	10^{-15}	10^{-23}	$\alpha_s \approx 1$
Electromagnetic	photon	0	1	electric charge	q, e, μ, τ, $W^{\pm}$	∞	10^{-18}	$\alpha = 1/137$
Weak	$W^{\pm}$, Z^0	80, 91	1, 1	weak charge	q, e, μ, τ, $W^{\pm}$, Z^0	10^{-18}	10^{-16} to 10^{-10}	$\alpha_w \approx 10^{-5}$
Gravity	graviton	0	2	mass	q, e, μ, τ, ν, $W^{\pm}$, Z^0	∞	?	$\alpha_g \approx 10^{-38}$

STUDENTS-HUB.com Uploaded By: Malak Obaid

EXPLORING
A Further Comment About Interaction Strengths

At the beginning of this section we defined the strengths of the interactions in terms of the coupling constants, relating their approximate values to the most familiar one, which is the fine-structure constant $\alpha = e^2/4\pi\epsilon_0\hbar c$. In QED the electric charge

$$e = \sqrt{4\pi\epsilon_0\hbar c\alpha} \propto \sqrt{\alpha}$$

is the amplitude of the coupling of the photon (the mediating boson) to the electron (the particle). Thus, the probability of events involving that coupling, such as the Compton effect, illustrated in Figure 12-5(a), is proportional to $e^2 \propto \alpha$.

The time-independent solution to the Klein-Gordon equation (Equation 11-52) can also be interpreted as the static potential $U(r)$ of the field of a point charge represented by the exchange particles. We then have

$$U(r) = \frac{Ae^{-r/R}}{r} \qquad \textbf{12-4}$$

where A is a constant of integration and $R = \hbar/mc$ is both the range of the force and the Compton wavelength $\lambda_c/2\pi$ of the mediating boson. For the electromagnetic interaction the range R is infinite and $U(r)$ becomes

$$U(r) = \frac{A}{r} \qquad \textbf{12-5}$$

Recalling from classical electromagnetism that the electrostatic potential of a point charge q is $U(r) = q/4\pi\epsilon_0 r$, we see that the constant A in Equation 12-5 plays the same role as the charge. In this manner a coupling constant proportional to A^2, just as $\alpha \propto e^2$, can be obtained for each of the interactions, albeit not without some difficulty. Doing so for the strong and weak interactions involves mathematics beyond the scope of our discussions, but as we will see in Section 12-4, this use of QED as a model is a powerful aid in understanding both the weak and the strong interaction. The coupling constants and other characteristics of the four interactions are given in Table 12-4.

One last comment before we leave this topic: The coupling constants are not actually constants. Again, this can be most clearly illustrated using the electromagnetic interaction. Consider a positive point charge q embedded in a dielectric as shown in Figure 12-10*a*. The charge q polarizes the nearby molecules of the dielectric. As a result, the charge q is partially screened by the negative ends of the polarized molecules and the electric field of q at a distance r away is correspondingly reduced. Thus, the value measured for q is the effective charge q_{eff}, which depends on how far from q the measurement is made, where q_{eff} is given by

$$q_{\text{eff}} = \frac{q}{\epsilon} \qquad \textbf{12-6}$$

and ϵ is the dielectric constant of the material, which you remember is a measure of how difficult it is to polarize the material. Only by measuring very close to q, roughly speaking within the molecular equilibrium separation r_0 (closer than the closest molecule so that there is no screening), will you actually measure the value q. This is shown in Figure 12-10*b*. Notice also that (1) measurements made at large values of r yield q/ϵ, not q, and (2) the value of q_{eff} *increases* for very small values of r.

STUDENTS-HUB.com Uploaded By: Malak Obaid

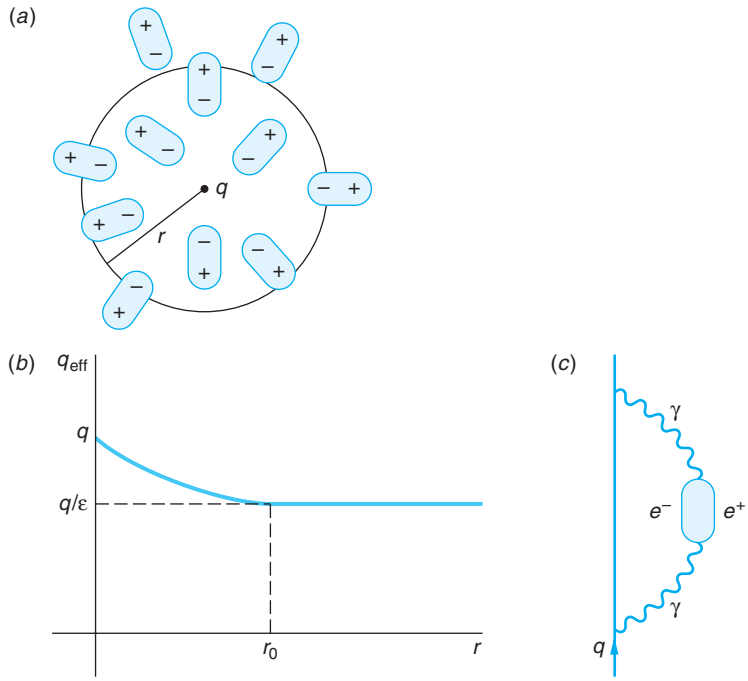

Figure 12-10 (*a*) A positive charge q placed in a dielectric material polarizes the dielectric by orienting the nearby molecules with their negative ends closest to q. An observer at some distance r from q sees a reduced electric field because of the screen of negative charges. (*b*) The value q_{eff} is measured for the charge. At small distances, those less than the equilibrium separation r_0 of the molecules of the dielectric, the value of q_{eff} approaches the value of q. (*c*) The vacuum also polarizes like a dielectric due to production of virtual electron-positron pairs by virtual photons. The effect is to increase the value of the fine-structure constant at very short interaction distances.

The production and absorption of virtual particles in QED results in the vacuum behaving like a dielectric. The positive charge q (or any charge) is continually emitting and absorbing virtual photons. Some of the photons occasionally create electron-positron pairs, which then annihilate, as the Feynman diagram in Figure 12-10*c* illustrates. The virtual electron and positron are attracted and repelled, respectively, by q, resulting in *vacuum polarization*, which partially screens q, just as it was screened when embedded in the dielectric. And just as in the dielectric, the full value of the charge q is not seen, or measured, until you get inside the screen. In vacuum polarization the role of the equilibrium separation r_0 is played by the Compton wavelength of the electron $\lambda_c = h/mc = 2.43 \times 10^{-12}$ m. Thus, even in a vacuum the "actual" value of q can only be measured at distances closer than about 2.43×10^{-12} m. What we measure experimentally and refer to as "the charge of the electron" is actually the completely screened effective charge. Thus, the fine-structure constant α, which is proportional to the square of the electric charge, will *increase* at very small distances from q.

A corresponding discussion can be given for the weak and strong interactions, but there are significant differences. The photon, which mediates the electromagnetic interaction, does not carry electric charge. However, the $W^{\pm}$ and Z^0, which mediate the weak interaction, have mass and carry weak charge. (The $W^{\pm}$ also carry electric charge.) The gluons, which mediate the strong force, carry color charge. This latter difference results in an important characteristic of the strong force called *quark confinement*, which we will discuss further in Section 12-4.

STUDENTS-HUB.com Uploaded By: Malak Obaid

Questions

3. How are baryons and mesons similar? How are they different?
4. What properties do all leptons have in common?
5. The mass of the muon is nearly equal to that of the pion. How do these particles differ?
6. The bonding of the electrons to nuclei to form atoms is an example of the electromagnetic interaction. Use the interaction's properties to explain why the dimensions of atoms are of the order of 10^{-10} m.
7. Describe a way the world would be different if electrons felt the strong interaction.
8. What might be the "technicality" that results in there being eight gluons instead of the expected nine?

EXAMPLE 12-4 **Neutron Decay** The free neutron decays via the weak interaction with a half-life of 10.4 min according to the reaction

$$n \longrightarrow p + e^- + \bar{\nu}_e$$

Use a Feynman diagram to illustrate the details of this decay.

SOLUTION

Since this decay involves a change in the charge of the hadron, the mediating boson is a W^-. The W^- then decays to the e^- and $\bar{\nu}_e$. The Feynman diagram describing these events is therefore as shown below, where particles shown moving backward in time are to be interpreted as the corresponding antiparticle moving forward in time. Notice that, as mentioned earlier, the charged weak interaction changes the quark flavor.

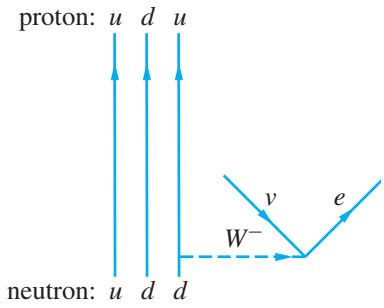

In words, this diagram is read like this: A d quark in the neutron emits a W^-, changing (decaying) to a u quark, thus changing the neutron into a proton. The W^- then decays to an e^- and an $\bar{\nu}_e$.

Remarks: *The mediating boson could also be a W^+. What would the diagram look like in that case?*

STUDENTS-HUB.com Uploaded By: Malak Obaid

EXAMPLE 12-5 **Estimate of Cross Section for Strong Interaction** Obtain a rough estimate for the cross section of a typical strong interaction scattering of two hadrons, such as pions by protons or protons by protons.

SOLUTION

1. The cross section σ for an interaction or reaction is given approximately by the area of a circle whose radius is the range of the interaction. (See Section 11-7.) For the strong interaction we can write, therefore, that
$$\sigma_S = \pi R_S^2$$
2. From Example 11-15 we found the range of the strong interaction R_S to be about 10^{-15} m. Therefore, σ_S is equal to
$$\sigma_S = \pi(10^{-15}\text{ m})^2 = 3.1 \times 10^{-30}\text{ m}^2 = 31\text{ mb}$$

Remarks: *The cross section, as noted in Section 11-7, is actually dependent on the collision energy, but typical values are of the order of tens of millibarns, in agreement with our approximation.*

12-3 Conservation Laws and Symmetries

One of the maxims of nature, sometimes referred to as the *totalitarian principle*, is "anything that can happen does happen." If a conceivable decay or reaction does *not* occur, then there must be a reason. The reason is usually expressed in terms of a conservation law. You are already familiar with several such laws. The *conservation of energy* rules out the decay of any particle for which the total mass of the decay products would be greater than the initial mass of the particle before decay. The *conservation of linear momentum* requires that when an electron and positron annihilate, two photons (at least) must be emitted. *Angular momentum* must also be conserved in a reaction or decay. A fourth conservation law that restricts the possible particle decays and reactions is that of *electric charge*. The net electric charge before a decay or reaction must equal the net charge after the decay or reaction.

Every conservation law is a consequence of a particular symmetry in the laws of physics that govern the universe. This is a paraphrased statement of a theorem proven in 1918 by Emmy Noether[11] for conjugate variables in classical mechanics. For instance, the laws of physics are symmetric (i.e., invariant) with respect to translations in time. That means they work the same today as they have in the past. Noether's theorem relates this particular invariance of the physical laws to the conservation of energy. The fact that the physical laws are symmetric under translations in space leads to the conservation of linear momentum. If a system is symmetric to rotations about a point, then the angular momentum is conserved. The conservation of electric charge is a consequence of the invariance of the laws of electrodynamics under a gauge (i.e., scale) transformation.

There is a quantum theory analog of Noether's theorem; however, as was the case in classical physics, the conservation law is often discovered empirically before the symmetry that is its origin is identified. For example, Herman von Helmholtz set forth the law of conservation of energy primarily on the basis of James Joules's experiments long before Emmy Noether had proven her theorem. This is also the situation today in particle physics. Most of the conservation laws discussed in this section are empirical discoveries since no symmetry has yet been identified that provides their foundation. We will point out a few of these as we proceed.

STUDENTS-HUB.com Uploaded By: Malak Obaid

Baryon Number

In Section 11-4 we mentioned two conservation laws in our discussion of radioactive decay: conservation of nucleon number and of lepton number. We now need to state these more explicitly. The first is a special case of the following more general law:

The baryon number is conserved.

All baryons have baryon quantum number $B = +1$, all antibaryons have $B = -1$, and all other particles are assigned $B = 0$. Conservation of baryon number requires that the total B for all particles before a decay or reaction occurs must be equal to that for all particles afterward. As an example of baryon conservation, consider the production of the antiproton in Figure 12-2 again. The reaction is

$$pp \longrightarrow ppp\,\bar{p} \qquad \textbf{12-7}$$

The total baryon number before the reaction is $B = +1 + 1 = +2$. That after the reaction is $B = +1 + 1 + 1 - 1 = +2$. Thus, conservation of B requires that three protons appear on the right side of Equation 12-7; that is, the production of an antiproton is always accompanied by the production of a proton. Conservation of baryon number together with the conservation of energy implies that the least massive baryon, the proton, must be stable. Whether that is in fact true is currently an active experimental question among particle physicists. There is no known symmetry requiring conservation of baryon number. There are several conceivable proton decay modes, all involving the proton decaying to a lepton and a meson, both of which have $B = 0$. To date, nonconservation of baryon number has never been observed. Current experiments place the lower limit of the proton lifetime at about 10^{32} years. We will return to this matter later in this chapter.

Lepton Number

In the original version of the Standard Model neutrinos have no mass and are polarized. Experiments had shown that neutrinos were left-handed; that is, their spin direction was antiparallel to their momentum, and antineutrinos were right-handed, their spin being parallel to their momentum (see Figure 12-11*a*). In the Standard Model mass arises from interaction with the Higgs boson. That interaction also changes right-handedness to left-handedness and vice versa, so the fact that neutrinos were always detected as left-handed meant that, like the photon, they did not interact with the Higgs and therefore had no mass. This in turn means that lepton number is conserved in the weak interactions and conservation of leptons applies independently to each of the three flavors.

The lepton number for each flavor of leptons is independently conserved.

The lepton quantum number for the electron and the electron neutrino is $L_e = +1$ and that for the positron and electron antineutrino is $L_e = -1$. All other particles, including the other leptons, have $L_e = 0$. In a similar fashion the lepton quantum numbers L_μ are assigned for the muon generation and L_τ for the tau generation. To see how conservation of lepton number works, consider the following decays:

$$p \longrightarrow \pi^0 e^+ \qquad \textbf{12-8}$$

$$\mu^+ \longrightarrow e^+ \nu_e \bar{\nu}_\mu \qquad \textbf{12-9}\boldsymbol{a}$$

$$\mu^+ \longrightarrow e^+ \gamma \qquad \textbf{12-9}\boldsymbol{b}$$

$$n \longrightarrow p e^- \bar{\nu}_e \qquad \textbf{12-10}$$

STUDENTS-HUB.com Uploaded By: Malak Obaid

The decay shown in Equation 12-8 (one of the conceivable proton decay modes) would conserve energy, charge, angular momentum, and linear momentum, but it has not been observed. It conserves neither baryon number B nor lepton number L_e. The decay of the μ^+, given by Equation 12-9*a*, results in both an electron neutrino and a muon antineutrino. The μ^+ has $L_\mu = -1$ and $L_e = 0$. The decay products also have $L_\mu = -1$ (the ν_μ) and $L_e = -1 + 1 = 0$ (the e^+ and ν_e). The μ^+ decay given in Equation 12-9*b* had been searched for by many groups without success for many years. Its absence was the first indicator that L_e and L_μ were independently conserved. Equation 12-10, the decay of the neutron, conserves both B and L_e. Conservation of lepton number implies that the neutrino emitted in the beta decay of a free neutron is an electron antineutrino.

However, during the past several years experiments at the Sudbury Neutrino Observatory and Super-Kamiokande have shown that neutrinos do in fact have mass and oscillate, albeit slowly, from one flavor to another as they travel. This discovery was the first experimental evidence that the Standard Model is an approximation of a more comprehensive, unknown theory. We will speculate briefly on what that theory might be in Section 12-5, but for our discussion here the implications are considerable. Since neutrinos have mass, their speeds are less than c. This implies that a left-handed neutrino can become a right-handed neutrino with respect to an observer and vice versa. Since we know of no fundamental symmetry that requires conservation of leptons, if lepton number is not conserved, then we have no way to distinguish between neutrinos and antineutrinos; the neutrino may be a Majorana particle, as was alluded to in Section 12-1. A number of theoretical extensions of the Standard Model have been suggested to deal with this problem, but as yet there is no clear solution. With this caveat in mind, we will for the remainder of this section use the lepton and baryon conservation laws stated above and defer discussion of the possible consequences of their violation until Section 12-5.

EXAMPLE 12-6 Conservation Laws What conservation laws (if any) are violated by the following reactions?

(a) $n \longrightarrow p\pi^-$ (b) $\Lambda^0 \longrightarrow \bar{p}\pi^+$ (c) $\pi^- \longrightarrow \mu^- \bar{\nu}_\mu$

SOLUTION

(a) There are no leptons in this decay, so there is no problem with the conservation of lepton number. The net charge is zero before and after the decay, so charge is conserved. Also, the baryon number is $+1$ before and after the decay. However, the rest energy of the proton (938.3 MeV) plus that of the pion (139.6 MeV) is greater than the rest energy of the neutron (939.6 MeV). Thus, this decay violates the conservation of energy.

(b) Again, there are no leptons involved, and the net charge is zero before and after the decay. Also, the rest energy of the Λ^0 (1116 MeV) is greater than the rest energy of the antiproton (938.3 MeV) plus that of the pion (139.6 MeV), thus energy is conserved with the loss in rest energy equaling the gain in kinetic energy of the decay products. However, this decay does not conserve baryon number, which is $+1$ for the Λ^0, -1 for the antiproton, and 0 for the pion.

(c) There are no baryons involved, so conservation of baryon number is not a problem. The net charge is -1 before and after the decay, so charge is conserved. Also, the rest energy of the π^- (139.6 MeV) is greater than that of the μ^- (105.7 MeV) and the $\bar{\nu}_\mu$, so energy is conserved, the difference appearing as kinetic energy of the muon and neutrino. Finally, $L_\mu = 0$ on the left side and $L_\mu = 1 - 1 = 0$ on the right side, therefore lepton number is also conserved. This is the reaction by which the π^- decays.

STUDENTS-HUB.com Uploaded By: Malak Obaid

More

Each conservation law results from a particular symmetry in the laws that govern the physical universe. Since it is not necessarily obvious under what mathematical operations the laws of physics will be symmetric, on a pragmatic level it is fair to ask, quantum mechanically, *When Is a Physical Quantity Conserved?* We provide an answer to this question on the home page: www.whfreeman.com/tiplermodernphysics5e. See also Equations 12-11 through 12-22 and Note 12 here, as well as Example 12-7.

More Conservation Laws

The quantum numbers and corresponding conservation laws of the hadrons described in this section arise logically from combinations of so-called *internal quantum numbers* of the quarks. These are listed in Table 12-5. They are the electric charge Q, baryon number B, strangeness S, charm C, bottom B', and top T. As we have noted above, electric charge and baryon number are conserved in all interactions. Strangeness, charm, bottom, and top are conserved in the strong and electromagnetic interactions but are not conserved in the weak interaction.

Strangeness There are some conservation laws that are not universal but apply only to certain kinds of interactions. In particular, there are quantities that are conserved in decays and reactions that occur via the strong interaction but not in decays or reactions that occur via the weak interaction. This is somewhat analogous to the selection rules discussed in atomic transitions. For example, the selection rule $\Delta\ell = \pm 1$ holds for electric dipole transitions from one atomic state to another. An atom in a state with $\ell = 2$ cannot decay to a lower energy state with $\ell = 0$ via electric dipole radiation because of this selection rule, but it can decay via an electric quadrupole transition, which is generally much slower than electric dipole transitions. One of the particularly important quantities conserved in strong interactions is *strangeness*. This quantity was introduced by M. Gell-Mann[13] and K. Nishijima in 1952 to explain the seemingly strange behavior of the heavy baryons and mesons.

Table 12-5 Internal quantum numbers of the quarks

Quark	Q	B	U	D	C	S	T	B'
u	2/3	1/3	1	0	0	0	0	0
d	−1/3	1/3	0	−1	0	0	0	0
c	2/3	1/3	0	0	1	0	0	0
s	−1/3	1/3	0	0	0	−1	0	0
t	2/3	1/3	0	0	0	0	1	0
b	−1/3	1/3	0	0	0	0	0	−1

STUDENTS-HUB.com Uploaded By: Malak Obaid

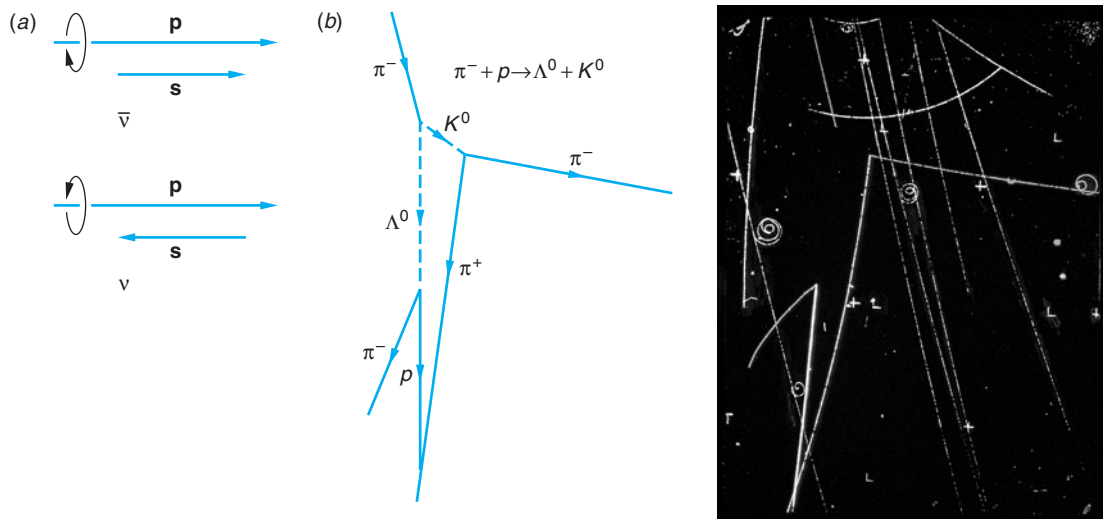

Figure 12-11 (*a*) The spin of antineutrinos is parallel to their momentum. The spin of neutrinos is antiparallel to their momentum. Described in terms of *helicity* $= m_s/s$ with the z axis in the direction of **p**, antineutrinos have helicity $+1$ and neutrinos have helicity -1. (*b*) An early photograph of bubble chamber tracks at the Lawrence Berkeley Laboratory, showing the production, represented by Equation 12-23, and decay of two strange particles, the K^0 and the Λ^0. These neutral particles are identified by the tracks of their decay particles. The lambda particle was so named because of the similarity of the tracks of its decay particles and the Greek letter Λ. The incident π^- meson had energy of 1 GeV. [*(b) Lawrence Berkeley Laboratory/Photo Researchers.*]

Consider the reaction in which a high-energy π^- interacts with a proton,

$$p\pi^- \longrightarrow \Lambda^0 K^0 \qquad \textbf{12-23}$$

shown in Figure 12-11*b*. The cross section for this reaction is large, as would be expected since it takes place via the strong interaction (see Example 12-5). However, the decay times for both Λ^0 and K^0 are of the order of 10^{-10} s, which is characteristic of the weak interaction. When first discovered, their unexpectedly long lifetimes were very strange, so these and other particles showing similar behavior were called *strange particles*. An early success of the quark model was the explanation of these unexpectedly long lifetimes. As an example, the Λ^0 is a *uds* quark combination, which corresponds to a particular set of the internal quark quantum numbers. If no lighter (i.e., lower-energy) hadron with that exact set of quantum numbers exists, then decay via the strong or electromagnetic interaction is not possible. Decay can only occur via the much slower weak interaction.

These particles are always produced in pairs and never singly, even when all other conservation laws are met. This behavior is described by assigning to them a new quantum number called *strangeness*. The strangeness of the ordinary hadrons—the nucleons and pions—was arbitrarily chosen to be zero. The strangeness of the K^0 was arbitrarily chosen to be $+1$. Therefore, the strangeness of the Λ^0 particle must be -1 so that strangeness is conserved in the reaction of Equation 12-23. The strangeness of other particles could then be assigned by looking at their various reactions and decays. In reactions and decays that occur via the strong and electromagnetic interactions, strangeness is conserved. In those that occur via the weak interaction, strangeness is not conserved but can only change by ± 1.

STUDENTS-HUB.com Uploaded By: Malak Obaid

Isospin As pointed out earlier, a striking feature of the hadrons is that they cluster into *charge multiplets*, groups of particles with nearly the same mass, such as the multiplet consisting of the proton ($p = uud$) and neutron ($n = udd$). Within each multiplet all of the particles have the same spin, parity (see below), baryon number, strangeness, charm, and bottom but differ in their electric charges. In addition, we learned in Section 11-5 that the strong (nuclear) force is independent of electric charge. Were it not for the masses of the quarks and the electromagnetic interaction, the masses of the particles in a given charge multiplet would be the same. We are thus led to the view that the members of the multiplet are simply different charge states of the same particle. The "splitting" of particle mass states is analogous to the splitting of atomic energy states due to the spin-orbit interaction. (See Section 7-5.) Because of the analogy with isotopes (atoms with the same Z but slightly different masses) and with the splitting of different spin states, the term *isospin* is used to describe this multiplicity. The isospin $\mathbf{I}$ is treated as a vector in a three-dimensional "charge space," just as the orbital angular momentum $\mathbf{L}$ is a vector in real space. The component of $\mathbf{I}$ in the "z direction" is called I_3 and is quantized, just as the z components of the orbital and intrinsic angular momenta of atomic electrons are quantized. Similarly, there are $(2I + 1)$ different I_3 states. The charge q on a particle is related to its value of I_3 by

$$q = eQ = e\left(I_3 + \frac{B + S}{2}\right) \qquad \textbf{12-24}$$

where Q is the charge quantum number. The value of I of the nucleon is $1/2$, with the two possible values $I_3 = +1/2$ for the proton and $I_3 = -1/2$ for the neutron. The isospin I is also $1/2$ for the xi doublet and 0 for the lambda and omega singlets. It is 1 for the Σ triplet (with $I_3 = +1$ for Σ^+, 0 for Σ^0, and -1 for Σ^-). In the case of the mesons, the pion isospin triplet has $I = 1$, the kaon doublet $I = 1/2$, and the eta singlet $I = 0$. The rules for combining isospin are the same as those for combining real spin or angular momentum. If only the strong interaction is present, then I_{op} and H_{op} commute and $\mathbf{I}$ is conserved. Decays and reactions in which the total isospin of the system is not conserved do not proceed via the strong interaction.

Hypercharge Four of the quantum numbers that we have discussed thus far turn out to be related to one another. These are strangeness, charge, isospin, and baryon number. The relation is

$$S = 2(Q - I_3) - B \qquad \textbf{12-25}$$

Strangeness is now used less frequently than a simpler quantity called *hypercharge* Y, which is defined as

$$Y \equiv B + S + C + B' + T \qquad \textbf{12-26}$$

With the aid of Equation 12-25 the hypercharge quantum number Y is then given by

$$Y = S + B = 2(Q - I_3) \qquad \textbf{12-27}$$

Stated simply, the hypercharge is twice the average charge of a given multiplet. For example, the average charge of the nucleon multiplet is $(1e + 0)/2 = (1/2)e$. Thus, for the nucleon, $Y = 1$, as given by Equation 12-27. Since baryon number is strictly conserved and strangeness is conserved only in strong interactions, hypercharge, too, is conserved only in strong interactions. Since $\Delta S = \pm 1$ or 0 in weak interactions,

STUDENTS-HUB.com Uploaded By: Malak Obaid

Table 12-6 Some quantum numbers of the hadrons that are stable against decay via the strong interaction

Particle	Spin ($\hbar$)	I	I_3	B	S	Y
p	1/2	1/2	+1/2	1	0	1
n	1/2	1/2	−1/2	1	0	1
Λ^0	1/2	0	0	1	−1	0
Σ^+	1/2	1	+1	1	−1	0
Σ^0	1/2	1	0	1	−1	0
Σ^-	1/2	1	−1	1	−1	0
Ξ^0	1/2	1/2	+1/2	1	−2	−1
$\Xi-$	1/2	1/2	−1/2	1	−2	−1
$\Omega-$	3/2	0	0	1	−3	−2
π^+	0	1	+1	0	0	0
π^0	0	1	0	0	0	0
π^-	0	1	−1	0	0	0
K^+	0	1/2	+1/2	0	+1	+1
K^0	0	1/2	−1/2	0	+1	+1
η^0	0	0	0	0	0	0

changes in hypercharge are similarly restricted to $\Delta Y = \pm 1$ or 0. Table 12-6 lists the values of these additional quantum numbers for those hadrons that are stable against decay via the strong interaction. Note that, if it were not for the conservation of strangeness or hypercharge in the strong interaction, all the baryons except the nucleons would decay via the strong interaction and live only for about 10^{-23} s.

The singlet, doublet, and triplet charge multiplets discussed above are clearly represented in graphs of Y versus I_3. Studies of the regularities apparent in such graphs (see Figure 12-12) were instrumental in the development of the quark model of fundamental particles to be discussed in Section 12-4. The regularities are analogous to those observed in the multiplet structure of atomic energy states that ultimately led to the understanding of atomic structure.

The conservation laws and the properties of charge Q, lepton number L, baryon number B, and strangeness S give us some insight into the relation between particles and their antiparticles. A particle and its antiparticle must have opposite signs for the values of each of these properties. Any particle that has a nonzero value for any of these properties will therefore have a distinct antiparticle. The photon, graviton, and the π^0 have $Q = 0$, $L = 0$, $B = 0$, and $S = 0$ and are therefore in some sense their own antiparticles. The π^+ and π^- mesons are somewhat special because they have charge but have zero values for L, B, and S. They are therefore antiparticles of each other, but since there is no conservation law for mesons, it is impossible to say which is the particle and which is the antiparticle.

STUDENTS-HUB.com Uploaded By: Malak Obaid

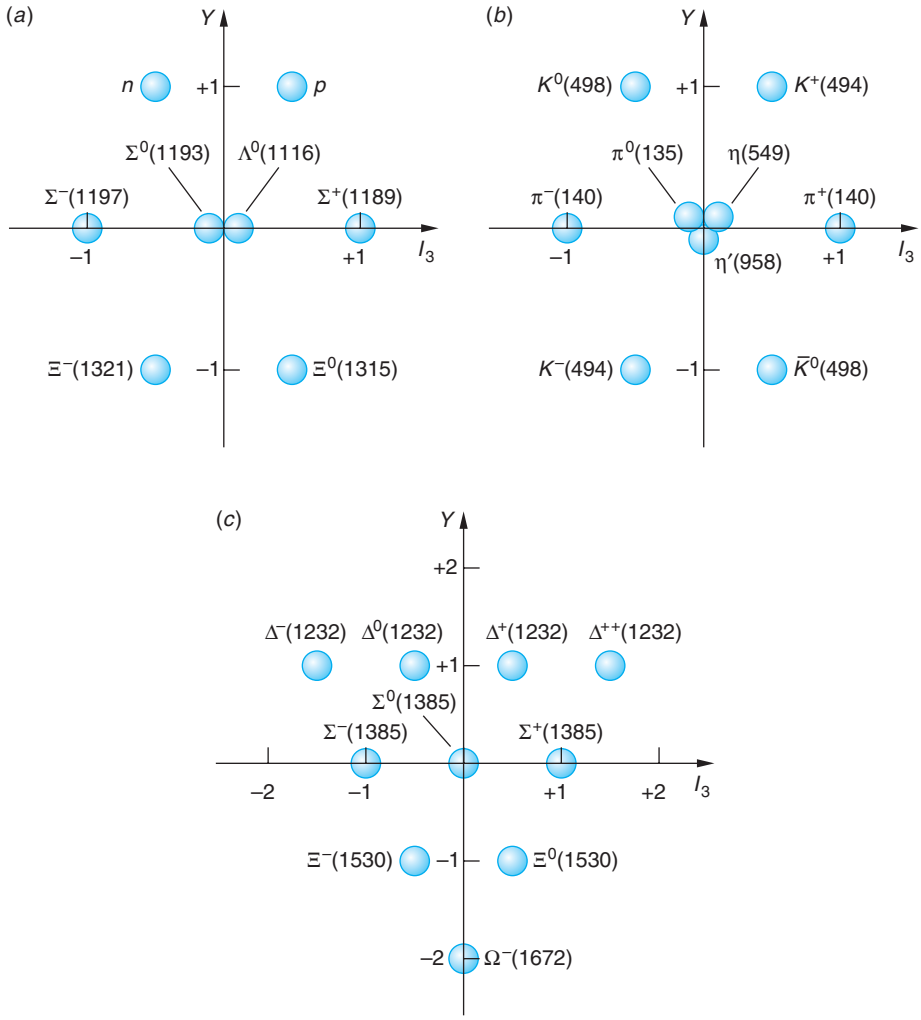

Figure 12-12 Graphs of hypercharge Y vs. the I_3 component of the isospin. (*a*) Baryons with spin 1/2. (*b*) Mesons with spin 0. (*c*) Baryons with spin 3/2. Except for the Ω^-, these are resonance particles, as discussed in Section 12-3 and on the home page. Masses in parentheses are in MeV/c^2. Notice in each case that particles of like charge lie along downward-sloping diagonals and particles of like hypercharge (and strangeness) lie along horizontal lines.

EXAMPLE 12-8 **Applying the Conservation Laws** State whether the following decays can occur via the strong interaction, via the electromagnetic interaction, via the weak interaction, or not at all:

(*a*) $\Sigma^+ \longrightarrow p\,\pi^0$ (*b*) $\Sigma^0 \longrightarrow \Lambda^0\gamma$ (*c*) $\Xi^0 \longrightarrow n\pi^0$

SOLUTION

We first note that the mass of each decaying particle is greater than that of the decay products, so there is no problem with energy conservation in any of the decays. In addition, there are no leptons involved in any of the decays, and charge and baryon number are both conserved in all the decays.

(*a*) From Figure 12-12, we can see that the hypercharge of the Σ^+ is 0, whereas the hypercharge of the proton is +1 and that of the pion is 0. This decay is possible via the weak interaction but not the strong interaction. It is, in fact, one of the decay modes of the Σ^+ particle, with a lifetime of the order of 10^{-10} s.

STUDENTS-HUB.com Uploaded By: Malak Obaid

(*b*) Since the hypercharge of both the Σ^0 and Λ^0 is 0, this decay can proceed via the electromagnetic interaction. It is the dominant mode of decay of the Σ^0 particle, with a lifetime of about 10^{-20} s.

(*c*) The hypercharge of the Ξ^0 is -1, whereas that of the neutron is $+1$ and that of the pion is 0. Since hypercharge cannot change by 2 in a decay or reaction, this decay cannot occur.

Questions

9. How can you tell if a decay proceeds via the strong, electromagnetic, or weak interactions?
10. Can the strangeness or hypercharge of a new particle be determined even if the number of particles in the multiplet is unknown? How or why not?

Parity The *parity* of a nucleus or particle is defined in the same way as for an atom. (See Section 6-5.) The parity operation reflects the space variables in the coordinate origin. If the parity operator acting on the wave function changes the sign of the wave function, the parity is said to be odd, or -1. If the wave function does not change sign, the parity is even, or $+1$. The parity quantum number P is different from the other quantum numbers we have been considering. It can have only the values $+1$ or -1. If the value of the parity of a system changes, the new value is -1 times the old value. Parity is therefore a multiplicative property rather than an additive property like baryon number, strangeness, or hypercharge. The parity of an atomic wave function is related to the orbital angular momentum by $P = (-1)^{\ell}$. The parity is odd or even depending on whether ℓ is odd or even. In our discussion of radiation from atoms, we saw that the parity of an atom can change just as the angular momentum of the atom changes when the atom emits light. For electric dipole transitions, $\Delta\ell = \pm 1$, so the parity and angular momentum quantum numbers always change. However, if the complete system, including the photon, is considered, the total angular momentum and the total parity do not change in atomic transitions; that is, parity is conserved in electromagnetic interactions. Parity is also conserved in the strong interaction.

Until 1956 it was assumed that parity is conserved in all nuclear reactions and radioactive decays. In that year, T. D. Lee and C. N. Yang suggested that parity might not be conserved in weak interactions. This suggestion grew out of attempts to understand the peculiar behavior of what were then known as the τ and θ mesons. These particles were identical in every way except that the θ meson decayed into two pions with positive parity, whereas the τ decayed into three pions with negative parity. (Each elementary particle can be assigned an intrinsic parity. That of the pion is negative.) The τ-θ puzzle was this: Are there two different particles with all properties identical except parity, or is it possible that parity is not conserved in some reactions? After careful study Lee and Yang found that all the experimental evidence for parity conservation pertained to strong or electromagnetic interactions and not for weak interactions. They suggested that the nonconservation of parity could be observed experimentally by measuring the angular distribution of electrons emitted in β decay of nuclei that have their spins aligned. Such an experiment was performed in December 1956 by a group led by C. S. Wu and E. Ambler. The results confirmed Lee and Yang's predictions, for which they received the Nobel Prize in Physics in 1957. The τ and θ mesons are a single particle, now known as the K^0 meson, which has two distinct modes of decay. The significance of the K^0 decay will be discussed further in the TCP Invariance section below.

STUDENTS-HUB.com Uploaded By: Malak Obaid

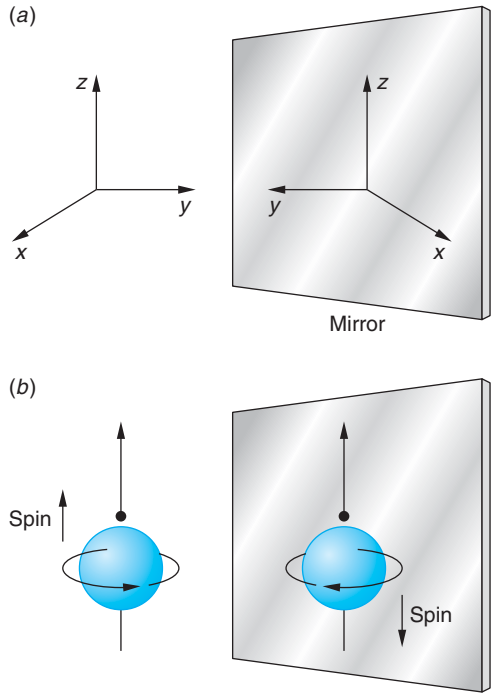

Figure 12-13 (*a*) The mirror image of a right-handed coordinate system ($\mathbf{x} \times \mathbf{y}$ in the $\mathbf{z}$ direction) is a left-handed coordinate system ($\mathbf{x} \times \mathbf{y}$ in the $-\mathbf{z}$ direction). No combination of translation and rotation can change a right-handed coordinate system into a left-handed system. (*b*) Spinning nucleus emitting an electron in the direction of its spin. In the mirror, the image nucleus is emitting the electron in the direction opposite to its spin because the mirror reverses the direction of the spin vector.

The conservation of parity essentially means that a process described by the coordinates x, y, and z appears the same if described by the coordinates $x' = -x$, $y' = -y$, and $z' = -z$. The system x, y, z is called a *right-handed coordinate system* because $\mathbf{x} \times \mathbf{y}$ is in the $+\mathbf{z}$ direction. Similarly, the system x', y', z' is called a *left-handed coordinate system* because $\mathbf{x}' \times \mathbf{y}'$ is in the negative $\mathbf{z}'$ direction. No rotation can change a right-handed coordinate system into a left-handed one, but reflection in a mirror does, as shown in Figure 12-13*a*. We can thus state the law of conservation of parity in more physical terms: If parity is conserved, the mirror image of a process cannot be distinguished from the process itself. Figure 12-13*b* shows a spinning nucleus emitting an electron in the direction of its spin. In the mirror, the nucleus appears to be emitting the electron in the direction opposite to that of its spin. If parity is conserved in β decay, the chance of emission in the direction of the nuclear spin must equal the chance of emission in the opposite direction; i.e., there can be no preferred direction. Whether or not one direction is actually preferred in β decay is usually not observable because the nuclear spins are randomly oriented. Wu and Ambler aligned the nuclei in ^{60}Co by placing their sample in a magnetic field at a very low temperature (about 0.01 K). They found that more particles were emitted opposite to the spin of the nucleus than in the direction of the spin, indicating that parity is not conserved in weak interactions. Table 12-7 summarizes the conservation laws discussed in this section.

TCP Invariance It is a property of any relativistic quantum theory in which signal speeds cannot exceed the vacuum speed of light, that the combined operations of *P*arity ($\mathbf{r} \rightarrow -\mathbf{r}$), *T*ime reversal ($t \rightarrow -t$), and *C*harge conjugation (particle $\rightarrow$ antiparticle) leave any wave function unchanged:

$$TCP\,\Psi(\mathbf{r}, t) = +1\,\Psi(\mathbf{r}, t) \quad \text{or} \quad TCP = +1 \qquad \textbf{12-28}$$

STUDENTS-HUB.com Uploaded By: Malak Obaid

Table 12-7 Conserved quantities in fundamental particle interactions

Conserved quantity	Interaction		
	Strong	Electromagnetic	Weak
Energy, Momentum, Charge (Q), Baryon number (B), Lepton number (L)	Yes	Yes	Yes
Isospin (I)	Yes	No	No ($\Delta I = \pm 1, 0$)
Hypercharge (Y)	Yes	Yes	No ($\Delta Y = \pm 1, 0$)
Strangeness (S)	Yes	Yes	No ($\Delta S = \pm 1, 0$)
Parity (P)	Yes	Yes	No

It makes no difference in what order the operations are performed. Invariance under these combined operations requires that particles and their antiparticles have the same masses and lifetimes. It was long thought that the invariance under the combined operations was the result of invariance of physical laws under each of the operations independently, i.e., $T = +1$, $P = +1$, and $C = +1$.

However, as we described in the previous section, it was discovered that parity was not conserved in weak interactions. For the weak interaction the parity operation yields $P = -1$. That immediately implies that one of the other operations must not be conserved in the weak interaction. Lee and Yang's solution to the $\tau - \theta$ puzzle revealed that there are two K^0 mesons (kaons) with nearly identical masses but very different decay modes and lifetimes. The K_S^0 (S for "short") decays to two pions with a lifetime of about 0.9×10^{-10} s. The K_L^0 (L for "long") decays to three pions with a lifetime of about 0.5×10^{-7} s. (See Table 12-3.)

Then in 1964 J. H. Christenson and his collaborators showed that in about 1 of every 1000 decays, the K_L^0 also decayed into just two pions. This result means that for the K_L^0 decay, the combined operation $CP = -1$ because the two-pion final system has $CP = +1$ and the three-pion final system has $CP = -1$.

The implications of this result are enormous and continue to be a focus of intense theoretical and experimental research. For example, within the framework of the Standard Model, CP violation requires that there be three generations of quarks and, correspondingly, the very large number of hadrons that can be assembled from them. The observed matter-antimatter asymmetry in the universe also requires CP violation. If $TCP = +1$ and $CP = -1$, $T = -1$ also, which establishes an absolute direction for the flow of time.

Questions

11. Suppose a new uncharged meson is discovered. What condition is necessary for it to have a distinct antiparticle?
12. How might Table 12-7 be different if strangeness were not conserved in interactions between hadrons?

STUDENTS-HUB.com Uploaded By: Malak Obaid

More

Particles and excited states of particles that decay via the strong interaction have mean lives of only 10^{-23} s or so, not nearly long enough to be tracked by a particle detector. Such particles are instead detected by measuring resonances in the scattering cross sections in a way analogous to J. Franck and G. Hertz's detection of the first excited state of the Hg atom by measuring the resonances in the electron scattering from Hg atoms. Many fundamental particles have been found in this way, as is described on the home page (www.whfreeman.com/tiplermodernphysics5e), *Resonances and Excited States*, which also includes a partial list of meson and baryon resonances. See also Figures 12-14 through 12-16, Table 12-8, Equations 12-29 through 12-31, and Examples 12-9 and 12-10 here.

12-4 The Standard Model

The Standard Model is currently (since 1978) the accepted theory of elementary particle physics. It includes the *quark model* of particle structure that had been developed earlier, the unified theory of electromagnetic and weak interactions called the *electroweak theory*, and the strong-interaction analog of quantum electrodynamics called *quantum chromodynamics* (QCD). It has been remarkably though not totally successful in explaining the characteristics of fundamental particles and the interactions between them and is second only to QED in the accuracy of its predictions. In our discussions thus far in this chapter we have had occasion to allude to a number of specific features of the Standard Model. In this section we will consider the three of its constituents noted above in further detail. Since the complexity of the Standard Model's mathematical detail is beyond the level of this book, our discussion will be largely qualitative and conceptual.

Searches for experimental support for the Standard Model led to the development of many new types of particle detectors. Several have found applications beyond particle physics, one example being BGO crystal detectors, used in medical diagnostic PET scanners (see Figure 11-65).

Quark Model of the Hadrons

The Eightfold Way The construction of large high-energy particle accelerators beginning in the 1950s made possible the production of a flood of previously unseen hadrons.[14] Among the many attempts at understanding and classifying the jumble of hadrons, the most successful scheme is known as the *eightfold way*.[15] It was suggested independently by Gell-Mann and Y. Ne'eman in 1961 and subsequently justified by the Standard Model. In this scheme, hadrons that make up the charge multiplets were arranged in groups, called *supermultiplets*, in which each member had the same intrinsic spin and parity, J^P, where J is the intrinsic spin and P is the parity. Three of Gell-Mann's supermultiplets are shown in Figure 12-12: (*a*) the eight lightest baryons, called the *baryon octet*; (*b*) the eight lightest mesons, the *meson octet* (actually a *nonet*); and (*c*) the next 10 heavier baryons, the *baryon decuplet*. Figure 12-17 shows the energies of the baryon octet in a diagram analogous to the fine-structure splitting of atomic states. The energy splittings between the isospin multiplets (from 78 to 176 MeV) are about 20 times the splitting within the multiplets. There are no completed baryon supermultiplets beyond the octet and decuplet, although there are several partially completed ones. The known mesons complete six nonets. Note that there is also an *antibaryon* octet, decuplet, etc., but for the mesons their antiparticles are members of the same nonet. Gell-Mann's accomplishment is the elementary

STUDENTS-HUB.com Uploaded By: Malak Obaid

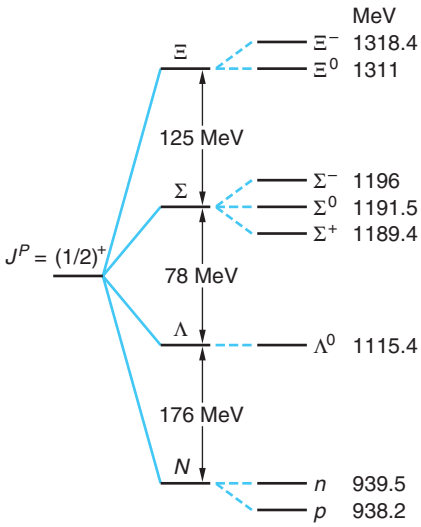

Figure 12-17 The energy-level diagram of the baryon octet, the supermultiplet of the hadronically stable $J^P = (1/2)^+$ baryons. In the absence of any interactions, all these particles should have the same mass. The different numbers of *s* quarks splits the mass state into four states, corresponding to the nucleon (*N*), lambda (Λ), sigma (Σ), and xi (Ξ) particles. The different quark masses and the weaker electromagnetic interaction further splits the particles into the *N* doublet, Σ triplet, and Ξ doublet.

particle analog of Mendeleev's development of the periodic table of the chemical elements, which was first published in 1869, nearly 100 years earlier, far in advance of the theoretical foundation for the periodic table provided by atomic theory and quantum mechanics.

The eightfold way is based on part of a mathematical theory known as the theory of continuous groups that was developed by the Norwegian mathematician S. Lie, among others. The simplest Lie group is known as SU(2), for *s*pecial *u*nitary group of 2×2 matrices. A special condition on the 2×2 arrays reduces the number of components from 4 to 3. The three independent components of these arrays correspond to the three components of angular momentum (or isospin). As we have seen previously, the various possible values of angular momentum J have corresponding states that occur in multiplets having 1, 2, 3, 4, . . ., $(2J + 1)$ elements, which we describe as having angular momentum of $0, 1/2, 1, 3/2, \ldots \hbar$ units. The next higher Lie group is known as SU(3), for *s*pecial *u*nitary group of 3×3 arrays. Again, a special condition reduces the number of components from 9 to 8 (hence the name *eightfold way*). The eight quantities in the application of SU(3) group theory to hadrons consist of the three components of isospin, the hypercharge, and four that are yet to be named. Without going into the details of group theory, we will merely state that the SU(3) group leads to multiplets of 1, 3, 8, 10, . . . elements. Rather than assigning a single number to these multiplets analogous to the angular momentum quantum number of SU(2), it is more useful to make two-dimensional diagrams called *weight diagrams*, which are the geometric patterns of points, triangles, and hexagons shown in Figure 12-18. In the application of SU(3) to particle theory, the axes are Y and I_3, as in Figure 12-12.

In the plot of Y versus I_3 for the $J^P = 3/2^+$ baryons (the decuplet shown in Figure 12-12*c*), neither the Ξ nor the Ω^- had been discovered prior to 1961. Note that the difference in rest energy between each line of the decuplet is about 140 MeV. A constant energy difference between successive multiplets in the decuplet is predicted by SU(3) theory. The prediction of the Ω^- particle by Gell-Mann in 1961 and its discovery in 1964 with just the mass and spin Gell-Mann had predicted was one of the spectacular successes of the pre–Standard Model eightfold way. Note that the Ω^- is the only particle in the decuplet that is not a resonance particle. The mass of the Ω^- is just small enough that energy conservation prevents it from decaying via a strangeness-conserving strong interaction such as $\Omega^- \longrightarrow \Xi^0 + K^-$.

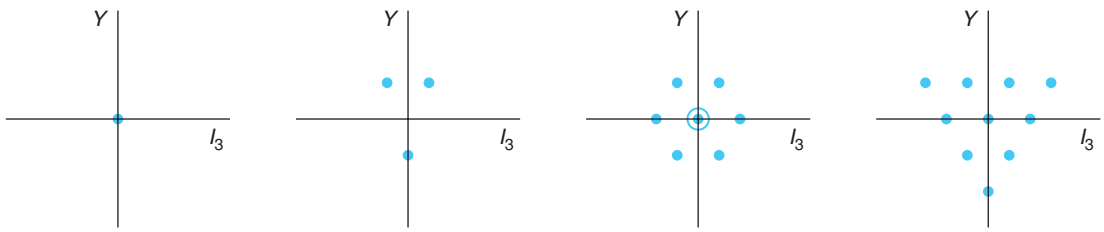

Figure 12-18 Weight diagrams occurring in SU(3) group theory. The circle and dot at the origin in the hexagon indicate two particles at the origin, making this pattern an octet.

STUDENTS-HUB.com Uploaded By: Malak Obaid

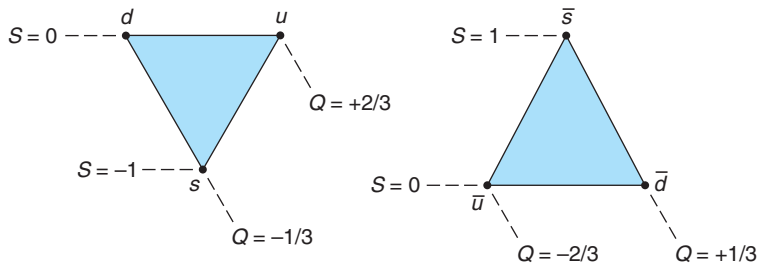

Figure 12-19 The SU(3) weight diagrams (Y vs. I_3) for the three light quarks and their antiquarks. As in the supermultiplet diagrams of the eightfold way, the downward-sloping lines are constant charge and the horizontal lines are constant strangeness.

Murray Gell-Mann, who proposed the existence of strangeness, developed the classification system for hadrons [SU(3)] and postulated the existence of fractionally charged particles, which he called quarks. He won the Nobel Prize in Physics in 1969. [*American Institute of Physics, Neils Bohr Library.*]

Other supermultiplets can be formed from the unstable baryons and mesons, but there are no observed groups of three particles corresponding to the triplet allowed by SU(3) theory, illustrated second from the left in Figure 12-18. This fact and the absence of a *reason* for the supermultiplets of the eightfold way led Gell-Mann and G. Zweig in 1964 to independently propose that all hadrons are composed of even more fundamental constituents called quarks.[16] Their proposal is the basis of the quark model, arguably the most important advance in our understanding of elementary particles.

In the original quark model, quarks came in three types labeled u, d, and s (for *u*p, *d*own, and *s*trange). Later discoveries, as we have seen, added three more quarks, labeled c, b, and t for *c*harm, *b*ottom, and *t*op. Recall that the charge of the u quark is $2e/3$ and that of the d and s quarks is $-e/3$. Each quark has $B = 1/3$. Each quark has spin $1/2$. The strangeness of the u and d quark is 0 and that of the s quark is -1. Each quark has an antiquark with the opposite electric charge, baryon number, and strangeness. The three types up, down, and strange form the triangular SU(3) weight diagram of Figure 12-18, as shown in detail in Figure 12-19. The properties of the quarks are listed in Table 12-2. The basic assertion of the quark model is that all baryons consist of three quarks (or three antiquarks for antiparticles), whereas mesons consist of a quark and an antiquark. The mesons thus have baryon number $B = 0$, as required. The proton consists of the combination uud and the neutron udd. Baryons with a strangeness $S = -1$ contain one s quark. All the particles listed in Table 12-3 can be constructed from the three original quarks and the corresponding three antiquarks.[17]

A great success of the quark model was that all of the allowed combinations of the three quarks and quark-antiquark pairs resulted in known hadrons. Strong evidence for the existence of quarks inside the nucleons is provided by high-energy scattering experiments called *deep inelastic scattering*. In these experiments, a nucleon is bombarded with electrons or muons of energies from 15 to 200 GeV. Analyses of particles scattered at large angles indicate the presence within the nucleon of spin-1/2 particles of sizes much smaller than that of the nucleon. These experiments are analogous to Rutherford's scattering of α particles by atoms in which the presence of a tiny nucleus in the atom was inferred from the large-angle scattering of the α particles.

STUDENTS-HUB.com Uploaded By: Malak Obaid

Table 12-9 Properties of three-quark combinations

Combination	Spin ($\hbar$)	Charge (e)	Baryon number	Strangeness	Hypercharge	I_3
uuu	3/2	+2	1	0	+1	+3/2
uud	1/2, 3/2	+1	1	0	+1	+1/2
udd	1/2, 3/2	0	1	0	+1	−1/2
uus	1/2, 3/2	+1	1	−1	0	+1
uss	1/2, 3/2	0	1	−2	−1	+1/2
uds	1/2, 3/2	0	1	−1	0	0
ddd	3/2	−1	1	0	+1	−3/2
dds	1/2, 3/2	−1	1	−1	0	−1
dss	1/2, 3/2	−1	1	−2	−1	−1/2
sss	3/2	−1	1	−3	−2	0

Since the conservation laws represented by the several quantum numbers in Table 12-5 are additive, it is simply a matter of arithmetic to determine the properties of the hadrons. For example, a particle formed by the combination uds can have a spin of either 1/2 or 3/2, charge equal to $+2/3 - 1/3 - 1/3 = 0$, and baryon number $B = 1/3 + 1/3 + 1/3 = 1$. Table 12-9 lists the possible three-quark combinations (baryons), and Table 12-10 lists the possible quark-antiquark combinations (mesons).

Table 12-10 Properties of quark-antiquark combinations for three quarks

Combination	Spin ($\hbar$)	Charge (e)	Baryon number	Strangeness	Hypercharge	I_3
$u\bar{u}$	0, 1	0	0	0	0	0
$u\bar{d}$	0, 1	+1	0	0	0	+1
$u\bar{s}$	0, 1	+1	0	+1	+1	+1/2
$d\bar{u}$	0, 1	−1	0	0	0	−1
$d\bar{d}$	0, 1	0	0	0	0	0
$d\bar{s}$	0, 1	0	0	+1	+1	−1/2
$s\bar{u}$	0, 1	−1	0	−1	−1	−1/2
$s\bar{d}$	0, 1	0	0	−1	−1	+1/2
$s\bar{s}$	0, 1	0	0	0	0	0

STUDENTS-HUB.com Uploaded By: Malak Obaid

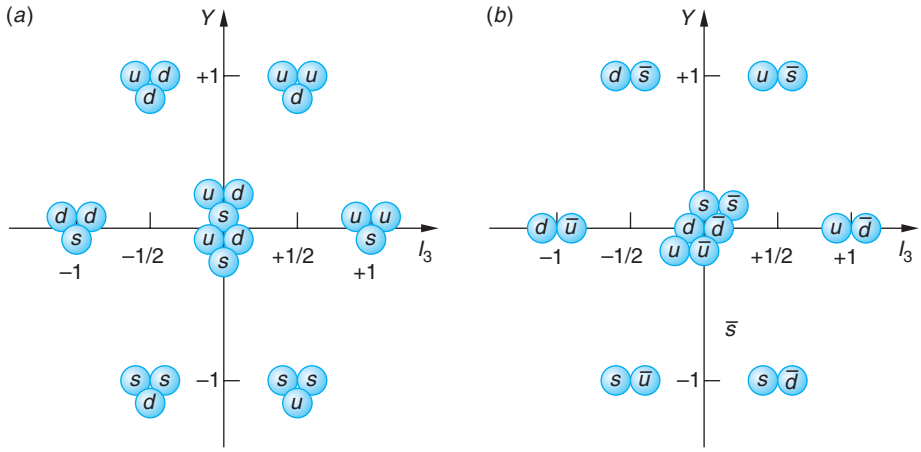

Figure 12-20 (*a*) The graph of Y vs. I_3 for the spin-1/2 three-quark combinations—the baryon octet. (*b*) The graph of Y vs. I_3 for the quark-antiquark combinations that form the lightest meson nonet.

The eight spin-1/2 baryons make up the baryon octet of Figure 12-12*a*. The three quarks of which each member is composed are shown in Figure 12-20*a*. Notice that Table 12-10 lists *nine* quark-antiquark combinations, rather than eight, as given by the eightfold way. The ninth meson identified by the quark model as a part of this group, the η', had already been found but had been thought to be a singlet in the eightfold way. Figure 12-20*b* shows the quark-antiquark composition of the first of the several meson nonets, the one illustrated in Figure 12-12*b*.

EXPLORING
Where Does the Proton Get Its Spin?

In the quark model of the hadrons the proton consists of two up quarks and a down quark, *uud*. The electric charge and quantum numbers of the proton, as with the neutron and other composite particles, are correctly given by summing the corresponding quantities for the constituent quarks. For example, the proton's charge is $+(2/3)e + (2/3)e - (1/3)e = +1e$, and its spin is the $+1/2\hbar$ combination of the three spin $1/2\hbar$ quarks. However, a series of deep inelastic scattering experiments of electrons and muons on protons have yielded a surprising result. Begun in 1987 at CERN and continued up to the present there and at Brookhaven National Laboratory (Relativistic Heavy Ion Collider, RHIC) and the Thomas Jefferson National Accelerator Facility, the experiments consist of scattering extremely high-energy (= very short wavelength) muons or electrons whose spins are polarized from protons and ^{3}He nuclei whose spins are also polarized. Measuring the exit angles and energies of the scattered particles is a rich source of information concerning the spin structure of both the proton and the neutron. Surprisingly, the experimental results indicate that the spins of the three constituent, or "valence," quarks account for only 20 to 30 percent of the proton's spin! The experiments show that the spins of the *u* quarks are aligned parallel with the proton's spin, but this is not true for the spin of the *d* quark, which is as one would expect it to be. These results suggest that the orbital angular momentum of the valence quarks and perhaps the spins of the gluons and the "sea" quarks make a significant contribution to the nucleon spin. Aptly called "the proton spin crisis," the results have underscored that our understanding of nucleon structure and quantum chromodynamics (QCD) is incomplete in some important respects.

STUDENTS-HUB.com Uploaded By: Malak Obaid

Nor does the spin crisis stop there. The results also show that the "sea" of virtual quark-antiquark pairs that surround the valence quarks (just as virtual pions surround the nucleons themselves in the nucleus) is strongly polarized with its collective spin direction *opposite* to the proton's net spin. Even more mysterious, the "sea" turns out to contain a significant number of strange (s) quarks. As one scientist put it, there is no simple "gee whiz" explanation for the spin crisis. Several theories have been advanced to account for the discovery, but thus far none have been successful. The spin crisis is currently the focus of vigorous experimental and theoretical research.

EXAMPLE 12-11 Predicting the Properties of Particles What are the properties of the particles made up of the following quarks: (*a*) $u\bar{d}$, (*b*) $\bar{u}d$, (*c*) dds, and (*d*) uss?

SOLUTION

(*a*) Since $u\bar{d}$ is a quark-antiquark combination, it has baryon number 0 and is therefore a meson. There is no strange quark here, so the strangeness of the meson is zero. The charge of the up quark is $+2/3e$ and that of the anti-down quark is $+1/3e$, so the charge of the meson is $+1e$. This is the quark combination of the π^+ meson.

(*b*) The particle $\bar{u}d$ is also a meson with zero strangeness. Its electric charge is $-2/3e + (-1/3e) = -1e$. This is the quark combination of the π^- meson.

(*c*) The particle dds is a baryon with strangeness -1 since it contains one strange quark. Its electric charge is $-1/3e - 1/3e - 1/3e = -1e$. This is the quark combination for the Σ^- particle.

(*d*) The particle uss is a baryon with strangeness -2. Its electric charge is $+2/3e - 1/3e - 1/3e = 0$. This is the quark combination for the Ξ^0 particle.

Color In Section 12-1 we briefly introduced the concept of the color charge of the quarks. In this section we will extend that discussion to include some important quark and hadron properties related to color. The quark model as described thus far in Section 12-4, essentially that developed over the decade following the introduction of Gell-Mann's quark hypothesis, contained two significant problems: despite numerous experimental searches, no free quarks had been found, and the model's construction of baryons was inconsistent with the Pauli exclusion principle. For example, the $\Delta^{++}(1232)$ has spin 3/2 and thus contains three u quarks (fermions) with exactly the same set of quantum numbers.

The solution to the exclusion-principle dilemma came from O. W. Greenberg, who postulated that each quark flavor (u, d, and s) came in three *colors* in addition to their other properties. The color charge of a quark has three possible values: *r*ed, *b*lue, and *g*reen. Thus, a blue quark would have blueness $+1$, redness 0, and greenness 0, and its antiquark would have blueness -1, and so on. The terms "color" and "color charge" are, of course, simply labels to describe a quark property analogous to electric charge and are in no way related to the usual meanings of the words. The use of the three primary colors for this purpose did, however, provide a very simple rule to ensure that the exclusion principle was obeyed:

All particles that occur in nature are colorless.

STUDENTS-HUB.com Uploaded By: Malak Obaid

The term "colorless" means that either

1. The total amount of color (i.e., the sum of the color quantum numbers) is zero, or
2. There are equal amounts of all three colors present (in analogy with the combining of the three primary colors to produce white).

Thus, for example, the three up quarks that compose the $\Delta^{++}(1232)$ are one each of u_r, u_b, and u_g.

The J/ψ Puzzle The solution provided by color seemed an artificial one, as did the explanation for seeing no free quarks described in the next subsection, but strong support for the model came late in 1974 from an unexpected quarter. Two groups independently discovered a new meson. The first, S. Ting and his co-workers at Brookhaven, called it the J, while the second group, B. Richter and his co-workers at SLAC,[18] called it the ψ. Now referred to as the J/ψ, the new meson had three times the mass of the proton and a lifetime of 10^{-20} s, extraordinarily long for a strongly interacting particle. The exceptionally long lifetime pointed to new physics,[19] and within months after its discovery it was recognized that the J/ψ was composed of a fourth quark and its antiquark. The fourth quark, which had been proposed by S. Glashow and others for compelling theoretical reasons some years earlier so as to make equal numbers of quarks and leptons (before the discovery of the τ and ν_τ), is called the *c*harm quark and $J/\psi = (c\bar{c})$.[20] Discovery of the first charm baryon, the Λ_C^+, is shown in Figure 12-21. Figure 12-22

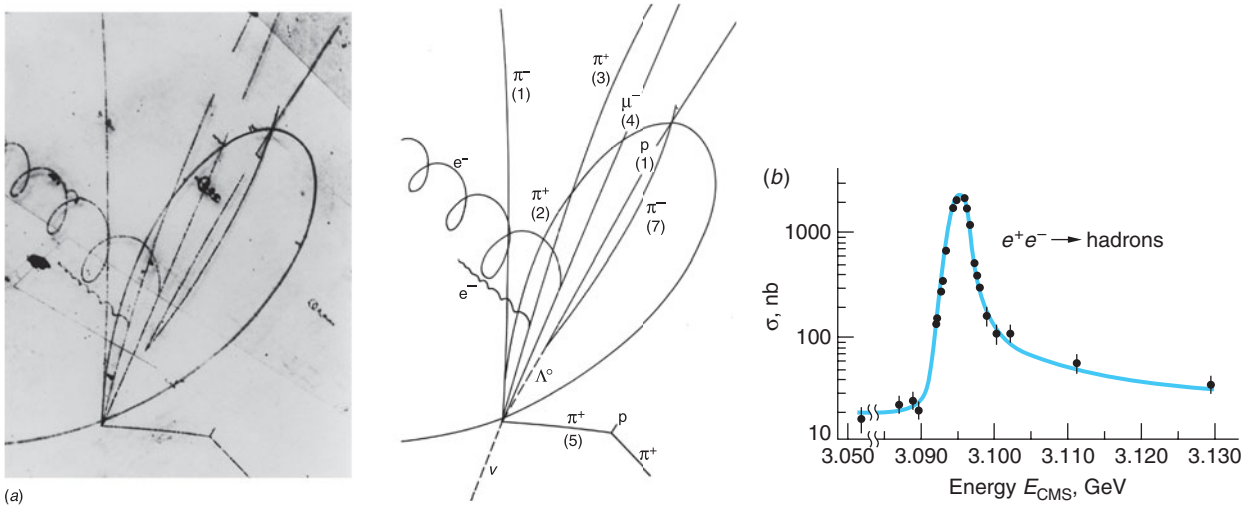

Figure 12-21 (*a*) Discovery of the first charm baryon, the Λ_c^+. The reaction is $\nu_\mu + p \rightarrow \Lambda_c^+ + \mu^- + \pi^+ + \pi^-$. The charm baryon decays via $\Lambda_c^+ \rightarrow \Lambda^0 + \pi^+$ too soon to leave a track, but the subsequent decay of the Λ^0 is easily seen. [*Brookhaven National Laboratory.*] (*b*) A portion of the experimental data obtained by B. Richter and his co-workers at SLAC showing the J/ψ resonance.

STUDENTS-HUB.com Uploaded By: Malak Obaid

shows some supermultiplets formed with four quarks. This discovery made two nicely symmetric sets of four leptons (e, ν_e, μ, ν_μ) and four quarks (u, d, s, c) and, of course, their antiparticles. Then in 1975 a new lepton was found! The new lepton, the τ, presumably had an associated neutrino, the ν_τ, and the numerical symmetry of the generations of particles was again upset. But within two years a new heavy meson, the upsilon Υ, was discovered and quickly recognized as being composed of a fifth quark-antiquark pair. The fifth quark is called the *b*ottom (or sometimes *b*eauty) quark, and $\Upsilon = (b\bar{b})$. The theory then predicts a sixth quark, called, as you might guess, the *t*op (or *t*ruth) quark. The *t* quark was found in 1995 by two groups at Fermilab, thus restoring Glashow's symmetry of fundamental quarks and leptons and completing the new periodic table of the constituents of fundamental particles. (See Figure 12-23.) At 176 MeV/c^2, the *t* quark is the most massive fundamental particle that has been discovered. There are substantial theoretical and experimental reasons to believe that there are no more quarks or leptons to be found. (See Figure 12-24.) Table 12-5 lists the up, down, strangeness, charm, top, and bottom internal quantum numbers for the six flavors of quarks and their antiquarks.

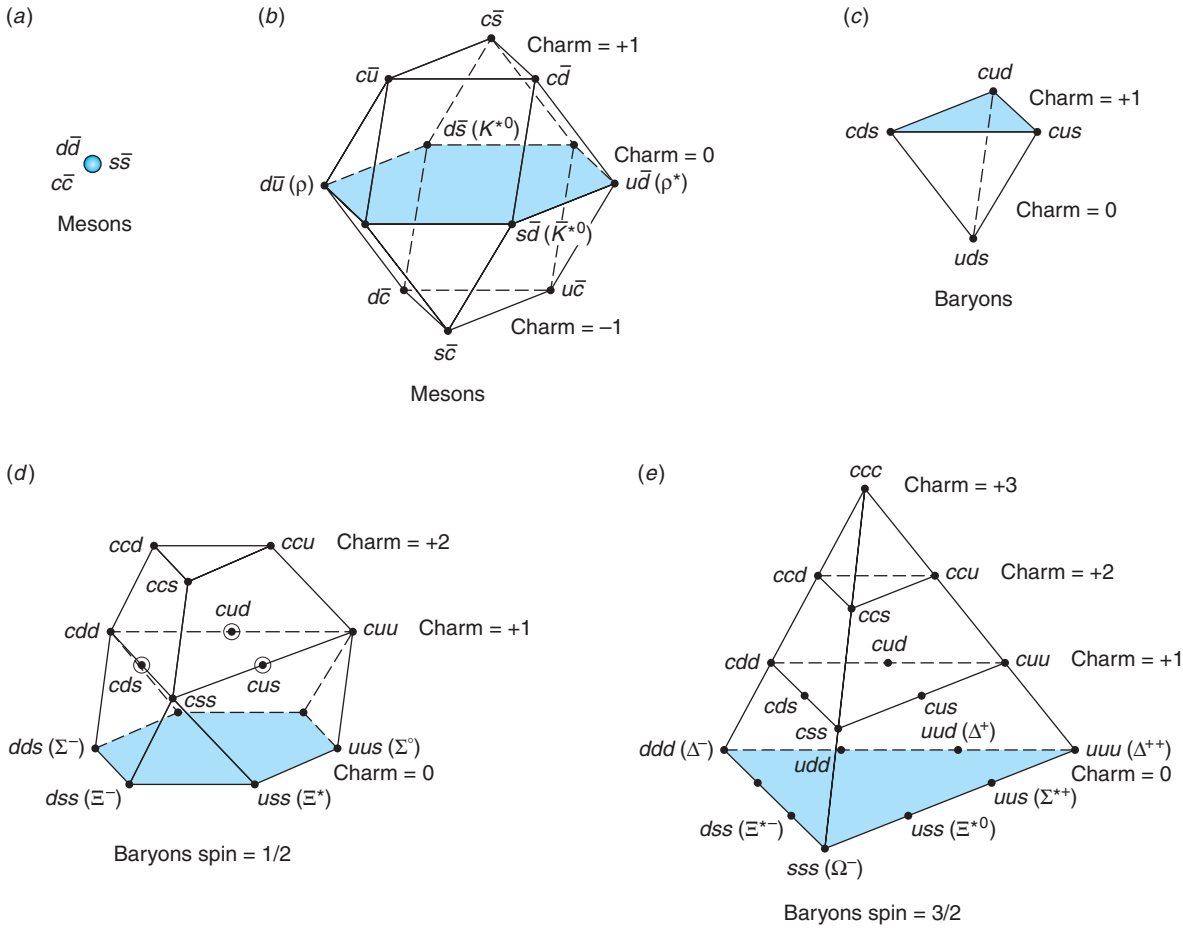

Figure 12-22 Supermultiplets formed from u, d, s, and c quarks. The circles indicate that there are two particles with the same quark composition and different energies.

STUDENTS-HUB.com Uploaded By: Malak Obaid

Charge	First generation	Second generation	Third generation
		Quarks	
+2/3	u_r u_b u_g	c_r c_b c_g	t_r t_b t_g
−1/3	d_r d_b d_g	s_r s_b s_g	b_r b_b b_g
		Leptons	
−1	e	μ	τ
0	ν_e	ν_μ	ν_τ

Figure 12-23 Periodic table of elementary particle constituents.

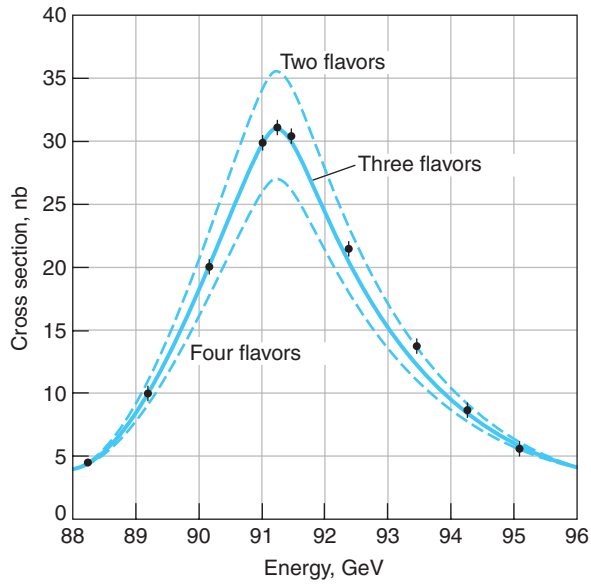

Figure 12-24 Both the shape and height of Z^0 resonance are theoretically related to the number of flavors of the leptons and quarks. As that number increases, the maximum cross section decreases and the energy width (at half the maximum height) becomes larger. Current measurements, shown by the black circles, are fully consistent with three flavors, or generations, excluding both two and four.

Quantum Chromodynamics

Quantum chromodynamics (QCD) is the modern theory that describes the strong interaction between quarks and gluons. It is directly analogous to quantum electrodynamics (QED), which so successfully accounts for the electromagnetic interaction. Indeed, QCD was modeled on QED. As stated earlier, the particle (boson) that mediates the strong quark-quark interaction is the gluon and the fundamental process (analogous

STUDENTS-HUB.com Uploaded By: Malak Obaid

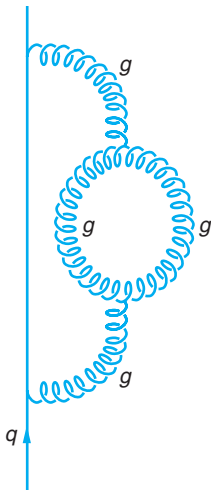

Figure 12-26 Feynman diagram of a quark emitting a gluon, which then creates two gluons that recombine, the resulting gluon being absorbed by the quark.

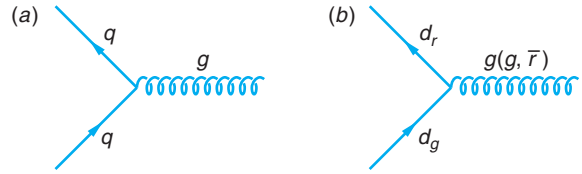

Figure 12-25 (*a*) The fundamental vertex of QCD, in which a quark emits a virtual gluon. (*b*) Since gluons carry a color and an anticolor, the emission of the gluon may also change the color of the quark.

to $e \rightarrow e + \gamma$ shown in Figure 12-4) is illustrated by the Feynman diagram in Figure 12-25*a*. The gluons are the QCD analog of the photon in QED. Like photons, they are massless and have spin 1; however, there is one crucial difference between the two particles. The gluons carry color charge, whereas the photon is electrically neutral. In fact, the gluons are bicolored, carrying one unit of a color charge and one of an anticolor charge and hence are not color neutral. Thus, in the process $q \rightarrow q + g$ the quark may change color (but not flavor), as shown in Figure 12-25*b*. Since the gluons carry net color charge, they can also interact with each other via the strong interaction *and* they form an octet in the SU(3) group theory representation, just as do the mesons.[21] This means that, in addition to the increase in the strong interaction coupling constant α_s at very short distances analogous to the vacuum polarization in QED discussed in Section 12-2 and shown in Figure 12-10, there are also gluon-gluon loops, as shown in Figure 12-26. The effect of such gluon loops is to, in a sense, dilute the strong force and decrease the value of the strong interaction coupling constant α_s at extremely short distances ($\leq 10^{-18}$ m). As it turns out, this latter effect predominates at very small quark separations. As a pair of quarks move extremely close to each other, their coupling decreases, a condition called *asymptotic freedom*. The result is that inside the nucleon, the quarks move more or less as free particles, a phenomenon that has been confirmed by electron deep scattering experiments. Indeed, hundreds of experiments have confirmed the property of asymptotic freedom.

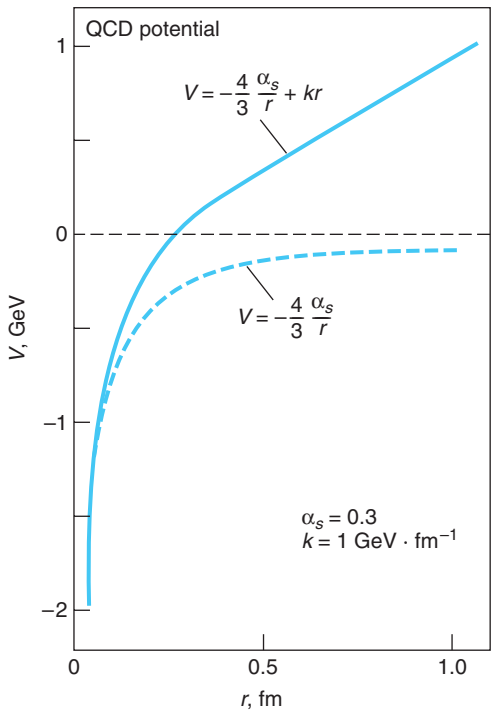

Figure 12-27 The potential seen by quarks in QCD. In this diagram the strong coupling constant $\alpha_s = 0.3$ and $k = 1$ GeV/fm in Equation 12-29.

One of the possible potential functions for the strong interaction has the approximate form

$$V_{QCD}(r) = -\frac{4\alpha_s}{3r} + kr \qquad \textbf{12-32}$$

It has been reasonably well tested experimentally at short distances. Notice that V_{QCD} increases indefinitely with r (see Figure 12-27), that is, the strong force at large r, $F_{QCD} = -\nabla V_{QCD} =$ constant, rather than going to zero, as do the Coulomb and gravitational forces. The result is to prevent the quarks from getting too far apart, effectively containing them inside the hadrons, a phenomenon called *quark confinement*. This is the QCD explanation for why free quarks have not yet been found. When a large amount of energy is added to a quark system such as a nucleon, a quark-antiquark pair is created and the original quarks remain confined within the original system. This is the origin of the virtual pions that were postulated by the Yukawa model of the nuclear force as the mediator of that interaction. (See Figure 12-28.)

STUDENTS-HUB.com Uploaded By: Malak Obaid

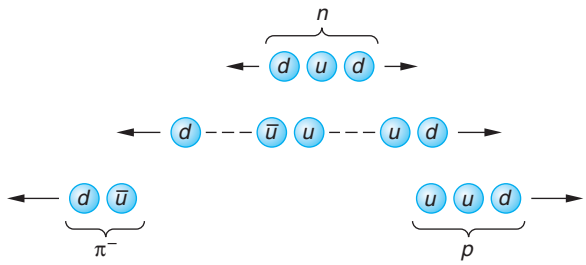

Figure 12-28 Shown is one possible illustration of quark confinement. If energy is added to remove a d quark from a neutron, a ($\bar{u}$, u) pair is created. The $\bar{u}$ and one of the d quarks combine to form a π^-, while the u from the pair and the original u and d combine to produce a proton and no free quark appears.

During particle decays and interactions quarks transform into one another. For example, the β^-decay of the neutron given by Equation 11-38 proceeds according to the quark model in which a d quark turns into a u quark, as illustrated by Example 12-4. All baryons eventually decay in one or more steps to the lightest (lowest-energy) baryon, the proton. The decay of the proton is prohibited by conservation of energy and baryon number, but searches for proton decay are continuing. Example 12-12 illustrates the decay of another baryon, the Λ^0.

Questions

13. How can you tell whether a particle is a meson or a baryon by looking at its quark content?
14. Are there any quark-antiquark combinations that result in nonintegral electric charge?
15. What experimental evidence exists to support the assertion that natural particles are colorless?

EXAMPLE 12-12 Decay of Λ^0 Draw a Feynman diagram that shows the quarks involved in the decay of the Λ^0, which goes according to

$$\Lambda^0 \longrightarrow pe^-\bar{\nu}_e$$

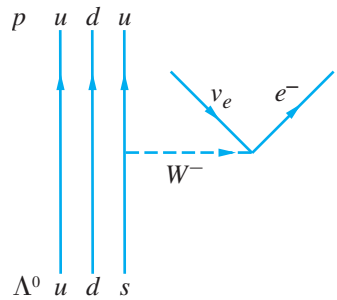

SOLUTION

From Table 12-10 we see that the Λ^0 is composed of a u quark, a d quark, and an s quark. The proton consists of two u quarks and a d quark. The decay results from the weak interaction, the s quark decaying to a u quark and a W^-. Note that strangeness is not conserved in the weak interaction that transforms the s quark into the u quark.

STUDENTS-HUB.com Uploaded By: Malak Obaid

Table 12-11 Quark composition of selected particles

Baryons	Quarks	Mesons	Quarks
p	uud	π^+	$u\bar{d}$
n	udd	π^-	$\bar{u}d$
Λ^0	uds	K^+	$u\bar{s}$
Δ^{++}	uuu	K^0	$d\bar{s}$
Σ^+	uus	$\overline{K}^0$	$s\bar{d}$
Σ^0	uds	K^-	$s\bar{u}$
Σ^-	dds	J/ψ	$c\bar{c}$
Ξ^0	uss	D^+	$c\bar{d}$
Ξ^-	dss	D^0	$c\bar{u}$
Ω^-	sss	D_s^+	$c\bar{s}$
Λ_c^+	udc	B^+	$u\bar{b}$
Σ_c^{++}	uuc	$\overline{B}^0$	$d\bar{b}$
Σ_c^+	udc	B^0	$d\bar{b}$
Ξ_c^+	usc	B^-	$\bar{u}b$

(*a*)

(*b*)

(*c*)

Figure 12-29 The plastic strip in (*a*) has left-right symmetry. Increased vertical force on the ends of the strip breaks the symmetry, causing the strip to take one or the other of the positions (*b*) or (*c*), neither of which has left-right symmetry.

The Electroweak Theory

In the *electroweak theory*, the electromagnetic and weak interactions are considered to be two different manifestations of a more fundamental electroweak interaction. At very high energies ($\gg 100$ GeV), the electroweak interaction is mediated by four bosons. From symmetry considerations, these would be a triplet consisting of W^+, W^0, and W^-, all of equal mass, and a singlet boson B^0 of some other mass. Neither the W^0 nor the B^0 would be observed directly, but one linear combination of the W^0 and the B^0 would be the Z^0, and another would be the photon. At ordinary energies, the symmetry is spontaneously broken.

By "spontaneously broken symmetry" we mean the following: the Hamiltonian H_{op} retains the complete symmetry, but the ground state computed from that H_{op} does not, or, as we say, the symmetry is broken. For example, magnetism in solids arises due to interaction of the spins of the atoms of the crystal lattice. For a ferromagnet, such as iron, the H_{op} describing that interaction is invariant under rotation, but in the ground state magnetic domains are spontaneously formed in the sample. The spin direction changes from domain to domain but is the same inside each domain. A domain is certainly not invariant to a rotation of the spins. Thus, the ground state spontaneously breaks the rotational symmetry. (To further help you visualize what "spontaneously broken symmetry" means, think of a small plastic strip, like a short ruler, gripped at the ends between your thumb and index finger. As you squeeze, the strip will snap into a curve to one side or the other, breaking the original left-right symmetry. See Figure 12-29.)

STUDENTS-HUB.com Uploaded By: Malak Obaid

The broken symmetry in the electroweak interaction leads to the separation of the electromagnetic interaction mediated by the photon and the weak interaction mediated by the W^+, W^-, and Z^0 particles. The fact that the photon is massless and that the W and Z particles have masses of the order of 100 GeV/c^2 shows that the symmetry assumed in the electroweak theory does not exist at lower energies. The symmetry-breaking agent is called a *Higgs field*, which requires a new boson, the *Higgs boson*, whose rest energy is expected to be of the order of 1 TeV (1 TeV = 10^{12} eV). According to the Standard Model, it is by interacting with the Higgs field that particles acquire their masses. The Higgs boson has not yet been observed. Calculations show that Higgs bosons (if they exist) should be produced in a head-on collision between protons of energies of the order of 20 TeV. While such energies are not available with existing accelerators, the Large Hadron Collider, which began operation at CERN in 2008, will be able to reach and exceed that energy by accelerating beams of a variety of nuclei. Searching for the Higgs boson is a primary goal for the LHC.

The Standard Model—A Summary

The *Standard Model* is the theoretical model of elementary particles and their interactions. It is based on a combination of the quark model, electroweak theory, and quantum chromodynamics. In this model, the fundamental particles are the leptons and quarks, each of which comes in three generations, as shown in Tables 12-1 and 12-2. The force carriers are the photon, the $W^{\pm}$ and Z^0 particles, and eight types of gluons. The leptons and quarks are all spin-1/2 fermions, which obey the Pauli exclusion principle. The force carriers are integral-spin bosons, which do not obey the Pauli exclusion principle. Every force in nature is due to one of the four basic interactions: strong, electromagnetic, weak, and gravitational. A particle experiences one of the basic interactions if it carries a charge associated with that interaction. Electric charge is the familiar charge that you have studied previously. It is carried by the quarks and charged leptons. Weak charge, also called flavor charge, is carried by leptons and quarks. The charge associated with the strong interaction is called color charge and is carried by quarks and gluons but not by leptons. The charge associated with the gravitational force is mass. It is important to note that the photon, which mediates the electromagnetic interaction, does not carry electric charge. The $W^{\pm}$ and Z^0 particles, which mediate the weak interaction, do carry weak charge, and the gluons, which mediate the strong interaction, carry color charge. This latter fact is related to the confinement of quarks.

All matter is made up of leptons and quarks. There are no known composite particles consisting of leptons bound together by the weak force. Leptons exist only as isolated particles. Hadrons (baryons and mesons) are composite particles consisting of quarks bound together by the color charge. A result of the QCD theory is that only color-neutral combinations of quarks are allowed. Three quarks of different colors can combine to form color-neutral baryons, such as the neutron and proton. Mesons contain a quark and an antiquark and are also color neutral. Excited states of hadrons are considered to be different particles. For example, the Δ^{++} particle is produced by $\pi^+ p \rightarrow \Delta^{++}$. The Δ^{++} must have the exact same set of internal quantum numbers as the $\pi^+ p$: $B = 1, C = S = T = B' = 0$, which from Equations 12-26 and 12-27 means $Y = 1$ and $I_3 = 3/2$. The three u quarks can be in the same spin state in the Δ^{++} without violating the exclusion principle because they have different colors.

The strong interaction can manifest itself in two ways: the fundamental, or color, interaction and the *residual strong interaction*. The fundamental interaction is responsible for the force exerted by one quark on another and is mediated by gluons.

STUDENTS-HUB.com Uploaded By: Malak Obaid

The residual strong interaction is responsible for the force between color-neutral nucleons, such as the neutron and proton. This force is due to the residual strong interactions between the color-charged quarks that make up the nucleons and can be viewed as being mediated by the exchange of mesons. The residual strong interaction between color-neutral nucleons is analogous to the residual electromagnetic interaction between neutral atoms that bind them together to form molecules.

For each particle there is an antiparticle. A particle and its antiparticle have identical mass and spin but opposite electric charge. For leptons, the leptons numbers L_e, L_μ, and L_τ of the antiparticles are the negatives of the corresponding numbers for the particles. For example, the lepton number for the electron is $L_e = +1$ and that for the positron is $L_e = -1$. For hadrons, the baryon number, strangeness, charm, topness, and bottomness are the sums of those quantities for the quarks that make up the hadron. The number for each antiparticle is the negative of the number for the corresponding particle. For example, the lambda particle Λ^0, which is made up of the *uds* quarks, has $B = 1$ and $S = -1$, whereas its antiparticle, $\overline{\Lambda}^0$, which is made up of the $\overline{uds}$ quarks, has $B = -1$ and $S = +1$. Particles such as the photon γ and the Z^0 that have zero electric charge, $B = 0$, $L = 0$, $S = 0$ and zero charm, top, and bottom, are each their own antiparticle. Note that the K^0 meson ($d\bar{s}$) has a zero value for all of these quantities except strangeness, which is $+1$. Its antiparticle, the $\overline{K}^0$ meson ($\bar{d}s$), has strangeness -1, which makes it distinct from the K^0. The π^+ ($u\bar{d}$) and π^-($\bar{u}d$) have electric charge but zero values for L, B, and S. They are antiparticles of each other, but since there is no conservation law for mesons, it is impossible to say which is the particle and which is the antiparticle. Similarly, the W^+ and W^- are antiparticles of each other. Table 12-11 lists the quark compositions of several particles.

EXAMPLE 12-13 **Decay of the Ω^-** The Ω^- decays according to the equation

$$\Omega^- \longrightarrow \Lambda^0 + K^-$$

and the resulting Λ^0 and K^- usually decay according to

$$\Lambda^0 \longrightarrow p + \pi^- \quad \text{and} \quad K^- \longrightarrow \mu^- + \overline{\nu}_\mu$$

Write each of these reactions in terms of quarks.

SOLUTION

Using Table 12-11, the Ω^- decay is given by

$$sss \longrightarrow uds + s\bar{u}$$

in which an *s* is changed to a *d* and a $u\bar{u}$ pair is created. The Ω^0 and K^- decay according to, for the Λ^0,

$$uds \longrightarrow uud + \bar{u}d$$

where again an *s* is changed to a *d* and a $u\bar{u}$ pair is created, and for the K^- meson,

$$s\bar{u} \longrightarrow \mu^- + \overline{\nu}_\mu$$

where the *s* and *u* annihilate, producing a W^-, which decays to the leptons.

STUDENTS-HUB.com Uploaded By: Malak Obaid

12-5 Beyond the Standard Model

Grand Unification Theories

At the beginning of Section 12-4 we noted that the Standard Model of particle physics, while correctly accounting for a wide range of observations, has left a number of fundamental questions unanswered. Of premier importance among these are why nature requires four interactions rather than one and why their strengths and properties should be so different. The successful unification of the electromagnetic and weak interactions into the electroweak theory discussed earlier has led to a number of efforts to include the strong interaction and, ultimately, the gravitational interaction into a single, so-called *grand unification theory*, or GUT.[22] As in the electroweak theory, the different strengths at energies well below the rest energies of the mediating bosons would be accounted for by spontaneous symmetry breaking. GUTs also explain the equality of the electron and proton charges.

A central feature of current GUTs is that the coupling constants of all four interactions approach the same value, approximately that of the fine-structure constant α, at some very high energy. It is a remarkable experimental observation that the measured values of the coupling constants do appear to be tending toward a common value. Unfortunately, extrapolation to the common point must be made over an extraordinarily large energy range, that point of common value being at about 10^{16} GeV, compared with about 10^4 GeV that can be reached with the largest existing accelerator, the LHC at CERN. (See Figure 12-30.) To assume that nature has no surprises or new physics to await us somewhere in that colossal energy range ignores the lessons of history.

Supersymmetry (SUSY)

A number of GUTs include a proposed new symmetry in addition to the symmetries we have discussed. Called *supersymmetry* (with the acronym SUSY), it assigns to each elementary particle a *superpartner*. The superpartner is in every way identical to the particle except for its spin. The leptons and quarks, both spin-1/2 fermions, have

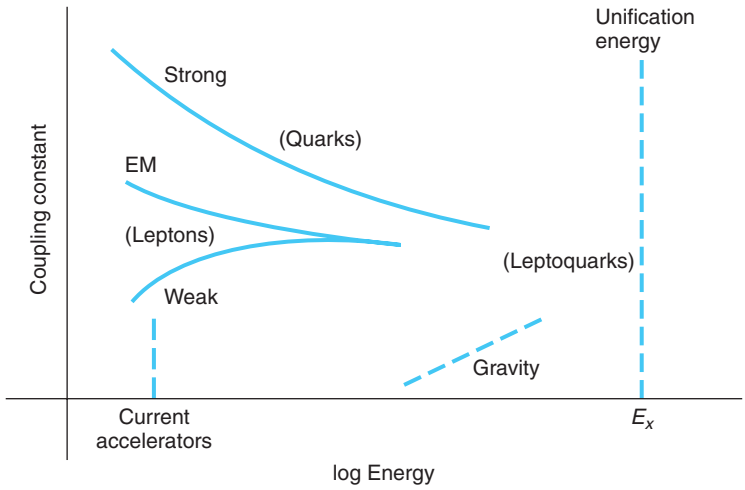

Figure 12-30 The coupling constants of the four interactions appear to be approaching a common value at some energy in the range 10^{16} to 10^{18} GeV. Since the largest existing accelerator, the Large Hadron Collider at CERN, can reach only about 14 TeV, the extrapolation to the unification energy E_x is highly uncertain.

STUDENTS-HUB.com Uploaded By: Malak Obaid

Table 12-12 Elementary particle and their superpartners

Particle	Symbol	Spin	Superpartner	Symbol	Spin
Quark	q	1/2	Squark	q	0
Electron	e	1/2	Selectron	e	0
Muon	μ	1/2	Smuon	μ	0
Tau	τ	1/2	Stau	τ	0
W	W	1	Wino	W	1/2
Z	Z	1	Zino	Z	1/2
Photon	γ	1	Photino	γ	1/2
Gluon	g	1	Gluino	g	1/2
Higgs	H	0	Higgsino	H	1/2

superpartners with spin 0. The spin-1 bosons have spin-1/2 superpartners. The superpartners of the fermions are given the same names with a prefix *s*; e.g., the electron's superpartner is the selectron. The superpartners of the bosons have the same names with a suffix *ino* added (sort of), e.g., the gluon's superpartner is the gluino. The particles and their superpartners are listed in Table 12-12.

Exact supersymmetry would equate the masses of the particles and their superpartners. However, this is apparently not true in nature or the superpartners would have been detected long ago. So SUSY is modified to account for that absence by postulating that the mass of the lightest superpartner would be very large indeed, of the order of the masses of the $W^{\pm}$ and the Z^0 bosons. Doing so ultimately predicts the GUT unification energy in the vicinity of the current extrapolated projections, predicts the proton lifetime in agreement with current experimental limits, and keeps the GUT unification coupling constant in line with current extrapolations. An important goal of the Large Hadron Collider is to test predictions of supersymmetry.

SUSY is also a component of current theories designed to include gravity within GUTs. These are the *string* and *superstring theories*. String theories replace pointlike elementary particles with tiny, quantized strings and require 10 or more dimensions. Their purpose is to surmount current theoretical problems in quantizing gravity. Currently, particle physicists are sharply devided over string theories, some heralding them as the "theory of everything," others dismissing them as "not even wrong." As of this date, there is no experimental evidence supporting any of the string theories.

Proton Decay

In GUTs the quarks and leptons are states of one particle, the leptoquark, and occur symmetrically in the same multiplet. This would account for why there are equal numbers of quark and lepton flavors and also lead to the prediction that each type of particle can be changed into the other. If that is the case, then baryon number is no longer a conserved quantity and the proton should not be stable. Current versions of GUTs place the lifetime of the proton at about 10^{30} to 10^{33} years, the long lifetime being the result of the large energy at which unification of the interactions occurs.

STUDENTS-HUB.com Uploaded By: Malak Obaid

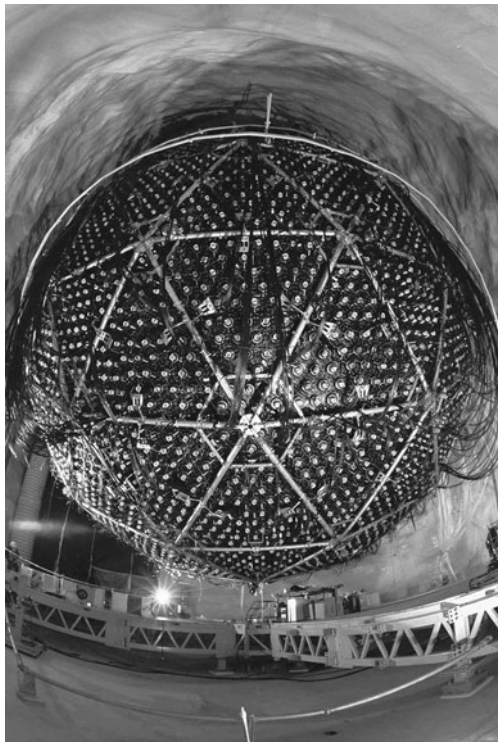

(*a*)

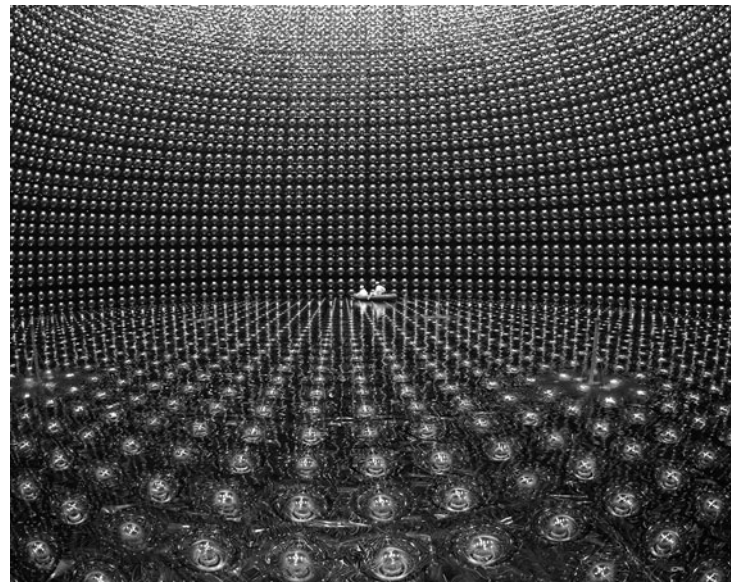

(*b*)

The Sudbury Neutrino Observatory (SNO) in Canada and the Super-Kamiokande (Super-K) neutrino detector in Japan collected data on neutrino interactions that confirmed neutrino oscillations. (*a*) The SNO neutrino detector is a spherical acrylic vessel 12 m in diameter and contains 1000 metric tons of ultrapure heavy water (D_2O) located 2000 m below ground. Cherenkov light produced by neutrino reactions in the water is viewed by 9456 photomultipliers, each 20 cm in diameter. (*b*) The Super-K neutrino detector, a cylindrical structure 41 m tall and 39 m in diameter, contains 45,000 metric tons of pure water (H_2O) viewed by 11,200 photomultipliers. [*(a) Courtesy of Sudbury Neutrino Observatory; (b) courtesy of Kamioka Observatory, University of Tokyo.*]

Current experiments have placed the lower limit on the proton lifetime at about 10^{32} years; to date, no proton decays have been detected. Searches for proton decay, such as that at Super-Kamiokande, generally involve monitoring very large volumes of pure water, watching for one of the several possible proton decay "signatures"; e.g., $p \rightarrow \pi^0 e^+$ or $p \rightarrow \pi^+ \overline{\nu}_e$. The nonconservation of baryon number in the early universe when energies were very high provides an explanation of a major cosmological problem, namely, why the present universe has many more baryons than antibaryons.

Lepton numbers would no longer be conserved at the unification energy, and currently forbidden reactions such as $\mu^- \rightarrow e^- + \gamma$ and $\mu^+ \rightarrow e^+ + e^+ + e^-$ would be allowed. Experimental searches have been made, but no lepton-number-nonconserving events have been found.

Massive Neutrinos

From the time Pauli first suggested their existence in 1930, neutrinos were thought to have zero mass. Then, based on Bahcall's theoretical calculation of the solar neutrino flux and Davis's remarkable measurement[23] of the flux at only about 30 percent of Bahcall's prediction, the *solar neutrino problem* emerged (see Section 11-8). Its recent solution through the detection of neutrino oscillations by the Sudbury Neutrino

STUDENTS-HUB.com Uploaded By: Malak Obaid

Observatory (SNO) and Super-Kamiokande (Super-K) experiments gives support to GUTs since most GUTs require that neutrinos have mass. The theories predict their mass to be given approximately by

$$m_\nu \approx \frac{M_{eW}^2}{M_x} \qquad \textbf{12-33}$$

where M_{eW} is a characteristic mass of the electroweak interaction, roughly $10^2\ \text{GeV}/c^2$, and M_x is the unification mass $E_x/c^2 \approx 10^{16}\ \text{GeV}/c^2$ (see Figure 12-30). Nearly all GUTs project M_x values of this order of magnitude, which in turn means that all neutrinos would have m_ν less than about 1 eV. The theories also predict $m(\nu_e) \ll m(\nu_\mu) \ll m(\nu_\tau)$. The impact of massive neutrinos on both the solar neutrino problem described briefly in Chapter 11 and the universe's "missing energy" (or "missing mass") problem discussed in Chapter 13 is substantial. S. Mikheyev, A. Smirnov, and L. Wolfenstein proposed a solution to the solar neutrino problem in particular in which an ν_e can oscillate to a ν_μ or ν_τ while propagating through the Sun's mass. For this complex process, called the *MSW effect*, to occur, the neutrino wave functions $\psi(\nu_e)$, $\psi(\nu_\mu)$, and $\psi(\nu_\tau)$ must each consist of superpositions of the three mass states. Similar processes can be described for neutrinos moving through space and the atmosphere. (See Exploring, Neutrino Oscillations and Mass.) The relative phases of the mass states may change for two reasons. (1) In passing through the solar matter (electrons and protons), the three mass states scatter differently; hence their relative phases change. (2) While propagating through space and the atmosphere, the mass states move at different speeds, which also results in a change in the relative phase. The phase changes result in interference of the neutrino matter waves, and as a consequence a neutrino emitted in the Sun as a ν_e may oscillate to a ν_μ or ν_τ before reaching Earth and therefore not be detected by experiments searching for electron neutrinos. Experimental evidence supporting the existence of oscillations was provided by the SNO and Super-K measurements.

Magnetic Monopoles

Magnetic monopoles, first suggested by Dirac in 1929, are also proposed by GUTs. Dirac showed that their existence in relativistic quantum mechanics leads to the quantization of both the electric charge e and the magnetic charge q_m. The magnetic charge of a monopole would be

$$q_m = n\frac{\hbar c}{2e} \quad \text{for } n = 1, 2, 3, \ldots \qquad \textbf{12-34}$$

It is important to note that $q_m^2/\hbar c \approx \hbar c/e^2 \propto 1/\alpha$. In the unified theories the quantization of electric charge occurs naturally in units of e, and magnetic monopoles of charge q_m and mass M_m are then predicted. The predicted values of M_m are very large, about $10^{16}\ \text{GeV}/c^2$, far beyond the energy achievable in any accelerator. Cosmic ray searches for monopoles place an upper limit on their flux at about $10^{-15}\ \text{cm}^{-2}\ \text{s}^{-1}$ per unit solid angle. Coincidentally, this value corresponds approximately to the maximum flux that could exist in the Milky Way without having long since destroyed the galactic magnetic field. As of this writing, only a single possible observation of a magnetic monopole has been reported in the literature, by B. Cabrera in 1982. This observation is inconsistent with current limits.

STUDENTS-HUB.com Uploaded By: Malak Obaid

Quantum Gravity

The addition of quantum gravity to grand unified theories is a formidable task. Called *superstring theories* because of their basic view of fundamental particles as strings rather than points, perhaps the most promising of the current versions is based on a 10-dimensional universe (nine space and one time dimension) in which six of the space dimensions have been collapsed or curled up on themselves. The string "lengths" are much shorter than can be measured, about 10^{-35} m. Besides the inclusion of quantum gravity, superstring theories also produce the *gauge theories*[24] with the correct mediating bosons; however, although they are the subject of considerable interest to theoretical physicists, there is as yet no experimental support for these theories, and it is not clear to what extent, if any, they represent physical reality.

Many questions are still unanswered. For example, do the quarks have internal structure? What is the origin of isospin? There is some indication that hadrons are surrounded by a "sea" of virtual quark-antiquark pairs. What is their role? Is the fractional charge of the quarks related to color? Investigating these problems experimentally will require new, higher-energy accelerators and more advanced detectors than currently exist anywhere in the world. Obviously, there is much to be done.

EXPLORING
Neutrino Oscillations and Mass

Quantum mechanics requires that, if neutrinos oscillate from one type, or flavor, to another, then they must have mass, whether they originate in the Sun, the atmosphere, a nuclear power reactor, an accelerator, or somewhere else in the cosmos. While the detailed justification of this requirement is beyond the scope of our discussions, an outline of why this must be true is presented here. The relationship between neutrino (flavor) wave functions and the mass eigenfunctions is given by

$$\psi_\alpha = \sum_i U^*_{\alpha i}\,\psi_i \qquad \psi_i = \sum_\alpha U_{\alpha i}\,\psi_\alpha \qquad \textbf{12-35}$$

where ψ_α are the wave functions of the neutrino flavors ($\alpha = \nu_e, \nu_\mu, \nu_\tau$), ψ_i are the mass eigenfunctions ($i = \nu_1, \nu_2, \nu_3$), and $U_{\alpha i}$ (and its complex conjugate) is a function that describes the extent to which mixing of the flavors or masses occurs, i.e., the phases of the oscillations. Note that, if there were no oscillations, $U_{\alpha i} = 1$ and the ψ_α would equal the mass eigenfunction for ν_α; however, the experiments noted above show that $U_{\alpha i} \neq 1$. The states with different mass eigenfunctions propagate at different speeds, the less massive moving faster than the more massive ones. Since the mass eigenfunctions are combinations of neutrino (flavor) wave functions, the difference in speeds results in interference between the neutrino waves in each mass eigenfunction. When, eventually, constructive interference occurs, one neutrino flavor has changed into another.

The mass eigenfunctions are plane wave solutions of the time-dependent Schrödinger equation. (See Equation 6-7.)

$$\psi_i(x, t) = e^{i(px - Et)/\hbar} \qquad \textbf{12-36}$$

STUDENTS-HUB.com Uploaded By: Malak Obaid

The dependence of the energy on the mass is given by Equation 2-31 and the extremely relativistic approximation of Equation 2-36

$$E = \sqrt{(pc)^2 + (mc^2)^2} \qquad \textbf{2-31}$$

written as

$$E = (pc)\left[1 + \frac{(mc^2)^2}{(pc)^2}\right]^{1/2}$$

Since for each of the neutrinos under discussion the total energy $E \gg mc^2$, the binomial expansion allows us to write

$$E \approx pc + \frac{(mc^2)^2}{2pc} + \ldots \qquad \textbf{12-37}$$

After time t moving at $v \approx c$, the neutrino has traveled a distance $x \approx ct = L$ and the mass wave functions become

$$\psi_i(L) = e^{-\frac{iL}{\hbar c}\frac{(mc^2)^2}{2E}}\psi_i(0) \qquad \textbf{12-38}$$

and the probability that a neutrino of flavor α at $t = 0$ will be observed to have changed or oscillated to flavor β is given by

$$P_{\alpha\to\beta} = |\psi_\beta\psi_\alpha|^2 = \left|\sum_i U^*_{\alpha i}U_{\beta i}e^{-\frac{iL}{\hbar c}\frac{(mc^2)^2}{2E}}\right|^2 \qquad \textbf{12-39}$$

If we confine our attention to the two-neutrino case (the three-neutrino case is more complex to describe), Equation 12-39 becomes (after some work!)

$$P_{\alpha\to\beta,\,\alpha\neq\beta} = \sin^2 2\theta \sin^2\left(1.267\frac{\Delta m^2 L}{E}\frac{\text{GeV}}{\text{eV}^2\text{km}}\right) \qquad \textbf{12-40}$$

where θ is the neutrino mixing angle and Δm is the difference in the masses of the two neutrinos. Although Equation 12-40 applies to a two-neutrino world, its is a decent approximation for the $\nu_\mu \leftrightarrow \nu_\tau$ oscillations in the atmosphere since electron neutrinos do not contribute significantly in this case. It is also reasonable for solar electron neutrinos oscillating to superpositions of ν_μ and ν_τ.

From Equation 12-40 we now can see why flavor-changing neutrinos must have mass. Since experiments show that $P_{\alpha\to\beta} \neq 0$ and measure for solar neutrinos $\theta(\nu_e, \nu_\mu) = 33.9°$ $(\neq 0)$ and for atmospheric neutrinos $\theta(\nu_\mu, \nu_\tau) = 45°$, then in both cases $\Delta m^2 \neq 0$. Thus, *neutrinos have mass*. The current values of Δm^2 are

$$\Delta m^2_{\text{solar}} = 8.0 \times 10^{-5}\ \text{eV}^2$$
$$\Delta m^2_{\text{atmo}} = 2.4 \times 10^{-3}\ \text{eV}^2$$

More

GUTs aren't the only avenue being actively explored by physicists in search of a deeper understanding of the structure of matter than we now have. The so-called *Theories of Everything* that seek to account for all of physics within a single theoretical construct are highly speculative, and none yet have any experimental support. On the home page at www.whfreeman.com/tiplermodernphysics5/e.

STUDENTS-HUB.com Uploaded By: Malak Obaid

Summary

TOPIC	RELEVANT EQUATIONS AND REMARKS
1. Particles and antiparticles	Each fundamental particle found in nature has an antiparticle; some are distinct, e.g., the electron and positron; some are the antiparticles of themselves, e.g., the photon.
Feynman diagrams	These are spacetime diagrams that provide a useful way of visualizing interactions between particles—for example, Coulomb repulsion of like charges.
Leptons and quarks	All visible matter is made of two types of elementary particles, leptons and quarks, each consisting of three generations.
2. Fundamental interactions Force carriers	1. Strong interaction—gluons 2. Electromagnetic interaction—photons 3. Weak interaction—$W^{\pm}$, Z^0 4. Gravitational interaction—graviton
Interaction "strengths"	This term refers to the magnitudes of the dimensionless coupling constants that multiply the space-dependent part of the potential energy functions.
3. Conservation laws and symmetries	Every symmetry of the particle Hamiltonians leads to a conservation law and vice versa (Noether's theorem). Energy, momentum, electric charge, and angular momentum are conserved in all interactions. Some quantities are conserved in some interactions but not in others. For example, isospin is conserved in the strong interaction but not in the weak interaction.
4. Standard Model	The Standard Model seeks to explain all matter in terms of the interactions among three types of elementary particles: quarks, leptons, and force carriers.
Color	All quarks and gluons have color charge with one of three possible values: red, blue, and green. The exclusion principle requires that all particles that occur in nature are colorless.
QCD	The potential function of the strong interaction has the approximate form $V_{\text{QCD}}(r) = -\frac{4\alpha_s}{3r} + kr$ **12-32**
5. Beyond the standard model	Grand unification theories (GUTs) attempt to unify all four basic interactions mathematically. While thus far unsuccessful, some predict, among other things, proton decay, magnetic monopoles, and massive neutrinos. The latter has been verified by experiments.

General References

The following general references are written at a level appropriate for the readers of this book.

Das, A., and T. Ferbel, *Introduction to Nuclear and Particle Physics*, Wiley, New York, 1994.

Eisberg, R., and R. Resnick, *Quantum Physics,* 2d ed., Wiley, New York, 1985.

Frauenfelder, H., and E. M. Henley, *Subatomic Physics,* 2d ed., Prentice Hall, Englewood Cliffs, N.J., 1991.

Fritzch, H., *Elementary Particles,* World Scientific, Singapore, 2005.

Griffiths, D. J., *Introduction to Elementary Particles*, Prentice Hall, New York, 1987.

Martin, B. R., and G. Shaw, *Particle Physics*, 2d ed., Wiley, New York, 1997.

Rubbia, C., and M. Jacob, "The Z^0," *American Scientist*, **78,** 502 (1990).

Veltman, M., *Facts and Mysteries in Elementary Particle Physics*, World Scientific, London, 2003.

Williams, W. S. C., *Nuclear and Particle Physics*, Oxford, New York, 1997.

STUDENTS-HUB.com Uploaded By: Malak Obaid

Notes

1. The word *atom* comes from the Greek word *atomos*, meaning indivisible, which was coined by the philosopher Democritus, a contemporary of Socrates, about 2400 years ago. In addition to suggesting that matter consisted of a variety of tiny atoms, he also suggested that the Milky Way was made of a large number of individual stars and that the Moon had mountains and valleys just like Earth.

2. Carl David Anderson (1905–1991), Swedish-American physicist. His discovery of the positron in cosmic ray cloud chamber tracks was followed three years later by his discovery of the muon in cloud chamber tracks recorded on Pikes Peak in Colorado. The former earned him a share of the 1936 Nobel Prize in Physics.

3. The Dirac equation for particles with 1/2-integral spin, like the electron, is the relativistic analog of the Schrödinger equation; however, it is not obtained by operator substitution into Equation 2-31 since the resulting wave function does not include the effects of spin.

4. Richard Phillips Feynman (1918–1988), American physicist who described himself as a "curious character." An almost legendary figure among physicists in the United States, he was one of many who worked on the Manhattan Project at Los Alamos during World War II, where he also became an accomplished safecracker. An excellent bongo drummer and a passable artist, he shared the 1965 Nobel Prize in Physics with Julian Schwinger and Sin-itiro Tomonaga, all of whom independently contributed to the development of quantum electrodynamics. His books *Surely You're Joking, Mr. Feynman!* and *What Do You Care What People Think?* provide delightful insights into his life.

5. Emilio Gino Segrè (1905–1989), Italian-American physicist. A lifelong friend and colleague of Fermi, Segrè shared the 1959 Nobel Prize in Physics with Owen Chamberlain, a member of his Berkeley research group, for the discovery of the antiproton. Of greater interest to most people might be his discovery of technetium ($Z = 43$), the first chemical element to be artificially created. The isomeric state of the isotope of technetium, ^{99}Tc, is by far the most widely used radioisotope in medical diagnosis, treatment, and research.

6. This process is called Møller scattering in QED.

7. In fact, an infinite number. The contribution that each possible diagram makes to the total process decreases sharply as the number of vertices increases, so complex diagrams may typically be ignored.

8. The name *lepton*, which means "light particle," was originally selected to reflect the small mass of these particles relative to that of the hadrons; however, the τ (discovered by M. Perl in 1975) has a mass nearly twice that of the proton, so the name is no longer an indicator of the mass of these particles.

9. The reason for making the coupling constants dimensionless is so all observers will measure comparable values, independent of the units they may have used.

10. Carlo Rubbia (b. 1934), Italian physicist. He shared the 1984 Nobel Prize in Physics with Simon van der Meer for their contributions to the discovery of the $W^{\pm}$ and Z^0.

11. Emmy A. Noether (1882–1935), German mathematician. Dismissed from her position at Göttigen by the Nazi regime, she came to the United States in 1933. Her obituary in the *New York Times* was written by Einstein.

12. Operators, like H_{op}, that result in real (i.e., observable) values are called *Hermitian* operators. They obey the rule

$$\int a(x)F_{op}b(x)\,dx = \int b(x)F^*_{op}a(x)\,dx$$

13. Murray Gell-Mann (b. 1929), American physicist. He received the 1969 Nobel Prize in Physics for this and other work on fundamental particles and their interactions.

14. The rate of discovery became so large that one physicist quipped that "by 1990 all physicists would be famous because there would be a particle named for each physicist" ($\approx$30,000). Most "discoveries" turned out to be spurious.

15. From a saying attributed to the Buddha: "Now this, O monks, is the noble truth of the way that leads to the cessation of pain: this is the noble *Eightfold Way*: namely, right views, right intention, right speech, right action, right living, right effort, right mindfulness, and right concentration."

16. The name "quark" was suggested to Gell-Mann by a quotation from *Finnegans Wake*, by James Joyce: "Three quarks for Muster Mark." Joyce did not tell us and the context does not make clear exactly what a quark is.

17. The correct quark combinations of hadrons are not always obvious because of the symmetry requirements on the total wave function. For example, the π^0 meson is represented by a linear combination of $u\bar{u}$ and $d\bar{d}$

18. Samuel Chao Chung Ting (b. 1936), American physicist, and Burton Richter (b. 1931), American physicist, shared the 1976 Nobel Prize in Physics for this important discovery.

19. One physicist put the long lifetime of the J/ψ in biological terms by comparing it with someone coming upon a remote mountain village where the average age of the inhabitants was 70,000 years. That would be a definite indication of new biology.

20. Particle physicists call the discovery of the J/ψ the "November revolution," referring to the enormous support of the quark model that its November 1974 publication provided.

21. They form nine combinations, just like the mesons, but for the gluons the ninth combination is really a singlet and hence is independent.

22. Since no theory of quantum gravity complementing QED and QCD exists, current efforts to develop GUTs include only the strong and electroweak interactions.

23. Raymond Davis, Jr. (1914–2006), American physicist, and John Bahcall (1934–2005) American physicist. Davis's measurements won him a share of the 2002 Nobel Prize in Physics.

STUDENTS-HUB.com Uploaded By: Malak Obaid

24. Theories in which the interaction is determined by the invariance of the theory (i.e., its mathematical equations) under particular transformations are called *gauge theories*. For example, classical electrodynamics is a gauge theory (although not usually referred to as such), as are QED and QCD. Historically, interactions were "figured out" by clever physicists on the basis of experimental evidence. A bit of a surprise, Schrödinger's wave mechanics is not a gauge theory.

Problems

Level I

Section 12-1 Basic Concepts

12-1. Two pions at rest annihilate according to the reaction $\pi^+ + \pi^- \rightarrow \gamma + \gamma$. (*a*) Why must the energies of the two gamma rays be equal? (*b*) Find the energy of each gamma ray. (*c*) Find the wavelength of each gamma ray.

12-2. Find the minimum energy of the photon needed for the following reactions: (*a*) $\gamma \rightarrow \Lambda^+ + \pi^-$, (*b*) $\gamma \rightarrow p + \bar{p}$, and (*c*) $\gamma \rightarrow \mu^- + \mu^+$.

12-3. Draw two different Feynman diagrams for each of the following events: (*a*) $e^+ + e^- \rightarrow e^+ + e^-$; (*b*) $\gamma + e^- \rightarrow \gamma + e^-$.

12-4. Draw a Feynman diagram illustrating each of the following scattering events: (*a*) electron-electron, (*b*) electron-positron, and (*c*) Compton effect.

12-5. Find (*a*) the energy of the electron, (*b*) the energy of the ^{32}S nucleus, and (*c*) the momentum of each in the decay $^{32}\text{P} \rightarrow {}^{32}\text{S} + e^-$, assuming no neutrino in the final state ($n \rightarrow p + e^-$). (The rest mass of ^{32}P is 31.973762 u.)

12-6. The fate of an antiproton is usually annihilation via the reaction $p + \bar{p} \rightarrow \gamma + \gamma$. Assume that the proton and antiproton annihilate at rest. (*a*) Why must there be two photons rather than just one? (*b*) What is the energy of each photon? (*c*) What is the wavelength of each photon? (*d*) What is the frequency of each photon?

12-7. Figure 12-2 shows the production of the first antiproton. It was produced by the reaction $p + p \rightarrow p + p + p + \bar{p}$ and required a minimum kinetic energy of 5.6 GeV. (The proton beam energy was actually 25 GeV.) Less energy would be required by either of the following reactions. Why is neither of them a possible alternative? Justify your answer.

(*a*) $p + p \longrightarrow p + e^- + e^+ + \bar{p}$ (*b*) $p + p \longrightarrow p + \bar{p}$

12-8. Positronium is a bound state of an electron and a positron (see Section 2-4). Its lifetime expressed in natural units used by particle physicists ($\hbar = c = 1$) is $\tau = 2/m\alpha^5$, where m = electron mass and α = the fine-structure constant. Use dimensional analysis (*a*) to include $\hbar$ and c in the expression for τ and (*b*) to compute the value of τ.

Section 12-2 Fundamental Interactions and the Force Carriers

12-9. Name the interaction responsible for each of the following decays:

(*a*) $n \longrightarrow p + e^- + \bar{\nu}_e$

(*b*) $\pi^0 \longrightarrow \gamma + \gamma$

(*c*) $\Delta^+ \longrightarrow \pi^0 + p$

(*d*) $\pi^+ \longrightarrow \mu^+ + \nu_\mu$

12-10. Which of the following decays—$\pi^0 \rightarrow \gamma + \gamma$ or $\pi^- \rightarrow \mu^- + \bar{\nu}_\mu$—would you expect to have the longer lifetime? Why?

12-11. Of the reactions below, which are allowed to proceed via the weak interaction and which are forbidden? Justify your answer.

(*a*) $K^+ \longrightarrow \pi^0 + \mu^+ + \nu_\mu$

(*b*) $p + e^- + \nu_e \longrightarrow e^- + \pi^+ + p$

(*c*) $\Lambda^0 \longrightarrow \pi^+ + e^- + \bar{\nu}_e$

(*d*) $p + \nu_\mu \longrightarrow \mu^+ + n$

STUDENTS-HUB.com Uploaded By: Malak Obaid

12-12. Which of the four fundamental interactions is most likely responsible for the following reactions?

(*a*) ^{16}O (excited state) $\longrightarrow$ ^{16}O (ground state) + γ

(*b*) $\nu_e + e \longrightarrow \nu_e + e$

(*c*) $p + \bar{p} \longrightarrow \gamma + \gamma$

(*d*) $p + \bar{\nu}_e \longrightarrow n + e^+$

(*e*) $\pi^0 + p \longrightarrow \pi^0 + p$

(*f*) $^3H \longrightarrow {}^3He + e^- + \bar{\nu}_e$

12-13. Using the information concerning the neutrinos from SN1987A, including Figure 12-31, compute an upper limit to the mass of the electron neutrino.

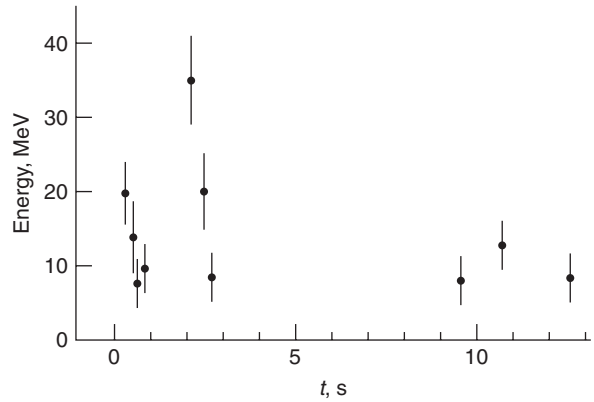

Figure 12-31 Problem 12-13. Electron antineutrino energy versus arrival time in the Kamiokande detector in Japan for antineutrinos emitted by the supernova 1987A. The spread in arrival times (about 13 s) permits a calculation of an upper limit to the mass of the $\bar{\nu}_e$.

12-14. The rest energies of the Σ^+ and Σ^- are slightly different, but those of the π^+ and π^- are exactly the same. Explain this difference in behavior.

12-15. Draw Feynman diagrams of the following decays:

(*a*) $\mu^+ \longrightarrow e^+ + \nu_e + \bar{\nu}_\mu$

(*b*) $\pi^- \longrightarrow \mu^- + \bar{\nu}_\mu$

(*c*) $\tau^- \longrightarrow \mu^- + \bar{\nu}_\mu + \nu_\tau$

Section 12-3 Conservation Laws and Symmetries

12-16. What is the uncertainty in the rest energies of the following particles?

(*a*) $\Lambda(1670)$, (*b*) $\Sigma(2030)$, (*c*) $\Delta(1232)$.

12-17. State which of the decays or reactions that follow violate one or more of the conservation laws, and give the law or laws violated in each case.

(*a*) $p \longrightarrow n + e^+ + \bar{\nu}_e$

(*b*) $n \longrightarrow p + \pi^-$

(*c*) $e^+ + e^- \longrightarrow \gamma$

(*d*) $p + \bar{p} \longrightarrow \gamma + \gamma$

(*e*) $\nu_e + p \longrightarrow n + e^+$

(*f*) $p \longrightarrow \pi^+ + e^+ + e^-$

12-18. Determine the change in strangeness in each reaction that follows, and state whether the reaction can proceed via the strong interaction, the electromagnetic interaction, the weak interaction, or not at all:

(*a*) $\Omega^- \longrightarrow \Xi^0 + \pi^-$

(*b*) $\Xi^0 \longrightarrow p + \pi^- + \pi^0$

(*c*) $\Lambda^0 \longrightarrow p + \pi^-$

12-19. Determine the change in strangeness for each decay, and state whether the decay can proceed via the strong interaction, the electromagnetic interaction, the weak interaction, or not at all: (*a*) $\Omega^- \longrightarrow \Lambda^0 + \bar{\nu}_e + e^-$, (*b*) $\Sigma^+ \longrightarrow p + \pi^0$, and (*c*) $\Sigma^0 \longrightarrow \Lambda^0 + \gamma$

STUDENTS-HUB.com Uploaded By: Malak Obaid

12-20. The rules for determining the isospin of two or more particles are the same as those for combining angular momentum. For example, since $T = 1/2$ for nucleons, the combination of two nucleons can have either $T = 1$ or $T = 0$ or may be a mixture of these isospin states. Since $T_3 = +1/2$ for the proton, the combination $p + p$ has $T_3 = +1$ and therefore must have $T = 1$. Find T_3 and the possible values of T for the following:
(*a*) $n + n$
(*b*) $n + p$
(*c*) $\pi^+ + p$
(*d*) $\pi^- + n$
(*e*) $\pi^+ + n$

12-21. Which of the following decays are allowed and which are forbidden? If the decay is allowed, state which interaction is responsible. If it is forbidden, state which conservation law its occurrence would violate.
(*a*) $\pi^- \longrightarrow e^- + \gamma$
(*b*) $\pi^0 \longrightarrow e^- + e^+ + \nu_e + \bar{\nu}_e$
(*c*) $\pi^+ \longrightarrow e^- + e^+ + \mu^+ + \nu_\mu$
(*d*) $\Lambda^0 \longrightarrow \pi^+ + \pi^-$
(*e*) $n \longrightarrow p + e^- + \bar{\nu}_e$

12-22. For each of the following particles, write down two possible decays that satisfy all conservation laws: (*a*) Ω^-, (*b*) Σ^+, (*c*) Λ^0, (*d*) π^0, and (*e*) K^+.

12-23. Consider the following reactions:

$$K^- + p \longrightarrow K^0 + K^+ + \Omega^-$$

followed by

$$\Omega^- \longrightarrow \Xi^0 + \pi^-$$

Given that $B = 1$ for the proton and $B = 0$ for mesons and that baryon number is conserved, determine the baryon number of the Ω^- and the Ξ^0.

12-24. Which of the following decays and reactions conserve strangeness?
(*a*) $\bar{p} + p \longrightarrow \gamma + \gamma$
(*b*) $\Xi^- \longrightarrow \pi^- + \Lambda^0$
(*c*) $\Sigma^+ \longrightarrow \Lambda^0 + \pi^+$
(*d*) $\pi^- + p \longrightarrow \pi^- + \Sigma^+$
(*e*) $\Omega^- \longrightarrow \Xi^- + \pi^0$

Section 12-4 The Standard Model

12-25. Find the baryon number, charge, isospin, and strangeness for the following quark combinations and identify the corresponding hadron: (*a*) *uud*, (*b*) *udd*, (*c*) *uuu*, (*d*) *uss*, (*e*) *dss*, (*f*) *suu*, and (*g*) *sdd*.

12-26. Find the baryon number, charge, isospin, and strangeness for the following quark combinations and identify the corresponding hadron (the charge and strangeness of the antiquarks are the negatives of those of the corresponding quarks, as with any other particle-antiparticle pair): (*a*) $u\bar{d}$, (*b*) $\bar{u}d$, (*c*) $u\bar{s}$, (*d*) $s\bar{s}$, and (*e*) $\bar{d}s$

12-27. Draw two Feynman diagrams that represent the decay of the antibottom quark.

12-28. Some quark combinations can exist in two or more isospin states, with each state corresponding to a different hadron. One such combination is *uds*. (*a*) What is the value of I_3 for this combination? (*b*) What are the possible values of total isospin I for this combination? (*c*) Find the baryon number, charge, and strangeness of this combination, and identify the hadron corresponding to each isospin state.

12-29. The Δ^{++} particle is a baryon that decays via the strong interaction. Its strangeness, charm, topness, and bottomness are all zero. What combination of quarks gives a particle with these properties?

12-30. Compute the approximate range of a weak interaction mediated by a W^+.

STUDENTS-HUB.com Uploaded By: Malak Obaid

12-31. One mode of weak decay of the $\overline{K}^0$ is

$$\overline{K}^0 \longrightarrow \pi^+ + \mu^- + \overline{\nu}_\mu$$

Showing the quark content of the particles, draw the Feynman diagram of this so-called semileptonic decay.

12-32. The Λ^0 undergoes a weak decay as follows: $\Lambda^0 \rightarrow p + \pi^-$. Showing the quark content of the particles, draw the Feynman diagram of this so-called nonleptonic decay.

12-33. Show that the neutron cannot undergo the weak decay shown for the Λ^0 in Problem 12-32.

12-34. The decay of the Λ^0 shown in Problem 12-32 can also proceed via the strong interaction. Showing the quark content of the particles, draw the Feynman diagram that illustrates the strong decay of the Λ^0.

12-35. The $X^0(1193)$ can be produced by the reaction $K^- + p \rightarrow \pi^0 + X^0$. (*a*) Determine the baryon, strangeness, charm, and bottom quantum numbers of the $X^0(1193)$. (*b*) From your answer to (*a*), what is the quark content of the $X^0(1193)$?

12-36. Find a possible combination of quarks that gives the correct values for electric charge, baryon number, and strangeness for (*a*) K^+ and (*b*) K^0.

12-37. The D^+ meson has strangeness 0, but it has charm of +1. (*a*) What is a possible quark combination that will give the correct properties for this particle? (*b*) Repeat (*a*) for the D^- meson, which is the antiparticle of the D^+.

12-38. The lifetime of the Σ^0 is 6×10^{-20} s. The lifetime of the Σ^+ is 0.8×10^{-10} s and that of the Σ^- is 1.48×10^{-10} s, nearly twice as long. How can these differences in lifetimes between members of the same isospin multiplet be explained?

Section 12-5 Beyond the Standard Model

12-39. Grand unification theories predict that the proton is unstable. If that turns out to be true, why does it mean that baryon number is not conserved? If leptons and quarks are interchangeable at the unification energy, does this mean that there is a new, conserved "leptoquark number"?

12-40. GUTs predict a lifetime of about 10^{32} y for the proton. If that is the case, how many protons will decay each year in the world's oceans? (Assume the average depth of the oceans to be 1 km and that they cover 75 percent of Earth's surface.)

12-41. Protons might decay via a number of different modes. What conservation laws are violated by the following possibilities?

(*a*) $p \longrightarrow e^+ + \Lambda^0 + \nu_e$

(*b*) $p \longrightarrow \pi^+ + \gamma$

(*c*) $p \longrightarrow \pi^+ + K^0$

Level II

12-42. Find a possible quark combination for the following particles: (*a*) $\overline{n}$, (*b*) Ξ^0, (*c*) Σ^+, (*d*) Ω^-, and (*e*) Ξ^-.

12-43. State the properties of the particles made up of the following quarks: (*a*) *ddd*, (*b*) $u\overline{c}$, (*c*) $u\overline{b}$, and (*d*) $\overline{sss}$.

12-44. Show that the Z^0 cannot decay into two identical zero-spin particles.

12-45. Consider the following decay chain:

$$\Xi^0 \longrightarrow \Lambda^0 + \pi^0$$
$$\Lambda^0 \longrightarrow p + \pi^-$$
$$\pi^0 \longrightarrow \gamma + \gamma$$
$$\pi^- \longrightarrow \mu^- + \overline{\nu}_\mu$$
$$\mu^- \longrightarrow e^- + \overline{\nu}_e + \nu_\mu$$

(*a*) Are all the final products shown stable? If not, finish the decay chain. (*b*) Write the overall decay reaction for Ξ^0 to the final products. (*c*) Check the overall decay reaction for the conservation of electric charge, baryon number, lepton number, and strangeness. (*d*) In the first step of the chain, could the Λ^0 have been a Σ^0?

STUDENTS-HUB.com Uploaded By: Malak Obaid

12-46. There are six hadrons with quantum numbers (Q,U,S,C,B) = (2,1,0,1,0); (0,1,−2,1,0); (0,0,1,0,−1); (0,−1,1,0,0); (0,1,−1,1,0); (−1,1,−3,0,0). Determine the quark content of each hadron.

12-47. Show that the following decays conserve all lepton numbers:

(*a*) $\mu^+ \longrightarrow e^+ + \nu_e + \bar{\nu}_\mu$

(*b*) $\tau^- \longrightarrow \mu^- + \nu_\mu + \nu_\tau$

(*c*) $n \longrightarrow p + e^- + \bar{\nu}_e$

(*d*) $\tau^- \longrightarrow \mu^- + \nu_\mu$

12-48. A π^0 with energy 850 MeV decays in flight via the reaction $\pi^0 \rightarrow \gamma + \gamma$. Compute the angles made by the momenta of the gammas with the original direction of the π^0.

12-49. Test the following decays for violation of the conservation of energy, electric charge, baryon number, and lepton number:

(*a*) $\Lambda^0 \longrightarrow p + \pi^-$

(*b*) $\Sigma^- \longrightarrow n + p^-$

(*c*) $\mu^- \longrightarrow e^- + \bar{\nu}_e + \nu_\mu$

Assume that linear and angular momentum are conserved. State which conservation laws (if any) are violated in each decay.

12-50. Consider the following decay chain:

$$\begin{aligned}
\Omega^- &\longrightarrow \Xi^0 + \pi^- \\
\Xi^0 &\longrightarrow \Sigma^+ + e^- + \bar{\nu}_e \\
\pi^- &\longrightarrow \mu^- + \bar{\nu}_\mu \\
\Sigma^+ &\longrightarrow n + \pi^+ \\
\pi^+ &\longrightarrow \mu^+ + \nu_\mu \\
\mu^+ &\longrightarrow e^+ + \nu_e + \bar{\nu}_\mu \\
\mu^- &\longrightarrow e^- + \bar{\nu}_e + \nu_\mu
\end{aligned}$$

(*a*) Are all the final products shown stable? If not, finish the decay chain. (*b*) Write the overall decay reaction for Ω^- to the final products. (*c*) Check the overall decay reaction for the conservation of electric charge, baryon number, lepton number, and strangeness.

Level III

12-51. The mass of the hydrogen atom is smaller than the sum of the masses of the proton and the electron, the difference being the binding energy. The mass of the π^+ is 139.6 MeV/c^2; however, the masses of the quarks of which it is composed are only a few MeV/c^2. How can that be explained?

12-52. (*a*) Calculate the total kinetic energy of the decay products for the decay $\Lambda^0 \rightarrow p + \pi^-$. Assume the Λ^0 is initially at rest. (*b*) Find the ratio of the kinetic energy of the pion to the kinetic energy of the proton. (*c*) Find the kinetic energies of the proton and the pion for this decay.

12-53. A Σ^0 particle at rest decays into a Λ^0 plus a photon. (*a*) What is the total energy of the decay products? (*b*) Assuming that the kinetic energy of the Λ^0 is negligible compared with the energy of the photon, calculate the approximate momentum of the photon. (*c*) Use your result for (*b*) to calculate the kinetic energy of the Λ^0. (*d*) Use your result for (*c*) to obtain a better estimate of the momentum and the energy of the photon.

12-54. In this problem, you will calculate the difference in the time of arrival of two neutrinos of different energy from a supernova that is 170,000 light-years away. Let the energies of the neutrinos be E_1 = 20 MeV and E_2 = 5 MeV, and assume that the mass of a neutrino is 2.2 eV/c^2. Because their total energy is so much greater than their rest energy, the neutrinos have speeds that are very nearly equal to c and energies that are approximately $E \approx pc$. (*a*) If t_1 and t_2 are the times it takes for neutrinos of speeds u_1 and u_2 to travel a distance x, show that

$$\Delta t = t_2 - t_1 = x\frac{u_1 - u_2}{u_1 u_2} \approx \frac{x\,\Delta u}{c^2}$$

STUDENTS-HUB.com Uploaded By: Malak Obaid

(*b*) The speed of a neutrino of mass m_0 and total energy E can be found from Equation 2-10. Show that when $E \gg m_0c^2$, the speed u is given by

$$\frac{u}{c} \approx 1 - \frac{1}{2}\left(\frac{m_0c^2}{E}\right)^2$$

(*c*) Use the result for (*b*) to calculate $u_1 - u_2$ for the energies and mass given, and calculate Δt from the result (*a*) for $x = 170{,}000\ c \cdot \text{y}$. (*d*) Repeat the calculation in (*c*) using $m_0c^2 = 40$ eV for the rest energy of a neutrino.

12-55. There are three possible decay modes for the τ^-. (*a*) Draw the Feynman diagrams for each mode. (*b*) Which mode is the most probable? Explain why.

12-56. In a large accelerator, such as the Large Hadron Collider at CERN, the momentum of a proton in a circular orbit of radius R is given by $\mathbf{p} = 0.3\ R\mathbf{B}\ \text{GeV}/c$, where $\mathbf{B}$ is the magnetic field. Derive this expression.

STUDENTS-HUB.com Uploaded By: Malak Obaid

CHAPTER 13

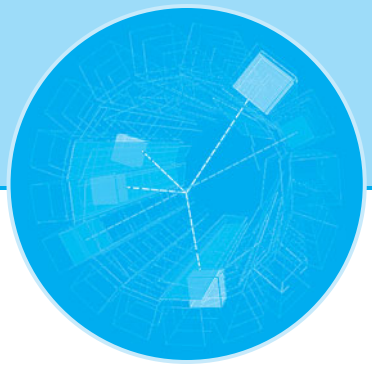

Astrophysics and Cosmology

13-1 The Sun 619
13-2 The Stars 630
13-3 The Evolution of Stars 639
13-4 Cataclysmic Events 644
13-5 Final States of Stars 647
13-6 Galaxies 653
13-7 Cosmology and Gravitation 662
13-8 Cosmology and the Evolution of the Universe 664

Physics is an experimental science. The formulation and acceptance of our current understanding of the physical world, from Newton's laws and Maxwell's equations to relativity theory and quantum mechanics, are based on countless experimental observations. In this chapter, we look outward from Earth into the cosmos and apply the principles and techniques of physics first to the composition and evolution of stars, a branch of physics called *astrophysics*, and then to the large scale structure and evolution of the universe, a field called *cosmology*. In doing so the scale of our discussions expands from the nanometer and femtometer dimensions of the molecules, atoms, and nuclei to the light-year and parsec dimensions of galaxies and space, a span of more than 40 orders of magnitude.

When observing stars and galaxies, astrophysicists and cosmologists are limited to examining the electromagnetic radiation and occasional particles emitted at times past that happen to have traveled to the vicinity of Earth so as to arrive at the moment of observation. The information thus gained, together with the fundamental assumption that the laws of physics discovered here on Earth are also valid throughout the universe, forms the basis for their work. During most of history, the instrument used for studying the cosmos was the human eye. Though well adapted to life on Earth, the eye is a relatively poor instrument for the scientific examination of the sky because it stores information for only a small fraction of a second before transmitting it to the brain for analysis, is sensitive to a very limited portion of the electromagnetic spectrum, and has limited resolution and light-gathering capacity. Today, most of our information about the distant universe is received through telescopes.

13-1 The Sun

As we look outward from Earth and beyond the Moon, the most obvious object in the sky is, of course, the Sun. It is important to us for several reasons. First, the light that reaches us from the Sun is responsible for life on Earth. It sustains a comfortable average temperature on Earth's surface and is the ultimate source of virtually all of our energy. Since the Sun contains nearly all of the mass of the solar system, it also provides the gravitational force that binds our planet to the system. But most important

STUDENTS-HUB.com
Uploaded By: Malak Obaid

for our purposes in this section, the Sun is the only star of the 100 billion or so in the Milky Way that is close enough for us to examine its surface in detail. The others are so far away that they appear only as point sources when viewed by even the largest telescopes. (The very recent exceptions are Alpha Orionis—Betelgeuse—which has been imaged by the Hubble Space Telescope, and Altar, which has been imaged by long-baseline interferometry.) What we learn from studies of our star not only provides a more complete understanding of the processes taking place in it, but surely applies to other stars as well.

The Surface and Atmosphere of the Sun

We can see only the thin outer layer of the Sun, the *photosphere*, which emits the light that makes the Sun visible. The photosphere is generally considered to be the surface of the Sun. The energy per second per square meter that arrives from the Sun at the top of Earth's atmosphere is called the *solar irradiance* or the *solar constant f*. It has been measured to be

$$f = 1.365 \times 10^3 \text{ W/m}^2 \qquad \textbf{13-1}$$

The corresponding quantity for stars other than the Sun is called the *radiant flux*, as we shall see in Section 13-2. Using the solar constant, the Earth-Sun distance of 1 astronomical unit (AU) $= 1.496 \times 10^8$ km, and conservation of energy, we can calculate the *luminosity L*, which is the total power radiated by the Sun or by any star. The area A of a sphere of 1 AU radius is

$$A = 4\pi r^2 = 4\pi(1.496 \times 10^{11})^2 \text{ m}^2$$

At that radius, each square meter receives energy from the Sun at the rate given by the solar constant. Therefore, the Sun's luminosity $L_\odot$ is given by

$$L_\odot = Af = 4\pi(1.496 \times 10^{11} \text{ m})^2(1.365 \times 10^3 \text{ W/m}^2)$$

$$L_\odot = 3.84 \times 10^{26} \text{ W} \qquad \textbf{13-2}$$

This is truly enormous power. If we could put a 1000-MW electricity-generating plant on each square meter of Earth's surface, all of them combined would only produce 0.1 percent of the power produced by the Sun.

If we assume that the Sun radiates as a blackbody, we can use the luminosity of the Sun along with its radius (6.96×10^8 m) to calculate the effective temperature at the surface of the Sun from the Stefan-Boltzmann law. It states that the power per unit area R (= intensity) radiated by a blackbody in thermal equilibrium is proportional to the fourth power of its surface temperature:

$$R = \sigma T^4 \qquad \textbf{3-4}$$

where Stefan's constant $\sigma = 5.67 \times 10^{-8} \text{ W/m}^2 \cdot \text{K}^4$ and T is the absolute temperature. If the radius of the Sun is $R_\odot$, the intensity radiated at the surface of the Sun is

$$R = \frac{L_\odot}{4\pi R_\odot^2} \qquad \textbf{13-3}$$

Take care not to confuse the intensity R with the solar radius $R_\odot$. The effective temperature T_e for the surface of the Sun is defined as the temperature for which the intensity radiated satisfies the Stefan-Boltzmann law for a blackbody:

STUDENTS-HUB.com Uploaded By: Malak Obaid

$$R = \frac{L_\odot}{4\pi R_\odot^2} = \sigma T_e^4$$

Solving for T_e, we obtain

$$T_e = \left(\frac{R}{\sigma}\right)^{1/4} = \left(\frac{L_\odot}{4\pi\sigma R_\odot^2}\right)^{1/4} \qquad \textbf{13-4}$$

EXAMPLE 13-1 **The Temperature of the Sun's Photosphere** Use the Stefan-Boltzmann law to calculate the effective temperature of the photosphere.

SOLUTION

Using $L_\odot = 3.84 \times 10^{26}$ W from Equation 13-2 in Equation 13-4, we have

$$T_e = \left(\frac{L_\odot}{4\pi\sigma R_\odot^2}\right)^{1/4} = \left[\frac{3.84 \times 10^{26}\ \text{W}}{4\pi(5.67 \times 10^{-8}\ \text{W/m}^2 \cdot \text{K}^4)(6.96 \times 10^{8}\ \text{m})^2}\right]^{1/4}$$

$$= 5780\ \text{K}$$

The intensity of solar radiation has been measured at wavelengths ranging from about 10^{-13} m in the gamma-ray region to nearly 10 m in the radio region, a range accounting for over 99 percent of the Sun's emitted power. Over much of this span, the solar spectrum is quite well predicted by Planck's law of blackbody radiation (see Chapter 3) with $T = 5800$ K, as shown in Figure 13-1. The distribution peaks in about the middle (yellow) region of the visible spectrum. This agreement between the measured and theoretical spectra is very constant and is one of the characteristics of the *quiet Sun*.

If we examine the edge of the solar disk, called the *limb*, we see that it is sharply demarcated and darker than the rest of the Sun. From the sharpness of the limb, we conclude from the following reasoning that the photosphere is very thin. Atmospheric turbulence during daylight limits the angular resolution of optical telescopes to about 1 arc second (1/3600 of a degree). At the distance of the Sun, this corresponds to about 700 km. As we look at the Sun, the angle over

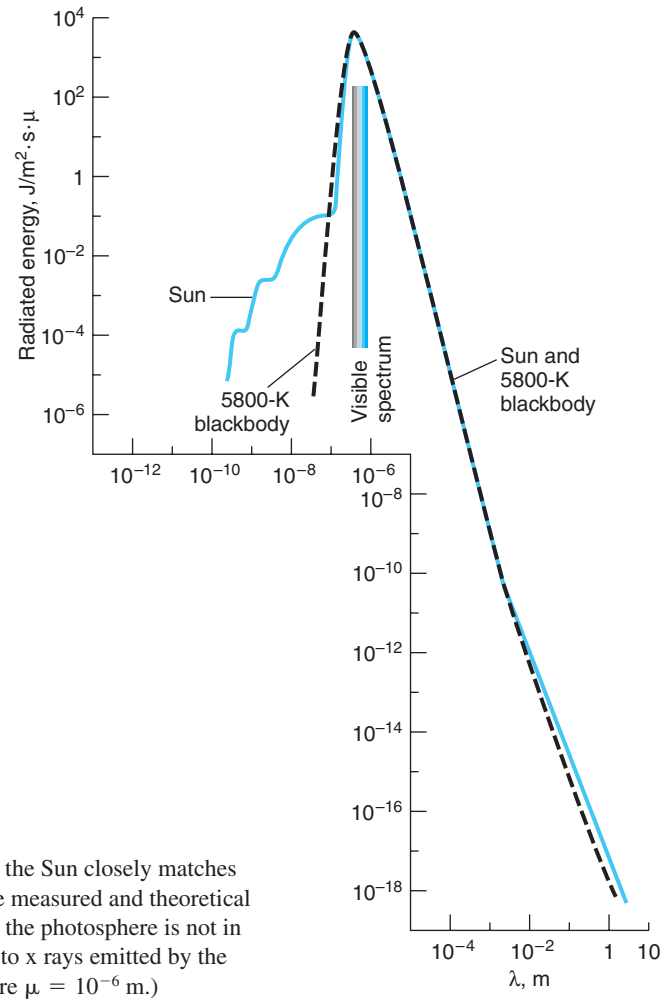

Figure 13-1 The spectral distribution of energy emitted by the Sun closely matches that of a blackbody at 5800 K. The discrepancy between the measured and theoretical curves in the region illustrated is due mainly to the fact that the photosphere is not in thermal equilibrium. The hump at short wavelengths is due to x rays emitted by the corona, which is at a much higher temperature. (In this figure $\mu = 10^{-6}$ m.)

STUDENTS-HUB.com Uploaded By: Malak Obaid

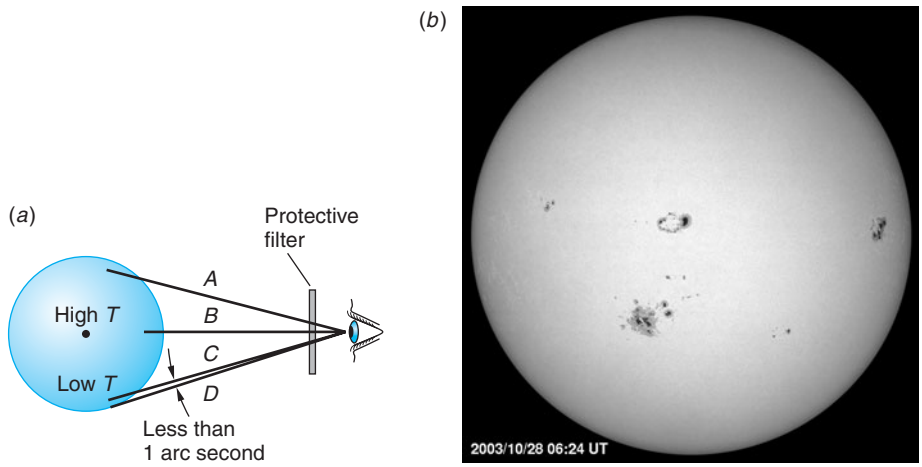

Figure 13-2 (*a*) Two sight lines of equal optical path length, *A* and *B*. Along *B* the observer sees deeper (= hotter = brighter) into the Sun than along *A*; therefore, path *B* looks brighter than path *A*, so the limb looks darker than the disk of the Sun. For paths *C* and *D*, the angle over which the gas of the photosphere changes from transparent to opaque is smaller than we can resolve, so the limb looks sharp. (*b*) A full disk image taken in the visible spectrum or white light at the National Solar Observatory/Sacramento Peak, New Mexico, on October 28, 2003. This image shows sunspot groups and evidence of limb darkening. [*SOHO (ESA & NASA).*]

which the gas of the photosphere changes from rarified and transparent to optically dense and opaque is smaller than we can resolve. Therefore, the photosphere must be less than 700 km thick, which is only about 0.1 percent of the solar radius.

The relatively dark appearance of the limb tells us about the temperature gradient in the Sun's atmosphere. Figure 13-2 shows two paths, *A* and *B*, for viewing the Sun. Because the photosphere is more transparent when viewed at normal incidence than when viewed at a grazing angle, the light traveling along path *B* originates deeper in the Sun than light traveling along path *A*. Since the interior is hotter than the outer layers, the light traveling path *B* originates in a hotter (brighter) part of the Sun than light traveling path *A*. Thus, the light from the limb appears less intense, hence darker (cooler). By measuring the change in brightness from path *A* to path *B*, we can determine the temperature gradient in the photosphere. It is shown in the left portion of Figure 13-3. Notice in the right portion of Figure 13-3 that the temperature begins to rise sharply, accompanying the transition from the Sun's surface, the photosphere, into the solar atmosphere.

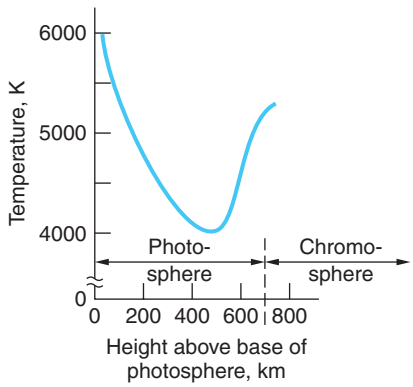

Figure 13-3 The temperature of the Sun decreases from the base of the photosphere outward to a minimum at about 500 km, then increases rather rapidly to about 15,000 K in the chromosphere.

Outside the photosphere are two layers of the Sun's atmosphere that are not generally seen because of the brightness of the photosphere. The inner most of the two layers of the solar atmosphere, the *chromosphere*, is visible for a few seconds just before totality during a solar eclipse. Under high resolution, the chromosphere resembles a field of burning grass, although each burning "blade" is about 700 km thick and 7000 to 10000 km high and lasts for only 5 to 15 minutes. Spectral examination indicates that the temperature of the chromosphere increases with distance above the photosphere, averaging about 15,000 K (Figure 13-4).

STUDENTS-HUB.com Uploaded By: Malak Obaid

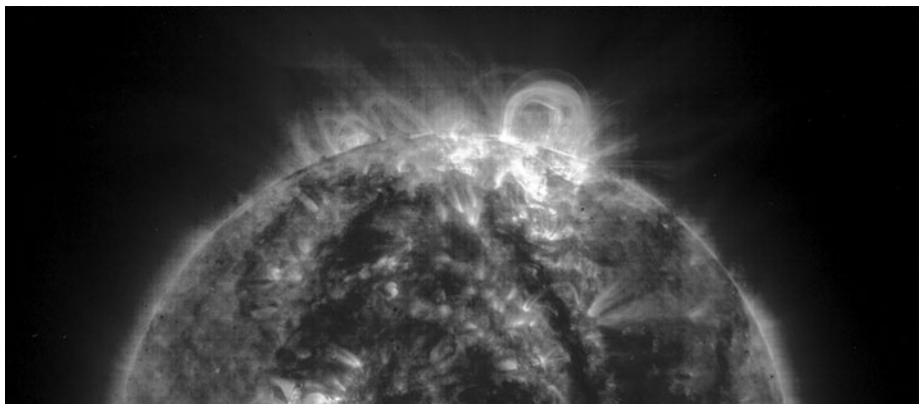

Figure 13-4 This ultraviolet image shows a loop in the magnetic field, seen circling back toward the Sun, trapping hot gas in the chromosphere. [*SOHO (ESA & NASA).*]

When the totality of the eclipse blocks out the chromosphere, the outer layer of the Sun's atmosphere, the *corona*, becomes visible. It is decidedly nonuniform in thickness, consisting of faint white streamers extending 2 to 3 solar diameters into space. The temperature of the corona is approximately 2,000,000 K. Radiation from the corona would overpower that from the 5800 K photosphere, except for the fact that the gas of the corona is so rarified that the total energy it emits is minuscule compared to that of the photosphere. It does, however, account for the relatively high intensity of x rays emitted by the Sun, which shows up in Figure 13-1 as a deviation from the spectral distribution of the blackbody at short wavelengths. It is thought that the extreme temperatures in the corona are produced by acoustic waves generated in the Sun's interior that build into shock waves in the corona. These shock waves heat the gases of the Sun's outer atmosphere and give the particles so much energy that even the Sun's enormous gravity cannot confine them. These high-energy particles, mostly protons and electrons, stream outward from the corona continuously. They form the *solar wind* that pervades the entire solar system.

The Sun's Interior

We cannot see through the photosphere into the interior of the Sun. Consequently, our understanding of the processes there is purely theoretical. With the single exception of solar neutrinos, no radiation or particles originating in the interior reach us directly. To understand the principle features of the current theory, we need first to determine the Sun's mass, as we can do easily with the aid of Newton's law of universal gravitation and the second law of motion. The result is that the Sun's mass $M_\odot = 1.99 \times 10^{30}$ kg.

For simplicity, theoretical models usually consider the Sun to be a nonrotating star in hydrostatic equilibrium. This means that the outward pressure at any point, which is presumed to be due to energy conversion processes occurring in the Sun's interior, is exactly balanced by the inward pressure of gravity. Although the mean density of the Sun (1.4 g/cm^3) is not much different from that of Earth (5.5 g/cm^3), the enormous pressures that exist in the solar interior substantially exceed those that correspond to the electrodynamic forces that bind the electrons to the nuclei. Thus, the matter in the interior of the Sun—and certainly within the *core*, the central region in which temperatures are high enough to allow hydrogen fusion—must surely be in the plasma (ionized) state.

STUDENTS-HUB.com Uploaded By: Malak Obaid

EXAMPLE 13-2 Hydrogen in the Sun's Core Show that neutral hydrogen is unlikely to exist in the Sun's interior.

SOLUTION

The pressure at the center of the Sun P_c is of the order $P_c = \mu g$, where

$$\mu = \text{mass/unit surface area} \approx \left(\frac{M_\odot}{R_\odot^2}\right)$$

and

$$g = \frac{1}{2}G\left(\frac{M_\odot}{R_\odot^2}\right)$$

is the average acceleration due to gravity in the Sun. The pressure turns out to be about 10^{15} N/m^2. This is the pressure pushing on the surface of a hydrogen atom near the Sun's center. The resistance to this gravitational pressure would come from the Coulomb force tending to hold the atom together. That pressure is given by the Coulomb attraction between the proton and electron per unit surface area of the atom. Using the Bohr radius a_0 for hydrogen, we have

$$\frac{F}{A} = \frac{ke^2/a_0^2}{4\pi a_0^2} = \frac{ke^2}{4\pi a_0^4} = \frac{(9 \times 10^9\ \text{N}\cdot\text{m}^2/\text{C}^2)(1.6 \times 10^{-19}\ \text{C})^2}{4\pi(0.5 \times 10^{-10}\ \text{m})^4} = 2.9 \times 10^{12}\ \text{N/m}^2$$

Thus, the gravitational pressure in the Sun's interior, at least near the center, exceeds that tending to hold the hydrogen atoms together by a factor of about 1000—making it unlikely that neutral hydrogen atoms could exist there.

Remarks: *Given the Sun's density, even the particles in the depths of the core are still relatively far apart, so that the plasma behaves much like an ideal gas. This allows calculation of the core temperature from the ideal-gas law. It is found to be about* 1.5×10^7 *K.*

The Source of the Sun's Energy

Using the value for the luminosity of the Sun that we computed earlier, Lord Kelvin was the first to point out that the present energy content of the Sun as calculated from thermodynamics would be radiated away in about 3×10^7 years. Since life has existed on Earth for approximately 100 times that long, we can conclude that the Sun has been radiating at close to its present luminosity for at least 3×10^9 years. Therefore, the Sun must have a supply of energy far larger than that represented by gravitational potential energy, the hot plasma, and the observed radiation field. The source of the Sun's energy is nuclear fusion.

Current theory proposes that, as the young Sun contracted, its temperature rose. To understand why the Sun contracted and why that caused its temperature to rise, we start with Newton's law of universal gravitation.

$$F_{\text{grav}} = G\frac{Mm}{R^2}$$

where F_{grav} is the attractive gravitational force between the masses M and m which are separated by a distance R, and G is the constant of gravitation.. Notice that, as R becomes smaller, F_{grav} becomes larger, which means that the masses M and m move

STUDENTS-HUB.com Uploaded By: Malak Obaid

toward one another with increasing acceleration. Conservation of energy requires that the resulting increase in kinetic energy must come from somewhere. That "somewhere" is the gravitational potential energy U_{grav} of the masses in their original positions; U_{grav} must decrease correspondingly. How might this account for the energy emitted by the Sun (and other stars)? A star is a huge ball of gas. The gas atoms near the surface feel the gravitational force attracting them toward the inner atoms of the star's core. The core atoms feel that force, too, but they are also attracted in the opposite direction by the gas atoms near the surface on the other side; hence, the core atoms don't move. (See Figure 13-5.) However, the entire surface of the star accelerates toward the core—the star undergoes gravitational contraction. The increasing kinetic energy of the accelerated atoms (heat) increases the star's temperature, radiating energy into space.

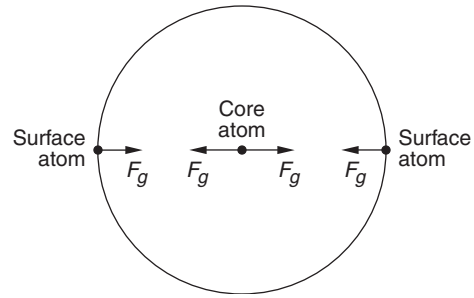

Figure 13-5 Atoms in the outer areas of stars feel a net gravitational force directed toward the core. The net gravitational force on the atoms in the core is essentially zero. In the absence of an outward-directed pressure, the star collapses.

Eventually the temperature of the core reached about 1.5×10^7 K, which is high enough for the hydrogen nuclei (protons) in the plasma to have sufficient energy on the average (about 1 keV) to fuse into helium nuclei. This reaction, actually a chain of reactions, was first proposed by H. A. Bethe[1] and is referred to as the *proton-proton cycle*. The first reaction in the chain is

$$^1\text{H} + {}^1\text{H} \longrightarrow {}^2\text{H} + e^+ + \nu_e + 0.42 \text{ MeV} \qquad \textbf{13-5}$$

Due to the height of the Coulomb barrier the probability for this reaction is very low except for those protons in the high-energy tail of the Maxwell-Boltzmann distribution. Fusion is possible only because of quantum mechanical tunneling. This sets a limit on the rate at which the Sun can produce energy and thus ensures a long lifetime for the Sun and similar stars. This limit is sometimes called the "bottleneck" of the solar fusion cycle. Once ^{2}H (deuterium) is formed via Equation 13-5, the following reaction becomes very probable:

$$^2\text{H} + {}^1\text{H} \longrightarrow {}^3\text{He} + \gamma + 5.49 \text{ MeV} \qquad \textbf{13-6}$$

It is followed by

$$^3\text{He} + {}^3\text{He} \longrightarrow {}^4\text{He} + 2\,{}^1\text{H} + \gamma + 12.86 \text{ MeV} \qquad \textbf{13-7}$$

This process by which hydrogen nuclei are "burned" to helium nuclei is shown schematically in Figure 13-6*a*. There are other possible reactions for converting ^{1}H to ^{4}He, all of which have the same net Q value. Their rates, however, differ depending on the composition and temperature of the Sun's interior. The most important of these is the CNO (carbon-nitrogen-oxygen) cycle, which accounts for about 1.5 percent of the total solar luminosity. The CNO cycle is very temperature dependent and is the dominant H-fusion cycle for stars slightly more massive than the Sun.

The neutrinos produced in the proton-proton cycle escape from the core, providing our only means for direct observation of the Sun's interior. The measured luminosity $L_\odot$ and the known total Q value of the proton-proton cycle enable a calculation of the total reaction rate. In addition, the alternative reactions for ^{3}He have different neutrino energy spectra, thus providing a way of determining the relative contributions of each reaction and gaining further information about the composition and temperature of the core. The neutrino flux arriving at Earth from all reactions in the proton-proton fusion cycle determined by John Bahcall's[2] definitive theoretical analysis of the solar neutrino spectrum based on the standard solar model is shown in Figure 13-6*b*.

STUDENTS-HUB.com Uploaded By: Malak Obaid

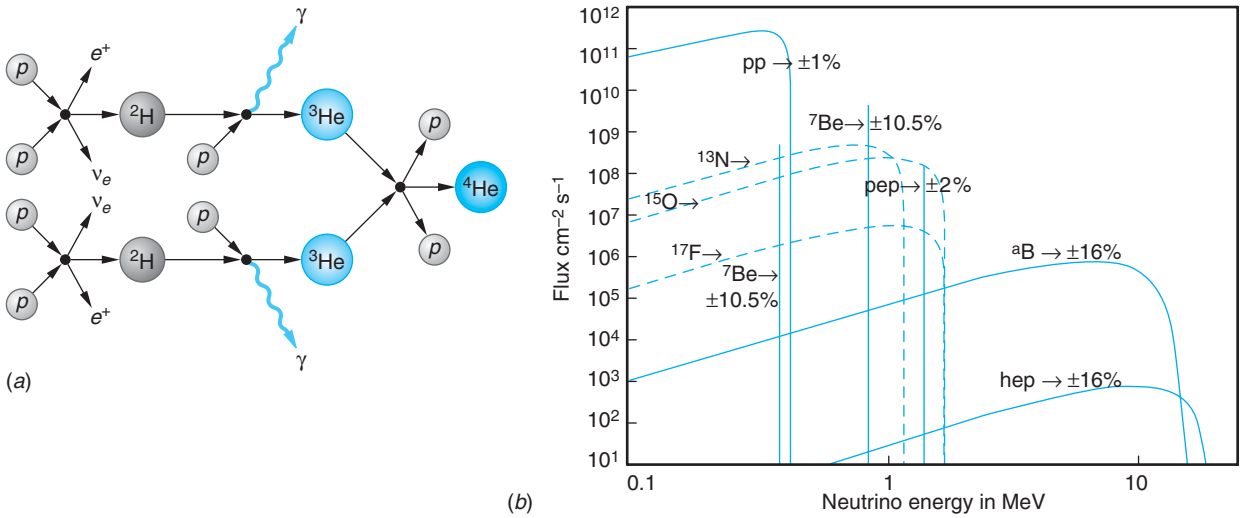

Figure 13-6 (*a*) The proton-proton cycle is the primary source of the Sun's energy. The neutrino created in the initial step escapes from the core. The net energy produced, including that released from orbital electron binding and $e^- e^+$ annihilation, is about 26.7 MeV per ^{4}He produced. (*b*) Neutrino flux at Earth predicted by the standard solar model. Neutrinos produced in the *p-p* cycle are shown by solid lines; those produced in the CNO cycle are shown by dotted lines. [*J. Bahcall and A. Serenilli, ApJ,* **621**, *L85 (2005).*]

For those neutrinos resulting from the $^8\text{B} + p \rightarrow {}^8\text{Be}^* + \text{e}^+ + \nu_e$ reaction (Table 13-1) the predicted intensity is 8.1 ± 1.3 *S*olar *N*eutrino *U*nits (1 SNU = 1 event per 10^{36} target atoms per second). However, experiments conducted by Ray Davis and his co-workers over more than 30 years using a chlorine radiochemical detector located deep inside a gold mine in South Dakota which was sensitive primarily to the ^{8}B-produced neutrinos[3] found the measured rate at which solar neutrinos from this reaction arrive at Earth to be 2.56 ± 0.16 SNU, only about 32 percent of the expected rate. Subsequently, experiments sensitive to other reactions in the *p-p* cycle performed at six other laboratories around the world confirmed this discrepancy. This discrepancy is referred to as the *solar-neutrino problem*. Davis shared the 2002 Nobel Prize in Physics for this discovery.

The discrepancy between the theoretical prediction of the standard solar model and the experimental results presented a very serious problem for both astrophysics and particle physics. In the words of John Bahcall, whose calculations provided the solar model prediction:

> Is the solar neutrino problem caused by unknown properties of neutrinos or by a lack of understanding of the interior of the Sun? In other words, is this a case of new physics or faulty astrophysics?

It turned out to be a case of "new physics." As was described in Section 12-5, the recent discovery of neutrino oscillations that enables neutrinos of one flavor to change into neutrinos of another flavor, means that electron neutrinos emitted in the Sun's *p-p* fusion cycle may oscillate to muon or tau neutrinos during their trip from the Sun to Earth. Davis's neutrino telescope was sensitive only to electron neutrinos. This accounts for the discrepancy and also, according to the Standard Model of particle physics, requires that neutrinos have a nonzero mass.

STUDENTS-HUB.com Uploaded By: Malak Obaid

Table 13-1 Proton-proton nuclear fusion cycle

	Reaction	% of events	ν energy (MeV)
1.	$p + p \longrightarrow {}^2\mathrm{H} + e^+ + \nu_e$	99.96	≤ 0.423
	or		
	$p + e^- + p \longrightarrow {}^2\mathrm{H} + \nu_e$	0.04	1.445
2.	${}^2\mathrm{H} + p \longrightarrow {}^3\mathrm{He} + \gamma$	100	
3.	${}^3\mathrm{He} + {}^3\mathrm{He} \longrightarrow {}^4\mathrm{He} + 2p$	85	
	or		
	${}^3\mathrm{He} + {}^4\mathrm{He} \longrightarrow {}^7\mathrm{Be} + \gamma$	15	
4.	${}^7\mathrm{Be} + e^- \longrightarrow {}^7\mathrm{Li} + \nu_e$	15	0.863 (90%) 0.385 (10%)
5.	${}^7\mathrm{Li} + p \longrightarrow 2\,{}^4\mathrm{He}$		
	or		
	${}^7\mathrm{Be} + p \longrightarrow {}^8\mathrm{B} + \gamma$	0.02	
6.	${}^8\mathrm{B} \longrightarrow {}^8\mathrm{Be}^* + e^+ + \nu_e$		<15
7.	${}^8\mathrm{Be}^* \longrightarrow 2\,{}^4\mathrm{He}$		
	or		
	${}^3\mathrm{He} + p \longrightarrow {}^4\mathrm{He} + e^+ + \nu_e$	0.00003	<18.8

Source: Data from J. Bahcall, *Phys. Rev. C*, **56**, 3391 (1997).

The Active Sun

In addition to the relatively stable phenomena that we have discussed, the Sun exhibits a number of transient phenomena, most of which are associated with its magnetism. We noted earlier that the solar interior must be primarily a plasma composed of protons and electrons. The Sun rotates with different angular velocities at different latitudes. At any given latitude, it probably has different angular velocities at different distances from the spin axis as well. The complex motions resulting from this differential rotation and from the rise and fall of charged particles in the convection zone between the core and the photosphere are probably the source of the Sun's chaotic magnetic field structure (Figure 13-7). This transient structure may have localized magnetic field strengths exceeding 1 T on occasion.

The transient structure is superimposed onto a general average magnetic field of about 10^{-4} T, roughly twice Earth's average magnetic field. The origin of this general field is not known, except that it is not a remnant of the Sun's formation, since a primeval field would likely have decayed away by now. Its presence poses formidable problems for any theoretical solar model. Not only must the model explain the origin of the general field, but it must also account for the fact that its polarity reverses every 11 years, in step with the *sunspot cycle*.

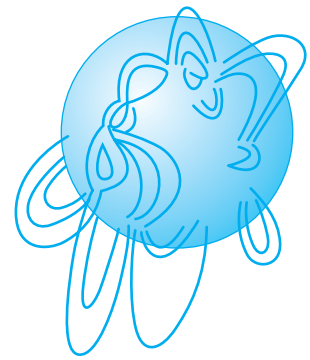

Figure 13-7 The field lines that describe the Sun's magnetic field structure at any given time are derived from ground-based measurements, e.g., Zeeman effect and the transport of charged matter. The high-intensity, chaotic structure is superimposed onto a constant general magnetic field of about 10^{-4} T.

STUDENTS-HUB.com Uploaded By: Malak Obaid

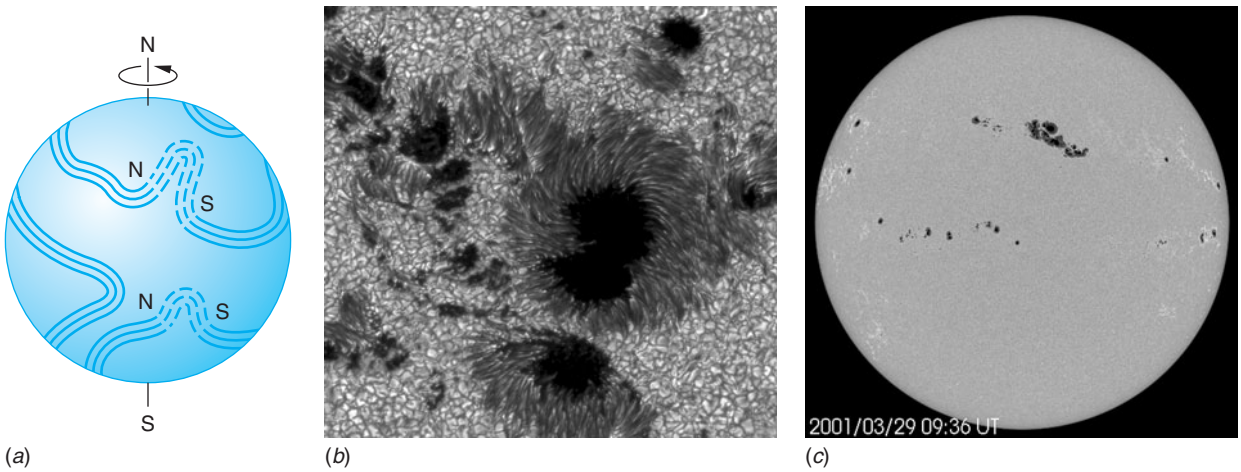

(*a*) (*b*) (*c*)

Figure 13-8 (*a*) Magnetic flux lines are distorted by the Sun's differential rotation and pushed up out of the surface by motion in the convection zone. (*b*) A sunspot occurs where a bundle of field lines leaves and reenters the surface. The areas where they leave and return to the surface become sunspots. This very large spot on this part of the Sun's surface is about 20 arc seconds in diameter. The granular appearance of the Sun's surface is very apparent. Sunspot activity on 29 March 2001. [(*b*) *Institute for Solar Physics of the Royal Swedish Academy of Sciences*. (*c*) *SOHO (ESA & NASA).*]

Sunspots, dark blemishes on the solar disk, were first reported in pretelescope times and were observed by Galileo in 1610. They originate in the following way, according to one of the current models: As shown in Figure 13-8, the Sun's magnetic field lines are distorted into bundles or tubes by the Sun's differential rotation. Occasionally vertical movements in the convection zone may push a bundle through the surface. The area where it leaves the surface and the area where it returns to the surface become the sunspots. They appear darker than the adjacent photosphere, which means that they are cooler, typically around 3800 K. One of the pair of spots will have a magnetic north pole, the other a south pole. If the bundle of field lines does not protrude completely through the photosphere, only a single sunspot is formed.

The number of spots per year varies regularly from about 20 to about 150 in a cycle of 11 years, as can be seen in Figure 13-9. Early in each new cycle, the sunspots form at a latitude of about 30°. As the Sun progresses through its 11-year cycle, the spots form progressively closer to the equator. There is an additional cyclical variation in the annual number of sunspots with a period of about 100 years that is also apparent in Figure 13-9. Currently, the theoretical explanation for these regularities, while in agreement with some features of the observations, is not complete.

Solar flares are violent, stormlike phenomena that appear to be associated with the large magnetic fields in the vicinity of sunspots. There is, however, no generally accepted model to explain them. Solar flares erupt explosively, ejecting particles and emitting radiation ranging from the x-ray through the radio regions of the spectrum. They last anywhere from a few minutes to a few hours and can have temperatures as high as 5×10^6 K. The particles ejected by solar flares reach Earth within a day or so and often produce auroras as they accelerate in Earth's magnetic field. Solar flares can disrupt some types of radio transmissions, and on rare occasions can generate surges in high-voltage transmission lines. A flare that happened to be directed toward Earth in 1996 caused, among other things, the failure of a communications satellite.

STUDENTS-HUB.com Uploaded By: Malak Obaid

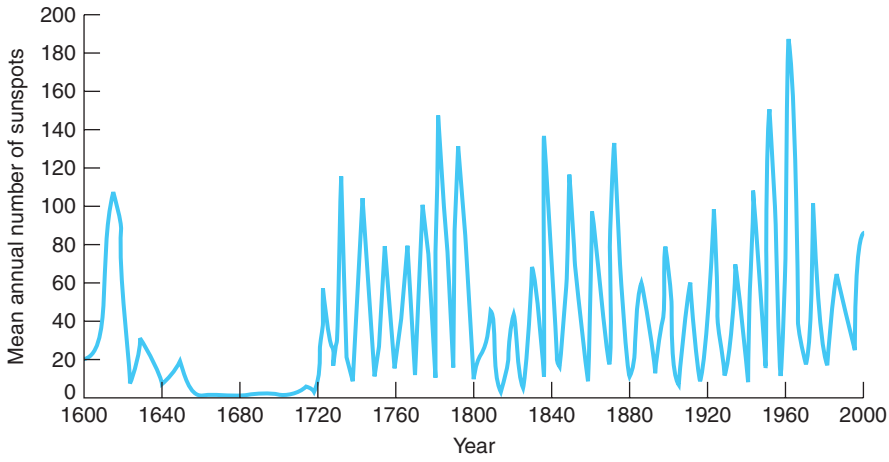

Figure 13-9 The number of sunspots that occur each year has varied regularly on an 11-year cycle for more than 270 years. The unexplained absence of spots between about 1650 and 1700, referred to as the Maunder minimum, approximately coincides with a period of unusually low temperatures in Europe referred to as the "Little Ice Age." Whether there exists a causal connection between the two phenomena is a matter of scientific debate. Sunspot cycle 23 began in 1996 and ended in 2007. (Counting the cycles began in 1775.) Sunspot activity is next expected to peak in 2011–2012.

Two other transient solar phenomena related to sunspots are plages and filaments. *Plages* are bright (hotter) areas adjacent to the dark sunspots. The evolution of plages suggests that they are areas of increased mass density, resulting perhaps from the movement of the magnetic field bundles generated from the sunspots. *Filaments* are dark, thin lines that seem to thread their way across the disk, sometimes for thousands of kilometers. They do not lie on the surface but extend out into space, sometimes more than 100,000 kilometers, in graceful loops and swirls. Filaments that are seen projecting into space at the Sun's edge are called *prominences*. They may erupt and disappear quickly or persist for several weeks. While prominences appear closely related to the shape of the magnetic field, as with other transient features, there is as yet no model that fully accounts for them.

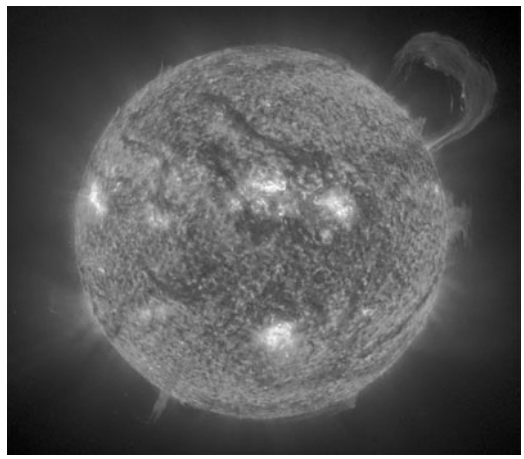

The huge handle-shaped prominence shown on the upper right was photographed in 304 Å [30.4 nm] light on 14 September 1999. It consists of charged particles confined by the magnetic field of the sun. [*SOHO (ESA & NASA).*]

STUDENTS-HUB.com Uploaded By: Malak Obaid

EXPLORING
Is There Life Elsewhere?

We are certainly not the first to ask that question. The Greek philosophers beginning with Thales and continuing through Plato and his student Aristotle thought and wondered about the structure of the heavens and the mysteries they might contain. Many scientists in the nineteenth century assumed that the other planets of the solar system, particularly Mars and Venus, were inhabited. In the twentieth century the term *Martian* became synonymous with "beings from outer space." An entire movie and television genre has flourished based on time travel, spaceships, aliens from outer space, and a plethora of weird science—pseudoscience.

The real issue, however, is much more serious: Is life "out there" possible? The answer is surely, Yes. Consider: With the development and evolution of telescopes we have learned that the motions of stars and galaxies obey the same laws of physics that have been discovered on Earth. Our location is in no way special. The physical processes that occur on Earth occur throughout the universe. All of the chemical elements discovered in our studies of the near and distant universe also occur on Earth. The relativistic and quantum physics we have developed works in the cosmos, too. So, then, must our biology—an application of physics and chemistry—work throughout the universe. On Earth we have learned that life-forms can survive and prosper in seemingly hostile environments. Sea animals thrive in the scalding hot water and enormous pressures of the deep ocean volcanic vents. Other organisms live in the rocks of deep mines and in the permanent ice of the Antarctic. Other creatures have been discovered that use sulfur in their metabolism, rather than oxygen. And the complex organic molecules that are the building blocks of life as we know it have been found in meteorites and identified in interstellar gas clouds. Thus, it would appear that the development of life elsewhere in the Galaxy and the universe may not be all that unusual.

If intelligent life has developed elsewhere, where is it and how do we find it? Since 1995 new technology and techniques have led to the indirect discovery (e.g., via stellar motion perturbations) of 229 extrasolar planets (called *exoplanets*) orbiting 194 relatively nearby stars (as of April 2007). While most of the discovered planets are hot and large, Neptune to Jupiter in size, at least two are cool and about 5 times Earth's mass orbiting a faint star in the Milky Way's central bulge. As of now, only one exoplanet has been imaged directly. If intelligent life on these planets (or the millions of others that must exist throughout the universe) are sending electromagnetic signals into space, as we are, detecting those signals could provide the first clue that we are not the only intelligent life that has existed in the universe. Listening for those signals is the objective of the Search for Extraterrestrial Intelligence (SETI) project. Look for SETI online to learn more.

13-2 The Stars

On clear, dark nights, we can see about 6000 stars without the aid of telescopes. The sight is incredibly beautiful and must surely have been just as awesome to our forebears. A cursory glance at the night sky reveals the following features: the distribution of stars is not uniform, the stars do not all have the same brightness, and there is a dim irregular band of light bisecting the sky. In this section, we will investigate these features.

The hazy band of light that stretches across the entire sky is the Milky Way. With the aid of a small telescope or even binoculars, the band is resolved into a mass of individual stars. It is part of a huge Galaxy[4] containing an estimated 10^{11} stars that are

STUDENTS-HUB.com Uploaded By: Malak Obaid

bound together gravitationally in our region of the universe. Most of the stars visible to the unaided eye seen in any direction are simply those members of the Galaxy close enough to Earth to be individually resolved by the eye.

Constellations Chance groupings in the celestial pattern, usually among the brighter individual stars, are called *constellations*. Ancient peoples associated them with persons, gods, and objects from their histories, religions, and myths, probably as mnemonic devices. The constellations, as well as several prominent stars, have always had practical uses. For centuries, seafarers have used the Pole Star (in the northern hemisphere) and the Southern Cross (in the southern hemisphere) as aids in navigation. In ancient Egypt the pharaoh's advisors learned to predict the life-sustaining annual flooding of the Nile by watching for the first appearance of the bright star Sirius[5] above the horizon in the early spring. Today, 88 constellations (see Figure 13-10 for some of them) are used by astronomers to identify sections of the sky. For example, the center of the Milky Way is said to be "in Sagittarius," meaning it is in the direction of the constellation Sagittarius. (The center of the Galaxy is actually more than 10 times farther from the Sun than are the stars that form that constellation.)

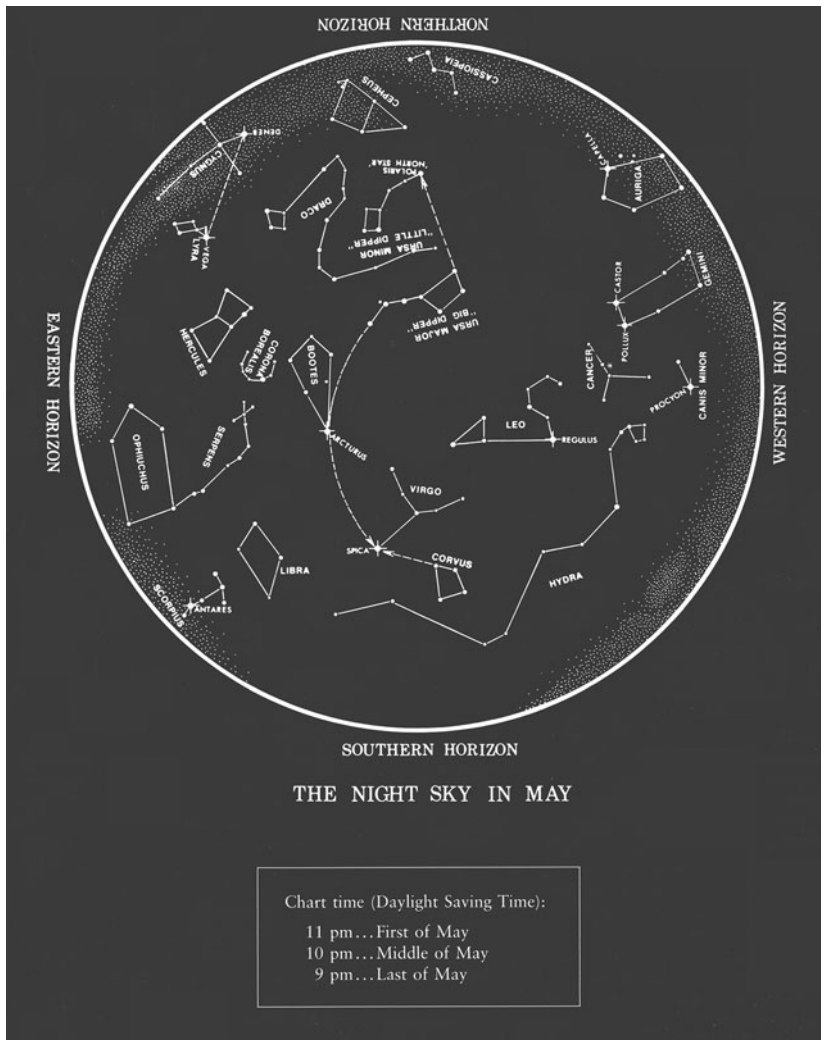

Figure 13-10 Star chart of the sky as it appears on a spring evening at latitude 40° north, showing many of the constellations visible. During the night, the entire pattern revolves about 120° about Polaris, the Pole Star. To use the chart, hold it (or a copy) in front of you with the S (south) at the bottom while you face south. Match the lower half to the stars that you see. Then rotate the chart, putting the W at the bottom, face west and again match the lower half to the stars you see, and so on. [*R. A. Freedman and W. J. Kaufmann III, Universe, 8e (New York: W. H. Freeman and Co., 2008), p. S-6.*]

STUDENTS-HUB.com Uploaded By: Malak Obaid

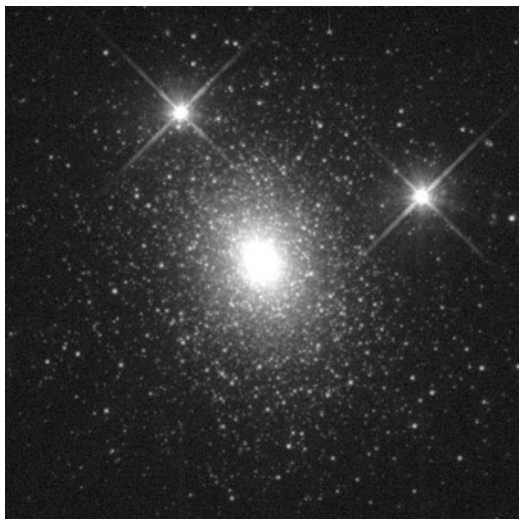

Globular cluster G1 in galaxy M31 contains more than 300,000 stars. G1 orbits the Andromeda galaxy, the nearest large spiral to Earth. The two bright stars with "spikes" are in the Milky Way. [*Michael Rich, Kenneth Mighell, and James D. Neill (Columbia University), and Wendy Freedman (Carnegie Observatories), and NASA.*]

Stellar Populations

One characteristic of our Galaxy is that certain regions of it have many more stars than other nearby regions. Such concentrations are called *star clusters*. There are two types of star clusters. *Galactic clusters*, also called *open clusters*, may contain from about 20 to several hundred stars. All stars in galactic clusters appear to have very similar compositions, as inferred from studies of their optical spectra. About 70 percent of their mass is hydrogen, another 28 percent or so is helium, and 2 to 3 percent consists of elements heavier than helium. Stars with this characteristic composition, like our Sun, are referred to as *population I stars*. *Globular clusters* may consist of 10^3 to 10^6 stars in a compact, roughly spherical group. Their concentrations of elements heavier than helium are all very similar and much lower than that of population I stars, typically 0.1 to 0.01 percent. These are called *population II stars*. One such cluster, photographed by the Hubble Space Telescope, is shown in the photo at the left.

Population I stars are thought to be current generation stars that formed after the gas and dust that exists between these stars had been enriched by the products of ancient fusion reactions in the early universe. The lower concentration of heavier elements in the population II stars suggests that they are of a previous generation, hence older than those of population I. The fact that they are found in regions of space where there is little dust or gas tends to support that interpretation.

Classification of Stars

Stars are grouped into classes based primarily on the spectral lines each emits and absorbs. That different stars have different spectra was discovered nearly 200 years ago by Joseph Fraunhofer who also measured numerous absorption lines in the solar spectrum. Over the years, advances in spectroscopy, instrumentation, and atomic theory enabled astrophysicists Edward Pickering and Annie Jump Cannon[6] to rearrange systematically the earlier classification scheme into a temperature sequence. Stars are grouped according to temperature categories (or spectral types) ranging from hot blue, so-called O stars, to cool red, so-called M stars. The seven categories are: O B A F G K M. Generations of students have memorized the classifications by using the phrase "Oh Be A Fine Girl/Guy, Kiss Me." Table 13-2 lists some of their important characteristics. Cannon also added ten subdivisions (0 to 9) within each category to provide for finer distinctions between the stars in each group. For example, B0 stars are hotter (called *early type*) than B9 stars (called *late type*). The physical basis for the distinction between the groups and early/late types lies in the quantum mechanical details of the spectra and the atomic electron excitations and ionizations of the elements comprising each star. Improved observational techniques and analytical methods have led to a number of additional classifications including several for hot blue emission stars and classes L, T, and Y for cool red and brown dwarfs.

Stellar Magnitudes

The Greek astronomer Hipparchus[7] devised the first classification of stars based on how bright each appeared. Called *apparent magnitude* and represented with the letter m, the values he assigned ranged from $m = 1$ for the brightest stars to $m = 6$ for the dimmest visible to his eye. (The telescope had not yet been invented.) As time passed and technology was developed and improved, astronomers extended and refined the apparent magnitude scale. The modern definition of the

STUDENTS-HUB.com Uploaded By: Malak Obaid

Table 13-2 Characteristics of star categories

Spectral type	Important characteristics
O	Hottest blue-white stars; helium absorption lines
B	Hot blue-white stars; helium and hydrogen absorption lines
A	White stars; hydrogen and calcium absorption lines
F	Yellow-white stars; calcium and some metal absorption lines
G	Yellow stars; solar-type spectra with calcium and iron absorption lines (The Sun is a G2 star.)
K	Cool orange stars; strong metal absorption lines
M	Coolest red stars; strong metal absorption lines

apparent magnitude scale is that a difference of 5 in the value of m corresponds to a factor of 100 in brightness; that is, a difference of 1 in the value of m between two stars means the *ratio* of their respective brightness is $100^{1/5} = 2.51$. Thus, star A with $m = 2$ is 2.51 times brighter than star B with $m = 3$, $2.51 \times 2.51 = 6.31$ times brighter than star C with $m = 4$, and so on. (Note that smaller m-values mean brighter, larger m-values mean dimmer.) Modern technology enables scientists to measure apparent magnitude with an accuracy of ± 0.01 and has vastly extended the range of m-values. For example, the brightest star in the sky, the Sun, has $m = -26.81$ and the faintest objects that can be observed have about $m = 29$.

Of course, apparent magnitudes are not the whole story. Two stars with the same luminosity, but located at different distances from us will have different m-values, the furthest away being the dimmer and, therefore, having the larger m-value. So we define a new, more basic quantity, the *absolute magnitude* M, in terms of the *radiant flux* F which includes both the star's luminosity L and its distance R from Earth (see Section 13-1). The radiant flux F is defined as

$$F = \frac{L}{4\pi R^2} \qquad \textbf{13-8}$$

Recall that $4\pi R^2$ is the surface area of a sphere of radius R and has SI units of meter squared (m^2). The units of radiant flux are then $J/s \cdot m^2$. Using Equation 13-8, the absolute magnitude M of a star is defined as being equal to the apparent magnitude the star would have, *if* it were located at a distance of 10 parsecs (pc; see Section 13-3) from Earth. Using the expression for the radiant flux and the definitions for the apparent and absolute magnitudes, one can eventually obtain the expression below connecting F, m, M, and R:

$$100^{(m-M)/5} = \frac{F_{10\text{ pc}}}{F} = \left(\frac{R}{10\text{ pc}}\right)^2 \qquad \textbf{13-9}$$

where R is the actual distance between the star and Earth (measured in pc).

STUDENTS-HUB.com Uploaded By: Malak Obaid

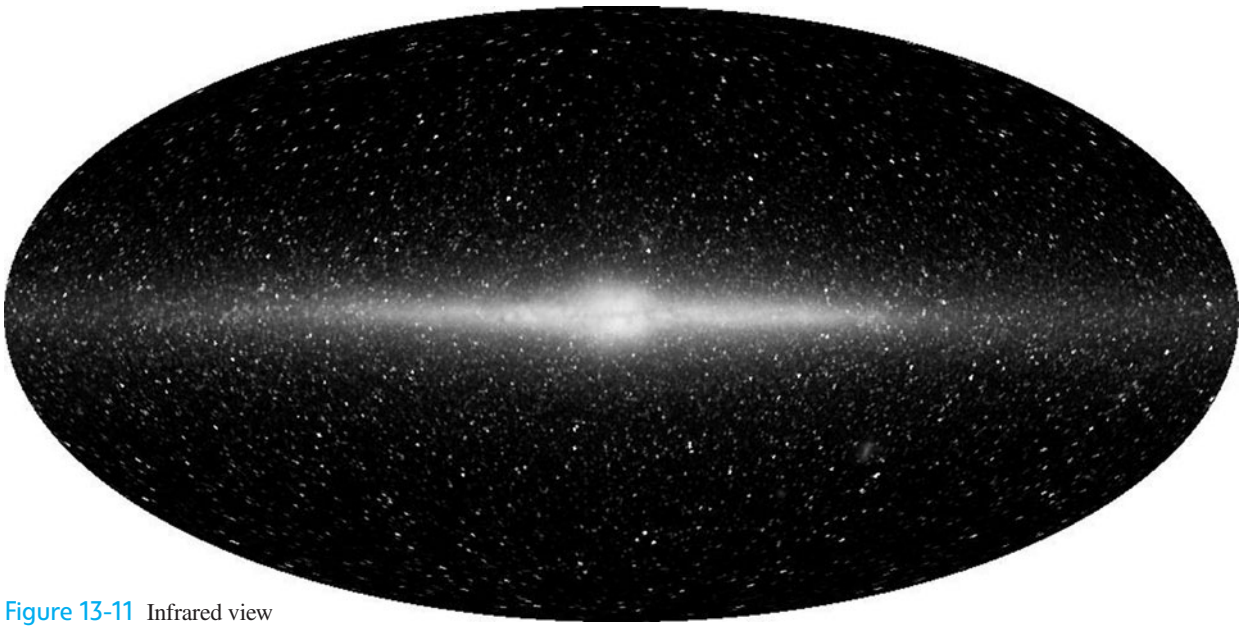

Figure 13-11 Infrared view of the Milky Way taken by the COBE satellite showing the disk and the central bulge. [*The COBE Project, DIRBE/NASA.*]

The Structure of the Milky Way

Figure 13-11 is a map of the Milky Way viewed from the location of the Sun. The size and shape of the Galaxy are not at all obvious in the picture—hardly surprising from the perspective of an observer inside the Galaxy itself.[8] However, painstaking counts of the number of stars per unit volume in various directions have revealed that the Milky Way is basically a huge disk. Up until the early 1900s, astronomers thought that the Sun was located at the disk's center. The true size and shape of the Galaxy (Figure 13-12) were deduced by H. Shapley[9] through a brilliant analysis of the distribution of globular clusters. He discovered that 200 or so globular clusters are distributed approximately spherically in space and proposed that the center of that distribution coincided with the center of our Galaxy. That center lies about 28,000 $c \cdot$ y (8 kpc; see Equation 13-12) from the Sun, which is approximately one-third of the way out from the center. The Milky Way is roughly 1.63×10^5 $c \cdot$ y in diameter. It has been said that Shapley dethroned the Sun from the center of the Galaxy in much the same way that Copernicus had dethroned Earth from the center of the universe.

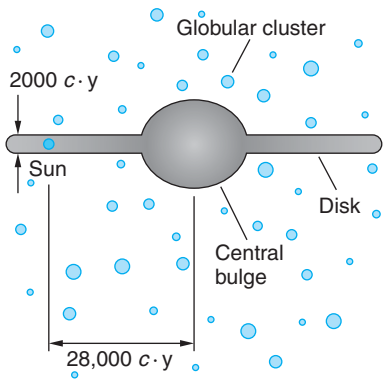

Figure 13-12 A diagram of the presently accepted structure of the Milky Way based on the work of Harlow Shapley. The Milky Way is brighter in the summer night sky in the northern hemisphere than in the winter because the summer night sky looks toward the center of the Galaxy, while the winter night sky is toward its outer edge.

Following Shapley's work, astronomers studying other nearby galaxies with the aid of new, high-resolution telescopes found that the distribution of stars within those systems, many of which had open spiral structures such as shown in Figure 13-24*b* (page 655), depends in part upon the ages and compositions of the stars, with open clusters being found mainly in the arms of the spirals. Making the reasonable assumption that such distribution patterns would also hold for the Milky Way and with meticulous measurements of the distances to about 200 galactic clusters, astronomers have identified three spiral arms and a bar associated with the central bulge for the Milky Way. Thus, if we could look down on the Milky Way from the Galactic north pole, it would look much like Figure 13-13*a*.

STUDENTS-HUB.com Uploaded By: Malak Obaid

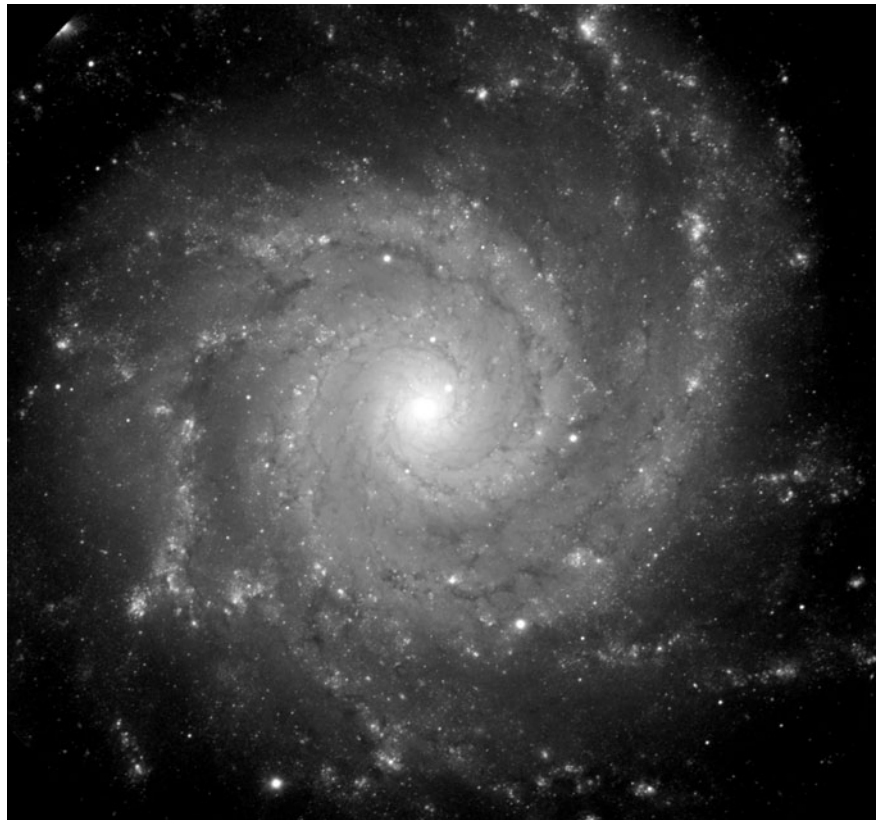

(*a*)

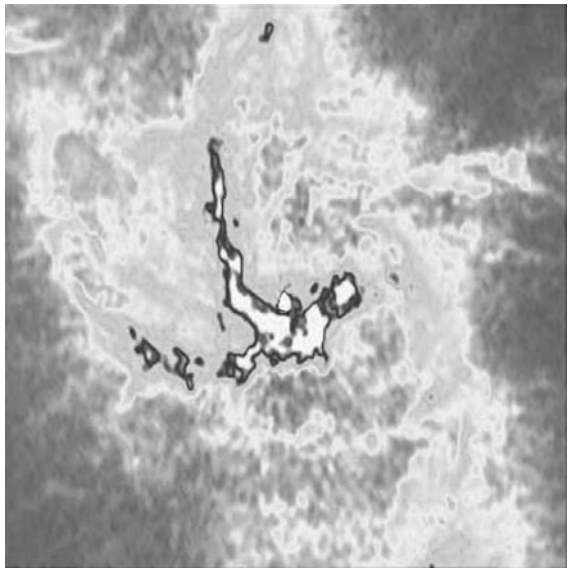

(*b*)

Figure 13-13 (*a*) The combination of observations in the visible and radio regions of the spectrum reveal a spiral structure with a faint bar for the Milky Way. To an observer looking down on the Galaxy from about 1 million parsecs, the Milky Way might look something like this. The Sun is 28,000 *c* · y from the center in one of the spiral arms. (*b*) Viewed from Earth, the center of the Galaxy is obscured by clouds of dust and gas that prevent most visible light from reaching us; however, it contains several areas of strong radio emission, the strongest of which is Sagittarius A*, a compact radio source that appears to dominate the large-scale motion of the galactic center. This radio image (taken at 6 cm wavelength) is of the inner 8 *c* · y of the Milky Way. The dark spot at the very center is Sagittarius A, which is very likely a huge black hole (see Section 13-5). This image was made using the Very Large Array, a radio frequency interferometer made of 27 synchronized antennae with an effective diameter of about 40 km, located in New Mexico. Its resolution is better than that of the best ground-based optical telescopes by about a factor of five. [*(a) Gemini Observatory-GMOS Team. (b) HST Astronomy Imaging Workbench/Farhad Yusef-Sadeh/ Northwestern University.*]

STUDENTS-HUB.com Uploaded By: Malak Obaid

EXPLORING
The Celestial Sphere

Copernicus's refined heliocentric model of the solar system and its subsequent verification by observations laid to rest for all time the geocentric model of Aristotle and Ptolemy. However, we still use one feature of the latter. Putting aside the motions of the planets and a few interplanetary space probes, our observations of the stars and specification of their locations in the sky are normally referred to a coordinate system centered on Earth, not the Sun. The distances to the stars are so great that the stars appear to us to be fixed relative to one another and collectively form the surface of a huge sphere—the *celestial sphere*—with Earth at its center.

The celestial sphere rotates regularly each night from east to west, its axis of rotation coinciding with Earth's rotational axis and its north and south poles oriented in the same way as Earth's poles. The locations of the stars on the celestial sphere, like towns on a road map and points on the surface of Earth, are specified with two coordinates. For locations on Earth the coordinates are called *latitude* and *longitude*. The former specifies how many degrees north or south of the equator (which is defined as zero degrees, 0° latitude) the point is located; the latter tells how many degrees west of zero degrees longitude the point lays. The longitude line (also called a meridian) that passes through Greenwich, United Kingdom, is defined as 0°. (See Figure 13-14*a*.)

Since there are 360° around Earth and our planet rotates on its axis once every 24 hours (1440 min), longitude is often expressed in time units (hours) rather than angle units (degrees or radians).

$$\frac{1440 \text{ min}}{360 \text{ deg}} = 4.0 \frac{\text{min}}{\text{deg}}$$

For example, Orlando, Florida, is located at 28.4° N latitude, 81.3° W longitude. In time units 81.3° W longitude is

$$81.3 \text{ deg} \times 4.0 \text{ min/deg} = 325.2 \text{ min} = 5.42 \text{ h}$$

Thus, Orlando is 5.42 hours west of (i.e., earlier than) Greenwich.

On the celestial sphere the locations of stars are described in an exactly analogous way. The analog of longitude on the celestial sphere is *right ascension*.[10] It is represented by the lower case Greek letter α. Right ascension is measured in hours, rather than degrees, from zero up to 24 as on Earth. The analog of latitude is *declination*, represented by the lower case Greek letter δ. Declination is measured in degrees north (+) or south (−) of the celestial equator. (See Figure 13-14*b*.)

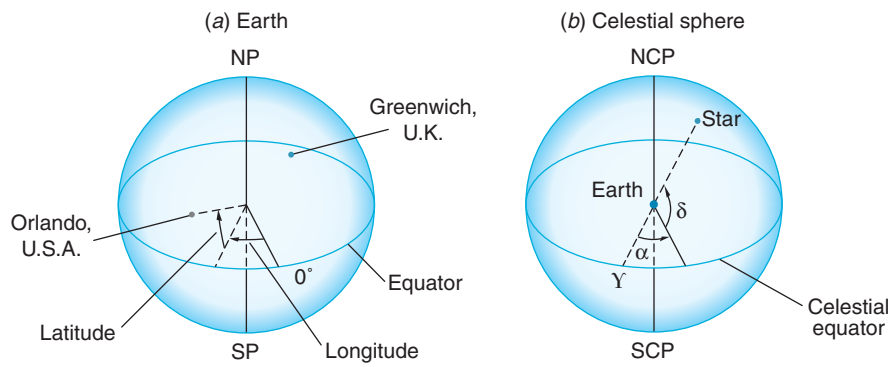

Figure 13-14
(*a*) Diagrammatic definition of longitude and latitude on Earth. (*b*) Corresponding definition of right ascension α and declination δ on the celestial sphere. ϒ marks the celestial sphere analog of Earth's 0° longitude, the meridian through Greenwich, United Kingdom.

STUDENTS-HUB.com Uploaded By: Malak Obaid

Choosing the analog of the Greenwich meridian, i.e., the 0° longitude, for the celestial sphere requires a bit of explanation. Since Earth rotates on its axis from west toward east, the stars fixed on the celestial sphere continually move across the sky from east toward west. Also, Earth orbits the Sun once every 365.26 days. This means that while Earth rotates on its axis once each 24 hours, it also advances along its orbit around the Sun slightly less than 1° during that 24-hour period. To bring the Sun directly over the same meridian as on the day before, Earth must rotate very nearly 361°; however, doing the same thing with a star on the celestial sphere requires only a 360° rotation, because the distances to the stars are vastly greater than Earth's daily motion in its orbit. As we noted above, 1° corresponds to 4.0 minutes, so a given star rises in the east each night 4.0 minutes earlier than it did the night before, as a result of Earth's orbital motion around the Sun.

In addition to the nightly advance of star rise, there is a gradual change in the orientation of the celestial sphere that varies with the seasons. This change is due to the fact that Earth's rotational axis is tilted at about 23.5° with respect to the plane of our orbit around the Sun. This means that over the course of one year as viewed from Earth, the Sun follows a path, called the *ecliptic*, on the celestial sphere that ranges from 23.5° north to 23.5° south of the celestial equator. Thus, the ecliptic intersects 0° declination twice each year (Figure 13-15), once on about March 20, the *vernal* (or *spring*) *equinox*, and again on about September 23, the *autumnal equinox*. The Sun reaches its maximum north declination of 23.5° N on about June 21, the *summer solstice* and its maximum south declination of 23.5° S on about December 21, the *winter solstice*[11] (see Figure 13-15).

By international agreement, the point at which the Sun's path projected against the celestial sphere (the ecliptic) crosses the celestial equator (0° declination) in the spring, the vernal equinox, is defined as zero hours (and 0°) right ascension. On the celestial sphere the vernal equinox is designated with the Greek capital letter ϒ (see Figure 13-14*b*). There are a number of other small motions of Earth that affect the appearance of the celestial sphere over very long periods of time, e.g., the slow wander of Earth's poles; however, those are beyond the scope of our discussions in this chapter.

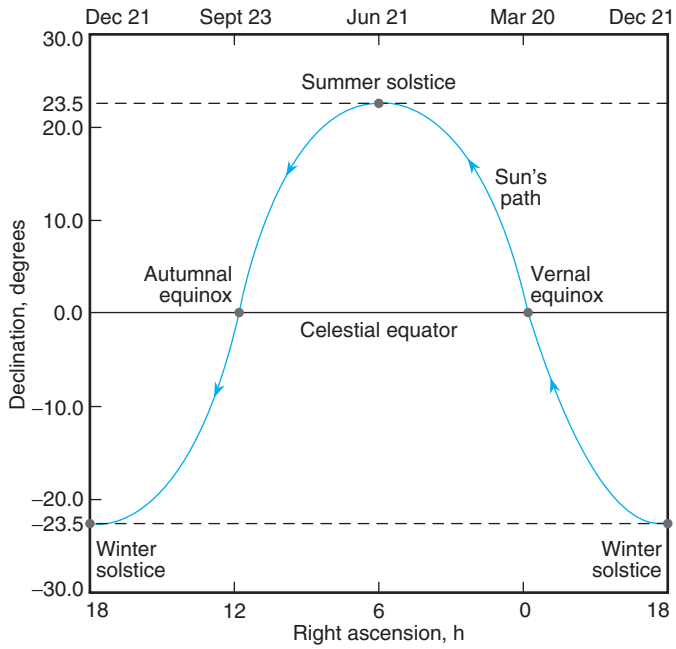

Figure 13-15 The Sun's path as projected onto the celestial sphere.

STUDENTS-HUB.com Uploaded By: Malak Obaid

The Mass (and Missing Mass) of the Milky Way

Using the Doppler effect, J. Oort and B. Lindblad first demonstrated in 1926 that the Galaxy is rotating. The Sun is apparently moving in a circular orbit at a speed of about 2.5×10^5 m/s toward the constellation Cygnus. Assuming that the Sun's speed is constant, we can compute the time for the Sun to complete one revolution around the center of the Milky Way (a "Sun year") and the mass of the Galaxy. Since the Sun is 28,000 $c \cdot$ y from the galactic center, a Sun year is 2.1×10^8 Earth years. (See Problem 13-4.)

EXAMPLE 13-3 **The Mass of the Galaxy** Calculate an approximate value for the mass of the Galaxy. Include in the calculation the mass that lies inside the Sun's orbit in the Milky Way.

SOLUTION

1. Using Newton's law of gravitation, where the gravitational force acting on the solar mass $M_\odot$ by the mass of the Galaxy M_G is given by:
$$F = G\frac{M_\odot M_G}{R^2}$$

2. This gravitational force provides the centripetal force that holds the Sun in its galactic orbit of radius R. Thus,
$$\frac{GM_\odot M_G}{R^2} = \frac{M_\odot v^2}{R}$$

3. Solving for M_G gives:
$$M_G = \frac{Rv^2}{G}$$

4. Substituting values for the Sun's orbital radius R and speed v and for the universal gravitational constant G gives:
$$M_G = \frac{(28{,}000\ c \cdot \text{y})(9.46 \times 10^{15}\ \text{m}/c \cdot \text{y})(2.5 \times 10^5\ \text{m/s})^2}{6.67 \times 10^{-11}\ \text{Nm}^2/\text{kg}^2}$$
$$= 2.48 \times 10^{41}\ \text{kg}$$

Remarks: *Thus, if the Sun's mass is a representative average for the stars of the Milky Way, the Galaxy contains about 1.3×10^{11} stars.*

A problem arises in that, if we add together the masses of all of the visible stars in the Galaxy, including those beyond the Sun's orbit, plus all of the dust and gas clouds, we can account for only about 4 percent of the gravitational mass necessary to hold the Galaxy together. This discrepancy is referred to as the *missing mass* or *dark matter problem*. It exists for all galaxies and, indeed, for the universe itself. The first hint of the problem came in 1933. Based on his studies of the motions of the galaxies in the Coma Cluster of galaxies (see Section 13-6), F. Zwicky found that the mass of the cluster, estimated from the brightness and number of galaxies it contained, was too small by a factor of about 400 to account for the observed motions. He inferred that there must be some kind of unseen gravitational mass in the cluster—dark matter. Various solutions to the problem, such as black holes and dark matter, are under intense investigation and debate. Possible dark matter candidates include massive neutrinos and *w*eakly *i*nteracting *m*assive *p*articles (called WIMPs). Among the WIMP

STUDENTS-HUB.com Uploaded By: Malak Obaid

candidates (out of many suggested possibilities) are *axions* and *neutralinos*, hypothetical elementary particles that many astrophysicists and cosmologists think may be the best choices. Although it is now certain that neutrinos have mass, they probably do not contribute significantly to solution of the dark matter problem because, being relativistic, they don't clump together into clouds like cold interstellar hydrogen does.

Axions were postulated more than 30 years ago as part of an elegant theoretical solution to a problem with quantum chromodynamics, namely that QCD predicted a large electric dipole moment for the neutron (that experiments show it does not have). The axion resulted from the breaking of a symmetry (see Section 12-4) in the theory that explained the absence of an electric dipole moment for the neutron. As proposed the axion would have no electric charge and interact only minimally with ordinary matter. As a contributor to the solution of the dark matter problem, its value may be limited, since recent experiments place an upper limit to its mass, if it exists, of $10^{-6}\ \text{eV}/c^2$.

The neutralino is considered by many astrophysicists and cosmologists as perhaps the best candidate to solve the dark matter problem. The neutralinos (there may be four of them) are the mass eigenstates that result from the quantum mixing of the supersymmetry partners of the W, Z, and Higgs bosons, the Wino, Zino, and Higgsino (see Table 12-11). One of the neutralinos may be the lightest possible supersymmetric particle and would, therefore, be stable. In some cosmological models it was produced copiously in the early universe and, with no decay channel available, it may have a relic abundance that could account for the dark matter. The lightest neutralinos mass is estimated at 10 to $10^4\ \text{GeV}/c^2$. (The proton mass is $0.938\ \text{GeV}/c^2$.) It would couple to other particles only via the weak interaction, so its behavior would be similar to that of the neutrino in that it would not be directly observable in existing detectors at the big accelerators. A significant portion of the experimental runs of the Large Hadron Collider will be searches for supersymmetry particles, including the energy/momentum discrepancy signature of the neutralinos.

13-3 The Evolution of Stars

While no universally accepted theory of stellar formation exists, it is generally agreed that stars are formed from massive clouds of dust and gas that exist throughout space. At some point in the swirling cloud, gravitational attraction begins to cause aggregations of matter to collect. These contract further due to gravity, attracting still more matter to them and eventually—if the cloud has sufficient mass—increasing the temperature to that necessary to initiate fusion as was described earlier, and a star is born.

In this section, we discuss how stars evolve once they have been formed. Two characteristics of stars are important for this discussion, the luminosity L and the effective temperature T_e. The effective temperature of a star is difficult to measure. It is usually inferred from a comparison of the spectral distribution of its radiation with that of a blackbody or from measurements of the absorption lines of hydrogen and helium in the atmosphere of the star.

The luminosity is the total power radiated by the star. It is determined from the radiant flux F of the star at Earth (remember, called the solar constant f for the Sun) and the distance r from Earth to the star (see Equation 13-2):

$$L = 4\pi r^2 F \qquad \textbf{13-10}$$

Determining the distance to a star is generally a very difficult task. For stars that are relatively close, the distance can be determined from the apparent motion of the star in the sky due to the motion of Earth around the Sun. During one complete revolution

STUDENTS-HUB.com Uploaded By: Malak Obaid

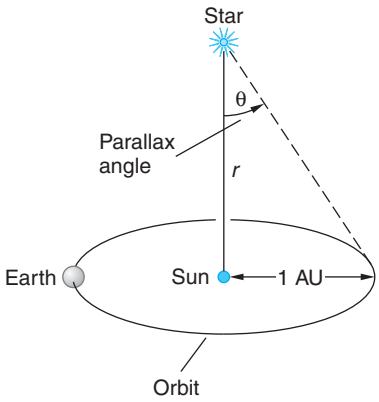

Figure 13-16 The parallax method of finding distances to nearby stars. A parsec is the distance r for which the parallax angle θ subtended by 1 AU is 1 arc second.

of Earth, a star appears to move in an ellipse of angular radius θ along the major axis called the *parallax angle* as shown in Figure 13-16. The parallax angle is given by

$$\theta = \frac{1 \text{ AU}}{r} \qquad \textbf{13-11}$$

Astronomical distances are measured in parsecs or light-years. One parsec (pc) is that distance at which 1 AU subtends an angle of 1 arc second (1″), which equals 1/3600 of a degree. Setting $\theta = 1''$ in Equation 13-11, we obtain

$$1 \text{ parsec} = \frac{1 \text{ AU}}{1''} \times \frac{3600''}{1^\circ} \times \frac{180^\circ}{\pi \text{ rad}} = 2.60 \times 10^5 \text{ AU} \qquad \textbf{13-12}$$

Using $1 \text{ AU} = 1.496 \times 10^{11}$ m and $1\ c \cdot \text{y} = 9.461 \times 10^{15}$ m, we can express the parsec in terms of meters or light-years:

$$1 \text{ pc} = 3.086 \times 10^{16} \text{ m} = 3.26\ c \cdot \text{y} \qquad \textbf{13-13}$$

EXAMPLE 13-4 **Distance to Proxima Centauri** Proxima Centauri is the star closest to the Sun. By measuring the maximum apparent change in the direction to Proxima Centauri between two observations made six months apart, the parallax angle is found to be 0.77233″. How far is it to Proxima Centauri? (Proxima Centauri's location: R. A. $14^h29^m43^s$, Dec. 16°41′58″.)

SOLUTION

Since $1 \text{ AU}/1'' = 1$ parsec, we have for $\theta = 0.77233''$,

$$r = \frac{1 \text{ AU}}{\theta} = \frac{1 \text{ AU}}{0.77233''} = \frac{1 \text{ AU}}{1''}\frac{1''}{0.77233''} = 1 \text{ pc} \times \frac{1''}{0.77233''} = 1.2948 \text{ pc}$$

$$= 4.22\ c \cdot \text{y}$$

Parallax angles as small as 0.001″ can be measured, which means that the parallax method of Example 13-4 can be used to measure stellar distances from the Sun out to about 1 kpc. Since it is about 8 kpc to the center of the Galaxy, the method can be used for only about 10,000 stars that are relatively close to the Sun and, thus, in the Milky Way. For the rest, the parallax angle is immeasurably small. In other situations, more indirect measurements of distance are necessary. One involves complex analyses of intensity variations over time for particular types of pulsating stars (Cepheid variables) found primarily in star clusters. Distances to clusters as far away as about 29 Mpc have been measured by this method. Supernovae (see Section 13-4) provide several methods for determining distances to the galaxies in which they are located. The most important of these makes use of the similarity of the light curves, that is, the emitted light intensity versus time, of so-called Type Ia supernovae. Such measurements enable calculations of the distances to supernovae that are accurate to within about 5 percent and recently provided the crucial evidence that the expansion of the universe is accelerating.

STUDENTS-HUB.com Uploaded By: Malak Obaid

Hertzsprung-Russell Diagram The various states of stars can be conveniently displayed by plotting the luminosity L versus the effective temperature T_e. The result is called the *Hertzsprung-Russell (H-R) diagram*. Figure 13-17*a* shows an H-R diagram for some stars of representative masses. The large majority of stars on an H-R diagram fall in the broad central band called the *main sequence*. Main sequence stars are normal in that they are homogeneous mixtures, except in the core, they have essentially the same chemical composition, and they are fusing hydrogen into helium via one or another of the nuclear reactions discussed earlier. Stars expand as they leave the main sequence. For that reason, stars in the main sequence are often called *main sequence dwarfs*. Between 80 and 90 percent of all stars are on the main sequence.

The location of a star along the main sequence in the H-R diagram depends on its luminosity, which is primarily dependent on the mass of the star. The masses of stars range from about 0.08 $M_\odot$ to about 60 $M_\odot$, where $M_\odot$ is the mass of the Sun. Gaseous objects with less than about 0.08 $M_\odot$ do not have enough gravity for their central cores to be compressed sufficiently to generate the temperature necessary to sustain the nuclear fusion reactions needed for energy emission. Objects with masses greater than 60 $M_\odot$ would generate such enormous internal temperatures that the outward radiation pressure would exceed the gravity-generated inward pressure. Such a system would be very unstable, if indeed it could form at all.

Evaluation of the masses of binary stars has shown that the luminosity of a star is approximately proportional to the fourth power of its mass:

$$L \propto M^4 \qquad \textbf{13-14}$$

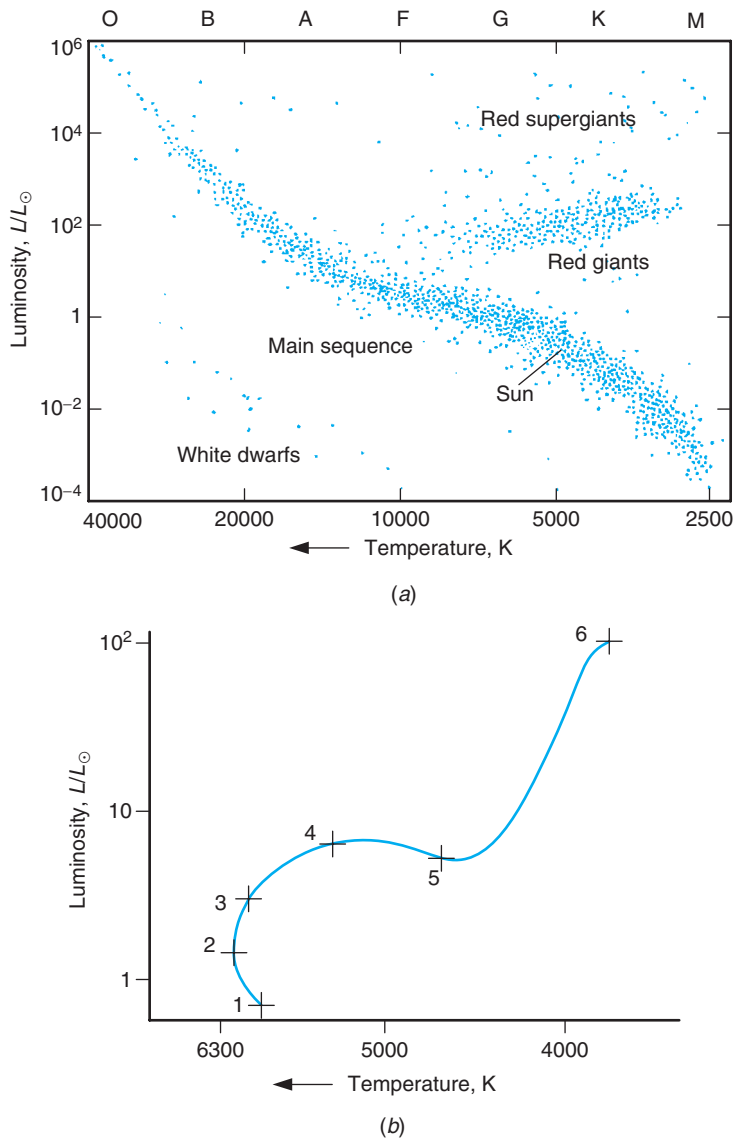

Figure 13-17 (a) The Hertzsprung-Russell (H-R) diagram for stars in the solar neighborhood. Most stars (80 to 90 percent) fall on the main sequence. Stars in the lower right end of the main sequence are cool and dim, those in the upper left are hot and bright. (*b*) The Sun's evolutionary track from the time it entered the main sequence at point 1. The Sun is currently between points 1 and 2. It will leave the main sequence at point 4. The time between successive points is approximately 10^9 years.

The lifetime of a star t_L is proportional to the total available energy, which is proportional to the star's mass ($E = Mc^2$), and inversely proportional to the rate of energy emission, which is the luminosity:

$$t_L = \frac{E}{L} \propto \frac{Mc^2}{M^4} \propto M^{-3} \qquad \textbf{13-15}$$

STUDENTS-HUB.com Uploaded By: Malak Obaid

Thus, more massive stars burn their hydrogen more quickly than do less massive stars. Thus, a star with twice the Sun's mass would be expected to have a lifetime only 1/8 as long as that of the Sun. (Equation 13-15 doesn't work for very small or very large stars because the luminosity-mass relationship of Equation 13-14 is only an average result. The exponent in Equation 13-15 is larger in magnitude for very small stars and smaller for very large stars.)

Considerations of energy balance for stars on the main sequence lead to the approximate proportionality of the radius and the mass, as can be demonstrated using the data in Table 13-3 (see Problem 13-6):

$$R \propto M \qquad \textbf{13-16}$$

Combining this with Equation 13-4, which relates the effective temperature to the luminosity per unit area, we can relate the effective temperature to the mass of the star:

$$T_e = \left(\frac{L}{4\pi R^2 \sigma}\right)^{1/4} \propto \left(\frac{M^4}{M^2}\right)^{1/4} \propto M^{1/2} \qquad \textbf{13-17}$$

Thus, stars with larger masses have higher effective temperatures and, hence, higher luminosities than those with lower masses. It is on the basis of Equations 13-15 and 13-17 that the stellar masses were plotted on the H-R diagram in Figure 13-17*a*. Table 13-3 lists properties of stars by spectral type. The following values for the Sun's characteristics will enable calculation of numerical values for the corresponding characteristics of individual stars: $L_\odot = 3.83 \times 10^{26}$ J/s; $R_\odot = 6.96 \times 10^8$ m; $M_\odot = 1.99 \times 10^{30}$ kg.

As the star ages, it consumes its primary fuel, hydrogen. What happens to it as the hydrogen supply in the core becomes exhausted depends on its initial mass. Low-mass and high-mass stars follow somewhat different evolutionary paths. In either case, however, the fundamental processes involved are successive nuclear reactions fueled by the product of the previous cycle. Thus, after the hydrogen in the core has fused to helium, the star must begin fusing helium in a cycle that eventually forms carbon.

Table 13-3 Selected properties of stars

Spectral type	Surface temperature (K)	$L/L_\odot$	$R/R_\odot$	$M/M_\odot$
O5	44,500	790,000	15	60
B0	30,000	52,000	8	18
A0	9,520	54	3	3
F0	7,200	6	2	2
G0	6,030	1.5	1.1	1.1
Sun (G2)	5,800	1.0	1.0	1.0
K0	5,300	0.4	0.8	0.8
M0	3,900	0.08	0.6	0.5
M8	2,600	0.001	0.17	0.06

STUDENTS-HUB.com Uploaded By: Malak Obaid

Before this can occur, the core must heat up still further to the 10^8 K necessary to initiate helium fusion. The chain of events involved in this process is complex and beyond the scope of this book. However, its result for low-mass stars is that the radius (and therefore the surface area) increases while luminosity remains nearly constant. Thus, the intensity (luminosity per unit area) and, consequently, the effective temperature decrease and the radiation emitted shifts to longer wavelengths as the star expands to become a *red subgiant*. The photosphere rapidly becomes more transparent as T_e and the density ρ decrease, increasing the luminosity and effectively limiting the decrease in temperature. The star is then a *red giant*. The track of a typical evolving low mass star such as the Sun is shown on the H-R diagram in Figure 13-17*b*.

Helium ignition results in the star again increasing its effective temperature and moving to the *horizontal branch*. When the helium in the core is exhausted, the star begins fusing carbon and ascends the red giant branch again, becoming a *red supergiant*. Betelgeuse, the bright star in the shoulder of the constellation Orion, is a red supergiant. Its density is about 1.5×10^{-5} kg/m^3, a hundred thousand times less than the air we breathe! What happens after this is not completely clear. Through a combination of events that includes the loss of considerable mass, perhaps including the ejection of an expanding shell of gas (called a *planetary nebula*), such as that shown in Figure 13-18, the star may become a white dwarf, slowly cooling toward thermal equilibrium with the universe. We will discuss white dwarfs further in Section 13-5.

High mass stars—those with masses greater than about $6M_\odot$—evolve much more quickly than low-mass ones, as predicted by Equation 13-15. In addition, they have sufficient initial mass to generate gravitationally the high pressures and temperatures necessary to ignite the fusion reactions with oxygen, neon, and then silicon to produce, ultimately, iron. These reactions occur with phenomenal speed and lead to catastrophic events that will be discussed in the next section. An extremely massive star, such as Betelgeuse, may become a supernova via core collapse (see Section 13-4).

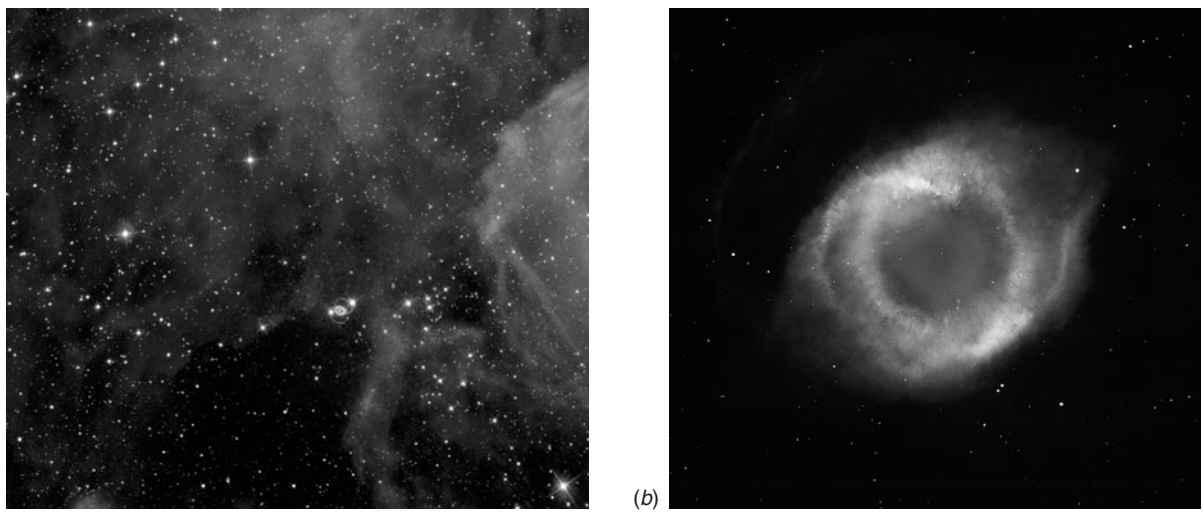

(*a*) (*b*)

Figure 13-18 The nebula 30 Doradus (*a*), also known as the Tarantula nebula, is believed to be older than nebula NGC 7293 (*b*), also known as the Helix nebula. The Tarantula nebula's rapidly expanding gas cloud consequently shows a greater degree of diffusion. Located in the Large Magellanic Cloud, the Tarantula contains one of the most massive stars known, as well as supernova SN1987A, the very bright star slightly below the center (of the left-hand photo). Ultraviolet radiation from stars heats the gas of a nebulae, causing it to radiate. [*(a) The Hubble Heritage Team (AURA/STScI/NASA). (b) NASA, NOAO, ESA, the Hubble Helix Nebula Team, M. Meixner (STScI), and T.A. Rector (NRAO).*]

STUDENTS-HUB.com Uploaded By: Malak Obaid

13-4 Cataclysmic Events

Huge explosions and other sorts of cataclysmic events are a natural part of the life cycle of stars. Stars formed in swirling clouds of gas move along the H-R diagram, incorporating such occurrences into their evolution and forming in the process the elements needed to form new stars. Why these cataclysmic events occur is the subject of this section.

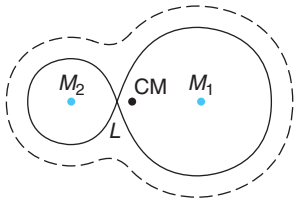

Figure 13-19 Cross sections of two gravitational equipotential surfaces for stars M_1 and M_2. The point labeled L is one of five Lagrangian points where the net gravitational potential is an extremum (a saddle point in this case) and the net force is zero.

Novae

More than half of all stars are members of *binary pairs* or even larger associations. These stars orbit their common center of mass as the group moves with the rotation of the Galaxy. The periods of binaries vary from a few hours for those with the companions very close to each other to millions of years for those with the companions separated by thousands of astronomical units. Here, we are interested in close binaries.

A complete analysis of the interactions between the two stars forming a close binary is beyond the scope of this book, but a qualitative explanation will suffice. Consider a binary whose stars of masses M_1 and M_2 rotate about their common center of mass in circular orbits. An observer at rest in the rotating system experiences a net force that is the sum of the gravitational forces due to the two stars and the pseudoforces due to the rotation. Figure 13-19 shows an equipotential surface about a binary pair. It is easy to visualize that there is a point along the line joining the centers of the two stars where the net potential is a minimum. At this point, the net force due to the combined effects of the rotation and the gravitational attraction by the masses M_1 and M_2 is zero. This point is a *Lagrangian point*. The three-dimensional equipotential surface that includes the Lagrangian point L forms an envelope around each star called the *Roche lobe*.[12]

Now consider what happens when, through natural evolution, one of the stars, say M_1, begins expanding and fills its Roche lobe. The photosphere of the star feels a vacuum outside the surface, the outward pressure at any point being balanced by gravity. But at the Lagrangian point there is no gravity. Thus, material from M_1 pours through the Langrangian point into the Roche lobe of M_2. Once inside it is gravitationally attracted toward M_2. Since the system is rotating, the material from M_1 doesn't simply move directly toward M_2 but, because of the Coriolis effect, forms a spiraling *accretion disk* (Figure 13-20).

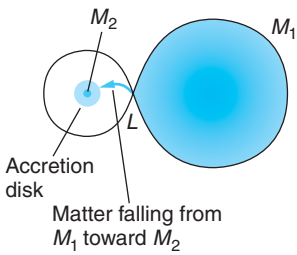

Figure 13-20 Material from M_1 pouring through the Lagrangian point into the Roche lobe of M_2 forms an accretion disk in M_2's equatorial plane. Material arriving later hits the disk, generating a high-temperature impact area. This causes novae to flicker irregularly.

If M_2 is a normal star, nothing of great consequence occurs, but if it is a white dwarf, then cataclysmic events called *novae* can occur. We will mention two possibilities. Material flowing through the Lagrangian point into the accretion disk is stored there until some instability occurs in the disk that results in the dumping of material onto the surface of the white dwarf. The impact heats the surface, causing a sudden luminosity increase by a factor of 10 to 100. Such events recur at intervals of a few weeks for *dwarf novae* to hundreds or thousands of years for *recurrent novae*. Between these sudden bursts in intensity, the novae flicker as described in the caption of Figure 13-20.

For *classical novae*, which eject substantial material into space and can brighten by a factor of a million within a few days, astrophysicists suggest that the sudden dumping of material from the accretion disk onto the hot surface may result in the buildup of sufficient hydrogen to initiate a thermonuclear explosion. After the blast the system returns to a more quiescent state, pending the accumulation of more hydrogen in the disk. The theoretical problems involved in explaining such an event are formidable, however, and no general agreement on the mechanism exists.

STUDENTS-HUB.com Uploaded By: Malak Obaid

Supernovae

A *supernova*—the catastrophic explosion of an entire star—is, perhaps surprisingly, somewhat more clearly understood than the nova. Supernovae are classified as Type I or Type II mainly on the basis of their spectra (Figure 13-21). The spectra of *Type I* supernovae do not contain hydrogen lines, indicating that they are devoid of hydrogen, or nearly so. In contrast, *Type II* supernovae exhibit strong hydrogen lines. Type I supernovae are further divided into Type Ia, which show a strong line of singly ionized Si at 615 nm, Type Ib whose spectra include strong He lines, and Type Ic whose spectra do not include He lines. Recalling that H and He are in that order the most abundant elements in the universe, these spectral differences indicated that there are significant differences in the progenitors of the Type I and Type II supernovae. Type II supernovae are subdivided into two groups based on the shape of their light intensity versus time curves following peak brightness. The light curves of Type II-L supernovae decline *l*inearly with time; the light curves of Type II-P exhibit an intermediate *p*lateau lasting 30 days or more before the intensity decline resumes.

Supernovae are not just big novae. Their origin is completely different. In Section 13-3, we saw what occurs in a star as it uses up the hydrogen in the core and begins moving off the main sequence of the H-R diagram. The star begins to fuse helium, then carbon. If it were a low-mass star, it would have insufficient gravitational energy to ignite the fusion of heavier nuclei in quantity. For massive stars, however, the situation is different. Type Ia supernovae originate in binary systems where one star is a massive white dwarf rich in carbon and oxygen (see Section 13-5). An expanding companion that fills its Roche lobe may dump a huge amount of gas directly onto the dwarf's surface, increasing the gravitational pressure in the core. If the pressure increases the core temperature enough to trigger carbon fusion, a runaway fusion reaction results, producing a massive thermonuclear explosion—a huge "carbon bomb." Depending on the characteristics of the particular binary, it may be possible that Type Ib and Type Ic supernovae result from gravitational core collapse. Type I supernovae occur among population II stars. (Don't be confused by the apparent inconsistency in nomenclature.) As noted earlier, Type Ia supernovae all have very similar maximum intensities and light curves which makes it possible for them to be identified even at very large distances, enabling them to be used as "standard candles" by astronomers. It is these features that have made it possible for astronomers to measure much greater distances to host galaxies than was previously possible.

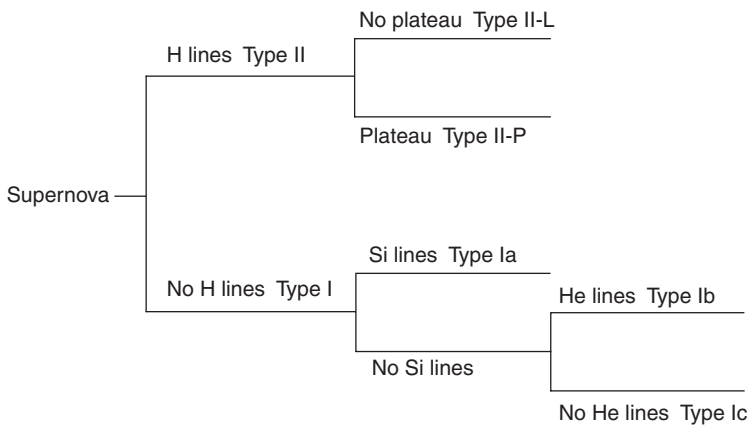

Figure 13-21 Schematic of the classifications of supernovae. Type I subgroups are based on their spectra at maximum brightness. Type II subgroups are based on the existence or absence of a plateau in the light curve.

STUDENTS-HUB.com Uploaded By: Malak Obaid

If a star's mass is greater than about $8M_{\odot}$, evolution toward a Type II supernova proceeds approximately as follows. Gravity is strong enough to continue to draw mass from the middle layers into the core as the core uses up fuel. The increasing temperatures, exceeding 10^8 K, are sufficient to ignite fusion in neon and silicon ultimately producing iron. As we saw in Chapter 11, the specific binding energy of iron is the highest in the periodic table. Fusing elements above iron doesn't emit energy, it absorbs energy. Thus, when the core has been fused to iron, there is nowhere else to go via thermonuclear reactions. With no counteracting outward pressure from nuclear reactions, gravitational contraction continues even more rapidly and the core consequently continues to heat up until it exceeds 10^9 K. At that point, the radiation within the star is intense and iron nuclei undergo photodisintegration into helium and neutrons, absorbing energy from the core and accelerating the gravitational collapse:

$$^{56}_{26}\text{Fe} \longrightarrow 13\,^{4}_{2}\text{He} + 4n \qquad \textbf{13-18}$$

The helium nuclei then begin to photodisintegrate, absorbing enormous amounts of energy to overcome the nuclear binding energy of helium:

$$^{4}_{2}\text{He} \longrightarrow 2p + 2n \qquad \textbf{13-19}$$

The core is now in gravitational free fall, compressing the electrons and protons into neutrons via inverse beta decay:

$$p + e^{-} \longrightarrow n + \nu_e \qquad \textbf{13-20}$$

What happens next to the core is a matter of intense theoretical conjecture that we will explore further in Section 13-5.

What happens to the envelope of the star—the material outside the core—although unclear theoretically, is certainly apparent visually. The entire envelope is blown away in an incredibly massive explosion. This is a Type II supernova. Supernovae are extremely rare, but scientists were fortunate enough to observe one in 1987 only 170,000 $c \cdot$ y away in the Large Magellanic Cloud, a small irregular galaxy that is a companion to the Milky Way. Called SN1987A (see Figure 13-18 and the photo at the left), it was the first to occur close enough to be visible to the unaided eye since 1604, when both Kepler and Galileo saw one. Two others were recorded earlier, in 1006 and 1054, the latter documented by Chinese astronomers and still visible as the Crab Nebula. Several others have been observed with telescopes. As a result of the enormous number of nuclear reactions and decays initiated by the supernova, the radiation emitted in the explosion is accompanied by a flood of neutrinos. Neutrinos emitted by SN1987A were detected by the Kamiokande neutrino observatory, bringing with them information about the core-collapse model of supernovae and a hint of the nonzero neutrino mass (see Problem 12-13).

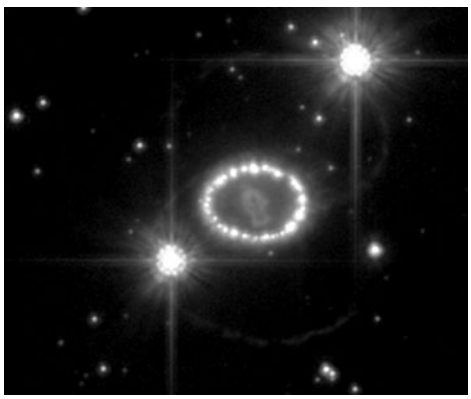

Supernova 1987A developed a set of rings some weeks after it was first seen. The rings are likely caused by a beam of high-energy radiation or particles sweeping across the gas. The source of the beam may be a previously unseen companion of the star that exploded. This Hubble Space Telescope photo was made with hydrogen Balmer alpha light. [*NASA, ESA, P. Challis and R. Kirshner (Harvard-Smithsonian Center for Astrophysics).*]

At its peak light output, a supernova typically shines more brightly than the entire galaxy in which it is located. The spectra of supernovae reveal the presence of elements throughout the entire periodic table. This indicates that some of the energy removed from the core following the production of iron is used to produce elements of even higher atomic numbers. The supernova ejects some of this material into space, where it eventually contributes to the formation of a new generation of stars and their planets via condensation. Such events undoubtedly preceded the birth of the Sun and the formation of Earth. We are, as has been said before, "made of the stuff of stars."

STUDENTS-HUB.com Uploaded By: Malak Obaid

13-5 Final States of Stars

The cataclysmic events that occur near the end of the life of a star lead to one of only three possible final states: a white dwarf, a neutron star, or a black hole. The mass of the star, particularly that of the core, appears to be the primary factor in determining the final state.

White Dwarfs

Stars whose masses are less than about $6M_\odot$ follow an evolutionary track on the H-R diagram that takes them through one or more periods of substantial mass loss from the outer layers of gas. How this occurs is not clear, but the ejected mass, which is heated to a glowing planetary nebula by the hot core, leaves behind a *white dwarf*, a term used because many, though by no means all, are literally white hot. Its mass is typically about $1M_\odot$ and its radius of the order of 10^7 m, which is about the same as the radius of Earth. Thus, the density of a typical white dwarf is about 5×10^5 g/cm^3 compared to Earth's average density of about 5.5 g/cm^3. A coin the size of a penny made from white dwarf material would have a mass of over 200 kg, one the size of a Euro over 400 kg.

Thermonuclear reactions have ceased in the white dwarf, leaving it with a core consisting primarily of carbon and oxygen, so there is no outward pressure due to them from within the star. The star therefore collapses because of the inward gravitational pressure until the exclusion principle prevents the atomic electrons from coming any closer together. This effect is similar to the exclusion-principle repulsion between atoms in a molecule that we discussed in Chapter 9. It results in an outward pressure that is larger even than the thermal pressure of the hot core. It is this *electron degeneracy pressure* that supports the white dwarf. When the outward electron degeneracy pressure equals the inward pressure due to gravity, the star stops contracting.

Explicit derivation of the expression for the electron degeneracy pressure leads to a nonrelativistic relation between the dwarf's radius R and mass M:

$$R = (3.1 \times 10^{17}\ \text{m} \cdot \text{kg}^{1/3})\left(\frac{Z}{A}\right)^{5/3} M^{-1/3} \qquad \textbf{13-21}$$

where Z is the atomic number and A is the atomic mass number of the material of the star. Note the interesting result that the larger the mass, the smaller the radius, a consequence of the gravitational contraction that was discussed earlier. For example, a white dwarf with a mass of $1M_\odot$ will have a radius smaller than one with a mass of $0.5M_\odot$! Equation 13-21 raises the interesting question of whether, when the electrons become relativistic, the mass might become large enough for the radius of the dwarf to shrink to zero. Although Equation 13-21 does not formally allow that possibility until M approaches infinity, S. Chandrasekhar[13] derived the corresponding relativistic relation and found that the radius would go to zero when the mass reached about $1.4M_\odot$. This quantity is called the *Chandrasekhar limit*. Its validity is strongly supported by the fact that the masses of all white dwarfs that have been measured are less than that value.

A lone white dwarf continually radiates heat to space and, without a nuclear furnace, slowly cools and dims. When it is no longer visible, it has become a *black dwarf*. It continues to cool toward thermal equilibrium with the universe. It is not likely that any white dwarfs have yet reached this final stage. However, if the white dwarf is a part of a binary, then in addition to the possibility of a nova described earlier, mass may flow from the companion directly onto the surface of the white dwarf. When the degenerate electron pressure can no longer support the white dwarf (at the Chandrasekhar limit), the star implodes, suddenly raising the core temperature and

STUDENTS-HUB.com Uploaded By: Malak Obaid

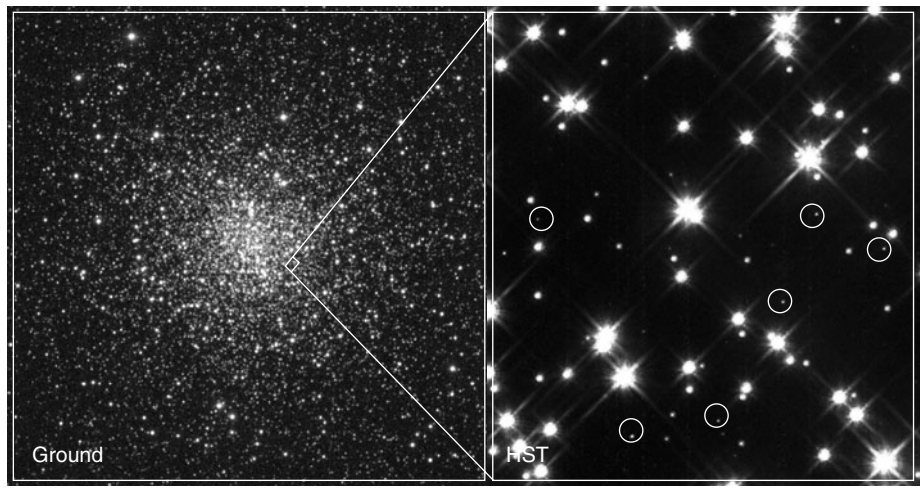

White dwarfs identified by the Hubble Space Telescope in M4, the globular cluster closest to Earth (7000 $c \cdot$ y). M4 contains more than 100,000 stars. [*(left) Kitt Peak National Observatory 0.9-meter telescope, National Optical Astronomy Observatories; courtesy M. Bolte (University of California, Santa Cruz). (right) Harvey Richer (University of British Columbia, Vancouver, Canada) and NASA.*]

detonating fusion in the carbon/oxygen core. The sudden energy release causes the white dwarf to explode as a Type Ia supernova. The common mass limit, 1.4 $M_\odot$, at which the white dwarfs explode, is a major factor in the resulting similarity of the Type Ia supernovae light curves that enables their use as a luminosity standard for measuring astronomical distances. Following the supernova explosion, about half of the residual core of the star is iron.

Neutron Stars

In the discussion of supernovae, we saw that the enormous pressures developed in the core forced inverse beta decay to occur, converting the core into neutrons. If the mass of the core following the explosion is greater than the Chandrasekhar limit, what happens? We can get an idea by considering the neutrons to be an ideal gas of fermions and derive a nonrelativistic expression for the mass-radius relation analogous to Equation 13-21. The result is

$$R = (1.6 \times 10^{14}\ \text{m} \cdot \text{kg}^{1/3}) M^{-1/3} \qquad \textbf{13-22}$$

where M is the mass in kilograms and R is the radius of the core in meters. Such a star is called a *neutron star*, since the envelope was blown away in the supernova and all that is left is the core consisting of neutrons. For $M = 1.0 M_\odot$, Equation 13-22 yields the radius $R = 1.27 \times 10^4$ m $= 12.7$ km.

The density of the neutron star is about 1.2×10^{14} g/cm^3. This is only slightly less than the density of the neutron itself, which is about 4×10^{14} g/cm^3. Thus, we can conclude that the gravitational pressure of the neutron star is balanced by the repulsive component (due to the exclusion principle) of the strong nuclear force between the neutrons. As you might guess from our earlier discussion, gravity can overcome even this resisting pressure. The mass corresponding to the gravity at which that occurs would be the maximum mass possible for a neutron star, a mass analogous to the Chandrasekhar limit for white dwarfs. Current theory puts the maximum mass of a neutron star between 1.7 $M_\odot$ and 3$M_\odot$. The few neutron stars that have been tentatively identified and measured all have masses below this limit.

STUDENTS-HUB.com Uploaded By: Malak Obaid

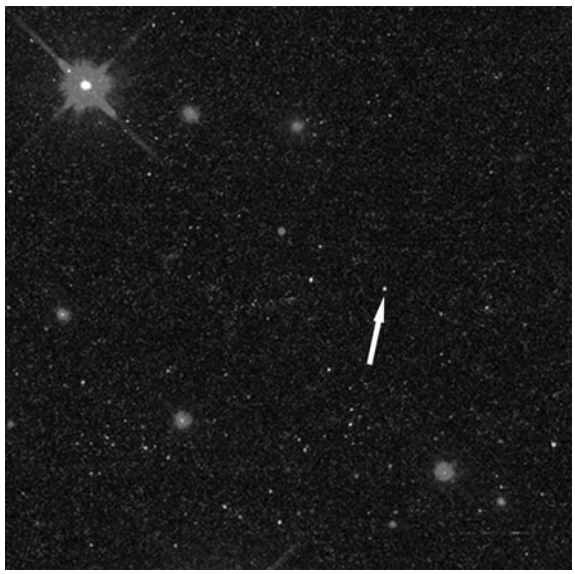

A lone neutron star, the first seen in visible light, is very hot (about 650,000 K at the surface) and may be no larger than 28 km in diameter. [*Fred Walter (State University of New York at Stony Brook) and NASA.*]

Regularly pulsing radio sources, called *pulsars*, discovered in 1967 in nebulae such as the Crab Nebula that are remnants of supernovae, are thought to be neutron stars. Current theory suggests that the radiation is emitted as the result of charged particles emitted by the neutron star that are accelerated along the star's magnetic field lines as a consequence of the star's rapid rotation as illustrated in Figure 13-22.

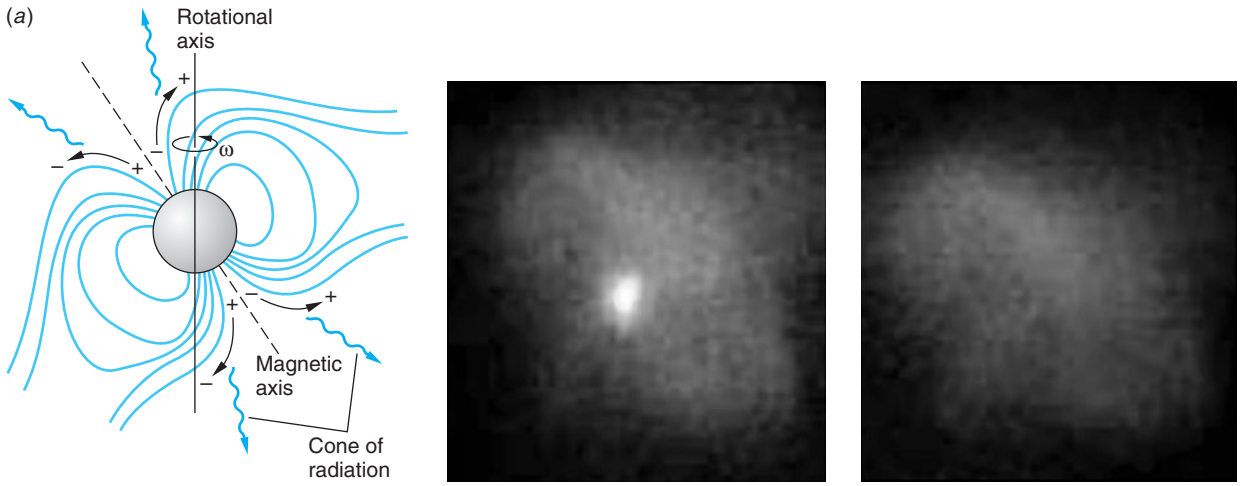

Figure 13-22 (*a*) The neutron star acquires much of the original star's angular momentum and magnetic field, causing it to rotate rapidly while dragging along a distorted magnetosphere. Accelerated charged particles radiate in a cone about the rotating magnetic axis like a cosmic lighthouse. (*b*) The pulsar in the Crab Nebula. As the cone of radiation swings to face Earth, light emitted from accelerated electrons becomes visible (the bright spot in the image). (*c*) A fraction of a second later, the pulsar has turned and this light is no longer directed toward Earth. Currently rotating about 30 times a second, the pulsar has a period that is increasing by about 10^{-5} s per year. [*(b) and (c) Harvard/Smithsonian Center for Astrophysics.*]

STUDENTS-HUB.com Uploaded By: Malak Obaid

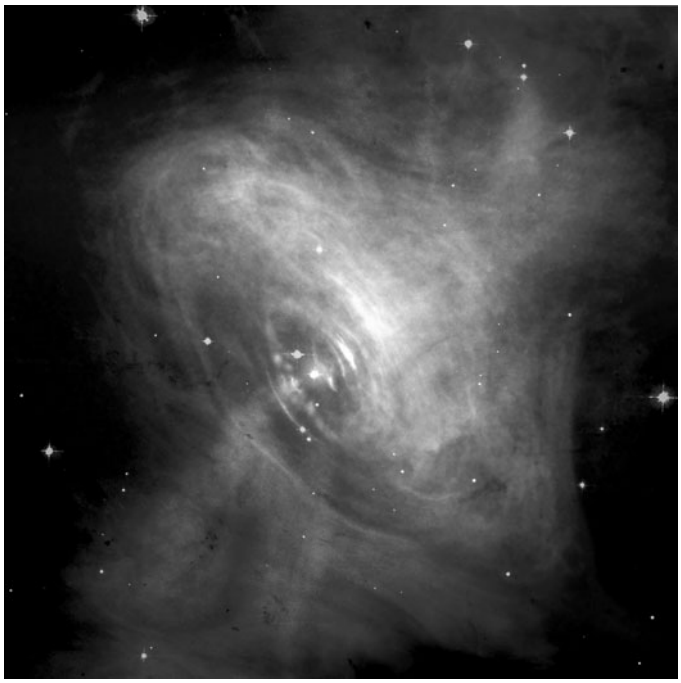

This composite image of the Crab Nebula was made from an x-ray image recorded by the Chandra X-Ray Observatory and an optical image from the Hubble Space Telescope. The inner ring is about 1 $c \cdot$ y across. [*Credits for X-ray Image: NASA/CXC/ASU/J. Hester et al. Credits for Optical Image: NASA/HST/ASU/J. Hester et al.*]

The Crab pulsar also corresponds to an optical variable as illustrated in Figures 13-22*b* and *c*. It emits energy at an incredible 3×10^{31} W. Its period is equally incredible, 0.033 seconds, one of the shortest known. As it emits energy into space, the neutron star also slowly cools, approaching thermal equilibrium with the universe.

Black Holes

What happens when the mass of the remaining core of a supernova exceeds the $1.7M_\odot$ to $3M_\odot$ upper limit for the formation of a neutron star? The velocity necessary for an object with mass to escape from an object of mass M is found by equating the gravitational potential energy at the surface of M to the kinetic energy necessary to escape. This results in the escape velocity

$$v_e = \left(\frac{2GM}{R}\right)^{1/2} \qquad \textbf{13-23}$$

For a neutron star with $M = 1.0M_\odot$, $v_e = 1.3 \times 10^8$ m/s, more than 40 percent of the speed of light. If there were no relativistic and quantum mechanical effects, the escape velocity would equal c when

$$R_S = \frac{2GM}{c^2} \qquad \textbf{13-24}$$

where R_S is called the *Schwarzschild radius*. Thus, if an incipient neutron star is so massive that its radius is less than R_S, no object with mass can escape from its surface. In addition, radiation of wavelength λ_0 emitted at some distance R from mass M is shifted to a longer wavelength λ according to the *gravitational redshift* described in Section 2-5; the ratio is given by

$$\frac{\lambda}{\lambda_0} = \left(1 - \frac{v_e^2}{c^2}\right)^{-1/2} = \left(1 - \frac{2GM}{c^2R}\right)^{-1/2} = \left(1 - \frac{R_S}{R}\right)^{-1/2} \qquad \textbf{13-25}$$

If R shrinks to the Schwarzschild radius, then λ approaches infinity and the energy ($E = hf = hc/\lambda$) approaches zero. Thus, if R is less than R_S, no energy can escape the surface as radiation, either. Such an object is called a *black hole*, because it neither emits nor reflects radiation or mass and, hence, appears absolutely black.[14]

The radius of a black hole with a mass of $1M_\odot$, if there is such an object, would be only about 3 km. Many astrophysicists currently believe that a massive black hole is located at the center of the Milky Way and may account for a very small part of the "missing mass" of the Galaxy. During the past decade astronomers at the Max Planck Institute (Germany) have tracked about a dozen individual stars (of more than 300) orbiting an unseen object at Sagittarius A*, a radio source near the center of the Milky Way (see Figure 13-13). One of these, for example, is called S2. Determining S2's orbital period to be 15.2 y enabled calculation of the mass of the unseen object to

STUDENTS-HUB.com Uploaded By: Malak Obaid

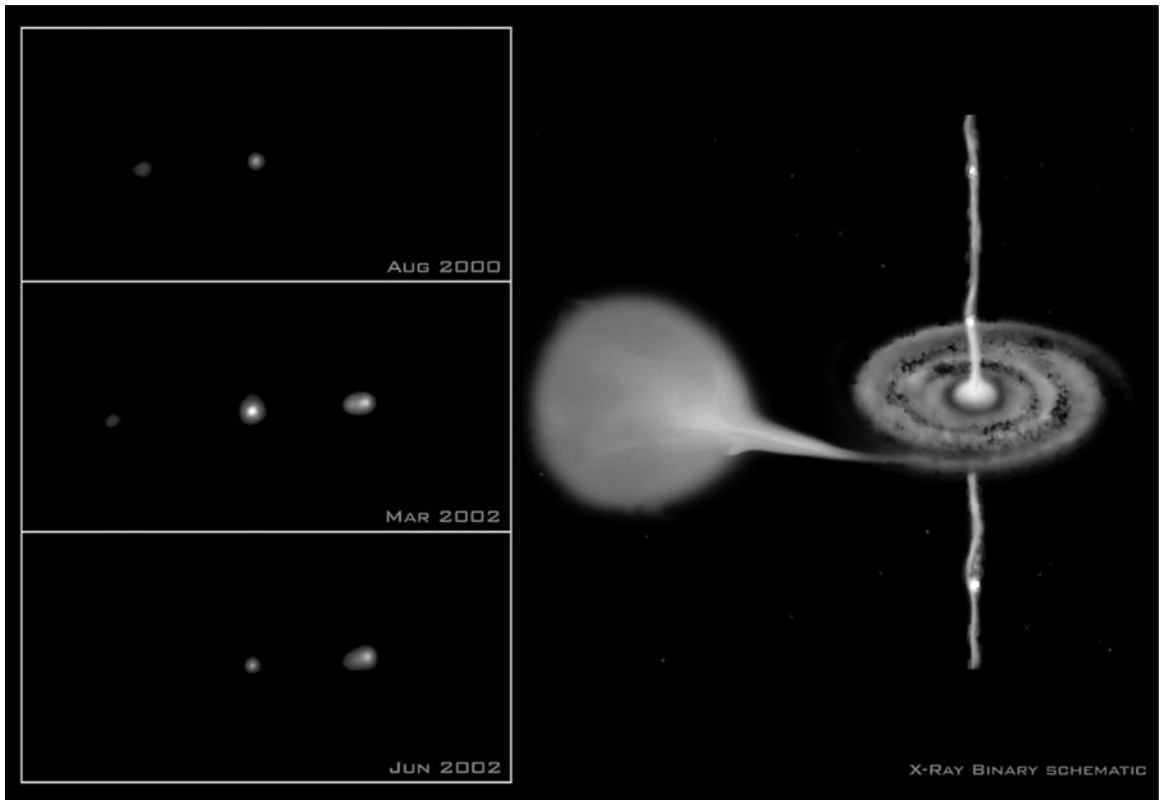

The series of Chandra X-Ray Observatory images on the left show jets of high-energy particles being produced near a black hole in a binary system, first on the left (top image), then on the right (middle image). The jets are moving away from each other at about 0.5 *c*. In the lower image the left jet has disappeared. The schematic on the right illustrates how the jets originate. The black hole draws mass from the normal companion, then intense electromagnetic forces in the accretion disk expel the jets of high-energy particles. [*Left: X-ray (NASA/CXC); Right: Illustration (CXC/M.Weiss).*]

be about $3 \times 10^6\ M_\odot$. S2's orbital speed of approximately 4×10^6 m/s "confines" the unseen mass of Sagittarius A* to such a small volume that there can be little doubt that it is an enormous black hole. Unlike white dwarfs and neutron stars, black holes are not cooling toward thermal equilibrium with the universe.

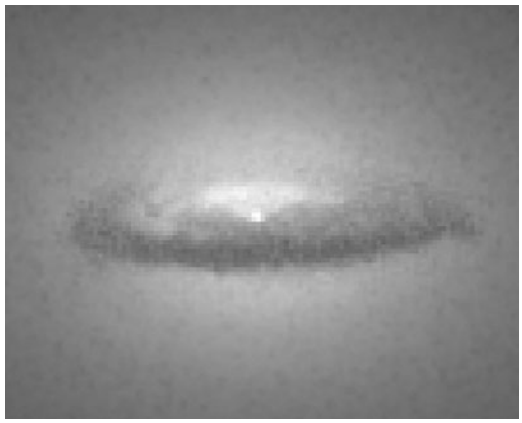

Black hole in the center of galaxy NGC 7052. The disk is 3700 $c \cdot$ y in diameter. The black hole, whose mass is about 300 million solar masses, will swallow the disk in a few billion years. [*Roeland P. van der Marel (STScI), Frank C. van den Bosch (Univ. of Washington), and NASA.*]

STUDENTS-HUB.com Uploaded By: Malak Obaid

Gamma-Ray Bursts

Flashes of gamma rays (and x rays) that occur about once a day at apparently random locations in the sky were discovered by Vela military satellites in 1967. They are short, lasting from less than a second to as long as a few minutes. During the burst they are by far the brightest gamma-ray sources in the sky, their fluxes exceeding those of the brightest steady sources, such as the Sun and the Crab Nebula, by a factor of a 1000 or more. Their brief lifetime makes it difficult to attempt to identify the bursts with individual stars or galaxies because of the inherent delay in processing the burst information and re-aiming the large telescopes. With a bit of good fortune, that problem was first solved in 1997 when the Dutch/Italian BeppoSAX satellite detector discovered an x-ray afterglow following burst GRB970228.[15] Then in 1999 burst GRB990510 was seen simultaneously by the Compton Gamma Ray Observatory and BeppoSAX satellites within the field of view of the Very Large Telescope (VLT) in Chile, the largest telescope in the southern hemisphere. The subsequent x-ray, optical, and radio wavelength afterglows told astronomers what to look for and, since then, many bursts have been studied more thoroughly via their afterglows, some lasting for several months.

Since that time the all-sky surveys of the Burst and Transient Source Experiment (BATSE) and Swift satellites have recorded more than 8000 gamma-ray bursts distributed isotropically over the sky (see the photo below). The uniform distribution of the GRBs across the sky is strong evidence that they occur in the distant universe, since only at great distances does the cosmos appear uniform. The VLT measured the redshift z of GBR990510 to be 1.61 implying a recession speed that places the source about halfway to the edge of the visible universe. The origin of the bursts and the mechanism for the enormous energy release implied by the gamma-ray flux are not yet clear. As of this writing approximately 100 afterglows have been located and for most of these a host galaxy has been identified. The GRBs in many cases appear to be the result of the supernova collapse of very large stars becoming neutron stars or black holes. This is an area of active current research.

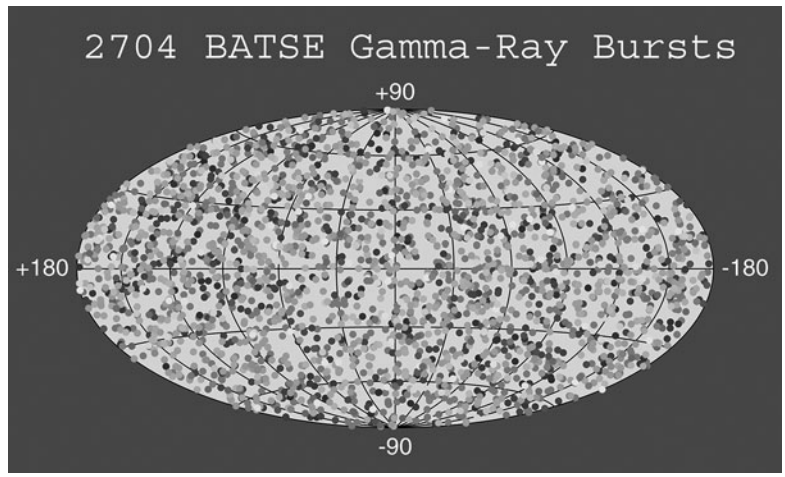

This map shows the locations of more than 2700 gamma-ray bursts recorded by BATSE aboard the Compton Gamma-Ray Observatory during its 9 years of operation. The projection is in galactic coordinates, the plane of the Milky Way being the horizontal line through the middle of the figure. The burst locations are color-coded based on the integrated energy over the duration of the burst. [*Image courtesy of the BATSE team, http://gammaray.nsstc.nasa.gov.*]

STUDENTS-HUB.com Uploaded By: Malak Obaid

13-6 Galaxies

In Section 13-2 we saw that the Milky Way is shaped like a spiral disk with a central bulge located about 28,000 $c \cdot y$ from the Sun. The disk is surrounded by a roughly spherical "halo" of globular clusters made up mostly of population II stars, which are also part of our Galaxy. We will now look at some of the characteristics of galaxies.

Material Between the Stars

"Holes in the sky"—regions where no stars are seen—have been observed since the early days of astronomy and were assumed to be empty space. However, studies of open clusters about 70 years ago led to the discovery of a more or less continuous distribution of tiny dust particles, called *interstellar dust*, between the stars. Consisting of solid specks of silicates and carbides averaging only a few hundred nanometers in diameter (approximately matching the wavelength of visible light), the interstellar dust both absorbs and scatters some of the starlight striking it. Thus, dust in the interstellar medium (ISM) dims starlight coming toward Earth and, since blue light scatters more efficiently than red light, starlight is reddened on its trip to us, just as sunlight is reddened at sunset. Although the dust seems to pervade the entire Galaxy, the concentrations are very low and its total mass makes only a very small contribution to the total mass of the ISM. The vacuum in interstellar space is far better than the best obtainable in the laboratory.

The ISM consists primarily of hydrogen and helium. Hydrogen as atomic hydrogen, ionized hydrogen (protons), and hydrogen molecules (H_2) makes up about 70 percent of the mass of the ISM. Atomic helium is most of the rest, while the carbide and silicate dust contribute only a few percent of the ISM's total mass. Spectroscopic studies of binaries reveal some absorption lines that are not Doppler-shifted. In 1904, J. F. Hartmann reasoned correctly, although not to universal acceptance, that the unshifted lines result from absorption of light from the binary by an intervening gas cloud, rather than by gas in the atmosphere of the star. Though still difficult to demonstrate conclusively in all cases, the existence of interstellar gas clouds is now generally accepted. As a result of temperature variations in the early universe and the subsequent continuous action of gravity, huge clouds of primarily hydrogen have formed throughout the ISM. They range in mass from about 1 to 1000 times the mass of the Sun and have temperatures of about 30 to 150 K. At these temperatures the hydrogen atoms in the clouds are in their ground states.

Even though the atoms are in their ground states, it is possible to see the clouds as a result of the hyperfine splitting of the hydrogen ground state due to the spins (i.e., magnetic moments) of the electrons and protons. If the spins of the electron and the proton in a particular atom are antiparallel, the atom's ground state energy is very slightly lower that it would be if the spins were parallel. (See Section 7-4 and Figure 13-23.) The energy difference between the two states is so small, 5.9×10^{-6} eV, that a collision with another atom or a dust grain can result in the atom absorbing enough energy to "flip" the electron's spin into the parallel configuration. Once the electron's spin is flipped, the atom has only two ways to return to the ground state: it can have another collision

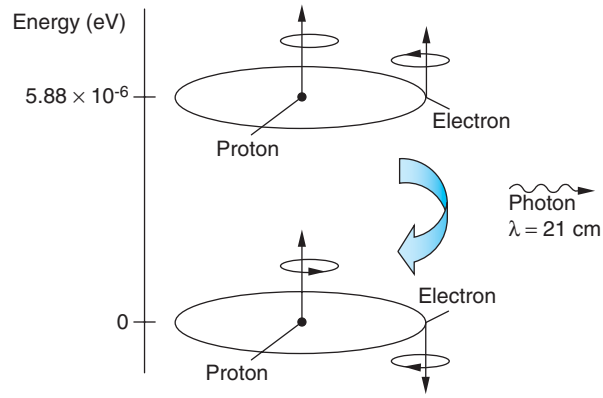

Figure 13-23 The hyperfine spitting of the hydrogen atom ground state is the origin of the 21-cm radiation used to map gas clouds in the ISM.

STUDENTS-HUB.com Uploaded By: Malak Obaid

enabling the atom to release the excess energy as heat or it can spontaneously flip the spin back antiparallel to that of the proton, emitting a photon with wavelength 21 cm in the process. The likelihood of either of these occurring is very small. For a given atom, collisions only occur every few hundred years and spontaneous return to the lower state may take millions of years. Even so, the number of atoms in the huge clouds is so large that there is a faint continuous emission of the 21-cm photons that enables mapping of the clouds by radiotelescopes.

Together, the interstellar dust and the clouds of gas account for an estimated 2 to 3 percent of the total mass (ordinary and dark matter) of our Galaxy. It is nearly certain that there is not enough unseen gas and dust to account for the Galaxy`s dark matter.

Gaseous Nebulae

Though most gas clouds, or nebulae, in interstellar space are irregular in shape, a few are circular, leading to speculation that they are self-gravitating and represent the very early stages of new star formation. Some large hydrogen clouds have spherical inner regions of ionized hydrogen, with a quite sharp demarcation between the H and H^+ regions. Astrophysicists believe that the ionized region is maintained by ultraviolet photons with frequencies above the Lyman limit emitted by a hot, newly formed star at the center of the region. The view that new stars form in the nebulae in an ongoing process is strongly supported by the observation that, although the Galaxy is of the order of 10^{10} years old, our Galaxy contains main sequence stars that are no more than 2 to 3×10^6 years old. Furthermore, high-resolution radioastronomy has in recent years located numerous newly forming stars embedded in clouds of dust and gas that are completely opaque to optical wavelengths.

Classification of Galaxies

Although fuzzy, extended objects, at one time called "nebulae" (not to be confused with planetary nebulae defined in Section 13-3), that were obviously not stars had been observed in the night sky since the 1700s, what and where they were was a matter of active scientific debate until well into the twentieth century. The answer had to await the development of telescopes with sufficient resolution and light gathering power and a theoretical means of computing distances from observations made with them. These came together in the mid-1920s when Edwin Hubble[16] used the 2.5 m telescope on Mount Wilson, the largest in existence at the time, to measure the intensities of rare stars, called Cepheid variables[17] that he discovered in three "nebulae." One of those nebulae, the great spiral Andromeda, he measured to be 2×10^6 light-years away. In one stroke, he was able to demonstrate that the "nebulae" were in fact galaxies much like our own, as had first been suggested by the philosopher Emmanuel Kant 150 years earlier, and that they were far outside the Milky Way. Exploring Hubble's discovery will take us into the realm of cosmology, the study of the large-scale structure of the universe.

Following his discovery that these "nebulae" were in reality distant galaxies, Hubble conducted a systematic study of the enormous number that were visible. He found that all but a very few fit into four general categories. Most had regular geometrical shapes and occur in two varieties: *ellipticals* which are roundish, rather like a football, and *disks*. The disks in turn had two subgroups, *ordinary spirals* and *barred spirals* (i.e., spirals with a "bar" of stars across the center). The small percentage that did not have regular shapes he called *irregular galaxies*. Figure 13-24 shows an example of each type of galaxy. The Milky Way is a large barred spiral.

STUDENTS-HUB.com Uploaded By: Malak Obaid

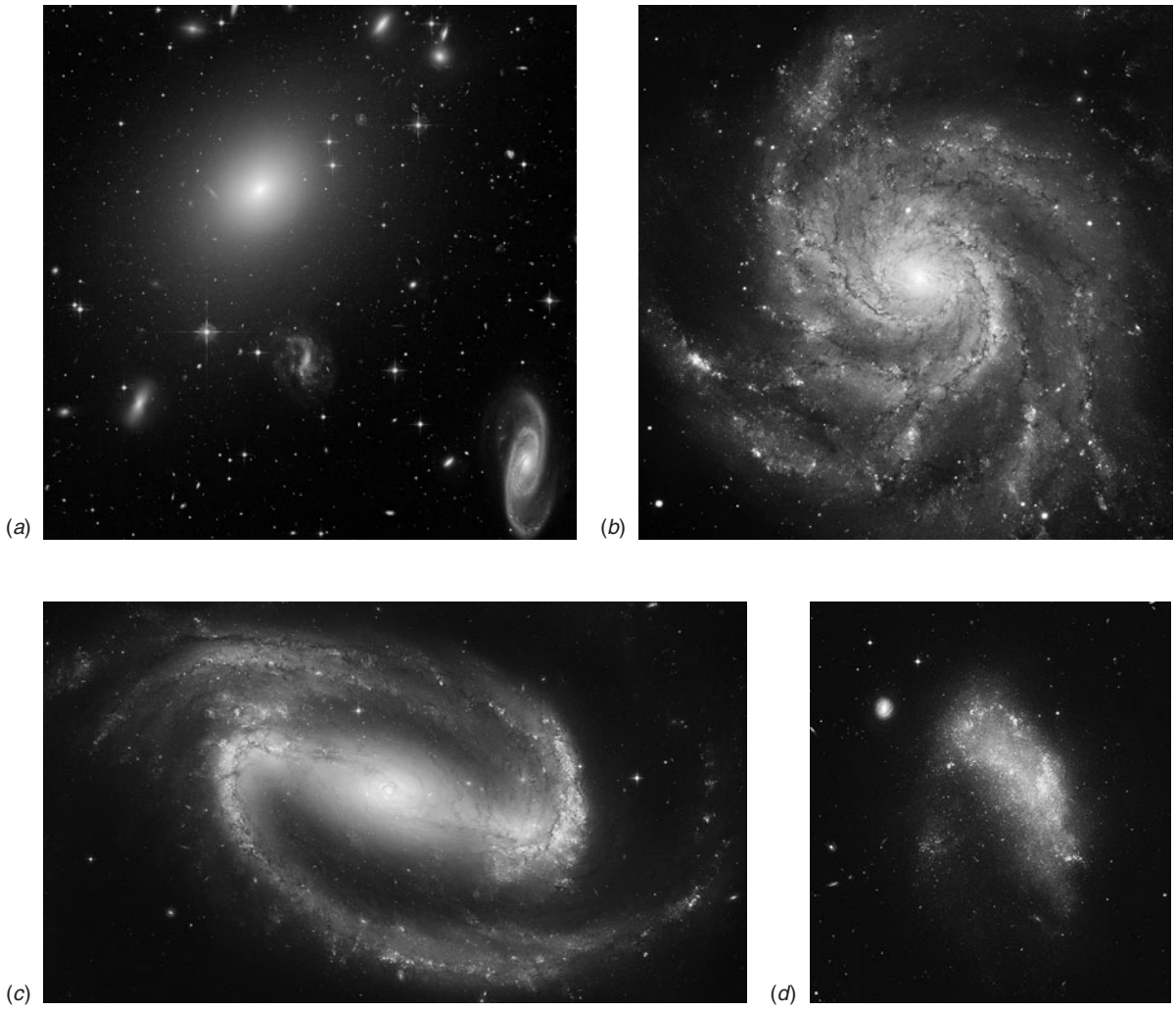

Figure 13-24 In Hubble's galaxy classification scheme, (*a*) is an example of an elliptical galaxy, (*b*) illustrates an ordinary spiral, (*c*) is a barred spiral, and (*d*) is an irregular galaxy. The Milky Way is thought to be a spiral with a faint bar. [*(a) NASA, ESA, and The Hubble Heritage Team (STScI/AURA). (b) NASA and ESA. (c) NASA, ESA, and The Hubble Heritage Team (STScI/AURA). (d) NASA, ESA, and The Hubble Heritage Team (STScI/AURA).*]

In addition to their geometrical differences, the four types of galaxies have other dissimilarities. A large fraction of the motion of the stars in spirals is rotational about the galactic center, whereas the motion of stars in ellipticals is generally random with only a relatively small rotational component. Ellipticals also seem to have very little interstellar gas and dust, while spirals and many irregulars have a substantial amount. The fact that most ellipticals have no young stars is probably a consequence of that absence. With a few exceptions, ellipticals are much smaller than spirals, typically having only about 20 percent of the diameter of an average spiral and only a thousandth of the mass.

STUDENTS-HUB.com Uploaded By: Malak Obaid

Quiet and Active Galaxies

Most of the approximately 10^{10} galaxies in the observable universe appear to be *quiet galaxies*—i.e., there is very little activity other than what might be expected for such dynamic systems. The vast majority of these galaxies are so distant that our instruments cannot resolve internal details. Therefore, only the composite spectra and radiant flux F for the entire galaxy can be observed. The range of velocities Δv that exists in the stars of the regular galaxies, measured by the Doppler broadening of the spectral lines, turns out to be related to the total luminosity L by

$$L \propto (\Delta v)^4 \qquad \textbf{13-26}$$

Since L is related to F and r, the distance to the galaxy, by Equation 13-8, the distance r can be found from measurements of the redshift and the apparent brightness of the galaxy, assuming that L is known.

In a very small percentage of galaxies something extremely violent, even by comparison with stellar supernovae, is occurring. Such systems are called *active galaxies*. There are several distinct types, some of which may not even be galaxies at all. The first discovered were *Seyfert galaxies*, named after Carl Seyfert, who first identified many of them. They are spirals with extremely bright, central starlike cores, or nuclei. In many of them, light coming from the core exceeds that from all of the stars in the galaxy and may vary in intensity by a factor of two or more in less than a year. Such a rapid variation in the total intensity means that the source must be less than one light-year in extent while producing as much energy as 10^{11} stars. Even more incredible, if possible, is the fact that the light emitted by a Seyfert galaxy consists of broad emission lines originating in both allowed and forbidden transitions in highly ionized atomic systems superimposed on a continuum, but without the absorption lines typical of stars. That suggests that its enormous energy is not coming from thermonuclear reactions. The source is not yet understood.

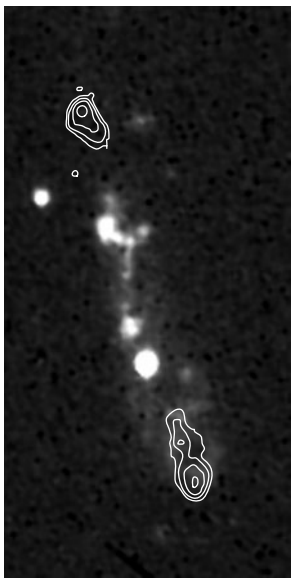

Radio galaxy 3C368. The contours show the centers of strong radio emission. The bright knots may be regions of star formation in this elliptical galaxy. [*NASA, NRAO, VLA, HST, WFPC 2, M. Longair (U. Cambridge).*]

A similar sort of extreme activity occurs in a few ellipticals called *N galaxies* and *BL Lac objects*. N galaxies are elliptical counterparts of Seyfert galaxies, that is, they have very bright centers. BL Lac objects seem to be like N galaxies, but exhibit substantial short-term intensity variations. In these, an intensity variation of a factor of two can occur within a week and a complete reversal of the polarization of the emitted light within one day, suggesting that the energy source is only one light-day in diameter. BL Lac objects are now thought to be giant ellipticals about 10^9 $c \cdot$ y from Earth.

Some of the giant ellipticals are also strong emitters in the radio region of the spectrum. Study of these *radio galaxies* has been intense, and the results have been astonishing. For example, the radio source Centaurus A is double-lobed with a small radio-emitting nucleus midway between the lobes. It is one of the brightest radio-emitting objects in the universe. Analyses of its spectra indicate that the initial energy release represented by the radiation that we now see amounted to 10^{56} J, which is about the equivalent of all the stars in the Milky Way undergoing supernova explosions simultaneously! The nature of such a colossal event is not currently understood.

In a universe of strange phenomena, *quasars*, short for quasi-stellar radio sources, are among the strangest. Discovered as radio sources, their optical images look like stars; that is, they have no resolved structure. Their spectra resemble that of a Seyfert galaxy. Resolved radio images of some quasars show that a few of them are double-lobed, like the radio galaxies, which makes their identification ambiguous. The Sloan Digital Sky Survey (SDSS) has catalogued 46,420 quasars; of those, 520 have redshifts ≥ 4, the most distant at a redshift of $z = 5.41$. There is also a group of objects about 10 times more numerous than quasars, radio sources that were earlier called

STUDENTS-HUB.com Uploaded By: Malak Obaid

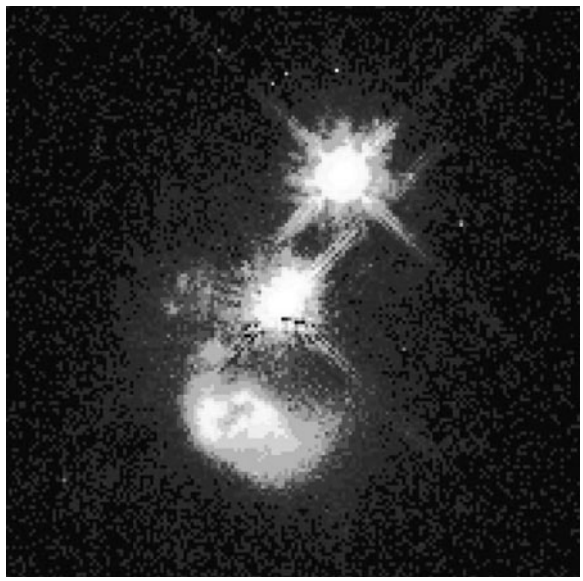

Debris from the catastrophic collision of two galaxies may be fueling quasar IRAS04505-2958. The quasar is about 3×10^9 $c \cdot$ y from Earth. Astronomers believe the collision ripped out the core of a spiral galaxy (bottom of the picture). The ring lies in front of the quasar (the bright object in the middle) at a distance of 15,000 $c \cdot$ y (one-seventh of the diameter of the Milky Way). The bright object just above the quasar is a foreground star. [*John Bahsall (Institute for Advanced Study, Princeton), Mike Disney (University of Wales), and NASA.*]

quasi-stellar objects. These are like quasars in every major way, except that they are not radio-emitters. Current terminology refers to both types as quasars, the radio sources as *radio-loud quasars* (QSRs) and the others as *radio-quiet quasars* (QSOs).

Perhaps the strangest thing about the quasars is the magnitude of the redshift of their spectra, which is very large. It implies that some quasars are receding directly away from us at greater than 0.95 c. This would make them the most distant massive objects, of the order of 10^{10} $c \cdot$ y from Earth. Their radiant flux F together with the great distance imply power outputs of 10^{40} W, greater than that of 10^{12} Suns. Not only that, but the intensities of some quasars vary over only a few hours, suggesting dimensions of only a few light-hours.

Hubble's law

E. P. Hubble was the first astronomer to recognize that there is a relation between the redshifts of the spectra of galaxies and their *distances* from us. This relation is illustrated in Figure 13-25 for a group of spiral galaxies used by astronomers for calibrating distances. The recession velocity v of a galaxy is related to its distance r from us by *Hubble's law:*

$$v = H_0 r \qquad \textbf{13-27}$$

where H_0 is the *Hubble constant*.

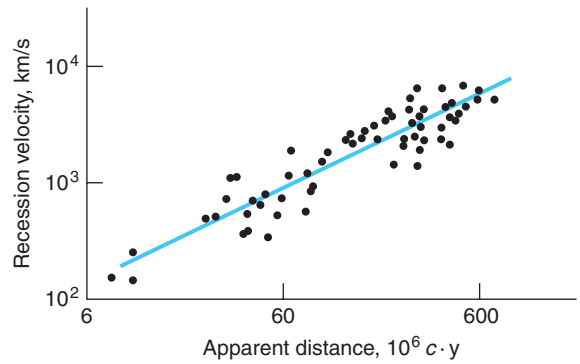

Figure 13-25 A plot of the recession velocities of individual galaxies versus apparent distance illustrates Hubble's law. The slope of the line is H_0.

STUDENTS-HUB.com Uploaded By: Malak Obaid

In principle, the value of H_0 is easy to obtain, since it relies on the direct calculation of v from redshift measurements. However, recall that astronomical distances are very difficult to obtain and that they have been measured for only a miniscule fraction of the 10^{10} or so galaxies in the observable universe. Thus, the value of H_0 changes as the interpretation of distance calibration data is refined. The currently accepted value of the Hubble constant is

$$H_0 = 71 \pm 4 \text{ km/s per Mpc} = 22 \pm 2 \text{ km/s per } 10^6\, c \cdot \text{y} \qquad \textbf{13-28}$$

Notice that the basic unit of H_0 is reciprocal time. The quantity $1/H_0$ is called the *Hubble time* and equals about 1.3×10^{10} years. This would correspond to the age of the universe if gravitational pull on the receding galaxies were ignored.

The redshift z, defined in Section 1-5, is given by

$$z = \frac{f_0 - f}{f} = \frac{\lambda - \lambda_0}{\lambda_0} \qquad \textbf{13-29}$$

where f_0 and λ_0 are measured in the rest system of the star or galaxy (the emitter) and f and λ are measured at Earth (the observer). Figure 13-26 shows the redshifted spectra of five galaxies whose distances from us range from 2.6 to 287.5 Mpc.

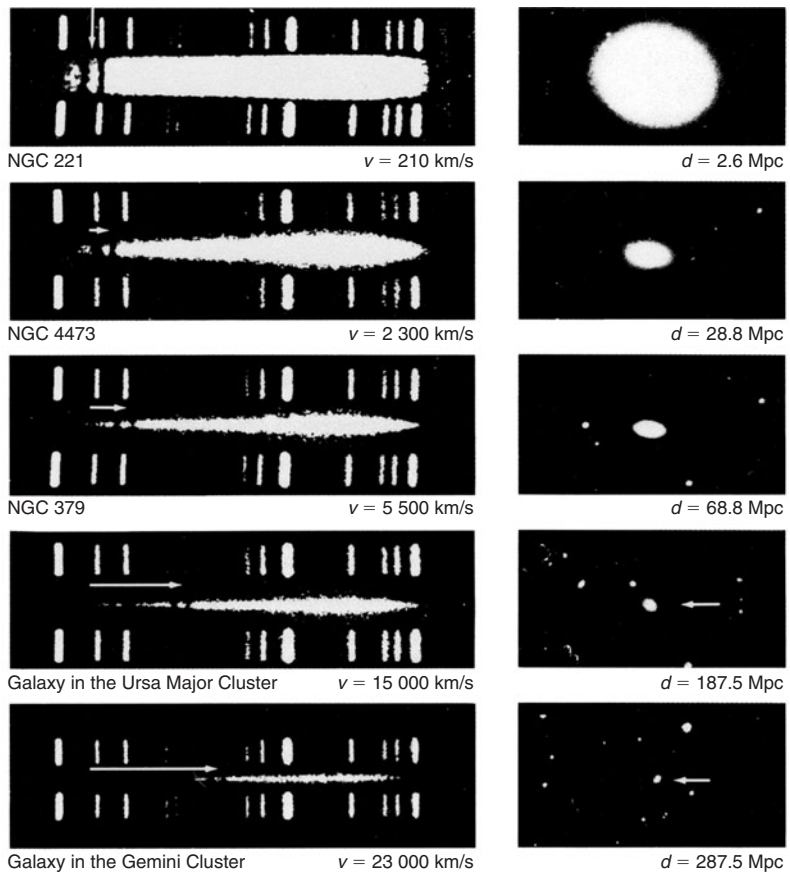

Figure 13-26 The redshifts of the Ca, H, and K absorption spectral lines are shown for five galaxies at different distances from us. The line spectra above and below the absorption spectrum are standards used for determining the amount of shift accurately. [*California Institute of Technology.*]

STUDENTS-HUB.com Uploaded By: Malak Obaid

EXAMPLE 13-5 **Distance to a Galaxy in Virgo** Redshift measurements on a galaxy in the constellation Virgo yields a recession velocity of 1200 km/s. How far is it to Virgo?

SOLUTION

Using Hubble's law, we obtain

$$r = \frac{v}{H_0} = \frac{1200 \text{ km/s}}{21 \text{ km/s per } 10^6\, c \cdot \text{y}} = \frac{(1200 \text{ km/s})(10^6\, c \cdot \text{y})}{21 \text{ km/s}} = 57 \times 10^6\, c \cdot \text{y}$$

$$= 17.5 \text{ Mpc}$$

Remarks: *Compare this result with distance measurements to Virgo made by some of the standard astronomical distance-measuring methods given in Table 13-4.*

Hubble's law tells us that the galaxies are all receding from us, with those the farthest away moving the fastest. However, there is no reason why our location in the universe should be special. An observer in any galaxy would make the same observations and compute the same Hubble constant. (See Problem 13-25.) Thus, Hubble's law states that all of the galaxies are receding from each other at an average speed of 71 km/s per Mpc of separation. In other words, *the universe—space itself—is expanding*. This is a profound discovery with enormous theoretical implications.

All galaxies participate in the general expansion of the universe. As a result, the wavelengths of light emitted toward Earth by galaxies (and stars and anything else out there) is lengthened or stretched along with the space through which it is moving, producing the *cosmological redshift*. It is the cosmological redshift that is described by Hubble's law. This redshift is not related to the galaxy's recessional velocity by the relativistic Doppler effect equation that we developed in Chapter 1 (Equation 1-38), even though astronomers often use that equation to express a measured redshift z as the radial velocity of a galaxy as if it were moving through space, rather than the actual velocity with which it receding from us due to the expansion of space. That this practice provides a reasonable estimate of relatively nearby distances can be seen as follows: Substituting Equation 13-27 into Equation 13-29 and solving for r yields

$$r = \frac{c}{H_0} \frac{(z+1)^2 - 1}{(z+1)^2 + 1} \qquad \textbf{13-30}$$

For $z \leq 2$, Equation 13-30 yields values of r within about 5 percent of the values measured by the methods listed in Table 13-4. If $z \ll 1$, then the nonrelativistic equation $r = cz/H_0$ can be used and, e.g., for $z < 0.1$ the error is about the same as above. However, always remember that the cosmological redshift has nothing to do with the Doppler effect.

Table 13-4 Distance measurements to Virgo

Method	Cepheids	Novae	Brightness fluctuations	Type Ia supernovae
Distance to Virgo (Mpc)	15 – 25	21.1 ± 3.9	15.9 ± 0.9	19.4 ± 5.0
Maximum useful distance (Mpc)	<29	<20	<50	> 1000

STUDENTS-HUB.com Uploaded By: Malak Obaid

The fractional change in the wavelength for the cosmological redshift is equal to the fractional change in the "size" or scale R of the universe since the time when the light was emitted. This allows us to also write the redshift as

$$z = \frac{\lambda - \lambda_0}{\lambda_0} = \frac{R - R_0}{R_0} = \frac{R_{\text{observed}} - R_{\text{emitted}}}{R_{\text{emitted}}} \quad \Rightarrow \quad \frac{R_{\text{observed}}}{R_{\text{emitted}}} = 1 + z \qquad \textbf{13-31}$$

Equation 13-31 says, for example, that a galaxy with $z = 2$ is now three times farther from Earth than it was when the observed light was emitted. Looking at regions in space that are cosmologically nearby or close to us provides a "snapshot" of what the universe looks like everywhere *now*. At Earth at the present time (t_0), $z = 0$. That is, galaxies close by the Milky Way have no (measurable) cosmological redshift. Looking at objects with higher z values corresponds to looking back in time. Thus, at redshift z we are seeing the universe as it appeared when it was $1/(1 + z)$ of its size now.

The discovery and analysis of the redshifts and luminosities of the quasars has significantly furthered our understanding of the expansion and evolution of the universe. Observations show that bright quasars are more numerous at large z than at small z, that is, the space or volume density of bright quasars was larger at earlier times than it is now. This could be because there where more of them in earlier times or their luminosities could have been higher or both. Or it could be that the observations are simply the result of the general expansion of space and the volume density and luminosities of the quasars have not changed over time. To remove the complicating effect of the expansion, astrophysicists and cosmologists define *comoving coordinates* and, correspondingly, for our purposes here *comoving space density*. The former we will return to in Section 13-8. The latter removes the effect of the expanding universe by dividing the number density of objects per cubic Mpc at redshift z by $(1 + z)^3$. This converts the number density of objects to the value it would have at $z = 0$ (today). Thus, if the number density and/or brightness have been constant over time, their comoving space density and brightness will be constant. Changes signal a change in the number density or an evolution of the quasars or both.

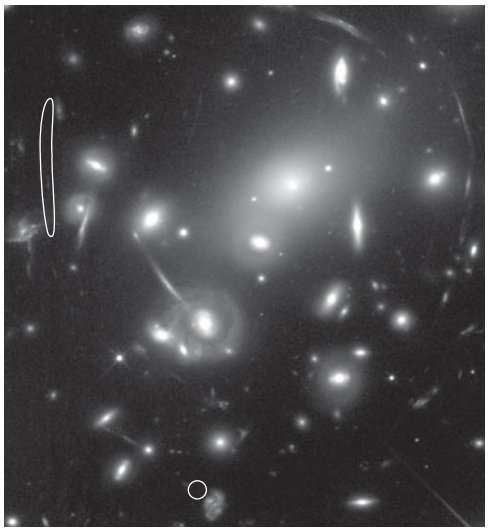

The oval encircles the most distant galaxy yet discovered (as of 2007). The faint streaks are the galaxy's image as gravitationally lensed by galaxy cluster Abell 2218. Its redshift of 6.6 puts it about 13×10^9 $c \cdot y$ from Earth moving away from us at about 0.97 c. The light that formed this image left the galaxy when the universe was only 700 million years old. [*NASA, Andrew Fruchter and the ERO Team [Sylvia Baggett (STScI), Richard Hook (ST-ECF), Zoltan Levay (STScI)] (STScI).*]

Observations of the comoving space density of bright quasars show that they are more than 1000 times more numerous at $z = 2$ than they are today (at $z = 0$), *but* the total number of quasars has not changed back to about $z = 2$. Therefore, observations indicate that the luminosity of quasars evolves over time, but not their comoving space density. That is, at least back to $z = 2$, there appears to be a constant number of quasars growing dimmer as the universe expands. Further back than $z = 2$, measurements have reached about $z = 6$. In this range the picture is more complicated, the comoving space density declining after about $z \approx 3$, diminishing by approximately a factor of 10 by $z = 4$. The meaning of the decrease is a focus of continuing research.

An obvious question is whether there are other observational results that support Hubble's conclusion. For example, is the observed expansion general, or could it be a statistical accident—a consequence of our having measured distances to only a fraction of the 250,000 (out of the 10^{10} galaxies in the observable universe) whose redshifts have been measured to date? Thus, redshift surveys of the universe are an important first step in studying Hubble's expansion.

STUDENTS-HUB.com Uploaded By: Malak Obaid

Redshift surveys establish the existence of large scale structure in the universe and, together with independent distance measurements for individual galaxies, determine the Hubble constant. Such surveys have been underway for several years and about 10^{-5} of the volume of the visible universe has now been mapped. These surveys have yielded several unexpected discoveries, but have not yet answered the question above conclusively. There are huge voids in space—regions where the density of galaxies is only 20 percent or so of the average for the universe. In addition, the galaxies themselves tend to be grouped into clusters and the clusters into superclusters. The Milky Way is a part of the Local Cluster that contains about a dozen galaxies. The galaxies also tend to lie on thin, sheetlike structures. How such structures might have evolved in the general expansion described by Hubble's law presents a challenge to cosmological models. The most successful cosmological model thus far has been the Λ Cold Dark Matter (ΛCDM) model, where Λ is Einstein's cosmological constant. One of the largest of the galaxy mapping projects has been the 2dF Galaxy Redshift Survey (2dF GRS; Figure 13-27). The project, completed in 2002, obtained high-quality spectra and redshifts for 245,591objects, mainly galaxies. Still underway is the largest survey, the Sloan Digital Sky Survey (SDSS). The SDSS first phase was completed in 2005 after measuring the spectra of 675,000 galaxies, 90,000 quasars, and 185,000 individual stars. The SDSS second phase of measurements is currently underway at the project's dedicated 2.5-m telescope in New Mexico.

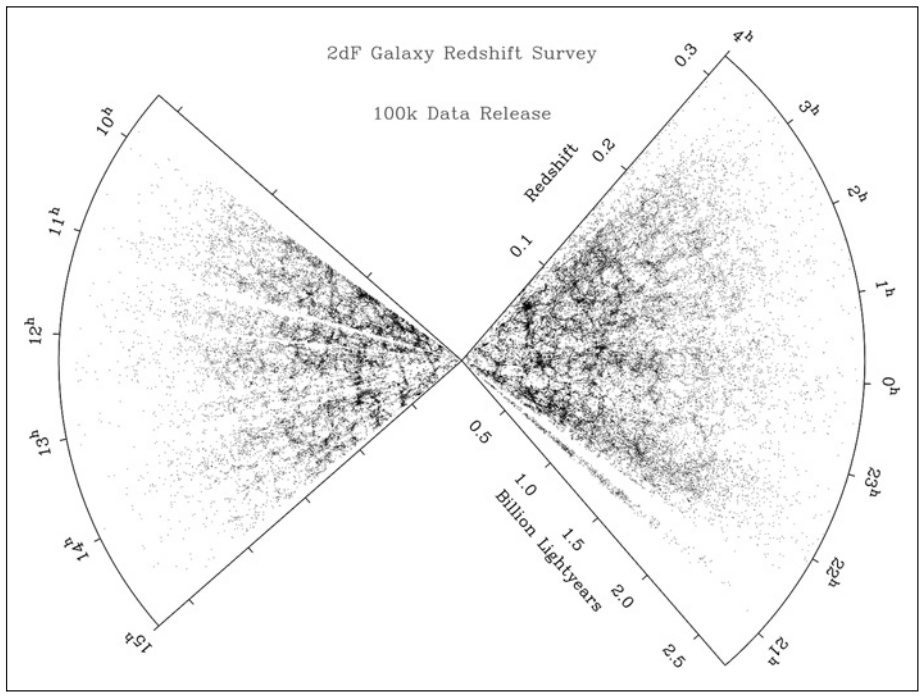

Figure 13-27 The 2dF Galaxy Redshift Survey (2dF GRS) is a major spectroscopic survey utilizing unique facilities built by the Anglo-Australian Observatory. By the survey's completion in 2002 it had recorded precise spectra for 245,591 objects enabling a wide range of new analyses including, for example, the first direct comparison with the microwave background anisotropy on the same spatial scale and studies of galaxy clustering to test inflationary cosmological models of the early universe. The survey is integrated with the 2dF Quasi Stellar Objects survey. [*Matthew Colless and the 2dF Galaxy Redshift Survey Team.*]

STUDENTS-HUB.com Uploaded By: Malak Obaid

13-7 Cosmology and Gravitation

We have seen that applying Hubble's law to the observations of galaxies leads inescapably to the conclusion that the universe is expanding and provides us with a measure, $1/H_0$, of how long ago that expansion began. In this section, we will examine the basic theoretical framework that suggests possible tests of that conclusion. The basis for this discussion is the philosophical view that at large scale the universe is homogeneous and isotropic at any instant in time. That is, at any given instant the universe has the same physical properties everywhere and looks the same in all directions from every location. This is called the *cosmological principle*. Note that Hubble's law is consistent with the cosmological principle.

We have already seen that the cosmological principle clearly does *not* hold on a local scale. Galaxies are clustered into local groups. Even on a scale of 10^8 $c \cdot$ y, the dimension typical of galactic superclusters, the universe is neither homogeneous nor isotropic. However, when maps of very distant space are examined (Figure 13-28), the distribution does appear to be statistically homogeneous and isotropic. Redshift survey maps like Figure 13-27, which extend to about 4×10^9 $c \cdot$ y, do indeed show homogeneity and isotropy in a statistical sense.

The Critical Energy Density of the Universe

Noting that the Hubble age $1/H_0 = 1.3 \times 10^{10}$ years ignores the effect of gravity and ignoring for the moment the recently discovered acceleration of the expansion, the expectation is that gravity tends to slow the expansion over time. Is the gravity in the universe strong enough to eventually reverse the expansion and cause the universe to collapse? Or will the expansion continue forever? The answer depends upon the mass density ρ_0 of the universe. We can understand this by considering the motion of a single galaxy of mass m at a very large distance R from Earth. Let M be the total mass of all the galaxies within the spherical volume of radius R. The gravitational potential energy of our single galaxy is $-GMm/R$. The total energy of the galaxy is

$$E = K + U = \frac{1}{2}mv^2 - \frac{GMm}{R} \qquad \textbf{13-32}$$

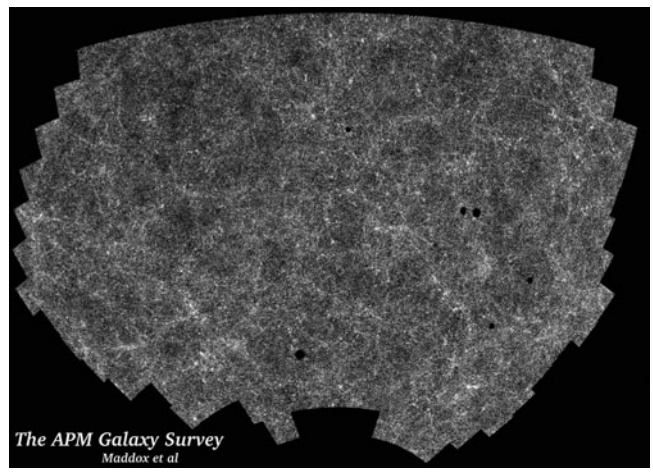

Figure 13-28 A map showing approximately 2 million galaxies ranging up to 2×10^9 $c \cdot$ y away. The distribution of the galaxies looks essentially homogeneous and isotropic. This is a composite of 185 contiguous photos taken by the Schmidt telescope at the European Southern Observatory. The south Galactic pole is at the bottom center. [*S. Maddox (Nottingham U.) et al., APM Survey, Astrophys. Dept. Oxford U.*]

STUDENTS-HUB.com Uploaded By: Malak Obaid

If we project an object with some speed v from Earth, the object will escape if its total energy is greater than or equal to zero, but if the total energy is negative, the particle will eventually stop and fall back to Earth. Similarly, if the total energy of the galaxy is greater than or equal to zero, it will continue to move away from Earth forever, but if the total energy is negative, the galaxy will eventually stop moving away from Earth and start moving back toward Earth. We can see from Equation 13-32 that the total energy of the galaxy depends on the mass density $\rho = M/(4/3\pi R^3)$. We can find the critical mass density of the universe ρ_c by setting the total energy in Equation 13-32 equal to zero:

$$\frac{1}{2}mv^2 = \frac{GMm}{R}$$

Substituting $v = H_0R$ from Hubble's law (Equation 13-27), we obtain

$$\frac{1}{2}m(H_0R)^2 = \frac{GMm}{R}$$

$$\frac{1}{2}H_0^2 = \frac{GM}{R^3}$$

Then

$$\rho_c = \frac{M}{\left(\frac{4}{3}\right)\pi R^3} = \frac{3H_0^2}{8\pi G} \qquad \textbf{13-33}$$

Substituting the values for H_0 and G, we obtain for the critical mass density of the universe:

$$\rho_c \approx 10^{-26}\ \text{kg/m}^3$$

This corresponds to about five hydrogen atoms per cubic meter of space.

Determining the present mass density ρ_0 of the universe is thus an important goal. If it is larger than ρ_c, the expansion will reverse and the universe will collapse. If it is smaller, then the expansion will continue forever. If it should happen that $\rho_0 = \rho_c$, the expansion will coast to a stop, but will not begin to contract. It should also be clear that if ρ_0 is greater than ρ_c now, it will always be so because it is actually the conservation of energy that determines whether contraction or continued expansion will occur. Since ρ_0 must decline over time as expansion progresses, the Hubble constant must also decline over time to ensure that ρ_0 remains larger than ρ_c. In other words, the Hubble constant must be a function of time $H(t)$, that is, $H_0 \equiv H(t_0)$. The value of ρ_0 based on the *visible* (baryonic matter) universe is only about 4 percent of ρ_c, suggesting that the universe will expand forever. However, the dark matter of the universe discussed earlier affects the value of ρ_0. Together, the visible matter and dark matter account for about 26 percent of the mass necessary to make $\rho_0 = \rho_c$. Examination of the recession rates of the Type Ia "standard candle" supernovae suggests that dark energy provides the additional 74 percent needed. Recalling that they have very similar brightness and light curves, the discovery that for a given brightness the redshifts of distant Type Ia supernovae are less than expected implies that the universe was expanding at less than the expected rate in the past. Therefore, the universe is expanding at an accelerated rate today. The implication is that dark energy corresponds to a repulsive force that is speeding up the expansion.

STUDENTS-HUB.com Uploaded By: Malak Obaid

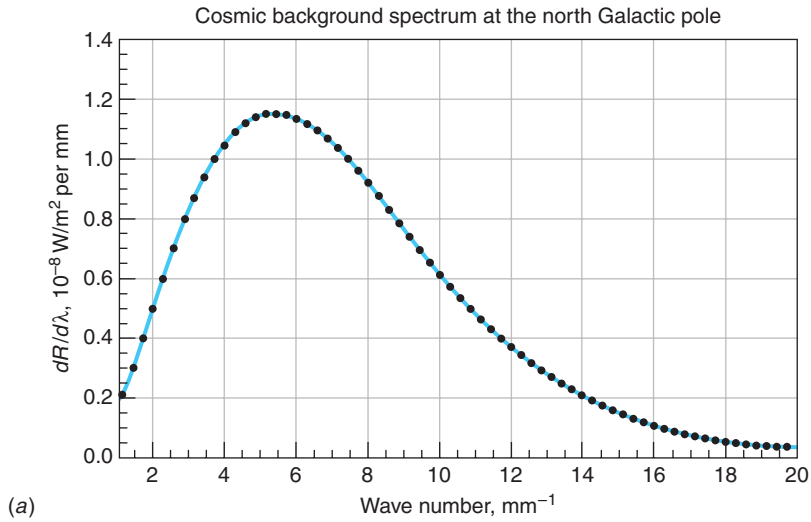

(*a*)

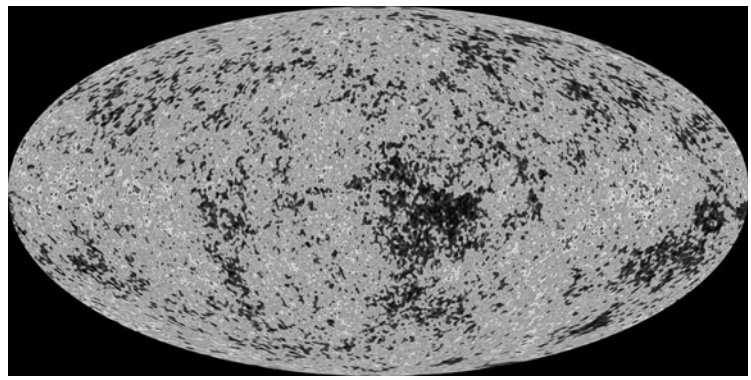

(*b*)

Figure 13-29 (*a*) The spectrum of the cosmic background radiation measured by NASA's *Cosmic Background Explorer* (COBE) spacecraft. The dots are the data points. The solid curve is the Planck radiation curve for a blackbody at 2.725 K. [*CERN Courier, June 1991, p. 2, courtesy of NASA.*] (*b*) This detailed all-sky picture of the infant universe includes three years of WMAP data. It shows 13.7×10^9-years-old temperature fluctuations that were the seeds that eventually became the galaxies and provides new clues regarding events that occurred in the first trillionth of a second following the Big Bang. The range of the temperature fluctuations is ± 200 μK. [*NASA/WMAP Science Team.*]

This view is independently supported by very recent research that compares the temperature fluctuations in the cosmic microwave background shown in Figure 13-29*b* with their origin in the "lumpiness" of matter in the 2dF GRS (see Figure 13-27).

13-8 Cosmology and the Evolution of the Universe

Following his completion of general relativity in 1915, Einstein turned to cosmology. He based his early work on the assumption that the universe was not only homogeneous and isotropic, but also constant in time. This is sometimes called the *perfect cosmological principle*. He quickly discovered that, like a universe described by Newton's gravitational theory, only an empty (no mass) universe can be static. He found that a static universe could be metastable if it contained mass and a *cosmological constant*, thereby committing what he later described as the biggest blunder of his life. On learning of Hubble's discovery of the expansion of the universe, he abandoned the cosmological constant. However, dark energy is essentially a revision of the cosmological constant for an expanding universe. Since the constant, in effect, generated the mass of the universe, adjusting its value could shift some of the predicted mass into energy, thereby accounting for the unseen mass.

STUDENTS-HUB.com Uploaded By: Malak Obaid

One difficulty with the steady-state model is a problem known as *Olber's paradox*, first posed by Edmund Halley in 1720, but named after the nineteenth-century physician-astronomer Wilhelm Olbers who publicized it widely. If there is a uniform distribution of stars throughout an infinite space, then no matter in which direction you look, you will eventually see a star. Since stars are bright, the night sky should look as bright as the surface of the average star. (This is analogous to standing in an infinitely large forest in which all the trees are painted white. Along any line of sight, you will eventually see a white tree, so you should see white in all directions.) Why then is the night sky dark? The solution offered by Olber himself was that interstellar dust absorbs the light from distant stars. But this is no help since the dust would eventually be heated to glowing, so the night sky should still be bright.

The solution to this problem came in part with Hubble's discovery of the expansion of the universe. The point is not that light is redshifted out of the visible region,[18] but that the energy of every photon is diminished, since $E = hc/\lambda$. However, redshift can account for only a very small part of the solution. The key is that, since the velocity of light is finite, looking into space means looking back in time. Looking deeper into space we eventually would be looking at a time before the stars began to form, that is, at a time greater than the Hubble age. (In terms of our forest analogy, the distant trees have not yet been painted white; therefore, if the separation of the trees is great enough, many lines of sight will end on dark trees.)

A Simple Cosmology Model[19]

To a considerable extent, descriptions of the origin and evolution of the universe depend on the cosmology model that is used to interpret observations. The appearance of galaxies at cosmological distances is directly affected by the curvature of spacetime through which the light travels on its trip to Earth. One would reasonably expect that the distortion of spacetime would be more complex at higher redshifts when the visible universe was smaller and the mass density larger than now, which is understandably a region of high interest to cosmologists. A proper interpretation of observations at high redshifts necessarily requires the use of the general theory of relativity. Such an application is beyond the scope of our discussions; however, we can develop a useful, albeit approximate view of the expansion of the universe with the aid of cosmological a model based on Newtonian mechanics and the cosmological principle, then follow up with a very brief look at the current state of the theory based on general relativity and measurements from the Wilkinson Microwave Anisotropy Project (WMAP).

Consider a thin spherical shell of radius r in our homogeneous, isotropic universe (Figure 13-30a). The shell contains and uniformly distributed total mass m.

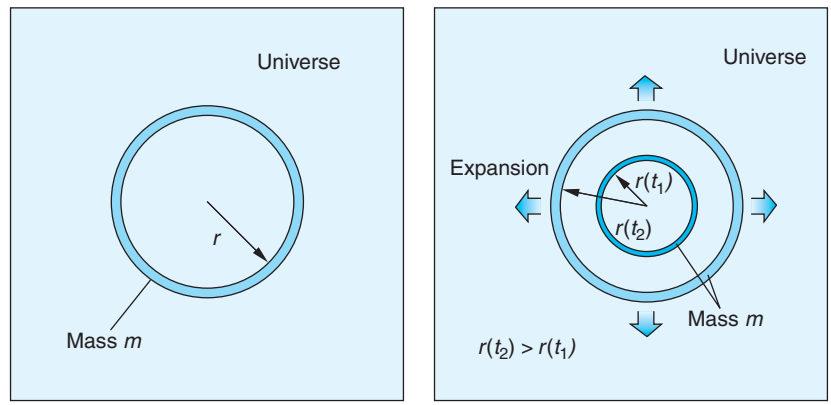

Figure 13-30 (*a*) Cross section of a thin spherical shell containing mass m in an isotropic, homogeneous universe. (*b*) The same shell as it has expanded from its size at time t_1 to time t_2. The thickness of the shell also expands; however, the mass in the shell is constant. The shell's comoving coordinate $r(t_0)$ remains unchanged.

STUDENTS-HUB.com Uploaded By: Malak Obaid

Our shell, like all such shells, expands along with the general expansion of the universe, becoming both large and thicker; however, m remains constant. Assuming gravity to be the only interaction present, the total energy of the mass m within the shell is the kinetic energy plus the gravitational potential energy:

$$E = K + U = \frac{1}{2}mv^2(t) - \frac{GM_r m}{r(t)} \qquad \textbf{13-34}$$

where $v(t)$ is the recessional velocity of the shell and M_r is the mass within the sphere that is enclosed by the shell. Like m, M_r also remains constant because $M_r = (4/3)\pi r^3\rho$ and, although r and ρ are both functions of time, $\rho \propto r^{-3}$. The mass of our universe outside the shell exerts no net gravitational force on m. (Why not?) As the shell expands the gravitational force due to M_r causes the kinetic energy of m to decrease and the gravitational potential energy to increase, i.e., to become less negative. Conservation of energy requires that the total energy E be unchanged, so we will, with remarkable foresight, write the total energy as

$$E = -\frac{1}{2}kmc^2r^2(t_0) \qquad \textbf{13-35}$$

where $r(t_0)$ is the radius of the shell at $t_0 = now$ and k is a constant with units (length)$^{-2}$. As we will see, the constant k determines the geometry of the universe. Combining Equations 13-34 and 13-35, substituting for M_r, and cancelling m yield

$$v^2(t) - \frac{8}{3}\pi G\rho(t)\, r^2(t) = -kc^2r^2(t_0) \qquad \textbf{13-36}$$

Referring to Equation 13-36, note that:

- If $k > 0$, then the total energy of the mass m is negative. In that event there is a radius $r(t)$ beyond which the shell cannot expand because v is (instantaneously) zero and we say that the universe is *closed* or *bounded*. The shell will then begin to contract due to the mass M_r interior to the shell and undergo a time-reversed copy of the expansion back to what is sometimes called the "Big Crunch."
- If $k = 0$, then the total energy of the mass m is zero. In that case as $t \longrightarrow \infty$, $r(t) \longrightarrow \infty$ the recession velocity $v\,(t) \longrightarrow 0$ and the shell (and universe) coast forever toward a halt. We refer to such a universe as *flat*.
- If $k < 0$, then the total energy of the mass m is positive. In that event, as $r(t)$ increases, the gravitational potential energy becomes steadily more negative. But $v^2(t)$ must continually increase in order to keep the total energy positive. We then say that the universe is *open* and will continue to expand forever.

Since the cosmological principle requires that all shells, including ours in Figure 13-30*a*, must expand in the same way, that is, the time required for the radii of all shells to, say, triple, must be the same, we can express the radius $r(t)$ of our shell (or any shell) as

$$r(t) = R(t)r(t_0) \qquad \textbf{13-37}$$

STUDENTS-HUB.com Uploaded By: Malak Obaid

where $r(t)$ is the distance from the coordinate origin to the shell (see Figure 13-30*a*) and $R(t)$ is the *scale factor* first introduced in Equation 13-31 which describes the expansion or contraction of the universe. Since there is nothing special about our shell, $R(t)$ is the same for *all* shells. The constant $r(t_0)$ that in effect labels the shell is called the *comoving coordinate* (see Figure 13-30*b*). Assuming that the present is t_0, $R(t_0) = 1$ and, as we have noted, the present radius of our shell is $r(t_0)$. In Equation 13-31 R refers to the rest frame of the observer and R_0 to that of the emitting star or galaxy. Since $R(t_0) = 1$, the scale factor $R(t)$ and the redshift z are related by

$$1 + z = \frac{1}{R(t)} \qquad \textbf{13-38}$$

For example, looking back in time to redshift $z = 2$, the scale factor $R = 1/3$, that is, the visible universe was one-third of its present size. Hubble's law can now be written as

$$v\,(t) = H(t)r(t) = H(t)R(t)r(t_0) \qquad \textbf{13-39}$$

Differentiating Equation 13-37 with respect to time, substituting into Equation 13-36, and cancelling $r^2(t_0)$ yield

$$\left(H^2(t) - \frac{8}{3}\pi G\,\rho(t)\right)R^2(t) = -kc^2 \qquad \textbf{13-40}$$

Cosmologists define the *density parameter* $\Omega = \rho(t)/\rho_c(t)$ whose present value is

$$\Omega_0 = \frac{\rho_0}{\rho_{c0}} = \frac{8\pi G\rho_0}{3H_0^3} \qquad \textbf{13-41}$$

and since, as you will show in Problem 13-26, $\rho(z) = \rho(1 + z)^3$,

$$\frac{\Omega}{\Omega_0} = (1 + z)^3\frac{H_0^2}{H^2} \qquad \textbf{13-42}$$

In relativistic cosmology models, universes are described in terms of three components: matter (including dark matter) Ω_m, relativistic particles (e.g., neutrinos) Ω_{rel}, and dark energy (the cosmological constant) Ω_Λ. Current data suggests that relativistic particles do not contribute significantly to the energy density at the present time. Cosmologists, like all scientists, use graphical representations whenever possible, in this situation employing a two-dimensional graph of $\Omega_{\Lambda 0}$ versus Ω_{m0} to assess the current state of the universe. It is reproduced as Figure 13-31. The coordinates $(\Omega_{\Lambda 0}, \Omega_{m0})$ for the best values of the density parameters based on current WMAP observations are $(0.73 \pm 0.04, 0.27 \pm 0.04)$. Delving further into this and related issues is on the leading edge of cosmological research, but regretfully beyond the scope of this book.

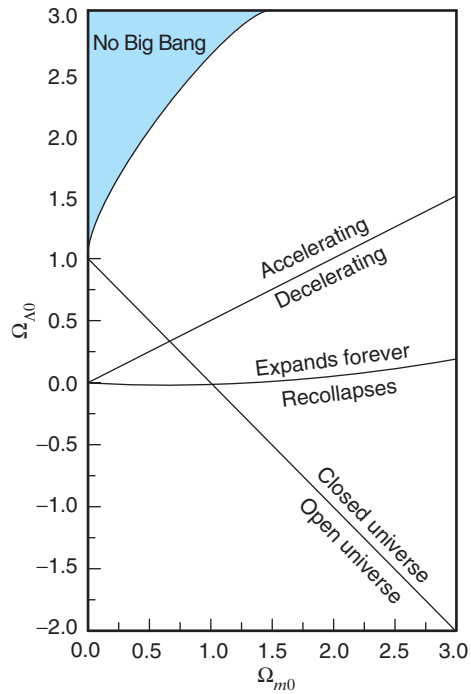

Figure 13-31 Every point in the $\Omega_{\Lambda 0} - \Omega_{m0}$ plane represents a possible universe. The lines drawn are based on various parameters from general relativity analyses. The line with negative slope starting in the lower right corner corresponds to the geometry parameter $k = 0$ (see Equation 13-36).

STUDENTS-HUB.com Uploaded By: Malak Obaid

The Big Bang

Over the past century cosmologists have developed a well-defined *standard model of the universe* that fits a comprehensive set of very precise, constraining measurements and observations. The foundation of the standard model is the Big Bang theory. It is the observational foundation of the theory that $(13.7 \pm 0.2) \times 10^9$ years ago[20] the universe was in a hot, dense state and at that particular time a single event, the Big Bang,[21] initiated an expansion and cooling that has continued to the present time. Two major astrophysical discoveries made in the 1960s were the first of several that have convinced most scientists that the model is correct. The first of the two discoveries that supported the evolving universe model was Martin Ryle's[22] observations revealing that there is a higher comoving space density of distant radio galaxies than nearby ones. Since distant observations correspond to earlier times, this meant that the universe had looked different at earlier times than it does now; that is, it has evolved over time.

The second discovery was monumental, as important as Hubble's discovery of the expansion of the universe itself. In investigating ways of accounting for the cosmic abundance of elements heavier than hydrogen, cosmologists recognized that nucleosynthesis in stars could explain the abundance of those heavier than helium but not that of helium itself. (See Figure 13-32.) Helium must therefore have been formed during the Big Bang. Synthesizing the amount of helium that would account for its present abundance requires that the Big Bang occurred at an extremely high initial temperature to provide the necessary reaction rate before the fusion was shut down by the decreasing density due to the very rapid initial expansion. The high temperature implies a corresponding thermal (blackbody) radiation field that would cool as the expansion progressed. Theoretical analysis predicted that from the Big Bang to the present, the remnants of the radiation field should have cooled to a temperature of

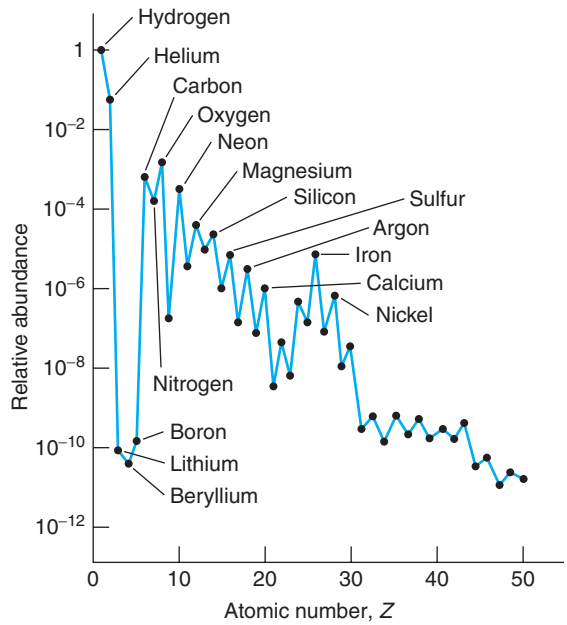

Figure 13-32 The abundances, relative to hydrogen, of elements in the Milky Way up to $Z = 50$ (tin). Note the peak at $Z = 26$ (iron), the sharp decline in abundances after iron, and the extremely low relative abundances of lithium, beryllium, and boron.

STUDENTS-HUB.com Uploaded By: Malak Obaid

about 3 K, corresponding to a blackbody spectrum with peak wavelength λ_{max} in the microwave region. In 1965, the predicted Cosmic Microwave Background (CMB) radiation was discovered by Arno Penzias and Robert Wilson[23] at Bell Labs. Since this landmark discovery, analysis of data from the Cosmic Background Explorer (COBE) satellite by John Mather and George Smoot[24] and by the Wilkinson Microwave Anisotropy Project (WMAP) collaborators have established the temperature of the background field at 2.725 ± 0.001 K with deviations from that value of no more than a few thousandths of a percent. These results show that the CMB has the isotropic distribution in space that is absolutely essential for a universe that satisfies the cosmological principle. Indeed, the Cosmic Microwave Background is the most precise blackbody known in nature (see Figure 13-29*a*). In addition, the WMAP detection of temperature fluctuations in the range of 30 μK (see Figure 13-29*b*) provided the first evidence for density inhomogeneities that cosmologists believe seeded all of the galactic structure of the universe.

The Very Early History of the Universe

What was the Big Bang like? The singular event that initiated the expansion of the universe must have been a huge explosion of space that occurred throughout the entire hot, dense state. Most cosmologists favor the standard model as the theoretical description of the evolution of the universe following the Big Bang. It relies heavily on recent experimental discoveries and theoretical advances in particle physics and reflects the increasing overlap of frontier research in those areas of physics over the past several years. The standard model's account of how the universe evolved from $t = 0$ to now, when $t \approx 10^{10}$ years, is outlined in the following discussion and illustrated in Figure 13-33.

In the beginning the universe was dominated by energy at negative pressure which led to an early exponentially accelerated expansion referred to as *inflation*. The theoretical basis for inflation comes from general relativity and the cosmological principle which together give the acceleration equation (not intended to be obvious) below.

$$\frac{1}{R(t)}\frac{d^2R}{dt^2} = -\frac{4\pi G}{3c^2}(\rho c^2 + 3P) \qquad \textbf{13-43}$$

where $R(t)$ is the dimensionless scale factor discussed earlier, ρc^2 is the energy density of the universe, and P is the pressure. Notice that in situations where negative pressure dominates, the expansion has positive acceleration. This very early period of inflation for which, bear in mind, we have no direct evidence, is nonetheless successful in resolving several cosmological questions, including (1) Why is the CMB temperature so uniform in every direction? (2) Why is the geometry of the universe so close to being flat? (3) Why do we not see magnetic monopoles? (4) What is the origin of the anisotropies measured by WMAP? Following that brief, but extremely rapid inflation, the universe was dominated by radiation, then subsequently by matter. Recently, cosmologically speaking, it has again become dominated by a negative energy pressure which is driving a new, but slower acceleration of the general expansion. Today, as we have alluded to earlier, matter accounts for only about 26 percent of the energy density of the universe, only 4 percent being ordinary matter. (See Figure13-34). The other 22 percent is the cold dark matter (CDM) discussed earlier that neither emits nor reflects light or is affected by radiation pressure, but does participate in the gravitational interaction. Figure 13-34*c* shows what may be the first indirect observation of dark matter. Dark energy, the remaining 74 percent of the energy density of the universe, is apparently driving the new acceleration.

STUDENTS-HUB.com Uploaded By: Malak Obaid

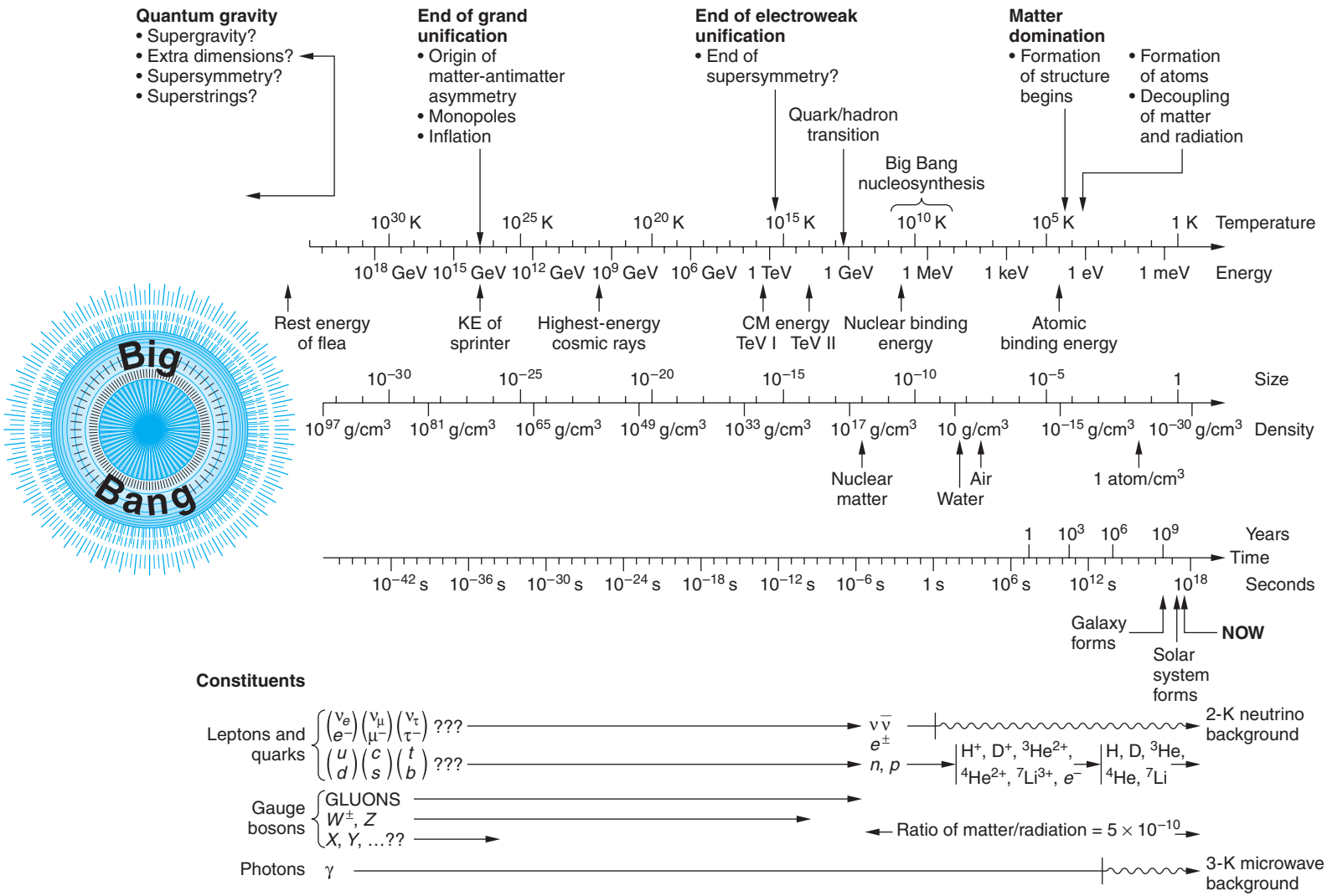

Figure 13-33 The evolution of the universe from time $t = 0$ to the present, according to the standard model.

STUDENTS-HUB.com Uploaded By: Malak Obaid

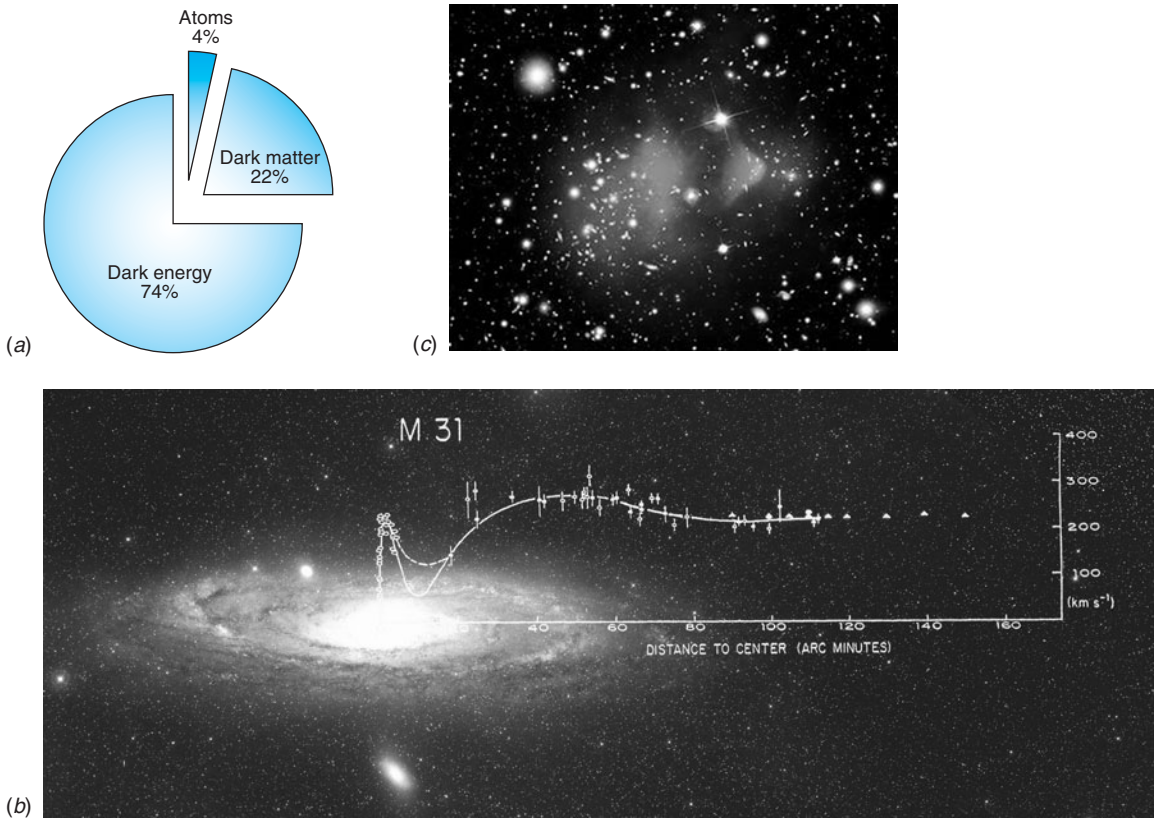

Figure 13-34 (*a*) The mass-energy content of the universe. Recent observations indicate that the dark energy is driving a renewed acceleration of the general expansion of the universe. (*b*) Stellar velocities in M31. Newton's law of gravitation requires that constant velocity implies $M \propto r$. Thus, in M31 much of the mass lies well beyond the visible extent of the galaxy, a very early indicator of dark matter. (*c*) Galaxy cluster 1E0657-558 resulted from a small cluster passing through a larger one some time in the past. Using this cluster as a gravitational lens for more distant galaxies made possible the mapping of the gravitational potential of 1E0657-588 (the large fuzzy "cloud"). X-ray emission recorded by the Chandra X-Ray Observatory of the two central, darker portions of the "cloud" reveal the hot gases (ordinary matter) of the two original colliding clusters. The lighter portions to the outside of the "cloud" are inferred to be dark matter. [The authors thank Vera Rubin for permission to use image (*b*). *(b) Vera Rubin and Janice Dunlap. (c) X-ray courtesy NASA/CXC/CfA/M Markevitch et al.; optical courtesy NASA/STScI; Magellan/U Arizona/D Clowe et al.; lensing map courtesy NASA/STScI; ESO WFI; Magellan/U Arizona/D Clowe et al.)*]

Initially, the four forces of nature (strong, electromagnetic, weak, and gravity) were unified into a single force. Physicists have been successful in developing theoretical descriptions that unify the first three, but a theory of quantum gravity, needed for the extreme densities of the single-force period, does not yet exist. Consequently, until the cooling universe "froze" or "condensed out" the gravitational force about 10^{-43} seconds after the Big Bang when the temperature was still 10^{32} K, we have no means of describing what was occurring. At this point the average energy of the particles would have been about 10^{19} GeV. As the universe continued to cool below 10^{32} K the three forces other than gravity remained unified and are described by grand unification theories (GUTs). Quarks and leptons were indistinguishable and particle quantum numbers were not conserved. It was during this period that a slight excess of quarks over antiquarks occurred, roughly 1 in 10^9, that ultimately resulted in the matter that we now observe in the universe.

STUDENTS-HUB.com Uploaded By: Malak Obaid

At 10^{-35} seconds, the universe had expanded sufficiently to cool to about 10^{27} K at which point another phase transition occurred as the strong force condensed out of the grand unified group, leaving only the electromagnetic and weak forces still unified as the *electroweak force*. During this period the previously free quarks in the dense mixture of roughly equal numbers of quarks, leptons, their antiparticles, and photons began to combine into hadrons and their antiparticles, including the nucleons. By the time the universe had cooled to about 10^{13} K, at about $t = 10^{-6}$ s, the hadrons had mostly disappeared through annihilation. This is because 10^{13} K corresponds to $kT \sim 1$ GeV, which is the minimum energy needed to create nucleons and antinucleons from the photons present via the reactions

$$\gamma \longrightarrow p^+ + p^- \qquad \textbf{13-44}\boldsymbol{a}$$

and

$$\gamma \longrightarrow n + \overline{n} \qquad \textbf{13-44}\boldsymbol{b}$$

The particle-antiparticle pairs annihilated and there was no new production to replace them. Only the slight earlier excess of quarks led to a slight excess of protons and neutrons over their antiparticles. The annihilations resulted in photons and leptons and after about $t = 10^{-4}$ seconds, those particles in roughly equal numbers dominated the universe. This was the *lepton era*. At about $t = 10$ seconds the temperature had fallen to 10^{10} K (kT $\sim$ 1 MeV). Further expansion and cooling dropped the average photon energy below that needed to form an electron-positron pair. Annihilation then removed all of the positrons as it had the antiprotons and antineutrons earlier, leaving only the small excess of electrons arising from charge conservation, and the *radiation era* began. The particles present were primarily photons and neutrinos.

Within a few more minutes, the temperature dropped sufficiently to enable fusing protons and neutrons to form nuclei that were not immediately photodisintegrated. Deuterium, helium, and a bit of lithium were produced in this *nucleosynthesis period*, but the rapid expansion soon dropped the temperature too low for the fusion to continue and the formation of heavier elements had to await the birth of stars.

A long time later, when the temperature dropped to about 3000 K as the universe grew to about 1/1000 of its present size, kT dropped below typical atomic ionization energies and atoms were formed. By then the expansion had cooled the radiation field so that the total radiation energy was now about equal to the energy represented by the remaining mass. This occurred when the scale factor $R(t)$ reached about 2.8×10^{-4}. As expansion and cooling continued, the energy of the steadily redshifting radiation declined until matter came to dominate the universe, its energy density exceeding that of today's 2.725 K radiation remaining from the Big Bang by about a factor of 1000. Now, once again, energy at negative pressure appears to dominate.

Unanswered Questions and the Limits of Knowledge

The standard model of the evolution of the universe and the current theories of stellar and galactic genesis and evolution have been amazingly successful. Still, some fundamental questions that have arisen during our discussions remain unanswered. Will the universe expand forever or rebound to its initial state and repeat the Big Bang? The answer depends on whether the present average matter density is greater or less than the critical density of about 10^{-26} kg/m^3. The uncertainty in the current measurements would allow either possibility, but the value is tantalizingly close to the critical value. If it does equal the critical value, an intriguing additional question is, Why? We have noted the serious problem of the dark matter and how it might be explained. Answering some of these questions requires that we probe at the current limits of physical knowledge.

STUDENTS-HUB.com Uploaded By: Malak Obaid

For example, near a mass m, general relativity prevents our seeing events occurring at dimensions less than the Schwarzschild radius, the *event horizon*,

$$R_S = \frac{2Gm}{c^2} \qquad \textbf{13-45}$$

On the other hand the uncertainty principle in quantum theory places this limit at the Compton wavelength λ_c:

$$\lambda_c = \frac{h}{mc} \qquad \textbf{13-46}$$

Equating these, $m = \sqrt{hc/2G}$, an expression for m that depends only on universal constants, where $m \approx 10^{-8}$ kg. That relation for m together with Equation 13-46 allows the corresponding definition of a length unit dependent only on universal constants. That length $L = \lambda_c \approx 10^{-35}$ m and the time for light to travel across that length can be similarly expressed as

$$t = \left(\frac{Gh}{c^5}\right)^{1/2} = 1.35 \times 10^{-43}\ \text{s} \qquad \textbf{13-47}$$

In terms of these units the mass density of the universe is such that a mass m is contained within a volume of dimensions $L^3 \sim (10^{-35})^3$ m^3. The definition of the units of mass, length, and time in terms of fundamental constants was originally pointed out by Planck[25] and are the basis for Planck units, the topic of the Exploring section that follows.

Some cosmologists have suggested that, if the universe had evolved even slightly differently than it has, perhaps due to a slightly different value for h or e or some other fundamental constant, life on Earth and maybe Earth itself would be impossible. This can be attributed to the *anthropic principle*, that the universe looks as it does because we are here to see it.

EXPLORING
"Natural" Planck Units

Not long after Max Planck had introduced the constant h in fitting physical theory to the emission spectrum of a blackbody, he pointed out that a system of "natural" units for the fundamental quantities of mass, length, time, and temperature could be constructed from the three fundamental constants $\hbar$, c, and G, where $\hbar$ = Planck's constant/2π, c = speed of light, and G = Newton's gravitation constant.

Planck mass:

$$M_P = (\hbar c/G)^{1/2} = 2.2 \times 10^{-8}\ \text{kg}$$

Planck length:

$$l_P = (\hbar G/c^3)^{1/2} = 1.6 \times 10^{-35}\ \text{m}$$

Planck time:

$$t_P = (\hbar G/c^5)^{1/2} = 5.4 \times 10^{-44}\ \text{s}$$

Planck energy:

$$E_P = M_P c^2 = 2.0 \times 10^{9}\ \text{J} = 1.2 \times 10^{22}\ \text{MeV}$$

Planck temperature:

$$T_P = \frac{E_P}{k_B} = \frac{\hbar^{1/2} c^{5/2}}{G^{1/2} k_B} = 1.4 \times 10^{32}\ \text{K}$$

STUDENTS-HUB.com Uploaded By: Malak Obaid

If length, mass, temperature, and time are measured in Planck units, the result is the "natural" units often used by particle physicists, astrophysicists, and cosmologists: $c = k_B = \hbar = G = 1$.

When first proposed, Planck's suggested units had little basis in fundamental physics, but over time that has changed. As Frank Wilczek[26] has pointed out, Planck's proposal has now become compelling: the constant $\hbar$ is now the fundamental unit of action and c the fundamental unit of velocity. These are the primary units of measurement in the two great theories of modern physics, quantum mechanics and special relativity. The corresponding unit in general relativity is G (actually $1/Gc^4$).

As Wilczek speculates, with the natural units of measure it may soon be possible to understand why, compared to the other forces in nature, the gravitational force is so weak and how we can account for the value of the proton's mass. In addition, he suggests that we have the beginnings of a quantum theory of gravity that agrees accurately with all existing experimental data. Thus, Einstein's goal of the unification of the four natural forces may be just over the horizon.

Summary

TOPIC	RELEVANT EQUATIONS AND REMARKS
1. The Sun	The solar energy received at the top of Earth's atmosphere, called the solar constant, is
	$f = 1.365 \times 10^3 \text{ W/m}^2$ **13-1**
	The rate at which the Sun emits energy is the luminosity $L_\odot$:
	$L_\odot = 3.85 \times 10^{26} \text{ W}$ **13-2**
Surface temperature	Assuming that the Sun radiates as a blackbody, its effective surface temperature T_e can be computed from the Stefan-Boltzmann law:
	$T_e = 5780 \text{ K}$
Source of Sun's energy	The source of the Sun's energy in nuclear fusion, mainly via the proton-proton cycle which starts with the reaction
	${}^1\text{H} + {}^1\text{H} \longrightarrow {}^2\text{H} + e^+ + \nu_e + 0.42 \text{ MeV}$ **13-5**
2. The stars	Stars are classed as either population I or population II, based on their composition. The former have 2 to 3 percent of their mass composed of elements heavier than helium; the latter are nearly devoid of those elements.
The Milky Way	Our galaxy, the Milky Way, consists of about 10^{10} stars. The Sun is about 28,000 $c \cdot$ y from the center of the Galaxy, which is in the direction of the constellation Sagittarius from us. Only about 4 percent of the mass of the Galaxy is accounted for by the visible stars and the gas and dust of the ISM.
3. Evolution of the stars	The Hertzsprung-Russell diagram displays the evolution of stars, relating their luminosities to their effective temperatures. Both quantities are related to the stellar mass.
	$L \propto M^4$ **13-14**
	$T_e = \left(\frac{L}{4\pi R^2 \sigma}\right)^{1/4} \propto M^{1/2}$ **13-17**
	Stars "burning" hydrogen to helium fall on the main sequence of the H-R diagram.

STUDENTS-HUB.com Uploaded By: Malak Obaid

TOPIC	RELEVANT EQUATIONS AND REMARKS
Final states of stars	Following exhaustion of their hydrogen fuel, stars evolve to one of three possible final states, dependent on their mass: white dwarf, neutron star, or black hole. It is in cataclysmic events accompanying evolution to these states that elements heavier than Fe are formed.
4. Galaxies	Edwin Hubble grouped galaxies into four general categories: ellipticals, spirals, barred spirals, and irregulars.
Hubble's law	Hubble showed that the universe was expanding and, using spectral redshifts to determine the velocities of galaxies, that the recession velocities v were proportional to the distance r from us according to $v = H_0 r$ **13-27** where the Hubble constant H_0 is $H_0 = 71 \pm 4$ km/s per Mpc $= 22 \pm 2$ km/s per $10^6\, c \cdot$ y **13-28** The quantity $1/H_0 = 1.3 \times 10^{10}$ y is the Hubble age. It would correspond to the age of the universe under a constant velocity expansion if gravitational pull on receding galaxies were ignored.
5. Gravitation and cosmology	The cosmological principle states that the universe has the same physical properties everywhere and looks the same in every direction from every location. The current theory of cosmology, called the standard model, describes the universe as having begun with the Big Bang 13.7×10^{10} years ago. It has substantial theoretical and observational support.
Inflation	The standard model holds that the very early universe underwent a period of exponentially accelerated growth which explains many features of the current universe. After a long period of slowing, the expansion of the universe is again accelerating.

General References

The following general references are written at a level appropriate for the readers of this book.

Akerlof, C. W., and M. A. Srednicki, *Relativistic Astrophysics and Particle Cosmology*, New York Academy of Sciences, New York, 1993.

Bahcall, J. N., *Neutrino Astrophysics*, Cambridge University Press, New York, 1989.

Bennett, J., M. Donahue, N. Schneider, and M. Voit, *Stars, Galaxies, and Cosmology*, 2d ed., Addison Wesley, San Francisco, 2002.

Carroll, B. W., and D. A. Ostlie, *An Introduction to Modern Astrophysics*, 2d ed., Pearson Addison Wesley, San Francisco, 2007.

Comins, N. F., and W. J. Kaufmann III, *Discovering the Universe*, 6th ed., W. H. Freeman, New York, 2003.

Frauenfelder, H., and E. M. Henley, *Subatomic Physics*, 2d ed., Prentice Hall, Englewood Cliffs, N.J., 1991.

Pasachoff, J. M., *Contemporary Astronomy*, Saunders, Philadelphia, 1977.

Rees, M., *Before the Beginning*, Addison Wesley, San Francisco, 1997.

Ryden, B., *Introduction to Cosmology*, Addison Wesley, San Francisco, 2003.

Shu, F. H., *The Physical Universe*, University Science Books, Mill Valley, Calif., 1982.

Weinberg, S., *The First Three Minutes*, updated ed., Basic Books, New York, 1993.

Notes

1. Hans Albrecht Bethe (1906–2005). He made the proposal concerning stellar energy sources in 1938. One of those who worked on the Manhattan Project during World War II, he received the Nobel Prize for his work on the Sun's energy source in 1967.

2. John Bahcall (1934–2005), American physicist. His definitive theoretical analysis of the solar neutrino spectrum provided the benchmark for experimentalists whose measurements ultimately confirmed neutrino oscillations.

STUDENTS-HUB.com Uploaded By: Malak Obaid

3. The reaction by which Davis's detector detected neutrinos is ${}^{37}_{17}\mathrm{Cl} + \nu_e \rightarrow {}^{37}_{18}\mathrm{Ar} + e^-$. Seventy-seven percent of the neutrinos producing this reaction were from the ${}^8\mathrm{B}$ decay, step 6 of the *p-p* cycle shown in Table 13-1.
4. The term *galaxy* is derived from the Greek word for milk.
5. Apart from the Sun, Sirius is the brightest star in the sky.
6. Annie Jump Cannon (1863–1941). An astronomer at the Harvard Observatory, her work on stellar classification systems forms the basis of the *Henry Draper Catalogue* which contains the spectral classifications of 225,300 stars.
7. Hipparchus (circa 190 B.C.–circa 120 B.C.). The greatest of the Greek astronomers, he created the stellar magnitude system of classifying stars by brightness. He measured the size and distance to the Sun and Moon and made the first accurate star map showing the positions of about 1000 of the brightest stars.
8. Astronomers customarily capitalize the word *Galaxy* when it refers to the Milky Way.
9. Harlow Shapley (1885–1972). A long-time director of the Harvard Observatory, he was an early and vocal supporter of civil liberties and peace movements in the United States.
10. The term "right ascension" for the celestial longitude apparently comes from the appearance of the stars as rising vertically, i.e., at a right angle to the line of sight to the horizon each night.
11. *Equinox* means day and night are equal; *solstice* means "standing Sun."
12. Edouard A. Roche (1820–1883). A French astronomer, he also showed that a small body orbiting a large body would be broken up by tidal forces if it comes within 2.5 times the radius of the larger body. The distance is referred to as Roche's limit. It corresponds approximately to the outer limit of planetary ring systems in the solar system.
13. Subrahmanyan Chandrasekhar (1910–1995). He received his Ph.D. under P. A. M. Dirac and spent most of his career at the University of Chicago. He shared the 1983 Nobel Prize in Physics for his work on the evolution of stars. The Chandra X-Ray Observatory is named for him.
14. The possibility of black holes was first suggested by Rev. John Mitchell, an English amateur astronomer, in 1783. He observed that a star with the same density, but 500 times the radius of the Sun would have an escape velocity greater than the speed of light. He speculated that light could not leave such a star. The name black hole was coined by physicist John Wheeler.
15. Gamma-ray bursts are named according to the first date of observation: GRB yymmdd
16. Edwin P. Hubble (1889–1953). Trained as a lawyer, he was influenced to take up astronomy partly by R. A. Millikan. In recognition of his many contributions, he was accorded the honor of being the first user of the 5-m Hale telescope on Mount Palomar.
17. Cepheid variables are rare stars for which a relation exists connecting the period of intensity variation to the brightness and, hence, to the distance from the Sun. They were one of the earliest means of measuring astronomical distances. Polaris, the current Pole Star, is a Cepheid variable.
18. Light beyond the blue of the visible region would be shifted into the visible. Indeed, the visible region might even get brighter!
19. This discussion is based on the development in the early part of Chapter 29 of Carroll and Ostlie (see General References).
20. This age of the universe results from measurements made by the Wilkinson Microwave Anisotropy Project.
21. The term *Big Bang* was coined by the eminent astronomer Fred Hoyle, a steadfast proponent of the steady-state universe, intending the term as derision of the expanding universe cosmology.
22. Sir Martin Ryle (1918–1984). His invention of long-baseline radiointerferometry resulted in his sharing the Nobel Prize in 1974.
23. Arno Allan Penzias (b. 1933), German-American physicist, and Robert Woodrow Wilson (b. 1936), American radioastronomer. Their discovery of the cosmic microwave background radiation, first predicted by George Gamow 20 years earlier, earned each of them a share of the 1978 Nobel Prize in Physics.
24. Frank C. Mather (b. 1946) and George F. Smoot (b. 1945), American physicists, shared the 2006 Nobel Prize in Physics for this work which provides very strong support for the Big Bang theory.
25. M. Planck, Sitzungsber. "Dtsh. Akad. Wiss," Berlin, *Math-Phys. Tech. Kl.*, 440 (1899).
26. Frank Wilczek, American physicist, in the series "Scaling Mount Planck" in *Physics Today*, June 2001, November 2001, and August 2002. He shared the Nobel Prize in Physics in 2004 for his contributions to quark theory.

Problems

Level I

Section 13-1 The Sun

13-1. Measurement of the Doppler shift of spectral lines in light from the east and west limbs of the Sun at the solar equator reveal that the tangential velocities of the limbs differ by 4 km/s. Use this result to compute the approximate period of the Sun's rotation. ($R_\odot = 6.96 \times 10^5$ km)
13-2. The gravitational potential energy U of a self-gravitating spherical body of mass M and radius R is a function of the details of the mass distribution. For the Sun $U_\odot = -2GM_\odot^2/R_\odot$. What would be the approximate lifetime of the Sun, radiating at its present rate, if the source of its emitted energy were entirely derived from gravitational contraction? ($M_\odot = 1.99 \times 10^{30}$ kg)

STUDENTS-HUB.com Uploaded By: Malak Obaid

Section 13-2 The Stars

13-3. Lithium, beryllium, and boron ($Z = 3$, 4, and 5, respectively) have very low abundances in the cosmos compared to many heavier elements. (See Figure 13-32.) Considering the fusion of He to C, explain these low abundances.

13-4. The Sun is moving with speed 2.5×10^5 m/s in a circular orbit about the center of the Galaxy. How long (in Earth years) does it take to complete one orbit? How many orbits has it completed since it was formed?

13-5. The reason that massive neutrinos were considered as a candidate for solving the missing mass problem is that, at the conclusion of the lepton era, the universe contained about equal numbers of photons and neutrinos. They are still here, for the most part. The former can be observed and their density is measured to be about 500 photons/cm^3; thus, there must be about that number density of neutrinos in the universe, too. If neutrinos have a nonzero mass and if the cosmological expansion has reduced their average speed so that their energy is now primarily mass, what would be the individual neutrino mass (in eV/c^2) necessary to account for the missing mass of the universe? Recall that the observed mass of the stars and galaxies (including the dust and gas) accounts for only about 4 percent of that needed to close the universe.

13-6. Using data from Table 13-3, construct a graph that demonstrates the validity of Equation 13-17.

13-7. Recalling that the light-year $c \cdot$ y is the distance light travels in one year, compute in meters the distance equivalent to 1 light-second, 1 light-minute, 1 light-hour, and 1 light-day.

Section 13-3 The Evolution of Stars

13-8. A unit of length often used by astronomers to measure distances in "nearby" space is the parsec (pc), defined as the distance at which a star subtends a parallax angle of one arc second due to Earth's orbit around the Sun. (See Equation 13-11 and Example 13-4.) The practical limit of such measurements is 0.01 arc second. (*a*) How many light-years is 1 pc? (*b*) If the density of stars in the Sun's region of the Milky Way is 0.08 stars/pc^3 , how many stars could, in principle, have their distances from us measured by the trigonometric parallax method?

13-9. Astronomers often use the *apparent magnitude m* as a means of comparing the visual brightness of stars and relating the comparison to the luminosity and distance to "standard" stars, such as the Sun. (See Equation 13-9.) The difference in the apparent magnitudes of two stars m_1 and m_2 is defined as $m_2 - m_1 = 2.5 \log (f_1/f_2)$, a relation based on the logarithmic response of the human eye to the brightness of objects. Pollux, one of the "twins" in the constellation Gemini, has apparent magnitude 1.16 and is 12 pc away. Betelgeuse, the star at Orion's right shoulder, has apparent magnitude 0.41. How far away is Betelgeuse, if they have the same luminosity?

13-10. Using the H-R diagram (Figure 13-17), determine the effective temperature and the luminosity of a star whose mass is (*a*) $0.3M_\odot$ and (*b*) $3M_\odot$. *(c)* Compute the radius of each star. (d) Determine their expected lifetimes, relative to that of the Sun.

13-11. Two stars in a binary system are located 100 $c \cdot$ y from Earth and separated from each other by 10^8 km. What is the angular separation of the stars in arc seconds? In degrees?

Section 13-4 Cataclysmic Events

13-12. Compute the energy required (in MeV) to produce each of the photodisintegration reactions in Equations 13-19 and 13-20.

13-13. The gas shell of a planetary nebula shown at the right in Figure 13-18 is expanding at 24 km/s. Its diameter is 1.5 $c \cdot$ y. (*a*) How old is the gas shell? (*b*) If the central star of the planetary nebula is 12 times as luminous as the Sun and 15 times hotter, what is the radius of the central star in units of $R_\odot$?

Section 13-5 Final States of Stars

13-14. Calculate the Schwarzschild radius of a star whose mass is equal to that of (*a*) the Sun, (*b*) Jupiter, (*c*) Earth. (The mass of Jupiter is approximately 318 times that of Earth.)

13-15. Consider a neutron star whose mass equals $2M_\odot$. (*a*) Compute the star's radius. (*b*) If the neutron star is rotating at 0.5 rev/s and assuming its density to be uniform, what is its rotational kinetic energy? (*c*) If its rotation slows by 1 part in 10^8 per day and the lost kinetic energy is all radiated, what is the star's luminosity?

STUDENTS-HUB.com Uploaded By: Malak Obaid

13-16. If the 90 percent of the Milky Way's mass which is "missing" resides entirely in a large black hole at the center of the Galaxy, what would be the black hole's (*a*) mass and (*b*) radius?

Section 13-6 Galaxies

13-17. Redshift measurements for a particular galaxy indicate that it has a recession velocity of 72,000 km/s. (*a*) Compute the distance to the galaxy. (*b*) The value of Hubble's constant depends critically on calibration distance measurements which are difficult to make. If the calibration distance measurements are in error by 10 percent, by how much is the age calculated from Equation 13-28 in error?

13-18. The bright core of a certain Seyfert galaxy had a luminosity of $10^{10}L_{\odot}$. The luminosity increased by 100 percent in a period of 18 months. Show that this means that the energy source of the core is less than 9.45×10^4 AU in diameter. How does this compare to the diameter of the Milky Way?

Section 13-7 Cosmology and Gravitation

13-19. Evaluate Equation 13-33 for the critical density of the universe.

Section 13-8 Cosmology and the Evolution of the Universe

13-20. Cosmological theory suggests that the average separation of galaxies, i.e., the scale of the universe, is inversely proportional to the absolute temperature. If that is true, relative to the present size, how large was the universe compared to the scale today (*a*) 2000 years ago, (*b*) 10^6 years ago, (*c*) $t = 10$ s after the Big Bang, (*d*) when $t = 1$ s and, (*e*) when $t = 10^{-6}$ s?

13-21. Determine the value of the mass density of the universe for $t =$ Planck time. How does this compare to the density of the proton? Of osmium?

13-22. At what wavelength is the blackbody radiation distribution of the cosmic microwave background at a maximum?

13-23. How long after the Big Bang did it take the universe to cool to the threshold temperature for the formation of muons? What would be the mass of a particle-antiparticle pair that could be formed by the average energy of the current 2.725 K background radiation?

13-24. Show that the present mass density of the universe $\rho_0 = R(t)\rho(t)$.

Level II

13-25. If Hubble's Law is true for an observer in the Milky Way (i.e., us), prove that it must also be true for observers in other galaxies. (Hint: Use the vector property of the velocity.)

13-26. Show that the mass density of the universe at redshift z is given by $\rho(z) = \rho(1 + z)^3$.

13-27. When the Sun was formed about 75 percent of its mass was hydrogen, of which only about 13 percent ever becomes available for fusion. (The rest is in regions of the Sun where the temperature is too low for fusion reactions to occur.) $M_{\odot} = 2 \times 10^{30}$ kg and the Sun fuses about 6×10^{11} kg/s. (*a*) Compute the total mass of hydrogen available for fusion during the Sun's lifetime. (*b*) How long (in years) will the Sun's initial supply of hydrogen last? (*c*) Since the solar system is currently about 4.6×10^9 years old, when should we begin to worry about the Sun running out of hydrogen for fusion?

13-28. Supernova SN1987A was first visible at Earth in 1987. (*a*) How many years B.P. (before present) did the explosion occur? (*b*) If protons with 100 GeV of kinetic energy were produced in the event, when should they arrive at Earth?

13-29. Assume that the Sun when it first formed was composed of 70 percent hydrogen. How many hydrogen nuclei were there in the Sun at that time? How much energy would ultimately be released if all of the hydrogen nuclei fused into helium? Astrophysicists have predicted that the Sun can radiate energy at its current rate until about 23 percent of the hydrogen has been "burned." What total lifetime for the Sun does that prediction imply? Compare these results with the corresponding ones from Problem 13-27.

13-30. Kepler's third law states that the square of a planet's orbital speed is proportional to the cube of its average orbital radius. Use Kepler's third law to answer each of the following questions. (*a*) The Moon's orbital radius is 3.84×10^5 km and it orbits Earth once every 27.3 d. Neglecting the Moon's mass, compute the mass of Earth. (*b*) Io (one of Jupiter's moons) orbits Jupiter once every 42.5 h in a near-circular orbit of average radius 4.22×10^5 km. Neglecting

STUDENTS-HUB.com Uploaded By: Malak Obaid

Io's mass, compute the mass of Jupiter. (*c*) Compute the orbital period of the International Space Station as it orbits 300 km above Earth's surface. (*d*) Charon, a moon of Pluto, orbits that planet once every 6.4 d at an average distance of 1.97×10^4 km. Compute the total mass of Pluto and Charon. What fraction of Earth's mass is this? (*e*) Using the data for the star S2, compute the volume (upper limit) that confines the black hole at the center of the Milky Way. Compare the result with the volume of the Sun.

13-31. Consider an eclipsing binary whose orbital plane is parallel to our line of sight. Doppler measurements of the radial velocity of each component of the binary are shown in Figure 13-35. Assume that the mass $m_1 > m_2$ and that the orbits of each component about the center of mass are circular. (*a*) What is the period T and the angular frequency ω of the binary? (*b*) Show that in this case $(m_1 + m_2) = (\omega^2 r^3)/G$, where r = separation of the binary. (*c*) Compute the values of m_1, m_2, and r from the data in the v versus t graph.

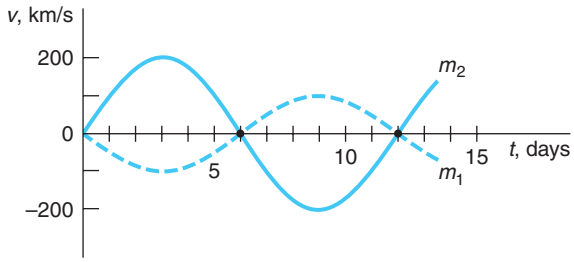

Figure 13-35

13-32. Prove that the total energy of Earth's orbital motion $E = (mv^2/2) + (-GM_\odot\, m/r)$ is equal to one-half of its gravitational potential energy $(-GM_\odot\, m/r)$, where r is Earth's orbit radius.

13-33. Given the currently accepted value of the Hubble constant and the fact that the average matter density of the universe is one H atom/m^3, what creation rate of new H atoms would be necessary in a steady-state model to maintain the present mass density, even though the universe is expanding? (Give your answer in H atoms/m^3 per 10^6 years.) Would you expect such a spontaneous creation rate to be readily observable?

Level III

13-34. The ability of a planet to retain particular gases in an atmosphere depends on the temperature that its atmosphere has (or would have) and the escape velocity for the planet. In general, if the average speed of a particular gas molecule exceeds 1/6 of the escape velocity, that gas will disappear from the atmosphere in about 10^8 years. (*a*) Graph the average speed of H_2O, CO_2, O_2, CH_4, H_2, and He from 50 K to 1000 K. On the same graph show the points representing 1/6 of the escape velocity versus average temperature of the atmosphere for the planets in Table 13-5 below. (*b*) Show that the escape speed v from a planet is given by

$$\frac{v}{v_{\text{Earth}}} = \sqrt{\frac{(M/M_{\text{Earth}})}{(R/R_{\text{Earth}})}}$$

Table 13-5 Atmospheric temperatures

Average T_{atmo}(K)	Planet	M/M_{Earth}	R/R_{Earth}
300	Earth	1.00	1.00
390	Venus	0.81	0.95
600	Mercury	0.06	0.38
150	Jupiter	318.00	11.00
60	Neptune	17.00	3.90
290	Mars	0.11	0.53

STUDENTS-HUB.com Uploaded By: Malak Obaid

(*c*) Which of the six gases plotted probably would and would not currently be found in the atmospheres of the solar system bodies in the table? Explain *each* answer briefly.

13-35. Using the parallax technique, compute the distance to (*a*) Alpha Centauri (parallax angle 0.742 arc seconds) and (*b*) Procyon (parallax angle 0.0286 arc second. Express each answer in both light-years and parsecs.

13-36. As the Sun evolves into a red giant star, suppose that its luminosity increases by a factor of 10^2. Show that Earth's oceans will evaporate, but that the water vapor will not escape from the atmosphere.

13-37. The approximate mass of dust in the Galaxy can be computed from the observed extinction of starlight. Assuming the mean radius of dust grains to be R with a uniform number density n grains/cm^3, (*a*) show that the mean free path d_0 of a photon in interstellar dust is given by $d_0 = 1/(n\pi R^2)$. (*b*) Starlight traveling toward an Earth observer a distance d from the star has intensity

$$I = I_0 e^{-d/d_0}$$

In the vicinity of the Sun, a measurement of I yields $d_0 = 3000\ c \cdot \text{y}$. If $R = 10^{-5}$ cm, calculate n. (*c*) The average mass density of solid material in the Galaxy is 2 g/cm^3 and in the disk the density of stars is about $1M_\odot/300\ (c \cdot y)^3$. Compute the ratio of the mass density of dust to the mass density of stars, assuming 1 $M_\odot$ in 300 $(c \cdot \text{y})^3$.

13-38. The supernova SN1987A certainly produced some heavy elements. Compared to the energy released in fusing 56 ^{1}H atoms into one ^{56}Fe atom starting from the proton-proton cycle, how much energy would be required to fuse two ^{56}Fe atoms into one ^{112}Cd atom?

13-39. Current theory suggests that black holes evaporate by the emission of Hawking radiation in a time t that depends on the mass M of the black hole according to the following relation:

$$t = (1.024 \times 10^4 \pi^2\ \text{m}^3/\text{s}^2) G^2 M^2 / hc^4$$

(*a*) Explain without calculating anything why the formula implies that high-mass black holes have longer lifetimes than low-mass ones and why the rate of evaporation accelerates as the black hole loses mass. (*b*) Compute the lifetime of a black hole whose mass equals $1M_\odot$. Compare this time with the current age of the universe. (*c*) According to some theories, the largest black hole that could conceivably form would have a mass $10^{12}\ M_\odot$, of the order of the mass of an entire galaxy. What would be the lifetime of a black hole that large?

STUDENTS-HUB.com Uploaded By: Malak Obaid

APPENDIX A

Table of Atomic Masses

Z	Element	Symbol	Chemical atomic weight	Mass number (* indicates radioactive)	Atomic mass	Percent abundance	Half-life and decay mode (if unstable)
0	(Neutron)	*n*		1*	1.008665		10.4 m β^-
1	Hydrogen	H	1.00798	1	1.007825	99.985	
	Deuterium	D		2	2.014102	0.015	
	Tritium	T		3*	3.016049		12.33 y β^-
2	Helium	He	4.00260	3	3.016029	0.00014	
				4	4.002602	99.99986	
				6*	6.018886		0.81 s β^-
				8*	8.033922		0.12 s β^-
3	Lithium	Li	6.941	6	6.015121	7.5	
				7	7.016003	92.5	
				8*	8.022486		0.84 s β^-
				9*	9.026789		0.18 s β^-
				11*	11.043897		8.7 ms β^-
4	Beryllium	Be	9.0122	7*	7.016928		53.3 d ec
				9	9.012174	100	
				10*	10.013534		1.5×10^6 y β^-
				11*	11.021657		13.8 s β^-
				12*	12.026921		23.6 ms β^-
				14*	14.042866		4.3 ms β^-
5	Boron	B	10.811	8*	8.024605		0.77 s β^+
				10	10.012936	19.9	
				11	11.009305	80.1	
				12*	12.014352		0.0202 s β^-
				13*	13.017780		17.4 ms β^-
				14*	14.025404		13.8 ms β^-
				15*	15.031100		10.3 ms β^-
6	Carbon	C	12.011	9*	9.031030		0.13 s β^+
				10*	10.016854		19.3 s β^+
				11*	11.011433		20.4 m β^+
				12	12.000000	98.90	
				13	13.003355	1.10	
				14*	14.003242		5730 y β^-
				15*	15.010599		2.45 s β^-
				16*	16.014701		0.75 s β^-
				17*	17.022582		0.20 s β^-

(*Continued*)

STUDENTS-HUB.com
Uploaded By: Malak Obaid

Z	Element	Symbol	Chemical atomic weight	Mass number (* indicates radioactive)	Atomic mass	Percent abundance	Half-life and decay mode (if unstable)
7	Nitrogen	N	14.0067	12*	12.018613		0.0110 s β^+
				13*	13.005738		9.96 m β^+
				14	14.003074	99.63	
				15	15.000108	0.37	
				16*	16.006100		7.13 s β^-
				17*	17.008450		4.17 s β^-
				18*	18.014082		0.62 s β^-
				19*	19.017038		0.24 s β^-
8	Oxygen	O	15.9994	13*	13.024813		8.6 ms β^+
				14*	14.008595		70.6 s β^+
				15*	15.003065		122 s β^+
				16	15.994915	99.71	
				17	16.999132	0.039	
				18	17.999160	0.20	
				19*	19.003577		26.9 s β^-
				20*	20.004076		13.6 s β^-
				21*	21.008595		3.4 s β^-
9	Fluorine	F	18.99840	17*	17.002094		64.5 s β^+
				18*	18.000937		109.8 m β^+
				19	18.998404	100	
				20*	19.999982		11.0 s β^-
				21*	20.999950		4.2 s β^-
				22*	22.003036		4.2 s β^-
				23*	23.003564		2.2 s β^-
10	Neon	Ne	20.180	18*	18.005710		1.67 s β^+
				19*	19.001880		17.2 s β^+
				20	19.992435	90.48	
				21	20.993841	0.27	
				22	21.991383	9.25	
				23*	22.994465		37.2 s β^-
				24*	23.993999		3.38 m β^-
				25*	24.997789		0.60 s β^-
11	Sodium	Na	22.98977	21*	20.997650		22.5 s β^+
				22*	21.994434		2.61 y β^+
				23	22.989767	100	
				24*	23.990961		14.96 h β^-
				25*	24.989951		59.1 s β^-
				26*	25.992588		1.07 s β^-
12	Magnesium	Mg	24.3051	23*	22.994124		11.3 s β^+
				24	23.985042	78.99	
				25	24.985838	10.00	
				26	25.982594	11.01	
				27*	26.984341		9.46 m β^-
				28*	27.983876		20.9 h β^-
				29*	28.375346		1.30 s β^-

STUDENTS-HUB.com Uploaded By: Malak Obaid

Z	Element	Symbol	Chemical atomic weight	Mass number (* indicates radioactive)	Atomic mass	Percent abundance	Half-life and decay mode (if unstable)
13	Aluminum	Al	26.98154	25*	24.990429		7.18 s β^+
				26*	25.986892		7.4×10^5 y β^+
				27	26.981538	100	
				28*	27.981910		2.24 m β^-
				29*	28.980445		6.56 m β^-
				30*	29.982965		3.60 s β^-
14	Silicon	Si	28.086	27*	26.986704		4.16 s β^+
				28	27.976927	92.23	
				29	28.976495	4.67	
				30	28.973770	3.10	
				31*	30.975362		2.62 h β^-
				32*	31.974148		172 y β^-
				33*	32.977928		6.13 s β^-
15	Phosphorus	P	30.97376	30*	29.978307		2.50 m β^+
				31	30.973762	100	
				32*	31.973762		14.26 d β^-
				33*	32.971725		25.3 d β^-
				34*	33.973636		12.43 s β^-
16	Sulfur	S	32.066	31*	30.979554		2.57 s β^+
				32	31.972071	95.02	
				33	32.971459	0.75	
				34	33.967867	4.21	
				35*	34.969033		87.5 d β^-
				36	35.967081	0.02	
17	Chlorine	Cl	35.453	34*	33.973763		32.2 m β^+
				35	34.968853	75.77	
				36*	35.968307		3.0×10^5 y β^-
				37	36.965903	24.23	
				38*	37.968010		37.3 m β^-
18	Argon	Ar	39.948	36	35.967547	0.337	
				37*	36.966776		35.04 d ec
				38	37.962732	0.063	
				39*	38.964314		269 y β^-
				40	39.962384	99.600	
				42*	41.963049		33 y β^-
19	Potassium	K	39.0983	39	38.963708	93.2581	
				40*	39.964000	0.0117	1.28×10^9 y β^+, ec, β^-
				41	40.961827	6.7302	
				42*	41.962404		12.4 h β^-
				43*	42.960716		22.3 h β^-

(*Continued*)

STUDENTS-HUB.com Uploaded By: Malak Obaid

Z	Element	Symbol	Chemical atomic weight	Mass number (* indicates radioactive)	Atomic mass	Percent abundance	Half-life and decay mode (if unstable)
20	Calcium	Ca	40.078	40	39.962591	96.941	
				41*	40.962279		1.0×10^5 y ec
				42	41.958618	0.647	
				43	42.958767	0.135	
				44	43.955481	2.086	
				46	45.953687	0.004	
				48	47.952534	0.187	
21	Scandium	Sc	44.9559	41*	40.969250		0.596 s β^+
				43*	42.961151		3.89 h β^+
				45	44.955911	100	
				46*	45.955170		83.8 d β^-
22	Titanium	Ti	47.88	44*	43.959691		49 y ec
				46	45.952630	8.0	
				47	46.951765	7.3	
				48	47.947947	73.8	
				49	48.947871	5.5	
				50	49.944792	5.4	
23	Vanadium	V	50.9415	48*	47.952255		15.97 d β^+
				50*	49.947161	0.25	1.5×10^{17} y β^+
				51	50.943962	99.75	
24	Chromium	Cr	51.996	48*	47.954033		21.6 h ec
				50	49.946047	4.345	
				52	51.940511	83.79	
				53	52.940652	9.50	
				54	53.938883	2.365	
25	Manganese	Mn	54.93805	53*	52.941292		3.74×10^6 y ec
				54*	53.940361		312.1 d ec
				55	54.938048	100	
				56*	55.938908		2.58 h β^-
26	Iron	Fe	55.847	54	53.939613	5.9	
				55*	54.938297		2.7 y ec
				56	55.934940	91.72	
				57	56.935396	2.1	
				58	57.933278	0.28	
				60*	59.934078		1.5×10^6 y β^-
27	Cobalt	Co	58.93320	57*	56.936294		271.8 d ec
				58*	57.935755		70.9 h ec, β^+
				59	58.933198	100	
				60*	59.933820		5.27 y β^-
				61*	60.932478		1.65 h β^-

STUDENTS-HUB.com Uploaded By: Malak Obaid

Z	Element	Symbol	Chemical atomic weight	Mass number (* indicates radioactive)	Atomic mass	Percent abundance	Half-life and decay mode (if unstable)
28	Nickel	Ni	58.693	58	57.935346	68.077	
				59*	58.934350		7.5×10^4 y ec, β^+
				60	59.930789	26.223	
				61	60.931058	1.140	
				62	61.928346	3.634	
				63*	62.929670		100 y β^-
				64	63.927967	0.926	
29	Copper	Cu	63.546	63	62.929599	69.17	
				64*	63.929765		12.7 h ec
				65	64.927791	30.83	
				66*	65.928871		5.1 m β^-
30	Zinc	Zn	65.39	64	63.929144	48.6	
				66	65.926035	27.9	
				67	66.927129	4.1	
				68	67.924845	18.8	
				70	69.925323	0.6	
31	Gallium	Ga	69.723	69	68.925580	60.108	
				70*	69.926027		21.1 m β^-
				71	70.924703	39.892	
				72*	71.926367		14.1 h β^-
32	Germanium	Ge	72.61	69*	68.927969		39.1 h ec, β^+
				70	69.924250	21.23	
				72	71.922079	27.66	
				73	72.923462	7.73	
				74	73.921177	35.94	
				76	75.921402	7.44	
				77*	76.923547		11.3 h β^-
33	Arsenic	As	74.9216	73*	72.923827		80.3 d ec
				74*	73.923928		17.8 d ec, β^+
				75	74.921594	100	
				76*	75.922393		1.1 d β^-
				77*	76.920645		38.8 h β^-
34	Selenium	Se	78.96	74	73.922474	0.89	
				76	75.919212	9.36	
				77	76.919913	7.63	
				78	77.917307	23.78	
				79*	78.918497		$\leq 6.5 \times 10^4$ y β^-
				80	79.916519	49.61	
				82*	81.916697	8.73	1.4×10^{20} y $2\beta^-$

(*Continued*)

STUDENTS-HUB.com Uploaded By: Malak Obaid

Z	Element	Symbol	Chemical atomic weight	Mass number (* indicates radioactive)	Atomic mass	Percent abundance	Half-life and decay mode (if unstable)
35	Bromine	Br	79.904	79	78.918336	50.69	
				80*	79.918528		17.7 m β^+
				81	80.916287	49.31	
				82*	81.916802		35.3 h β^-
36	Krypton	Kr	83.80	78	77.920400	0.35	
				80	79.916377	2.25	
				81*	80.916589		2.11×10^5 y ec
				82	81.913481	11.6	
				83	82.914136	11.5	
				84	83.911508	57.0	
				85*	84.912531		10.76 y β^-
				86	85.910615	17.3	
37	Rubidium	Rb	85.468	85	84.911793	72.17	
				86*	85.911171		18.6 d β^-
				87*	86.909186	27.83	4.75×10^{10} y β^-
				88*	87.911325		17.8 m β^-
38	Strontium	Sr	87.62	84	83.913428	0.56	
				86	85.909266	9.86	
				87	86.908883	7.00	
				88	87.905618	82.58	
				90*	89.907737		29.1 y β^-
39	Yttrium	Y	88.9058	88*	87.909507		106.6 d ec, β^+
				89	88.905847	100	
				90*	89.914811		2.67 d β^-
40	Zirconium	Zr	91.224	90	89.904702	51.45	
				91	90.905643	11.22	
				92	91.905038	17.15	
				93*	92.906473		1.5×10^6 y β^-
				94	93.906314	17.38	
				96	95.908274	2.80	
41	Niobium	Nb	92.9064	91*	90.906988		6.8×10^2 y ec
				92*	91.907191		3.5×10^7 y ec
				93	92.906376	100	
				94*	93.907280		2×10^4 y β^-
42	Molybdenum	Mo	95.94	92	91.906807	14.84	
				93*	92.906811		3.5×10^3 y ec
				94	93.905085	9.25	
				95	94.905841	15.92	
				96	95.904678	16.68	
				97	96.906020	9.55	
				98	97.905407	24.13	
				100	99.907476	9.63	

STUDENTS-HUB.com Uploaded By: Malak Obaid

Z	Element	Symbol	Chemical atomic weight	Mass number (* indicates radioactive)	Atomic mass	Percent abundance	Half-life and decay mode (if unstable)
43	Technetium	Tc		97*	96.906363		2.6×10^6 y ec
				98*	97.907215		4.2×10^6 y β^-
				99*	98.906254		2.1×10^5 y β^-
44	Ruthenium	Ru	101.07	96	95.907597	5.54	
				98	97.905287	1.86	
				99	98.905939	12.7	
				100	99.904219	12.6	
				101	100.905558	17.1	
				102	101.904348	31.6	
				104	103.905428	18.6	
45	Rhodium	Rh	102.9055	102*	101.906794		207 d ec
				103	102.905502	100	
				104*	103.906654		42 s β^-
46	Palladium	Pd	106.42	102	101.905616	1.02	
				104	103.904033	11.14	
				105	104.905082	22.33	
				106	105.903481	27.33	
				107*	106.905126		6.5×10^6 y β^-
				108	107.903893	26.46	
				110	109.905158	11.72	
47	Silver	Ag	107.868	107	106.905091	51.84	
				108*	107.905953		2.39 m ec, β^+, β^-
				109	108.904754	48.16	
				110*	109.906110		24.6 s β^-
48	Cadmium	Cd	112.41	106	105.906457	1.25	
				108	107.904183	0.89	
				109*	108.904984		462 d ec
				110	109.903004	12.49	
				111	110.904182	12.80	
				112	111.902760	24.13	
				113*	112.904401	12.22	9.3×10^{15} y β^-
				114	113.903359	28.73	
				116	115.904755	7.49	
49	Indium	In	114.82	113	112.904060	4.3	
				114*	113.904916		1.2 m β^-
				115*	114.903876	95.7	4.4×10^{14} y β^-
				116*	115.905258		54.4 m β^-

(*Continued*)

STUDENTS-HUB.com Uploaded By: Malak Obaid

Z	Element	Symbol	Chemical atomic weight	Mass number (* indicates radioactive)	Atomic mass	Percent abundance	Half-life and decay mode (if unstable)
50	Tin	Sn	118.71	112	111.904822	0.97	
				114	113.902780	0.65	
				115	114.903345	0.36	
				116	115.901743	14.53	
				117	116.902953	7.68	
				118	117.901605	24.22	
				119	118.903308	8.58	
				120	119.902197	32.59	
				121*	120.904237		55 y β^-
				122	121.903439	4.63	
				124	123.905274	5.79	
51	Antimony	Sb	121.76	121	120.903820	57.36	
				123	122.904215	42.64	
				125*	124.905251		2.7 y β^-
52	Tellurium	Te	127.60	120	119.904040	0.095	
				122	121.903052	2.59	
				123*	122.904271	0.905	1.3×10^{13} y ec
				124	123.902817	4.79	
				125	124.904429	7.12	
				126	125.903309	18.93	
				128*	127.904463	31.70	$>8 \times 10^{24}$ y $2\beta^-$
				130*	129.906228	33.87	1.2×10^{21} y $2\beta^-$
53	Iodine	I	126.9045	126*	125.905619		13 d ec, β^+, β^-
				127	126.904474	100	
				128*	127.905812		25 m β^-, ec, β^+
				129*	128.904984		1.6×10^7 y β^-
54	Xenon	Xe	131.29	124	123.905894	0.10	
				126	125.904268	0.09	
				128	127.903531	1.91	
				129	128.904779	26.4	
				130	129.903509	4.1	
				131	130.905069	21.2	
				132	131.904141	26.9	
				134	133.905394	10.4	
				136	135.907215	8.9	
55	Cesium	Cs	132.9054	133	132.905436	100	
				134*	133.906703		2.1 y β^-
				135*	134.905891		2×10^6 y β^-
				137*	136.907078		30 y β^-

STUDENTS-HUB.com Uploaded By: Malak Obaid

Z	Element	Symbol	Chemical atomic weight	Mass number (* indicates radioactive)	Atomic mass	Percent abundance	Half-life and decay mode (if unstable)
56	Barium	Ba	137.33	130	129.906289	0.106	
				132	131.905048	0.101	
				133*	132.905990		10.5 y ec
				134	133.904492	2.42	
				135	134.905671	6.593	
				136	135.904559	7.85	
				137	136.905816	11.23	
				138	137.905236	71.70	
57	Lanthanum	La	138.905	137*	136.906462		6×10^4 y ec
				138*	137.907105	0.0902	1.05×10^{11} y ec, β^+
				139	138.906346	99.9098	
58	Cerium	Ce	140.12	136	135.907139	0.19	
				138	137.905986	0.25	
				140	139.905434	88.43	
				142	141.909241	11.13	
59	Praseodymium	Pr	140.9076	140*	139.909071		3.39 m ec, β^+
				141	140.907647	100	
				142*	141.910040		25.0 m β^-
60	Neodymium	Nd	144.24	142	141.907718	27.13	
				143	142.909809	12.18	
				144*	143.910082	23.80	2.3×10^{15} y α
				145	144.912568	8.30	
				146	145.913113	17.19	
				148	147.916888	5.76	
				150	149.920887	5.64	
61	Promethium	Pm		143*	142.910928		265 d ec
				145*	144.912745		17.7 y ec
				146*	145.914698		5.5 y ec
				147*	146.915134		2.623 y β^-
62	Samarium	Sm	150.36	144	143.911996	3.1	
				146*	145.913043		1.0×10^8 y α
				147*	146.914894	15.0	1.06×10^{11} y α
				148*	147.914819	11.3	7×10^{15} y α
				149	148.917180	13.8	
				150	149.917273	7.4	
				151*	150.919928		90 y β^-
				152	151.919728	26.7	
				154	153.922206	22.7	

(*Continued*)

STUDENTS-HUB.com Uploaded By: Malak Obaid

Z	Element	Symbol	Chemical atomic weight	Mass number (* indicates radioactive)	Atomic mass	Percent abundance	Half-life and decay mode (if unstable)
63	Europium	Eu	151.96	151	150.919846	47.8	
				152*	151.921740		13.5 y ec, β^+
				153	152.921226	52.2	
				154*	153.922975		8.59 y β^-
				155*	154.922888		4.7 y β^-
64	Gadolinium	Gd	157.25	148*	147.918112		75 y α
				150*	149.918657		1.8×10^6 y α
				152*	151.919787	0.20	1.1×10^{14} y α
				154	153.920862	2.18	
				155	154.922618	14.80	
				156	155.922119	20.47	
				157	156.923957	15.65	
				158	157.924099	24.84	
				160	159.927050	21.86	
65	Terbium	Tb	158.9253	158*	157.925411		180 y ec, β^+, β^-
				159	158.925345	100	
				160*	159.927551		72.3 d β^-
66	Dysprosium	Dy	162.50	156	155.924277	0.06	
				158	157.924403	0.10	
				160	159.925193	2.34	
				161	160.926930	18.9	
				162	161.926796	25.5	
				163	162.928729	24.9	
				164	163.929172	28.2	
67	Holmium	Ho	164.9303	165	164.930316	100	
				166*	165.932282		1.2×10^3 y β^-
68	Erbium	Er	167.26	162	161.928775	0.14	
				164	163.929198	1.61	
				166	165.930292	33.6	
				167	166.932047	22.95	
				168	167.932369	27.8	
				170	169.935462	14.9	
69	Thulium	Tm	168.9342	169	168.934213	100	
				171*	170.936428		1.92 y β^-
70	Ytterbium	Yb	173.04	168	167.933897	0.13	
				170	169.934761	3.05	
				171	170.936324	14.3	
				172	171.936380	21.9	
				173	172.938209	16.12	
				174	173.938861	31.8	
				176	175.942564	12.7	

STUDENTS-HUB.com Uploaded By: Malak Obaid

Z	Element	Symbol	Chemical atomic weight	Mass number (* indicates radioactive)	Atomic mass	Percent abundance	Half-life and decay mode (if unstable)
71	Lutetium	Lu	174.967	173*	172.938930		1.37 y ec
				175	174.940772	97.41	
				176*	175.942679	2.59	3.8×10^{10} y β^-
72	Hafnium	Hf	178.49	174*	173.940042	0.162	2.0×10^{15} y α
				176	175.941404	5.206	
				177	176.943218	18.606	
				178	177.943697	27.297	
				179	178.945813	13.629	
				180	179.946547	35.100	
73	Tantalum	Ta	180.9479	180	179.947542	0.012	
				181	180.947993	99.988	
74	Tungsten (Wolfram)	W	183.85	180	179.946702	0.12	
				182	181.948202	26.3	
				183	182.950221	14.28	
				184	183.950929	30.7	
				186	185.954358	28.6	
75	Rhenium	Re	186.207	185	184.952951	37.40	
				187*	186.955746	62.60	4.4×10^{10} y β^-
76	Osmium	Os	190.2	184	183.952486	0.02	
				186*	185.953834	1.58	2.0×10^{15} y α
				187	186.955744	1.6	
				188	187.955744	13.3	
				189	188.958139	16.1	
				190	189.958439	26.4	
				192	191.961468	41.0	
				194*	193.965172		6.0 y β^-
77	Iridium	Ir	192.2	191	190.960585	37.3	
				193	192.962916	62.7	
78	Platinum	Pt	195.08	190*	189.959926	0.01	6.5×10^{11} y α
				192	191.961027	0.79	
				194	193.962655	32.9	
				195	194.964765	33.8	
				196	195.964926	25.3	
				198	197.967867	7.2	
79	Gold	Au	196.9665	197	196.966543	100	
				198*	197.968217		2.70 d β^-
				199*	198.968740		3.14 d β^-

(*Continued*)

STUDENTS-HUB.com Uploaded By: Malak Obaid

Z	Element	Symbol	Chemical atomic weight	Mass number (* indicates radioactive)	Atomic mass	Percent abundance	Half-life and decay mode (if unstable)
80	Mercury	Hg	200.59	196	195.965806	0.15	
				198	197.966743	9.97	
				199	198.968253	16.87	
				200	199.968299	23.10	
				201	200.970276	13.10	
				202	201.970617	29.86	
				204	203.973466	6.87	
81	Thallium	Tl	204.383	203	202.972320	29.524	
				204*	203.973839		3.78 y β^-
				205	204.974400	70.476	
		(Ra E″)		206*	205.976084		4.2 m β^-
		(Ac C″)		207*	206.977403		4.77 m β^-
		(Th C″)		208*	207.981992		3.053 m β^-
		(Ra C″)		210*	209.990057		1.30 m β^-
82	Lead	Pb	207.2	202*	201.972134		5×10^4 y ec
				204	203.973020	1.4	
				205*	204.974457		1.5×10^7 y ec
				206	205.974440	24.1	
				207	206.975871	22.1	
				208	207.976627	52.4	
		(Ra D)		210*	209.984163		22.3 y β^-
		(Ac B)		211*	210.988734		36.1 m β^-
		(Th B)		212*	211.991872		10.64 h β^-
		(Ra B)		214*	213.999798		26.8 m β^-
83	Bismuth	Bi	208.9803	207*	206.978444		32.2 y ec, β^+
				208*	207.979717		3.7×10^5 y ec
				209	208.980374	100	
		(Ra E)		210*	209.984096		5.01 d α, β^-
		(Th C)		211*	210.987254		2.14 m α
				212*	211.991259		60.6 m α, β^-
		(Ra C)		214*	213.998692		19.9 m β^-
				215*	215.001836		7.4 m β^-
84	Polonium	Po		209*	208.982405		102 y α
		(Ra F)		210*	209.982848		138.38 d α
		(Ac C′)		211*	210.986627		0.52 s α
		(Th C′)		212*	211.988842		0.30 μs α
		(Ra C′)		214*	213.995177		164 μs α
		(Ac A)		215*	214.999418		0.0018 s α
		(Th A)		216*	216.001889		0.145 s α
		(Ra A)		218*	218.008965		3.10 m α
85	Astatine	At		215*	214.998638		$\approx$ 100 μs α
				218*	218.008685		1.6 s α
				219*	219.011297		0.9 m α

STUDENTS-HUB.com Uploaded By: Malak Obaid

Z	Element	Symbol	Chemical atomic weight	Mass number (* indicates radioactive)	Atomic mass	Percent abundance	Half-life and decay mode (if unstable)
86	Radon	Rn					
		(An)		219*	219.009477		3.96 s α
		(Tn)		220*	220.011369		55.6 s α
		(Rn)		222*	222.017571		3.823 d α
87	Francium			221*	221.01425		4.18 m α
		Fr		222*	222.017585		14.2 m β^-
		(Ac K)		223*	223.019733		22 m β^-
88	Radium	Ra		221*	221.01391		29 s α
		(Ac X)		223*	223.018499		11.43 d α
		(Th X)		224*	224.020187		3.66 d α
				225*			14.9 d β^-
		(Ra)		226*	226.025402		1600 y α
		($MsTh_1$)		228*	228.031064		5.75 y β^-
89	Actinium	Ac		225*			10 d α
		($Ms\ Th_2$)		227*	227.027749		21.77 y β^-
				228*	228.031015		6.15 h β^-
				229*			1.04 h β^-
90	Thorium	Th	232.0381				
		(Rd Ac)		227*	227.027701		18.72 d α
		(Rd Th)		228*	228.028716		1.913 y α
				229*	229.031757		7300 y α
		(Io)		230*	230.033127		75,000 y α, sf
		(UY)		231*	231.036299		25.52 h β^-
		(Th)		232*	232.038051	100	1.40×10^{10} y α
		(UX_1)		234*	234.043593		24.1 d β^-
91	Protactinium	Pa		231*	231.035880		32,760 y α
		(UZ)		234*	234.043300		6.7 h β^-
92	Uranium	U	238.0289	231*	231.036264		4.2 d β^+
				232*	232.037131		69 y α
				233*	233.039630		1.59×10^5 y α
		(UII)		234*	234.040946	0.0055	2.45×10^5 y α
		(Ac U)		235*	235.043924	0.720	7.04×10^8 y α
		(UI)		236*	236.045562		2.34×10^7 y α
				238*	238.050784	99.2745	4.47×10^9 y α
				239*	239.054290		23.5 m β^-
93	Neptunium	Np		235*	235.044057		396 d α
				236*	236.046559		1.54×10^5 y ec
				237*	237.048168		2.14×10^6 y α

(*Continued*)

STUDENTS-HUB.com Uploaded By: Malak Obaid

Z	Element	Symbol	Chemical atomic weight	Mass number (* indicates radioactive)	Atomic mass	Percent abundance	Half-life and decay mode (if unstable)
94	Plutonium	Pu		236*	236.046033		2.87 y α, sf
				238*	238.049555		87.7 y α, sf
				239*	239.052157		24,120 y α, sf
				240*	240.053808		6560 y α, sf
				241*	241.056846		14.4 y β^-
				242*	242.058737		3.7×10^5 y α, sf
				244*	244.064200		8.1×10^7 y α, sf
95	Americium	Am		240*	240.055285		2.12 d ec
				241*	241.056824		432 y α, sf
96	Curium	Cm		247*	247.070347		1.56×10^7 y α
				248*	248.072344		3.4×10^5 y α, sf
97	Berkelium	Bk		247*	247.070300		1380 y α
				249*	249.074979		327 d β^-
98	Californium	Cm		250*	250.076400		13.1 y α, sf
				251*	251.079580		898 y α
99	Einsteinium	Es		252*	252.082974		1.29 y α
				253*	253.084817		2.02 d α, sf
100	Fermium	Fm		253*	253.085173		3.00 d ec
				254*	254.086849		3.24 h α, sf
101	Mendelevium	Md		256*	256.093988		75.6 m ec, β^+
				258*	258.098594		55 d α
102	Nobelium	No		257*	257.096855		25 s α
				259*	259.100932		58 m α, sf
103	Lawrencium	Lr		259*	259.102888		6.14 s α, sf
				260*	260.105346		3.0 m α, sf
104	Rutherfordium	Rf		260*	260.160302		24 ms sf
				261*	261.108588		65 s α, sf
105	Dubnium	Db		261*	261.111830		1.8 s α
				262*	262.113763		35 s α
106	Seaborgium	Sg		263*	263.118310		0.78 s α, sf
107	Bohrium	Bh		262*	262.123081		0.10 s α, sf
108	Hassium	Hs		265*	265.129984		1.8 ms α
				267*	267.131770		60 ms α
109	Meitnerium	Mt		266*	266.137789		3.4 ms α, sf
				268*	268.138820		70 ms α

STUDENTS-HUB.com Uploaded By: Malak Obaid

Z	Element	Symbol	Chemical atomic weight	Mass number (* indicates radioactive)	Atomic mass	Percent abundance	Half-life and decay mode (if unstable)
110	Darmstadtium	Ds		269* 271* 273*	269.145140 271.146080 272.153480		0.17 ms α 1.1 ms α 8.6 ms α
111	Roentgenium	Rg		272*	272.153480		1.5 ms α
112	Ununbium	Unb		277*	?		0.2 ms α
113	Ununtrium	Unt		284*	?		? α
114	Ununquadium	Unq		289*	?		? α
115	Ununpentium	Unp		288*	?		? α
116	Ununhexium	Unh		292*	?		? α
117							
118	Ununoctium	Uno		294*	?		? α

STUDENTS-HUB.com Uploaded By: Malak Obaid

Probability Integrals

When calculating various average values using the Maxwell-Boltzmann distribution, integrals of the following type occur:

$$I_n = \int_0^\infty x^n e^{-\lambda x^2} dx$$

where n is an integer. These can be obtained from I_0 and I_1 by differentiation. Consider I_n to be a function of λ and take the derivative with respect to λ:

$$\frac{dI_n}{d\lambda} = \int_0^\infty -x^2 x^n e^{-\lambda x^2} dx = -I_{n+2} \qquad \textbf{B1-1}$$

Thus, if I_0 is known, all the I_n for even n can be obtained, and if I_1 is known, all the I_n for odd n can be obtained from Equation B1-1. I_1 can easily be evaluated. Using the substitution $u = \lambda x^2$, then $du = 2\lambda x\, dx$ and

$$I_1 = \int_0^\infty x e^{-\lambda x^2} dx = \frac{1}{2}\lambda^{-1} \int_0^\infty e^{-u} du = \frac{1}{2}\lambda^{-1}$$

Then I_3 and I_5 are

$$I_3 = -\frac{d\left(\frac{1}{2}\lambda^{-1}\right)}{d\lambda} = \frac{1}{2}\lambda^{-2} \qquad \text{and} \qquad I_5 = -\frac{dI_3}{d\lambda} = \lambda^{-3}$$

The evaluation of I_0 is more difficult, but it can be done using a trick. We evaluate I_0^2:

$$I_0^2 = \int_0^\infty e^{-\lambda x^2} dx \int_0^\infty e^{-\lambda y^2} dy = \int_0^\infty \int_0^\infty e^{-\lambda(x^2+y^2)} dx\, dy \qquad \textbf{B1-2}$$

where we have used y as the dummy variable of integration in the second integral. If we now consider this to be an integration over the xy plane, we can change to polar coordinates $r^2 = x^2 + y^2$ and $\tan\varphi = y/x$. The element of area $dx\, dy$ becomes $r\, dr\, d\varphi$ and the integration over positive x and y becomes an integration from $r = 0$ to $r = \infty$ and from $\varphi = 0$ to $\varphi = \pi/2$. Then we have

$$I_0^2 = \int_0^\infty \int_0^{\pi/2} e^{-\lambda r^2} r\, dr\, d\varphi = \frac{\pi}{2} I_1 = \frac{\pi}{4}\lambda^{-1}$$

and

$$I_0 = \frac{1}{2}\sqrt{\pi}\,\lambda^{-1/2}$$

STUDENTS-HUB.com

Uploaded By: Malak Obaid

We then obtain I_2, I_4, . . . by differentiation. For example,

$$I_2 = -\frac{dI_0}{d\lambda} = \frac{1}{4}\sqrt{\pi}\,\lambda^{-3/2}$$

Table B1-1 lists the values of the integral I_n calculated as above for values of n from 0 to 5.

Table B1-1 Values of the integral $I_n = \int_0^\infty x^n e^{-\lambda x^2}\,dx$ for $n = 0$ to $n = 5$

n	I_n
0	$\frac{1}{2}\pi^{1/2}\lambda^{-1/2}$
1	$\frac{1}{2}\lambda^{-1}$
2	$\frac{1}{4}\pi^{1/2}\lambda^{-3/2}$
3	$\frac{1}{2}\lambda^{-2}$
4	$\frac{3}{8}\pi^{1/2}\lambda^{-5/2}$
5	λ^{-3}
If n is even	$\int_{-\infty}^{+\infty} x^n e^{-\lambda x^2}\,dx = 2I_n$
If n is odd	$\int_{-\infty}^{+\infty} x^n e^{-\lambda x^2}\,dx = 0$

STUDENTS-HUB.com Uploaded By: Malak Obaid

Binomial and Exponential Series

Binomial Series

$$(1 + x)^m = 1 + mx + \frac{m(m-1)}{2!}x^2 + \frac{m(m-1)(m-2)}{3!}x^3 + \cdots + \frac{m(m-1)(m-2)\cdots(m-n+2)}{(n-1)!}x^{n-1} + R_n$$

where

$$R_n = \frac{m(m-1)(m-2)\cdots(m-n+1)}{n!}x^n(1 + ax)^{m-n}$$

for all cases where $0 < a < 1$.

$$R_n < \left|\frac{m(m-1)(m-2)\cdots(m-n+1)}{n!}x^n\right| \quad \text{if } x > 0$$

$$R_n < \left|\frac{m(m-1)(m-2)\cdots(m-n+1)}{n!}\frac{x^n}{(1+x)^{n-m}}\right| \quad \text{for } x < 0, \quad n > m$$

$$R_n < |x^n|(1+x)^m \quad \text{if} \quad -1 < m < 0$$

If m is a negative integer or a positive or negative fraction, the binomial expansion is valid only when $|x| < 1$. Except when m is a positive integer, a binomial such as $(a + b)^m$ must be written in one of the following forms before expanding it:

$$a^m\left(1 + \frac{b}{a}\right)^m \quad \text{if} \quad a > b \qquad b^m\left(1 + \frac{a}{b}\right)^m \quad \text{if} \quad b > a$$

Exponential Series

$$e^x = 1 + x + \frac{x^2}{2!} + \frac{x^3}{3!} + \cdots + \frac{x^{n-1}}{(n-1)!} + \frac{x^n}{n!} + \cdots$$

$$a^x = 1 + x\log a + \frac{(x\log a)^2}{2!} + \cdots + \frac{(x\log a)^{n-1}}{(n-1)!} + \frac{(x\log a)^n}{n!} + \cdots$$

STUDENTS-HUB.com

Uploaded By: Malak Obaid

Diagrams of Crystal Unit Cells

Crystalline solids are classified according to their symmetries into 7 crystal systems and 14 lattices. A **lattice** is defined as an infinite array of points each of which has surroundings identical to those of all other points. In three dimensions this definition is expressed by three **translation vectors a**, **b**, and **c**, such that the array of atoms in the crystal when viewed from point **r** looks the same when viewed from any other point **r′**, where **r′** is reached by translations of integer multiples of the $\mathbf{a}_i$, that is,

$$\mathbf{r}' = \mathbf{r} + m_1\mathbf{a} + m_2\mathbf{b} + m_3\mathbf{c}$$

where m_i are integers. The translation vectors are usually (but not always) used to specify the three axes of the crystal's **unit cell**. The volume of the unit cell is $\mathbf{a} \cdot (\mathbf{b} \times \mathbf{c})$, and no cell of smaller volume can serve as the unit to assemble the crystal.

Figure B3-1 illustrates the orientations of the translation vectors and the standard designations of the angles between them. Figure B3-2 illustrates diagrams of the 14 lattices.

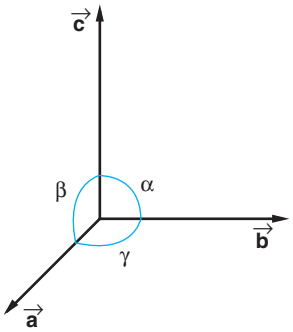

Figure B3-1 The directions of the translation vectors are often used to define the directions of the crystal axes, the angles between each axis pair defining the shape of the cell.

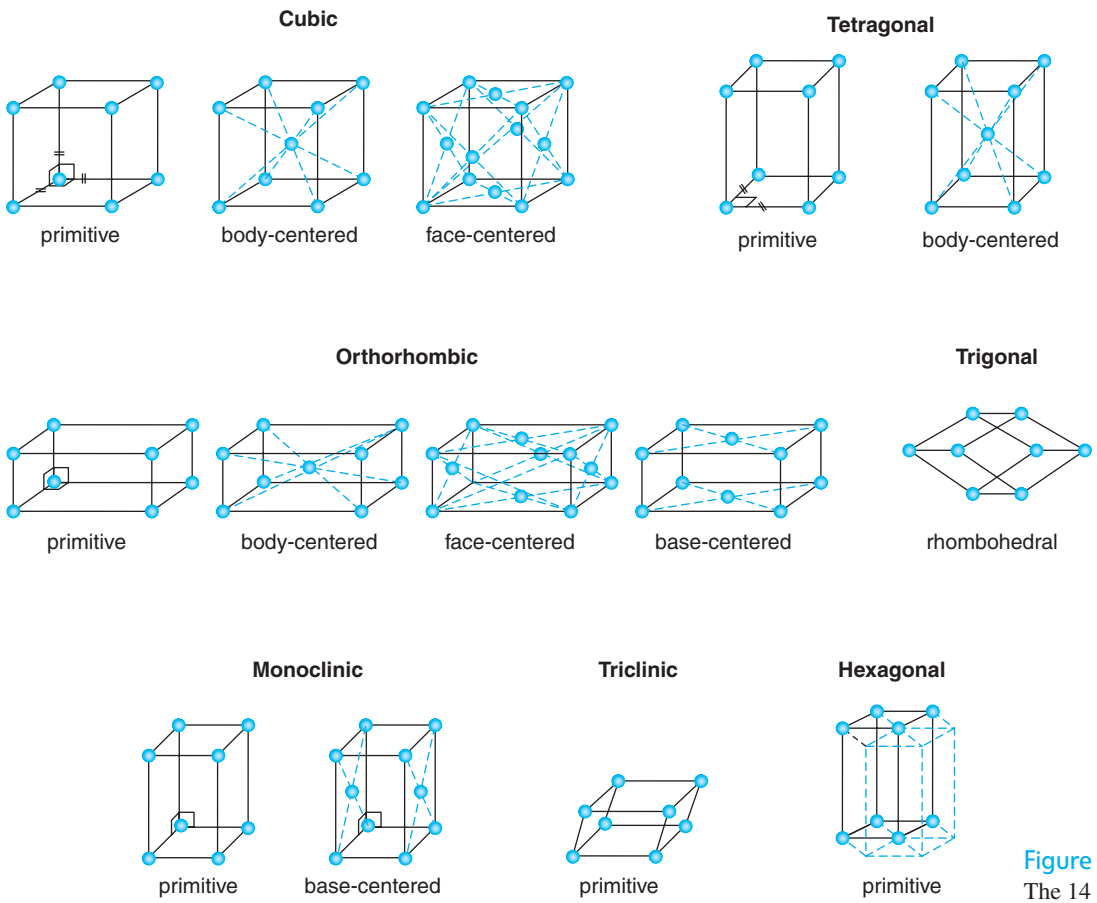

Figure B3-2
The 14 crystal lattices.

STUDENTS-HUB.com
Uploaded By: Malak Obaid

Electron Configurations

Electron configurations of the atoms in their ground states. For a few of the rare earth elements ($Z = 57$ to 71) and the heavy elements ($Z > 89$), the configurations are not firmly established.

Z	Element	Ionization energy (eV)	K $n:1$ $l:s$	L 2 sp	M 3 spd	N 4 $spdf$	O 5 $spdf$	P 6 spd	Q 7 sp
1	H (hydrogen)	13.6	1						
2	He (helium)	24.5	2						
3	Li (lithium)	5.4	2	1					
4	Be (beryllium)	9.3	2	2					
5	B (boron)	8.3	2	2 1					
6	C (carbon)	11.3	2	2 2					
7	N (nitrogen)	14.5	2	2 3					
8	O (oxygen)	13.6	2	2 4					
9	F (flourine)	17.4	2	2 5					
10	Ne (neon)	21.6	2	2 6					
11	Na (sodium)	5.1	2	2 6	1				
12	Mg (magnesium)	7.6	2	2 6	2				
13	Al (aluminum)	6.0	2	2 6	2 1				
14	Si (silicon)	8.1	2	2 6	2 2				
15	P (phosphorus)	10.5	2	2 6	2 3				
16	S (sulfur)	10.4	2	2 6	2 4				
17	Cl (chlorine)	13.0	2	2 6	2 5				
18	Ar (argon)	15.8	2	2 6	2 6				

STUDENTS-HUB.com

Uploaded By: Malak Obaid

Z	Element	Ionization energy (eV)	K n : 1 l : s	L 2 s p	M 3 s p d	N 4 s p d f	O 5 s p d f	P 6 s p d	Q 7 s p
19	K (potassium)	4.3	2	2 6	2 6 .	1			
20	Ca (calcium)	6.1	2	2 6	2 6 .	2			
21	Sc (scandium)	6.5	2	2 6	2 6 1	2			
22	Ti (titanium)	6.8	2	2 6	2 6 2	2			
23	V (vanadium)	6.7	2	2 6	2 6 3	2			
24	Cr (chromium)	6.8	2	2 6	2 6 5	1			
25	Mn (manganese)	7.4	2	2 6	2 6 5	2			
26	Fe (iron)	7.9	2	2 6	2 6 6	2			
27	Co (cobalt)	7.9	2	2 6	2 6 7	2			
28	Ni (nickel)	7.6	2	2 6	2 6 8	2			
29	Cu (copper)	7.7	2	2 6	2 6 10	1			
30	Zn (zinc)	9.4	2	2 6	2 6 10	2			
31	Ga (gallium)	6.0	2	2 6	2 6 10	2 1			
32	Ge (germanium)	7.9	2	2 6	2 6 10	2 2			
33	As (arsenic)	9.8	2	2 6	2 6 10	2 3			
34	Se (selenium)	9.8	2	2 6	2 6 10	2 4			
35	Br (bromine)	11.8	2	2 6	2 6 10	2 5			
36	Kr (krypton)	14.0	2	2 6	2 6 10	2 6			
37	Rb (rubidium)	4.2	2	2 6	2 6 10	2 6 . .	1		
38	Sr (strontium)	5.7	2	2 6	2 6 10	2 6 . .	2		
39	Y (yttrium)	6.4	2	2 6	2 6 10	2 6 1 .	2		
40	Zr (zirconium)	6.8	2	2 6	2 6 10	2 6 2 .	2		
41	Nb (niobium)	6.9	2	2 6	2 6 10	2 6 4 .	1		
42	Mo (molybdenum)	7.1	2	2 6	2 6 10	2 6 5 .	1		
43	Tc (technetium)	7.3	2	2 6	2 6 10	2 6 6 .	1		

(*Continued*)

STUDENTS-HUB.com Uploaded By: Malak Obaid

Z	Element	Ionization energy (eV)	K n : 1 l : s	L 2 s p	M 3 s p d	N 4 s p d f	O 5 s p d f	P 6 s p d	Q 7 s p
44	Ru (ruthenium)	7.4	2	2 6	2 6 10	2 6 7 .	1		
45	Rh (rhodium)	7.5	2	2 6	2 6 10	2 6 8 .	1		
46	Pd (palladium)	8.3	2	2 6	2 6 10	2 6 10 .			
47	Ag (silver)	7.6	2	2 6	2 6 10	2 6 10 .	1		
48	Cd (cadmium)	9.0	2	2 6	2 6 10	2 6 10 .	2		
49	In (indium)	5.8	2	2 6	2 6 10	2 6 10 .	2 1		
50	Sn (tin)	7.3	2	2 6	2 6 10	2 6 10 .	2 2		
51	Sb (antimony)	8.6	2	2 6	2 6 10	2 6 10 .	2 3		
52	Te (tellurium)	9.0	2	2 6	2 6 10	2 6 10 .	2 4		
53	I (iodine)	10.5	2	2 6	2 6 10	2 6 10 .	2 5		
54	Xe (xenon)	12.1	2	2 6	2 6 10	2 6 10 .	2 6		
55	Cs (cesium)	3.9	2	2 6	2 6 10	2 6 10 .	2 6 . .	1	
56	Ba (barium)	5.2	2	2 6	2 6 10	2 6 10 .	2 6 . .	2	
57	La (lanthanum)	5.6	2	2 6	2 6 10	2 6 10 .	2 6 1 .	2	
58	Ce (cerium)	5.6	2	2 6	2 6 10	2 6 10 1	2 6 1 .	2	
59	Pr (praseodymium)	5.5	2	2 6	2 6 10	2 6 10 3	2 6 . .	2	
60	Nd (neodymium)	5.5	2	2 6	2 6 10	2 6 10 4	2 6 . .	2	
61	Pm (promethium)	5.5	2	2 6	2 6 10	2 6 10 5	2 6 . .	2	
62	Sm (samarium)	5.6	2	2 6	2 6 10	2 6 10 6	2 6 . .	2	
63	Eu (europium)	5.7	2	2 6	2 6 10	2 6 10 7	2 6 . .	2	
64	Gd (gadolinium)	6.2	2	2 6	2 6 10	2 6 10 7	2 6 1 .	2	
65	Tb (terbium)	6.0	2	2 6	2 6 10	2 6 10 9	2 6 . .	2	
66	Dy (dysprosium)	6.8	2	2 6	2 6 10	2 6 10 10	2 6 . .	2	
67	Ho (holmium)	6.0	2	2 6	2 6 10	2 6 10 11	2 6 . .	2	

STUDENTS-HUB.com Uploaded By: Malak Obaid

Z	Element	Ionization energy (eV)	*K* *n* : 1 *l* : *s*	*L* 2 *s p*	*M* 3 *s p d*	*N* 4 *s p d f*	*O* 5 *s p d f*	*P* 6 *s p d*	*Q* 7 *s p*
68	Er (erbium)	6.1	2	2 6	2 6 10	2 6 10 12	2 6 . .	2	
69	Tm (thulium)	5.8	2	2 6	2 6 10	2 6 10 13	2 6 . .	2	
70	Yb (ytterbium)	6.2	2	2 6	2 6 10	2 6 10 14	2 6 . .	2	
71	Lu (lutetium)	5.1	2	2 6	2 6 10	2 6 10 14	2 6 1 .	2	
72	Hf (hafnium)	7.0	2	2 6	2 6 10	2 6 10 14	2 6 2 .	2	
73	Ta (tantalum)	7.9	2	2 6	2 6 10	2 6 10 14	2 6 3 .	2	
74	W (tungsten)	8.0	2	2 6	2 6 10	2 6 10 14	2 6 4 .	2	
75	Re (rhenium)	7.9	2	2 6	2 6 10	2 6 10 14	2 6 5 .	2	
76	Os (osmium)	8.5	2	2 6	2 6 10	2 6 10 14	2 6 6 .	2	
77	Ir (iridium)	9.0	2	2 6	2 6 10	2 6 10 14	2 6 7 .	2	
78	Pt (platinum)	9.0	2	2 6	2 6 10	2 6 10 14	2 6 9 .	1	
79	Au (gold)	9.2	2	2 6	2 6 10	2 6 10 14	2 6 10 .	1	
80	Hg (mercury)	10.4	2	2 6	2 6 10	2 6 10 14	2 6 10 .	2	
81	Tl (thallium)	6.1	2	2 6	2 6 10	2 6 10 14	2 6 10 .	2 1	
82	Pb (lead)	7.4	2	2 6	2 6 10	2 6 10 14	2 6 10 .	2 2	
83	Bi (bismuth)	7.3	2	2 6	2 6 10	2 6 10 14	2 6 10 .	2 3	
84	Po (polonium)	8.4	2	2 6	2 6 10	2 6 10 14	2 6 10 .	2 4	
85	At (astatine)	9.5	2	2 6	2 6 10	2 6 10 14	2 6 10 .	2 5	
86	Rn (radon)	10.7	2	2 6	2 6 10	2 6 10 14	2 6 10 .	2 6	
87	Fr (francium)	4.0	2	2 6	2 6 10	2 6 10 14	2 6 10 .	2 6 .	1
88	Ra (radium)	5.3	2	2 6	2 6 10	2 6 10 14	2 6 10 .	2 6 .	2
89	Ac (actinium)	6.9	2	2 6	2 6 10	2 6 10 14	2 6 10 .	2 6 1	2
90	Th (thorium)	7.0	2	2 6	2 6 10	2 6 10 14	2 6 10 .	2 6 2	2
91	Pa (protactinium)		2	2 6	2 6 10	2 6 10 14	2 6 10 1	2 6 2	2

(*Continued*)

STUDENTS-HUB.com Uploaded By: Malak Obaid

Z	Element	Ionization energy (eV)	K n : 1 l : s	L 2 s p	M 3 s p d	N 4 s p d f	O 5 s p d f	P 6 s p d	Q 7 s p
92	U (uranium)	6.1	2	2 6	2 6 10	2 6 10 14	2 6 10 3	2 6 1	2
93	Np (neptunium)		2	2 6	2 6 10	2 6 10 14	2 6 10 4	2 6 1	2
94	Pu (plutonium)	5.8	2	2 6	2 6 10	2 6 10 14	2 6 10 6	2 6 .	2
95	Am (americium)	6.0	2	2 6	2 6 10	2 6 10 14	2 6 10 7	2 6 .	2
96	Cm (curium)		2	2 6	2 6 10	2 6 10 14	2 6 10 7	2 6 1	2
97	Bk (berkelium)		2	2 6	2 6 10	2 6 10 14	2 6 10 8	2 6 1	2
98	Cf (californium)		2	2 6	2 6 10	2 6 10 14	2 6 10 10	2 6 .	2
99	Es (einsteinium)		2	2 6	2 6 10	2 6 10 14	2 6 10 11	2 6 .	2
100	Fm (fermium)		2	2 6	2 6 10	2 6 10 14	2 6 10 12	2 6 .	2
101	Md (mendelevium)		2	2 6	2 6 10	2 6 10 14	2 6 10 13	2 6 .	2
102	No (nobelium)		2	2 6	2 6 10	2 6 10 14	2 6 10 14	2 6 .	2
103	Lw (lawrencium)		2	2 6	2 6 10	2 6 10 14	2 6 10 14	2 6 1	2
104	Rf (rutherfordium)		2	2 6	2 6 10	2 6 10 14	2 6 10 14	2 6 2	2
105	Du (dubnium)		2	2 6	2 6 10	2 6 10 14	2 6 10 14	2 6 3	2
106	Sg (seaborgium)		2	2 6	2 6 10	2 6 10 14	2 6 10 14	2 6 4	2
107	Bh (bohrium)		2	2 6	2 6 10	2 6 10 14	2 6 10 14	2 6 5	2
108	Hs (hassium)		2	2 6	2 6 10	2 6 10 14	2 6 10 14	2 6 6	2
109	Mt (meitnerium)		2	2 6	2 6 10	2 6 10 14	2 6 10 14	2 6 7	2
110	Ds (darmstadtium)		2	2 6	2 6 10	2 6 10 14	2 6 10 14	2 6 9	1
111	Rg (roentgenium)		2	2 6	2 6 10	2 6 10 14	2 6 10 14	2 6 10	1
112	Unb (ununbium)		2	2 6	2 6 10	2 6 10 14	2 6 10 14	2 6 10	2
113	Unt (ununtrium)		2	2 6	2 6 10	2 6 10 14	2 6 10 14	2 6 10	2 1
114	Unq (ununquadium)		2	2 6	2 6 10	2 6 10 14	2 6 10 14	2 6 10	2 2
115	Unp (ununpentium)		2	2 6	2 6 10	2 6 10 14	2 6 10 14	2 6 10	2 3

STUDENTS-HUB.com Uploaded By: Malak Obaid

Z	Element	Ionization energy (eV)	*K* *n* : 1 *l* : *s*	*L* 2 *s p*	*M* 3 *s p d*	*N* 4 *s p d f*	*O* 5 *s p d f*	*P* 6 *s p d*	*Q* 7 *s p*
116	Unh (ununhexium)		2	2 6	2 6 10	2 6 10 14	2 6 10 14	2 6 10	2 4
117									
118	Uno (ununoctium)		2	2 6	2 6 10	2 6 10 14	2 6 10 14	2 6 10	2 6

STUDENTS-HUB.com Uploaded By: Malak Obaid

APPENDIX D

Fundamental Physical Constants

This set of fundamental physical constants consists of selected values recommended by CODATA, the Committee on Data for Science and Technology of the International Council of Scientific Unions, resulting from the most recent (2002) compilation and computations. The digits in parentheses are the one-standard-deviation uncertainties in the last digits. (Reference: P. J. Mohr and B. N. Taylor, http://www.physicstoday.org/guide/fundconst.pdf.)

Quantity	Symbol	Value	Units
Universal constants			
Speed of light in vacuum (exact)	c	299,792,458	$m \cdot s^{-1}$
Permeability of vacuum (magnetic constant) (exact)	μ_0	$4\pi \times 10^{-7} = 12.566370614 \times 10^{-7}$	$N \cdot A^{-2}$
Permittivity of vacuum (electric constant) (exact)	ϵ_0	$1/\mu_0 c^2 = 8.854187817$	$10^{-12}\ F \cdot m^{-1}$
Newtonian constant of gravitation	G	6.6742 (10)	$10^{-11}\ m^3 \cdot kg^{-1} \cdot s^{-2}$
Planck constant	h	6.6260693 (11)	$10^{-34}\ J \cdot s$
in electron volts, $h/\{e\}$		4.13566743 (35)	$10^{-15}\ eV \cdot s$
$h/2\pi$	$\hbar$	1.05457168 (18)	$10^{-34}\ J \cdot s$
in electron volts, $\hbar/\{e\}$		6.58211915 (56)	$10^{-16}\ eV \cdot s$
Planck mass, $(\hbar c/G)^{1/2}$	m_p	2.17654 (16)	10^{-8} kg
Planck temperature, $(\hbar c^5/G)^{1/2}/k$	T_p	1.41679 (11)	10^{32} K
Planck length, $\hbar/m_p c = (\hbar G/c^3)^{1/2}$	l_p	1.61624 (12)	10^{-35} m
Planck time, $(l_p/c) = (\hbar G/c^5)^{1/2}$	t_p	5.39121 (40)	10^{-44} s
Electromagnetic constants			
Elementary charge	e	1.60217653 (14)	10^{-19} C
	e/h	2.41798940 (21)	$10^{14}\ A \cdot J^{-1}$
Magnetic flux quantum, $h/2e$	Φ_0	2.06783372 (18)	10^{-15} Wb
Josephson constant $2e/h$	K_J	483597.879 (41)	$10^9\ Hz \cdot V^{-1}$
von Klitzing constant, $h/e^2 = \mu_0 c/2\alpha$	R_K	25812.807449 (86)	Ω
Bohr magneton, $e\hbar/2m_e$	μ_B	927.400949 (80)	$10^{-24}\ J \cdot T^{-1}$
in eV/T		5.788381804 (39)	$10^{-5}\ eV \cdot T^{-1}$
Nuclear magneton, $e\hbar/2m_p$	μ_N	5.05078343 (43)	$10^{-27}\ J \cdot T^{-1}$
in eV/T		3.152451259 (24)	$10^{-8}\ eV \cdot T^{-1}$
Atomic constants			
Fine-structure constant, $e^2/4\pi\epsilon_0\hbar c$	α	7.297352568 (24)	10^{-3}
inverse fine-structure constant	α^{-1}	137.03599911 (46)	
Rydberg constant, $m_e c\alpha^2/2h$	R_∞	10,973,731.568525 (73)	m^{-1}
in hertz, $R_\infty c$		3.289841960360 (22)	10^{15} Hz
in joules, $R_\infty hc$		2.17987209 (37)	10^{-18} J
in eV, $R_\infty hc/\{e\}$		13.6056923 (12)	eV
Bohr radius	a_0	0.5291772108 (18)	10^{-10} m
Electron			
Mass	m_e	9.1093826 (16)	10^{-31} kg
		5.4857990945 (24)	10^{-4} u
in electron volts, $m_e c^2/\{e\}$		0.510998918 (44)	MeV

STUDENTS-HUB.com
Uploaded By: Malak Obaid

Quantity	Symbol	Value	Units
Electron-muon mass ratio	m_e/m_μ	4.83633167 (13)	10^{-3}
Electron-tau mass ratio	m_e/m_τ	2.87564 (47)	10^{-4}
Electron-proton mass ratio	m_e/m_p	5.4461702173 (25)	10^{-4}
Electron-deuteron mass ratio	m_e/m_d	2.7244371095 (13)	10^{-4}
Electron-α-particle mass ratio	m_e/m_α	1.37093355575 (61)	10^{-4}
Specific charge	$-e/m_e$	−1.75882012 (15)	10^{11} C · kg^{-1}
Molar mass	$M(e)$	5.4857990945 (24)	10^{-7} kg · mol^{-1}
Compton wavelength, $h/m_e c$	λ_C	2.426310238 (16)	10^{-12} m
$\lambda_C/2\pi = \alpha a_0 = \alpha^2/4\pi R_\infty$	$\lambda\!\!\!^{-}{}_C$	386.1592678 (26)	10^{-15} m
Classical radius, $\alpha^2 a_0$	r_e	2.817940325 (28)	10^{-15} m
Thomson cross section, $(8\pi/3)r_e^2$	σ_e	0.665245873 (13)	10^{-28} m^2
Magnetic moment	μ_e	−928.476412 (80)	10^{-26} J · T^{-1}
in Bohr magnetons	μ_e/μ_B	−1.0011596521859 (38)	
in nuclear magnetons	μ_e/μ_N	−1838.28197107 (85)	
Magnetic moment anomaly, $\lvert\mu_e\rvert/\mu_B - 1$	a_e	1.1596521859 (38)	10^{-3}
g factor, $-2(1 + a_e)$	g_e	−2.0023193043718 (75)	
Electron-muon magnetic moment ratio	μ_e/μ_μ	206.7669894 (54)	
Electron-proton magnetic moment ratio	μ_e/μ_p	−658.2106862 (66)	
Muon			
Mass	m_μ	1.88353140 (33)	10^{-28} kg
		0.1134289264 (30)	u
in electron volts, $m_\mu c^2/\{e\}$		105.6583692 (94)	MeV
Muon-electron mass ratio	m_μ/m_e	206.7682838 (54)	
Muon-tau mass ratio	$m_\mu/m\tau$	5.94592 (97)	
Molar mass	$M(\mu)$	1.134289264 (34)	10^{-4} kg · mol^{-1}
Magnetic moment	μ_μ	−4.49044799 (40)	10^{-26} J T^{-1}
in Bohr magnetons	μ_μ/μ_B	4.84197085 (15)	10^{-3}
in nuclear magnetons	μ_μ/μ_N	8.89059770 (27)	
Magnetic moment anomaly, $\lvert\mu_\mu\rvert/(e\hbar/2\,m_\mu) - 1$	a_μ	1.16591981 (62)	10^{-3}
g factor, $-2(1 + a_\mu)$	g_μ	−2.0023318396 (12)	
Muon-proton magnetic moment ratio	μ_μ/μ_p	−3.183345118 (89)	
Tau			
Mass	m_τ	3.16777 (52)	10^{-27} kg
		1.90768 (31)	u
in electron volts		1776.99 (29)	MeV
Proton			
Mass	m_p	1.67262171 (29)	10^{-27} kg
		1.00727646688 (13)	u
in electron volts		938.272029 (80)	MeV
Proton-electron mass ratio	m_p/m_e	1836.15267261 (85)	
Proton-muon mass ratio	m_p/m_μ	8.88024333 (23)	
Specific charge	e/m_p	9.57883376 (82)	10^7 C · kg^{-1}
Molar mass	$M(p)$	1.00727646688 (13)	10^{-3} kg · mol^{-1}
Compton wavelength, $h/m_p c$	$\lambda_{C,p}$	1.3214098555 (88)	10^{-15} m
$\lambda_{C,p}/2\pi$	$\lambda\!\!\!^{-}{}_C$	2.103089104 (14)	10^{-16} m

(*Continued*)

STUDENTS-HUB.com Uploaded By: Malak Obaid

Quantity	Symbol	Value	Units
Magnetic moment	μ_p	1.41060671 (12)	10^{-26} J · T^{-1}
in Bohr magnetons	μ_p/μ_B	1.521032206 (15)	10^{-3}
in nuclear magnetons	μ_p/μ_N	2.792847351 (28)	
Diamagnetic shielding correction for protons			
(H_2O spherical sample, 25°C), $1 - \mu'_p/\mu_p$	σ_{H_2O}	25.687 (15)	10^{-6}
Shielded proton moment			
(H_2O spherical sample, 25°C)	μ'_p	1.41057047 (12)	10^{-26} J · T^{-1}
in Bohr magnetons	μ'_p/μ_B	1.520993132 (16)	10^{-3}
in nuclear magnetons	μ'_p/μ_N	2.792775604 (30)	
Gyromagnetic ratio	γ_p	26,752.2205 (23)	10^4 sec^{-1} · T^{-1}
	$\gamma_p/2\pi$	42.5774813 (37)	MHz · T^{-1}
uncorrected (H_2O, spherical sample, 25°C)	γ'_p	26,751.5333 (23)	10^4 sec^{-1} · T^{-1}
	$\gamma'_p/2\pi$	42.5763875 (37)	MHz · T^{-1}
Neutron			
Mass	m_n	1.67492728 (29)	10^{-27} kg
		1.00866491560 (55)	u
in electron volts, $m_nc^2/\{e\}$		939.565360 (81)	MeV
Neutron-electron mass ratio	m_n/m_e	1838.6836598 (13)	
Neutron-proton mass ratio	m_n/m_p	1.00137841870 (58)	
Molar mass	$M(n)$	1.00866491560 (55)	10^{-3} kg · mol^{-1}
Compton wavelength, h/m_nc	$\lambda_{C,n}$	1.3195909067 (88)	10^{-15} m
$\lambda_{C,n}/2\pi$	$\lambda\!\!\!^{-}_{C,n}$	2.100194157 (14)	10^{-16} m
Magnetic moment	μ_n	−0.96623645 (24)	10^{-26} J · T^{-1}
in Bohr magnetons	μ_n/μ_B	−1.04187563 (25)	10^{-3}
in nuclear magnetons	μ_n/μ_N	−1.91304273 (45)	
Neutron-electron magnetic moment ratio	μ_n/μ_e	1.04066882 (25)	10^{-3}
Neutron-proton magnetic moment ratio	μ_n/μ_p	−0.68497934 (16)	
Deuteron			
Mass	m_d	3.34358335 (57)	10^{-27} kg
		2.01355321270 (35)	u
in electron volts, $m_dc^2/\{e\}$		1875.61282 (16)	MeV
Deuteron-electron mass ratio	m_d/m_e	3670.4829652 (18)	
Deuteron-proton mass ratio	m_d/m_p	1.99900750082 (41)	
Molar mass	$M(d)$	2.01355321270 (35)	10^{-3} kg · mol^{-1}
Magnetic moment	μ_d	0.433073482 (38)	10^{-26} J · T^{-1}
in Bohr magnetons	μ_d/μ_B	0.4669754567 (50)	10^{-3}
in nuclear magnetons	μ_d/μ_N	0.8574382329 (92)	
Deuteron-electron magnetic moment ratio	μ_d/μ_e	−0.4664345548 (50)	10^{-3}
Deuteron-proton magnetic moment ratio	μ_d/μ_p	0.3070122084 (45)	
Alpha particle			
Mass	m_α	6.6446565 (11)	10^{-27} kg
in electron volts		3727.37917 (32)	MeV
Physiochemical constants			
Avogadro constant	N_A, L	6.0221415 (10)	10^{23} mol^{-1}
Atomic mass constant, $m(C^{12})/12$	m_u	1.66053886 (28)	10^{-27} kg
in electron volts, $m_uc^2/\{e\}$		931.494043 (80)	MeV

STUDENTS-HUB.com Uploaded By: Malak Obaid

Quantity	Symbol	Value	Units
Faraday constant	F	96,485.3383 (83)	$C \cdot mol^{-1}$
Molar Planck constant	$N_A h$	3.990312716 (27)	$10^{-10}\ J \cdot s \cdot mol^{-1}$
	$N_A hc$	0.11962656572 (80)	$J \cdot m \cdot mol^{-1}$
Molar gas constant	R	8.314472 (15)	$J \cdot mol^{-1} \cdot K^{-1}$
Boltzmann constant, R/N_A	k	1.3806505 (24)	$10^{-23}\ J \cdot K^{-1}$
in electron volts, $k/\{e\}$		8.617343 (15)	$10^{-5}\ eV \cdot K^{-1}$
in hertz, k/h		2.0836644 (36)	$10^{10}\ Hz \cdot K^{-1}$
in wavenumbers, k/hc		69.50356 (12)	$m^{-1}\ K^{-1}$
Molar volume (ideal gas),			
RT/p (at 273.15 K, 101 325 Pa)	V_m	22.413996 (39)	$10^{-3}\ m^{-3} \cdot mol^{-1}$
Loschmidt constant, N_A/V_m	n_0	2.6867773 (47)	$10^{25}\ m^{-3}$
Stefan-Boltzmann constant, $(\pi^2/60)k^4/h^3c^2$	σ	5.670400 (40)	$10^{-8}\ W \cdot m^{-2} \cdot K^{-4}$
First radiation constant, $2\pi hc^2$	c_1	3.74177138 (64)	$10^{-16}\ W \cdot m^2$
Second radiation constant, hc/k	c_2	1.4387752 (25)	$10^{-2}\ m \cdot K$
Wien displacement law constant,			
$\lambda_{max} T = c_2/4.96511423\ldots$	b	2.8977686 (51)	$10^{-3}\ m \cdot K$
Conversion factors and units			
Electron volt, $(e/C)J = \{e\}J$	eV	1.60217653 (14)	10^{-19} J
Atomic mass unit (unified), $m_u = m(C^{12})/12$	u	1.66053886 (28)	10^{-27} kg
Standard atmosphere	atm	101,325	Pa
Standard acceleration of gravity	g_n	9.80665	$m \cdot s^{-2}$

STUDENTS-HUB.com Uploaded By: Malak Obaid

APPENDIX E

Conversion Factors

Conversion factors are written as equations for simplicity; relations marked with an asterisk are exact.

Length

1 km = 0.6215 mi
1 mi = 1.609 km
1 m = 1.0936 yd = 3.281 ft = 39.37 in
*1 in = 254 cm
*1 ft = 12 in = 30.48 cm
*1 yd = 3 ft = 91.44 cm
1 light-year = 1 $c \cdot$ y = 9.467×10^{15} m
*1 Å = 0.1 nm

Area

*1 $m^2 = 10^4$ cm^2
1 km^2 = 0.3861 mi^2 = 247.1 acres
1 hectare = 10^4 m^2 = 2.471 acres
*1 in^2 = 6.4516 cm^2
1 $ft^2 = 9.29 \times 10^{-2}$ m^2
1 m^2 = 10.76 ft^2
*1 acre = 43,560 ft^2
1 mi^2 = 640 acres = 2.590 km^2

Volume

*1 $m^3 = 10^6$ cm^3
*1 L = 1000 $cm^3 = 10^{-3}$ m^3
1 gal = 3.786 L
1 gal = 4 qt = 8 pt = 128 oz = 231 in^3
1 in^3 = 16.39 cm^3
1 ft^3 = 1728 in^3 = 28.32 L = 2.832×10^4 cm^3

Time

*1 h = 60 min = 3.6 ks
*1 d = 24 h = 1440 min = 86.4 ks
1 y = 365.24 d = 31.56 Ms

Speed

1 km/h = 0.2778 m/s = 0.6215 m/h
1 mi/h = 0.4470 m/s = 1.609 km/h
1 mi/h = 1.467 ft/s

Angle and angular speed

*π rad = 180°
1 rad = 57.30°
1° = 1.745×10^{-2} rad
1 rev/min = 0.1047 rad/s
1 rad/s = 9.549 rev/min

Mass

*1 kg = 1000 g
*1 metric ton = 1000 kg = 1 Mg
1 u = 1.6606×10^{-27} kg
1 kg = 6.022×10^{26} u
1 slug = 14.59 kg
1 kg = 6.852×10^{-2} slug
1 u = 931.50 MeV/c^2

Density

*1 g/cm^3 = 1000 kg/m^3 = 1 kg/L
(1 g/cm^3)g = 62.4 lb/ft^3

Force

1 N = 0.2248 lb = 10^5 dyn
1 lb = 4.4482 N
(1 kg)g = 2.2046 lb

Pressure

*1 Pa = 1 N/m^2
*1 atm = 101.325 kPa = 1.01325 bars
1 atm = 14.7 lb/in^2 = 760 mmHg
= 29.9 inHg = 33.8 ftH_2O
1 lb/in^2 = 6.895 kPa
1 torr = 1 mmHg = 133.32 Pa
1 bar = 100 kPa

Energy

*1 kW · h = 3.6 MJ
*1 cal = 4.1840 J
1 ft · lb = 1.356 J = 1.286×10^{-3} Btu
*1 L · atm = 101.325 J
1 L · atm = 24.217 cal
1 Btu = 778 ft · lb = 252 cal = 1054.35 J
1 eV = 1.602×10^{-19} J
1 u · c^2 = 931.50 MeV
*1 erg = 10^{-7} J

Power

1 horsepower = 550 ft · lb/s = 745.7 W
1 Btu/min = 17.58 W
1 W = 1.341×10^{-3} horsepower
= 0.7376 ft · lb/s
1 W = 1 J/s

Magnetic field

*1 G = 10^{-4} T
*1 T = 10^4 G

Thermal conductivity

1 W/m · K = 6.938 Btu · in/h · ft^2 · F°
1 Btu · in/h · ft^2 · F° = 0.1441 W/m · K

STUDENTS-HUB.com
Uploaded By: Malak Obaid

Nobel Laureates in Physics

Listed are the names and a brief quotation from the award citation for all Nobel laureates in physics. Included, too, are a few Nobel laureates in chemistry whose work was very closely related to physics, this latter group with a (C) following their names. (The Royal Swedish Academy of Sciences, which awards the prizes, has generally considered the discovery of new elements to be chemistry rather than physics.)

Year	Nobel laureate		Citation for
1901	Wilhelm Konrad Roentgen	1845–1923	discovery of X rays
1902	Hendrik Antoon Lorentz Pieter Zeeman	1853–1928 1865–1943	their researches into the influence of magnetism upon radiation phenomena
1903	Antoine Henri Bequerel Pierre Curie Marie Sklowdowska-Curie	1852–1908 1859–1906 1867–1934	his discovery of spontaneous radioactivity their joint researches on the radiation phenomena discovered by Henri Bequerel
1904	Lord Rayleigh (John William Strutt) Sir William Ramsay (C)	1842–1919 1851–1939	investigations of the densities of the most important gases and his discovery of argon his discovery of the inert gaseous elements in air and his determination of their place in the periodic system
1905	Philipp Eduard Anton von Lenard	1862–1947	his work on cathode rays
1906	Joseph John Thomson	1856–1940	his theoretical and experimental investigations on the conduction of electricity by gases
1907	Albert Abraham Michelson	1852–1931	his optical precision instruments and the spectroscopic and metrological investigations carried out with their aid
1908	Gabriel Lippman Ernest Rutherford (C)	1845–1921 1871–1937	his method of reproducing colors photographically based on the phenomena of interference his investigations into the disintegration of the elements and the chemistry of radioactive substances
1909	Guglielmo Marconi Carl Ferdinand Braun	1874–1937 1850–1918	their contributions to the development of wireless telegraphy
1910	Johannes Diderik van der Waals	1837–1923	his work on the state of equations of gases and liquids
1911	Wilhelm Wien Marie Curie (C)	1864–1928 1867–1934	his discoveries regarding the laws governing the radiation of heat her services to the advancement of chemistry by the discovery of the elements radium and polonium and by the isolation of radium and the study of its nature and compounds
1912	Nils Gustaf Dalén	1869–1937	his invention of automatic regulators for use in conjunction with gas accumulators for illuminating lighthouses and buoys

(*Continued*)

STUDENTS-HUB.com
Uploaded By: Malak Obaid

Year	Nobel laureate		Citation for
1913	Heike Kamerlingh Onnes	1853–1926	his investigations of the properties of matter at low temperatures, which led, *inter alia,* to the production of liquid helium
1914	Max von Laue	1879–1960	his discovery of the diffraction of X rays by crystals
1917	Charles Glover Barkla	1877–1944	his discovery of the characteristic X rays of the elements
1918	Max Planck	1858–1947	his discovery of energy quanta
1919	Johannes Stark	1874–1957	his discovery of the Doppler effect in canal rays and of the splitting of spectral lines in electric fields
1920	Charles-Édouard Guillaume	1861–1938	the service he has rendered to precise measurement in physics by his discovery of anomalies in nickel steel alloys
1921	Albert Einstein	1879–1955	his services to theoretical physics, and especially for his discovery of the law of the photoelectric effect
	Frederick Soddy (C)	1877–1956	his contributions to our knowledge of the chemistry of radioactive substances, and his investigations into the origin and nature of isotopes
1922	Neils Bohr	1885–1962	his investigation of the structure of atoms and the radiation emanating from them
	Francis W. Aston (C)	1877–1945	his discovery, by means of his mass spectrograph, of isotopes in a large number of nonradioactive elements, and for his enunciation of the whole-number rule
1923	Robert Andrews Millikan	1868–1953	his work on the elementary charge of electricity and on the photoelectric effect
1924	Karl Manne Georg Siegbahn	1886–1978	his discoveries and researches in the field of X-ray spectroscopy
1925	James Franck Gustav Hertz	1882–1964 1887–1975	their discovery of the laws governing the impact of an electron upon an atom
1926	Jean-Baptiste Perrin	1870–1942	his work on the discontinuous structure of matter, and especially for his discovery of sedimentation equilibrium
1927	Arthur Holly Compton Charles Thomson Rees Wilson	1892–1962 1869–1959	his discovery of the effect named after him his method of making the paths of electrically charged particles visible by condensation of vapor
1928	Owen Willans Richardson	1879–1959	his work on the thermionic phenomenon, and especially for the discovery of the law named after him
1929	Prince Louis-Victor de Broglie	1892–1987	his discovery of the wave nature of electrons
1931	Werner Heisenberg	1901–1976	the creation of quantum mechanics, the application of which has, *inter alia*, led to the discovery of the allotropic forms of hydrogen
1933	Erwin Schrödinger Paul Adrien Maurice Dirac	1887–1961 1902–1984	their discovery of new productive forms of atomic theory

STUDENTS-HUB.com Uploaded By: Malak Obaid

Year	Nobel laureate		Citation for
1934	Harold C. Urey (C)	1893–1991	his discovery of heavy hydrogen
1936	Victor Franz Hess	1883–1964	his discovery of cosmic radiation
	Carl David Anderson	1905–1991	his discovery of the positron
	Peter Debye (C)	1884–1966	his contributions to our knowledge of molecular structure through his investigations on dipole moments and on the diffraction of X rays and electrons in gases
1937	Clinton Joseph Davisson	1881–1958	their experimental discovery of the diffraction of electrons
	George Paget Thomson	1892–1975	by crystals
1938	Enrico Fermi	1901–1954	his demonstrations of the existence of new radioactive elements produced by neutron irradiation, and for his related discovery of nuclear reactions brought about by slow neutrons
1939	Ernest Orlando Lawrence	1901–1958	the invention and development of the cyclotron and for results obtained with it, especially with regard to artificial radioactive elements
1943	Otto Stern	1888–1969	his contributions to the development of the molecular ray method and his discovery of the magnetic moment of the proton
1944	Isidor Issac Rabi	1898–1988	his resonance method for recording the magnetic properties of atomic nuclei
	Otto Hahn (C)	1879–1968	his discovery of the fission of heavy nuclei
1945	Wolfgang Pauli	1900–1958	his discovery of the exclusion principle, also called the Pauli principle
1946	Percy Williams Bridgman	1882–1961	the invention of an apparatus to produce extremely high pressures and for the discoveries he made in the field of high pressure physics
1947	Sir Edward Victor Appleton	1892–1965	his investigations of the physics of the upper atmosphere, especially for the discovery of the Appleton layer
1948	Patrick Maynard Stuart Blackett	1897–1974	his development of the Wilson cloud chamber method and his discoveries therewith in nuclear physics and cosmic radiation
1949	Hideki Yukawa	1907–1981	his prediction of the existence of mesons on the basis of theoretical work on nuclear forces
1950	Cecil Frank Powell	1903–1969	his development of the photographic method of studying nuclear processes and his discoveries regarding mesons made with this method
1951	Sir John Douglas Cockcroft	1897–1967	their pioneer work on the transmutation of atomic nuclei by
	Ernest Thomas Sinton Walton	1903–1995	artificially accelerated atomic particles their discoveries in
	Edwin M. McMillan (C)	1907–1991	the chemistry of the transuranium elements
	Glenn T. Seaborg (C)	1912–1999	
1952	Felix Bloch	1905–1983	the development of new methods for nuclear magnetic precision
	Edward Mills Purcell	1912–1997	measurements and discoveries in connection therewith

(*Continued*)

STUDENTS-HUB.com
Uploaded By: Malak Obaid

Year	Nobel laureate		Citation for
1953	Frits Zernike	1888–1966	his demonstration of the phase contrast method, especially for his invention of the phase contrast microscope
1954	Max Born	1882–1970	his fundamental research in quantum mechanics, especially his statistical interpretation of the wave function
	Walter Bothe	1891–1957	the coincidence method and his discoveries made therewith
1955	Willis Eugene Lamb Jr.	b. 1913	his discoveries concerning the fine structure of the hydrogen spectrum
	Polykarp Kusch	1911–1993	his precision determination of the magnetic moment of the electron
1956	William Shockley	1910–1989	their investigations on semiconductors and their discovery of the transistor effect
	John Bardeen	1908–1991	
	Walter Houser Brattain	1902–1987	
1957	Chen Ning Yang	b. 1922	their penetrating investigation of the parity laws, which led to important discoveries regarding elementary particles
	Tsung Dao Lee	b. 1926	
1958	Pavel Alekseyevich Cherenkov	1904–1990	their discovery and interpretation of the Cherenkov effect
	Ilya Mikhaylovich Frank	1908–1990	
	Igor Yevgenyevich Tamm	1895–1971	
1959	Emilio Gino Segrè	1905–1989	their discovery of the antiproton
	Owen Chamberlain	1920–2006	
1960	Donald Arthur Glaser	b. 1926	the invention of the bubble chamber
	Willard F. Libby (C)	1908–1980	his method to use ^{14}C for age determination in several branches of science
1961	Robert Hofstadter	1915–1990	his pioneering studies of electron scattering in atomic nuclei and for his discoveries concerning the structure of the nucleon achieved thereby
	Rudolf Ludwig Mössbauer	b. 1929	his researches concerning the resonance absorption of γ rays his discovery in this connection of the effect that bears his name
1962	Lev Davidovich Landau	1908–1968	his pioneering theories of condensed matter, especially liquid helium
1963	Eugene Paul Wigner	1902–1995	his contributions to the theory of the atomic nucleus and the elementary particles, particularly through the discovery and application of fundamental symmetry principles
	Maria Goeppert Mayer	1906–1972	their discoveries concerning nuclear shell structure
	J. Hans D. Jensen	1907–1973	
1964	Charles H. Townes	b. 1915	fundamental work in the field of quantum electronics, which has led to the construction of oscillators and amplifiers based on the maser-laser principle
	Nikolai G. Basov	1922–2001	
	Alexander M. Prokhorov	1916–2002	
1965	Shin'ichiro Tomonaga	1906–1979	their fundamental work in quantum electrodynamics, with profound consequences for the physics of elementary particles
	Julian Schwinger	1918–1994	
	Richard P. Feynman	1918–1988	

STUDENTS-HUB.com Uploaded By: Malak Obaid

Year	Nobel laureate		Citation for
1966	Alfred Kastler	1902–1984	the discovery and development of optical methods for studying Hertzian resonance in atoms
1967	Hans Albrecht Bethe	1906–2005	his contributions to the theory of nuclear reactions, especially his discoveries concerning the energy production in stars
1968	Luis W. Alvarez	1911–1988	his decisive contributions to elementary particle physics, in particular the discovery of a large number of resonance states made possible through his development of the techniques of using the hydrogen bubble chamber and data analysis
1969	Murray Gell-Mann	b. 1929	his contributions and discoveries concerning the classification of elementary particles and their interactions
1970	Hannes Alfvén	1908–1995	fundamental work and discoveries in magnetohydrodynamics with fruitful applications in different parts of plasma physics
	Louis-Eugène-Félix Néel	1904–2000	fundamental work and discoveries concerning antiferromagnetism and ferrimagnetism, which have led to important applications in solid-state physics
1971	Dennis Gabor	1900–1979	his invention and development of the holographic method
1972	John Bardeen	1908–1991	their theory of superconductivity, usually called the BCS theory
	Leon N. Cooper	b. 1930	
	J. Robert Schrieffer	b. 1931	
1973	Leo Esaki	b. 1925	their experimental discoveries of tunneling phenomena in semiconductors and superconductors, respectively
	Ivar Giaever	b. 1929	
	Brian D. Josephson	b. 1940	his theoretical predictions of the properties of a supercurrent through a tunnel barrier, in particular those phenomena which are generally known as Josephson effects
1974	Antony Hewish	b. 1924	the discovery of pulsars
	Sir Martin Ryle	1918–1984	his observations and inventions in radio astronomy
1975	Aage Bohr	b. 1922	the discovery of the connection between collective motion and particle motion in atomic nuclei and for the theory of the structure of the atomic nucleus based on this connection
	Ben R. Mottleson	b. 1926	
	L. James Rainwater	1917–1986	
1976	Burton Richter	b. 1931	their pioneering work in the discovery of a heavy elementary particle of a new kind
	Samuel Chao Chung Ting	b. 1936	
1977	Philip Warren Anderson	b. 1923	their fundamental theoretical investigations of the electronic structure of magnetic and disordered systems
	Nevill Francis Mott	1905–1996	
	John Hasbrouck Van Vleck	1899–1980	
1978	Pyotr L. Kapitza	1894–1984	his basic inventions and discoveries in the area of low-temperature physics
	Arno A. Penzias	b. 1933	their discovery of cosmic microwave background radiation
	Robert Woodrow Wilson	b. 1936	

(*Continued*)

STUDENTS-HUB.com Uploaded By: Malak Obaid

Year	Nobel laureate		Citation for
1979	Sheldon Lee Glashow Abdus Salam Steven Weinberg	b. 1932 1926–1996 b. 1933	their contributions to the theory of the unified weak and electromagnetic interaction between elementary particles, including, *inter alia*, the prediction of the weak neutral current
1980	James W. Cronin Val L. Fitch	b. 1931 b. 1923	the discovery of violations of fundamental symmetry principles in the decay of neutral K-mesons
1981	Nicolaas Bloembergen Arthur L. Schawlow Kai M. Siegbahn	b. 1920 1921–1999 b. 1918	their contributions to the development of laser spectroscopy his contribution to the development of high-resolution electron spectroscopy
1982	Kenneth G. Wilson	b. 1936	his theory for critical phenomena in connection with phase transitions
1983	Subrahmanyan Chandrasekhar William A. Fowler	1910–1995 1911–1995	his theoretical studies of the physical processes of importance to the structure and evolution of the stars his theoretical and experimental studies of the nuclear reactions of importance in the formation of the chemical elements in the universe
1984	Carlo Rubbia Simon van der Meer	b. 1934 b. 1925	their decisive contributions to the large project, which led to the discovery of the field particles W and Z, communicators of the weak interaction
1985	Klaus von Klitzing	b. 1943	the discovery of the quantized Hall effect
1986	Ernst Ruska Gerd Binnig Heinrich Rohrer	1906–1988 b. 1947 b. 1933	his fundamental work in electron optics and for the design of the first electron microscope their design of the scanning tunneling microscope
1987	J. Georg Bednorz Karl Alex Müller	b. 1950 b. 1927	their important breakthrough in the discovery of superconductivity in ceramic materials
1988	Leon M. Lederman Melvin Schwartz Jack Steinberger	b. 1922 1932–2006 b. 1921	the neutrino beam method and the demonstration of the doublet structure of the leptons through the discovery of the muon neutrino
1989	Hans G. Dehmelt Wolfgang Paul Norman F. Ramsey	b. 1922 1913–1993 b. 1915	their development of the ion trap technique the invention of the separated oscillatory fields method and its use in the hydrogen maser and other atomic clocks
1990	Jerome I. Friedman Henry W. Kendall Richard E. Taylor	b. 1930 1926–1999 b. 1929	their pioneering investigations concerning deep inelastic scattering of electrons on protons and bound neutrons which have been of essential importance for the development of the quark model in particle physics

STUDENTS-HUB.com Uploaded By: Malak Obaid

Year	Nobel laureate		Citation for
1991	Pierre-Gilles de Gennes	1932–2007	his discovering that methods developed for studying ordered phenomena in simple systems can be generalized to more complex forms of matter, in particular, to liquid crystals and polymers
1992	Georges Charpak	b. 1924	his invention and development of particle detectors, particularly multi-wire proportional counters
1993	Joseph H. Taylor, Jr. Russell A. Hulse	b. 1941 b. 1950	their discovery of rare binary pulsars
1994	Bertram N. Brockhouse Clifford G. Shull	1918–2003 1915–2001	their pioneering contributions to the development of neutron scattering techniques for studies of condensed matter
1995	Martin Perl Frederick Reines	b. 1927 1918–1998	for his discovery of the tau lepton for his discovery of the neutrino
1996	David Lee Douglas Osheroff Robert Richardson	b. 1931 b. 1945 b. 1937	for their discovery of the superfluid phase of ^{3}He
1997	Steven Chu Claude Cohen-Tannoudji William Phillips	b. 1948 b. 1933 b. 1948	for their development of techniques to chill atoms to millionths of a kelvin above absolute zero and to trap them with laser light
1998	Robert B. Laughlin Horst L. Störmer Daniel C. Tsui	b. 1950 b. 1949 b. 1939	for their discovery of a new form of quantum fluid with fractiionally charged excitations
1999	Gerardus ‘t Hooft Martinus J. G. Veltman	b. 1946 b. 1931	for elucidating the quantum structure of electroweak interactions in physics
2000	Zhores I. Alferov Herbert Kroemer Jack S. Kilby	b. 1930 b. 1928 1923–2005	for basic work on information technology for his part in the invention of the integrated circuit
2001	Eric A. Cornell Wolfgang Ketterle Carl E. Weiman	b. 1961 b. 1957 b. 1951	for the achievement of Bose-Einstein condensation in dilute gases of alkali atoms and early fundamental studies of the properties of the condensates
2002	Raymond Davis, Jr. Masatoshi Koshiba Riccardo Giacconi	1914–2006 b. 1926 b. 1931	their pioneering contributions to astrophysics, in particular the detection of cosmic neutrinos his pioneering contributions to astrophysics, which have led to the discovery of cosmic x-ray sources
2003	Alexei A. Abrikosov Vitaly L. Ginzburg Anthony J. Leggett	b. 1928 b. 1916 b. 1938	for pioneering contributions to the theory of superconductors and superfluids

(*Continued*)

STUDENTS-HUB.com Uploaded By: Malak Obaid

Year	Nobel laureate		Citation for
2004	David J. Gross H. David Politzer Frank Wilczek	b. 1941 b. 1949 b. 1951	for the discovery of asymptotic freedom in the theory of the strong interaction
2005	Roy J. Glauber John L. Hall Theodor W. Hänsch	b. 1925 b. 1934 b. 1941	for his contribution to the quantum theory of optical coherence for their contributions to the development of laser-based precision spectroscopy, including the optical frequency combo technique
2006	John C. Mather George F. Smoot	b. 1946 b. 1945	for their discovery of the blackbody form and anisotropy of the cosmic microwave background radiation

STUDENTS-HUB.com Uploaded By: Malak Obaid

Answers

These results are usually rounded to three significant figures. Differences in the third significant figure may result from rounding and are not important. When the solution is a diagram, graph, derivation, or proof, reference is made to the *Students Solution Manual* (*SSM*) where the solution appears.

Chapter 1

1-1. (a) 4.4×10^8 m/s (b) No, since the droid is moving faster than light speed relative to Hoth.

1-5. (a) At $t = 2$ s, a bright circle reflected from great circle perpendicular to the motion. (b) At $t = 2$ s, the entire interior lights up.

1-9. $\Delta t \approx 4.63 \times 10^{-13}$ s

1-13. (a) 3.76×10^{-5} s (b) 2.0×10^{-5} s

1-17. (a) See *Students Solution Manual (SSM)* (b) When 10 s have passed on the rocket's clock, only 6 s have passed on the lab clock.

1-21. $0.14c$

1-25. $0.527c$

1-29. (a) In S': $V' = 16$ m^3; in S: $V = 12.2$ m^3 (b) See *SSM*

1-33. 657.0 nm, 662.9 nm, 725.6 nm

1-37. 3.0 m

1-41. 9.6 ms

1-45. (a) See *SSM* (b) $v = 1.44 \times 10^8$ m/s (c) 4.39 μs (d) 4.39 μs

1-49. (a) $v = 0.5c$ in the $-x$ direction (b) 0.58 y (c) 0.866 $c \cdot$ y (d) spacelike (e) 0.866 $c \cdot$ y

1-53. $\theta' = 0.494\, v_y/c$

1-57. (a) 120 min (b) 240 min (c) identical

1-61. (a) $A \rightarrow B$: $T/2 + 2vL/(c^2 - v^2)$; $B \rightarrow A$: $T/2 + 2vL/(c^2 - v^2)$ (b) $4vL/(c^2 - v^2)$

Chapter 2

2-1. See *SSM*

2-5. 1.1×10^{-16} kg, mass increases

2-9. (a) $0.99998898c$ (b) 3.94×10^4 GeV/c (c) 3.31×10^9 GeV; -3.31×10^9 GeV/c

2-13. (a) 3.5×10^{-7} (b) 0.0079

2-17. 6.26 MeV

2-21. 280 MeV

2-25. See *SSM*

2-29. $m = 1673$ MeV/c^2, $u = 0.286c$

STUDENTS-HUB.com
Uploaded By: Malak Obaid

2-33. (c) is correct.
2-37. 8.62 ms
2-41. (a) 1.73×10^5 m/s (b) 1.5×10^5 m/s (c) 155 kg
2-45. See *SSM*
2-49. (a) $v = E/Mc$ (b) $\Delta x = EL/Mc^2$ (c) $m \approx E/c^2$
2-53. (a) See *SSM* (b) See *SSM*

Chapter 3

3-1. proton 6.5×10^{-2} m; electron 3.6×10^{-5} m; deuteron 0.13 m; H_2 0.13 m; helium 0.26 m
3-5. (a) 2.2 mm (b) 9.1×10^9 Hz, 1.1×10^{-10} s
3-9. See *SSM*
3-13. 5.67×10^{-8} W/m^2 K^4
3-17. 16 R_1
3-21. 278.3 K (5.3 °C)
3-25. (a) 255 nm (b) 1.4×10^{-4}
3-29. (a) 1.03×10^{15} Hz (b) ultraviolet
3-33. 4.14×10^{-3} nm; 5.8%
3-37. 0.243 nm
3-41. (a) electron 0.00243 nm; proton 1.32 fm (b) electron 0.510 MeV; proton 939 MeV
3-45. (a) 2.08 eV (b) 4.95×10^{14} Hz (c) 4.19×10^{-15} eV/Hz
3-49. See *SSM*
3-53. See *SSM*
3-57. (a) 0.0309 nm, 0.1259 nm (b) 9.90 keV

Chapter 4

4-1. Lyman 91.16 nm; Balmer 364.6 nm; Paschen 820.4 nm
4-5. 4103 nm
4-9. 45.5 fm; 29.5 fm; 19.0 fm
4-13. (a) 1.91 nm (b) 0.95 nm
4-17. 8.22×10^{14} Hz, 8.22×10^6 revolutions
4-21. See *SSM*
4-25. (a) 19.0 μm (b) 3.65×10^3 m/s
4-29. 680 fm
4-33. 1.90×10^{-8} Hz$^{-1/2}$
4-37. 10.2 V
4-41. (a) 1.054×10^{-3} A (b) 9.27×10^{-24} A · m^2
4-45. (a) Lyman α: $n = 6 \rightarrow n = 3$ Lyman β: $n = 9 \rightarrow n = 3$ (b) $\Delta\lambda = 0.056$ nm
4-49. (a) $b = R\cos(\theta/2)$ (b) $I_0R^2\cos^2(\theta/2)$ (c) πR^2 (d) See *SSM*
4-53. For $n = 1$: $v = 0.0075cZ^{1/2}$; $E = -14.4Z$ eV
4-57. 10; 1,042

STUDENTS-HUB.com Uploaded By: Malak Obaid

Chapter 5

5-1. (a) 2.1×10^{-23} m (b) 2.1×10^{-21} m/y
5-5. 0.0276 nm
5-9. (a) 0.445 fm (b) 6.18×10^{-3} fm
5-13. $\lambda = 0.523$ nm; $E_k = 3.0 \times 10^{-3}$ eV
5-17. (a) See *SSM* (b) 50 m/s (c) 50 m/s (d) $\Delta x = 5\pi$ m; $\Delta k = 0.4$ m^{-1}
5-21. 3.2×10^{-5} s
5-25. (a) $A^2\,dx$ (b) $0.61A^2\,dx$ (c) $0.14A^2\,dx$ (d) $x = 0$
5-29. 1.99×10^{-21} eV
5-33. (a) 5.3×10^{-10} (b) 1.32×10^{-7} eV
5-37. See *SSM*
5-41. (a) See *SSM* (b) See *SSM*
5-45. (a) 1840 MeV (b) 2.02 fm (c) 1.22 fm (d) 0.76 fm
5-49. (a) 0.243 nm (b) 0.511 MeV (c) 0.511 MeV/c (d) 2.43×10^{-3} nm
5-53. 1.2×10^{-6} eV, 1.2 eV

Chapter 6

6-1. See *SSM*
6-5. See *SSM*
6-9. (a) 0.021 eV (b) 205 MeV
6-13. (a) $\Delta x = 10^{-6}$ m; $\Delta p = 10^{-16}$ kg · m/s (b) 9×10^{11}
6-17. See *SSM*
6-21. 1.21×10^{-7} N
6-25. 0.87 nm
6-29. (a) $L/2$ (b) $0.320L^2$
6-33. $\langle x \rangle = 0$; $\langle x^2 \rangle = \hbar/(2m\omega)$
6-37. (a) See *SSM* (b) $\langle x \rangle = 0$ (c) $\langle x^2 \rangle = 3\hbar/(2m\omega)$ (d) $\langle V(x) \rangle = 3\hbar\omega/4$
6-41. (a) 2.33×10^{-34} J (b) 2.1×10^{28} (c) 0.70 Hz
6-45. (a) 4.3×10^{-6} is the transmitted fraction (b) See *SSM*
6-49. (a) $R = 0.111$; $T = 0.889$ (b) $R = 0.111$; $T = 0.889$
6-53. $\langle E_k \rangle = \hbar^2/(2mL^2)$
6-57. (a) 4.95×10^{-13} (b) 0.197
6-61. (a) $0.39c$ (b) See *SSM* (c) 8.03×10^5 eV (d) 3.76×10^5 eV

Chapter 7

7-1. $11E_0$, $12E_0$, $14E_0$, The 1st, 2nd, 3rd, and 5th excited states are degenerate.
7-5. (a) See *SSM* (b) 1, 1, 4 and 1, 2, 2
7-9. (a) 0, 1, 2 (b) For $\ell = 0$, $m = 0$; for $\ell = 1$, $m = \pm 1, 0$; for $\ell = 2$, $m = \pm 2, \pm 1, 0$ (c) 18
7-13. (a) $2\hbar^2$ (b) $6\hbar^2$ (c) $5\hbar^2$ (d) $n = 3$
7-17. (a) $n = 6$, $\ell = 3$ (b) -0.38 eV (c) 3.65×10^{-34} J · s (d) $\pm 3\hbar$, $\pm 2\hbar$, $\pm\hbar$, 0
7-21. See *SSM*

STUDENTS-HUB.com Uploaded By: Malak Obaid

7-25. (a) $0.606(1/a_0)^{3/2}/\sqrt{32\pi}$ (b) $0.368(1/a_0)^3/(32\pi)$ (c) $0.368/(8a_0)$
7-29. See *SSM*
7-33. (a) 4 (b) 3
7-37. See *SSM*
7-41. See *SSM*
7-45. Sn: $1s^22s^22p^63s^23p^63d^{10}4s^24p^64d^{10}5s^25p^2$
Nd: $1s^22s^22p^63s^23p^63d^{10}4s^24p^64d^{10}5s^25p^64f^46s^2$
Yb: $1s^22s^22p^63s^23p^63d^{10}4s^24p^64d^{10}4f^{14}5s^25p^66s^2$
7-49. (a) silicon, Si (b) calcium, Ca
7-53. Similar to H: Li, Rb, Ag, and Fr
Similar to He: Ca, Ti, Cd, Ba, Hg, and Ra
7-57. $D_{5/2} \rightarrow P_{1/2}$ is *j*-forbidden
7-61. (a) 2.90×10^{-6} eV (b) 7.83×10^{-4} nm (c) 0.638 T
7-65. (a) 1.67×10^6 m/s^2 (b) 1.95 cm
7-69. (a) See *SSM* (b) See *SSM*
7-73. (a) through (e) See *SSM*

Chapter 8

8-1. (a) 1930 m/s (b) 1.01×10^4 K
8-5. (a) 3400 J (b) One mole of any gas has the same translational energy at the same temperature.
8-9. See *SSM*
8-13. $C_v = R$, $C_p = 2R$, and $\gamma = 2$
8-17. (a) n_2/n_1 and n_3/n_1 are both ≈ 0 (b) 19,760 K (c) 0.7%
8-21. See *SSM*
8-25. See *SSM*
8-29. See *SSM*
8-33. See *SSM*
8-37. (a) $f_{FD}(E) = [e^{10(E-E_F)/E_F} + 1]^{-1}$ (b) See *SSM*
8-41. $\langle E_{K(\text{escape})} \rangle = 2kT$
8-45. See *SSM*

Chapter 9

9-1. (a) 23.06 kcal/mol (b) 98.5 kcal/mol (c) 1.08 eV/molecule
9-5. (a) −5.39 eV (b) 4.83 eV (c) 0.46 eV
9-9. For KBr: 0.19 eV For RbCl: 0.23 eV
9-13. 2.63×10^{-29} C · m
9-17. (a) 0.67 nm (b) 55 nm (c) See *SSM*
9-21. 1.78×10^{-4} eV
9-25. (a) 18.6 u (b) 0.280 nm
9-29. 0.04×10^{-5} eV
9-33. about 5.5×10^{31}
9-37. 1.28×10^{16}/s
9-41. (a) 8.47×10^{-5} radians (b) 5.08×10^{-3} W/cm^2

STUDENTS-HUB.com Uploaded By: Malak Obaid

9-45. (a) $E_3 = 1.44 \times 10^{-3}$ eV, $E_2 = 9.61 \times 10^{-4}$ eV, $E_1 = 4.79 \times 10^{-4}$ eV, vibrational states (note equal spacing); See *SSM* (b) 0.215 nm

9-49. 480 N/m

9-53. (a) 0.31 eV (b) 8.9×10^{-14} eV · nm[20]

9-57. (a) 4.58×10^{-48} kg · m^2 (b) 1.32×10^{14} Hz

Chapter 10

10-1. 4.64

10-5. 4.09 eV/atom

10-9. 4.18

10-13. (a) 5.86×10^{22}/cm^3 (b) 5.90×10^{22}/cm^3

10-17. 1.87 eV

10-21. (a) 34.2 nm (b) 41.4 nm (c) 43.1 nm

10-25. 6.7×10^{-3}

10-29. (a) 0.37 eV (b) 4300 K

10-33. See *SSM*

10-37. (a) 27.8 mV (b) −12.0 mV

10-41. For ^{206}Pb: 7.217 K; for ^{207}Pb: 7.200 K; for ^{208}Pb: 7.183 K

10-45. (a) 0.95 (b) 0.71 (c) 0.32

10-49. (a) See *SSM* (b) *See SSM* (c) 0.0055

10-53. silicon: 3.17 nm; germanium: 8.46 nm

10-57. (a) 1.28×10^{13} Hz (b) 23.4 μm

Chapter 11

11-1. See *SSM*

11-5. See *SSM*

11-9. (a) 6.46 MeV/nucleon (b) 7.47 MeV/nucleon (c) 8.77 MeV/nucleon

11-13. (a) 2.70 fm; 3.53 fm (b) 4.26 fm; 5.57 fm (c) 6.34 fm; 8.30 fm

11-17. (a) 5.21 h (b) 3.11×10^6 atoms

11-21. 33.2 min

11-25. $A = 191$; $B = -72.2$

11-29. 1.00 MeV

11-33. 93 keV

11-37. 789 MeV/c^2

11-41. ^{36}S, ^{53}Mn, ^{82}Ge, ^{88}Sr, ^{94}Ru, ^{131}In, ^{145}Eu

11-45. $^{30}_{14}$Si, $j = 0$; $^{37}_{17}$Cl, $j = 3/2$; $^{55}_{27}$Co, $j = 7/2$; $^{90}_{40}$Zr, $j = 0$; $^{107}_{49}$In, $j = 9/2$

11-49. (a) −4.97 MeV (b) 1.92 MeV

11-53. 224 MeV

11-57. 1.78×10^{14} atoms/s

11-61. (a) 8.78×10^{12} J (b) 145 y

11-65. 1.90×10^9 y

11-69. (a) 10^{13} (b) 0.149 mg (c) 2.15×10^4 y

11-73. See *SSM*

11-77. (a) 5.06×10^{-6} eV (b) 4.71×10^{-2} eV (c) 1.17 cm/s

STUDENTS-HUB.com Uploaded By: Malak Obaid

11-81. (a) ^{141}Ba: 6.24×10^{-15} m; ^{92}Kr: 5.42×10^{-15} m (b) 249 MeV
11-85. 7.03×10^{8} y
11-89. (a) See *SSM* (b) 51.7 MeV (c) 1.43 MeV (c) 96.5 MeV
11-93. (a) See *SSM* (b) See *SSM* (c) See *SSM* (d) See *SSM* (e) See *SSM*
11-97. (a) See *SSM* (b) 8.66×10^{4}
11-101. (a) 137% (b) 0.00498

Chapter 12

12-1. (a) See *SSM* (b) 139.6 MeV (c) 8.88 fm
12-5. (a) 1.711 MeV (b) 78.5 eV (c) 2.16 MeV/c
12-9. (a) weak (b) electromagnetic (c) strong (d) weak
12-13. $m \approx 22$ eV/c^2
12-17. (a) Conservation of energy and lepton number are violated. (b) Conservation of energy is violated. (c) Conservation of linear momentum is violated. (d) No conservation laws are violated. (e) Conservation of lepton number is violated. (f) Conservation of baryon number is violated.
12-21. (a) Conservation of lepton number is violated. (b) Allowed. (c) Allowed. (d) Conservation of baryon number and angular momentum are violated. (e) Allowed.
12-25. See *SSM*
12-29. *uuu*
12-33. −138.3 MeV Energy is not conserved.
12-37. (a) $c\bar{d}$ (b) $\bar{c}d$
12-41. (a) Energy is not conserved. (b) Angular momentum is not conserved. (c) Angular momentum is not conserved.
12-45. (a) The final products are all stable. (b) See *SSM* (c) See *SSM* (d) No. Energy is not conserved.
12-49. (a) No conservation laws are violated. (b) Conservation of energy and baryon number are violated. (c) No conservation laws are violated.
12-53. (a) 1193 MeV (b) 77 MeV/c (c) 2.66 MeV (d) 74.3 MeV/c

Chapter 13

13-1. 25.3 d
13-5. 10.4 eV/c^2
13-9. 17.0 pc
13-13. (a) 9400 y (b) $R_{\text{star}} = 1.96R_{\odot}$ using the T_e relation
13-17. (a) $3.27 \times 10^{9}\ c \cdot$ y (b) 10%
13-21. 5.5×10^{97} kg/m^3; 1.67×10^{18} kg/m^3; 2.45×10^{4} kg/m^3
13-25. See *SSM*
13-29. (a) 8.33×10^{56} (b) 8.89×10^{44} J (c) 1.7×10^{10} y
13-33. $\approx$ 0.001 "new" H atoms/m$^3 \cdot 10^6$ y; No.
13-37. (a) See *SSM* (b) 1.1×10^{-12} cm^3 (c) $\approx 0.1\%\ M_{\odot}$

STUDENTS-HUB.com Uploaded By: Malak Obaid

INDEX

boldface indicates a definition
italics indicates a figure
t indicates a table
* indicates a MORE section on the home page: www.whfreeman.com/tiplermodernphysics5e
# indicates a Classical Concept Review section on the home page: www.whfreeman.com/tiplermodernphysics5e

Absolute magnitude (*M*), **633**
Absorption, 393
Absorption spectra. *See* Spectra
ac Josephson effect, **467**–468
Accelerator mass spectroscopy (AMS), **537,** 545, 546–548, *548*
Accelerators, particle, *71,* 477, *516,* 561–562
  and liquid helium, 336
  and the quark model of hadrons, 591
  and relativistic momentum, 67
  and superconductivity, 458
Acceptor levels, **448**
Accretion disks, **644,** *644*
Active galaxies, *656,* **656**–657, *657*
Active Sun, 627–629
Akimitsu, Jun, 458
Alkali atoms, excited states of, 301–303, *302*
Alley, C. O., 33
Alpha decay, 258–259, 496–499
  and decay chains, 497–498, *498*
  energetics of, 498*
Alpha particles (α), 178, 477
  scattering of, and atomic models, *151,* 151–159, *152, 153, 154, 156, 157,* 477
Amaldi, Edoardo, 553
Ambler, E., 588, 589
Ammonia inversion spectra, **392**
Amorphous solids, **414**
AMS. *See* Accelerator mass spectroscopy (AMS)
Anderson, Carl David, 356, 477, 552, 561, 562–563, 612
Anglo-Australian Observatory, 661
Angular frequency (ω), **196**
Angular momentum (**L**), 379
  conservation of, 275
  nuclear (**I**), 489–492
  quantization of, 161, 275–277
  relativistic (**L**), 80–81
  spin (**S**), 285–290
  and spin-orbit effect, **293**–295
  total (**J**), 291–293
Angular momentum operators, 245*t*
Angular momentum quantum number (ℓ), **276**
  spin (m_s), **285**
  total (j), **291**
Annihilation of particles, **90**–93, *91,* 565–566
  Feynman diagram for, *567*
Anthropic principle, **673**
Antibaryons, **591**
Antibonding orbitals, **373,** *373*
Antielectrons. *See* Positrons (e^+)
Antiferromagnetism, **436**
Antihydrogen, 565
  and lasers, 403
Antineutrons, 564
Antiparticles, **90, 500,** 562–566, 573*t,* 604
Antiprotons, 114, 612
Apparent magnitude (*m*), **632**–633, **677**
Approximations
  first-order perturbation theory, **298**
  in nuclear physics, 507, 514, 519
  in relativity, 94–97, 610
  and the Schrödinger equation, 228, 230, 269, 295, 297
  in statistical physics, 356
Aristotelian physics, 1, 3
Aristotle, 1, 6, 630, 636
Artwork
  authentication of, *537,* 537–539
  dating of, *543,* 543–544
Associated Legendre functions, **274,** 281
Astronomical units (AU), 620
Astrophysics, **619**–661. *See also* Cosmology; Stars; Sun
  and cataclysmic events, 644–646
  and galaxies, 653–661
  and radiometric dating, 545–546
  and stars, 630–643, 647–652
  and the Sun, 619–630
  and surface temperatures of stars, 121
Asymptotic freedom, **600**
Atomic beam fluorescence spectroscopy, 490
Atomic clocks, **260,** 392, 396
  testing relativity with, 33
Atomic lasers, **343,** *343*
Atomic mass number (*A*), **478**
Atomic mass units (u), 83
Atomic models, 147–184
  and atomic spectra, 147–150
  Bohr, 159–169, 176*
  and the Franck-Hertz experiment, 174–176
  Rutherford, 150–159
  Sommerfeld, 167
  Thomson, 150–151, *151*
  and x-ray spectra, 169–173
Atomic number (*Z*), **478**
Atomic physics, 269–314
  and atomic spectra, 301–305
  and electron spin, 285–290
  and hydrogen atom wave functions, 281–285
  and the periodic table, 297–301
  and quantization of angular momentum and energy, 272–281
  and the Schrödinger equation for multiple particles, 295–297
  and the Schrödinger equation in three dimensions, 269–272
  and the spin-orbit effect, 291–295
Atomic radii, 300, *301*
Atomic spectra, 148–150, *149*
  and excited states, 301–303, *302*
Auger, Pierre, 173
Auger effect, **173,** *173*
Auger electrons, 173, 548
Auroras, 628
Autumnal equinox, **637,** *637*
Avalanche breakdown, **454**
Average speed ‹*v*›, 320, *320*
Avogadro's hypothesis, 115
Avogadro's number (N_A), **116,** 214
Awschalom, David, 452
Axions, **639**

BL Lac objects, **656**
Bahcall, John, 607, 612, 625, 626, 675
Balmer, Johann, 149
Balmer series, **149,** *149, 163,* 164
  and density of states, 318
  redshift of, 44
Band spectra, **147**
Band theory of solids, 438*–445*, **440,** *440*
  and conductors, 441–442, *442*
  and impurity semiconductors, 445–452
  and insulators, 442, *442*
  and intrinsic semiconductors, *442,* 442–445
  Kronig-Penney model of, *438,* **438**–441, *439*
Bands. *See* Band theory of solids
Bardeen, John, 456, 463, 471
Barkla, Charles G., 172, 179, 307
Barns, **521**
Barred spiral galaxies, **654**–655, *655*
Barrier penetration. *See* Tunneling
Barrier potentials, *256,* 256–257
Baryon decuplet, *587,* **591**
Baryon number, **564,** 569*t,* 583, 583*t,* 586*t*
  conservation of, 581
  nonconservation of, 607
Baryon octet, *587,* **591,** *592, 595*
Baryons, **569,** 573*t, 587,* 594*t*
  supermultiplets of, *598*
Bases, transistor, **456,** *456*
BATSE. *See* Burst and Transient Source Experiment (BATSE)
BCS theory of superconductivity, **463**–465, 510
BEC. *See* Bose-Einstein condensates (BEC)
Becquerel, Antoine Henri, 477, 495, 552
becquerels (Bq), **493**
Bednorz, Johannes G., 466
Bennet, W. R., Jr., 401
BeppoSAX satellite, 652
Beta decay, 499–504
  β^+, 501
  β^-, 499–500
  double, 503
  electron capture, 502–504
  inverse, 646, 648
Beta particles (β), 151, 477
Betelgeuse, 620, 643
Bethe, Hans Albrecht, 535, 625, 675
Big Bang, 668–672, *670,* 676
  and blackbody radiation, *126,* 126–127, 664, *664,* 668–669
  fusion reactions during, 556, 668, *668*
  and inflation, **669**
  and quantum fluctuations, 206

STUDENTS-HUB.com
Uploaded By: Malak Obaid

Big Crunch, 666
Binary pairs, **644,** *644*
Binding energy (E_b), 81–84, **83, 163**
  nuclear (B), 488–489, *489,* 495, *495,* 513, *514*
Binnig, Gerd, 257
Black dwarfs
Black holes, 105–106, **650**–651, *651*
  at center of the Milky Way, *635,* 650–651
  simulating, 305
Blackbody radiation, 119–127, 129
  from Big Bang, 664, *664,* 668–669
  energy density in, 122
  ideal, **120**
  as photon gas, 344–351
  solar, 620–621, *621*
Bloch, Felix, 221, 262, 439, 470
Bloch functions, **439**
Blueshift, **42, 43**
  gravitational, 104–105
Body-centered cubic (bcc) crystal symmetry, 418
Bohr, Aage N., 527
Bohr, Niels H. D., *159,* 179, 215
  and atomic model, 159–162, 164, 165, 170, 176*, 226
  and nuclear reactions, 521
Bohr frequency condition, **160**
Bohr magneton (μ_B), **182, 287,** 552
  and magnetism, 435
Bohr radius (a_0), **161,** 279
  and probability density, 282–283
Boks, J., 335
Boltzmann, Ludwig, 356
  and kinetic theory, 316, 319
  and thermodynamics, 120
Boltzmann constant (k), 122, **316**
Boltzmann distributions ($f_B(E)$), **316**
  and conduction, 425, 430
  and quantization of energy states, 346
  vs. other distributions, 329–333, *331*
Boltzmann factor ($e^{-E/kT}$), **316**
  and energy-level populations, 385, 388–389, 394
Bond lengths (r_0), 366, 368*t*
  and rotational spectra, 380
Bonding orbitals, **373,** *373*
Bonds, molecular, 416*t*. *See also* Covalent bonds; Ionic bonds
  dipole-dipole, **364, 375**–379, *377, 378*
  and electron configurations, 363
  hydrogen, **377,** *378*
  metallic, **364, 375, 415, 421**–422, *422*
  other types, 375*–379
  saturated, **374**
  and wave functions, 284, *285*
Born, Max, 192, 215, 225, 307
Born exponents (n), **470**
Bose, Satyendra Nath, 329, 356
Bose-Einstein condensates (BEC), 335–343, **341,** *343,* 354
  fermion analog of, 353–354, *354*
  and lasers, 403
  and photon gases, 344–351
  and slowing of light, 304–305, *305*
Bose-Einstein distributions ($f_{BE}(E)$), **316,** 328–**329**
  and composition of the nucleus, 479
  vs. other distributions, 329–333, *331*
Bosons, **329**–332
  as force mediators, 571, 602
  Higgs, 568, 581, **603**
  $W^{\pm}$ and Z^0, 575, *575,* 576*t,* 602–603
Bottom (B'), 570, 583, 583*t*
Boundary conditions, **230**
  and energy quantization, 225
  in three dimensions, 270
Brackett, F. S., 164
Brackett series, 180
Bragg, William H., 141, 169
Bragg, William L., 134, 141, 169
Bragg condition, **135,** *135*
  and band theory of solids, 440–441
  for electrons, 188–189, *189*
Bragg planes, **134,** *134*
Brattain, Walter H., 456, 471
Bremsstrahlung, **134,** 136, *136,* 511
Brillouin zones, **441**
Brookhaven National Laboratory, 564, 595, 597
Bubble chambers, *564, 572, 584*
Burst and Transient Source Experiment (BATSE), 652

Cabrera, B., 608
Cannon, Annie Jump, 632, 676
Carbon dating, *543,* 543–545
  and accelerator mass spectroscopy, 546–547
Carnot, Nicolas Léonard Sadi, 1
CAT. *See* Computer assisted tomography (CAT)
Cathode-ray tubes (CRTs), 117
Causality, and special relativity, 37, 39, *39,* 54–55, *55*
CDs. *See* Compact discs (CDs)
CEBAF. *See* Continuous Electron Beam Accelerator Facility (CEBAF)
Celestial sphere, *636,* **636**–637
Center-of-mass reference frames, *519,* **519,** 522
Cepheid variables, as standard candles, 640, 654, 676
CERN. *See* European Organization for Nuclear Research (CERN)
Chadwick, James, 477, 479, 500, 552, 561
Chain reactions, 527, **530**
Chamberlain, Owen, 564, 612
Chandra X-Ray Observatory, 650, 651
Chandrasekhar, Subrahmanyan, 647, 676
Chandrasekhar limit, **647,** 648
Characteristic rotational energy (E_{0r}), **380,** 389*t*
Characteristic spectra, **135,** *136*
Charge
  color, **569**–570, 576*t,* **596**–597
  density of, in nucleus, *482*
  electric, 118–119, 569*t,* 576*t,* 583, 583*t*
  flavor, **568,** 569*t,* **574**
  gravitational, 576, 576*t*
  magnetic, 608
  weak, **570, 574,** 576*t*
Charge multiplets, 572, **585**–586, 606
Charged current, ***574***
Charged weak force, **574**
Charm (C), 570, 583, 583*t,* 597, *597*
Chirped pulse amplification, **403**
Christenson, J. H., 590
Chromosphere, *622,* **622**–623, *623*
Classical Concept Reviews. *See also* Exploring; More
  charge-to-mass ratio (e/m) of electrons, 116#
  conduction, 423#
  Fourier integrals, 199#
  Galilean transformation of coordinates, 6#
  inertial reference frames, 6#
  interference fringes, 9#
  kinetic theory, 315#, 316#, 319#, 328#
  Millikan oil-drop experiment, 119#
  relativity, 6#
Classical novae, **644**
Classical physics. *See also* Newtonian physics
  conduction, **422**–426, 423#
  dynamics, 65–66, 81
  failures of, 325, 327, 346–347, 422, 425
  history of, 1–2
  particles, 212
  and relativistic approximations, 95–96
  statistical, 316–328
  uncertainty relations, 199–201, **200**
  wave equation, **196,** 202, 212
Classical relativity, 4–6#, 8–9, 11
Clausius, Rudolf, 325
Clocks. *See also* Time
  atomic, 33, **260,** 392, 396
  in gravitational fields, 103–105
  light, **29,** *30*
  local, **15**
  reference, **13,** *14*
Closed universe, **666**
Clusius, K., 337
COBE. *See* Cosmic Background Explorer (COBE) satellite
Coblenz, W. W., 123
Cockcroft, John D., 477, *516,* 552
Coefficient of reflection (R), 253, *254*
Coefficient of transmission (T), 253, *254*
  and alpha decay, 259, 497
  and tunneling, 257
Coherent radiation, *391,* **394**
Cohesive energy, **417,** 420
Collectors, transistor, **456,** *456*
Collisions. *See also* Scattering
  and atomic energy levels, *174,* 174–175
  elastic, 66–67, *67*
  between electromagnetic radiation and matter, 137–139
  inelastic, *76,* 76–77
  and relativistic energy, *76,* 76–77
  and relativistic momentum, 66–67, *67*
Color charge, **569**–570, 576*t*
  and quark model of hadrons, **596**–597
  and strong interaction, 570, 571
Comoving coordinates, **660,** *665,* **667**
Comoving space density, **660,** 668
Compact discs (CDs), 404, 437
Complex conjugates, 204, 225, 262
Complex numbers, 109, 205, 224–225, 262, 407
Compound doublets, **303**
Compound nucleus, **517,** 521–522, *522*
Compton, Arthur H., 133, 137, *138,* 141, 407, 531, 561
Compton edge, **146**
Compton effect, *137,* 137–139, *138,* 390, *391*
  Feynman diagram for, *567*
Compton Gamma Ray Observatory, 652
Compton wavelength (λ_c), **137,** 195
  and limits of knowledge, 673
  and range of strong interaction, 510, 578
Compton's equation, **137,** 138*
Computer assisted tomography (CAT), **478,** 540–542, *541, 542*
Conant, James B., 531
Condon, Edward U., 258, 477
Conduction
  and band theory of solids, 441–442, *442*
  classical, **422**–426, 423#
  electrical, 423–424
  quantum, 430–434
  thermal, 337, 434*
Conduction bands, **441,** *441, 442*
Conductivity (σ), **424**–425. *See also* Superconductivity
Conservation laws, 583*
  of electric charge, **580**
  of energy, 76–81, 517–520, **580,** 663, 666
  and invariant quantities, 66, 73, 580
  of linear and angular momentum, **580**
  in particle physics, 500, 568, 580–591, 590*t,* 594
  in radioactive decay, 496, 500
Constellations, **631,** *631*
Continuity conditions, 228, 252
Continuous Electron Beam Accelerator Facility (CEBAF), *71*
Continuous spectra, **147**–148
Continuous wave lasers, 400–**401**
Conversion electrons, **505**
Cooper, Leon N., 463, 471
Cooper pairs, *463,* **464**–465
  and exchange forces, 510
  in fermion gases, 354
  in Josephson junctions, 467
Coordinate systems
  celestial, *636,* **636**–637

STUDENTS-HUB.com Uploaded By: Malak Obaid

comoving, **660,** *665,* **667**
polar, 101
right-handed *vs.* left-handed, **589,** *589*
spherical, 271–272, *272, 282*
Copernicus, Nicolaus, 3, 57, 636
Core, solar, **623**
Cormack, Allan, 541, 553
Cornell, Eric A., 341, 343
Corona, **623**
Corpuscles, **118**
Correspondence principle, **160**–161
and Bohr atoms, 166
for infinite square wells, 233–234, 236
and Rydberg atoms, 168
for simple harmonic oscillators, 248, *248*
Cosmic Background Explorer (COBE) satellite, 126, 664, 669
Cosmic background radiation, *126,* 126–127, 664, *664*
anisotropies in, 664, *664,* 669
Cosmic rays, **141**
and carbon dating, 543–545
as charged particles, 138
de Broglie wavelength of, 195–196
and pair-production, 90
relativistic speeds of, 22–23
Cosmological constant (Λ), 661, **664,** 667
Cosmological principle, *662,* **662,** 666–667, 669
perfect, **664**
Cosmological redshift, **659**–661
Cosmology, **619,** 662–674. *See also* Astrophysics
and the Big Bang, 126–127, 206
and evolution of the universe, 664–674
and expansion of the universe, 43–44
and general relativity, 101–105, *104*
and gravitation, 662–664
and headlight effect, 52
Coulomb's law
and alpha decay, 258–259, *259*
and atomic models, 159–160, 161
and covalent bonds, *370,* 370–371
Feynman diagrams for, 566–567, *567*
and fission, 528, *528*
and fusion, 625
and phonons, 464
and scattering of charged particles, 153–154, 156*
Coupling constants, **570**–571, 577–578, *605,* 612
for electromagnetic interactions (α), 571, 577
for strong interactions (α_s), 571, 600
Covalent bonds, **364,** 369–375, **374**
other types, 375*, 420*
vs. ionic bonds, 374
Covalent solids, 415–421
Cowan, Clyde, 500
CP violations, 590
Crab nebula, 646, *649,* 649–650, *650*
Creation of particles. *See* Pair production of particles
Creeping films, **338,** *338*
Critical magnetic fields (B_c), 458, 458*t, 459,* 460, *461*
Critical mass density (ρ_0) of the universe, 662–663, 672
Critical population inversion density (Δn_c), **400,** 404–405
Critical temperature (T_c)
for Bose-Einstein condensates, 340–341
for superconductivity, **458,** 458*t, 459,* 466*t*
Cross sections (σ), *154,* **154,** 484, **521,** *523*
differential ($d\sigma/d\Omega$), **178**
for neutron capture, 514, *514*
partial, **521**
for strong interaction, 580
CRT. *See* Cathode-ray tubes (CRTs)
Crystallography, 134–136
Crystals, *414,* 414–415, 416*t*
symmetry of, *415,* 415–421, 416*t, 418, 419, 420*
Curie, Marie, 552
Curie, Pierre, 435, 552
Curie temperature (T_C), **436**
curies (Ci), **493**
Curie's law, **435**
Current, charged *vs.* neutral, ***574***
Current density (*j*), **424**
Current loops, 286
Curvature of wave functions, 239, *239*
Cyclotrons, 477, *516*
and accelerator mass spectroscopy, 547
and medical isotopes, 542

dc Josephson effect, **467**
Dalton, John, 561
Dark energy, 185, 663, 664, 667, 669, *671*
Dark matter, 185, **638**–639, 663, 667, *671*
and black holes, 650
and interstellar dust, 654
Darwin, C. G., 47
Davis, Raymond, Jr., 607, 612, 626, 676
Davisson, Clinton J., 186, 188–193, *191,* 214
Davisson-Germer experiment, *188,* 188–192
de Broglie, Louis, 2, 185–188, *186,* 191–193, 214
de Broglie, Maurice, 214
de Broglie relations, **185**–187
and Bose-Einstein condensates, *341,* 343
and distinguishability of particles, 332
and Schrödinger equation, 223
de Broglie wavelength (λ), **185,** 195–196
Debye, Peter J. W., 221, 262, 348
Debye frequency (f_D), *348,* **348,** 351
Debye temperature (T_D), **348,** *348*
Decay, radioactive, 495*. *See also* Radioactivity
alpha, 496–499
beta, 499–504
electron capture, 502–504
gamma, 504–506
hadron, 572, *572*
internal conversion, 505
Decay constants (λ), **492**
Declination (δ), **636,** *636*
Deep inelastic scattering, **593**
Degeneracy, **250, 271,** 316
of energy eigenvalues, **250**
in fermion gases, 353–354, *354*
and molecular spectra, 388–389
Degeneracy pressure, electron, **647**
Degrees of freedom, **324,** 346, 348
DeMarco, Brian, 354
Democritus, 115, 141, 561, 612
Density. *See also* Probability density ($P(x, t)$)
comoving space, **660,** 668
critical (Δn_c), of population inversions, **400**
critical mass (ρ_0), of the universe, 662–663, 672
current (*j*), **424**
energy, 122, 123
nuclear, 484, 489
number, **427,** 428, 429*t*
photon, 345
Density of states ($g(E)$), **317**
and distribution functions, 333–335
and electron gases, 428–429
Density parameter (Ω), **667,** *667*
Depleted regions, **452,** *452*
Deuterium, **165**
fusion of, 526, 533, 536
Deuterons, 479*t*
binding energy of, 83
Diamagnetism, **436**
and superconductivity, 460
Dielectric breakdown, **442**
Dielectric constant (κ or ε), 445*t,* 577
Differential cross section ($\sigma/d\Omega$), **178**
Diffraction. *See also* Interference; Superposition
of atoms, 193–196, *194*
of electrons, 186–188–192, *192,* 481, *481*
of x rays, *134,* 134–135
Digital versatile discs (DVDs), 404, 437
Diode lasers, 403, 456, *456*
Diodes, 452–456
light-emitting (LEDs), *455,* **455**–456, *456, 457*
solar cells, **455,** *455*
tunnel, 257, 260*, 453, **454**
Zener, *453,* **454**
Dipole moment. *See* Electric dipole moment (*p*)
Dipole-dipole bonds, **364, 375**–379, *377, 378*
Dirac, Paul A. M., 262, 356, 676
and Fermi-Dirac distributions, 329
and magnetic monopoles, 608
and positrons, 90, 562–563
and relativistic wave equation, 222, 288, 491
Direct interactions, **517**
Disk galaxies, **654**–655, *655*
Dispersion, **147,** *147*
of wave packets, 204, *204*
Dispersive media, **199**
Dissociation energy (E_d), **366,** 368*t,* **417**
Distortion of shapes, relativistic, *35,* 35–36
Distribution functions. *See* Boltzmann distributions ($f_B(E)$); Bose-Einstein distributions ($f_{BE}(E)$); Energy density distributions; Fermi-Dirac distributions ($f_{FD}(E)$); Maxwell distributions; Maxwell-Boltzmann distributions; Probability distribution functions ($P(x)$)
DNA molecules, 377, *378*
Donor levels, **447,** *447*
Doped semiconductors. *See under* Semiconductors
Doping, **445,** *447,* 447–448
Doppler effect, 41–45
applications of, 42
and gravitational redshift, 104
for light, 12
and rotation of the Milky Way, 638
for sound, 7, 41
transverse, *41,* 44–**45**
and twin paradox, 47–48
Down (*D*), 570, 583, 583*t*
Down-type quarks, 569*t,* **570**
Drift velocity (v_d), **423**–424
and Hall effect, 449, *449*
Driplines, **495,** *495*
Drude, Paul, 422
Duane-Hunt rule, **136**
Dulong, P., 327
Dulong-Petit law, **327,** 347, 351, 426
DVDs. *See* Digital versatile discs (DVDs)
Dwarf novae, **644**
Dynamic states, **85**

Weak interaction
and beta decay, 501
charged *vs.* neutral, **574**
mediation of, 574
Early type stars, **632**
EAST. *See* Experimental Advanced Superconducting Tokamak (EAST)
Ecliptic, **637,** *637*
Eddington, Arthur, 100, 101, 102, 110
EELS. *See* Electron energy loss spectroscopy (EELS)
Effective mass (*m**), **444**–445
Effective nuclear charge (Z_{eff}), 299, 301
Ehrenfest, Paul, 57, 58, 307
Eigenfunctions ($\psi_n(x)$), **233,** 609
Eigenstates, **226**
Eigenvalues, **273**
angular momentum, 273
energy, **232,** 273
Eightfold way, **591**–596, **592, 612**
Einstein, Albert, *13, 127*
and absorption, 393
and atomic spectra, 148, 159
and Bose-Einstein condensates, 341

STUDENTS-HUB.com Uploaded By: Malak Obaid

Einstein, Albert, *(continued)*
and Bose-Einstein distributions, 329
career of, 109, 141, 262, 307, 356, 407, 612
and cosmological constant, 661, 664
and de Broglie relations, 214
and general relativity, 97–102, 105*, 108, 110, 114
and heat capacities, 346–347, 356
and mass-energy equivalence, 81–82
and photoelectric effect, 125, 128–129, 130, 136, 561
and relativistic mass, 69
and special relativity, 2, 3, 11–12, 15, 34
and stimulated emission, 394
and transverse Doppler effect, 45
and unified field theories, 570, 674
and wave equations, 202, 225
Einstein temperature (T_E), *347,* **347,** 432–433
Einstein's coefficients of absorption and emission, 393, 394
and lasers, 399
Einstein's postulates, 11–17
Elastic collisions
and relativistic momentum, 66–67, *67*
Elastic scattering, **390,** *391,* **516**–517, *517*
Electric charge (e), 116, 118–119, 576*t*
of hadrons, 573*t*
quantization of, 115–119
of quarks, 569*t,* 583, 583*t*
Electric dipole moment (p), *376,* 376–378
average, **378**
average square, **378**
and bond character, 374–375
and rotational spectra, 380
Electric field ($\mathscr{E}$), 423
Electric quadrupole moment (Q), *485,* **485,** 552
Electrical conduction, 423–424, 431–433. *See also* Conduction
Electrodynamics, and special relativity, 11
Electromagnetic interaction, 509–510, 511, 574, 576*t*. *See also* Fundamental interactions
and cosmology, 671
Electromagnetic radiation
detection of, 127
particle description of, 127
slowing, 304–305, *305*
transmission of, 89–90
wave description of, 127
Electron affinity, **364,** 365*t*
Electron capture, 502–504, 552
Electron configurations, **297**–301
and bonding, 363
Electron degeneracy pressure, **647**
Electron energy loss spectroscopy (EELS), **175**–176, *176*
Electron gases, 352, 421, *422*. *See also* Band theory of solids
Electron holography, *462*
Electron spin. *See* Spin angular momentum (**S**)
Electron volts (eV), 78
Electrons (e^-), **116, 118,** 479*t,* **561**
Auger, 173
charge-to-mass ratio (e/m)of, 116#–118
conversion, **505**
diffraction of, 186, 188–192
intrinsic angular momentum of, 285–290
and photoelectric effect, 127–132
relativistic mass of, 78, *79*
speed of relativistic, 86–87
Electroweak interaction, **672**
Electroweak theory, **570, 591, 602**–603
Elliott, Steven, 503
Elliptical galaxies, **654**–655, *655*
Elsasser, Walter, 188, 192
Emission. *See also* Radiation
field, **257**
spontaneous, **393**
stimulated, *391,* **394**–396
Emission spectra. *See* Spectra
Emissivity (ε), **120**
Emitters, transistor, **456,** *456*
Endothermic reactions, **518**
Energy bands. *See* Band theory of solids
Energy density distributions, 122
and Planck's law, 123
Energy (E). *See also* Kinetic energy (E_k); Potential energy (U)
binding (E_b), 81–84, **83**
characteristic rotational (E_{0r}), **380,** 389*t*
cohesive, **417,** 420
conservation of, 76–81, 517–520, 663, 666
density, blackbody, 122
dissociation (E_d), **366,** 368*t,* **417**
Fermi (E_F), **352,** 426–429, 429*t*
first ionization, **298,** *300*
lattice, **417**
Lorentz transformation of, 73–76, **74,** 85
quantization of, 124–125, 129, 225, 230, 238, 278–279
relativistic (E), **70**–81, 563
rest (mc^2), **72**–73, 84*t,* 86, 90
in Schrödinger equation, 226–227
zero point, 208–**209**
Energy eigenvalues, **232**
degenerate, **250**
Energy gaps (E_g), *440,* **440**–441
and conductivity, 443–444, 445*t*
superconducting (E_g), **464**–465, *465*
Energy levels for diatomic molecules, 379–384
rotational, 379–382, *380*
vibrational, *382,* 382–384
Energy-level diagrams, **163**
and alpha decay, *499*
for atomic spectra, *302*
for atoms, *297, 311*
for the baryon octet, *592*
for fine-structure splitting, *294*
for helium-neon lasers, *402*
for hydrogen, *163, 278, 280*
for infinite square wells, *232, 238*
for nuclei, *515*
for quantum wells, *242*
for simple harmonic oscillators, *249*
Entrance channels, **522**
Entropy, 319*
Equilibrium separations (r_0), 366, 368*t*
and rotational spectra, 380, 381–382, 389*t*
in solids, 416–418, 416*t*
Equinoxes, *637,* **637, 676**
Equipartition theorem, **324***
Equivalence, principle of, **98**–99, *99*
and gravitational redshift, 103–104
Esaki, Leo, 263, 471
Escape velocity (v_e)
and planetary atmospheres, 323–324, 679
and Schwarzschild radius, 106, 650
Estermann, I., 193
Ether, **6,** 7–11
Ether drag, 61
Euler, Leonhard, 407
European Organization for Nuclear Research (CERN), *91,* 336, *563, 565,* 575
European Southern Observatory, 662
Evaporation, 322
Event horizons, **673**
Events, in special relativity, **13**–14, 23, 32, 50
Excited states (E_n), **175, 223**
and atomic spectra, 301–303, *302*
and fission, 528
of hadrons, 572–573
of the hydrogen atom, 281–283, 318
of molecules, 368
of nuclei, 504–506, 521–523, *522*
Exclusion principle. *See* Pauli exclusion principle
Exclusion-principle repulsion, 365, 367, 416
Exit channels, **522**
Exoplanets, **630**
Exothermic reactions, **517**
Expectation values $\langle x \rangle$, 242–**243**
in kinetic theory, 319–320
Experimental Advanced Superconducting Tokamak (EAST), 532
Experiments. *See* Burst and Transient Source Experiment (BATSE); Davisson-Germer experiment; Franck-Hertz experiment; Gedanken experiments; Ice Cube experiment; Michelson-Morley experiment; Millikan oil-drop experiment; Stern-Gerlach experiment; Thomson experiment
Exploring. *See also* Classical Concept Reviews; MORE
alpha decay, 258–259
atomic clocks, **260**
calibration spacetime axes, 28–29
celestial sphere, *636,* **636**–637
deflection of light in a gravitational field, 100–103, *101, 102*
extraterrestrial life, 630
fluxoids, **462,** *462*
frozen light, 304–305, *305*
gamma-ray microscopes, 206–208, *207*
gravitational redshift, *103,* 103–105, *104*
Hall effect, *449,* 449–452
interaction strengths, 577–578
Josephson junctions, 466–468, **467**
liquid helium, 336–339, *338, 339*
neutrino oscillations and mass, 609–610
other bonding mechanisms, 375–379
parity, 250
Planck units, 673–674
probability density of exchange mesons, 512–513, *513*
proton spin, 595–596
Rydberg atoms, **168,** *168*
spintronics, **437,** *437*
Stern-Gerlach experiment, 288–290, *289, 290*
superluminal speeds, 52–55, *54*
transverse Doppler effect, 44–**45**

Fabry-Pérot cavities, 106, 107
Face-centered cubic (fcc) crystal symmetry, *415,* **415,** *420*
Face-centered cubic structure, **134**
Faraday, Michael, 115–116
faradays (F), **116**
Faraday's law, 115–116
and flux quantization, 462
and superconductivity, 459
Fermi, Enrico, 329, *329,* 356, 500, 530, *531,* 553, 612
Fermi energy (E_F), **352**
and band theory of solids, *442,* 444
and free-electron gas in metals, 426–429, 429*t*
of nucleons, 515
Fermi speed (u_F), **431**
Fermi temperature (T_F), **430**
Fermi-Dirac distributions ($f_{FD}(E)$), **316,** 328–**329**
and band theory of solids, 444, 444*t*
and conduction, 425, 430, *431*
and fermion gases, *352,* 352–353, *353*
vs. other distributions, 329–333, *331*
Fermi-Dirac particles. *See* Fermions
Fermilab, 336, 598
Fermion gases, 351–354, *354*
and lasers, 403
neutron stars as, 648
Fermions, **329**–332
Ferrimagnetism, **436**
Ferromagnetism, **434, 436**
Feynman, Richard P., 213*, 215, *566,* 612
and quantum electrodynamics, 563
Feynman diagrams, **566**–568, *567*
examples of, *510, 511, 574, 578, 579, 600, 601*
Field emission, **257**
Filaments, **629,** *629*

STUDENTS-HUB.com Uploaded By: Malak Obaid

Fine structure, **167, 285,** 288
Fine-structure constant (α), 166–168, **167,** 571, 577
Fine-structure splitting, **167, 293**–295, *294*
  and emission spectra, 385, *385*
Finite square wells, 238–242, *239*
  and alpha decay, 258–259, *259*
  and covalent bonding, 369, *369*
  graphical solution of, 241*
  and Kronig-Penney model, 438, *438, 439*
  and quantum wells, **242**
  and strong interaction, 507–508, *508*
  and vibrational energy levels, *382,* 382–383, *383*
First ionization energies, **298,** *300*
First-order perturbation theory, **298**
Fissile nuclides, **528**
Fission, **478,** *527,* 527–531
  and energy conversion, 81
FitzGerald, George F., 34
Flash memory, 437
Flat universe, **666**
Flavor charge, **568,** 569*t,* **574,** *599,* 609
Fluorescence, *391,* **393**
Flux lines, *628*
Flux quantization, 462
Flux tubes, **461,** *461, 462*
Fluxoids (ϕ_0), **462,** *462*
Force carriers. *See* Mediation of forces
Force constants (*K*)
  and vibrational energy levels, 383, 384, 389
Forces (**F**). *See also* Electromagnetic interaction; Fundamental interactions; Gravitational interaction; Strong interaction; Weak interaction
  coupling constants for, 570–571
  inverse-square, 279
  relativistic, 70–71
  saturated, **488,** 507, 509
  short-range, **509**
Forward biasing, **452,** *452*
Fountain effect, **338,** *339*
Fourier analysis, 197–198#
Four-vectors, **85**
FQHE. *See* Fractional quantized Hall effect (FQHE)
Fractional quantized Hall effect (FQHE), 451
Frames of reference. *See* Reference frames
Franck, James, 169, 174–175, 179, 188, 192, 591
Franck-Hertz experiment, 174–176
Fraunhofer, Joseph von, 147, 178, 393, 632
Fraunhofer D lines, 393, 490, *491. See also* Sodium (Na)
Free-electron lasers, 404
Free-electron theory, 426–430
  failures of, 351
  and Fermi temperature, 430
  one-dimensional, 426–428
  three-dimensional, 428–429
Frequency (*f*)
  control of, 201
  Debye (f_D), *348,* **348,** 351
  proper (f_0), **42**
  quantization of, 230
Friction, 378
Fringes, interference, **9#,** *10. See also* Interference
Fuller, R. Buckminster, 407
Fullerenes, 375*, 407, *420,* 420–421
Fundamental interactions, 570–580, 576*t. See also* Electromagnetic interaction; Gravitational interaction; Strong interaction; Weak interaction
  unification of, 671
Fundamental particles, 479
Fusion, **478,** 531–536. *See also* Proton-proton cycle
  during the early universe, 556, 668, *668,* 672
  and metallic hydrogen, 421
  as stellar energy source, 624, 642–643
  and supernovae, 645–646, 648

g factor (*g*), **287**–288
  and magnetism, 435
Galactic clusters, **632**
Galaxies, 630, 653–661, **676**. *See also* Milky Way
  classification of, 654–661, 656
  and interstellar medium, 653–654
  quiet *vs.* active, *656,* **656**–657, *657*
2dF Galaxy Redshift Survey, 661, *661*
Galilean transformation of coordinates, **5**–6#, 11
Galilei, Galileo, 1, 3, 4, 646
Gamma decay, 504–506
Gamma rays, **91,** 477
Gamma-ray bursts (GRBs), 652, *652*
Gamma-ray microscopes, 206–208, *207*
Gamow, George, 217, 258, *299,* 477, 676
Gaseous nebulae, 654
Gases
  electron, 352, 421, *422*
  fermion, 351–354, *354*
  free-electron, 426–430
  heat capacities (C_V) of, 325–327, 325*t,* 348–351
  kinetic theory of, 115, 316–328
  photon, 344–351
Gassendi, Pierre, 115
Gauge theories, 580, **609, 613**
Gedanken experiments, **109**
  flash of light inside a sphere, 58
  gamma-ray microscopes, 206–208, *207*
  headlight effect, *51,* 51–52
  knowledge creation paradox, 54–55, *55*
  lever paradox, *80,* 80–81
  lightning strikes train, *15,* 15–17, *16, 28,* 28–29
  Olbers' paradox, **665**
  pole and barn paradox, 48–51, *49*
  pregnant elephant, 32–33
  scissors paradox, 52–54, *54*
  twin paradox, 45–48*, *46*
Geiger, Hans W., *151*
  and alpha decay, 496
  and nuclear charge, 172
  and Rutherford scattering, 151–153, 155–156, 159, 477
  and size of nucleus, 157
Geiger-Nuttall rule, 496, *496*
Gell-Mann, Murray, 583, 591–593, *593,* 596, 612
General relativity, 47, **97**–108
  and cosmology, 665
Generations of leptons, **568,** 569*t, 599*
Geochemistry, 545–548
Geometry of space, 39, 57, 84, 666
Geosynchronous satellites, *5,* 112
Gerlach, Walther, 286, 289–290, 307
Germer, Lester H., 186, 188–191, *191,* 193, 214
Giaever, I., 471
Giant magnetoresistance (GMR), 437
Glashow, Sheldon L., 570, 597, 598
Glass, 414
Global positioning systems (GPS), 97, 98, 110
Globular clusters, **632,** *632*
  and structure of the Milky Way, 634
Gluon-gluon loops, 600, *600*
Gluons, **90, 511, 568**
  and force mediators, **571,** 576*t,* 603
  and quantum chromodynamics, 599–600, *600*
GMR. *See* Giant magnetoresistance (GMR)
Goeppert-Mayer, Maria, 552; *see also* Mayer, M.
Gordon, Walter, 512
Goudsmit, Samuel A., 285, 307
GPS. *See* Global positioning systems (GPS)
Grand unification theories (GUTs), **605**–610
  and the early universe, 671
Graphite, 420, *420*
Gravitational blueshift, 104–105
Gravitational charge, 576, 576*t. See also* Mass (*m*)
Gravitational interaction, 576, 576*t. See also* Fundamental interactions
  and astrophysics, 623, 624–625
  and cosmology, 662–664, 671
  deflection of light by, 100–103, *101, 102*
  quantum, 609, 671, 674
  transmission of, 90
Gravitational length contraction, **101**
Gravitational lensing, 100, **102,** *102, 104*
Gravitational redshift, *103,* 103–105, **104,** *104,* **650**
Gravitational time dilation, **101,** 105*
Gravitational waves, *106,* **106**–108, 576
Gravitons, 57, **90, 576,** 576*t*
GRBs. *See* Gamma-ray bursts (GRBs)
Greenberg, D. W., 596
Ground states (E_0), **163, 175, 233**
  of hadrons, 572
  of the hydrogen atom, 281–283
  of molecules, 368
  of nuclei, 480–492
  and the periodic table, 297–301
Group theory, 592
Group velocity (v_g), **197,** 199
  for particle waves, 202
Gurney, R. W., 258, 477
GUTs. *See* Grand unification theories (GUTs)
Gyromagnetic ratio (*g*), **287**–288

h-bar (ħ), 161. *See also* Planck's constant (*h*)
H-R diagrams. *See* Hertzsprung-Russell (H-R) diagrams
Hadronic force. *See* Strong interaction
Hadrons, **568**–569, 573*t*
  quantum numbers of, 586*t*
  quark model of, **591**–599
  and the strong interaction, 571–573
Hahn, Otto, 527, 530, 553
Hale, George, 110
Half-life ($t_{1/2}$), **493,** 543*t,* 547*t*
  and charge-carriers, 449
  quantum, 450–451, *451*
  spin, **437,** 452
Hall effect, *449,* 449–452
Hall resistance (R_H), 450, *451*
Halley, Edmund, 665
Hamiltonian operators (H_{op}), 245, 245*t,* 370
  and symmetry breaking, 602
Hanford Observatory, 107
Hard core, **509**
Hard superconductors, **460,** *460*
Harmonic waves, **196,** 222, 224
Hartmann, J. F., 653
Hawking, Stephen, 356
Hawking radiation, 680
Heat capacities (C_V), 324–328
  for gases, 325–327, 325*t,* 348–351
  for metals, 422, 426, 433–434
  and phase transitions, 337, *337*
  for solids, *327,* 327–328, 347–348, *348*
Heisenberg, Werner K., 205, 206, 215, 221, 307, 407
Helicity, ***584***
Helium (He)
  formation of, 668, *668*
  in interstellar medium, 653
  liquid, 336–339, *338, 339*
  wave functions for, 297–298
Helium-neon lasers, *401,* 401–402
Helix nebula, *643*
Helmholtz, Hermann von, 109, 141, 580
Hermite polynomials, 248
Hermitian operators, **612**
Herriott, D. R., 401
Hertz, Gustav L., 169, 174–175, 179, 591
Hertz, Heinrich R., 127, 132, 141, 179
Hertzsprung-Russell (H-R) diagrams, *641,* **641**–643
Hess, Victor, 552
Heteropolar (heteronuclear) molecules, **407**
Hexagonal close-packed (hcc) crystal symmetry, **419,** *419*

STUDENTS-HUB.com Uploaded By: Malak Obaid

Higgs bosons, 568, 581, **603**
Higgs field, **603**
High-temperature superconductivity, *460,* 466, 466*t*
Hipparchus, 632, 676
Hofstadter, Robert, 481, 552
Holes, 443, 448
Holography, electron, *462*
Homopolar (homonuclear) molecules, **407**
Hooke, Robert, 115
Horizontal branch, in stellar evolution, **643**
Hounsfield, Godfrey, 541, 553
Hoyle, Fred, 676
Hubble, Edwin P., 43, 654, 657, 676
Hubble constant (H_0), **657**–658, 661
Hubble Space Telescope, 620, 632, 646, 648, 650
Hubble time, **658**
Hubble's law, *657,* **657**–661
Hulse, R. A., 106
Hybridization of orbitals, 420, **470**
Hydrogen bonds, **377,** *378*
Hydrogen (H) atoms
  binding energy of, 83
  Bohr model of, 159–169, 176*
  energy-level diagrams for, *163, 278, 280*
  excited states of, 281–283, 318
  fine-structure splitting in, **293**–295, *294*
  probability density in, 282–285, *283, 284, 285*
  quantization of angular momentum in, 275–277
  quantization of energy in, 278–279
  Schrödinger equation for, 272–274
  size of, 209–210
  spectra of, *149,* 150
  wave functions for, 281–285, 290
Hydrogen (H_2) molecules
  escape of, from Earth's atmosphere, 323–324
  heat capacity of, 326, *326*
  in interstellar medium, 653
  wave functions for, 370–374, *371*
Hypercharge (*Y*), **585**–586, 586*t, 587*
  and group theory, 592
Hyperfine splitting, **314**
  and interstellar dust, *653,* 653–654
  and masers, 396, *397*
Hyperfine structure, **304, 479, 490**

Ice, dipole-dipole bonds in, 377, *377*
Ice Cube experiment, 129
Ideal blackbodies, **120**
Imaginary numbers. *See* Complex numbers
Impact parameters (*b*), **154,** *154*
Impurity semiconductors. *See under* Semiconductors
Indistinguishable particles, 295–296, 328, *329,* 330, 332
Inelastic collisions
  and relativistic energy, *76,* 76–77
Inelastic scattering, **390,** *391*
Inertial confinement, **533**
Inertial reference frames, *4,* **4**–6#
  and simultaneity, 14–17
  and special relativity, 12–14, *14,* 47
Infinite square wells, 229–238, *230*
  complete wave function for, 235–238
  and correspondence principle, 233–234, 236
  energy levels of, 231–232, *232*
  and free-electron gas in metals, 426, *427*
  and line of stability, 487
  minimum energy of, 208–209
  in three dimensions, 270–271
Inflation, **669**
Insulators, and band theory of solids, 442, *442*
Integral quantized Hall effect (IQHE), 451
Intensity (*I*), 407, 521
  of electron diffraction, *190, 191*
  and photoelectric effect, 131–132
Interaction times, **571**
Interactions. *See also* Fundamental interactions
  and Feynman diagrams, **566**
Interference. *See also* Diffraction; Superposition
  double-slit, 202–204, *203,* 213*
  by electrons, 186, 188–189, *203*
  fringes produced by, **9#**, *10, 203*
  and linear equations, 223
  quantum, **304**–305, *305*
Interferometers, Michelson, **7,** *9,* 9–11, *10*
Internal conversion, **505**
Internal quantum numbers, **583,** 583*t*
International Thermonuclear Experimental Reactor (ITER), 532, *533*
Interstellar dust, **653**–654
Interstellar medium (ISM), 653–654
Intrinsic semiconductors. *See under* Semiconductors
Invariance, **4**
  and conservation laws, 66, 73, 580
  and gauge theories, 613
  of mass, 84–97
  TCP, 589–590
Inverse beta decay, 646, 648
Ionic bonds, **364**–369
  vs. covalent bonds, 374–375
Ionic solids, 415–421
Ionization energy, **163**
  and ionic bonds, *364,* 364–365, 365*t*
Ionizing radiation, 536*, 549*
IQHE. *See* Integral quantized Hall effect (IQHE)
Irregular galaxies, **654**–655, *655*
Island of stability, **488,** 515–516
ISM. *See* Interstellar medium (ISM)
Isobars, **480**
Isomers, **505**
Isospin (**I**), **585,** 586*t, 587*
  and group theory, 592
  weak (T_z), **568,** 570
Isotones, **480,** 513
Isotope effect, **463**
Isotopes, **165,** 471, **480**
ITER. *See* International Thermonuclear Experimental Reactor (ITER)

J/ψ puzzle, 597–599
Javan, Ali, 401
Jefferson National Accelerator Facility, 595
Jensen, Johannes Hans Daniel, 514, 515, 552
Jin, Deborah, 354
Joos, Georg, 11
Josephson, Brian D., 467, 471
Josephson effect
  ac, **467**–468
  dc, **467**
Josephson junctions, 466–468, **467**
Joule, James, 109, 580
Junction lasers, 403
Junctions
  Josephson, 466–468, **467**
  semiconductor, **452,** *452*

K series, *170,* **171**
K shell, **171**
Kamerlingh Onnes, Heike, 335, 336, *336,* 356, 458
Kant, Emmanuel, 654
Kaons (K^0), 588, 590
Keesom, Willem H., 335, 337
Kelvin, William Thompson, Lord, 2, 307, 624
Kepler, Johannes, 646
Ketterle, Wolfgang, 343, 403
Kinematic states, **85**
Kinetic energy (E_k)
  Maxwell distributions of, *323,* **323**–324
  minimum, 208–209
  negative, 240, 255
  in nuclear reactions, 522
  and photoelectric effect, 128
  relativistic, 71–**72,** *72*
  of rotation, 379
  vs. potential energy, 81–83
Kinetic energy operators, 245*t*
Kinetic theory, 315#, 316#, 319#, 328#
  and blackbody radiation, 119–122
  of gases, 115, 316–328
  and Planck's law, 123
Klein, Oskar, 512
Klein-Gordon relativistic wave equation, 512, 564, 577
Klitzing, Klaus von, 450–451, 471
Kronig-Penney model, *438,* **438**–441, *439*
Kündig, Walter, 45
Kusch, P., 322

L series, *170,* **171**
Laboratory frames of reference, **518,** *519,* 522
Lagrangian points, **644,** *644*
Laguerre polynomials, 279, 279*t,* 281, 284
Lamb, W., 307
Lamb shift, 307
Lambda points, **335**–336, *337,* **337,** 341
Λ Cold Dark Matter (ΛCDM), 661
Landé, Alfred, 307
Landé factor (g_N), 490
Langevin, Paul, 214
Laplace, Pierre, 106
Large Hadron Collider (LHC), *563,* 568, 603, 605, 639
Larmor theorem, **286**
Laser Interferometer Gravitational-Wave Observatory (LIGO), 106–107, *108*
Lasers, 396–405
  applications of, 402–405
  atomic, **343,** *343*
  continuous wave, 400–**401**
  diode, 403, 456, *456*
  helium-neon, *401,* 401–402
  other types of, 403–404
  ruby, *397,* 397–401, *398*
  tunable dye, 168, 490
Late type stars, **632**
Latitude, **636,** *636*
Lattice energy, **417**
Laue, Max von, 80, 134
Laue patterns, *134, 192, 194,* 418
Laughlin, R. B., 471
Law of atmospheres, **317**–318
Law of inertia, **4**
Lawrence, Ernest O., *516*
Lawrence Livermore Laboratory, 564, 584
Laws of motion, Newtonian, 4–6
Lawson, J. D., 532
Lawson's criterion, **532**
LEDs. *See* Light-emitting diodes (LEDs)
Lee, David M., 338
Lee, T. D., 588, 590
Left-handed coordinate systems, **589,** *589*
Legendre polynomials, **274**
Lenard, Philipp, 127, 128
Lenard-Jones potential, 411
Length, proper (L_p), **33,** 38, 85
Length contraction, *33,* 33–36
  gravitational, **101**
Lepton era, **672**
Lepton number
  conservation of, 581–582
  nonconservation of, 607
Leptons, **500,** 568–570, 569*t,* 598, *599,* **612**
  and weak interaction, 574
Leptoquarks, 606, 671
Leucippus, 115
LHC. *See* Large Hadron Collider (LHC)
Libby, Willard F., 553
Lie, S., 592
Life, extraterrestrial, 630
Lifetime (τ), **210, 493**
  of excited energy states, 393
  and force ranges, 572
  of protons, 606–607
  for spontaneous emission (t_s), 399–400

STUDENTS-HUB.com Uploaded By: Malak Obaid

of strange particles, 584
and tunneling, 259
Light. *See* Electromagnetic radiation; Speed of light (*c*)
Light clocks, **29,** *30*
Light curves, 640
Light-emitting diodes (LEDs), *455,* **455**–456, *456, 457*
Lightlike spacetime intervals, **37, 39**
LIGO. *See* Laser Interferometer Gravitational-Wave Observatory (LIGO)
Limbs, solar, **621,** *622*
Lindblad, Bertil, 638
Line of stability, *486,* **487**
and fission, 528, *529*
Line spectra, **147**–148, *148*
Linear combinations, 223, 262
Liquid lasers, 404
Liquid-drop model, 489*, 513
and fission, 527, *527*
Liquids
helium, 336–339, *338, 339*
structure of, 413
surface tension of, 378
Livingston, M. S., *516*
Livingston Observatory, 106
Local clocks, **15**
London, Fritz, 335, 378
London dispersion forces, **378**. *See also* van der Waals attraction
Longitude, **636,** *636*
Lorentz, Hendrik A., 34, 102, 214
and conduction, 422
and coordinate transformations, 18
and electrons, 118, 141
and Michelson-Morley experiment, 57, 61
and Zeeman effect, 295, 307
Lorentz transformation, **18**
and dynamics, 65, 73–76
of four-vectors, 85
of mass-energy, 88
and nuclear reactions, 519
of space and time coordinates, 17–29
Lorentz-FitzGerald contraction, **34**
Luminosity (*L*), **620,** 639
of galaxies, 656
and Hertzsprung-Russell diagrams, 641, *641*
of quasars, 660
Lyman, Theodore, 150, 164
Lyman series, *163,* 164

Macroscopic quantum wave functions, **342,** *342*
Madelung constant (α), **368, 415,** 416*t,* 418, 419
Magic numbers, **488,** 513–514
Magnetic confinement, **532**
Magnetic fields (*B*)
charged particles in, 116–117
critical (B_c), 458, 458*t, 459,* 460, *461*
and fine-structure splitting, 293–295
inhomogeneous, *289*
at the nucleus, 490*t*
relativistic electrons in, 94–95, *95*
solar, *627,* 627–629, *628*
Magnetic moment (μ), **286**–290
nuclear, **489**–492
quantization of, 287
Magnetic monopoles, 608, 669
Magnetic quantum number (*m*), **276,** 280
Magnetic resonance imaging (MRI), **491, 540**
and liquid helium, 336
and superconductivity, 458, 562
Magnetic susceptibility (χ), **435**
Magnetic traps, 342
Magnetic tunnel junctions, **437,** *437*
Magnetism, 287, 434–437
Magnetization (*M*), 476
Magnetons
Bohr (μ_B), **182**
nuclear (μ_N), **314**
Magnetoresistance, giant (GMR), 437
Magnetoresistive random access memory (MRAM), 437
Magnitude, stellar
absolute (*M*), **633**
apparent (*m*), **632**–633, **677**
Maiman, Theodore, 397
Main sequence dwarfs, **641,** *641*
Main sequence stars, **641,** *641*
Majorana neutrinos, 568, 582
Marsden, Ernest
and nuclear charge, 172
and Rutherford scattering, 151–153, 155–156, 159, 477
and size of nucleus, 157
Masers, **396,** *397. See also* Lasers
Mass (*m*)
effective (*m**), **444**–445
as gravitational charge, 576, 576*t*
gravitational *vs.* inertial, 98–99, *99*
and Higgs boson, 603
invariance of, 84–97
of the Milky Way, 638–639
of neutrinos, 500, 536, 581–582, 607–608, 609–610, 626
of nuclei, 488–489
reduced (μ), **165**–166
relativistic (*m*(*u*)), 67–69, **68**
rest (*m*), **78**
stellar, 623, 641–642
units of, 78, 83, **380,** 673
Massless particles, 89–90. *See also* Gluons; Gravitons; Photons
Mather, John C., 669, 676
Matter waves, **187**–196
Matter-antimatter asymmetry
and *CP* violations, 590
Max Planck Institute, 650
Maxwell, James Clerk, 1, 6, 316, 319
Maxwell distributions
and Bose-Einstein condensates, 342
and electromagnetism, 570
and fusion, 532, 536, 625
of kinetic energy, *323,* **323**–324
of molecular speeds, 319–322, **320,** *320,* 359
Maxwell-Boltzmann distributions
and diode currents, 453
and Planck's law, 123–124
Maxwell's equations, 6, *6,* 11
Mayer, M., 514, 515
Mean free path (λ), **424,** 432
Mediation of forces, 570–580
and Feynman diagrams, 566–567, *567*
and the uncertainty principle, 510
Medicine
nuclear, 478, 529, 540–542, 612
and x rays, 133, 136
Meissner, H. Walther, 459
Meissner effect, *459,* 459–462, **460,** *461*
Mendeleev, Dmitri, 172, 592
Mercury [element], spectra of, *149,* 175
Mercury [planet], precession of orbit of, 100, 105*
Meson fields, **510**
Meson octet (nonet), *587,* **591,** *595*
Mesons, **510, 569,** 573*t, 587,* 594*t*
as force mediators, 604
probability density of, 512–513, *513*
supermultiplets of, *598*
Metallic bonds, **364, 375, 415, 421**–422, *422*
Metals, free-electron gases in, 351, 426–430
Metastable states, **505**
and lasers, 397, *397,* 401
Michelson, Albert A., 1, 7, *7,* 9, 11, 57, *127*
Michelson interferometer, **7,** *9,* 9–11, *10*
and gravity waves, 106–107, *107*
Michelson-Morley experiment, 7–11*
Microscopes
gamma-ray, 206–208, *207*
photoelectric-effect, 132
resolving power of, 215
scanning tunneling (STMs), *257,* 257–258
Mikheyev, S., 608
Milky Way, 630, *634, 635. See also* Galaxies
mass of, 638–639
structure of, *634,* 634–635, 654
Miller, R. C., 322
Millikan, Robert A., *127,* 141, 676
and electron charge, 116, 118–119
and photoelectric effect, 130, 561
Millikan oil-drop experiment, 118–119#, *119*
Minkowski, Hermann, 109
Mirror nuclides, **480,** *481*
Missing mass. *See* Dark matter
Mitchell, John, 676
Molecular orbitals. *See* Orbitals
Molecules, 363–412
and covalent bonds, 369–375
energy levels and spectra of, 379–390
and ionic bonds, 364–369
and lasers and masers, 396–405
and other bonds, 375–379
and scattering, absorption, and stimulated emission, 390–396
Moment of inertia (*I*), 379
and rotational spectra, 380, 387, 389
Momentum operators (p_{op}), **244,** 245*t*
Momentum (**p**)
of electromagnetic radiation, 137
Lorentz transformation of, 73–76, **74**
relativistic (**p**), 66–70, **67,** *68*
MORE. *See also* Classical Concept Reviews; Exploring
alpha-decay energetics, 498*
Bohr atomic model, 176*
conservation laws, 583*
delay of light in a gravitational field, 105*
derivation of Compton's equation, 138*
double-slit interference, 213*
energy bands, 438*, 445*
entropy, 319*
equipartition theorem, 324*
graphical solution of the finite square well, 241*
ionizing radiation, 536*
liquid-drop model, 489*
Michelson-Morley experiment, 11*
Mössbauer effect, 505*
multielectron atoms, 303*, 401
nuclear power, 530*
other covalent bonds, 375*, 420*
perihelion of Mercury's orbit, 105*
radiation dosages, 549*
radioactive decay, 495*
relativity of simultaneity, 48*
resonances and excited states, 591*
Rutherford scattering, 156*
Schrödinger's differential equation trick, 249*
shell model, 516*
spectroscopic notation, 292*
temperature, 319*
theories of everything, 610*
thermal conduction, 434*
transcendental equations, 241*
transistors, 457*
transitions between energy states, 246*, 393*, 395*
tunnel diodes, 260*
twin paradox, 48*
wave-particle duality, 213*
Weizsächer formula, 489*
Zeeman effect, 303*
Morley, Edward W., 7, 9, 11, 57
Moseley, Henry G.-J., *169,* 169–170, 172–173, 179, 181, 478, 542
Moseley plots, **170,** *170*

STUDENTS-HUB.com Uploaded By: Malak Obaid

Mössbauer, Rudolf Ludwig, 505*, 552
Mössbauer effect, **211,** 505*, 557
  measuring gravitational red- and blueshift with, 105, 505
  measuring natural line widths with, 211
  measuring transverse Doppler effect with, 45, 505
Most probable speed (v_m), 320, *320*
Mott, N. F., 437
Mourou, Gérhard, 403
MRAM. *See* Magnetoresistive random access memory (MRAM)
MRI. *See* Magnetic resonance imaging (MRI)
MSW effect, **608**
Müller, Karl A., 466
Multielectron atoms, 303*, 401
Multiplets, charge, 572, **585**–586, 606
Muons (mu (μ) mesons), 561
  decay of, *36,* 36–37
  mass of, 78

N galaxies, **656**
npn transistors, **456,** *456*
n-type semiconductors, **447,** *447*
NAA. *See* Neutron activation analysis (NAA)
Nanostructures, **242,** *420,* 421
Natural line width (Γ_0), 210–**211**
  and gamma decay, 504–505
  and nuclear resonances, 522
Néel temperature (T_N), **436**
Ne'eman, Yuval, 591
Neutral current, ***574***
Neutral weak force, **574**
Neutralinos, **639**
Neutrinos (ν), **90**
  as dark matter, 638
  and density parameter, 667
  discovery of, **500,** 562
  Majorana, 568, 582
  mass of, 500, 536, 581–582, 607–608, 609–610, 626
  oscillations of, 582, 607–608, 609–610, 626
  in proton-proton cycle, 536
  and solar-neutrino problem, **536, 607**–608, 625–**626,** *626*
  from supernovae, 646
  types of, 500, 568, 569*t*
Neutron activation analysis (NAA), **478,** 524, *537,* **537**–539
Neutron capture, *524,* 524–525
  cross section for, 514, *514,* 524
Neutron number, **479**
Neutron stars, 352, **484, 648**–650, *649*
Neutrons (*n*), 479*t*
  decay of, 579
  diffraction of, 193, *194*
  discovery of, **477, 479, 561**
  reactions of, 524–525
  thermal, **524**
Newton, Isaac, 1, 3, 4, 147, 356
Newtonian physics, 4–6, 70–71. *See also* Classical physics
Nichols, Ernest F., 137
Nicholson, J. W., 161
Nishijima, K., 583
NMR. *See* Nuclear magnetic resonance (NMR)
Noether, Emmy, 580, 612
Nondispersive media, **199**
Nonpolar molecules, 377–379, *378*
Normalization
  of Bose-Einstein distribution, 339
  and hydrogen atom wave functions, 282
  of Maxwell-Boltzmann distribution, 124
  of probability amplitude, **225,** 227, 228, 232, 240, 512
Novae, **60, 644,** *644*
Nuclear binding energy (*B*), 488–489, *489*
  and driplines, 495, *495*
  and shell model, 513, *514*
Nuclear exchange force, 509–511
Nuclear force. *See* Strong interaction
Nuclear magnetic moment, **489**–492
Nuclear magnetic resonance (NMR), 470, 539–**540**. *See also* Magnetic resonance imaging (MRI)
Nuclear magneton (μ_N), **314**
Nuclear physics, 477–560
  applications of, 537–549
  and composition of the nucleus, 478–479
  and fission and fusion, 526–536
  and ground-state properties of nuclei, 480–492
  history of, 477–478
  and nuclear decay, 495–506
  and nuclear reactions, 516–525
  and radioactivity, 492–495
  and the shell model, 513–516
  and the strong interaction, 506–513
Nuclear power, 478, 530*
Nuclear reactions, 516–525
Nuclear reactors
  fission, 81, 524, 525, 530, *531*
  fusion, *534*
  natural, 553
Nuclear spectra, 480, 508, *523*
Nuclear spin angular momentum (**I**), 304, **489**
Nuclear weaponry, 478, 530
Nucleons, **479,** 509
  mass differences between, 526, *526*
Nucleosynthesis era, **672**
Nucleus
  composition of, 478–479
  compound, **517,** 521–522, *522*
  density of, 484, 489
  discovery of, 153–156
  excited states of, 504–506, 521–523, *522*
  ground state of, 480–492
  shape of, 485
  size of, 156–159, 480–484
  stability of, *486,* 486–488
  structure of, 191
Nuclides, **480**
  fissile, **528**
  mirror, **480,** *481*
Number density, **427,** 428, 429*t*
Nurmia, M., 497
Nuttall, John Mitchell, 496

Observers
  in special relativity, **13**–14
  and wave-particle duality, 212
Ochsenfeld, Robert
Ohm's law, 422, 424, 425
  and Josephson junctions, 467
Oil-drop experiment. *See* Millikan oil-drop experiment
Olbers, Wilhelm, 665
Olbers' paradox, **665**
OLEDs. *See* Organic semiconductor light-emitting diodes (OLEDs)
Oort, Jan, 638
Open clusters, **632**
Open universe, **666**
Operators, **243**–246, 245*t*
Oppenheimer, J. Robert, 105
Optical barrier penetration, *257*
Optical pumping, **396**
Optical traps, **403**
Optical tweezers, 403
Orbital quantum number. *See* Angular momentum quantum number (ℓ)
Orbitals, **363, 373, 407**
  bonding *vs.* antibonding, **373,** *373*
  hybridization of, 420, **470**
Orbits
  circular atomic, 159–160, *169*
  elliptical atomic, 166–167, 279
Ordinary spiral galaxies, **654**–655, *655*
Organic semiconductor light-emitting diodes (OLEDs), *455,* 456
Oscilloscopes, 117
Osheroff, Douglas D., 338
Ötzi the Iceman, 548, *548*

P branches, **407**
pn junctions, **452,** *452*
pnp transistors, **456,** *456*
p-type semiconductors, *447,* **448**
Pair production of particles, 90–93, *91, 92,* 564, *564*
  Feynman diagram for, 567, *567*
Paradoxes in relativity. *See* Gedanken experiments
Parallax angles (θ), **640,** *640*
Paramagnetism, **435,** 476
Parity operations, **250,** 588
Parity (*P*), **588**–589, *589*
  nonconservation of, 588
Parsecs (pc), 633, 640, *640*
Partial cross sections, **521**
Particle physics, 561–618
  basic concepts for, 562–570
  conservation laws and symmetries in, 580–591
  fundamental interactions and force carriers in, 570–580
  and grand unified theories, 605–610
  history of, 561–562
  Standard Model of, 591–604
Particle waves, 185–220, **187**
  and the de Broglie hypothesis, 185–187
  measurements of, 187–196
  probabilistic interpretation of, 202–205
  and the uncertainty principle, 205–211
  and wave packets, 196–202
  and wave-particle duality, 212–213
Particle-in-a-box. *See* Infinite square wells
Particle-induced x-ray analysis (PIXE), 548–549, *549*
Particles. *See also* Alpha particles (α); Antiparticles; Beta particles (β); Virtual particles
  annihilation of, **90**–93, *91,* 565–566, *567*
  indistinguishable, 295–296, 328, *329,* 330, 332
  massless, 89–90
  pair production of, 90–93, *91, 92,* 564, *564, 567*
Paschen, Friedrich, 150, 164
Paschen series, *163,* 164
Pauli, Wolfgang, *299,* 303, 307
  and electron spin, 285, 286
  and neutrinos, 500, 607
Pauli exclusion principle, **295,** 296–**297**
  and baryons, 596
  and bosons, 329, 330
  and fermions, 329, 331, 429
  and line of stability, 487
  and neutron stars, 648
  and white dwarfs, 647
Pauli paramagnetism, **435**
Penzias, Arno Allan, 126, 669, 676
Perfect cosmological principle, **664**
Periodic table, 172
  of elementary particle constituents, *599*
  and ground states of atoms, 297–301
Perl, M., 612
Perrin, Jean-Baptiste, 116, 187, 214
Perturbation theory, first-order, **298**
PET. *See* Positron emission tomography (PET)
Petit, A., 327
Pfund, A. H., 164
Phase transitions, 336, 672
Phase velocity (v_p), **196,** 199
  for particle waves, 201
Phonons, **463**–465, 510
Photodisintegration, 646
Photoelectric effect, 125, 127–132, *391,* 392

STUDENTS-HUB.com Uploaded By: Malak Obaid

and de Broglie wavelength, 190
Photomultipliers, 129
Photon gases, 344–351
Photons, 57, **89**–90, **129, 141, 561**
as force mediators, 574, 576*t*
and Schrödinger equation, 222
virtual, **509**–510
Photosphere, **620**–622, *622*
Photovoltages, **455**
Photovoltaics. *See* Solar cells
π mesons. *See* Pions (π)
Pickering, Edward, 632
Pions (π), **511,** 561, 564, 571
in Feynman diagrams, 566
virtual, 600
PIXE. *See* Particle-induced x-ray analysis (PIXE)
Plages, solar, **629,** *629*
Planck, Max K. E. L., 141, 215, 262
and energy distributions, 123–125, 344–345
and energy quantization, 129–130, 148, 159, 226, 249, 346, 561
and fundamental constants, 673
Planck units, 673–674
Planck's constant (h), **124,** 125
Planck's law, *123,* 123–127, **124**
and stellar temperatures, 621
and stimulated emission, 394
Planetary nebulae, **643,** *643*
Plasma, **532**
confinement of, 532–533
metals as, 470
solar, 623, 625
structure of, 413
Plato, 630
Polar coordinates, 101
Polar molecules, **376**–377, *377*
Polaris, 631, 676
Polarizability (α), **377**
Polycrystalline solids, 414
Polyelectrons, **110**
Polynomials
Hermite, 248
Laguerre, 279, 279*t*
Legendre, **274**
Population densities (n), **400**
Population I stars, **632**
Population II stars, **632**
Population inversions, **396,** 401
critical density (Δn_c) of, **400,** 404–405
Positron emission tomography (PET), **478,** 501, 542
Positronium, ***91,*** **181**
Positrons (e^+), 90, *91,* 110, 562–563
discovery of, **477, 561**
Potential energy (U), 81. *See also* Finite square wells; Infinite square wells; Simple harmonic oscillators
and alpha decay, 497, *497*
and coupling constants, 570–571, 577
and covalent bonding, 370–374, *372, 373*
of electric dipoles, 376, 377
gravitational, 625
and ionic bonding, 365–366, *366*
Kronig-Penney, *438,* 438–439
Lenard-Jones, 411
for quarks, 600, *600*
and Schrödinger equation, 223, 227–228
and solids, 415–417
of strong interaction, *479,* 506, *508, 515*
and vibrational energy levels, *382,* 382–383, *383*
vs. kinetic energy, 81–83
Pound, R. V., 100, 105, 552
Primitive vertices, *566,* **566,** *600*
Principle of equivalence, **98**–99, *99*
and gravitational redshift, 103–104
Principle quantum number (n), 161, **278**
Probability, and particle waves, 196, 201–205, 224–225
Probability amplitude ($\Psi(x, t)$), **225**
Probability density ($P(x, t)$)
in band theory of solids, *441*
for electron gases, 421, *422*
of exchange mesons, 512–513, *513*
in finite square wells, 241, *241*
for the hydrogen atom, 282–283, *283, 284, 285*
and indistinguishable particles, 295–296, 328, *329,* 330, 332
in infinite square wells, *233, 234,* 236–237, *237*
in simple harmonic oscillators, 248, *248*
Probability distribution functions ($P(x)$), 204–205
for exchange mesons, 512–513, *513*
for infinite square wells, 234, *234*
Prominences, solar, **629,** *629*
Proper frequency (f_0), **42**
Proper length (L_p), **33,** 38
as four-vector, 85
Proper time interval (τ), **21, 24, 31,** 38
as four-vector, 85
Proton-proton cycle, **535**–536, **625**–626, *626,* 627*t*
Protons (p), 479*t,* **561**
decay of, 606–607
diffraction of, 193, *194*
in interstellar medium, 653
Proxima Centauri, 640
Ptolemy, 636
Pulsars, **649,** *649*
Pump levels, in lasers, **397,** *397*
Purcell, E. M., 470
Pure rotational spectra, **380**

Q branches, **390**
Q-switching, **399**
Q values, **517**–520, 535
QED. *See* Quantum electrodynamics (QED)
QSOs. *See* Radio-quiet quasars (QSOs)
QSRs. *See* Radio-loud quasars (QSRs)
Quality factors (Q), **399**
Quantization, **115**–146
of angular momentum, 161, 275–277
and blackbody radiation, 119–127
and the Compton effect, 133–139
of electric charge, 115–119
of energy, 124–125, 129, 225, 238, 278–279
of energy states of matter, 346–351
of magnetic flux, 462
of magnetic moment, 287
and the photoelectric effect, 127–132
Quantum chromodynamics (QCD), **591,** 599–602
failures of, 595
and Feynman diagrams, 566
Quantum computers, **242,** 437
Quantum dots, **242**
Quantum electrodynamics (QED), 566
and antiparticles, 563
and dark matter, 639
and electron magnetic moment, 552
and interaction strengths, 577–578
and mediation of forces, 574
Quantum fluctuations, 206
Quantum gravity, 609, 671, 674
Quantum Hall effect, 450–451, *451*
Quantum interference, **304**–305, *305*
Quantum numbers, **161, 233,** 279–281
angular momentum (ℓ), **276**
energy (n), 161, 233
internal, **583,** 583*t*
magnetic (m), **276,** 280
in particle physics, 580–591
and Pauli exclusion principle, 296–297
principle (n), 161, **278**
rotational (ℓ), **379**
spin (m_s), **285**
total angular momentum (j), **291**
vibrational (v), **383**
Quantum statistics, 328–335
Quantum wells, **242,** *242*
Quantum wires, **242**
Quark confinement, **578, 600,** *601*
Quark model of hadrons, **591**–599
Quarks, **90, 479, 511, 568**–570, 569*t,* 593, *599,* 602*t*
discovery of, 154, **561**
internal quantum numbers of, **583,** 583*t*
naming of, 612
and quantum chromodynamics, 599–602
up-type *vs.* down-type, 569*t,* **570**
and weak interaction, 574
Quasars, **656**–657, *657,* 660
Quiet galaxies, **656**
Quiet Sun, **621**

R branches, **407**
Radial Schrödinger equation, **273**
Radiant flux (F), **620, 633,** 639
of quasars, 657
Radiation. *See also* Blackbody radiation; Cosmic background radiation; Electromagnetic radiation; Emission; Radioactivity
coherent, *391,* **394**
Hawking, 680
ionizing, 536*, 549*
radio-frequency (RF), **540**
resonance, *391,* **393**
thermal, **119**
Radiation dosages, 549*
Radiation era, **672**
Radio galaxies, **656,** *656*
Radioactivity, 492–495, **552**
decay modes of, 495–506
discovery of, 477
statistical nature of, 36–37, 492–493
units of, 493
Radio-frequency (RF) radiation, **540**
Radiography, **540**–542, *541, 542*
Radio-loud quasars (QSRs), **657**
Radiometric dating, 542–546, *543*
Radio-quiet quasars (QSOs), **657**
RAM. *See* Random access memory (RAM)
Raman, Chandrasekhara V., 390, 407
Raman scattering, **390**–392, *391, 392,* 407
Raman spectra, 392, *392*
Ramsauer-Townsend effect, 259
Random access memory (RAM), 437
Rayleigh, John W. Strutt, Lord, 122, 123, 141, 390
Rayleigh scattering, **390,** *391*
Rayleigh-Jeans equation, **122,** *123,* 125
Rayleigh's criterion, 215
Reactors. *See* Nuclear reactors
Rebka, G. A., 552
Recurrent novae, **644**
Red giants, **643**
Red subgiants, **643**
Red supergiants, **643**
Redshift, **42, 43**–44
cosmological, **659**–661
of galaxies, 656
of gamma-ray bursts, 652
gravitational, *103,* 103–105, **104,** *104,* **650**
and Hubble's law, 657–659, *658*
of quasars, 657
Reduced mass (μ), **165**–166
in moments of inertia, 380, 381
in Schrödinger equation, 272
in simple harmonic oscillators, 383
Reference clocks, in special relativity, **13,** *14*
Reference frames, 57
center-of-mass, *519,* **519,** 522
inertial, *4,* **4**–6#
laboratory, **518,** *519,* 522
non-inertial, 97
rest, 667
zero momentum (S′), **76**
Reflection of wave functions, 250–260

STUDENTS-HUB.com Uploaded By: Malak Obaid

Refraction
by electromagnetic waves, 147
index of, 304–305
Reines, Frederick, 500
Relativistic force (**F**), 70–71
Relativistic Heavy Ion Collider (RHIC), 111, 562, 595
Relativistic kinetic energy (E_k), 71–**72,** *72*
Relativistic mass ($m(u)$), 67–69, **68**
Relativistic mechanics, 222, 288
and de Broglie relations, 186
Relativistic momentum (**p**), 66–70, **67,** *68*
and fine-structure splitting, 167
Relativistic multiplier (γ), 19, 68
Relativistic speed ratio (β), 19, 43
Relativistic wave equations, 222, 288, 491, 512, 562, 564
Relativity, **3**–114
classical, 4–6#, 8–9, 11
and coordinate transformations, 17–29
and the Doppler effect, 41–45
and dynamics, 65–97
and Einstein's postulates, 11–17
and energy, 70–81
experimental basis of, 4–11
and gedanken experiments, 45–55
general, 47, **97**–108
and invariant mass, 84–97
and the Lorentz transformation, 17–29
and mass/energy conversion, 81–84
and momentum, 66–70
and motion, 3–64
of simultaneity, **14**–17, *15, 16, 17,* 48*, 50
special, **4**–97
and time dilation and length contraction, 29–40
Relaxation time (τ), **424**
Residual strong interaction, **603**–604
Resistance (*R*), 424
standard of, 451
Resistivity (ρ), **424**–425
and superconductivity, 458
temperature dependence of, 432–433, *433,* 443
Resonance absorption, **393**
Resonance radiation, *391,* **393**
Resonances, **522**–523, *524*
of hadrons, **573,** *587,* 591*, *599*
Response time-bandwidth relation, **199**
Rest energy (mc^2), **72**–73, 84*t*
of massless particles, 90
of moving objects, 86
Rest mass (*m*), **78**
and conservation of energy, 81–83
of moving objects, 86
Reverse biasing, *452,* **453**
RHIC. *See* Relativistic Heavy Ion Collider (RHIC)
Richardson, Robert C., 338
Richter, Burton, 597, 612
Right ascension (α), **636,** *636*
Right-handed coordinate systems, **589,** *589*
Rindler, W., 48, 50
Ritz, Walter, 150
Roche, Edouard A., 676
Roche lobes, *644,* **644,** 645
Rocks, radiometric dating of, 545–546
Roentgen, Wilhelm K., 133, 141, 477, 540
Rohrer, Heinrich, 257
Roosevelt, Franklin D., 531
Root-mean-square speed (v_{rms}), *320,* 320–321
Rotational energy levels, 379–382, *380*
Rotational quantum numbers (ℓ), **379**
Rubbia, Carlo, 574, 575, 612
Ruby lasers, *397,* 397–401, *398*
Rumford, Benjamin Thompson, Count, 89
Rutherford, Ernest, *151,* 178, 179
and atomic model, 141, 151, 153–156, 159, 263
and the nucleus, 157–159, 479, 480, *480,* 496, 517, 561, 593
and radiation, 477
Rutherford scattering, 153–156*
Rydberg, Johannes R., 150
Rydberg atoms, **168,** *168*
Rydberg constant (*R*), **150,** 162, 165–166
Rydberg-Ritz formula, **150,** 162
Ryle, Martin, 668, 676

SN1987A [supernova], *643, 646*
Sagittarius A*, *635,* 650–651
Salam, Abdus, 570
Satellites
BeppoSAX, 652
Cosmic Background Explorer (COBE), 126, 664, 669
geosynchronous, *5*
Saturated bonds, **374**
Saturated forces, **488,** 507, 509
s-bonding, **373**
Scale factor ($R(t)$), **667**
Scanning tunneling microscopes (STMs), *257,* 257–258
Scattered fraction (*f*), 155
Scattering, 390–392. *See also* Collisions
deep inelastic, **593**
elastic, **390,** *391,* **516**–517, *517*
and the nucleus, 508–509
Scattering angles (θ), **154,** *154*
Schrieffer, J. Robert, 463, 471
Schrödinger, Erwin R. J. A., *223,* 262
and de Broglie relations, 186, 192
and wave equation, 221–222, 225–226, 246, 269, 272, 288, 512
Schrödinger equation, 221–268, **224**. *See also* Wave equations
and acceptable wave functions, 227–229
and expectation values and operators, 242–246
and the finite square well, 238–242
and the infinite square well, 229–238
for multiple particles, 295–297
in one dimension, 222–229
radial, **273**
and reflection and transmission of waves, 250–260
and the simple harmonic oscillator, 246–250
in spherical coordinates, 271–272
in three dimensions, 269–272
time-independent, 226–**227**
and wave-particle duality, 212
Schwarzschild radius (R_S), **106, 650**
and limits of knowledge, 673
Schwinger, Julian, 612
SDSS. *See* Sloan Digital Sky Survey (SDSS)
Search for Extraterrestrial Intelligence (SETI), 630
Seasons, 637
Segrè, Emilio, 542, 553, 564, 612
Selection rules, **249**
for hydrogen atoms, **280,** *280*
and molecular spectra, *382,* 384, 385, *387,* 392
for nuclear transitions, 490, 583
for simple harmonic oscillators, 249, *249*
Semiconductor lasers, 403
Semiconductors
devices of, 452–459
impurity, **445**–452, *447*
intrinsic, *442,* 442–445, **443**
junctions of, **452,** *452*
n-type, **447,** *447*
p-type, *447,* **448**
Semimetals, **442**
Separation of variables, 226–227, **262,** 273
constant for (*C*), **226**–227
Series limits, **149,** *149,* **163,** *163*
SETI. *See* Search for Extraterrestrial Intelligence (SETI)
Seyfert, Carl, 656
Seyfert galaxies, **656**
Shapiro, I. I., 100
Shapley, Harlow, 634, 676
Shells
electronic, **293,** 301
nuclear, 488, 513–516*
Shielding, 299
Shock waves, 623
Shockley, William B., 456, 471
Short-range forces, **509**
Shroud of Turin, 548
Signal processing, 199
Silicon (Si), and impurity semiconductors, *446,* 446–448
Simple cubic (sc) crystal symmetry, **418,** *418*
Simple harmonic oscillators, *246,* 246–250
correspondence principle for, 248, *248*
and equipartition theorem, 324*
and heat capacities, 346–348
and Planck's law, 123–124, 125
and vibrational energy levels, *383*
Simultaneity
relativity of, **14**–17, *15, 16, 17,* 48*, 50
in spacetime, 28, *28*
Single-photon emission computer tomography (SPECT), **541**
Sirius, 631
SLAC. *See* Stanford linear accelerator (SLAC)
Sloan Digital Sky Survey (SDSS), 656, 661
Smirnov, A., 608
Smoke detectors, 496
Smoot, George F., 669, 676
Snell's law, 214
SNO neutrino observatory, 90, 129
Snyder, H., 105
Socrates, 612
Sodium (Na)
and band theory of solids, *441,* 441–442
spectra of, *149, 302,* 302–303, 490, *491*
Soft superconductors, **460,** *460*
Solar cells, **455,** *455*
Solar constant (*f*), **143, 620,** 639
Solar flares, **628,** *629*
Solar wind, **623**
Solar-neutrino problem, **536, 607**–608, 625–**626,** *626*
Solid angle (Ω), 178
Solid state physics, 413–476
and band theory of solids, 438–445
and conduction, classical, 422–426
and conduction, quantum, 430–434
and the free-electron gas in metals, 426–430
and impurity semiconductors, 445–452
and magnetism, 434–437
and semiconductor junctions and devices, 452–457
and the structure of solids, 413–422
and superconductivity, 458–468
Solids
amorphous, **414**
covalent, 415–421
ionic, 415–421
polycrystalline, 414
structure of, 413–422
Solstices, *637,* **637, 676**
Sommerfeld, Arnold, 167, 215, 285, 434
Southern Cross, 631
sp^2 and sp^3 hybridization, 420
Spacelike spacetime intervals, **37, 38**
Spacetime, **14**
Spacetime diagrams, 23–29, *24*. *See also* Feynman diagrams
calibrating axes of, 28–29
Spacetime intervals (Δs), **37**–40
as four-vector, 84–85
lightlike, **37, 39**

STUDENTS-HUB.com Uploaded By: Malak Obaid

spacelike, **37, 38**
timelike, **37, 38**
Special relativity, **4**–97
Specific heat. *See* Heat capacities (C_V)
SPECT. *See* Single-photon emission computer tomography (SPECT)
Spectra, **147**
absorption, of diatomic molecules, 385–390, *388*
ammonia inversion, **392**
atomic, 148–150, *149*
band, **147**
characteristic, **135,** *136*
continuous, **147**–148
emission, of diatomic molecules, 384–385, *385, 386*
line, **147**–148, *148*
nuclear, 480, 508, *523*
pure rotational, **380**
Raman, 392, *392*
of supernovae, 645
vibrational-rotational, **385,** *386*
x-ray, 169–173, *172*
Spectral distributions, **120**–121, *121*
Spectral lines, **116**
Doppler broadening of, 328, 656
and Hubble's law, *658*
natural width (Γ_0) of, 210–**211,** 504–505, 522
and stellar classification, 632
Spectroscopic notation, 292*–293
Spectroscopy, **147**
accelerator mass (AMS), **537,** 545, 546–548, *548*
atomic beam fluorescence, 490
electron energy loss (EELS), **175**–176, *176*
Speed. *See also* Velocity
Fermi (u_F), **431**
molecular, 319–322
superluminal, 52–55, *54*
Speed of light (c), 6–7, 57
and ether, 7–11
slowing of, 304–*305*
and special relativity, 12
and time dilation, 31
and worldlines, *26*
Spherical coordinates, 271–272, *272, 282*
Spherical harmonic functions, **274,** 274*t,* 281
Spin angular momentum (**S**), **167,** 285–290
of antineutrinos, *584*
of hadrons, 573*t,* 586*t*
and magnetism, 434–437
nuclear (**I**), 304, **489**
of protons, 595–596
of quarks, 569*t*
Spin Hall effect, **437,** 452
Spin quantum numbers (m_s), **285**
Spin valves, **437**
Spin-orbit effect, **293**–295
nuclear, 515, *515*
Spintronics, **437,** *437*
Spontaneous emission, **393**
vs. stimulated emission, 395
Spring equinox, **637,** *637*
SQUIDs. *See* Superconducting quantum interference devices (SQUIDs)
Standard candles, 640, 645, 648, 663
Standard Model, 511, **562,** 591–604
and conservation laws, 581, 590
failures of, 605
and mass, 603
and mediation of forces, 571, 603
and quarks and gluons, 568, 570
summary of, **603**–604
Standing waves
and de Broglie relations, 186, *186*
and lasers, 398, *398*
and Planck's law, 123
and Schrödinger equation, 226
Stanford linear accelerator (SLAC), 113, 481, 597
Star clusters, **632**
Stars, 630–652, 642*t*. *See also* Astrophysics; Cosmology; Galaxies; Sun
and cataclysmic events, 644–646
classification of, 632, 633*t*
composition of, 149, 302
constellations of, **631,** *631*
evolution of, 639–643
final states of, 647–652
and Hertzsprung-Russell diagrams, *641,* **641**–643
magnitude of, **632**–**633**
neutron, **484**
populations of, **632**
surface temperature of, 121, 639, 641, *641*
Stationary states, **160,** 226
Statistical physics, 315–360
and Bose-Einstein condensates, 335–343
classical, 316–328
and fermion gases, 351–354
and nuclear reactions, 521–522
and photon gases, 344–351
quantum mechanical, 328–335
and radioactivity, 36–37, 492–493
Stefan, Josef, 120, 356
Stefan-Boltzmann law, 120, 126
and stellar temperatures, 620
Stefan's constant (σ), 120, 126, 620
Stellar aberration, 61
Stellar populations, **632**
Step potentials, *251,* 251–255, *253, 254*
Stern, Otto, 193, 286, 289–290, 307, 359
Stern-Gerlach experiment, 286, 288–290, *289, 290*
Stimulated emission, *391,* **394**–396. *See also* Lasers
vs. spontaneous emission, 395
STMs. *See* Scanning tunneling microscopes (STMs)
Stoney, George J., 116, 141
Stopping potential (V_0), **128**–130, *130*
Stormer, H. L., 471
Strangeness (S), **564, 583–584,** 583*t,* 586*t*
Strassmann, Fritz, 527, 530, 553
String theories, **606**
Strong interaction, **506**–513, 571–573, 576*t*. *See also* Fundamental interactions
and alpha decay, 258–259
and beta decay, 501
and cosmology, 671–672
range of, 484, 510–511, 578
residual, **603**–604
transmission of, 90
Strutt, John W., Lord Rayleigh, 122, 123, 141, 390
SU(2) group theory, 592
SU(3) group theory, 592–595
Sudbury Neutrino Observatory, 536, 582, *607,* 607–608
Summer solstice, **637,** *637*
Sun, 619–629. *See also* Astrophysics; Stars
active, 627–629
change in mass of, 79
chromosphere of, *622,* **622**–623, *623*
core of, **623**
corona of, **623**
energy source of, 535–536, 624–627
interior of, 623–624
limbs of, **621,** *622*
magnetic field of, *627,* 627–629, *628*
mass of, 623
photosphere of, **620**–622, *622*
proton-proton cycle in, **535**–536, **625**–626, *626,* 627*t*
quiet, **621**
spectrum of, 328
surface and atmosphere of, 125, 620–623, *622, 623*
x rays from, *621,* 623
Sunspot cycle, **627**–628, *629*
Sunspots, *622,* **628,** *628*
Superclusters, 661, 662
Superconducting energy gaps (E_g), **464**–465, *465*
Superconducting quantum interference devices (SQUIDs), **468,** *468*
Superconductivity, **458**–468
BCS theory of, **463**–465
high-temperature, *460,* 466, 466*t*
type I *vs.* type II, **460,** *460*
Supercurrents, **459**
Superfluids, **336**–339, **338,** *338, 339*
Super-Kamiokande Neutrino Observatory, 90, 129, 536, 582, *607,* 608, 646
Superleaks, **356**
Superluminal speeds, 52–55, *54*
Supermultiplets, **591,** 598, *598*
Supernovae, 484, *643,* **645**–646, *646*
as standard candles, 640, 645, 648, 663
Superpartners, 568, **605**–606, 606*t*
and dark matter, 639
Superposition. *See also* Diffraction; Interference
and stationary states, 235, 262
and wave packets, 198, *198*
Superstring theories, **606, 609**
Supersymmetry (SUSY), 568, **605**–606
Surface tension, 378
Surface-barrier detectors, **454**
Symmetry
breaking of, *602,* 602–603
and conservation laws, 66, 580–591
and crystallography, *415,* 415–421, 416*t, 418, 419, 420*
and three-dimensional square wells, 271, *271*
and wave-particle duality, 185
Synchronization, in special relativity, **13,** *14,* 15

Taagepera, B., 497
Tachyons, **54**–55
Tarantula nebula, *643*
Taylor, E. F., 48
Taylor, J. H., 106
TCP invariance, 589–590
Temperature (T), 319*
critical (T_c), for Bose-Einstein condensates, 340–341
critical (T_c), for superconductivity, **458,** 458*t, 459,* 466*t*
Curie (T_C), **436**
Debye (T_B), **348,** *348*
Einstein (T_E), *347,* **347,** 432–433
Fermi (T_F), **430**
Néel (T_N), **436**
stellar, 639, 641, *641*
of the Sun, 125, *621,* 621–623
Thales, 630
Theories of everything, 610*
Thermal conduction, 337, 434*
Thermal equilibrium, 119–120
Thermal neutrons, **524**
Thermal radiation, **119**
Thermomechanical effect, **338,** *339*
Thompson, Benjamin, Count Rumford, 89
Thompson, C., 542
Thompson, William, Lord Kelvin, 2, 307
Thomson, George P., 192, 214
Thomson, Joseph J., *117,* 141, 178, 179, 192
and atomic model, 150–151
and discovery of electrons, 116, 118, 127, 214, 422, 561, 568
and polyatomic molecules, 374
Thomson experiment, 116–118, *117,* **117**
Thought experiments. *See* Gedanken experiments
Time. *See also* Clocks
absolute direction of, 590
interaction, **571**
relativistic, 18–21
relaxation (τ), **424**

STUDENTS-HUB.com Uploaded By: Malak Obaid

Time dilation, *30,* 30–33, **31**
  and Doppler effect, 45
  gravitational, **101**
Time intervals, proper (τ), **21**
Time-independent Schrödinger equation, 226–**227,** 245
Timelike spacetime intervals, **37, 38**
Timelike worldlines, **38**
Ting, Samuel Chao Chung, 597, 612
Tokamaks, **532,** *533*
Tomography, **552**. *See also* Computer assisted tomography (CAT); Positron emission tomography (PET); Single-photon emission computer tomography (SPECT)
Tomonaga, Sin-itiro, 612
Top (*T*), 570, 583, 583*t*
Torque (τ)
  and magnetic moments, 287, *287*
  and precession, 291
  relativistic, 80–81
Total angular momentum quantum numbers (*j*), **291**
Totalitarian principle, **580**
Townes, Charles, 396
Townsend, John S. E., 118
Tracers, isotopic, 179
Transcendental equations, 241*
Transformation of coordinates. *See also* Coordinate systems; Lorentz transformation
  Galilean, **5**–6#, 11
Transistors, 456, *456,* 457*
Transition elements, **300**
Transitions between energy states, 246*, 393*, 395*
Transmission of wave functions, 250–260
Tritium, 526, 533
Tsui, Daniel C., 451, 471
Tunnel diodes, 257, 260*, 453, **454**
Tunneling, 241, *256,* 256–**257**
  and alpha decay, 258–259, 497, *497*
  and fission, 528
  and fusion, 532, 625
  and Josephson junctions, 466–467
  and scanning tunneling microscopes (STMs), *257,* 257–258
  and semiconductor devices, 454, *454*
Tunneling current, *453,* **454**
  and Josephson junctions, *467*
Type I superconductors, **460,** *460*
Type I supernovae, **645**
  of white dwarfs, 647–648
Type II superconductors, **460,** *460*
Type II supernovae, *645,* **645**–646

Uhlenbeck, George E., 285, 307
Uncertainty principle, **205**–208
  and angular momentum, 277, 292
  classical, 199–201, **200**
  consequences of, 208–211
  and finite square wells, 240–241
  and infinite square wells, 234
  and limits of knowledge, 673
  and mediation of forces, 510
Unified mass unit (u), **380**
Unit cells, **415**
Universe. *See also* Big Bang
  acceleration of expansion of, 640, 662
  evolution of, 302
  expansion of, 659–660, 668
  geometry of, 666
  photon density of, 345
Up (*U*), 570, 583, 583*t*
Up-type quarks, 569*t,* **570**
Uranium
  diffusion of, 320
  fission of, 526, 528–530, *529*
  isotopes of, 267
Urey, Harold C., 165, 179

Vacuum polarization, *578,* **578,** 600
Valence bands, **441,** *441, 442*
Van de Graaff generators, 477, *518*
  and accelerator mass spectroscopy, 547, *547*
van der Meer, Simon, 612
van der Waals, Johannes D., *336,* 376, 378, 407
van der Waals attraction, 368, 374, **378, 407**
Vector models, **277,** *277*
Velocity. *See also* Speed
  drift (v_d), **423**–424
  escape (v_e), 106, 323–324, 650, 679
  group (v_g), **197,** 199
  phase (v_p), **196,** 199
  relativistic transformations of, 21–23
Vernal equinox, **637,** *637*
Very Large Array, 635
Very Large Telescope (VLT), 652
Vessot, R. F. C., 105
Vibrational energy levels, *382,* 382–384
Vibrational quantum numbers (v), **383**
Vibrational-rotational spectra, **385,** *386*
Virtual particles, **206**
  and exchange forces, 509–511
  Feynman diagrams for, **566,** *567, 574*
  and vacuum polarization, 578, *578*
Virtual photons, **509**–510
VLT. *See* Very Large Telescope (VLT)
von Fraunhofer, Joseph, 147, 178, 393, 632
von Helmholtz, Hermann, 109, 141, 580
von Klitzing, Klaus, 450–451, 471
von Klitzing constant (R_K), **450**–451
von Laue, Max, 80, 134
Vortices, **461,** *461, 462*

$W^{\pm}$ bosons, 575, *575,* 576*t*
Walsh, D., 103
Walton, Ernest T. S., 477, *516,* 552
Wave equations. *See also* Schrödinger equation
  classical, **196,** 202, 212, 222
  relativistic, 222, 288, 491, 512, 562, 564
Wave functions ($\psi_n(x)$)
  and alpha decay, 497, *497*
  for barrier potentials, 256, *256*
  and covalent bonding, *369,* 369–370
  for finite square wells, 239–241, *240, 241*
  for the hydrogen atom, 281–285
  for hydrogen molecules, 370–374, *371*
  for infinite square wells, 230–233, *233*
  macroscopic, **342,** *342*
  for neutrinos, 608
  for plane waves, 439
  reflection and transmission of, 250–260
  for simple harmonic oscillators, 246–248, *247*
  for step potentials, *252,* 252–255, *254*
  and *TCP* invariance, 589–590
Wave number (k), **178, 196, 214**
Wave packets
  dispersion of, 204, *204*
  for particles, 201–202
  reflection and transmission of, *253*
  for waves ($\Psi(x, t)$), 196–199, **197**
Wave vectors (k), 439–**441**
Wave velocity. *See* Phase velocity (v_p)
Wave-particle duality, 185, 212–213*
  and Compton effect, 138
  and photon gases, 345
  and uncertainty principle, 206
Waves. *See also* Particle waves
  gravitational, *106,* **106**–108
  harmonic, **196,** 222, 224
  matter, **187**–196
  shock, 623
Weak charge, **570, 574,** 576*t*
Weak interaction, **501,** 574–576, 576*t*. *See also* Fundamental interactions
  and cosmology, 671
  Feynman diagrams for, *574*
  range of, 576
Weak isospin (T_z), **568,** 569*t,* 570
Weakly interacting massive particles (WIMPs), 638–639
Weight diagrams, **592,** *592, 593*
Weinberg, Steven, 570
Weizsächer semiempirical mass formula, 489*, *489,* 502, 559
Wheeler, John A., 48, 527, 676
White dwarfs, 643, **647**–648, *648*
Wieman, Carl E., 341, 343
Wien, Wilhelm, 121
Wien's displacement law, 120–121, 125
Wigner, Eugene, 552
Wilczek, Frank, 674, 676
Wilkinson Microwave Anisotropy Project (WMAP), 127, 664, 665, 669
Wilson, Robert Woodrow, 126, 669, 676
WIMPs. *See* Weakly interacting massive particles (WIMPs)
Winter solstice, **637,** *637*
WMAP. *See* Wilkinson Microwave Anisotropy Project (WMAP)
Wolfenstein, L., 608
Wolfke, Mieczysl̂ aw, 335
Wollaston, William H., 178
Work
  and relativity, 71, 80–81
  and torque, 287
Work function (ϕ), **129,** 130, 130*t,* 136
Worldlines, **24**–27, *25, 26, 27*
  of tachyons, *55*
  timelike, **38**
Wu, C. S., 588, 589

X rays, *133,* 133–136
  discovery of, 477
  and particle-induced x-ray analysis (PIXE), 548–549, *549*
  from solar corona, *621,* 623
  spectra of, 169–173, *172*

Yang, C. N., 588, 590
Yukawa, Hideki, 552
  and exchange forces, 509–511, 566, 571, 600

Z^0 bosons, *91,* 575, *575,* 576*t, 599*
Zeeman, Pieter, 57, 116, 117, 295, 307
Zeeman effect, **116,** 280, **295,** 303*
  nuclear analog of, 491
Zener breakdown, *453,* **454**
Zener diodes, *453,* **454**
Zero momentum frames (S′), **76**
Zero point energy, 208–**209,** 336, 368
Zweig, George, 593
Zwicky, Fritz, 638

STUDENTS-HUB.com Uploaded By: Malak Obaid

The Greek Alphabet

Alpha	A	α	Iota	I	ι	Rho	P	ρ
Beta	B	β	Kappa	K	κ	Sigma	Σ	σ
Gamma	Γ	γ	Lambda	Λ	λ	Tau	T	τ
Delta	Δ	δ	Mu	M	μ	Upsilon	Υ	υ
Epsilon	E	ϵ	Nu	N	ν	Phi	Φ	ϕ
Zeta	Z	ζ	Xi	Ξ	ξ	Chi	X	χ
Eta	H	η	Omicron	O	o	Psi	Ψ	ψ
Theta	Θ	θ	Pi	Π	π	Omega	Ω	ω

Prefixes for Powers of 10

Multiple	Prefix	Abbreviation
10^{18}	exa	E
10^{15}	peta	P
10^{12}	tera	T
10^{9}	giga	G
10^{6}	mega	M
10^{3}	kilo	k
10^{2}	hecto	h
10^{1}	deka	da
10^{-1}	deci	d
10^{-2}	centi	c
10^{-3}	milli	m
10^{-6}	micro	μ
10^{-9}	nano	n
10^{-12}	pico	p
10^{-15}	femto	f
10^{-18}	atto	a

Mathematical Symbols

$=$	is equal to	Δx	change in x
$\neq$	is not equal to	$\lvert x \rvert$	absolute value of x
$\approx$	is approximately equal to	$n!$	$n(n-1)(n-2)\cdots 1$
$\sim$	is of the order of	Σ	sum
$\propto$	is proportional to	lim	limit
$>$	is greater than	$\Delta t \rightarrow 0$	Δt approaches zero
$\geq$	is greater than or equal to	$\frac{dx}{dt}$	derivative of x with respect to t
$\gg$	is much greater than		
$<$	is less than	$\frac{\partial x}{\partial t}$	partial derivative of x with respect to t
$\leq$	is less than or equal to		
$\ll$	is much less than	$\int$	integral

STUDENTS-HUB.com Uploaded By: Malak Obaid

Abbreviations for Units

A	ampere	keV	kilo-electron volts
Å	angstrom (10^{-10} m)	L	liter
atm	atmosphere	m	meter
Btu	British thermal unit	MeV	mega-electron volts
Bq	becquerel	min	minute
C	coulomb	mm	millimeter
°C	degree Celsius	ms	millisecond
cal	calorie	N	newton
Ci	curie	nm	nanometer (10^{-9} m)
cm	centimeter	rev	revolution
eV	electron volt	R	roentgen
°F	degree Fahrenheit	Sv	seivert
fm	femtometer, fermi (10^{-15} m)	s	second
G	gauss	T	tesla
Gy	gray	u	unified mass unit
g	gram	V	volt
H	henry	W	watt
h	hour	Wb	weber
Hz	hertz	y	year
J	joule	μm	micrometer (10^{-6} m)
K	kelvin	μs	microsecond
kg	kilogram	μC	microcoulomb
km	kilometer	Ω	ohm

Some Useful Combinations

$hc = 1.9864 \times 10^{-25}\ \text{J}\cdot\text{m} = 1239.8\ \text{eV}\cdot\text{nm}$

$\hbar c = 3.1615 \times 10^{-26}\ \text{J}\cdot\text{m} = 197.33\ \text{eV}\cdot\text{nm}$

Bohr radius $a_0 = \dfrac{4\pi\varepsilon_0\hbar^2}{m_e e^2} = 5.2918 \times 10^{-11}\ \text{m}$

$ke^2 = 1.440\ \text{eV}\cdot\text{nm}$

Fine structure constant $\alpha = \dfrac{e^2}{4\pi\varepsilon_0\hbar c} = 0.0072974 \approx \dfrac{1}{137}$

$kT = 2.5249 \times 10^{-2}\ \text{eV} \approx \frac{1}{40}\ \text{eV}$ at $T = 293\ \text{K}$

STUDENTS-HUB.com Uploaded By: Malak Obaid

Some Physical Constants

(See Appendix D for a complete list of fundamental constants.)

Avogadro's number	N_A	6.022142×10^{23} particles/mol
Boltzmann's constant	k	1.380650×10^{-23} J/K
Bohr magneton	$m_B = e\hbar$	$9.2740095 \times 10^{-24}$ J/T
Coulomb constant	$k = 1/4\pi\varepsilon_0$	$8.987551788 \times 10^{9}$ N·m²/C²
Compton wavelength	$\lambda_c = h/m_e c$	$2.42631024 \times 10^{-12}$ m
Fundamental charge	e	1.602176×10^{-19} C
Gas constant	$R = N_A k$	8.31447 J/mol·K = 1.987 22 cal/mol·K
		$= 8.20578 \times 10^{-2}$ L·atm/mol·K
Gravitational constant	G	6.6742×10^{-11} N·m²/kg²
Mass, of electron	m_e	9.109382×10^{-31} kg
		$= 510.9989$ keV/c^2
of proton	m_p	1.672622×10^{-27} kg
		$= 938.2722$ MeV/c^2
of neutron	m_n	1.674927×10^{-27} kg
		$= 939.5653$ MeV/c^2
Permeability of free space	μ_0	$4\pi \times 10^{-7}$ N/A²
Planck's constant	h	6.626069×10^{-34} J·s
		$= 4.135667 \times 10^{-15}$ eV·s
	$\hbar$	1.054572×10^{-34} J·s
		$= 6.582119 \times 10^{-16}$ eV·s
Speed of light	c	2.99792458×10^{8} m/s
Unified mass unit	u	1.660539×10^{-27} kg
		$= 931.49401$ MeV/c^2

Some Conversion Factors

1 yr = 3.156×10^7 s	1 T = 10^4 G
1 light-year = 9.461×10^{15} m	1 Ci = 3.7×10^{10} Bq
1 cal = 4.186 J	1 barn = 10^{-28} m²
1 MeV/c = 5.344×10^{-22} kg·m/s	1 u = 1.66054×10^{-27} kg
1 eV = 1.6022×10^{-19} J	1 parsec = 3.26 light-years
1 kW·h = 3.6 MJ	1 rad = 57.30°

Some Particle Masses and Rest Energies

	kg	**MeV/c^2**	**u**
Electron	9.1094×10^{-31}	0.51100	5.4858×10^{-4}
Muon	1.8835×10^{-28}	105.66	0.11343
Proton	1.6726×10^{-27}	938.27	1.00728
Neutron	1.6749×10^{-27}	939.57	1.00866
Deuteron	3.3436×10^{-27}	1875.61	2.01355
α particle	6.6447×10^{-27}	3727.38	4.00151
W	1.43×10^{-25}	80×10^3	85.9
Z°	1.63×10^{-25}	91.2×10^3	97.9

STUDENTS-HUB.com Uploaded By: Malak Obaid

Periodic Table

1																	18
1 H Hydrogen 1.007 94(7)	2											13	14	15	16	17	2 He Helium 4.002 602(2)
3 Li Lithium 6.941(2)	4 Be Beryllium 9.012 182(3)											5 B Boron 10.811(7)	6 C Carbon 12.0107(8)	7 N Nitrogen 14.0067(2)	8 O Oxygen 15.9994(3)	9 F Fluorine 18.998 4032(5)	10 Ne Neon 20.1797(6)
11 Na Sodium 22.989 769 28(2)	12 Mg Magnesium 24.3050(6)	3	4	5	6	7	8	9	10	11	12	13 Al Aluminum 26.981 538 6(8)	14 Si Silicon 28.0855(3)	15 P Phosphorus 30.973 762(2)	16 S Sulfur 32.065(5)	17 Cl Chlorine 35.453(2)	18 Ar Argon 39.948(1)
19 K Potassium 39.0983(1)	20 Ca Calcium 40.078(4)	21 Sc Scandium 44.955 912 (6)	22 Ti Titanium 47.867(1)	23 V Vanadium 50.9415(1)	24 Cr Chromium 51.9961(6)	25 Mn Manganese 54.938 045(5)	26 Fe Iron 55.845(2)	27 Co Cobalt 58.933 195(5)	28 Ni Nickel 58.6934(2)	29 Cu Copper 63.546(3)	30 Zn Zinc 65.409(4)	31 Ga Gallium 69.723(1)	32 Ge Germanium 72.64(1)	33 As Arsenic 74.921 60(2)	34 Se Selenium 78.96(3)	35 Br Bromine 79.904(1)	36 Kr Krypton 83.798(2)
37 Rb Rubidium 85.4678(3)	38 Sr Strontium 87.62(1)	39 Y Yttrium 88.905 85(2)	40 Zr Zirconium 91.224(2)	41 Nb Niobium 92.906 38 (2)	42 Mo Molybdenum 95.94(2)	43 Tc Technetium [97.9072]	44 Ru Ruthenium 101.07(2)	45 Rh Rhodium 102.905 50(2)	46 Pd Palladium 106.42(1)	47 Ag Silver 107.8682(2)	48 Cd Cadmium 112.411(8)	49 In Indium 114.818(3)	50 Sn Tin 118.710(7)	51 Sb Antimony 121.760(1)	52 Te Tellurium 127.60(3)	53 I Iodine 126.904 47(3)	54 Xe Xenon 131.293(6)
55 Cs Cesium 132.905 451 9 (2)	56 Ba Barium 137.327(7)	57-71 Lanthanoids	72 Hf Hafnium 178.49(2)	73 Ta Tantalum 180.947 88(2)	74 W Tungsten 183.84(1)	75 Re Rhenium 186.207(1)	76 Os Osmium 190.23(3)	77 Ir Iridium 192.217(3)	78 Pt Platinum 195.084(9)	79 Au Gold 196.966 569(4)	80 Hg Mercury 200.59(2)	81 Tl Thallium 204.3833(2)	82 Pb Lead 207.2(1)	83 Bi Bismuth 208.980 40(1)	84 Po Polonium [208.9824]	85 At Astatine [209.9871]	86 Rn Radon [222.0176]
87 Fr Francium [223]	88 Ra Radium [226]	89-103 Actinoids	104 Rf Rutherfordium [261]	105 Db Dubnium [262]	106 Sg Seaborgium [266]	107 Bh Bohrium [264]	108 Hs Hassium [277]	109 Mt Meitnerium [268]	110 Ds Darmstadtium [271]	111 Rg Roentgenium [272]	112 UUb [277]	113 Uut [284]	114 Uuq [289]	115 Uup [288]	116 Uuh [292]		118 Uuo [294]

57 La Lanthanum 138.905 47(7)	58 Ce Cerium 140.116(1)	59 Pr Praseodymium 140.907 65(2)	60 Nd Neodymium 144.242(3)	61 Pm Promethium [145]	62 Sm Samarium 150.36(2)	63 Eu Europium 151.964(1)	64 Gd Gadolinium 157.25(3)	65 Tb Terbium 158.925 35(2)	66 Dy Dysprosium 162.500(1)	67 Ho Holmium 164.930 32(2)	68 Er Erbium 167.259(3)	69 Tm Thulium 168.934 21(2)	70 Yb Ytterbium 173.04(3)	71 Lu Lutetium 174.967(1)
89 Ac Actinium [227]	90 Th Thorium 232.038 06(2)	91 Pa Protactinium 231.035 88(2)	92 U Uranium 238.028 91(3)	93 Np Neptunium [237]	94 Pu Plutonium [244]	95 Am Americium [243]	96 Cm Curium [247]	97 Bk Berkelium [247]	98 Cf Californium [251]	99 Es Einsteinium [252]	100 Fm Fermium [257]	101 Md Mendelevium [258]	102 No Nobelium [259]	103 Lr Lawrencium [262]

Notes

- Symbols for elements 112 through 118 are temporary placeholders. The corresponding Latin names are, using 115 as an example, Ununpentium, meaning element one, one, five.

STUDENTS-HUB.com

Uploaded By: Malak Obaid